Methods in Molecular Biology 2450

Springer Protocols



Simon Blanchoud
Brigitte Galliot *Editors*

Whole-Body Regeneration

Methods and Protocols

OPEN ACCESS

Humana Press

METHODS IN MOLECULAR BIOLOGY

Series Editor
John M. Walker
School of Life and Medical Sciences
University of Hertfordshire
Hatfield, Hertfordshire, UK

For further volumes:
http://www.springer.com/series/7651

For over 35 years, biological scientists have come to rely on the research protocols and methodologies in the critically acclaimed *Methods in Molecular Biology* series. The series was the first to introduce the step-by-step protocols approach that has become the standard in all biomedical protocol publishing. Each protocol is provided in readily-reproducible step-by-step fashion, opening with an introductory overview, a list of the materials and reagents needed to complete the experiment, and followed by a detailed procedure that is supported with a helpful notes section offering tips and tricks of the trade as well as troubleshooting advice. These hallmark features were introduced by series editor Dr. John Walker and constitute the key ingredient in each and every volume of the *Methods in Molecular Biology* series. Tested and trusted, comprehensive and reliable, all protocols from the series are indexed in PubMed.

Whole-Body Regeneration

Methods and Protocols

Edited by

Simon Blanchoud

Department of Biology, University of Fribourg, Fribourg, Fribourg, Switzerland

Brigitte Galliot

Dept Génétique et Evolution, Université de Genève, Genève, Geneva, Switzerland

Humana Press

Editors
Simon Blanchoud
Department of Biology
University of Fribourg
Fribourg, Fribourg, Switzerland

Brigitte Galliot
Dept Génétique et Evolution
Université de Genève
Genève, Geneva, Switzerland

ISSN 1064-3745 ISSN 1940-6029 (electronic)
Methods in Molecular Biology
ISBN 978-1-0716-2171-4 ISBN 978-1-0716-2172-1 (eBook)
https://doi.org/10.1007/978-1-0716-2172-1

© The Editor(s) (if applicable) and The Author(s) 2022, Corrected Publication 2022
Open Access This book is licensed under the terms of the Creative Commons Attribution 4.0 International License (http://creativecommons.org/licenses/by/4.0/), which permits use, sharing, adaptation, distribution and reproduction in any medium or format, as long as you give appropriate credit to the original author(s) and the source, provide a link to the Creative Commons license and indicate if changes were made.
The images or other third party material in this book are included in the book's Creative Commons license, unless indicated otherwise in a credit line to the material. If material is not included in the book's Creative Commons license and your intended use is not permitted by statutory regulation or exceeds the permitted use, you will need to obtain permission directly from the copyright holder.
The use of general descriptive names, registered names, trademarks, service marks, etc. in this publication does not imply, even in the absence of a specific statement, that such names are exempt from the relevant protective laws and regulations and therefore free for general use.
The publisher, the authors and the editors are safe to assume that the advice and information in this book are believed to be true and accurate at the date of publication. Neither the publisher nor the authors or the editors give a warranty, expressed or implied, with respect to the material contained herein or for any errors or omissions that may have been made. The publisher remains neutral with regard to jurisdictional claims in published maps and institutional affiliations.

Cover Caption: The drawing visible on the cover of this book was created by Rosalie Fortabat, 10 year-old CM2 student from École du Port de la Ville de Nice, in the context of the multidisciplinary project "WORKSTATION NICE. MARINE MODELS. DRAWING REGENERATION" by the artist Irene Kopleman. Irene Kopleman's project was a collaboration between the artist, the Musée d'Art Moderne et d'Art Contemporain in Nice (MAMC, FR), the Tiozzo Lab at the Institute de la Mer de Villefranche-sur-Mer (FR), and the Röttinger Lab at the Institute for Research on Cancer and Aging in Nice (FR). The project allowed the public to experience, to participate, and to contribute to the progress of research on the regenerative capacities of marine invertebrates. May such multidisciplinary projects continue to flourish to stimulate the curiosity of young generations for art, for science and for regeneration research in particular.

This Humana imprint is published by the registered company Springer Science+Business Media, LLC, part of Springer Nature.
The registered company address is: 1 New York Plaza, New York, NY 10004, U.S.A.

Preface

Whole-body regeneration (WBR) is the ability of an adult organism to restore a complete, functional body from a fragment of itself. Since Trembley's pioneering work in 1744, this amazing process has intrigued scientists who continue to characterize the mechanisms underlying spontaneous regeneration, with the hope that understanding them will open up avenues to human therapies. Although it is one of the oldest areas of experimental research in the life sciences, WBR retains enormous appeal as well as much of its mystery. One of the most puzzling aspects of WBR is the wide diversity of forms and species it involves. This phylogenetic dispersion is a fantastic asset for piecing together the puzzle of WBR origins and evolutions through comparative analyses. Indeed, each WBR context appears to be a mixture of evolutionarily conserved processes and species-specific innovations. From this perspective, the study of WBR in these aquatic invertebrates, which are generally not established model systems, is a major experimental and conceptual challenge.

This book aims to provide a comprehensive overview of the many tools available to scientists to study the numerous facets of WBR. The first part of this book provides information on the diversity of WBR, on the main challenges of this research, and on the variety of approaches used to address this topic over time. The second and third parts present a series of zoological contexts where WBR is well established and can be studied in the lab with appropriate cellular tools (Fig. 1). By including as many phyla as possible and

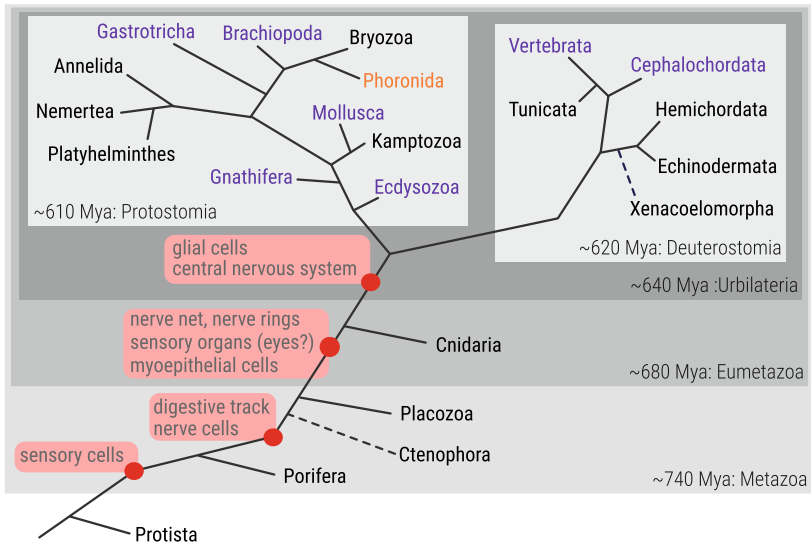


Fig. 1 Whole-body regeneration (WBR) across metazoan phyla. Taxa written in black are exemplified in the current issue, those in orange are not represented in this book, and the ones in purple do not have known examples of WBR. The phylogenetic tree is overlaid with key developmental innovations highlighted by red boxes. Debated phylogenetic relations are indicated by dashed lines. Phylogeny of the depicted taxa and the estimated times of divergence were adapted from (**1**) dos Reis *et al.*, 2015, Current Biology 25, 2939–2950, DOI: 10.1016/j.cub.2015.09.066 and (**2**) Marlétaz *et al.*, 2019, Current Biology 29, 312–318, DOI: 10.1016/j.cub.2018.11.042

Table 1
Techniques and taxa covered by every chapter

		All	Protista	Porifera		Ctenophora	Placozoa	Cnidaria				Kamptozoa	Bryozoa	Annelida				Nemertea	Platyhelminthes			Xenacoelo-morpha		Echinodermata		Hemichordata	Tunicata		
Techniques	**Species**	Review	*Physarum polycephalum*	*Ephydatia fluviatilis*	*Leucosolenia sp.*	*Mnemiopsis leidyi*	*Trichoplax adhaerens*	*Acropora hyacinthus*	*Hydra vulgaris*	*Hydractinia symbiolongicarpus*	*Nematostella vectensis*	all	all	*Aeolosoma viride*	*Diopatra neapolitana*	*Platynereis dumerilii*	*Lineus sanguineus*	all	*Macrostomum lignano*	*Schmidtea mediterranea*	*Hofstenia miamia*	*Isodiametra pulchra*	*Echinaster sepositus*	*Marthasterias glacialis*	*Ptychodera flava*	*Botryllo̲ides anceps*	*Botryllo̲ides diegensis*	*Botryllo̲ides leachii*
Animal handling	algae culture											7																	
	anesthesia	2							33				8		10							13				16		
	animal collection				4	5						7	8		10		12						14		15	16		
	breeding		3		4	5	6			22		7	8	9	10		12		26				14			16		
	maze		3																										
	spawning					5				22			8			11			26										
	surgery	2	3		4	5,18	6		33		30	7		9	10	11	12			27		13	14		15	16			
Organismal	drug treatment	2				5										11													
	histological sectioning				4																		14			16			
	immunohistochemistry				4																	13							
	injection									22	23			9					26								21		
	staining						6					7	8													16	21		
	electron microscopy				4								8										14						
	electroporation								34																				
	fixation			17	4	5						7	8	9		11						13	14		15				
	live imaging		3		4	5			33																				
Cellular	cell cycling activity								20																				
	cell extraction					18																		31			21		
	tissue dissociation				4	18	6		20,33,34		30							25		28									
	cell proliferation				4				20					9		11						13							
	flow cytometry								20		30																21		
	primary cell culture					18																							
	reaggregation				4				33,34																				
Genomic	ATAC-seq															11					29								
	ChIP-seq																			28									
	Comet assay																	25											
	CRISPR/Cas9									22	23																		
	DNA barcoding																									16			
	DNA electrophoresis																	25											
	DNA extraction													24							29	13							
	genotyping									22	23																		
	transgenesis																		26										
	telomeres monitoring													24															
Transcriptomic	in situ hybridization			17				19						9,24		11						13			15				
	real time PCR								34																				
	RNA extraction								34			7										13	14						
	RNA interference								34					9						27		13							
	RNA sequencing																												32
	RNA synthesis			17						22	23									27									
	single-cell RNA-seq										30																		
Proteomic	immunoprecipitation																			28									
	protein extraction		3											24										31			21		
	proteomics																							31					
Computational	database										35																		
	differential expression																												32
	evolution	1																											
	formalization																	36											
	gene ontology																												32
	image analysis		3															36											
	image quantification								33						10														

giving a focus to rather uncommon organisms, including a protist one, we have tried to foster diversity and interdisciplinarity for WBR research. Table 1 determines which species is covered by which technique. In Parts IV, V, and VI, we have selected what we believe to be the future of WBR research with cutting-edge techniques from established model organisms that open to broad and integrated molecular and systems biology approaches. These parts include genetics, omics, and synthetic techniques, which according to the species are or will become instrumental to address some of the central questions in WBR.

Thanks to the contributions of all the authors, whom we warmly praise here, this book will provide a source of reference laboratory protocols for WBR research, essential for both experienced scientists and those new to the field. With the new conceptual and technical tools described here, a new impetus is given to this nearly 300-year-old field of research to shed unprecedented light on the biological and biophysical mechanisms underlying this fascinating developmental process.

We believe that Open Access is essential for the whole community to benefit from the contributions made by the authors of this book. Open Access to the entire book was made possible by the support of the authors as well as a substantial contribution from the MARISTEM Cost Action CA16203. We are grateful for this important support, which makes science accessible to everyone.







Funded by the Horizon 2020
Framework Programme of the
European Union

Fribourg, Switzerland — *Simon Blanchoud*
Geneva, Switzerland — *Brigitte Galliot*

Contents

Preface . . . . . *v*
Contributors . . . . . *xiii*

PART I HISTORICAL OVERVIEWS

1 The Hazards of Regeneration: From Morgan's Legacy to Evo-Devo 3
Chiara Sinigaglia, Alexandre Alié, and Stefano Tiozzo

2 Studying Regeneration in Ascidians: An Historical Overview 27
Virginia Vanni, Loriano Ballarin, Fabio Gasparini, Anna Peronato, and Lucia Manni

PART II ZOOLOGICAL APPROACHES

3 Studying Protista WBR and Repair Using *Physarum polycephalum* 51
Megan M. Sperry, Nirosha J. Murugan, and Michael Levin

4 Studying Porifera WBR Using the Calcerous Sponges *Leucosolenia* 69
Andrey I. Lavrov and Alexander V. Ereskovsky

5 Studying Ctenophora WBR Using *Mnemiopsis leidyi* 95
Julia Ramon-Mateu, Allison Edgar, Dorothy Mitchell, and Mark Q. Martindale

6 Studying Placozoa WBR in the Simplest Metazoan Animal, *Trichoplax adhaerens* 121
Hans-Jürgen Osigus, Michael Eitel, Karolin Horn, Kai Kamm, Jennifer Kosubek-Langer, Moritz Jonathan Schmidt, Heike Hadrys, and Bernd Schierwater

7 Collecting and Culturing Kamptozoans for Regenerative Studies 135
Achim Meyer, Julia Merkel, and Bernhard Lieb

8 Collecting and Culturing Bryozoans for Regenerative Studies 151
Abigail M. Smith, Peter B. Batson, Katerina Achilleos, and Yuta Tamberg

9 Studying Annelida Regeneration in a Novel Model Organism: The Freshwater *Aeolosoma viride* 179
Chiao-Ping Chen, Sheridan Ke-Wing Fok, Cheng-Yi Chen, Fei-Man Hsu, Yu-Wen Hsieh, and Jiun-Hong Chen

10 Studying Annelida Body Regeneration Under Environmental Stress in *Diopatra neapolitana* 195
Adília Pires

11 Studying Annelida Regeneration Using *Platynereis dumerilii* 207
Michel Vervoort and Eve Gazave

12 Collecting and Culturing *Lineus sanguineus* to Study Nemertea WBR. 227
Eduardo E. Zattara and Fernando A. Fernández-Alvarez

13 Studying Xenacoelomorpha WBR Using *Isodiametra pulchra* 245
Bernhard Egger

14 Studying Echinodermata Arm Explant Regeneration Using *Echinaster sepositus* 263
Cinzia Ferrario, Yousra Ben Khadra, Michela Sugni, M. Daniela Candia Carnevali, Pedro Martinez, and Francesco Bonasoro

15 Studying Hemichordata WBR Using *Ptychodera flava* 293
Asuka Arimoto and Kuni Tagawa

16 Studying Tunicata WBR Using *Botrylloides anceps* 311
Arzu Karahan, Esra Öztürk, Berivan Temiz, and Simon Blanchoud

Part III Cellular Approaches

17 In Situ Hybridization to Identify Stem Cells in the Freshwater Sponge *Ephydatia fluviatilis*. 335
Chiaki Kojima and Noriko Funayama

18 Isolation and Maintenance of In Vitro Cell Cultures from the Ctenophore *Mnemiopsis leidyi* 347
Abigail C. Dieter, Lauren E. Vandepas, and William E. Browne

19 Analysis of Spatial Gene Expression at the Cellular Level in Stony Corals 359
Nikki Traylor-Knowles and Madison Emery

20 Studying Stem Cell Biology in Intact and Whole-Body Regenerating *Hydra* by Flow Cytometry 373
Wanda Buzgariu, Jean-Pierre Aubry-Lachainaye, and Brigitte Galliot

21 Noninvasive Intravascular Microtransfusion in Colonial Tunicates 399
Lluìs Albert Matas Serrato, Alessandro Bilella, and Simon Blanchoud

Part IV Genetic Approaches

22 Gene Manipulation in *Hydractinia*. 419
Eleni Chrysostomou, Febrimarsa, Timothy DuBuc, and Uri Frank

23 Manipulation of Gene Activity in the Regenerative Model Sea Anemone, *Nematostella vectensis* 437
Eric M. Hill, Cheng-Yi Chen, Florencia del Viso, Lacey R. Ellington, Shuonan He, Ahmet Karabulut, Ariel Paulson, and Matthew C. Gibson

24 Monitoring Telomere Maintenance During Regeneration of Annelids 467
Nithila A. Joseph, Chi-Fan Chen, Jiun-Hong Chen, and Liuh-Yow Chen

25 Analysis of DNA Double-Stranded Breaks Using the Comet Assay in Planarians 479
Paul G. Barghouth, Salvador Rojas, Lacey R. O'Dell, Andrew M. Betancourt, and Néstor J. Oviedo

26 Random Integration Transgenesis in a Free-Living Regenerative Flatworm *Macrostomum lignano* 493
Jakub Wudarski, Kirill Ustyantsev, Filipa Reinoite, and Eugene Berezikov

27 RNAi Screening to Assess Tissue Regeneration in Planarians 509
Rachel H. Roberts-Galbraith

28 Monitoring Chromatin Regulation in Planarians Using Chromatin Immunoprecipitation Followed by Sequencing (ChIP-seq) 529
Divya Sridhar and Aziz Aboobaker

29 Assessing Chromatin Accessibility During WBR in Acoels. 549
Andrew R. Gehrke and Mansi Srivastava

Part V OMICS Approaches

30 Single-Cell Transcriptomic Analysis in the Regenerating Cnidarian *Nematostella vectensis* 565
Flora Plessier, Sandrine Schmutz, Sophie Novault, and Heather Marlow

31 Characterization of Soluble Cell-Free Coelomic Fluid Proteome from the Starfish *Marthasterias glacialis* 583
Laidson Paes Gomes, Catarina Gouveia e Silva, Jean-Charles Gaillard, Jean Armengaud, and Ana Varela Coelho

32 Using RNA-Seq for Transcriptome Profiling of *Botrylloides* sp. Regeneration 599
Michael Meier and Megan J. Wilson

Part VI Integrative Approaches

33 Studying Mechanical Oscillations During Whole-Body Regeneration in *Hydra* 619
Jaroslav Ferenc and Charisios D. Tsiairis

34 Combining RNAi-Mediated β-Catenin Inhibition and Reaggregation to Study *Hydra* Whole-Body Regeneration 635
Matthias Christian Vogg and Brigitte Galliot

35 Creating a User-Friendly and Open-Access Gene Expression Database for Comparing Embryonic Development and Regeneration in *Nematostella vectensis* 649
Olivier Croce and Eric Röttinger

36 Formalizing Phenotypes of Regeneration 663
Daniel Lobo

Correction to: Assessing Chromatin Accessibility During WBR in Acoels. C1

Index *681*

Contributors

Aziz Aboobaker • *Department of Zoology, University of Oxford, Oxford, UK*

Katerina Achilleos • *Department of Marine Science, University of Otago, Dunedin, New Zealand*

Alexandre Alié • *Sorbonne Université, CNRS, Laboratoire de Biologie du Développement de Villefranche-sur-Mer (LBDV), Villefranche-sur-Mer, France*

Asuka Arimoto • *Marine Biological Laboratory, Graduate School of Integrated Sciences for Life, Hiroshima University, Onomichi, Hiroshima, Japan*

Jean Armengaud • *Département Médicaments et Technologies pour la Santé, Université Paris-Saclay, Bagnols-sur-Cèze, France*

Jean-Pierre Aubry-Lachainaye • *Flow Cytometry Facility, Faculty of Medicine, University of Geneva, Geneva, Switzerland*

Loriano Ballarin • *Department of Biology, University of Padova, Padova, Italy*

Paul G. Barghouth • *Department of Molecular & Cell Biology, University of California, Merced, CA, USA; Quantitative and Systems Biology Graduate Program, University of California, Merced, CA, USA*

Peter B. Batson • *Department of Marine Science, University of Otago, Dunedin, New Zealand*

Yousra Ben Khadra • *Laboratory of Genetics, Biodiversity, and Valorization of Bioresources, Higher Institute of Biotechnology, University of Monastir, Monastir, Tunisia*

Eugene Berezikov • *European Research Institute for the Biology of Ageing, University of Groningen, University Medical Center Groningen, Groningen, The Netherlands; Institute of Cytology and Genetics SB RAS, Novosibirsk, Russia*

Andrew M. Betancourt • *Department of Molecular & Cell Biology, University of California, Merced, CA, USA*

Alessandro Bilella • *Department of Biology, University of Fribourg, Fribourg, Switzerland*

Simon Blanchoud • *Department of Biology, University of Fribourg, Fribourg, Switzerland*

Francesco Bonasoro • *Department of Environmental Science and Policy, University of Milan, Milan, Italy; GAIA 2050, Department of Environmental Science and Policy, University of Milan, Milan, Italy*

William E. Browne • *Department of Biology, University of Miami, Miami, FL, USA*

Wanda Buzgariu • *Department of Genetics and Evolution, iGE3, Faculty of Sciences, University of Geneva, Geneva, Switzerland*

M. Daniela Candia Carnevali • *Department of Environmental Science and Policy, University of Milan, Milan, Italy; GAIA 2050, Department of Environmental Science and Policy, University of Milan, Milan, Italy*

Cheng-Yi Chen • *Department of Life Science, National Taiwan University, Taipei, Taiwan; Stowers Institute for Medical Research, Kansas City, MO, USA*

Chi-Fan Chen • *Department of Life Sciences, National Taiwan University, Taipei, Taiwan*

Chiao-Ping Chen • *Department of Life Science, National Taiwan University, Taipei, Taiwan*

Jiun-Hong Chen • *Department of Life Science, National Taiwan University, Taipei, Taiwan*

Liuh-Yow Chen • *Institute of Molecular Biology, Academia Sinica, Taipei, Taiwan*

Eleni Chrysostomou • *Centre for Chromosome Biology, School of Natural Sciences, National University of Ireland Galway, Galway, Ireland*
Ana Varela Coelho • *Instituto de Tecnologia Química e Biológica António Xavier, Universidade Nova de Lisboa, Oeiras, Portugal*
Olivier Croce • *Institute for Research on Cancer and Aging in Nice (IRCAN), Université Côte d'Azur, CNRS, INSERM, Nice, France; Institut Fédératif de Recherche—Ressources Marines (IFR MARRES), Université Côte d'Azur, Nice, France*
Florencia del Viso • *Stowers Institute for Medical Research, Kansas City, MO, USA*
Abigail C. Dieter • *Department of Biology, University of Miami, Miami, FL, USA*
Timothy DuBuc • *Biology Department, Swarthmore College, Swarthmore, PA, USA*
Allison Edgar • *The Whitney Laboratory for Marine Bioscience, St. Augustine, FL, USA*
Bernhard Egger • *Research Unit Evolutionary and Developmental Biology, Institute of Zoology, University of Innsbruck, Innsbruck, Austria*
Michael Eitel • *Department of Earth and Environmental Sciences, Paleontology and Geobiology, GeoBio-Center, Ludwig-Maximilians Universität München, Munich, Germany*
Lacey R. Ellington • *Stowers Institute for Medical Research, Kansas City, MO, USA*
Madison Emery • *Department of Marine Biology and Ecology, Rosenstiel School of Marine and Atmospheric Science, University of Miami, Miami, FL, USA; Department of Biology, University of Texas at Arlington, Arlington, TX, USA*
Alexander V. Ereskovsky • *Department of Embryology, Faculty of Biology, Saint-Petersburg State University, Saint-Petersburg, Russia; Institut Méditerranéen de Biodiversité et d'Ecologie marine et continentale (IMBE), Aix Marseille University, CNRS, IRD, Avignon University, Station Marine d'Endoume, Marseille, France; Koltzov Institute of Developmental Biology of Russian Academy of Sciences, Moscow, Russia*
Febrimarsa • *Centre for Chromosome Biology, School of Natural Sciences, National University of Ireland Galway, Galway, Ireland*
Jaroslav Ferenc • *Friedrich Miescher Institute for Biomedical Research, Basel, Switzerland; University of Basel, Basel, Switzerland*
Fernando A. Fernández-Alvarez • *Marine Science Institute (ICM), Spanish National Research Council (CSIC), Barcelona, Spain*
Cinzia Ferrario • *Department of Environmental Science and Policy, University of Milan, Milan, Italy; Department of Physics, Center for Complexity and Biosystem, University of Milan, Milan, Italy*
Sheridan Ke-Wing Fok • *Department of Life Science, National Taiwan University, Taipei, Taiwan*
Uri Frank • *Centre for Chromosome Biology, School of Natural Sciences, National University of Ireland Galway, Galway, Ireland*
Noriko Funayama • *Department of Biophysics, Graduate School of Science, Kyoto University, Kitashirakawa-Oiwake, Sakyo-ku, Kyoto, Japan*
Jean-Charles Gaillard • *Département Médicaments et Technologies pour la Santé, Université Paris-Saclay, Bagnols-sur-Cèze, France*
Brigitte Galliot • *Department of Genetics and Evolution, iGE3, Faculty of Sciences, University of Geneva, Geneva, Switzerland*
Fabio Gasparini • *Department of Biology, University of Padova, Padova, Italy*
Eve Gazave • *CNRS, Institut Jacques Monod, UMR 7592, Université de Paris, Paris Cedex, France*

Andrew R. Gehrke • *Department of Organismic and Evolutionary Biology, Harvard University, Cambridge, MA, USA*
Matthew C. Gibson • *Stowers Institute for Medical Research, Kansas City, MO, USA; Department of Anatomy and Cell Biology, The University of Kansas School of Medicine, Kansas City, KS, USA*
Laidson Paes Gomes • *Instituto de Tecnologia Química e Biológica António Xavier, Universidade Nova de Lisboa, Oeiras, Portugal*
Catarina Gouveia e Silva • *Instituto de Tecnologia Química e Biológica António Xavier, Universidade Nova de Lisboa, Oeiras, Portugal*
Heike Hadrys • *Institut für Tierökologie, Stiftung Tierärztliche Hochschule Hannover, Hannover, Germany*
Shuonan He • *Stowers Institute for Medical Research, Kansas City, MO, USA*
Eric M. Hill • *Stowers Institute for Medical Research, Kansas City, MO, USA*
Karolin Horn • *Institut für Tierökologie, Stiftung Tierärztliche Hochschule Hannover, Hannover, Germany*
Yu-Wen Hsieh • *Department of Life Science, National Taiwan University, Taipei, Taiwan*
Fei-Man Hsu • *Department of Life Science, National Taiwan University, Taipei, Taiwan*
Nithila A. Joseph • *Institute of Molecular Biology, Academia Sinica, Taipei, Taiwan*
Kai Kamm • *Institut für Tierökologie, Stiftung Tierärztliche Hochschule Hannover, Hannover, Germany*
Ahmet Karabulut • *Stowers Institute for Medical Research, Kansas City, MO, USA*
Arzu Karahan • *Institute of Marine Sciences, Middle East Technical University, Erdemli, Mersin, Turkey*
Chiaki Kojima • *Department of Biophysics, Graduate School of Science, Kyoto University, Kitashirakawa-Oiwake, Sakyo-ku, Kyoto, Japan*
Jennifer Kosubek-Langer • *Institut für Tierökologie, Stiftung Tierärztliche Hochschule Hannover, Hannover, Germany; Department of Animal Behavior, Freie Universität Berlin, Berlin, Germany*
Andrey I. Lavrov • *Pertsov White Sea Biological Station, Biological Faculty, Lomonosov Moscow State University, Moscow, Russia; Department of Embryology, Faculty of Biology, Saint-Petersburg State University, Saint-Petersburg, Russia*
Michael Levin • *Wyss Institute for Biologically Inspired Engineering at Harvard University, Boston, MA, USA; Department of Biology, Tufts University, Medford, MA, USA; Allen Discovery Center at Tufts University, Medford, MA, USA*
Bernhard Lieb • *Johannes Gutenberg-Universität, Institut für Molekulare Physiologie, Mainz, DE, Germany*
Daniel Lobo • *Department of Biological Sciences, University of Maryland, Baltimore County, Baltimore, MD, USA*
Lucia Manni • *Department of Biology, University of Padova, Padova, Italy*
Heather Marlow • *(Epi)genomics of Animal Development, Department of Developmental and Stem Cell Biology, Institut Pasteur, Paris, France; Department of Organismal Biology and Anatomy, The University of Chicago, Chicago, IL, USA*
Mark Q. Martindale • *The Whitney Laboratory for Marine Bioscience, St. Augustine, FL, USA*
Pedro Martinez • *Department of Genetics, Microbiology and Statistics, University of Barcelona, Barcelona, Spain; ICREA, Catalan Institute for Research and Advanced Studies, Barcelona, Spain*

Lluìs Albert Matas Serrato • *Department of Biology, University of Fribourg, Fribourg, Switzerland*
Michael Meier • *Developmental Genomics Laboratory, Department of Anatomy, School of Biomedical Sciences, University of Otago, Dunedin, New Zealand*
Julia Merkel • *Johannes Gutenberg-Universität, Institut für Molekulare Physiologie, Mainz, DE, Germany*
Achim Meyer • *Leibniz Centre for Tropical Marine Research (ZMT), Bremen, DE, Germany*
Dorothy Mitchell • *The Whitney Laboratory for Marine Bioscience, St. Augustine, FL, USA*
Nirosha J. Murugan • *Department of Biology, Algoma University, Sault Ste. Marie, ON, Canada; Allen Discovery Center at Tufts University, Medford, MA, USA*
Sophie Novault • *Cytometry and Biomarkers, Center for Technological Resources and Research, Institut Pasteur, Paris, France*
Lacey R. O'Dell • *Department of Molecular & Cell Biology, University of California, Merced, CA, USA*
Hans-Jürgen Osigus • *Institut für Tierökologie, Stiftung Tierärztliche Hochschule Hannover, Hannover, Germany*
Néstor J. Oviedo • *Department of Molecular & Cell Biology, University of California, Merced, CA, USA; Quantitative and Systems Biology Graduate Program, University of California, Merced, CA, USA; Health Sciences Research Institute, University of California, Merced, CA, USA*
Esra Öztürk • *Institute of Marine Sciences, Middle East Technical University, Erdemli, Mersin, Turkey*
Ariel Paulson • *Stowers Institute for Medical Research, Kansas City, MO, USA*
Anna Peronato • *Department of Biology, University of Padova, Padova, Italy*
Adília Pires • *Centre for Environmental and Marine Studies (CESAM) & Department of Biology, University of Aveiro, Aveiro, Portugal*
Flora Plessier • *Committee on Development, Regeneration and Stem Cell Biology, The University of Chicago, Chicago, IL, USA; École Doctorale "Complexité du Vivant" ED515, Sorbonne Université, Paris, France; Département de Biologie, École Normale Supérieure de Lyon, Lyon, France; (Epi)genomics of Animal Development, Department of Developmental and Stem Cell Biology, Institut Pasteur, Paris, France; Department of Organismal Biology and Anatomy, The University of Chicago, Chicago, IL, USA*
Julia Ramon-Mateu • *The Whitney Laboratory for Marine Bioscience, St. Augustine, FL, USA; Sorbonne Université, CNRS, Laboratoire de Biologie du Développement de Villefranche-sur-mer (LBDV), Villefranche-sur-mer, France*
Filipa Reinoite • *European Research Institute for the Biology of Ageing, University of Groningen, University Medical Center Groningen, Groningen, The Netherlands*
Rachel H. Roberts-Galbraith • *Department of Cellular Biology, University of Georgia, Athens, GA, USA*
Salvador Rojas • *Department of Molecular & Cell Biology, University of California, Merced, CA, USA; Quantitative and Systems Biology Graduate Program, University of California, Merced, CA, USA*
Eric Röttinger • *Institute for Research on Cancer and Aging in Nice (IRCAN), Université Côte d'Azur, CNRS, INSERM, Nice, France; Institut Fédératif de Recherche—Ressources Marines (IFR MARRES), Université Côte d'Azur, Nice, France*

Bernd Schierwater • *Institut für Tierökologie, Stiftung Tierärztliche Hochschule Hannover, Hannover, Germany*
Moritz Jonathan Schmidt • *Institut für Tierökologie, Stiftung Tierärztliche Hochschule Hannover, Hannover, Germany*
Sandrine Schmutz • *Cytometry and Biomarkers, Center for Technological Resources and Research, Institut Pasteur, Paris, France*
Chiara Sinigaglia • *Institut de Génomique Fonctionnelle de Lyon, ENS Lyon, Lyon, France*
Abigail M. Smith • *Department of Marine Science, University of Otago, Dunedin, New Zealand*
Megan M. Sperry • *Wyss Institute for Biologically Inspired Engineering at Harvard University, Boston, MA, USA; Department of Biology, Tufts University, Medford, MA, USA*
Divya Sridhar • *Department of Zoology, University of Oxford, Oxford, UK*
Mansi Srivastava • *Department of Organismic and Evolutionary Biology, Harvard University, Cambridge, MA, USA*
Michela Sugni • *Department of Environmental Science and Policy, University of Milan, Milan, Italy; Department of Physics, Center for Complexity and Biosystem, University of Milan, Milan, Italy; GAIA 2050, Department of Environmental Science and Policy, University of Milan, Milan, Italy*
Kuni Tagawa • *Marine Biological Laboratory, Graduate School of Integrated Sciences for Life, Hiroshima University, Onomichi, Hiroshima, Japan*
Yuta Tamberg • *Department of Marine Science, University of Otago, Dunedin, New Zealand*
Berivan Temiz • *Institute of Marine Sciences, Middle East Technical University, Erdemli, Mersin, Turkey*
Stefano Tiozzo • *Sorbonne Université, CNRS, Laboratoire de Biologie du Développement de Villefranche-sur-Mer (LBDV), Villefranche-sur-Mer, France*
Nikki Traylor-Knowles • *Department of Marine Biology and Ecology, Rosenstiel School of Marine and Atmospheric Science, University of Miami, Miami, FL, USA*
Charisios D. Tsiairis • *Friedrich Miescher Institute for Biomedical Research, Basel, Switzerland*
Kirill Ustyantsev • *Institute of Cytology and Genetics SB RAS, Novosibirsk, Russia*
Lauren E. Vandepas • *Benaroya Research Institute, Seattle, WA, USA; National Oceanographic and Atmospheric Administration, Manchester, WA, USA*
Virginia Vanni • *Department of Biology, University of Padova, Padova, Italy*
Michel Vervoort • *CNRS, Institut Jacques Monod, UMR 7592, Université de Paris, Paris Cedex, France*
Matthias Christian Vogg • *Department of Genetics and Evolution, iGE3, Faculty of Sciences, University of Geneva, Geneva, Switzerland*
Megan J. Wilson • *Developmental Genomics Laboratory, Department of Anatomy, School of Biomedical Sciences, University of Otago, Dunedin, New Zealand*
Jakub Wudarski • *European Research Institute for the Biology of Ageing, University of Groningen, University Medical Center Groningen, Groningen, The Netherlands*
Eduardo E. Zattara • *Instituto de Investigaciones en Biodiversidad y Medio Ambiente (INIBIOMA), CONICET-Universidad Nacional del Comahue, Bariloche, Argentina; Department of Invertebrate Zoology, National Museum of Natural History, Smithsonian Institution, Washington, DC, USA*

Part I

Historical Overviews



Chapter 1

The Hazards of Regeneration: From Morgan's Legacy to Evo-Devo

Chiara Sinigaglia, Alexandre Alié, and Stefano Tiozzo

Abstract

In his prominent book *Regeneration* (1901), T.H. Morgan's collected and synthesized theoretical and experimental findings from a diverse array of regenerating animals and plants. Through his endeavor, he introduced a new way to study regeneration and its evolution, setting a conceptual framework that still guides today's research and that embraces the contemporary evolutionary and developmental approaches.

In the first part of the chapter, we summarize Morgan's major tenets and use it as a narrative thread to advocate interpreting regenerative biology through the theoretical tools provided by evolution and developmental biology, but also to highlight potential caveats resulting from the rapid proliferation of comparative studies and from the expansion of experimental laboratory models. In the second part, we review some experimental evo-devo approaches, highlighting their power and some of their interpretative dangers. Finally, in order to further understand the evolution of regenerative abilities, we portray an adaptive perspective on the evolution of regeneration and suggest a framework for investigating the adaptive nature of regeneration.

Key words Whole-body regeneration, Evolution, Phylogeny, Adaptation, Homology, Character, Ecology, Development

1 Introduction

Thomas Hunt Morgan is considered one of the fathers of modern genetics. He is best known for demonstrating that chromosomes carry the mechanical basis of heredity, the genes. He also has the merit of introducing and developing a successful laboratory model for genetic studies, the fruit fly *Drosophila*. Yet, in his early career, while working at the Bryn Mawr women's college (1891–1904), Morgan devoted a significant amount of time to studying the problem of regeneration, focusing on a diverse array of regenerating animals (Fig. 1). Morgan's experimental and theoretical findings are synthesized in his now-classic book *Regeneration* [1]. Despite his extensive experiments and the diversity of the organisms studied, Morgan failed to identify a universal mechanism

Simon Blanchoud and Brigitte Galliot (eds.), *Whole-Body Regeneration: Methods and Protocols*, Methods in Molecular Biology, vol. 2450, https://doi.org/10.1007/978-1-0716-2172-1_1, © The Author(s) 2022

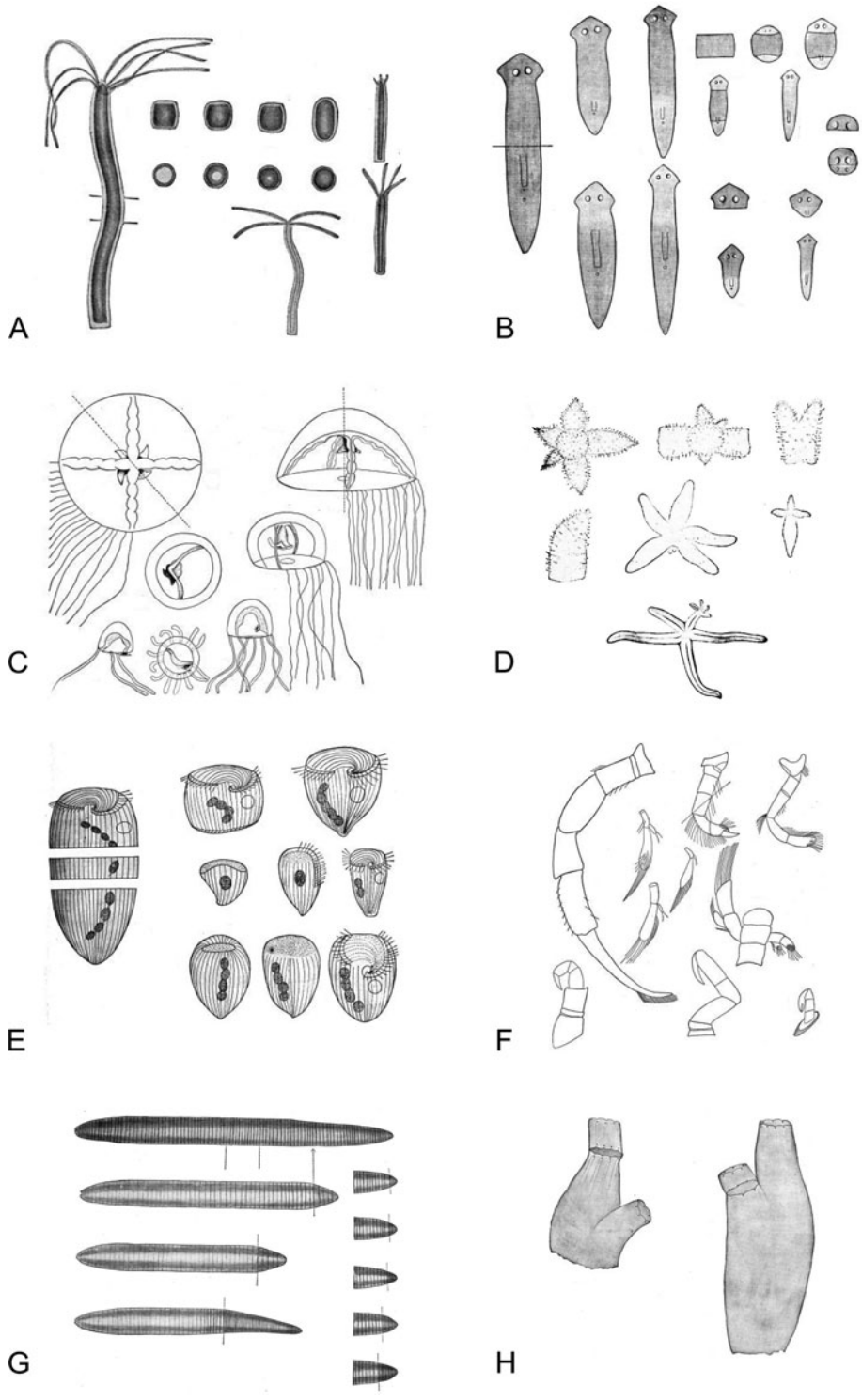


Fig. 1 Example of regenerating animal models reported in Morgan's *Regeneration* (1901). (**a**) *Hydra viridis*, (**b**) *Planaria maculata*, (**c**) *Gonionemus vertens*, (**d**) *Linckia multiformis*, (**e**) *Stentor coeruleus*, (**f**) *Eupagurus longicarpus*, (**g**) *Allolobophora fœtida*, (**h**) *Ciona intestinalis*. (Modified from Morgan (1901) [1])

governing regeneration. Probably in a lighter moment, he allegedly said that since he had been unable to solve the problem of regeneration, he had decided to try something easier such as the problem of heredity [2]. The fascination and the struggle of understanding regenerative phenomena and their evolution remain as alive today as it was then.

Over the last two decades, new cell and molecular biology tools have become available, allowing the exploration of a broader range of metazoan regenerative mechanisms and prompting a (re)-expansion of the field of regenerative biology [3, 4]. A unifying theory of regeneration is nevertheless still lacking. Why do not all species regenerate? Does regeneration have a single or multiple (evolutionary) origin? Are the mechanisms of regeneration co-opted from other developmental phenomena (i.e., embryogenesis)? To what extent asexual reproduction, coloniality, cancer, and regeneration can be seen as different facets of the same phenomenon? Can we decipher the mechanisms of regeneration and reenable them in nonregenerating species? Such compelling questions are still waiting for satisfactory answers.

Morgan's book [1] is as relevant today as it was in the previous century, as, besides providing a historical perspective on regeneration studies across the nineteenth and the twentieth century, it lays down the conceptual and theoretical framework guiding our current research on regenerative phenomena.

2 The Legacy of Morgan's *Regeneration*

In *Regeneration*, Morgan synthesized and critically revised the work of his colleagues and predecessors. By analyzing classical studies, including the work of Trembley, Spallanzani and Bonnet, and the ongoing work of his contemporary scholars, such as Roux, Barfurth, and Driesch, Morgan realized how the results diverged significantly in relation to the organism studied and the methodology adopted, often leading to controversial interpretations. Through his exercise of synthesis, Morgan first attempted to group organism-specific processes into a general phenomenon of regeneration, framing his comparative approach into general questions concerning growth and differentiation, and eventually providing new insights to a theory of development. Indeed, one of the most important contributions of Morgan's book was the idea that regeneration should be considered as a growth property, and therefore approached as a developmental phenomenon. This approach to regeneration actively opposed the adaptationist view endorsed by August Weismann [5, 6], who considered regeneration as a phenomenon of adaptation and not a primary quality of the organism [7], and supported the existence of a causal relationship between the tendency to be injured and the capacity

to "*re-grow*." With the filter of time, the inflamed debate between the two scientists was most likely rooted on methodological and epistemological grounds, with Morgan criticizing Weismann for his adherence to a "theory," instead of starting from a purely experimental approach [5]. These originally discordant approaches are not mutually exclusive, and studying regeneration today as a form of development does not mean that this process has to be considered irrespectively of its adaptive value [8].

Morgan advocated and emphasized the importance of comparing the widest diversity of organisms in order to recast the questions about development in terms of experimentally testable hypotheses. His view of regeneration was supported by a striking array of experiments that he and his students performed on a substantial number of vertebrate and invertebrate species (Fig. 1). Undeniably, the tenet that emerges in *Regeneration* and that is still acutely pertinent 120 years later is to challenge any general hypothesis about regenerative phenomena by performing comparative experiments using different model organisms [1, 6, 9].

2.1 Partial Versus Whole-Body Regeneration

In the pursuit of a coherent explanation of regenerative phenomena, one of the priorities in Morgan's work was to introduce a clearer and more consistent terminology, able to reflect the variety of regenerative processes and to compare the many models that he and his students were describing. Even if Morgan's most famous dichotomous subdivision of regeneration based on cellular rearrangements (morphallaxis) and cell proliferation (epimorphosis) turned out to be too restrictive [10], some of his terminology and classifications are still relevant today. For instance, Morgan classified regenerative ontogenies according to the new anatomical structures that resulted from regeneration [1]. Another general classification provided by Morgan is based on the causality of the regenerative process. He distinguished between "restorative regeneration," which include post-traumatic regeneration and is the result of some exogenous injury to the organism, and "physiological regeneration," which occurs during body homeostasis, such as the turnover cycle of epithelial dermal cells in mammals, or during the "life cycle of the individual," like for example during budding, molting or feather replacements.

To our knowledge, the expression whole-body regeneration (WBR) was not used in Morgan's work. It has been introduced relatively recently and spread widely in the scientific literature [11–18]. The term WBR has been loosely used to describe regenerative processes that involve a "large" portion of an animal body, without adhering to a strict definition. According to Cary and colleagues, an organism undergoes WBR when it "[…] *can re-grow all body parts following amputation*," which is opposed to "*partial regeneration*," when regeneration is restricted to only some body structure [16]. Bely and colleagues also define WBR as the ability to

regenerate "*all body parts*," and considered that regeneration of the primary body axis is not by itself sufficient to define WBR [4]. When using WBR most authors refer to restorative regeneration but it has also been used for physiological regenerative processes [19, 20]. The expression is also employed regardless of the stages of an organism's life cycle [16, 17].

While venturing into a clearer definition of WBR we run into some classical philosophical problems. WBR brings to the forefront the problem of biological individuality and, more specifically, the issue of establishing criteria for the persistence over time of biological individuals [21, 22]: to which and how many changes an organism can go through and still be considered the same individual? When WBR leads to two or more individuals how regeneration can be considered different from reproduction, and which one is the original individual? Indeed, the expression "WBR" is rather idiomatic since, if an injury leaves some cells or tissues behind, the regeneration then cannot be "whole." It appears that the amount of regenerated material is the main property defining WBR, but what is the threshold above which regeneration can be labeled "whole"? We could consider, for example, that at least half of the original individual has to regenerate. Following this rule, in a beheaded *Planaria maculata* the head reforming the body would be a case of WBR, but not the body reforming the head [23] (Fig. 1b). Yet such a threshold would be clearly arbitrary, leading to conclusions that would need to be justified.

The term "whole-body regeneration" has become popular only in the last few decades. Just like the use of "regeneration," it is rich in emphasis, but not accurate and nor fully definable. Regardless of the criteria to define it, WBR in different species clearly refers to different processes.

2.2 Regeneration: Function Versus Process

While attempting to introduce a language that accommodates the various regenerative phenomena that had been studied so far, Morgan used the term *regeneration* to indicate diverse and heterogeneous phenomena of organ renewal, replacements of body parts, or asexual development [6]. He wrote that "regeneration" could constitute an umbrella term encompassing "*not only the replacement of a lost part, but also the development of a new, whole organism, or even a part of an organism, from a piece of an adult, or of an embryo, or of an egg*," and even including instances of imperfect regeneration: "[…] *must include also those cases in which the part replaced is less than the part removed, or even different in kind*" [1]. This broad definition of regenerative phenomena is still applied today. Just like WBR, it should however be regarded as a "working definition," encompassing a heterogeneous class of events, not necessarily shared among taxa [24, 25]. Despite the complexity of the phenomena considered and the blurriness of definitions, often there has been a tendency to map regeneration as a character on

phylogenetic trees. However, regeneration cannot be reduced to a single trait, and plotting onto an existing phylogeny its presence or absence has no more value than charting the capacity of animals to fly instead of focusing on the mechanisms and structures that allow the flight. Indeed, functions can arise convergently by multiple means rather than by historical continuity [26]. Instead, regeneration must be considered as a spatiotemporal organized process, or assemblies of processes into modules [27, 28] that can be used as individual evolutionary characters [29, 30]. Then, only characters on which we can do a reasonable hypothesis of primary homology [31], for example morphological, cellular, or molecular characters associated with regeneration, can be plotted on a tree.

To identify characters associated with regeneration it may be convenient to move toward a more reductionist approach, and break down the regenerative process along its ontogenetic and evolutionary paths. In the first case, each regenerative process could be split into conserved subprocesses such as wound-healing (when present), precursor(s) mobilization, and morphogenesis [32]. The latter involves comparing these artificial ontogenetic steps between closely related phylogenetic clades, for example class, order, or family, minimizing divergence time [25, 33, 34]. The definition and the breakdown of components, and the identification of which, if any, descend from a common ancestor are among the key interests of the field of evo-devo.

2.3 Help from Evo-Devo Theoretical Tools

If, as Morgan firstly suggested, regenerative phenomena can be considered as developmental processes, then the conceptual and methodological approaches developed by evo-devo research are valuable also to explore the evolution of regenerative processes [3, 19, 25, 35]. First, the use of an extended concept of homology, such as "process homology" [29] or "character identity networks" [26], which links characters from different biological hierarchies (e.g., gene, GRN, morphological characters), and, for instance, can help to describe relationships between homologous proteins and homologous molecular pathways, even if they do not necessarily lead to homologous anatomical structures [29, 36]. This more nuanced concept of homology is a powerful tool to refine comparisons of apparently unrelated regenerative processes, potentially also among phylogenetically distant and divergent species.

Second, another useful concept that captures the different levels and types of heterogeneity of an organism is the notion of *modularity* [27, 37, 38]. Regeneration, just like development can be divided into discrete and interacting modules, which can be tissues, fields (i.e., cells committed to forming the same structure), elements of gene enhancers, parts of gene regulatory networks, or any other "*basic structural entities or regulatory phenomena necessary to assemble a complex morphological structure*" [39]. The

concept of modules also helps to distinguish the processes occurring during regeneration from the function of regeneration itself [25].

Third, conjointly with modularity comes the concept of *developmental constraint*, which restrains phenotype production due to a limited interaction among existing modules [29, 40]. For example, a limited or restrained propagation of morphogens, or bioelectric signals through voltage gradients, due to the increased histological and cytological complexity could prevent regeneration [41, 42]. The possible inhibitory effect of the immune system on regeneration is also another little-studied potential constraint [43–45]. The existence of developmental constraints should also be taken into account when comparing regenerative processes across different species.

The conceptual tools that regenerative biology can borrow from the field of evo-devo are powerful. Comparative approaches however entail interpretive caveats, as illustrated in the following examples.

3 The Difficult Task of Reconstructing WBR Evolution

The evolutionary questions concerning regeneration ultimately provide a complete narrative of the phenomenon. They are far from being just theoretical, and they can change the approach to the mechanistic study and guide the experimental design on a given model organism [8]. The three following examples illustrate the power of evo-devo experimental approaches to infer the evolution of regeneration—and of WBR in particular—but also point out some possible interpretive caveats.

3.1 Far from Basal: Diversity of Regeneration in Sponges

Sponges are emblematic organisms to study the early evolution of regeneration because they have excellent regenerative abilities [46] and likely represent the monophyletic sister group of all other metazoans [47, 48]. Sponges are often considered as basal metazoans, or ancestral representative of animals. However, they are not more basal to eumetazoans than eumetazoans are basal to sponges (Fig. 2a), and there is no fossil evidence that their body plan represents an ancient state [49, 50]. As any organism, modern sponges are nothing but a mosaic of characters in their ancestral or derived state. This holds true for their regenerative mechanisms that show great inter-species variations. For instance, the proverbial ability of cell aggregates to generate a functional sponge varies even between closely related species [51–54]: *Halisarca dujardini* can reconstruct its body from cell suspension, whereas *Halisarca panicea* is unable to do so [53]. Whether or not cell reaggregation is ancestral to Porifera will remain unsolved without phylum-level comparative studies.

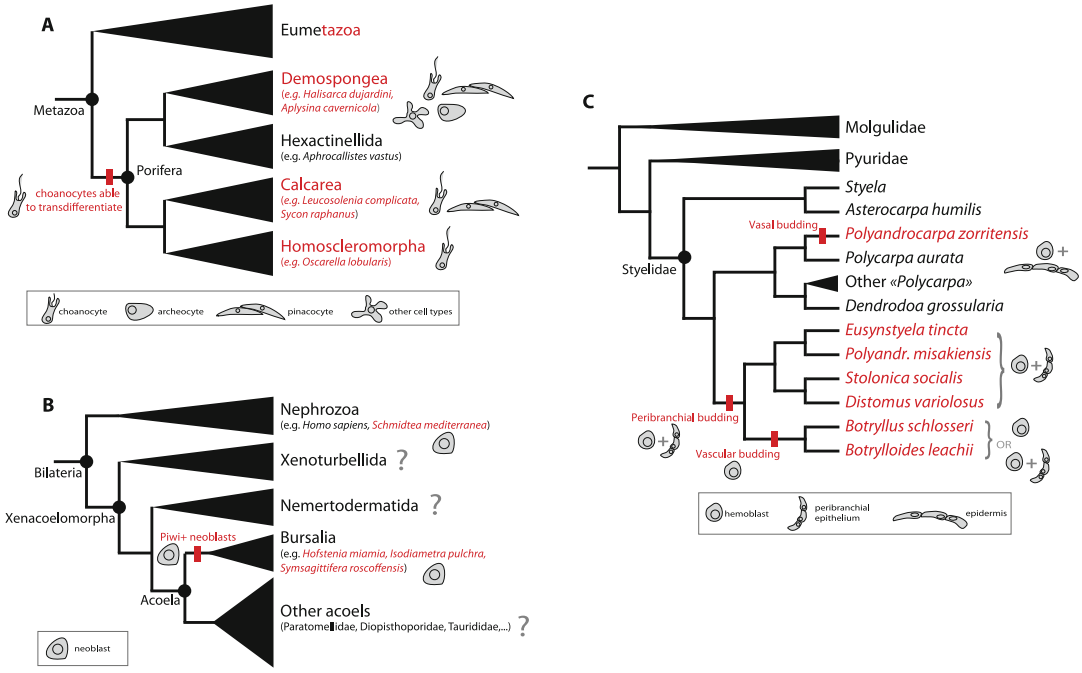


Fig. 2 Phylogenetic relationships between species cited in the text, and cell types involved in WBR, in sponges (**a**), xenacoelomorphs (**b**), and ascidians (**c**). The species that are reputed for their extensive ability to regenerate are represented in red. The cells drawn represent the cell types known to supplement more tissues during regeneration, by proliferation and/or differentiation. On branches are shown ancestral reconstruction regarding the role of each cell type in WBR based on parsimonious optimization

The mechanisms of WBR from body fragment also varies between the four sponges classes. Many demosponges use massive proliferation and migration of archaeocytes with the participation of dedifferentiated choanocytes, which all together form a regenerative blastema [55, 56]. In some other demosponges (e.g., *Halisarca dujardini* and *Aplysina cavernicola*) the cell plasticity is even greater, with dedifferentiation of various cell types that also participate in blastema formation [57, 58]. In contrast to demosponges, neither archaeocytes nor tissue regeneration has yet been observed in their sister group, the Hexactinellida [59]. Calcareous sponges, who also do not possess archaeocytes, regenerate through epithelial morphogenesis by spreading and transdifferentiation of pinacocytes and choanocytes (e.g., in *Leucosolenia complicata*) with minor cell proliferation and no blastema formation [60]. Finally, among the homoscleromorphs, the sister group of calcareous sponges, only *Oscarella lobularis* has been reported to regenerate [61, 62]. As in Calcarea, it involves choanocyte transdifferentiation and tissue rearrangement, without blastema formation or local proliferation. Due to this phylum-level variability in regenerative capability and mechanisms, reconstructing the origin and evolution of WBR in sponges is far from being a straightforward task (Fig. 2a).

Nevertheless, choanocyte dedifferentiation and/or transdifferentiation seem to be a common theme in regenerative species, which may be in line with the suspected stem cell nature of choanocytes [63]. Comparative investigations focused on choanocyte dynamics (e.g., time series of single-cell RNAseq) could unravel fundamental sets of genes regulating WBR potentially inherited from the last common ancestor of Porifera.

3.2 Acoels and Planarians: Lessons from Faraway Cousins

Recent work on acoels and Platyhelminthes has provided fresh insights on the possible ancestral mechanisms of WBR in the last common ancestor of Bilateria. Acoels are flatworms belonging to a larger clade named Xenacoelomorpha, together with Xenoturbellids and Nemertodermatids (Fig. 2b). Some authors consider Xenacoelomorpha as the sister group of all other Bilateria [64, 65] and others the sister group of Ambulacraria. Despite being distantly related, acoels share a superficial morphological resemblance with Platyhelminthes, a group of lophotrochozoan flatworms. Their regenerative mechanisms also show extensive similarities. In acoels and planarians, regeneration involves the proliferation-dependent formation of a regenerative blastema by mesenchymal multipotent and totipotent stem cells, the neoblasts, which express homologous genes such as *Piwi* paralogs and other members of the Germline Multipotency Programs [66–68]. In both acoels and planarians, muscles play a contraction-independent role by secreting position control proteins (e.g., wnt and bmp ligands), thus providing positional information for correct body plan restoration upon WBR [69–72]. These shared characters suggest ancestral features inherited from the last common ancestor of Bilateria. However, proposing the homology of regenerative processes at such a large phylogenetic scale remains risky. For instance, while neoblast-like stem cells are present in several bilaterian lineages [68], their phylogenetic distribution is much more parsimoniously explained by convergent acquisition, rather than as an ancestral presence with multiple losses. Transcriptomic and genomic characterization of neoblasts in various animals may additionally reveal shared molecular signatures that also result from convergent acquisition. Also, the orthology of the position-control genes expressed by muscles during planarian and acoel regeneration has not been established [69], and therefore it's not clear if their role in regeneration is inherited from a common ancestor or not.

To date, regeneration studies on acoels have been mainly done in species belonging to the Bursalia suborder (e.g., *Hofstenia miamia, Isodiametra pulchra*). But, to our knowledge, regeneration power is not yet reported in the ca. other 400 acoel species nor in other Xenacoelomorphs (Xenoturbellids and Nemertodermatids) [73]. The example of sponges clearly demonstrates the intraphylum plasticity of WBR and highlights the importance of studying more related models. This may be the case for acoels too, as

they are known to evolve relatively fast [74] and to harbor many derived characters among Xenacoelomorphs, such as the organization of body muscles, or the presence of epidermal eyespots [75, 76]. Consequently, acoels alone cannot be taken as a proxy for Xenacoelomorpha and ancestral reconstruction of bilaterian WBR will not be possible without exploring anatomical, cellular and molecular diversity across Xenacoelomorpha.

Despite these caveats, the comparison between acoels and planarians is highly relevant to reconstruct the ancestral mechanisms of WBR in Bilateria. It is important to note that this holds regardless of the position of acoels as the sister group of Nephrozoa or Ambulacraria, since in both cases the last common ancestor of acoels and planarians is the ancestor of all Bilateria (Fig. 2b).

3.3 Plastic Families: Convergent Acquisition of WBR in Tunicates

Increasing the phylogenetic resolution and comparing multiple closely related species is crucial to assign confidently the directionality of evolutionary transitions. Tunicates include so-called solitary species, where regeneration is limited to some tissue and organs [77] and colonial species, which are all able to undergo WBR via different types of budding [78]. Tracking WBR evolution in tunicates benefits from numerous anatomical studies on many species combined with well-resolved and robust phylogenies that allowed to infer multiple independent acquisitions of WBR in the whole subphylum [34, 78, 79]. For example, the evolution of budding in the family of Styelidae remained largely speculative until recently. Berrill [80] considered that all colonial species belonging to this family should be unified as a natural group because he assumed that they all perform the same kind of budding. In contrast, Kott suspected that budding modes may be more diverse than expected and advocated for "*accurate resolution of their taxonomy [and] information on the process of vegetative reproduction*" [81]. Recent phylogenetic reconstruction of Styelidae [34], as well as a closer look at the budding tissues in the species *Polyandrocarpa zorritensis* [82] showed that the fundamental differences in the mechanisms of bud formation, as well as their phylogenetic distribution, are more parsimoniously explained by convergent acquisition [34]. Thus, according to these data, three modes of WBR have been independently acquired (Fig. 2c) from a solitary, nonbudding, ancestor of Styelidae. Therefore, the question is to know whether homologous modules (e.g., GRN made of orthologous genes) have been convergently deployed in these three nonhomologous budding modes. The discovery of such shared GRN or budding cell types between the different budding modes in Styelidae will be interpreted as independent co-options, as long as the phylogenetic topology makes the convergent acquisition of budding the most parsimonious hypothesis.

3.4 A Roadmap to Investigate WBR Evolution

These three examples clearly show that, in the attempt to infer the evolution of regenerative phenomena, the phylogenetic relationships between the considered organisms must be used as an interpretative framework to formulate hypotheses on evolutionary trajectories. Then, each defined character should be first considered independently (presence/absence of neoblasts, expression of Wnt orthologs, a given morphogenetic movement, etc.) in order to reconstruct the mosaic of derived and ancestral states that make up the regenerative process and its phylogenetic distribution. Combining several lines of evidence such as histology, morphology, molecular signatures (e.g., by RNAseq) and phylogenetic analyses of genes of interest is, therefore, an informative way to refine homology hypotheses. When possible, multiple species must be considered in parallel to cover the diversity of the regenerative mechanisms (including absences) across the studied taxa. Finally, a particularly informative ontogenetic step to collect characters related to regeneration may be the earliest steps after the injury, at the interface between the wound healing (when present) and the mobilization of the precursors (i.e., stem cells or dedifferentiating cells). For instance, recent RNA-seq and ATAC-seq analyses on fine-grained time series have shown that several species of bilaterian and cnidarians overexpress *immediate-response genes* such as EGR or Runt homologs, and establish Wnt signaling centers at the onset of regeneration [11, 83–86]. However, Wnt genes expressed in different regenerative contexts across species are not orthologous and are likely under the control of nonhomologous mechanisms [83]. This and the patchy distribution of WBR may point toward an evolutionary scenario where WBR arose multiple times independently during metazoan evolution, often reusing similar modules co-opted from embryogenesis (e.g., Wnt canonical pathway) while also assembling original modules specific to each regenerative strategy.

4 What Is the Significance of WBR? An Integrative and Practical Approach

Regardless of the phylogenetic context—single or multiple acquisitions/losses of regenerative capacities—the advantages of regenerating a large portion of the body, or of multiplying individuals by budding, might seem self-evident. These advantages were largely assumed by early scholars, as Reaumur [87] and Bonnet [88], long before any theorization of evolution by means of natural selection. Yet, trade-offs between costs and benefits of regeneration might exist—and sometimes the benefits themselves might be difficult to identify, as in the case of the constant cycles of zooids destruction and regeneration in the colonial ascidian *Botryllus schlosseri* [89]. The challenges in understanding the evolution of WBR among metazoans depend thus also on the difficulties in answering an

apparently elementary question: what are the consequences of regeneration on the survival and/or reproductive fitness of an individual? In other words, is regeneration, or the loss of it, adaptive?

Following Darwin's work [90], Weismann explicitly regarded regeneration as an adaptive phenomenon "*the degree to which it is present is mainly in proportion to the liability of the part to injury*" [7]. Morgan, who was skeptical of untested theoretical explanations, set out to validate experimentally this prediction. In order to test whether the regenerative potential of a body part correlated with its risk of being injured in nature, he chose as a study model the hermit crab *Pagurus longicarpus* (Fig. 1f), as its anterior appendages were exposed to damage, while its posterior ones were "*naturally protected*" by the host gastropod shell. All appendages proved to regenerate well, which led Morgan to reject any adaptive value for regeneration. Morgan's experimental setup was however criticized for oversimplifying the parameters of the problem. Needham, in particular, argued that for a correct estimation of the evolutionary pressures, the "*indispensability*" of each appendage had to be considered. After recapitulating the experiments on *Pagurus* [91] and other crustaceans [92], Needham remarked that, (1) the frequency of regeneration in posterior, more protected, appendages was indeed lower (in *Pagurus* it was 21% vs. 83%), and that (2) each pair of posterior appendages was essential to locomotion (and thus for survival of the crab). Thus, not only there was a correlation between risk of injury and regenerative potential, but the maintenance of a complete pair of posterior appendages was likely under strong selective pressure, supporting the old idea that regenerative abilities had an adaptive value [92]. The question was thus far from being settled because if purely adaptive interpretations could explain the patchy distribution of regenerative potential among metazoans, it remained difficult to account for the similarities among regenerative processes [8]. Goss crystallized this idea and argued that if regeneration was truly an adaptive phenomenon, it must have arisen (and been positively selected) from nonregenerating ancestors multiple times, which would entail substantial differences between developmental mechanisms [8]. Shared features between diverse regenerative processes had instead been demonstrated, such as the requirement for innervation [93, 94]. Previous research had further highlighted a certain degree of similarity between embryonic and regenerating limbs, notably concerning patterning [95, 96] and morphogenesis [97]. Goss, like Morgan, favored a scenario where regeneration would be an inherent feature of metazoan life, and most likely a derivative of a core embryonic developmental program [98].

In his view, the modern phylogenetic pattern of regenerating taxa could be interpreted as the result of repeated losses of potential—themselves the consequence of other adaptive processes, for

instance, the evolution of better brains in vertebrates [99], or the transition from aquatic to terrestrial habitats [8]. While some similarities among regenerative processes do exist, for example with regard to wound healing [100], it is today clear that the comparison is far from being trivial, as also concluded by Morgan, and that the answer cannot derive from the "mere" addition of further, diverse types of data. The previous examples on sponges, flatworms, and tunicates show that the identification of the relevant comparisons, at all the different scales, is key. Regarding the shared features of regeneration and embryogenesis, for example, recent transcriptomic approaches have indeed highlighted some degree of conservation in sequential gene usage between embryonic processes and regeneration [101–104]. On the other hand, regeneration is broadly thought to display specific features, such as an involvement of the immune response [105], of the nervous system [106], and perhaps of muscle cells [69].

4.1 The Puzzle of "Restriction and Absence" of WBR: Eco-Evo-Evo Perspectives

Representatives of sponges, acoels, planarians, tunicates but also cnidarians, ctenophores, annelids, echinoderms, and placozoans display different WBR capacities. The ability to regenerate large portions of the body is conversely lacking in arthropods, which nevertheless can regenerate their appendages until they reach a terminal molting stage—suggesting a possible trade-off between a protective cuticle and WBR, probably emerging at the origin of Ecdysozoa [107]. The problem with the "*restriction and absence*" [108] of regenerative potential among taxa remains central to the study of the evolution of regeneration [4]. As highlighted in the previous sections, the fragmentary taxonomic sampling is a major limit in understanding the evolutionary trajectories of WBR. The absence of regeneration is particularly difficult to address, and any explanatory research would need to take into account three parameters:

1. *Evolutionary parameters*, in the form of a robust and well-resolved phylogeny for discriminating between putative losses and de novo acquisitions;
2. *Developmental parameters*—for example, taxon-specific anatomical features, such as the cuticle of ecdysozoans.
3. *Ecological parameters*—for example, the presence of environmental turbulence, such as the wind-generated waves fragmenting naked coral embryos after mass spawning events [109].

Habitat, body size, reproduction modes, anatomy, and defense mechanisms might all be factors to consider. The intersection of ecological, developmental, and phylogenetic parameters poses a methodological challenge, and an eco-evo-devo approach has the potential for providing a common framework for tackling the issue [110].

Recent works have extensively discussed the ultimate causes of a reduced regenerative potential [4]. These works argue either that some selective pressure could play against the preservation of regenerative capacities, or that no particular pressure would maintain it, so that it becomes a neutral trait. The studies directly addressing the ultimate causes of regeneration are rare. A famous example is the loss of regenerative capacity in some groups of spiders, including the black widow (*Latrodectus mactans*). Spiders usually regenerate well their injured legs [111], with the notable exception of few orb-weaving genera, where it has been hypothesized that a regenerated appendage could impair web-making more than a missing one [112]. In this case, a strong pressure, the need for a geometrically accurate spider-web, selected against the maintenance of regenerative capacities. Conversely, if no particular pressure maintains regenerative capacities, for example, if predation is low [113, 114], these could be lost. Neutrality could also emerge if regenerative phenomena were essentially a by-product (an epiphenomenon) of other developmental processes under selective pressure and if the molecular link between modules was lost, for instance due to the activity of selfish genetic elements [115]. Continued tissue growth [116], agametic reproduction, or core embryonic mechanisms [117] have all been proposed as processes from which regeneration might have derived.

A taxon-restricted loss of regenerative capacities does not necessarily imply an elimination of the genetic program for regeneration. Are there any latent or inhibited regenerative capacities in taxa that usually do not display them—and which could thus be reactivated? In naidine annelids, both comparative regeneration experiments and phylogeny indicate multiple events of loss of head regeneration. Interestingly, in one species, amputation during asexual fission within a small proliferative region harboring activated stem cells could elicit regeneration of a normal head [118]. This indicates that, despite the loss of regeneration, the capacity remained latent in these annelids, and could be reactivated. This study is a further reminder that a comparative experimental approach is essential for understanding the evolutionary trajectories of regeneration.

The problems with the loss of regenerative capacities, its significance for the fitness of organisms, and the question of whether regeneration is an attribute of all organisms are not purely theoretical. Indeed, our hopes of inducing regeneration where it does not occur, for example in adult humans, ultimately rests on the assumption that potential for regeneration might remain latent in organisms who are currently unable to do it [119].

4.2 Questions and Approaches to Investigate WBR Evolution

Regardless of the evolutionary scenario, WBR constitutes a particular category of regenerative phenomena, whose links to physiology and reproduction are blurred. Here we have considered WBR in its most inclusive sense, including physiological regeneration and asexual reproduction, and effectively adopting the functional definition of regeneration that—by replacing essential body parts—significantly delays an organism's death. But how to practically study WBR, placing this phenomenon in its evolutionary, developmental, and ecological context? The questions raised through the Weismann vs. Morgan adaptive/innate debate are still highly relevant today. The criteria and strategies then proposed can represent today the starting points for practically shaping an integrative research program on the complex issue of whole-body regeneration.

1. *Does the regenerating structure/body part experience frequent injuries in nature?* Injuries, for example, due to sublethal predation, are frequent in marine invertebrates, either planktonic or benthic [113, 120, 121]. In several demosponges, the rate of regeneration was shown to vary across species and to be inversely correlated to the frequency of injury [122], and, interestingly, not to be a consequence of phylogeny or physiological growth rate [122, 123].
2. *Is functionality fully recovered after WBR?* Restoration of key functions, more than a perfect "replica" of the missing parts, is necessary for survival, as also identified by Needham [91]. The hydrozoan jellyfish *Clytia hemisphaerica* has recently been shown to efficiently recover buoyancy and feeding after large injuries, while the original body symmetry is not necessarily restored [124].
3. *Is WBR significantly expanding the life span of an organism?* Arguably, recovering from large injuries extends an organism's life expectancy, but other phenomena can be considered. The physiological regeneration of the colonial ascidian *Botryllus schlosseri* represents an interesting case, where the succession of generations could contribute to eliminating the senescence of the single individuals, rejuvenating the tissues but preserving the preadaption of the colony to its surrounding environment [125]. An alluring corollary to this argument is that regeneration time is expected to be significantly shorter than the life span of an organism.
4. *How is WBR ecologically relevant?* This question needs to consider that organisms are affected by their environment, and in turn, they modify it. Increasingly frequent episodes of mortality sweep through marine ecosystems due to extreme climatic events [126], which locally destroy benthic communities. The strategies of recovery, for example between marine

invertebrates undergoing WBR or recruiting new larvae, have a key impact on the dynamics of the benthic community. With regard to the second point, annelids have an important biogeomorphic impact on marine sediments, and regeneration negatively impacts their reworking of sediments [127]. Additionally, as WBR is tightly linked to the production of new individuals, it might represent a dispersal strategy [128], allowing organisms to colonize rapidly a novel or changing habitat, as it has been shown for forest recovery after fires [129]. The consequences of WBR on the invasiveness of a species and perhaps on the emergence of new species following reproductive isolation have been poorly studied, but constitute an interesting avenue for future research.

The extreme nature of WBR poses unique challenges, in particular when we try to investigate and measure the ecological and physiological implications. The resources required during WBR cannot be made available to other processes [130] This suggests important trade-offs for the organisms concerned, which need to be identified and quantified. These trade-offs concern the regenerative events, but also the loss of a body part itself. With regard to the cost-benefits of the regenerative process itself, regeneration subtracts resources from growth and reproduction, the so-called regenerative load [131]. In sponges and corals, injuries inflicted when food is scarce or when the animal had been previously injured regenerate less well, showing that resource allocation is critical [132]. On the other hand, besides the obvious benefit in avoiding looming death, WBR might provide some specific advantages, for example, a rapid adaptation to changing environments [125, 133]. In heteromorphic colonies of hydrozoans and bryozoans, changing environmental conditions could cause the regression of existing individuals and the generation of a different type of specialized zooid [125, 134]. Interestingly, given the colonial nature of these organisms, the costs of the process would be reduced by the reutilization of regressing individuals [20] as a source of materials and energy for the growing ones.

The loss of body parts is more difficult to quantify. Energy loss is a multifaceted variable, but the dry weight of the removed body part has been used as an estimate [135]. Short-term, acute, costs include the loss of foraging or motility, of body mass, risk of infection, behavioral disruption, and impaired self and nonself recognition, while lower fecundity or growth (due to loss of germ cells or energy storage) might be seen in the long term [136]. The loss of an arm, for example, has a greater cost for asteroids than for crinoids or ophiuroids, as they bear gonads [135]. As for the eventual benefits, it might seem difficult to imagine any advantage in losing a body part. Yet autotomy, the active breaking of a body part along a predetermined "plane," suggests a possible scenario:

crustaceans, annelids, holothurians and other animals shed body parts as a defense mechanism, in order to escape predators or to isolate infected or malfunctioning body parts (reviewed [137]).

5 Conclusions

When, later in his life, Morgan heard that a 24-year-old Norman John Berrill was working on marine worms and ascidian development and regeneration, he reproached him saying, "*You are being very foolish [...] At your age you cannot waste your time. We will never understand the phenomena of development and regeneration.*" [138]. Perhaps, if he had access to the theoretical tools of eco-evo-devo and to the technological resources available today, he would have thought otherwise. Morgan's emphasis on exploring the vast diversity of both developmental and regenerative phenomena, and experimenting with testable hypotheses in models, represents the assets of his legacy. The very same *modus operandi* could help to avoid hasty interpretation and to remove anthropomorphic biases in how we interpret natural phenomena. Luckily, the young Berrill did not take Morgan's advice and "[...] *continued watching in wonder to my heart's content and I am even more bewildered, though more sophisticated, by what I see*" [138].

Acknowledgments

The authors want to thank Evelyn Houliston, Lucas Leclere, and Elena Casetta for their valuable comments on the manuscript. This work was supported by ANR (ANR-14-CE02-0019-01).

References

1. Morgan TH (1901) Regeneration. Macmillan & Co., London
2. Bonner JT (1952) Morphogenesis: and essay on development. Princeton University Press, Princeton, New Jersey
3. Lai AG, Aboobaker AA (2018) EvoRegen in animals: time to uncover deep conservation or convergence of adult stem cell evolution and regenerative processes. Dev Biol 433: 118–131. https://doi.org/10.1016/j.ydbio.2017.10.010
4. Bely AE, Nyberg KG (2010) Evolution of animal regeneration: re-emergence of a field. Trends Ecol Evol 25:161–170. https://doi.org/10.1016/j.tree.2009.08.005
5. Esposito M (2013) Weismann versus Morgan revisited: clashing interpretations on animal regeneration. J Hist Biol 46:511–541. https://doi.org/10.1007/s10739-012-9341-9
6. Sunderland ME (2010) Regeneration: Thomas Hunt Morgan's window into development. J Hist Biol 43:325–361. https://doi.org/10.1007/s10739-009-9203-2
7. Weismann A (1893) The germ-plasm: a theory of heredity. Charles Sc, New York
8. Goss RJ (1992) The evolution of regeneration: adaptive or inherent? J Theor Biol 159: 241–260. https://doi.org/10.1016/S0022-5193(05)80704-0
9. Jenner RA, Wills MA (2007) Opinion: the choice of model organisms in evo-devo. Nat Rev Genet 8:311–319

10. Agata K, Saito Y, Nakajima E (2007) Unifying principles of regeneration I: epimorphosis versus morphallaxis. Develop Growth Differ 49: 73–78. https://doi.org/10.1111/j.1440-169X.2007.00919.x
11. Gehrke AR, Neverett E, Luo YJ et al (2019) Acoel genome reveals the regulatory landscape of whole-body regeneration. Science 363:eaau6173. https://doi.org/10.1126/science.aau6173
12. Johnson EM, Gorman RM, Gabel BEG, George ME (1982) The *hydra aftenuata* system for detection of teratogenic hazards. Teratog Carcinog Mutagen 2:263–276. https://doi.org/10.1002/1520-6866(1990)2:3/4<263::AID-TCM1770020308>3.0.CO;2-I
13. Rinkevich B, Shlemberg Z, Fishelson L (1995) Whole-body protochordate regeneration from totipotent blood cells. Proc Natl Acad Sci U S A 92:7695–7699. https://doi.org/10.1073/pnas.92.17.7695
14. Kassmer SH, Langenbacher AD, De Tomaso AW (2020) *Integrin-alpha-6*+ candidate stem cells are responsible for whole body regeneration in the invertebrate chordate *Botrylloides diegensis*. Nat Commun 11:1–11. https://doi.org/10.1038/s41467-020-18288-w
15. Blanchoud S, Rinkevich B, Wilson MJ (2018) Whole-body regeneration in the colonial tunicate *Botrylloides leachii*. Results Probl Cell Differ 65:337–355. https://doi.org/10.1007/978-3-319-92486-1_16
16. Cary GA, Wolff A, Zueva O et al (2019) Analysis of sea star larval regeneration reveals conserved processes of whole-body regeneration across the metazoa. BMC Biol 17:16. https://doi.org/10.1186/s12915-019-0633-9
17. Ramon-Mateu J, Ellison ST, Angelini TE, Martindale MQ (2019) Regeneration in the ctenophore *Mnemiopsis leidyi* occurs in the absence of a blastema, requires cell division, and is temporally separable from wound healing. BMC Biol 17:80. https://doi.org/10.1186/s12915-019-0695-8
18. Amiel AR, Röttinger E (2021) Experimental tools to study regeneration in the sea anemone *Nematostella vectensis*. Methods Mol Biol 2219:69–80
19. Sánchez Alvarado A, Yamanaka S (2014) Rethinking differentiation: stem cells, regeneration, and plasticity. Cell 157:110–119
20. Lauzon RJ, Brown C, Kerr L, Tiozzo S (2012) Phagocyte dynamics in a highly regenerative urochordate : insights into development and host defense. Dev Biol:1–17. https://doi.org/10.1016/j.ydbio.2012.11.006
21. Clarke E (2010) The problem of biological individuality. Biol Theory 5:312–325. https://doi.org/10.1162/biot_a_00068
22. Bouchard F, Huneman P (2013) From groups to individuals evolution and emerging individuality. MIT Press, Boston
23. Morgan TH (1898) Experimental studies of the regeneration of *Planaria maculata*. Arch für Entwickelungsmechanik der Org 7: 364–397. https://doi.org/10.1007/BF02161491
24. Sanchez-Alvarado A (2000) Regeneration in the metazoans: why does it happen? BioEssays 22:578–590
25. Tiozzo S, Copley RR (2015) Reconsidering regeneration in metazoans: An evo-devo approach. Front Ecol Evol 3:1–12. https://doi.org/10.3389/fevo.2015.00067
26. Wagner GP (2007) The developmental genetics of homology. Nat Rev Genet 8:473–479
27. Wagner GP, Pavlicev M, Cheverud JM (2007) The road to modularity. Nat Rev Genet 8: 921–931. https://doi.org/10.1038/nrg2267
28. Bolker JA (2000) Modularity in development and why it matters to Evo-devo. Integr Comp Biol 40:770–776. https://doi.org/10.1093/icb/40.5.770
29. Gilbert SF, Bolker JA (2001) Homologies of process and modular elements of embryonic construction. J Exp Zool 291(1):1–12
30. Waddington CH (1975) The evolution of an evolutionist. Cornell Un, Ithaca, NY
31. Rieppel O (2013) Homology: a philosophical and biological perspective. In: Handbook of paleoanthropology. Springer, Berlin Heidelberg, pp 1–19
32. Brockes JP, Kumar A, Velloso CP (2001) Regeneration as an evolutionary variable. J Anat 199:3–11. https://doi.org/10.1017/S0021878201008299
33. Zattara EE, Scientific N, Hiebert T, Bely AE (2019) A phylum-wide survey reveals multiple independent gains of head regeneration in Nemertea. Proc Biol Sci 286(1898): 20182524. https://doi.org/10.1098/rspb.2018.2524
34. Alié A, Hiebert LS, Simion P et al (2018) Convergent acquisition of nonembryonic development in styelid ascidians. Mol Biol Evol 35:1728–1743. https://doi.org/10.1093/molbev/msy068
35. Wagner GP, Zhang J (2011) The pleiotropic structure of the genotype-phenotype map: the

evolvability of complex organisms. Nat Rev Genet 12:204–213. https://doi.org/10.1038/nrg2949

36. Postlethwait JH, Schneiderman HA (1971) Pattern formation and determination in the antenna of the homoeotic mutant Antennapedia of *Drosophila melanogaster*. Dev Biol 25:606–640. https://doi.org/10.1016/0012-1606(71)90008-X
37. Bolker JA (2000) Modularity in development and why it matters to Evo-devo. Am Zool 40:770–776. https://doi.org/10.1093/icb/40.5.770
38. Raff RA (2000) Evo-devo: the evolution of a new discipline. Nat Rev Genet 1:74–79. https://doi.org/10.1038/35049594
39. Atchley WR, Hall BK (1991) A model for development and evolution of complex morphological structures. Biol Rev Camb Philos Soc 66:101–157. https://doi.org/10.1111/j.1469-185X.1991.tb01138.x
40. Richardson MK, Chipman AD (2003) Developmental constraints in a comparative framework: a test case using variations in phalanx number during amniote evolution. J Exp Zool B Mol Dev Evol 296:8–22. https://doi.org/10.1002/jez.b.13
41. Levin M, Stevenson CG (2012) Regulation of cell behavior and tissue patterning by bioelectrical signals: challenges and opportunities for biomedical engineering. Annu Rev Biomed Eng 14:295–323. https://doi.org/10.1146/annurev-bioeng-071811-150114
42. Beane WS, Morokuma J, Lemire JM, Levin M (2013) Bioelectric signaling regulates head and organ size during planarian regeneration. Development 140:313–322. https://doi.org/10.1242/dev.086900
43. Eming SA, Hammerschmidt M, Krieg T, Roers A (2009) Interrelation of immunity and tissue repair or regeneration. Semin Cell Dev Biol 20:517–527. https://doi.org/10.1016/j.semcdb.2009.04.009
44. Harty M, Neff AW, King MW, Mescher AL (2003) Regeneration or scarring: an immunologic perspective. Dev Dyn 226:268–279
45. Mescher AL, Neff AW, King MW (2017) Inflammation and immunity in organ regeneration. Dev Comp Immunol 66:98–110. https://doi.org/10.1016/j.dci.2016.02.015
46. Simpson T (1984) The cell biology of sponges. Springer-V, New York
47. Pick KS, Philippe H, Schreiber F et al (2010) Improved phylogenomic taxon sampling noticeably affects nonbilaterian relationships. Mol Biol Evol 27:1983–1987. https://doi.org/10.1093/molbev/msq089
48. Simion P, Philippe H, Baurain D et al (2017) A large and consistent Phylogenomic dataset supports sponges as the sister group to all other animals. Curr Biol 27:958–967. https://doi.org/10.1016/j.cub.2017.02.031
49. Sperling EA, Robinson JM, Pisani D, Peterson KJ (2010) Where's the glass? Biomarkers, molecular clocks, and microRNAs suggest a 200-Myr missing Precambrian fossil record of siliceous sponge spicules. Geobiology 8:24–36. https://doi.org/10.1111/j.1472-4669.2009.00225.x
50. Erwin DH (2020) The origin of animal body plans: a view from fossil evidence and the regulatory genome. Development 147:dev182899. https://doi.org/10.1242/dev.182899
51. Eerkes-Medrano D, Feehan CJ, Leys SP (2015) Sponge cell aggregation: checkpoints in development indicate a high level of organismal complexity. Invertebr Biol 134:1–18. https://doi.org/10.1111/ivb.12072
52. Lavrov AI, Kosevich IA (2014) Sponge cell reaggregation: mechanisms and dynamics of the process. Russ J Dev Biol 45:205–223
53. Lavrov AI, Kosevich IA (2016) Sponge cell reaggregation: cellular structure and morphogenetic potencies of multicellular aggregates. J Exp Zool Part A Ecol Genet Physiol 325:158–177. https://doi.org/10.1002/jez.2006
54. Soubigou A, Ross EG, Touhami Y et al (2020) Regeneration in sponge *Sycon ciliatum* mimics postlarval development. Development 147(22):dev193714. https://doi.org/10.1101/2020.05.04.061218
55. Boury-Esnault N (1976) Morphogenese experimentale des papilles inhalantes de l'eponge *Polymastia mamillaris* (Muller). Arch Zool Exp Gen 117:181–196
56. Diaz JP (1979) Variations, differentiations et functions des categories cellulaires de lademosponge d'eaux saumatres, *Suberites massa*, Nardo, au cours du cycle biologique annuel et dans des conditions experimentales. Université Montpellier, Montpellier
57. Borisenko IE, Adamska M, Tokina DB, Ereskovsky AV (2015) Transdifferentiation is a driving force of regeneration in *Halisarca dujardini* (Demospongiae, Porifera). PeerJ 3:e1211. https://doi.org/10.7717/peerj.1211
58. Ereskovsky AV, Tokina DB, Saidov DM et al (2020) Transdifferentiation and mesenchymal-to-epithelial transition during regeneration in Demospongiae (Porifera). J

Exp Zool Part B Mol Dev Evol 334:37–58. https://doi.org/10.1002/jez.b.22919

59. Leys SP, Mackie GO, Reiswig HM (2007) The biology of glass sponges. Adv Mar Biol 52:1–145
60. Ereskovsky AV, Lavrov AI, Bolshakov FV, Tokina DB (2017) Regeneration in white sea sponge *Leucosolenia complicata* (Porifera, calcarea). Invertebr Zool 41:108–113. https://doi.org/10.15298/invertzool.14.2.02
61. Ereskovsky AV, Borisenko IE, Lapébie P et al (2015) *Oscarella lobularis* (Homoscleromorpha, Porifera) regeneration: epithelial morphogenesis and metaplasia. PLoS One 10: e0134566. https://doi.org/10.1371/journal.pone.0134566
62. Caroline R, Amélie V, Laura F-C, et al (2020) The buds of *Oscarella lobularis* (Porifera): a new convenient model for sponge cell and developmental biology. bioRxiv 2020.06.23.167296. https://doi.org/10.1101/2020.06.23.167296
63. Funayama N (2013) The stem cell system in demosponges: suggested involvement of two types of cells: archeocytes (active stem cells) and choanocytes (food-entrapping flagellated cells). Dev Genes Evol 223:23–38. https://doi.org/10.1007/s00427-012-0417-5
64. Cannon JT, Vellutini BC, Smith J et al (2016) Xenacoelomorpha is the sister group to Nephrozoa. Nature 530:89–93. https://doi.org/10.1038/nature16520
65. Rouse GW, Wilson NG, Carvajal JI, Vrijenhoek RC (2016) New deep-sea species of Xenoturbella and the position of Xenacoelomorpha. Nature 530:94–97. https://doi.org/10.1038/nature16545
66. De Mulder K, Pfister D, Kuales G et al (2009) Stem cells are differentially regulated during development, regeneration and homeostasis in flatworms. Dev Biol 334:198–212. https://doi.org/10.1016/j.ydbio.2009.07.019
67. Srivastava M, Mazza-Curll KL, Van Wolfswinkel JC, Reddien PW (2014) Whole-body acoel regeneration is controlled by Wnt and bmp-Admp signaling. Curr Biol 24: 1107–1113. https://doi.org/10.1016/j.cub.2014.03.042
68. Gehrke AR, Srivastava M (2016) Neoblasts and the evolution of whole-body regeneration. Curr Opin Genet Dev 40:131–137
69. Raz AA, Srivastava M, Salvamoser R, Reddien PW (2017) Acoel regeneration mechanisms indicate an ancient role for muscle in regenerative patterning. Nat Commun 8:1260. https://doi.org/10.1038/s41467-017-01148-5
70. Witchley JN, Mayer M, Wagner DE et al (2013) Muscle cells provide instructions for planarian regeneration. Cell Rep 4:633–641. https://doi.org/10.1016/j.celrep.2013.07.022
71. Cebrià F (2016) Planarian body-wall muscle: regeneration and function beyond a simple skeletal support. Front Cell Dev Biol 4:8
72. Lucila Scimone M, Cote LE, Reddien PW (2017) Orthogonal muscle fibres have different instructive roles in planarian regeneration. Nature 551:623–628. https://doi.org/10.1038/nature24660
73. Nakano H (2019) Development of Xenoturbellida. In: Results and problems in cell differentiation. Springer Verlag, Berlin, pp 251–258
74. Philippe H, Brinkmann H, Copley RR et al (2011) Acoelomorph flatworms are deuterostomes related to Xenoturbella. Nature 470: 255–258. https://doi.org/10.1038/nature09676
75. Hejnol A, Pang K (2016) Xenacoelomorpha's significance for understanding bilaterian evolution. Curr Opin Genet Dev 39:48–54
76. Jondelius U, Raikova OI, Martinez P (2019) Xenacoelomorpha, a key group to understand Bilaterian evolution: morphological and molecular perspectives. In: Evolution, origin of life, concepts and methods. Springer International Publishing, Cham, pp 287–315
77. Jeffery WR (2015) Closing the wounds: one hundred and twenty five years of regenerative biology in the ascidian *Ciona intestinalis*. Genesis 53:48–65. https://doi.org/10.1002/dvg.22799
78. Alié A, Hiebert LS, Scelzo M, Tiozzo S (2020) The eventful history of nonembryonic development in tunicates. J Exp Zool Part B Mol Dev Evol 336(3):250–266. https://doi.org/10.1002/jez.b.22940
79. Delsuc F, Philippe H, Tsagkogeorga G et al (2018) A phylogenomic framework and timescale for comparative studies of tunicates. BMC Biol 16:1–14. https://doi.org/10.1186/s12915-018-0499-2
80. Berrill NJ (1948) The gonads, larvae, and budding of the Polystyelid ascidians Stolonica and Distomus. J Mar Biol Assoc U.K. 27:633. https://doi.org/10.1017/S002531540005606X
81. Kott P (1985) The australian ascidiacea part I. Mem Queensl Mus 23:1–440

82. Scelzo M, Alié A, Pagnotta S et al (2019) Novel budding mode in *Polyandrocarpa zorritensis*: a model for comparative studies on asexual development and whole body regeneration. EvoDevo 10:7. https://doi.org/10.1186/s13227-019-0121-x
83. Ramirez AN, Loubet-Senear K, Srivastava M (2020) A regulatory program for initiation of Wnt signaling during posterior regeneration. Cell Rep 32:108098. https://doi.org/10.1016/j.celrep.2020.108098
84. Chera S, Ghila L, Dobretz K et al (2009) Apoptotic cells provide an unexpected source of Wnt3 signaling to drive *hydra* head regeneration. Dev Cell 17:279–289. https://doi.org/10.1016/j.devcel.2009.07.014
85. Wenger Y, Buzgariu W, Perruchoud C, et al (2019) Generic and context-dependent gene modulations during *Hydra* whole body regeneration bioRxiv 587147. https://doi.org/10.1101/587147
86. Cazet J, Juliano C (2020) Oral Regeneration Is the Default Pathway Triggered by Injury in *Hydra* bioRxiv 2020.07.06.189811. https://doi.org/10.1101/2020.07.06.189811
87. René Antoine Ferchault de Réaumur, << Sur les diverses reproductions qui se font dans les Ecrevisses, les Omars, les Crabes, etc. Et entre autres, sur celles de leurs jambes et de leurs Ecailles >>, in Histoire de l'Académie Royale des Sciences, Paris, Imprimerie Royale, 1731, p. 235
88. Bonnet C (1745) Traité d'insectologie ou observations sur les pucerons: Traité d'insectologie ou observations sur quelques espéces de vers d'eau douce, qui coupés par morceaux deviennent autant d'animaux complets. Paris, Chez Durand, M.DCC.XLV. https://doi.org/10.5962/bhl.title.51914
89. Lauzon RJ, Ishizuka KJ, Weissman IL (2002) Cyclical generation and degeneration of organs in a colonial urochordate involves crosstalk between old and new : a model for development and regeneration. Dev Biol 348:333–348. https://doi.org/10.1006/dbio.2002.0772
90. Darwin C (1875) The variation of animals and plants under domestication, 2nd edn. John Murray, London
91. Needham AE (1961) Adaptive value of regenerative ability. Nature 191:720–721. https://doi.org/10.1038/191720a0
92. Needham AE (1952) The incidence and adaptive value of autotomy and of regeneration in Crustacea. Proc Zool Soc London 123:111–122. https://doi.org/10.1111/j.1096-3642.1953.tb00159.x
93. Huet M (1975) Le rôle du système nerveux an cours de la régénération du bras chez une Etoile de mer: *Asterina gibbosa* Penn.(Echinoderme, Astéride). J Embryol Exp Morph 33:535–552
94. Schotté OE, Butler EG (1944) Phases in regeneration of the urodele limb and their dependence upon the nervous system. J Exp Zool 97:95–121. https://doi.org/10.1002/jez.1400970202
95. Muneoka K, Bryant SV (1982) Evidence that patterning mechanisms in developing and regenerating limbs are the same. Nature 298:369–371
96. Muneoka K, Sassoon D (1992) Molecular aspects of regeneration in developing vertebrate limbs. Dev Biol 152:37–49. https://doi.org/10.1016/0012-1606(92)90154-9
97. Tank PW, Carlson BM, Connelly TG (1977) A scanning electron microscopic comparison of the development of embryonic and regenerating limbs in the axolotl. J Exp Zool 201:417–429. https://doi.org/10.1002/jez.1402010308
98. Barr HJ (1964) Regeneration and natural selection. Am Nat 98:183–186. https://doi.org/10.1086/282317
99. Elder D (1979) Why is regenerative capacity restricted in higher organisms? J Theor Biol 81:563–568. https://doi.org/10.1016/0022-5193(79)90053-5
100. Fumagalli MR, Zapperi S, La Porta CAM (2018) Regeneration in distantly related species: common strategies and pathways. NPJ Syst Biol Appl 4:5. https://doi.org/10.1038/s41540-017-0042-z
101. Bryant DM, Johnson K, DiTommaso T et al (2017) A tissue-mapped axolotl De novo transcriptome enables identification of limb regeneration factors. Cell Rep 18:762–776. https://doi.org/10.1016/j.celrep.2016.12.063
102. Hutchins ED, Markov GJ, Eckalbar WL et al (2014) Transcriptomic analysis of tail regeneration in the lizard *Anolis carolinensis* reveals activation of conserved vertebrate developmental and repair mechanisms. PLoS One 9:e105004. https://doi.org/10.1371/journal.pone.0105004
103. Rodius S, Androsova G, Götz L et al (2016) Analysis of the dynamic co-expression network of heart regeneration in the zebrafish. Sci Rep 6:26822. https://doi.org/10.1038/srep26822
104. Warner JF, Amiel AR, Johnston H, Röttinger E (2019) Regeneration is a partial

redeployment of the embryonic gene network. bioRxiv. https://doi.org/10.1101/658930
105. Aurora AB, Olson EN (2014) Immune modulation of stem cells and regeneration. Cell Stem Cell 15:14–25
106. Sinigaglia C, Averof M (2019) The multifaceted role of nerves in animal regeneration. Curr Opin Genet Dev 57:98–105. https://doi.org/10.1016/j.gde.2019.07.020
107. Goss RJ (1969) Principles of regeneration. Elsevier, Amsterdam
108. Huxley J (1943) Evolution : the modern synthesis. Harper & Brothers, New York
109. Heyward AJ, Negri AP (2012) Turbulence, cleavage, and the naked embryo: a case for coral clones. Science 335:1064. https://doi.org/10.1126/science.1216055
110. Gilbert SF, Epel D (2009) Ecological developmental biology: Intregrating epigenetics, medicine and evolution. Sinauer As. Sinauer Associates Inc., Sunderland
111. Edwards GB, Foelix RF (2001) Biology of spiders. Florida Entomol 84:324. https://doi.org/10.2307/3496196
112. Vollrath F (1988) Altered geometry of webs in spiders with regenerated legs. Nature Publishing Group, Berlin
113. Lindsay SM (2010) Frequency of injury and the ecology of regeneration in marine benthic invertebrates. Integr Comp Biol 50:479–493. https://doi.org/10.1093/icb/icq099
114. Gahn FJ, Baumiller TK (2010) Evolutionary history of regeneration in crinoids (Echinodermata). Integr Comp Biol 50:514–514. https://doi.org/10.1093/icb/icq155
115. Ågren JA, Clark AG (2018) Selfish genetic elements. PLOS Genet 14:e1007700. https://doi.org/10.1371/journal.pgen.1007700
116. Tanaka EM, Ferretti P (2009) Considering the evolution of regeneration in the central nervous system. Nat Rev Neurosci 10:713–723. https://doi.org/10.1038/nrn2707
117. Brockes JP, Kumar A (2008) Comparative aspects of animal regeneration. Annu Rev Cell Dev Biol 24:525–549. https://doi.org/10.1146/annurev.cellbio.24.110707.175336
118. Sikes JM, Bely AE (2010) Making heads from tails: development of a reversed anterior-posterior axis during budding in an acoel. Dev Biol 338:86–97. https://doi.org/10.1016/j.ydbio.2009.10.033
119. Dimmeler S, Ding S, Rando TA, Trounson A (2014) Translational strategies and challenges in regenerative medicine. Nat Med 20:814–821
120. Hays GC, Doyle TK, Houghton JDR (2018) A paradigm shift in the trophic importance of jellyfish? Trends Ecol Evolution 33:874–884
121. Clark MS, Dupont S, Rossetti H et al (2007) Delayed arm regeneration in the antarctic brittle star *Ophionotus victoriae*. Aquat Biol 1:45–53. https://doi.org/10.3354/ab00004
122. Wulff J (2010) Regeneration of sponges in ecological context: is regeneration an integral part of life history and morphological strategies? Integr Comp Biol 50:494–505
123. Ayling AL (1983) Growth and regeneration rates in thinly encrusting Demospongiae from temperate waters. Biol Bull 165:343–352. https://doi.org/10.2307/1541200
124. Sinigaglia C, Peron S, Eichelbrenner J et al (2020) Pattern regulation in a regenerating jellyfish. elife 9:e54868. https://doi.org/10.7554/eLife.54868
125. Sabbadin A (1966) Aspetti e problemi della vita coloniale. Bolletino di Zool 33:23–38. https://doi.org/10.1080/11250006609440508
126. Herring SC, Christidis N, Hoell A et al (2020) Explaining extreme events of 2018 from a climate perspective. Bull Am Meteorol Soc 101:S1–S140. https://doi.org/10.1175/bams-explainingextremeevents2018.1
127. Van Regteren M, Ten Boer R, Meesters EH, De Groot AV (2017) Biogeomorphic impact of oligochaetes (Annelida) on sediment properties and *Salicornia* spp. seedling establishment. Ecosphere 8:e01872. https://doi.org/10.1002/ecs2.1872
128. Gravier-Bonnet N (1992) Cloning and dispersal by buoyant autotomised hydranths of a *Thecate* hydroid (Cnidaria; hydrozoa). Sci Mar 56:229–236
129. Wells PV (1969) The relation between mode of reproduction and extent of speciation in Woody genera of the California chaparral. Evolution (N Y) 23:264. https://doi.org/10.2307/2406790
130. Garland T (2014) Trade-offs. Curr Biol 24:R60–R61
131. Juanes F, Smith LD (1995) Ecological consequences of limb damage and loss in decapod crustaceans: a review and prospectus. J Exp Mar Biol Ecol 193:197–223

132. Henry LA, Hart M (2005) Regeneration from injury and resource allocation in sponges and corals - a review. Int Rev Hydrobiol 90:125–158
133. Sabbadin A (1958) Experimental analysis of the development of colonies of *Botryllus schlosseri* (Pallas) , Ascidiacea. Arch Ital Anat Embriol 63:178–221
134. Saito Y, Mukai H, Watanabe H (1981) Studies on Japanese compound Styelid ascidians -ii. a new species of the genus *Botrylloides* and Redescription of *B. violaceus* Oka. Publ Seto Mar Biol Lab 26:357–368. https://doi.org/10.5134/176032
135. Lawrence JM (2010) Energetic costs of loss and regeneration of arms in stellate echinoderms. Integr Comp Biol 50:506–514
136. Maginnis TL (2006) The costs of autotomy and regeneration in animals: a review and framework for future research. Behav Ecol 17:857–872. https://doi.org/10.1093/beheco/arl010
137. Fleming PA, Muller D, Bateman PW (2007) Leave it all behind: a taxonomic perspective of autotomy in invertebrates. Biol Rev 82: 481–510
138. Berrill NJ (1983) The pleasure and practice of biology. Can J Zool 61:947–951. https://doi.org/10.1139/z83-127

Open Access This chapter is licensed under the terms of the Creative Commons Attribution 4.0 International License (http://creativecommons.org/licenses/by/4.0/), which permits use, sharing, adaptation, distribution and reproduction in any medium or format, as long as you give appropriate credit to the original author(s) and the source, provide a link to the Creative Commons license and indicate if changes were made.

The images or other third party material in this chapter are included in the chapter's Creative Commons license, unless indicated otherwise in a credit line to the material. If material is not included in the chapter's Creative Commons license and your intended use is not permitted by statutory regulation or exceeds the permitted use, you will need to obtain permission directly from the copyright holder.





Chapter 2

Studying Regeneration in Ascidians: An Historical Overview

Virginia Vanni, Loriano Ballarin, Fabio Gasparini, Anna Peronato, and Lucia Manni

Abstract

Ascidians are sessile tunicates, that is, marine animals belonging to the phylum Chordata and considered the sister group of vertebrates. They are widespread in all the seas, constituting abundant communities in various ecosystems. Among chordates, only tunicates are able to reproduce asexually, forming colonies. The high regenerative potentialities enabling tunicates to regenerate damaged body parts, or the whole body, represent a peculiarity of this taxon. Here we review the methodological approaches used in more than a century of biological studies to induce regeneration in both solitary and colonial species. For solitary species, we refer to the regeneration of single organs or body parts (e.g., siphon, brain, gonad, tunic, viscera). For colonial species, we review a plethora of experiments regarding the surgical manipulation of colonies, the regeneration of isolated colonial entities, such as single buds in the tunic, or part of tunic and its circulatory system.

Key words Colonial circulatory system, Evisceration, Gonad, Neural complex, Partial regeneration, Siphon, Thorax, Tunic, Whole body regeneration

1 Introduction

Within the phylum Chordata, which includes the three subphyla Vertebrata, Cephalochordata, and Tunicata (Fig. 1), the latter exhibits the more striking regenerative abilities. This feature, widely recognized by the scientific community since the end of the nineteenth century, raised renewed interests in the last 15 years, thanks to the availability of new methodological tools enabling the dissection of its molecular and cellular bases [1, 2]. In tunicates, the regenerative ability shows remarkable differences in various clades, even in different tissues and organs of the same organism [3]. Nonetheless, in some species, it can extend to extremes of complete individuals formed, from a small group of stem cells in the case of whole-body regeneration (WBR) [4, 5].

Tunicates are filter feeding, marine organisms, widespread in all the seas, constituting abundant communities in various ecosystems.

Simon Blanchoud and Brigitte Galliot (eds.), *Whole-Body Regeneration: Methods and Protocols*,
Methods in Molecular Biology, vol. 2450, https://doi.org/10.1007/978-1-0716-2172-1_2, © The Author(s) 2022

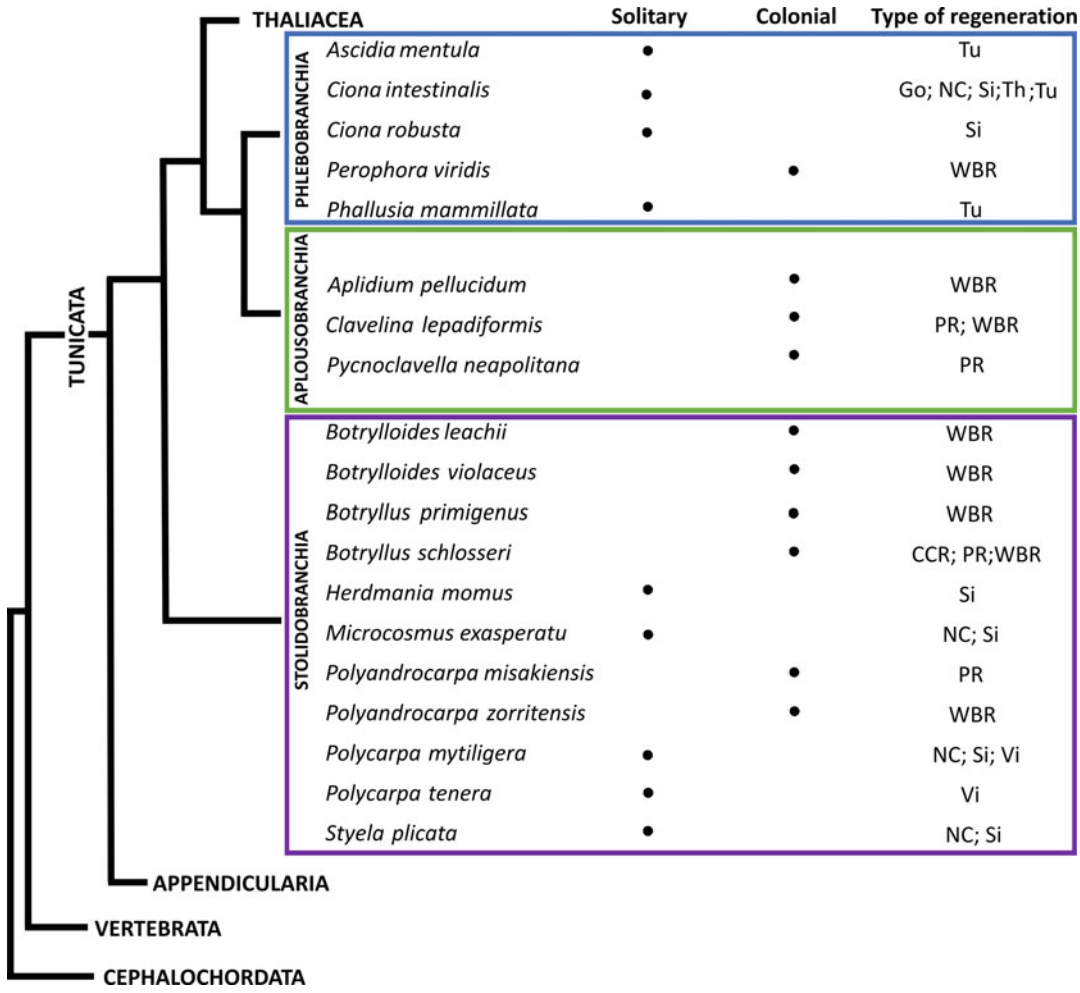


Fig. 1 Phylogenetic tree of chordates (modified from [7]) reporting the ascidian species studied for regeneration. Dots indicate if species are solitary or colonial. Types of regeneration induced in the various species include the following: regeneration of the colonial circulatory system (CCS), gonads (Go), neural complex (NC), partial regeneration (PR), regeneration of the siphons (Si), thorax (th), tunic (tu), viscera (Vi). WBR: whole body regeneration

They are considered the sister group of vertebrates (Fig. 1) [6, 7], therefore representing, from an evolutionary point of view, an intriguing taxon for comparative studies on regeneration, a limited process in vertebrates [8, 9]. Tunicates include both solitary and colonial species, the latter representing the only chordates capable of asexual reproduction (also called budding) [10].

Ascidians represent the main tunicate group, now considered paraphyletic by several authors. Their life cycle includes a swimming larva, which exhibits the typical chordate body plan and is the dispersal phase of the species. The larva is lecithotrophic and swims for a few hours to select an appropriate substrate on which

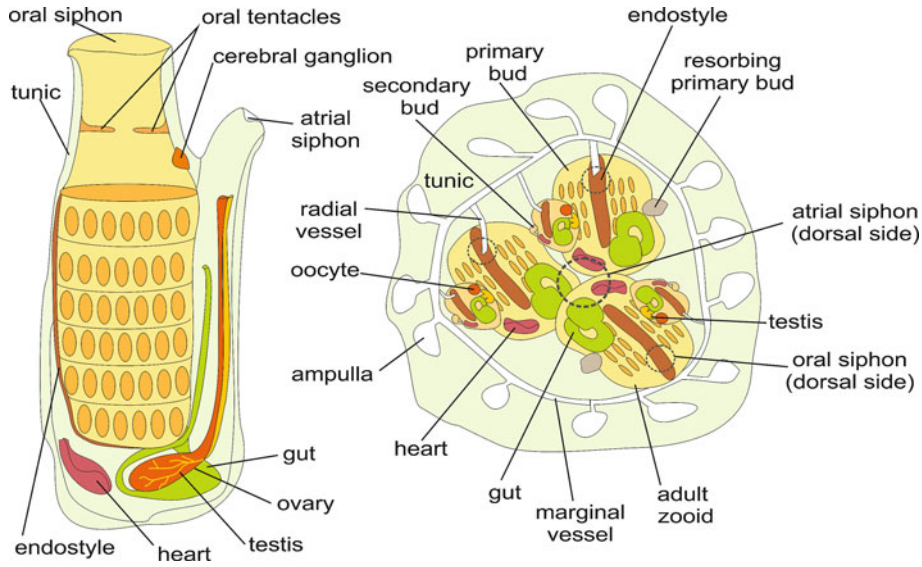


Fig. 2 Schematic representation of a solitary (left) and a colonial (right) ascidian (in ventral view). In the colonial tunicate, three adult zooids are represented, each one bearing one primary bud and one secondary bud

to adhere. Then, it undergoes a deep metamorphosis becoming a sessile individual, the juvenile, which possesses the capacity to regenerate.

Ascidian adult body is cylindrical, with an anterior inhalant (oral) siphon and a dorsal exhalant (atrial) siphon (Figs. 2 and 3). The brain (called cerebral ganglion) is located between the two siphons. The brain, together with the associated neural gland, forms the neural complex. The majority of the body is occupied by a large branchial chamber (pharynx) perforated by numerous ciliated stigmata [11]. The inhaled water enters the branchial chamber and, passing through the stigmata, is filtered by a mucous net produced by the endostyle. The latter is a glandular groove located in the ventral floor of the branchial chamber. The filtered seawater passes then to the atrial chamber and is expelled through the atrial siphon. Nutrients, entrapped in the mucous net, are agglutinated in a mucous cord that is conveyed to the U-shaped gut, located posteriorly, below the branchial chamber. The anus opens into the atrial chamber, so that the fecal pellets are removed by the exhalant water flow. Ascidians are hermaphrodites; gonads can be located in the posterior body, close to the gut, or in the lateral body wall.

In solitary ascidians, the cylindrical, tube-like body shape suggested a wide range of regeneration experiments involving mainly distal body parts, such as the siphons and the neural complex (Table 1) (Fig. 3b–f). In the solitary species of the genus *Ciona*, *C. intestinalis* and *C. robusta*, for which very advanced methodological tools are available, regeneration has been comprehensively

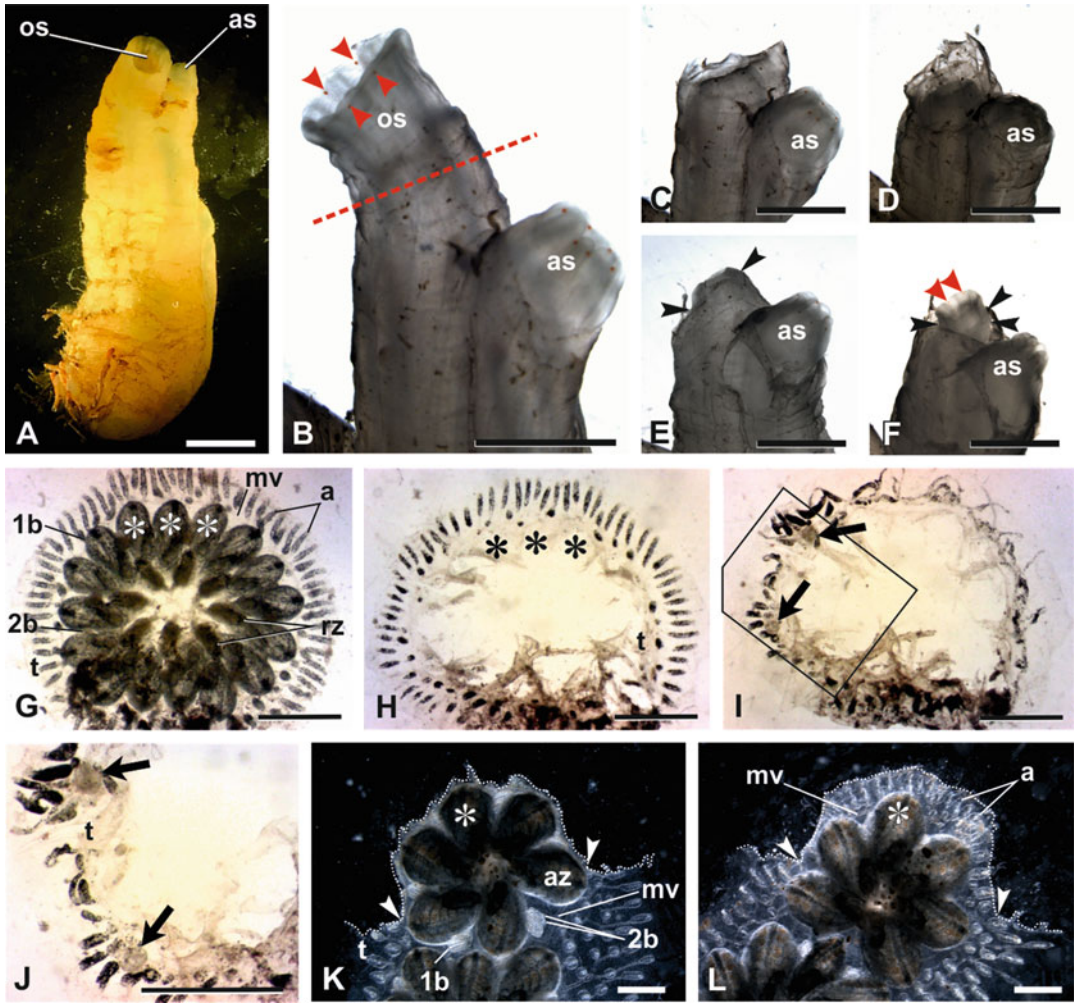


Fig. 3 (**A**–**F**). Oral siphon regeneration in *Ciona robusta*. (**A**) Individual showing the typical cylindrical, tube-like body shape of solitary ascidians. The oral siphon (os) individuates the anterior side, the atrial siphon (as) the dorsal side. (**B**–**F**). Details of siphons of an individual before (**B**), and after 0 (**C**), 1 (**D**), 3 (**E**), and 6 days (**F**) from the amputation of the oral siphon. The red line in **B** labels the level of amputation. One day after amputation (**D**), the wound is closed. In (**E**, **F**), black arrowheads mark the basal limit of the regenerating oral siphon. In (**B**) and (**F**), red arrowheads label some of the eight orange-pigmented sensory organs located in the notches between the lobes of the oral siphon rim. Six similar organs are also on the atrial siphon. Note that after 6 days from oral siphon ablation (**F**), the organs are present. (**G**–**J**). WBR in *Botryllus schlosseri*. In a colony at takeover phase (**G**; ventral view), regressing adult zooids (rz) are in form of dense masses at the center of the colony; primary buds (1b) are almost ready to open their siphons becoming the new generation of filtering individuals; small secondary buds (2b) are recognizable on primary buds. The colony is embedded by the tunic (t), where the colonial circulatory system is located. A marginal vessel (mv) extends all around the colony, connecting and coordinating the zooids. Blind ampullae (a) elongate from the marginal vessel toward the periphery. (**H**) colony (dorsal view) showed in **G** 2 days after the ablation of all the zooids (regressing zooids, primary and secondary buds). The circulation is restored. Asterisks in **H** individuate the position of the three primary buds marked by asterisks in **G**. (**I**–**J**) 3 days post ablation, two new vascular buds (arrows) are recognizable close to the marginal vessel. Square area in **I** is enlarged in **J**. (**K**–**L**) Tunic and colonial circulatory system regeneration in *Botryllus schlosseri* (ventral view). (**K**) a portion of the tunic (t) with its marginal vessel (mv) and blood ampullae has been removed (dotted line) in front of three adult zooids (az).

Table 1
Types of regeneration studies in solitary ascidians

Regenerating organ	Species	Outcome	References
Tunic	*Ascidia mentula*	Full regeneration	[19]
	Phallusia mammillata	Full regeneration	[20]
	Ciona intestinalis	Full regeneration	[23]
Thorax	*Ciona intestinalis*	Full regeneration only if fragments of the pharynx remains and in posterior toward anterior direction	[18]
	Polycarpa mytiligera	Full regeneration from posterior toward anterior direction	[14]
Siphon (oral/atrial)	*Ciona intestinalis*	Full regeneration (short/long distance regeneration for oral siphon)	[32, 33]
	Polycarpa mytiligera	Full regeneration	[13, 31]
	Styela plicata	Full regeneration	[31]
	Microcosmus exasperatus	Full regeneration	[31]
	Herdmania momus	Scrubby regeneration	[31]
Neural complex	*Styela plicata*	Full regeneration	[31, 70]
	Ciona intestinalis	Full regeneration	[16, 67–69]
	Microcosmus exasperatus	Full regeneration	[31]
	Polycarpa mytiligera	Full regeneration	[31]
Gonad	*Ciona intestinalis*	Full regeneration	[66]
Viscera	*Polycarpa mytiligera*	Full regeneration	[13, 31]
	Polycarpa tenera	Full regeneration	[12]
Body parts with multiple organs	*Polycarpa mytiligera*	Full regeneration of complete individuals from body fragments obtained by cutting animals longitudinally and transversely	[14]

Fig. 3 (continued) Arrowheads individuate the lateral cut edges. (**L**) the same colony showed in (**K**), 6 days after ablation: new tunic covers the previously exposed zooids. (**L**) in the regenerated tunic, the marginal vessel and a crown of new ampullae (a) are recognizable. Asterisks in **K** and **L** individuate the same zooid, as reference. Scale bar = 1 mm in **a**, (**G–J**); 5 mm in (**B–F**); 100 μ in (**K**, **L**).

explored in terms of both its morphological and cellular/molecular aspects (Table 2) [1]. Among other emerging model species, *Polyandrocarpa mytiligera* is a solitary ascidian of the Red Sea that, for example, can regenerate the whole gut after its evisceration [12–14].

In colonial ascidians, several individuals (zooids) are organized in large colonies exhibiting astonishing morphologies and colors (Fig. 3g) [10]. Usually, regeneration is seen as the ability of an organism to regrow or repair its cells, tissues and organs after their loss or severe injury. However, to some extent, asexual reproduction in colonial ascidians is considered an expansion of regeneration, as a nonembryonic development of new individuals. Indeed, the ability of colonial ascidians to activate unusual developmental pathways in both natural and/or induced conditions makes the border between asexual reproduction and a true, injury-induced, regeneration quite faint [2, 11].

In colonial ascidians, a plethora of regeneration experiments has been performed regarding, in general, the removal of single individuals from colonies (single buds, adult individuals, both buds and adult zooids) (Table 3; Fig. 3g–j) [2]. However, the regeneration of isolated colonial entities (e.g., isolated buds in the tunic, the whole tunic with its circulatory system without any zooid) and the regeneration of part of the tunic and its circulatory system have also been studied (Fig. 3k–l). The latter is a network of hemolymphatic vessels (Fig. 3g) connected to a marginal vessel that extends along the periphery of the colony. Several radial vessels emerge from each zooid and connect them to the marginal vessel. Blind, sausage-like ampullae elongate toward the tunic periphery. Among colonial ascidians, *Botryllus schlosseri* is one of the most studied species. However, several ascidians species can be maintained in laboratory culture throughout their life cycle and used for regeneration experiments (Table 3). Thanks to their recurrent budding, the ability to survive in aquaria also beyond their natural lifespan (useful to study ageing), the possibility to be split in fragments to analyze different conditions in the same genetic environment, their sequenced genome, and the availability of some molecular tools for unbiased results (Table 4), colonial ascidians provide valuable models for an integrated approach to regeneration.

On the whole, studies on both solitary and colonial species are shedding light in outstanding challenging topics of contemporary biological science, such as the connections between animal regeneration and regenerative medicine, stem cells biology, aging, and tissue homeostasis [1, 15].

Here, we briefly review the different types of regeneration experiments performed in ascidians in more than a century. Moreover, we present, in an historical perspective, the methodological approaches used to induce regeneration in both solitary and colonial ascidians.

Table 2
Experimental procedures used in the study of regeneration of solitary ascidians

Experimental procedure	Species	Methods	References
Tunic removal	*Ascidia mentula*	In vivo observations	[19]
	Phallusia mammillata	In vivo observations	[20]
	Ciona intestinalis	In vivo observations	[23]
Thorax	*Ciona intestinalis*	In vivo observations	[18]
Siphon (oral/atrial) ablation	*Ciona intestinalis*	In vivo observations	[80]
		Histological analysis	[32, 33]
		EdU labeling for proliferating cells	[32, 80]
		pH 3 labeling for proliferating cells	[80]
		Inhibition of cell proliferation with colchicine or nocodazole	[32]
		UV irradiation to study the involvement and the origin of stem cells	[80, 81]
		Anti-piwi antibody to label stem cells	[32]
		Alkaline phosphatase histoenzymology to reveal stem cells	[32]
		In vitro cultures of siphon explants	[80, 81]
		Distal, middle, basal, or oblique amputations to study the origin of the orange-pigmented sensory organ progenitor cells	[80]
		Branchial sac transplantation to assess the role of the pharynx as source of stem cells	[32, 80]
		Repeated ablation to study the effects of a possible depletion of stem cells	[80]
		Amputation in young and aged animals to study the effect of aging	[32, 81, 82]
		Treatment of animals in notch inhibitors to study the role of the notch pathway in regeneration	[83]
		Exposure of TGFβ inhibitors to study the involvement of TGFβ-mediated signal transduction in regeneration	[84]
		Use of transgenic animals to study the role of the nervous system in the process	[69]
		RNAseq of regenerating fragments to reveal differentially expressed genes	[83]
	Polycarpa mytiligera	In vivo observations	[13, 31]
		Histological analysis	[31]
	Styela plicata	In vivo observations and histological analysis	[31]
	Microcosmus exasperatus	In vivo observations and histological analysis	[31]
	Herdmania momus	In vivo observations and histological analysis	[31]

(continued)

Table 2
(continued)

Experimental procedure	Species	Methods	References
Neural complex ablation and brain chemical degeneration	*Styela plicata*	Induction of brain degeneration using 3-acetylpyridine and recovery study by means of behavioral experiments, TEM analysis, immunohistochemistry, Western blotting	[70]
	Ciona intestinalis	Histology, monoclonal antibodies, BrdU labeling, colchicine treatment	[67, 68]
		Live imaging and EdU labeling	[33, 80, 82]
		Use of old animals to study the effects of aging	[82]
		Live imaging, Nomarski images, confocal imaging, EdU incubations and staining for GFP, behavioral responses	[69]
Gonad removal	*Ciona intestinalis*	In vivo observation and histological analysis	[66]
Evisceration	*Polycarpa tenera*	In vivo observation and histological analysis	[12]
	Polycarpa mytiligera	In vivo observation and histological analysis	[13]
Dissection of individuals in fragments	*Polycarpa mytiligera*	In vivo observation, histological analysis, EdU labeling for proliferating cells, confocal imaging	[14]

2 Regeneration in Solitary Ascidians

The study of regeneration in solitary ascidians has a long story as it began at the end of the nineteenth and the early beginning of the twentieth century, with the experiments carried out by a series of German scientists working at the Stazione Zoologica, in Naples (Italy), newly founded by Anthon Dohrn [16–18]. With the establishment of a series of new French marine stations at the beginning of the last century, the contributions of the Belgian-French scientists appeared and, rapidly, acquired a predominance that was maintained throughout the first half of the century [19–24]. Then, the American school arose and, quickly, reached the visibility that it still has [25–27].

Solitary ascidians are capable of partial body regeneration (Table 1). In all the studied species, the epidermis can easily regenerate the tunic once the latter is removed [19, 20, 23]. When part of the body is removed, in most cases it can be reformed quite rapidly. *C. intestinalis* has been the reference model for the study of solitary ascidian regeneration for more than a century. In this species, when an animal is bisected, only the basal part can

Table 3
Types of regeneration studies in colonial ascidians

Type of regeneration	Species	Outcome	References
WBR			
Regeneration from colonial vasculature	*Botryllus schlosseri*	Vascular bud development	[5, 48–51]
	Botryllus primigenus	Vascular bud development	[45–47]
	Botrylloides leachii	Vascular bud development	[71, 73, 74, 76, 77]
	Botrylloides violaceus	Vascular bud development	[72]
	Botrylloides diegensis	Vascular bud development	[52]
Regeneration from zooid fragments	*Botryllus schlosseri*	Development of budlets from the remaining tissues	[50, 53, 54]
	Clavelina lepadiformis	Remodeling of remaining tissues and development of new buds	[21, 55]
	Aplidium pellucidum	Remodeling of remaining tissues and development of new buds	[39]
	Perophora viridis	Resorption of mature zooids and development of new buds	[39, 40]
Regeneration from postaddomen and stolon	*Clavelina lepadiformis*	New buds formation	[21]
Regeneration from isolated stolon fragments	*Polyandrocarpa zorritensis*	New buds formation	[56]
	Clavelina lepadiformis	New buds formation	[21, 36–38, 85–89]
	Perophora viridis	New buds formation	[25, 39, 40]
Partial regeneration			
Damaged bud regeneration	*Botryllus schlosseri*	Regeneration of the damaged parts	[27]
	Clavelina lepadiformis	Regeneration of damaged part from esophageal fragments	[21]
	Pycnoclavella neapolitana	Regeneration of damaged parts from the anterior end of the epicardium	[59]
	Polyandrocarpa misakiensis	Regeneration of amputated parts from the atrial epithelium	[60, 61]
Regeneration of the colonial circulatory system			
Colonial circulatory system regeneration	*Botryllus schlosseri*	Regeneration of vessels and ampullae	[62–65, 78]

regenerate the missing one, provided that part of the pharyngeal basket is conserved; conversely, the distal part is unable to regenerate any basal structure. The regeneration includes organs such as the siphons, the neural complex, the gonads and the missing part of the digestive system.

Table 4
Experimental procedures used in the study of regeneration of colonial ascidians

Experimental procedure	Species	Methods	References
WBR			
Isolation of colonial vasculature	*Botryllus schlosseri*	In vivo observations	[5, 48–50]
		Live imaging, microinjection of cells from isogenic colonies, circulation parameters measurements, histology	[5]
		Immunohistochemistry, in situ hybridization, knockdown by siRNA of GATAa	[51]
	Botryllus primigenus	In situ hybridization (Vasa, Nanos, Piwi) Immunohistochemistry (Vasa, Nanos) TEM, Knockdown by siRNA of Piwi and Nanos	[45–47]
	Botrylloides leachii	Live imaging and histology	[71, 74, 77]
		Transcriptome profiling	[73]
		In situ hybridization	[73, 74, 77]
		Serin protease inhibition	[73]
		Immunohistochemistry, Western blot, blood cells collection and Dil staining, RNAi, Citral and DEAB administration, Mitomycin C treatment	[74]
		Chemical inhibition of HDAC activity, measurement of nuclear acetyl-proteins-proliferating cell antigen (PCNA) staining	[77]
	Botrylloides violaceus	Microscopy and live imaging, histology, immunocytochemistry (Piwi, PCNA), Western blot (Piwi)	[72]
	Botrylloides diegensis	Gene expression (qPCR for Vasa, Piwi1, Piwi2, IA6, pou3, Cyclin B, Histone 3,Notch and Wnt pathways components), in situ hybridization (IA6, Pou3, h3), immunohistochemistry (IA6, Pou3, histone h3 phospho S10), isolation via FACS of IA6 positive cells and proliferating cells, limit dilution of sorted cells, injection in mitomycin C treated colonies of sorted cells, tracking of EdU labeled cells, Notch and Wnt signaling inhibition (DAPT and endo-IWR1)	[52]
Isolation of regressing zooids in the colony	*Botryllus schlosseri*	Immunohistochemistry (Vasa, Pl10, IAP28, pH 3), gene expression (qPCR for IAP genes, PI3K/Akt pathway), IAP genes chemical inhibition (GDC-0152 and Birinapant)	[53]
Isolation of bud fragments	*Botryllus schlosseri*	Histology	[54]
	Clavelina lepadiformis	In vivo observation and histological analysis	[55]
	Aplidium pellucidum	In vivo observations	[39]
	Perophora viridis	In vivo observations	[39, 40]

(continued)

Table 4
(continued)

Experimental procedure	Species	Methods	References
Esophagus isolation	*Clavelina lepadiformis*	In vivo observations and histological analysis	[21]
Stolon isolation	*Clavelina lepadiformis*	In vivo observations	[21, 38]
		Histology	[21]
	Perophora viridis	In vivo observations	[25, 39, 40]
		Histology	[25]
	Polyandrocarpa zorritensis	Histology	[56]
Partial regeneration			
Damaging of individuals	*Botryllus schlosseri*	In vivo observations	[27]
	Clavelina lepadiformis	In vivo observations and histological analysis	[21]
	Pycnoclavella neapolitana	In vivo observations	[59]
	Polyandrocarpa misakiensis	X-ray irradiation, histology, immunohistochemistry	[60]
		Inhibition of retinoic acid, detection of the activity of b-gal, knockdown by siRNA of retinoic acid receptors, in situ hybridization	[61]
Regeneration of the colonial circulatory system			
Removal of tunic, vessels, and ampullae	*Botryllus schlosseri*	In vivo observations	[62–65, 78]
		Histology	[65]
		Immunohistochemistry	[63, 65, 78]
		TEM	[62, 65]
		Knockdown by siRNA	[62]
		In situ hybridization and qPCR	[62, 63]

The regeneration of the *Ciona* siphons attracted the attention of many researchers for the simplicity of the technique required: a scalpel and some anesthetic [28–30]. A full regeneration of the siphons has also been described in *P. mytiligera*, *Styela plicata* and *Herdmania momus*, whereas, *Microcosmus exasperatus* show a scrubby siphon reconstitution, suggesting an unequal distribution of the regenerative abilities among solitary species [31].

Jeffery and collaborators [32, 33] reinvestigated in detail the regeneration of the oral siphon in *C. intestinalis* (formerly called *Ciona intestinalis* type B) [34]. They demonstrated that both short-distance and long-distance processes are involved in oral siphon regeneration, the former based on the presence, in the

remaining siphon stump, of a local pool of progenitor cells, the latter relying on the migration of progenitor cells from niches in the pharynx. Short-distance recruitment of progenitor cells is mainly involved in the formation of the orange-pigmented sensory organs (Fig. 3b, f) and is much more influenced by the depletion of the progenitor cell reservoir through repeated ablations [32]. When the siphon is amputated at its base, only long-distance recruitment of progenitor cells occurs [32].

A spectacular example of regeneration regards the two congeneric species *P. mytiligera* and *P. tenera* that can eject their viscera when subjected to stress conditions and rebuild them in less than 3 weeks [13]. Moreover, individuals of *P. mytiligera* can be separated in fragments by cutting along the longitudinal or transverse body axes. Each fragment then is able to regenerate completely the missing organs forming independent functional individuals [14].

As stated above, the methods used for studying regeneration in solitary ascidians were, in the past, quite simple: a scalpel or a razor blade to cut the animals or ablate the siphon(s), a dissection microscope to observe the anesthetized animals after the operation, eventually equipped with a camera lucida apparatus to record the regenerating steps in the recovering specimens (see the following "methodological approaches" section for a detailed historical overview on the methods used to induce regeneration). Today, the experimental procedure is not greatly different. The only relevant change is the introduction of in vivo imaging, which renders reporting much easier, and of electron microscopy analysis that allows detailed observations of the events at cellular levels. In addition, it must be stressed that, today, research on regeneration can exploit the abundance of biochemical and biomolecular toolkits offering the possibility to study in detail the events occurring during recovery. Table 2 reports the various approaches used for the study of regeneration and the attempt to elucidate the cells, genes, signaling pathways involved in the process.

3 Regeneration in Colonial Ascidians

The first studies on regeneration in colonial ascidians are those of Giard [35] in the second half of the nineteenth century, cited by [36]. Driesh [36], using *Clavelina lepadiformis*, observed that, dividing the animals in two, each fragment was able to regenerate the missing parts. *C. lepadiformis* was also used as a model organism for regeneration studies by Della Valle [37, 38]. In 1921, Huxley was one of the first authors to study regeneration in *Perophora viridis*, by recording the regenerative process after splitting the zooids in two [39]. The same author also investigated the regenerative capability of *Aplidium pellucidum* by isolating small colonial fragments. More detailed studies were carried out on the

regeneration processes of *P. viridis* by Deviney, in 1934 [25], and by Goldin, in 1948 [40].

In the second half of the twentieth century, new model organisms, such as *B. schlosseri* and *Botrylloides leachii*, became the main protagonists of regeneration studies in colonial ascidians. Even today these two organisms are widely used for regeneration studies. Over the years, studies have focused on three aspects (Table 3):

1. WBR
2. Partial regeneration
3. Circulatory system regeneration

3.1 WBR

WBR was studied in *B. schlosseri*, *B. leachii*, *Botrylloides violaceus* and *Botrylloides diegensis* following the surgical removal of all zooids and buds from a colony (Fig. 3g–j) or isolating small fragments of the colonial vasculature. This type of regeneration closely resembles vascular budding, a spontaneous formation of new buds from the vessels of the vascular system, first described in botryllid ascidians more than 200 years ago [41] and observed and described again by Giard [35], Bancroft [42], and Herdman [43]. This type of budding is constitutive in *Botryllus primigenus* [44], but it can also be induced through the isolation of small vascular fragments containing part of the colonial circulatory system [45–47]. In WBR, a bud, that eventually reconstitutes the whole colony, develops in the colonial vasculature from the aggregation of hemoblasts [5, 48–52]. Recently, Rosner and collaborators observed and studied an additional form of WBR in *B. schlosseri*, termed "budectomy induced WBR." When, in a colony at takeover (the phase in which the adult zooids are being resorbed and replaced by their primary buds), all the buds are surgically removed leaving only old zooids undergoing resorption, new budlets can develop from the latter [53]. In this view, even the experiments performed on *B. schlosseri* colonies by Majone in 1977 can be considered as WBR [54]. In this case, new budlets develop from anterior bud fragments connected to the colonial vasculature. These new budlets eventually grow further to actively filter-feeding adults [54].

In species in which zooids are connected by stolons, such as *Polyandrocarpa zorritensis*, *C. lepadiformis* and *P. viridis*, WBR has been induced through the isolation of part of the stolon from the rest of the colony [21, 25, 37–39, 55, 56]. The success and timing of regeneration depend on the dimension of isolated stolon fragments [25, 38, 40]. Full recovery can require a period of time ranging from a few days, as in *P. zorritensis* [56], to several weeks, as in the case of small pieces of stolon of *C. lepadiformis* [37]. In *A. pellucidum* and *P. viridis*, Huxley [39] isolated small fragments of colonies or even of zooids, and observed what he called the "dedifferentiation" of the latter to undifferentiated structures from which new buds eventually

developed [39]. These processes were further studied by Deviney in 1934 [25] and Goldin in 1948 [40].

In *B. schlosseri,* it is also possible to observe the regeneration of bud residuals. When, in a colony, a single adult individual is left and its primary and secondary buds are removed, bud residuals can reverse the degeneration process and start regeneration. This phenomenon, described for the first time by Sabbadin in 1956 [57, 58], probably occurs for the absence of competition among buds, allowing the residuals to rescue development. In this case, a constitutive degeneration of budlets is reversed in a regenerative process induced by the new colony condition. This is an example in which it is difficult to mark the border between asexual reproduction and typical regeneration, and it stresses the high homeostatic capacity of colonial organisms to survive adverse conditions.

3.2 Partial Body Regeneration

Partial body regeneration can also be observed in colonial species. In *B. schlosseri* [27], *C. lepadiformis* [21], *Pycnoclavella neapolitana* [59] and *P. misakiensis* [60, 61], the regeneration of the missing parts of amputated buds have been studied (Table 3). In these cases, no regression and development of new budlets are observed.

3.3 Tunic and Colonial Circulatory System Regeneration

Colonial ascidians have also been studied for the ability to regenerate their tunic and the colonial circulatory system. In *B. schlosseri*, the full regeneration of the tunic and circulatory system occur in few hours when the peripheral matrix (i.e., the tunic and the enclosed portion of vasculature) is removed [62, 63] or days, when also marginal and radial vessels are ablated from the colony (Fig. 1k, l) [64, 65].

As in solitary species, in more than a century of studies the surgical procedures employed to induce whole body or partial regeneration in colonial ascidians are roughly unchanged. However, the development of imaging and molecular tools allowed, in the last decades, the detailed study of the kinetics of regeneration, and the investigation of the molecular pathways involved in many aspects of WBR, as stem cells maintenance and differentiation (Table 4).

4 Methodological Approaches to Induce Regeneration: An Historical Overview

4.1 Solitary Ascidians

The first reports on induction of regeneration in solitary ascidians comes from Loeb (1892, cited in [36]), who observed siphon regeneration in *Ciona*, and Schultze [16], who documented siphon and brain regeneration and studied the process both in vivo and at the histological level. Almost 15 years later, Hirschler [18] cut individuals of *Ciona* transversely and obliquely through the thorax and utilized camera lucida drawings to record the regeneration process. Unfortunately, we do not have any information on the

methodological approach used by these authors to induce regeneration. In 1930, Wermel published some methodological notes to study the regeneration of the oral siphon: he anesthetized animals of 4–7 cm in length (with MS222 or 10% chloral hydrate) and used fine dissection scissors to cut tissues [28].

Similar approaches for inducing regeneration were followed by later authors up to the more recently published reports, with some minor differences, such as the use of a scalpel to perform the ablations after the anesthetizing step [31].

Consecutive amputations of the oral siphon were used to study the recruitment of progenitor cells required for regeneration in *Ciona* [32].

In 1915, Sélys-Longchamps described the evisceration in individuals of *Polycarpa tenera* kept in aquaria [12], also induced in the congeneric species *P. mytiligera* by Shenkar and Gordon [13], whereas Bourchard-Mandrelle [66] observed gonad regeneration in *Ciona* after their removal through a small hole in the body wall.

In 1992, Bollner and collaborators [67] set up the methodological approach for inducing brain regeneration in *Ciona*, used also in subsequent works [68]: after anesthesia with MS222 (0.02%) they first cut the epidermis and the nerves anterior to the neural complex to expose the anterior neural gland (ciliated funnel), and then proceeded through the epidermis toward the posterior part of the neural complex that was finally separated from the pharyngeal basket and the posterior nerves.

Dahlberg et al. [69] obtained better results than traditional microdissection in the induction of brain regeneration in *Ciona* by anesthetizing animals in MS222 (0.4 g/L) or propylene phenoxetol (0.06%) in seawater for 15–30 min before ablation, dissection or live imaging. For the ablation, they used fine forceps and biopsy punch tools (2 and 3 mm diameter). Animals were placed in silicone-coated Petri dishes and the entire cerebral ganglion was removed (with the associated neural gland, its ciliated funnel and the dorsal tubercle), in a single action to minimize the trauma. A different method to produce a brain lesion and induce its regeneration in *S. plicata* was described in 2015 by Medina and collaborators [70]: it consisted on the systematic injection in the pharyngeal region of the neurotoxin 3-acetylpyridine (3-AP; 65 mg/kg body weight), diluted in sterilized artificial seawater. This compound is a niacinamide antagonist that inhibits ATP synthesis, resulting lethal to the high metabolic rate of neurons. At selected time points following injection, they anesthetized, killed, and dissected the animals to collect their brains, which were then processed for their analysis.

Some general methodological approaches to induce regeneration in solitary ascidian can be summarized as follow:

1. Anesthetization of specimens, leave the animals in:
   (a) MS222 (e.g., 0.4 g/L in [69]) or
   (b) 10% (w/v) chloral hydrate [28] or
   (c) 0.06% (v/v) propylene phenoxetol [69] or
   (d) menthol crystals (e.g., 0.4% (w/v) in [31]).
2. Removal of body parts:
   (a) For amputations (siphons, thorax, etc.)
      - Dissection scissors and/or [28].
      - Scalpels (see for example [31]).
      - Forceps and biopsy punch tools (2 and 3 mm diameter) [69].
      - Dissection on petri dishes (e.g., Sylgard®-coated) [69].
   (b) For chemical induction of brain degeneration.
      - Injection, in the pharyngeal region, of 3-acetylpyridine (3-AP; 65 mg/kg body weight) diluted in sterilized artificial seawater [70].
   (c) For evisceration.
      - Specimens kept alive in aquaria [12].
      - Gently squeezing [13].

4.2 Colonial Ascidians

Up to the half of the nineteenth century, publications reporting experiments on colonial ascidians did not provide details on the methodological approaches used to induce regeneration. Publications simply report that individuals or stolons were cut and observed in vivo. Sometimes, regenerating fragments could be labeled with vital stains such as neural red, whereas fixed specimens were labeled with carminium for whole mount analysis [21]. Below, we report the available information on the three main kinds of regeneration in colonial ascidians.

One of the first studies on partial regeneration in *B. schlosseri* was that of Sabbadin, in 1956 [57]. In his study, he removed all the budlets (budectomy) of a colony except one with thin tungsten needles and razor blades under a dissecting microscope. The only remaining budlet was then removed when, after 72 h, it became a bud. The atrophied buds which are normally resorbed restarted their development and, eventually, became adults. Since 1956, numerous studies used *B. schlosseri* as a model organism to study WBR in colonial ascidians. In 1975, Sabbadin and Zaniolo [50] removed all the zooids and buds from colonies, with needles and razor blades under a dissecting microscope, leaving only the peripheral colonial matrix, that is, the tunic and its vasculature. They observed that, in a few days, a vascular bud developed from aggregation of blood cells and generated a new zooid. The same method

was used by Rinkevich and collaborators [71] in *B. leachii,* Brown and collaborators [72] in *B. violaceus*, and Sunanaga and collaborators [45–47] in *B. primigenus*. Over the past 20 years, studies on regeneration using *B. schlosseri* and *B. leachii* have been implemented using molecular and biochemical techniques, studying in detail the involvement and function of some genes in regenerative processes of this two colonial ascidian [5, 53, 73–77].

Studies on partial regeneration in *B. schlosseri* were performed by Watkins [27], who damaged, with sharpened steel needles, the colonial buds and observed that about half of them regenerated the damaged part and reached maturity. The same method was used by Kaneko and collaborators [61] to induce partial regeneration in *P. misakiensis*.

Up to now, the regeneration of the vascular system was studied only in *B. schlosseri*. Zaniolo and Trentin [64] removed the entire colonial matrix (tunic, vessels and ampullae) around some zooids using a tungsten needle under a dissection microscope and observed the full regeneration of the peripheral vessels and tunic in 5 days. The same method was used in later studies [62, 63, 65, 78].

A general methodological approach to induce regeneration in colonial ascidian can be summarized as follow:

1. Collect swimming larvae and induce their metamorphosis by osmotic shock (30 s in diluted seawater 1% (w/v) of salinity) and let them to adhere on glass slide where they can grow [79].
2. Maintain animals in aerated aquaria filled with filtered seawater (FSW) at a 14:10 h light–dark regimen under constant (18–20 °C) temperature. Daily, feed them with unicellular algae (e.g., *Tetraselmis chuii*) and change water.
3. Keep colony-containing slides vertically, using plastic racks and clean them with a brush at each change of water.
4. Perform operations using thin tungsten needles and razor blades under a dissection microscope.
5. After surgery, keep the colonies in FSW in aerated aquaria as previously described.

For WBR

1. Remove all the zooids, buds, and budlets from the colony, leaving only the colonial matrix [50].

For partial body regeneration

1. Remove the parts of interest of the animal from the colonies [27, 61].

For circulatory system regeneration

1. Remove the colonial matrix after cutting the radial vessels and the test all around the zooids [64].

5 Concluding Remarks

As evidenced by the studies reported here, tunicates exhibit remarkable regenerative abilities, which have been studied from many points of view in over a century of researches. Besides their easy rearing and maintenance under laboratory conditions, the methods to induce regeneration are relatively simple and require few and cheap tools. Moreover, among chordates, only tunicates regenerate complete adult individuals from small tissue fragments. Despite these important characteristics, many molecular tools are still missing for this group of organisms. Transgenesis is one example: this technique would allow the in vivo study of gene expression during regeneration phases. However, it is still not developed especially for colonial ascidians and many solitary species as well. Today, the improvement of imaging techniques, and the broad application of some molecular biology tools, like RNA sequencing, can speed up the advancement of knowledge in the regenerative biology of ascidians. The studies summarized here will serve as a reference and a starting point for future researches aimed to uncover the biological basic properties of the astonishing regeneration in these chordates.

Acknowledgments

The authors wish to thank the COST Action MARISTEM 16203 community for supporting short term scientific missions and useful discussions.

References

1. Jeffery WR (2018) Regeneration and aging in the tunicate *Ciona intestinalis*. In: Conn's handbook of models for human aging, second Edi. Elsevier Inc., Amsterdam, pp 521–531
2. Manni L, Anselmi C, Cima F, Gasparini F, Voskoboynik A, Martini M, Peronato A, Burighel P, Zaniolo G, Ballarin L (2019) Sixty years of experimental studies on the blastogenesis of the colonial tunicate *Botryllus schlosseri*. Dev Biol 448:293–308. https://doi.org/10.1016/j.ydbio.2018.09.009
3. Carnevali MDC, Burighel P (2010) Regeneration in echinoderms and ascidians. In: Encyclopedia of life sciences. John Wiley & Sons, Ltd, Chichester
4. Tiozzo S, Brown FD, De Tomaso AW (2008) Regeneration and stem cells in ascidians. In: Stem Cells: From Hydra to Man. Springer, Dordrecht, pp 95–112
5. Voskoboynik A, Simon-Blecher N, Soen Y, Rinkevich B, De Tomaso AW, Ishizuka KJ, Weissman IL (2007) Striving for normality: whole body regeneration through a series of abnormal generations. FASEB J 21: 1335–1344. https://doi.org/10.1096/fj.06-7337com
6. Delsuc F, Brinkmann H, Chourrout D, Philippe H (2006) Tunicates and not cephalochordates are the closest living relatives of vertebrates. Nature 439:965–968. https://doi.org/10.1038/nature04336
7. Delsuc F, Philippe H, Tsagkogeorga G, Simion P, Tilak M, Turon X, López-legentil S, Piette J, Lemaire P, Douzery EJP (2018) A phylogenomic framework and timescale for comparative studies of tunicates. BMC Biol 16(1):39
8. Alvarado AS, Tsonis PA (2006) Bridging the regeneration gap: genetic insights from diverse

animal models. Nat Rev Genet 7:873–884. https://doi.org/10.1038/nrg1923
9. Seifert AW, Muneoka K (2018) The blastema and epimorphic regeneration in mammals. Dev Biol 433:190–199. https://doi.org/10.1016/j.ydbio.2017.08.007
10. Alié A, Hiebert LS, Scelzo M, Tiozzo S (2020) The eventful history of nonembryonic development in tunicates. J Exp Zool Part B Mol Dev Evol 336(3):250–266. https://doi.org/10.1002/jez.b.22940
11. Burighel P, Cloney RA (1997) Urochordata: Ascidiacea. Microsc Anat Invertebr Vol 15 Hemichordata. Chaetognatha, Invertebr chordates 15:221–347
12. Selys-Longchamps M (1915) Autotomie et régénération des viscères chez *Polycarpa tenera* Lacaze et Delage. C R Acad Sci Paris 160: 566–569
13. Shenkar N, Gordon T (2015) Gut-spilling in chordates: evisceration in the tropical ascidian *Polycarpa mytiligera*. Sci Rep 5:9614. https://doi.org/10.1038/srep09614
14. Gordon T, Upadhyay AK, Manni L, Huchon D, Shenkar N (2021) And then there were three…: extreme regeneration ability of the solitary chordate *Polycarpa mytiligera*. Front Cell Dev Biol 9:652466. https://doi.org/10.3389/fcell.2021.652466
15. Voskoboynik A, Weissman IL (2015) *Botryllus schlosseri*, an emerging model for the study of aging, stem cells, and mechanisms of regeneration. Invertebr Reprod Dev 59:33–38. https://doi.org/10.1080/07924259.2014.944673
16. Schultze LS (1899) Die Regeneration Des Ganglions Von *Ciona intestinalis* L. und. Jena Z f Naturwiss 33:263–344
17. Schultze LS (1900) Die Regeneration des Ganglions von *Ciona intestinalis* L. und über das Verhältnis der Regeneration und Knospung zur Keimblätterlehre. Jena Z Med Naturwiss 33:263–344
18. Hirschler J (1914) Über die Restitutions-und Involutionsvoränge bei operierten Exemplaren von *Ciona intestinalis* Flem. (Teil I) nebst Bemurkungen über den Wert des Negativen für das Potenzproblem. Arch Mikrosk Anat 85:205–227
19. Fol A (1908) Note sur la régénération de la tunique chez les Tuniciers. Bull Soc Zool Fr 33:79–81
20. Azéma M (1927) Sur le role des prolongements vasculaires au cours de la régénération de la tunique chez *Ascidiella aspersa*. Bull Soc Zool Fr 52:549–557
21. Brien P (1930) Régénération naturelle et expérimentale chez les Clavelinidae. Ann la Société R Zool Belgique 61:20–112
22. Brien P (1932) L'heteromorphose chez les Tuniciers. La regeneration bithoracique et monothoracique des fragments oesophagiens de *Clavelina lepadiformis* (Muller). Bull la Cl des Sci Académie R Belgique 18:975–1005
23. Peres JM (1948) Recherches sur la genese et la regeneration de la tunique chez *Ciona intestinalis* L. Bull Inst Oceanogr Monaco 145:1–12
24. Wagers AJ, Christensen JL, Weissman IL (2002) Cell fate determination from stem cells. Gene Ther 9:606
25. Deviney EM (1934) The behavior of isolated pieces of ascidian (*Perophora viridis*) stolon as compared with ordinary budding. J Elisha Mitchell Sci Soc 49:185–224
26. Berrill NJ (1951) Regeneration and budding in tunicates. Biol Rev 26:456–475. https://doi.org/10.1111/j.1469-185X.1951.tb01207.x
27. Mj W (1958) Regeneration of buds in *Botryllus*. Biol Bull 115:147–152. https://doi.org/10.2307/1539101
28. Wermel J (1930) Über den Einfluss der Regeneration und Überernährung auf die Siphonenlänge bei *Ciona Intestinalis* L. - Ein Beitrag zu Kammerers Experimenten. Wilhelm Roux Arch Entwickl Mech Org 122:22–47. https://doi.org/10.1007/BF00576964
29. Whittaker JR (1975) Siphon regeneration in *Ciona*. Nature 255:224–225. https://doi.org/10.1038/255224a0
30. Sutton MF (1953) The regeneration of the siphon of *Ciona intestinalis*. J Mar Biol Ass UK 32:249–268
31. Gordon T, Manni L, Shenkar N (2019) Regeneration ability in four stolidobranch ascidians: ecological and evolutionary implications. J Exp Mar Bio Ecol 519:151184. https://doi.org/10.1016/j.jembe.2019.151184
32. Jeffery WR (2015) Distal regeneration involves the age dependent activity of branchial sac stem cells in the ascidian *Ciona intestinalis*. Regeneration 2:1–18. https://doi.org/10.1002/reg2.26
33. Jeffery WR (2015) Closing the wounds: one hundred and twenty-five years of regenerative biology in the ascidian *Ciona intestinalis*. Genesis 53:48–65. https://doi.org/10.1002/dvg.22799
34. Brunetti R, Gissi C, Pennati R, Caicci F, Gasparini F, Manni L (2015) Morphological evidence that the molecularly determined *Ciona intestinalis* type a and type B are different species: *Ciona robusta* and *Ciona*

intestinalis. J Zool Syst Evol Res 53:186–193. https://doi.org/10.1111/jzs.12101

35. Giard A (1872) Recherches sur les Ascidies composées. Arch zool exp 1:566 ff
36. Driesch H (1902) Über ein neues harmonisch-äquipotentielles System und über solche Systeme überhaupt. Arch Entwickleungsmechanik der Org 14:227–246. https://doi.org/10.1007/BF02162038
37. Della Valle P (1914) Studii sui rapporti fra differenziazione e rigenerazione - 3. Lo sviluppo di segmenti isolati di stolone di *Clavelina* di lunghezza diversa e di calibro eguale. Boll della Soc di Nat Napoli 27:195–237
38. Della Valle P (1915) Studii sui rapporti fra differenziazione e rigenerazione - 4. Le restituzioni dei cespugli di ramificazioni stoloniali di *Clavelina*. Boll della Soc dei Nat Napoli 28: 49–82
39. Huxley JS (1921) Studies in dedifferentiation. II. Dedifferentiation and resorption in *Perophora*. J Cell Sci 65(260):643–697
40. Goldin A (1948) Regeneration in *Perophora viridis*. Biol Bull 94:184–193. https://doi.org/10.2307/1538246
41. Savigny JC (1816) Recherches anatomiques sur les ascidies composées et sur les ascidies simples - Système de la classe des Ascidies. In: Mémoires sur les Animaux sans Vertèbres, vol 2. G. Dufour, Paris, pp 1–229
42. Bancroft FW (1903) Aestivation of *Botrylloides gascoi* Della Valle. Mark Anniv, vol 147–166. H. Holt, New York
43. Herdman EC (1925) Botryllus. Trans Liverp Biol Soc Proc 39:201–236
44. Oka H, Watanabe H (1957) Vascular budding, a new type of budding in *Botryllus*. Biol Bull 112:225–240. https://doi.org/10.2307/1539200
45. Sunanaga T, Saito Y, Kawamura K (2006) Post-embryonic epigenesis of vasa-positive germ cells from aggregated hemoblasts in the colonial ascidian, *Botryllus primigenus*. Develop Growth Differ 48:87–100. https://doi.org/10.1111/j.1440-169X.2006.00849.x
46. Sunanaga T, Satoh M, Kawamura K (2008) The role of Nanos homologue in gametogenesis and blastogenesis with special reference to male germ cell formation in the colonial ascidian, *Botryllus primigenus*. Dev Biol 324:31–40. https://doi.org/10.1016/j.ydbio.2008.08.023
47. Sunanaga T, Inubushi H, Kawamura K (2010) Piwi -expressing hemoblasts serve as germline stem cells during postembryonic germ cell specification in colonial ascidian, Botryllus primigenus. Dev Growth Differ 52:603–614. https://doi.org/10.1111/j.1440-169X.2010.01196.x
48. Milkman R, Byrne S (1961) Recent observations on Botryllus schlosseri. Biol Bull 121:376
49. Milkman R (1967) Genetic and developmental studies on *Botryllus schlosseri*. Biol Bull 132: 229–243. https://doi.org/10.2307/1539891
50. Sabbadin A, Zaniolo G, Majone F (1975) Determination of polarity and bilateral asymmetry in palleal and vascular buds of the ascidian *Botryllus schlosseri*. Dev Biol 46:79–87. https://doi.org/10.1016/0012-1606(75)90088-3
51. Ricci L, Cabrera F, Lotito S, Tiozzo S (2016) Redeployment of germ layers related TFs shows regionalized expression during two non-embryonic developments. Dev Biol 416: 235–248. https://doi.org/10.1016/j.ydbio.2016.05.016
52. Kassmer SH, Langenbacher AD, De Tomaso AW (2020) Integrin-alpha-6+ candidate stem cells are responsible for whole body regeneration in the invertebrate chordate *Botrylloides diegensis*. Nat Commun 11:4435. https://doi.org/10.1038/s41467-020-18288-w
53. Rosner A, Kravchenko O, Rinkevich B (2019) IAP genes partake weighty roles in the astogeny and whole body regeneration in the colonial urochordate *Botryllus schlosseri*. Dev Biol 448:320–341. https://doi.org/10.1016/j.ydbio.2018.10.015
54. Majone F (1977) Regeneration of isolated bud fragments of *Botryllus schlosseri*. Acta Embryol Exp (Palermo):11–19
55. Ries E (1937) Untersuchungen Über den Zelltod II - Das Verhalten differenzierter und undifferenzierter Zellen bei der Regeneration, Reduktion und Knospung von *Clavelina lepadiformis*. Wilhelm Roux Arch Entwickl Mech Org 137:327–362. https://doi.org/10.1007/BF00593065
56. Scelzo M, Alié A, Pagnotta S, Lejeune C, Henry P, Gilletta L, Hiebert LS, Mastrototaro F, Tiozzo S (2019) Novel budding mode in *Polyandrocarpa zorritensis*: a model for comparative studies on asexual development and whole body regeneration. EvoDevo 10:7. https://doi.org/10.1186/s13227-019-0121-x
57. Sabbadin A (1956) Effetti dell'estirpazione delle gemme sulla durata del ciclo vitale in *Botryllus schlosseri* (pallas). Bolletino di Zool 23:331–342. https://doi.org/10.1080/11250005609439244
58. Sabbadin A (1958) Analisi sperimentale dello sviluppo delle colonie di *Botryllus schlosseri*

(Pallas) [Ascidiacea]. Arch Ital Anat Embriol 58:177–221

59. Brien P (1933) Regeneration thoracique chez *Archiascidia neapolitana* (Julin) Structure du Système nerveux central. Bull Biol Fr Belg 67: 100–124
60. Kawamura K, Hashimoto K, Nakauchi M (1995) Development of irradiated tunicate buds: is cell division cycle required for morphallaxis? Develop Growth Differ 37: 487–496. https://doi.org/10.1046/j.1440-169X.1995.t01-4-00003.x
61. Kaneko N, Katsuyama Y, Kawamura K, Fujiwara S (2010) Regeneration of the gut requires retinoic acid in the budding ascidian *Polyandrocarpa misakiensis*. Develop Growth Differ 52: 457–468. https://doi.org/10.1111/j.1440-169X.2010.01184.x
62. Tiozzo S, Voskoboynik A, Brown FD, De Tomaso AW (2008) A conserved role of the VEGF pathway in angiogenesis of an ectodermally-derived vasculature. Dev Biol 315:243–255. https://doi.org/10.1016/j.ydbio.2007.12.035
63. Braden BP, Taketa DA, Pierce JD, Kassmer S, Lewis DD, De Tomaso AW (2014) Vascular regeneration in a basal chordate is due to the presence of immobile, bi-functional cells. PLoS One 9:e95460. https://doi.org/10.1371/journal.pone.0095460
64. Zaniolo G, Trentin P (1987) Regeneration of the tunic in the colonial ascidian, *Botryllus schlosseri*. Acta Embryol Morphol Exper 8: 173–180
65. Gasparini F, Burighel P, Manni L, Zaniolo G (2008) Vascular regeneration and angiogenic-like sprouting mechanism in a compound ascidian is similar to vertebrates. Evol Dev 10: 591–605. https://doi.org/10.1111/j.1525-142X.2008.00274.x
66. Bourchard-Madrelle C (1966) Régéneration de l'ovaire chez une ascidie simple *Ciona intestinalis* L. (Protochordé). Bull Soc Zool Fr 91: 107–114
67. Bollner T, Beesley PW, Thorndyke MC (1992) Pattern of substance P- and cholecystokinin-like immunoreactivity during regeneration of the neural complex in the ascidian *Ciona intestinalis*. J Comp Neurol 325:572–580
68. Bollner T, Howalt S, Thorndyke MC, Beesley PW (1995) Regeneration and post-metamorphic development of the central nervous system in the protochordate *Ciona intestinalis*: a study with monoclonal antibodies. Cell Tissue Res 279:421–432. https://doi.org/10.1007/BF00318500
69. Dahlberg C, Auger H, Dupont S, Sasakura Y, Thorndyke M, Joly JS (2009) Refining the *Ciona intestinalis* model of central nervous system regeneration. PLoS One 4:e4458. https://doi.org/10.1371/journal.pone.0004458
70. Medina BNSP, Santos de Abreu I, Cavalcante LA, Silva WAB, da Fonseca RN, Allodi S, de Barros CM (2015) 3-acetylpyridine-induced degeneration in the adult ascidian neural complex: reactive and regenerative changes in glia and blood cells. Dev Neurobiol 75:877–893. https://doi.org/10.1002/dneu.22255
71. Rinkevich B, Shlemberg Z, Fishelson L (1995) Whole-body protochordate regeneration from totipotent blood cells. Proc Natl Acad Sci U S A 92:7695–7699. https://doi.org/10.1073/pnas.92.17.7695
72. Brown FD, Keeling EL, Le AD, Swalla BJ (2009) Whole body regeneration in a colonial ascidian, *Botrylloides violaceus*. J Exp Zool Part B Mol Dev Evol 312:885–900. https://doi.org/10.1002/jez.b.21303
73. Rinkevich Y, Paz G, Rinkevich B, Reshef R (2007) Systemic bud induction and retinoic acid signaling underlie whole body regeneration in the urochordate *Botrylloides leachi*. PLoS Biol 5:e71. https://doi.org/10.1371/journal.pbio.0050071
74. Rinkevich Y, Rosner A, Rabinowitz C, Lapidot Z, Moiseeva E, Rinkevich B (2010) Piwi positive cells that line the vasculature epithelium, underlie whole body regeneration in a basal chordate. Dev Biol 345:94–104. https://doi.org/10.1016/j.ydbio.2010.05.500
75. Ricci L, Chaurasia A, Lapébie P, Dru P, Helm RR, Copley RR, Tiozzo S (2016) Identification of differentially expressed genes from multipotent epithelia at the onset of an asexual development. Sci Rep 6:1–10. https://doi.org/10.1038/srep27357
76. Zondag LE, Rutherford K, Gemmell NJ, Wilson MJ (2016) Uncovering the pathways underlying whole body regeneration in a chordate model, *Botrylloides leachi* using de novo transcriptome analysis. BMC Genomics 17: 114. https://doi.org/10.1186/s12864-016-2435-6
77. Zondag L, Clarke RM, Wilson MJ (2019) Histone deacetylase activity is required for Botrylloides leachii whole-body regeneration. J Exp Biol 222:jeb203620. https://doi.org/10.1242/jeb.203620
78. Gasparini F, Caicci F, Rigon F, Zaniolo G, Manni L (2014) Testing an unusual in vivo vessel network model: a method to study angiogenesis in the colonial tunicate *Botryllus*

schlosseri. Sci Rep 4:1–11. https://doi.org/10.1038/srep06460

79. Rinkevich B, Weissman IL (1987) The fate of Botryllus (Ascidiacea) larvae co-settled with parental colonies: beneficial or deleterious consequences? Biol Bull 173:474–488
80. Auger H, Sasakura Y, Joly J-S, Jeffery WR (2010) Regeneration of oral siphon pigment organs in the ascidian *Ciona intestinalis*. Dev Biol 339:374–389. https://doi.org/10.1016/j.ydbio.2009.12.040
81. Jeffery WR (2015) Regeneration, stem cells, and aging in the tunicate Ciona: Insights from the Oral Siphon. Int Rev Cell Mol Biol 319:255–282
82. Jeffery WR (2015) The tunicate *Ciona*: a model system for understanding the relationship between regeneration and aging. Invertebr Reprod Dev 59:17–22. https://doi.org/10.1080/07924259.2014.925515
83. Hamada M, Goricki S, Byerly MS, Satoh N, Jeffery WR (2015) Evolution of the chordate regeneration blastema: differential gene expression and conserved role of notch signaling during siphon regeneration in the ascidian *Ciona*. Dev Biol 405:304–315. https://doi.org/10.1016/j.ydbio.2015.07.017
84. Spina EJ, Guzman E, Zhou H, Kosik KS, Smith WC (2017) A microRNA-mRNA expression network during oral siphon regeneration in *Ciona*. Development 144:1787–1797. https://doi.org/10.1242/dev.144097
85. Driesch H (1905) Skizzen zur Restitutionslehre. Arch Entwicklungsmechanik der Org 20:21–29. https://doi.org/10.1007/BF02162639
86. Driesch H (1902) Studien über das Regulationsvermögen der Organismen. Arch Entwicklungsmechanik der Org 14:532–538. https://doi.org/10.1007/bf02188502
87. Schultz E (1907) Über Reductionen - III. Die Reduction und Regeneration des abgeschnittenen Kiemenkorbes von *Clavellina lepadiformis*. Arch Entwicklungsmechanik der Org 24:503–523. https://doi.org/10.1007/BF02289889
88. Spek J (1927) Über die Winterknospenentwicklung, Regeneration und Reduktion bei *Clavellina lepadiformis* und die Bedeutung besonderer "omnipotenter" Zellelemente für diese Vorgänge. Wilhelm Roux'Archiv Entwicklungsmechanik der Org 111(119):172
89. Fischer I (1937) Über das Verhalten des stolonialen Gewebes der Ascidie *Clavelina lepadiformis* in vitro. Wilhelm Roux Arch Entwickl Mech Org 137:383–403. https://doi.org/10.1007/BF00593068

Open Access This chapter is licensed under the terms of the Creative Commons Attribution 4.0 International License (http://creativecommons.org/licenses/by/4.0/), which permits use, sharing, adaptation, distribution and reproduction in any medium or format, as long as you give appropriate credit to the original author(s) and the source, provide a link to the Creative Commons license and indicate if changes were made.

The images or other third party material in this chapter are included in the chapter's Creative Commons license, unless indicated otherwise in a credit line to the material. If material is not included in the chapter's Creative Commons license and your intended use is not permitted by statutory regulation or exceeds the permitted use, you will need to obtain permission directly from the copyright holder.



Part II

Zoological Approaches



Chapter 3

Studying Protista WBR and Repair Using *Physarum polycephalum*

Megan M. Sperry, Nirosha J. Murugan, and Michael Levin

Abstract

Physarum polycephalum is a protist slime mould that exhibits a high degree of responsiveness to its environment through a complex network of tubes and cytoskeletal components that coordinate behavior across its unicellular, multinucleated body. *Physarum* has been used to study decision making, problem solving, and mechanosensation in aneural biological systems. The robust generative and repair capacities of *Physarum* also enable the study of whole-body regeneration within a relatively simple model system. Here we describe methods for growing, imaging, quantifying, and sampling *Physarum* that are adapted for investigating regeneration and repair.

Key words Slime mould, Networks, Signaling, Extract, Regeneration, Injury

1 Introduction

The protist slime mould *Physarum polycephalum* (which we will refer to as *Physarum*) exhibits generative capacities that permit the study of the basis of regeneration without the complexities of multi-cellular model systems. Although the multinucleated single-celled slime mould lacks a fixed shape and nervous system, *Physarum* relays signals throughout its body using a network of branching cytoskeletal tubes that expand and contract to distribute biochemicals (Fig. 1) [1]. That intracellular communication method, known as shuttle streaming, acts as an intrinsic cellular oscillator that drives synchronization across the cell and allows for collective behavior of the organism (Table 1) [1]. The coordination of activities over short and long distances gives rise to more complex mechanosensing, problem solving, and decision-making capabilities that optimize the slime mould's ability to find food and avoid danger [2–6]. The coordinated oscillations also seem necessary for regeneration and repair capacities [7], however, the prior use of *Physarum* to study regeneration is limited.

Simon Blanchoud and Brigitte Galliot (eds.), *Whole-Body Regeneration: Methods and Protocols*,
Methods in Molecular Biology, vol. 2450, https://doi.org/10.1007/978-1-0716-2172-1_3, © The Author(s) 2022

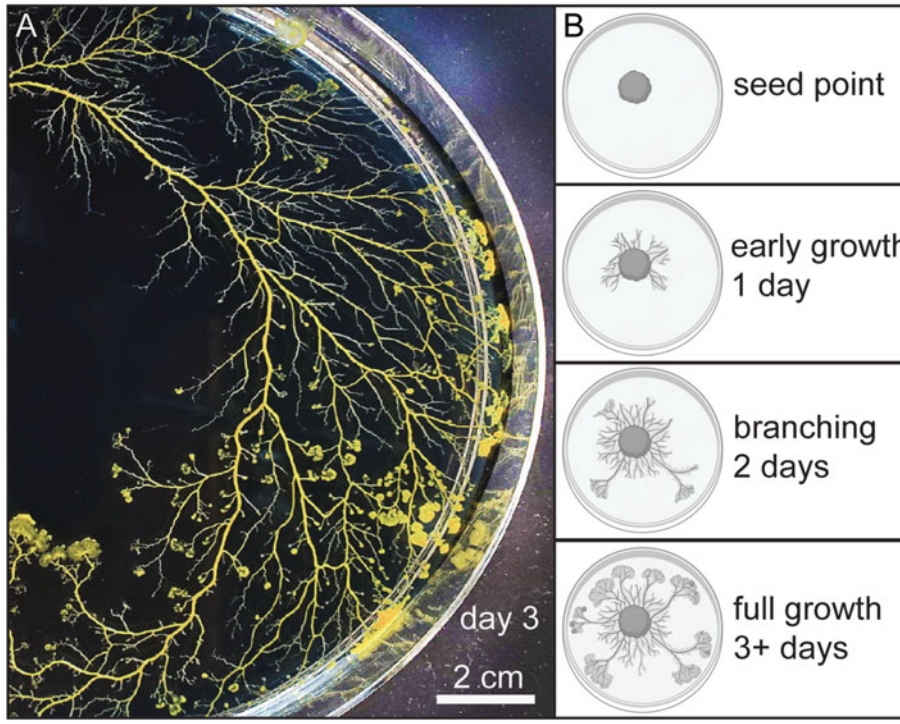


Fig. 1 *Physarum* culture. (**a**) Plasmodial *Physarum* growing on agar substrate on day 3 (seed point out of frame). (**b**) *Physarum* undergoes plasmodial proliferation and builds branching networks to explore its environment

Relatively simple to culture, image, and sample, the single-cell *Physarum* is capable of regeneration in its most basic form [7]. *Physarum* can grow from discrete drops of liquid protoplasm to form a single plasmodial cell [7], develop an entire plasmodial network from a small seed point by plasmodial proliferation [8], fuse with separate plasmodial networks [9], and rapidly heal from injuries within its vein network (Table 1). Furthermore, *Physarum* takes multiple forms that allow hibernation under stressful conditions and growth when environmental conditions are optimal [10]. In suboptimal conditions (low humidity, lack of food, and in the presence of light), *Physarum* will reconfigure into a dormant, encrusted state known as sclerotia (Table 1) [10], where it can hibernate for months to years. Sclerotia rapidly transforms to a vegetative plasmodial state in the presence of humidity and food sources (Table 1), forming a branching slime mould network. In this dynamic state, *Physarum* uses shuttle streaming to distribute biochemicals throughout the plasmodial network and is capable of kinase signaling typically observed in eukaryotic organisms [11].

In contrast to regeneration programs that advance toward a large-scale target morphology [12, 13], *Physarum* has a strong generative capacity with consistent regeneration of hierarchical

Table 1
Definitions of *Physarum* States & Anatomy

***Physarum* States & Anatomy**	**Definition**
Myxamoebae	The uninucleate, haploid spores released from *Physarum* sporangia
Plasmodial network	*Physarum* growing into an interconnected network of protoplasmic strands
Plasmodial state	A slime mold enclosed within a single membrane without cell walls. In this state, the slime mould is a syncytium with a cytoplasm containing thousands of individual nuclei
Protoplasm	Contents of the cell enclosed by the cellular membrane
Sclerotia	A dry and dormant state that *Physarum* enters in low-humidity conditions
Seed point	The starting point for a *Physarum* culture
Shuttle streaming	Periodic movement of cytoplasmic fluid throughout the *Physarum* network
Slime mould	Eukaryotic organisms that can live freely as single cells but can aggregate together to form multicellular structures
Sporangia	Enclosure in which asexual spores form
Syncytium	A single cell containing several nuclei formed by fusion of cells or by division of nuclei
Vegetative	Reproduction or propagation achieved by asexual means, such as by culturing a plasmodial network from a small fragment of *Physarum*
Vein	Branches of the *Physarum* network that participate in food foraging and shuttle streaming activities

branching patterns [14]. Similar to *Physarum*, plants possess a high degree of developmental plasticity, exhibiting consistent, reproducible shoot and root systems from leaf cuttings, with a shoot on one side and a root on the other and small variations in shape from its original body (regeneration in plants fully reviewed in [15]). In this chapter, we define whole-body regeneration as the development of an entire plasmodial network from a small seed point by plasmodial proliferation. In addition, we present methods for transforming sclerotia into a vegetative state and for regeneration of *Physarum* veins, which are methods for revival and tissue repair, but do not represent regeneration of the entire organism.

Also similar to plants, the large-scale morphology of *Physarum* is strongly driven by conditions in its local environment, such as attractants, repellants, and substrate stiffness [4, 16]. *Physarum* is extremely capable of growing and retracting in response to its surroundings and seemingly prioritizes efficient sampling of its surroundings and reinforcement of its beneficial branches over growing into a precise shape [16]. However, given the same environmental conditions, like a maze, *Physarum* will repeatedly

identify the minimum-length solution by retracting veins that reach dead ends [17–19]. Therefore, in this chapter, we offer examples of fixed environmental conditions that can be used to assess repair and regrowth in the context of functional patterning, such as the Salt Bridge. Salt interferes with the ionic homeostatic mechanisms of *Physarum* and therefore exposure to salt will cause *Physarum* to generate unique whole-body morphologies in its presence [9].

The strong generative capacity of plants relies on stem cells that form at the cut site, elongate and proliferate, and produce new plant bodies [15]. Dissimilar to plants that possess a meristem region of undifferentiated cells, the entire plasmodial *Physarum* network exists as an undifferentiated single cell. Nuclei of plasmodial *Physarum* divide without passing through cytokinesis, giving rise to a large multinuclear syncytium [8]. Although plasmodial *Physarum* and its encrusted state, sclerotia, do not undergo cellular differentiation or even cytokinesis, when *Physarum* mature or food becomes limited, plasmodia will differentiate into sporangia in the presence of light [11]. The sporangia release haploid spores, which germinate, form flagellated myxamoebae, genetically recombine with myxamoebae from other plasmodia, and fuse into a zygote that develops into a new plasmodium [11].

In this chapter, we present methods for regenerating *Physarum* from its dormant sclerotia state, culturing plasmodia, and drying plasmodia to sclerotia. We describe methods for the modeling of injury and regeneration, particularly in complex environments like mazes and salt bridges. We also present methods for automated macrophotography to monitor *Physarum* growth and form. For more detailed analysis of *Physarum* form and function, we introduce microscopy approaches, including the injection of fluorescent polymers and beads prior to imaging. Those fluorescent materials can be used to observe the response of *Physarum* to localized nutrient or chemical stimuli via cytoplasmic shuttle streaming, which is the primary method of information transfer throughout the organism's body [1]. Methods to quantify both the structural and functional *Physarum* networks during growth and repair are also described. Finally, we outline techniques to sample *Physarum networks* and plasmodial slime for downstream use in mass spectrometry metabolomics or gene expression measurements like polymerase chain reaction or RNA sequencing [11, 20].

2 Materials

Prepare all solutions using ultrapure water (0.2 μm-filtered and deionized). Prepare and store all reagents at room temperature (unless indicated otherwise).

2.1 Physarum Culture Environments

1. Sample of *Physarum* as plasmodia or sclerotia (*see* **Note 1**).
2. 1% (w/v) agar plate medium: 3 g bacteriological agar powder ($C_{12}H_{18}O_9$) in 300 mL water. Heat until complete dissolution (*see* **Note 2**).
3. Oatmeal flakes (*see* **Notes 3** and **4**).
4. Spray bottle of water.
5. Humidity and temperature-controlled plant growth incubator (*see* **Note 5**).
6. 10% (w/v) flan medium: 10 g blended oat flakes in boiling 1% agar plate medium. Pour the mixture into molds to set and allow to acclimate to room temperature prior to use for experiments.
7. Maze: 1 cm wide lanes cut out from 1 cm thick acrylic sheet. Fill lanes with a 0.25 cm thick layer 1% agar plate medium.
8. Agar bridge: round food patch of 10% flan medium (diameter = 15 mm), round patch 1% agar (diameter = 15 mm). Inside a Petri dish, separate the patches by a rectangular platform composed of 1% agar gel, 1% agar gel with 150 mM NaCl, or other noxious substance (*see* **Note 6**). Keep agar bridges in individual Petri dishes for experiments. Adhere black paper to the inside of each Petri dish to absorb moisture in the dish, forcing the hydrophilic *Physarum* to traverse along the agar bridge, and providing clear contrast for imaging.

2.2 Physarum Imaging and Analysis

1. Macro-photography setup (e.g. scanner, camera, or webcam): For continuous imaging, install the macro-photography setup inside of a dark, environmentally controlled chamber.
2. Upright widefield microscope with brightfield & fluorescent channels.
3. 1× commercially available phosphate-buffered saline (PBS) (*see* **Note 7**).
4. Non-toxic fluorescent polymer for visualization of shuttle streaming in plasmodial *Physarum*: Dilute to desired concentration using 1× PBS.
5. Fluorescent beads: Dilute to desired concentration using 1× PBS.
6. Glass capillary needle.
7. Pressurized injector.
8. Dissection microscope.
9. Physarum Network Analysis Program (*see* **Note 8**).
10. MATLAB, Octave, Scikit-Image or other high-level programming language with image analysis functions.
11. Bioformats Package (Open Microscopy) for image import.

12. Java (latest version).
13. Ghostscript for exporting images in vector formats.
14. Pdftops (Xpdf Suite; Foo Labs) for eps file export.

3 Methods

Carry out all procedures at room temperature unless otherwise specified.

3.1 Physarum Culture

1. Pour 2 mL of sterile water onto a 1 cm^2 filter paper containing dehydrated *Physarum* sclerotia (*see* **Note 9**).
2. Place moistened filter paper, sclerotia-side down, at the center of a 1% agar-filled plate.
3. Arrange 4–6 oatmeal flakes 3–5 cm from the sclerotia.
4. Apply a single spray of sterile water on the plate to moisten, but not soak, the environment.
5. Maintain cultures at 22 °C and 90% humidity in a dark incubator (*see* **Note 5**).
6. Wait 2 days for the *Physarum* plasmodia to start growing toward the oat flake food sources (*see* **Note 10**).
7. Add 10 to 12 oat flakes to cover the rest of the plate.
8. Apply a single spray of sterile water to the plate.
9. Return to incubator.
10. Add fresh oat flakes every 2 days (*see* **Note 10**).
11. Return to incubator.
12. Wait a total of 5 days for *Physarum* to completely cover the plate.
13. Cut a 1 cm^2 cube of *Physarum*-coated agar using a sterile toothpick.
14. Transfer the piece of agar, *Physarum*-up, to the center of a fresh 1% agar plate (Fig. 2a, b) to sub-culture the *Physarum* to a new plate.
15. Spread 10 to 12 oat flakes across the agar.
16. Apply a single spray with sterile water.
17. Incubate at 22 °C and 90% humidity in the dark.
18. Repeat **steps 14–17** to maintain a growing culture of *Physarum* (*see* **Note 11**).
19. Allow plasmodium to grow over filter paper to begin transition to the sclerotia state for long-term storage.
20. Move the filter paper with plasmodium to dry, dark conditions for at least 2 days to produce sclerotia.

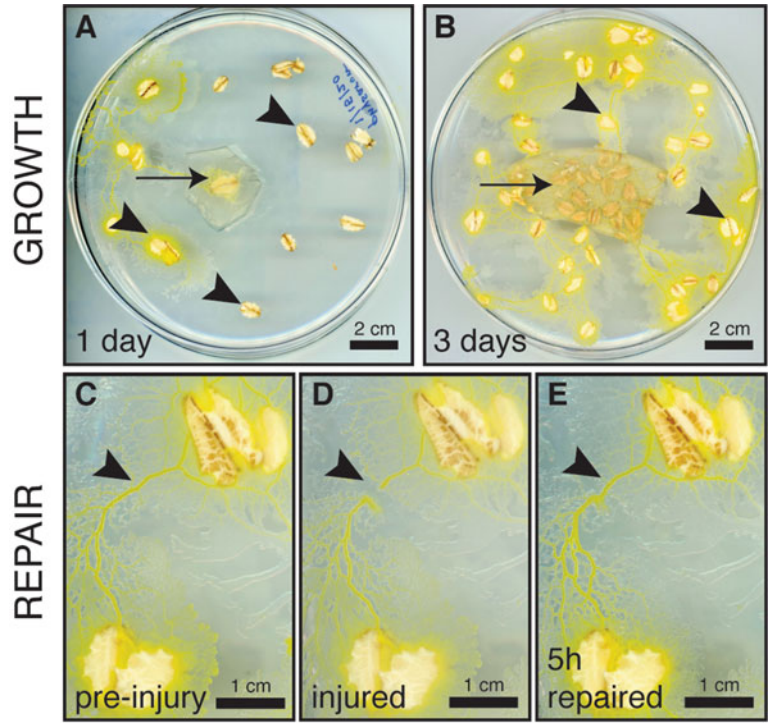


Fig. 2 *Physarum* growth and repair. (**a**) *Physarum* grows from a single seed point (arrow) towards food sources (arrowheads) one day after sub-culturing. (**b**) After 3 days, the plasmodial *Physarum* covers the plate, forming a network that includes the seed point (arrow) and all food sources (arrowheads). (**c**) Before injury, a vein connects two food sources. The food source in the upper right corner is proximal to the *Physarum* seed point compared to the food source in the lower left corner. (**d**) An injury to the vein that leaves the underlying agar intact can be (**e**) rapidly repaired within 5 h

21. Keep the sclerotia in dry and dark conditions for long-term storage. The dry sclerotia can remain dormant for up a year.

3.2 Models of Vein Repair After Injury & Amputation

The repair processes described here can be monitored using the imaging approaches outlined in Subheading 3.4.

1. Take a growing *Physarum* from the culture incubator to be used for vein injury.
2. Select a vein to be injured.
3. Scrape the vein gently to create a 1 cm gap using a cell scraper without disrupting the underlying agar layer (Fig. 2c, d) (*see* **Notes 12** and **13**).
4. Return the plate to its incubator.
5. Image the plate hourly by automated, time-lapsed imaging using the macro-photography setup (Fig. 2e) as described in Subheading 3.4.

6. Wait 5 h, or more, until the vein has repaired (*see* **Note 13**).
7. Take a growing *Physarum* from the culture incubator to be used for vein amputation.
8. Select a vein to be amputated.
9. Scrap gently the whole vein to amputate it using a cell scraper without disrupting the underlying agar layer (*see* **Notes 12** and **13**).
10. Image the plate hourly by time-lapsed imaging using the macro-photography setup (Fig. 2e).
11. Repeat **step 10** until the vein has repaired (*see* **Note 13**).

3.3 Generation in Complex Environments: Maze & Salt Bridge Experiments

The generative processes described here can be monitored using the imaging approaches outlined in Subheading 3.4.

1. Take a growing *Physarum* from the culture incubator to be used for maze growth.
2. Identify one oat flake that is evenly covered in *Physarum*.
3. Place the *Physarum*-covered oat at the entrance of the maze.
4. Add 2 fresh oat flakes at the maze's endpoint and 3 at points equidistant from the start of the maze to induce growth away from the source (Fig. 3b).
5. Move the maze to the incubator.
6. Image the plate hourly by time-lapsed imaging using the macro-photography setup (Fig. 2e) as described in Subheading 3.4.
7. Wait 48 h.
8. Take a growing *Physarum* from the culture incubator to be used for a bridge experiment.
9. Prepare one normal 1% agar bridge (control) and one 150 mM NaCl agar bridge.
10. Place a *Physarum* sample on the 1% agar side of both agar bridges (Fig. 3c).
11. Move plates to the incubator and allow 24 h for *Physarum* to traverse the bridge (Fig. 3d).

3.4 Structural & Functional Imaging

1. Store the macro-photography set-up inside of a temperature and humidity-controlled incubator for automated time-lapse imaging over multiple days.
2. Place the *Physarum* dish(es) in the field of view of the macro-photography set-up inside the incubator.
3. Set the image acquisition rate and total imaging time to automatically acquire images (Fig. 4a) (*see* **Note 14**).
4. Wait until the total imaging time has elapsed.

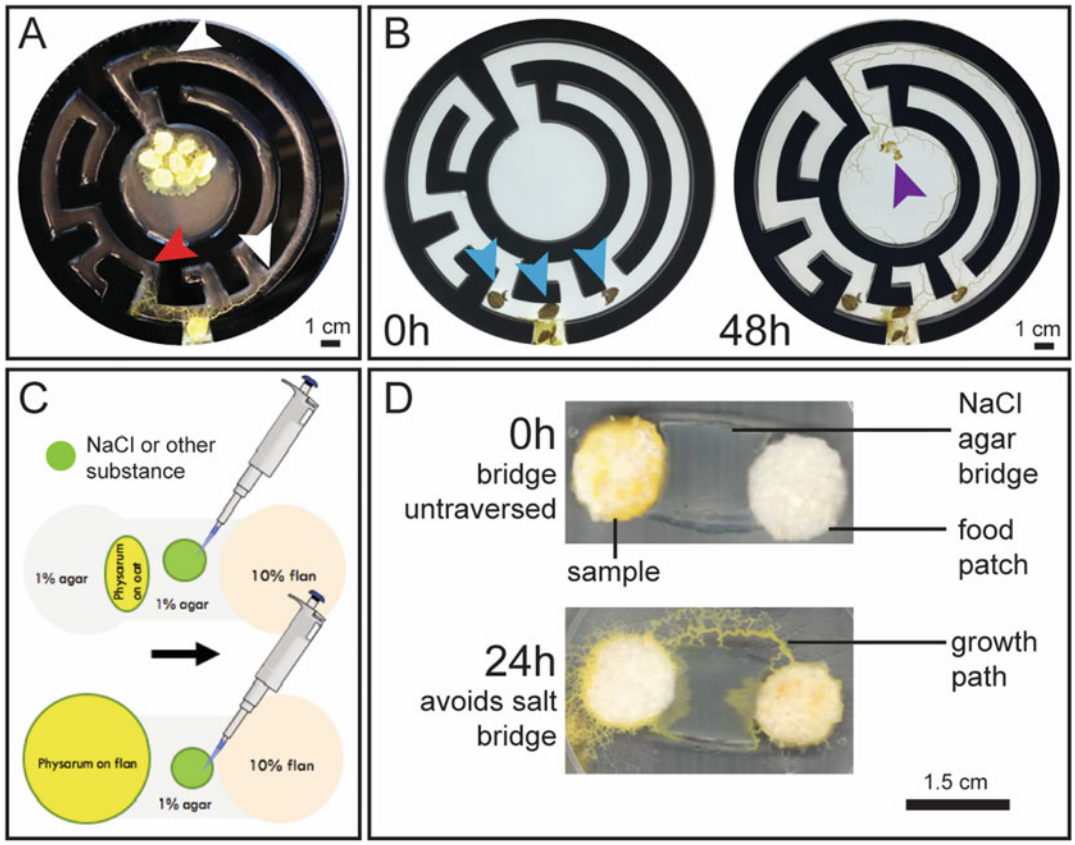


Fig. 3 *Physarum* generation in complex environments. (**a**) Physarum grows within the confines of the maze (white arrows) toward the food source and retreats from areas lacking food (red arrow), building an optimized morphology based on the environmental conditions. (**b**) The oat flakes at the primary maze entrance points (blue arrows) are placed to encourage *Physarum* growth in three directions. Despite this, after 48 h *Physarum* only grows toward the maze endpoint (purple arrow; oatmeal flake removed). (**c**) The agar bridge connects *Physarum* samples to the 10% flan medium. Salt or other substances may be added to the bridge to induce morphological changes, such as (**d**) growth around the noxious salt bridge after 24 h

5. Stop time-lapse imaging.
6. Before brightfield and darkfield imaging, remove Petri dish lid to minimize reflection artifacts in images.
7. Illuminate from above the microscope stage and place the Petri dish flat in the field of view.
8. Use the brightfield view to visualize the outer architecture of the plasmodial network (Fig. 4b).
9. To visualize the interior compartments of *Physarum* veins, use darkfield microscopy (Fig. 4c).
10. Load fluorescent dextran or bead solution into glass capillary needle using a pressurized injection system for visualizing shuttle streaming within *Physarum* plasmodial networks.

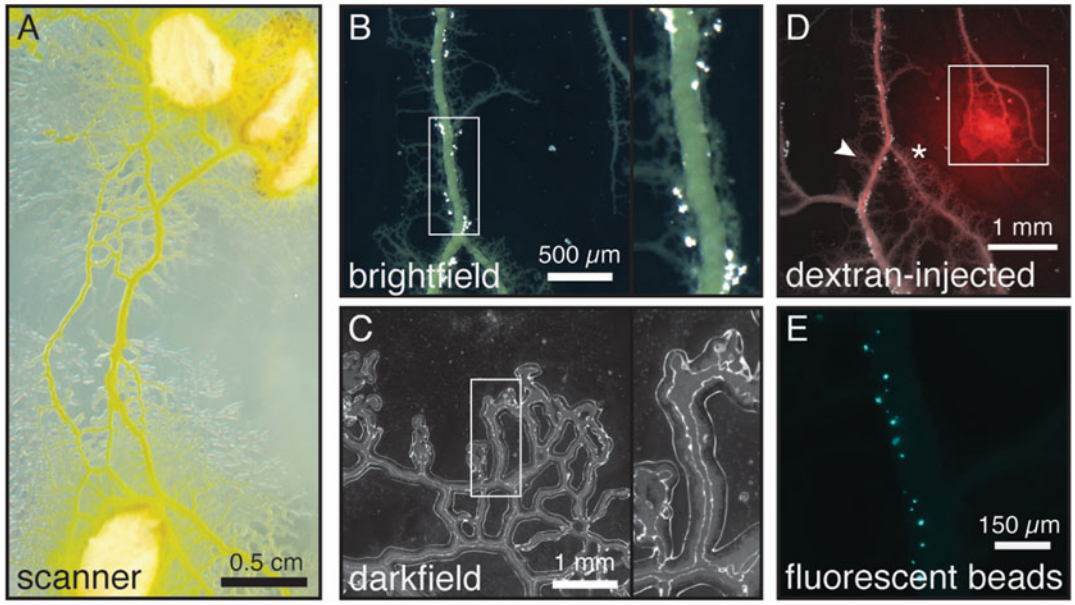


Fig. 4 Structural and functional visualization of *Physarum* plasmodium. Physarum structure visualized using (**a**) a scanner, (**b**) brightfield microscopy, or (**c**) darkfield microscopy. Brightfield imaging captures the outer architecture of the *Physarum*, whereas darkfield imaging shows compartments within each vein (*insets*). (**d**) Fluorescent dextran travels through the *Physarum* network, with preference for certain paths (arrow) over others (star). Dextran can be shuttled through the network and deposited in slime secretions (box). (**e**) Fluorescent beads travel through the *Physarum* network (shown at high magnification)

11. Place the tip of the glass capillary needle into a large, primary vein of the *Physarum*.
12. Inject labeling solutions into the vein using short pulses (150 ms) at 140 kPa pressure.
13. If necessary, clean and clear the capillary needle (*see* **Notes 15** and **16**).
14. Repeat injections in other regions of the plasmodium, as needed.
15. Visualize shuttle streaming using fluorescent microscopy in the same way described for brightfield and darkfield imaging (Fig. 4d, e; *see* **Note 17**).
16. Set the microscopy software to acquire images at a high frame rate (typically ≥1 frame/s) to capture movement.

3.5 Quantification of Growth & Repair

This section outlines a general protocol for *Physarum* image processing and network analysis.

1. Launch the Physarum_network application (*see* **Note 8**).
2. Import 8-bit images in the Directory panel (Fig. 5a).

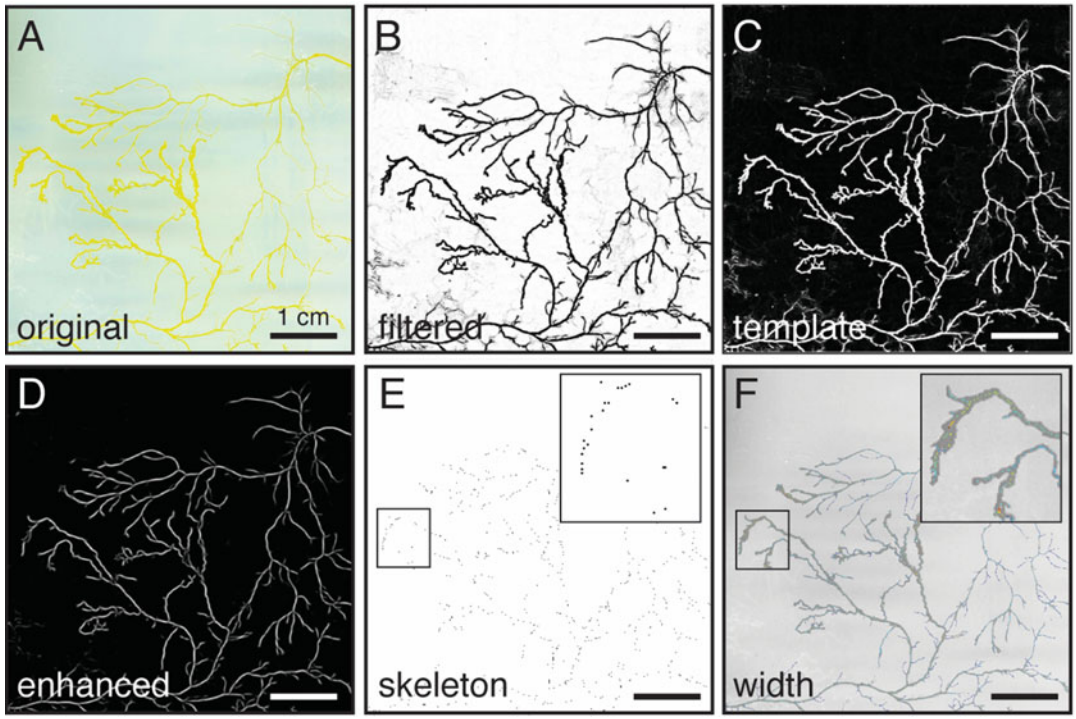


Fig. 5 Image processing and network analysis pipeline to quantify *Physarum* shape and connectivity. (**a**) Images saved from a scanner are imported and (**b**) filtered, (**c**) used to create a template, and (**d**) processed to enhance vein structure. The single pixel-wide skeleton is extracted and used to form a (**e**) network graph for evaluation using metrics, like (**f**) vein width. Scale bar = 1 cm for all panels

3. Input the *microns per pixel* in the Profile panel to calibrate the image size.
4. Calculate the *full width half maximum* value for the smallest and largest veins in the network in the Profile panel to appropriately set the scaling and filtering operations for the network.
5. Set the *number of scales* and *resampling* in the Image processing panel based on the *full width half maximum* values determined in the Profile panel.
6. Select the *opening* function for background correction in the Image processing panel (*see* **Note 18**).
7. Select the *guided* filtering algorithm in the Imaging processing panel to improve signal to noise in the image (*see* **Note 18**).
8. Select *process* to visualize the filtered output in the image display panel (Fig. 5b).
9. Select *single* projection in the network template panel to for converting a single original image to a network skeleton in the network template panel (Fig. 5c). For time series, a template can be constructed from a projection of the data along the time dimension (*see* **Note 19**).

10. Leave the *boundary mask* options unchecked in the Skeleton extract panel (default) if there are no boundaries, regions to exclude, or food sources in the image. If there are non-*Physarum* objects in the image, use this panel to define boundaries, exclude regions, or delineate food sources (*see* **Note 20**).
11. Use the *Frangi kernel* algorithm in the skeleton extract panel to improve the relative contrast of the network veins by enhancing vessel-like features through calculating the eigenvectors of the Hessian (Fig. 5d; *see* **Note 21**).
12. Use the *hysteresis* algorithm to extract the skeleton network. This algorithm uses intensity information and pixel connectivity to derive a single-pixel skeleton.
13. Check that the single-pixel skeleton accurately reflects the network in the original images (Fig. 5e).
14. Manually edit the network skeleton if connections are incorrect or missing using the binary editing tool in the skeleton extract panel.
15. Estimate vein diameter across the network using the *distance* approach, which estimates the local full-width half max from the original tubule intensity for each pixel in the skeleton.
16. Convert the skeleton into a weighted graph representation of the *Physarum* network with nodes defined by the junctions between the veins and edges defined by each vein that joins nodes.
17. Visualize graph edge metrics in the display panel or in the parameter panel (Fig. 5f).
18. Output images and graph metrics for additional analysis.

3.6 Sampling Physarum

1. Remove oat flakes from the *Physarum* plate of interest.
2. Using a cell scrapper, carefully remove the plasmodial network from the agar to sample the *Physarum*.
3. Record the total mass of *Physarum* sample.
4. Combine the sample with water or media of choice at a concentration of 1 g/mL.
5. Vortex for 30 s to combine.
6. Continue with sample centrifugation and storage in **step 11**.
7. Remove oat flakes from an additional *Physarum* plate.
8. Add water or other media to cover the plate in a thin layer (5 mL for a 140 mm plate) to sample water-soluble *Physarum* secretions.
9. Mildly shake *Physarum* plates for 30 min to collect water-soluble components of the *Physarum* and its secretions.

10. Holding the plate at an angle, collect liquid from the plate using a pipette.
11. Centrifuge each sample at 3000 rcf for 15 min to separate large particulates.
12. Collect the supernatant liquid from each centrifuged sample.
13. Store samples at −80 °C for downstream analyses.

4 Notes

1. *Physarum* culture kits can be purchased from several scientific retailers. We purchase sclerotia from Carolina Biological Supply Company.
2. This recipe makes enough 1% agar medium for six 140 mm diameter dishes filled with 50 mL/dish.
3. *Physarum* prefer nutrition from old fashioned or whole-oat oatmeal and will not grow as well using instant (processed) oatmeal flakes or irradiated oatmeal.
4. An alternative to feeding *Physarum* with oatmeal flakes is to make or purchase oatmeal agar. The distribution of nutrition throughout the plate will cause *Physarum* to grow in dense clusters as opposed to networks. Shuttle streaming and the production of slime may be reduced using this method; however, oatmeal agar can be useful for culturing stock plates of *Physarum*.
5. *Physarum* will grow most optimally if stored in a dark, humidity-controlled plant growth chamber. However, humid conditions can also be achieved in a standard incubator using a humidifier with automatic feedback control. Dry conditions can cause the plasmodial *Physarum* to revert to the dried, sclerotia state. Light can trigger spore formation instead of plasmodial growth [11].
6. In addition to salt, other noxious substances can be integrated into the agar bridge, such as quinine and caffeine [9, 21].
7. 1× PBS is purchased in a formulation buffered to pH 7.4 and free of calcium chloride, magnesium chloride, and phenol red.
8. The Physarum_network algorithm was developed by Fricker et al., 2017 and additional details about the algorithm are available [22].(Download website: https://markfricker.org/77-2/software/physarum-network-analysis/).
9. Cultures can become contaminated, so inspect each plate for foreign cultures before subculturing or sampling for downstream analyses. To avoid contamination, use sterile instruments and keep Petri dishes covered when not actively working with them. Aliquot oatmeal flakes into 50 mL air-tight containers to prevent contamination of the food stocks.

10. Some *Physarum* may grow faster. Once cultures cover all flakes, proceed to next steps. Because *Physarum* grow toward fresh food sources, add new flakes every 1–3 days for optimal growth.
11. We recommend that *Physarum* undergo subculture weekly. *Physarum* can undergo continuous subculture cycles, however, the organism will exhibit signs of aging after extended subculture, such as slowing of growth within 162 days for some strains [23]. We initiate new cultures from sclerotia quarterly throughout the year to avoid any slowing of growth due to senescence.
12. The induction of injury in *Physarum* can be done with any number of blunt tools. However, we do not recommend using very sharp instruments, like a scalpel, which may damage the underlying agar and prevent rapid repair of *Physarum* veins.
13. We have observed faster and more robust repair mechanisms in newly plated *Physarum* (less than 48 h since sub-culture). Therefore, we recommend that vein injury and amputation be performed early after sub-culture.
14. Exposure to light can alter the growth patterns of *Physarum*, such as photoavoidance and sporulation [24]. To reduce the effects of light exposure during imaging, we recommend increasing the scanning time interval and therefore acquiring images at the lowest allowable rate. We typically image *Physarum* plates for 1–3 days at intervals of 15 min or longer.
15. *Physarum* lacks cell walls and their slime sheath is the primary layer of protection from injury and the environment. Positioning the needle in the slime sheath can cause it to clog and therefore we recommend frequent cleaning of the needle or delivering the dextran or bead by pipette on or near the *Physarum* veins.
16. Alternatively, fluorescent dextran and bead solutions can also be delivered to the surface of the *Physarum* using a pipette. Deposit a 1–2 μL droplet of dextran or bead solution on the surface of a large, primary vein of the *Physarum*. The *Physarum* vein will absorb the droplet and distribute it throughout the plasmodium using shuttle streaming. This technique avoids the challenges of pressure injection, such as needle clogging. However, the injection technique provides greater specificity in delivery location.
17. 2 μm-diameter fluorescent beads (FluoSpheres carboxylate-modified microspheres, 2 μm; Life Technologies) and 10,000 molecular weight fluorescent dextran (Dextran, Rhodamine B, 10,000 MW, Neutral; Invitrogen) were used in the microscopy images shown in this chapter.

18. When performing image processing, we used the *opening* function to correct the background and *guided* to improve signal-to-noise. The *opening* function uses a disk-shaped kernel to remove features smaller than the thinnest veins and estimates the local background surrounding each pixel in the *Physarum* network image. The background is subtracted from the original image. The *guided* algorithm applies an edge-preserving smoothing filter according to the intensities in the original image.
19. Creating a template for a time series using the projection algorithm can be helpful since it will permit the construction of a network with consistent node and edge definitions across the whole image series.
20. We recommend selecting *manual* to exclude boundaries (such as a plate edge) using drawing tools to outline the image bounds. Features (such as a food source) in the *Physarum* image can be selected using the *manual* tool and will be included as a node during network construction.
21. When extracting the *Physarum* network skeleton, we found the *neuriteness* algorithm to produce excellent network images. However, this algorithm produced a network comprised of two parallel lines, forming the outline of each vein, instead of a single-pixel wide binary skeleton. Instead, we suggest using the *Frangi enhancement* algorithm.

Acknowledgements

This research was also supported by the Allen Discovery Center program through The Paul G. Allen Frontiers Group (12171). We also gratefully acknowledge the Defense Advanced Research Projects Agency (DARPA) under Cooperative Agreement Number HR0011-18-2-0022. The content of the information does not necessarily reflect the position or the policy of the Government, and no official endorsement should be inferred. Approved for public release; distribution is unlimited. The authors also thank Melanie Chien for assistance with experiments and Cuong Nguyen for training in laser cutting during preparation of the maze.

References

1. Alim K, Andrew N, Pringle A, Brenner MP (2017) Mechanism of signal propagation in Physarum polycephalum. Proc Natl Acad Sci U S A 114:5136–5141. https://doi.org/10.1073/pnas.1618114114
2. Vallverdú J, Castro O, Mayne R et al (2018) Slime mould: the fundamental mechanisms of biological cognition. Biosystems 165:57–70. https://doi.org/10.1016/j.biosystems.2017.12.011
3. Whiting JGH, Jones J, Bull L et al (2016) Towards a Physarum learning chip. Sci Rep 6:1–14. https://doi.org/10.1038/srep19948

4. Murugan NJ, Kaltman DH, Jin H et al (2020) Mechanosensation mediates long-range spatial decision-making in an aneural organism. Adv Mater 33(34):e2008161. https://doi.org/10.1101/2020.03.20.985523
5. Iwayama K, Zhu L, Hirata Y et al (2016) Decision-making ability of Physarum polycephalum enhanced by its coordinated spatio-temporal oscillatory dynamics. Bioinspir Biomim 11:036001. https://doi.org/10.1088/1748-3190/11/3/036001
6. Reid CR, Latty T, Dussutour A, Beekman M (2012) Slime mold uses an externalized spatial "memory" to navigate in complex environments. Proc Natl Acad Sci U S A 109:17490–17494. https://doi.org/10.1073/pnas.1215037109
7. Tsuda S, Jones J (2011) The emergence of synchronization behavior in Physarum polycephalum and its particle approximation. Biosystems 103:331–341. https://doi.org/10.1016/j.biosystems.2010.11.001
8. Doerhoefer S, Khodyreva S, Safronov IV et al (1998) Molecular constituents of the replication apparatus in the plasmodium of Physarum polycephalum: identification by photoaffinity labelling. Microbiology 144:3181–3193. https://doi.org/10.1099/00221287-144-11-3181
9. Vogel D, Dussutour A (2018) Brainless learners. In: Adams DS, Levin M (eds) Ahead of the curve, vol 2. IOP Publishing, Bristol, pp 6-2–6-12
10. Dove W, Rusch H (2017) Growth and differentiation in Physarum Polycephalum. Princeton University Press, Princeton, New Jersey
11. Schaap P, Barrantes I, Minx P et al (2016) The physarum polycephalum genome reveals extensive use of prokaryotic two-component and metazoan-type tyrosine kinase signaling. Genome Biol Evol 8:109–125. https://doi.org/10.1093/gbe/evv237
12. Lobo D, Solano M, Bubenik GA, Levin M (2014) A linear-encoding model explains the variability of the target morphology in regeneration. J R Soc Interface 11:20130918. https://doi.org/10.1098/rsif.2013.0918
13. Levin M (2012) Morphogenetic fields in embryogenesis, regeneration, and cancer: non-local control of complex patterning. Biosystems 109:243–261. https://doi.org/10.1016/j.biosystems.2012.04.005
14. Jones J (2015) From pattern formation to material computation: multi-agent modelling of Physarum Polycephalum, vol 15. Springer, Berlin
15. Ikeuchi M, Ogawa Y, Iwase A, Sugimoto K (2016) Plant regeneration: cellular origins and molecular mechanisms. Dev 143:1442–1451. https://doi.org/10.1242/dev.134668
16. Takamatsu A, Takaba E, Takizawa G (2009) Environment-dependent morphology in plasmodium of true slime mold Physarum polycephalum and a network growth model. J Theor Biol 256:29–44. https://doi.org/10.1016/j.jtbi.2008.09.010
17. Zhu L, Kim SJ, Hara M, Aono M (2018) Remarkable problem-solving ability of unicellular amoeboid organism and its mechanism. R Soc Open Sci 5:180396. https://doi.org/10.1098/rsos.180396
18. Nakagaki T, Yamada H, Tóth A (2000) Maze-solving by an amoeboid organism. Nature 407:470
19. Bonifaci V, Mehlhorn K, Varma G (2012) Physarum can compute shortest paths. J Theor Biol 309:121–133. https://doi.org/10.1016/j.jtbi.2012.06.017
20. Golderer G, Werner ER, Leitner S et al (2001) Nitric oxide synthase is induced in sporulation of physarum polycephalum. Genes Dev 15:1299–1309. https://doi.org/10.1101/gad.890501
21. Boisseau RP, Vogel D, Dussutour A (2016) Habituation in non-neural organisms: evidence from slime moulds. Proc R Soc B Biol Sci 283:2–8. https://doi.org/10.1098/rspb.2016.0446
22. Fricker MD, Akita D, Heaton LLM et al (2017) Automated analysis of Physarum network structure and dynamics. J Phys D Appl Phys 50:1–15. https://doi.org/10.1088/1361-6463/aa72b9
23. Nakagawa CC, Jones EP, Miller DL (1998) Mitochondrial DNA rearrangements associated with mF plasmid integration and plasmodial longevity in Physarum polycephalum. Curr Genet 33:178–187. https://doi.org/10.1007/s002940050325
24. Nakagaki T, Umemura S, Kakiuchi Y, Ueda T (1996) Action Spectrum for sporulation and Photoavoidance in the plasmodium of Physarum polycephalum, as modified differentially by temperature and starvation. Photochem Photobiol 64:859–862

Open Access This chapter is licensed under the terms of the Creative Commons Attribution 4.0 International License (http://creativecommons.org/licenses/by/4.0/), which permits use, sharing, adaptation, distribution and reproduction in any medium or format, as long as you give appropriate credit to the original author(s) and the source, provide a link to the Creative Commons license and indicate if changes were made.

The images or other third party material in this chapter are included in the chapter's Creative Commons license, unless indicated otherwise in a credit line to the material. If material is not included in the chapter's Creative Commons license and your intended use is not permitted by statutory regulation or exceeds the permitted use, you will need to obtain permission directly from the copyright holder.





Chapter 4

Studying Porifera WBR Using the Calcerous Sponges *Leucosolenia*

Andrey I. Lavrov and Alexander V. Ereskovsky

Abstract

Sponges (Porifera), basal nonbilaterian metazoans, are well known for their high regenerative capacities ranging from reparation of a lost body wall to whole-body regeneration from a small piece of tissues or even from dissociated cells. Sponges from different clades utilize different cell sources and various morphological processes to complete the regeneration. This variety makes these animals promising models for studying the evolution of regeneration in Metazoa. However, there are few publications concerning the regenerative mechanisms in sponges. This could be partially explained by the delicacy of sponge tissues, which requires modifying and fine adjusting of common research protocols. The current chapter describes various methods for studying regeneration processes in the marine calcareous sponge, *Leucosolenia*. Provided protocols span all significant research steps: from sponge collection and surgical operations to various types of microscopy and immunohistochemical studies.

Key words Regeneration, Sponges, Protocols, Microscopy, Surgical operations, Ultrastructure, Proliferation, Apoptosis

1 Introduction

Sponges (Phylum Porifera) are thought to be the sister group of all other animals and the earliest branching multicellular lineage of extant animals [1]. As such, they represent a key group for the understanding of the evolutionary history of animals, including the origin and evolution of regeneration mechanisms. The body shape of sponges is very diverse; they may be film-like, encrusting, lumpy or spherical, tubular, branching, flabellate, and so on. The body size of sponges varies as much as their body shapes: from 3–10 mm to 1.5–2 m [2]. Their organization is peculiar: they have no distinct gut, muscles, gonads, nervous system, or respiratory system. The surface of a sponge is covered by a simple single-layered flat epithelium (called exopinacoderm), while the internal parts of the animal body are occupied by a highly complex mesenchymal tissue (called mesohyl) that comprises numerous mobile cell

Simon Blanchoud and Brigitte Galliot (eds.), *Whole-Body Regeneration: Methods and Protocols*,
Methods in Molecular Biology, vol. 2450, https://doi.org/10.1007/978-1-0716-2172-1_4, © The Author(s) 2022

types embedded in its extracellular matrix [3]. The rigidity of the sponge body is ensured by the collagen and spongin fibrils (in some Demospongiae orders) and by the internal inorganic skeleton, consisting of either calcium carbonate ($CaCO_3$) (Calcarea, some Demospongiae) or silica (SiO_2) (Hexactinellida, Demospongiae, many Homoscleromorpha).

The mesohyl is penetrated by a complex system of canals and choanocyte chambers (termed the aquiferous system), which is the most characteristic feature of the poriferan anatomy. Sponges use this constant water pumping system to obtain food and oxygen and to remove metabolic wastes. Surrounding water is drawn into the inhalant canals via numerous pores (ostia) in the exopinacoderm. Water then circulates through choanocyte chambers, where it is filtered, before leaving the sponge via the system of exhalant canals that converge to large exhalant openings (osculum) [4]. The choanocyte chambers are lined by flagellated collar cells (called choanocytes). The constant beating of choanocytes' flagella generates the water flow through the whole aquiferous system, and their collars serves as an ultimate filter for retaining particles from the pumped water [2].

Five types of the body organization have been described in sponges: (1) asconoid, (2) solenoid, (3) syconoid, (4) sylleibid, and (5) leuconoid [3]. These types differ by the complexity of the aquiferous system and the extent of the mesohyl development. In the simplest asconoid sponges, ostia lead directly to a single cavity completely lined with the choanocytes, and the mesohyl is represented only by thin, mostly acellular layer. The more complex leuconoid sponges are characterized by an elaborated aquiferous system with highly developed canals and numerous choanocyte chambers and thick mesohyl with numerous specialized cell types.

A characteristic feature distinguishing sponges from other Metazoa is the high plasticity of cellular differentiation, anatomical, and tissue structures throughout their life cycle. Various differentiated cells of the sponge can move, transdifferentiate, and switch functions. The direction of the differentiation depends on the current needs of the organism. Thus, the sponge is constantly in the state of rearrangements of all its structures [5–9]. This "chronic morphogenesis" contributes to the growth of the animal, for instance, by reconstructing its somatic tissue after degradation during sexual and asexual reproduction, as well as during regeneration [10–13]. Besides, sponges are not equipped with protective tissues or structures like cuticles, scales, or shells, but are covered only by a single-cell layer. It has been suggested that this lack of protection against injury closely correlates with the high regenerative capacity of sponges [14].

Sponges are known to possess remarkable reconstitutive abilities ranging from restoration of a lost body part to a complete organism development from a small piece of tissue and even from

the cell suspension. However, only few reliable data on the regeneration mechanisms (morphogenesis, cell behavior, and regulation) and their distribution among sponge clades currently exists [10, 12, 15–18].

We provided complex and detailed investigations of reparative regeneration in homoscleromorphs [10], calcareous sponges [13, 19], and demosponges [11, 12]. These studies included various approaches: transmission electron microscopy (TEM), scanning electron microscopy (SEM), epifluorescent and light microscopy, immunohistochemistry, and time-lapse recordings. The obtained results show a high diversity of morphogenesis, cell mechanisms, and cell turnover, accompanying the regeneration processes.

The model sponges presented in this chapter belong to the genus *Leucosolenia*, an abundant species broadly distributed in the White Sea and in the North of Europe, where they are accessible throughout the year. *Leucosolenia* are calcareous sponges, characterized by a calcium carbonate mineral skeleton and the asconoid aquiferous system (Fig. 1a).

The body wall of *Leucosolenia* has a thickness of 15–30 μm and is composed of three layers: an outer layer—the exopinacoderm, a central region—the loose mesohyl, and an inner layer—the choanoderm (Fig. 2b). Inhalant pores (ostia) are scattered throughout the exopinacoderm. They are formed by tubular cylindrical cells (porocytes), which connect the external milieu with the internal choanocyte cavity. The mesohyl of *Leucosolenia* contains a variety of

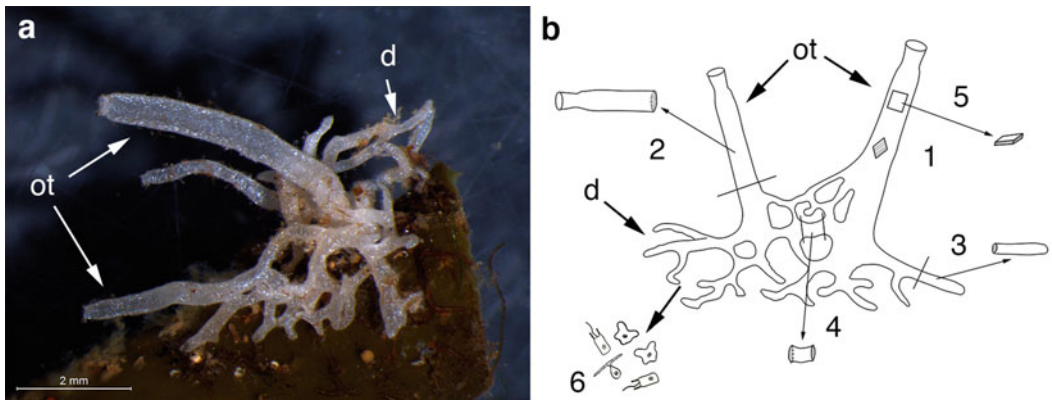


Fig. 1 Surgical operations in *Leucosolenia variabilis*. (**a**) sponge in vivo; (**b**) scheme of a sponge with different types of surgical operations: (1) body wall regeneration, (2) whole-body regeneration (WBR) from an amputated oscular tube, (3) WBR from an amputated diverticulum, (4) WBR from an amputated cormus tube, (5) WBR from a small fragment of the body wall, (6) cell reaggregation after mechanical tissue dissociation. WBR could be observed during the restorative process in amputated body tubes (2–4), small fragments of the body wall (5) and during cell reaggregation after dissociation (6). WBR from amputated body tubes requires minimal rearrangements of intact tissues, while cell reaggregation is accompanied by complete destruction of intact tissue structure. WBR from small fragments of the body wall represents an intermediate type. *d* diverticula, *ot* oscular tubes

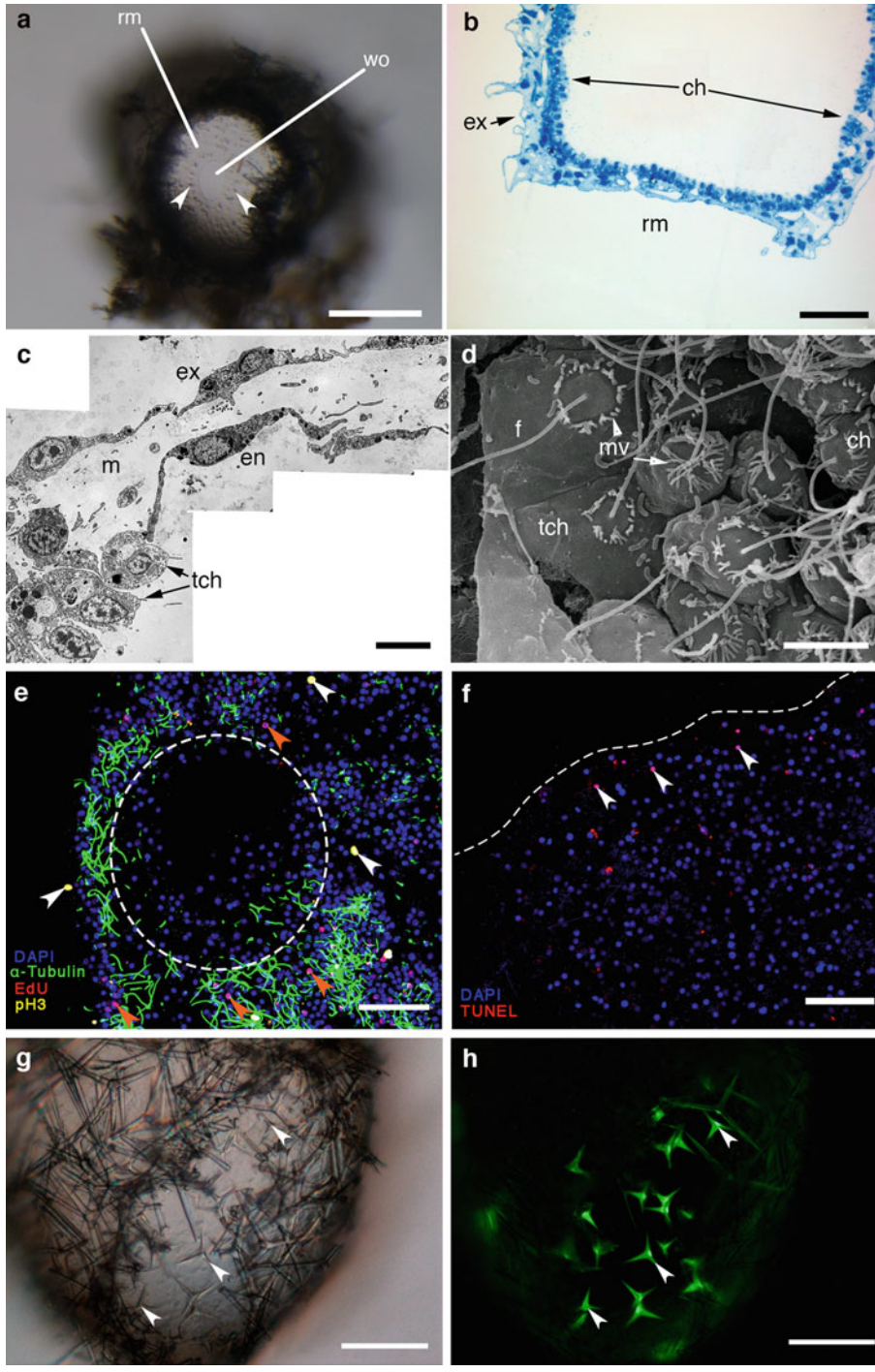


Fig. 2 Various methods for investigations of *Leucosolenia variabilis* regeneration. (**a**) regenerative membrane growing from the periphery to the center of the wound orifice, stereomicroscope (in vivo), white arrowheads mark mesohyl cells inside the regenerative membrane. (**b**) Semithin section of regenerative membrane transformed into intact body wall (96 hpo). (**c**) TEM micrograph of complete regenerative membrane (24 hpo) consisting of the flattened exopinacocytes and endopinocytes transdifferentiated from choanocytes. (**d**) SEM micrograph of choanocytes transdifferentiating into endopinacocytes during growth of regenerative

cell types, including sclerocytes, rare amoeboid cells, symbiotic bacteria, spicules, as well as gametes and developing embryos during the reproduction season.

The rapid wound healing and high regeneration capacity after different surgical interventions were demonstrated, indicating that *Leucosolenia* are a promising model for sponge regeneration investigations [20]. *Leucosolenia complicata* and *L. variabilis* have been successfully used for different experiments concerning the study of restoration morphogenesis [13, 19, 21–26].

In a recent publication, we revisited various regenerative processes of *L. variabilis* from the White Sea using electron microscopy, laser confocal microscopy, epifluorescence microscopy, and time-lapse microscopy. These approaches allowed us to precisely address the issues of morphogenetic mechanisms, cell transdifferentiations, movements, and proliferation. Our study reveals the contributions of cell types to reparative regeneration in this species and demonstrates a central role of epithelial morphogenesis and transdifferentiations in the regeneration process [13].

Leucosolenia demonstrate high and diverse regenerative capacity after various surgical operations. In this chapter, we provide methods to study the reparative regeneration of the body wall, whole-body regeneration (WBR) from amputated tubes and small fragments of the body wall, as well as cell reaggregation and primmorph formation after tissue dissociation. We also provide protocols for cell proliferation, apoptosis, and immunohistochemical studies. Finally, we present approaches for functional analysis of cell proliferation and skeleton synthesis during regeneration.

2 Materials

1. Castroviejo scissors.
2. 50 μm nylon mesh.

Fig. 2 (continued) membrane (24 hpo). (**e**) Cell proliferation is neither affected nor contributes to the regeneration at any stage of the process, for example, during transformation of regenerative membrane into intact body wall (36 hpo), white dashed line delimits regenerative membrane, orange arrowheads mark cells in S phase of cell cycle (EdU-positive cells), white arrowheads—cells in late G_2/M-phase of cell cycle (pH3-positive cells). (**f**) Apoptosis during early stages (3 hpo) of regeneration, white dashed line marks wound surface, white arrowheads mark apoptotic (TUNEL-positive) cells. (**g**, **h**) Spicule secretion in the regenerative membrane during its transformation into intact body wall (72 hpo), (**g**) general view under bright field microscopy, (**h**) epifluorescence view with FITC filter set with newly synthesized spicules showing bright green emission, white arrowheads marks the same spicules in (**g**) and (**h**). (**a**, **b**, **c**, **d**, **g**, **h**) WBR from an amputated oscular tube; (**e**) WBR from an amputated cormus tube; (**f**) body wall regeneration. Scale bars: (**a**) 200 μm, (**b**, **e**, **f**, **g**, **h**) 50 μm, (**c**, **d**) 5 μm. *ch* choanocyte, *en* endopinacocyte of regenerative membrane, *ex* exopinacocyte of intact tissue, *f* flagellum, *m* mesohyl, *mv* microvilli of choanocyte, *rm* regenerative membrane, *tch* transdifferentiated choanocyte, *wo* wound orifice

3. Hemocytometer.
4. Orbital shaker.
5. Sterile filtered seawater (FSW): filter fresh seawater through sterile 0.22 μm syringe filter with PES membrane.
6. Laboratory aquarium.
7. Stereomicroscope.
8. Inverted microscope with phase-contrast or DIC objectives.
9. Digital camera compatible with microscopes.
10. Thermo-controlling plate.
11. Glass-bottom Petri dishes.
12. Clearing agent like xylene or similar (e.g., Neo-Clear, Sigma-Aldrich) (*see* **Note 1**).
13. Paraffin waxes or similar (e.g., Paraplast, Sigma-Aldrich).
14. Bouin fixative: 15 mL saturated solution of picric acid, 5 mL 35–40% formalin, 1 mL 100% acetic acid. Store at RT.
15. 0.1 M Millonig phosphate buffer: 13 mM NaH_2PO_4, 87 mM Na_2HPO_4, 85.55 mM NaCl in distilled water, adjust pH to 7.4–7.5 with 0.1 M HCl. Store at 4 °C, shelf life—up to 1 month.
16. 0.1 M Na-Cacodylate buffer: 0.1 M Na-cacodylate, 85.55 mM NaCl, 5 mM $CaCl_2$, 5 mM $MgCl_2$ in distilled water, adjust pH to 7.0–7.5 with 0.1 M HCl. Store at RT, shelf life—virtually unlimited.
17. 10% (w/v) ruthenium red aquiferous solution: 0.1 g dry ruthenium red, 1 mL distilled water. Heat solution up to 60 °C for 20 min and cool to RT, centrifuge at max speed and accurately transfer supernatant into a new vessel. Store at 4 °C, shelf life—up to several months.
18. 2.5% (v/v) glutaraldehyde: 1 mL 25% commercially available glutaraldehyde aquiferous solution, 9 mL either buffer. Use freshly prepared or store at 4 °C, shelf life—up to 1 month (*see* **Note 2**).
19. 2.5% (v/v) glutaraldehyde +0.1% (w/v) ruthenium red in Na-Cacodylate buffer: 1 mL 25% commercially available glutaraldehyde aquiferous solution, 0.1 mL 10% (w/v) ruthenium red aquiferous solution, 8.9 mL 0.1 M Na-Cacodylate buffer. Use freshly prepared or store at 4 °C, shelf life—up to 1 month.
20. 1% (v/v) OsO_4: 1 mL 4% commercially available OsO_4 aquiferous solution, 3 mL either buffer. Use freshly prepared (*see* **Note 2**).
21. 1% (v/v) OsO_4 + 0.1% (w/v) ruthenium red in Na-Cacodylate buffer: 1 mL 4% commercially available OsO_4 aquiferous

solution, 0.04 mL 10% (w/v) ruthenium red aquiferous solution, 2.96 mL 0.1 M Na-Cacodylate buffer. Use freshly prepared.

22. 5% (w/v) ethylenediaminetetraacetic acid (EDTA) aquiferous solution: 5 g dry EDTA, 50 mL distilled water. Constantly mix with a magnetic stirrer and add 10 M NaOH drop by drop until EDTA completely dissolve, adjust pH to 7.5–8.0 with 1 M and 0.1 M NaOH, fill up to 100 mL with distilled water. Store at RT, shelf life—virtually unlimited.
23. Dehydration Mix 1 (DM1): 3 mL 96% ethanol, 1 mL acetone.
24. Dehydration Mix 2 (DM2): 2 mL 96% ethanol, 2 mL acetone.
25. Dehydration Mix 3 (DM3): 1 mL 96% ethanol, 3 mL acetone.
26. Infiltration Mix 1 (IM1): 2 mL acetone, 1 mL resin.
27. Infiltration Mix 2 (IM2): 2 mL acetone, 2 mL resin.
28. Infiltration Mix 3 (IM3): 1 mL acetone, 2 mL resin.
29. Toluidine blue—methylene blue mixture: 0.5 g sodium tetraborate, 0.5 g toluidine blue, 0.1 g methylene blue in 50 mL distilled water. Mix first the sodium tetraborate with a magnetic stirrer until sodium tetraborate completely dissolve, then add the toluidine blue and methylene blue. Mix with a magnetic stirrer until complete dissolution. Store in the dark at RT, shelf life—virtually unlimited.
30. 4% (w/v) uranyl acetate: 2 g uranyl acetate, 50 mL distilled water. Vigorously mix until completely dissolution. Store in the dark at 4 °C, shelf life—several months.
31. 0.4% (w/v) lead citrate: 0.2 g lead citrate, 50 mL distilled water, 0.5 mL 10 N NaOH. Vigorously mix until completely dissolution. Store in the dark at 4 °C, shelf life—several months.
32. 10× phosphate buffered saline (10× PBS): 1370 mM NaCl, 27 mM KCl, 100 mM Na_2HPO_4, 18 mM KH_2PO_4 in distilled water, adjust pH to 7.4–7.5 with 0.1 M HCl. Store at RT, shelf life—virtually unlimited.
33. 1× phosphate buffered saline (1× PBS): 10% (v/v) 10× PBS in distilled water. Store at 4 °C, shelf life—up to 1 month.
34. 16% (w/v) paraformaldehyde (PFA) aquiferous solution: 16 g PFA powder, 50 mL distilled water. Add several drops of 1 M NaOH, heat to 60 °C and mix on a magnetic stirrer until complete dissolution of the powder. Adjust pH to 7.4–7.5 with NaOH, fill up to 100 mL with distilled water. Store at 4 °C, shelf life—up to several months.
35. 4% PFA PBS: 1 mL 16% PFA aquiferous solution, 0.4 mL 10× PBS, 2.6 mL distilled water. Use freshly prepared or store at 4 °C, shelf life—up to 1 month (*see* **Note 2**).

36. 0.5% (v/v) Triton X-100 in PBS (PBSt): 0.5 mL Triton X-100, 99.5 mL 1× PBS. Store at 4 °C, shelf life—up to several months.
37. 1% (w/v) BSA PBS: 1 g BSA, 50 mL distilled water. Mix on a magnetic stirrer until complete dissolution, add 10 mL 10× PBS, fill up to 100 mL with distilled water. Filter solution through sterile 0.22-μm syringe filter with PES membrane into a sterile vessel. Store at 4 °C, shelf life—up to 1 month.
38. Blocking solution (BS): 1 g BSA, 0.1 g gelatin from cold water fish skin, 50 mL distilled water. Mix on a magnetic stirrer until complete dissolution of powders, add 0.5 mL Triton X-100, 0.05 mL Tween 20, 10 mL 10× PBS, fill up to 100 mL with distilled water. Filter solution through sterile 0.22-μm syringe filter with PES membrane into a sterile vessel. Store at 4 °C, shelf life—up to 1 month.
39. 30% (v/v) glycerol-PBS/DABCO: 0.25 g DABCO, 7 mL 1× PBS. Mix solution until complete dissolution, add 3 mL glycerol.
40. 60% (v/v) glycerol-PBS/DABCO: 0.25 g DABCO, 4 mL 1× PBS. Mix solution until complete dissolution, add 6 mL glycerol.
41. 90% (v/v) glycerol-PBS/DABCO: 0.25 g DABCO, 1 mL 1× PBS. Mix solution until complete dissolution, add 9 mL glycerol.
42. Anti-phospho-Histone H3 ($pSer^{10}$) primary antibodies produced in rabbit (e.g., H0412, Sigma-Aldrich).
43. Anti-acetylated-α-tubulin primary antibodies produced in mouse (e.g., T6793, Sigma-Aldrich).
44. Fluorescent conjugated anti-mouse (e.g., A21202, Thermo Fisher Scientific) and anti-rabbit (e.g., A-31573, Thermo Fisher Scientific) secondary antibodies.
45. 10 mM EdU stock solution: 50 mg EdU, 19.83 mL DMSO (cell culture grade). Aliquot solution in 500 μL and store at −20 °C, shelf life—up to several years.
46. 0.1 M $CuSO_4$ stock solution: 249.7 mg $CuSO_4 \bullet 5H_2O$, 10 mL distilled water. Store at 4 °C, shelf life—virtually unlimited.
47. 200 mg/mL sodium L-ascorbate stock solution: 2 g sodium L-ascorbate, 10 mL distilled water. Aliquot solution in 200 μL and store it at −20 °C, shelf life—up to several months.
48. 1 mM Sulfo-Cyanine3 Azide stock solution: 1 mg Sulfo-Cyanine3 azide, 1.357 mL distilled water. Aliquot solution in 10 μL and store it at −20 °C, shelf life—virtually unlimited.

49. Click-reaction cocktail: 850 μL 1× PBS, 40 μL 0.1 M $CuSO_4$, 10 μL 1 mM Sulfo-Cyanine3 azide, 100 μL 200 mg/mL sodium L-ascorbate (*see* **Note 3**).
50. TUNEL Imaging Kit (e.g., Click-iT TUNEL Imaging assay, Thermo Fisher Scientific, or In Situ Cell Death Detection Kit, Merck).
51. DNase reaction buffer: 0.1 M Tris–HCl, 25 mM $MgCl_2$, 1 mM $CaCl_2$ in Milli-Q grade water, adjust pH to 7.4–7.5 with 0.1 M HCl. Aliquot buffer in 1 mL and store at −20 °C, shelf life—up to several years.
52. 1 mg/mL aphidicolin stock solution: 1 mg dry aphidicolin, 1 mL DMSO. Aliquot solution in 10 μL and store at −20 °C, shelf life—up to several years.
53. 0.5 M hydroxyurea stock solution: 380 mg dry hydroxyurea, 10 mL distilled water. Aliquot solution in 100 μL and store at −20 °C, shelf life—up to several years.
54. 1 g/L Calcein disodium salt solution: 100 mg dry Calcein, 100 mL distilled water. Store at 4 °C, shelf life—up to several months.

3 Methods

3.1 Collection, Manipulation, and Laboratory Maintenance of Sponges

1. Collect sponges in the upper subtidal zone (0–2 m) at low tide with their brown algal substrate (*Ascophyllum, Fucus*).
2. During collection, pay special attention to avoid contact of the sponges with air.
3. Maintain collected sponges in a 100 L laboratory aquarium with natural seawater (daily change of half-volume) and biological filters at a temperature of 6–12 °C, not longer than 4 days (*see* **Note 4**).
4. Before surgery, clean the sponge thoroughly of detritus, epibionts, and fouling, using tweezers, soft brush, and pipetting, washed several times with a large volume of FSW.

3.2 Surgical Operations and Subsequent Cultivation

The surgical operations are carried out manually under a stereomicroscope, while a sponge is carefully supported with forceps. Four types of surgical operations were performed (Fig. 1b).

3.2.1 Excision of a Small Part

Approximately 0.3–0.5 × 0.3–0.5 cm^2 of the body wall is removed (*see* **Note 5**). It could be made in different parts of sponge: at the oscular tube, tubes of cormus or diverticula (Fig. 1b).

1. Make two oblique incisions using Castroviejo scissors to excise a square piece of the sponge body wall.

2. Remove the cut fragment from the Petri dish.
3. Maintain operated sponge in the Petri dish with FSW at 10–12 °C.
4. Change half of FSW with fresh one every 12 h.
5. Inspect and photograph the sponge using a stereomicroscope equipped with a digital camera to monitor regeneration processes. Observations should be done at 3, 6, 12, 18, 24, 36, 48 h postoperation (hpo), and then every 24 h.

3.2.2 Amputation of Oscular Tubes

Removal of an oscular tube (Fig. 1b). After this operation, the regeneration of the basal parts in the amputated oscular tubes could be studied.

1. Cut oscular tubes perpendicular to the main axis using scissors.
2. Remove sponge from the Petri dish.
3. Maintain the amputated oscular tubes in the Petri dish with FSW at 10–12 °C.
4. Change half of FSW with fresh one every 24 h.
5. Inspect and photograph the amputated oscular tubes as indicated above.

3.2.3 Whole-Body Regeneration

Excision and cultivation of fragments of the body wall (Fig. 1b 5) will allow for studying the whole-body regeneration (WBR) of the sponge.

1. Cut off numerous square fragments of the sponge body wall by oblique incisions using Castroviejo scissors.
2. Remove sponge from the Petri dish.
3. Maintain the fragments of the body wall in the Petri dish with FSW at 10–12 °C.
4. Change half of FSW with fresh one every 24 h.
5. Inspect and photograph the fragments of the body wall as indicated above.

3.2.4 Cell Reaggregation

This type of operation (Fig. 1b 6) (*see* **Note 6**) will allow for studying the WBR of the sponge:

1. Cut a sponge in small fragments with scalpel and forceps in FSW.
2. Squeeze fragments of sponge tissues through 50 μm nylon mesh into vessels with fresh FSW to obtain cell suspension.
3. Determine the cell concentration in the obtained suspension using a hemocytometer.

4. Dilute the obtained suspension with FSW up to concentrations of 1×10^7 to 3×10^7 cells/mL and cultured in 30 mm Petri dishes (5 mL of suspension in each dish).
5. Change half of FSW with fresh one every 48 h.
6. Inspect and photograph the cell aggregates as indicated above at 12, 24, 36, 48 h postdissociation (hpd), and then every 24 h.

3.3 Time-Lapse Recordings

Time-lapse recordings represent a useful tool for long-term continuous observations of regeneration processes (*see* **Note 7**).

1. Place a specimen in a Petri dish under a microscope and provide it with appropriate orientation, allowing for observation of a wound site (Fig. 2a).
2. Use a thermo-controlling plate for controlling the temperature of specimens, keeping it around the normal range for sponges.
3. Use a lateral moderate-intensity illumination as the main light source and the recording period of 0.5–5 min for time-lapse recording using a stereomicroscope.
4. Use objectives 20× and 40× allowing for phase-contrast or DIC observations and the recording period of 10–30 s for time-lapse recording using an inverted microscope.
5. Regularly check the recording scene to monitor the regeneration process stage, the orientation of a specimen, and a focal plane of a microscope.

3.4 Methods of Tissue Fixation and Processing for Histological Investigation

1. Fix in Bouin fixative for 2 h at room temperature (RT). Fixative volume should be at least tenfold higher than that of tissues.
2. Rinse specimens with 70% ethanol several times at RT until the yellow color disappear (*see* **Note 8**).
3. Dehydrate specimens in ethanol series (70–70–96–96%) for 15 min each stage at RT.
4. Dehydrate specimens three times in absolute ethanol 20 min each time at RT.
5. Incubate specimen twice in clearing agent for 1 h each time at RT.
6. Infiltrate specimens with the first wax for 1 h at 58 °C.
7. Infiltrate specimens with the second wax for 30 min at 58 °C.
8. Embed specimens in a fresh portion of wax in molds at RT.

3.5 Methods of Tissue Fixation and Processing for Transmission Electron Microscopy (TEM)

Two methods of fixations are possible: (a) for conventional observations and (b) for extracellular matrix (ECM) and cell junction studies (*see* **Note 9**). For conventional observation (Fig. 2b, c), the fixation and subsequent treatments can be done using either 0.1 M Millonig phosphate buffer or 0.1 M Na-Cacodylate buffer. Both

buffers provide equal quality of fixations. However, the same one should be used during fixation and treatments of a single specimen. Unless specified, all incubations and rinses are performed at RT "with shaking," that is, with constant orbital shaking at 70 rpm.

1. Fix tissues in 2.5% glutaraldehyde overnight at +4 °C without shaking.
2. Rinse specimens three times with the selected buffer, for 30 min each time.
3. Postfix specimens in 1% OsO_4 for 2 h at RT in the dark.
4. Rinse specimens three times with the selected buffer for 30 min each time.
5. Quickly rinse specimens with distilled water at RT.
6. Incubate specimens in 5% EDTA solution for calcareous spicule dissolution for 2 h (*see* **Note 10**).
7. Quickly rinse specimens with distilled water at RT.
8. Rinse specimens three times with the selected buffer for 30 min each time.

The fixation and subsequent treatments for ECM and cell junction visualization should be done using 0.1 M Na-Cacodylate buffer, as phosphate ions block ruthenium red interactions with tissues.

1. Fix tissues in 2.5% glutaraldehyde + 0.1% ruthenium red for 2 h at +4 °C without shaking (*see* **Note 11**).
2. Rinse specimens three times with the Na-cacodylate buffer for 30 min each time.
3. Postfix specimens in 1% OsO_4 + 0.1% ruthenium red for 3 h at RT (*see* **Note 11**).
4. Rinse specimens three times with the Na-cacodylate buffer for 30 min each time.
5. Quickly rinse specimens with distilled water at RT.
6. Incubate specimens in 5% EDTA solution for spicule dissolution for 2 h.
7. Quickly rinse specimens with distilled water at RT.
8. Rinse specimens three times with Na-cacodylate buffer for 30 min each time.

After fixation, specimens should be dehydrated and embedded "with shaking" until **step 14**:

9. Dehydrate specimens in ethanol series (10–20–30–40–50–60–70–70–82–96–96%) 15 min each stage at +4 °C.
10. Dehydrate specimens in dehydration mixes (DM1-DM2-DM3) 20 min each stage at +4 °C.

11. Dehydrate specimens twice in acetone 20 min each time.
12. Infiltrate specimens in infiltration mixes (IM1-IM2-IM3) 2–12 h each stage at +4 °C in tightly sealed containers.
13. Infiltrate specimens with resin in open containers for 6 h at RT.
14. Infiltrate specimens with fresh resin for additional 4 h at RT.
15. Fill a flat embedding mold with fresh resin without shaking.
16. Transfer specimens in the flat embedding mold and orient them properly.
17. Polymerize resin according to the manufacturer's instructions (typically 1–2 days at +60 °C).
18. Trim a resin block with a razor blade to remove excessive resin around the specimen and form a truncated pyramid.
19. Cut semithin sections 0.5–1 μm thick using an ultramicrotome (e.g., Leica EM UC6) and transfer then onto a clean object slide.
20. Stain semithin sections with toluidine blue—methylene blue mixture 30–90 s at +60 °C using a hotplate.
21. Wash stained sections twice with distilled water, dry them and make permanent preparation using the resin as a mounting medium.
22. Polymerize the resin in the permanent preparations for 1–2 days at +60 °C.
23. Study the preparations with a brightfield microscope (e.g., Leica DM2500) and localize the region of interest for TEM.
24. Cut ultrathin sections of the region of interest from the same resin block using an ultramicrotome and transfer them onto grids for electron microscopy.
25. Stain grids with 4% aqueous uranyl acetate for 30–60 min at +37 °C (*see* **Note 12**).
26. Carefully wash grids three times with distilled water and dry them.
27. Stain grids with 0.4% lead citrate for 15–30 min in the dark and in the presence of granulated NaOH at RT.
28. Carefully wash grids three times with distilled water and dry them.
29. Study grids with a transmission electron microscope.

The fixation, postfixation, and dehydration of specimens should be done as detailed in **steps 1–11** in Subheading 3.5 (*see* **Note 13**).

3.6 Methods of Tissue Fixation and Processing for Scanning Electron Microscopy (SEM)

1. Dry specimens in CO_2 critical point using critical point drier (e.g., Hitachi HCP-2).
2. Mount samples on metal specimen mounts or stabs with carbon adhesive glue, carbon adhesive tabs, or nail polish.
3. Metalize mounted specimens using ion coater (e.g., Eiko IB-3).
4. Study specimens using a scanning electron microscope (Fig. 2d).

3.7 Cell Proliferation and Immunohistochemical Studies

For cell proliferation studies, a combination of 5-ethynyl-2-′-deoxyuridine (EdU), labeling cells in S-phase of the cell cycle (DNA-synthesizing cells), and anti-phospho-histone H3 antibodies, labeling cells in lateG_2/M-phase of the cell cycle (dividing cells), is used (Fig. 2e). Unless specified, all incubations and rinses are performed at RT "with shaking," that is, with constant orbital shaking at 70 rpm.

1. Incubate alive regenerating specimens in a 30 mm plastic Petri dish with 5 mL of 20 μM EdU solution in FSW for 6 h at 10–14 °C without shaking (*see* **Notes 14** and **15**).
2. Rinse the specimens twice with fresh FSW, 10–15 min each time, at 10–14 °C.
3. Fix specimens with 4% PFA PBS for 2–12 h at 4 °C without shaking (*see* **Note 16**).
4. Rinse fixed specimens three times with 1× PBS, 30 min each time.
5. Incubate specimens in 5% EDTA solution for calcareous spicule dissolution for 2 h (*see* **Note 10**).
6. Rinse fixed specimens three times with 1× PBS, 30 min each time.
7. Incubate specimens twice in 1% BSA PBS, 20 min each time.
8. Permeabilize specimen with PBSt for 10–15 min.
9. Incubate specimens twice in 1% BSA PBS, 20 min each time.
10. Incubate specimens in freshly prepared Click-rection cocktail for 30–60 min in the dark.
11. Rinse specimens three times with BS, 1 h each time, in the dark.
12. Incubate specimens in the mix of primary antibodies, anti-phospho-histone H3 (rabbit; 1:500–1:1000 dilution) + anti-acetylated-α-tubulin (mouse; 1:1000–1:2000 dilution), in BS overnight in the dark at 4 °C (*see* **Notes 17** and **18**).
13. Rinse specimens twice with BS, 1 h each time, in the dark.
14. Incubate specimen in fresh BS overnight in the dark at 4 °C.

15. Incubate specimens in the mix of secondary antibodies, donkey anti-mouse IgG Alexa Fluor 488 (1:2000 dilution) + donkey anti-rabbit IgG Alexa Fluor 647 (1:2000 dilution), in BS overnight in the dark at 4 °C.
16. Rinse specimens twice with 1× PBS, 1 h each time, in the dark.
17. Incubate specimen in fresh 1× PBS overnight in the dark at 4 °C.
18. Counterstain nuclei with 2 μg/mL DAPI solution in 1× PBS for 1 h in the dark.
19. Rinse specimens three times with 1× PBS, 30 min each time, in the dark.
20. Infiltrate specimens in 30%–60%–90% glycerol-PBS/DABCO series, 30–60 min at each step (until specimens completely submerge into each solution) in the dark at RT without shaking.
21. Mount specimens in fresh 90% glycerol-PBS/DABCO, using small plasticine spacers in-between object and cover slide to avoid severe deformations of specimens.
22. Seal preparation with nail polish.
23. Study preparations with a confocal microscope using following (or close) excitation wavelengths: 405 nm (DAPI), 488 nm (acetylated-α-tubulin), 555 nm (EdU), 647 nm (phosphohistone H3) (*see* **Note 19**).

3.8 Cell Proliferation Blocking

1. Incubate sponge tissue in FSW with 1 μg/mL for aphidicolin or 5 mM for HU for at least 12 h at 10–12 °C to completely block cell proliferation (*see* **Notes 14** and **20**).
2. Change media every 12–24 h, maintaining a constant concentration of a blocking agent, if prolonged blocking is required.
3. Wash sponge tissues in a large volume of fresh FSW and incubate it for at least 24 h at 10–12 °C to release cell proliferation.

3.9 Apoptosis Studies

The following protocol is a slightly modified manufacturer's protocol for Click-iT TUNEL Imaging assay (Thermo Fisher Scientific) and In Situ Cell Death Detection Kit (Merck) (*see* **Notes 21** and **22**). Unless specified, all incubations and rinses are performed at RT "with shaking," that is, with constant orbital shaking at 70 rpm.

1. Fix specimens with 4% PFA PBS for 2–12 h at 4 °C without shaking (*see* **Note 16**).
2. Rinse fixed specimens three times with 1× PBS, 30 min each time.
3. Incubate specimens in 5% EDTA solution for calcareous spicule dissolution for 2 h (*see* **Note 10**).

4. Rinse fixed specimens three times with 1× PBS, 30 min each time.
5. Permeabilize specimens with PBSt for 20 min.
6. Rinse fixed specimens three times with 1× PBS, 10 min each time.
7. Incubate specimens in TdT buffer for 30 min.
8. Incubate specimens in TdT-cocktail for 8–12 h (*see* **Notes 23** and **24**).
9. Skip **steps 10** and **11** if not using the Click-iT TUNEL Imaging assay (Thermo Fisher Scientific).
10. Incubate specimens twice in 3% BSA PBS, 10 min each time.
11. Incubate specimens in freshly prepared Click-reaction cocktail for 30–60 min in the dark (*see* **Note 24**).
12. Rinse fixed specimens three times with 1× PBS, 30 min each time, in the dark.
13. Counterstain nuclei with 2 μg/mL DAPI solution in 1× PBS for 1 h in the dark.
14. Rinse specimens three times with 1× PBS, 30 min each time, in the dark.
15. Infiltrate specimens in 30%–60%–90% glycerol-PBS/DABCO sequence, 30–60 min at each step (until specimens completely submerge into each solution) in the dark at RT without shaking.
16. Mount specimens in fresh 90% glycerol-PBS/DABCO, using small plasticine spacers in-between object and cover slide to avoid severe deformations of specimens.
17. Seal preparation with nail polish.
18. Study preparations with a confocal microscope using 405 nm excitation wavelengths for DAPI and excitation wavelength recommended in the manufacturer's protocol for apoptotic cells (Fig. 2f) (*see* **Note 19**).

3.10 Skeleton Synthesis Studies

As spicules of *Leucosolenia* are composed of calcium carbonate ($CaCO_3$), their synthesis could be visualized in vivo, using Calcein disodium salt solution (*see* **Note 25**).

1. Incubate regenerating specimen in 100 mg/L Calcein disodium salt solution in FSW at 10–12 °C (*see* **Note 14**).
2. Rinse specimen twice with FSW, 10 min each time at 10–12 °C.
3. Study specimen in an epifluorescent microscope, using a standard FITC filter set (Fig. 2g, h) (*see* **Note 25**).

4 Notes

1. Many reagents used in the protocols are health hazardous and requires safety precautions. All fixative solutions (glutaraldehyde, OsO_4, PFA, Bouin fixative) should be manipulated with laboratory gloves to avoid damaging skin and in a fume hood, as they are corrosive to the respiratory tract. Similar precautions should be kept during work with acids and alkali. Uranyl acetate is a radioactive substance. DAPI and EdU incorporate in DNA and aphidicolin and HU interferes with DNA synthesis, thus these reagents could potentially have carcinogenic effects.
2. Properly prepared solutions are the first essential step in any protocol. Storage conditions and the state of solutions are no less important. Always check state of solutions before applying them to specimens: all solutions should be clean, without any precipitate or other foreign particles. While the majority of solutions could be preliminary prepared and stored in the appropriate conditions, some of them are recommended to use freshly prepared. We highly recommend using all aldehyde-based fixatives (2.5% glutaraldehyde and 4% PFA PBS) freshly prepared. OsO_4-based fixatives must be used only freshly prepared, as OsO_4 is quickly reduced in solution, becoming ineffective for tissue fixation.
3. The way of the preparation of the Click-cocktail for Click-reaction is essential. This solution should be freshly prepared for each treatment, and the reagents should be added into 1× PBS in the strict order: $CuSO_4$, Sulfo-Cyanine3 Azide, sodium L-ascorbate; otherwise, the reaction will not proceed. After the addition of $CuSO_4$, some precipitate can appear; this precipitate should dissolve after the addition of sodium L-ascorbate. The stock solution of sodium L-ascorbate should be light-ochre. If the solution changes color to dark-ochre or brown during storage, it should be discarded.
4. A successful experimental study of any organism in a laboratory usually requires adaptation of widely known protocols. Firstly, the conditions during maintaining and experimental manipulation with an organism should be similar to the natural conditions in which the organism lives. In the case of *L. variabilis* from the White Sea, we use natural seawater and maintain physiological for the sponge range of temperatures (6–12 °C). Secondly, all solutions for fixations and treatments should be adopted to the water salinity normal to the studied organism. Here we use solutions adapted to the salinity of 25–26‰ (~750–800 mOsm).
5. The reparative regeneration of the body wall is the best-studied regeneration process in *Leucosolenia* (Fig. 1b1). This type of

regeneration occurs after the excision of a small part of the body wall or amputation of an oscular tube. The process ends within 4–6 days post-operation (hpo) with complete restoration of the lost body wall. Three main stages could be distinguished in this type of regeneration: (1) internal milieu isolation (3—12 hpo), (2) wound orifice healing (regenerative membrane formation) (12—24 hpo) (Fig. 2a), and (3) transformation of the regenerative membrane into an intact body wall (48—144 hpo) [13].

6. Every cell suspension for cell reaggregation experiments should be obtained from only one individual to avoid undesired allorecognition effects. The optimal cell concentrations in obtained suspensions are 1×10^7 to 3×10^7 cells/mL. The cell reaggregation will be slowed or even impossible with lower concentrations, while higher concentrations will lead to the formation of single large cell aggregate with low viability [27, 28]. We also recommend maintaining cell cultures on an orbital shaker (70 rpm) for the first 24 h for intensification the cell reaggregation process.
7. Time-lapse recordings represent a powerful instrument for directly assessing morphogenetic events and cellular behavior in a living specimen. Depending on the level at which a regeneration process should be observed, time-lapse recordings could be done using either a stereomicroscope or inverted microscope equipped with a digital camera. Time-lapse recording made with stereomicroscope allows for making a general description of the regeneration process and some morphogenetic events, while recordings with an inverted microscope allow for observing the behavior of single cells. The maintaining of appropriate conditions for a living specimen during long-term time-lapse recordings is of paramount importance. For constant temperature management in microscope systems, thermo-controlling plates represent the best solution. However, a microscope for time-lapse recordings could be placed directly to thermo-stable conditions: into a fridge (for smaller microscope models) or cold-room (for large microscope models). Additionally, the medium in which a specimen is maintained should be periodically changed with fresh one.

   The illumination is no less important. Not all light sources are equally suitable to observe living specimens, especially long term during time-lapse recordings. Avoid using heating light sources, as they will quickly raise the temperature of a specimen. Also, pay attention to the wavelength profile of a light source, as a light source with high intensities in the “blue” part of the spectrum may have deleterious effects on a living specimen. For time-lapse recording with a stereomicroscope, a lateral illumination gives a better contrast to the specimens. It also

could be combined with transmission illumination. The light intensity should be set to a moderate level, as too bright illumination could negatively affect the viability of a specimen. The optimal recording period depends on the studied process: the quicker process—the shorter period should be used. Usually, a set of preliminary recordings are required to determine the optimal period.

8. Complete rinse of specimens after Bouin fixative with 70% ethanol could take up to several days.
9. For the best fixation quality for transmission electron microscopy, specimens should be treated and embedded in resin as soon as possible. However, if necessary, specimens can be stored in the buffer after postfixation or spicule dissolution for weeks and in 96% ethanol after dehydration for days. The storage temperature should be +4 °C.
10. Spicule dissolution with 5% EDTA solution is appropriate only for calcium carbonate spicules. If you study demosponges, hexactinellids, or homoscleromorphs with silica spicules, use 4–10% HF solution to dissolve spicules. If you study a sponge without an inorganic skeleton, omit step with spicule dissolution.
11. Pay special attention to the fixation timing in the protocol of ECM and cell junction fixation for electron microscopy, as it is essential to successful results (especially postfixation in buffered 1% OsO_4 + 0.1% ruthenium red).
12. During the staining of ultrathin sections, special attention should be paid to avoid the appearance of dust on the sections. We recommend working in a laboratory with minimal air movement. Wash working space before the start of the staining, and filter all used solutions (including distilled water) with 0.22 μm syringe filters with PES membrane. The uranyl acetate is a radioactive substance and requires special precautions during working with. Otherwise, it could be substituted with nonradioactive analogs (e.g., UranyLess EMS). Special attention should be paid to minimize contact of lead citrate solution (especially during staining) with air. Lead citrate will form an insoluble precipitate upon interaction with air CO_2. We recommend staining ultrathin sections with lead citrate in close Petri dish in the presence of granulated NaOH, which will reduce CO_2 concentration in the dish. In general, staining with lead citrate could be omitted, but ultrathin sections stained with it will show more contrast.
13. If it is necessary to retain spicules for scanning electron microscopy studies, the **steps 5–8** in Subheading 3.5 should be omitted.

14. After the addition of a reagent into the FSW with a living specimen, mix the solution well by pipetting or short incubation (10–20 min) on an orbital shaker (70 rpm). It is especially important for reagents with stock solutions made in DMSO.
15. Several technical control specimens should be used to control the quality of EdU staining and correctly interpret obtained Z-stacks, discriminating between specific and unspecific signals:
    (a) Negative control specimen (NCS), an alive regenerating specimen, which is incubated in DMSO solution in FSW at **step 1** (instead of EdU solution, as in experimental specimens). Each batch of experimental specimens should be supplemented with NCS. Incubate NCS in a 30 mm plastic Petri dish with 5 mL of FSW supplemented with DMSO for 6 h at 10–14 °C in parallel with the experimental specimens according to Subheading 3.7. The volume of added DMSO is equal to the volume of the EdU stock solution added to the experimental specimens. After incubation, treat NCS similarly to experimental specimens. The staining patterns in EdU-channel (555 nm) in NCS should be recognized as unspecific, and similar patterns in experimental specimens should not be considered.
    (b) Positive control specimen (PCS), any alive specimen, which admittedly contains DNA-synthesizing cells. We recommend supplying each batch of experimental specimens with PCS. Treat PSC similarly and parallel to the experimental specimens, starting from **step 1** of Subheading 3.7. If, during the study with a confocal microscope PCS shows, no EdU-positive cells, then experimental specimens should be discarded as some issues with EdU incubation or Click-reaction arose.
16. Specimens fixed for cell proliferation studies could be stored up to 6 months and for immunohistochemical studies—up to 1–6 months, depending on an antigen of interest. Storage conditions: 4% PFA PBS, 4 °C. Specimens for apoptosis studies should be processed as soon as possible, as prolonged storage could lead to the intensive DNA fragmentation and, subsequently, to the false-positive results of TUNEL assay.
17. The sponge tissues could be studied by immunohistochemical methods, using antibodies. Although no sponge-specific primary antibodies are commercially available, numerous commercial primary antibodies, recognizing epitopes in various vertebrates and invertebrates, work properly in sponge tissues.

Immunohistochemical studies could be done in parallel with EdU cell proliferation studies (in this case, apply primary and secondary antibodies at **steps 10** and **12** in Subheading 3.7, respectively) or separately (in this case, omit **steps 1–2**, **5**, and **7–8** in Subheading 3.7).

At least at several first treatments, two negative control specimens should be used to control the quality of immunohistochemical staining and correctly interpret obtained Z-stacks, discriminating between specific and unspecific signals:

(a) Primary antibodies NCS. Incubate this specimen in BS instead of primary antibodies at **step 10**.

(b) Secondary antibodies NCS. Incubate this specimen in BS instead of secondary antibodies at **step 12**.

(c) The staining patterns in both NCS should be recognized as unspecific, and similar patterns in experimental specimens should not be considered.

18. If several primary antibodies are used in immunohistochemical studies, they should be produced in different host species (mouse, rabbit, chicken, etc.). In turn, secondary antibodies should be chosen according to host specificity of primary antibodies and carry fluorescent dyes with excitation wavelengths not overlapping with each other and Click-reaction azide (in the case of parallel staining with EdU).

19. Preparations of stained specimens for cell proliferation, apoptosis, or immunohistochemical studies could be stored up for 1–2 months in the dark at 4 °C.

20. Functional tests are an essential step required to make conclusions about the involvement of cell proliferation into a regenerative process. Two chemical agents, aphidicolin and hydroxyurea (HU), allow for complete blocking of cell proliferation at S phase of the cell cycle in intact and regenerating tissue of *L. variabilis*. Aphidicolin is a reversible inhibitor of DNA polymerase α and δ, while HU is a reversible inhibitor of ribonucleotide reductase (RNR). The minimal effective concentrations were determined as 1 μg/mL for aphidicolin and 5 mM for HU. Both agents do not show evident negative effects on the general viability of sponges even during prolonged expositions up to 5 days. 0.5 M HU stock solution could be prepared directly in FSW, instead of distilled water.

21. Two commercially available apoptosis detection kits, which use TUNEL assay, are suitable for sponge tissues: Click-iT TUNEL Imaging assay (Thermo Fisher Scientific) and In Situ Cell Death Detection Kit (Merck). Both kits label double-strand DNA breaks generated during the late stages of

apoptosis. In Situ Cell Death Detection Kit is based on one-step labeling through the incorporation of dUTP conjugated with fluorescent dye in cell DNA at double-strand break sites. In turn, Click-iT TUNEL Imaging assay is based on two-step labeling: at the first step, dUTP modified with alkyne (EdUTP) is incorporated in cell DNA at double-strand break sites, at the second—Click-reaction visualizes EdUTP with Alexa Fluor azide. While In Situ Cell Death Detection Kit offers simpler and shorter treatments, Click-iT TUNEL Imaging assay gets an advantage of better penetration in tissue due to the small size of both EdUTP and Alexa Fluor azide.

22. Two technical control specimens should be used to control the quality of TUNEL staining and correctly interpret obtained Z-stacks, discriminating between specific and unspecific signals:
    (a) Negative control specimen (NCS), a specimen, in which the TdT reaction at **step 6** is blocked. Treat NCS similarly to experimental specimens but incubate it TdT-cocktail devoid of TdT-enzyme. The staining patterns in TUNEL-channel in NCS should be recognized as unspecific, and similar patterns in experimental specimens should not be considered.
    (b) DNase positive control specimen (DNase-PCS), a specimen (intact sponge tissues), in which dsDNA breaks are artificially introduced by DNase I. Treat DNase-PCS similarly to experimental specimens but incubate it in DNase I solution containing 1–2 U of the enzyme for 30 min at 37 °C immediately prior to **step 5**. DNase I incubation solution could be prepared by mixing commercially available DNase I enzyme, 10× DNase reaction buffer, and appropriate volume of MilliQ. After DNase treatment, rinse DNase-PCS three times with 1× PBS, 10 min each time, and proceed to **step 5**.
    (c) As DNase I is highly volatile, to avoid contamination of experimental samples with it (which will generate pseudo-positive staining) use a separate set of instruments for manipulations with DNase-PCS. If during the study with a confocal microscope, DNase-PCS shows no TUNEL-positive cells, then experimental specimens should be discarded as some issues with TdT-reaction or Click-reaction arose.
23. TUNEL assay for apoptotic cell detection is based on an enzymatic reaction of TdT. DNase-PC processing also includes an enzymatic reaction of DNase I. The activity of both enzymes highly depends on the storage conditions and could vary from batch to batch. Thus, if you have issues with TUNEL assay, you

should try to change enzymes on fresh ones. Also, you could try to extend the duration of enzymatic reactions and raise reaction temperature to 37 °C.

24. The composition and preparation instructions for TdT- and Click-iT cocktails vary in Click-iT TUNEL Imaging assay (Thermo Fisher Scientific) and In Situ Cell Death Detection Kit (Merck) and should be checked in the manufacturer's protocol for a particular kit. Use only Milli-Q grade water to prepare both cocktails.
25. Only Calcein disodium salt (not Calcein-AM) is appropriate for in vivo studies of spicule synthesis. The stock solution of Calcein disodium salt solution could be prepared directly in FSW, instead of distilled water. Incubation time in Calcein solution could be varied: short incubation time (several hours) is suitable for studies of spicule synthesis rate, prolonged incubation time (1–2 days)—for studies localization of spicule synthesis sites and description of general patterns of skeleton restoration. If needed, after in vivo study, the specimen could be further incubated in the Calcein solution for additional labeling. Alternatively, specimens could be fixed and processed for immunohistochemical studies (*see* Subheading 3.7; omit **step 5** in this protocol to retain spicules in the specimen).

Acknowledgments

We gratefully thank our colleagues Fyodor Bolshakov, Veronika Frolova, Nikolai Melnikov, Ksenia Skorentseva, Alexandra Koynova, and Igor Kosevich (Moscow State University, Russia); Daria Tokina and Ilia Borisenko (Saint-Petersburg State University, Russia); and Emilie Le Goff and Stephen Baghdiguian (Université de Montpellier, France) for their invaluable advices and help. The light microscopy studies were conducted using equipment of the Center of microscopy WSBS MSU, electron microscopy studies—in the Electron Microscopy Laboratory of the Shared Facilities Center of Lomonosov Moscow State University sponsored by the RF Ministry of Education and the Common Service of morphology in IMBE, France. We are also indebted to the COST Action 16203 MARISTEM, which facilitated author discussions over the course of its periodic meetings. Studies were supported by the grants of the Russian Science Foundation no. 17-14-01089 (in vivo regeneration experiments), RFBR nos. 19-04-563 and 19-04-00545, and Fund of President RF no. MK-1096.2021.1.4.

References

1. Simion P, Philippe H, Baurain D, Jager M, Richter DJ, Di Franco A, Roure B, Satoh N, Quéinnec É, Ereskovsky AV et al (2017) A large and consistent Phylogenomic dataset supports sponges as the sister group to all other animals. Curr Biol 27:1–10. https://doi.org/10.1016/j.cub.2017.02.031
2. Simpson TL (1984) The cell biology of sponges. Springer-Verlag, New York
3. Ereskovsky A, Lavrov A (2021) Porifera. In: LaDouceur EB (ed) Invertebrate histology. John Wiley & Sons, Inc. (In press)
4. Morganti TM, Ribes M, Yahel G, Coma R (2019) Size is the major determinant of pumping rates in marine sponges. Front Physiol 10: 1474. https://doi.org/10.3389/fphys.2019.01474
5. Gaino E, Burlando B (1990) Sponge cell motility: a model system for the study of morphogenetic processes. Boll Zool 57:109–118
6. Bond C (1992) Continuous cell movements rearrange anatomical structures in intact sponges. J Exper Zool 263:284–302
7. Gaino E, Manconi R, Pronzato R (1995) Organizational plasticity as a successful conservative tactics in sponges. Anim Biol 4:31–43
8. Maldonado M, Uriz MJ (1999) An experimental approach to the ecological significance of microhabitat-scale movement in an encrusting sponge. Mar Ecol Prog Ser 185:239–255
9. Galera J, Turton X, Uriz MJ, Becerro M (2000) Microstructure variation in sponges sharing growth form: the encrusting demosponges *Dysidea fragilis* and *Crambe*. Acta Zool 81:93–107
10. Ereskovsky AV, Borisenko IE, Lapébie P, Gazave E, Tokina DB, Borchiellini C (2015) *Oscarella lobularis* (Homoscleromorpha, Porifera) regeneration: epithelial morphogenesis and metaplasia. PLoS One 10(8):e0134566. https://doi.org/10.1371/journal.pone.0134566
11. Ereskovsky AV, Tokina DB, Saidov DM, Baghdiguian S, Le Goff E, Lavrov AI (2020) Transdifferentiation and mesenchymal-to-epithelial transition during regeneration in Demospongiae (Porifera). J Exp Zool Pt B: Mol Dev Evol 334:37–58. https://doi.org/10.1002/jez.b.22919
12. Borisenko IE, Adamska M, Tokina DB, Ereskovsky AV (2015) Transdifferentiation is a driving force of regeneration in *Halisarca dujardini* (Demospongiae, Porifera). PeerJ 3: e1211. https://doi.org/10.7717/peerj.1211
13. Lavrov AI, Bolshakov FV, Tokina DB, Ereskovsky AV (2018) Sewing wounds up: the epithelial morphogenesis as a central mechanism of calcaronean sponge regeneration. J Exp Zool Pt B: Mol Dev Evol 330:351–371. https://doi.org/10.1002/jezb.22830
14. Korotkova GP (1997) Regeneration in animals. Saint-Petersburg University Press, Saint-Petersburg. [in Russian]
15. Alexander BE, Achlatis M, Osinga R, van der Geest HG, Cleutjens JPM et al (2015) Cell kinetics during regeneration in the sponge *Halisarca caerulea*: how local is the response to tissue damage? PeerJ 3:e820. https://doi.org/10.7717/peerj.820
16. Borisenko IE, Adamski M, Ereskovsky AV, Adamska M (2016) Surprisingly rich repertoire of Wnt genes in the demosponge *Halisarca dujardini*. BMC Evol Biol 16:123
17. Kenny NJ, de Goeij JM, de Bakker DM, Whalen CG, Berezikov E, Riesgo A (2017) Towards the identification of ancestrally shared regenerative mechanisms across the Metazoa: a transcriptomic case study in the demosponge *Halisarca caerulea*. Mar Genom 44:1–35
18. Thiney Y (1972) Morphologie et cytochimie ultrastructurale de l'oscule d'Hippospongia communis LMK et de sa régénération (Ph.D. thesis, University Claude Bernard, Lyon)
19. Ereskovsky AV, Lavrov AI, Bolshakov FV, Tokina DB (2017) Regeneration in White Sea sponge *Leucosolenia complicata* (Porifera), (Calcarea). Invert Zool 14:108–113. https://doi.org/10.15298/invertzool.14.2.02
20. Korotkova GP (1961a) Regeneration and somatic embryogenesis in the calcareous sponge *Leucosolenia complicata* Mont. Acta Biol Acad Sci Hungar 11:315–334
21. Jones WC (1957) The contractility and healing behaviour of pieces of Leucosotenia complicata. Quart J Microsc Sci 98:203–217
22. Korotkova GP (1961b) Regeneration and cellular proliferation in calcareous sponge *Leucosolenia complicata* Mont. Vestnik Leningr Univ 4:39–50. [in Russian]
23. Korotkova GP (1962) Behaviour of the cellular elements in the calcareous sponge *Leucosolenia complicata* Mont. During regeneration. Acta Biol Acad Sci Hungar 13:1–30
24. Korotkova GP (1969) Peculiarities of morphogenesis during the development of the calcareous sponge *Leucosolenia complicata* Mont. From a small pieces of the body wall. Vestnik Leningr Univ 15:15–22. [in Russian]

25. Korotkova GP, Gelihovskaia MA (1963) Recherches Experimentales sur le Phenomene de Polarite Chez les Eponges Calcaires du Type Ascon. Cah Biol Mar 4:47–60
26. Ereskovsky A, Borisenko IE, Bolshakov FV, Lavrov AI (2021) Whole-body regeneration in sponges: diversity, fine mechanisms, and future prospects. Genes 12(4):506. https://doi.org/10.3390/genes12040506
27. Lavrov AI, 2016. The ability of sponges from Demospongiae and Calcarea to develop after tissue dissociation. Ph.D. thesis, Lomonosov Moscow State University. [in Russian]
28. Lavrov AI, Kosevich IA (2016) Sponge cell reaggregation: cellular structure and morphogenetic potencies of multicellular aggregates. J Exp Zool A Ecol Genet Physiol 325:158–177

Open Access This chapter is licensed under the terms of the Creative Commons Attribution 4.0 International License (http://creativecommons.org/licenses/by/4.0/), which permits use, sharing, adaptation, distribution and reproduction in any medium or format, as long as you give appropriate credit to the original author(s) and the source, provide a link to the Creative Commons license and indicate if changes were made.

The images or other third party material in this chapter are included in the chapter's Creative Commons license, unless indicated otherwise in a credit line to the material. If material is not included in the chapter's Creative Commons license and your intended use is not permitted by statutory regulation or exceeds the permitted use, you will need to obtain permission directly from the copyright holder.





Chapter 5

Studying Ctenophora WBR Using *Mnemiopsis leidyi*

Julia Ramon-Mateu, Allison Edgar, Dorothy Mitchell, and Mark Q. Martindale

Abstract

Ctenophores, also known as comb jellies, are a clade of fragile holopelagic, carnivorous marine invertebrates, that represent one of the most ancient extant groups of multicellular animals. Ctenophores show a remarkable ability to regenerate in the adult form, being capable of replacing all body parts (i.e., whole-body regeneration) after loss/amputation. With many favorable experimental features (optical clarity, stereotyped cell lineage, multiple cell types), a full genome sequence available and their early branching phylogenetic position, ctenophores are well placed to provide information about the evolution of regenerative ability throughout the Metazoa. Here, we provide a collection of detailed protocols for use of the lobate ctenophore *Mnemiopsis leidyi* to study whole-body regeneration, including specimen collection, husbandry, surgical manipulation, and imaging techniques.

Key words Ctenophore, *Mnemiopsis leidyi*, Wound healing, Whole-body regeneration, Husbandry, Surgeries, Live imaging, Time-lapse

1 Introduction

While regenerative capabilities are common across the animal kingdom, the ability to regenerate all the structures of the body (i.e., whole-body regeneration) is a rather unique feature only found in some species. Ctenophores (comb jellies) are one such animal with impressive whole-body regenerative capabilities; they are holopelagic, carnivorous marine invertebrates that represent one of the oldest extant metazoan lineages [1]. Ctenophores have a unique body plan characterized by a biradial symmetry (with no planes of mirror symmetry) and one primary body axis (the oral–aboral axis) delimited by a mouth (oral) and an apical sensory organ (aboral). The ctenophore body is composed of two epithelial layers: the ectoderm—including the epidermis, apical organ, pharynx, nerve net, ctene plates (or comb plates), and tentacle sheath—and the endoderm primarily composed of a system of endodermal canals that distribute nutrients to the periphery of the animal. The

Simon Blanchoud and Brigitte Galliot (eds.), *Whole-Body Regeneration: Methods and Protocols*, Methods in Molecular Biology, vol. 2450, https://doi.org/10.1007/978-1-0716-2172-1_5, © The Author(s) 2022

ectodermal and endodermal tissues are separated by a thick mesoglea mostly composed of extracellular matrix, but also containing several types of individual muscle and mesenchymal cells [2]. The characteristics of the mesoglea differ between ctenophore species. For example, in *Pleurobrachia* species (the sea gooseberry), the mesoglea is rather rigid, while in lobate ctenophores the mesoglea is highly pliable, presumably due to differences in hydration characteristics. Ctenophores' main mode of locomotion is via the coordinated beating of their comb plates. They possess eight longitudinally oriented rows of locomotory ctene plates, each plate composed of thousands of laterally arranged cilia which they coordinately beat to propel through the water column. Ctenophores have been accurately described morphologically for over a century, with the first volume of the *Flora and Fauna of the Statione de Napoli* being dedicated to Ctenophora by one of the world's first experimental embryologists, Carl Chun [3].

One of the best-studied species of ctenophores in the regenerative field is the lobate ctenophore *Mnemiopsis leidyi* [4–10]. Like the majority of ctenophores [11], *M. leidyi* is a self-fertile hermaphrodite, meaning that a single animal carries both female and male gonads. The eggs and sperm are released freely into a common sinus under each comb row and fertilization takes place upon release into the water column [12]. Like most ctenophores, *M. leidyi* produces embryos which are optically clear and, like all ctenophores, it has a very stereotyped, clade-specific cleavage program where rounds of division occur every 20 min at room temperature and the juvenile cydippid stage hatches from the fertilization envelope within 18–24 h after the first cleavage [13–15]. The cydippid is a feeding form characterized by a pair of long branching muscular tentacles that define the tentacular axis and bear specialized adhesive cells called colloblasts, used to capture prey [16, 17]. In lobate ctenophores like *Mnemiopsis*, the tentacles are progressively reduced and internalized during the transition to adulthood as the animal forms two large oral lobes that are extremely efficient at prey capture (Fig. 1). Under optimal conditions, the adult form can get sexually mature at ~4 weeks of age, though sexual reproduction at the juvenile morphological stage, termed "dissogeny," has been documented as early as 2 weeks [18, 19].

Our recent study shows that in *M. leidyi* cell proliferation is activated (after wound-healing) at the wound site and is indispensable for whole-body regeneration. EdU pulse and chase experiments after surgery together with the removal of the two main regions of active cell proliferation suggest a local source of cells in the replacement of missing structures. Time-lapse live imaging during *M. leidyi* wound healing shows evidence of cells forming actin-based protrusions while migrating to the wound site [10]. While lobate ctenophores show an outstanding capacity to

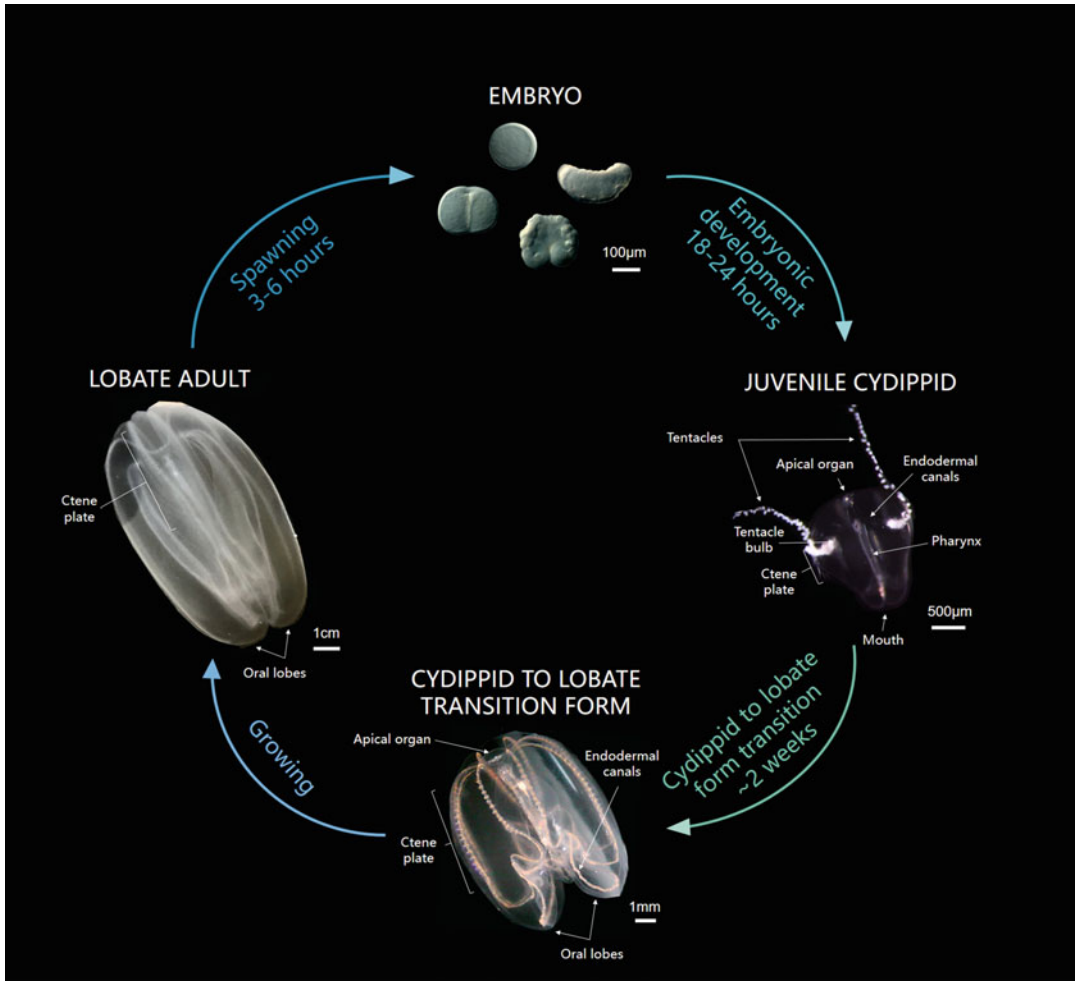


Fig. 1 The life cycle of *Mnemiopsis leidyi*. The adult body plan is referred to as "lobate," describing their prey-capture tissues (oral lobes) that extend from the oral end. Adults produce both eggs and sperm. Embryos are ~150 µm in diameter and develop from single cell to hatching over ~24 h. The hatched, free-swimming feeding juvenile body plan is referred to as "cydippid" and characterized by a relatively shortened body and long prey-capture tentacles. The cydippids will start to transition into the lobate body plan as their tentacles retract, body lengthens and lobes form. Adult lobates will continue to grow until they reach a maximum size of around 6–18 cm

regenerate all body parts, another group of ctenophores, the Beroids, have lost the ability to regenerate [9]. Hence, the comparison of cellular and molecular responses after amputation between lobate ctenophores and Beroids provides an ideal system to elucidate the core cellular and molecular responses required for the process (and loss) of adult regenerative potential.

The many favorable experimental features provided by ctenophores (optical clarity, stereotyped cell lineage, multiple cell types, sequenced genome available [20], comparative and functional

genomics [21–27], rapid regeneration (48–72 h) and their early branching phylogenetic position (potentially the earliest extant animal clade [1, 20, 28, 29]) make them a new powerful research organism for the study of regeneration at a cellular and evolutionary level. Here we provide a detailed protocol to use ctenophores to study the process of whole-body regeneration from the collection of specimens and husbandry in the laboratory to the deployment of basic techniques for the study and monitoring of regeneration at a cellular level.

2 Materials

2.1 Equipment

1. Ctenophore dipper: 1 L plastic beaker fixed at the tip of a 2-meter pole (Fig. 2A).
2. 20 L plastic bucket.
3. Ctenophore tank system: 200 L tank made of plexiglass (PMMA) walls consisting of an inner tank module enclosed between two outer compartments with drains both at the bottom and the top of the tank (Fig. 2B, C).
4. 6″ diameter glass bowls (Fig. 3).
5. 2 L glass beaker (Fig. 3).
6. 1 mL transfer plastic pipettes.
7. Rotifer culture system: 2 L glass beaker, a 5 × 5 cm piece of rotifer floss (e.g., Reed Mariculture, Inc), air pump (e.g., Tetra Whisper Aquarium Air Pump) connected by plastic tubing to a 1 mL serological pipette.
8. A coarse filter: 30-μm nylon mesh screening (e.g., Nitex) affixed to a section of pipe or plastic container with the bottom removed.
9. *Artemia* hatching system: 1.5 L plastic cone with a stopcock (valve) at the bottom placed inside a support, aeration system made from a 1 mL plastic pipette attached at one end to a plastic tube connected to a standard aquarium air pump from the other end.
10. Operating dish: 35-mm plastic petri dish, coated with a 2-mm thick silicon (SYLGARD-184) layer.
11. Microburner: 16-gauge syringe needle inserted into latex tubing attached to a propane source (Fig. 4A).
12. Pulled glass needles from Pyrex capillaries (Fig. 4A).
13. Pair of fine forceps (e.g., World Precision Instruments, Cat#500341).
14. Siliconized slide: microscope glass slide treated with a synthetic hydrophobic surface-applied product (e.g., Rain-X, Inc.).

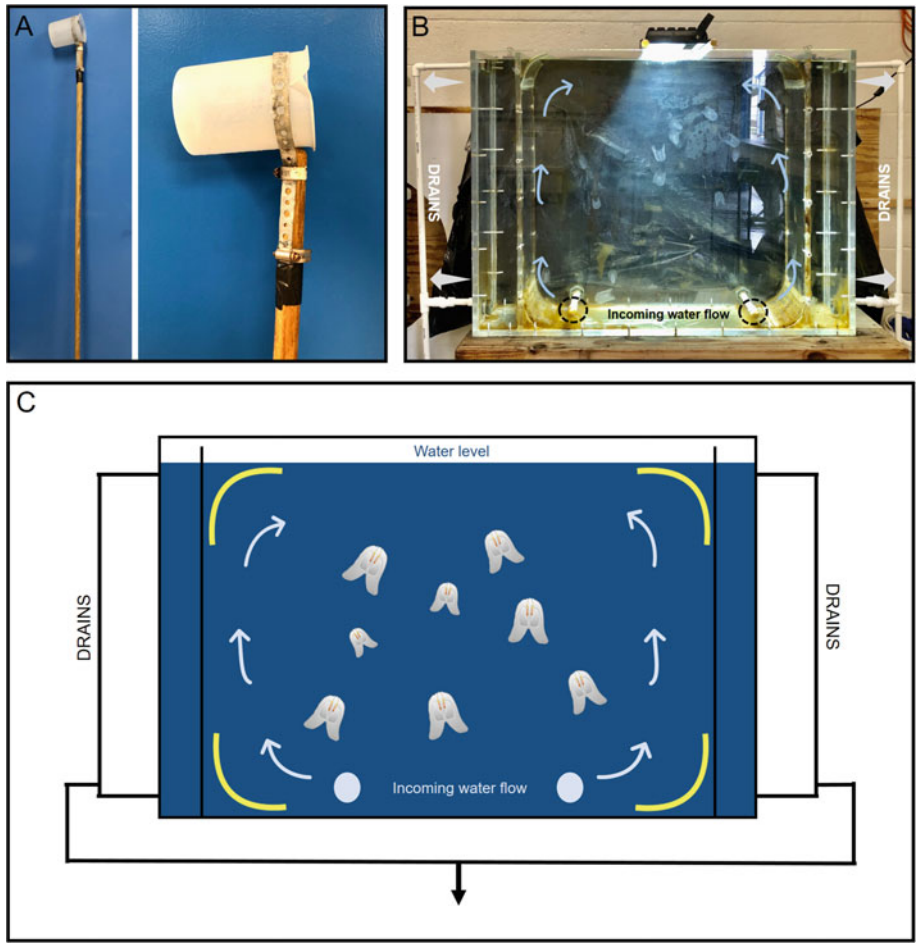


Fig. 2 Ctenophore collection and culturing materials. **(A)** A "ctenophore dipper" constructed to collect ctenophores from the field. Ctenophores located close to the surface of the water are gently scooped into the beaker portion of the dipper. (**B**) The pseudo-kreisel tank system used to contain adult ctenophores. (**C**) Diagram of a pseudo-kreisel tank system for culturing adult *M. leidyi* at the lab. Two water inlets located in the tank bottom generate a continuous flow that pushes water up the sides of the tank. Drains on the top and bottom of each side displace the input of water, while two partially perforated plexiglass sheets contain the animals in the central space. The flow of water keeps the ctenophores toward the tank's center, while constant water flow through the system prevents fouling

15. 35-mm plastic petri dishes.
16. Dissection microscope.
17. Microscope attached to a time-lapse camera—We use a Zeiss M2 Axio Imager coupled with a Rolera EM-C2 camera.

2.2 Reagents

1. 1× UV-FSW: UV treated 1.0-μm filtered full strength seawater (e.g., 35 g/L).
2. 1× 0.2-μm UV-FSW: UV treated 0.2-μm filtered full strength seawater.

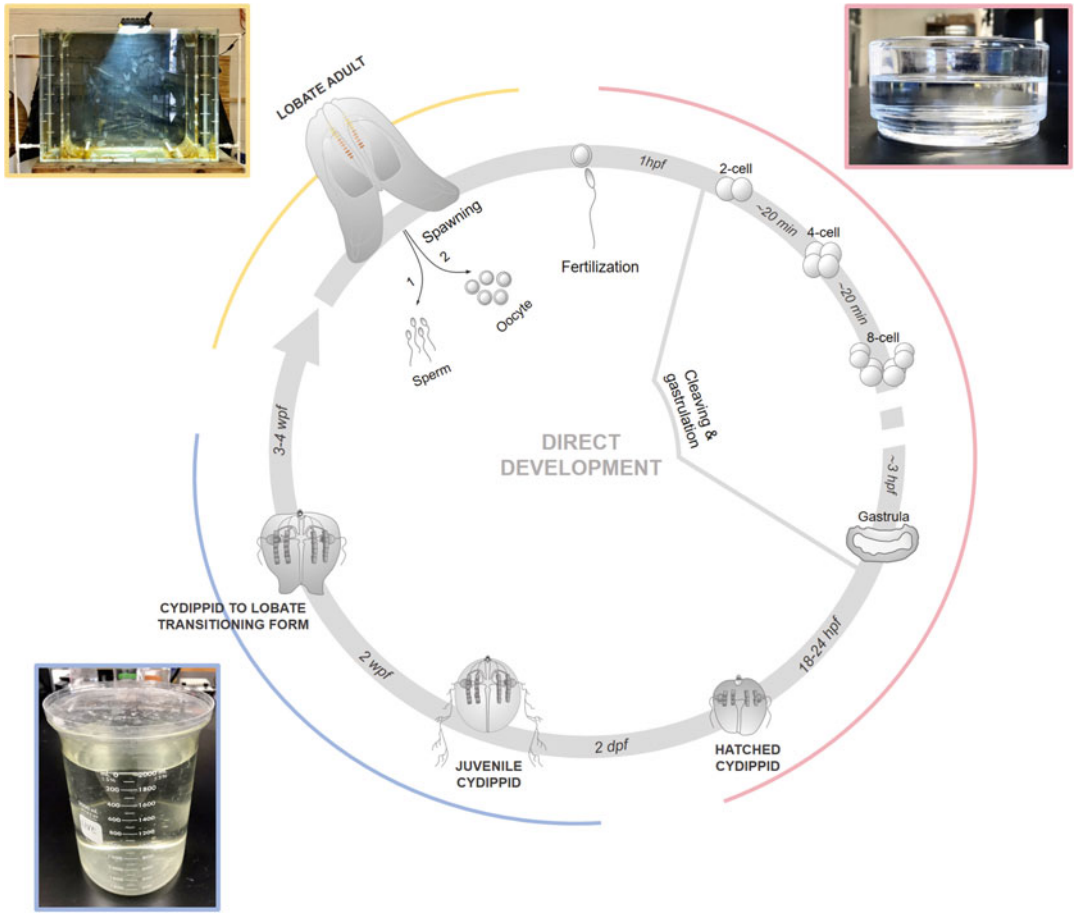


Fig. 3 Husbandry and culture of *Mnemiopsis leidyi*. Culturing conditions for each stage of the *M. leidyi* life cycle. Spawning is induced in wild-caught or captive adults by manipulating their light exposure. Embryos are collected and placed in a 6″ diameter glass finger bowl in 1× UV-FSW. Hatching occurs 18–24 h post-fertilization (hpf). Hatched cydippids (*M. leidyi* juveniles) are grown in 2 L glass beakers to provide space for hunting behavior as their tentacles tend to get tangled with other individuals in smaller containers. Cydippids grow into adults in the next 3–4 weeks postfertilization as they grow in size, retract their tentacles, and develop oral lobes for prey capture

3. 20 ppt FSW: 500 mL 1× UV-FSW, 500 mL deionized water (*see* **Note 1**).
4. Rotifers: one million *Brachionus plicatilis* (L-type) starting bag.
5. Concentrated microalgal based rotifer feed (e.g., RGcomplete, Reed Mariculture, USA). Store at 4 °C.
6. *Artemia* nauplii larvae. We use *Artemia franciscana* from Great Salt Lake Origin (www.brineshrimpdirect.com).
7. Mysid shrimps (*Americamysis bahia*, U.S. Mysids, Saint Augustine, FL USA).

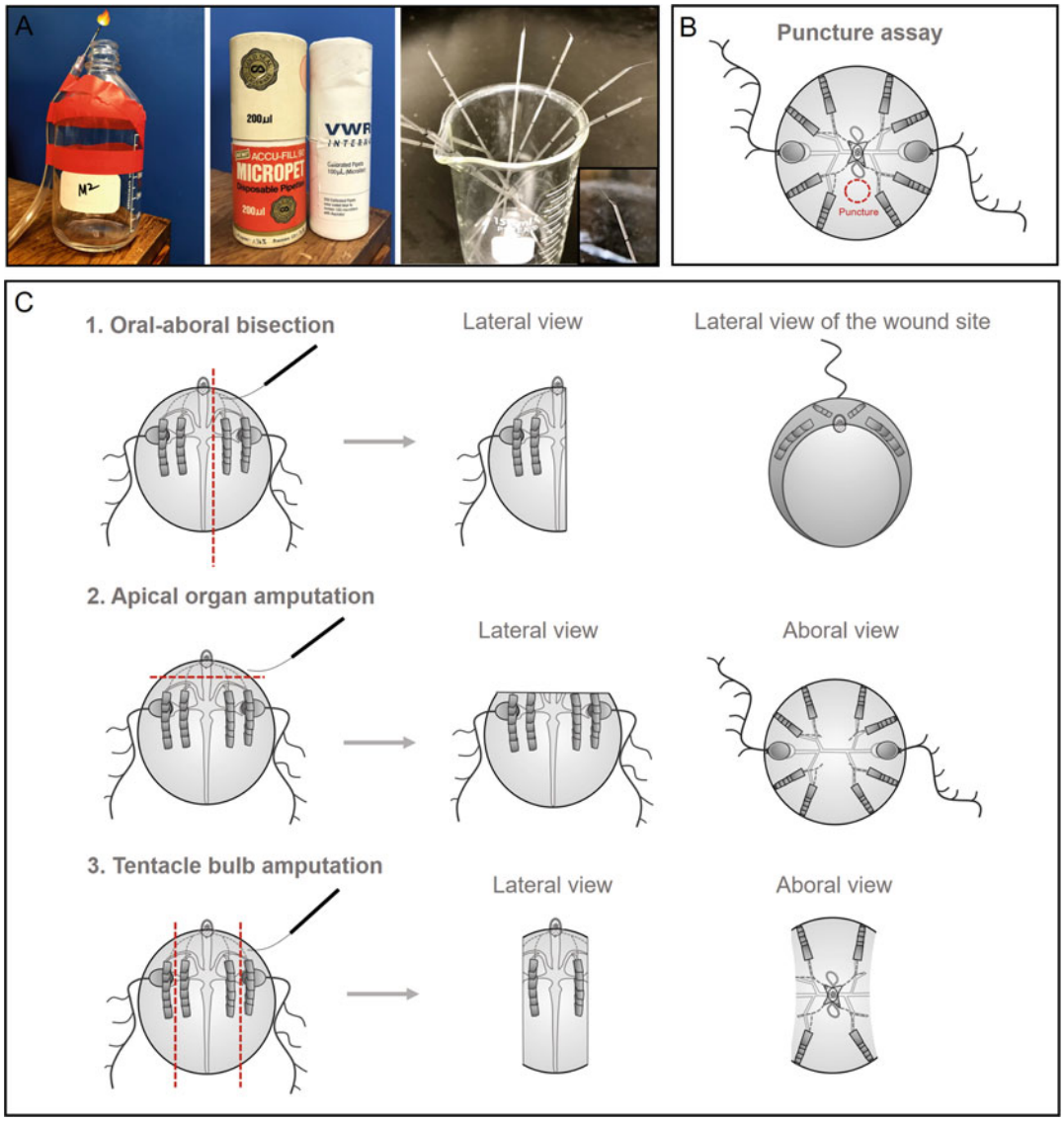


Fig. 4 Methods for ctenophore tissue regeneration assays. (**A**) Surgery instruments. Glass needles are hand-pulled using a microburner. (**B**) Puncture assay for *M. leidyi* cydippids. Tissue is punctured in a space that is clear of organs (tentacle bulb, comb rows, etc.) to assay wound healing of the epithelia. (**C**) Designs for multiple types of amputations. Oral–aboral bisection is performed by cutting tissue parallel to the esophageal canal and slightly to the side of the apical organ. This is so one half of the animal maintains an intact apical organ, as it is more likely to regenerate with this feature. Apical organ amputation includes cutting the space between the top of the comb rows and the base of the apical organ. Careful attention should be taken to ensure that the canals connected to the comb rows are not damaged. Tentacle bulb amputation requires cutting tissue between two adjacent comb rows, cutting out one or both tentacle bulbs on either side of the body and leaving behind 4 of the 8 comb rows. Make sure the tentacle bulbs are completely removed, including the dense cluster of cells at the base of the bulb

8. 100× hydroxyurea (HU) stock solution: 500 mM HU in distilled water. 1 mL aliquots can be kept at −20 °C for several months. Keep at 4 °C once thawed.
9. 1× HU: 100× HU stock solution in 1× UV-FSW.
10. 25 °C low-melt agarose (e.g., Sea-Plaque).
11. 1.2% (w/v) low-melt agarose in 1× UV-FSW.
12. 1× PBS: 137 mM NaCl, 2.7 mM KCl, 10 mM Na_2HPO_4, 1.8 mM KH_2PO_4 in 800 mL of H_2O. Adjust the pH to 7.4 with HCl, add H_2O to 1 L. Autoclave and store at room temperature (*see* **Note 2**).
13. Fixative solution: 100 mM HEPES-HCl, pH 6.9, 0.05 M EGTA, 5 mM $MgSO_4$, 200 mM NaCl, 1× PBS, 3.7% (w/v) formaldehyde (e.g., Sigma-Aldrich, #F8775), 0.2% (v/v) glutaraldehyde (e.g., EMS #16216), 0.2% (v/v) Triton X-100 (e.g., Sigma-Aldrich,#X100-500ML) in 1× 0.2-μm UV-FSW.
14. PBS-0.02% Triton X-100: 0.02% (v/v) Triton X-100 in 1× PBS.
15. Optically transparent jammed microgel: 7.5% (w/w) azobisisobutyronitrile and *N*′-methylene bisacrylamide microgel dried powder dispersed in 1× 0.2-μm UV-FSW. Kept at 4 °C. *See* [10] for details on microgel elaboration.
16. Mounting clay for microscope slides.
17. Vaseline.

3 Methods

3.1 Sources and Collection

We collect *M. leidyi* on the northeast coast of Florida, around the Saint Augustine area where the University of Florida's Whitney Lab for Marine Bioscience is located. The confluence of the Matanzas intercoastal river with the Atlantic Ocean creates a system of estuarine saline waters which favors the appearance of *M. leidyi* specimens all year long. *M. leidyi* can also be found in coastal waters along the Atlantic coast of North and South America and it has become an invasive species in European waters through ballast water introduction, most notably in the Black Sea, eastern Mediterranean, and Caspian Sea [30]. Collecting ctenophores is an art, but once an experienced collector has seen several in the wild it is relatively easy to find them.

1. Choose optimal environmental conditions for ctenophore collection (*see* **Notes 3** and **4**).
2. Navigate to a calm marine area (*see* **Note 5**).
3. Orient yourself with the sun at your back.

4. Spot ctenophores by the light reflection generated by the movement of the comb plates creating a colorful rainbow-like iridescence running down the comb rows or from food in the gut.
5. Collect the animal using the ctenophore dipper (Fig. 2A, *see* **Note 6**).
6. Transfer the specimen into a plastic bucket filled with seawater (*see* **Note 6**).
7. Repeat **steps 4–6** until sufficient specimens are collected (*see* **Note 7**).
8. Transfer the ctenophores to the laboratory.

3.2 Laboratory Setup for Mnemiopsis leidyi *Culture*

Different culturing systems have been optimized for each *M. leidyi* life cycle stage. Adult specimens prefer to move vertically on an hourly regime, so keeping them in a large volume, with a tall height aspect to cross sectional area is optimal. If adult animals are allowed to interact with the bottom surface of their container, they will erode their epidermal surface and die. For example, *M. leidyi* can be kept in 20 L buckets for short periods of time as long as the water is changed once or twice daily, but after several days animals will start to deteriorate. The ideal situation is to keep them in a tank installed in open sea water system room at ambient temperatures that allows continual sea water circulation keeping adults off tank surfaces. Hatchlings and juvenile cydippid stages can be grown and cultured in the laboratory (room temperature, 20–22 °C) in a variety of different types of glassware, but low-density cultures (~1 embryo/5 mL) are preferred. Generally, we dilute embryonic cultures to 2× larger volumes every 2–3 days to give them more space to set their tentacles and feed (*see* Subheading 3.4).

We keep both *M. leidyi* and the atentaculate *Beroe ovata* in pseudo-kreisel tanks made of clear 2 cm thick plexiglass sheets connected with stainless steel screws and sealed with silicone, that generate a circular flow which keeps animals suspended in the water column. In the pseudo-kreisel depicted (Fig. 2C), the inner tank module where the animals are kept is 90 cm in diameter and has rounded corners with small perforations allowing water to exchange into two outer compartments (10 cm each) that have drains both at the top (that also serve as water level overflows) and the bottom of the tank. Upwelling inlets at the bottom of the inner tank introduce fresh sea water and direct it to the edges. By controlling the volume of water entering and exiting the tank, the overall position of the ctenophores can be controlled. For example, if the flow rate is too high, all of the animals are concentrated in the center of the tank and if it is too low the animals may sink to the bottom. The optimal flow rate allows animals to swim freely but prevents them from approaching the bottom because abrasion of

ctenophore epidermis on the bottom of the tank causes wounds that lead to death. Incoming seawater at Whitney is naturally sand filtered and devoid of zooplankton or phytoplankton.

Water quality is important for the successful culturing of ctenophore embryos and adults. We routinely rear embryos and early hatched cydippids in glass bowls (Fig. 3) filled with 1× UV-FSW until they reach ~1.5–2 mm diameter (1 week old). They are then transferred to 2 L glass beakers in order to give them more vertical space for swimming and feeding and are kept in this container until they transition into the lobate state (Fig. 3) (*see* Subheading 3.4).

3.3 *Culturing Live Feed for* Mnemiopsis leidyi *Husbandry*

Juvenile and adult ctenophores feed on zooplankton present in the water column. Adults typically feed on copepods and other pelagic organisms (including larval fish). In captivity, the best first food source for *M. leidyi* is rotifers (e.g., *Brachionus plicatilis)* because of their small size and the ability of *M. leidyi* cydippids to catch them with their tentacles. We feed adults with *Artemia* and/or mysid shrimp daily. Note that feeding *Mnemiopsis* on *Artemia* is not sufficient to maintain reproductive ability, so mysids must be fed at least 1–2 times per week and ideally daily. Other labs use fish eggs and larvae rather than mysids. This nutritional requirement is currently a bottleneck in the rearing of reproductive colonies of *Mnemiopsis* in laboratory culture (*see* **Notes 8–10**).

A small-scale rotifer culture is sufficient to cover the feeding regimes of growing cydippids. We follow the instructions provided by the supplier (Reed Mariculture, Inc) except that we keep a smaller culture volume (*see* **Note 11**).

1. Fill two separate rotifer culture systems with 1 L of 20 ppt FSW.
2. Place the closed rotifer starting bag in the culture system.
3. Wait 30 min for the animals to acclimate.
4. Open the bag releasing the rotifers into each beaker.
5. Top up each beaker with 20 ppt FSW.
6. Shake the microalgal concentrate rotifer feed.
7. Pipette 2 mL of microalgal concentrate into each beaker.
8. Wait 6 h for the rotifers to feed.
9. Repeat **steps 6** and **7** to feed the rotifers again.
10. Wait 24 h for the culture to expand, feeding twice per day (morning and afternoon).
11. To harvest fresh rotifers, filter ~30–40% (600 mL) of the culture through the coarse 30-μm nylon mesh.
12. Backwash the mesh into a small glass beaker using a squirt bottle filled with 10 mL 1× UV-FSW.

13. Use these isolated rotifers to feed the juvenile ctenophores (Subheading 3.4). Stir rotifers with a plastic transfer pipette to make concentration uniform before feeding.
14. Repeat **steps 6–13** to culture the rotifers for a week.
15. Pour the cultures into clean 2 L glass beakers avoiding the transfer of waste deposited at the bottom.
16. Clean the glass beaker wiping the green residue on the sides and bottom with deionized water, avoiding any kind of soap.
17. Repeat **steps 14–16** for three more weeks.
18. For deeper cleaning, once a month, filter the whole culture through the 30-micron nylon mesh.
19. Backwash the mesh into two clean 2 L glass beaker filled with 20 ppt FSW.
20. Feed the clean culture following **steps 6** and **7**. It is convenient to perform the cleaning before feedings.
21. Follow **steps 11** and **12** to isolate a backup culture of rotifers.
22. Pipette 5 mL of microalgal concentrate into the backup culture.
23. The backup culture may be kept uncovered at 4 °C for a week.
24. Repeat **steps 6–23** to maintain the rotifer culture.

We use just-hatched *Artemia* to complement the diet of growing cydippids once they reach a certain size (Subheading 3.4) as well as to feed adult ctenophores.

1. Set up the *Artemia* hatching system by placing the plastic cone inside a support.
2. Fill the hatchery cone with 1 L of 1/3× FSW.
3. Add 6.5 g/L of *Artemia* cysts to the hatchery cone.
4. Start the aeration system.
5. Incubate for 20 h.
6. Stop the aeration, turn on the light source and wait for 5 min for the unhatched cysts to sink and accumulate at the bottom of the cone (*see* **Note 12**).
7. Open the water flow using the valve at the end of the cone to discard the unhatched cysts.
8. Collect hatched *Artemia* nauplii larvae from the bottom of the cone.
9. Use these isolated *Artemia* to feed growing cydippids and adult ctenophores (*see* Subheading 3.4).

We use mysid shrimps to feed adult ctenophores (*see* Subheading 3.4). We obtain the mysids directly from a shrimp farm and feed adult specimens with ~2 mysid shrimps per ctenophore twice a week (*see* **Note 13**).

3.4 Spawning and Husbandry of *Mnemiopsis leidyi*

M. leidyi has a natural circadian rhythm and spawns according to the light-dark cycle. Our protocol for *M. leidyi* spawning at the Whitney Lab in St. Augustine, FL. has been modified from Pang and Martindale, 2008 [31]. Under normal summer conditions in Cape Cod, MA (Woods Hole), *M. leidyi* spawning is triggered by the onset of darkness and it normally occurs ~8 h after sunset. In northeast Florida, spawning occurs after 3–4 h of darkness. In order to get *M. leidyi* to spawn at any time of the day, we keep animals under constant light conditions and then place them in the dark to induce spawning. It takes 2–3 days of constant light exposure to erase the endogenous circadian rhythm of wild caught animals so they reliably spawn 3–4 h after putting them in the dark. When spawning freshly caught specimens, wild caught adult ctenophores are kept in a 20 L bucket filled with 1× UV-FSW in the laboratory under constant light for 48–72 h (more detailed protocol in [32]). Here we describe the protocol to spawn adult ctenophores cultured in captivity at the lab. All steps are performed at room temperature (20–22 °C).

1. Take adult lobate stage animals from the tank and transfer them into a plastic bucket filled with fresh 1× UV-FSW using a plastic or glass beaker (*see* **Note 14**).
2. Transfer the specimens into individual 6″ glass culture bowls filled with fresh 1× UV-FSW. We place 2 ctenophores per bowl when specimens are ~5 cm long, up to three animals if they are smaller or only one for larger animals (*see* **Notes 15** and **16**).
3. Repeat **step 2** to fill 4 more bowls with adult ctenophores (*see* **Note 17**).
4. Place the bowls into complete darkness (*see* **Note 18**).
5. Wait 3 h for the animals to start spawning.
6. Check for cloudy meridional canals which indicate the presence of sperm (*see* **Notes 19** and **20**).
7. Wait 20–30 min for spawning to complete.
8. Transfer up to 200 fertilized embryos with a transfer pipette into a 6″ bowl filled with fresh 1× UV-FSW.
9. Cover the glass bowl with a plastic lid to avoid evaporation of water.
10. Place the bowl at room temperature in the lab.
11. Return the adult specimens to the pseudo-kreisel tank (*see* **Notes 21** and **22**).
12. Repeat **steps 8–10** to process all the fertilized embryos.
13. Wait for 24 h for the embryos to hatch (*see* **Note 23**).

14. Transfer about two freshly isolated rotifers (*see* Subheading 3.3) per embryo in each bowl within 24 h after fertilization to ensure food availability immediately after hatching.
15. Wait for 24 h for cydippids to grow.
16. Transfer 1-day old cydippids using a plastic transfer pipette into a clean glass bowl filled with fresh 1× UV-FSW (*see* **Notes 24** and **25**).
17. Feed about two freshly rotifers isolated per cydippid in each bowl.
18. Repeat **steps 15–17** for three more days.
19. Transfer 4-day old cydippids (about ~1.5–2 mm in size) into a 2 L glass vertical beaker (*see* **Note 26**).
20. Complement feeding with just-hatched *Artemia* nauplii larvae (1 *Artemia* per cydippid, *see* Subheading 3.3). Alternate rotifer and *Artemia* feedings every other day (*see* **Note 27**). This is a convenient size to perform regeneration experiments (*see* **Note 28**) (*see* Subheading 3.5).
21. Wait 12–24 h for animals to feed.
22. Clean the cultures by transferring the animals into a clean 2 L glass beaker filled with fresh 1× UV-FSW.
23. Repeat **steps 19–22** for two more weeks (*see* **Note 29**).
24. Transfer the lobate stage ctenophores into the ctenophore adult tank using a beaker.
25. Feed lobate ctenophores with a diet combining *Artemia*, mysid shrimps, and wild zooplankton and/or fish larvae if possible (*see* Subheading 3.3).

3.5 Animal Surgeries to Study Wound Healing and Whole-Body Regeneration

Although lobate stage adults have a high capacity to regenerate, we utilize *M. leidyi* cydippid stages due to their smaller size, speed of complete regeneration, and ease of visualization [5].

1. Use the microburner to hand-pull several Pyrex glass needles utilized for surgical operations (*see* **Notes 30–32**).
2. Collect cydippids of 1.5–3 mm diameter (~6–14 days postfertilization) and place them in a separate small glass dish (*see* **Note 33**).

Follow the steps described below according to the type of operation. All operations are performed at room temperature (20–22 °C).

Puncture assay (Fig. 4B):

3. Place one cydippid in a small drop of water on a siliconized microscope slide.

4. Using a pair of sharp forceps, puncture the animal by pinching the epithelium layer.
5. Check for the presence of an epithelial gap with the edges of the wound forming a small gap (diameter ~200–400 μm), exposing the mesoglea (*see* **Note 34**) [10].
6. Immediately after puncture, mount animals for live imaging (*see* Subheading 3.7 for details).

Whole-body regeneration studies (WBR):

7. Transfer cydippids using a plastic or glass pipette larger than the diameter of the specimen to an operating dish filled with just enough 1× 0.2-μm UV-FSW to cover the specimens (*see* **Note 35**).

We use three types of operations to recover all the structures/cell types of the cydippid's body.

8. To perform **oral–aboral bisections**, cut the cydippid longitudinally through the esophageal plane generating two "half animals" (*see* **Note 36**). The operations are performed such that one half retains an intact apical organ while the remaining half lacks the apical organ. Only the halves retaining the apical organ are kept for studies of WBR as these halves regenerate to whole animals in a high percentage of the cases (Fig. 4C) [5, 10]. Oral–aboral cuts that lack the apical organ either regenerate complete animals, or remain as "half" animals [5, 33] (*see* **Note 37**).
9. To perform **apical organ amputations,** remove the whole apical organ structure (including the entire statolith system, dome cilia and ciliated grooves) by cutting perpendicular to the oral–aboral axis above the level of the tentacle bulbs (Fig. 4C).
10. To perform **tentacle bulb amputations**, dissect the epidermis surrounding the tentacle bulb so the entire sheath and endodermal tentacular canal are removed (Fig. 4C) [10].
11. Transfer operated cydippids into a 35-mm plastic petri dish filled with 1× 0.2-μm UV-FSW using a pipette larger than the diameter of the specimen.
12. Clean operated cydippids once a day every day during regeneration by transferring them into a new small plastic petri dish filled with fresh 1× 0.2-μm UV-FSW (*see* **Notes 38** and **39**).

3.6 Cell Proliferation Inhibitor Treatment with Hydroxyurea (HU)

The role of cell proliferation in replacement of missing cell types was first proposed by TH Morgan more than 100 years ago [34]. Cell proliferation inhibitor experiments are a straightforward way to evaluate the requirement of cell proliferation in regeneration. We expose amputated cydippids to hydroxyurea (HU) treatments, a drug that inhibits cell proliferation by inhibiting the ribonucleotide reductase enzyme and thereby arresting cells in S-phase [35].

1. Prepare a 500 mM stock solution of HU by dissolving HU powder in distilled water.
2. Dilute the HU stock 1:100 to a working concentration of 5 mM in 1× UV-FSW (*see* **Note 40**). Once you have thawed an aliquot of stock solution for use, keep it at 4 °C.
3. Add 3 mL of 5 mM HU into a 35 mm plastic petri dish and transfer the amputated cydippids (not more than 50 per dish) (*see* **Note 41**).
4. Incubate HU treatments at room temperature for the desired time (*see* **Note 42**).
5. Replace HU working solution with fresh HU every 12 h (*see* **Note 43**).
6. You may now process the animals with downstream treatments like fixation (*see* Subheading 3.7) or wash out the HU to continue the experiment with living animals (*see* **Notes 44** and **45**).

3.7 Fixation of Mnemiopsis leidyi *Cydippids*

The gelatinous body of *M. leidyi* cydippids is mostly composed of mesoglea with varying osmotic proprieties, which makes standard fixation protocols challenging; standard fixative preparations in direct contact with the cydippid's body generate osmotic changes that cause the structural mesoglea to collapse and tissue to disintegrate. To preserve both the cellular and gross anatomic integrity, we use a fixation protocol based on embedding of specimens in a low melting point agarose [32].

1. Melt the 1.2% low melt agarose by warming the solution to 30 °C in a water bath (*see* **Notes 46** and **47**).
2. Place the specimens with the minimum volume (~10 μL FSW) in a 35-mm plastic petri dish.
3. Carefully add 100 μL of liquid agarose (approximately 10:1 agar:water drop volume) to the specimens (*see* **Note 48**).
4. Mix well but gently until the mixtures is homogenous and the specimens are fully embedded into the agar.
5. Let the embedded cydippids in agar cool for ~2 min (*see* **Note 49**).
6. Carefully place a coverslip over the agar drop and press down to form an agar lamina of homogenous thickness with the cydippids embedded inside. This step will facilitate mounting for microscopy.
7. Let the agar cool completely by incubating the petri dish on ice for ~5 min.
8. Once the agar is solidified, carefully remove the coverslip with forceps to allow better penetration of the fixative solution.

9. Add 3 mL of ice-cold fixative solution to the plastic petri dish (*see* **Note 50**).
10. Incubate for 1.5–2 h on a rocking platform at room temperature.
11. Discard the fixative solution and wash twice with PBS-0.02% Triton X-100 for 10 min on a rocking platform at room temperature.
12. Using a razor blade, carefully cut the agar lamina into cubes such that each cube contains an intact cydippid.
13. Transfer the agar cubes into a 2 mL tube using a plastic transfer pipette with a widened opening.
14. Specimens may now be labeled as desired. Fixed cydippids are kept in agar for all downstream preparations.

3.8 Live Imaging During Wound Healing and Regeneration

The remarkable optical clarity and small size of *M. leidyi* cydippids make them an ideal system for live-imaging experiments. Here we describe a combination of differential interference contrast (DIC) live-imaging and time-lapse techniques to monitor wound healing. *M. leidyi* wound healing involves cell migration and formation of actin-based cellular protrusions, resulting in a scar-less wound epithelium [10]. Under normal conditions wound healing is completed in around 30 min to 1 h after injury, depending on the size of the cut.

1. Place one punctured cydippid on a siliconized slide in the minimum volume (~10 μL drop of FSW).
2. Immobilize the animal by slowly applying 100 μL of optically transparent jammed microgel around the drop of water.
3. Carefully mix using the pipette tip until the specimen is surrounded by homogenous microgel (*see* **Note 51**).
4. Using a pair of fine forceps, orient the animal so that the epithelial wound faces upward (*see* **Note 52**).
5. Prepare a coverslip with clay feet on each of the four corners and place it over the preparation.
6. Press down the coverslip gently, being careful not to overcompress the animal.
7. For longer live-imaging times (>2 h), seal the edges of the coverslip with Vaseline to prevent evaporation (*see* **Note 53**).
8. Mount the slide on the microscope for image acquisition.
9. Locate the specimen using the bright-field mode of your microscope in ocular position and a low magnification objective (e.g., 5× or 10×).
10. Bring the region of interest (wound gap) into focus.

11. Change to a higher 20× magnification objective for wound-healing time-lapse experiments (*see* **Note 54**).
12. We recommend acquiring a z-stack at each time point. The z-stack should go into the mesoglea in order to visualize migration of cells from the mesoglea to the wound edges (*see* **Note 55**).
13. We found wound healing to be sufficiently resolved with a time-lapse setting of 30 s to 1-min intervals over 2 h.

4 Notes

1. Ratios of FSW: deionized water might need to be adapted depending on the starting salinity of the seawater.
2. PBS can be made directly as a 1× solution or diluted 1/10 from a 10× PBS stock solution.
3. Optimal conditions for ctenophore collection consist of a clear, sunny day (to avoid cloud reflections in the water) with no wind and slow water currents at ebb tide.
4. The best time of the day for collecting is when the sun is high in the sky and at your back. Polarized sunglasses can improve visibility.
5. Ctenophores swim to the surface of the water column during sunny hours, however, even the slightest wave action will make them sink to calmer water.
6. Ctenophores are extremely fragile animals and care must be taken to avoid touching specimens with nets or bare hands which could damage their outer epidermis. They should always be kept submerged and transferred gently between containers (e.g., plastic or glass beakers).
7. Ctenophores are open ocean animals but some species, like *M. leidyi,* are relatively common along the coast and can be found in a wide variety of different salinities (e.g., salt marshes). Ctenophores tend to be found in groups. If you see one *M. leidyi* it is likely you will see others.
8. In the wild, ctenophores feed on a diverse diet consisting in all types of zooplankton, fish eggs and larvae, so a diet of *Artemia* alone is not sufficient for maintaining healthy *M. leidyi* for long periods of time. Hatchlings can be efficiently grown with a diet of rotifers, however, a diverse diet including *Artemia* brine shrimp accelerates their growth rate. Wait until cydippids are larger than the brine shrimp (>1.5 mm diameter) before attempting to feed *Artemia*. Once cydippids transition into the lobate state, their diet should be diversified with foods such as mysid shrimp, fish larvae, and ideally wild plankton.

9. If adult *M. leidyi* are starved, they will begin to resorb their oral lobes and slowly shrink in size.
10. Overfeeding should also be avoided. Overfed *M. leidyi* will regurgitate ingested food and the undigested food will foul the water.
11. Rotifers:
    (a) We use *Brachionus plicatilis* (L-type) rotifers (Reed Mariculture, Campbell, CA, USA).
    (b) We recommend growing two asynchronous rotifer cultures at the same time and alternate harvesting between them. Excessive repeated harvesting (>50%) in one single culture could lead to the crash of the culture.
    (c) In order to maintain the productivity, it is important to not let the rotifers run out of food. Maintain a detectable light green tint in the water between feedings (https://reedmariculture.com/support_rotifers.php).
    (d) It is recommended to feed rotifers every day. If this is not possible, add the volume of food required for the days they will not be fed (ideally not more than 4). The accumulation of debris at the bottom could be a sign of overfeeding.
    (e) The stability of the rotifer culture is based on finding the right balance between harvesting and feeding. In a healthy culture all or the majority of the rotifers will be females and will reproduce clonally. An increase in the proportion of males (smaller individuals) in the culture is indicative of an unbalanced and stressed culture.
    (f) In case the rotifer culture cannot be maintained/harvested for longer than 4 days, there is a way to put rotifers in "hibernation mode" by setting up a backup culture. Harvest ~40% of your culture and transfer it into a 1 L container filled with 20 ppt FSW. Add a bit of extra algae concentrate to darken the culture. Let the culture uncovered or cover loosely to allow oxygen to enter and keep it at 4 °C to slower the metabolism of rotifers. After 7 days 50% of your rotifers should be alive.
12. Brine shrimp show positive phototaxis so hatched swimming *Artemia* larvae will concentrate at the light point high in the water column after few minutes.
13. Feeding the adult ctenophores with ~2 mysid shrimps per ctenophore the day before spawning increases the success and rate of gamete production.

14. Use plastic or glass beakers to dip out individual animals when transferring animals between tanks and containers in order to avoid damage to their gelatinous body.
15. *M. leidyi* are self-fertile hermaphrodites—a single animal carries both female and male gonads—and viable embryos can be obtained from the spawning of a single individual but they produce more viable offspring in the presence of conspecifics [36].
16. It is important to keep specimens in clean water while spawning in order to avoid debris and mucus which could interfere with fertilization and development.
17. One single healthy and well-fed specimen can give up to 500 embryos. We recommend using between 5 and 10 adults for spawning taking into account that from the starting number of embryos, around 2/3 end up developing into the cydippid stage.
18. You can place the bowls inside an incubator or cover them with a cardboard box.
19. Before spawning, the meridional canals below the comb rows may turn cloudy indicating the presence of sperm. Sperm is released before the eggs. After sperm are released the water of the bowl gets cloudy. Then the eggs are released 10–15 min after and are fertilized upon release.
20. Ctenophores can sometimes release a few eggs before the bulk of spawning starts. To ensure a batch of synchronously developing embryos, animals can be checked after 1.5–2 h of dark treatment and transferred into a bowl of fresh 1× UV-FSW if gametes are detected early.
21. Avoid keeping adult specimens in the small glass culture bowls after spawning otherwise both adult and embryo quality will deteriorate rapidly as the adult's waste and mucus accumulate. As soon as the eggs are released, remove adult specimens from the bowl and transfer fertilized embryos into another glass bowl filled with fresh 1× UV-FSW.
22. *M. leidyi* adults can be spawned multiple times a week if fed well and given sufficient time to recover between spawning cycles. We recommend waiting 1–2 days to spawn the animals again and feed them with shrimps within this time period.
23. Embryo development should be relatively synchronous, with the first cleavage occurring 1 h after fertilization and subsequent cleavages every 20 min thereafter. Gastrulation occurs at 3–4 h and hatching at 18–24 h [31].
24. Embryos are very sensitive and exposure to any type of chemical could drastically affect their development. Make sure that all culturing glassware and solutions are dedicated to this purpose

and kept free of detergents or any other harmful chemicals. Culturing materials should be cleaned exclusively with tap water followed by a final rinse with distilled water.

25. Clean water is essential to ensure the survival of just-hatched cydippids. Cleaning should be done once a day during the first 3 days and every other day thereafter. Use a plastic transfer pipette two times the diameter of the specimens for transferring cydippids into the clean glass bowl. To fit cydippids into the pipette as they grow, the plastic pipette opening can be widened by cutting with a razor blade.
26. Transfer growing cydippids into a larger volume and taller container (e.g., 2 L glass beaker) ~4 days after hatching in order to give them more space for swimming vertically and feeding in the water column. Cydippids feed by setting their tentacles and if they are too crowded their tentacles get tangled.
27. Use newly hatched *Artemia* (18–20 h after starting the culture) for feedings. *Artemia* rapidly loose nutritional value after hatching due to their use of internal stores for swimming. They can be fed with live algae and grown to larger sizes if desired.
28. We find that 1.5–3 mm diameter animals are a good size for performing regeneration experiments, since at this stage cydippids have completely developed all the organs of their body. Moreover, cydippids at this size have high fitness and the ability to withstand starvation which increases the success of regeneration.
29. Properly fed cydippids transition to the lobate state 3–4 weeks after hatching. To culture into adulthood, animals at this stage should be transferred to the ctenophore adult tank and feeding must be complemented with foods such as wild zooplankton, mysid shrimps, and/or fish larvae.
30. Pyrex glass is stiffer than borosilicate/aluminosilicate needle stock used for microinjection.
31. We recommend pulling several operating needles before you start. Because every needle will be a little bit different than the others, you will find the size and length that works best for you. Plus, if you break a needle during a surgery, you will have "backups" so that you can finish your experiment. Once you learn what shape you like, you can continue to pull additional needles that work best for you.
32. We like needles that are flexible enough so that you can put the tip on the bottom of the dish on the opposite side of the region you want to remove, and then move the needle down, sort of like a paper cutter. You can drive the needle down into the bottom of the dish to complete the cut.

33. Stop feeding the day before the operations and starve animals during regeneration in order to avoid food particles that can interfere with live imaging and cause nonspecific staining.
34. For live-imaging of wound healing, we puncture animals to generate small epithelial gaps approximately 200–400 μm in diameter which have been consistently proven to heal rapidly when exposed to the live-imaging setup conditions and can be visualize with high magnification objectives.
35. Keeping a low level of water in the surgical dish can help reduce the mobility of animals when cutting. If more immobilization is required, the dish with cydippids can be incubated on ice ~10 min before cutting.
36. We find it effective to use two glass needles when cutting, one for immobilizing and orienting the animal and the other for performing the cut.
37. When juvenile or adult ctenophores are bisected along the oral–aboral axis, an incomplete regeneration event will occur in a substantial percentage of the cases [4, 5]. Wound healing proceeds normally, but instead of replacing the missing parts, a stable "half-animal" forms. These animals possess half the typical complement of body structures, that is, one tentacle, four comb rows and a half apical organ. They are considered stable since they can feed, grow, and reproduce. We found that bisected cydippids containing an intact apical organ regenerate into whole animals in nearly 100% of cases in contrast to bisected cydippids with a half or missing apical organ which are more likely to forego whole-body regeneration and remain instead as "half animals" [10].
38. Accumulation of debris in the water can inhibit regeneration. Clean regenerating cydippids daily by transferring them into a new small plastic petri dish filled with 1× 0.2-μm UV-FSW.
39. We do not feed during regeneration as food in the gut could interfere with sample imaging but amputated animals could be fed when used for other experimental purposes (i.e., scoring ability to regenerate after amputation).
40. We set 5 mM HU as the working concentration for our cell proliferation inhibitor experiments since at this concentration control nonamputated cydippids remain in good condition, swimming normally, with no cell death over a 72 h time course incubation. We found concentrations higher than 5 mM to cause the degeneration and eventually death of most of the animals during the first 24 h of incubation [10].
41. Start incubating cydippids with 5 mM HU ~30 min before performing the surgeries to be sure that cell proliferation is completely blocked from the very beginning of the regenerative response.

42. HU is light-sensitive so dishes need to be protected from light (wrapped with aluminum foil or covered with a cardboard box).
43. HU loses efficacy over time so 5 mM HU working solution must be replaced every 24 h or less when doing a continuous incubation. Make 5 mM HU working concentration fresh each time you replace the solution.
44. Always confirm that HU treatments were effective by checking for cell proliferation in treated animals (e.g., with EdU labeling).
45. The inhibition of the ribonucleotide reductase enzyme by HU is reversible [37]. Wash out the HU working solution and replace it with 1× 0.2-μm UV-FSW to allow proliferation to resume.
46. It is important to homogenize the liquid agar very well (e.g., by vortexing) when first preparing the 1.2% agarose solution and again just before use when melting previously prepared 1.2% agarose. Incomplete homogenization can lead to irregular agar concentrations within the solution, impairing the embedding process.
47. The temperature of the liquid agar is crucial for the success of embedding. Too hot liquid agar disintegrates the cydippids while too cool agar sets before it can be thoroughly mixed with the sample. We recommend melting the agar at higher temperature (water bath above 30 °C or submerge in boiling water in a glass beaker) to ensure complete melting, and then letting it cool down for ~5 min until reaching a temperature slightly above the working temperature of 25 °C (~30–40 °C).
48. Do not pour the liquid agar directly on top of the drop containing live cydippids since the high temperature can cause instant disintegration. Instead, gently pipet the liquid agar from the sides surrounding the drop containing the sample and allow it to merge with the seawater. It is also important to homogenize the agar with the cydippids in seawater by carefully pipetting up and down 2 or 3 times.
49. Let the agar cool down for ~2 min before placing the coverslip on top. This helps in creating a small resistance from the agar when placing the coverslip on top which favors the formation of a homogeneous agar lamina with intact cydippids inside. If the agar is too liquid, cydippids get squished when placing the coverslip on top.
50. Use fresh fixative solution; it can be kept at 4 °C for up to 3 days.
51. For time lapse imaging immobilizing the specimen is of critical importance. For some experiments, increasing the viscosity

with methyl cellulose can suffice. For longer periods synthetic hydrogels [10] may be of use. We find 7.5% hydrogel as described the optimal concentration for our wound-healing time-lapse experiments, in terms of keeping a good balance between osmolarity of the medium and immobilization of the specimen. However, we recommend trying different hydrogel concentrations depending on the mobility of the animal and the length of the experiment. Lower hydrogel concentrations are more osmotically compatible with the animal but they also are less effective for immobilization while higher hydrogel concentrations allow for better immobilization but tend to dehydrate the specimens. Optimize this tradeoff for specific experiments.

52. It is convenient when orienting and immobilizing the animals to make the epithelial puncture on the aboral side of the cydippid's body since cydippids mounted with the aboral pole facing upward tend to stay more still compared to laterally mounted cydippids.
53. A coverslip with clay feet placed over the microgel drop is sufficient for maintaining humidity during short live-imaging experiments. For longer time-lapse experiments (>2 h) seal the edges of the coverslip with Vaseline to prevent evaporation. Under ideal circumstances, we have been able to image regeneration in *M. leidyi* for 12–16+ h. Specimens can also be mounted into a glass depression slide with a larger volume of microgel in order to maintain greater humidity; however, animals are less immobilized in this system and the sample is thicker which may restrict the magnification to lower-powered objectives.
54. For wounds of approximately 200–400 μm in diameter, we recommend using a 20× objective which provides sufficient magnification for detailed visualization of individual cell crawling and cytoskeletal extensions with a large enough field of view to include the complete epithelial gap.
55. Specimens are likely to move out of focus during the acquisition so setting up a range of stacks along the *z* axis will allow you to select the better planes upon playback.

References

1. Dunn CW, Hejnol A, Matus DQ, Pang K, Browne WE, Smith SA et al (2008) Broad phylogenomic sampling improves resolution of the animal tree of life. Nature 452(7188): 745–749. https://doi.org/10.1038/nature06614
2. Pang K, Martindale MQ (2008) Comb jellies (Ctenophora): a model for basal metazoan evolution and development. Cold Spring Harb Protoc 3(11):1–11. https://doi.org/10.1101/pdb.emo106
3. Chun C (1880) Fauna und flora des golfes von Neapel: Die ctenophoren des golfes von Neapel und der angrenzenden meeres-abschnitte. W. Engelmann, Leipzig. https://doi.org/10.5962/bhl.title.10162

4. Coonfield BR (1936) Regeneration in Mnemiopsis Leidyl Agassiz. Biol Bull 71:421–428
5. Martindale MQ (1986) The ontogeny and maintenance of adult symmetry properties in the ctenophore, *Mnemiopsis mccradyi*. Dev Biol 118:556–576. https://doi.org/10.1016/0012-1606(86)90026-6
6. Martindale MQ, Henry JQ (1996) Development and regeneration of comb plates in the ctenophore Mnemiopsis leidyi. Biol Bull 191(2):290–292. https://doi.org/10.1086/BBLv191n2p290
7. Henry JQ, Martindale MQ (2000) Regulation and regeneration in the ctenophore Mnemiopsis leidyi. Dev Biol 227(2):720–733. https://doi.org/10.1006/dbio.2000.990
8. Tamm SL (2012) Regeneration of ciliary comb plates in the ctenophore *Mnemiopsis leidyi*. I. Morphology. J Morphol 273:109–120. https://doi.org/10.1002/jmor.11016
9. Martindale MQ (2016) The onset of regenerative properties in ctenophores. Curr Opin Genet Dev 40:113–119. https://doi.org/10.1016/j.gde.2016.06.017
10. Ramon-Mateu J, Ellison ST, Angelini TE, Martindale MQ (2019) Regeneration in the ctenophore Mnemiopsis leidyi occurs in the absence of a blastema, requires cell division, and is temporally separable from wound healing. BMC Biol 17(1):1–25. https://doi.org/10.1186/s12915-019-0695-8
11. Harbison GR, Miller RL (1986) Not all ctenophores are hermaphrodites. Studies on the systematics, distribution, sexuality and development of two species of *Ocyropsis*. Mar Biol 90:413–424. https://doi.org/10.1007/BF00428565
12. Dunlap Pianka H (1974) Ctenophora. In: Giese AC, Pearse JS (eds) Reproduction of marine invertebrates. Academic Press Inc., Cambridge, pp 201–265
13. Martindale MQ, Henry JQ (1997) Reassessing embryogenesis in the Ctenophora: the inductive role of e1 micromeres in organizing ctene row formation in the "mosaic" embryo, *Mnemiopsis leidyi*. Development 124(10): 1999–2006
14. Martindale MQ, Henry JQ (1999) Intracellular fate mapping in a basal metazoan, the ctenophore Mnemiopsis leidyi, reveals the origins of mesoderm and the existence of indeterminate cell lineages. Dev Biol 214:243–257. https://doi.org/10.1006/dbio.1999.9427
15. Fischer AHL, Pang K, Henry JQ, Martindale MQ (2014) A cleavage clock regulates features of lineage-specific differentiation in the development of a basal branching metazoan, the ctenophore Mnemiopsis leidyi. EvoDevo 5(1):4. https://doi.org/10.1186/2041-9139-5-4
16. Hernandez-Nicaise M-L (1991) Ctenophora. In: Harrison FW, Westfall JA (eds) Microscopic anatomy of invertebrates: placozoa, porifera, cnidaria, and ctenophora, vol 2. Wiley, New York, pp 359–418
17. Babonis LS, DeBiasse MB, Francis WR, Christianson LM, Moss AG, Haddock SHD et al (2018) Integrating embryonic development and evolutionary history to characterize tentacle-specific cell types in a ctenophore. Mol Biol Evol 35(12):2940–2956. https://doi.org/10.1093/molbev/msy171
18. Chun C (1892) Die Dissogonie, eine neue Form der geschlechtlichen Zeugung. In: Festsch Zum siehenzigsten Geburtstage Rudorf Leuckarts. Engelmann, Leipzig, pp 77–108
19. Martindale MQ (1987) Marine biology larval reproduction in the ctenophore Mnemiopsis mccradyi (order Lobata). Mar Biol 94: 409–414. https://doi.org/10.1007/BF00428247
20. Ryan JF, Pang K, Schnitzler CE, Nguyen AD, Moreland RT, Simmons DK et al (2013) The genome of the ctenophore Mnemiopsis leidyi and its implications for cell type evolution. Science 342(6164):1242592. https://doi.org/10.1126/science.1242592
21. Yamada A, Martindale MQ, Fukui A, Tochinai S (2010) Highly conserved functions of the Brachyury gene on morphogenetic movements: insight from the early-diverging phylum Ctenophora. Dev Biol 339(1):212–222. https://doi.org/10.1016/j.ydbio.2009.12.019
22. Pang K, Ryan JF, Mullikin JC, Baxevanis AD, Martindale MQ (2010) Genomic insights into Wnt signaling in an early diverging metazoan, the ctenophore Mnemiopsis leidyi. EvoDevo 1(1):1–15. https://doi.org/10.1186/2041-9139-1-10
23. Schnitzler CE, Pang K, Powers ML, Reitzel AM, Ryan JF, Simmons D et al (2012) Genomic organization, evolution, and expression of photoprotein and opsin genes in Mnemiopsis leidyi: a new view of ctenophore photocytes. BMC Biol 10:107. https://doi.org/10.1186/1741-7007-10-107
24. Schnitzler CE, Simmons DK, Pang K, Martindale MQ, Baxevanis AD (2014) Expression of multiple sox genes through embryonic development in the ctenophore Mnemiopsis leidyi is spatially restricted to zones of cell proliferation. EvoDevo 5(1):1–17. https://doi.org/10.1186/2041-9139-5-15

25. Moroz LL, Kocot KM, Citarella MR, Dosung S, Norekian TP, Povolotskaya IS et al (2014) The ctenophore genome and the evolutionary origins of neural systems. Nature 510(7503):109–114. https://doi.org/10.1038/nature13400
26. Fidler AL, Pedchenko VK, Boudko SP, Brown KL, Rokas A, Hudson BG et al (2017) Collagen IV and basement membrane at the evolutionary dawn of metazoan tissues. Elife 6:1–24. https://doi.org/10.7554/eLife.24176
27. Sebé-Pedrós A, Chomsky E, Pang K, Lara-Astiaso D, Gaiti F, Mukamel Z et al (2018) Early metazoan cell type diversity and the evolution of multicellular gene regulation. Nat Ecol Evol 2(7):1176–1188. https://doi.org/10.1038/s41559-018-0575-6
28. Dunn CW (2017) Ctenophore trees news-and-views. Nat Ecol Evol 1(11):1600–1601. https://doi.org/10.1038/s41559-017-0359-4
29. Shen X, Hittinger CT, Rokas A (2017) Contentious relationships in phylogenomic studies can be driven by a handful of genes. Nat Ecol Evol 1(5):126. https://doi.org/10.1038/s41559-017-0126
30. Costello JH, Bayha KM, Mianzan HW, Shiganova TA, Purcell JE (2012) Transitions of Mnemiopsis leidyi (Ctenophora: Lobata) from a native to an exotic species: a review. Hydrobiologia 690(1):21–46. https://doi.org/10.1007/s10750-012-1037-9
31. Pang K, Martindale MQ (2008) Mnemiopsis leidyi spawning and embryo collection. Cold Spring Harb Protoc 3(11):1052–1054. https://doi.org/10.1101/pdb.prot5085
32. Salinas-Saavedra M, Martindale MQ (2018). Improved protocol for spawning and immunostaining embryos and juvenile stages of the ctenophore *Mnemiopsis leidyi*. https://doi.org/10.1038/protex.2018.092
33. Bading KT, Kaehlert S, Chi X, Jaspers C, Martindale MQ, Javidpour J (2017) Food availability drives plastic self-repair response in a basal metazoan-case study on the ctenophore Mnemiopsis leidyi A. Agassiz. Sci Rep 7(1):1–9. https://doi.org/10.1038/s41598-017-16346-w
34. Morgan TH (1901) Regeneration. The Macmillan Company, New York
35. Young CW, Hodaas S (1964) Hydroxyurea: inhibitory effect on DNA metabolism. Science 146:1172–1174. https://doi.org/10.1126/science.146.3648.1172
36. Sasson DA, Ryan JF (2016) The sex lives of ctenophores: the influence of light, body size, and self-fertilization on the reproductive output of the sea walnut, *Mnemiopsis leidyi*. PeerJ 4:e1846. https://doi.org/10.7717/peerj.1846
37. Adams RLP, Lindsay J (1967) Hydroxyurea. Reversal of inhibition and use as a cell-synchronizing agent. J Biol Chem 242(6):1314–1317

Open Access This chapter is licensed under the terms of the Creative Commons Attribution 4.0 International License (http://creativecommons.org/licenses/by/4.0/), which permits use, sharing, adaptation, distribution and reproduction in any medium or format, as long as you give appropriate credit to the original author(s) and the source, provide a link to the Creative Commons license and indicate if changes were made.

The images or other third party material in this chapter are included in the chapter's Creative Commons license, unless indicated otherwise in a credit line to the material. If material is not included in the chapter's Creative Commons license and your intended use is not permitted by statutory regulation or exceeds the permitted use, you will need to obtain permission directly from the copyright holder.





Chapter 6

Studying Placozoa WBR in the Simplest Metazoan Animal, *Trichoplax adhaerens*

Hans-Jürgen Osigus, Michael Eitel, Karolin Horn, Kai Kamm, Jennifer Kosubek-Langer, Moritz Jonathan Schmidt, Heike Hadrys, and Bernd Schierwater

Abstract

Placozoans are a promising model system to study fundamental regeneration processes in a morphologically and genetically very simple animal. We here provide a brief introduction to the enigmatic Placozoa and summarize the state of the art of animal handling and experimental manipulation possibilities.

Key words Placozoa, *Trichoplax adhaerens*, Regeneration, Vital Staining, Transplantation

1 Introduction

The phylum Placozoa [1] comprises flat (approx. 20–30 μm in height) discoid animals with a body size commonly less than 4 mm in diameter [2–5] (Fig. 1). One recently described species, *Polyplacotoma mediterranea*, can reach a size of up to 10 mm by adopting a highly ramified and highly flexible body shape [6]. In contrast, specimens of the other described species, *Trichoplax adhaerens* [2] and *Hoilungia hongkongensis* [7], as well as all other undescribed species never grow larger than 3–4 mm in diameter. The sandwich-like body of placozoans lacks any kind of symmetry but possesses a clear top-bottom polarity (Fig. 2a) [4, 8, 9]. The upper epithelium is facing the water column while the lower epithelium adheres to the substrate [2, 3, 10]. Upside-down flipped animals rotate and bring their lower epithelium back into contact with the surface quickly. Flipped animals perform this rotation by beating with the cilia of the upper epithelium. During this phase, the lower epithelium glides along itself until it regains contact with the ground [2, 3].

The three-layered placozoan bauplan consists of at least nine differentiated somatic cell types: upper and lower epithelial cells,

Simon Blanchoud and Brigitte Galliot (eds.), *Whole-Body Regeneration: Methods and Protocols*,
Methods in Molecular Biology, vol. 2450, https://doi.org/10.1007/978-1-0716-2172-1_6, © The Author(s) 2022



Fig. 1 Different vital stages of placozoans. (**a**) Light microscopy image of the morphologically most simple metazoan animal, the placozoan *Trichoplax adhaerens* ("Grell clone"). (**b**) Degenerative stage of *Trichoplax adhaerens* ("Grell clone"). Under unfavorable conditions the upper epithelium of the animal lifts up and forms a hollow bubble (red arrow). In most cases the specimen will die shortly thereafter. (**c**) Degenerative stage of *Trichoplax* sp. H2 ("Vieste clone"). These thread-shaped stages can be frequently found in old placozoan cultures and are likely caused to some extend by unfavorable water chemistry

fiber cells, sphere cells, three types of gland cells, lipophil cells, and crystal cells [2, 3, 11–13] (Fig. 2a). Noteworthy, multiple other somatic (sub)cell types are awaiting their description [13, 14]. In addition to the so far identified differentiated somatic cell types, pluri- or omnipotent stem cells are found near the contact zone between lower and upper epithelium [15, 16]. The fiber cell layer, which is sandwiched between the upper and lower epithelium, plays a major role, for instance, in animal body contraction [3, 17]. The inter-connected fiber cells are the contractile elements and therefore also play a major role in animal locomotion. Lipophil cells secrete enzymes for extracellular digestion (Fig. 2b) and are exclusively found in the lower epithelium [11]. The lower epithelium also harbors three different types of gland cells (type 1, 2 and 3), which synthesize neuropeptides or mucus (in case of type 2 gland cells) [12]. Given that gland cells of type 1 and 3 possess a cilium, they have been suggested to be secretory sensory cells [12]. It is worth mentioning that type 3 gland cells can also be found in the upper epithelium [12]. The recently described sphere cells in the upper epithelium [13] include the shiny spheres, which might play a role in predator defense [18]. Finally, the so-called crystal cells are located at the margin of the animal body [11] and serve functions in gravity perception [19]. Besides morphological studies, a single-cell RNAseq study has indicated the existence of even more somatic cell types in placozoans [14].

A shared feature of all placozoans is the exceptionally high degree of body plasticity due to the absence of any kind of skeleton or other solid body parts [2, 4, 5]. Placozoans constantly change shape by contracting and relaxing their flat body which causes locomotion. Another mode of locomotion is mediated by ciliary beats of the lower epithelial cells, which is not accompanied, however, by shape changes [2]. It has recently been suggested that the

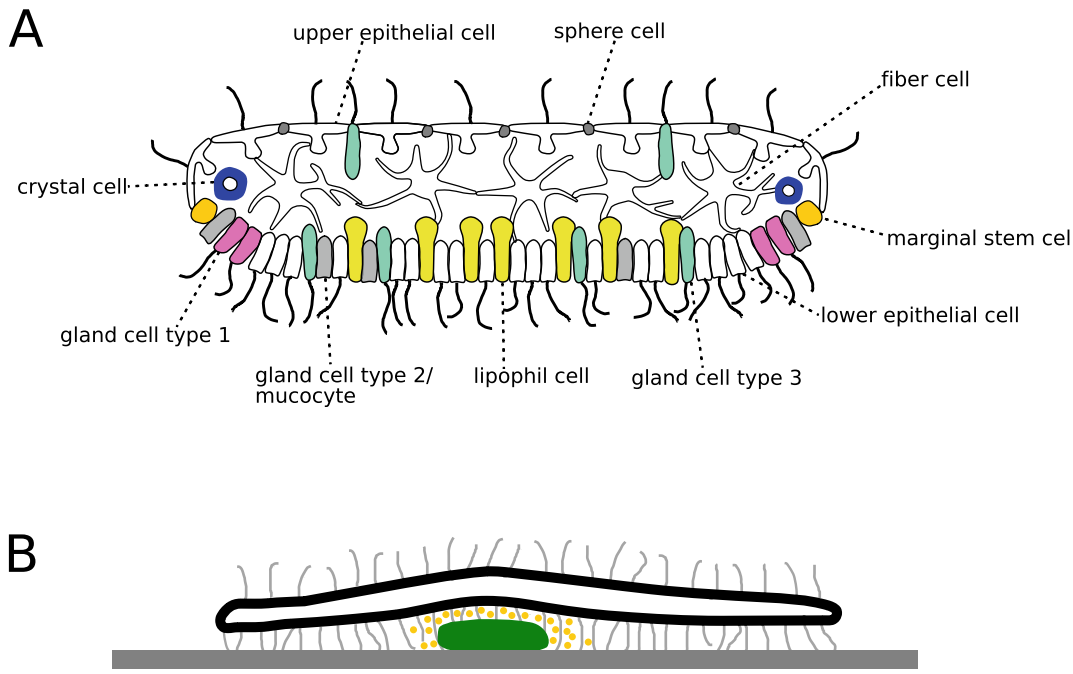


Fig. 2 Ultrastructure and feeding behavior of placozoans. (**a**) Schematic cross section of *Trichoplax adhaerens*. The typical placozoan bauplan consists of an upper epithelium, a lower epithelium and a fiber cell layer between both epithelia. The shown schematic bauplan and cell types are a synthesis of recent studies on the placozoan ultrastructure [11–13]. Please note that the actual number of placozoan somatic cell types is likely even higher and that each respective major cell type might summarize multiple sub-cell types. (**b**) Illustration of the typical placozoan feeding behavior. The animal glides over a food particle (green) to form an external digestion cavity. Digestive enzymes (yellow) are secreted into this extracorporeal feeding cavity and nutrition uptake is performed by the lower epithelium by means of phago- and likely pinocytosis. Panels **a** and **b** are modified after [40]

amino acid glycine induces fiber cell contractions and also the activation of ciliated locomotion in *Trichoplax adhaerens* [20]. The locomotion activity of placozoans mirrors the vitality of the animals and is correlated to food availability and food uptake [21–24]. Locomotion pauses for different reasons, for example, during the phase of extracellular digestion of food particles [21–24]. This extracellular digestion (Fig. 2b) is carried out by release of secreted enzymes of so far unknown composition (*for further details, see* [23]). Although the cells involved and the underlying physiological mechanisms are yet unknown, placozoans are able to perceive light [25].

Placozoans show exceptional regeneration capacities. For instance, partial mechanical disruptions will usually heal very rapidly within minutes [26] (*see* **Note 1**). This high regeneration capacity relates to the simple body architecture, which lacks any kind of organs or other complex morphological structures, even a basal membrane and a complex extracellular matrix are missing

[17]. The high regenerative capacity of the animals allows placozoans to reproduce very efficiently by binary fission, which is the dominant mode of reproduction under laboratory conditions [2, 3, 5] (*see* **Note 2**). For this type of vegetative reproduction, animals constrict in the center region of the body to form two daughter individuals of approximately the same size. The plane of each fission is orthogonal to the previous division plane [27] and a certain ratio of inner vs. marginal cells is required to trigger fission [26]. Daughter individuals stay connected for several hours by a cellular thread, which mechanically breaks when the daughter individuals move in different directions at the very end of the fission process [2, 3]. The resulting wounds heal rapidly and the original wound borders cannot be traced back under the light microscope 30 min after regeneration. The critical step of the wound healing process of both the outer margin as well as the central region of the animal body is the contraction of the adjacent epithelial cells which brings the cells within the cell layers in close contact [26].

Comprehensive studies on whole body regeneration in *Trichoplax adhaerens* have been conducted by Ruthmann and Terwelp (1979) [28], and by Schwartz (1984) [26]. Both studies applied procedures outlined by Miller in 1971 [29], but without citing this original work. Miller has been a methodical pioneer for modern placozoan regeneration experiments, although some of his results contradict findings by Ruthmann and Terwelp [28] and Schwartz [26]. Ruthmann and Terwelp [28] tested different chemicals (using for example colchicine or trypsin–EDTA-supplemented calcium−/magnesium-free ASW, *see* **Note 3**) to dissociate the placozoan body. Succeeding dissociation of animals into small cell clusters or even single cells, their reaggregation was studied after bringing the cells into close proximity via gentle centrifugation.

Studies from Kuhl and Kuhl (1963, 1966) [30, 31] reported first observations on the healing process of animals after cutting off a small piece from the animal body. The second key study on placozoan regeneration by Schwartz (1984) [26] focused on mechanical manipulation of the animal body. Schwartz studied the regeneration capacities of placozoan specimens after selective removal of marginal and/or center cells in a quantitative fashion and identified an approximately 20–25 μm thick circumferential marginal zone of presumably particular relevance for regeneration processes. This morphologically cryptic (i.e., macroscopically indistinguishable) zone consists of specific cell types, which cannot be found in the center of the animal. The differential cell type distribution from the edge to the center of the animal implies that cell type populations from both areas are needed to allow full recovery of animals after mechanical disruption. Schwartz also conducted a series of transplantation experiments (*see* **Note 4**). For example, parts of the marginal zone from a donor animal were transplanted into the central body region of an acceptor animal (Fig. 3). An

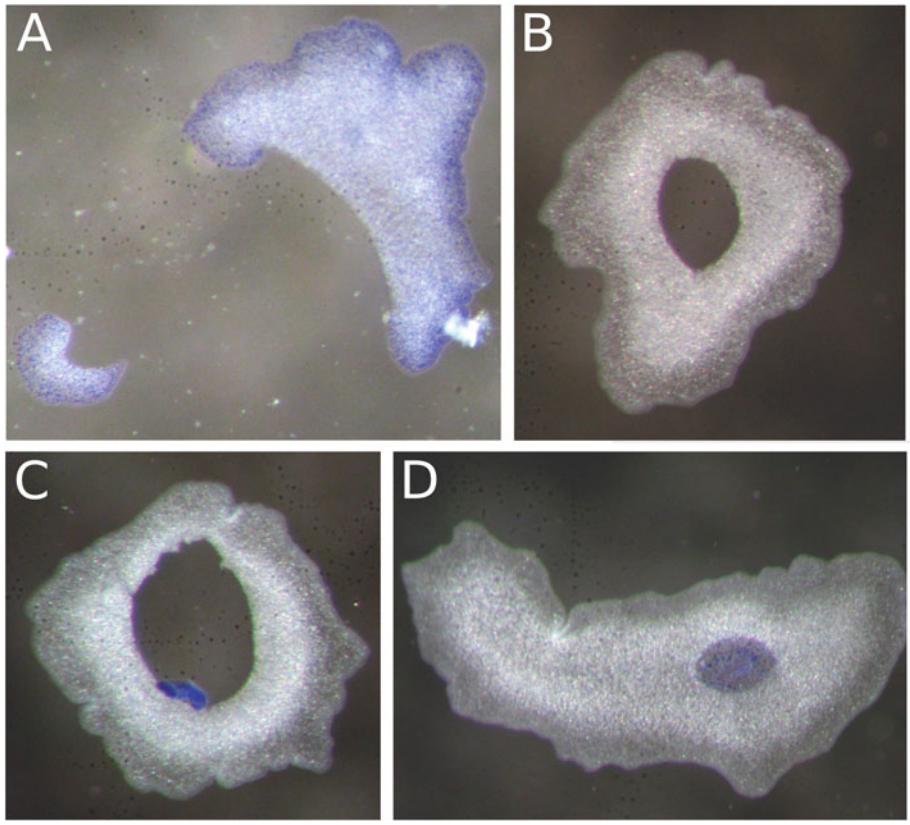


Fig. 3 Tissue transplantation in *Trichoplax adhaerens*. (**a**) From the "donor" animal, which has been stained with methylene blue, a piece consisting of marginal as well as center cells (lower left) has been cut off with an acupuncture needle. (**b**) The "acceptor" animal (unstained) has been prepared for the transplantation by means of cutting a hole into the center of its body. (**c**) The "donor" fragment is placed into the body hole of the "acceptor" animal. (**d**) Complete intergrowth of the "donor" fragment and the "acceptor" animal (18 h posttransplantation). Please note that the marginal cells of the "donor" fragment keep their state and form a new small margin in the central body region of the "acceptor" animal. (Picture taken from [33])

important result from these experiments was the observation that cells from the animal margin do not de- or redifferentiate when transplanted into the center of the animal. Successfully integrated marginal body fragments led to a hole in the central part of the body, resembling a doughnut-like appearance, with marginal cells lining the central hole. Eventually, such holes were shifted (by an unknown mechanism of active cell movement) toward the outer margin of the animal where the transplanted and the original marginal zones fused [26]. Due to the microscopic size of placozoans, only body parts comprising all three cell layers have so far been successfully transplanted into an acceptor animal. Body parts consisting just of the upper or lower epithelium alone, respectively, have not yet been successfully isolated and transplanted. Schwartz [26] also showed that even small animal fragments keep their

top-bottom polarity after excision, that is, that these fragments tightly reattach to the substrate by means of the lower epithelium.

The following protocols are based on previously published animal handling and manipulation techniques and may serve as an updated basic guideline to perform whole-body regeneration experiments in placozoans.

2 Materials

1. Stereomicroscope (magnification from 6.5× to 50×).
2. Cold light source with gooseneck light guide.
3. Glass petri dishes (4 cm and 15 cm diameter).
4. Handheld salinometer.
5. Food source: algae culture of *Pyrenomonas helgolandii* (or *Rhodomonas salina*) or rice grains [25].
6. Artificial sea water (ASW): 35 g/L commercial Ocean Sea Salt in ddH_2O.

   Filter at 4 μm, adjust to pH 7.8 and leave at least 24 h to settle (*see* **Note 5**). Autoclave if needed for downstream application. Store at room temperature.
7. Filter paper (retention range > 4 μm).
8. Methylene blue stock solution (MBSS): 0.5 g methylene blue powder in 100 mL ddH_2O.
9. Lipophilic membrane dye stock solution: 2 g dye (e.g., *DiI*, Invitrogen) in 200 μL 70% (v/v) EtOH in ddH_2O.
10. Single depression microscope slides.
11. Acupuncture needle (0.18 mm diameter or thinner, length ideally >30 mm).
12. Calcium- and magnesium-free artificial seawater (CMF-ASW) + egtazic acid (EGTA): 26.24 g NaCl, 0.671 g KCl, 4.687 g Na_2SO_4, 2.15 mM $NaHCO_3$, 10 mM Tris–HCl, 2.5 mM EGTA in 1 L ddH_2O (*see* **Note 6**).
13. High-salt ASW: 1 g NaCl in 100 mL ASW.
14. Fixative A: ice-cold 4% (w/v) paraformaldehyde (PFA), 0.2% (v/v) glutaraldehyde in high-salt ASW.
15. Fixative B: ice-cold 4% (w/v) PFA, in high-salt ASW.

3 Methods

Placozoan specimens are extremely fragile which is highly relevant when working with live animals. The standard procedure for transferring placozoans from one place (e.g., culture dish) to another

(e.g., microscopy slide) is to first detach the animal by means of a focused water jet gently pipetted from the side of the animal (*see* **Note 7**). Afterward, floating specimens can be pipetted into the designated place. Sometimes placozoans adhere very strongly to their substrate (the name giving feature for *Trichoplax adhaerens*, the "sticky hairy plate" [2, 3]), and cannot be detached without body disruptions. Another, even more disruptive, threat to the fragile animal body is the exposure to air—attached placozoans that fall dry for 1 s only get irreversibly disrupted. Therefore, the regular exchange of artificial seawater (ASW) in the culture dishes must be performed as rapidly and as cautiously as possible and an uninterrupted liquid film has to constantly cover the placozoans. Direct contact of placozoans to large underwater air bubbles, for example, as generated by algae in the culture dishes, is not harmful to the animals. Obviously, it is the rapid change of surface tension, and not the air itself, that is disruptive.

3.1 Animal Cultivation

Clonal animal material can be accessed through the corresponding author Bernd Schierwater who cultures a variety of placozoan model species in his lab. Alternatively, nonmodel placozoans can be randomly acquired from the walls of tropical sea water aquaria in pet shops, zoos, or even private aquaria. In these cases, a clonal lineage from one single starting animal has to be established and this clone has to be genetically characterized in advance of usage [32].

1. Fill a glass petri dish (*see* **Notes 8** and **9**) 2/3 with ASW.
2. Add 1 mL of food source (*see* **Notes 10** and **11**).
3. Cover the petri dish to minimize evaporation.
4. Detach placozoans from the wall of the shipment vessel (e.g., a 50 mL tube) by gently pipetting a focused water jet on their side (*see* **Note 7**).
5. Transfer floating placozoans into the petri dish by pipetting.
6. Store the culture at room temperature (ideally at 23 °C, tolerable range from 20 °C to 25 °C) under a 12:12 h light–dark cycle (*see* **Note 12**).
7. Every two weeks replace half of the ASW with fresh ASW to prevent the accumulation of waste products.
8. Add 1 mL of food source after replacement of ASW.
9. Repeat **steps 7** and **8** until the animal density reaches 300 specimens per dish (*see* **Notes 13** and **14**).
10. Follow **step 4** to detach 50 animals.
11. Pour 50% of the volume (including detached animals) to a new petri dish.
12. Add fresh ASW to the original and the new culture dishes.

13. Add 1 mL of food source to both cultures.
14. Repeat **steps 6–13** to maintain the placozoan culture.

3.2 DiI *Staining*

Dyes like *DiI* can be used to trace placozoan cells or transplants in live specimens [27, 33]. The following protocol refers to the procedures as already described in [33] as well as own unpublished data.

1. Pipet 30 µL of the membrane dye stock solution onto a depression microscope slide.
2. Wait for 1 h for the solution to dry completely at room temperature.
3. Detach placozoans from their culture dish by gently pipetting a focused water jet on their side.
4. Transfer the detached placozoans to the dried slide.
5. Do not cover the slide since removal of the cover glass might disrupt the animals.
6. Incubate at room temperature in the dark for 7 h in a wet chamber.
7. Transfer stained animals into a petri dish filled with ASW to wash them.
8. Proceed with mechanical manipulation experiments (*see* Subheading 3.4).

3.3 Methylene Blue Staining

Different vital stainings, such as Janus Green, Neutral Red, Cresyl Blue, Crystal Violet, or Methylene Blue, have been successfully tested for placozoans (e.g., [26, 27, 34]). The protocol below refers to the protocol from Schwartz 1984 [26].

1. Transfer placozoans into a 4 cm petri dish filled with 8 mL ASW.
2. Add 200 µL MBSS to the dish for the liquid to become dark blue.
3. Stain animals for 45–60 min.
4. Transfer stained specimens by pipetting into a new petri dish containing fresh ASW to wash the animals.
5. Proceed with mechanical manipulation experiments (*see* Subheading 3.4).

3.4 Mechanical Manipulation

The following protocol refers to the procedures described in Schwartz 1984 [26].

1. Transfer live specimens into a glass petri dish prefilled 2/3 with fresh ASW to remove algae.

2. Wait for 5 min for the animals to attach and become completely flattened.
3. Cut a small piece from one (stained) animal by using an acupuncture needle (Fig. 3a).
4. Create a hole in the center of another animal by using an acupuncture needle (Fig. 3b).
5. Immediately transfer the small animal fragment by pipetting into the middle of the hole of the other animal (Fig. 3c).
6. Follow the wound healing/regeneration process (Fig. 3d) by visual inspection and taking pictures/time-lapse videos (*see* **Note 15**).

3.5 Animal Fixation

This protocol follows [35].

1. Follow **steps 4** and **5** in Subheading 3.1 to transfer animals to be fixed into separate petri dishes.
2. Wait until all animals have settled on the bottom of the petri dishes.
3. Remove as much ASW as possible before adding fixative.
4. Carefully add ice-cold fixative A until the petri dishes are filled 2/3.
5. Incubate at room temperature for 90 s.
6. Carefully remove fixative A.
7. Carefully add ice-cold fixative B.
8. Incubate at 4 °C for 1 h.
9. Carefully remove fixative B.
10. Wash animals three times in ice-cold DEPC-treated H_2O.
11. Immediately proceed with respective downstream protocols (e.g., in situ hybridization).

3.6 Animal Body Dissociation and Reaggregation

In general, the success of regeneration, with the eventual rebuilding of a vital whole animal, is highly dependent on the random aggregation of all cell types (potentially including pluri- or omnipotent stem cells). The protocol below refers to the procedures as described in Ruthmann and Terwelp [28] as well as Sebe-Pedros et al. [14].

1. Transfer 50 live animals into a petri dish containing fresh ASW to remove algae.
2. Transfer animals by pipetting into a new petri dish prefilled 2/3 with CMF-ASW + EGTA (*see* **Note 3**).
3. Wait for 2–5 min until the cells start to disperse, beginning from the margin of the animal.

4. Carefully pipet animals 5–10 times up and down to accelerate the complete dissociation process of the entire animal body.
5. Pipet cell suspension into 1.5 mL tube and add fresh ASW.
6. Centrifuge the dissociated cells for 2 min at 150 rcf in a table centrifuge.
7. Remove and discard the excess ASW from the tube.
8. Leave the concentrated cell suspension for reaggregation overnight.
9. Monitor the ongoing reaggregation process under the stereomicroscope.

4 Notes

1. The recently reported "spontaneously occurring body disruptions" in *Trichoplax adhaerens* [36] are likely the result of inappropriate culture conditions.
2. Neither age nor any kind of developmental stages can be deduced from placozoan morphology. Likewise, division (i.e., vegetative reproduction) cannot be precisely predicted as it does not seem to be size-related.
3. CMF-ASW can be supplemented with 0.1% (v/v) trypsin to improve animal body dissociation [28].
4. The rate of success of mechanical manipulation/transplantation experiments on placozoans is strongly related on the vitality of acceptor animals; moving acceptor animals are frequently repelling the donor fragment.
5. Alternatively, we have successfully used the following composition for ASW: 26.29 g NaCl, 0.74 g KCl, 0.99 g $CaCl_2$, 6.09 g $MgCl_2 \bullet 6H_2O$, 3.94 g $MgSO_4 \bullet 7H_2O$ in 1 L ddH_2O [37]. ASW should be prepared at least 24 h in advance of usage. Ideally, ASW should settle for 3–5 days.
6. We took the composition of CMF-ASW from a previously published recipe [38].
7. The process of picking and transferring large numbers of placozoans can be simplified by stepwise adding 1 M $MgCl_2$ or alternatively 5% (v/v) total volume of ethanol [39] into the culture petri dish. After gently shaking, animals will detach and can be pipetted in large batches into a new petri dish. Remaining $MgCl_2$−/ethanol-enriched seawater has to be replaced afterward by regular ASW. Avoid adding an excess of $MgCl_2$, and application times longer than 2 min, since both will increase disintegration of animals.

8. Rinse glassware with ASW before usage to remove remnants of detergents.
9. For most experiments sterile working conditions are not necessary, that is, glassware does not need to be autoclaved unless downstream analyses require sterile work.
10. In addition to standard algae as food sources, placozoans can also be cultured on glass slides which are covered with a natural marine biofilm. Biofilm-covered slides can be obtained by placing clean (new) slides into a seawater aquarium or (if possible) a natural marine environment for at least seven days. Before usage, the biofilm-covered slides should be washed in ddH_2O for several hours to avoid placozoan contamination from the field/aquarium.
11. Depending on the food source, coloring of placozoans may look transparent/light white, pink, light yellow, light green, light brown, or blue. Healthy animals fed with *P. helgolandii* usually acquire a pinkish coloring due to the storage of breakdown products of algae digestion.
12. Frequently measure salinity in the culture dishes and adjust with ddH_2O to keep salinity constant at 35‰ ± 2‰. Avoid dropping of ddH_2O directly onto the animals.
13. The sporadically occurring sudden decline of a particular placozoan culture due to unfavorable conditions can be minimized by the weekly split of cultures and by keeping multiple cultures at different places.
14. Indicators of unfavorable culture conditions are animals with a large central bubble between the upper and lower epithelium or elongated placozoans (thread-shaped) (Fig. 1b and c, respectively).
15. The exposure of animals to a directional light source may cause an increase of animal movement activity, which has to be taken into account during the regeneration process.

References

1. Grell KG (1971) *Trichoplax adhaerens* F.E. Schulze und die Entstehung der Metazoan. Naturwissenschaftliche Rundschau 24(4):160–161
2. Schulze FE (1883) *Trichoplax adhaerens*, nov. gen., nov. spec. Zool Anz 6:92–97
3. Schulze FE (1891) Über *Trichoplax adhaerens*. In: Reimer G (ed) Abhandlungen der Königlichen Preuss. Verlag der königlichen Akademie der Wissenschaften, Berlin, Akademie der Wissenschaften zu Berlin, pp 1–23
4. Schierwater B (2005) My favorite animal, *Trichoplax adhaerens*. BioEssays 27(12): 1294–1302. https://doi.org/10.1002/bies.20320
5. Schierwater B, DeSalle R (2018) Placozoa. Curr Biol 28(3):R97–R98. https://doi.org/10.1016/j.cub.2017.11.042
6. Osigus HJ, Rolfes S, Herzog R, Kamm K, Schierwater B (2019) *Polyplacotoma mediterranea* is a new ramified placozoan species. Curr Biol 29(5):R148–R149. https://doi.org/10.1016/j.cub.2019.01.068

7. Eitel M, Francis WR, Varoqueaux F, Daraspe J, Osigus HJ, Krebs S, Vargas S, Blum H, Williams GA, Schierwater B, Worheide G (2018) Comparative genomics and the nature of placozoan species. PLoS Biol 16(7):e2005359. https://doi.org/10.1371/journal.pbio.2005359
8. Schierwater B (2013) Placozoa, Plattentiere. In: Westheide W, Rieger R (eds) Spezielle Zoologie. Teil 1: Einzeller und Wirbellose Tiere. 3rd edn. Springer Spektrum Berlin pp. 103–107
9. Schierwater B, Eitel M, Osigus HJ, von der Chevallerie K, Bergmann T, Hadrys H et al (2010) *Trichoplax* and Placozoa: one of the crucial keys to understanding metazoan evolution. In: DeSalle R, Schierwater B (eds) Key transitions in animal evolution. CRC Press, Boca Raton, FL, pp 289–326
10. Schierwater B, Eitel M (2015) Placozoa. In: Wanninger A (ed) Evolutionary developmental biology of invertebrates 1: introduction, non-Bilateria, Acoelomorpha, Xenoturbellida. Chaetognatha. Springer Vienna, Vienna, pp 107–114. https://doi.org/10.1007/978-3-7091-1862-7_5
11. Smith CL, Varoqueaux F, Kittelmann M, Azzam RN, Cooper B, Winters CA, Eitel M, Fasshauer D, Reese TS (2014) Novel cell types, neurosecretory cells, and body plan of the early-diverging metazoan *Trichoplax adhaerens*. Curr Biol 24(14):1565–1572. https://doi.org/10.1016/j.cub.2014.05.046
12. Mayorova TD, Hammar K, Winters CA, Reese TS, Smith CL (2019) The ventral epithelium of *Trichoplax adhaerens* deploys in distinct patterns cells that secrete digestive enzymes, mucus or diverse neuropeptides. Biol Open 8(8):bio045674. https://doi.org/10.1242/bio.045674
13. Romanova DY, Varoqueaux F, Daraspe J, Nikitin MA, Eitel M, Fasshauer D, Moroz LL (2021) Hidden cell diversity in Placozoa: ultrastructural insights from *Hoilungia hongkongensis*. Cell Tissue Res 385(3):623–637. https://doi.org/10.1007/s00441-021-03459-y
14. Sebe-Pedros A, Chomsky E, Pang K, Lara-Astiaso D, Gaiti F, Mukamel Z, Amit I, Hejnol A, Degnan BM, Tanay A (2018) Early metazoan cell type diversity and the evolution of multicellular gene regulation. Nat Ecol Evol 2(7):1176–1188. https://doi.org/10.1038/s41559-018-0575-6
15. Jakob W, Sagasser S, Dellaporta S, Holland P, Kuhn K, Schierwater B (2004) The Trox-2-Hox/ParaHox gene of *Trichoplax* (Placozoa) marks an epithelial boundary. Dev Genes Evol 214(4):170–175. https://doi.org/10.1007/s00427-004-0390-8
16. Schierwater B, de Jong D, Desalle R (2009) Placozoa and the evolution of Metazoa and intrasomatic cell differentiation. Int J Biochem Cell Biol 41(2):370–379. https://doi.org/10.1016/j.biocel.2008.09.023
17. Grell KG, Benwitz G (1971) Die Ultrastruktur von *Trichoplax adhaerens* F.E. Schulze. Cytobiologie 4:216–240
18. Jackson AM, Buss LW (2009) Shiny spheres of placozoans (*Trichoplax*) function in anti-predator defense. Invertebr Biol 128(3):205–212. https://doi.org/10.1111/j.1744-7410.2009.00177.x
19. Mayorova TD, Smith CL, Hammar K, Winters CA, Pivovarova NB, Aronova MA, Leapman RD, Reese TS (2018) Cells containing aragonite crystals mediate responses to gravity in *Trichoplax adhaerens* (Placozoa), an animal lacking neurons and synapses. PLoS One 13(1):e0190905. https://doi.org/10.1371/journal.pone.0190905
20. Romanova DY, Heyland A, Sohn D, Kohn AB, Fasshauer D, Varoqueaux F, Moroz LL (2020) Glycine as a signaling molecule and chemoattractant in *Trichoplax* (Placozoa): insights into the early evolution of neurotransmitters. Neuroreport 31(6):490–497. https://doi.org/10.1097/WNR.0000000000001436
21. Ueda T, Koya S, Maruyama YK (1999) Dynamic patterns in the locomotion and feeding behaviors by the placozoan *Trichoplax adhaerence*. Biosystems 54(1–2):65–70
22. Fortunato A, Aktipis A (2019) Social feeding behavior of *Trichoplax adhaerens*. Front Ecol Evol 7:19. https://doi.org/10.3389/fevo.2019.00019
23. Smith CL, Pivovarova N, Reese TS (2015) Coordinated feeding behavior in *Trichoplax*, an animal without synapses. PLoS One 10(9):e0136098. https://doi.org/10.1371/journal.pone.0136098
24. Smith CL, Reese TS, Govezensky T, Barrio RA (2019) Coherent directed movement toward food modeled in *Trichoplax*, a ciliated animal lacking a nervous system. Proc Natl Acad Sci U S A 116(18):8901–8908. https://doi.org/10.1073/pnas.1815655116
25. Heyland A, Croll R, Goodall S, Kranyak J, Wyeth R (2014) *Trichoplax adhaerens*, an enigmatic basal metazoan with potential. Methods Mol Biol 1128:45–61. https://doi.org/10.1007/978-1-62703-974-1_4
26. Schwartz V (1984) The radial polar pattern of differentiation in *Trichoplax adhaerens*

F.E. Schulze (Placozoa). Z. Naturforsch. C 39: 818–832

27. Zuccolotto-Arellano J, Cuervo-Gonzalez R (2020) Binary fission in *Trichoplax* is orthogonal to the subsequent division plane. Mech Dev 162:103608. https://doi.org/10.1016/j.mod.2020.103608
28. Ruthmann A, Terwelp U (1979) Disaggregation and reaggregation of cells of the primitive metazoan *Trichoplax adhaerens*. Differentiation 13:185–198
29. Miller RL (1971) Observations on *Trichoplax Adhaerens* Schulze, 1883. Am Zool 11(4): 698–699
30. Kuhl W, Kuhl G (1963) Bewegungsphysiologische Untersuchungen an *Trichoplax adhaerens* F. E. Schulze. Zoologischer Anzeiger Suppl 26:460–469
31. Kuhl W, Kuhl G (1966) Untersuchungen über das Bewegungsverhalten von *Trichoplax adhaerens* F.E.Schulze. Z Morphol Oekol Tiere 56: 417–435
32. Eitel M, Schierwater B (2010) The phylogeography of the Placozoa suggests a taxon-rich phylum in tropical and subtropical waters. Mol Ecol 19(11):2315–2327. https://doi.org/10.1111/j.1365-294X.2010.04617.x
33. von der Chevallerie K (2013) Experimental studies on the tumor suppressor p53, the myc protooncogene and tissue compatibility in the basal metazoan phylum Placozoa. PhD Thesis
34. Rassat J, Ruthmann A (1979) *Trichoplax adhaerens* F. E. Schulze (Placozoa) in the scanning electron microscope. Zoomorphology 93: 59–72
35. DuBuc TQ, Ryan JF, Martindale MQ (2019) "dorsal-ventral" genes are part of an ancient axial patterning system: evidence from *Trichoplax adhaerens* (Placozoa). Mol Biol Evol 36(5):966–973. https://doi.org/10.1093/molbev/msz025
36. Prakash VN, Bull MS, Prakash M (2021) Motility-induced fracture reveals a ductile-to-brittle crossover in a simple animal's epithelia. Nat Phys 17(4):504. https://doi.org/10.1038/s41567-020-01134-7
37. Artificial Seawater (2012). Cold Spring Harbor protocols 2012 (2):pdb.rec068270. https://doi.org/10.1101/pdb.rec068270
38. Calcium- and magnesium-free artificial seawater (CMF-ASW) (2009). Cold Spring Harbor Protocols 2009 (12):pdb.rec12053. https://doi.org/10.1101/pdb.rec12053
39. Miyazawa H, Nakano H (2018) Multiple surveys employing a new sample-processing protocol reveal the genetic diversity of placozoans in Japan. Ecol Evol 8(5):2407–2417. https://doi.org/10.1002/ece3.3861
40. Schierwater B, Kamm K, Wysocki K, Osigus HJ (2021) Phylum Placozoa. In: Schierwater B, DeSalle R (eds) Invertebrate zoology: a tree of life approach. Taylor & Francis, Abingdon-on-Thames, Oxfordshire

Open Access This chapter is licensed under the terms of the Creative Commons Attribution 4.0 International License (http://creativecommons.org/licenses/by/4.0/), which permits use, sharing, adaptation, distribution and reproduction in any medium or format, as long as you give appropriate credit to the original author(s) and the source, provide a link to the Creative Commons license and indicate if changes were made.

The images or other third party material in this chapter are included in the chapter's Creative Commons license, unless indicated otherwise in a credit line to the material. If material is not included in the chapter's Creative Commons license and your intended use is not permitted by statutory regulation or exceeds the permitted use, you will need to obtain permission directly from the copyright holder.



Chapter 7

Collecting and Culturing Kamptozoans for Regenerative Studies

Achim Meyer, Julia Merkel, and Bernhard Lieb

Abstract

Kamptozoa, also known as Entoprocta, are small aquatic filter-feeders that belong to the Lophotrochozoan superphylum, which also contains other acoelomate phyla including Annelida, Nemertea, and Mollusca. The study of Kamptozoa is thus of great interest to understand the early Lophotrochozoan evolution. Moreover, many kamptozoans have been shown to possess great regeneration capacities, including whole-body regeneration. In addition, and in particular for colonial cosmopolitan species such as *Barentsia benedeni*, kamptozoans are highly suitable as laboratory model organisms because of their simple culture, low space requirements, transparency and rapid life cycle. This chapter provides a brief introduction into field collection, culturing techniques for both the animals as well as the algae required for their feeding, fixation, staining, and sequencing.

Key words Entoprocta, Kamptozoa husbandry, *Cryptomonas baltica*, Filtration feeding

1 Introduction

Kamptozoans are aquatic acoelomate filter-feeding invertebrates. These animals have a typically minute body, called zooid, ranging from 0.1 mm (Loxosomatidae) to 15 mm (Barentsiidae), composed of a stalk part containing the stolon, and a head part called calyx that contains the other organs (Fig. 1). The calyx of kamptozoans is crowned by solid tentacles, which covering cilia generate a flow of water that brings food particles into the atrium of the animal for feeding. Although most of the approximately 180 described kamptozoan species are found in the marine environment (25 *Loxosoma* spp., 118 *Loxosomella* spp., 50 species from the families Loxosomatidae, Pedicellinidae, and Barentsiidae [1, 2]), some species such as the cosmopolitan *Barentsia benedeni* can retreat into brackish water and two species are found exclusively in freshwater (*Urnatella gracilis* [3], and *Loxosomatoides sirindhornae* [4]). All Kamptozoa bear ovoviviparous trochophore larvae

Simon Blanchoud and Brigitte Galliot (eds.), *Whole-Body Regeneration: Methods and Protocols*,
Methods in Molecular Biology, vol. 2450, https://doi.org/10.1007/978-1-0716-2172-1_7, © The Author(s) 2022

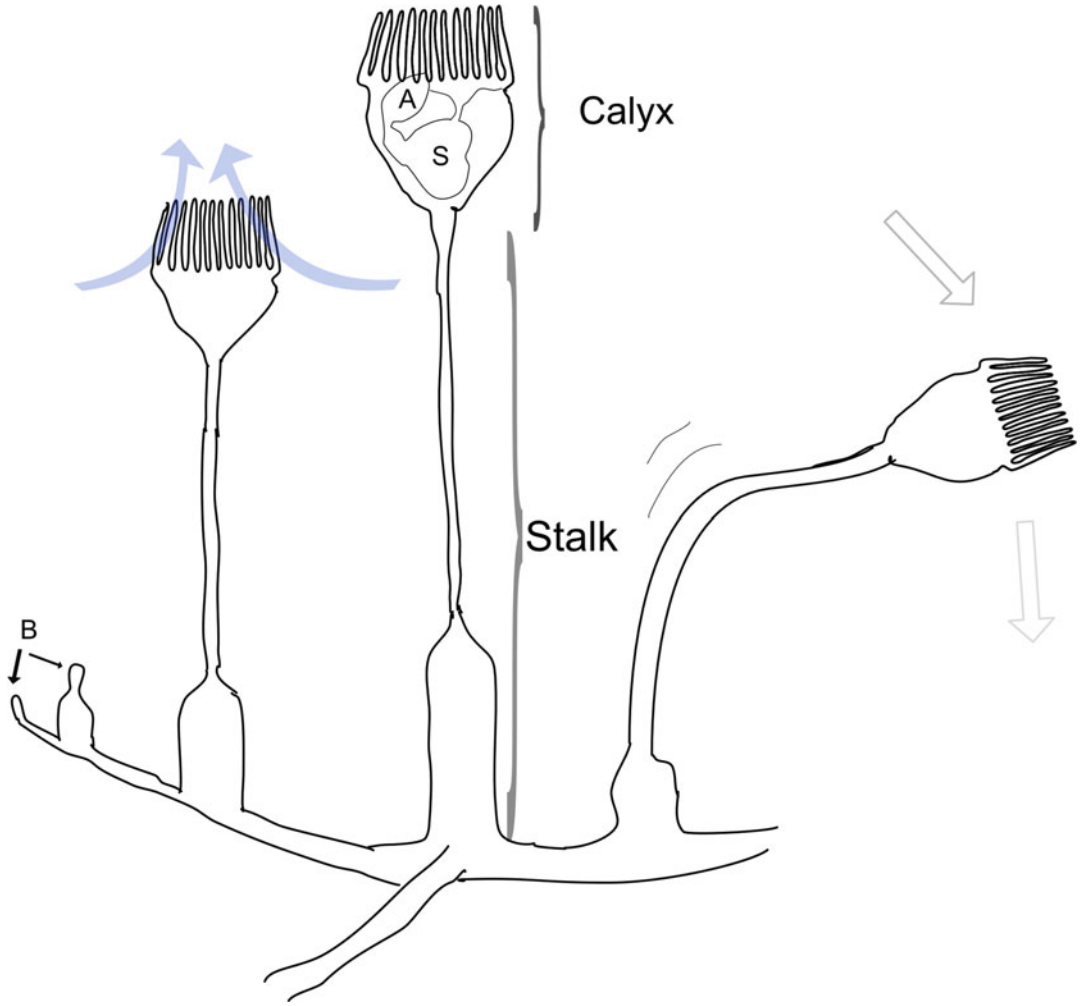


Fig. 1 Sketch of a colonial kamptozoan. A: Anus, B: Budding zooids, S: Stomach. Blue arrows indicate the aspiration current and filtration mode

which are similar to the mollusk and polychaete larvae. Additionally, all known species propagate by budding.

Kamptozoa, also currently known as Entoprocta, initial classifications (e.g., van Beneden 1845 [5]) described colonial species such as *Pedicellina cernua* as an ingroup of the "moss animals," or bryozoans, also currently known as Ectoprocta. Contradiction was firstly raised by Nitsche 1869 [6] pointing out some fundamental differences between these two groups of animals. One of the most readily observable difference is the location of the anus, which is position inside the atrium in Kamptozoa and outside of it in Bryozoa. Consequently, Nitsche suggested the names Entoprocta and Ectoprocta, and these names are still well accepted. However, the mode of filtration generated by cilia on the tentacles is opposed between Entoprocta and Ectoprocta, thus the name-giving

position of the anus is inevitably a consequence of this divergent filtration feeding pattern. Related to the fundamentally divergent adult body plan is also the reorganization of the alimentary system during metamorphosis of the kamptozoan trochophora, when the gut becomes U-shaped, the mouth opening breaks through at a new position and the anus finally settles down within the crown of solid tentacles of the adult zooid [7]. The alternative name Kamptozoa was dropped by Cori 1936 [7] from the Greek κμπτώ = bent and refers to the curved stolon which is observed as reaction to external stimuli. Thus, kamptozoa describes a feature which is related to the unique behavior of the disturbed living animal that facilitates their identification both in the field as well as below the stereomicroscope. Because Kamptozoa provides a friendlier semantic for a researcher focusing on these taxa, we tend to favor the use of this more recent nomenclature.

Phylogenetically, Kamptozoa belong to the Lophotrochozoan superphylum, which contains other phyla including Annelida, Nemertea, and Mollusca. Kamptozoa are thus of great interest to understand the early Lophotrochozoan evolution. Bleidorn [8] summarizes the current knowledge about Lophotrochozoan systematics including the description of characters which define Mollusca as the sister group of Kamptozoa. The internal kamptozoan phylogeny (Fig. 2) agrees on the distinction of Solitaria (130 species) and Coloniales (50 species) [9, 10]. Many colonial species and one solitary species, *Loxosomella antarctica*, have been shown to be capable of whole-body regeneration [11–13]. Whole-body regeneration can take place both under natural conditions (e.g., low salinity leads to the dropping off the calyx during winter [14]) or after zooid loss due to predation of the calyx [15]).

Understanding the regenerative pattern of Kamptozoa could shed light on general developmental processes. Their pronounced regeneration capacity together with the transparent and minute body size makes Kamptozoa an ideal organism for research on whole-body regeneration using modern laboratory procedures such as advanced labeling and staining methods (Fig. 3).

In this chapter, we present protocols for the isolation, culture and feeding of the colonial species *Barentsia benedeni*. In addition, we provide protocols for the monitoring of WBR as well as for the fixation, staining, and DNA extraction of whole zooids. These protocols can easily be adopted for the study of other colonial species, as it works well for *B. elongata*, and will enable short-term (several weeks) work with most solitary species.

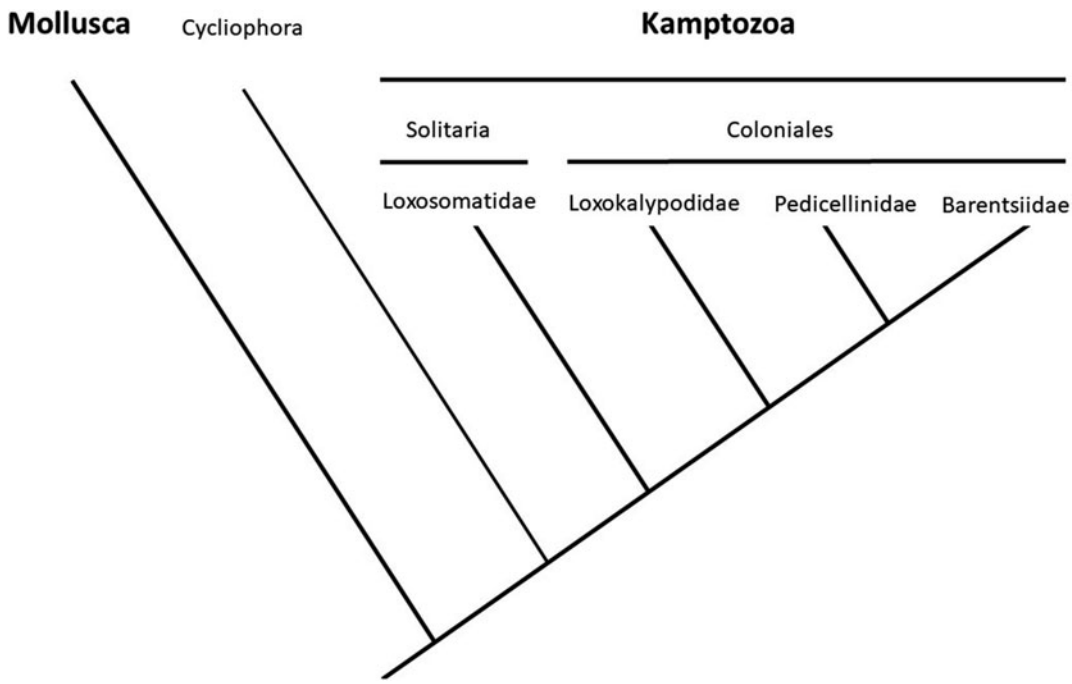


Fig. 2 Phylogenetic relationships of recent kamptozoan families, modified after [8, 9]

2 Material

2.1 Barentsia benedeni *Collection and Culture*

1. Long fine-meshed fishing net.
2. Wide-mouth Kautex jars (e.g., 500 mL).
3. Stereomicroscope.
4. Orbital shaker for kamptozoan culture bowls.
5. Covered glass culture vessel: glass bowl (e.g., Ø 12.5 cm; H: 5.8 cm; 0.36 L) with petri dish as lid and a small piece of cut-in air tubing ø 2/6 mm on the edge of the bowl to provide passive aeration (Fig. 4).
6. Filtered natural seawater (FNSW): natural seawater, 0.22 μm sterile-filtered (*see* **Note 1**). Store in a cool and dark place with air access for up to 1 year (e.g., in a fridge with a cotton plug).
7. Relaxing medium [16]: 79 mM (7.5 g/L) $MgCl_2$ in double-distilled water (ddH_2O). Mix 1:1 with FNSW.

2.2 Live Cryptophyta Algae Stock

Kamptozoans can feed on a variety of live Cryptophyta algae (*see* **Note 2**).

1. 250 mL wide-mouth Erlenmeyer flasks with cotton wool plugs.
2. Luer-lock syringes with sterile 0.22 μm filter unit.

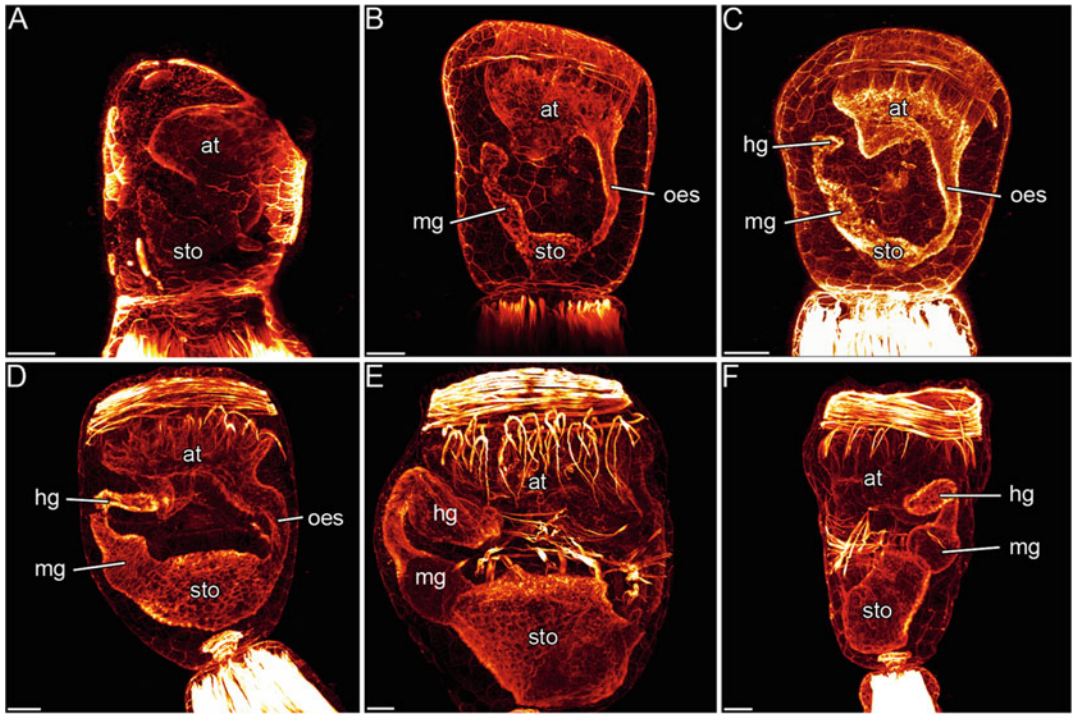


Fig. 3 Confocal micrographs of regeneration stages of *P. cernua* (thesis J. Merkel 2014). Scale bars 20 μm. (**a–e**) lateral view. (**f**) Laterofrontal view. (**a**) First regeneration stage. (**b**) Second regeneration stage. (**c**) Third regeneration stage. (**d**) Fourth regeneration stage. (**e, f**) Fifth regeneration stage. Indicated organs are atrium (at), stomach (sto), esophagus (oes), midgut (mg), and hindgut (hg). Micrographs were gained with a Leica SP5 II confocal microscope



Fig. 4 Culturing bowl with tools for cleaning. Note the green cut-in air tubing

3. Light cabinet with fluorescence bulb: one warm white 18 W T8 fluorescence bulb, 20 cm distance between the light source and the algae is required.
4. 50× Guillard's (F/2) medium [17]: 44.1 mM $NaNO_3$, 1.81 mM NaH_2PO_4, 5.30 mM Na_2SiO_3, 0.585 mM $FeCl_3$, 0.585 mM ethylenediaminetetraacetic acid disodium salt dihydrate (Na_2EDTA), 45.5 μM $MnCl_2$, 3.82 μM $ZnSO_4$, 2.10 μM $CoCl_2$, 1.96 μM $CuSO_4$, 1.30 μM Na_2MoO_4, 14.8 μM thiamine hydrochloride(vitamin B1), 0.102 μM biotin (vitamin H), 0.0184 μM cyanocobalamin (vitamin B12). Store at −20 °C for up to 2 years.

2.3 Fixation for F-Actin Staining

1. 0.1 M PBS (phosphate-buffered saline): 1.4 M NaCl, 26.8 mM KCl, 80.9 mM Na_2HPO_4 in H_2O, adjust to pH 7.4 using HCl or NaOH. Can be stored at room temperature for at least 1 year but should be discarded if turbid.
2. Fixative solution: 4% (v/v) paraformaldehyde (PFA) in 0.1 M phosphate buffered saline. Long-term storage (>2 weeks) in plastic containers at −20 °C and short term at 4 °C.
3. PBT: 0.2% (v/v) Triton X-100 in 0.1 M PBS. If stored at 4 °C in the dark it is usable for months.
4. Conjugated phalloidin: dissolve (usually comes as a powder; e.g., Alexa Fluor 488 phalloidin; Invitrogen, BODYPI R6G phalloidin, Oregon Green 514 phalloidin, BODIPY FL phallacidin) in methanol to yield a final concentration of 200 units/mL. This stock solution is stable for at least 1 year when stored at −20 °C.
5. Staining solution (1:20 diluted): 50 μL conjugated phalloidin, 950 μL PBT. Store at 4 °C in the dark for up to 1 week.

2.4 RNA Extraction and Target Gene Amplification

1. Mortar and pestle.
2. Sterile filter tips.
3. TRIzol™ Reagent (Invitrogen).
4. Chloroform.
5. 2-Propanol.
6. Ice-cold (−20 °C) 75% ethanol.
7. Liquid nitrogen.
8. Coprecipitant (e.g., Vivid Violet®, Roboklon; pellet paint®, Novagen; glycogen).
9. DEPC water: 1 mL diethyl pyrocarbonate (DEPC) in 1000 mL water. Mix in a screw-cap glass bottle. Incubate for ~2 h at room temperature in a fume hood with occasional swirling. Autoclave.

10. Reverse Transcriptase Kit (e.g., Super Script III, Invitrogen) which includes reaction buffer, 25 mM $MgCl_2$, DTT, and the reverse transcriptase enzyme.
11. RNase inhibitor.
12. 10 mM anchored oligoT primer oligodT-T7I. (GAGAGAG GATCCAAGTACTAATACGACTCACTATAGGGAGAT$_{25}$V) and 10 mM anchor primer oligodT-T7II (GAGAGAGGATC CAAGTACTAATACGACTCACTATAGG).
13. 10 mM gene-specific forward primer.
14. Taq polymerase master mix (e.g., 2× OptiTaq PCR Master Mix, Roboklon).
15. TAE buffer: 40 mM Tris, 20 mM acetic acid, 1 mM EDTA.
16. 1% (w/v) agarose (for molecular biology) in TAE buffer.

3 Methods

3.1 Collection and Identification

There are pronounced species-specific settlement preferences such as epizoic growth on sponges, bryozoans, polychaetes, and sipunculids or attachment to macroalgae, and for a few species also inanimate surfaces such as rocks or shells. Known substrate preferences will guide the collection of animals in the field. For example, the cosmopolitan colonial freshwater Kamptozoa *Urnatella gracilis* prefers shells of *Dreissena polymorpha* in the area around Berlin [3] and the solitary kamptozoan *Loxosomella murmanica* live epizoically on the sipunculan *Phascolion strombus* which inhabits empty shells of the gastropod *Turritella* sp. and the scaphopod *Antalis* sp.. Such shells can be dredged from about 30 m depth from muddy and rocky bottom in the North Sea [18]. We here present our protocol for the collection of *Barentsia benedeni* colonies.

1. Identify sheltered microhabitats suitable for the presence of *Barentsia benedeni*. Successful collection sites are at the bottom of wooden pier pilings, groynes, and old macroalgae in low-tide pools.
2. Retrieve material attached to the promising substrate either by scrapping it using a fishing net or by hand if within reach.
3. Transfer the sample to a small container filled with seawater.
4. Isolate suspicious samples with whitish material on them to a transport vessel (e.g., Kautex flask).
5. Bring the collected samples back to the lab.
6. Transfer one sample into a large petri dish or tray filled with FNSW.
7. Screen the whitish material under a dissecting microscope.

8. Confirm that identified zooids are kamptozoans by disturbing them using a fine paintbrush and observing their unique bending behavior.
9. Detach the kamptozoans from their substrate using a scalpel blade. Solitary kamptozoans such as *Loxosomella vivipara* immediately glue themselves with their foot on the glass wall of the container and in such cases the relaxing medium must be applied. Wait 1 to 3 min for the animals to relax (*see* **Note 3**).
10. Flush the detached animals using a Pasteur pipette while holding its stolon with curved tweezers to clean them from associated macrofauna such as Gammaridae or other small crustaceans.
11. Pool the cleaned kamptozoans in a container filled with FNSW and continue with either Subheadings 3.3, 3.4, or 3.5, respectively.

3.2 Food Algae Culture

Wear gloves to avoid contamination.

1. Pour a 200 mL aliquot of the algae stock on a petri dish.
2. Screen for obvious signs of contamination with a microscope.
3. Discontinue contaminated cultures, start with a new stock in **step 1**.
4. Transfer 150 mL NFSW into a 250 mL Erlenmeyer flask with a cotton plug.
5. Heat up for 1 min at 600 W in a microwave. Do not let the water boil or salts will precipitate [17].
6. Add 3 mL of freshly filter-sterilized 50X F/2 medium to the hot seawater (*see* **Note 4**).
7. Mix gently by swirling without wetting the cotton plug.
8. Wait 1 h for the medium to cool down to culturing temperature (RT or lower).
9. Inoculate with up to 50 mL algae stock.
10. Place the culture on an orbital shaker (~120 rpm) in the light cabinet (*see* **Note 5**).
11. Leave the culture to grow for 2 weeks before using it for feeding kamptozoans.
12. Algae cultures can be kept up to 1 month.
13. Renew the culture by starting with **step 1** using the old culture as stock.
14. Keep two 50 mL cultures at lower light, without shaking nor routine opening, for up to 2 months as backups.

3.3 Barentsia benedeni Culture

In our culturing setup, collected colonies will not attach themselves again to the walls of the culture vessel but will become floating ball-like structures.

1. Gently shake colonies within the culturing water using curved tweezers to remove detritus and filamentous algae.
2. Gently flush the colonies with a Pasteur pipette while holding them to remove potential unwanted macrofauna.
3. Transfer the cleaned colony to a tray filled with FNSW.
4. Confirm cleanness and health condition under a stereo microscope.
5. Discard sick or contaminated colonies.
6. Transfer the colony to a clean culturing bowl filled with FNSW (Fig. 4).
7. Place the culture bowl on a rotating shaker with low speed <100 rpm at 16–19 °C and dim indirect light during daytime (12 h/12 h) (*see* **Notes 6** and **7**).
8. Add once a week 5 mL of a dense algae culture with a Pasteur pipette to the *Barentsia* culture vessel (*see* **Notes 8** and **9**).
9. Leave the animals to feed for 24 h.
10. Gently shake colonies within the culturing water using curved tweezers to remove detritus and uneaten algae.
11. Clean the colonies and maintain the culture by restarting at **step 1**.

3.4 Tissue Isolation and Regeneration

1. Transfer a cleaned colony to a container filled with fresh FNSW.
2. Starve the colony for 1 week to fully isolate the zooid (*see* **Note 10**).
3. Clean the colony and the culture vessel twice during the starvation.
4. Amputate the tissue to be isolated using a fine pair of Vannas scissors.
5. Transfer the colony back to a clean culture vessel, without feeding.
6. Monitor the regenerating colony every 48 h.
7. In the case of whole-body regeneration induced by a stalk cut, regeneration will proceed as follows (Fig. 3).
8. 2 days postamputation (dpa): first regeneration stage, atrium and stomach have already formed.
9. 4 dpa: second regeneration stage, the esophagus has elongated, midgut is formed, and atrium is bulged on the anal side.
10. 6 dpa: third regeneration stage, developing hindgut and atrium converge.
11. 8 dpa: fourth regeneration stage, hindgut and atrium are interconnected.
12. 10 dpa: fifth regeneration stage, intestinal tract is again fully developed.

3.5 Fixation and F-Actin Staining

This protocol describes staining against F-actin but can be generalized to other conjugated probes by adapting the composition and incubation time of the staining medium. Thus staining with other primary and secondary antibodies could be applied to study different structures such as nuclei or keratin.

1. Transfer a fresh tissue sample to a 2 mL tube containing 1.5 mL of fixative solution.
2. Incubate for 1 h at room temperature.
3. Rinse the sample for 15 min in 0.1 M PBS.
4. Rinse the sample two more times by repeating **step 3**.
5. Store for up to 1 week at 4 °C in 0.1 M PBS containing 0.1% sodium azide (NaN_3) if subsequent developmental stages need to be collected (optional).
6. If sample was stored in NaN_3 repeat **step 3** and **4**.
7. Replace the solution with 1.5 mL of PBT.
8. Incubate for 1 h at room temperature to permeabilize the cell walls.
9. Replace the solution with 1 mL of staining solution.
10. Incubate for 4 h in the dark at room temperature.
11. Rinse three times in PBS for 15 min.
12. Transfer the sample onto a glass slide.
13. Mount with aqueous mounting medium.
14. Cover with a coverslip.
15. Image on a fluorescence microscope.

3.6 Total RNA Extraction and Target Gene Amplification

Although RNA can be extracted from any piece of tissue, we obtained good yields by pooling together tissue from approximately 40 clonal zooids. The sample volume should not exceed 10% of the volume of the TRIzol used for lysis. You may wash your bench and pipettes with RNase erase solution before work. All steps at room temperature unless otherwise specified. Wear protective gloves and googles when working with liquid nitrogen or deep-frozen devices. Use a fume hood during processing of phenol. Wear disposable gloves while handling organic reagents such as TRIzol (contains phenol) and RNA samples to prevent RNase contamination from the surface of the skin; change gloves frequently, particularly as the protocol progresses from crude extracts to more purified materials.

1. Precool mortar and pestle at −80 °C for several hours or overnight.
2. Fill a 2 mL reaction tube with 1 mL of TRIzol.
3. Dab the isolated tissue onto a paper wipe.

4. Transfer the tissue to a 2 mL tube.
5. Shock-freeze the tube in liquid nitrogen.
6. Store the frozen tissue at −80 °C until needed.
7. Transfer the deep-frozen tissue to the precooled mortar.
8. Grind the frozen tissue to a fine powder. You may carefully add liquid nitrogen using a ladle if signs of thawing occur during homogenization (*see* **Note 11**).
9. Transfer the powdered tissue to the prepared reaction tube with TRIzol using a spatula below a fume hood.
10. Incubate for 5 min.
11. Add 0.2 mL of chloroform.
12. Securely cap the tube and shake hard for 30 s while securing the lid with your thumb.
13. Incubate for 2–3 min.
14. Centrifuge the sample for 15 min at 12,000 rcf at 4 °C. The mixture separates into a lower red phenol–chloroform, an interphase, and a colorless upper aqueous phase containing the RNA.
15. Transfer the upper aqueous phase to a new sterile tube by angling the tube at 45° and avoid touching the interphase. Be generous to sacrifice RNA containing aqueous phase to the benefit of avoiding carry over contaminations from the interphase or the red organic phase.
16. Add 2 μL of coprecipitant to the aqueous phase in the new tube.
17. Add 0.5 mL of isopropanol.
18. Vortex briefly.
19. Incubate for 10 min.
20. Centrifuge for 10 min at 12,000 rcf at 4 °C. Total RNA precipitates as a pink pellet or a white gel-like pellet (if using glycogen) at the bottom of the tube.
21. Discard the supernatant using a pipette.
22. Resuspend the RNA pellet in 1 mL cold 75% ethanol by vortexing and flicking the tube.
23. The tube can be stored up to 1 year at −20 °C.
24. Centrifuge for 5 min at 7500 rcf at 4 °C.
25. Discard the supernatant using a pipette. Avoid touching or detaching the pellet.
26. Let the RNA pellet dry for 5–10 min by opening the lid in a dust free space.

27. Resuspend the pellet in 20–50 μL DEPC water and store the RNA solution at −80 °C or proceed to the next step setting up a rtPCR.
28. Thaw the following tubes from the cDNA synthesis kit at room temperature: 10× RT buffer, 25 mM $MgCl_2$ and 0.1 M DTT but keep the RNase inhibitor and the reverse transcriptase at −20 °C until needed (**step 32**).
29. Combine the following in a 0.2- or 0.5-mL tube: 1–4 μL RNA solution, 1 μL oligodT-T7I primer, 1 μL dNTP mix.
30. Fill up to 10 μL using DEPC water.
31. Incubate the tube at 65 °C for 5 min.
32. Prepare the following cDNA Synthesis Mix, adding each component in the indicated order in a 0.2 mL tube on ice: 2 μL 10× RT buffer, 4 μL 25 mM $MgCl_2$, 2 μL 0.1 M DTT, 1 μL RNase inhibitor, 1 μL reverse transcriptase.
33. Place the incubated RNA on ice for at least 1 min.
34. Add the 10 μL cDNA Synthesis Mix to the RNA/primer mix.
35. Incubate 50 min at 50 °C.
36. Terminate the reactions at 85 °C for 5 min.
37. Chill on ice for 1–5 min.
38. cDNA synthesis reaction can be stored at −20 °C or used for PCR immediately.
39. For PCR, add each component in the indicated order in a 0.2 mL tube on ice: 25 μL Master Mix, 1 μL gene specific forward primer, 1 μL oligodT-T7II, 1–4 μL cDNA mix and fill up to 50 μL using sterile water.
40. Amplify the PCR product using the following temperature settings in a thermocycler: Denaturation at 93–95 °C 2 min, 30× (denaturation at 93–95 °C 15 s, annealing at 50–68 °C for 30 s, elongation at 72 °C for 20 s/kb), final extension 7 min. Store at 4–16 °C.
41. Control visually for the presence of a single sharp PCR product band on an agarose gel.
42. Send 50 ng up to 200 ng DNA (e.g., 2 μL of a 1/10 diluted PCR reaction) in a 10 pmol primer solution to a Sanger sequencing company (*see* **Note 12**).

4 Notes

1. In our lab, we use commercially available FNSW which is shipped in 5 L containers. Natural seawater is mandatory for long term culture of the species, but not for the algae. For algal culture, it is thus possible to use artificial seawater instead.

2. Published lab culture of kamptozoans are based on feedings with algae suspensions from strains such as *Isochrysis*, *Monochrysis* [19], and *Cryptomonas* or for freshwater species *Ankistrodesmus*, *Scenedesmus*, and *Chlorella* [3]. In our lab, we have been using successfully *Cryptomonas baltica* for over 5 years. If this specific algae cannot be obtained, we would suggest as an alternative *Pyrenomonas helgolandii*. It can be assumed that this alga is just as suitable as *Cryptomonas* as complete feed, but it might require another medium than F/2 to grow as the advice of the SAG (Culture Collection of Algae at Göttingen University) is to use media including soil extract for this species.
3. Proceed with steps under anesthesia as efficiently as possible. Although $MgCl_2$ anesthesia is reversible, such a treatment is stressful for the animal. Thus, living healthy individuals for culturing purpose are best obtained without or very short $MgCl_2$ incubation times.
4. Although high temperatures might be harmful to the vitamins, we have been introducing the 50× F/2 medium shortly after heating without obvious negative effects. On the contrary, the high temperature appears to be helpful in avoiding contaminations.
5. Algae can alternatively be cultured without shaking but with daily manual swirling of the flasks. If no light cabinet is available, algae can be cultured simply using daylight from a northern window avoiding direct sun and high temperatures (Fig. 5).
6. *B. benedeni* can be kept in brackish water with a salinity of 20 ppt to allow slight evaporation to reduce the risk of losing the animals in times of lower maintenance due to excessive increase in salinity.
7. Animals can be placed on the same shaker as the algae flasks but draw-off should take place in another room to reduce the contamination risk. If a separate room isn't available, clean thoroughly the opening of the algae flask either by flaming or by using ethanol before collecting out of the flask.
8. Increase feeding rate if stronger growth is desired. Increased feeding must be done with more frequent feeding, not higher algae quantity in a single feeding, and needs always be accompanied by subsequent water exchange.
9. There are concentrated algae paste commercially available (e.g., Shellfish Diet 1800, Reed Mariculture). We have no experience using instant algae paste for Kamptozoa, but it might be possible to skip the algae culture part by using such products. Nonliving feed will increase the risk of water deterioration and will require careful water exchange and transfer to clean bowls more often.



Fig. 5 Simple algae culturing unit using natural light without shaker. Bottles are shaken manually once every working day because algae tend to settle on the bottom. *Isochrysis* sp. (left bottle) and *Nannochloropsis* sp. (right bottle)

10. Starvation time might be reduced because it has been shown that Kamptozoa have fast digesting times of a few hours [7].
11. In case of low tissue amount the tissue can be grinded directly in a 2 mL reaction tube using an EPPI-Pistill.
12. In case of heterogenous or low signal reads, PCR cleanup using SAP digestion or agarose gel clean up should be applied to improve the quality of the sequencing reads.

Acknowledgments

We are grateful for the detailed and comprehensive help from Simon Blanchoud turning our first draft into the desired style and language of the final manuscript. We thank Andreas Wanninger for sharing his experience in labeling marine invertebrates with us.

References

1. Nielsen C (2010) A review of the taxa of solitary entoprocts (Loxosomatidae). Zootaxa 2395:45–56
2. Schmidt-Rhaesa A (2019) Miscellaneous invertebrates. De Gruyter, Berlin
3. Emschermann P (1965) Über die sexuelle Fortpflanzung und die Larve von *Urnatella gracilis*, Leidy (Kamptozoa). Z Morphol Oekol Tiere 55(1):100–114
4. Wood TS (2005) *Loxosomatoides sirindhornae*, new species, a freshwater kamptozoan from Thailand (Entoprocta). Hydrobiologia 544(1):27–31
5. Van Beneden PJ (1845) Recherches sur l'anatomie, la physiologie et le developpment des Bryozoaires du cote d'Ostende. Histoire naturelle du genre Pedicellina. Nouv Mem Acad R Sci Bruxelles 19(2):1–31
6. Nitsche H (1869) Beiträge zur Kenntniss der Bryozoen I-II. Z Wiss Zool 20:1–36
7. Cori CJ (1936) Kamptozoa. Bronns Klassen und Ordnungen des Tierreichs. Bd. 4, Abt. II. Buch 4. Akademische Verlagsgesellschaft, Leipzig
8. Bleidorn C (2019) Recent progress in reconstructing lophotrochozoan (spiralian) phylogeny. Org Divers Evol 19(4):557–566
9. Emschermann P (1972) *Loxokalypus socialis* gen. et sp. nov. (Kamptozoa, Loxokalypodidae fam. nov.), ein neuer Kamptozoentyp aus dem nördlichen Pazifischen Ozean. Ein Vorschlag zur Neufassung der Kamptozoensystematik. Mar Biol 12:237–254. https://doi.org/10.1007/BF00346772
10. Wasson K (2002) A review of the invertebrate phylum Kamptozoa (Entoprocta) and synopsis of kamptozoan diversity in Australia and New Zealand. T Roy Soc South Aust 126:1–20
11. Emschermann P (1969) Ein Kreislauforgan bei Kamptozoen. Z Zellforsch 97:567–607
12. Emschermann P (1993) On Antarctic Entoprocta: nematocyst-like organs in a Loxosomatid, adaptive developmental strategies, host specificity and bipolar occurrence of species. Biol Bull 184:153–185
13. Mukai H, Makioka T (1978) Studies on regeneration of an Entoproct, Barentsia-discreta. J Exp Zool 205(2):261–275
14. Nassanoc N (1926) *Arthropodaria kovalevskii* n. sp. (Entoprocta) und die Regeneration ihrer Organe. Trav Lab Zool Sta Biol Séhastopol Acad Sei URSS Ser.2) 5:1–38
15. Canning MH, Carlton JT (2000) Predation on kamptozoans (Entoprocta). Invertebr Biol 119(4):386–387
16. Messenger JB, Nixon M, Ryan KP (1985) Magnesium chloride as an anaesthetic for cephalopods. Comp Biochem Physiol C 82(1):203–205
17. Andersen RA (2005) Algal culturing techniques. Elsevier/Academic Press, Burlington
18. Merkel J, Wanninger A, Lieb B (2018) Novel and conserved features of the Hox cluster of Entoprocta (Kamptozoa). J Phylogenetics Evol Biol 2018(6):1. https://doi.org/10.4172/2329-9002.1000194
19. Nielsen C, Rostgaard J (1976) Structure and function of an entoproct tentacle with discussion of ciliary feeding types. Ophelia 15:115–140

Open Access This chapter is licensed under the terms of the Creative Commons Attribution 4.0 International License (http://creativecommons.org/licenses/by/4.0/), which permits use, sharing, adaptation, distribution and reproduction in any medium or format, as long as you give appropriate credit to the original author(s) and the source, provide a link to the Creative Commons license and indicate if changes were made.

The images or other third party material in this chapter are included in the chapter's Creative Commons license, unless indicated otherwise in a credit line to the material. If material is not included in the chapter's Creative Commons license and your intended use is not permitted by statutory regulation or exceeds the permitted use, you will need to obtain permission directly from the copyright holder.



Check for updates

Chapter 8

Collecting and Culturing Bryozoans for Regenerative Studies

Abigail M. Smith, Peter B. Batson, Katerina Achilleos, and Yuta Tamberg

Abstract

Among marine invertebrates, bryozoans are small, not well known, and complex to identify. Nevertheless, they offer unique opportunities for whole-body generation research, because of their colonial, modular mode of growth. Here, we describe detailed methods for collection of bryozoans from a range of environments, sample preparation and identification, culture and feeding, spawning and breeding, marking colonies for growth studies, and histological preparation.

Key words Bryozoans, Culture, Collection, Growth, Feeding, Whole-body regeneration, Budding, Regression, Brown bodies, Anatomy, Histology, Larvae, Spawning, Settlement

1 Introduction

The Bryozoa (moss animals) is a diverse phylum of colonial aquatic invertebrates found in almost all freshwater and marine environments. The phylum comprises ~6000 living species [1] which grow into a bewildering array of colony types, including soft (weedy or gelatinous) and hard (calcified) forms, which may be moss-, sponge-, or coral-like in overall appearance. Numerous taxa grow as thin crusts or delicate lace-like encrustations over suitable substrates (Fig. 1) [2]. Although often overlooked, bryozoans are often among the most diverse and abundant members of marine communities, especially in the Southern Hemisphere. All bryozoans are suspension feeders, extracting small food particles from the water column, and colonies typically live attached to seafloor substrates (e.g., shells, rocks, algae) or on surfaces in freshwater ponds, rivers, and lakes [3]. Three of the main extant clades are the freshwater Phylactolaemata, the marine Stenolaemata, and the predominantly marine Gymnolaemata (Fig. 2). All three offer possibilities for the study of WBR and related phenomena.

Simon Blanchoud and Brigitte Galliot (eds.), *Whole-Body Regeneration: Methods and Protocols*, Methods in Molecular Biology, vol. 2450, https://doi.org/10.1007/978-1-0716-2172-1_8, © The Author(s) 2022

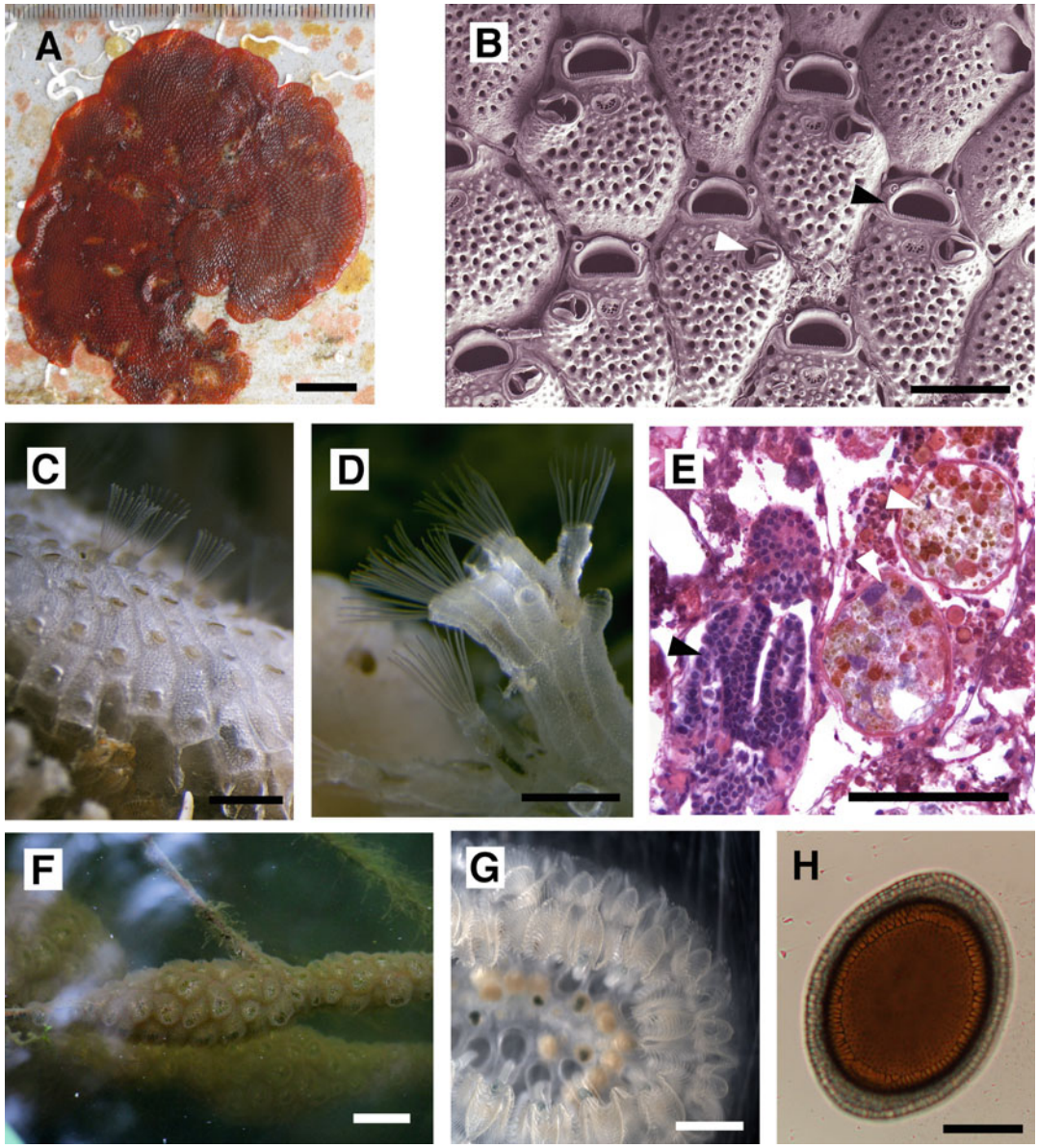


Fig. 1 Morphology of bryozoans. (**a**) An encrusting colony of the marine cheilostome bryozoan *Watersipora subatra*. (**b**) SEM image of the calcified autozooids of a *Microporella discors* colony (marine Cheilostomatida) showing ~6 polygonal autozooids; black arrowhead—autozooidal aperture; white arrowhead—avicularium (defensive polymorphic zooid). (**c**) Part of a living colony of the marine cheilostome *Hippomenella vellicata* showing feeding autozooids with extended lophophores (top); retracted autozooids with closed lid-like opercula (middle); and developing asexually budded autozooids at the colony margin (bottom). (**d**) Living colony of *Hastingsia* sp. This well-calcified continental shelf cyclostome was successfully grown in a laboratory culture system using natural seawater supplemented by cultured microalgae. (**e**) Two polypide regression products (brown bodies), indicated with white arrowheads; the adjacent zooidal chamber contains a developing polypide that will replace the previous polypide, which has degenerated (*Hornera* sp., marine cyclostomate, H&E stained). (**f**) Large colony of the gelatinous freshwater phylactolaemate *Pectinatella magnifica*. (**g**) Living colony of *Cristatella mucedo*, a freshwater phylactolaemate bryozoan; several rows of horseshoe-shaped lophophores line the periphery of the colony, which is capable of creeping along the

Bryozoan colonies are composed of iterated (mostly) submillimeter animals called zooids, which are budded as asexual clones from a single founder zooid, the ancestrula, itself derived from a free-swimming larva [4]. Depending on the species, a single colony may contain several to many hundreds of thousands of zooids. Autozooids are the zooid polymorphs responsible for feeding within a bryozoan colony; each has a lophophore bearing a crown of ciliated tentacles that captures microscopic food particles [5], typically microalgae. This feeding apparatus is normally extended into the water column on a flexible sheath, but can be retracted into a protective box-like or tubular zooid chamber, which may be gelatinous, leathery, or rigid in marine species that secrete a calcified skeleton [3]. The remaining parts of an autozooid include the polypide (comprising the lophophore, u-shaped unidirectional gut, a ganglion, and retractor muscles), and the cystid, the living and nonliving structural parts of the body wall (Fig. 3) [5]. Species identification of bryozoans often relies upon examination of the individual zooid architecture, and commonly requires the use of a dissecting microscope.

Zooids are physiologically interconnected via tissue strands (funiculus) which pass through pores in shared body walls, or via shared body cavities in budding zones [6, 7]. Autozooids possess variable degrees of physiological integration within the colony, while retaining a basic functional autonomy. Nonfeeding polymorphic zooids are common in marine bryozoans, and include

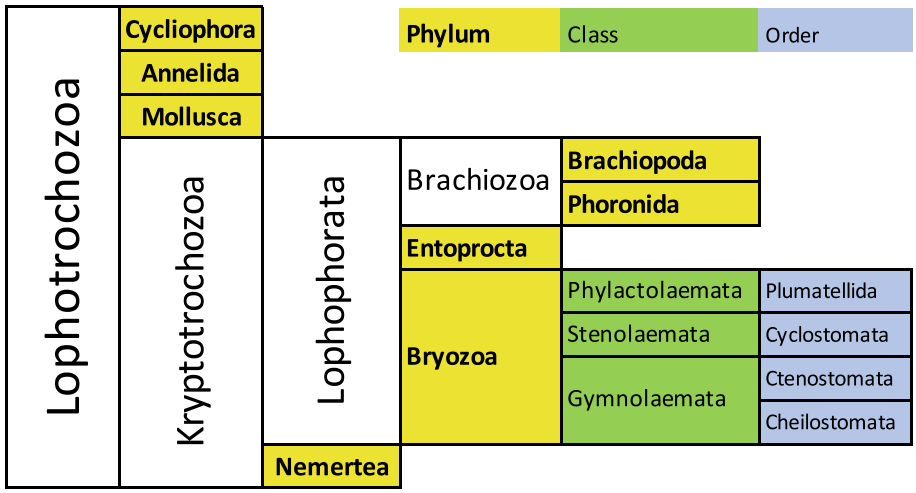


Fig. 2 Generalized phylogeny and relationships of the phylum Bryozoa (includes only extant taxa)

Fig. 1 (continued) substratum. (**h**) Statoblast (asexually produced resting propagule) of the freshwater bryozoan *Plumatella* cf. *geimermassardi* (fixed but unstained whole mount, imaged under compound microscope). Scale bars: **a**, 10 mm; **b**, 200 μm; **c**, 1 mm; **d**, 1 mm; **e**, 50 μm; **f**, 5 cm; **g**, 1 mm; **h**, 100 μm

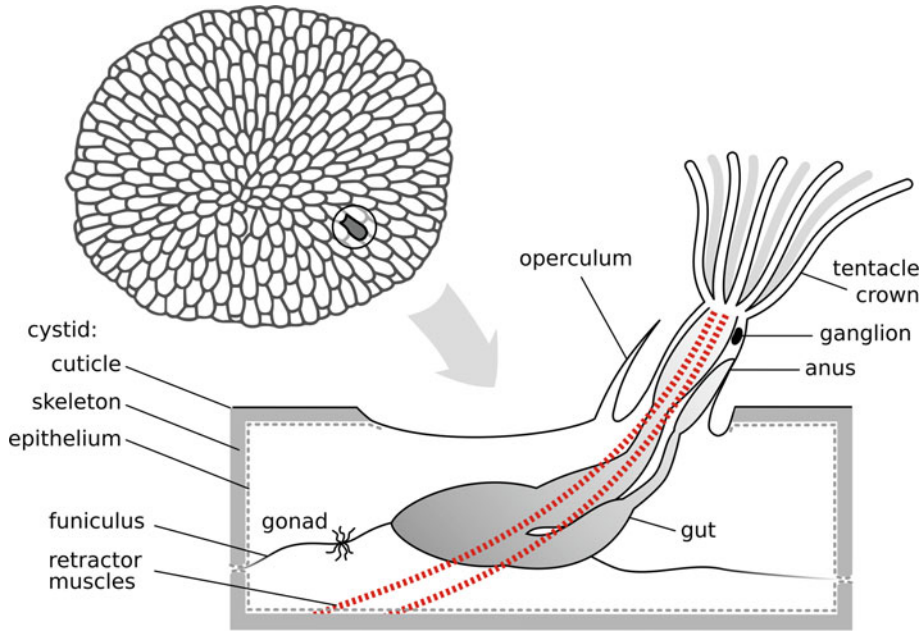


Fig. 3 Generalized anatomy of a cheilostomate bryozoan individual zooid. Scale: zooids generally range from 0.1 to 1.0 mm in length

reproductive, defensive, and structural modules [8] that rely on autozooids for nutrition. Bryozoans may undergo seasonal sexual reproduction, while asexual budding occurs all year. Freshwater and a few marine bryozoans produce clonal resting propagules (statoblasts and hibernacula) containing stem cells [9].

This group offers unique opportunities for whole-body regeneration (WBR) research, but has been underutilized compared to other invertebrate models. Studies of WBR in this phylum could focus on zooid-scale processes in the context of the whole colony. Autozooids undergo agametic cloning to produce new zooids by budding, resulting in new colony growth, and subsequently undergo one or more polypide degeneration–regeneration cycles, which replace senescent polypides within existing zooids of the colony. The latter process occurs throughout the functional life of a zooid and involves full breakdown of the incumbent polypide into a residual "brown body," and development of a polypide replacement, which arises from a blastema on the cystid [10]. Individual polypides typically last 1–10 weeks before regression commences, and the regression phase lasts 3–20 days, depending on the species [10].

Little is known of bryozoan regenerative processes at the subzooidal scale, for example, following partial injury to a polypide, but both WBR and body organ/tissue (= "structure") regeneration has been reported for this phylum by Bely & Nyberg [11]. In *Cristatella*, at least, surgical damage to zooids is repaired rapidly

without apparent damage. It is relatively easy to surgically separate living colonies into multiple ramets (clonal subcolonies), which will heal and continue to grow by budding [12]. Some bryozoans (e.g., *Cupuladria exfragminis*) are known to naturally autofragment as a clonal propagation strategy [13]. Bryozoans usually maintain budding along a given body axis during normal growth [14], but some taxa can undergo reversed-polarity budding and lateral budding during repair of individual zooids or during regeneration of mechanically broken branches [15]. At the colony scale, reversed-polarity budding can happen following breakage in branching forms. The precise extent of WBR in bryozoans remains to be determined.

In this chapter we present methods to study bryozoans, starting with how to find and collect bryozoans. Intertidal and shallow subtidal bryozoans can be scraped off rocks, picked from macroalgae or collected by divers, whereas shelf and deep-sea bryozoans are commonly collected via dredge or grab sampling. Preliminary on-board classification and sorting of bryozoans is achieved using overall colony form and colour, but proper species determination requires either light microscopy (difficult but can be nondestructive if done carefully) or scanning electron microscopy (lethal). Keeping living bryozoans in tanks requires careful preparation and maintenance of water quality, regular feeding of mixed phytoplankton cultures and, in some cases, regular gentle cleaning of colonies. Some encrusting bryozoans grow well in culture, but many are capable of surviving a long time without growing at all. It is possible to spawn at least some species of bryozoans, settle larvae, and raise colonies in a laboratory setting. Growth in bryozoans can be difficult to ascertain [16], but nontoxic marking of colonies using Calcein can be effective [17]. Deeper study into the structure of soft-parts (histology) and hard parts (micro-CT, SEM) allows for evaluation of life-cycle and effect of experimentation. In this contribution we provide the basic techniques for bryozoan collection, culture, and maintenance.

2 Materials

Not all materials presented in this section are required for every study. Researchers will need to choose the required materials based on their project specifications.

2.1 Colony Collection

1. Cool bag or insulated box for transport.
2. Airtight container(s) with lids, 1–3 L capacity.
3. Frozen cold-packs.
4. Thin wet protective layer (e.g., fresh seaweed, damp blotting paper).

5. Sampling kit: pocket knife, chisel, forceps, dropper.
6. Recording equipment: log book, waterproof paper.
7. Imaging equipment: camera with macrolens, scale bar, 10 × 10 cm black velvet.
8. Hand lens.
9. Collection permits (if necessary).
10. Underwater sampling equipment: dredge, grab sampler, grapnel.
11. Sorting and storage equipment: trays, 2 cm deep, about 30 × 20 cm^2, buckets, padding material (polystyrene or Styrofoam).
12. 95% analytical grade ethanol in dispensing bottle, triple-contained, except when in use.
13. 6–10 shallow trays.
14. Cool freshly collected seawater.
15. Small lab equipment: tweezers, scissors, pencil.
16. Blotting paper.

2.2 Identification of Bryozoans

1. Small fragments of dried bryozoans.
2. 12% NaClO solution: commercially available bleach.
3. 0.6% (w/v) bleaching solution: 5 mL 12% NaClO solution in 95 mL water.
4. 2.5 cm diameter mounting stubs for scanning electron microscope.
5. Mount-holding tweezers.
6. Lint-free cotton gloves.
7. 1 cm-wide double-sided carbon tape.
8. Silver paint.
9. Thin paintbrush.
10. Spray air duster.
11. Pick or fine tweezers.
12. Microscope.
13. Fine black indelible pen.
14. Sputter coater with gold-palladium source.
15. Scanning electron microscope (SEM).

2.3 Culture and Feeding

1. Tanks (e.g., glass, acrylic, PVC or opaque plastic).
2. Water circulation systems: pumps, hoses, spigots.
3. Aeration or bubble-free stirrers (not in all cases).
4. Residual-current device (RCD).

5. Temperature logger.
6. Temperature control mechanism (e.g., controller + heaters, chillers, or both).
7. Water supply (e.g., flow-through, recirculating or semiclosed recirculating) for filtered or artificial seawater.
8. Food supply (e.g., natural or cultured sources of microalgae).
9. Cell counter.
10. Tank cleaning tools (e.g., large-bore pipette).
11. Growth media for culture food and/or bryozoans.
12. Colony-cleaning tools: ultrafine brushes, disposable pipettes.
13. Black plastic containers (2–5 L).
14. Black plastic sheets.
15. Material for settlement substrates (e.g., acetate or glass slides).
16. Attachment system for substrates (rails, clips, etc.; avoid metals, especially copper).
17. Glass tank.
18. Intense light source (e.g., fluorescent or incandescent).
19. Disposable 3 mL pipette.

2.4 Marking

1. Living calcified bryozoans.
2. 10 L tank with bubbler.
3. Seawater at same temperature as bryozoans in squeeze bottle.
4. Sheets of black plastic.
5. Calcein solution: $C_{30}H_{26}N_2O_{13}$ (Fluorexon) at 50 to 150 mg/L in seawater (*see* **Note 1**).
6. 5% (v/v) diluted bleach: 417 mL 12% NaClO solution in 583 mL water.
7. Fluorescent light-source at wavelength 495 nm (*see* **Note 2**).

2.5 Anesthetizing and Fixing for Histology

Solutions should be prepared using ultrapure water and analytical grade reagents. Solutions should be stored at room temperature unless otherwise stated. Chemicals used in this section, with a single exception of $MgCl_2$, are toxic. Use fume hood for preparation and store tightly stoppered.

1. $MgCl_2$ solution: 73.2 g $MgCl_2 \bullet 6H_2O$ in 1 L H_2O.
2. Filtered sea water (FSW): 20 μm filtered fresh sea water.
3. Marine buffered formalin: 40 mL formalin, 100 g chalk, 960 mL FSW. Prepare 2 days before use.
4. 1–3 mL pipette.

5. 4% buffered formalin: 40 mL formalin, 100 g chalk, 960 mL H_2O. Prepare 2 days before use.
6. 0.1 M NaOH.
7. 16% PFA stock solution: Stir 70 mL distilled water at 60 °C with 16 g paraformaldehyde (PFA) for 1–2 h. Add one drop of 0.1 M NaOH at a time until the solution stops being opalescent. Bring the volume to 100 mL with distilled water.
8. 0.2 M phosphate buffered saline (PBS): one commercially available 2 g tablet in 200 mL purified water. Dissolve for 10 min to achieve a pH of 7.4.
9. 4% PFA fixative: 50% (v/v) 0.2 M PBS, 25% (v/v) 16% PFA stock solution (s*ee* **Note 3**).
10. PFA–glutaraldehyde (GA) mixture in buffer: 5 mL commercially available 25% GA, 12.5 mL 16% PFA stock solution, 25 mL 0.2 M PBS, 7.5 mL distilled water (*see* **Note 4**). Store refrigerated and use within days of preparation.

3 Methods

3.1 Onshore Collection

Bryozoan colonies are very diverse in terms of external appearance (Fig. 1). Encrusting bryozoans are generally small roundish patches, 1–3 cm in diameter, and variable in colour. When poked, they are predominantly hard to the touch, but some species are filamentous, weedy or gelatinous. It is easy to confuse these bryozoans with patches of algae—examination with a hand lens will show the regular openings (like pinpricks) on the surface of bryozoans, whereas most algae are smooth. Bryozoans prefer undersides of hard substrate, while algae need sunlight. Erect bryozoans tend to occur in deeper waters, and come in a multitude of shapes: fans, nets, fingers, trees, feathers. They can be confused with corals, macroalgae. Again, if they are hard/rigid and covered with small openings, found on undersides and overhangs, they are likely to be bryozoans.

1. Select an appropriate sampling site (*see* **Note 5**).
2. Record location details in log book, including time, date, latitude, longitude, water depth and relevant features or observations.
3. Fill an airtight container with water from the sampling site.
4. Scout around looking for orangish erect or encrusting roundish patches.
5. Look at piers, piles, bottles, cans, pieces of plastic and other human-made items.

6. Photograph specimens in situ, using macro lens and a ruler or scale bar.
7. Collect specimens with their substrate if possible (*see* **Note 6**).
8. Sample animals attached to large objects by gently scraping them off the surface using tools from the sampling kit (*see* **Note 7**).
9. Place the specimens into airtight container, covered with seaweed or blotting paper.
10. Repeat **steps 3** to **9** until sufficient colonies are collected.
11. Add a paper label indicating the sampling location into airtight containers (*see* **Note 8**).
12. Transport the colonies back to the lab within 3 h if possible (*see* **Note 9**).

3.2 Offshore Collection

1. Sail to a sampling location of interest (*see* **Note 10**).
2. Once on station, record location details in log book, including time, date, latitude, longitude, water depth, relevant features or observations.
3. Deploy a dredge, grab or grapnel (*see* **Note 11**).
4. Turn on deck hose (*see* **Note 12)**.
5. Retrieve collection device without dumping its content on the deck.
6. Gently run deck hose at low pressure over top surface of the contents.
7. Follow **steps 7** to **9** of Subheading 3.1, choosing complete unbroken colonies (*see* **Note 13**).
8. Dump contents onto the deck.
9. Photograph the material on deck with a label indicating location number (*see* **Note 14**).
10. Follow **steps 7** to **11** of Subheading 3.1.
11. Keep living colonies, cool, wet and aerated until able to sort them out (Subheading 3.3).
12. Store colonies for molecular analysis in ethanol, triple-contained while on boat and in transit.

3.3 Postcollection Sorting

1. Fill sorting trays with cool water from the sampling site.
2. Transfer morphologically similar samples from the transport container into the sorting trays using tweezers, one group per tray (*see* **Note 15**).
3. Repeat **steps 1** and **2** until the contents of the transport container has been processed.

4. Examine specimens with hand lens to ensure each tray contains similar-looking specimens.
5. Prepare two location labels for each group of bryozoans with pencil and small pieces of waterproof paper (*see* **Note 16**).
6. Place one location label inside each tray.
7. Transfer one complete representative colony onto a piece of black velvet and blot dry.
8. Place the second location label next to the sample.
9. Place a ruler or scale bar next to the sample.
10. Take one or more pictures with the camera using macro lens, including the label and scale bar in each photo.
11. Place this sample and its paper label in a labeled dry 15 mL tube for identification using SEM.
12. Place the SEM tube into a plastic bag labeled with sample location number and the note "For SEM."
13. Transfer a second representative colony into a labeled 10 mL tube filled with 95% AR grade ethanol for Genetic Archive.
14. Place the Genetic Archive sample into a plastic bag labeled with sample location number and the note "Genetic Archive."
15. Transfer remaining colonies and the paper location label into a labeled 50 mL tube filled with clean water from sample locations.
16. Place the container into a cool and dark container.
17. Repeat **steps 4** to **16** until all sorting trays have been processed.
18. Place the bag for Genetic Archive into a second plastic bag.
19. Store this Genetic Archive at 4 °C.
20. Transfer the live colonies from their seawater container into the aquarium system within the next hour.

3.4 Identification

Bryozoans are difficult to identify in the field and in hand specimen. There are many species which are superficially similar. Acquiring a bryozoan expert for confirming IDs is an excellent plan. If you need to send images for ID, scanning electron microscope images are best. Methodical comparison of SEM photos with species descriptions in specialist literature is, unfortunately, the only reliable way to identify bryozoans.

1. Pick one SEM tube from the plastic bag.
2. Transfer the sample into a plastic dish using a pair of tweezers.
3. Divide the specimen in half.
4. If the specimen is rigid and heavily calcified, soak one half in bleaching solution for 1 h. If it is soft, fluffy, goopy, or pliable, omit this step.

5. Rinse the bleached sample for a few seconds with tap water.
6. Transfer both halves of the colony onto a labeled glass dish.
7. Warm the glass dish to no more than 60 °C.
8. Wait 1 h for the samples to dry slowly.
9. Cut two pieces of double-sided carbon tape, each 2.5 cm long.
10. Wear fabric gloves.
11. Label a mounting stub on the bottom with the location (on the label in the tube) using indelible pen.
12. Hold the mounting stub using mount-holding tweezers (*see* **Note 17**).
13. Stick one piece of tape down to cover half of the mounting stub, without touching the mounting stub.
14. Stick the second piece of tape down so that there is a small gap between the two tapes, running across the middle of the stub surface.
15. Under binocular microscope, position the bryozoan specimens on either side of the seam (*see* **Note 18**).
16. Use spray air duster to remove any dust or crumbs..
17. Use silver paint to fill any gaps under large specimens, or to connect any loose branches to the carbon tape.
18. Allow 10 min to dry.
19. Coat the specimen with a thin layer of metal conductor (e.g., C, Au:Pd) using sputter coater according to instructions (*see* **Note 19**).
20. Draw the stub in the Notebook, showing the orientation and shape of each fragment relative to the seam, and label them.
21. Load the stub(s) into the SEM and pump down.
22. Modify your working distance, focus, and contrast to obtain high-contrast well-focused images (*see* **Note 20**).
23. For each species, take a photomicrograph of three different areas at magnification of 30×, making sure to show numerous zooids and heterozooids and their orientation to each other.
24. Take photomicrographs of ten single zooids at a magnification of 100–150× (so that the zooid fills the photo). Include both autozooids and heterozooids (*see* **Note 21**).
25. Every SEM micrograph should be recorded in the notebook, with photo date, photo number, specimen details, voltage, working distance and magnification.
26. Download photos onto flash drive and name each file with the photo number and date.

3.5 Culture and Feeding

Bryozoans are not easy to culture, so careful planning needs to be undertaken to design and run a laboratory-based culturing set-up (*see* **Note 22**). Useful summaries for culturing of bryozoans include [15] for marine and freshwater species, and [18] for freshwater species.

1. Select species to be cultured (*see* **Note 23**).
2. Develop a multitank system, based on environmental parameters (e.g., light levels, circulations, aeration, temperature) where species is found naturally (*see* **Note 24**). Examples of multitank systems are given in Fig. 4.
3. Set up the tank and allow it to run without bryozoans for at least 48 h.
4. Decide on a feeding strategy (*see* **Note 25**), and ensure a good supply of the food source.
5. Collect living bryozoans (*see* Subheadings 3.1 and 3.2).
6. Position colonies carefully in the tank, away from aeration systems (*see* **Note 26**).
7. Establish feeding and tank maintenance schedule for 2 weeks before beginning experiments or measurements (*see* **Note 27**).

3.6 Spawning

1. Find out what kind of larvae is produced by the species you wish to spawn (*see* **Note 28**).
2. Keep colonies in seawater, undisturbed at a constant temperature in the dark for at least 24 h prior to spawning.
3. Induce spawning in marine bryozoans by sudden exposure to bright light; freshwater species will spawn overnight, but must be watched as the larvae can be very short-lived. The time until larval release can vary between 5 and 60 min depending on the species [19–25] (*see* **Note 29**).
4. Collect larvae by gentle pipetting and transfer to prepared aquarium set-up or experiment (*see* **Note 30**). Provide many different substrate options (*see* **Note 28**), as they may settle fairly randomly when competent.

3.7 Marking Colonies

Calcein is taken up during calcification and retained in the skeleton, so this technique is useful for growth or skeletal regeneration studies in calcified marine bryozoans (*see* **Note 31**).

1. Fill tank (leaving headspace) with 8 L Calcein in seawater solution (*see* **Note 1**).
2. Adjust the water temperature to the one of the tank where bryozoans have been living.
3. Add bubbler for aeration and circulation.

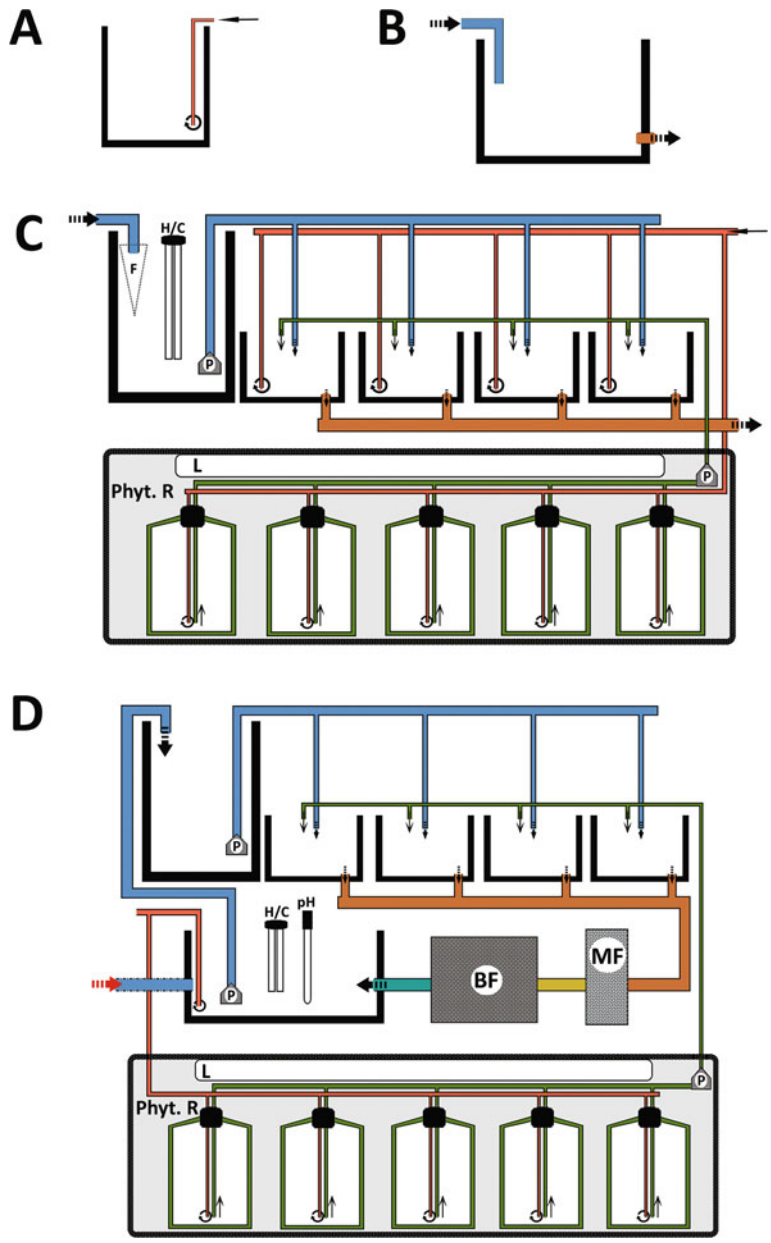


Fig. 4 Tank-based culture systems for bryozoans. (**a**) Short-term culture system using individual tanks. (**b**) Flow-through tank system. (**c**) Slow flow-through system. (**d**) Recirculating system. The option of a semirecirculating system is also shown with a red arrow. *BF* biological filter, *F* filter sock, *H/C* heating/cooling system, *L* light source, *MF* mechanical filter, *Phyt. R* phytoplankton room/area, *pH* pH meter, *P* pump. Colors: red = aeration system, blue = sea water inflow, brown: sea water outflow or waste water, yellow and light blue: water purification steps, green: phytoplankton as food

4. Gently place well-fed living bryozoans in Calcein tank, taking care that bubbles do not disturb or damage them (*see* **Note 32**).
5. Wrap tank with black plastic or keep in dark room for 8 to 24 h.
6. Gently rinse colonies in seawater at the same temperature and then place back in seawater culture tank.
7. When ready to measure growth rate, kill bryozoans in 5% bleach solution for 1 h.
8. Rinse in freshwater.
9. Dry gently in oven or under light at <60 °C.
10. Examine under fluorescence microscope at 495 nm wavelength.
11. Measure growth since marking date as distance from bright glowing band (Calcein mark) to growth edge.

3.8 Anesthetizing and Fixing for Histology

The process of relaxing the colony in such a way that the lophophores can be fixed in a protruded position needs to be controlled under the stereomicroscope, with minimal disturbance to the colony. A typical relaxation interval should not exceed 2–2.5 h.

1. Place the living colony in a container with 3/4 sea water and 1/4 $MgCl_2$ solution. The ratio of the colony to medium volume need not be large, indeed a smaller amount of medium is easier to replace and requires less relaxant.
2. After the polypides begin to protrude, gradually replace the medium: with a pipette gently withdraw a small (~1–3 mL) amount of the medium and slowly replace it with the same volume of $MgCl_2$ solution every 2–5 min, depending on the initial volume.
3. Check if the colony is relaxed, by giving the extended tentacles a gentle tap with a dissection needle or gently shake the container (*see* **Note 33**).
4. If the lophophores have lost sensitivity, wait an additional 10–15 min for $MgCl_2$ to further penetrate the polypides and immobilize the retractor muscles. It is common for a partly anesthetized polypide to lose sensitivity to touch, yet withdraw on contact with the fixative.
5. Briefly lift the whole colony and then return it back into the container. If the polypides remain everted, the colony is ready for fixation.
6. Fix specimens *for paraffin-based histology* in 4% buffered formalin at room temperature in a fume cupboard. The volume ratio of the material to medium should be no more than 1 to 10. Store at room temperature (*see* **Note 34**).

7. Fix specimens *for immunocytochemistry* using 4% PFA in buffer at room temperature for a minimum of 4 h, or at 4 °C overnight. The volume of the fixative should be 10 or more times larger than the volume of the sample. Remove colonies from the fixative within 10 days and store refrigerated in the same, but osmolarity-adjusted buffer.
8. Fix specimens *for electron microscopy* using GA or PFA-GA in buffer at room temperature.
9. Rinse specimens after fixing.
10. Store at +4 °C. Samples are best used within a month, but can be stored in the fixative for longer if needed (*see* **Note 35**).
11. Decalcify the specimen (if it is calcified) (*see* **Note 36**).
12. For subsequent processing stages please refer to methodology-specific protocols.

4 Notes

1. Concentrations of Calcein vary depending on organism and purpose of the study. Refer to [17] for review and recommendations.
2. Stained preparations can be observed under a microscope using the appropriate excitation filter for the stain used.
3. Store both the stock and resulting fixative refrigerated, use within days of preparation.
4. For marine species, adjust osmolarity with sucrose to be isotonic with local seawater. Since 1‰ = 30 mOsmol, convert target salinity, say 39‰, into osmolarity: 39*30 = 1170 mOsmol. Make up the fixative, measure its osmolarity and compare with sea water. The osmolarity of the fixative would be different depending on concentration of GA and the buffer used, so it is best to measure. Let us say the fixative has 974 mOsmol. Calculate the difference between it and the target, 1170–974 = 196 mOsmol. This is the amount that has to be added. Knowing that 0.342 g sucrose per 10 mL solution adds 100 mOsmol and knowing the volume of the fixative (in our case 50 mL) calculate the amount of sucrose: 0.342 * (196/100) * 5 = 3.35 g. Having a small difference of ~50 mOsmol between actual and target osmolarities is not a problem.
5. Bryozoans prefer the dark and are thus most easily found on the undersides of shells, on rocky overhangs, in submarine caves, on underwater vegetation and on the undersides of objects. In general they need hard substrate such as rocks or piers or bottles.

6. Freshwater bryozoans are not calcified, hard or rigid. They look like brown globs on logs, moss-like weeds or balls floating in the water. They are tricky: it is best to consult an expert for identification. In order to collect undisturbed colonies of the motile bryozoan *Cristatella mucedo* (Fig. 1), one can use a 3 mL plastic pipette with a cutoff tip. An opening (5–6 mm in diameter) should be large enough to take the colony in lengthwise, but small enough to provide enough suction. Other freshwater species live attached to the substrate and can be picked off (with or without substrate fragments) by hand, knife or forceps. Places to check: underwater vegetation and submerged surfaces (rotting wood, stones, plastic, cans, bottles) in streams, lakes, and ponds. In a fast-moving water, colonies are commonly located on the undersides of objects. Freshwater bryozoans are commonly identified using their reproductive resting stages: statoblasts. A very young colony may retain the valves of the original statoblast from which it "hatched." Older colonies, especially near the end of the reproductive season, often contain numerous statoblasts in the body cavity. In nature, these near-microscopic propagules can be collected from the water's edge, where they can form a brown "tideline," or they might be found on floating items (e.g., wood, litter) or in foam. If you want to collect statoblasts particularly, tether a piece of polystyrene foam (Styrofoam) in the water and collect it a few days later, then rinse off the statoblasts—they adhere to it especially well. For microscopic examination, statoblasts should be opened and both valves placed in a drop of water on a glass slide. Coverslips are usually unnecessary as dry objectives (magnifications up to 40×) are sufficient.
7. For many purposes, it does not matter if specimens break as you collect them. Because bryozoans are modular, even a small fragment contains enough information for identification or genetic analysis. Many collectors choose to leave half the colony behind, as it will continue to grow after sampling.
8. Labeling specimens well is critical. We use this protocol: three-letters for general location (e.g., Otago Shelf would be OSH), number for exact location which will be detailed in log book, (e.g., 08), letters for bryozoan species if known (*Cinctipora elegans* would be CE) or random if not (XX). So, the sample label would read: OSH-08-CE. As ethanol dissolves ink, we use pencil on waterproof paper, and label everything at least twice (once in the container, once in the bag containing the containers from that location, and often writing on the container in permanent marker).
9. After collection, guard against transport-related damage: overheating, oxygen deprivation and mechanical damage associated

with shaking. Overheating can be avoided with the use of cold packs and thermo-isolating boxes. Over short travel times, oxygen depletion is not significant if the density of animals is low, so we recommend filling the containers almost to the brim with water. This makes the colonies more resistant to shaking and mechanical damage. For long travel times, however, leave some air above the water and take extra care not to shake the containers.

10. Bryozoans can be dredged from the seafloor or collected from rocks or macroalgae.
11. When working in shelf depths from a sea-going vessel, a dredge is a quick way to get a huge volume of sediment on deck. Run the dredge for a very short time (2 min). If the location turns out to be full of bryozoans, then deploy the grab sampler to get discrete, less damaged samples. In the subtidal (water depths of 5–15 m), you can work from a smaller vessel and deploy a small hand-held grab or grapnel to collect macroalgae (on which the bryozoans may be living). Throw the grapnel far overboard, holding it parallel to the water. If collecting in the area with strong currents, throw the grapnel upstream. When the grapnel hits the bottom, release some additional rope (~5–10 m), then move the boat, dragging the grapnel along the bottom for about 2 min. Collected macroalgae can be roughly sorted and the epibiont-rich fragments placed into buckets with sea water for future processing.
12. Picking bryozoans from a heap of dredged material on a heaving boat while the deck hose is running is a messy job. Full waterproofs are needed.
13. Fill shallow trays with cool seawater and put the sampled specimens in there, grouping by apparent species. If hands are sensitive, use rubber gloves.
14. It is sometimes useful to collect 1–2 L of unsorted dredged material as a record of the sediment type and other taxa present. This can be transported dry, in seawater, or in ethanol. Ethanol will reduce the smell as the living material rots, and allows for future molecular analysis.
15. Morphologically similar colonies might be classified by colour (orange, purple), texture (soft, fluffy), or growth habit (e.g., branching, net-like). They may belong to multiple species, but often are the same family or genus.
16. Ethanol dissolves pen, so be sure to use pencil. It works to precut long thin (3–4 mm) strips of waterproof paper. Then write each location number (e.g., SE4) and place it straight into the container. Easier to handle than tiny rectangles of paper.

17. Avoid touching the mounting stub or anything that will go into the SEM, because grease from fingers will diminish the vacuum. If you do touch it, wipe with ethanol and start over.
18. When mounting bryozoans on the carbon tape, be gentle; they will break easily. Orient them to show zooids which are undamaged and variable, and try to include heterozooids, especially avicularia and gonozooids/ovicells. In the case of statoblasts, make sure some are upside down and some are right side up. For small specimens, it is possible to fit more than one species on a single stub. Use silver paint to close any gaps between the bryozoan and the tape—you are aiming to let electrons conduct.
19. If you have an Environmental SEM, coating is not required, and very low voltages can be used. Check with technician what best practice is for a fairly conductive substance like calcium carbonate.
20. You will need to develop the best protocol for your own SEM. We recommend voltage of 12–15 kV and a working distance in the range of 12–20 mm.
21. Orient photos so that the growing edge of the branch/colony is "up." Usually the orifice is nearer the top of the zooid. If there are interesting details (such as a tooth or process in the orifice, or an elaborate pore), zoom in and get a photo of it, often at about 300×. Sometimes you might want a photo of the ultrastructure of the surface or of a broken part, that would be at about 1000×.
22. For marine species, the most practical approach is to work at a dedicated marine laboratory, using available, locally common species, along with a locally obtained seawater supply pumped ashore into the facility and into a dedicated flow-through or semiclosed recirculating tank system. Use of a continuous supply of "natural" seawater alleviates some of the practical difficulties associated with food culturing and maintaining appropriate environmental parameters. However, this method comes with some risks—such as introducing predators or competitors into tanks, and increased vulnerability to episodic perturbations, such as heatwaves or storms, which can rapidly change in-tank water quality by changing the temperature or smothering colonies with fine sediments if seawater is piped directly into the system. Potentially, colony recruitment and culturing can be done in situ, using artificial settlement substrates attached to the seafloor or suspended beneath artificial structures such as buoys and wharves. Exclusion cages can be used to reduce mechanical damage and predation of colonies, although these may be largely ineffective against bryozoan micropredators. A hybrid strategy is to settle larvae in the

natural environment, then transfer the developing colonies, along with their substrates, to a culture system. If research objectives require tightly controlled conditions, or the absence of contaminating organisms, a closed aquarium system will be required. However, provision of artificial or sterilized natural seawater and a cultured microalgal diet adds a significant level of time investment to a project. Furthermore, some bryozoans have been shown to develop different and often-unusual colony morphology when kept in highly controlled laboratory conditions and fed microalgal monocultures [26].

23. The most tolerant and logistically feasible bryozoan species come from near-shore or intertidal environments, or from freshwater habitats. It is useful to conduct a pilot culturing study using a variety of locally obtained species to determine which taxa are best-suited for your system. When collecting colonies, make a note of the conditions in the microenvironments in which they occur, to help inform system design. Among the fast-growing encrusting genera are *Watersipora*, *Electra*, and *Einhornia*. *Cryptosula pallasiana* is a moderately well-studied, cosmopolitan and intertidal cheilostome [10] able to be cultured in the laboratory [27]. Ctenostomes amenable to culture include victorellids and *Amathia* [28, 29]. Among the cyclostomes, short-lived, fast-growing "weedy" species, such as *Tubulipora*, *Crisia*, and *Filicrisia*, are probably the most amenable to laboratory experimentation [30]. Heavily calcified marine taxa and deep-water species have proven to be very challenging to culture in the laboratory. Lack of knowledge regarding their natural environment (e.g., aquatic chemistry, food source) means that aquarium conditions can only be an educated guess. In some cases, culturing the specific phytoplankton species found in their natural environment might be the tipping point between failure and success. Freshwater bryozoans are abundant but have few genera. *Cristatella*, *Plumatella*, *Fredericella*, *Lophopus*, and *Pectinatella* in particular are among the most ubiquitous and easy to find taxa; and techniques for their culture have been refined [18]. *Cristatella mucedo* and *Fredericella sultana* have potential as a model species for WBR research, as they are common, easy to grow, and have fully sequenced genomes [31, 32].
24. Numerous commercial tank systems are available, and it is relatively easy to make custom systems. Tanks do not need to be large, but as a general rule, larger volumes (~20–50 L) tend to be more stable in terms of temperature and water quality and, for the same biomass of colonies, will require less frequent feeding at a given microalgal cell concentration if pulse feeding is used. Various low-volume rearing apparatus have been successfully developed [15], although these designs are relatively

sophisticated. Tanks and other components in contact with the water should be nonmetallic and should not contain natural rubber, as both can be toxic to bryozoans. It is good practice to "condition" immersed system parts, especially new plastics, by placing them under running (sea)water for 24 h; this removes soluble residues and encourages the establishment of biofilms. Recirculating, semirecirculating and flow-through tanks can be used for bryozoan culture. These options have different advantages and drawbacks. Flow-through tanks are preferable if using natural seawater as the food source. Cultured food, however, can also be used in the case of a slow flow-through system. Recirculating or semirecirculating systems are ideal if precise control of water quality conditions is needed. Depending on the objectives, a very simple system can be effective: for example, plastic buckets can be used as tanks, and manual water changes every ~24 h can work for short-term studies. A good general principle for culturing bryozoans is to replicate natural conditions as much as possible. Many marine and freshwater bryozoans prefer low-light levels and shaded environments, growing best on underhanging substrates. If culturing is taking place in a well-lit room, a light cover over tanks should be considered. Note that exposure to high-intensity light can induce spawning in some species (*see* Subheading 3.4). Water movement is another consideration. Linear or oscillating currents can be generated using various methods, including submersible pumps, wavemakers, aerators and mechanical stirrers. Some species grow well in still water, although a small amount of water movement is beneficial to ensure that food particles do not sink to the bottom. In our experience care should be taken to ensure microbubbles are not introduced into the system during aeration, as these can adhere to colonies, disrupting normal function. Similarly, high current speeds can be damaging. For many bryozoan species, management of water temperature is important. Nearshore marine and freshwater bryozoans tend to be eurythermal. For stenothermal taxa, a responsive temperature controller heating and/or cooling system should be used. Tanks can also be housed in a controlled-temperature environment.

25. Bryozoan colonies can be fed simply by the provision of natural seawater in flow-through systems, or by adding cultured food (usually microalgae) to tanks. For freshwater culturing, Wood [18] describes use of a closed mixed culture system using a tank containing well-fed goldfish and a rich microbiota; food-rich water from this reservoir is supplied to bryozoan culture tanks via an airlift pump. Marine bryozoan culture requires cultured microalgae, using commercially obtained strains developed for the aquaculture industry. Conveniently their nutritional

content is usually well-documented. Many marine laboratories maintain a dedicated phytoplankton culture room, and requests for culture of specific strains should be made 1–2 months in advance to allow time for culturing. Common microalgal genera used for feeding bryozoans include *Dunaliella*, *Rhodomonas*, *Tetraselmis*, and *Pavlova*. It is important to supply appropriate cell concentrations of the cultured microalgae to the bryozoan tank, taking into account the dilution volume of the tank itself. Feeding can be done by manual daily additions of cultured cells, or ideally, by a drip feed system, which can be applied both to closed and flow-through systems. Microalgal monocultures are commonly used for experimental studies of growth and feeding, but mixed microalgal diets may be more appropriate for some studies. It should be noted that abrupt changes in diet from one monoculture to another is reported to induce colony-wide polypide regeneration in some taxa [15]. Optimal cell concentrations can be found in the literature for some commonly studied species, such as *Electra pilosa* [33] or *Cryptosula pallasiana* [27]. To calculate the volume of cultured algae required for feeding, cell counts can be made using a cavity slide or an automated cell counter.

26. Bryozoan colonies are delicate, and must avoid direct contact with hard surfaces other than the attachment substrate. If colonies are grown on slides or plates they can be suspended vertically or upside-down in the water column. Wood [18] recommends use of inverted petri dishes as substrates for freshwater bryozoans. An attachment system, such as a frame, rails, Velcro, or even Lego, makes it easy to remove and replace colonies. Cyanoacrylate glue is a safe adhesive for bryozoans; aquarium silicone works as a strong and flexible glass adhesive, but requires curing and conditioning before use. If tank aeration is used, ensure that colonies are placed away from the bubble stream, and away from the strong flows generated by submersible pumps and inlets.

27. Cleaning of bryozoan culture tanks and the colonies themselves is necessary, especially in closed systems. Excess food and fecal pellets from colonies can contribute to rapid buildup of bacteria, which can inhibit normal function in some bryozoans [15]. Cleaning may also reduce the buildup of ciliates, which can often be problematic in marine culture systems. Regular siphoning of detritus from the tank floor is recommended, as well as regular water changes in closed systems. Cleaning of bryozoan colonies requires care and is best done in response to observed detritus clinging to the colony (some bryozoans appear quite adept at cleaning themselves). Common practice is to use an ultrafine artist's brush or a dissecting needle to gently sweep away sticking detritus. An

alternative is to employ gentle puffs from a disposable plastic pipette that has had the tip cut off to enlarge the opening. In both cases great care should be taken to avoid damaging the colonies, and it is prudent to do some "test cleans," followed by examination of colonies several hours later to ensure they are undamaged (e.g., feeding normally). Some bryozoans, such as free-walled cyclostomes, are prone to having their membranous body walls scraped off, and individual brush hairs can easily enter zooidal tubes, damaging terminal membranes and polypides. Water filtration can reduce the buildup of mobile detritus in a closed or semirecirculating system; however, doing so also removes food particles. One method is to run a timer-activated power filter once a day for a short period (~1 h) before feeding or turn off the water filtration system for a short period of time (~2 h) while feeding.

28. Most gymnolaemates, and all stenolaemates, produce lecithotrophic (nonfeeding) coronate larvae, but other species produce planktotrophic (feeding) cyphonautes [34]. Refer to [19] to identify the two larva types. A pilot study might be required prior to spawning the species of interest, in order to understand the type of larvae produced and potential settlement intervals.

29. Most marine bryozoans are light-induced spawners, [20–22, 34, 35] while spawning in freshwater bryozoans is dark-induced instead of light-induced [23]. Sheet-encrusting marine species such as *Membranipora membranicea* can be prepared for spawning with the "one-zooid-row preparation." It includes cutting portions of colonies with a scalpel blade into strips one-zooid wide and several zooids long [20, 36]. This method provides biological replicates (clones, ramets) for experiments. The "one-zooid strips" can then be placed in a small petri dish with seawater for spawning and observation. When choosing encrusting colonies growing on algae such as *M. membranacea*, it is advisable to choose algae which do not secret large amount of mucus when they are cut [20, 36]. If the "one-zooid-row preparation" is not possible, different colonies or colony parts can be kept in separate containers with the chosen substrate for settlement such as acetate sheets, glass slides, a chicken egg-shell membrane previously soaked for 24 h in seawater, other adult non–sexually reproductive bryozoan species (preferably dead) or any other calcified substrate (e.g., bivalve shells) [19, 37, 38]. Similar principles apply for freshwater species; each colony can be placed in a separate container or petri dish until spawning [23, 24]. For both marine and freshwater species, regular check-ups are required (every ~2 h) to ensure whether settlement has occurred. Spawning and settlement intervals can also be recorded with

a microscope camera, either by video recordings or photo time frames [36]. Settlement intervals vary, but planktotrophic cyphonautes larvae produced by the marine ctenostome species *Amathia gracilis* may swim up to 10 h before settlement [37].

30. Larvae of marine bryozoans are phototactic, and therefore a light source can be used to lure the larvae so they can be easily collected using a pipette. Care should be taken so that larvae do not swim to the air–water interface, where they can be trapped, therefore leading to larval mortality. In order to prevent that, the water–air interface can be taped over with black tape or tinfoil, all around the glass jar or aquarium. Apply the light source laterally below the tape line, which makes it possible to concentrate and collect the swimming larvae.
31. Calcein binds to $CaCO_3$ so this method generally works best on well-calcified species. Calcein concentration should be 50–150 mg/L. Higher concentrations work in a shorter time, but have a higher chance of being toxic [17].
32. Calcein marking can be done in situ—surround bryozoans with a plastic bag, sealed against the substrate or around them, then inject with concentrated Calcein to achieve necessary concentration.
33. If partially anesthetized polypides retract, they are often unable to evert again and the process needs to be started over with a different colony. Bryozoan species vary significantly in their sensitivity. While some are relatively hard to disturb, others may prove extremely skittish. In the latter case one may consider doing relaxation after hours or on a weekend. Both marine and freshwater species can be successfully relaxed in the regular lab settings, although a temperature-controlled room may be a better option for deep-water species. If done at room temperature, container may need to be cooled locally with a freezer pack. Have a reserve pack ready for long relaxations.
34. Freshwater species are more difficult to anesthetize. $MgCl_2$ can be used but is less effective for these bryozoans since solution isotonic to freshwater has very few Mg^{2+} ions, and increasing concentration causes osmotic shock. Instead, use one of the other two substances which work better: menthol and chloral hydrate solutions. Keep in mind that freshwater bryozoans are even more easily damaged by overexposure. Living tissues begin to macerate: the epidermal layer on the tentacle loses cohesion and the cells slough off. A polypide with visibly narrowed or uneven tentacle surfaces is too damaged to fix. A typical relaxation should not exceed 1 h. There are two methods using menthol for relaxation. Menthol is not easily soluble in water, so one may prepare a solution beforehand and add it

gradually, or else place small menthol crystals on the water surface of the culture container. It is important to keep the container covered, because menthol is an irritant and evaporates easily. The lid should be transparent to allow microscopic observation and cover the container in such a way as to be removed without shaking the colony. A large upturned Petri dish is usually good for this purpose. Use of a benchtop extraction hood during relaxation with menthol is recommended. The same procedure of gradually adding the relaxant applies for chloral hydrate solution. Chloral hydrate: 20 g $C_2H_3Cl_3O_2$ in 1 L H_2O, prepared 1 month before use to saturate properly.

35. 4% Formalin and Bouin's solution (150 mL filtered saturated solution of picric acid, 50 mL formalin, 10 mL glacial acetic acid, use within a few days of preparing) both work well for fixation of both marine and freshwater bryozoans for paraffin based histological sectioning. Samples can be stored in formalin for several months, but prolonged storage in Bouin's solution is not recommended, as it will dissolve skeletal carbonate. Histological handbooks such as [39] provide more background and details on specific fixatives and processing methods. Formalin-fixed material can also be processed for aceto-orcein staining. For immunocytochemical studies with the use of confocal laser scanning microscope, Triton X-100 is a common permeabilization agent, with goat or bovine serum albumin as common blocking solutions. Primary antibodies successfully used with bryozoans include rabbit anti-serotonin and mouse anti-acetylated α-tubulin; secondary antibodies include goat and donkey anti-rabbit as well as goat and donkey anti-mouse (e.g., [40]). For SEM examination of larvae, use 2.5% GA fixative, osmolarity-adjusted and buffered with 0.2 M Milloning's phosphate buffer (pH 7.4) for 1 h at 20 °C. Freshwater and ctenostome bryozoans may require stronger concentrations. Postfix the animals in 2% osmium tetroxide and 1.25% sodium bicarbonate (pH = 7.2 with 1 N HCL immediately before use) at 20 °C, for 1–2 h, then follow standard protocols for rinsing, dehydration, critical-point drying and coating [37]. Fixation and processing for visualization of ovaries, oocytes and nuclei requires some very specialized stains. For DNA-specific fluorochrome Bisbenzimide H333342 use samples fixed with buffered 4% formalin, stain with Bisbenzimide H333342 (10 pg/mL) for 5 min or more at room temperature. Rinse three times with filtered seawater [20]. The specimens can be stored at 4 °C until imaging. For aceto-orcein staining, specimens can be fixed either directly with 3:1 methanol–acetic acid for 30 min, or in two stages. For the latter method, first fix with 4% formalin with 0.2 M PBS for 20 min and rinse thoroughly with any phosphate

buffer, then postfix with 3:1 methanol–acetic acid for 60 min. Use 45% solution of aceto-orcein to stain the samples for 30 min. Rinse with 20% acetic acid [20, 34].

36. Most marine bryozoan taxa are biomineralized, with skeletons comprising $CaCO_3$ in the form of calcite and/or aragonite. For histological and EM sectioning purposes, the skeleton must be fully removed. Failure to properly decalcify can lead to wholesale destruction of the expensive diamond knives used for ultramicrotomy. Decalcification can have harsh effects on delicate bryozoan tissues, and lead to mechanical damage and extraction of cell contents, so gentler, longer-period protocols generally work best for heavily calcified taxa if excellent-quality sections are required. Immersion of samples in decalcification solution in the absence of $CaCO_3$ is especially damaging to tissues, so close monitoring of progress is recommended. Typically, a weak acid or a chelating agent is used to remove the skeleton. Popular acids for decalcification include ascorbic acid and formic acid, and these are used in diluted form (~2–4%), in a seawater-isotonic solution; this process can take several weeks and requires regular changes of solution. Calcium chelation is a highly regarded method, especially for TEM, and the preferred agent is EDTA (in 5–20% range). As decalcification protocols are required for marine bryozoans only, decalcifying solutions should done in a seawater isosmotic environment, ideally similar to that used for fixation and washing stages, so buffers should be used during this procedure, for example, PBS/cacodylate buffer. An osmometer is useful, and the osmolarity of local seawater should be used as a target. In most cases decalcification will be undertaken after the initial fixation, but can be done either before or after postfixation, in the case of TEM. Following decalcification, samples should be washed several times in seawater-isotonic buffer. As a general rule, further processing of the decalcified material is best done by hand, rather than with a tissue processor. For the most delicate specimens, embedding in low- or ultralow temperature agarose before decalcification dramatically improves overall sample integrity.

References

1. Bock PE, Gordon DP (2013) Phylum Bryozoa Ehrenberg, 1831. In: Zhang Z-Q (Ed) Animal biodiversity: an outline of higher-level classification and survey of taxonomic richness (Addenda 2013). Zootaxa 3703:67–74
2. Gordon DP, Taylor PD, Bigey FP (2009) Phylum Bryozoa: moss animals, sea mats, lace corals. Kingdom Animalia: Radiata, Lophotrochozoa, Deuterostomia. In: Gordon DP (ed) New Zealand inventory of biodiversity, vol 1. Canterbury University Press, Christchurch, NZ, pp 271–279
3. McKinney FK, Jackson JCB (1991) Bryozoan evolution. University of Chicago Press, Chicago
4. Ryland JS (1970) Bryozoans. Hutchinson University Press, London

5. Borg F (1926) Studies on recent cyclostomatous Bryozoa. Almqvist & Wiksells Boktryckeri AB, Stockholm, pp 1–506
6. Banta WC (1969) The body wall of cheilostome Bryozoa. II. Interzooidal communication organs. J Morphol 129:149–169
7. Boardman RS, Cheetham AH (1973) Degrees of colony dominance in stenolaemate and gymnolaemate Bryozoa. In: Oliver WA, Cheetham AH, Boardman RS (eds) Animal colonies. Downden, Hutchinson & Ross, Stroudsburg, PA, pp 121–220
8. Schack CR, Gordon DP, Ryan KG (2018) Modularity is the mother of invention: a review of polymorphism in bryozoans. Biol Rev 94: 773–809
9. Giangrande A, Licciano M (2014) Regeneration and clonality in Metazoa. The price to pay for evolving complexity. Invertebr Reprod Dev 58:1–8
10. Gordon DP (1977) The aging process in bryozoans. In: Woollacott RM, Zimmer RL (eds) Biology of bryozoans. Academic, New York, pp 335–376
11. Bely AE, Nyberg KG (2010) Evolution of animal regeneration: re-emergence of a field. Trends Ecol Evol 25:161–170
12. Hughes RN, Manríquez PH, Morley S, Craig SF, Bishop JD (2004) Kin or self-recognition? Colonial fusibility of the bryozoan *Celleporella hyalina*. Evol Dev 6:431–437
13. O'Dea A (2006) Asexual propagation in the marine bryozoan *Cupuladria exfragminis*. J Exp Mar Biol Ecol 335:312–322
14. Sköld HN, Obst M, Sköld M, Åkesson B (2009) Stem cells in asexual reproduction of marine invertebrates. In: Rinkevich B, Matranga V (eds) Stem cells in marine organisms. Springer, Dordrecht, pp 105–137
15. Jebram D (1977) Experimental techniques and culture methods. In: Woollacott RM, Zimmer RL (eds) Biology of Bryozoans. Academic, New York, pp 273–306
16. Smith AM, Key MM Jr (2020) Growth geometry and measurement of growth rates in marine bryozoans: a review. In: Wyse Jackson P, Zágoršek K (eds) Bryozoan Studies 2019. Czech Geological Survey, Brno, pp 139–156
17. Smith AM, Key MM, Wood ACL (2019) Culturing large erect shelf bryozoans: skeletal growth measured using calcein staining in culture. Aust Paleontol Mem 52:131–138
18. Wood TS (2005) The pipeline menace of freshwater bryozoans. Denisia 16:203–208
19. Bullard SG, Whitlatch RB (2004) A guide to the larval and juvenile stages of common Long Island sound ascidians and bryozoans. Connecticut Department of Environmental Protection, Sea Grant Connecticut, Groton, CT
20. Temkin MH (1994) Gamete spawning and fertilization in the gymnolaemate bryozoan *Membranipora membranacea*. Biol Bull 187: 143–155
21. Woollacott RM, Pechenik JA, Imbalzano KM (1989) Effects of duration of larval swimming period on early colony development in *Bugula stolonifera* (Bryozoa: Cheilostomata). Mar Biol 102:57–63
22. Pecquet A, Dorey N, Chan KYK (2017) Ocean acidification increases larval swimming speed and has limited effects on spawning and settlement of a robust fouling bryozoan, *Bugula neritina*. Mar Pollut Bull 124:903–910
23. Freeland JR, Lodge RJ, Okamura B (2003) Sex and outcrossing in a sessile freshwater invertebrate. Freshw Biol 48:301–305
24. Wood TS (2007) Development and metamorphosis of cyphonautes larvae in the freshwater ctenostome bryozoan, *Hislopia malayensis* Annandale, 1916. In: Bryozoan studies 2007, Virginia Museum of Natural History special publication 15, pp 339–346
25. Wendt DE (2000) Energetics of larval swimming and metamorphosis in four species of Bugula (Bryozoa). Biol Bull 198:346–356
26. Jebram D (1978) Preliminary studies on abnormities in bryozoans from the point of view of experimental morphology. Zool Jb Anat Bd 100:245–275
27. Amui-Vedel AM, Hayward PJ, Porter JS (2007) Zooid size and growth rate of the bryozoan *Cryptosula pallasiana* moll in relation to temperature, in culture and in its natural environment. J Exp Mar Biol Ecol 353:1–12
28. Jebram D (1975) Effects of different foods on *Conopeum seurati* (Canu) (Bryozoa Cheilostomata) and *Bowerbankia gracilis* Leidy (Bryozoa Ctenostomata), vol 3. doc lab Geol Fac Sci Lyon, HS, Lyon, pp 97–108
29. Jebram D, Everitt B (1982) New victorellids (Bryozoa, Ctenostomata) from North America: the use of parallel cultures in bryozoan taxonomy. Biol Bull 163:172–187
30. Jenkins HL, Bishop JD, Hughes RN (2015) Prudent female allocation by modular hermaphrodites: female investment is promoted by the opportunity to outcross in cyclostome bryozoans. Biol J Linn Soc 116:593–602
31. Starunov VV, Predeus AV, Barbitoff Y, Kutiumov VA, Maltseva AL, Vodiasova EA, Kohn AB, Moroz LL, Ostrovsky AN (2019) Comparative genomic analysis of *Cristatella mucedo* provides insights into bryozoan evolution and

nervous system function. Preprint. https://doi.org/10.1101/869792
32. Kumar G, Erti R, Bartholomew JL, El-Matbouli M (2020) First transcriptome analysis of bryozoan *Fredericella sultana*, the primary host of myxozoan parasite *Tetracapsuloides bryozalmonae*. Peer J 8:e9027
33. Riisgård HU, Goldson A (1997) Minimal scaling of the lophophore filter-pump in ectoprocts (Bryozoa) excludes physiological regulation of filtration rate to nutritional needs. Test of hypothesis. Mar Ecol Prog Ser 156:109–120
34. Temkin MH (1996) Comparative fertilization biology of gymnolaemate bryozoans. Mar Biol 127:329–339
35. Manríquez PH, Hughes RN, Bishop JD (2001) Age-dependent loss of fertility in water-borne sperm of the bryozoan *Celleporella hyalina*. Mar Ecol Prog Ser 224:87–92
36. Temkin MH, Bortolami SB (2004) Waveform dynamics of spermatozeugmata during the transfer from paternal to maternal individuals of *Membranipora membranacea*. Biol Bull 206: 35–45
37. Reed CG (1988) Organization of the nervous system and sensory organs in the larva of the marine bryozoan *Bowerbankia gracilis* (Ctenostomata: Vesiculariidae): functional significance of the apical disc and pyriform organ. Acta Zool 69:177–194
38. Batson PB, Taylor PD, Smith AM (2019) Early astogeny in *Hornera* (Bryozoa; Cyclostomata; Cancellata). Aust Palaeontol Mem 52:23–30
39. Suvarna SK, Layton C, Bancroft JD (2019) Bancroft's theory and practice of histological techniques, 8th edn. Elsevier, Amsterdam
40. Temereva EN, Kosevich IA (2018) The nervous system in the cyclostome bryozoan *Crisia eburnea* as revealed by transmission electron and confocal laser scanning microscopy. Front Zool 15:48

Open Access This chapter is licensed under the terms of the Creative Commons Attribution 4.0 International License (http://creativecommons.org/licenses/by/4.0/), which permits use, sharing, adaptation, distribution and reproduction in any medium or format, as long as you give appropriate credit to the original author(s) and the source, provide a link to the Creative Commons license and indicate if changes were made.

The images or other third party material in this chapter are included in the chapter's Creative Commons license, unless indicated otherwise in a credit line to the material. If material is not included in the chapter's Creative Commons license and your intended use is not permitted by statutory regulation or exceeds the permitted use, you will need to obtain permission directly from the copyright holder.





Chapter 9

Studying Annelida Regeneration in a Novel Model Organism: The Freshwater *Aeolosoma viride*

Chiao-Ping Chen, Sheridan Ke-Wing Fok, Cheng-Yi Chen, Fei-Man Hsu, Yu-Wen Hsieh, and Jiun-Hong Chen

Abstract

Aeolosoma viride, a globally distributed freshwater annelid, has a semitransparent appearance with 10 to 12 segments, about 2 to 3 mm in length. It is easy to raise and handle in laboratory conditions. Due to its robust regenerative capacity and applicability of various molecular tools including EdU labeling, whole-mount in situ hybridization (WISH), and RNA interference (RNAi), it rises as a promising model for studying whole-body regeneration.

Key words Annelid, *Aeolosoma viride*, Asexual reproduction, EdU labeling, Whole-mount in situ hybridization, RNA interference

1 Introduction

Earthworms are known form their regenerative capabilities [1, 2]. However, after testing several earthworm species in Taiwan, we could not find a robust model for studying annelid regeneration. The possibility of interrogating annelid regeneration came true with the presence of *Aeolosoma viride*. The discovery of this worm was an unexpected event when we collected *Daphnia* sp. from water ponds at National Taiwan University. Since these annelids exhibit asexual fission, and regeneration is recognized as one type of asexual reproduction [3], we inferred that this annelid may have regenerative abilities, which, to our knowledge, was not systematically documented previously. We tested its regenerative capability by amputating at the foregut-midgut or midgut-hindgut junctions (Fig. 1). Surprisingly, we found that this annelid can regrow anterior and posterior segments within 1 week.

Chiao-Ping Chen and Sheridan Ke-Wing Fok have contributed equally to this work.

Simon Blanchoud and Brigitte Galliot (eds.), *Whole-Body Regeneration: Methods and Protocols*, Methods in Molecular Biology, vol. 2450, https://doi.org/10.1007/978-1-0716-2172-1_9, © The Author(s) 2022

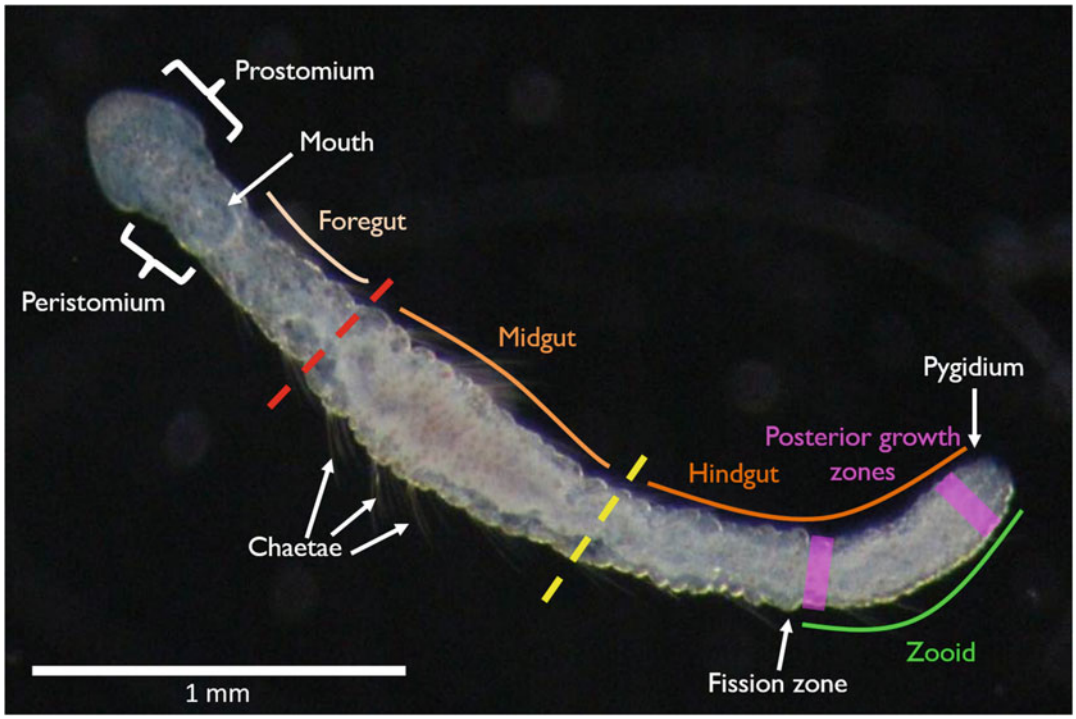


Fig. 1 Morphology and paratomic fission in *Aeolosoma viride*. The intact worm has a prostomium and a peristomium with the mouth in the first segment. The enlarged midgut locates at the center of its alimentary canal, and the fission zone locates between the parental chain and zooid. The posterior growth zone is located in the last segment before pygidium. The red dashed lines indicate the amputation sites in the experiment of anterior regeneration. The yellow dashed lines indicate the amputation sites in the synchronization and experiment of posterior regeneration

A. viride is a semitransparent, freshwater annelid of length 2–3 mm, comprising 10–12 segments [4]. Phylogenetically, *A. viride* is defined as a "clitellate-like polychaete" [5, 6]. Consistent with previous reports, *A. viride* reproduces exclusively by paratomic fission under our laboratory conditions (Fig. 1) [3, 7]. Paratomy is a form of agametic reproduction that produces multiple zooids simultaneously by fission in posterior segment. Species reproducing by paratomy have different regenerative capacities to regenerate anterior and posterior segments [8, 9]. Given their small size and transparency, as well as their strong regenerative ability together with applicability of various molecular tools including EdU labeling, whole-mount in situ hybridization (WISH), and RNA interference (RNAi) [4, 10], we anticipate that *A. viride* will be informative in comparative studies focused on whole-body regeneration. In this chapter, we will provide detailed steps on how to manipulate and conduct this novel model in regenerative research.

2 Materials

All solutions are prepared using analytical grade reagents and dissolved in deionized ultrapure water at room temperature (RT).

2.1 Regeneration in Aeolosoma viride

1. Artificial spring water (ASW): 48 mg/L $NaHCO_3$, 24 mg/L $CaSO_4 \cdot 2H_2O$, 30 mg/L $MgSO_4 \cdot 7H_2O$, 2 mg/L KCl. Adjust to pH 7.4 using 1 M HCl, sterilize before use.
2. 1× phosphate buffered saline (PBS): 40 g/L NaCl, 1 g/L KCl, 7.2 g/L Na_2HPO_4, 1.2 g/L KH_2PO_4. Sterilize before use.
3. Ground oatmeal.
4. Saturated menthol in ASW (*see* **Note 1**).
5. 4% (w/v) paraformaldehyde (PFA) in saturated menthol (*see* **Note 2**).
6. 4% (w/v) PFA in 1× PBS.
7. Mounting solution (e.g., 100% glycerol).
8. Sterile needles 27 G × 1/2″.
9. Microscope glass slides (e.g., 8 well-slide).
10. Culture plate (e.g., 6, 12 or 24 wells).
11. 25 °C incubator.
12. Dissection microscope (e.g., WILD M8, Leica).
13. DIC microscope.

2.2 Cell Proliferation Assay

1. 0.5% (v/v) Triton X-100 in 1× PBS.
2. PBS-T: 0.1% (v/v) Triton X-100 in 1× PBS.
3. 0.1 mM 5-ethynyl-2′-deoxyuridine (EdU) in 10% (v/v) DMSO.
4. 3% (w/v) bovine serum albumin (BSA) in 1× PBS.
5. EdU Imaging kit (e.g., Click-iT® EdU Imaging kit, Invitrogen).
6. 18 mg/mL Hoechst 33342.
7. Mounting solution (e.g., Fluoromount-G™, eBioscience).
8. 1× EdU buffer additive: 2 μL 10× ascorbic acid stock solution, 18 μL ddH_2O. Prepare fresh every time.
9. EdU reaction cocktail: 172 μL 1× EdU reaction buffer, 8 μL 100 mM $CuSO_4$, 0.48 μL Alexa Fluor® azide, 20 μL 1× EdU buffer additive. Prepare fresh every time.
10. Fluorescent microscope.

2.3 Whole-Mount In Situ Hybridization (WISH)

1. Primers for target gene.
2. T7 primer.
3. Trizol (e.g., TRIzol reagent).
4. Chloroform.
5. Isopropanol.
6. 0.0001% (v/v) diethyl pyrocarbonate (DEPC)-H_2O.
7. 75% ethanol in DEPC-H_2O.
8. Reverse transcriptase (e.g., SuperScript III).
9. DNA polymerase (e.g., SuperTherm Taq).
10. Thymine and adenine (TA) cloning vector (e.g., Yeastern yT&A).
11. T7 RNA polymerase (e.g., Ambion).
12. RNA digoxigenin (DIG) labeling mix (e.g., Roche).
13. DNase I (e.g., Promega).
14. 0.5 M EDTA in DEPC-H_2O, pH 8.4.
15. 6 M lithium chloride (LiCl) in DEPC-H_2O.
16. Anhydrous alcohol.
17. 1× PBS in DEPC-H_2O.
18. 10 μg/mL proteinase K in PBS-T: dilute from 10 mg/mL proteinase K stock solution. Prepare fresh before use.
19. 20× saline sodium citrate (SSC): 3 M NaCl, 0.3 M sodium citrate in DEPC-H_2O.
20. HYB^+ buffer: 5 mL 100% formamide, 2.5 mL 20× SSC, 0.1 mL 5 mg/mL heparin, 0.1 mL 50 mg/mL torula RNA type VI, 92 μL 1 M citric acid, 0.1 mL 10% tween-20 in DEPC-H_2O. Add 2.108 mL DEPC-H_2O to a final 10 mL solution, store at 4 °C.
21. HYB^- buffer: HYB^+ buffer without heparin and torula RNA.
22. HYB^+ W/O: HYB^+ without DEPC-H_2O.
23. 0.1% tween-20 in DEPC- H_2O.
24. 2× SSCTW: 10% (v/v) 20× SSC in 0.1% tween-20.
25. 0.2× SSCTW: 1% (v/v) 20× SSC in 0.1% tween-20.
26. 5% (w/v) BSA in PBS-T.
27. 1:5000 anti-DIG-alkaline phosphatase (AP) Fab fragments in 5% BSA. Prepare fresh every time.
28. Staining buffer: 100 mM Tris-HCl, pH 9.0, 150 mM NaCl, 1 mM $MgCl_2$ in DEPC-H_2O. Prepare fresh every time before use.

29. Alkaline phosphatase substrate: 50 mg/mL nitro blue tetrazolium (NBT), 50 mg/mL 5-bromo-4-chloro-3-indolyl-phosphate (BCIP). Prepare fresh every time.
30. 65 °C incubator.

2.4 RNA Interference (RNAi)

1. PCR product of target gene.
2. L4440 plasmid.
3. HT115 (DE3) competent cells.
4. Sterilized LB broth.
5. 20 mg/mL ampicillin in ddH_2O.
6. LB agar plate: 1.5% (w/v) agar with 20 μg/mL ampicillin in LB broth. Pour hot in 9 cm petri dishes, store at 4 °C after solidification.
7. 1 M IPTG in ddH_2O.
8. Electroporation system (e.g., Bio-Rad Pulse Controller Plus).
9. Glass capillary: borosilicate thin wall with filament, outside diameter 1.0 mm, inside diameter 0.78 mm, length 150 mm.
10. Needle puller (e.g., P-97, Sutter Instrument).
11. Microinjector (e.g., Nanoliter 2000 microinjector).
12. 1.5% agarose-based plates: 1.5% (w/v) agar in ASW. Pour hot in 6 cm petri dishes, store at 4 °C after solidification.

3 Methods

3.1 Animal Husbandry

1. Raise worms (*see* **Note 3**) in ASW under a regime of 12: 12 h day–night cycles at 22 ± 1 °C (*see* **Note 4**).
2. Provide 20 mg ground oatmeal (dry weight) to 500 ± 200 worms three to five times per week.
3. Replace one-half to one-fifth of old ASW with new ASW every week (*see* **Note 5**).
4. Check weekly the cultures for healthy 2–3 mm long actively swimming worm populations.
5. Discard unhealthy cultures.
6. If necessary, pick healthy worms in fresh ASW to create new culture.

3.2 Regeneration in *Aeolosoma viride*

1. Move worms to fresh tap water for 10 min to remove coexisting protozoa.
2. Move the worms into ASW.
3. Starve overnight to excrete their ingested food.

4. To synchronize the growth phase of posterior segments and remove potential fission progeny, amputate worms at the segment anterior to the fission zone by sterile needles on microscope glass slide under stereo microscope (Fig. 1).
5. Move the amputated worms into ASW for synchronization.
6. Keep at 25 °C for 3 days.
7. Amputate the worms again at the fourth segment for anterior regeneration experiment. or at the segment posterior to the midgut for posterior regeneration experiment.
8. Transfer the regenerating animals to fresh ASW in culture plate.
9. Keep at 25 °C for subsequent experiment and observation (*see* **Notes 6** and **7**).

3.3 Animal Fixation

1. Place a maximum of 10 intact or amputated worms in 20 μL ASW per well on a 8 well-slide under a dissection microscope.
2. Wash each well twice with 20 μL ASW.
3. Add 20 μL cold (4 °C) saturated menthol for anaesthetization.
4. Gently pipette for around 20 s to prevent the worms from curling up.
5. Remove 20 μL of the menthol solution.
6. Add 20 μL 4% PFA in saturated menthol.
7. Pipette gently for around 30 s.
8. Move the worms into 1.5 mL microcentrifuge tube with 200 μL 4% PFA in PBS.
9. Keep at 4 °C until further treatment.
10. Transfer to a microscope glass slide using a pipette.
11. Mount the worms in mounting solution on the slide.
12. Monitor its morphology using a DIC microscope (Fig. 2).

3.4 Cell Proliferation Assay

1. Incubate worms with 0.1 mM EdU in culture plate at 25 °C for 12 h (*see* **Notes 8** and **9**).
2. Follow **steps 1** to **8** in Subheading 3.3 to fix the animals.
3. Wash the worms with PBS-T five times, for 5 min each time.
4. Remove the PBS-T.
5. Incubate with 3% BSA for 5 min.
6. Remove the 3% BSA.
7. Incubate with 0.5% Triton X-100 for 20 min.
8. Remove the 0.5% Triton X-100.
9. Wash twice with 3% BSA, for 5 min each time.
10. Remove the 3% BSA.

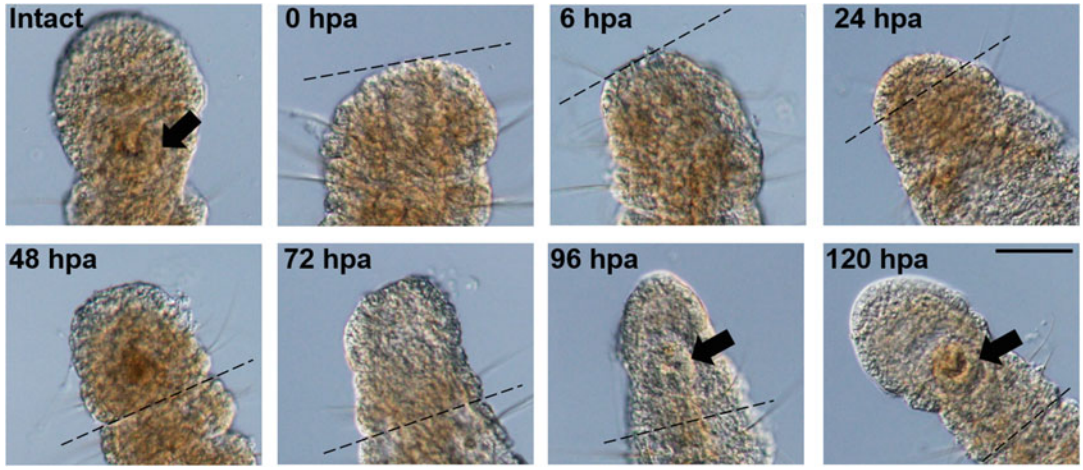


Fig. 2 Anterior regeneration in *A. viride*. Morphology was observed in intact and regenerating worms after amputation. The protruding blastema becomes visible 24–48 h after amputation (hpa). Mouth formation can be detected around 96 hpa as indicated with black arrows. The amputation site is marked by a black dotted line. Scale bar: 50 μm

11. Add EdU reaction cocktail, incubate in the dark for 30 min.
12. Remove the EdU reaction cocktail.
13. Wash five times with PBS-T, for 5 min each time.
14. Remove the PBS-T.
15. Add 18 ng/μL Hoechst 33342, incubate in the dark for 30 min.
16. Remove the Hoechst solution.
17. Wash the worms five times with PBS-T, for 5 min each time.
18. Mount the worms in mounting solution on slide.
19. Images are collected using a fluorescent microscope (Fig. 3).

3.5 Whole-Mount In Situ Hybridization (ISH)

1. Design gene specific primers for target gene according to an unpublished transcriptome database from *A. viride*. Target length is around 200–800 bp. For example, *Avi*-caspase *X* [11].
2. Place a maximum of 50 intact or amputated worms in 200 μL ASW per tube.
3. Wash twice with ASW, for 5 min each time.
4. Remove the ASW and add 200 μL TRIzol.
5. Vortex for 20–40 s until the tissue is completely liquefied without visible particles.
6. Add 40 μL chloroform.
7. Gently invert 10 times.
8. Keep at 25 °C for 15 min.

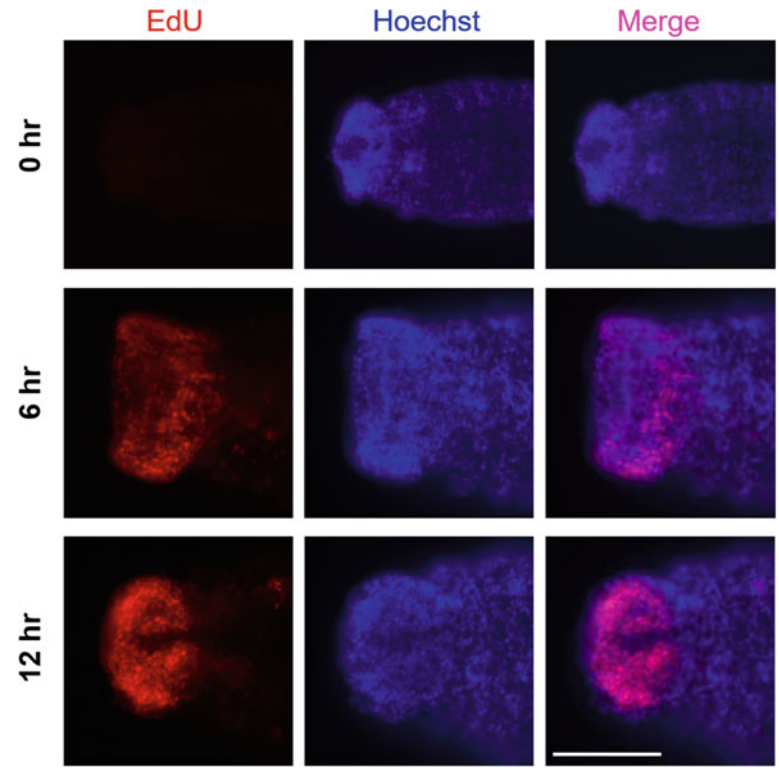


Fig. 3 EdU labeling of blastema cells at 48 h postamputation. Animals were incubated in EdU for 0, 6, or 12 h and then immediately fixed at 48 hpa. EdU-labeled nuclei are detected red and costained with Hoechst 33342 (blue). Amputation plane is on the left. Scale bar: 100 μm

9. Centrifuge tubes at 10,000 rcf at 4 °C for 15 min.
10. Transfer 120 μL of the clear supernatant to a new tube.
11. Add 120 μL isopropanol.
12. Gently invert 10 times.
13. Incubate for 30 min at −20 °C to precipitate total RNA.
14. Centrifuge tubes at 10,000 rcf at 4 °C for 30 min.
15. Remove the supernatant carefully.
16. Wash twice with 200 μL cold (−20 °C) 75% ethanol, for 5 min each time.
17. Remove the supernatant carefully and air dry.
18. Dissolve RNA pellet with 10 μL DEPC-H_2O.
19. Quantify the RNA concentration.
20. Synthesize cDNA from 0.1–5 μg total RNA using a reverse transcriptase.
21. Amplify DNA with gene specific primers and DNA polymerase by using PCR.

22. Clone riboprobe fragment into TA vector.
23. Select sense and antisense clone from TA vector.
24. Amplify DNA with T7 primers and DNA polymerase by using PCR.
25. Synthesize sense and antisense RNA probe using T7 RNA polymerase with RNA DIG labeling mix.
26. Digest DNA template with DNase I at 37 °C, for 20 min.
27. Mix with EDTA, LiCl and anhydrous alcohol sequentially to reach 50 mM, 100 mM, and 75% final concentration.
28. Precipitate sense and antisense RNA probes at −20 °C for 30 min.
29. Repeat **steps 14–18** to produce RNA probe.
30. Quantify the RNA concentration.
31. Add HYB^+ W/O to store at −20 °C.
32. Wash the fixed worms in microcentrifuge tube (see Subheading 3.3) five times with PBS-T, for 5 min each time.
33. Dilute proteinase K with PBS-T to 10 μg/mL.
34. Treat the worms with diluted proteinase K at room temperature for 10 min.
35. Replace proteinase K with 4% PFA.
36. Incubate at room temperature for 20 min.
37. Remove 4% PFA.
38. Wash five times with PBS-T, for 5 min each time.
39. Replace with HYB^+ buffer.
40. Incubate the microcentrifuge tube 65 °C for 1 to 3 h (*see* **Note 10**).
41. Hybridize worms with sense or antisense riboprobes (1 to 3 ng/μL) in HYB^+ at 65 °C for 16–24 h (*see* **Note 11**).
42. Remove HYB^+ buffer with riboprobes under dissection microscope carefully.
43. Add HYB^- buffer at 65 °C for 5 min.
44. Remove HYB^- buffer under dissection microscope carefully.
45. Transfer serially (5 min each time) into 66%, and 33% HYB^- buffer in 2× SSCTW at 65 °C.
46. Remove supernatant.
47. Wash the worms with 2× SSCTW at 65 °C for 5 min.
48. Remove 2× SSCTW.
49. Wash twice in 0.2× SSCTW at 65 °C, for 15 min each time.
50. Remove 0.2× SSCTW.

51. Transfer serially (for 5 min each time) into 66%, and 33% 0.2× SSCTW in PBS-T at room temperature.
52. Remove supernatant.
53. Wash the worms with PBS-T at room temperature for 5 min.
54. Block with 5% BSA at 4 °C overnight or at room temperature for 2 h.
55. Dilute anti-DIG-AP Fab fragments 1:5000 with 5% BSA.
56. Remove 5% BSA.
57. Incubate overnight with 1:5000 anti-DIG-AP Fab fragments at 4 °C.
58. Remove anti-DIG-AP Fab fragments.
59. Wash ten times with PBS-T, for 5 min each time.
60. Prepare fresh staining buffer.
61. Remove PBS-T.
62. Wash the worms twice with staining buffer, for 5 min each time.
63. Prepare fresh staining solution, add NBT (final 220 μg/mL) and BCIP (final 170 μg/mL) to staining buffer in the dark.
64. Remove the staining buffer.
65. Stain the worms with staining solution at 4 °C or room temperature in the dark.
66. Check the staining status under a dissection microscope.
67. Mount the worms in mounting solution.
68. Images are collected using a microscope (Fig. 4).

3.6 RNA Interference (RNAi) by Feeding Method

1. Design 300 bp gene specific primers for yellow fluorescent protein (YFP, as control group) and target gene. For example, *Avi-beta tubulin isoform 1* [4].
2. Amplify DNA with gene specific primers and DNA polymerase by using PCR.
3. Clone DNA fragment into L4440 plasmid (see **Note 12**).
4. Transform the L4440 vector (1 μL containing 100 ng) into 50 μL HT115 (DE3) competent cell through electroporation system under the following conditions: 2.0 kV, 100 Ω, and 25 μF.
5. Add 200 μL of LB broth to a cuvette.
6. Mix gently by pipetting.
7. Transfer to 1.5 mL microcentrifuge tube.
8. Shake vigorously (200 rpm) on an orbital shaker at 37 °C for 1 h.
9. Dilute the cells 20 times with LB broth.

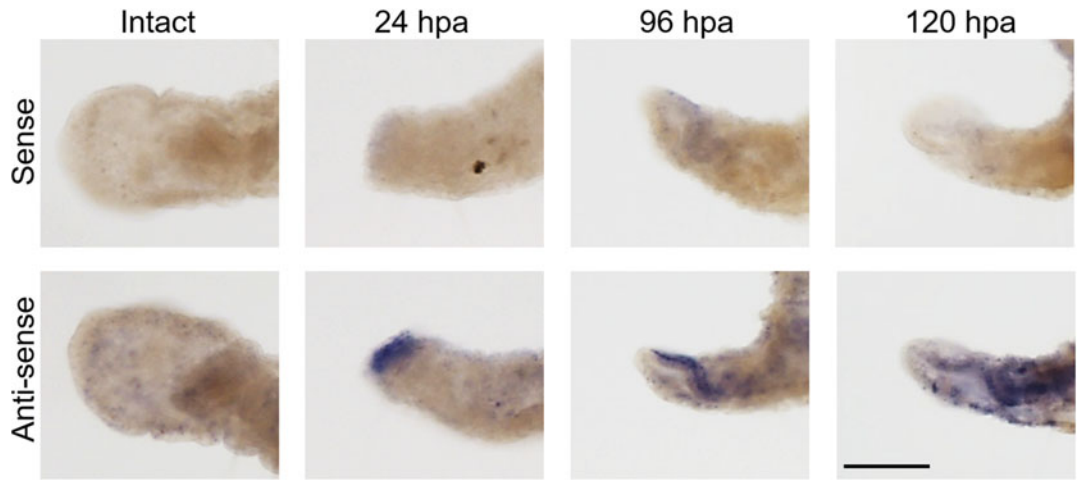


Fig. 4 Expression of the *Avi-caspase X* gene during anterior regeneration. Whole-mount ISH was performed on intact and regenerating worms with sense (upper row) or antisense (lower row) riboprobe. The amputation site is located on the left. Note the *Avi-caspase X* expressing cells (blue purple) observed from 24 hpa and at later time-points. Scale bar: 100 μm

10. Spread cells on LB agar plates.
11. Incubate at 37 °C for 16 h to overnight.
12. Pick single colony from LB plate into an LB broth containing 20 μg/mL ampicillin.
13. Incubate at 37 °C for 16 h.
14. Subculture at a 1:100 dilution with shaking until OD_{600} reaches 0.4–0.6.
15. Add 1 M IPTG to reach 0.1 mM final concentration.
16. Express target dsRNA at 37 °C for 4 h.
17. Collect the bacteria expressing the dsRNA into 2 mL tubes.
18. Spin at 3000 rcf for 1 min.
19. Replace the supernatant with fresh LB broth.
20. Repeat **steps 18** and **19** to wash bacteria a second time.
21. Dilute 1 μL of bacteria in 99 μL of LB broth.
22. Plate the serially diluted bacteria on an LB agar plate.
23. Incubate at 37 °C for 16 h.
24. Count the number of colony forming units (CFU).
25. This is the number of CFU per μL in the original solution.
26. Place the undiluted bacteria in their 2 mL tubes on a hot plate at 100 °C for 10 min.
27. Cool the tubes on ice for 5 min.
28. Store the bacteria at −20 °C (*see* **Note 13**).

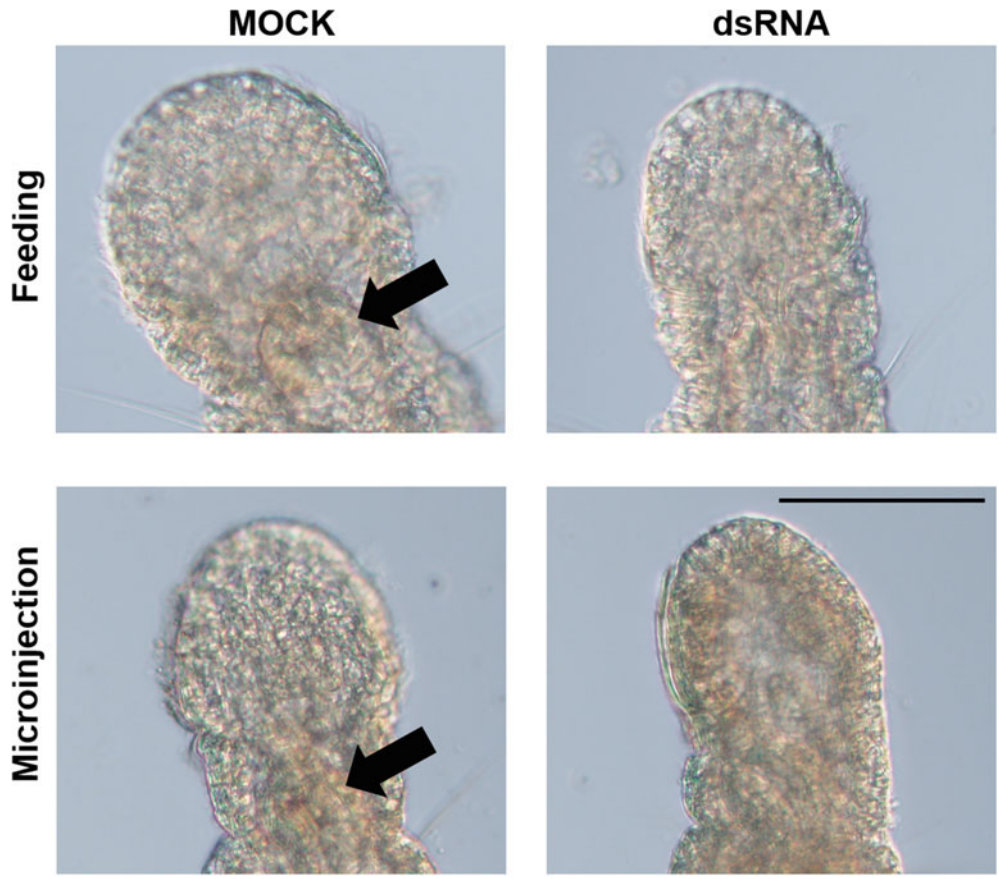


Fig. 5 *Avi-beta tubulin isoform 1* RNAi inhibited regeneration in *A. viride*. The inhibitory effect of regenerates by *Avi-beta tubulin isoform 1* RNAi feeding or microinjection was observed at 7 days postamputation. The head morphology of regenerating worms was obviously affected by feeding or dsRNA microinjection method. The black and white arrow respectively indicated the mouth. Scale bar: 100 μm

29. Fed worms with 1×10^8 CFU/mL bacteria containing dsRNA for three consecutive days, renewed every 24 h.
30. To validate the knock-down efficiency of the target gene, real time quantitative polymerase chain reaction (RT-qPCR) or ISH (see Subheading 3.5) can be performed after the feeding procedure (*see* **Note 14**).
31. Mount the fed worms in mounting solution.
32. Images are collected using a microscope (Fig. 5).

3.7 RNAi by Microinjection

1. Produce control and target dsRNA from L4440 vector (follow **steps 1** and **2** in Subheading 3.6 and **steps 23–26** in Subheading 3.5).
2. Dissolve RNA pellet with DEPC-H_2O.
3. Store at −20 °C.

4. Pull the microinjection pipette with the following settings: pressure 500, heat 640, pull 125.
5. Set the microinjector in slow mode with an injection volume of 27.6 nL. Each injection will contain roughly 100 ng dsRNA.
6. Open the tip of the microinjecting pipette using a pair of tweezers.
7. Load the dsRNA into the microinjecting pipette.
8. Move the worms onto a 1.5% agarose-based plate.
9. Remove ASW to limit movements of the worms on the agar surface.
10. Inject the dsRNA at the fourth segment of the worms (*see* **Note 15**) for two consecutive days to optimize intake of the dsRNA.
11. Allow the worms to recover in fresh ASW for 24 h after the final injection.
12. Validate the knock-down efficiency of the target gene by RT-qPCR or ISH (see Subheading 3.5).
13. Mount the injected worms in mounting solution.
14. Images are collected using a microscope (Fig. 5).

4 Notes

1. Preparation of saturated menthol in ASW by add 0.2 g menthol in 10 mL ASW, and placed at 4 °C for more than 24 h, make sure at least a piece of crystal menthol is still visible in the saturated solution before use.
2. Prepare 4% (w/v) PFA by adding 2 g PFA in 40 mL ASW, mix well and adjust to pH 11 using 1 M NaOH to help dissolution. Incubate at 65 °C overnight, adjust to pH 7.4 and then add ASW to a final volume of 50 mL. Finally, filter this 4% (w/v) PFA by 0.22 μm membrane and store at 4 °C.
3. Sample worms for initiating a laboratory culture of *A. viride* can be obtained from our lab, from Dr. Dian-Han Kuo at National Taiwan University or from Dr. Chia-Liang Cheng at National Dong Hwa University. Please contact the corresponding author if interested.
4. In our laboratory, *A. viride* was cultured in a glass bottle with ASW, the suitable volume of ASW filling about 70% capacity of the glass bottle. For bulk culture, we initially mix 200 worms in 30 mL ASW with 320 mL ASW in a 500 mL glass bottle. After 3 weeks, we can harvest around 30 times more worms for the experiment. In the meantime, we will change one-half to one-fifth of fresh ASW according to the water quality every week.

5. One habitual behavior of this worm is to adhere to the wall of the glass container. Therefore, most *A. viride* will remain on the wall when the old ASW is poured out.
6. Two morphological and behavioral criteria were used to confirm complete regeneration: (1) bulged head formation with a circular mouth at the ventral side of the peristomium; and (2) free swimming.
7. More than 80% of worms can complete anterior regeneration from the remaining 6 or 9 segments at 120 h postamputation (hpa) [1].
8. Both bromodeoxyuridine (BrdU) and EdU are commonly used reagents for incorporation in most vertebrates and invertebrates [12, 13]. However, we found that BrdU labeling did not work well in *A. viride*.
9. Commonly applied concentrations and duration of EdU labeling are 1–10 μM for 0.5–5 h in cell lines and annelids [14, 15]. However, these conditions did not work for *A. viride*. Instead, we used a high concentration (100 μM) and long incorporation time (12 h), which resulted in the regenerating blastema being observed at 48 hpa (Fig. 3).
10. The hybridization temperature commonly used in our lab was 65 °C, however, it depends on the condition of each riboprobe.
11. The probe concentration commonly used in our lab was 1 ng/μL, however, it depends on the concentration of each riboprobe. Typically, we use 3 ng/μL of newly synthesized riboprobe.
12. There are various ways to produce double-stranded RNA. The most common way is to amplify the target gene fragment with PCR using specific primers that contain SP6, T3, or T7 promoters. Then, both strands of the gene fragment can be synthesized using specific in vitro transcription enzymes. Finally, the two products can be mixed to form dsRNA. This approach has the benefit that each strand can be proofread by gel electrophoresis and the concentration of each strand can be varied. However, producing both strands separately using different enzymes is time-consuming. Both strands can be produced simultaneously using only T7 RNA transcriptase and L4440 vector. Gel electrophoresis can be used to separate the two strands, enabling validation that both strands have been synthesized successfully.
13. To confirm the expression of dsRNA of the target gene, collect 1 mL cultured bacteria and lyse with Trizol to extract total RNA. Finally, assess the quality and length of the dsRNA by gel electrophoresis using 1% (w/v) agarose gel.

14. Evaluate the knock-down efficiency of dsRNA by feeding or microinjection method through RT-qPCR and WISH (see Subheading 3.5). In RT-qPCR, *Avi*-actin was selected as internal control with specific primers: 5′-AT GGAGAAGATCTGG CATCA -3′ and 5′- GGAGTACTTGCGCTCAGGTG -3′ designed from *Avi*-actin (NCBI # KY079092.1). The gene expression relative to *Avi-actin* was calculated by the ΔΔCT method.
15. The injected material diffuses through the entire body cavity of annelids because they lack internal septa.

References

1. Bely AE (1999) Decoupling of fission and regeneration capabilities in an asexual oligochaete. Hydrobiologia 406:243–251. https://doi.org/10.1007/978-94-011-4207-6_24
2. Özpolat BD, Bely AE (2016) Developmental and molecular biology of annelid regeneration: a comparative review of recent studies. Curr Opin Genet Dev 40:144–153. https://doi.org/10.1016/j.gde.2016.07.010
3. Falconi R, Gugnali A, Zaccanti F (2015) Quantitative observations on asexual reproduction of *Aeolosoma viride* (Annelida, Aphanoneura). Invertebr Biol 134:151–161. https://doi.org/10.1111/ivb.12087
4. Chen CP, Fok SKW, Hsieh YW et al (2020) General characterization of regeneration in *Aeolosoma viride* (Annelida, Aeolosomatidae). Invertebr Biol 139:e12277. https://doi.org/10.1111/ivb.12277
5. Hessling R, Purschke G (2000) Immunohistochemical (cLSM) and ultrastructural analysis of the central nervous system and sense organs in *Aeolosoma hemprichi* (Annelida, Aeolosomatidae). Zoomorphology 120:65–78. https://doi.org/10.1007/s004350000022
6. Zrzavý J, Říha P, Piálek L et al (2009) Phylogeny of Annelida (Lophotrochozoa): total-evidence analysis of morphology and six genes. BMC Evol Biol 9:1–14. https://doi.org/10.1186/1471-2148-9-189
7. Falconi R, Renzulli T, Zaccanti F (2006) Survival and reproduction in *Aeolosoma viride* (Annelida, Aphanoneura). Hydrobiologia 564:95–99. https://doi.org/10.1007/s10750-005-1711-2
8. Bely AE, Sikes JM (2010) Latent regeneration abilities persist following recent evolutionary loss in asexual annelids. Proc Natl Acad Sci U S A 107:1464–1469. https://doi.org/10.1073/pnas.0907931107
9. Zattara EE, Bely AE (2016) Phylogenetic distribution of regeneration and asexual reproduction in Annelida: regeneration is ancestral and fission evolves in regenerative clades. Invertebr Biol 135:400–414. https://doi.org/10.1111/ivb.12151
10. Chen CF, Sung TL, Chen LY et al (2018) Telomere maintenance during anterior regeneration and aging in the freshwater annelid *Aeolosoma viride*. Sci Rep 8:18078. https://doi.org/10.1038/s41598-018-36396-y
11. Fok SKW, Chen CP, Tseng TL et al (2020) Caspase dependent apoptosis is required for anterior regeneration in *Aeolosoma viride* and its related gene expressions are regulated by the Wnt signaling pathway. Sci Rep 10:10692. https://doi.org/10.1038/s41598-020-64008-1
12. Gratzner HG (1982) Monoclonal antibody to 5-bromo- and 5-iododeoxyuridine: a new reagent for detection of DNA replication. Science 218:474–475. https://doi.org/10.1126/science.7123245
13. Salic A, Mitchison TJ (2008) A chemical method for fast and sensitive detection of DNA synthesis *in vivo*. Proc Natl Acad Sci U S A 105:2415–2420. https://doi.org/10.1073/pnas.0712168105
14. Buck SB, Bradford J, Gee KR et al (2008) Detection of S-phase cell cycle progression using 5-ethynyl-2′-deoxyuridine incorporation with click chemistry, an alternative to using 5-bromo-2′-deoxyuridine antibodies. Biotechniques 447:927–929. https://doi.org/10.2144/000112812
15. Planques A, Malem J, Parapar J et al (2019) Morphological, cellular and molecular characterization of posterior regeneration in the marine annelid *Platynereis dumerilii*. Dev Biol 445:189–210. https://doi.org/10.1016/j.ydbio.2018.11.004

Open Access This chapter is licensed under the terms of the Creative Commons Attribution 4.0 International License (http://creativecommons.org/licenses/by/4.0/), which permits use, sharing, adaptation, distribution and reproduction in any medium or format, as long as you give appropriate credit to the original author(s) and the source, provide a link to the Creative Commons license and indicate if changes were made.

The images or other third party material in this chapter are included in the chapter's Creative Commons license, unless indicated otherwise in a credit line to the material. If material is not included in the chapter's Creative Commons license and your intended use is not permitted by statutory regulation or exceeds the permitted use, you will need to obtain permission directly from the copyright holder.





Chapter 10

Studying Annelida Body Regeneration Under Environmental Stress in *Diopatra neapolitana*

Adília Pires

Abstract

The polychaete *Diopatra neapolitana* is a cosmopolitan annelid that can robustly regenerate both its anterior and posterior body part depending on the position of the amputation. Previous studies demonstrated that body regeneration represents a sensitive and unspecific response to environmental stresses, including contaminants and climate alterations.

The posterior body regeneration of *D. neapolitana* is thus a suitable, ecological and relevant biomarker in ecotoxicological and ecological risk assessment assays. Here we describe the amputation process, the monitoring of the regeneration process of the polychaete *D. neapolitana* and the quantification of the impact of environmental stresses on its regenerative capacity.

Key words Polychaetes, Posterior regeneration, Biomarker, Endpoint, Environmental alterations

1 Introduction

Annelids are known for their efficient wound healing and their capacity to regenerate both anterior and posterior segments after loss by injury [1, 2]. This regenerative ability varies significantly within the phylum, and some species can regenerate an entire individual from a single segment while others are much more limited [3]. Previous works demonstrated that species of the genus *Diopatra* could regenerate anterior and posterior segments and prostomial structures [3–6]. This mechanism performs a critical role in survivorship after tissue loss due to sublethal predation and harvesting [5, 7]. Additionally, it can also aid in recovery from injuries due to physical alterations [8].

Several studies demonstrated that exposure to environmental stressors such as contaminants or abiotic alterations reduced the regenerative capacity of polychaetes [9–17], with organisms regenerating slower and usually fewer chaetigers (segments that have chaetae). Nusetti et al. [9] observed that the polychaete *Eurythoe complanata* exposed to crankcase oil took longer to regenerate a

Simon Blanchoud and Brigitte Galliot (eds.), *Whole-Body Regeneration: Methods and Protocols*, Methods in Molecular Biology, vol. 2450, https://doi.org/10.1007/978-1-0716-2172-1_10, © The Author(s) 2022

new region and regenerated fewer segments. Exposure to micro- and nanoplastics reduced the capacity of *Perinereis aibuhitensis* and *Hediste diversicolor* to regenerate their posterior ends [14, 15]. *Diopatra neapolitana* exposed to several contaminants, such as metals, pharmaceuticals, carbon nanotubes, and environmental enrichment presented a delay in posterior segments regeneration, taking longer to achieve complete regeneration, and regenerated fewer segments [10–13, 16, 18]. Moreover, exposure to abiotic alterations, including pH variations and salinity changes, also reduced the regenerative ability of *D. neapolitana* [17].

Although the majority of toxicity studies with polychaetes have been conducted using the species *H. diversicolor* [14, 19–23], most of those regarding the use of the regenerative ability as a biomarker were carried out with the species *D. neapolitana* due to this process being well documented for *Diopatra* species (e.g., [3, 5, 24]). Additionally, this species represents a wide spatial distribution, being reported in intertidal and shallow subtidal habitats, namely, in the Red Sea and Indian Ocean [25], Mediterranean Sea [26–28], and the Atlantic Ocean [6, 29–31]. Furthermore, *Diopatra* species play an important ecological and economic role. Their tubes stabilize the sediments, increasing their structural complexity and thus their biodiversity, by supplying refugia from disturbance and predation [32] and facilitating the settlement and the attachment of some algal species [33]. Moreover, this species is commonly harvested to be sold as fish bait [31, 34, 35]. Altogether, these studies suggest that the regenerative capacity of polychaetes is a suitable biomarker in ecotoxicological and ecological risk assessment assays since it is sensitive to environmental stressors, including organic and inorganic contaminants and climate alterations.

The mechanisms behind this sensitive yet unspecific response to environmental stresses in *Diopatra* remain to be elucidated. Some authors suggested that the delay in regenerative capacity could be related to exposure to oxidative stress [10, 11, 14, 17] since free radicals may damage the biochemical and cellular functions that underlie the regenerative process. Moreover, Soneja et al. [36] reported that oxidative stress prolonged chronic wound inflammation as it stimulates cells of the immune system. Delayed regeneration may impact the sexual reproduction of individuals, as organisms will canalize their reserves toward tissue regeneration rather than producing gametes [5–7]. Also, the delay of organisms in starting gamete production compromises population maintenance, with consequences for communities and ecosystems [8].

Consequently, due to this species' ecological importance, understanding the interplay between environmental stresses and regenerative capacity is particularly pertinent since delays in regenerative capacity may negatively impact population and ecosystem function.

This chapter presents a detailed protocol to study the impacts of environmental stressors in the posterior regenerative capacity in field-collected organisms of the polychaete *D. neapolitana*.

2 Materials

All reagents should be prepared with sterile reverse osmosis water and stored at room temperature (RT) unless otherwise stated.

1. 20 × 15 × 40 cm (W × L × H) glass aquariums (*see* **Note 1**).
2. Sediments: clean medium or fine sand with low organic matter content. Collect from nonpolluted organisms' sampling site (*see* **Note 2**).
3. Artificial seawater (ASW): 30 g/L commercial synthetic sea salt (e.g., Tropic Marin Sea Salt) (*see* **Note 3**). Prepare at least 1 day before use.
4. Aeration system.
5. Acclimated culture room: photoperiod (12 h light:12 h dark), controlled temperature, constant aeration.
6. *Diopatra* food: collect shellfish in a clean site, cut in 2 mm^3 cubes, store until needed at −20 °C (*see* **Note 4**).
7. Contaminated ASW (e.g., 0 to 0.25 μg/L of arsenic).
8. Contaminated sediments (e.g., 0 to 9 mg/kg of lead).
9. Anesthetizing solution: 4% (w/v) $MgCl_2 \cdot 6H_2O$ in ASW.
10. Imaging setup: stereomicroscope with a camera attached and a ruler for measuring organisms.

3 Methods

3.1 Collection of Organisms and Acclimation

1. Setup the acclimated culture room to the desired conditions (*see* **Note 5**).
2. Fill each aquaria to be used with 3 L of sediment (*see* **Note 6**).
3. Add 9 L of ASW.
4. Add aeration to the aquaria.
5. Choose a sampling site where *D. neapolitana* can be found (*see* **Note 7**).
6. Identify a tube containing a specimen (Fig. 1a, *see* **Note 8**).
7. Pitch a shovel 10 cm away from the tube, with an inclination of about 45° and deep up to 30 cm (Fig. 1b).
8. Expose the tube by digging the shovel.

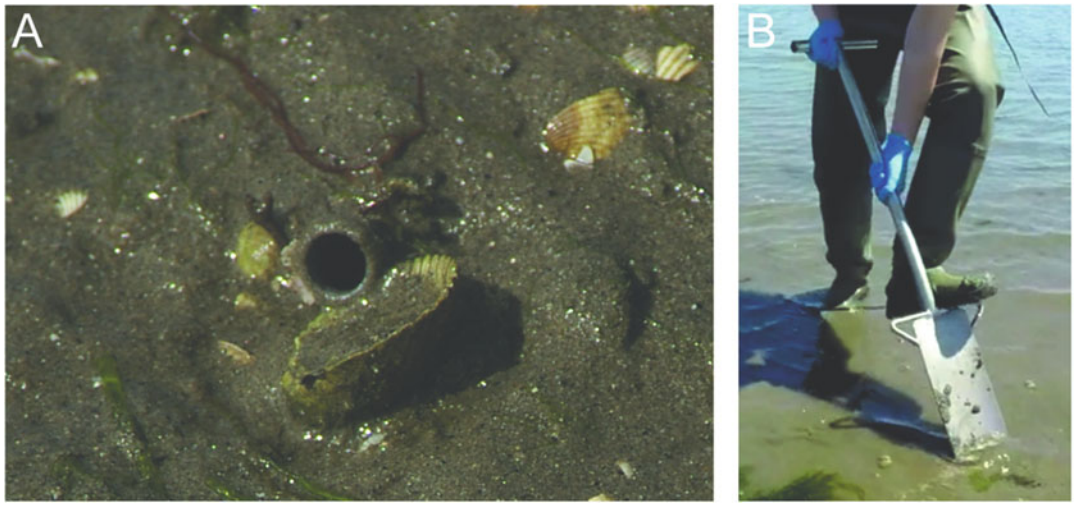


Fig. 1 (**a**) Tube of *Diopatra neapolitana* at sediment surface and (**b**) shovel with the inclination that should be used to catch *D. neapolitana* specimens

9. Transfer *Diopatra neapolitana* inside their tube into a transport bucket (*see* **Note 9**).
10. Repeat **steps 6** to **9** until sufficient specimens are collected.
11. Repeat **steps 5** to **10** until all the target sampling sites have been explored.
12. Transfer the animals to the lab (*see* **Note 10**).
13. Fill a beaker with 2 L ASW.
14. Pick a *Diopatra* tube using a pair of tweezers.
15. Flush the anterior end of the tube to force the specimen out of its tube into the beaker using ASW (*see* **Note 11**).
16. Transfer organisms with more than 60 chaetigers into the prepared aquaria but discard regenerating specimens (Fig. 2a, b, *see* **Note 12**).
17. Repeat **steps 14** to **16** until all tubes are processed.
18. Repeat **steps 13** to **17** until all transfer buckets are emptied of their animals.
19. Wait 24 h.
20. Discard animals that have not rebuilt a new tube.
21. Discard unhealthy animals (*see* **Note 13**).
22. Wait 24 h.
23. Repeat **steps 21** and **22** for 5 more days.
24. Renew water of every aquarium.
25. Place a piece of *Diopatra* food near the entrance of each tube as such as organisms can detect it.

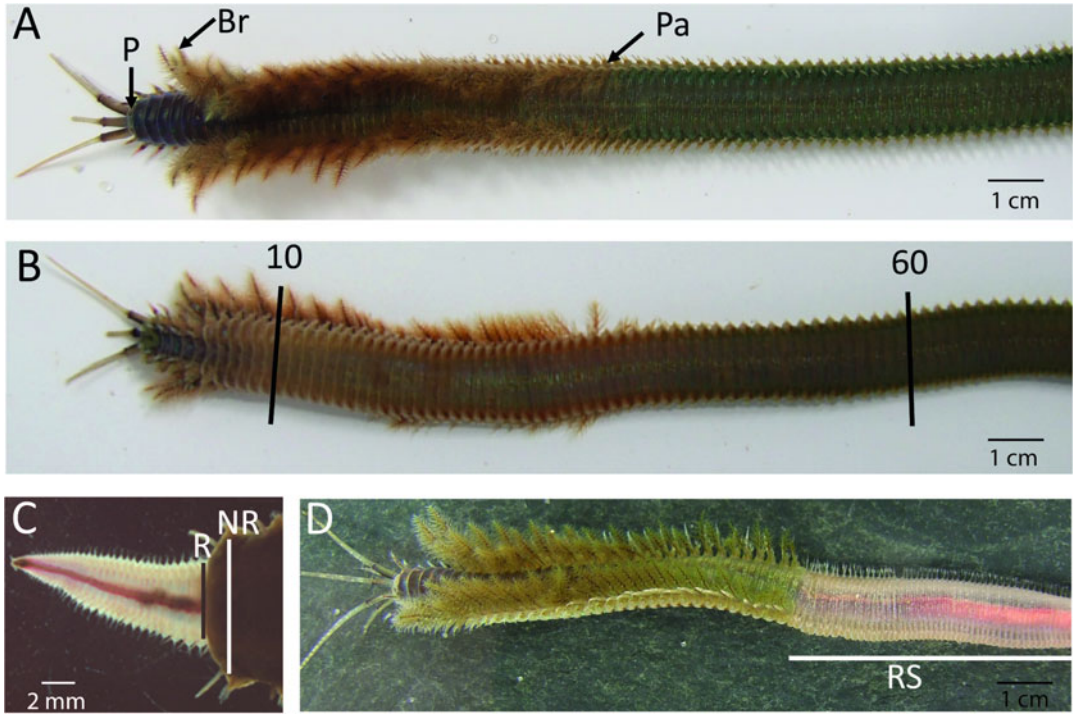


Fig. 2 *Diopatra neapolitana* anterior end ventral view (**a**) and dorsal view (**b**); (**c**) *D. neapolitana* specimen regenerating the posterior end, (**d**) *D. neapolitana* with posterior end regenerated. The newly regenerated chaetigers have a lighter color, being possible to observe the blood vessels through the body wall. 10—chaetiger 10, 60—chaetiger 60, P—Prostomium, Br—Branchiae, Pa—parapode, R—width of the regenerated chaetiger; NR—width of the not regenerated chaetiger (chaetiger 60); RS—specimen with posterior end fully regenerated

26. Wait 2 h for the animals to consume the food.
27. Remove the food that is not consumed.
28. Repeat **steps 21** and **22** for 2 more days (*see* **Note 14**).
29. Repeat **steps 25** to **28** two more times.
30. Renew water of every aquarium.
31. Discard animals that have not healed their damaged posterior part (*see* **Note 15**).
32. Repeat **steps 25** to **30** to maintain the culture of *Diopatra* (*see* **Note 16**).

3.2 Regeneration Assay

Experiments should be carried out with acclimatized specimens of similar size. The impacts of environmental stresses are tested by exposing the regenerating organisms to contaminated sediments and/or contaminated water.

1. Follow **steps 1** to **4** in Subheading 3.1 to prepare the aquariums for each condition that will be tested and for the controls (*see* **Note 17**).
2. Follow **steps 13** to **15** in Subheading 3.1 to remove the specimens from their tubes.
3. Transfer an animal to a petri dish filled with 100 mL of anesthetizing solution.
4. Wait 15 min for the animal to anesthetize (*see* **Note 18**).
5. Transfer the dish under a stereomicroscope.
6. Measure the width of the tenth chaetiger (without parapodia) using the ruler (Fig. 2b, *see* **Notes 19** and **20**).
7. Amputate the anesthetized organism at the 60th chaetiger (*see* **Note 21**) (Fig. 2b) with a scalpel.
8. Transfer the animal into a beaker filled with 100 mL ASW.
9. Wait 20 min for the animal to "wake up" and start to swim in ASW.
10. Select organisms with similar sizes for the regeneration assay (*see* **Note 20**).
11. Place the amputated specimen in the experiment aquarium.
12. Repeat **steps 3** to **11** to measure and amputate at least nine individuals per condition.
13. Follow **steps 25** to **30** in Subheading 3.1 to feed the regenerating animals.
14. Renew the water of each tank with the corresponding culture condition.
15. Repeat **steps 3** to **5** to anesthetize an animal.
16. Measure the width of the regenerated body part (R), the width of the last nonregenerated segment (NR) (Fig. 2c) and count the number of regenerating segments (RS), identified by the lighter color and/or the narrower width compared to the rest of the body (Figs. 2c and 3a–f, *see* **Note 22**).
17. Return the anesthetized animal to its experiment aquarium.
18. Repeat **steps 15** to **17** to measure all animals.
19. Repeat **steps 14** to **18** once a week until complete regeneration (*see* **Notes 23** and **24**).
20. Quantify the regenerative capacity of each condition through three parameters: the percentage of body regenerated (R/NR, Figs. 2c and 3a–f), the number of segments regenerated (RS), and the time needed to achieve complete regeneration (i.e., when R = NR, Fig. 2d).



Fig. 3 Different levels of posterior regeneration of *Diopatra neapolitana* exposed to sediments contaminated with lead (0.0, 3.0, 9.0 mg/kg). Photographic record of the regeneration process 14 (left column) and 28 days (right column) after amputation at control (**a** and **b**), 3.0 mg/kg (**c** and **d**), and 9.0 mg/kg (**e** and **f**)

4 Notes

1. Keep animals at a maximum density of 50 individuals/m^2. For example, this 20 × 15 cm aquarium can contain 14 organisms. Vary the size of the aquaria based on the number of organisms that will be used in each experiment.
2. If possible, use the sediments of the same sampling site where organisms will be collected. If these sediments do not have good characteristics, use sediment from another clean site. Alternatively, use commercial sand.

3. Salinity and pH should be adapted to parameters recorded in the sampling site. Alternatively, 0.22 μm filter-sterilized seawater (FSW) collected from the sampling site can be used.
4. Cockles and mussels are *Diopatra*'s preferred shellfish. Make sure to collect in a clean site. Alternatively, use commercial fish food (46% protein, 11% lipids) as feed. If commercial fish food is adopted, feed each organism with about 10 mg.
5. Organisms should be maintained at a constant temperature, salinity and pH similar to those measured in the collection site. In our case, experiments are usually carried out at a temperature between 17–20 °C, salinity between 28 and 30, and pH 7.8.
6. The height of the sediment in the aquarium should be about 10–12 cm. *Diopatra neapolitana* adults are very long, but organisms are not collected whole. Additionally, organisms construct their tubes with some inclination; thus, this height of sediment is suitable.
7. *D. neapolitana* are cosmopolitan tubiculous animals that live in muddy or muddy sand intertidal areas. They can be easily detected by the presence of their tubes on the sediment surface since they protrude a few millimeters above the surface of the sediment (Fig. 1a).
8. A tube with water is an inhabited tube. On the other hand, if the tube contains sediment inside, it is not inhabited by the polychaete.
9. Organisms are not collected entire, as they are very long; only the anterior end is usually collected. Avoid collecting organisms during the reproductive period (usually during summer months [27, 37]).
10. Animals can stand up to 2 h in transport buckets. The tubes could be complemented with macroalgae to maintain the organisms up to 6 h in the buckets.
11. It is important to remove the organisms from their tubes because their tubes usually have attached pieces of algae and other materials in the vicinity of the tube that will decompose and contaminate the clean sand. Organisms without tube will construct a new tube with the sand in a few hours.
12. Sampled specimens that show signs of undergoing regeneration will not be used in the experiment. They can be distinguished by the lighter color and/or the narrower regenerating chaetigers compared to the rest of the body (Fig. 2c).
13. In dead or dying organisms, the anterior end (antennae and some segments) usually remains outside the tube. To check their vitality, touch them in the portion located outside of the tube. If the polychaete runs into the tube, it means that it is

alive. However, if it does not run into the tube, it means that it is dying. In this situation, remove the organism from the aquarium with its tube. Dead organisms should be immediately removed from the aquarium because they begin to decompose very quickly and contaminate water and sediment.

14. If needed, animals can be fed every 2 days.
15. Since organisms are very long, they cannot be harvested as a whole; consequently, it is necessary to ensure that their integrity is reestablished. This period is critical to understand if the organisms have already started to heal the posterior end. Healthy organisms should have at least healed the damaged part after 1 week. Do not use specimens that have not healed after these 2 weeks.
16. *Diopatra* can be maintained in culture for several months. Healthy organisms will heal and completely regenerate the posterior end in 2 months [38]. In this case, organisms should be changed for larger aquaria, with 20 cm of sediment (height).
17. We advise to prepare at least three aquariums per condition.
18. Organisms take about 15 to 20 min to become anesthetized. Do not maintain organisms anesthetized longer than 1 h because they may not recover.
19. The width of the tenth chaetiger is commonly used as the unit of size among *Diopatra* species as it is challenging to capture entire *Diopatra* animals [39, 40].
20. Organisms can differ by a margin of about 2 mm; for example, choose organisms with the width of the tenth chaetigers between 6 and 8 mm.
21. Studies conducted by Pires et al. [5] further revealed that, under laboratory conditions simulating environmental conditions, *D. neapolitana* specimens are able to regenerate the anterior body part only when organisms are amputated up to the 15th chaetiger, where the posterior end can regenerate the missing anterior part. Polychaetes, when amputated at chaetiger 3, 10 and 15 have a survival capacity of 87.5%, 75% and 50%, respectively and regenerated the anterior end. Individuals amputated around chaetiger 20 cannot regenerate and do not survive. *D. neapolitana* organisms amputated at chaetiger 25 and beyond only regenerated the posterior part. Individuals amputated between the 25th chaetiger, 40th and after branchial region (around 60th chaetiger) are able to regenerate and present a survival capacity ranging from 50%, 81.3% and 100%, respectively [5]. Considering these results, we suggest to amputate the animals at chaetiger 60 for all organisms to survive the procedure.

22. On the first week, the regenerated portion does not form individualized segments; therefore, it is not possible to count the chaetigers.
23. Full regeneration as evidenced by the same width between the older and the newly formed chaetigers (Fig. 2d) is observed for *D. neapolitana* organisms (not exposed to stressful conditions) between day 50 and 60 after amputation [38]. The regenerated portion appears lighter than the original segments (Fig. 2d).
24. Shorter experiments could be conducted for 28 days only, but regeneration speed will not be measurable.

Acknowledgments

Thanks to FCT/MCTES for the financial support to CESAM (UIDP/50017/2020+UIDB/50017/2020+ LA/P/0094/2020) through national funds. This work was also financially supported by the project BIOGEOCLIM —PTDC/CTA-GQU/29185/2017 (POCI-01-0145-FEDER-029185) funded by FEDER, through COMPETE2020—Programa Operacional Competitividade e Internacionalização (POCI), and by national funds (OE), through FCT/MCTES. Adília Pires was contracted by national funds (OE), through FCT—Fundação para a Ciência e a Tecnologia, I.P., in the scope of the framework contract foreseen in the numbers 4, 5, and 6 of the article 23, of the Decree-Law 57/2016, of August 29, changed by Law 57/2017, of July 19.

References

1. Bely AE (2014) Early events in annelid regeneration: a cellular perspective. Integr Comp Biol 54(4):688–699. https://doi.org/10.1093/icb/icu109
2. Zattara EE, Bely AE (2016) Phylogenetic distribution of regeneration and asexual reproduction in Annelida: regeneration is ancestral and fission evolves in regenerative clades. Invertebr Biol 135(4):400–414. https://doi.org/10.1111/j.1525-142X.2010.00458.x
3. Bely AE (2006) Distribution of segment regeneration ability in the Annelida. Integr Comp Biol 46(4):508–518. https://doi.org/10.1093/icb/icj051
4. Berke SK, Mahon AR, Lima FP, Halanych KM, Wethey DS, Woodin SA (2010) Range shifts and species diversity in marine ecosystem engineers: patterns and predictions for European sedimentary habitats. Glob Ecol Biogeogr 19(2):223–232. https://doi.org/10.1111/j.1466-8238.2009.00509.x
5. Pires A, Freitas R, Quintino V, Rodrigues AM (2012) Can Diopatra neapolitana (Annelida: Onuphidae) regenerate body damage caused by bait digging or predation? Estuar Coast Shelf Sci 110:36–42. https://doi.org/10.1016/j.ecss.2011.12.039
6. Pires A, Quintino V, Gentil F, Freitas R, Rodrigues AM (2012) Reproductive biology of a brooding Diopatra species: *Diopatra marocensis* Paxton et al., 1995. Estuar Coast Shelf Sci 110:85–92. https://doi.org/10.1111/j.1439-0485.2011.00463.x
7. Zajac RN (1985) The effects of sublethal predation on reproduction in the spionid polychaete *Polydora ligni* Webster. J Exp Mar Biol Ecol 88(1):1–19
8. Lindsay SM (2010) Frequency of injury and the ecology of regeneration in marine benthic invertebrates. Integr Comp Biol 50(4):479–493. https://doi.org/10.1093/icb/icq099

9. Nusetti O, Zapata-Vívenes E, Esclapés MM, Rojas A (2005) Antioxidant enzymes and tissue regeneration in *Eurythoe complanata* (Polychaeta: Amphinomidae) exposed to used vehicle crankcase oil. Arch Environ Contam Toxicol 48(4):509–514. https://doi.org/10.1007/s00244-004-0041-0
10. Carregosa V, Velez C, Pires A, Soares AMVM, Figueira E, Freitas R (2014) Physiological and biochemical responses of the Polychaete *Diopatra neapolitana* to organic matter enrichment. Aquat Toxicol 155:32–42. https://doi.org/10.1016/j.aquatox.2014.05.029
11. Coppola F, Pires A, Velez C, Soares AMVM, Pereira E, Figueira E et al (2016) Biochemical and physiological alterations induced in *Diopatra neapolitana* after a long-term exposure to arsenic. Comp Biochem Physiol Pt C Toxicol Pharmacol 189:1–9. https://doi.org/10.1016/j.cbpc.2016.06.006
12. Pires A, Almeida Â, Correia J, Calisto V, Schneider RJ, Esteves VI et al (2016) Long-term exposure to caffeine and carbamazepine: impacts on the regenerative capacity of the polychaete *Diopatra neapolitana*. Chemosphere 146:565–573. https://doi.org/10.1016/j.chemosphere.2015.12.035
13. Pires A, Velez C, Figueira E, Soares AMVM, Freitas R (2017) Effects of sediment contamination on physiological and biochemical responses of the polychaete *Diopatra neapolitana*, an exploited natural resource. Mar Pollut Bull 119(1):119–131. https://doi.org/10.1016/j.marpolbul.2017.03.014
14. Silva MSS, Oliveira M, Lopéz D, Martins M, Figueira E, Pires A (2020) Do nanoplastics impact the ability of the polychaeta *Hediste diversicolor* to regenerate? Ecol Indic 110 (September 2019):105921. https://doi.org/10.1016/j.ecolind.2019.105921
15. Leung J, Chan KYK (2018) Microplastics reduced posterior segment regeneration rate of the polychaete *Perinereis aibuhitensis*. Mar Pollut Bull 129(2):782–786. https://doi.org/10.1016/j.marpolbul.2017.10.072
16. De Marchi L, Neto V, Pretti C, Figueira E, Chiellini F, Soares AMVM et al (2017) Physiological and biochemical responses of two keystone polychaete species: *Diopatra neapolitana* and *Hediste diversicolor* to multi-walled carbon nanotubes. Environ Res 154(December 2016):126–138. https://doi.org/10.1016/j.envres.2016.12.018
17. Pires A, Figueira E, Moreira A, Soares AMVM, Freitas R (2015) The effects of water acidification, temperature and salinity on the regenerative capacity of the polychaete *Diopatra neapolitana*. Mar Environ Res 106(1):30–41. https://doi.org/10.1016/j.marenvres.2015.03.002
18. Freitas R, Coelho D, Pires A, Soares AMVM, Figueira E, Nunes B (2015) Preliminary evaluation of *Diopatra neapolitana* regenerative capacity as a biomarker for paracetamol exposure. Environ Sci Pollut Res 22(17): 13382–13392. https://doi.org/10.1007/s11356-015-4589-1
19. Moreira SM, Lima I, Ribeiro R, Guilhermino L (2006) Effects of estuarine sediment contamination on feeding and on key physiological functions of the polychaete *Hediste diversicolor*: laboratory and in situ assays. Aquat Toxicol 78(2):186–201. https://doi.org/10.1016/j.aquatox.2006.03.001
20. Solé M, Kopecka-Pilarczyk J, Blasco J (2009) Pollution biomarkers in two estuarine invertebrates, *Nereis diversicolor* and *Scrobicularia plana*, from a marsh ecosystem in SW Spain. Environ Int 35(3):523–531. https://doi.org/10.1016/j.envint.2008.09.013
21. Gomes T, Gonzalez-Rey M, Rodríguez-Romero A, Trombini C, Riba I, Blasco J et al (2013) Biomarkers in *Nereis diversicolor* (Polychaeta: Nereididae) as management tools for environmental assessment on the southwest Iberian coast. Sci Mar 77(S1):69–78. https://doi.org/10.3989/scimar.03731.27F
22. Silva MSS, Pires A, Almeida M, Oliveira M (2020) The use of *Hediste diversicolor* in the study of emerging contaminants. Mar Environ Res 159:105013. https://doi.org/10.1016/j.marenvres.2020.105013
23. Silva MSS, Oliveira M, Valente P, Figueira E, Martins M, Pires A (2020) Behavior and biochemical responses of the polychaeta *Hediste diversicolor* to polystyrene nanoplastics. Sci Total Environ 707:134434. https://doi.org/10.1016/j.scitotenv.2019.134434
24. Berke SK, Cruz V, Osman RW (2009) Sublethal predation and regeneration in two onuphid polychaetes: patterns and implications. Biol Bull 217(3):242–252
25. Wehe T, Fiege D (2002) Annotated checklist of the polychaete species of the seas surrounding the Arabian peninsula: Red Sea, Gulf of Aden, Arabian Sea, Gulf of Oman. Arab Gulf Fauna Arab 19:7–238
26. Arvanitides C (2000) Polychaete fauna of the Aegean Sea: inventory and new information. Bull Mar Sci 66:73–96
27. Dağli E, Ergen Z, Çinar ME (2005 Sep) One-year observation on the population structure of *Diopatra neapolitana* Delle Chiaje (Polychaeta: Onuphidae) in Izmir Bay (Aegean Sea, eastern Mediterranean). Mar Ecol

26(3–4):265–272. https://doi.org/10.1111/j.1439-0485.2005.00055.x
28. Gambi M, Giangrande A (1986) Distribution of soft-bottom polychaetes in two coastal areas of the Tyrrhenian Sea (Italy): structural analysis. Estuar Coast Shelf Sci 23:847–862. https://doi.org/10.1016/0272-7714(86)90076-4
29. Fauvel P (1923) Polychétes errantes. In: Fauna de France V, vol 5. Le Chevalier, Paris, 488 p
30. Lourido A, Cacabelos E, Troncoso JS (2008) Patterns of distribution of the polychaete fauna in subtidal soft sediments of the Ría de Aldán (North-Western Spain). J Mar Biol Assoc 88(2):263–275. https://doi.org/10.1017/S0025315408000696
31. Cunha T, Hall A, Queiroga H (2005) Estimation of the *Diopatra neapolitana* annual harvest resulting from digging activity in canal de Mira, Ria de Aveiro. Fish Res 76(1):56–66. https://doi.org/10.1016/j.fishres.2005.05.008
32. Bailey-Brock JH (1984) Ecology of the tube-building polychaete *Diopatra leuckarti* Kinberg, 1865 (Onuphidae) in Hawaii: community structure, and sediment stabilizing properties. Zool J Linn Soc 80(2–3):191–199. https://doi.org/10.1111/j.1096-3642.1984.tb01972.x
33. Thomsen MS, McGlathery K (2005) Facilitation of macroalgae by the sedimentary tube forming polychaete *Diopatra cuprea*. Estuar Coast Shelf Sci 62(1–2):63–73. https://doi.org/10.1016/j.ecss.2004.08.007
34. Gambi MC, Castelli A, Giangrande A, Lanera P, Prevedelli D, Vandini RZ (1994) Polychaetes of commercial and applied interest in Italy: an overview. Mèmoires du Musèum Natl dHistoire Nat 162(July):593–603
35. Conti MF (1998) Experienze de allavamento del polichete Diopatra neapolitana Delle Chiaje, 1841 nella Laguna di S. Gilla (Sardegna Meridionale). Biol Mar Mediterr 5:1473–1480
36. Soneja A, Drews M, Malinski T (2005) Role of nitric oxide, nitroxidative and oxidative stress in wound healing. Pharmacol Rep 57:108–119. https://doi.org/10.1016/j.freeradbiomed.2013.04.024
37. Pires A, Gentil F, Quintino V, Rodrigues AM (2012) Reproductive biology of *Diopatra neapolitana* (Annelida, Onuphidae), an exploited natural resource in ria de Aveiro (northwestern Portugal). Mar Ecol 33(1):56–65. https://doi.org/10.1111/j.1439-0485.2011.00463.x
38. Pires A, Freitas R, Quintino V, Rodrigues AM (2012) Can *Diopatra neapolitana* (Annelida: Onuphidae) regenerate body damage caused by bait digging or predation? Estuar Coast Shelf Sci 110:36–42. https://doi.org/10.1016/j.ecss.2011.12.039
39. Arias A, Paxton H (2015) The cryptogenic bait worm *Diopatra biscayensis* Fauchald et al., 2012 (Annelida: Onuphidae)—Revisiting its history, biology and ecology. Estuar Coast Shelf Sci 163(PB):22–36. https://doi.org/10.1016/j.ecss.2015.05.033
40. Pires A, Paxton H, Quintino V, Rodrigues AM (2010) Diopatra (Annelida: Onuphidae) diversity in European waters with the description of *Diopatra micrura*, new species. Zootaxa 2395:17–33

Open Access This chapter is licensed under the terms of the Creative Commons Attribution 4.0 International License (http://creativecommons.org/licenses/by/4.0/), which permits use, sharing, adaptation, distribution and reproduction in any medium or format, as long as you give appropriate credit to the original author(s) and the source, provide a link to the Creative Commons license and indicate if changes were made.

The images or other third party material in this chapter are included in the chapter's Creative Commons license, unless indicated otherwise in a credit line to the material. If material is not included in the chapter's Creative Commons license and your intended use is not permitted by statutory regulation or exceeds the permitted use, you will need to obtain permission directly from the copyright holder.





Chapter 11

Studying Annelida Regeneration Using *Platynereis dumerilii*

Michel Vervoort and Eve Gazave

Abstract

Regeneration, the ability to restore body parts after an injury or an amputation, is a widespread property in the animal kingdom. This chapter describes methods used to study this fascinating process in the annelid *Platynereis dumerilii*. During most of its life, this segmented worm is able to regenerate upon amputation the posterior part of its body, including its pygidium (terminal non-segmented body region bearing the anus) and a subterminal posterior growth zone which contains stem cells required for the formation of new segments. Detailed description of *Platynereis* worm culture and how to obtain large quantity of regenerating worms is provided. We also describe the staging system that we established and three important methods to study regeneration: whole mount in situ hybridization to study gene expression, 5-ethynyl-2′-deoxyuridine (EdU) labeling to characterize cell proliferation, and use of pharmacological treatments to establish putative roles of defined signaling pathways and processes.

Key words Regeneration, Annelid, *Platynereis dumerilii*, Whole mount in situ hybridization, Gene expression, EdU, Cell proliferation, Pharmacological inhibitors

1 Introduction

Regeneration, the ability to restore a lost or damaged body part is a fascinating process that has intrigued scientists since the pioneering study of *Hydra* regeneration by A. Trembley during the 1700s [1]. While having been intensively studied during the first part of the twentieth century, reparative regeneration has been less investigated since the rise of genetic and molecular studies of development in the 70s. This is intrinsically linked to the limited regenerative potential of the main developmental biology models, with the noticeable exception of zebrafish [2], which have emerged at that time. These last years, there has been a strong revival of the interest for regeneration, in part driven by possible applications for regenerative medicine [3].

Annelida (annelids) constitute a major lineage of the Lophotrochozoa super phylum, a group of primary importance to understand animal and especially bilaterian evolution [4]. Annelids represent a quite large phylum, with over 22,000 species including

Simon Blanchoud and Brigitte Galliot (eds.), *Whole-Body Regeneration: Methods and Protocols*,
Methods in Molecular Biology, vol. 2450, https://doi.org/10.1007/978-1-0716-2172-1_11, © The Author(s) 2022

ragworms, earthworms and leeches. They can live in various ecosystems, mostly in the sea, but also in fresh water and humid terrestrial environments. They present a diversity of forms and life history traits; some live in a tube, while others are burrowed deep in the sand, stuck on algae or even parasitic [4, 5].

Interestingly, annelids, with the noticeable exception of leeches, are among the Metazoa that show the most important regenerative abilities [6, 7]. Indeed, many annelids are able to regenerate, after an amputation or injury, the posterior part of their body, their anterior part (including the head), or both, as well as appendages (named parapodia) and all kind of tentacles and cirri [6]. While the capacity to regenerate their posterior parts is almost shared by all annelids, anterior or head regeneration is less widespread [6].

There is a quite long history of experimental and descriptive morphological studies of regeneration in many annelid species [8, 9]. Many of these studies notably investigated possible sources of the cells involved in regeneration [8, 10], as well as the importance of the nervous system to allow a proper regeneration [11]. More recently, cellular and molecular aspects of annelid regeneration have been studied in a couple of model species, *Pristina leydyi, Capitella teleta*, and *Enchytraeus japonensis*, all belonging to the same group of annelids, the Sedentaria (for review see [6, 12]). While these studies provided interesting information, there is, however, still a crucial need for additional annelid models that allow to address fundamental and mechanistic questions about regeneration.

One major model species that has been successfully developed for decades is the Nereididae *Platynereis dumerilii*, which was originally described by Audouin and Milne Edwards in 1834 (Fig. 1) [13], and belongs to the Errantia lineage. *Platynereis dumerilii* is a medium-sized marine annelid that is easily maintained in laboratories world-wide. Like many other marine animals, such as corals, sea urchins and fishes, *Platynereis*'s life cycle is synchronized with the lunar cycle [14]. Each worm will reproduce only once in its life before dying, and the timing of this reproduction is tightly regulated by this circalunar life cycle. *Platynereis* has emerged as an intensely studied model organism for developmental, marine, neuro, and evolutionary biology, as well as to study regeneration [15, 16]. *Platynereis* worms have indeed extensive regenerative capabilities: after amputation of the posterior part of their body, which leads to the removal of the pygidium (terminal non-segmented body part of the worm), the stem cell–rich subterminal growth zone (responsible for the continuous growth of the worms [17]) and several segments, *Platynereis* worms are able to regenerate both pygidium and growth zone which will in turn produce new segments [18]. *Platynereis* is also able to regenerate various body outgrowths, such as tentacles and appendages



Fig. 1 *Platynereis dumerilii*. Pictures of juvenile and adult (male and female) worms. Males and females harbor specific morphological features linked to sexual metamorphosis, notably their color. While juveniles are mainly brownish, females are bright yellow, as they are full of oocytes. Males are white in their anterior part, as they are full of sperm, and red in their posterior part, due to extensive accessory blood capillaries. Morphological differences between juveniles and maturing worms are not limited to their color. Indeed, during sexual maturation, the whole intestine of the worm regresses and the trunk of the animal is progressively modified to become a bag full of gametes. In addition, mature worms harbor bigger and darker eyes compared to juveniles

(parapodia), but not its head. *Platynereis* worms can thus properly regenerate both complex differentiated structures which includes different types of tissues or organs (pygidium and parapodia, for example) and stem cells (posterior growth zone) [17, 18]. In this chapter, we will describe protocols routinely used to breed and maintain *Platynereis* in the laboratory and prepare biological materials required for regeneration studies. We will also introduce molecular biology and functional tools used to address key questions about regeneration.

2 Materials

Prepare all solutions using ultrapure autoclaved water (H_2O). Prepare and store all reagents at room temperature (unless indicated otherwise).

2.1 Platynereis Worms Culture and Biological Material Production

1. Filtered natural fresh seawater (NFSW): filter seawater with a 0.22 μm filter.
2. Dried adult fish food (e.g., TetraMin flakes, Tetra).
3. Dried fish fry food (e.g., Micron Growth Food, Sera).
4. Live Chlorophyta algae (e.g., *Tetraselmis marina*).
5. 7.5% $MgCl_2$: 75 g $MgCl_2$ hexahydrated powder in 1 L H_2O.
6. 1× Phosphatase buffer saline (1× PBS): 800 mL H_2O, 8 g NaCL, 200 mg KCl, 1.44 g Na_2HPO_4, 240 mg KH_2PO_4, HCl to pH 7.4, H_2O until volume is 1 L. Autoclave the solution.
7. 2 M NaOH: 80 g NaOH in 1 L H_2O (*see* **Note 1**).
8. 16% Paraformaldehyde (PFA) stock solution: 80 g PFA, 450 mL 1× PBS (*see* **Note 2**), stir and heat at 60 °C until dissolution of the powder. Add droplets of 2 M NaOH until solution turns quite clear. Cool at room temperature, adjust pH to 7 with HCl, add 1× PBS until volume is 500 mL, filter using a 0.20 μm filtration column, aliquot as 12 mL in 15 mL tubes and store at −20 °C. Thaw aliquots at 60 °C, leftover can be stored at 4 °C and used within 2 weeks.
9. 0.1% Tw 1× PBS (1× PBST): 1 mL Tween 20 in 1 L 1× PBS (*see* **Note 3**).
10. Fixation solution: 1 mL 16% PFA, 3 mL 1× PBST. Prepare fresh.
11. Dehydration solution: 2 mL MeOH, 2 mL 1× PBST. Prepare fresh.

2.2 Whole Mount In Situ Hybridization and EdU Labelling

1. 25% rehydration solution: 30 mL MeOH, 10 mL 1× PBST. Prepare fresh.
2. 50% rehydration solution: 20 mL MeOH, 20 mL 1× PBST. Prepare fresh.
3. 75% rehydration solution: 10 mL MeOH, 30 mL 1× PBST. Prepare fresh.
4. Digestion buffer: 50 μL 20 μg/μL Proteinase K (PK) in 25 mL 1× PBST. Prepare fresh.
5. 10× glycine: 4 g glycine in 200 mL of 1× PBS, adjust pH to 7.5 with HCl. Aliquot in 15 mL tubes, store at −20 °C.
6. 1× glycine: 5 mL 10× glycine, 45 mL 1× PBST. Prepare fresh.
7. 20× SSC: 175.3 g NaCl, 88.2 g $Na_3C_6H_5O_7$ in H_2O, adjust pH to 7.5 with HCl, add H_2O until volume is 1 L. Autoclave the solution.
8. Heparin: 50 mg Heparin, 1 mL H_2O. Prepare fresh.
9. Hybridization buffer (HB): 25 mL formamide, 12.5 mL 20× SSC, 125 μL Heparin, 250 mg Torula (yeast) RNA powder, 50 μL Tween 20. Adjust to 50 mL with H_2O. Store at −20 °C.

10. Working solution of RNA probes: 1000 to 1500 ng of probes in 1 mL of HB. Store at −20 °C.
11. 4× wash buffer: 10 mL 20× SSC, 25 mL formamide, 50 µL Tween 20, 15 mL H_2O. Prepare fresh.
12. 2× wash buffer: 5 mL 20× SSC, 50 µL Tween 20, 45 mL H_2O. Prepare fresh.
13. 0.2× wash buffer: 500 µL 20× SSC, 50 µL Tween 20, 49.5 mL H_2O. Prepare fresh.
14. Blocking solution: 50 µL sheep serum, 1 mL 1× PBST. Prepare fresh.
15. Anti-digoxigenin-alkaline phosphatase (AP) conjugate solution: 1 µL Anti-Digoxigenin-AP antibody, 3999 µL 1× PBST. Prepare fresh.
16. 1 M Tris: 121.14 g Tris–HCl, pH 9.5, 1 L H_2O. Autoclave the solution.
17. 3 M NaCl: 87.75 g NaCl, 500 mL H_2O. Autoclave the solution.
18. 1 M $MgCl_2$: 101.75 g $MgCl_2$, 500 mL H_2O. Autoclave the solution.
19. Staining buffer: 10 mL 1 M Tris–HCl pH 9.5, 10 mL 3 M NaCl, 5 mL 1 M $MgCl_2$, 100 µL Tween 20, 75 mL H_2O. Prepare fresh.
20. 1× Coloration solution: 1 µL nitro blue tetrazolium chloride (NBT), 3.5 µL 5-brom-4-chloro-3′-indolyphosphate p-toluidine salt (BCIP), 1 mL staining buffer. Prepare fresh.
21. Stop solution: 100 mL 1 M Tris-HCl pH 7.5, 100 mL 3 M NaCl, 1 mL Tween 20, 799 mL H_2O.
22. Mounting solution: 90 mL of glycerol, 10 mL 1× PBST.
23. 10 mM EdU stock solution: 5 mg EdU powder, 2 mL DMSO. Mix well. Aliquot in 1 mL and store at −20 °C.
24. 5 µM EdU incorporation solution: 1 µL EdU stock solution, 1999 µL NFSW. Prepare fresh (*see* **Note 4**).
25. EdU reaction solution: Follow specific manufacturer's instructions (e.g., Invitrogen Click-iT® EdU Imaging Kits). Prepare fresh every time.
26. Counterstaining solution: 1 µL of fluorescent nuclear-specific dye (e.g., Hoechst or DAPI); 999 µL of 1× PBST.
27. DABCO antiphotobleaching solution: 625 mg $N_2(C_2H_4)_3$ (1,4-Diazabicyclo[2.2.2]octane, DABCO), 225 mL glycerol, 25 mL H_2O. Stir for several hours until complete dissolution. Protect from light with aluminum foil. Store at 4 °C for months.

3 Methods

3.1 Platynereis Worms Culture

Platynereis dumerilii is a marine worm found worldwide in temperate seas [19]. Since decades researchers have no longer taken animals directly from the sea (except if information related to environmental cues are needed), as *Platynereis*'s full life cycle is completed easily and successfully in laboratory settings (*see* **Note 5**) [20]. To raise *Platynereis* worms, always rinse glassware with distilled water and never use detergents.

1. Prepare a thermostatic room at 18 °C, with light control and equipped with shelves.
2. Set up a daily illumination regime in the room to 8 h of full darkness and 16 h of full light.
3. Place worms in a Tupperware-like box of middle size (30 × 20 × 10 cm) filled with 800 mL of NFSW.
4. Switch on a low-light lamp 7 nights per month (on a 28-days monthly cycle) in the worm room during the whole night to artificially reproduce the moon illumination (*see* **Note 6**).
5. 3 days after the end of the moon illumination regime, collect sexually mature worms. Maturing males become red and white (full of sperm), while females become yellow (full of eggs) (Fig. 1). Both males and females display an increase of their eyes size as compared to juvenile worms.
6. Transfer the collected male and female worms in separate boxes supplied in air by a pump, using a large pipette (*see* **Note 7**).
7. Do not feed them as mature worms do not eat anymore (sexual maturation leads to a complete regression of the gut).
8. Collect sexually mature worms following **steps 5–7** every 2 days for 2 weeks (*see* **Note 8**).
9. Monitor maturation boxes daily to identify mature animals ready to reproduce. They can easily be recognized as they start to swim.
10. Collect one swimming sexually mature male and one swimming sexually mature female and put them in a 300 mL beaker filled with NFSW (*see* **Note 9**).
11. Wait 5 to 10 min for the elegant nuptial dance of the worms to complete, several thousands of gametes to be released and fertilization to occur (*see* **Note 10**).
12. When the fertilization is done, the female body looks empty and it is not swimming anymore, remove both the female and the male (*see* **Note 11**).
13. Put the beaker in a thermostatic room at 18 °C.

14. 15 min after fertilization, check the beaker for a substantial egg jelly that covers the whole developing egg batch. This is a clear indicator of a successful fertilization.
15. Discard unfertilized eggs, if any, from the content of the beakers using a pipette.
16. 24 h postfertilization (hpf), pour the content of the beaker through a 100 μm sieve. The net will retain small ciliated larvae that have developed from fertilized eggs.
17. Rinse larvae three times with 1 L NFSW to carefully remove all the jelly.
18. Transfer cleaned larvae back to a clean beaker by rinsing the sieve upside-down.
19. Check them every 24 h during the three following days and remove dead individuals if needed.
20. 5 days postfertilization (dpf), start feeding larvae with 1 mL of live algae. Algae will form a mat at the bottom of the beaker embedding the larvae.
21. Feed again larvae with 1 mL of live algae at 7 dpf and 9 dpf.
22. At 10 dpf, using a pencil, carefully shift the algae mat containing the larvae to a box filled with 1 L of NFSW, 25 mL of algae and supplied in air by a pump.
23. Until 30 dpf, fed twice a week with 5 mL of algae per box. Do not change the water during this period of time.
24. Until 60 dpf, fed twice a week with a mix of 5 mL of algae and 0.2 mg of fry food per box. Do not change the water during this period of time.
25. At 60 dpf, transfer up to 40 small worms per new box, filled with 800 mL of NFSW (*see* **Notes 12** and **13**). Change seawater every 2 weeks.
26. Feed the worms three times per week, alternating between adult fish food (twice per week) and mashed spinach (once per week) (*see* **Notes 14** and **15**).

3.2 Production and Fixation of Samples at Specific Stages of Regeneration

To minimize, as much as possible, variability, notably due to the age and the size of the animals, strict procedures for worm selection and amputation should be followed.

1. Select worms long of 30–40 segments and 3–4 month-old (*see* **Note 16**).
2. Transfer selected worms to a beaker filled with 100 mL of 7.5% $MgCl_2$.
3. Wait 20 min until worms are anesthetized (*see* **Note 17**).
4. Transfer anesthetized worms to a glass plate.
5. Using a pencil, spread a worm on a glass plate (*see* **Note 18**).

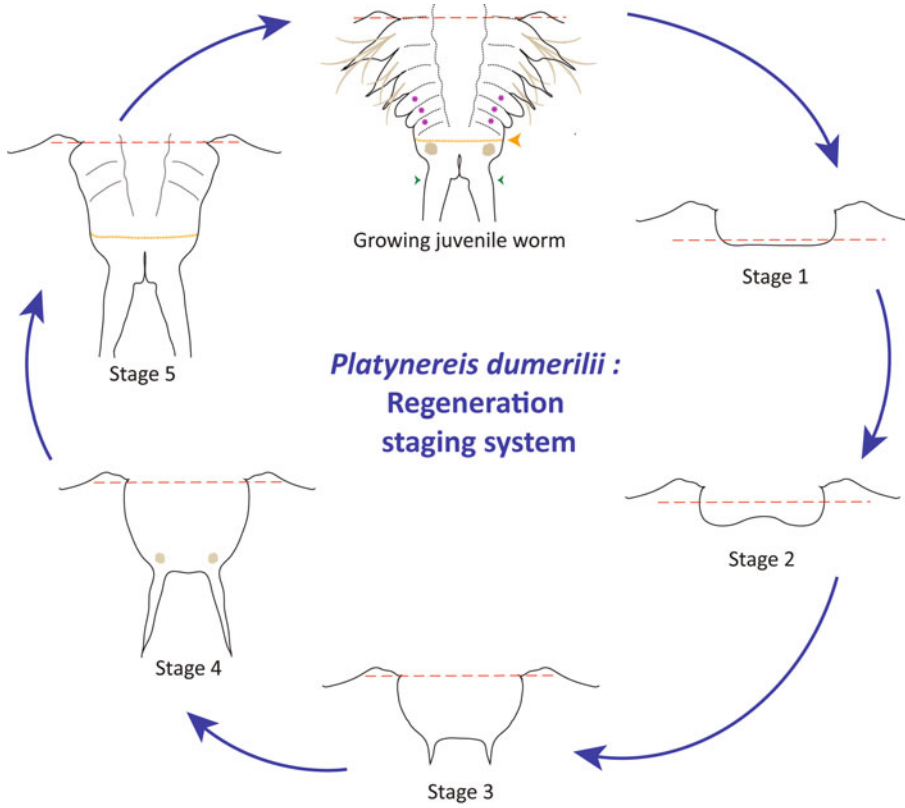


Fig. 2 Regeneration stages. On the top of the figure is drawn a growing juvenile worms with its posterior growth zone (orange line and arrowhead) and, anterior to the growth zone, developing segments (purple asterisks) and, posterior to the growth zone, the pygidium characterized by the presence of two specific outgrowths, anal cirri (green arrowheads) and two large glands (gray circles). Amputation plane is represented by red dotted lines. The five stages of regeneration are depicted. At stage 1, wound healing is achieved. At stage 2, a small blastema composed of proliferating cells is formed and its size increases during subsequent stages. At stage 3, small anal cirri can be observed. They strongly extend at stage 4 and some signs of pygidium differentiation become obvious (e.g., presence of glands). At stage 5, pygidium differentiation has pursued and a few segments delimited by faint segmental boundaries are observed. Growth continues and an increasing number of differentiating segments (with obvious segmental boundaries and developing parapodia) can subsequently be observed

6. Under a dissecting scope, perform a sharp amputation to remove the 6 posterior-most segments of worms using a micro-knife (*see* **Note 19**, Fig. 2).
7. Transfer to a clean box filled with NFSW at 18 °C and fed them normally three times per week.
8. Monitor amputated worms daily under a dissecting scope to determine the current stage of regeneration (*see* **Note 20**, Fig. 2).
9. Stage 1 (1 dpa): wound healing is achieved but no posterior outgrowth is present.

10. Stage 2 (2 dpa): a small regenerated region (blastema) is visible with a notch, corresponding to the anus, in its central part.
11. Stage 3 (3 dpa): presence of a larger blastema and two small anal cirri.
12. Stage 4 (4 dpa): large blastema and long anal cirri are present.
13. Stage 5 (5 dpa): presence of an indentation separating the differentiating pygidium from the anterior part of the regenerated region, faint segmental boundaries can be seen (*see* **Note 21**).
14. To collect regenerating tissue, identify a worm in the desired stage of regeneration following **steps 9** to **13**.
15. Amputate the worm two segments more anterior than the primary amputation plane following **steps 2** to **7**.
16. Transfer the sample using a pencil in a 5 mL tube containing 4 mL of fixation solution.
17. Incubate for 1.5 h while agitating on a rotating wheel.
18. Rinse twice with PBST.
19. Dehydrate for 20 min in dehydration solution at room temperature (RT) while agitating on a rotating wheel.
20. Replace the solution by 4 mL of 100% MeOH for 1 h while agitating on a rotating wheel.
21. Transfer sample to a 2 mL tube with 1 mL of 4 °C MeOH.
22. Store at −20 °C.

3.3 Whole Mount In Situ Hybridization

Whole mount in situ hybridization (WMISH) is the specific annealing of a labeled RNA probe to complementary sequence of a target mRNA in a fixed specimen, followed by detection and visualization of the nucleic acid hybrids [21] (*see* **Note 22**) (Fig. 3).

1. Transfer fixed samples to large baskets placed in a box containing 40 mL of 100% MeOH, under a fume hood and with orbital agitation (*see* **Note 23**).
2. Move baskets to a box containing 40 mL of the 25% rehydration solution.
3. Incubate for 5 min at RT.
4. Move baskets to a box containing 40 mL of the 50% rehydration solution.
5. Incubate for 5 min at RT.
6. Move baskets to a box containing 40 mL of the 75% rehydration solution.
7. Incubate for 5 min at RT.
8. Move baskets to a box containing 40 mL of 1× PBST.

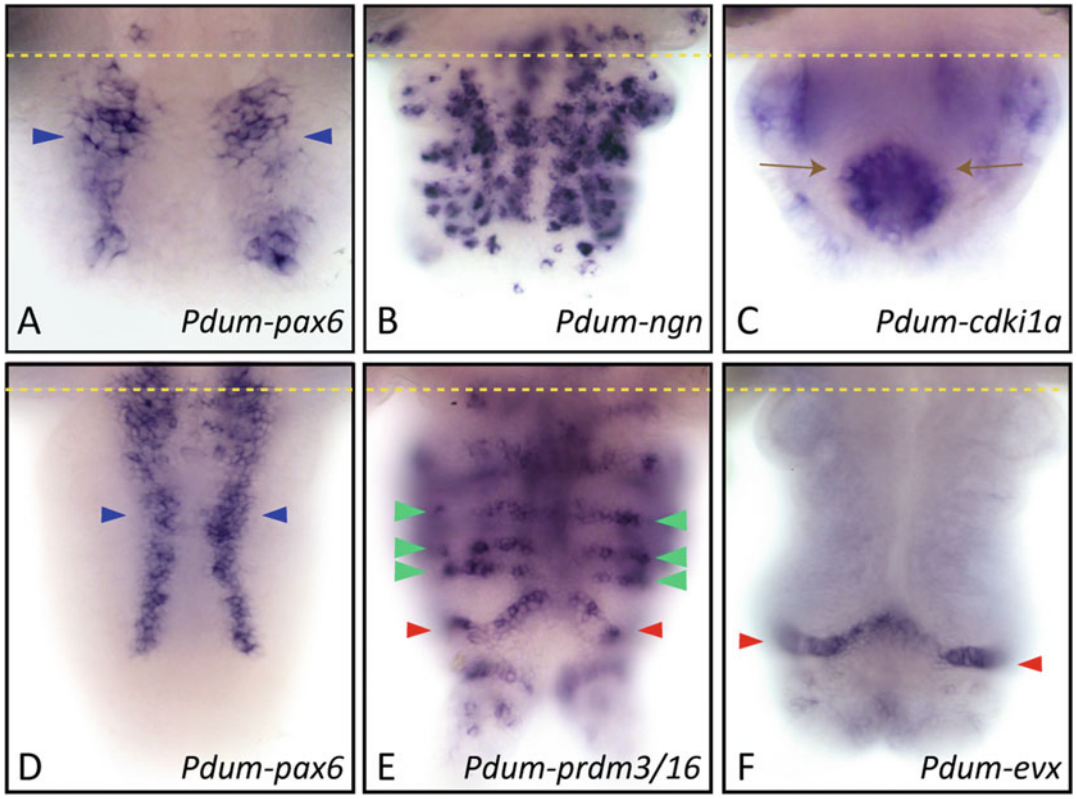


Fig. 3 Whole mount in situ hybridization. Whole mount in situ hybridization for the genes whose name is indicated are shown for two posterior regeneration stages, stage 3 (**a**–**c**) and stage 5 (**d**–**f**). All panels are ventral views (anterior is up). Amputation plane is represented by yellow dotted lines. In **a** and **d**, blue arrowheads point to expression of *Pdum-pax6* in two longitudinal rows of neuroectodermal cells which will give rise to ventral neurons of the ventral nerve cord. In **b** is shown the expression of *Pdum-neurogenin* in a large number of neuronal precursor cells of the both the central and peripheral nervous system. In **c**, brown arrows point to the expression of *Pdum-cdki1a* in internal cells located in the anal region. In **e**, green arrowheads point to segmental ectodermal stripes of cells expressing *Pdum-prdm3/16* which is also expressed in cells of the posterior growth zone (red arrowheads). These cells also express *Pdum-evx* (red arrowheads in **f**)

9. Incubate for 5 min at RT.
10. Repeat **steps 8** and **9**.
11. Move baskets to a box containing 25 mL of digestion buffer.
12. Incubate for 10 min at RT without agitation.
13. Move baskets to a box containing 50 mL of 1× glycine.
14. Incubate for 1 min.
15. Move baskets to a box containing 50 mL of fixation solution.
16. Incubate for 20 min.
17. Repeat **steps 8** and **9**, five times.

18. Transfer samples from a large basket to a pillbox with 2 mL 1× PBST.
19. Using a pipette, place up to 10 samples per small basket (one basket per probe) under a dissecting scope (*see* **Notes 24** and **25**).
20. Transfer small baskets to 2 mL tubes containing 1 mL of HB using forceps.
21. Incubate at 65 °C for 1 h.
22. Denature working solution of RNA probes at 80 °C during 10 min in a wet bath.
23. Transfer small baskets to 2 mL flat bottom tubes containing 300 µL of denaturated probe.
24. Place in an oven at 65 °C with orbital agitation (100 rpm) for 16 h (*see* **Notes 26** and **27**).
25. Transfer small baskets to 2 mL tubes containing 1 mL of 4× wash solution.
26. Incubate for 30 min at 65 °C (*see* **Note 28**).
27. Similarly perform in 2 mL tubes a second wash of 30 min at 65 °C in new 4× wash buffer.
28. Similarly perform in 2 mL tubes another two 15 min washes in 2× wash buffer at 65 °C, followed by two more 30 min washes in 0.2× wash buffer.
29. Transfer small baskets to 2 mL tubes containing 800 µL of blocking solution.
30. Incubate for 1 h at RT with orbital agitation.
31. Transfer small baskets to 2 mL tubes containing 800 µL of AP conjugate solution.
32. Incubate for 1 h at RT with orbital agitation (*see* **Note 29**).
33. Transfer the samples to 12 wells plates with 1 mL of staining buffer.
34. Add 1 mL of 1× coloration solution to each well (*see* **Note 30**).
35. Allow blue staining to appear at RT (*see* **Note 31**), which can take from few hours to few days depending on probes (*see* **Note 32**).
36. Check coloration every 30 min under a dissecting scope.
37. Transfer samples to a 2 mL tube containing 2 mL of stop solution to arrest the reaction.
38. Replace stop solution with 2 mL of 1× PBST.
39. Incubate 5 min while agitating on a rotating wheel.
40. Repeat 4 times **steps 36** and **37**.

41. Transfer samples to a 2 mL tube containing 2 mL of mounting solution.
42. Agitate on a rotating wheel at 4 °C overnight.
43. Select samples to be mounted under a dissecting scope.
44. Place 2 or 3 samples on a slide with 20 µL of mounting solution.
45. Place a small piece of clay under each corner of a coverslip and cover samples with it.
46. Press the corners of coverslip to flatten them (*see* **Note 33**).
47. Image the samples under a bright field microscope (Fig. 3).

3.4 EdU Labelling for Investigating Cell Proliferation During Platynereis *Regeneration*

5-ethynyl-2′-deoxyuridine (EdU) is a nucleoside analog that is widely used to detect cells that are in the S-phase of their cell cycle in various species (*see* **Note 34**). In *Platynereis*, EdU labeling has been used to study cell proliferation in whole mount animals during development, postembryonic growth, and regeneration (e.g., [17, 18, 22]) (Fig. 4).

1. Select live worms at desired regeneration stages.
2. Place one worm per well in 12-well plastic plates filled with 2 mL of EdU incorporation solution.
3. Incubate for 1 h at RT (*see* **Note 35**).
4. Discard EdU incorporation solution.
5. Rinse each well with 10 mL of NFSW.
6. Repeat 2 times **step 5** (*see* **Note 36**).
7. Follow the aforementioned fixation procedure (Subheading 3.2, **steps 16** to **22**) (*see* **Note 37**).
8. Follow the aforementioned rehydration and digestion procedures (Subheading 3.3, **steps 1** to **17**).

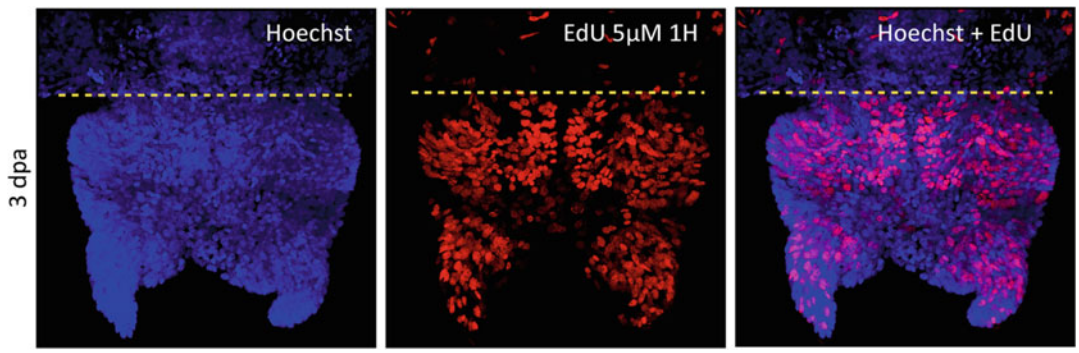


Fig. 4 EdU Labeling. Confocal image of the posterior part of a stage 3 worm (3 dpa) incubated in 5 µM EdU for 1 h before fixation. Hoechst counterstaining has been performed and allows to visualize all nuclei (in blue). EdU labeling is shown in red. Amputation plane is represented by yellow dotted lines. Anterior is up

9. Place up to 10 samples in the bottom of a 1.5 mL tube filled with 1 mL 1× PBST.
10. Remove the 1× PBST using a pipette.
11. Add 300 µL of EdU reaction solution in the tube.
12. Incubate 1 h in the dark at RT.
13. Remove EdU reaction solution.
14. Add 1 mL of 1× PBST in the tube.
15. Incubate for 5 min at RT in the dark under orbital agitation.
16. Remove 1× PBST.
17. Repeat 2 times **steps 13** to **15**.
18. Add 800 µL of counterstaining solution to the tube.
19. Incubate overnight at 4 °C in the dark under orbital agitation.
20. Remove counterstaining solution.
21. Perform 5 times **steps 14** to **16**.
22. Add 2 mL of DABCO anti-photobleaching solution.
23. Incubate overnight at 4 °C in the dark while agitating on a rotating wheel.
24. Follow the aforementioned mounting procedure (Subheading 3.3, **steps 42** to **45**).
25. Observe your samples under epifluorescent or confocal microscope (Fig. 4).

3.5 Pharmacological Treatments for Functional Studies During Platynereis *Regeneration*

Performing functional studies during postembryonic developments used to be challenging for many organisms in which genetic tools are not easily or fully mastered. One way to alter or modify various molecular signaling pathways or cellular mechanisms is to soak regenerating animals in specific pharmacological inhibitors or activators (*see* **Notes 38** and **39**). An initial and crucial step consists in defining the efficient concentration that induces defects in the regeneration process (e.g., morphological abnormalities) and/or in its timing, without (or with minimal) toxic effects (i.e., with a minimal number of dead or autotomized animals (*see* **Note 40**)).

1. Define three to four different inhibitor/activator concentrations to be tested (*see* **Note 41**).
2. Prepare fresh inhibitor/activator solutions and control solution (*see* **Note 42**).
3. Define your negative control condition (*see* **Note 43**).
4. Follow the aforementioned procedure for worm amputations (Subheading 3.2, **steps 1** to **6**).
5. Place amputated worms in 12-wells plates, one worm per well filled with 2 mL of solution.

6. Use at least 12 worms per concentrations and 12 worms as controls.
7. Incubate the worms for 24 h.
8. Remove the solution from each well.
9. Add 2 mL of 7.5% $MgCl_2$ per well.
10. Observe individually each worm under a dissecting scope.
11. Record their regeneration score according to the regeneration stage that has been reached (stages 1–5) following the procedure describe previously (Subheading 3.2, **steps 9** to **13**) (*see* **Notes 44** and **45**).
12. Remove the 7.5% $MgCl_2$ solution in each well.
13. Add 2 mL of fresh inhibitor / activator / control solution.
14. Repeat **steps 7** to **12** for 3 more days (*see* **Note 46**).
15. On day 5, repeat **steps 7** to **10** and discard worms.
16. Based on the results obtained, choose concentration with the greatest regeneration defects and the lowest toxicity.
17. Following the aforementioned procedure of pharmacological treatment and scoring (**steps 2** to **14**), repeat at least twice the regeneration experiment with the selected concentration using at least 24 worms per experiment (*see* **Note 47**).
18. Perform statistical analysis of the obtained data (*see* **Note 48**).

4 Notes

1. Pay attention to the exothermic reaction induced by mixing sodium hydroxide and water. Use borosilicate glasses free of any scratches, chips or breaks.
2. PFA is highly toxic. PFA solution must be prepared under a fume hood. It is very important to wear lab coat, spectacles and gloves during the whole procedure.
3. Tween 20 is a highly viscous product. Cut the end of the tip before pipetting and mix well.
4. Let EdU stock solution thaw at room temperature and be aware that this can last about 2 h.
5. If you want to establish your own culture, worm larvae are easily shared by the *Platynereis* community.
6. Be extremely careful to respect illumination and moonlight regimes, as any change in these regimes have long term negative effects on the worm culture; prepare a worm room schedule and follow it meticulously.

7. Some worms in the course of maturation may harbor an orange color and it may be difficult to morphologically categorized them as females or males yet. In such a case, place the "undetermined" worms either in a separated box (with an air supply) or in the "males" box. Do not place them in the "females" box as if one of them turns to be a male, it will release gametes and induce reproduction of most or all of the females of this box.
8. Illumination regime triggers sexual maturation for 2 weeks per month. The other 2 weeks of the month, there is no sexually mature worms available. Set up two culture rooms with alternate illumination regime in order to have mature animals all month long.
9. Every month, perform fertilization to replenish the worm culture after the sexual maturation period, which leads to the death of many animals.
10. When unfertilized eggs are released by a female, they have to be fertilized almost immediately to induce proper embryogenesis. If males are late to release sperm, you can press their body to manually induce release of sperm. Do that directly in the beaker, trap the male against the beaker wall with your finger and press anywhere on the male body until sperm is ejected. This procedure is not possible for females.
11. Males are able to release sperm a couple of times, and thus to fertilize several batch of eggs before dying.
12. Avoid putting more than 40 worms in a box, otherwise they will not grow enough before maturation and few gametes will be produced per animal.
13. While fertilization should be done in NFSW, adults/juveniles worms (>2-month-old) can be raised in a mix of 50% NFSW and 50% artificial seawater.
14. Use organic spinach as *Platynereis* worms are very sensitive to pesticides.
15. Alternative feeding using powdered spirulina (1.0 g/L) is possible [23].
16. Exclude worms that are already in the process of regeneration due to accidental injury as they may regenerate differently if amputated a second time.
17. Properly anesthetized worms are not moving anymore (while contractions of the gut are still present), even when put under the light of the dissecting scope. If this is not the case, increase anesthesia incubation time by a couple of minutes.
18. There is no need to hold them, they will stay in place if well anesthetized.

19. Pay attention to perform amputation between two segments and perpendicularly to the body axis. Avoid amputating parapodia from one side and not the other, as this will affect posterior regeneration timing.
20. More than 90% of amputated worms follow this timeline, but some worms from a specific box/batch are occasionally delayed for yet undetermined reason.
21. The regeneration process is finished at this stage; the next steps are considered as posterior elongation [17], that is, production of new segments from the regenerated posterior growth zone.
22. As an extension of the WMISH procedure, a technique named whole-body gene expression pattern registration allows the rigorous comparison of expression patterns, at a specific developmental stage, of an animal which harbors invariant development. It requires a standardized reference template at the desired developmental stage and allows the production of a standardized digital anatomical atlases of gene expression patterns, at near-cellular resolution [24].
23. Home-made large baskets are made of a plastic cylinder (diameter: 4 cm) with a heat-sealed 100 μM mesh at its bottom. This allows to incubate samples in solution while still contained in the basket and to move them easily from one solution to another, by moving the basket itself using forceps. Place all samples of the same stage in a same basket. Annotate each basket to avoid confusion. Consider to use five samples per stage per gene.
24. Home-made small baskets are composed of the largest part of a P1000 tip (8 mm long) with a heat-sealed 100 μM mesh at its bottom.
25. You can mix up to 2 stages within a same small basket (5 samples per stage, same probe). You can perform easily a WMISH experiment with up to 30 small baskets.
26. Hybridization temperatures as well as probe concentrations can be modulated to optimize coloration intensity and signal to background ratio.
27. After use, small baskets and flat bottom tubes are treated with 0.5 M NaOH overnight with agitation then carefully washed and rinsed with H_2O, so they can be reused. Regular tubes are washed with H_2O only and also reused.
28. Pay attention to perform the first four washes at 65 °C.
29. Alternatively, **steps 29** and **31** can be done at 4 °C overnight.
30. Pay attention that staining solution should be pH 9.5, otherwise the enzymatic reaction will not work.

31. Staining can be slowed down by putting plates at 18 °C and even 4 °C.
32. It is possible to stop coloration for the night or the week-end and to resume it later. To do that, remove all the 1× coloration solution, rinse with agitation with 1 mL of stop solution, then replace by another 1 mL of stop solution and leave in the dark at 4 °C. To resume coloration, make a wash with staining buffer before adding 1× coloration solution and resuming on **step 35**.
33. Depending of the thickness of the sample (notably the non-amputated anterior part), you will have to press more or less on the coverslip. Carefully check flattening of the sample in order not to smash it.
34. Unlike other labeling methods of S-phase cells using modified nucleosides, such as Bromodeoxyuridine (BrdU), EdU labeling has the advantage not to be antibody-based and therefore does not require DNA denaturation (usually achieved by treatment with a strong acid, often HCl) for its detection, which is harmful for tissue integrity and may therefore hamper further microscopic observations.
35. Longer incubation times can be envisioned to obtained more labeled (EdU+) cells. For regenerating worms, we used incubation times up to 5 h.
36. Fixation can be done immediately after incorporation or worms can be kept for defined period of time in NFSW (without EdU) before fixation. In the latter case, a so-called pulse and chase experiment is performed.
37. Samples can be stored at −20 °C or directly used for the subsequent steps.
38. Cell permeable small molecule inhibitors of various signaling pathways were also successfully used during *Platynereis* embryonic development [22, 25, 26]. One advantage to use pharmacological inhibitors relies on the fact they allow to specifically target the period of inhibition while avoiding interferences with earlier functions. Always try to use inhibitors at the lowest concentration producing significant and reproducible effects, to minimize off-target effects and toxicity.
39. To further characterize pharmacological treatment effects on regeneration, you can perform EdU labeling to assess cell proliferation and WMISH using specific markers (for example of particular tissue or cell types) on treated and control worms at different time points after amputation, as described in Subheadings 3.3 and 3.4.
40. Autotomy or self-amputation, is the discarding of a portion of the body containing several segments. This process usually

occurs when animals are facing stressful conditions (or are mechanically damaged). Autotomy can happen in normal culture conditions, at a low rate. When scoring worms during treatments, autotomy is easily visible as worms are separated in at least two fragments, the one bearing the head may start to regenerate again, while the other will not.

41. This is done based on previous experiments during regeneration or on larvae, or using information from the literature on other organisms.
42. Depending on the type of chemical used, stock solutions have to be made by dissolving it in a specific chemical product. Dimethylsulfoxide (DMSO) is widely used to dissolve various drugs. Working solutions are then made from this stock solution diluted in NFSW. Control solution is composed of NFSW supplemented by the chemical product used to initially dissolve the chemical to produce the stock solution.
43. Negative control worm condition consists in amputated worms soaked in control solution that contains the chemical used to dissolve the drug (typically DMSO) at a concentration corresponding to that of the solution with the highest concentration. In general, DMSO is not affecting regeneration nor development in most organisms, but this needs to be confirmed. Perform an initial experiment with a batch of animals soaked in NFSW and a batch of animals in NFSW with DMSO, follow them individually every day and compare regeneration scores obtained from the two series of animals.
44. Some worms may show a morphology that is intermediate between that of two successive stages of regeneration and therefore they can be scored as 1.5, 2.5, 3.5, and 4.5.
45. List any morphological abnormalities that may be visible on treated worms. Pay attention and count every day the number of worms that may have died or performed autotomy during the treatment, as these are indicators of toxicity and therefore important parameters to help choosing the most efficient concentration. To further test a possible toxicity of the inhibitors, you can also perform additional experiments: (1) treat non-amputated worms 5 days with the inhibitor (at the different tested conditions) and count the number of autotomized or dead worms, if any; (2) treat amputated worms with the inhibitors for 5 days, then place them in NFSW and check for potential regeneration recovery at 7, 10, and 15 dpa.
46. Drug solutions have to be replaced every 24 h to maintain their activity for the whole experiment.
47. When possible, use at least two different drugs to confirm effects on regeneration and its timing.

48. For inhibitor treatments, perform two-way ANOVA multiple comparisons between control *versus* treated worms per scoring day. Comparisons between different inhibitor concentrations are also interesting to perform.

Acknowledgments

Work in our team is supported by funding from Labex "Who Am I" laboratory of excellence (No. ANR-11-LABX-0071) funded by the French Government through its "Investments for the Future" program operated by the Agence Nationale de la Recherche under grant No. ANR-11-IDEX-0005-01, Centre National de la Recherche Scientifique, INSB (grant Diversity of Biological Mechanisms), Agence Nationale de la Recherche (grant TELO BLAST no. ANR-16-CE91-0007). The authors warmly thank all current and past members of the "Stem cells, Development and Evolution" team at the Institut Jacques Monod, Paris, France.

References

1. Galliot B (2012) Hydra, a fruitful model system for 270 years. Int J Dev Biol 56(6-8): 411–423. https://doi.org/10.1387/ijdb.120086bg
2. Marques IJ, Lupi E, Mercader N (2019) Model systems for regeneration: zebrafish. Development 146(18):dev167692. https://doi.org/10.1242/dev.167692
3. Gazave E, Rottinger E (2021) 7th Euro Evo devo meeting: report on the "evolution of regeneration in Metazoa" symposium. J Exp Zool B Mol Dev Evol 336(2):89–93. https://doi.org/10.1002/jez.b.22897
4. Ferrier DE (2012) Evolutionary crossroads in developmental biology: annelids. Development 139(15):2643–2653. https://doi.org/10.1242/dev.074724
5. Brusca RC, Brusca GJ (eds) (2003) Invertebrates, 2nd edn. Sinauer Associates, Sunderland
6. Ozpolat BD, Bely AE (2016) Developmental and molecular biology of annelid regeneration: a comparative review of recent studies. Curr Opin Genet Dev 40:144–153. https://doi.org/10.1016/j.gde.2016.07.010
7. Bely AE (2014) Early events in annelid regeneration: a cellular perspective. Integr Comp Biol 54(4):688–699. https://doi.org/10.1093/icb/icu109
8. Boilly B (1969) Sur l'origine des cellules régénératrices chez les annélides polychètes. Archives de Zoologie expérimentale et générale 110(1): 127–143
9. Hyman LH (1940) Aspects of regeneration in annelids. Am Nat 74:513–527
10. Boilly B (1969) Experimental study of the localization, by relation to the amputation plan, of the source of mesodermal regeneration cells in an annelid polychaete (Syllis amica Quatrefages). J Embryol Exp Morphol 21(1): 193–206
11. Boilly B, Boilly-Marer Y, Bely AE (2017) Regulation of dorso-ventral polarity by the nerve cord during annelid regeneration: a review of experimental evidence. Regeneration (Oxf) 4(2):54–68. https://doi.org/10.1002/reg2.78
12. Bely AE, Zattara EE, Sikes JM (2014) Regeneration in spiralians: evolutionary patterns and developmental processes. Int J Dev Biol 58(6–8):623–634. https://doi.org/10.1387/ijdb.140142ab
13. Audouin JV, Milne Edwards H (1833) Classification des annélides, et description de celles qui habitent les côtes de la France. Ann Sci Nat 29: 195–269
14. Zantke J, Ishikawa-Fujiwara T, Arboleda E, Lohs C, Schipany K, Hallay N, Straw AD, Todo T, Tessmar-Raible K (2013) Circadian and circalunar clock interactions in a marine annelid. Cell Rep 5(1):99–113. https://doi.org/10.1016/j.celrep.2013.08.031

15. Raible F, Tessmar-Raible K (2014) Platynereis dumerilii. Curr Biol 24(15):R676–R677. https://doi.org/10.1016/j.cub.2014.06.032
16. Williams EA, Jekely G (2016) Towards a systems-level understanding of development in the marine annelid Platynereis dumerilii. Curr Opin Genet Dev 39:175–181. https://doi.org/10.1016/j.gde.2016.07.005
17. Gazave E, Behague J, Laplane L, Guillou A, Preau L, Demilly A, Balavoine G, Vervoort M (2013) Posterior elongation in the annelid Platynereis dumerilii involves stem cells molecularly related to primordial germ cells. Dev Biol 382(1):246–267. https://doi.org/10.1016/j.ydbio.2013.07.013
18. Planques A, Malem J, Parapar J, Vervoort M, Gazave E (2019) Morphological, cellular and molecular characterization of posterior regeneration in the marine annelid *Platynereis dumerilii*. Dev Biol 445(2):189–210. https://doi.org/10.1016/j.ydbio.2018.11.004
19. Simakov O, Larsson TA, Arendt D (2013) Linking micro- and macro-evolution at the cell type level: a view from the lophotrochozoan Platynereis dumerilii. Brief Funct Genomics 12(5):430–439. https://doi.org/10.1093/bfgp/els049
20. Fischer A, Dorresteijn A (2004) The polychaete Platynereis dumerilii (Annelida): a laboratory animal with spiralian cleavage, lifelong segment proliferation and a mixed benthic/pelagic life cycle. Bioessays 26(3):314–325. https://doi.org/10.1002/bies.10409
21. Baumgart E, Schad A, Grabenbauer M (2001) In situ hybridization: general principles and application of Digoxigenin-labeled cRNA for the detection of mRNAs. In: Beesley JE (ed) Immunocytochemistry and in situ hybridization in the biomedical sciences. Birkhäuser, Boston, MA, pp 108–137. https://doi.org/10.1007/978-1-4612-0139-7_6
22. Demilly A, Steinmetz P, Gazave E, Marchand L, Vervoort M (2013) Involvement of the Wnt/beta-catenin pathway in neurectoderm architecture in Platynereis dumerilii. Nat Commun 4:1915. https://doi.org/10.1038/ncomms2915
23. Kuehn E, Stockinger AW, Girard J, Raible F, Ozpolat BD (2019) A scalable culturing system for the marine annelid Platynereis dumerilii. PLoS One 14(12):e0226156. https://doi.org/10.1371/journal.pone.0226156
24. Asadulina A, Panzera A, Veraszto C, Liebig C, Jekely G (2012) Whole-body gene expression pattern registration in Platynereis larvae. Evo-Devo 3(1):27. https://doi.org/10.1186/2041-9139-3-27
25. Gazave E, Lemaître Q, Balavoine G (2017) The notch pathway in the annelid Platynereis: insights into chaetogenesis and neurogenesis processes. Open Biol 7(2):160242
26. Zantke J, Bannister S, Rajan VB, Raible F, Tessmar-Raible K (2014) Genetic and genomic tools for the marine annelid Platynereis dumerilii. Genetics 197(1):19–31. https://doi.org/10.1534/genetics.112.148254

Open Access This chapter is licensed under the terms of the Creative Commons Attribution 4.0 International License (http://creativecommons.org/licenses/by/4.0/), which permits use, sharing, adaptation, distribution and reproduction in any medium or format, as long as you give appropriate credit to the original author(s) and the source, provide a link to the Creative Commons license and indicate if changes were made.

The images or other third party material in this chapter are included in the chapter's Creative Commons license, unless indicated otherwise in a credit line to the material. If material is not included in the chapter's Creative Commons license and your intended use is not permitted by statutory regulation or exceeds the permitted use, you will need to obtain permission directly from the copyright holder.



Chapter 12

Collecting and Culturing *Lineus sanguineus* to Study Nemertea WBR

Eduardo E. Zattara and Fernando A. Fernández-Alvarez

Abstract

Whole-body regeneration, the ability to reconstruct complete individuals from small fragments, is rare among ribbon worms (phylum Nemertea) but present in the pilidiophoran species *Lineus sanguineus*. This species can regenerate complete individuals from a tiny midbody section, and even from a quarter of a piece, provided it retains a fragment of a lateral nerve cord. While a few other unrelated species of ribbon worms are also excellent regenerators, *L. sanguineus* is unique in having evolved its regenerative abilities quite recently and thus offers an exceptional opportunity to gain insight into the evolutionary mechanisms of regeneration enhancement. Interestingly, both its sister species *Lineus lacteus* and *Lineus pseudolacteus,* a third species derived from the recent hybridization of the other two, differ in their regeneration abilities: while *L. lacteus* is uncapable of regenerating a lost head, *L. pseudolacteus* is capable of anterior regeneration, albeit at a slower rate than *L. sanguineus. L. sanguineus* has a worldwide distribution in temperate shores of both hemispheres, is readily found at intertidal habitats, and can survive, feed and be bred through asexual replication with minimal effort in laboratory settings. All the above make this species a superb candidate for studies of regenerative biology. In this chapter, we present protocols to collect, identify and breed *L. sanguineus* to study the extraordinary whole-body regeneration abilities found in this species.

Key words Heteronemertea, Intertidal, Invertebrate rearing, Pilidiophora, Spiralia

1 Introduction

Regeneration, the ability of organism to regrow lost body parts, is widespread across metazoan groups [1–3]. Regeneration varies broadly both in restorative potential and phylogenetic distribution: while many lineages are only capable of physiological tissue turnover or restoration of smaller amounts of lost tissues, others are capable of amazing regeneration feats, from restoring lost appendages to reconstructing whole new individuals from very small fragments. This later ability, known as whole-body regeneration, is well exemplified by planaria and other turbellarian flatworms, but is also commonplace in many cnidarians, ctenophores, sponges, xenacoelomorphs, and colonial tunicates. Some other groups, such as annelids and echinoderms, also show members with more

Simon Blanchoud and Brigitte Galliot (eds.), *Whole-Body Regeneration: Methods and Protocols*,
Methods in Molecular Biology, vol. 2450, https://doi.org/10.1007/978-1-0716-2172-1_12, © The Author(s) 2022

limited but still exceptional regenerative powers [3]. Such broad array of regenerative potential across animals suggests that regenerative abilities have a rich evolutionary history that is mostly unexplored.

Understanding how regeneration evolves can help elucidate the cellular and molecular underpinnings of this developmental ability. One particularly informative approach is through comparative studies of regenerative ability in species that span an evolutionary transition in regenerative potential. Candidate mechanisms can be gleaned from comparing developmental and molecular genetic differences across such species and correlating them with changes in extent of regeneration. Mechanisms can then be experimentally assessed to test whether they inhibit or enhance regeneration. Studies on species spanning an evolutionary loss or reduction of regenerative ability can inform how the potential to regenerate might have become blocked or dampened, and eventually lead to strategies to lift or alleviate such blocks and allow for better regeneration and healing in systems that do not regenerate well (including most mammals in general, and humans in particular). In contrast, studies on species spanning an evolutionary gain or enhancement of regenerative ability can give insight on how organisms might be able to reboot embryonic developmental capabilities in a postembryonic context and inspire novel tools to induce regeneration after traumatic injury. While many evolutionary transitions leading to diminished or lost regenerative ability have been identified, there are very few examples of increased or gained regeneration [4, 5]. Thus, while we have many systems where we can study how regeneration is lost, we lack good models of how it is gained.

Ribbon worms (phylum Nemertea) are a phylum of about 1300 known species of elongated, primarily marine predatory worms [6–8]. While most species of nemerteans are capable of restoring a lost posterior end after a transverse amputation behind the brain, only a few have so far been shown to be able of restoring their anterior end after a similar injury [9]. The few species capable of anterior regeneration are taxonomically scattered across the phylum; ancestral trait reconstruction strongly suggests that lack of anterior regeneration is the ancestral and most common condition for nemerteans. Thus, species capable of regrowing a lost anterior end represent lineages that experienced evolutionary gains in regenerative ability.

Among anteriorly regenerating species, *Lineus sanguineus* (Rathke, 1799) stands out, unquestionably one of the champions of regeneration possessing some of the highest regenerative abilities known among animals [2]. A single worm of this species can be repeatedly amputated to obtain a complete regenerated worm just 1/200,000th of the volume of the original individual. Furthermore, a complete worm can regenerate not only from a thin

transverse slice of the body, but even from just one *quadrant* of a thin slice [10]. Regeneration rate varies with the size and condition of the fragment, but a recognizable head and tail can be rebuilt in around a week or two.

Lineus sanguineus individuals tend to have a slender body, often a 100 times longer than their body width (Fig. 1a). They are slightly flattened dorsoventrally with a pair of long lateral grooves at the anterior end, followed by a reddish brain region. They have about 2 to 8 pairs of dorsolateral ocelli arranged in a bilateral pair of rows extending along the anterior half of the head, over the lateral cephalic slits. The mouth opens ventrally some distance behind the brain. Except for the frontal margin and lateral borders of the head, worms tend to be uniform in color. Color itself varies across the species' distribution, showing olive, green, brown or red hues. *L. sanguineus* inhabits sheltered stony regions, among algae, lurking within shellfish beds, or inside the fouling/encrusting community growing over natural and manmade substrates of the intertidal zones of the marine shore. It can be found on temperate seashores around the world [9, 11–15] (Fig. 1d). At the Southern Hemisphere, it has been found on the South Atlantic shores of Uruguay and Argentina, and the South Pacific shores of Chile and New Zealand. In the Northern Hemisphere, it has been reported from the North Atlantic shores of North America (from the Gulf of Mexico and Florida to Newfoundland, Canada), Europe (along the Bay of Biscay, English Channel and North Sea) and Eastern Asia (South and East China Seas, Yellow and Bohai Seas, Sea of Japan and eastern Japanese Atlantic shores). This widespread distribution makes it more readily available for collection by researchers near most temperate locations around the world.

Lineus sanguineus belongs to the class Pilidiophora, the nemertean group that contains the highest number of species with whole-body regenerative ability [9]. This cosmopolitan species [12] belongs to a mostly European species group that also includes *Riseriellus occultus* (described from NW Spanish and N Welsh shores), *Lineus longissimus* (found all along European Atlantic shores), two cryptic species known as *Lineus lacteus* (*L. lacteus A*, associated with the Bay of Biscay and English Channel shores, and *L. lacteus M*, found in the Mediterranean Sea), and the endemic *Lineus pseudolacteus* (found only at the French Atlantic shores near Roscoff, Bretagne) [12, 13]. Of the above species, only *L. sanguineus* and *L. pseudolacteus* are capable of anterior regeneration. The other species are limited to regenerate posterior ends [9].

Lineus sanguineus and *L. lacteus A* are sister species, estimated to have diverged about 10 My ago, while *L. pseudolacteus* likely emerged from a much more recent (12–25 Ky ago) single hybridization event between *L. sanguineus* and *L. lacteus*—likely after fertilization of an unreduced *L. sanguineus* oocyte by a *L. lacteus* sperm [13, 16]. Due to its triploid condition, *L. pseudolacteus* has

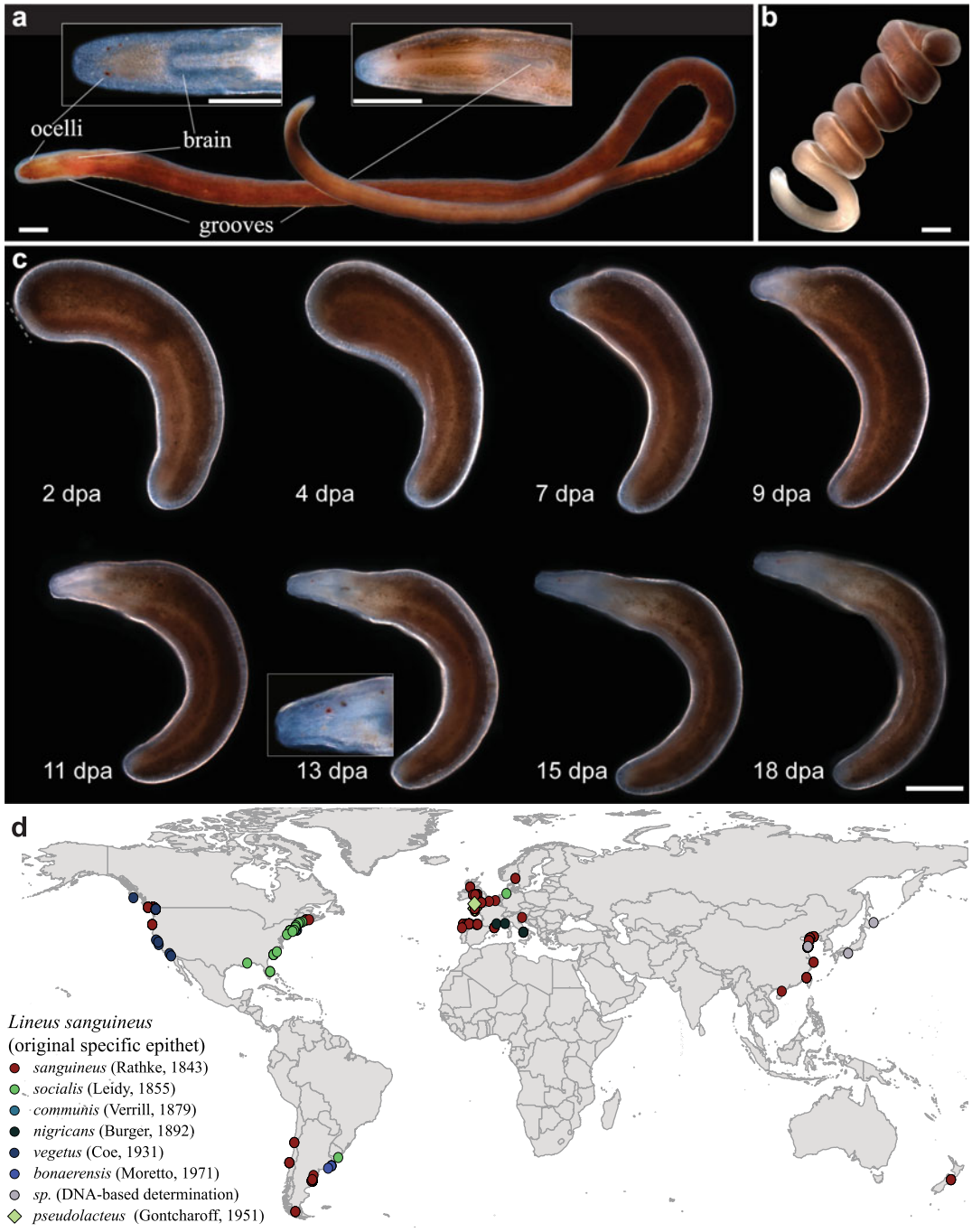


Fig. 1 Live and regenerating examples of *Lineus sanguineus*. (**a**) Live, extended individual of *L. sanguineus*; this specimen is relatively short—much longer specimens can be found. Anterior end at the left. The left inset shows a detail of the head in dorsal view. The right inset shows a detail of the head on lateral view (**b**) Live, coiled individual of *L. sanguineus*. Head toward upper right (**c**) Example of anterior regeneration from a posterior fragment, shown from 2 through 18 days postamputation (dpa); the red dashed line at 2 dpa shows the location of the healed anterior wound. Notice first ocelli appearing at 7 dpa, proboscis apparatus formed by 11 dpa and brain visible by 13 dpa (inset showing detail of head on lateral view); also note how the stump elongates and becomes slenderer to match the width of the regenerating anterior end. (**d**) Current known

been reproducing exclusively asexually since that event, a regeneration-dependent strategy inherited from their maternal species. Lack of anterior regeneration in *L. lacteus* places an upper bound on how long ago did the *L. sanguineus* lineage evolve anterior regeneration. Both parent species have been shown to possess private alleles, that is, unique haplotypic variants found only in one of the species. This should give a considerable fraction of their genome a specific signature which could facilitate detection of allelic bias in genes differentially expressed during regeneration of *L. pseudolacteus*, complementing gene expression studies comparing postamputation responses between *L. lacteus* and *L. sanguineus*. Furthermore, populations of *L. sanguineus* display different morphotypes with corresponding differences in regeneration potential, that are not obviously correlated with genetic differences [9, 12, 13]. For example, two ecologically isolated morphotypes with the same genotypic structure are present in Iberian shores: smaller individuals (<5 cm of total length) can be found among algae in lower, mid and sub-tidal regions, while the larger ones (5–20 cm) are found among sand below boulders in the high intertidal region. Interestingly, larger individuals regenerate more slowly than the smaller ones, suggesting that regenerative potential might be modulated by physiological trade-offs and local adaptations. All the above make *L. sanguineus, L. lacteus* and *L. pseudolacteus* a unique and powerful three-species system to inquire into the molecular and developmental mechanisms that evolved to enable the spectacular whole-body regeneration currently found in *L. sanguineus*.

In this chapter, we present simple and inexpensive methods to collect, keep and experiment on *Lineus sanguineus*. Most of these methods are applicable also to *L. lacteus* and *L. pseudolacteus* (except of course for asexual propagation, which cannot be used in *L. lacteus*). Many of these methods might also apply to a variable degree to other nemertean species too.

2 Materials

2.1 Field Collection of Specimens

1. Several medium sized, light colored (preferably white) buckets or deep trays.
2. Gallon-sized bottle or can (one to several).
3. Quarter-gallon, sturdy zipper bags or similar.

Fig. 1 (continued) distribution of *Lineus sanguineus*. Occurrence data obtained from the Global Biodiversity Information Facility and other sources [9, 11–14, 25] and curated by the authors. Occurrences are color-coded to show the different species under which the specimens had been originally described; all but *Lineus pseudolacteus* are now synonymized to *Lineus sanguineus*

4. Small sturdy knife (preferably of rust-resistant steel).
5. Soft round art paintbrush.
6. Pasteur plastic pipettes.
7. Clean plastic or glass vials.
8. Hammer and chisel and/or spatula.
9. Magnifying glass (optional, used to examine smaller specimens more closely).
10. Insulated cooler filled with ice.

2.2 Specimen Rearing

1. Filtered sea water (FSW): 0.45 μm filtered either natural or artificial seawater (*see* **Note 1**).
2. Glass dessert bowls, crystallizer dishes or fingerbowls.
3. Petri dishes (glass or plastic) with a diameter larger than that of the bowls.
4. Labeling tape.
5. Calf liver: ~250 g, ideally from organic-certified sources.
6. 200–400 μm mesh for tissue homogenization.
7. Disposable syringe (without the needle).
8. Polyethylene film or Parafilm.
9. #10 scalpel blades and scalpel handle.

3 Methods

3.1 Field Collection of Specimens

Lineus sanguineus inhabit rocky or pebbly areas of the intertidal zone, the region left exposed by receding waters during low tides (*see* **Note 2**, Fig. 2a). They often co-occur with other, sometimes similar looking species (*see* **Note 3**), like *Lineus ruber*, *L. viridis*, or *L. clandestinus*. In some places and locations, worms can be found and collected directly behind rocks and pebbles. This method is typically suitable for large specimens from the high intertidal zone (*see* **Note 4**). In most other occasions, however, they lurk within encrusting and fouling communities growing over large rocks and cannot be easily retrieved directly. In those cases, the most successful strategy is to cause hypoxia-induced migration (*see* Subheading 3.2).

1. Wait for waters to recede from the collecting area (Fig. 2a).
2. Pick up boulders and smaller pebbles (*see* **Note 5**; Fig. 2b).
3. Carefully examine the lower surface and any fissures of the boulder to see if there are worms.
4. Inspect the sand or mud that was below the boulder.



Fig. 2 Field collection of nemerteans. (**a**) A typical intertidal area where *L. sanguineus* can be found. (**b**) Direct collection of specimens under pebbles, rocks and shells. (**c**) Large specimen of *Lineus lacteus* inside a mollusk shell while eating its owner; the anterior end is deep within the shell. (**d**) Removal of a sample of the fouling community encrusted on the pylons of a pier. (**e**) Removed rubble is placed in trays and covered with sea water. (**f**) Rubble is spread out on the bottom of the tray, and allowed to become hypoxic, forcing nemerteans to come out of their shelter and allowing their collection

5. If you find one or more worms (Fig. 2c), gently collect the specimens using a paintbrush (*see* **Note 6**). A knife can be used to extract specimens from fissures in the boulder.
6. Place the individual(s) in a vial with seawater (*see* **Note 7**).
7. Remove most ice from an ice-filled insulated cooler.
8. Place vials with worms in the cold cooler, keeping it between 4 and 15 °C.
9. Bring cooler with worms to the lab or rearing facility.

3.2 Hypoxia-Induced Migration

This method, proposed by Kirsteuer [17], is suitable for smaller specimens from the low and mid intertidal region inhabiting within the encrusting community formed by algae, mussels, barnacles or other creatures adhering to a hard substrate (natural rocks and outcrops, or manmade structures like pilons and jetties). This strategy induces them to migrate out to the open by falling oxygen concentrations.

1. Use a chisel, spatula or knife to remove part of the encrusting community from the substrate (Fig. 2d).
2. Place removed rubble into a bucket or sturdy zipper bag.
3. Fill the container with seawater.
4. Repeat 1 and 2 until filling several bags.

5. Fill an additional bucket with seawater from the collection location.
6. (optional) Fill quarter-sized cans or bottles with seawater.
7. Bring back rubble bags, cans/bottles, and/or buckets to the lab or other work area.
8. Set up several deep trays or buckets on a table or the floor.
9. Empty rubble bags on trays/buckets, spreading the rubble evenly into a layer not thicker than 15–20 cm from the bottom of the container.
10. Add seawater to trays/buckets until the water level is twice higher than the rubble layer (Fig. 2e).
11. Fragment rubble into smaller pieces with hands or the help of a chisel or a spatula.
12. Spread fragments on bottom (Fig. 2e, f).
13. Keep at room temperature.
14. Monitor trays for the following 24 h for worms coming out of the rubble and crawling up the walls of the recipient (*see* **Note 8**).
15. Pick the worms gently using plastic pipettes or a soft paintbrush and place them in vials.
16. Keep the vials with worms between 4 and 15 °C until rearing bowls are set up (see Subheading 3.3).
17. Check periodically the trays/buckets for additional worms emerging from the rubble, until no more worms emerge, or the water becomes foul and turbid (*see* **Note 9**).
18. Discard the water and rubble (*see* **Note 10**).

3.3 Specimen Rearing

Collected specimens can be kept in the laboratory for many months and up to several years with minimal maintenance (*see* **Note 11**).

1. Set up clean, dry culture bowls (*see* **Note 12**).
2. Label bowls using labeling tape with date and source of specimens.
3. Add tempered FWS to fill about one half of the bowl.
4. Move 5–20 specimens (*see* **Note 13**) from collection vials to the bowl using either a paintbrush or Pasteur plastic pipettes (*see* **Note 14**).
5. Examine the behavior of the transferred worms (*see* **Note 15**).
6. Cover bowls with either plate of a petri dish to reduce evaporation; lids should sit loosely and not form an airtight seal.
7. Store the bowls at a cool (12 to 18 °C) location protected from direct sunlight. A temperature-controlled, constant-humidity chamber or incubator is optimal.

8. Check bowls daily, and use a soft paintbrush or plastic pipette to move any worms that have crawled up the walls over the water level back underwater (*see* **Note 16**).
9. Replace culture water with fresh FSW at least weekly (*see* **Note 17**).

3.4 Feeding

Although many nemerteans, including *Lineus sanguineus* can survive for many months without feeding, keeping well-fed worms will improve overall condition, yield more reliable experimental results and allow increasing population numbers through clonal propagation (see Subheading 3.5). *L. sanguineus* is a voracious predator, and likely a scavenger too, and will feed readily once it learns the nature of its food. It can be fed a variety of items, including live annelids, processed liver, minced scallops or mussels as well as eggs/oocytes from other invertebrates. In this protocol, we detail preparation of and feeding with liver homogenate, since this is a well-established method used to rear and perform dsRNA- or drug-mediated interference experiments on the planarian *Schmidtea mediterranea* [18, 19].

1. Cut a 100–250 g slice of calf liver into small (~3 cm) cubes.
2. Trim all fat, blood vessels, and other connective tissues.
3. Grind cubes using mortar and pestle, a potato masher, or a blender. If using a blender, use a slow speed to avoid formation of bubbles.
4. Pass the ground liver through a sieve with a 200–500 μm mesh to remove coarse fragments, bubbles and other tissue remains.
5. Cut out pieces of polyethylene film so they fit flat in a freezer container.
6. Remove the plunger from a disposable syringe.
7. Load the liver homogenate into the barrel.
8. Replace the plunger.
9. Place a first sheet of polyethylene film on the bench.
10. Push the plunger to extrude a round, long strip of homogenate over the plastic film (*see* **Note 18**).
11. Repeat to lay parallel strips of liver until completely depleting the barrel of homogenate.
12. Reload the barrel and repeat **steps 8** to **11** until all area of the film is covered with parallel stripes of liver.
13. Put another piece of polyethylene film on top of the liver stripes.
14. Repeat **steps 7** to **13** until all liver homogenate is laid down.
15. Place the stack of strips in a freezer container.
16. Store the freezer container at −20 °C.

17. At feeding time, thaw approximately 1 cm of liver homogenate strips per worm to be fed.
18. Label as many glass dishes as there are culture dishes to be fed.
19. Fill the feeding dishes to about half with FWS.
20. Move worms from their culture dish to the corresponding feeding dish using a paintbrush or plastic pipette.
21. Divide the liver strip into small pieces no larger than the worms are thick.
22. Add 2–3 pieces per worm to each feeding dish (*see* **Note 19**).
23. Sink any floating pieces of liver to the bottom of the feeding dish with a plastic pipette.
24. Replace water in culture dishes with fresh FSW.
25. Keep worms to feed for 1–2 h in feeding dish (*see* **Note 20**).
26. Return worms to their respective culture dishes (*see* **Note 21**).
27. Clean the feeding dishes.
28. Check culture dishes every 12 h for the presence of feces, remove them with a pipette.
29. Change the FWS from the culture dishes about a day or two after feeding the worms.

3.5 Propagation

Lineus sanguineus are known to reproduce asexually in the wild, and will readily do so in culture conditions [20]. Since they are capable of whole-body regeneration, population numbers can also be expanded by cutting worms into several fragments. Each fragment will regenerate the missing ends and result in a complete, albeit smaller worm. This technique allows not only to quickly expand the number of individuals, but also to generate smaller individuals that are better fit for experimentation, whole mount immunohistochemical procedures and imaging.

1. Label one glass dish per worm to be cut (*see* **Note 22**).
2. Fill the dishes to about half of their volume with FSW.
3. Add cold (4 °C) FSW to a shallow petri dish plate up to about 5 mm.
4. Move the worm to be amputated into the cold petri dish (*see* **Note 23**).
5. Wait until the worm starts crawling and extends.
6. Using a #10 scalpel blade (or similar curved edge blade), make a single transverse cut at about one third of the total body length from the anterior end.
7. Move the anterior fragment into a new, labeled culture dish (see Subheading 3.3).

8. Use the scalpel to make a cut approximately 1 cm posterior to the anterior cut surface (*see* **Note 24**).
9. Move the ~1 cm worm fragment to a glass dish.
10. Repeat **steps 8** and **9** until the length of the remaining posterior portion of the worm is about one third of its original length.
11. Move the posterior portion of the worm to the same culture dish used in **step 7**.
12. Discard water from the petri dish.
13. Wipe clean the bottom of the petri dish with a paper towel.
14. Repeat **steps 3** to **13** for each worm to be amputated.
15. Transfer with a plastic pipette all healthy amputated fragments (*see* **Note 25**) to small culture bowls, using one bowl per glass dish.
16. Keep worms at room temperature (*see* **Note 26**).
17. Check culture bowls 4 h after cutting and remove any dead or dying fragments.
18. Examine fragments in culture bowls 24 h after cutting and remove any dead or dying fragments (*see* **Notes 25** and **27**).
19. Replace water from culture bowls with fresh FSW (*see* **Note 28**).
20. Repeats **steps 18** and **19** at 48 h, 72 h, and 96 h after amputation, and then every 2 days thereafter.
21. When fragments have regenerated into worms in which ocelli, brains, mouth and a proboscis can be seen (Fig. 1c; *see* **Note 29**), move the culture bowls to the rearing chamber (see Subheading 3.3).

4 Notes

1. Clean sea water is the main requirement for successful maintenance and rearing of *Lineus sanguineus* and other nemerteans. While most marine research stations are fitted with sea tables and a constant supply of natural sea water, other locations are unlikely to have such facilities. If located near the ocean, sea water can be procured from the shore, brought in tanks or bottles, filter-sterilized and stored. Worm cultures use relatively small amounts of water, so unless there are many specimens being kept, only occasional trips would be needed. If located inland, then procuring natural sea water might not be practical. In such a case, it is possible to use instead one of the many formulations for artificial sea waters sold for aquariums. However, formulations not always yield an artificial sea water

equivalent to the one which the worms are habituated and might even prove lethal to them. Specific formulations should be tested on one or two individuals, by passing the worms through a graduated replacement from the natural seawater in which they were placed after collection to the artificial sea water. Even if the worms appear to survive the artificial medium, specifics of the formulation could affect regenerative ability. Thus, if setting up worm cultures for a research project at an inland location, it might be advisable to bring natural seawater from the collection sites and test that regenerative responses are similar in both natural and artificial media.

2. Several other species of nemerteans also inhabit the same habitats in which *Lineus sanguineus* can be found. Which species may be found will depend on the geographic location. Most of them can be collected and kept in the laboratory using the same methodologies described here.
3. Since several co-occurring *Lineus* species vary in coloration depending on the geographic region, sometimes determining if *L. sanguineus* is present may not be obvious. A useful behavioral test is to gently poke or disturb the worm with a jet of water from a pipette: while most species will contract their longitudinal muscles, becoming shorter and broader, *L. sanguineus* instead contracts diagonal muscles and coils into a spiral (Fig. 1b). If further confirmation is desired and resources are available, it is advisable to collect all specimens, bring them back to the lab and use molecular barcoding tools. Since most nemertean species readily regenerate lost posterior ends, the posterior end of each worm can be amputated and subject to DNA extraction without sacrificing the whole specimen. The barcoding fragment of cytochrome oxidase unit I (COI) can then be amplified using Folmer's L/H primer pair [21], sequenced and compared against other nemertean sequences deposited at NCBI's GenBank database (https://blast.ncbi.nlm.nih.gov).
4. Best collection sites are those with ample intertidal zones. Plan collection trips ahead of time, and always consult the tide tables for the area you will be collecting. Begin fieldwork well ahead of the time the tide will reach its low point, as waters are receding. Do not attempt to collect at a spot that is still close to where waves are breaking, and always retire from the area once the tide begins to rise. If you are new to the area, it is always advisable to try finding advice or help from someone with experience on local tide patterns.
5. Worms can also be found hiding or feeding inside mollusk shells, or even inside live or freshly dead mollusks and other animals.

6. Nemerteans are prone to breaking into pieces either during collection, or when placed in stressful conditions. Usually, the fragment containing the anterior end of the worm is necessary for morphological identification, except for some species with very distinctive pigmentation patterns (e.g., *Siphonenteron bilineatum*, *Lineus grubei*, *Kulikovia torquatus*). Specific identity of headless fragments can be determined using molecular barcoding (*see* **Note 3**).
7. If keeping track of the number of individuals, or maintaining individual identity is important, then use a single vial per collected individual. Nemerteans often fragment after collection, altering the original number and size of collected worms.
8. It might take several hours for worms to emerge, depending on how many of them were in the rubble, how much rubble is in each tray, air and water temperature.
9. As the rubble decays, water quality may degrade rapidly. There is a trade-off between waiting for a longer period to catch any straggler worms and allowing advancing putrefaction to generate a pungent foul smell.
10. It is highly advisable not to wait more than 24 h before disposing of the rubble, especially in warmer weather. When disposing of the rubble, return it as close to its source as possible, to avoid translocating organisms.
11. This is true for many species of nemerteans, though others might survive for only days or hours. Ability to survive for long periods without feeding is fundamental to survey regeneration capabilities: since anteriorly amputated worms usually lack a mouth to feed, they must be able to tolerate starvation long enough to regenerate a mouth. Specimens dying shortly (i.e., <2 days) after amputation lead to weaker inferences about an absence of anterior regeneration in a species. In contrast, beheaded specimens surviving for weeks or months without any signs of regeneration yield stronger evidence of absent anterior regeneration.
12. Nemertean cultures usually perform better when glass rather than plastic containers are used.
13. *Lineus sanguineus* individuals can tolerate a large range of densities, from single specimens to over a 100 worms in a single dish. Unless rearing resources are limited (i.e., limited bowls or shelf space), it is probably best not to keep more than 10–20 worms per culture dish. Although intraspecific aggression or cannibalism has not been reported, it is harder to keep track of a larger numbers of worms, as they tend to aggregate in dense "knots" from which it is quite difficult to isolate individual specimens.

14. Worms secrete a sticky mucus and will easily stick to the inside of the plastic pipette during transfers. To avoid this, try to use swift movements to aspire worms into the pipette and expel them into the container they are being transferred to. If worms stick to the inside of the pipette, try to energetically squeeze and release the bulb so that fast moving water dislodges them from their gooey grasp. If that fails, a last resort option is to cut open the pipette and rescue the worm with a paintbrush.
15. *L. sanguineus* individuals usually coil into a spiral (shorter animals) or knot (longer animals) when kept in vials. After being transferred to the glass bowls, worms should eventually begin to crawl around the bowl. Sometimes worms will curl themselves into a knot and secrete a mucus cocoon. If needed, the cocoon can be opened carefully with tweezers under a dissecting scope.
16. Some nemerteans tend to crawl upward, moving above the water level and sometimes lodging between the edge of the container and the covering lid. While they might survive for some time outside of the water in humid environments, they will eventually dry up and die. It is a good idea to check frequently after an initial culture is setup to see if this behavior shows up. Worms clinging on the container wall out of the water can be pushed back down by squirting them with water using a plastic pipette.
17. Keep an eye for evaporation or fouling of the water. Always make additional checks after feeding the worms (see Subheading 3.4), as food particles transferred to the culture dish along with recently fed worms can quickly spoil and foul the water. If a layer or biofilm of mucus and bacteria builds up over the surface of the bowl, move the worms to a new, clean bowl and add filtered sea water.
18. Laying out the liver homogenate in stripes before freezing facilitates feeding standardized amounts, and avoids freeze–thaw cycles by allowing thawing only the necessary amount of homogenate.
19. Many more worms can be placed into a single feeding dish, but as the number increases it becomes increasingly difficult to keep track of each individual's feeding performance and thus to ensure that all individuals are feeding adequately.
20. Allow worms time to detect the presence of food. Different individuals may take different time to do so, especially recently collected worms. Once they detect food, they will usually approach the liver piece and start eating. Worms in recently established cultures may initially not accept or eat the food being offered. A learning period involving several tries is sometimes required before they first try a new food item. Once they

successfully pass this period, they usually become much more eager to feed on the same substrate in subsequent occasions. However, if worms keep rejecting the food after several attempts, it might be worth trying with a different item.

21. If less manipulation of worms is desired, it is also possible to add the food directly to the culture dishes, and then remove uneaten food pieces. This however tends to accelerate fouling of water, so more care in changing sea water will be needed.
22. The number and size of fragments that can be obtained from a single individual varies with the original size of the specimen (i.e., long worms might yield over two dozen small fragments). In turn, the size of the fragments determines the size of the regenerated individuals.
23. Cold water will slow down worms enough to make a reasonable accurate cut. However, if highly precise amputations are needed, cold might not be enough to keep the worm in position. In those cases, animals can be anesthetized using <1.5% ethyl carbamate, <5% chloral hydrate, <1.5% chlorobutanol or 7.5% MgCl [17, 22]. To avoid passive displacement, the worm can also be placed over wet filter paper [23].
24. The size of the fragments can be as small or large as needed, but the probability of successful regeneration often decreases if a fragment's length is less than its width, or if it is made too close to the posterior end [10, 24]. If very small worms are desired, it might be necessary to make two successive rounds of amputation and regeneration.
25. Fragments that do not survive the amputation usually die within the next few hours. Dead or dying fragments stop all muscular and ciliary movements and usually start changing color and begin disintegrating.
26. *L. sanguineus* can live at a wide range of temperatures, if temperature does not change too abruptly. However, warmer temperatures (e.g. room temperature, ~24 °C) promote the growth of microorganisms and accelerate physiological processes of worms, which might be detrimental for cultures. Warmer temperatures, however, also accelerate developmental processes, including regeneration.
27. It is very common for regenerating fragments to secrete protective mucus and surround themselves in a spherical cocoon. They will complete regeneration within the cocoon, but if observation of the progress of the regeneration process is desired, can might be removed from the cocoon by carefully prying it open with a couple of sharp tweezers under a dissecting scope.
28. Change water sooner if microbial growth is observed.

29. Time to complete regeneration varies, depending on the size of the fragments, temperature, and condition and strain of the original individual, but usually by 2 weeks it should be possible to see ocelli, brains, mouth and a proboscis on the regenerate (Fig. 1c).

Acknowledgments

We are grateful to Jon L. Norenburg (National Museum of Natural History, Smithsonian Institution) and Nuria Anadón (Departamento de Organismos y Sistemas, Universidad de Oviedo) for inducing each of us into the depths of nemertean lore. E.E.Z. was supported through his training by a University of Maryland & Smithsonian Institution Seed Grant, and by the Smithonian Tropical Research Institute. F.Á.F.-Á. was supported by a JdC-I Postdoctoral Fellowship Grant (ref. IJC2020-043170-I) awarded by CIN/AEI/10.13039/501100011033 and the European Union NextGenerationEU/PRTR. This research was supported by the Spanish government through the 'Severo Ochoa Centre of Excellence' accreditation (CEX2019-000928-S).

References

1. Bely AE, Nyberg KG (2010) Evolution of animal regeneration: re-emergence of a field. Trends Ecol Evol 25:161–170
2. Bely AE, Zattara EE, Sikes JM (2014) Regeneration in spiralians: evolutionary patterns and developmental processes. Int J Dev Biol 58: 623–634
3. Zattara EE (2020) Axial regeneration in segmented animals: a post-embryonic reboot of the segmentation process. In: Cellular processes in segmentation. CRC, Boca Raton, FL, pp 255–292
4. Bely AE (2010) Evolutionary loss of animal regeneration: pattern and process. Integr Comp Biol 50:515–527
5. Zattara EE, Bely AE (2016) Phylogenetic distribution of regeneration and asexual reproduction in Annelida: regeneration is ancestral and fission evolves in regenerative clades. Invertebr Biol 135:400–414
6. Gibson R (1972) Nemerteans. Hutchinson, London
7. Gibson R (1995) Nemertean genera and species of the world: an annotated checklist of original names and description citations, synonyms, current taxonomic status, habitats and recorded zoogeographic distribution. J Nat Hist 29:271–561
8. Kajihara H, Chernyshev AV, Sun S-C et al (2008) Checklist of nemertean genera and species published between 1995 and 2007. Species Divers 13:245–274
9. Zattara EE, Fernandez-Alvarez FA, Hiebert TC et al (2019) A phylum-wide survey reveals multiple independent gains of head regeneration in Nemertea. Proc R Soc B Biol Sci 286: 20182524
10. Coe WR (1929) Regeneration in nemerteans. J Exp Zool 54:411–459
11. Runnels C (2013) Phylogeography and species status of *Ramphogordius sanguineus*. Theses and Dissertations
12. Kang X-X, Fernández-Álvarez FÁ, Alfaya JEF et al (2015) Species diversity of *Ramphogordius sanguineus/Lineus ruber*-like Nemerteans (Nemertea: Heteronemertea) and geographic distribution of *R. sanguineus*. Zoolog Sci 32: 579–589
13. Ament-Velásquez SL, Figuet E, Ballenghien M et al (2016) Population genomics of sexual and asexual lineages in fissiparous ribbon worms (*Lineus*, Nemertea): hybridization, polyploidy and the Meselson effect. Mol Ecol 25: 3356–3369
14. Bierne J, Tarpin M, Vernet G (1993) A reassessment of the systematics and a proposal for

the phylogeny of some cosmopolitan *Lineus* species (Nemertea). Hydrobiologia 266: 159–168

15. Moretto HJA (1997) A new heteronemertean from the argentine coast of the southern Atlantic. Hydrobiologia 365:215–222
16. Leasi F, da Andrade SC, Norenburg J (2016) At least some meiofaunal species are not everywhere. Indication of geographic, ecological and geological barriers affecting the dispersion of species of *Ototyphlonemertes* (Nemertea, Hoplonemertea). Mol Ecol 25:1381–1397
17. Kirsteuer E (1967) Marine, benthonic nemerteans: how to collect and preserve them. Am Mus Novit 2290:1–10
18. Rouhana L, Weiss JA, Forsthoefel DJ et al (2013) RNA interference by feeding in vitro-synthesized double-stranded RNA to planarians: methodology and dynamics. Dev Dyn 242:718–730
19. Basquin C, Orfila A-M, Azimzadeh J (2015) Chapter 13. The planarian *Schmidtea mediterranea* as a model for studying motile cilia and multiciliated cells. In: Basto R, Marshall WF (eds) Methods in cell biology. Academic Press, New York, pp 243–262
20. Coe WR (1930) Asexual reproduction in Nemerteans. Physiol Zool 3:297–308
21. Folmer O, Black M, Hoeh W et al (1994) DNA primers for amplification of mitochondrial cytochrome c oxidase subunit I from diverse metazoan invertebrates. Mol Mar Biol Biotechnol 3:294–299
22. Herrera Bachiller A (2016) Los nemertinos de España y Portugal. https://ebuah.uah.es/dspace/handle/10017/25884
23. Bierne J (1985) Histocompatibility in Nemertines: fates of multiparental *Lineus* constructed by grafting of pieces from many donors. Am Zool 25:135–144
24. Coe WR (1930) Regeneration in nemerteans. II. Regeneration of small sections of the body split or partially split longitudinally. J Exp Zool 57:109–144
25. GBIF.org (2020) GBIF occurrence download. https://doi.org/10.15468/dl.3jmymm

Open Access This chapter is licensed under the terms of the Creative Commons Attribution 4.0 International License (http://creativecommons.org/licenses/by/4.0/), which permits use, sharing, adaptation, distribution and reproduction in any medium or format, as long as you give appropriate credit to the original author(s) and the source, provide a link to the Creative Commons license and indicate if changes were made.

The images or other third party material in this chapter are included in the chapter's Creative Commons license, unless indicated otherwise in a credit line to the material. If material is not included in the chapter's Creative Commons license and your intended use is not permitted by statutory regulation or exceeds the permitted use, you will need to obtain permission directly from the copyright holder.





Chapter 13

Studying Xenacoelomorpha WBR Using *Isodiametra pulchra*

Bernhard Egger

Abstract

Xenacoelomorpha are a phylogenetically and biologically interesting, but severely understudied group of worm-like animals. Among them, the acoel *Isodiametra pulchra* has been shown to be amenable to experimental work, including the study of stem cells and regeneration. The animal is capable of regenerating the posterior part of the body, but not its head. Here, methods such as nucleic acid extractions, in situ hybridisation, RNA interference, antibody and cytochemical stainings, and the general handling of the animals are presented.

Key words Acoela, Isodiametra, Regeneration, Neoblast stem cells, Antibody stainings, Phalloidin, In situ hybridization, RNA and DNA extraction, Anesthesia

1 Introduction

Xenacoelomorpha are one of the few remaining phyla with an unresolved, contested position in the Tree of Life. The group is either recovered as sister group of all other bilaterian animals, or as a member of Deuterostomia [1, 2]. Three groups constitute the Xenacoelomorpha: Xenoturbellida with 6 described species in one genus, Nemertodermatida with 18 described species, and Acoela with more than 300 described species being by far the largest and best known of the three groups. Their simple body plan—lacking a coelom, a circulatory system, a skeleton or respiratory organs other than the epidermis—can either be seen as plesiomorphic, or as a series of reductions [3]. In either case, they are an interesting and still poorly studied group of almost exclusively marine animals.

The regeneration capacity of the few studied xenacoelomorphs varies, where only a few species were shown to be able to completely regenerate their head, including brain and statocyst (a gravity sensing organ), such as *Hofstenia miamia* [4]. Regeneration capacity is possibly linked to the mode of reproduction, where obligatorily sexually reproducing species are often less capable of regeneration than asexually reproducing species. In different acoels, all modes of

Simon Blanchoud and Brigitte Galliot (eds.), *Whole-Body Regeneration: Methods and Protocols*,
Methods in Molecular Biology, vol. 2450, https://doi.org/10.1007/978-1-0716-2172-1_13, © The Author(s) 2022

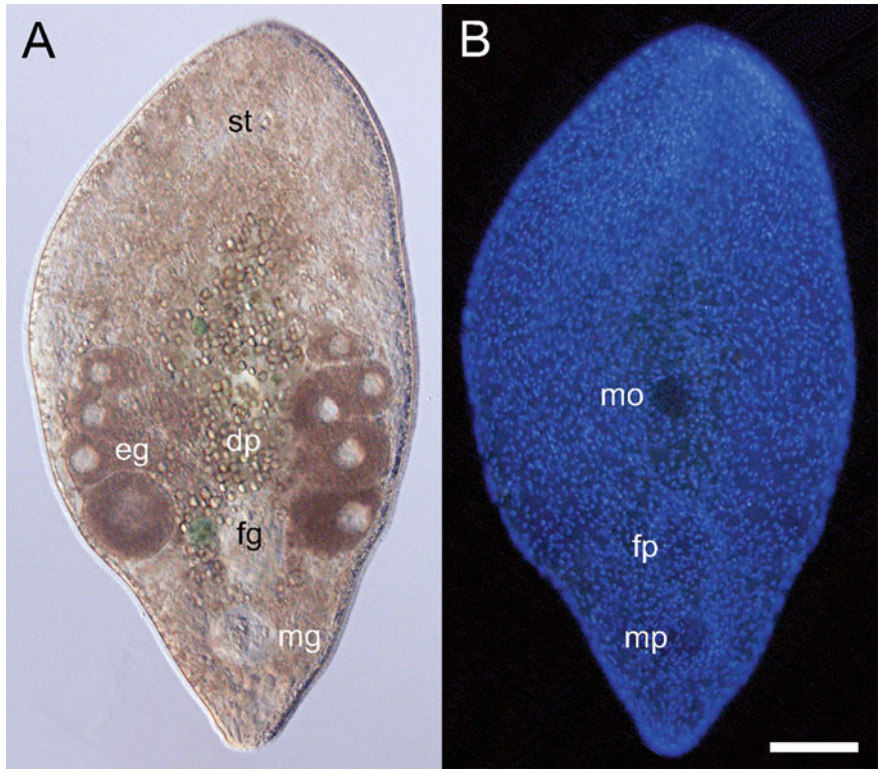


Fig. 1 (**a**) Squeeze preparation of a live adult specimen of *Isodiametra pulchra*. (**b**) Same specimen as in **a**, nuclei of the epidermis stained blue with DAPI. Anterior is up. *dp* digestive parenchyma, *eg* developing eggs, *fg* female genital opening, *mg* male genital apparatus, *mo* mouth, *mp* male genital opening, *st* statocyst. Scale bar is 100 μm

asexual reproduction occur: architomy (fission happens before new organs have been built), paratomy (fission happens after new organs have been built), and budding [5].

Regeneration, growth and homeostasis in acoels is powered by neoblast stem cells, the only proliferating cells in the body, located exclusively in the mesenchymal space and thus lacking in the epidermis [4–7].

One of the better studied acoels is *Isodiametra pulchra*, an animal less than a millimeter in length, transparent, bearing a single statocyst near the anterior end (Fig. 1). It belongs to the species-rich family Isodiametridae (comprising about 100 species), and can be cultured in large numbers in the laboratory. It is sexually reproducing, and cannot regenerate its head, but posterior body parts [8]. The following protocols are tested with adult and juvenile *I. pulchra*, or its close (and even smaller) relative, *Aphanostoma pisae*, or both [6–11].

In particular, RNA and DNA extraction, anesthesia, amputation, fixation, in situ hybridization (Fig. 2), RNA interference, and antibody and cytochemical stainings (Fig. 3) are covered in this



Fig. 2 Wholemount in situ hybridisation of an adult specimen of *Isodiametra pulchra* against *Ipiwi1*, a stem-cell gene. (Picture is courtesy of Thomas Zauchner). Anterior is up. Scale bar is 100 μm

chapter. While all methods included here have been published elsewhere, this chapter serves to bring them together in a compact format and to provide tricks and tips and notes on critical steps.

2 Materials

2.1 Nucleic Acid Extractions

Use nuclease-free (but not DEPC (diethyl pyrocarbonate)-treated) water. Only use nuclease-free sterile tubes, pestles and pipet tips. Only use molecular biology graded reagents. Work under the fume hood if indicated on the reagent's safety data sheet.

1. *Isodiametra pulchra* worms (*see* **Note 1**) and culture system (*see* **Note 2**).
2. DNA/RNA extraction buffer (e.g., TRIzol, Thermo Fisher Scientific; TRI Reagent, Sigma-Aldrich): store at 4 °C.
3. Glycogen, nuclease-free (e.g., Thermo Fisher Scientific, AM9510). Keep at −20 °C.
4. Isopropanol (2-propanol).

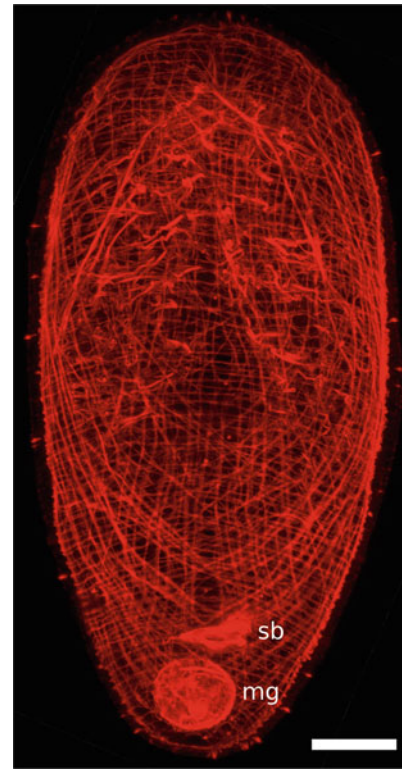


Fig. 3 Confocal laser scanning projection of the body wall and genital musculature of *Aphanostoma pisae* stained with rhodamine-conjugated phalloidin. (Picture is courtesy of Thomas Zauchner). Anterior is up. *mg* male genital apparatus, *sb* seminal bursa. Scale bar is 50 μm

5. 80% (v/v) Ethanol.
6. Sodium dodecyl sulfate (SDS) buffer: 0.5% (w/v) SDS, 200 mM Tris, 25 mM ethylenediaminetetraacetic acid (EDTA), 250 mM NaCl. Store at RT.
7. Protease XIV stock solution: 20 mg/mL protease XIV. Aliquot in 10 μL and store at −20 °C.
8. Protease XIV working solution: 1% (v/v) protease XIV stock solution in PBS-Tx. Prepare fresh.
9. 25:24:1 (v/v/v) Phenol–chloroform–isoamyl alcohol: either prepare the mixture yourself, or purchase a premixed solution. Store at 4 °C.
10. 3 M sodium acetate: 40.83 g sodium acetate in 80 mL deionized water (dH_2O). Adjust to pH 5.2 with glacial acetic acid, fill up to 100 mL with deionized water, autoclave and store aliquots at −20 °C.

2.2 Antibody and Cytochemical Stainings

There is no requirement to use purified water other than dH_2O.

1. Artificial seawater (ASW): 3.2% (w/v) aquarium salt in dH_2O. Mix well and let oxygenize for at least 6 h.
2. $MgCl_2$: 7% (w/v) $MgCl_2 \bullet 6\ H_2O$ in dH_2O.
3. 10× PBS: 2.4 g KH_2PO_4, 14.4 g Na_2HPO_4, 2 g KCl, 80 g NaCl in 800 mL dH_2O. Adjust pH to 7.4 with HCl, fill up to 1 L with dH_2O, autoclave, store at RT.
4. Formaldehyde (FA): 4% (w/v) paraformaldehyde in 1× PBS. Dissolve at 53 °C for 1 h, shake every 15 min, adjust to pH 7.4 with HCl and NaOH and store 1 mL aliquots at −20 °C.
5. PBS-Tw: 0.1% (v/v) Tween in 1× PBS.
6. PBS-Tx: 0.1% (v/v) Triton X-100 in 1× PBS.
7. BSA-Tx: 1% (w/v) bovine serum albumin (BSA) in PBS-Tx. Dissolve BSA powder by stirring, store at 4 °C and renew solution every 2 weeks.
8. 5-bromo-2′-deoxyuridine (BrdU) stock solution: 50 mM BrdU in dH_2O. Store at −20 °C.
9. 5 mM BrdU working solution: 10% (v/v) 50 mM BrdU stock solution in ASW. Prepare fresh.
10. 5-Ethynyl-2′-deoxyuridine (EdU): prepare and store all solutions of the Click-iT kit according to manufacturer's protocol (Thermo Fisher Scientific, C10337).
11. 0.4 mM EdU working solution: 25% (v/v) 10 mM EdU stock in ASW. Prepare fresh.
12. 2 M HCl: 16.6 mL 37% (v/v) HCl in 83.4 mL water.
13. Primary antibodies: mouse-anti-BrdU and rabbit-anti-pH 3.
14. Primary antibodies solution: mouse anti-BrdU antibody 1:600, rabbit anti-pH3 antibody 1:150 in BSA-Tx (*see* **Note 3**). Prepare fresh.
15. Secondary antibodies: goat anti-mouse FITC-conjugated and swine anti-rabbit TRITC-conjugated.
16. Secondary antibodies solution: goat anti-mouse FITC-conjugated 1:250, swine anti-rabbit TRITC-conjugated 1:250 in BSA-Tx (*see* **Note 4**). Prepare fresh.
17. TRITC-conjugated phalloidin.
18. 4′,6-Diamidino-2-phenylindole (DAPI).
19. Triple staining solution: 1:500 phalloidin TRITC-conjugated, 1:10,000 DAPI in Click-iT solution according to the manufacturer's instructions. Prepare fresh.
20. Mounting medium (e.g., Vectashield, VectorLabs, or 80% (v/v) glycerol in PBS).

2.3 In Situ Hybridization and RNA Interference

All solutions are to be prepared with either nuclease-free or DEPC-treated water (1 mL DEPC per liter solution; stir over night and autoclave).

1. 100%, 75%, 50%, 25% methanol.
2. Proteinase K stock solution: 10 mg/mL proteinase K in 1× PBS-Tw. Aliquot in 10 µL and store at −20 °C.
3. 20 µg/mL proteinase K working solution: 10 µL proteinase K stock solution in 5 mL PBS-Tw. Prepare fresh right before use.
4. 4% (w/v) glycine stock solution: 4 g glycine in 100 mL. Filter-sterilize and store at 4 °C.
5. 4 mg/mL glycine working solution: 50 µL glycine stock solution in 450 µL PBS-Tw. Prepare fresh right before use.
6. 1 M triethanolamine (TEA) stock solution: 18.57 g TEA in 100 mL. Adjust pH to 7.8, Filter-sterilize and store at RT.
7. 0.25% acetic anhydride: 0.25% (v/v) acetic anhydride in TEA. Prepare fresh.
8. 0.5% acetic anhydride: 0.5% (v/v) acetic anhydride in TEA. Prepare fresh.
9. 1% (w/v) heparin: 1 g heparin in 100 ml. Filter-sterilize and store at −20 °C.
10. 10× 3-[(3-Cholamidopropyl)dimethylammonio]-1-propanesulfonate (CHAPS) stock solution: 1 g CHAPS in 100 mL. Filter-sterilize, aliquot in 50 mL and store at −20 °C.
11. 20× saline sodium citrate buffer (SSC): 175.3 g NaCl, 88.2 g sodium citrate in 1 L. Adjust to pH 7.0, treat with 1 mL DEPC, stir over night, autoclave and store at RT.
12. SSC–CHAPS: 10% (v/v) 20× SSC, 10% (v/v) 10× CHAPS. Prepare fresh.
13. 50× Denhardt's solution: 1% (w/v) nuclease-free BSA, 1% (w/v) Ficoll 400, 1% (w/v) PVP-40, stir strongly until dissolved. Store at −20 °C.
14. 1% tRNA stocks: 1 g commercially available tRNA in 100 mL, shake over night at 60 °C. Store 1 mL aliquots at −20 °C.
15. Hybridisation mix (hybmix): 1000 mL 100% formamide, 500 mL 20× SSC, 40 mL 1% tRNA, 2 mL 100% Tween, 200 mL 10× CHAPS, 40 mL 50× Denhardt's, 20 mL 1% heparin, 198 mL water. Store in 50 mL aliquots at −80 °C. Can be stored for 1 month at −20 °C.
16. Hybmix/PBS-Tw: 50% (v/v) hybmix in PBS-Tw. Prepare fresh.
17. 75% (v/v), 50% (v/v), 25% (v/v) hybmix in 20× SSC. Prepare fresh.

18. 100 mM maleic acid buffer (MAB): 11.62 g maleic acid, 8.76 g NaCl in 1 L. Adjust pH to 7.5, treat with 1 mL DEPC overnight, autoclave, and store at RT.
19. 10× blocking solution: 10 g blocking reagent (Roche, 11,096,176,001) in MAB. Heat at 60 °C until dissolved, autoclave and store at −20 °C.
20. Alkaline phosphatase stock I: 1 M NaCl. Autoclave and store at RT.
21. Alkaline phosphatase stock II: 0.5 M $MgCl_2 \bullet 6H_2O$. Autoclave and store at RT.
22. Alkaline phosphatase stock III: 1 M Tris. Adjust pH to 9.5, autoclave and store at RT.
23. Alkaline phosphatase buffer (NTMT): 5 mL alkaline phosphatase stock I, 5 mL alkaline phosphatase stock II, 5 mL alkaline phosphatase stock III, 50 µL Tween. Prepare fresh.
24. Anti-digoxigenin-alkaline phosphatase antibody (anti-DIG-AP antibody).
25. Anti-DIG-AP staining solution: 1:2000 anti-DIG-AP antibody in blocking solution. Prepare fresh every time.
26. NBT (nitro-blue tetrazolium chloride)/BCIP (5-bromo-4-chloro-3′-indolyphosphate p-toluidine salt) stock solution: 18.75 mg/mL NBT, 9.4 mg/mL BCIP, 67% (v/v) dimethyl sulfoxide (DMSO).
27. NBT/BCIP working solution: 15 µL NBT/BCIP stock solution, 0.1 M Tris-HCl, pH 9.5, 0.1 M NaCl in 1 mL. Prepare fresh.
28. In vitro RNA production kit.
29. 3–50 µg/µL gene-specific double-stranded RNA (dsRNA) (*see* **Note 5**).
30. 10 mg/mL antibiotic stock solutions: kanamycin, streptomycin, and ampicillin in separate stocks.

3 Methods

Work at RT and use a pipette, if not stated otherwise.

3.1 Anesthesia (Relaxation), Amputation, and Fixation

The soft-bodied animals will contract to unsightly balls when exposed to a fixative without prior anesthesia. In the literature and in the following protocols, anesthesia is referred to as "relaxation." Relaxing animals is not only necessary before fixation but also comes in handy for amputations to stop the animals from bending and turning around.

1. Isolate culture worms to be processed in an unfed culture vessel.
2. Starve the worms for 2 days.
3. Transfer animals to an embryo dish filled with ASW using a pipette.
4. Remove most ASW, so that the animals are barely covered in ASW.
5. Add 500 µL of $MgCl_2$ over the animals (*see* **Note 6**).
6. Repeat **steps 4** and **5** two times.
7. Wait 10 min for the animals to relax (*see* **Note 7**).
8. Clean a razor blade with 70% ethanol to remove oil (*see* **Note 8**).
9. Wait 2 min for the ethanol on the razor blade to evaporate.
10. Transfer a single relaxed animal to an object slide in a small, flat droplet.
11. Amputate animal with a razor blade at the desired body level.
12. Quickly add a drop of ASW onto the amputated animal on the object slide.
13. Return the amputated animal to a petri dish or well plate filled with ASW.
14. Let the animals regenerate for a desired period of time.
15. Repeat **steps 3** to **7**.
16. Remove most $MgCl_2$ (*see* **Note 9**).
17. Immerse animals in cold FA (4 °C) (*see* **Note 10**).
18. Incubate for 1 h at RT.
19. Remove FA.
20. Rinse specimens in PBS-Tx for 5 min.
21. Repeat **step 20** five times.

3.2 In Situ Hybridization

In situ hybridization is used to detect mRNA in the tissue where it is expressed, using labeled RNA probes. Probe design and synthesis can be done after standard protocols (e.g., [6]).

If not otherwise specified, procedures are done at RT. Pipet liquids, not the animals, that is, the animals stay in the same container (microcentrifuge tube, petri, or embryo dish if not otherwise specified. Liquids are to be removed before adding new liquids.

1. Wash fixed animals with distilled water for 1 min.
2. Dehydrate animals in 50% methanol for 10 min.
3. Repeat **step 2** in a graded methanol series (70%, 90%, 100% methanol).

4. Store animals in 100% methanol in microcentrifuge tubes at −20 °C overnight or until further use (*see* **Note 11**).
5. Wash in 100% methanol for 5 min (*see* **Note 12**).
6. Wash in a graded methanol series (75%, 50%, 25%) for 5 min each.
7. Wash animals with PBS-Tw for 5 min.
8. Repeat **step 7** five times.
9. Incubate animals in proteinase K working solution for 3–4 min at 25 °C (*see* **Note 13**).
10. Quickly stop proteinase treatment with glycine working solution for 20 min.
11. Wash with PBS-Tw for 5 min.
12. Repeat **step 11** five times.
13. Wash in TEA for 5 min.
14. Repeat **step 13**.
15. Incubate in 0.25% acetic anhydride for 5 min.
16. Incubate in 0.5% acetic anhydride for 5 min.
17. Washes in PBS-Tw for 5 min.
18. Repeat **step 17**.
19. Postfix in FA for 20 min.
20. Wash with PBS-Tw for 5 min.
21. Repeat **step 20** five times.
22. Incubate in PBS-Tw at 80 °C for 20 min (heat fixation).
23. Incubate in hybmix/PBS-Tw for 10 min.
24. Incubate in hybmix at 55 °C for 10 min.
25. Incubate in new hybmix for 2 h at 55 °C.
26. Denature mRNA probe for 7 min at 96 °C.
27. Snap chill probe on ice.
28. Add probe to the specimens in hybmix.
29. Hybridize at 55 °C for 1–2 days, shaking on an orbital shaker at 300 rpm (*see* **Note 14**).
30. Wash out probe with new hybmix at 62 °C for 5 min.
31. Wash with 75% hybmix at 62 °C for 5 min (*see* **Note 15**).
32. Wash with 50% hybmix at 62 °C for 5 min.
33. Wash with 25% hybmix at 62 °C for 5 min.
34. Wash with SSC–CHAPS at 62 °C for 30 min.
35. Repeat **step 34**.
36. Wash with MAB for 10 min.

37. Repeat **step 36**.
38. Incubate in blocking solution at 4 °C for 2 h.
39. Incubate in anti-DIG-AP staining solution at 4 °C overnight.
40. Wash with MAB for 10 min.
41. Repeat **step 40** five times.
42. Develop colour with NBT/BCIP working solution until pattern emerges.
43. Stop colour development with 100% ethanol for 5 min.
44. Wash in PBS-Tw for 15 min.
45. Repeat **step 44**.
46. Mount animals on object slides with mounting medium.

3.3 RNA Interference (RNAi)

This method is used to knock down expression of targeted genes in vivo with double-stranded RNA (dsRNA). In *Isodiametra*, RNAi can be simply performed by soaking the animals in a seawater solution with dsRNA. Use 25–40 animals per well of a 24-well plate (*see* **Note 16**).

1. Add 400 μL ASW per well of a 24-well plate.
2. Transfer live animals from culture dishes to the prepared wells.
3. Add the dsRNA to a well at a final concentration of 3–50 ng/μL.
4. Add 2 μL of one of the antibiotic stocks to each well.
5. Put lid on well plate and place it in the culture room at 20 °C.
6. Wait for 24 h.
7. Observe behavioral or morphological changes.
8. Replace ASW containing dsRNA and antibiotics with 400 μL of fresh ASW.
9. Repeat **steps 3** to **8**, alternating the type of antibiotics, until the dsRNA treatment is over.
10. Transfer animals to embryo dishes filled with ASW.
11. Process the animals as required for downstream analysis.

3.4 Antibody Stainings

Different to in situ hybridization reagents, there is no requirement for using nuclease-free or DEPC-treated water. While many combinations of antibody stainings are possible, here a double fluorescent wholemount staining using antibodies against BrdU and phosphorylated histone H3 (pH3) is presented.

1. Incubate live animals in 5 mM BrdU working solution for 1 h at RT in darkness (*see* **Note 17**).
2. Wash animals with ASW to remove excessive BrdU.
3. Repeat **step 2**.

4. Follow **steps 4** to **21** in Subheading 3.1 to fix the animals,
5. Incubate animals in protease XIV working solution for 20 min at 37 °C under visual control (*see* **Note 18**).
6. Add 1 mL 2 M HCl to stop the protease treatment when epidermis becomes slightly ragged, that is, the smooth line of the epidermis on the side of the animals turns into a slightly rippled line.
7. Replace 2 M HCl once.
8. Incubate in 2 M HCl for 1 h at 37 °C (*see* **Note 19**).
9. Wash with PBS-Tx for 5 min (*see* **Note 20**).
10. Repeat **step 9** five times.
11. Block in BSA-Tx for 30 min.
12. Incubate in primary antibody solution at 4 °C overnight.
13. Transfer antibody dilution to a microcentrifuge tube for recycling (*see* **Note 21**).
14. Wash animals with PBS-Tx for 5 min.
15. Repeat **step 14** five times.
16. Block in BSA-Tx for 30 min.
17. Incubate in secondary antibody solution for 1 h at RT in darkness.
18. Wash with PBS-Tx for 5 min.
19. Repeat **step 18** five times.
20. Coverslip with mounting medium (*see* **Note 22**).

3.5 Cytochemical Stainings

Again, a great variety of cytochemical stainings can be performed. Here, a triple fluorescent wholemount staining using EdU, DAPI and phalloidin is presented.

1. Incubate live animals in EdU working solution for 1 h at RT in darkness.
2. Follow **steps 2** to **4** in Subheading 3.4.
3. Follow **steps 9** to **11** in Subheading 3.4.
4. Incubate in triple staining solution for 1 h at RT in darkness.
5. Follow **steps 18** to **20** in Subheading 3.4.

3.6 RNA Extraction

When preparing animals for an RNAseq experiment, antibiotics can be used to remove (or reduce) bacterial RNA. Animals can be starved for several days to avoid contaminating algal RNA. Take care not to breathe in opened tubes to prevent RNases from breaking up RNA.

1. Pipette live animals (typically 10–100) into a microcentrifuge tube (*see* **Note 23**).

2. Carefully remove as much ASW as possible with a pipette.
3. Add 1 mL RNA extraction buffer.
4. Use a clean (RNase-free) pestle to mash tissue.
5. Pipette up and down to separate tissue clumps.
6. Centrifuge at max speed at 4 °C for 10 min.
7. Let tube rest at RT for 6 min.
8. Add 200 µL chloroform.
9. Close tube tightly.
10. Vigorously shake tube for 1 min (*see* **Note 24**).
11. Let tube rest at RT for 10 min.
12. Centrifuge at max speed at 4 °C for 15 min.
13. Transfer upper (transparent) phase (ca. 500 µL) into new tube (*see* **Note 25**).
14. Add 10 µg glycogen and mix.
15. Add 1 mL isopropanol.
16. Incubate at RT for 8 min.
17. Centrifuge at max speed at 4 °C for at least 1 h.
18. Take off supernatant (be careful not to pipette away pellet).
19. Add 1 mL 80% ethanol.
20. Centrifuge at max speed at 4 °C for 20 min.
21. Repeat **steps 18** to **20**.
22. Take off all supernatant.
23. Let air dry for 10–30 min (*see* **Note 26**).
24. Add 40–100 µL nuclease-free water.
25. Let rest on ice for 5 min.
26. Store at −80 °C.

3.7 DNA Extraction

For genome sequencing, antibiotics can be used on live animals to remove or reduce bacterial contamination.

1. Pipette live animals (typically 10–100) in microcentrifuge tube (*see* **Note 27**).
2. Carefully remove as much ASW or ethanol as possible.
3. Add 500 µL SDS buffer.
4. Add 5 µL 20 mg/mL protease XIV stock solution.
5. Incubate at 50 °C for at least 1 h to dissolve tissue.
6. Add 240 µL phenol–chloroform–isoamyl alcohol.
7. Tightly close tube.
8. Invert tube several times.

9. Centrifuge tube at max speed at RT for 20 min.
10. Transfer upper transparent phase into new tube (*see* **Note 28**).
11. Add 50 μL sodium acetate.
12. Mix by inverting tube.
13. Add 830 μL chilled 100% ethanol.
14. Leave at −20 °C overnight.
15. Centrifuge at max speed for 1 h.
16. Take off ethanol.
17. Add 1 mL 80% ethanol.
18. Centrifuge at max speed for 20 min.
19. Repeat **steps 16** to **18**.
20. Take off all ethanol.
21. Let air dry for at least 30 min.
22. Elute in 40–100 μL nuclease-free water.
23. Let rest on RT for 5 min.
24. Store at 4 °C if you plan to use the DNA within the next month, otherwise store at, −20 °C or − 80 °C.

4 Notes

1. *Isodiametra pulchra* was originally described as *Convoluta pulchra* and can be found in marine muddy sand beaches on the North American east coast [12]. Currently, lab cultures can be obtained from Andreas Hejnol (University of Bergen, Norway), Pedro Martinez (University of Barcelona, Spain), Simon Sprecher (University of Fribourg, Switzerland), and Peter Ladurner and Bernhard Egger (University of Innsbruck, Austria).
2. *Isodiametra pulchra* can be maintained in glass or plastic Petri dishes with 3.2% ASW, feeding on the diatom *Nitzschia curvilineata* in a light/dark cycle of 10/14 h at 20 °C. *Isodiametra* is an obligatorily sexually reproducing hermaphrodite. For detailed culture conditions, especially for the algae, see [13].
3. Avoid freeze–thaw cycles whenever possible; either store thawed tubes at 4 °C until further use or make small aliquots that will be used up for a single experiment.
4. Pretty much any kind of conjugation can be used with secondary antibodies; the presented protocol presents the combination most often used in *Isodiametra*. It is important to avoid light as much as possible to ensure the longevity of the fluorophores.

5. Gene-specific double-stranded RNA (dsRNA) first needs to be synthesized for RNAi interference experiments. We had good results following [6], using an in vitro RNA transcription system.
6. If the experimenter is skilled, it is preferable to amputate without relaxing animals in $MgCl_2$. Take care to add the relaxant gradually to avoid "freezing" the animals in awkward positions. Toward this end, also make sure to add the fixative at RT, to prevent animals contracting ring muscles in the middle of the body ("wasp waist").
7. Incubating animals in relaxans for an extended period of time (longer than 20 or 30 min) in $MgCl_2$ will lead to loss of epidermal cells and eventually to the partial dissociation of the whole animal; younger animals are more susceptible to $MgCl_2$ than older animals.
8. It is important to clean razor blades from oil (that is covering the blades to prevent rust) with 70% ethanol, but care has to be taken not to blunt the blade during cleaning, and to let the ethanol evaporate before the blade is being used for amputations; after cleaning the blades, they will start rusting. For better handling, double-sided razor blades can be broken into four smaller pieces by bending the ends toward each other by touching them on the unsharpened sides; take special care not to cut yourself! The blades can be used in a guillotine-like movement to separate body parts of the specimens, or attached to the end of a small chopstick for a halberd-like amputation movement. Immediately after amputation, ASW needs to be returned on the object slide to prevent surface tension to destroy the animals.
9. Never remove the complete liquid from the dish/tube before fixation, as surface tension will flatten the animals and may even rip them apart. It is better to exchange the fixative shortly after adding it to dilute the remaining relaxant.
10. Reagents prepared for in situ hybridisation, such as FA, can also be used for antibody stainings, but not the other way round. It is better to use FA made in the lab from PFA instead of buying FA as a solution. For best results, prepare fresh FA for each use.
11. Even if you can continue immediately, always store animals at −20 °C in methanol at least over night before continuing with the in situ protocol; for rehydration of stored specimens, ethanol can be used instead of methanol.
12. All steps can be done in 1.5 mL tubes or in 24-well plates with or without meshes, but also embryo dishes can be used for better visibility of the specimens. Specimens are denser than the surrounding liquid and sink to the bottom of the container (e.g., tube). After pipetting or steps where specimens were

disturbed, it is advisable to wait for the next pipetting step until specimens have sunken to the bottom again.

13. The protease step during in situ hybridizations is a critical step and has to be carefully timed. If the protocol is not successful, first try making fresh FA, and allow for different batches with slightly differently treated animals regarding protease incubation duration, temperature and concentration. The maximum activity of proteinase K is at a temperature of about 37 °C. Take special care if working with juveniles, as they are more susceptible to protease.
14. The length of hybridisation can vary considerably for different probes, probably linked to gene expression levels in the animals. As a rule of thumb, shorter incubation times lead to lower background, so it is not advisable to always use a very long incubation time. Too much background can be addressed with treating the specimens with RNase A after the stringency washes, as the enzyme only digests single stranded RNA.
15. All washing steps in PBS can be extended for potentially even better stainings. Wash often, wash long, with the exception of SSC washing steps during in situ hybridizations.
16. Animals can be maintained in 24-well plates or in embryo dishes for RNAi treatment; smaller containers are preferable due to the amount of required dsRNA. Feeding animals with algae during treatment is not detrimental to the effects of RNAi treatment [6]. Antibiotics may be used to prevent premature degradation of dsRNA.
17. The presented protocol describes a BrdU and EdU pulse staining, that is, animals are killed after the BrdU/EdU pulse. For a pulse-chase staining, animals are kept alive for a period of time after the BrdU/EdU pulse.
18. For BrdU stainings, the protease step is the most critical step. Carefully observe the epidermis before adding protease, and only stop the protease if a difference in the epidermal surface can be seen. EdU labeling is much less critical regarding the protease treatment and generally gives more consistent results than BrdU labeling—however, EdU labeling is much more expensive.
19. This step ensures that the DNA strands become denatured for the BrdU antibody to be able to bind.
20. For the binding affinity of the antibodies, it is important that the pH is close to neutral.
21. Recycle primary antibodies to save money and to obtain better stainings with less background in subsequent stainings. Store recycled antibodies at 4 °C. Typically, antibodies can be reused 2–3 times. If available, use a slow shaker for incubation and washing steps.

22. Use 20 μL mounting medium for coverslips measuring 21 × 26 mm, for small animals like *Isodiametra* it will be the exact amount of liquid needed for coverslipping.
23. Also animals stored in an RNA preservation buffer can be used, but we have better results with live animals.
24. It is advisable to use more expensive microcentrifuge tubes for extracting RNA or DNA, as to avoid leaky tubes during shaking steps.
25. In case of visible contaminations, repeat the chloroform step.
26. Take care to not let the RNA pellet in RNA extractions air dry for longer than ca. 30 min, as hardened RNA pellets are very difficult to elute. This problem does not exist for DNA pellets.
27. Also animals stored in 70% or higher ethanol can be used.
28. In case of visible contaminations, repeat the phenol–chloroform–isoamyl alcohol step.

Acknowledgments

I gratefully acknowledge the hard work of former students, working with and painstakingly improving protocols, namely Simona Migliano, Isabel Dittmann, Lucy Nevard, Lucy Neumann, Thomas Zauchner, and Jochen Hilchenbach. I am especially grateful to Peter Ladurner and to Katrien De Mulder, who adapted and established many protocols with *Isodiametra*.

References

1. Cannon JT, Vellutini BC, Smith J 3rd, Ronquist F, Jondelius U, Hejnol A (2016) Xenacoelomorpha is the sister group to Nephrozoa. Nature 530:89–93
2. Philippe H, Poustka AJ, Chiodin M et al (2019) Mitigating anticipated effects of systematic errors supports sister-group relationship between Xenacoelomorpha and Ambulacraria. Curr Biol 29:1818–1826
3. Achatz JG, Chiodin M, Salvenmoser W, Tyler S, Martinez P (2013) The Acoela: on their kind and kinships, especially with nemertodermatids and xenoturbellids (Bilateria incertae sedis). Org Divers Evol 13:267–286
4. Srivastava M, Mazza-Curll KL, van Wolfswinkel JC, Reddien PW (2014) Whole-body acoel regeneration is controlled by Wnt and Bmp-Admp signaling. Curr Biol 24: 1107–1113
5. Egger B, Gschwentner R, Rieger R (2007) Free-living flatworms under the knife: past and present. Dev Genes Evol 217:89–104
6. De Mulder K, Kuales G, Pfister D et al (2009) Characterization of the stem cell system of the acoel *Isodiametra pulchra*. BMC Dev Biol 9:69
7. Egger B, Steinke D, Tarui H et al (2009) To be or not to be a flatworm: the acoel controversy. PLoS One 4:e5502
8. Perea-Atienza E, Botta M, Salvenmoser W et al (2013) Posterior regeneration in *Isodiametra pulchra* (Acoela, Acoelomorpha). Front Zool 10:64
9. Moreno E, De Mulder K, Salvenmoser W, Ladurner P, Martínez P (2010) Inferring the ancestral function of the posterior Hox gene within the bilateria: controlling the maintenance of reproductive structures, the musculature and the nervous system in the acoel flatworm *Isodiametra pulchra*. Evol Dev 12: 258–266

10. Zauchner T, Salvenmoser W, Egger B (2015) A cultivable acoel species from the Mediterranean, *Aphanostoma pisae* sp. nov. (Acoela, Acoelomorpha). Zootaxa 3941:401–413
11. Dittmann IL, Zauchner T, Nevard LM, Telford MJ, Egger B (2018) SALMFamide2 and serotonin immunoreactivity in the nervous system of some acoels (Xenacoelomorpha). J Morphol 279:589–597
12. Smith JPS, Bush L (1991) *Convoluta pulchra* n. sp. (Turbellaria: Acoela) from the East Coast of North America. Trans Am Microsc Soc 110: 12–26
13. Egger B, Ishida S (2005) Chromosome fission or duplication in *Macrostomum lignano* (Macrostomida, Plathelminthes)—remarks on chromosome numbers in "Archoophoran turbellarians". J Zoolog Syst Evol Res 43: 127–132

Open Access This chapter is licensed under the terms of the Creative Commons Attribution 4.0 International License (http://creativecommons.org/licenses/by/4.0/), which permits use, sharing, adaptation, distribution and reproduction in any medium or format, as long as you give appropriate credit to the original author(s) and the source, provide a link to the Creative Commons license and indicate if changes were made.

The images or other third party material in this chapter are included in the chapter's Creative Commons license, unless indicated otherwise in a credit line to the material. If material is not included in the chapter's Creative Commons license and your intended use is not permitted by statutory regulation or exceeds the permitted use, you will need to obtain permission directly from the copyright holder.



Chapter 14

Studying Echinodermata Arm Explant Regeneration Using *Echinaster sepositus*

Cinzia Ferrario, Yousra Ben Khadra, Michela Sugni, M. Daniela Candia Carnevali, Pedro Martinez, and Francesco Bonasoro

Abstract

Echinoderms are marine invertebrate deuterostomes known for their amazing regenerative abilities throughout all life stages. Though some species can undergo whole-body regeneration (WBR), others exhibit more restricted regenerative capabilities. Asteroidea (starfish) comprise one of the few echinoderm taxa capable of undergoing WBR. Indeed, some starfish species can restore all tissues and organs not only during larval stages, but also from arm fragments as adults. Arm explants have been used to study cells, tissues and genes involved in starfish regeneration. Here, we describe methods for obtaining and studying regeneration of arm explants in starfish, in particular animal collection and husbandry, preparation of arm explants, regeneration tests, microscopic anatomy techniques (including transmission electron microscopy, TEM) used to analyze the regenerating explant tissues and cells plus a downstream RNA extraction protocol needed for subsequent molecular investigations.

Key words Echinoderms, Starfish, Regeneration, Arm explants, Transmission electron microscopy, Semithin and ultrathin sectioning, TEM grid staining, RNA extraction

1 Introduction

Echinodermata is a well-known phylum of benthic marine deuterostome invertebrates that includes sea lilies, starfish, brittle stars, sea urchins, and sea cucumbers. Echinoderms and vertebrates belong to the same super phylum named deuterostomes, which includes the chordates and therefore vertebrates, and for this reason share common ancestral traits that were retained during evolution in both lineages. This makes them relevant alternative non-vertebrate models to study potential shared biological mechanisms/processes or to study loss of specific "functions" (e.g., remarkable regenerative abilities, including whole-body regeneration—WBR) along the different evolutionary lineages. Echinoderms have developed phylum-specific morphological

Simon Blanchoud and Brigitte Galliot (eds.), *Whole-Body Regeneration: Methods and Protocols*, Methods in Molecular Biology, vol. 2450, https://doi.org/10.1007/978-1-0716-2172-1_14, © The Author(s) 2022

features, such as secondary radial symmetry, pentameric organization, a miniaturized and modular hydraulic system, that is, the water vascular system, a calcareous endoskeleton (stereom structure), and mutable connective tissues, namely, collagenous tissues that can rapidly modify their intrinsic mechanical properties under nervous system control [1]. Echinoderms are very common and distributed worldwide at almost all depths and latitudes in all marine environments. Indeed, brittle stars can be the dominant macrobenthic fauna on many muddy seafloors and sea cucumbers sometimes account for up to 90% of biomass in the deep oceans [2]. Successful colonization of such diverse biotopes, despite the presence of different predators, may be explained by echinoderms' incredible adaptive capabilities, including their ability to regenerate lost body parts after predation. Although regeneration is observed in all echinoderm taxa, asexual reproduction followed by whole-body regeneration (WBR) is much less common. Notably, some starfish species, primarily *Linckia* spp. and *Coscinasterias spp.*, are capable of extensive WBR: the ability to regenerate the entire individual from a single arm [2–4].

Several starfish species (class Asteroidea), such as *Leptasterias hexactis*, *Asterias rubens, Marthasterias glacialis*, and, more recently, *Echinaster sepositus*, represent the most used models for regeneration studies. Molecular analyses have been recently added to the range of well-known morphological approaches, namely, light and electron microscopy, to identify the mechanisms involved in both developmental and regenerative processes [5–10]. While regeneration studies were traditionally performed in animals with distally amputated arms, nowadays we have developed the better controlled model of arm explants. A double-amputated arm explant (an amputated arm reamputated at its distal tip) represents a simplified and easy-to-use model to investigate the regenerative process, including the relevant cells and tissues plus the activity of different regulatory molecules, that is, signaling and transcription factors, involved. Of particular importance is that the regenerative potential of the arm is tested in the absence of any systemic control by the rest of the body, including its supporting metabolic contribution [11–15]. Remarkably, in starfish arm explants, the distal end/tip initiates regeneration following the same stages observed in standard arm-tip regeneration, thus proving the validity of this cultured model. Furthermore, although to a much less extent, both distalization (namely, the regeneration of the distal-most structures (terminal tube foot and ossicle)) and intercalation (the regeneration of new tissues between the terminal differentiated structures and the stump) apparently occur in both the distal tip of the arm explants and the tip of single amputated arms. On the contrary, at the proximal end of the arm explants, only the terminal elements are regenerated (distalization) with no signs of intercalation being detectable [16] (Fig. 1). This can provide information on the ability

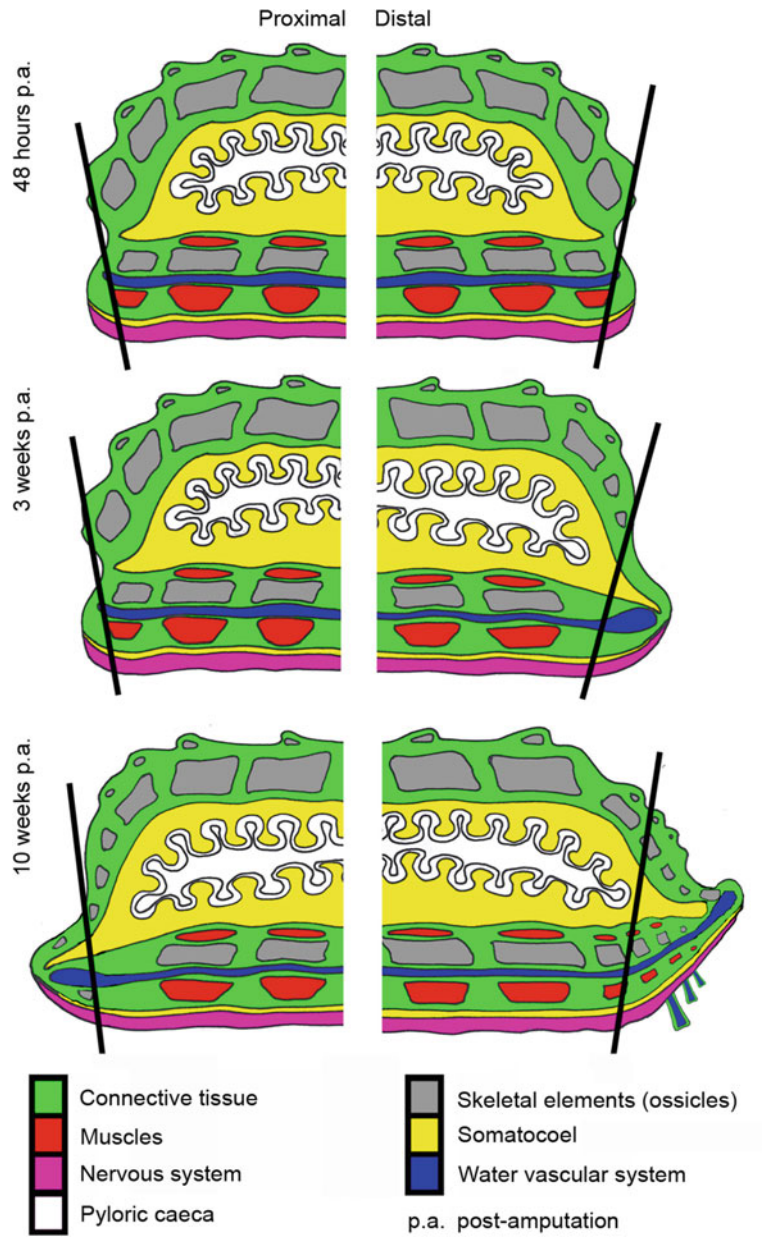


Fig. 1 Longitudinal section schemes of *E. sepositus* arm explants at three selected regenerative stages. For clarity, the tube feet of the nonregenerating arm explant portions have been omitted. Left column: regenerating proximal end. Right column: regenerating distal end. First line: 48 h p.a. Second line: 3 weeks p.a. Third line: 10 weeks p.a. Proximal and distal ends regenerate differently: indeed, while the distal end shows distalization (both terminal ossicle and tube foot) and intercalation (new tube feet), the proximal end shows only distalization (terminal tube foot only) without intercalation. For color coding of tissues, see legend embedded in the figure. Black lines = amputation planes

to "manage" the directionality/polarity of regeneration (i.e., unidirectional vs bidirectional).

Echinaster sepositus, known as the red starfish, is found in the East Atlantic Ocean and in the Mediterranean Sea, where it is one of the most common starfish species. *E. sepositus* inhabits shallow waters, between 1 and 250 m deep, in a wide range of habitats, including rocky and sandy bottoms and seagrass meadows [17]. Its diurnal habits and evident coloration make it clearly visible on any substrate. They live in habitats that are easily accessible and, hence, their collection does not present logistic problems. Its size is sufficiently large to allow easy experimental manipulation and observation of regenerating stages, but still small enough to allow advanced microscopic analyses (e.g., transmission electron microscopy) of the regenerates. Although, as all echinoderms, it is difficult and time-consuming to achieve a full life cycle in the laboratory, adult specimens are rather robust and can be easily maintained in laboratory conditions for long periods (several months or up to 1 year). Overall, these practical features make it a valid and easy-to-handle research model. Indeed, it has been used for many years as model species to study arm tip regeneration using both morphological [18, 19] and molecular [20] approaches. Now we have extended the potential of the species by introducing the culture of arm explants, allowing a more efficient control over the regenerative process. Critical aspects of arm regeneration, such as the control of polarity, the dependence on positional cues, the origin of cells contributing to the different tissues and the regulatory aspects controlling the patterning of newly grown structures, are here more easily studied. In fact, the WBR potential of a single arm or arm piece can be better investigated using arm explants since culturing them allows both better control and easy reproducibility of growing conditions. A seemingly trivial, but extremely useful, characteristic of our model is that, being pentamerous animals, experimentally manipulated and control arm fragments can always be derived from the same animal.

In this chapter, we report methods for collecting and maintaining *E. sepositus* in the laboratory, preparing double-amputated arm explants, and studying the histology/ultrastructure of the regenerative processes using light and transmission electron microscopy (TEM), methods that we complement with those for extracting RNA used for intensive molecular analyses, such as transcriptomics.

2 Materials

All reagents should be prepared using autoclaved filtered distilled water (dH_2O) and kept at room temperature (RT), unless otherwise specified.

2.1 Starfish Collection and Husbandry

1. SCUBA diving equipment: gloves, net.
2. Coolers.
3. Husbandry setup: 50 L glass aquaria, circulation pump, chemical filter (activated charcoal), biological filter (ceramic rings), mechanical filter (filter wool), water oxygenator.
4. Artificial Sea Water (ASW): 37 g commercial marine salts (e.g., Sea Salt, Instant Ocean®) in 1 L deionized water (*see* **Note 1**).
5. Aquarium refrigeration system.
6. Aquarium illumination system with photoperiod control.
7. pH meter.
8. Salinity meter: densimeter or refractometer.
9. Water quality measuring kits: NO_2, NO_3, Cl_2, GH (general hardness), KH (carbonate hardness).
10. Marine oligo-elements (e.g., Marine trace, Seachem).
11. Nitrifying bacteria (e.g., Bactiva, Aquaristica).
12. 1 M $Ca(OH)_2$.
13. Starfish food: 1 cm^3 pieces of squid. Store at −20 °C for up to 1 month.

2.2 Fixation and Epoxy Resin Embedding

Wear gloves and a lab coat and work under a fume hood.

1. 0.2 M sodium cacodylate stock solution: 0.2 M sodium cacodylate trihydrate in dH_2O—pH 7.4 (use drops of 1 M NaOH to adjust pH).
2. 0.1 M sodium cacodylate buffer: 1:1 (v:v) 0.2 M sodium cacodylate stock solution in dH2O. Use a freshly prepared solution, store at 4 °C.
3. Fixative solution: 2% (v/v) glutaraldehyde, 1.4% (w/v) NaCl, in 0.1 M sodium cacodylate buffer (*see* **Note 2**). Use a freshly prepared solution, store at 4 °C.
4. Postfixative solution: 1:1:2 (v:v:v) 4% (v/v) osmium tetroxide, dH_2O and 0.2 M sodium cacodylate stock solution. Osmium tetroxide is highly toxic and must be handled with care. Use a freshly prepared solution, store at 4 °C in darkness.
5. Decalcifying solution: 1:1 (v:v) 4% (w/v) L-ascorbic acid with 0.6 M NaCl. Use a freshly prepared solution, store at 4 °C in darkness.
6. UA solution: 2% (w/v) uranyl acetate in 25% ethanol (EtOH). Uranyl acetate is radioactive and must be handled with care (*see* **Note 3**). Use a freshly prepared solution, store at RT in darkness.
7. Propylene oxide (commercially available solution). Allow to equilibrate at RT before use. Store at 4 °C (*see* **Note 4**).

8. Propylene oxide–Epoxy resin mixture solutions: mix propylene oxide and Epoxy resin in different proportions: 3:1, 1:1, and 1:3. Use a vortex to mix the different solutions and wait until small air bubbles have completely disappeared.
9. Epoxy resin: Epon Araldite-812 (e.g., Fluka-Merck) four components (called A/M, B, C, and Epon). Mix under a fume hood at RT 10 mL A/M, 30 mL B, 12 mL Epon, and 0.8 mL C. Gently mix, avoiding formation of air bubbles, until the resin reaches a homogeneous orange color and honey-like consistency (*see* **Note 5**). Aliquot, store for long term at −20 °C and for short term at 4 °C. Allow to equilibrate at RT under a fume hood before use.
10. Stereomicroscope.
11. Large (at least 1 cm^3) labeled embedding molds (*see* **Note 6**).

2.3 Semithin and Ultrathin Sectioning and Staining

1. Sodium methoxide.
2. 100% methanol (MeOH).
3. 100% EtOH.
4. Crystal violet stain: 1% (w/v) crystal violet in dH_2O, add few drops of 100% EtOH to help dissolving the powder.
5. Basic fuchsin stain: 1% (w/v) basic fuchsin in dH_2O, add few drops of 100% EtOH to help dissolving the powder.
6. Embedding medium (e.g., Eukitt®).
7. 1% (w/v) uranyl acetate in dH_2O (*see* **Note 3**).
8. Lead citrate solution: 1.33 g $Pb(NO_3)_2$, 1.76 g $Na_3(C_6H_5O_7)$ $\bullet 2H_2O$ in 30 mL dH_2O. Shake vigorously for 1–2 min. After 30 min, add 8 mL 1 N NaOH and dH_2O to a final volume of 50 mL. Mix by inversion. Faint turbidity, if present, can be removed by centrifugation.
9. Ultramicrotome.
10. Heater.
11. Light microscope.
12. Disposable glass knife with plastic knife boats (fixed with wax).
13. Glass pipette with round tip (prepared rounding the tip on a flame).
14. Eyelash tool: pull one eyelash, insert it in a glass pipette tip, fix it with a drop of melted wax.
15. Circle tool: prepare a small copper circle (diameter around 3 mm), insert it in a glass pipette tip, fix it with a drop of melted wax.
16. TEM grids (*see* **Note 7**).
17. TEM grid storage box.

2.4 RNA Extraction

1. TRIzol (e.g., Thermo Fisher).
2. Chloroform.
3. RNA *later* (e.g., Thermo Fisher)/liquid nitrogen.
4. Isopropanol.
5. RNase-free water.
6. 75% EtOH in dH_2O.
7. Handheld homogenizer (Pellet Pestle Motor).
8. Pellet pestles.
9. Refrigerated centrifuge.
10. Microvolume spectrophotometer (e.g., NanoDrop, Thermo Fisher Scientific). Agilent 2100 Bioanalyzer System.

3 Methods

3.1 Starfish Collection and Husbandry

1. SCUBA dive in an unpolluted marine area inhabited by *Echinaster sepositus*.
2. Identify a healthy adult specimen (10–12 cm in diameter).
3. Transfer the animal using SCUBA gloves into an appropriate SCUBA net.
4. Repeat **steps 2** and **3** to collect other specimens (see **Note 8**).
5. Transfer the animals into coolers half-filled with fresh seawater (see **Note 9**).
6. Transport them to the laboratory/aquaria facility within the next 2–3 h (see **Note 10**).
7. Add the same volume of ASW as there is natural seawater in each cooler.
8. Wait 2 h for the starfish to acclimate to both the ASW and the new temperature.
9. Transfer 4–5 animals per husbandry setup.
10. Set the photoperiod at 12 h:12 h light–dark.
11. Feed each animal by placing a piece of starfish food (e.g., squid pieces) directly in its mouth.
12. Check that the ASW temperature is about 17 °C.
13. Check that salinity is between 37 and 38‰.
14. Check that pH is between 8–8.2 (see **Note 11**).
15. Use the water quality measuring kits to monitor the chemical parameters of the husbandry systems.

16. Replace half of the aquarium ASW volume in each system with new ASW if NO_2 and NO_3 levels are higher than 0 mg/L and 100 mg/L, respectively.
17. Add nitrifying bacteria elements following manufacturer's instructions.
18. Add marine oligo-elements following manufacturer's instructions.
19. Repeat **steps 11** to **18** for a second week of acclimatization.
20. Continue the maintenance following the same schedule until the end of the experiments.

3.2 Arm Explants

1. Place a starfish on a flat and hard support for amputation (*see* **Note 12**).
2. Amputate one arm proximally at one third of the arm's length with a razor blade (Fig. 2a).
3. Amputate the isolated arm a second time distally at the level of two third of the arm within the next 5 min (Fig. 2a).
4. Repeat **steps 2** and **3** to double amputate all four other arms of the starfish.
5. Collect the five "central" arm segments (the double-amputated arm explants), about 2 cm long.
6. Place the arm explants in properly labeled glass containers filled with ASW (Fig. 2b).

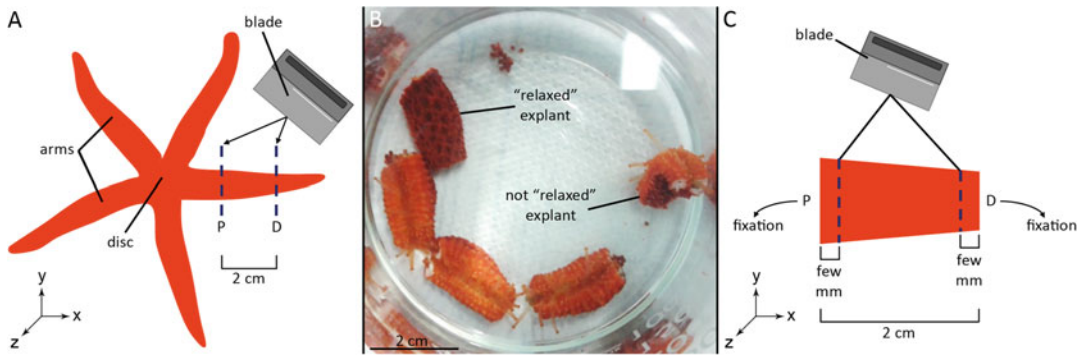


Fig. 2 Starfish arm explant preparation, collection and fixation. (**a**) Top view (*x*–*z*) scheme of *E. sepositus* (aboral side), in which the disc and five slender arms are visible. Using a blade, the central third of each arm is traumatically amputated proximally (P) and distally (D) to obtain five arm explants approximately 2 cm long. For clarity, the amputation of only a single arm is shown. (**b**) After amputation, arm explants are placed back in the aquaria and left to regenerate for the prefixed time-points. They are then collected from the aquaria and placed in glass containers filled with ASW until they are completely "relaxed" (neither curled nor twisted). (**c**) Top view (*x*–*z*) scheme of a "relaxed" regenerating arm explant sectioned using a blade in three portions: proximal, central, and distal. The proximal and distal portions (smaller than the central one) of each explant are fixed and will be processed according to TEM protocols, whereas the central portion can be discharged. *Abbreviations*: D, distal end; P, proximal end. Dashed lines = amputation planes

7. Rapidly place the donor starfish in properly labeled glass containers filled with ASW.
8. Repeat this procedure for all experimental starfish. Use a different glass container for each animal.
9. Do not touch the arm explants or move the container for 30–60 min.
10. Gently transfer the arm explants into the aquaria. Avoid touching the amputated ends and allow them to regenerate over the prefixed time-points (see **step 17**).
11. Keep the five arm explants belonging to the same donor starfish separated from those from other specimens using different aquaria (*see* **Note 13**).
12. Place the donor starfish (with all five arms amputated) in the aquarium with the corresponding arm explants (*see* **Note 14**).
13. During the regeneration period, ASW chemical parameters must be checked and promptly adjusted if necessary (as described in **steps 12–18**, Subheading 3.1).
14. Check and annotate the arm explant health status and behavior.
15. Repeat **step 14** every 2–3 days.
16. Remove dead arm explants (showing connective tissue "melting" or whitish spots on the epidermis) from the aquarium; immediately check ASW parameters (as described in **steps 12–14**, Subheading 3.1) and, if necessary, promptly perform ASW changes to avoid NO_2/NO_3 or pathogen contamination of the whole system (as described in **step 16**, Subheading 3.1).
17. Define at least three regeneration time-points, for example: 48 h post-amputation (p.a.), 3 weeks p.a. and 10 weeks p.a. (see also Fig. 1 and [16, 18, 19]). Based on our experience, arm explants can be successfully maintained in laboratory conditions for 5–6 months.
18. At each prefixed time-point, collect one arm explant from each donor starfish and process them for downstream analyses, both morphological or molecular.

3.3 Fixation for Transmission Electron Microscopy (TEM)

From now on, always wear gloves and a lab coat and work under a fume hood. All solutions should be carefully and gently transferred using clean disposable glass pipettes. All steps should be performed on an orbital shaker (gentle shaking) to facilitate solution penetration and washes. Prepare glass containers with proper labeling for each sample. Before starting, heat the oven at 65 °C. Troubles possibly arising during protocol performance and corresponding troubleshooting are listed in Table 1.

Table 1
Table summarizing common problems arising during microscopy protocol and corresponding troubleshooting

Trouble	Troubleshooting
Poor fixation (possibly due to wrong component concentrations, pH, storage conditions, or contamination) *See* Fig. 4a, b	1. Make sure that the fixative solution is not contaminated (precipitates or debris should not be present) 2. Make sure that the fixative solution has been properly stored, namely, at 4 °C. if so, go to **step 3** 3. Measure the pH of the in 0.2 M sodium cacodylate buffer used to prepare the fixative solution. Adjust to 7.4, using NaOH or HCl depending on recorded value, and use it to prepare a fresh fixative solution 4. Measure the pH of the fixative solution. Adjust to 7.4, using NaOH or HCl depending on recorded value If fixation is still unsatisfactory, prepare fresh fixative solution. Pay particular attention to NaCl concentration and pH. Use the correct ratio of fixative solution per sample volume (1:20). Timing of fixation can be increased up to 2–3 days at 4 °C. Avoid longer fixation to prevent tissue shrinkage
Poor decalcification (possibly due to wrong component concentrations, storage conditions, or contamination) *See* Fig. 4c, d	1. Make sure that the decalcifying solution is not contaminated (precipitates or debris should not be present) 2. Make sure that the decalcifying solution has been properly stored, namely, at 4 °C in darkness If decalcification is still unsatisfactory, prepare fresh decalcifying solution. It is recommended to use larger volumes of solution and change it more frequently to facilitate the decalcification process. Avoid decalcification longer than 3 days at 4 °C in darkness. As suggested, perform the decalcification step on an orbital shaker
Poor dehydration (possibly due to wrong ethanol concentrations or storage conditions)	1. Make sure that the dehydration steps have been properly performed, namely, ethanol has been properly stored and used glass containers have been properly dried before use If dehydration is still unsatisfactory, it is recommended to use larger volumes of ethanol solutions and increase time of each dehydration step. Avoid leaving the samples in direct contact with air during solution changes to prevent tissue rehydration
Poor embedding medium infiltration (possibly due to wrong component concentrations or storage conditions)	1. Make sure that epoxy resin aliquots have been properly stored, namely, well closed, at RT during use, at 4 °C for short-term storage and at

(continued)

Table 1
(continued)

Trouble	Troubleshooting
	−20 °C for long-term storage 2. If epoxy resin does not show the typical honey-like viscosity/consistency and color, prepare fresh epoxy resin and discharge the previous stock If necessary, the proportions of epoxy resin and propylene oxide could be changed to have a more gradual medium infiltration. Perform all steps in the orbital shaker to facilitate embedding medium infiltration
Poor embedding medium polymerization (possibly due to wrong polymerization temperature or timing)	1. Make sure that the temperature of the oven has been properly set, namely, at 65 °C 2. Make sure that the oven has not been opened during the polymerization days 3. Make sure that the oven temperature is stable during the whole polymerization period, namely, 3 days 4. Make sure that polymerization has been performed for the right number of days, namely, 3 If polymerization is still poor, change oven. Note that epoxy resin polymerization can occur also at RT but it will last much longer. Therefore, when possible, prefer polymerization in stable conditions of temperature and humidity that the oven guarantees
Problems with semithin sectioning (possibly due to glass knife damages or ultramicrotome problems). Figure 4e, f	1. Make sure that the glass knife is not compromised. If so, use a new one 2. Make sure that all ultramicrotome parts are well fixed and oriented 3. Make sure that thickness of the section is around 1 μm 4. Make sure that the plastic knife boat is properly fixed to the glass knife, sectioning speed and glass knife orientation are correct in order to avoid on the sample surface the presence of drops that can compromise the sectioning. If so, change it Semithin section thickness and ultramicrotome section speed can be optimized during sectioning. Indeed, both slightly thicker and thinner sections as well as slightly faster and slower section speed can result in better semithin sections. The researcher has to try different combinations to obtain satisfactory results

(continued)

Table 1
(continued)

Trouble	Troubleshooting
Poor semithin section staining (possibly due to wrong solution concentrations or storage). *See* Fig. 4i, j	1. Make sure that sodium methoxide and staining solutions have been properly stored, namely, at RT 2. If debris are present on the glass slides, filter the staining solutions using a syringe and a 0.2 μm filter If staining is still unsatisfactory, both timing of sodium methoxide and staining, and staining solution concentrations can be increased or decreased. Sodium methoxide should be usually increased. Note that differences in staining can be present between samples simply due to sample variability, therefore, the researcher can perform few trials before finding right staining timing and concentrations
Problems with ultrathin sectioning (possibly due to glass knife damages or ultramicrotome problems). *See* Fig. 4g, h	1. Make sure that the glass knife is not compromised. If so, use a new one 2. Make sure that all ultramicrotome parts are well fixed and oriented 3. Prefer using the left side of the glass knife for ultrathin sectioning 4. Make sure that the plastic knife boat is properly fixed to the glass knife in order to avoid on the sample surface the presence of drops that can compromise the sectioning. If so, change it Ultrathin section thickness and ultramicrotome section speed can be optimized during sectioning. Indeed, both slightly thicker and thinner sections as well as slightly faster and slower section speed can result in better ultrathin sections. The researcher has to try different combinations to obtain satisfactory results, namely, ultrathin sections of the following colors: Gold, silver, and white
Poor ultrathin section staining (possibly due to wrong solution concentrations and storage or contamination). *See* Fig. 4k, l	1. Make sure that solutions are not contaminated (precipitates or debris should not be present) 2. Make sure that solutions have been properly stored, namely, UA solution at RT and lead citrate solution at 4 °C 3. If debris are present on the ultrathin sections, filter again the staining solutions using a syringe and a 0.2 μm filter If staining is still unsatisfactory, the researcher can increase the timing of staining, namely, up to 30 min for UA solution and up to 15 min for lead citrate. If so, the following washes in dH_2O can be increased to guarantee the complete elimination of both solutions

(continued)

Table 1
(continued)

Trouble	Troubleshooting
Poor ultrathin section carbon-coating (possibly due to wrong carbon-coating procedure)	1. Make sure that carbon-coating procedure has been properly performed following manufacturer's instructions 2. Perform a second carbon-coating Note that this step of the protocol can be omitted if the transmission electron microscope (TEM) ensures a good level of contrast. Check TEM characteristics with the TEM technician before performing carbon-coating, since it can result unnecessary to obtain micrographs of high quality, in terms of contrast

1. Immediately after collecting the regenerating arm explants, use tweezers to gently transfer them to labeled glass containers filled with ASW.
2. Wait for at least 30 min until they are completely "relaxed"—not curled or twisted, since this can impair fixation and precisely orientated sectioning (Fig. 2b).
3. Gently transfer the arm explants to labeled glass containers filled with fixative solution, avoiding to touch the regenerating tissues with the tweezers.
4. Leave the arm explants in fixative solution for at least 30 min at RT. Place one arm explant on a flat and hard support for amputation (*see* **Note 15**).
5. Rapidly section the arm explant into three portions using a blade: the proximal third, the central third, and the distal third (Fig. 2c) (*see* **Note 16**).
6. Using tweezers, place samples in properly labeled glass containers filled with fresh fixative solution.
7. Discard the central portion.
8. Repeat **steps 3** to **7** for all arm explants.
9. Leave samples in fixative solution for 2 h at 4 °C (*see* **Note 17**). Use a 1:20 volume ratio of fixative solution to sample volume (*see* **Note 18**). Samples can be stored in the fixative solution at 4 °C up to 3 days before further processing.
10. Perform two rapid washes followed by two washes of 15 min in 0.1 M sodium cacodylate buffer to completely remove all traces of fixative solution.
11. Leave samples in the same buffer overnight at 4 °C (*see* **Note 19**).
12. Let samples equilibrate to RT.

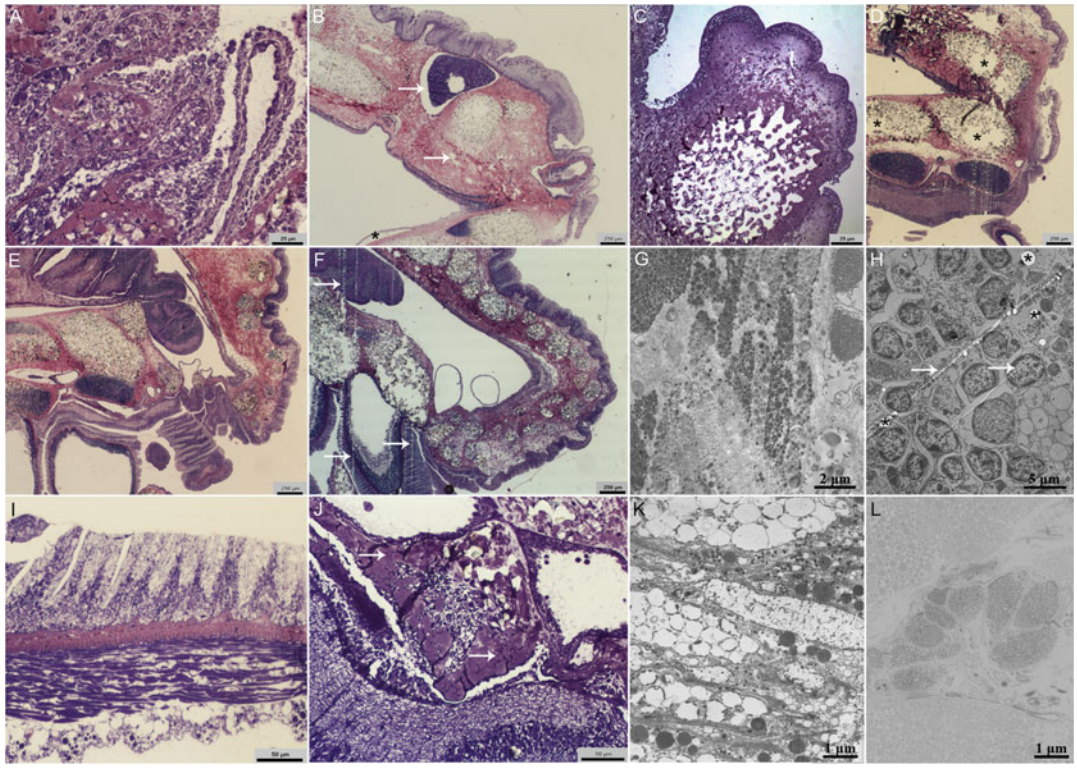


Fig. 4 Example pictures. Light microscopy images (**a**–**f**, **i**, **j**) and TEM micrographs (**g**, **h**, **k**, **l**) showing examples of satisfactory and unsatisfactory results in terms of sample fixation and decalcification, and semithin and ultrathin sectioning and staining. (**a**) Semithin section showing satisfactory sample fixation. All tissues are well preserved. (**b**) Semithin section showing unsatisfactory sample fixation. Artifacts are visible as lacunae and spaces in the tissues (arrows) as well as epithelium detachment (asterisk). (**c**) Semithin section showing satisfactory sample decalcification. The skeletal tissues of a spine, that is, trabeculae are well preserved and no signs of calcium carbonate crystals are visible. (**d**) Semithin section showing unsatisfactory sample decalcification. Skeletal tissues of the ossicles (asterisks) are not well preserved and tissue integrity is therefore lost. (**e**) Semithin section showing satisfactory semithin sectioning. All tissues are well preserved. (**f**) Semithin section showing unsatisfactory semithin sectioning. Vertical lines (arrows) are artifacts due to the sectioning, in particular, to the damaged glass knife edge. (**g**) TEM micrograph showing satisfactory ultrathin sectioning. All tissues are well preserved. (**h**) TEM micrograph showing unsatisfactory ultrathin sectioning. Lines (arrows) and holes (asterisks) are artifacts due to the sectioning, in particular, to the damaged glass knife edge. (**i**) Semithin section showing satisfactory semithin staining. The difference between diversely stained tissues is well visible and different tissue identification is therefore easy and clear. (**j**) Semithin section showing unsatisfactory semithin staining. Basic fuchsin staining (arrows) is not clearly distinguishable from crystal violet staining. Therefore, tissue identification can be more difficult or even wrong. (**k**) TEM micrograph showing satisfactory ultrathin staining. Contrast between electron-dense and electron-lucent cellular elements is well defined. (**l**) TEM micrograph showing unsatisfactory ultrathin staining. Low contrast between electron-dense and electron-lucent portions make it difficult to distinguish among different tissues/cellular elements

13. Remove the 0.1 M sodium cacodylate buffer.
14. Add the postfixative solution.

15. Leave samples immersed in this solution for 2 h at RT in darkness (*see* **Note 20**).
16. Remove the postfixative solution.
17. Perform four gentle washes with autoclaved filtered dH_2O to completely remove traces of osmium tetroxide of the postfixative solution (*see* **Note 21**).
18. Remove dH_2O from the previous wash.
19. Add the decalcifying solution.
20. Leave samples in this solution for at least 24 h in darkness at 4 °C (*see* **Note 22**), changing the solution at least twice a day.
21. Remove the decalcifying solution.
22. Perform several rapid washes in autoclaved filtered dH_2O to completely remove the decalcifying solution.
23. Remove dH_2O from the previous wash.
24. Add 2% (w/v) uranyl acetate in 25% EtOH; leave samples in this solution for 2 h at RT in darkness.
25. Remove the 2% (w/v) uranyl acetate in 25% EtOH.
26. Perform at least 3–4 rapid washes in 25% EtOH to completely remove all traces of the previously used solution.
27. Remove the 25% EtOH from the previous wash.
28. Perform a dehydration in an increasing scale of ethanol: 25%, 50%, 70%, 90%, 95% (two washes of 15 min each), and 100% (three washes of 20 min each) (*see* **Note 23**) at RT. Be sure that samples are never left in direct contact with air, to prevent their rehydration (Table 1).
29. Remove the 100% EtOH from the previous wash.
30. Perform 3–4 rapid washes in propylene oxide at RT.
31. Transfer each of the propylene oxyde-Epoxy resin solutions in the order specified at **step 8** of Subheading 2.2 and leave samples for 1 h in each solution at RT (*see* **Note 24**). When samples are immersed in the first two solutions, glass containers should be left closed; when samples are immersed in the third solution, glass containers should be left partially opened to allow the propylene oxide to evaporate at RT.
32. Remove the remaining 1:3 propylene oxide and Epoxy resin solution.
33. Add pure Epoxy resin and leave samples in pure Epoxy resin overnight at RT under a fume hood.
34. Prepare properly labeled silicon/plastic molds according to the sample size.
35. Add pure Epoxy resin to each mold.

36. Transfer each sample to the corresponding mold using tweezers, avoiding touching the regenerating tissues. During embedding, properly orient samples to facilitate subsequent sectioning. Work under a stereomicroscope positioned under a fume hood, if necessary (*see* **Note 25**).
37. After a final check of the samples' orientation, carefully transfer them to an oven set at 65 °C.
38. Wait 2 days for the resin blocks to polymerize. To avoid changing the temperature and humidity in the oven chamber, do not open the oven during this period (Table 1).
39. Remove the resin blocks from the oven.
40. Store the samples at RT in darkness (*see* **Note 26**).

3.4 Semithin Sectioning and Staining

From now on, always wear gloves and a lab coat.

1. Remove the resin block containing the sample selected for sectioning from the mold.
2. Insert the resin block into the ultramicrotome's sample holder, properly orienting it according to the desired sectioning plane (longitudinal, transverse, frontal, etc.).
3. Fix the resin block tightly to prevent movement during sectioning.
4. Using a blade and working under the stereomicroscope of the ultramicrotome, shape (trim) the resin block to create a pyramid trunk carefully removing excess of resin around the sample (Fig. 3a).
5. Tightly fix the sample holder to the ultramicrotome arm.
6. Fix the glass knife with the plastic boat to the knife stage (*see* **Note 27**).
7. Using a 1 mL syringe add autoclaved filtered dH_2O to the plastic knife boat.
8. Using the proper wheels of the ultramicrotome, orient the knife and the resin block to achieve the desired sectioning orientation.
9. After adjusting the needed parameters of the ultramicrotome, begin sectioning semithin sections of 1 μm in thickness (Fig. 3b). If sectioning is unsatisfactory, the thickness of semithin sections and the speed of sectioning can be modified—a slightly higher thickness than 1 μm and a slower ultramicrotome sectioning speed may result in better semithin sections, considering their quite large square surface (Table 1).
10. Collect semithin sections on properly labeled glass slides (*see* **Note 6**) using a glass pipette. Slowly approach the sections from below, collecting them from below with the glass pipette rounded tip; gently place them in the autoclaved filtered dH_2O drops, prepared using a 1 mL syringe (Fig. 3c).

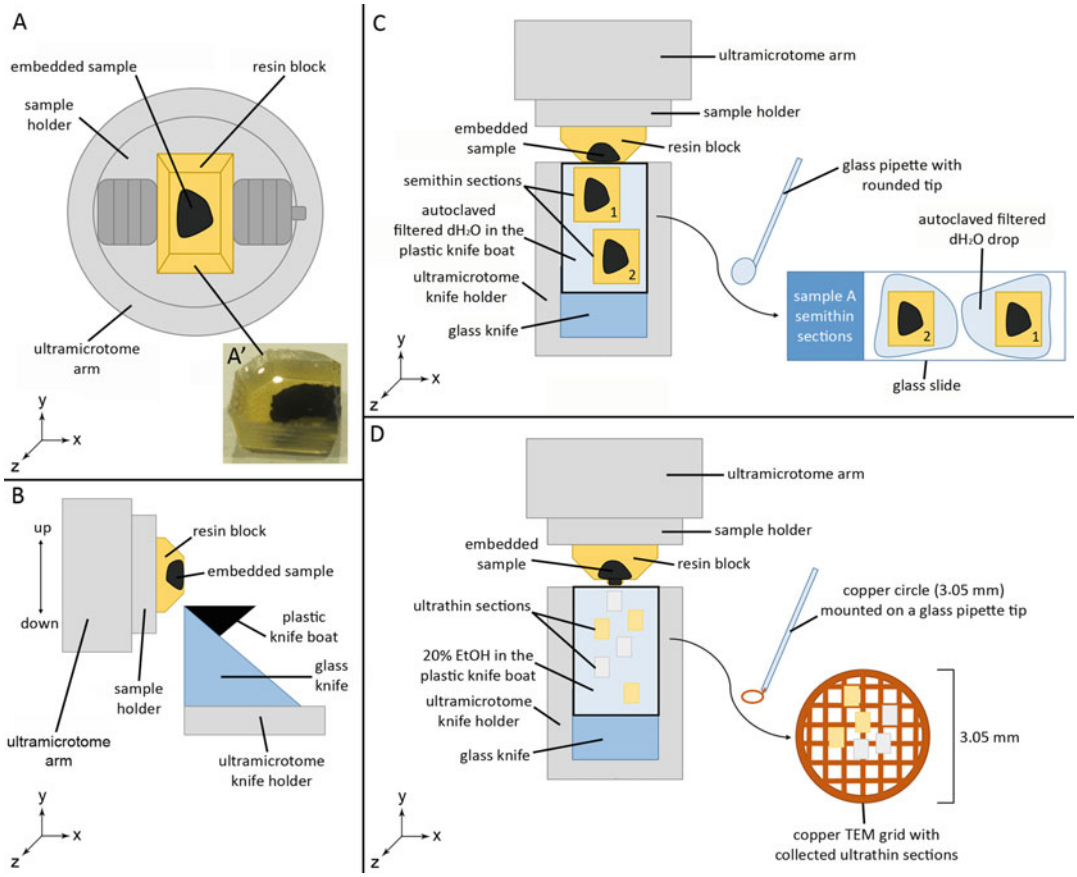


Fig. 3 Procedures to follow for semithin and ultrathin sectioning and semithin and ultrathin section collection. (**a**) Frontal view (*x*–*y*) scheme of the resin block with the embedded sample (black) tightly fixed in the ultramicrotome sample holder, which is positioned in the ultramicrotome arm. (A') Top view (*x*–*z*) image of a resin block with an embedded sample of starfish arm explant. The embedded sample appears black due to postfixation in osmium tetroxide. (**b**) Lateral view (*y*–*z*) scheme of the resin block with the embedded sample (black) positioned in the ultramicrotome arm and of the glass knife (with the plastic knife boat) fixed on the ultramicrotome knife holder. Each time the ultramicrotome arm goes up and down (black arrow on the left), a section (1 μm for semithin sections and 50–90 nm for ultrathin sections) is sectioned by the glass knife and floats onto the liquid within the plastic knife boat, which contains autoclaved filtered dH_2O for semithin sections or 20% EtOH in autoclaved filtered dH_2O for ultrathin sections. (**c**) Semithin section collection. Top view (*x*–*z*) scheme of the glass knife with a plastic knife boat; two semithin sections are floating onto the autoclaved filtered dH_2O inside. Using a disposable glass pipette with a rounded tip, semithin sections can be transferred into autoclaved filtered dH_2O drops on a labeled glass slide (top view; *x*–*z*). (**d**) Ultrathin section collection. Top view (*x*–*z*) scheme of the glass knife with a plastic knife boat; six ultrathin sections are floating onto the 20% EtOH in autoclaved filtered dH_2O inside. Ultrathin sections are much smaller than semithin sections. Using a copper circle mounted on a disposable glass pipette tip, ultrathin sections can be collected from above (maintaining the copper circle parallel to the liquid surface) and positioned on the copper TEM grid (top view; *x*–*z*)

11. Allow the water drops to dry on a heater (70 °C) in a horizontal position.
12. Using a disposable glass pipette place several drops of sodium methoxide on the sections, allowing it to completely remove the resin for at least 30 s.
13. Insert slides into a glass Coplin jar filled with 100% MeOH for 1 min to remove the sodium methoxide.
14. Insert slides into a glass Coplin jar filled with 100% EtOH for 1 min to remove the 100% MeOH.
15. Rapidly wash the slides with tap water followed by autoclaved filtered dH_2O.
16. Allow the dH_2O to dry on a heater (70 °C) in a horizontal position.
17. Using a disposable glass pipette place several drops of 1% (w/v) crystal violet on the sections, allowing it to stain for 30–60 s. The staining time must be optimized according to the type of tissue either changing crystal violet concentration or staining time (Table 1 and Fig. 4).
18. Rapidly wash the slides with tap water and autoclaved dH_2O.
19. Allow the dH_2O to dry on a heater (70 °C) in a horizontal position.
20. Using a disposable glass pipette place several drops of 1% (w/v) basic fuchsin on the sections, allowing it to stain for 15–30 s. The staining time must be optimized according to the type of tissue either changing basic fuchsin concentration or staining time (Table 1 and Fig. 4).
21. Rapidly wash the slides with tap water followed by autoclaved dH_2O.
22. Allow the dH_2O to dry on a heater (70 °C) in a horizontal position.
23. Mount the slides using few drops of Eukitt® and glass coverslips according to the number of sections present on the glass slides.
24. Let the Eukitt® dry for several minutes on the heater (70 °C) in a horizontal position.
25. Observe the slides under a light microscope. If staining is not satisfactory, modify the staining concentrations (both lower and higher than 1% (w/v)), as well as the staining time (both lower and higher than 15–60 s) on the following slide (Table 1 and Fig. 4).
26. Repeat **steps 8** to **25** to continue sectioning, collection, and observation of semithin sections until the desired sample plane with tissues of interest has been reached.

27. Leave mounted glass slides overnight at RT in a horizontal position.
28. Store mounted glass slides indefinitely in proper glass slide boxes at RT in darkness.

3.5 Ultrathin Sectioning

From now on, always wear gloves and a lab coat.

1. After reaching the desired sample plane, performing the semithin sectioning, and checking the tissues of interest under the light microscope, remove the sample holder from the ultramicrotome arm.
2. Place the sample holder on the sample stage.
3. Using a thin blade and working under the ultramicrotome's stereomicroscope, shape (trim) the sample surface to create a small pyramid trunk (less than 1 square mm) only on the desired tissues (*see* **Note 28**).
4. Place the sample holder back on the ultramicrotome arm and close tightly.
5. Using a 1 mL syringe remove autoclaved filtered dH_2O from the plastic knife boat.
6. Using a 1 mL syringe add 20% EtOH in autoclaved filtered dH_2O to the plastic knife boat.
7. After adjusting the needed parameters of the ultramicrotome, begin sectioning ultrathin sections of 50–90 nm in thickness (Fig. 3d). If sectioning is not satisfactory, modify the thickness of ultrathin sections and the speed of sectioning; slightly higher or lower thickness than 50–90 nm and a slower ultramicrotome sectioning speed may result in better ultrathin sections (Table 1 and Fig. 4).
8. Ultrathin sections floating on the 20% EtOH inside the plastic knife boat can be serially and carefully collected on a TEM grid.
9. Only white, silver, or gold ultrathin sections must be collected: indeed, the color of the section indicates the correct thickness (between 50 and 90 nm). Sections that are too thick (more than 100 nm) show a different color, namely, blue, green, or pink.
10. To collect ultrathin sections, use an eyelash mounted on a glass pipette. Do not directly touch the sections with the eyelash. It is better to use the eyelash to move the 20% EtOH around the sections to group them before collection.
11. Decide which side of the TEM grid to use to collect the sections; use the same side for all grids.
12. Using tweezers (without excessive pressure to avoid deformation), pick a TEM grid.

13. Slowly collect all sections inside using a small copper circle by approaching them from above.
14. Maintaining the copper circle parallel to the TEM grid surface, slowly approach the TEM grid and allow the sections to adhere to the grid surface (Fig. 3d).
15. Once sections have been attached to the grid surface, gently remove excess 20% EtOH using a small piece of filter paper.
16. After the grid has completely dried, store it in a TEM grid storage box with proper labeling (*see* **Note 29**).
17. Repeat **steps 7** to **16** to continue sectioning and collecting ultrathin sections of the tissues of interest.
18. If desired, after ultrathin sectioning, some semithin sections can also be collected, stained, and observed (as described in Subheading 3.4) in order to determine if ultrathin sectioning of the tissue of interest is complete.

3.6 Ultrathin Section Staining and TEM Grid Carbon-Coating

From now on, always wear gloves and a lab coat and work under a fume hood for the ultrathin section staining.

1. Insert 1 mL of 1% (w/v) uranyl acetate in a 1 mL syringe covered with aluminum foil to block radiation.
2. Prepare a piece of Parafilm® in a large glass petri dish.
3. Using this syringe with the 0.2 μm filter, prepare a droplet of 1% (w/v) uranyl acetate on the Parafilm® for each grid that must be stained (*see* **Note 30**).
4. Transfer the selected grids face down on the single droplets using tweezers (do not touch ultrathin sections while handling the grids). Be sure that the side of the grids with ultrathin sections is in direct contact with the staining solution. If properly done, the grids will float on the droplets due to surface tension (Fig. 5a).
5. Close the large glass petri dish and cover it with aluminum foil to block radiation.
6. Wait for 20 min.
7. Use a 1 mL syringe with a 0.2 μm filter to prepare (on another piece of Parafilm®) 10 droplets of autoclaved filtered dH_2O for each grid.
8. Use a 1 mL syringe with a 0.2 μm filter to prepare (on another piece of Parafilm®) a droplet of lead citrate solution for each grid that must be stained.
9. In the large glass petri dish where the piece of Parafilm® is positioned, insert 3–4 NaOH pellets in order to keep the glass petri dish dry.

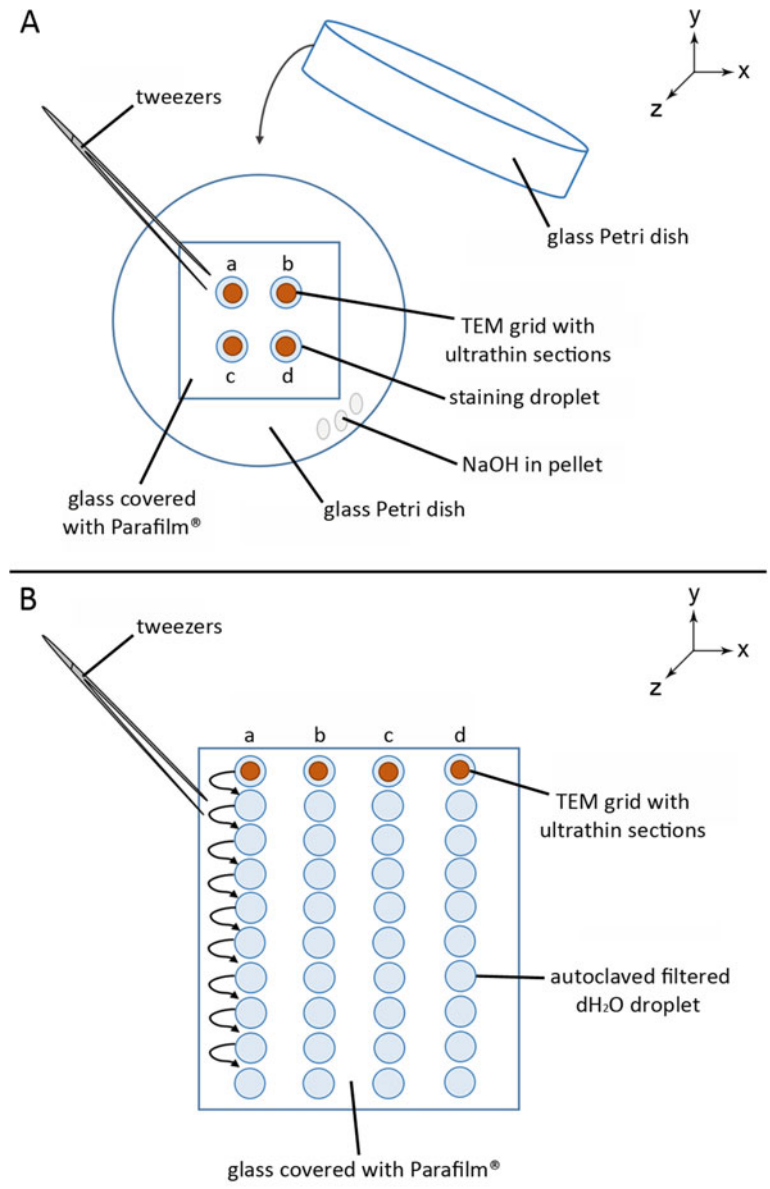


Fig. 5 Ultrathin section staining procedure. (**a**) Top view (*x*–*z*) scheme of TEM grid staining. TEM grids are gently placed in droplets of staining solution using tweezers. The TEM grid position is accurately labeled. When exposed to 1% uranyl acetate, the glass petri dish must be covered with aluminum foil and must not contain NaOH pellets. The latter are needed only in the lead citrate step. (**b**) Top view (*x*–*z*) scheme of TEM grid-washing steps after staining. TEM grids are gently washed in subsequent autoclaved filtered dH_2O droplets, using tweezers (arrows) to completely remove traces of staining solution (1% uranyl acetate or lead citrate). During all steps, ultrathin sections face the liquid. The droplets of various solutions are prepared on a glass covered with Parafilm®, using 1 mL syringes with a 0.2 μm filters. The TEM grid position is accurately labeled

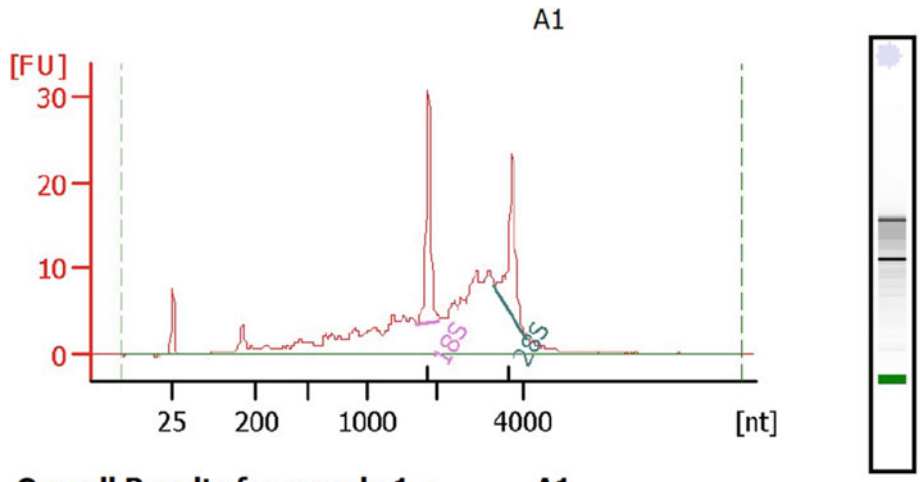
10. Wait until the grids have been in the staining solution for 20 min.
11. Gently using tweezers, sequentially transfer each grid (always face down) to the 10 droplets to rapidly wash the ultrathin sections and eliminate all traces of 1% (w/v) uranyl acetate. If properly done, the grids will float on the droplets due to surface tension (Fig. 5b).
12. When all grids have been washed, gently use tweezers to transfer them (face down) to the single droplets of lead citrate solution. If properly done, the grids will float on the droplets due to surface tension (Fig. 5a).
13. Wait for 8–12 min, depending on the level of contrast needed (Table 1 and Fig. 4).
14. During this time, use a 1 mL syringe with a 0.2 μm filter to prepare (on another piece of Parafilm®) 10 droplets of autoclaved filtered dH_2O for each grid.
15. Gently using tweezers, sequentially transfer each grid (always face down) to the 10 droplets to rapidly wash the ultrathin sections and eliminate all traces of lead citrate solution. If properly done, the grids will float on the droplets due to surface tension (Fig. 5b).
16. Gently dry for few seconds all grids using a small piece of filter paper. Avoid direct contact between the filter paper and ultrathin sections positioning the grid face up on the filter paper.
17. Transfer the grids face up on a properly labeled piece of filter paper.
18. Transfer the grids to a carbon-coater and follow the manufacturer's instructions to coat the ultrathin sections with a thin layer of carbon that will stabilize the ultrathin sections under the TEM beam. This step can be omitted (Table 1).
19. Store the grids in the TEM grid storage box at RT in darkness until observation under TEM.
20. Image the sections using TEM following the manufacturer's instructions.
21. If ultrathin section staining (contrast) results are not satisfactory during observation under TEM, increase the staining times for both 1% (w/v) uranyl acetate and lead citrate (Table 1 and Fig. 4).

3.7 RNA Extraction

The following protocol has been successfully employed to perform RNA extraction from regenerating arm tips of both asteroids and ophiuroids. It has been performed on *E. sepositus* regenerating arm explants, with the same success (*see* **Note 31**). The extraction protocol final aim has been either the cloning of fragments by

conventional PCR [21] or obtaining RNA of high quality for transcriptome analysis [22]. From now on, always wear gloves and a lab coat and work under a fume hood.

1. Using a scalpel, dissect out the regenerating tissues from both sides (proximal and distal) of each regenerating explant, and avoid collection of nonregenerating tissues or stump tissue.
2. Immediately freeze each piece (regenerating tissue) in a properly labeled 1.5 mL tube in liquid nitrogen or in RNA *later* or go to **step 5** to start RNA extraction from fresh tissue.
3. Store samples at −80 °C (liquid nitrogen) or at −20 °C (RNA *later*) for up to several months until use.
4. Remove the samples from the freezer and keep on ice.
5. Add 1 mL of TRIzol per approximatively 100 mg of tissue. Once the TRIzol is added it is not needed to work on ice any more.
6. Homogenize each sample using the Pellet Pestle Motor.
7. Mix the sample by pipetting up and down a few times using a P1000.
8. Add 200 µL of chloroform per each mL of TRIzol added in **step 5**.
9. Close the tube and shake it vigorously for 15 s.
10. Incubate 2–3 min at RT.
11. Centrifuge the homogenate at 11,000 rcf for 15 min at 2–8 °C.
12. Collect the upper aqueous phase and place it into a new properly labeled 1.5 mL tube.
13. Discard the other phases.
14. Add 500 µL of isopropanol to the solution and incubate at room temperature for 10 min.
15. Spin at 10000 rcf for 10 min at 2–8 °C; a gel-like pellet should form at the bottom of the tube.
16. Carefully remove the supernatant.
17. Add 1 mL of 75% EtOH.
18. Vortex for 5 s at RT.
19. Spin at 10,000 rcf for 5 min at 2–8 °C.
20. Carefully remove the supernatant.
21. Air dry the pellet for 5 min at RT.
22. Dissolve the pellet in 50–100 µL of RNase free water (*see* **Note 32**).
23. Quantify and qualify the obtained RNA using a spectrophotometer (*see* **Note 33** and Fig. 6).



Overall Results for sample 1 : A1

RNA Area:	245,7
RNA Concentration:	149 ng/µl
rRNA Ratio [28s / 18s]:	0,9
RNA Integrity Number (RIN):	6.6 (B.02.07)
Result Flagging Color:	
Result Flagging Label:	RIN: 6.60

Fragment table for sample 1 : A1

Name	Start Size [nt]	End Size [nt]	Area	% of total Area
18S	1.705	2.076	26,8	10,9
28S	3.329	4.092	23,9	9,7

Fig. 6 Sample electropherogram of RNA extract from regenerating tissue of *E. sepositus*. A total RNA sample is analyzed on the Agilent 2100 Bioanalyzer System using the Eukaryote Total RNA Nano assay. RIN (RNA Integrity Number) software algorithm allows for the quality determination of eukaryotic total RNAs, based on a numbering system from 1 to 10, with 1 being the most degraded profile and 10 being the most intact

24. Synthesize cDNA following standard procedures for downstream experiments, that is, transcriptome analysis or RNA probe synthesis for in situ hybridization. Samples with highest RIN values should be selected, as they are of the highest quality.

4 Notes

1. ASW should be prepared 2–3 weeks before introducing animals into the aquaria and left to run in aquaria that are completely equipped with all filters. This time is necessary to stabilize the chemical/physical parameters and allow the growth of a sufficient population of nitrifying bacteria. To facilitate this process,

the researcher can add commercially available bacteria useful for both initial set up of the aquarium and long-term maintenance and partial water renewal. In the latter case, ASW should be prepared 2–3 days in advance before adding it to the system.

2. The concentration of NaCl may change depending on the salinity of the seawater where starfish were collected. For example, if the recorded salinity at the collection site is approximately 37‰, 1.4% (w/v) NaCl should be used, whereas at 33‰ salinity, 1.2% (w/v) NaCl is preferred.
3. Only specialized personnel can prepare this solution; waste must be handled and treated as radioactive (e.g., aluminum foil should be used to cover all disposables and materials used in order to block radiations). Before starting the protocol, the researcher must be aware of the risks connected with handling this reagent, verify that authorizations are valid, and strictly follow the instructions of the radioactive laboratory manager.
4. Propylene oxide is highly volatile. Open and use only under a fume hood. Once opened, store at 4 °C. Propylene oxide melts plastic and Parafilm®. Therefore, avoid direct contact with these materials; before use, check if the plastic tubes are resistant to this reagent. If not, use glass tubes instead.
5. This is a crucial step: a nonhomogeneous embedding medium will not perfectly infiltrate the tissues and polymerize (Table 1).
6. Glass containers and plastic disposable materials used during the protocol should be properly labeled using pencils on paper tape, since several of the solvents employed (e.g., EtOH) remove the ink. Prefer pencils also to label the glass slides used to collect the semithin sections.
7. The researcher can choose among many types of TEM grids (usually 3.05 mm in diameter) that vary in terms of materials (copper, nickel, silver, gold, etc.), meshes (50, 100, 150, 200, 300, 400, etc.), and cost. For standard TEM analyses, copper grids with meshes from 200 to 400 are generally preferred.
8. Avoid pressing and crowding of the starfish during collection.
9. A good water–animal's ratio is about 10 L per starfish.
10. Since *E. sepositus* has a delicate epidermis, avoid shaking the animals during transportation. Moreover, avoid abrupt changes in seawater temperature during transport. Ice packs can be added to the coolers to help maintain the same temperature as that of the sampling site. Starfish tolerate these transport conditions for several hours.
11. Organic materials (uneaten food, feces, etc.) can cause a decrease in sea water pH. This can be adjusted using drops of 1 M $Ca(OH)_2$.

12. This step should be completed in "dry" conditions. The animals should not be immersed in ASW to facilitate specimen handling.
13. One large aquarium provided with proper internal separators can be used as well.
14. The donor animals will regenerate. Note that after some days, the arm explants may begin moving throughout the aquarium.
15. This step should be completed in "dry" conditions. The arm explants should not be immersed in ASW to facilitate specimen handling.
16. Both proximal and distal portions should be large enough to avoid tissue deformation/rupture when sectioned with the blade but should not exceed 5–7 millimeters in thickness, to allow the fixative solution to penetrate all tissues. Use a different blade for each arm explant.
17. The researcher can leave samples in the fixative solution for a maximum of 2–3 days at 4 °C, to prevent shrinkage of the tissues.
18. To facilitate fixative penetration, a glass pipette can be used to gently insert the fixative solution into the perivisceral coelomic cavity (somatocoel), where tissues, such as the pyloric caeca (*see* Fig. 1), may partially block fixative solution infiltration into deep tissues.
19. If samples are small and the researcher must shorten the protocol times, the researcher can also leave the samples in 0.1 M sodium cacodylate trihydrate buffer for just 3–4 h and then proceed with the following protocol step.
20. When samples contact the postfixative solution, due to the presence of osmium tetroxide, they rapidly turn black. After 2 h, check that samples are totally black to be sure that all tissues have been properly postfixed.
21. The researcher should also carefully wash (with dH_2O) the inner walls of the glass containers where samples are immersed, since small crystals of osmium tetroxide can cause artifacts under TEM.
22. Depending on the sample size, the researcher can leave samples in decalcifying solution for a maximum of 3 days (at 4 °C in darkness). Large volumes are preferable to facilitate the decalcification process. Therefore, if necessary, use tweezers to gently transfer samples in labeled glass containers bigger than those used for the previous steps.
23. The researcher can stop the protocol when samples are immersed in 70% EtOH and leave them at 4 °C in darkness for several weeks. In this case, glass containers completely filled

with 70% EtOH should be tightly closed with Parafilm® to prevent EtOH evaporation.

24. If the samples are particularly small, the researcher can skip the steps involving the 3:1 propylene oxide and Epoxy resin, and the 1:3 propylene oxide and Epoxy resin, instead performing only the 1:1 propylene oxide and Epoxy resin step for at least 2 h.
25. Because the samples are black, we recommend orienting the samples with the oral side face down in the mold (tube feet are always easily recognizable) and properly labeling the mold so that it will be easy to distinguish the arm explant proximal and distal ends.
26. Samples embedded in Epoxy resin can be stored at RT in darkness for at least several years, virtually forever.
27. The researcher should consider that semithin sections will be several millimeters wide; therefore, a glass knife wider than the sample width must be used to avoid problems during sectioning. Fix the knife tightly to prevent it from moving during sectioning; adjust the knife-stage inclination degrees.
28. The researcher should be careful in shaping (trimming) the small pyramid trunk with the thin blade to avoid damage to the samples, especially the tissues of interest. Moreover, when possible, the researcher should avoid including skeletal (calcitic/mineralized) tissues, such as ossicle or spines in the small pyramid trunk—even after the decalcifying step, microscopic traces of calcium carbonate crystals may remain present in these tissues and impair sectioning, ruining the blade edge. If skeletal elements are the tissues of interest, the researcher should be aware that the edges of glass knives may be damaged. Therefore, they must be frequently changed to obtain proper ultrathin sections. The edges of diamond knives may be permanently damaged, with consequent high costs for repair and/or new purchase.
29. TEM grids can be stored in the TEM grid storage box virtually forever at RT in darkness.
30. The researcher must properly label the position of each grid on the piece of Parafilm®, especially if grids belong to different samples.
31. At this stage no specific results are reported since the isolated RNA can be processed for different analyses, that is, transcriptomics or cDNA synthesis.
32. Optional step: heat the tube to 55 °C for 10 min to help dissolve the RNA.
33. The quality of extracted RNAs is routinely tested in an Agilent 2100 Bioanalyzer System. Measures of integrity are given as

RIN (RNA integrity number) values. RINs are calculated based on the mobility run of an RNA sample through a capillary electrophoresis.

Acknowledgments

The authors are grateful to Greta Valoti for providing the image of *Echinaster sepositus* double-amputated arm explants. The laboratory of Pedro Martinez is supported with a Grant from "Agencia Estatal de Investigación, Spain" (PGC2018-094173-B-I00).

References

1. Wilkie IC (2005) Mutable collagenous tissue: overview and perspectives. In: Matranga V (ed) Echinodermata. Progress in molecular and subcellular biology. Marine molecular biotechnology, vol 5. Springer, Berlin, pp 221–250
2. Emson RH, Wilkie IC (1980) Fission and autotomy in echinoderms. Ocean Mar Biol Ann Rev 18:155–250
3. Ruppert EE, Fox RS, Barnes RD (2004) Invertebrate zoology: a functional evolutionary approach. Thomson Brooks/Cole, Belmont
4. Cortés Rivera Y, Hernández RI, Martin S, del Angel P et al (2016) Regenerative potential of the sea star *Linckia guildinguii*. Hidrobiológica 26(1):95–100
5. Thorndyke MC, Chen W-C, Beesley PW et al (2001) Molecular approach to echinoderm regeneration. Microsc Res Tech 55:474–485
6. Hinman VF, Nguyen AT, Cameron RA et al (2003) Developmental gene regulatory network architecture across 500 million years of echinoderm evolution. Proc Natl Acad Sci 100(23):13356–13361
7. Czarkwiani A, Ferrario C, Dylus DV et al (2016) Skeletal regeneration in the brittle star *Amphiura filiformis*. Front Zool 13:18
8. Ben Khadra Y, Sugni M, Ferrario C et al (2017) An integrated view of asteroid regeneration: tissues, cells and molecules. Cell Tissue Res 370(1):13–28
9. Ferrario C, Ben Khadra Y, Czarkwiani A et al (2018) Fundamental aspects of arm repair phase in two echinoderm models. Dev Biol 433(2):297–309
10. Gildor T, Cary GA, Lalzar M et al (2019) Developmental transcriptomes of the sea star, *Patiria miniata*, illuminate how gene expression changes with evolutionary distance. Sci Rep 9:16201
11. Candia Carnevali MD, Bonasoro F, Patruno M et al (1998) Cellular and molecular mechanisms of arm regeneration in crinoid echinoderms: the potential of arm explants. Dev Genes Evol 208:421–430
12. Bonasoro F, Candia Carnevali MD, Sala F et al (1999) Regenerative potential of crinoid arm explants. In: Candia Carnevali MD, Bonasoro F (eds) Echinoderm research 1998. Balkema, Rotterdam, Brookfield, pp 133–138
13. Candia Carnevali MD, Bonasoro F (2001) Microscopic overview of crinoid regeneration. Microsc Res Tech 55:403–426
14. Candia Carnevali MD (2006) Regeneration in echinoderms: repair, regrowth and cloning. Invert Surviv J 3:64–76
15. Ben Khadra Y, Sugni M, Ferrario C et al (2018) Regeneration in stellate echinoderms: Crinoidea, Asteroidea and Ophiuroidea. Results Probl Cell Differ 65:285–320
16. Valoti G, Ferrario C, Candia Carnevali MD et al (2016) Regenerative potential of *Echinaster sepositus* (Retzius, 1783) arm explants: macro- and microscopic analyses. In: Proceedings of the LXXVII National Congress of the Italian Zoological Union (UZI)
17. Villamor A, Becerro MA (2010) Matching spatial distributions of the sea star *Echinaster sepositus* and crustose coralline algae in shallow rocky Mediterranean communities. Mar Biol 157:2241–2251
18. Ben Khadra Y, Ferrario C, Di Benedetto C et al (2015) Wound repair during arm regeneration in the red starfish *Echinaster sepositus*. Wound Repair Regen 23:611–622
19. Ben Khadra Y, Ferrario C, Di Benedetto C et al (2015) Re-growth, morphogenesis, and differentiation during starfish arm regeneration. Wound Repair Regen 23:623–634

20. Ben Khadra Y, Dimassi N, Martinez P (2018) Expression of Wnt genes in *Echinaster sepositus* arm regeneration. Int J Biochem Physiol 3(1): 1–10
21. Ben Khadra Y, Said K, Thorndyke M, Martinez P (2014) Homeobox genes expressed during echinoderm arm regeneration. Biochem Genet 52(3–4):166–180
22. Gabre JL, Martinez P, Sköld HN, Ortega-Martinez O, Abril JF (2015) The coelomic epithelium transcriptome from a clonal sea star, *Coscinasterias muricata*. Mar Genomics 3:245–248

Open Access This chapter is licensed under the terms of the Creative Commons Attribution 4.0 International License (http://creativecommons.org/licenses/by/4.0/), which permits use, sharing, adaptation, distribution and reproduction in any medium or format, as long as you give appropriate credit to the original author(s) and the source, provide a link to the Creative Commons license and indicate if changes were made.

The images or other third party material in this chapter are included in the chapter's Creative Commons license, unless indicated otherwise in a credit line to the material. If material is not included in the chapter's Creative Commons license and your intended use is not permitted by statutory regulation or exceeds the permitted use, you will need to obtain permission directly from the copyright holder.





Chapter 15

Studying Hemichordata WBR Using *Ptychodera flava*

Asuka Arimoto and Kuni Tagawa

Abstract

Hemichordates are benthic marine invertebrates closely related to chordates. Several species, including *Ptychodera flava* in the phylum Hemichordates, can undergo whole body regeneration from a small fragment. *P. flava* is widely distributed in the warm Indo-Pacific region and is easily collected in the lower tidal zone of a shallow beach with a coral reef. Here, we describe the methods for animal collection and preparation of regenerating tissues. The prepared tissues can be used for various molecular and/or histological experiments. We also demonstrate how to examine gene expression patterns in the tissues using whole mount in situ hybridization.

Key words Hemichordates, Gene expression, Whole mount in situ hybridization, DIG-labeled RNA probes, Preabsorbed antibodies, NBT/BCIP staining

1 Introduction

Hemichordates, which are commonly known as acorn worms or pterobranchs, are benthic marine invertebrates. These animals belong to deuterostome and show morphological similarities to chordates such as branchial gills. Moreover, the orthology of some of these features is supported by gene expression and whole-genome analyses [1, 2]. In contrast to the limited capability of regeneration in solitary chordates, hemichordates can undergo whole body regeneration from a fragment of their body [3]. The regeneration of acorn worms tends to occur in anterior-posterior direction rather than other body axes, especially, two complete individuals are formed through regeneration if the body is split into two pieces behind the hepatic region. Although regeneration is observed in many hemichordates, asexual reproduction through the regenerative process or regeneration from a small piece occurs only in a few species [4, 5]. In addition, although acorn worms are found in the sea floor of various environments, only a few species can be easily collected. By combining these two advantages,

Simon Blanchoud and Brigitte Galliot (eds.), *Whole-Body Regeneration: Methods and Protocols*,
Methods in Molecular Biology, vol. 2450, https://doi.org/10.1007/978-1-0716-2172-1_15, © The Author(s) 2022

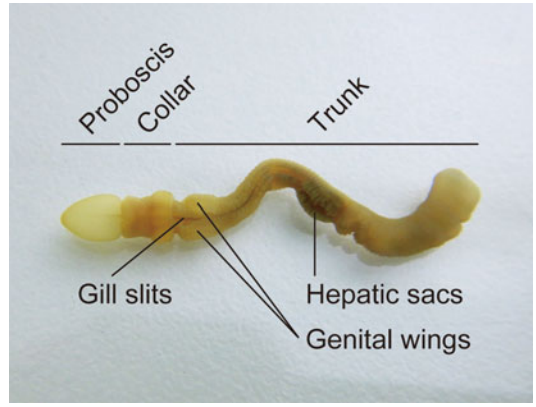


Fig. 1 External morphology of *Ptychodera flava*. This figure shows the dorsal view of the animal and left is the anterior tip. The body consists of three parts, proboscis, collar and trunk. The posterior end of trunk is terminated at the anus. The genital wings swell up in the reproductive season. The hepatic sacs are small projections in dark brown

Ptychodera flava is thus a suitable species for the study of regeneration (Fig. 1).

Here, we demonstrate how to collect the animal and prepare regenerating tissues in the laboratory. *P. flava* is widely distributed in the Indo-Pacific region, and some populations have been reported in the temperate zone [6]. This species generally lives just under a sand flat in the intertidal zone of the coral reef with a relatively high population density [7]. These ecological characteristics allow easy access to the habitats and efficient collection of the worms. We also describe the techniques to handle the fragile worms. Although the body is very fragile, the small body size of *P. flava* reduces the difficulties of avoiding animal damage during collection on the beach. *P. flava* can be kept without any special aquarium equipment during regeneration. Physiological tolerance allows a high-density system for preparing regenerating tissues at a low cost.

Several hemichordates, including *P. flava*, have been used for studies using molecular techniques [8–11]. Extensive studies of gene expression patterns using embryonic and/or larval specimens have helped elucidate the mechanisms of animal evolution and development. However, visualization of gene expression in adult tissues is still challenging. In this chapter, we also describe the method of whole mount in situ hybridization of regenerating tissues. This method displays gene expression patterns without ambiguous staining.

2 Materials

All solutions should be prepared with ultrapure deionized water unless otherwise stated. RNase-free solutions and equipment are used for RNA probe synthesis and procedures of whole mount in situ hybridization before RNase treatment.

2.1 Animal Husbandry

1. Plastic sandwich bags.
2. 9 cm diameter plastic petri dishes.
3. 10 mL disposable plastic pipettes.
4. Filtered seawater (FSW): 5 μm filtered natural seawater.
5. Anesthetic seawater: 150 mM $MgCl_2$ in FSW.
6. Fixative: 4% (w/v) paraformaldehyde, 0.1 M NaCl, 0.1 M 3-(N-morpholino) propanesulfonic acid (MOPS) buffer, pH 7.5. We recommend using freshly prepared fixative.

2.2 Preparation of RNA Probes

1. Heat stable DNA polymerase.
2. dNTPs.
3. Forward primer.
4. Reverse primer.
5. Plasmids containing gene of interest.
6. RNA polymerase.
7. Digoxigenin (DIG) RNA labeling mixture.
8. 0.5 M ethylenediaminetetraacetic acid (EDTA) pH 8.0.
9. 8 M LiCl.
10. RNase inhibitor.
11. Fluorometer supporting RNA-specific quantification.

2.3 Preparation of Preabsorbed Antibodies

1. Liquid nitrogen.
2. Pestle and mortar.
3. Acetone.
4. 10× maleic acid buffer: 1 M maleic acid, pH 7.5, 1.5 M NaCl. Adjust pH with NaOH.
5. MABT: 10% (v/v) 10× maleic acid buffer, 0.1% (v/v) Tween 20.
6. Blocking reagent A: 1% (w/v) blocking reagent in MABT. Store in aliquots of 1 mL at −20 °C.
7. 20 mg/mL bovine serum albumin.
8. Sheep serum.
9. Anti-digoxigenin-alkaline phosphatase Fab fragments from sheep.

2.4 Whole Mount In Situ Hybridization

1. PBST: 3.2 mM Na_2HPO_4, 0.5 mM KH_2PO_4, 1.3 mM KCl, 135 mM NaCl, 0.1% (v/v) Tween 20.
2. 20× saline sodium citrate (SSC) buffer: 3 M NaCl, 0.3 M sodium citrate.
3. Bleaching solution: 1% (v/v) hydrogen peroxide in PBST. Prepare just before use.
4. Permeabilization solution: 10 μg/mL proteinase K in PBST. Prepare just before use.
5. Postfixing solution: 4% (w/v) paraformaldehyde in PBST. Store in aliquots of 1 mL at −20 °C.
6. 0.1 M triethanolamine.
7. Acetylation solution: 0.25% (v/v) acetic anhydride in 0.1 M triethanolamine. Prepare just before use.
8. Hybridization buffer: 50% (v/v) formamide, 30% (v/v) 20× SSC buffer, 0.1 mg/mL yeast total RNA, 0.1% (v/v) Tween 20, 0.1% (w/v) Ficoll 400, 0.1% (w/v) polyvinylpyrrolidone, 0.1% (w/v) bovine serum albumin. Store at −20 °C.
9. Digoxigenin (DIG)-labeled RNA probes.
10. Washing buffer: 50% (v/v) formamide, 5% (v/v) 20× SSC buffer, 0.1% (v/v) Tween 20. Store in aliquots of 10 mL at −20 °C. Warm up to 65 °C before use.
11. Solution A: 500 mM NaCl, 10 mM Tris-HCl, 5 mM ethylenediaminetetraacetic acid (EDTA), pH 8.0, 0.1% (v/v) Tween 20. Warm up to 37 °C before use.
12. RNase A solution: 20 μg/mL RNase A, 500 mM NaCl, 10 mM Tris-HCl, 5 mM EDTA, pH 8.0, 0.1% (v/v) Tween 20. Prepare just before use.
13. 2× SSCT: 10% (v/v) 20× SSC buffer, 0.1% (v/v) Tween 20. Warm up to 37 °C before use.
14. 1× SSCT: 5% (v/v) 20× SSC buffer, 0.1% (v/v) Tween 20. Warm up to 65 °C before use.
15. 0.2× SSCT: 1% (v/v) 20× SSC buffer, 0.1% (v/v) Tween 20. Warm up to 65 °C before use.
16. Blocking reagent B: 2 mg/mL bovine serum albumin, 10% (v/v) sheep serum in blocking reagent A. Store in aliquots of 1 mL at −20 °C.
17. Preabsorbed anti-digoxigenin-alkaline phosphatase Fab fragments.
18. TNT buffer: 0.1 M Tris-HCl, pH 8.0, 0.15 M NaCl, 0.1% (v/v) Tween 20. Warm up to 37 °C before use.

19. TMNT buffer: 0.1 M Tris-HCl, pH 9.5, 0.1 M NaCl, 50 mM $MgCl_2$, 0.1% (v/v) Tween 20. Prepare just before use and warm up to 37 °C.
20. Nitroblue tetrazolium (NBT) stock solution: 100 mg/mL NBT in N, N-dimethylformamide (DMF). Store in aliquots of 100 μL in the dark at −20 °C.
21. 5-bromo-4-chloro-3-indolyl phosphate (BCIP) stock solution: 50 mg/mL BCIP in DMF. Store in aliquots of 100 μL in the dark at −20 °C.
22. Staining solution: 1/4000 NBT, 1.75/1000 BCIP in TMNT buffer. Prepare just before use.
23. PBST–EDTA: 1 mM EDTA, pH 8.0 in PBST.

3 Methods

3.1 Animal Collection

1. Dig in sand using a trowel at the low tide zone to collect animals (*see* Fig. 2a and **Note 1**).
2. Pour seawater in the sand on the trowel to wash out the animals (Fig. 2b).
3. Transfer the collected animal from the trowel to a plastic sandwich bag filled with seawater (*see* **Note 2**).
4. Ten to fifteen animals can be kept in the same 1000 mL plastic bag during collection and transportation (*see* **Note 3**).
5. Avoid shaking the plastic bags during transportation to prevent shearing the animal body.
6. Transport the collected animals to the laboratory (*see* **Note 4**).
7. Treated FSW with bubble aeration for at least 30 min.
8. Add 30 mL of FSW in a 9 cm diameter plastic petri dish.
9. Transfer the collected animals into the dish one by one using a 10 mL disposable plastic pipette in which the conical tip is cut off (*see* **Notes 5** and **6**).
10. If the animals are tangled with each other in the plastic bag, dissociate the animals by gently pipetting up and down (Fig. 3a, b).
11. Remove sand attached to the surface of the animals using tweezers (Fig. 3c).
12. Pick up undamaged individuals after removing sand (*see* **Note 7**).
13. Keep the undamaged animals at 25 °C until the sand in the intestine of the animal has completely passed from the body (*see* **Note 8**).

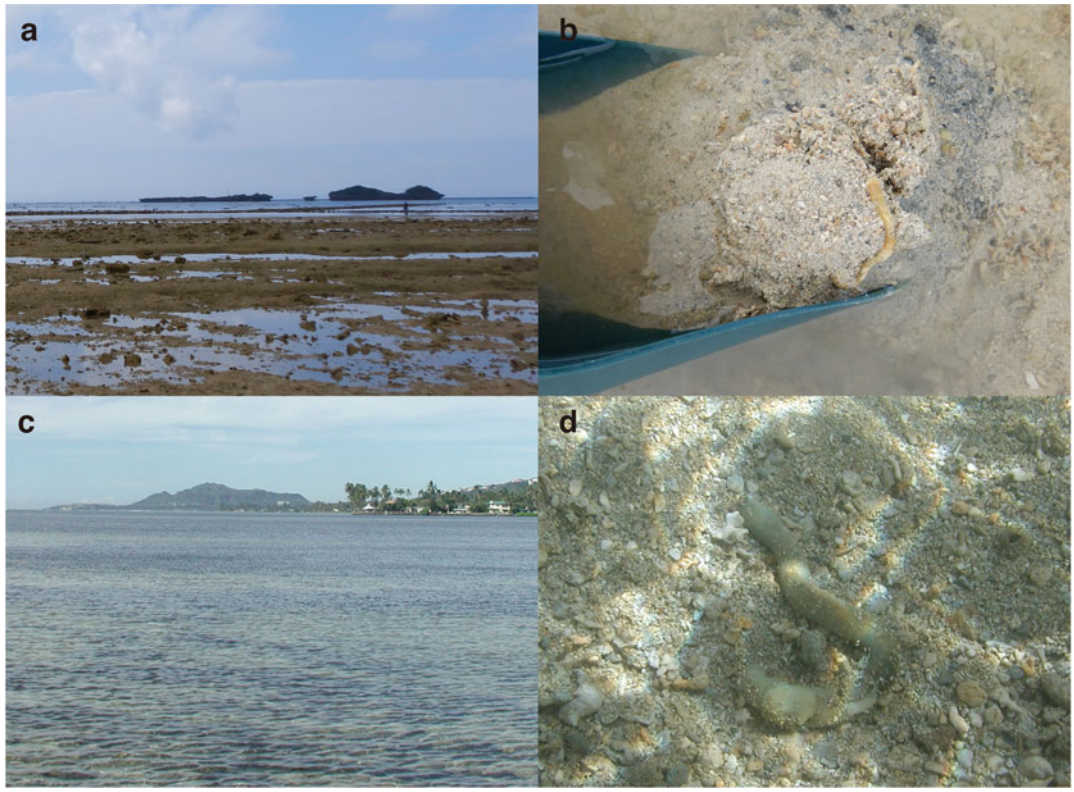


Fig. 2 Comparison of the habitat and the sampling methods of *Ptychodera flava*. (**a**, **b**) Animal collection on a tidal flat in Okinawa, Japan. A trowel is used to dig the sand. The animals in the dug sand are exposed by addition of seawater. (**c**, **d**) The animals were collected by snorkeling in shallow water in Hawaii, USA. In this case, the sand was dug using a vigorous wave of the hand to find the animals

14. Remove the excreted sand using a 1000 μL pipette with a wide-bore tip every day.
15. Loosen possible knots in the animal body using toothpicks (Fig. 3d).

3.2 Preparation of Regenerating Tissues

1. Select undamaged individuals (*see* **Note 9**).
2. Remove the filmy mucus attached on the surface of the animals using tweezers (*see* **Note 10**).
3. Replace seawater in the dish with 30 mL of anesthetic seawater (*see* **Note 11**).
4. Incubate at 25 °C for 10 min (*see* **Note 12**).
5. Cut the body into two pieces using iris scissors (*see* Fig. 4a and **Note 13**).
6. Transfer each piece immediately to a new 9 cm diameter plastic petri dish filled with 30 mL of FSW (*see* **Note 14**).

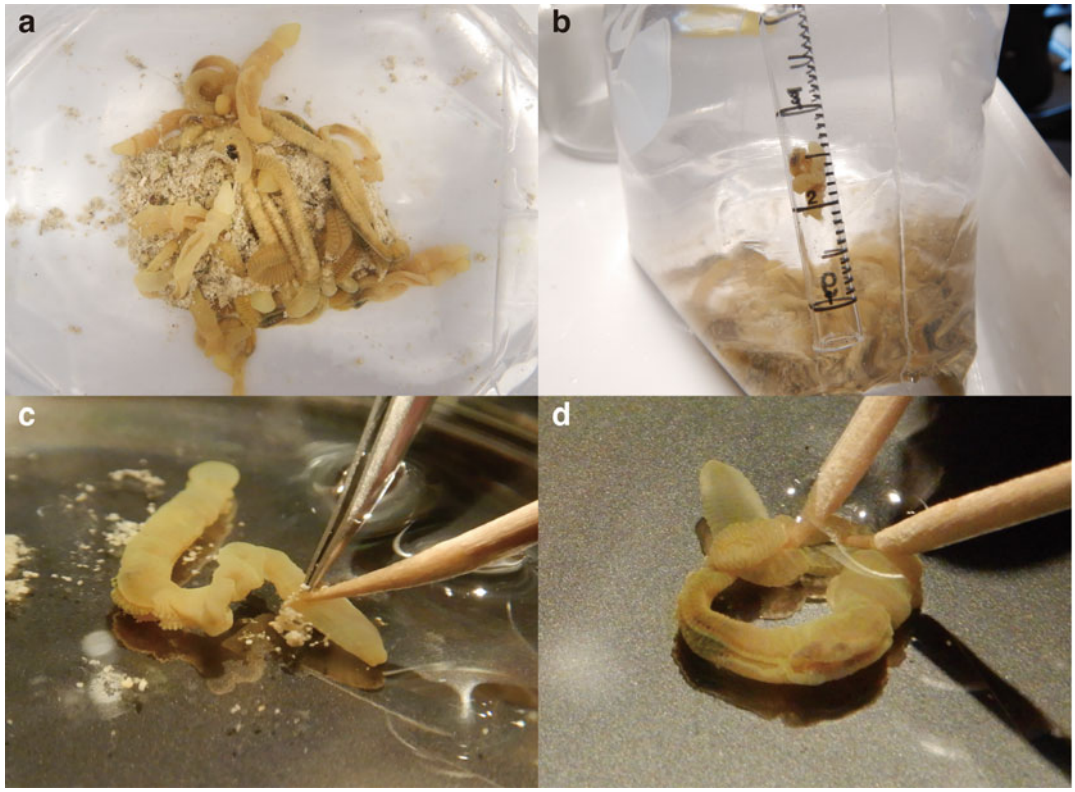


Fig. 3 Animal treatment and maintenance at the laboratory. (**a**, **b**) The tangled animals in the plastic bag after transportation and a dissociated individual in a pipette. (**c**) The sand with filmy mucus attached on the surface of the animal was removed using tweezers and a toothpick. (**d**) A knot made in the animal body was loosened by toothpicks



Fig. 4 Preparation of regenerating tissues of *Ptychodera flava*. (**a**) An undamaged animal was cut into two pieces using iris scissors behind the hepatic sacs. The sand which are indicated arrowheads remaining in the intestine can be confirmed from the outside of the body as in Panel (**b**). (**c**) Collection of a regenerating tissue using iris scissors. The animal was not treated with anesthetic seawater. The arrowhead indicates the regenerating proboscis

7. Keep the fragments at 25 °C until a target stage in regeneration (*see* Fig. 5, **Notes 15** and **16**).
8. Transfer the regenerating tissue into a clean 1.5 mL plastic tube containing 1 mL of fixative (*see* Fig. 4c, and **Note 17**).

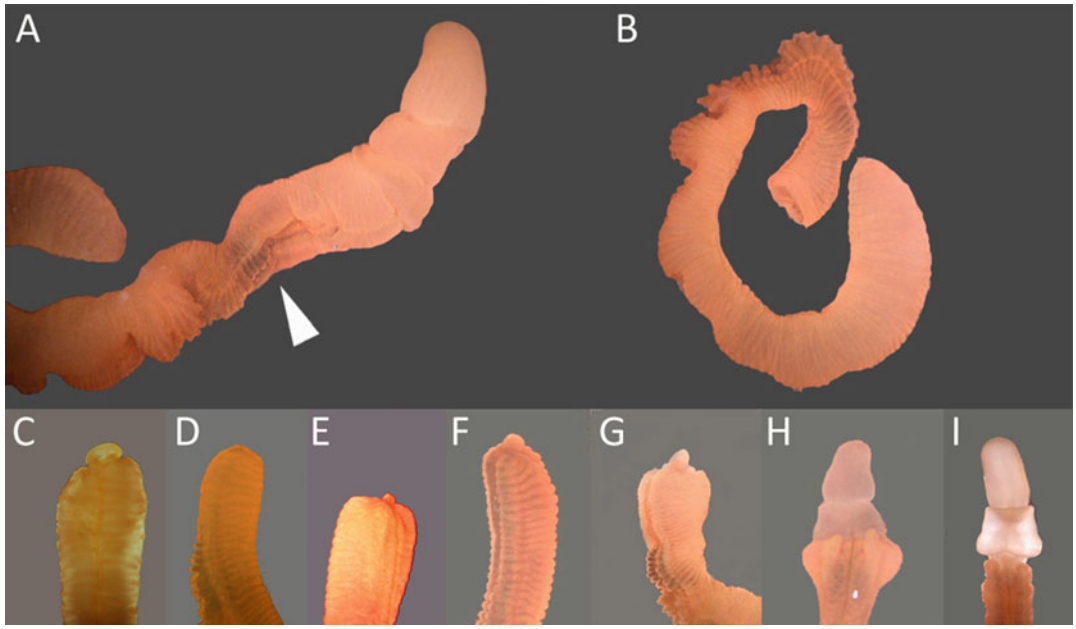


Fig. 5 Anterior regeneration process of *Ptychodera flava*. (**a**) An undamaged individual before amputation. (**b**) A posterior piece just after amputation. (**c**) The wound is healing at 2 days postamputation (dpa). (**d**) The completion of wound healing at 3 dpa. (**e**) The regenerating tissue called blastema becomes visible at 4 dpa. (**f**) Two rudiments of collar are swelled on both lateral sides of the blastema at 5 dpa. (**g**) The collar rudiment surrounds the most prominent mass of the blastema at 7 dpa. The mouth opens at the ventral region between the regenerating proboscis and collar. (**h**) Complete function of proboscis and collar are recovered at 12 dpa. (**i**) At 17 dpa, the missing branchial region becomes visible. The process of gill regeneration continues for approximately 2 months. (Reprinted by permission from the Zoological Society of Japan: Zoological Science, Regeneration in the Hemichordate *Ptychodera flava,* Humphreys et al., 2010)

9. Incubate at 4 °C for 16 h.
10. Remove and discard all of the fixative from the tube.
11. Dehydrate the samples in 1 mL of an ethanol series (30% EtOH, 50% EtOH, 80% EtOH) at 4 °C for 30 min each step.
12. Replace the medium with 1 mL of 80% EtOH.
13. Incubate at 4 °C for 30 min (*see* **Note 18**).

3.3 Preparation of RNA Probes

The method for preparation of digoxigenin-labeled RNA probes is modified from [12].

1. Amplify 10 ng of the template plasmid through PCR (*see* **Note 19**).
2. Mix 2.5 μL of the amplified solution and 7.5 uL of DIG labeling solution thoroughly using a 20 μL pipette (*see* **Note 20**).
3. Incubate at 37 °C for 16 h (*see* **Note 21**).
4. Adjust volume to 51.8 μL with RNase-free water.

5. Add 3.2 μL of 0.5 M EDTA and 25 μL of 8 M LiCl.
6. Mix thoroughly using a vortex mixer.
7. Incubate at −20 °C for 20 min.
8. Centrifuge the sample at 16,000 rcf at 4 °C for 20 min.
9. Discard the supernatant.
10. Add 200 μL of 80% EtOH.
11. Centrifuge the sample at 16,000 rcf at 4 °C for 5 min.
12. Discard the supernatant completely.
13. Vacuum dry the pellet for 10 min.
14. Add 50 μL of RNase-free water containing 10 units of RNase inhibitor (*see* **Note 22**).
15. Measure the concentration of the RNA probe using a fluorometer.

3.4 Preparation of Preabsorbed Antibodies

The method for preparation of preabsorbed antibodies is modified from [13].

1. Chill a pestle and mortar using liquid nitrogen.
2. Put a whole body of adult *P. flava* in the chilled mortar (*see* **Note 23**).
3. Immediately add liquid nitrogen to the mortar.
4. Grind the frozen sample to a fine powder using the pestle and mortar.
5. Transfer the powder to a clean, prechilled 50 mL plastic tube.
6. Add four volumes of the powder of prechilled acetone.
7. Incubate on ice for 30 min.
8. Centrifuge the sample at 10,000 rcf at 4 °C for 5 min.
9. Discard the supernatant.
10. Repeat **steps 6** to **9** again.
11. Transfer the pellet to a clean 5 μm filter paper.
12. Dry up the pellet at room temperature (*see* **Note 24**).
13. Add 1.5 mg of the completely dried powder into a clean 1.5 mL plastic tube containing 400 μL of blocking reagent A.
14. Incubate at 70 °C for 30 min.
15. Add 50 μL of 20 mg/mL bovine serum albumin and 50 μL of sheep serum.
16. Cool down the solution to room temperature.
17. Add 0.5 μL of anti-digoxigenin-alkaline phosphatase Fab fragments.
18. Incubate at 4 °C for 16 h with gentle agitation.

19. Add 900 μL of blocking reagent A, 50 μL of 20 mg/mL bovine serum albumin and 50 μL of sheep serum.
20. Mix thoroughly using a 1000 μL pipette.
21. Centrifuge the sample at 10,000 rcf at 4 °C for 1 min.
22. Transfer the supernatant to clean 1.5 mL plastic tubes in 200 μL aliquots.
23. Store the aliquots at −20 °C.

3.5 Whole Mount In Situ Hybridization

1. Transfer dehydrated tissues to a clean 1.5 mL plastic tube with 100 μL of 80% EtOH using a 1000 μL pipette with a wide-bore tip (*see* **Note 25**).
2. Rehydrate tissues in an ethanol-PBST series (75% EtOH–25% PBST, 50% EtOH–50% PBST, 30% EtOH–70% PBST, 100% PBST) with 200 μL of each solution for 10 min.
3. Replace the medium with 200 μL of bleaching solution.
4. Incubate at room temperature for 10 min (*see* **Note 26**).
5. Rinse the sample twice in 200 μL of PBST.
6. Replace with 200 μL of permeabilization solution.
7. Incubate at 37 °C for 30 min.
8. Rinse the sample three times in 200 μL of PBST.
9. Perform postfixation in 200 μL of postfixing solution at room temperature for 1 h.
10. Rinse the sample twice in 200 μL of PBST.
11. Immerse the samples twice in 200 μL of 0.1 M triethanolamine at room temperature for 10 min.
12. Incubate in 200 μL of acetylation solution at room temperature for 10 min at room temperature.
13. Rinse the sample three times in 200 μL of PBST.
14. Replace PBST in the tube with 200 μL of 50% hybridization buffer/50% PBST.
15. Incubate at room temperature for 10 min.
16. Replace with 200 μL of hybridization buffer.
17. Incubate at room temperature for 10 min.
18. Replace the hybridization buffer with 200 μL of fresh hybridization buffer.
19. Incubate at 60 °C for 2 h (*see* **Note 27**).
20. Replace the buffer with 100 μL of hybridization buffer containing 0.1 ng/μL RNA probe (*see* **Note 28**).
21. Incubate at 60 °C for at least 16 h (*see* **Note 29**).
22. Remove the excess RNA probe in 200 μL of washing buffer at 65 °C for 20 min.

23. Repeat this wash for a total of three times (*see* **Note 30**).
24. Replace the buffer with 200 µL of solution A.
25. Incubate at 37 °C for 10 min.
26. Repeat this buffer replacement for a total of three times.
27. Replace with 200 µL of RNase A solution.
28. Incubate the sample at 37 °C for 30 min.
29. Rinse the sample three times in 200 µL of 2× SSCT at 37 °C.
30. Replace with 200 µL of 1× SSCT.
31. Incubate at 65 °C for 20 min.
32. Repeat **steps 30** and **31** again.
33. Replace with 200 µL of 0.2× SSCT.
34. Incubate at 65 °C for 10 min.
35. Repeat **steps 33** and **34** again.
36. Replace with 200 µL of MABT.
37. Incubate at room temperature for 10 min.
38. Repeat **steps 36** and **37** for a total of three times.
39. Replace with 200 µL of blocking reagent A.
40. Incubate at room temperature for 20 min.
41. Replace with 200 µL of blocking reagent B.
42. Incubate at room temperature for 1 h.
43. Replace with 100 µL of preabsorbed antibody solution.
44. Incubate at room temperature for 2 h (*see* **Note 31**).
45. Rinse the sample twice in 200 µL of MABT at room temperature.
46. Remove the excess antibody in 1 mL of MABT at 37 °C for 16 h.
47. Replace the buffer with 1 mL of MABT (*see* **Note 32**).
48. Incubate at 37 °C for 20 min.
49. Repeat **steps 47** and **48** for a total of four times.
50. Replace with 200 µL of TNT buffer.
51. Incubate at 37 °C for 10 min.
52. Repeat **steps 50** and **51** again.
53. Replace with 200 µL of TMNT buffer.
54. Incubate at 37 °C for 10 min.
55. Repeat **steps 53** and **54** again.
56. Replace with 200 µL of staining solution.
57. Incubate the samples at 37 °C (*see* **Note 33**).

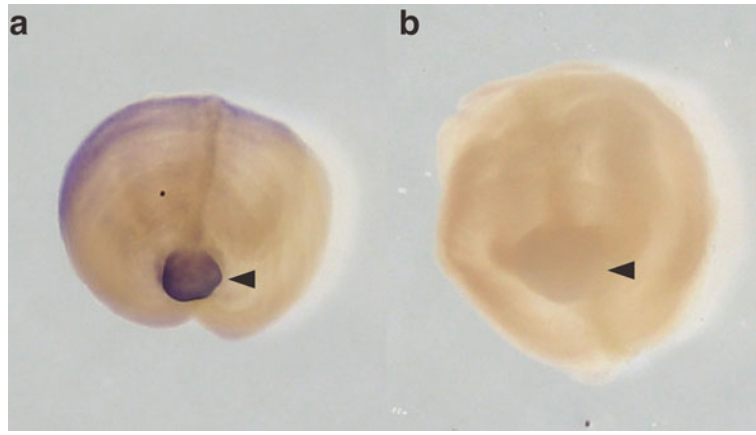


Fig. 6 Examples of whole mount in situ hybridization using regenerating tissues of *Ptychodera flava*. Gene expressions of *soxb1* at 7 days postamputation were examined using an antisense probe (**a**) and a sense probe (**b**), respectively. The upper side is dorsal. The arrowheads show regenerating proboscis in each panel. The gene expressions of *soxb1* were identified at regenerating rudiments of proboscis and collars located at the tip of anterior and surrounding region of them

58. Rinse the samples twice in 200 μL of PBST–EDTA at room temperature.
59. Replace with 200 μL of PBST twice.
60. Incubate at 37 °C for 12 h.
61. Replace with 1 mL of 30% EtOH–70% PBST.
62. Incubate at room temperature for 30 min.
63. Repeat incubation in fresh 30% EtOH–70% PBST for 90 min (*see* **Note 34**).
64. Rinse the sample twice in 200 μL of PBST (*see* **Note 35**).
65. Transfer the samples to a plastic petri dish filled with PBST using a 1000 μL pipette with a wide-bore tip.
66. Imaging on the samples using a camera mounted on a stereomicroscope (Fig. 6).

4 Notes

1. The animals are commonly found in the low tide zone of a shallow beach with a coral reef (Fig. 2). Small individuals that are suitable for preparing regenerating tissues prefer a place where fine coral sand accumulates. These animals are abundant in sand less than 10 cm in depth and are rarely found in an anaerobic bottom layer. We generally collect small individuals with a 2–4 mm diameter of the trunk. Prominent fecal castings

are accompanied by burrow systems of some large-sized acorn worms; however, *P. flava* does not form such a structure. The animals can also be collected in high tide conditions by snorkeling (Fig. 2c, d and [13]). Key points of species identification are shapes and colors of proboscis, genital wings and hepatic sacs. Any closely related species has not been reported in habitats of *P. flava* [6].

2. An animal should not be picked up with fingers to prevent shearing of the body by its own weight. The entire body of the animal should be held on a palm.
3. If a transportation longer than 3 h is expected, the plastic bags are put in a Styrofoam box with ice packs wrapped cushioning materials. The Styrofoam box has to be treated at temperature between 10 °C to 30 °C. This procedure can extend transportation period up to 2 days.
4. The color of animals sometimes changes from vivid yellow to light brown after transportation; however, this phenomenon does not affect the success rate of regeneration. All procedures were carried out at 20–25 °C after transportation. Cold conditions lower than 20 °C resulted in a lower success rate of regeneration.
5. We recommend using collected animals for experiments of regeneration as soon as possible. Five to ten animals can be kept in a 1 L tank with 800 mL of filtered seawater with gentle bubble aeration and fed 50 mL of the diatom *Chaetoceros calcitrans* once a week, however, the worms gradually become smaller and show a lower success rate of regeneration. The seawater in the tank should be replaced the next day of feeding. A 5 mm thick layer of fine coral sand in the tank suppresses autotomy. Collected animals can be maintained in the lab to prepare regenerating tissues using the compromise culture method up to 3 months.
6. Sharp tweezers should not be used to transfer the animals. The tweezers can easily damage the animal body. A conical tip of joining molded pipette (e.g., Corning) can be easily picked by hands, otherwise cut off using a razor blade. For transferring large animals, round disposable chopsticks are more suitable than pipettes. Artificial seawater is also acceptable for storage of the collected animals.
7. Any scale of damage is not allowed. A stereomicroscope can be used to assess the damage to animals smaller than 1 mm in diameter at the trunk. Damaged individuals will die or show signs of autotomy accompanying trunk constriction within a few days. A white or pale colored proboscis or posterior tip suggests that the individual is regenerating or has just completed regeneration. We do not use these individuals to collect regenerating tissues.

8. The treatment period is shorter than 3 days in many cases.
9. Animals changing to dark brown show a lower success rate of regeneration.
10. The presence of mucus layer on the surface of the animals can be distinguished by the refractive index differences. If a such layer is not be observed, this procedure can be omitted.
11. Anesthesia is not an essential treatment for amputation. Therefore, although the technical difficulties of amputation are increased, it is possible to prepare specimens for assessing the gene expression of early wound responses under natural conditions.
12. Increasing the incubation time to up to 30 min does not affect the rate of regeneration.
13. We usually cut an animal body behind the hepatic sacs (Fig. 4a, b). The body should be cut at once to avoid warping of the cut section. Although the success rate of regeneration depends on the cutting position [6, 14], the common success rate of regeneration is higher than 80% in our routine method.
14. Researchers should minimize carry-over of anesthetic seawater. Antibiotics do not significantly increase the success rate of regeneration.
15. The seawater in the dish should be replaced when its color changes to yellow or brown. The water change should be done with great care because a newly formed region can be broken by water current.
16. The stage of anterior regeneration can be identified based on the morphologies. On the other hand, it is difficult to distinguish the stage of posterior regeneration based on external structures. The difficulties come from the absence of characteristic structures in the posterior region even in undamaged individuals.
17. The dissected specimens should be smaller than a cube three millimeters on a side. Five to ten tissue specimens can be kept in the same 1.5 mL plastic tube. The composition of the fixative is suitable for in situ hybridization specimens. The dissected tissues for RNA extraction are dissolved in TRIzol reagent. We recommend a flash freezing method using liquid nitrogen rather than fixative for DNA extraction samples.
18. Dehydrated samples in 80% EtOH can be stored at −20 °C for at least 1 year.
19. The PCR is carried out in 20 μL scale. The composition of PCR solution and settings of thermal cycler follow the recommendation of manufacturer of employed DNA polymerase. Universal primers for the plasmid are suitable for the PCR. The specificity of PCR is confirmed using agarose gel electrophoresis.

20. The composition of DIG labeling solution containing RNA polymerase which recognizes promoter sequences on the plasmid follows manufacturer's instruction.
21. The results of in vitro transcription are examined using native agarose gel electrophoresis.
22. The purified RNA probe can be stored at −80 °C.
23. Sands remaining in the intestine should be completely removed in advance of the antibody preparation.
24. Residual acetone deactivates antibodies. Breaking down the pellet using a clean medicine spoon helps to be shortened the incubation time. The completely dried powder can be stored at −20 °C.
25. Hydrophobic coating for plastic tubes is not necessary.
26. Hydrogen peroxide treatment reduces mucus secretion from tissues during high temperature incubation. The color of the samples is slightly bleached; however, it is still brownish after this step.
27. The viscosity of the solution is slightly increased after incubation. The solution in the 1.5 mL tube should be removed slowly using a 200 μL pipette.
28. The standard concentration of RNA probe in hybridization buffer is 0.1 ng/μL, however, the concentration should be optimized in the range of 0.01 to 1 ng/μL based on preliminary experiments.
29. If the viscosity of the solution is significantly increased than the prehybridization step, it suggests the failure of hydrogen peroxide treatment. The viscosity is gradually decreased by washing buffer and solution A. We do not reuse the hybridization buffer containing an RNA probe. The mucus released from the tissues denatures the integrity of the hybridization buffer.
30. The samples should be kept in warm conditions until **step 36**.
31. The incubation time should not be increased. A long incubation even at 4 °C gives rise to nonspecific staining.
32. The MABT is warmed to 37 °C before use.
33. The samples should be kept in dark conditions during incubation until **step 63**. The alkaline phosphatase binding to digoxigenin-labeled RNA probe produces purple or dark blue pigments. In contrast, light reddish-purple pigments are produced by the nonenzymatic reaction. The staining generally takes 30 min to 3 h. The samples should be rinsed using PBST–EDTA before changing the color of nonspecific staining to dark purple. Insufficient washing after RNA probe hybridization and/or antibody reaction induces false positive staining of grooves on the surface of the trunk region even in a negative control sample.

34. Although the standard procedure described in **step 63** is effective to remove nonspecific staining, dehydration and rehydration using a series of 30% EtOH–70% PBST, 50% EtOH–50% PBST, and 80% EtOH–20% H_2O improve the contrast of the staining after postfixation (*see* **Note 35**).
35. Stained specimens can be stored at 4 °C for at least 1 month after performing postfixation again. The procedure is the same as **step 9**. The postfixation procedure also helps to fix stained pigments. In other words, the visibility of nonspecific staining is increased by postfixation if such staining remains.

Acknowledgement

We wish to express our sincere thanks to the Zoological Society of Japan for allowing us to reproduce their data as Fig. 5 in this chapter. Special thanks to Prof. Nori Satoh for his continued support of our research.

References

1. Ogasawara M, Wada H, Peters H et al (1999) Developmental expression of *Pax1/9* genes in urochordate and hemichordate gills: insight into function and evolution of the pharyngeal epithelium. Development 126:2539–2550
2. Simakov O, Kawashima T, Marlétaz F et al (2015) Hemichordate genomes and deuterostome origins. Nature 527:459–465
3. Rychel AL, Swalla BJ (2009) Regeneration in hemichordates and echinoderms. In: Rinkevich B, Matranga V (eds) Stem cells in marine organisms. Springer, Dordrecht
4. Dawydoff C (1909) Beobachtungen über den Regenerationsprozess bei den Enteropneusten. Z Wiss Zool 93:237–305
5. Tweedell KS (1961) Regeneration of the enteropneust, *Saccoglossus kowalevskii*. Biol Bull 120: 118–127
6. Nishikawa T (1977) Preliminary report on the biology of the enteropneust, *Ptychodera flava* Eschscholtz, in the vicinity of Kushimoto, Japan. Publ Seto Mar Biol Lab 23:393–419
7. Kohn AJ (1994) Ecology of *conus* in Hawaii. In: Kay EA (ed) A natural history of the Hawaiian islands: selected readings II. University of Hawaii Press, Hawaii
8. Tagawa K, Humphreys T, Satoh N (1998) Novel pattern of *Brachyury* gene expression in hemichordate embryos. Mech Dev 75: 139–143
9. Lowe CJ, Wu M, Salic A et al (2003) Anteroposterior patterning in hemichordates and the origins of the chordate nervous system. Cell 113:853–865
10. Miyamoto N, Nakajima Y, Wada H et al (2010) Development of the nervous system in the acorn worm *Balanoglossus simodensis*: insights into nervous system evolution. Evol Dev 12: 416–424
11. Gonzalez P, Uhlinger KR, Lowe CJ (2016) The adult body plan of indirect developing hemichordates develops by adding a Hox-patterned trunk to an anterior larval territory. Curr Biol 27:87–95
12. Ogasawara M, Minokawa T, Sasakura Y et al (2001) A large-scale whole-mount *in situ* hybridization system: rapid one-tube preparation of DIG-labeled RNA probes and high throughput hybridization using 96-well silent screen plates. Zoolog Sci 18:187–193
13. Lowe CJ, Tagawa K, Humphreys T, Kirschner M, Gerhart J (2004) Hemichordate embryos: procurement, culture, and basic methods. In: Ettensohn CA, Wray GA, Wessel GM (eds) Methods cell biol, vol 74. Elsevier, Amsterdam, pp 171–194
14. Humphreys T, Sasaki A, Uenishi G et al (2010) Regeneration in the hemichordate *Ptychodera flava*. Zoolog Sci 27:91–95

Open Access This chapter is licensed under the terms of the Creative Commons Attribution 4.0 International License (http://creativecommons.org/licenses/by/4.0/), which permits use, sharing, adaptation, distribution and reproduction in any medium or format, as long as you give appropriate credit to the original author(s) and the source, provide a link to the Creative Commons license and indicate if changes were made.

The images or other third party material in this chapter are included in the chapter's Creative Commons license, unless indicated otherwise in a credit line to the material. If material is not included in the chapter's Creative Commons license and your intended use is not permitted by statutory regulation or exceeds the permitted use, you will need to obtain permission directly from the copyright holder.



Chapter 16

Studying Tunicata WBR Using *Botrylloides anceps*

Arzu Karahan, Esra Öztürk, Berivan Temiz, and Simon Blanchoud

Abstract

Tunicates are marine filter-feeding invertebrates that can be found worldwide and which are the closest phylogenetic group to the vertebrates (Craniata). Of particular interest, colonial tunicates are the only known chordates that can undergo Whole-Body Regeneration (WBR) via vascular budding. In *Botrylloides anceps*, a fully functional adult regenerates from a fragment of the vascular system in around 2 weeks after amputation. In this chapter, we present protocols to collect *B. anceps* colonies, confirm their species, breed them in the lab, monitor WBR and perform histological staining on cryosections.

Key words Whole-body regeneration, *Botrylloides anceps*, Vascular budding, DNA barcoding, Chordate, Histological section

1 Introduction

Tunicates are filter-feeding invertebrates that have colonized virtually all marine habitats. Although they were classified in the Mollusca phylum during the early twentieth century, the Tunicata subphylum belong to the Chordata and is the closest phylogenetic group to the vertebrates (Craniata) [1]. Consequently, and despite their apparently simpler body morphologies, tunicates display all chordate features (notochord, post-anal tail, endostyle, neural tube and gill slits) as well as a relatively high tissue complexity (heart, neural ganglion, tunic, circulatory system) [2]. Tunicates is a very diverse group of animals that displays quite different reproductive features, repair abilities, development strategies, and life cycles [3–5]. The majority of tunicates are sessile hermaphrodites that reproduce through a motile tadpole larval stage. After a short free-swimming life stage [2], the tadpole settles on a substrate using the adhesive papillae located at tip of its head. It undergoes a rapid metamorphosis during which its tail and notochord are resorbed, its organs mature and filter-feeding starts. Water enters through the oral siphon, is filtered by the pharyngeal basket and is evacuated through the atrial siphons [6, 7].

Simon Blanchoud and Brigitte Galliot (eds.), *Whole-Body Regeneration: Methods and Protocols*,
Methods in Molecular Biology, vol. 2450, https://doi.org/10.1007/978-1-0716-2172-1_16, © The Author(s) 2022

In addition to sexual reproduction, a number of tunicates can reproduce asexually by budding in a process termed blastogenesis (reviewed in [8]). The adult animal, called zooid, starts the development of its daughter, called bud, by the thickening of its epithelium together with that of the underlying layer of tissue. The location of the bud and thus the origin of the underlying tissue can vary depending on the species [8]. These tissue invaginate until forming a double vesicle stage common to all types of asexual reproduction in tunicates. The inner layer will then further invaginate to produce the various organs and the whole bud will mature until it becomes a filter-feeding zooid. In some species of budding tunicates, buds remain connected to its zooid, typically through an interzooidic vascular system, thus forming colonies. In some colonial tunicates, in particular among members of the *Botrylloides* and *Botryllus* sister genera, blastogenesis is a highly synchronized process where the new generation of buds matures simultaneously throughout the colony to replace the old zooids that get resorbed during the so-called takeover stage.

In botryllid tunicates, researchers have identified a second nonembryonic development that can lead to the formation of zooids. Botryllids can undergo whole-body regeneration (WBR) from a fragment of their interzooidic vascular system [4, 9]. Most notably, this is the only know occurrence of WBR in the Chordata phylum. WBR is a type of vascular budding, which is initiate by an injury that leads to the loss of all zooids and buds from the colony [9–11]. Many of the up-regulated metabolic pathways during the WBR play a crucial role in stem cell maintenance, proliferation, differentiation, and tissue organization [12–15]. Pluripotent stem cells (potentially undifferentiated hemoblasts) are assumed to be the precursor cells for WBR [4, 9, 16, 17]. It has been reported that regeneration in *Botrylloides leachii* is initiated by the activation of population of dormant stem-like cells that line the surface of the vascular epithelium [14, 16, 18]. In *Botrylloides diegensis*, a population of *Integrin alpha 6* positive circulating stem cells have been shown to be the source of the WBR capacity [19]. In both cases, upon activation, these cells migrate to the vessel lumen where regeneration begins, and these precursor cells differentiate and eventually transform into a single adult individual within the regeneration lumen [9, 16, 17, 20]. The epithelial layer close to the wound area is generally thought to be the origin of the activation source for regeneration [13, 21].

Vascular budding has also been reported in *Botrylloides gascoi* and *Botrylloides leachii* under field conditions when colonies recover from their aestivation during which all zooids are lost [22, 23]. Interestingly, vascular budding is a part of the life history of *Botryllus primigenus* where it happens spontaneously throughout its adult life cycle [24–26]. Altogether, botryllid ascidians display the rare feature of using three distinct developmental

pathways to produce the same final organism. This property is of particular interest for comparative developmental studies. Moreover, botryllid ascidians are used as model organisms in a wide range of studies including apoptosis, immunobiology, allorecognition and angiogenesis [4, 18, 20, 27–32]. These animals are thus highly suitable as research specimens, their usage will be widely popularized in the near future.

To promote these exciting organisms, we here present a number of protocols for the study of colonial tunicates that we developed for *Botrylloides anceps*. The species originates from the Pacific Ocean. It was recorded for the first time in the Mediterranean Sea along the coastline of Israel in 2009, most likely after an opportunistic migration through the Suez channel [7]. More recently, we logged this species on Turkish coasts in 2018. In this chapter, we present protocols to collect, identify, induce WBR and study the regenerative process using histological staining of cryosections. These protocols should be readily applicable to other botryllids, and likely to other sessile colonial tunicates as well.

2 Materials

2.1 Animals Collection, Handling, Feeding, and DNA Barcoding

All solutions should be prepared with ultrapure water and stored at room temperature unless otherwise state.

1. Filtered seawater (FSW): 20 μm filtered natural seawater.
2. Husbandry system: containers filled with FSW, air pump, air stones, flexible hose.
3. Cotton thread.
4. Salinity meter (e.g., a seawater refractometer).
5. Single-edged razor blades.
6. Large 75 × 50 mm glass microscopy slides.
7. Freeze-dried rotifer powder.
8. Commercial culture of Ochrophyta single-cell algae (e.g., *Nannochloropsis sp.*).
9. Powdered food for filter feeders (e.g., Coral food SPS, Tropical Marine).
10. Food mixture: 13 mL algae, 1 g powdered food, 1 g freeze-dried rotifer powder in 487 mL H_2O, aliquot in 15 mL tubes, store at −20 °C.
11. 1× Phosphate Buffer Solution (PBS): 1.9 mM NaH_2PO_4, 8.4 mM Na_2HPO_4, 175.0 mM NaCl, adjust pH to 7.4 with HCl.
12. Stereomicroscope equipped with a camera.

13. Lysis stock solutions: Prepare separately 1 M Tris–borate (pH 8.2) solution, 0.5 M EDTA solution, 10% (w/v) SDS solution, and 0.5 M NaCl solution. Use within 2 months.
14. Lysis buffer: 12.5 mL 1 M Tris–borate solution, 10 mL 0.5 M EDTA, 10 mL 10% (w/v) SDS, 1 mL 0.5 M NaCl. Adjust the volume to 50 mL with double distillated H_2O.
15. 5 M $NaClO_4$ stock solution. Prepare fresh every time.
16. Chloroform–isoamyl alcohol: 24 mL chloroform, 1 mL isoamyl alcohol.
17. Phenol–chloroform–isoamyl alcohol: 25 mL phenol (saturated pH 7.5–8.0), 24 mL chloroform, 1 mL isoamyl alcohol.
18. Nanodrop spectrophotometer (A230/A260/A280 nm wavelength).
19. 2× PCR master mix: 20 mM Tris–HCI, pH 8.3, 100 mM KCI, 3 mM $MgCI_2$, 0.002% (w/v) gelatin, 0.4 mM dNTP mix (dATP, dGTP, dCTP, dTTP), stabilizers, 0.06 unit/μL Taq DNA polymerase.
20. Cytochrome oxidase I primer mix: 10 pmol/μL Forward primer 5-AMWAATCATAAAGATATTRGWAC-3, 10 pmol/μL Reverse primer 5- AARAARGAMGTRTTRAAATTHC GATC-3 (*see* **Note 1**).
21. Tris/Borate/EDTA (TBE) buffer: 89 mM Tris–borate, 2 mM EDTA, pH 8.3.
22. Agarose gel: 1.25 g agarose in 100 mL TBE buffer. Heat until the solution is completely clear, add 5 μL of nucleic acid staining solution, gently mix the solution. Pour into a gel tray with comb, cool until solidified.
23. 6× agarose loading dye: 10 mM Tris–HCl, pH 7.6, 0.15% (w/v) orange G, 0.03% (v/v) xylene cyanol FF, 60% (v/v) glycerol, 60 mM EDTA.
24. PCR purification kit.
25. Sanger sequencing service (e.g., supplied from a commercial sequencing company).

2.2 Histological Cryosectioning and Staining

1. Cryostat microtome sectioning machine.
2. Crystal menthol.
3. Bouin's fixative: 75 mL saturated picric acid, 25 mL formalin, 5 mL glacial acetic acid (*see* **Note 2**).
4. Dehydration solution: 30% (w/v) sucrose.
5. Optimal cutting temperature (OCT) compound (e.g., Polar-Stat Plus, Ted Pella).
6. Embedding molds (e.g., Peel-a-way, Polysciences).
7. Coated microscopy glass slides (e.g., Superfrost Plus, VWR).

8. Groat's hematoxylin: 1 g ammonium iron (III) sulfate in 50 mL of H_2O, 0.8 g sulfuric acid mixed with 0.5 g hematoxylin in 50 mL EtOH, mix both solutions, filter. Stain can be reused virtually endlessly if filtered every 20–30 stains.
9. Differentiation solution: 0.1% (v/v) HCl in 70% (v/v) EtOH. Can be used to differentiate up to 30 slides.
10. Eosin: 0.1 g Eosin Y, 0.5 mL glacial acetic acid in 100 mL H_2O. Filter, store in a light-protected container.
11. 80% (v/v) EtOH: 20 mL H_2O in 80 mL EtOH.
12. Histological clearing agent (e.g., HistoClear II, National Diagnostics).
13. Mounting medium.

3 Methods

3.1 Sampling and Adaptation

Botrylloides anceps colonies can be found in stony areas of the intertidal zone, less than 1 m deep. So far, we collected this species from three different stations (Konacık-Iskenderun, Mezitli-Mersin, and Alanya-Antalya) but we have found other suitable colonial ascidians in different sites of the North-eastern Mediterranean coastlines (Fig. 1a, *see* **Note 3**).

1. Chose a rocky shore that *B. anceps* possibly inhabits (Fig. 1b, *see* **Note 4**).
2. Sample the selected shore at low tide.
3. Record the salinity of the water (*see* **Note 5**).
4. Record the water temperature.
5. Carefully lift submerged stones to check for colonies on its substrate-facing side.
6. Place back empty stones in the exact same place where collected.
7. Place a marker on the spot of a suitably inhabited rocks (*see* **Note 6**).
8. Carry the stone to the shore for easier manipulations.
9. Give a unique identification code to the colony.
10. Write the code on a glass slide and on a 1.5 mL tube using a waterproof pen.
11. Place the slide and tube nearby to the colony.
12. Take a picture of the whole setup (Fig. 1c).
13. Peel a 1 mm stretch of the colony from its substrate using single-edged razor blades.
14. Place the animals onto the labeled slide (*see* **Note 7**).



Fig. 1 Collecting wild botryllids. (**a**) The map shows the sampling locations from the southern part of Turkey. *Botrylloides* were observed in all four location, but *B. anceps* could not be found in Kızkalesi-Mersin. (**b**) A picture from the Kızkalesi station. (**c**) A picture of a complete setup with an inhabited rock, a fragment transferred on a glass slide and a tube with a sample for DNA barcoding. (**d**) Attaching a sample on a slide. (**e**) Magnification of a *B. anceps* colony secured on a slide by using fine cotton thread

15. Gently tie the colony to the slide using a cotton thread (Fig. 1e, *see* **Note 8**).
16. Put the slide vertically in the fitted slots of the glass staining racks placed inside an insulated plastic container filled up with seawater (*see* **Note 9**).

17. Peel another 1 mm stretch of the colony.
18. Place the sample in the labeled tube filled with 70% ethanol. Keep at room temperature until DNA isolation for DNA barcoding (*see* **Note 10**).
19. Bring back the stone to that exact same place where it was collected from.
20. Transfer the animals and the samples to an aquaculture room within the next 24 h (*see* **Note 11**).
21. Fill the husbandry system with FSW of the same salinity as at the collection place.
22. Put the slides with their staining racks into the husbandry system (Fig. 2a, b, *see* **Note 12**).
23. Aerate the system with a medium bubbling level (Fig. 2a).
24. Maintain the water of the system at a constant temperature similar to that at the collection place (between 20 and 25 °C).
25. Illuminate the animals with a low light on 12 h day and 12 h night photoperiod.
26. Pipette daily 2.5 mL of food mixture per 3 L of FSW.
27. Replace the FSW with fresh FSW every other day.
28. Wait 1 week after the collection for the colonies to attach to the glass slide.
29. Remove the cotton thread.
30. Transfer the new colonies to the main husbandry system.

3.2 DNA Barcoding

Total DNA isolation uses handmade buffers adapted from a previously published protocol [33].

1. Centrifuge the sample to be used for DNA barcoding for 2 min at max speed.
2. Discard the supernatant and leave it under a hood until ethanol completely evaporate (~1 h).
3. Add 150 µL of lysis buffer.
4. Homogenize with a single use pestle.
5. Add another 150 µL of lysis buffer.
6. Add 60 µL $NaClO_4$ stock solution.
7. Add 360 µL of phenol–chloroform–isoamyl alcohol.
8. Vortex the tube for 10 min at 600 rcf in a hood.
9. Centrifuge for 10 min at 14,000 rcf, 4 °C.
10. Transfer the upper phase (around 350 µL) in a new 1.5 mL tube.
11. Add 350 µL of chloroform–isoamyl alcohol to the isolated phase.

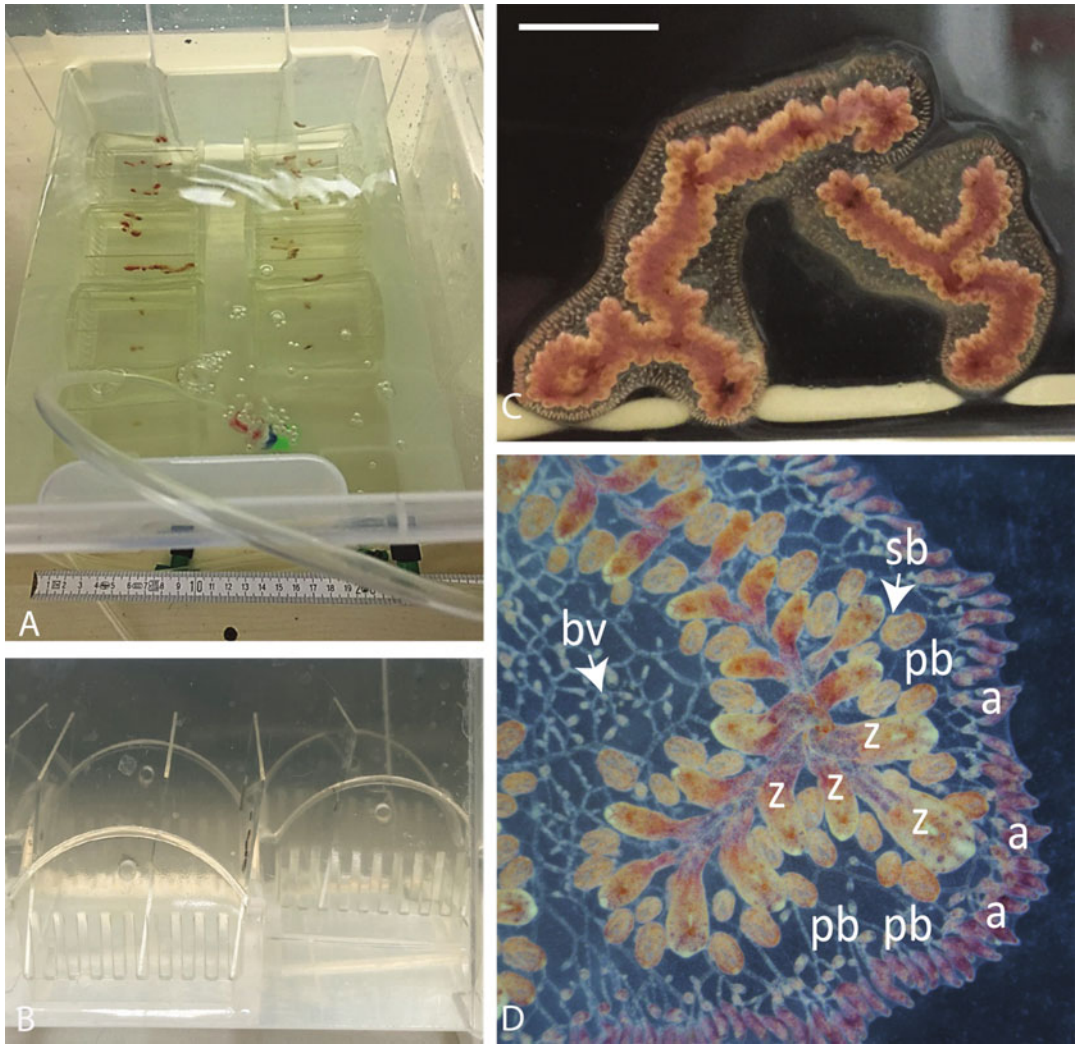


Fig. 2 Colony maintenance. (**a**) A *B. anceps* husbandry setup in our aquaculture room. (**b**) A side-view of a staining rack with *botryllid* colonies in it. (**c**) A top view of a *Botrylloides anceps* colony. Scale bar is 1 cm. (**d**) Magnification of a part of a system during the "takeover" (main zooids are being resorbed while the primary buds replace them). *a* ampulla, *bv* blood vessel, *pb* primary bud, *sb* secondary bud, *Z* zooid

12. Mix gently by shaking for 30 s.
13. Centrifuge for 10 min at 14,000 rcf, 4 °C.
14. Transfer the upper phase in a new 1.5 mL tube.
15. Add 350 µL of cold 100% EtOH to the isolated phase and mix gently (*see* **Note 13**).
16. Centrifuge the sample for 30 min at 16,000 rcf, 4 °C.
17. Replace the supernatant with 700 µL of cold 70% ethanol.
18. Centrifuge the sample for 30 min at 16,000 rcf, 4 °C.

19. Discard the supernatant.
20. Leave the sample under a hood overnight to dry.
21. Resuspend the DNA in 50 μL of ultrapure water.
22. Quantify the DNA concentration and quality using a spectrophotometer or equivalent tool (e.g., Qubit fluorometer).
23. Make sure the quality of DNA is within acceptable range (*see* **Note 14**).
24. Dilute the DNA with ultrapure water to reach a concentration between 10 to 100 ng/μL (*see* **Note 15**).
25. Transfer 25 μL of 2× PCR mater mix to a PCR tube.
26. Add 2 μL of DNA template.
27. Add 1 μL of cytochrome oxidase I primer mix.
28. Add 23 μL of ultrapure water.
29. Run a PCR program with the following parameters: 95 °C 5 min; 35 cycle × (95 °C 45 s; 45 °C 45 s; 72 °C 90 s), 72 °C for 10 min and infinite hold at 12 °C.
30. Load 4 μL of the PCR product with 1 μL of loading dye into a well of agarose gel.
31. Load 2 μL 100 bp DNA ladder into another well.
32. Run the electrophoresis for 60 min at 100 V.
33. Visualize the results of the PCR amplification on the gel (*see* **Note 16**).
34. Identify PCR positive samples by the presence of a 600 bp amplification band in the visualized gel by comparison with the DNA ladder.
35. Use a PCR clean-up kit to purify the positive PCR products (*see* **Note 17**).
36. Perform the Sanger sequencing for both directions (forward and reverse) of the purified COI amplifications (*see* **Note 18**).
37. Trim the primer sections from the raw sequencing results (*see* **Note 19**).
38. Run your trimmed sequences through the BOLD Identification System [34] (*see* **Notes 20** and **21**).
39. Record the Probability of Placement to determine the species of your sample (*see* **Note 22**).
40. Assign your sample to the species with a sequence match of 97% or above and a query cover of at least 85% (*see* **Note 23**).
41. Submit your DNA barcode to the BOLD with all the information about sampling areas, specimen and if possible, a voucher ID from a fragment of your sample deposited in a museum (*see* **Note 24**).

3.3 Colonies Maintenance

Our maintenance protocol has been adapted from the work by Rosner et al. (2019) [35].

1. Pipette daily 2.5 mL of food mixture per 3 L of FSW.
2. Replace the FSW with fresh FSW every other day.
3. Once a week, transfer the colonies to a smaller container filled with FSW for maintenance.
4. Prepare a humidity chamber for the subcloning by placing a glass staining rack onto a wet tissue inside a sealable container.
5. Take one slide out of the water.
6. Clean the glass slide around the colony by scratching it using a razor blade.
7. Gently brush the colony with a soft paint brush to remove debris and dirt.
8. Check the colony under a stereomicroscope (*see* **Note 25**).
9. Ablate portions of the colony that are degrading, dirty or unattached to the glass slide.
10. If the cleaned colony is smaller than 2 cm in diameter, put it back into the husbandry system.
11. For larger colonies, detach a small piece of the main colony containing between 5 and 10 zooids using a razor blade (Fig. 2c, *see* **Note 26**).
12. Transfer the fragment (called subclone) onto a new glass slide using a brush.
13. Gently dry out the water around the colony fragment without touching the animal using paper tissue.
14. Give a unique identification code to the fragment.
15. Write the code on the glass slide.
16. Place the slide in the humidity chamber.
17. Wait 30 min for the colony to attach onto the slide.
18. Place the new slide carefully into the husbandry system.
19. Repeat **steps 5** to **18** until all slides have been processed.
20. Handle the new slides very carefully during the first week.

3.4 Whole-Body Regeneration

Our regeneration protocol has been adapted from the work by Rinkevich et al. (2007) [36].

1. Transfer *B. anceps* sub-clones into a container filled with FSW (*see* **Note 27**).
2. Place a slide upside-down under a stereomicroscope.
3. Observe the buds and budlets (the buds' buds) to determine the blastogenic stages (Fig. 2d, *see* **Note 28**).

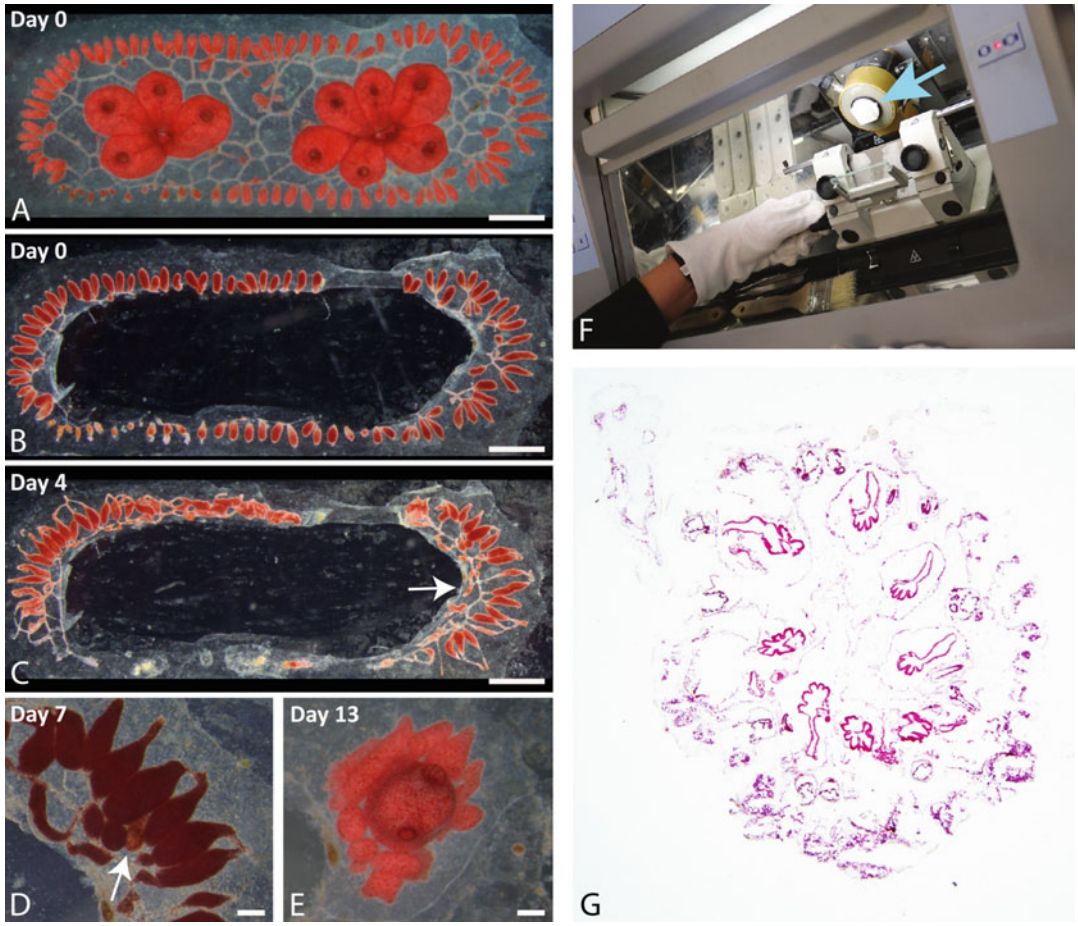


Fig. 3 Whole-body regeneration. (**a**) A *B. anceps* colony before removing zooids and buds. Scale bar is 1 mm. (**b**) The same colony after removal all the zooids and buds. (**c**) Fourth day post ablation. (**d**) Magnification of a portion of the regenerating colony where a regeneration niche is developing (arrow). Scale bar is 200 μm. (**e**) Fully completed WBR (day 13th). (**f**) The frozen mold (blue arrow) attached to the cryostat for sectioning. (**g**) A section of *B. anceps* colony at 1.2× magnification

4. Turn the slide to have the colony facing upwards.
5. Take a picture of the whole colony together with a scale (Fig. 3a).
6. Remove all the zooids and buds by carefully cutting all the blood vessels between the zooid, buds and ampullas with the pointy side of a fine needle, leaving only ampullas and peripheral blood vessels (Fig. 3b).
7. Record the date and time.
8. Transfer the regenerating colonies to a dedicated husbandry system.
9. Do not feed them (they will not take it) but change the water with fresh FSW every other day (*see* **Note 29**).

10. Wait until the desired stage of WBR is reached (*see* **Note 30**).
11. Take pictures from both sides of the regenerating colonies (Fig. 3a–e).
12. Proceed with the desired downstream analysis.

3.5 Histological Sectioning

Although the most common protocols for histology use paraffin embedding, we prefer to use cryosectioning for its quick turn-around time.

1. Transfer the colony to be fixed into a container filled with 100 mL of FSW.
2. Add a few menthol crystals to the water.
3. Wait 10 min for the colony to anesthetize.
4. Detach the colony from the glass using razor blade.
5. Transfer into a 2 mL tube filled with 1.5 mL of Bouin's fixative (*see* **Note 31**).
6. Fix overnight at 4 °C.
7. Replace the fixative with PBS.
8. Discard the rinsing medium.
9. Fill the tube with PBS.
10. Wait 2 h for the sample to wash.
11. Repeat **steps 8** to **10** three more times (*see* **Note 32**).
12. Transfer the sample to a 2 mL tube filled with 1.5 mL dehydration solution.
13. Leave 1 h at 4 °C to dehydrate (*see* **Note 33**).
14. Precool a metal block in a closed container filled half-way with liquid nitrogen (*see* **Note 34**).
15. Fill a labeled embedding mold with OCT (*see* **Note 35**).
16. Transfer the colony into the mold using a pair of tweezers (*see* **Note 36**).
17. Center the colony at the bottom of the mold with a pair of tweezers (*see* **Notes 37** and **38**).
18. Place the mold onto the cold metal block.
19. Wait 5 min until it becomes fully opaque.
20. Store up to 12 months at −80 °C until sectioning.
21. Transfer the block into the cryostat.
22. Peel the mold to release the block of frozen OCT.
23. Glue the block onto the cryostat's sample holder using a few drops of OCT.
24. Freeze the sample holder.
25. Label 10 coated microscopy glass slides (*see* **Note 39**).

26. Fix the sample holder onto the cryostat (Fig. 3f).
27. Cut the excess OCT around the sample using a razor blade (*see* **Note 40**).
28. Bring the sample close to the blade.
29. Section until the blade cuts the block twice.
30. Move the blade backwards.
31. Realign the sample in the direction of the last cut to place it perpendicular to the blade (*see* **Note 41**).
32. Repeat **steps 28** to **31** until the cryostat cuts through the whole surface of the block (*see* **Note 42**).
33. Cut a section of the block (*see* **Note 43**).
34. Transfer it to the next available position on the slides (*see* **Note 44**).
35. Brush the blade to remove debris and ice.
36. Brush the sample to remove leftover OCT.
37. Repeat **steps 33** to **36** until no sample is visible in the last section.
38. Wait 20 min for the slides to dry.
39. Clean the cryostat following the manufacturer's instructions.
40. Store the dried sections at −20 °C until needed.

3.6 Hematoxylin-Eosin Stain

1. Thaw the cryosectioned slide on the bench (*see* **Note 45**).
2. Transfer the slides into a Coplin jar filled with tap water (*see* **Note 46**).
3. Leave the section to rehydrate for 5 min.
4. Transfer to another Coplin jar filled with Groat's hematoxylin.
5. Stain for 12 min (*see* **Note 47**).
6. Shake vigorously each slide in the differentiation solution for 20 s.
7. Transfer into a Coplin jar filled with tap water.
8. Place the Coplin jar in the sink under a stream of running tap water.
9. Leave 10 min to color.
10. Rinse the slides in distilled water.
11. Transfer into a Coplin jar filled with Eosin.
12. Stain for 5 min.
13. Rinse the slides in 80% EtOH.
14. Transfer the slides to 100% EtOH (*see* **Note 48**).
15. Wash for 3 min.

16. Transfer to a bath filled with clearing agent.
17. Wash for 3 min.
18. Repeat **steps 16** and **17** twice.
19. Place a slide flat on a paper tissue.
20. Pour 3 drops of mounting medium over the sections.
21. Hold a sufficiently long coverslip over the stained sections.
22. Rest one side of the coverslip on the corresponding side of the slide, still holding the other side.
23. Hold the other side of the coverslip using a short needle placed under the coverslip.
24. Slowly lower the coverslip until it rests fully flat on the slide (*see* **Note 49**).
25. Identify bubbles trapped under the coverslip.
26. Swipe the air out of the mounting medium by pressing on the coverslip with the needle while holding the coverslip in place with the other hand (*see* **Note 50**).
27. Cover the mounted slide with a paper tissue.
28. Gently press uniformly on the coverslip to remove any excess mounting medium.
29. Leave the slide to dry for 30 min.
30. Use a paper tissue dipped in clearing agent to clean the dried mounting medium on the slide.
31. Image the slide under a brightfield microscope.
32. H&E sections will have dark DNA stains and purple to red cytoplasm (Fig. 3g).

4 Notes

1. These primers have been designed specifically for botryllids [37]. Universal invertebrate primers (Forward: GGTCAA CAAATCATAAAGATATTGG, Reverse: TAAACTTCAGGG TGACCAAAAAATCA, [38]) and tunicate specific primers (Forward: TCGACTAATCATAAAGATATTA, Reverse: AAC TTGTATTTAAATTACGATC, [39]) can also be used using the same protocol.
2. Handle the saturated solution of picric acid very carefully and do not let it dry in the bottle as picric acid crystals are explosive! To circumvent this issue, we favor the use of commercially available Bouin's fixative.
3. Although *B. anceps* colonies were the only species found in some locations, they more typically share their habitat with

other invertebrates (mostly sponge) and other botryllids (e.g., *Botryllus schlosseri, Botrylloides aff. leachii, Didemnum* sp.). All of them can be collected and kept in the aquaculture room using the same protocol.

4. Sometimes the species cannot be found even in very suitable rocky habitat. You may need to check many coastlines to find this particular species.
5. The salt concentration is one of the main requirements for thriving botryllid ascidian culture. Both artificial and natural seawater can be used. In our institute, we are using natural seawater collected on the Mediterranean Sea coastline. However, likely because of the presence of multiple freshwater streams in the area, we have observed that the salinity on our shores is not stable. To circumvent this issue, we measure the salinity of each new batch of FSW, correct it by adding sea salt and keep it in our aquaculture room for 1 week before use.
6. To preserve the biodiversity, we recommend to collect only part of each identified colonies, typically around 1 mm of zooids. Consequently, only colonies larger than 2–3 mm long are suitable for collection.
7. *B. anceps* colony is prone to folding during the sampling. Make sure that once on the glass slide, all zooids of the colony are facing upwards. Like on the stone, their atrial and buccal siphons should be facing towards the water and not towards the glass.
8. This technique is adapted from a previously published protocol for the collection of colonial ascidians [40].
9. We recommend placing only three slides on each rack, to give them enough place for an effective water circulation.
10. Species identification is one of the main issues when working with botryllid ascidians. Indeed, many species have a similar external morphology, color patterning is not a good discriminant and chimerism is common in Botryllid ascidians. Consequently, DNA barcoding should be used to overcome this identification problem. Tissue fragment for DNA barcoding can either be isolated directly during sampling (Fig. 1d) or from a sub-cloned colony in the husbandry system.
11. There is no need to use air stone while transferring the animals to the lab.; they can survive hours without oxygen support.
12. Botryllid cultures are typically done in plastic container. These vessels are easy to handle, to carry, and to wash. However, prefer food-grade containers to avoid chemicals leaking in the water.

13. You should see the DNA precipitating as white strings. If you do not see any precipitation, store the sample overnight at −20 °C to increase the precipitation.
14. In the nanodrop spectrophotometer, the value 1.8 from 260/280 ratio represents the pure DNA and 2.0–2.2 from 260/230 ratio pure nucleic acid. Be sure your DNA in this range or close these values. If not, you may need to isolate the DNA from the beginning (if you have some remaining sample) or clean the isolated DNA by bringing the volume to 100 μL by adding lysis buffer and restart from **step 4**.
15. Dilution of the DNA is necessary because high DNA concentrations inhibit the reaction. Besides, it may yield big shining plums (smears) of nonamplified DNA scattered along the agarose gel.
16. If you record double PCR products for one sample, set the PCR again, and rearrange the annealing temperature between the 46 to 49 °C, it will help reduce nonspecific PCR products.
17. After a PCR reaction, purification of the targeted genes is necessary for downstream use, and it facilitates removing enzymes, nucleotides, detergents, primers, and buffer components.
18. Performing the sequencing to both directions allows you to double-check your sequences by reducing nucleotide assignment errors.
19. Without trimming, you may get less coverage from the blast analysis. So, we highly recommend trim off the primer sites and use only the central sequence.
20. The NCBI BLAST engine can be used as alternative or as complement to the BOLD identification system [41].
21. It is also possible to use these sequences to build a reference DNA barcode library for a known species as identified by an expert taxonomist. This approach has the advantage of providing a trustful reference to the entire community.
22. Probability of Placement (%): how similar the query sequence is to the target sequence, that is, how many characters in each sequence are identical. The higher the percent identity is, the more significant the match.
23. Be aware that there are some mislabeled sequences in public reference databases [42]. In the case your sequence matches several different species, favor the references uploaded by expert taxonomists.
24. If you encounter a big enough colony during the sampling, take the third fragment beside the aquaculture and DNA barcoding's processes and preserve it into a 10% formalin solution

Table 1
Staging method of the blastogenic cycle

Stages	Features
A	It starts with the opening of the buccal and atrial siphons
B	Initiates with the beginning of heartbeats in the primary buds
C	It begins with the onset of organogenesis in secondary buds and the accumulation of pigment cells in the primary buds' epithelium
D	Commences with the shutdown of buccal and atrial siphons

and submit it in a museum with a unique voucher ID. Load this ID to NCBI or the BOLD system when you upload your barcodes.

25. Sometimes large number of Ciliates can be observed on the slides. In case of such invasion, transfer the concerned colonies to a temporary container, wash all the husbandry system, glass racks and brushes with 10% (v/v) bleach. Clean the dead parts of each colony with a single edge razor blade and a soft brush using fresh seawater. Finally, transfer the cleaned colonies into a new husbandry system.
26. When a colony covers more than 1/4 of the slide, make sub-clones with half of its zooids and put the resulting new slides in a new husbandry system.
27. We recommend starting a WBR experiment with at least 8 colonies from the same original clone to provide sufficient material for histological sectioning and biological replica.
28. We divide the blastogenic cycle into four major stages as previously published [43]. The details about each stage are given in Table 1.
29. During WBR there are no zooids left to consume the food. The decaying food will contaminate the entire container.
30. Monitoring WBR progression at least on a daily basis. Record the time of observation precisely to match it with the defined stages of WBR ([44], Table 2). Alternatively, film the whole processes with a high-quality camera to monitor WBR.
31. Fixing the colonies at different stages of WBR for immunohistochemistry analysis will help to observe this process at the cellular and sub-cellular level [15].
32. Large samples might require more washing steps. Repeat washing until the PBS has a no more yellow taint.
33. Dehydration time depends on the size of the sample. Dehydration is complete when the sample sinks in the sucrose.
34. A block of dry ice can also be used instead of the cooled metal block.

Table 2
The whole-body regeneration stages of *B. anceps*

Stages	Time	Features
Stage 0	0–30 m	Hemorrhagic period; after removing all the zooids and buds, hemorrhagic period stopped in 1 min (Fig. 3b)
Stage 1	30 m–24 h	Formation of the new vessels (Fig. 3b)
Stage 2	48 h–120 h	Reorganization; the tissue underwent considerable restructuring as it condenses together inside the tunic (Fig. 3c)
Stage 3	144 h–168 h	Formation of the regeneration niches (Fig. 3d)
Stage 4	192 h–384 h	Formation of the functional zooid (Fig. 3e)

(*m* minute, *h* hours)

35. It is very important to avoid bubbles at this step. The best approach to do so is to pour the OCT in one continuous streak in one corner of the mold. In case bubbles get trapped in the OCT, group them at the surface of the OCT in one corner of the mold.
36. Do not squeeze the sample during this transfer or it will get damaged.
37. Alignment of the colony is typically done with its tunic lying flat at the bottom of the mold and its zooids facing upwards. Other alignments to suit different types of histological sections can easily be produced using the same approach.
38. OCT is highly viscous so moving the submerged sample can be a bit difficult as any movement of the tweezers will move it. We advise to push the sample using a pair of tweezers and to use how much they are open to modulate how gentle the strokes are.
39. The exact number of slides that your sample will occupy depends on the thickness of your sectioning and of your sample. In our hands, for relatively flat colonies and a sectioning at 12 μm, 10 slides were optimal. We also tested 12 slides at 10 μm and 8 slides at 14 μm.
40. Removing OCT around the sample allows to have more sections on the same glass slide, which is very useful for downstream analyses. However, removing too much OCT will cause the sections to be teared during sectioning. We recommend having at least 1 mm of OCT surrounding the sample.
41. The direction and the amplitude of the realignment will need to be adapted to your cryostat and your current sample. Make

sure that the blade is secured and the sample is blocked before you start moving it.

42. Be aware that for blocks with colonies aligned at the bottom of the block, this realignment should be done efficiently as you will start cutting into the sample almost immediately.
43. Obtaining good sections requires a bit of practice. The sharpness of the blade is obviously very important, but the speed and fluidity of the movement of the sample are crucial too. Typically, we advise moving the sample in one continuous movement that lasts about 2 s. Some of the main issues observed during sectioning are that sections can be teared, they can fold, they can curl or they can stay attached to the main block. In the first case, try varying the speed of the cut. If that does not suffice, sample might have required a stronger fixation or embedding included small bubbles. Increasing the thickness of the sections is the most effective solution to this problem. For the folding, try to clean the blade some more as even very small debris can prevent the section from sliding properly on the blade. Curling was mainly observed when room temperature and humidity was too high. Curled sections can be flattened using a thin paint brush. However, curling takes a few seconds to occur so we rather recommend that the transfer be done very quickly. Attachments are typically due to excess OCT at the top of the block. Brushing out this material should solve the issue. If not, a small bezel cut with a razor blade to remove this upper edge should be very effective.
44. We use two main organizations for the sections. First a continuous one, where each section follows the previous one. This has the advantage of being very flexible in terms of the number of slides that are used. Second, a parallel one, where all the slides are filled in parallel. This has the advantage of yielding slides that are almost perfect replica of one another. This approach is particularly useful for comparing different stainings.
45. Thawing typically takes around 2 min. Wait until all condensation has evaporated from the slides.
46. The minerals present in tap water are beneficiary to the staining process. For the specified steps, better results were obtained with tap water than with deionized/distilled water.
47. Although H&E is one of the most straightforward and reproducible histological stain, the intensity of the stain could be influenced by many parameters including the thickness of your section, the type of OCT or the fixation of your sample. It might thus be necessary to modify the duration of the staining steps.

48. At this step, the slides could be checked under a microscope for the quality of their staining. Staining of both hematoxylin and eosin could be increased by repeating the corresponding steps.
49. Mounting medium are typically highly viscous. It is thus necessary to lower the coverslip slowly to avoid trapping air bubbles under it.
50. The point is to push the air bubbles toward the boundaries of the coverslip by pressing around it and following it as it moves. Note that only bubbles in contact with the sample will be an issue during imaging. Other bubbles could be left where they are.

Acknowledgments

The study was supported by the YÖP-701-2018-2666 project (Middle East Technical University support program) and by the MARISTEM European COST Action (CA16203). The experiments were done in the IMS-METU, DEKOSIM laboratory (BAP-08-11-DPT2012K120880-Turkey) and the Blanchoud Group laboratory, University of Fribourg (Switzerland). We are grateful to Prof. Rinkevich (Israel Oceanographic and Limnologic research center) and his research group; Dr. Amalia Rosner, Dr. Jacob Douek, Dr. Ziva Lapidot, and Mr. Guy Paz for the original protocols adapted in this chapter. We appreciate the support of the Erdemli Municipality in protecting the Kızkalesi sampling area.

References

1. Delsuc F, Brinkmann H, Chourrout D et al (2006) Tunicates and not cephalochordates are the closest living relatives of vertebrates. Nature 439:965–968. https://doi.org/10.1038/nature04336
2. Millar RH (1971) The biology of ascidians. In: Russell FS, Yonge M (eds) Advances in marine biology, vol 9. Academic Press, London, New York, pp 1–100
3. Rinkevich B, Shlemberg Z, Lilker-levav T et al (1993) Life history characteristics of *Botryl-loides* (tunicata) populations in Akko bay, Mediterranean coast of Israel. Isr J Zool 39: 197–212. https://doi.org/10.1080/00212210.1993.10688712
4. Rinkevich B, Shlemberg Z, Fishelson L (1995) Whole-body protochordate regeneration from totipotent blood cells. Proc Natl Acad Sci U S A 92(17):7695–7699. https://doi.org/10.1073/pnas.92.17.7695
5. Lemaire P, Smith WC, Nishida H (2008) Ascidians and the plasticity of the chordate developmental program. Curr Biol 18(14): R620–RR63. https://doi.org/10.1016/j.cub.2008.05.039
6. Davidson B, Swalla BJ (2002) A molecular analysis of ascidian metamorphosis reveals activation of an innate immune response. Development 129(20):4739–4751
7. Brunetti R (2009) Botryllid species (Tunicata, Ascidiacea) from the Mediterranean coast of Israel, with some considerations on the systematics of Botryllinae. Zootaxa 2289(1):18–32. https://doi.org/10.11646/zootaxa.2289.1.2
8. Alié A, Hiebert LS, Scelzo M et al (2021) The eventful history of nonembryonic development in tunicates. J Exp Zool Pt B Mol Dev Evol 336:250–266. https://doi.org/10.1002/jez.b.22940

9. Brown FD, Keeling EL, Le AD et al (2009) Whole body regeneration in a colonial ascidian, *Botrylloides violaceus*. J Exp Zool B Mol Dev Evol 312B(8):885–900. https://doi.org/10.1002/jez.b.21303
10. Blanchoud S, Zondag L, Lamare MD et al (2017) Hematological analysis of the ascidian *Botrylloides leachii* (Savigny, 1816) during whole-body regeneration. Biol Bull 232(3):143–157. https://doi.org/10.1086/692841
11. Voskoboynik A, Simon-Blecher N, Soen Y et al (2007) Striving for normality: whole body regeneration through a series of abnormal generations. FASEB J 21(7):1335–1344. https://doi.org/10.1096/fj.06-7337com
12. Rinkevich Y, Rinkevich B, Reshef R (2008) Cell signaling and transcription factor genes expressed during whole body regeneration in a colonial chordate. BMC Dev Biol 8(1):100. https://doi.org/10.1186/1471-213X-8-100
13. DuBuc TQ, Traylor-Knowles N, Martindale MQ (2014) Initiating a regenerative response; cellular and molecular features of wound healing in the cnidarian *Nematostella vectensis*. BMC Biol 12(1):24. https://doi.org/10.1186/1741-7007-12-24
14. Tiozzo S, Brown FD, Tomaso D (2008) Regeneration and stem cells in ascidians. In: Bosch TCG (ed) Stem cells: from hydra to man. Springer, Dordrecht. https://doi.org/10.1007/978-1-4020-8274-0_6
15. Rosner A, Moiseeva E, Rinkevich Y et al (2009) Vasa and the germ line lineage in a colonial urochordate. Dev Biol 331(2):113–128. https://doi.org/10.1016/j.ydbio.2009.04.025
16. Rinkevich Y, Rosner A, Rabinowitz C et al (2010) Piwi positive cells that line the vasculature epithelium, underlie whole body regeneration in a basal chordate. Dev Biol 345(1):94–104. https://doi.org/10.1016/j.ydbio.2010.05.500
17. Knapp D, Tanaka EM (2012) Regeneration and reprogramming. Curr Opin Genet Dev 22(5):485–493. https://doi.org/10.1016/j.gde.2012.09.006
18. Rinkevich Y, Douek J, Haber O et al (2007a) Urochordate whole body regeneration inaugurates a diverse innate immune signaling profile. Dev Biol 312(1):131–146. https://doi.org/10.1016/j.ydbio.2007.09.005
19. Kassmer SH, Langenbacher AD, De Tomaso AW (2020) Integrin-alpha-6+ candidate stem cells are responsible for whole body regeneration in the invertebrate chordate *Botrylloides diegensis*. Nat Commun 11:4435. https://doi.org/10.1038/s41467-020-18288-w
20. Rinkevich Y, Paz G, Rinkevich B et al (2007b) Systemic bud induction and retinoic acid signaling underlie whole body regeneration in the urochordate *Botrylloides leachii*. PLoS Biol 5(4):e71. https://doi.org/10.1371/journal.pbio.0050071
21. Zondag LE, Rutherford K, Gemmell NJ et al (2016) Uncovering the pathways underlying whole body regeneration in a chordate model, *Botrylloides leachii* using de novo transcriptome analysis. BMC Genomics 17(1):114. https://doi.org/10.1186/s12864-016-2435-6
22. Bancroft FW (1903) Variation and fusion of colonies in compound ascidians, vol 3. The Academy, Harward University, Cambridge, MA
23. Burighel P, Brunetti R, Zaniolo G (1976) Hibernation of the colonial ascidian *Botrylloides leachii* (Savigny): histological observations. Ital J Zool 43(3):293–301
24. Oka H, Watanabe H (1959) Vascular budding in *Botrylloides*. Biol Bull 117(2):340–346. https://doi.org/10.2307/1538913
25. Okuyama M, Saito Y (2001) Studies on Japanese Botryllid ascidians. I. a new species of the genus *Botryllus* from the Izu Islands. Zoolog Sci 18(2):261–267. https://doi.org/10.2108/zsj.18.261
26. Mukai H, Watanabe H (1976) Studies on the formation of germ cells in a compound ascidian *Botryllus primigenus* oka. J Morphol 148(3):337–361. https://doi.org/10.1002/jmor.1051480306
27. Ballarin L, Franchini A, Ottaviani E et al (2001) Morula cells as the major immunomodulatory hemocytes in ascidians: evidences from the colonial species *Botryllus schlosseri*. Biol Bull 201(1):59–64. https://doi.org/10.2307/1543526
28. Manni L, Zaniolo G, Cima F et al (2007) *Botryllus schlosseri*: a model ascidian for the study of asexual reproduction. Dev Dyn 236(2):335–352. https://doi.org/10.1002/dvdy.21037
29. Gasparini F, Burighel P, Manni L et al (2008) Vascular regeneration and angiogenic-like sprouting mechanism in a compound ascidian is similar to vertebrates. Evol Dev 10(5):591–605. https://doi.org/10.1111/j.1525-142X.2008.00274.x
30. Ballarin L, Menin A, Tallandini L et al (2008) Haemocytes and blastogenetic cycle in the colonial ascidian *Botryllus schlosseri*: a matter of life and death. Cell Tissue Res 331(2):555–564. https://doi.org/10.1007/s00441-007-0513-4

31. Franchi N, Schiavon F, Carletto M et al (2011) Immune roles of a rhamnose-binding lectin in the colonial ascidian *Botryllus schlosseri*. Immunobiology 216(6):725–736. https://doi.org/10.1016/j.imbio.2010.10.011
32. Lauzon RJ, Brown C, Kerr L et al (2013) Phagocyte dynamics in a highly regenerative urochordate: insights into development and host defense. Dev Biol 374(2):357–373. https://doi.org/10.1016/j.ydbio.2012.11.006
33. Paz G, Douek J, Mo C et al (2003) Genetic structure of *Botryllus schlosseri* (Tunicata) populations from the Mediterranean coast of Israel. Mar Ecol Prog Ser 250:153–162. https://doi.org/10.3354/meps250153
34. Ratnasingham S, Hebert PDN (2007) BARCODING: BOLD: the barcode of life data system (http://www.barcodinglife.org). Mol Ecol Notes 7:355–364. https://doi.org/10.1111/j.1471-8286.2007.01678.x
35. Rosner A, Kravchenko O, Rinkevich B (2019) IAP genes partake weighty roles in the astogeny and whole-body regeneration in the colonial urochordate *Botryllus schlosseri*. Dev Biol 448:320–341. https://doi.org/10.1016/j.ydbio.2018.10.015
36. Rinkevich Y, Paz G, Rinkevich B et al (2007) Systemic bud induction and retinoic acid signaling underlie whole body regeneration in the Urochordate *Botrylloides leachii*. PLoS Biol 5:e71. https://doi.org/10.1371/journal.pbio.0050071
37. Reem E, Douek J, Rinkevich B (2018) Ambiguities in the taxonomic assignment and species delineation of botryllid ascidians from the Israeli Mediterranean and other coastlines. Mitochondrial DNA Pt A 29:1073–1080. https://doi.org/10.1080/24701394.2017.1404047
38. Folmer O, Black M, Hoeh W et al (1994) DNA primers for amplification of mitochondrial cytochrome c oxidase subunit I from diverse metazoan invertebrates. Mol Mar Biol Biotechnol 3:294–299
39. Stefaniak L, Lambert G, Gittenberger A et al (2002) (2009) genetic conspecificity of the worldwide populations of *Didemnum vexillum* Kott. Aquat Invasions 4(1):29–44. https://doi.org/10.3391/ai.2009.4.1.3
40. Hyams Y, Paz G, Rabinowitz C et al (2017) Insights into the unique torpor of *Botrylloides leachii*, a colonial urochordate. Dev Biol 428:101–117. https://doi.org/10.1016/j.ydbio.2017.05.020
41. Johnson M, Zaretskaya I, Raytselis Y et al (2008) NCBI BLAST: a better web interface. Nucleic Acids Res 36:W5–W9. https://doi.org/10.1093/nar/gkn201
42. Viard F, Roby C, Turon X et al (2019) Cryptic diversity and database errors challenge non-indigenous species surveys: an illustration with *Botrylloides spp.* in the English Channel and Mediterranean Sea. Front Mar Sci 6:1–13. https://doi.org/10.3389/fmars.2019.00615
43. Mukai H, Watanabe H (1976) Relation between sexual and asexual reproduction in the compound ascidian, *Botryllus primigenus*. Sci Rep Fac Educ Gumma Univ 25:61–79
44. Zondag LE, Rutherford K, Gemmell NJ et al (2016) Uncovering the pathways underlying whole body regeneration in a chordate model, *Botrylloides leachi* using de novo transcriptome analysis. BMC Genomics 17:114. https://doi.org/10.1186/s12864-016-2435-6

Open Access This chapter is licensed under the terms of the Creative Commons Attribution 4.0 International License (http://creativecommons.org/licenses/by/4.0/), which permits use, sharing, adaptation, distribution and reproduction in any medium or format, as long as you give appropriate credit to the original author(s) and the source, provide a link to the Creative Commons license and indicate if changes were made.

The images or other third party material in this chapter are included in the chapter's Creative Commons license, unless indicated otherwise in a credit line to the material. If material is not included in the chapter's Creative Commons license and your intended use is not permitted by statutory regulation or exceeds the permitted use, you will need to obtain permission directly from the copyright holder.



Part III

Cellular Approaches



Chapter 17

In Situ Hybridization to Identify Stem Cells in the Freshwater Sponge *Ephydatia fluviatilis*

Chiaki Kojima and Noriko Funayama

Abstract

Sponges (Porifera) are a large phylum that includes an enormous number of species. They are classified into four classes. Among these four classes, class Demospongiae is the largest and contains more than 90% of sponge species. In the last decade, methodologies for molecular studies and sequencing resources in sponge biology have dramatically advanced and made it possible to clearly define particular types of cells based on the genes they are expressing. Here we describe in detail the method of high-resolution WISH (whole mount in situ hybridization) and dual color fluorescent detection of in situ hybridization (dual color FISH) that we have established to detect particular types of cells, especially their stem cells known as archeocytes, in juveniles of freshwater demosponge, *E. fluviatilis*.

Key words Stem cells, *Piwi*, *Musashi*, Porifera, WISH, FISH, Archeocyte

1 Introduction

Molecular studies of sponges are important for both evolutionary developmental biology (since sponges are one of the earliest branching metazoan phyla) and ecological developmental biology (since sponges are sessile organisms). Furthermore, many sponges have high regenerative ability and thus potentially have totipotent/pluripotent stem cells. Uncovering the cellular and molecular bases of sponge stem cells will not only be crucial for understanding the ancestral gene repertoire of animal stem cells, but will also give us clues for understanding the evolution of molecular mechanisms for maintaining multipotency (pluripotency) and for elucidating the regulatory mechanisms of their differentiation.

Molecular and cellular studies in juveniles of the freshwater *Ephydatia fluviatilis* suggested that demosponges, which contain more than 90% of all sponge species, have two types of stem cells: mesenchymal Archaeocytes/Archeocytes and food-entrapping Choanocytes [1–4]. Recent studies of sponges in other classes, suggest that this model could be generalized at least in three classes

Simon Blanchoud and Brigitte Galliot (eds.), *Whole-Body Regeneration: Methods and Protocols*,
Methods in Molecular Biology, vol. 2450, https://doi.org/10.1007/978-1-0716-2172-1_17, © The Author(s) 2022

of sponges, demosponges, calcareous sponges, and homoscleromorpha [4]. However, the type of cells (archaeocytes or choanocytes) that acts as stem cells seems variable, depending on the cellular organization of each class of sponges. Traditionally, both "archeocytes" and "archaeocytes" are used as terms meaning amoeboid cells that contain a large nucleus with a large nucleolus, and are capable of phagocytosis [5, 6]. These cells are suggested to be totipotent somatic stem cells based on microscopic analysis. They are suggested to produce both somatic differentiated cells and gametes [5–7], just like the multipotent stem cells "interstitial stem cells" in hydra, and "neoblasts" in planarians.

In situ hybridization enables the detection of mRNA and thus it is a powerful tool to characterize cells expressing a particular gene, or to identify specific types of cells that express a particular gene. Actually, by the establishment of the methods of WISH and FISH with high resolution ([8, 9] respectively), together with the identification of cell-type specific genes [8–13], cells with morphological features of Archaeocytes/Archeocytes were defined as at least multipotent stem cells that can undergo self-renewal and directly differentiate into multiple types of cells [1]. Thus, *EflPiwiA*-, *EflPiwiB*-, *EflMusashiA*-expressing cells have been defined as at least multipotent stem cells in demosponges [1–4, 11, 12]. It has also been suggested on the basis of their gene expression and microscopic analysis that these cells are in fact totipotent stem cells.

Here we describe in detail the method of WISH and dual color fluorescent detection of in situ hybridization (dual color FISH) that we have established to detect particular types of cells, especially stem cells, in juveniles of freshwater demosponge, *E. fluviatilis*.

2 Materials

Prepare all solutions using ultrapure water (deionized water) or RNase-free deionized water (when necessary) and analytical grade reagents.

1. M-Medium: 1.47 g $CaCl_2 \bullet 2H_2O$, 1.23 g $MgSO_4 \bullet 7H_2O$, 0.71 g $Na_2SiO_3 \bullet 9H_2O$, 0.42 g $NaHCO_3$, 0.037 g KCl in 10 L. Adjust to pH 7.3–7.8 using 2 M HCl.
2. Stage 2 to 4 juvenile sponges (*see* **Note 1**).
3. 1/4 Holtfreter's solution (HS): 875 mg NaCl, 12.5 mg KCl, 25 mg $CaCl_2$, 50 mg $NaHCO_3$ in 1 L.
4. Fixative solution: 4% (w/v) paraformaldehyde in 1/4 HS.
5. 50% MetOH: 50% (v/v) MetOH in 1/4 HS.
6. 100% MetOH.
7. 0.5 μg template DNA for RNA probe synthesis (*see* **Note 2**).
8. 100 mM DTT Molecular Grade (e.g., Promega).
9. Resuspension mix: 3 μL 100 mM DTT, 50 μL RNase-free water.

10. 40 U/μL RNase inhibitor (e.g., Toyobo).
11. T3 and/or T7 polymerase with 5× transcription buffer (e.g., Takara Bio).
12. Dig RNA labeling mix (e.g., Roche).
13. RNA synthesis reaction mix: 0.5 μg template linear DNA, 4 μL 5× transcription buffer, 2 μL Dig RNA labeling mix, 2 μL 100 mM DTT, 0.5 μL 40 U/μL RNase inhibitor, 1.5 μL polymerase, 9 μL RNase-free Water. Prepare fresh.
14. 0.5 M EDTA: 46.5 g ethylenediaminetetraacetic acid (EDTA) •2Na•2H_2O in 250 mL ultrapure water. Adjust to pH 8.0 using 5 M NaOH.
15. 1 mg/mL yeast RNA: 1 mL commercial 10 mg/mL yeast RNA (e.g., Thermo Fisher scientific), 9 mL RNase-free water.
16. 10 M NH_4OAc: 77 g NH_4OAc in 100 mL ultrapure water.
17. 100% EtOH.
18. 70% EtOH: 70% (v/v) EtOH in ultrapure water.
19. 50× TAE: 242 g Tris (hydroxymethyl)aminomethane (TAE), 57.1 mL acetic acid, 100 mL 0.5 M EDTA in 1 L ultrapure water.
20. 1× TAE: Mix 20 mL 50× TAE and 980 mL ultrapure water.
21. 0.7% agarose gel for electrophoresis: 0.7% (w/v) agarose (e.g., Takara Bio) in 1× TAE.
22. DNA loading buffer for electrophoresis (e.g., ThermoFisher).
23. Nucleic acid stain reagent (e.g., Midori green Xtra, Nippon genetics).
24. 50% (v/v) xylene in EtOH.
25. 35 mm glass petri dishes (*see* **Note 3**).
26. 10% (v/v) Tween 20 in ultrapure water.
27. 10 mg/mL heparin in ultrapure water.
28. Phosphate buffered saline (PBS): 0.2 g KCl, 8 g NaCl, 2.9 g $NaHPO_4$•12H_2O, 0.24 g KH_2PO_4. Adjust to pH 7.4 using 1 M HCl.
29. TPBS: 0.1% (v/v) Tween 20 in 1 L PBS.
30. 20× SSC: 175.3 g NaCl, 88.2 g trisodium citrate dihydrate in 1 L. Adjust to pH 7.0 using 1 M HCl.
31. 1 M DTT: 15.4 g in 100 mL ultrapure water.
32. Hybridization solution: 25 mL formamide, 500 μL 1 mg/mL yeast RNA, 500 μL 10 mg/mL heparin, 500 μL 10% Tween 20, 500 μL 1 M DTT, 12.5 mL 20× SSC, 10.5 mL H_2O.
33. WASH buffer: 250 mL formamide, 125 mL 20× SSC, 5 mL 10% Tween 20, 120 mL freshly obtained ultrapure water.

34. Buffer I: 11.6 g maleic acid, 8.8 g NaCl, 10 mL 10% (v/v) Triton X-100 in 1 L. Adjust to pH 7.5 using 1 N NaOH.
35. Buffer II: 1% blocking reagent (e.g., Sigma Aldrich) in Buffer I. Sterilize by autoclaving 20 min at 121 °C and store at 4 °C.
36. TMN: 0.1 M Tris-HCl pH 9.5, 0.05 M $MgCl_2$, 0.1 M NaCl in 10 mL.
37. Alkaline phosphatase conjugated Anti-Digoxigenin antibody, Fab fragments (Roche).
38. DMFA: *N*, *N*-Dimethylformamide (e.g., Roche).
39. 50 mg/mL 5-bromo-4-chloro-3-indolyl-phosphate (BCIP) in DMFA.
40. 100 mg/mL 4-Nitro blue tetrazolium chloride (NBT): 100 mg/mL NBT, 70% (v/v) DMFA in ultrapure water.
41. BCIP-NBT solution: 35 μL 50 mg/mL BCIP, 18 μL 100 mg/mL NBT in 10 mL TMN.
42. TE: 10 mM Tris-HCl, pH 8.0, 1 mM EDTA, pH 8.0 in 1 L.
43. Peroxidase-conjugated Anti-Digoxigenin antibody, Fab fragments (e.g., Roche).
44. Peroxidase-conjugated streptavidin (e.g., PerkinElmer).
45. 1% (v/v) peroxidase-conjugated streptavidin in Buffer II.
46. Fluorescent Tyramide Signal Amplification (TSA) kit (e.g., Molecular Probes).
47. 1% (w/v) H_2O_2: 1% (w/v) H_2O_2 in TPBS.
48. Nuclear staining dye (e.g., Hoechst 33342, Invitrogen) in TPBS.
49. Anti-fade reagent (e.g., Fluoro KEEPER, Nacalai Tesque).
50. Shaker/Rotator.
51. Hybridization incubator with rocking platform.

3 Methods

3.1 Preparation of Sponge Samples

1. Transfer juvenile sponges to a 24 well plate filled with fixative solution.
2. Fix the animal overnight at 4 °C.
3. Replace the fixative with 1/4 HS.
4. Gently shake plate at 4 °C for 30 min.
5. Replace the solution with ice-cold 50% MetOH.
6. Gently shake plate at 4 °C for 30 min.
7. Replace the solution with ice-cold 100% MetOH.
8. Store the sample at −30 °C.

3.2 RNA Probe Synthesis

1. Prepare the RNA synthesis reaction mix in sterile 1.5 mL or 250 μL tube (*see* **Notes 4** and **5**). High quality of the template DNA is important to obtain a high-quality RNA probe.
2. Incubate the reaction mixture at 37 °C for 3 h for RNA synthesis.
3. Add 2 μL of 0.5 M EDTA to stop the RNA synthesis.
4. Add 2 μL of 1 mg/mL yeast RNA, 5.5 μL of 10 M NH_4OAc and 70 μL 100% EtOH for ethanol precipitation.
5. Keep the reaction mixture at −80 °C for 10 min or − 30 °C for 30 min.
6. Centrifuge for 10 min at 17,500 rcf, 4 °C.
7. Remove the supernatant.
8. Add 100 μL of ice-cold 70% EtOH.
9. Centrifuge for 10 min, at 17,500 rcf, 4 °C.
10. Remove the supernatant.
11. Dry the pellet briefly on ice.
12. Dissolve the pellet in RNase-free water.
13. Load 1 μL of the reaction mixture (synthesized RNA probe) with DNA loading buffer according to manufacturer's instruction in 0.7% agarose gel.
14. Store the remaining reaction mixture at −30 °C.
15. Perform electrophoresis using 1× TAE buffer.
16. Stain the agarose gel using the nucleic acid stain reagent according to the manufacture's instruction.
17. Confirm the RNA probe is efficiently synthesized. You should see thick band of RNA probe.

3.3 Whole Mount In Situ Hybridization (BCIP-NBT Detection)

Specificity of RNA probes and the RNA expression pattern of the gene of interest had better to be first determined by NCBI-NBT detection. Since the fluorescent detection reaction using TSA system is very quick (the time window of the reaction is 5–10 min), nonspecific signals can easily be obtained. Thus, the conditions of fluorescent detection, such as RNA probe concentration and duration of detection reaction, should be optimized for each gene, by comparison of the signals of RNA expression detected by NCBI-NBT.

Day 1

1. Prepare 100% EtOH in 35 mm glass petri dishes at room temperature (RT).
2. Transfer specimens from −30 °C 100% MetOH to glass dishes containing 100% EtOH.
3. Replace the solution to 50% xylene in EtOH in a chemical safety hood (*see* **Note 6**).

4. Keep the petri dishes in a chemical safety hood at RT for 30 min.
5. Prepare ice-cold 100% EtOH in each well of a 12-well plate.
6. Transfer a specimen to each well.
7. Gently shake the plate for 15 min at 4 °C.
8. Replace the solution to ice-cold 75% EtOH in 1/4 HS.
9. Gently shake the plate for 15 min at 4 °C.
10. Replace the solution to ice-cold 50% EtOH in 1/4 HS.
11. Gently shake the plate for 15 min at 4 °C.
12. Replace the solution to ice-cold 25% EtOH in 1/4 HS.
13. Gently shake the plate for 15 min at 4 °C.
14. Replace the solution to ice-cold 1/4 HS.
15. Gently shake the plate for 5 min at 4 °C.
16. Fix specimen with ice-cold fixative solution for 30 min at 4 °C.
17. Replace the solution to ice-cold TPBS.
18. Gently shake the plate for 15 min at 4 °C.
19. Replace the solution to hybridization solution.
20. Incubate the plate at 50 °C (42–55 °C) with gentle rocking with a seesaw-like motion for 1 h using Hybridization incubator (e.g., TAITEC).
21. Replace the solution in each well with 1 mL of hybridization solution containing RNA probe (*see* **Note 7**).
22. Incubate the plate at 50 °C (42–55 °C) with gentle rocking with a seesaw-like motion for overnight.

Day 2

23. Warm wash buffer to 50 °C (42–55 °C).
24. Replace the solution with the prewarmed wash buffer.
25. Gently rock a plate with a seesaw-like motion at 50 °C (42–55 °C) for 5 min using Hybridization incubator.
26. Repeat **steps 24** and **25** for 2 times (wash using wash buffer 3 times at 50 °C (42–55 °C), in total).
27. Warm wash buffer to 65 °C during **step 4**.
28. Replace the solution with 65 °C wash buffer.
29. Gently rock plate with a seesaw-like motion at 65 °C (55–65 °C) for 10 min.
30. Repeat **steps 28** and **29** for 2 times (10 min × 3 times, in total).
31. Replace solution with 50 °C (42–55 °C) wash buffer.
32. Gently rock the plate with a seesaw-like motion at 50 °C (42–55 °C) for 30 min.

33. Repeat **steps 31** and **32** at least 11 times (at least 30 min × 12 times, in total).
34. Replace solution with 1 mL of Buffer I.
35. Gently rock the plate at RT for 5 min.
36. Repeat **steps 34** and **35** for 2 times (5 min × 3 times, in total).
37. Replace solution to Buffer II.
38. Incubate specimens for 1 h (pre-blocking).
39. Replace solution to 1/2000 (v/v) anti-DIG-Alkaline phosphatase (AP) in Buffer II.
40. Incubate at 4 °C overnight (about 16 h).

Day 3

41. Replace solution to Buffer I.
42. Gently shake the plate at RT for 5 min.
43. Repeat **steps 41** and **42** for 2 times (5 min × 3 times, in total).
44. Change Buffer I.
45. Gently shake the plate at RT for 60 min.
46. Repeat **steps 44** and **45** for at least 5 times (30 min × 6 times, in total).
47. Replace the solution to TMN.
48. Gently shake the plate at RT for 5 min.
49. Repeat **steps 47** and **48** for 2 times (5 min × 3 times, in total).
50. Replace the solution to BCIP-NBT solution.
51. Develop color at RT while preventing light exposure (shading) by wrapping a plate with aluminum foil until signals in each cell can be easily detected. Do not shake.
52. Stop the coloring reaction by replacing the solution to TE at RT.
53. Gently shake plate for 5 min.
54. Repeat **steps 52** and **53** for × 2 times (5 min × 3 times, in total).
55. Examine signals using a high-resolution stereomicroscope.
56. Take photos at least within several days.

3.4 Dual-Color Fluorescent Whole Mount In Situ Hybridization

1. Prepare 100% EtOH in 35 mm glass petri dishes at room temperature (RT).
2. Remove a gemmule coat from each sponge body using a sharpened tungsten needle (*see* **Note 8**).
3. Follow the steps from **steps 2** to **37** in Subheading 3.3, replacing the hybridization solution containing RNA probes in **step 21** with a hybridization solution containing Dig-labeled RNA probe and biotin-labeled RNA probe.

4. Incubate specimens with Buffer II by gently shaking at 4 °C overnight for pre-blocking.
5. Transfer specimens on parafilm in the plastic dish.
6. Cover the specimen with 100 μL the mixture of 1/100 (v/v) Anti-DIG-HRP in Buffer II.
7. Keep the specimens at RT for 30–60 min.
8. Add 2 mL TPBS in each well of 12 well plate.
9. Transfer specimens to 12 well plate.
10. Gently shake the plate at RT for 10 min.
11. Change solution to TPBS.
12. Gently shake the plate at RT for 10 min.
13. Repeat **steps 45** and **46** for 2 times (10 min × 3 times, in total).
14. Transfer specimens on Parafilm in the plastic dish.
15. Cover specimens with 100 μL of TSA mixture (e.g., Alexa 488) according to the manufacturer's instructions.
16. Keep the specimens at RT for 5–10 min while shading with aluminum foil, for first color detection. Hereafter, all the steps should be performed with shading.
17. Add 2 mL TPBS in each well of 12-well plate.
18. Transfer specimens to 12-well plate.
19. Gently shake the plate at RT for 10 min.
20. Change to TPBS.
21. Gently shake the plate at RT for 10 min.
22. Repeat **steps 54** and **55** for 2 times (10 min × 3 times, in total).
23. Replace the solution to 1 mL 1% H_2O_2 in TPBS.
24. Gently shake at RT for 30 min.
25. Replace the solution to 1 mL Buffer II for secondary pre-blocking.
26. Gently shake at RT for 30 min.
27. Transfer specimens on parafilm in the plastic dish.
28. Cover the specimens with 100 mL 1% (v/v) peroxidase-conjugated streptavidin (*see* **Note 9**).
29. Keep the specimens at RT for 30–60 min.
30. Add 2 mL TPBS in each well of 12 well plate.
31. Transfer specimens to 12 well plate.
32. Gently shake the plate at RT for 10 min.
33. Change solutions to TPBS.

34. Gently shake the plate at RT for 10 min.
35. Repeat **steps 67** and **68** for 2 times (10 min × 3 times, in total).
36. Transfer specimens on parafilm in the plastic dish.
37. Cover specimens with 100 μL of TSA mixture (e.g., Alexa 594) according to the manufacturer's instructions.
38. Keep the specimens at RT for 5–10 min for second color detection.
39. Repeat **steps 65–70**.
40. Add 100 mL of nuclear staining dye to each specimen.
41. Keep at RT for 30 min.
42. Add 2 mL TPBS in each well of 12 well plate.
43. Transfer specimens to 12 well plate.
44. Gently shake the plate at RT for 10 min.
45. Mount specimens on glass slides with antifade reagent.
46. Examine the fluorescent signals using fluorescence microscopy.

4 Notes

1. Gemmules were isolated as described previously [1]. For the samples for WISH and FISH, gemmules were cultivated on round coverslips (e.g., Fisherbrand), and allowed to develop in M-medium. Developmental stages of juvenile sponges were determined as described previously [1].
2. High quality of template DNA is necessary for synthesis of high-quality RNA probes. Digested linearized plasmid DNA should be purified by phenol/chloroform extraction followed by EtOH precipitation to eliminate enzyme(s).

   PCR DNA fragments should be purified by agarose gel electrophoresis followed by extraction from the gel to eliminate the template circular DNA that was used for PCR. Alternatively, plasmid DNA ($G^{m}ATC$ methylated DNA) in the reaction mixture of PCR can be specifically digested by DpnI (e.g., Takara Bio), and then PCR fragments can be column purified using a Gene gel/PCR Extraction kit (e.g., Nippon Genetics). Do not use the PCR reaction solution without such purification, because contamination by the RNA that was synthesized using the PCR template could cause nonspecific signals in WISH or FISH.
3. To prepare RNase-free glass dishes, cover the glass dishes with aluminum foil and heat them at 200 °C for 2 h to eliminate RNase.
4. For negative control probe, we usually prepare sense RNA probe of gene of interest, or sense RNA probe of GFP gene.

5. For dual color FISH, use Biotin RNA Labeling Mix (Sigma-Aldrich) instead of Dig NTP mix for the second RNA probe.
6. Since xylene dissolves plastics, **steps 2** and **3** of Day 1 should be performed in RNase-free glass dishes.
7. We generally use 1 μL of the reaction mixture of RNA probe synthesis in 1 mL of hybridization solution. When mRNA expression of the gene of interest seems to be high (too quick development of color during detection), we optimize the concentration of the reaction mixture of RNA probe synthesis from 0.1 to 1 μL/mL of hybridization solution. If the RNA expression of the gene of interest is low, the reaction mixture of RNA probe synthesis might be increased up to 10 μL/mL hybridization solution.
8. Removing the gemmule coat from the sponge body is useful to avoid autofluorescence for FISH. Removing gemmules is not necessary for WISH.
9. For dual color Fish detection, we previously used a biotin-labeled RNA probe and anti-biotin antibody [2, 4, 12], but the commercial production of anti-biotin antibody was terminated. Thus, we re-examined possible combinations of a nucleotide analogue and its detection (antibody or chemical binding between biotin and streptavidin, Fig. 1). Although the biotin

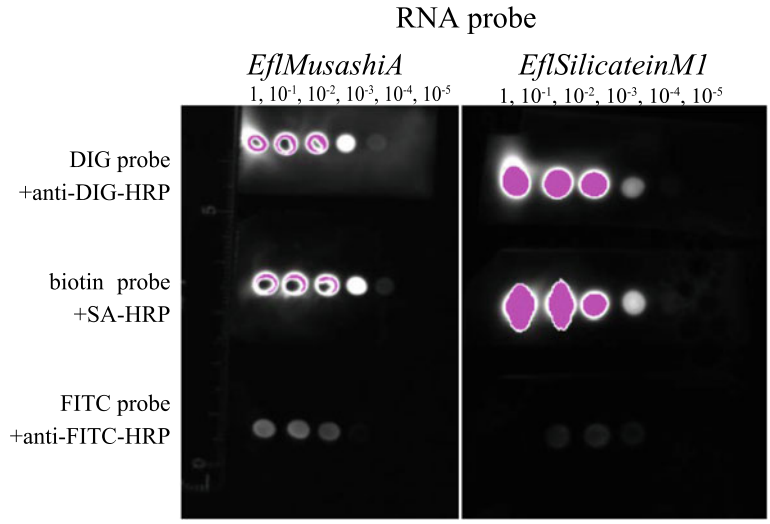


Fig. 1 Evaluation of the detection efficiency of the combinations of nucleotide analogue and peroxidase-conjugated antigen, or streptavidin. After RNA synthesis, the reaction mixture was dot blotted on a nitrocellulose membrane at dilutions from 1× to 10^{-5}×, and then heated at 80 °C for 2 h, and rinsed with Buffer I. After blocking using 1% blocking reagent in Buffer I for 30 min at RT, RNA probes were fluorescently detected using TSA. Note that the combination of biotin-streptavidin gave a stronger detection signal than the combination of FITC-RNA probe and anti-FITC-HRP

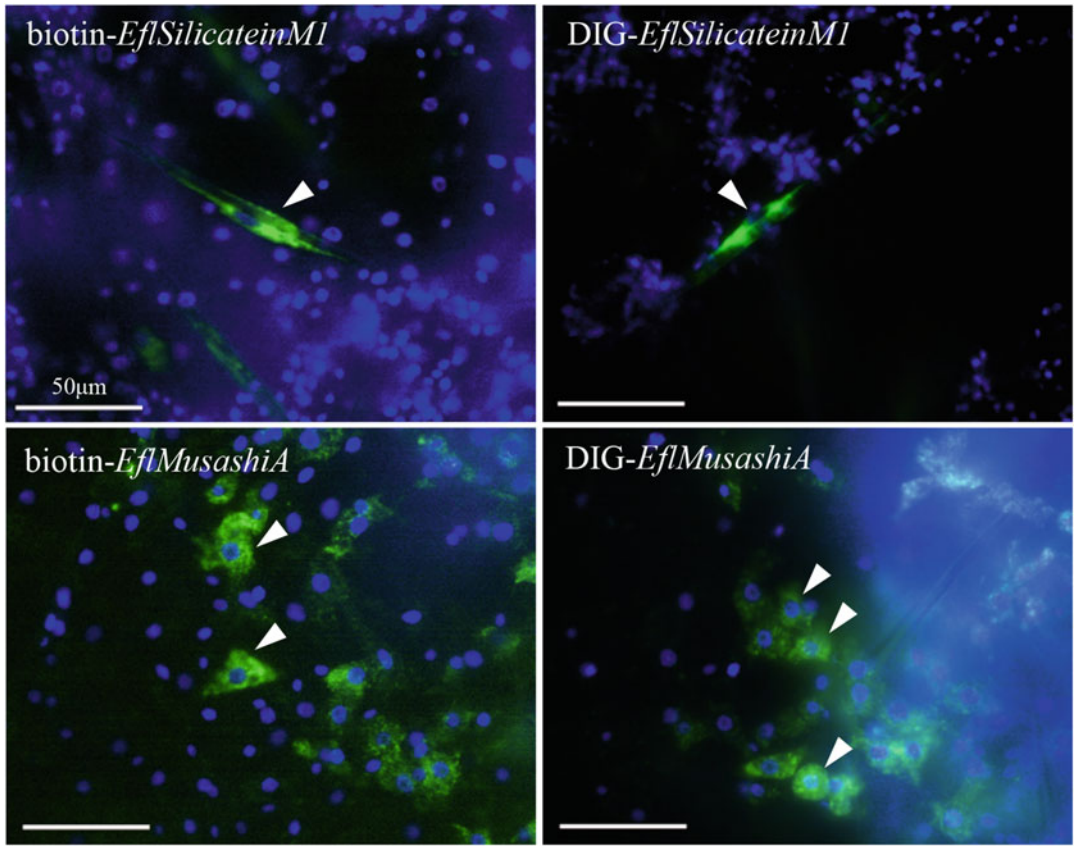


Fig. 2 Fluorescent detection of biotin-RNA probe by streptavidin-HRP in FISH. Our previous studies suggested that the expression of *EflSlicateinM1* in sclerocytes is much higher than that of *EflMusashiA* in archaeocytes (probably more than 10 times). Thus, *EflSlicateinM1*was used as a positive control for FISH. As shown in the dot blot analysis shown in Fig. 1, biotin-RNA probe detected with streptavidin-HRP did not have high background signals, and the sensitivity of detecting specific signals was as high as the sensitivity using a DIG biotin-RNA probe with anti-DIG-HRP for FISH

and streptavidin-HRP combination can give high background signals in several freshwater organisms such as planarians (personal communication), that was not the case in juveniles of *E. fluviatilis*, and *EflMusashiA*-expressing archeocytes and *EflSilicateinM1*-expressing sclerocytes could be specifically detected (Fig. 2). Thus, recently we are using the combination of biotin-labeled RNA probe and streptavidin-HRP [3].

Acknowledgments

I thank Drs. Simon Blanchoud and Brigitte Galliot for giving me the opportunity to contribute to this book. I also thank Dr. Elizabeth Nakajima for her proofreading of the manuscript. This work was supported by MEXT/JSPS KAKENHI grants 20H05942, 19H00994, and 17KT0019 to N. F.

References

1. Funayama N, Nakatsukasa M, Mohri K, Masuda Y, Agata K (2010) Piwi expression in archeocytes and choanocytes in demosponges: insights into the stem cell system in demosponges. Evol Dev 12:275–287
2. Funayama N (2010) The stem cell system in demosponges: insights into the origin of somatic stem cells. Dev Growth Differ 52:1–14
3. Funayama N (2013) The stem cell system in demosponges: suggested involvement of two types of cells: Archeocytes (active stem cells) and choanocytes (food-entrapping flagellated cells). Dev Genes Evol 223:23–38
4. Funayama N (2018) The cellular and molecular bases of the sponge stem cell systems underlying reproduction, homeostasis and regeneration. Int J Dev Biol 62:513–525
5. Simpson TL (1984) The cell biology of sponges. Springer-Verlag, New York
6. Ereskovsky A (2010) The comparative embryology of sponges. Springer, Berlin
7. Leys SP, Ereskovsky AV (2006) Embryogenesis and larval differentiation in sponges. Can J Zool 84:262–287
8. Funayama N, Nakatsukasa M, Hayashi T, Agata K (2005a) Isolation of the choanocyte in the fresh water sponge, *Ephydatia fluviatilis* and its lineage marker, Ef annexin. Dev Growth Differ 47:243–253
9. Mohri K, Nakatsukasa M, Masuda Y, Agata K, Funayama N (2008) Toward understanding the morphogenesis of siliceous spicules in freshwater sponge: differential mRNA expression of spicule-type-specific silicatein genes in *Ephydatia fluviatilis*. Dev Dyn 237:3024–3039
10. Nakayama S, Arima K, Kawai K, Mohri K, Inui C, Sugano W, Koba H, Tamada K, Nakata YJ, Kishimoto K, Arai-Shindo M, Kojima C, Matsumoto T, Fujimori T, Agata K, Funayama N (2015) Dynamic transport and cementation of skeletal elements building up pole-and-beam structured skeleton of sponges. Curr Biol 25: 2549–2554
11. Funayama N, Nakatsukasa M, Kuraku S, Takechi K, Dohi M, Iwabe N, Miyata T, Agata K (2005b) Isolation of *Ef silicatein* and *Ef lectin* as molecular markers for sclerocytes and cells involved in innate immunity in the fresh water sponge, *Ephydatia fluviatilis*. Zoolog Sci 22:1113–1122
12. Okamoto K, Nakatsukasa M, Alié A, Masuda Y, Agata K, Funayama N (2012) The active stem cell specific expression of sponge Musashi homolog *EflMsiA* suggests its involvement in maintaining the stem cell state. Mech Dev 129: 24–37
13. Alié A, Hayashi T, Sugimura I, Manuel M, Sugano W, Mano A, Satoh N, Agata K, Funayama N (2015) The ancestral gene repertoire of animal stem cells. Proc Natl Acad Sci 112(51):E7093–E7100

Open Access This chapter is licensed under the terms of the Creative Commons Attribution 4.0 International License (http://creativecommons.org/licenses/by/4.0/), which permits use, sharing, adaptation, distribution and reproduction in any medium or format, as long as you give appropriate credit to the original author(s) and the source, provide a link to the Creative Commons license and indicate if changes were made.

The images or other third party material in this chapter are included in the chapter's Creative Commons license, unless indicated otherwise in a credit line to the material. If material is not included in the chapter's Creative Commons license and your intended use is not permitted by statutory regulation or exceeds the permitted use, you will need to obtain permission directly from the copyright holder.



Chapter 18

Isolation and Maintenance of In Vitro Cell Cultures from the Ctenophore *Mnemiopsis leidyi*

Abigail C. Dieter, Lauren E. Vandepas, and William E. Browne

Abstract

The ability to isolate, monitor, and examine specific cells of interest enables targeted experimental manipulations that would otherwise be difficult to perform and interpret in the context of the whole organism. In vitro primary cell cultures derived from ctenophores thus serve as an important tool for understanding complex cellular and molecular interactions that take place both within and between various ctenophore cell types. Here we describe methods for reliably generating and maintaining primary cell cultures derived from the lobate ctenophore *Mnemiopsis leidyi* that can be used for a wide variety of experimental applications.

Key words Ctenophore, *Mnemiopsis leidyi*, Suspension culture, Serum, Nonbilaterian

1 Introduction

Ctenophora, also known as comb jellies, are gelatinous invertebrates that inhabit marine ecosystems and represent one of the earliest diverging branches of metazoans [1–3]. The unique rotationally symmetric body plan of ctenophores is composed of two germ layers—an outer ectodermal layer and an inner endodermal layer—separated by a thick collagenous mesoglea populated with a variety of cell types, including muscle and motile stellate cells (Fig. 1) [4]. Recent studies in ctenophores have begun to characterize the range of cell types identifiable by both morphological and functional criteria [5–8] as well as gene expression criteria [9].

Across the metazoan tree of life, the extent to which organisms can heal and regenerate varies dramatically. All animals retain some capacity to repair and replace damaged cells, and the ability to restore injured tissues and organs is widespread among metazoan lineages [10]. Ctenophores have remarkable wound healing and regenerative capabilities (Fig. 2) [11–13]. Among ctenophores, *Mnemiopsis leidyi* has become a model system for understanding a variety of cellular, molecular, and developmental phenomena. *Mnemiopsis* can regenerate wounded tissues, restore entire organ

Simon Blanchoud and Brigitte Galliot (eds.), *Whole-Body Regeneration: Methods and Protocols*,
Methods in Molecular Biology, vol. 2450, https://doi.org/10.1007/978-1-0716-2172-1_18, © The Author(s) 2022

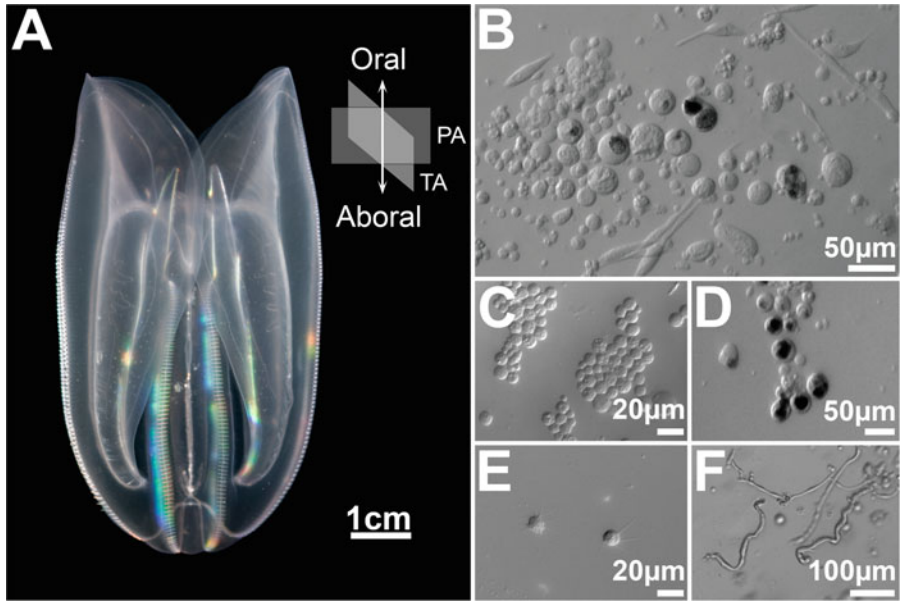


Fig. 1 *Mnemiopsis leidyi*. (**a**) Adult *M. leidyi*, axes labelled on the right, oral oriented up. (**b**) Representative field from primary cell culture 96 h postisolation. (**c**) Isolated proliferating ectodermal cells. (**d**) Isolated proliferating endodermal cells. (**e**) Isolated motile stellate cells. (**f**) Isolated giant smooth muscle cells

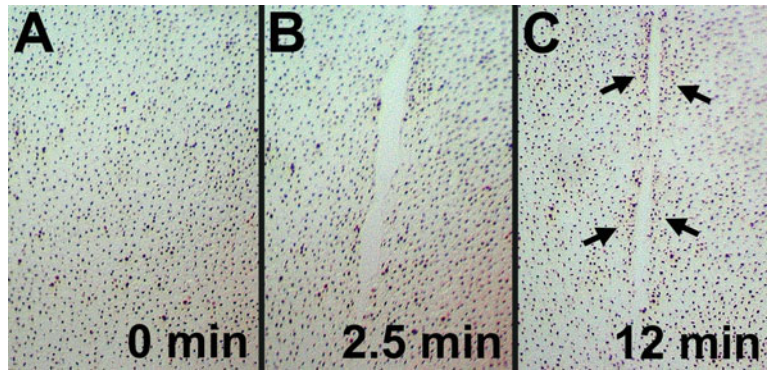


Fig. 2 *Mnemiopsis leidyi* ectoderm epithelium stained with neutral red vital dye. (**a**) Area of contiguous ectodermal epithelium prewounding. (**b**) 2.5 min postwounding with scalpel blade. (**c**) 12 min postwounding. Arrows indicate sites of cell aggregations along edges of the healing wound

systems, and recover large scale deletions of their body plan via whole-body regeneration (WBR) [10, 14]. WBR encompasses a complex set of context dependent cellular activities that includes wound healing, immune response, signaling, proliferation, and differentiation that ultimately result in tissue growth and reorganization of the affected region [14–18]. The phylogenetic position of the ctenophore lineage suggests that an improved understanding of WBR in ctenophores will offer unique insight into the evolution of metazoan regeneration [13, 14, 19].

Primary cell cultures provide a useful tool for the study of ctenophore cell biology. Reliable methods for generating and maintaining primary cell cultures from the model lobate ctenophore *Mnemiopsis leidyi* opens the door for assaying cell biological attributes in specific cell types of interest. In this chapter, we detail cell culture techniques for the selection and preparation of cell sources, the preparation of tissue explants, the dissociation of cells for small and large scale preparations, and cell culture maintenance. These protocols provide simple robust techniques to generate in vitro cell cultures (e.g., Fig. 1b) that can be used for a wide variety of downstream applications including live cell imaging, gene expression profiling, pharmacological assays, flow cytometry, and next-generation sequencing applications.

2 Materials

Store all solutions at 4 °C unless indicated otherwise.

1. Dounce homogenizer with tight and loose fitting pestles (15 mL).
2. Cell culture dishes (30 mm, 60 mm diameter).
3. Cell strainers with nylon mesh pore size of 300 μm, 100 μm, and 70 μm.
4. Filter sterilized artificial seawater (FSW): 35.9 g/L of commercial sea salt in deionized water, 0.2 μm filter-sterilized.
5. 3.125 mg/mL penicillin.
6. 5 mg/mL streptomycin
7. FSW P/S: 1% penicillin, 1% streptomycin in FSW.
8. Minimal Media: 2% (v/v) fetal bovine serum (FBS) in FSW P/S.
9. 10× Phosphate Buffer Solution (PBS): 18.6 mM NaH_2PO_4, 84.1 mM Na_2HPO_4, 1750.0 mM NaCl. Mix phosphates in deionized H_2O and adjust pH to 7.4 with either NaOH or HCl. Store at room temperature (RT).
10. Flow Cytometry Buffer Media: 10 mL FBS, 2.5 mL penicillin, 2.5 mL streptomycin, 2 mL 0.5 M ethylenediaminetetraacetic acid (EDTA), 50 mL 4 M NaCl, fill to 500 mL final volume with 0.2 m filter-sterililized 1 × PBS.
11. 10× dissociation solution: 25 g trypsin, 2 g EDTA • 4Na, 8.5 g NaCl in 1 L of dH_2O.
12. Dissociation media: 9 mL FSW P/S, 1 mL 10× dissociation solution.

3 Methods

Carry out all procedures at RT unless otherwise specified.

3.1 Ctenophore Mesogleal Serum (CMS)

This serum is used to supplement media in which ctenophore cells are maintained in culture.

1. Transfer animal tissue for CMS production to glass Dounce.
2. Dissociate tissue thoroughly using the Dounce homogenizer with 15–20 strokes of a tightly fitted pestle.
3. Spin homogenate at 7000 rcf for 30 min.
4. Carefully transfer the supernatant to appropriately sized conical tubes, leaving sedimented cellular debris behind.
5. Heat-inactivate the collected supernatant for 30 min on low rotation at 56 °C.
6. Mix heat-inactivated supernatant 1:2 with FSW P/S.
7. Allow the CMS to cool to room temperature.
8. Briefly vortex CMS before use.
9. CMS can be stored at 4 °C for 72 h.

3.2 Animal Preparation

1. Screen selected animals for visible parasites, ectosymbionts, and endosymbionts under a light microscope (*see* **Note 1**).
2. Rinse selected animals three times with FSW P/S.
3. Isolate washed animals in fresh FSW P/S overnight (*see* **Note 2**).
4. Perform 4 additional washes with FSW P/S immediately prior to use (*see* **Note 3**).
5. Prepare cell extracts using one of the approaches presented in Subheadings 3.2 to 3.6.

3.3 Tissue Explant Preparation for Small-Scale Cultures

1. Shear the bottom 2–3 mm off a microcentrifuge tube using a razor blade to create a jagged coring instrument (*see* **Note 4**).
2. Make a shallow cut along the surface of the ctenophore's epidermis with a scalpel under a light microscope (*see* **Note 5**).
3. Use the cut microcentrifuge tube to core out a small tissue explant at the wound site (*see* **Note 6**).
4. Place and incubate tissue explants in culture media supplemented with CMS at 16 °C (*see* **Notes 7–10**).
5. Remove explant remnants from cultures 24–48 h postplating with a pipette (*see* **Note 11**).
6. Maintain cell cultures as detailed in Subheading 3.7.

3.4 Mechanical Cell Dissociation for Small-to-Medium Scale Cultures

1. Dissect the tissue of interest under a light microscope using a scalpel or razor blade into small fragments that can be easily loaded into microcentrifuge tubes (*see* **Note 12**).
2. Divide the excised tissue among microcentrifuge tubes, filling no more than half of the total microfuge tube volume (*see* **Notes 13** and **14**).
3. Gently homogenize collected excised tissue until the consistency becomes uniformly smooth. Ensure that the pestle does not fully lift out of the sample to prevent introduction of air bubbles into the homogenate (*see* **Note 15**).
4. Spin resulting homogenate at 800 rcf for 10 min.
5. Carefully collect the loosely sedimented cell pellet using a trimmed pipette tip (*see* **Note 16**).
6. Transfer the cell pellet to 30 mm cell culture dishes with 2.5 mL of culture media supplemented with CMS (*see* **Notes 7–9** and **12**).
7. Gently swirl dishes to disperse the cell pellets.
8. Maintain cell cultures as detailed in Subheading 3.7 (*see* **Note 10**).

3.5 Mechanical Cell Dissociation for Large-Scale Cultures

1. Subdivide the prepared animal into tissue fragments using a clean razor blade (*see* **Note 17**).
2. Place prepared tissues in a Dounce homogenizer using a clean trimmed pipette.
3. Gently homogenize with 10–15 strokes of a loosely fitted pestle.
4. Funnel the resulting homogenate through a series of stacked mesh filters (300 μm, 100 μm, and 70 μm) arranged in descending order on a low pressure ring adapter with Luer-Lok port into a 50 mL tube (Fig. 3).
5. Use an appropriately sized syringe mounted to the Luer-Lok port to gently "pull" the viscous homogenate through the filter stack (*see* **Note 18**).
6. Distribute the filtered homogenate into 4 mL aliquots in 15 mL conical tubes for centrifugation.
7. Bring the volume of each conical tube to 8 mL with FSW P/S (*see* **Note 19**).
8. Gently swirl the contents of the tube with a sterile P1000 (or similar) pipette tip to resuspend cells.
9. Spin the tubes at 800 rcf at 16 °C for 8 min to sediment cells. (*see* **Note 20**).

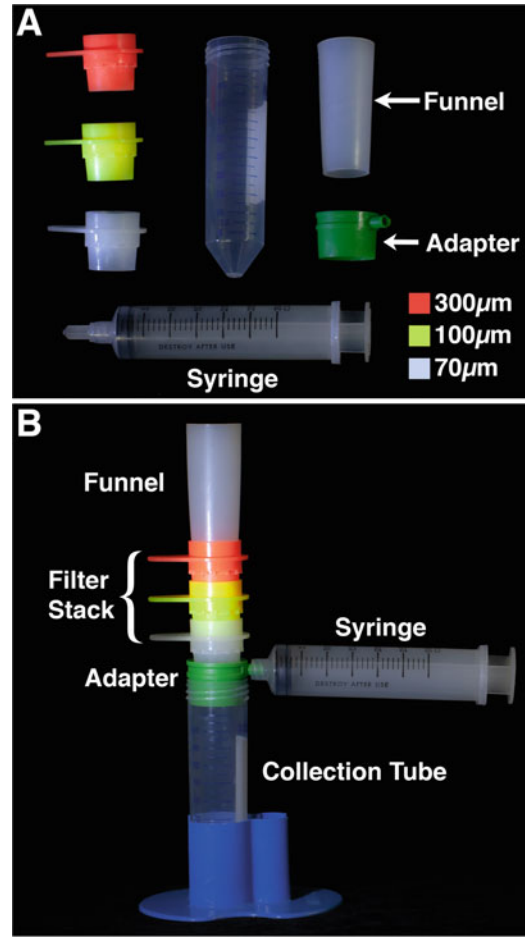


Fig. 3 Filter stack used for cell suspension size selection. (**a**) Filter stack components. The adapter includes a plug for syringe attachment. Legend at lower right indicates filter screen sizes. (**b**) Assembled filter stack with descending 300 μm, 100 μm and terminal 70 μm screens for cell size selection. Mounted syringe allows for the application of light suction below the filter stack to "pull" the initial viscous cell homogenate through the filter screens

10. Remove and discard the upper 4 mL of supernatant, retain the lower 4 mL containing a loose cushion of concentrated cells (*see* **Note 21**).
11. Repeat **steps 7** to **9**.
12. Carefully remove the upper 7 mL of supernatant, making sure not to disturb the lower 1 mL containing the loosely compacted cell pellet (*see* **Note 22**).
13. Carefully add 3 mL of culture media supplemented with CMS to the tube (*see* **Notes 7–9**).
14. Gently resuspend cells using a sterile P1000 (or similar) pipette tip (*see* **Note 23**).

15. Plate the cells in 30 mm cell culture dishes (*see* **Note 12**).
16. Maintain cell cultures as detailed in Subheading 3.7.

3.6 Preparing Enzymatically Dissociated Cells

1. Prepare glass slides for cell adherence and subsequent imaging by incubating slides with any desired collagenous matrices, according to manufacturers' instructions (*see* **Note 24**).
2. Excise tissue fragments using a razor blade.
3. Transfer the excised tissue to a glass Dounce.
4. Add 500 μL of FSW P/S.
5. Gently homogenize with 10–15 strokes of a loosely fitted pestle.
6. Centrifuge the resulting homogenate for 10 min at 350 rcf at RT to pellet cells.
7. Remove and discard the supernatant.
8. Add 10 mL of dissociation media.
9. Pipet up and down gently to break up cell pellet.
10. Transfer homogenate to a 15 mL tube.
11. Place tube on its side on an orbital shaker and agitate at 75 rpm for 10–15 min at RT.
12. Pellet cells by centrifuging for 10 min at 350 rcf at 16 °C.
13. Inactivate residual trypsin by resuspending the cell pellet in media (*see* **Note 12**; for example in FSW P/S + 10% CMS or 10% FBS).
14. Centrifuge for 10 min at 350 rcf at 16 °C.
15. Resuspended the enzymatically dissociated cells in culture media supplemented with CMS and plate as desired for downstream assays (*see* **Notes 7–9** and **12**).
16. Maintain cell cultures as detailed in Subheading 3.7 (*see* **Note 10**).

3.7 Primary Cell Culture Maintenance

1. Incubate cell cultures in humidified chambers at 12–16 °C (*see* **Note 10**).
2. Perform a ~50% media exchange every 48–72 h. To retain loosely attached and/or unattached cells, allow cell culture dishes to rest at a slight angle for at least an hour prior to performing media exchange (*see* **Note 25**).
3. Ctenophore primary cell and tissue cultures can be maintained under a wide range of CMS concentrations (*see* **Notes 6**, **26** and **27**). CMS with high mesogleal serum content will yield a higher-viscosity media.

4 Notes

1. Cultured animals are the preferred source of tissue for generating primary cell cultures in part due to decreased parasite loads. When the use of wild-caught animals is necessary, screening for visible parasites, epibionts, and/or endobionts is recommended. The translucent tissue of *Mnemiopsis* allows for rapid screening by light microscope for areas of discoloration and/or melanization that can often accompany infestations. Tissues that appear to be affected and heavily parasitized animals should be avoided.
2. Isolating selected animals overnight in fresh FSW will allow time for gut clearance and will reduce food debris contaminants in cell cultures.
3. After overnight incubation in FSW, additional washing of animals selected for cell preparations helps remove excess mucus and any loosely attached epibionts from the surface of the ctenophore.
4. Using a crude coring instrument generated from a cut microcentrifuge tube is advantageous for generating explants as the resulting explants have uneven/rough edges that slow wound healing. Delaying wound closure allows time for cells to migrate into the culture media before wound sites seal.
5. The shallow cut made in the epidermis serves to mark the site from which the explant will be taken and helps to keep the coring instrument in place over the desired explant tissue.
6. Align the cut end of the microcentrifuge tube over the wound site. Forceps may be used to hold the ctenophore in place. Press down and twist to tear the tissue generating a small explant.
7. CMS is an undefined media that partially recapitulates the in vivo environment and supports both cell growth and survival. CMS can be diluted with FSW P/S over a wide range of concentrations (1×–6×) without significant adverse effects on primary cell cultures. CMS is typically generated from the entire animal. CMS aliquots stored at 4 °C remain useful for 72 h.
8. Minimal media is highly reduced, has a significantly lower viscosity than CMS and aliquots stored at 4 °C remain useful for 2 weeks.
9. The flow cytometry buffer media is ideal for short term exposure in cell cultures that are explicitly prepared for flow cytometry processing. This media is pH and salinity buffered and also reduces cell clumping.

10. Cell cultures are incubated at approximately 16 °C in humidified chambers to prevent rapid changes in media osmolarity due to evaporation. This temperature was found to be optimal for long term cell culture maintenance. Low incubation temperatures also reduce metabolic load and slow bacterial and fungal growth in cultures.
11. In cell cultures prepared from tissue explants, after 24–48 h the remaining explant tissue should be removed to reduce metabolic load and potential cell crowding. Explant remnants are most easily removed from the culture dish using a pipette.
12. Specific tissues can be targeted for dissection and placed in culture. The tissue type, amount, as well as the destination plate/well size will depend on the assay or downstream application being performed. Thus cell density seeding should be optimized prior to performing downstream experiments.
13. A trimmed plastic transfer pipette, with an opening large enough to mitigate shearing effects that can lyse cells, can be used to transfer tissue segments.
14. Dissected tissues are divided across multiple tubes so that no more than half of a tube volume is filled prior to homogenization to prevent overflow/spilling.
15. Manual homogenization using a pestle and microcentrifuge tube takes approximately 2 min to produce a uniform smooth homogenate. As the homogenate becomes more uniform in consistency, its relative viscosity/stickiness should reduce along with the absence of visible tissue fragments.
16. Many ctenophores are relatively transparent. Thus, the loose cell pellet is often not clearly visible. Retaining the lower portion of the microcentrifuge volume will ensure the recovery of loosely sedimented cells.
17. Subdividing an animal into several tissue fragments makes it easier to load into the Dounce. For generating cultures other than from the whole organism or pharyngeal specific cultures, exclude the pharynx region. The proximal third of the pharynx produces digestive enzymes and is a relatively low pH environment. In small cultures the inclusion of high numbers of pharyngeal cells may alter the pH environment and introduce proteolytic enzymes that can have a negative effect on cell culture maintenance.
18. The initial ctenophore tissue homogenate is typically very viscous. Using a ring adapter with Luer-Lok port and a syringe to provide light suction significantly reduces the time required to filter viscous homogenates. Stacking progressively restrictive filter meshes allows for efficient size selection. This filtering method can be optimized to collect desired cell fractions based on a fixed upper cell size limit.

19. Ctenophore cell cultures are vulnerable to bacterial contamination. To inhibit bacterial growth within cultures, remove small noncellular particulates, and reduce the viscosity of filtrated cell homogenate, cell suspension homogenates are mixed with FSW P/S.
20. Centrifugation at 800 rcf results in a loose cell pellet at the bottom of the tube. When a whole animal is used, the final cell suspension after washing will yield approximately one million cells/mL.
21. Discarding the upper supernatant removes lysed cell material and small particulates. The bottom half of the initial homogenate volume is retained to ensure the concentrated cells will be collected.
22. The cells will be concentrated in a loose pellet. Often this cell pellet is not clearly visible. After two spin steps, the bottom 1 mL of the initial homogenate volume will contain a loose cell cushion.
23. Carefully resuspend cells in media by using a cut P1000 tip or wide tip transfer pipet. Carefully disperse the cells by slowly and gently pipetting up and down, high shear forces will lyse cells.
24. To promote cell attachment, glass slides can be coated with a collagenous matrix diluted in FSW P/S following manufacturer's instructions.
25. For media exchanges, set culture dishes on a ramp with a slight angle (we use a small 3D printed wedge with a 4° slope) and leave undisturbed for 1 h to allow nonadherent cells to settle and collect at the lowest point of the dish. Carefully and slowly remove ~50% of the culture media and replace with fresh media.
26. Long-term cell culture health is visually assessed during 50% media exchanges. When incubated at 12–16 °C with 50% media exchanges every 2–3 days, *M. leidyi* primary cell cultures can be maintained for >20 days. Primary cell cultures represent complex mixtures of cell types, including those competent for proliferation and also terminally differentiated cell types that will senesce [6]. Thus, the composition of *M. leidyi* primary cell cultures maintained over extended time periods is dynamic.
27. The described tissue explant, cell preparation, and cell culture maintenance protocols have been successfully applied to additional ctenophore species; *Bolinopsis infundibulum*, *Bolinopsis vitrea*, and *Pleurobrachia bachei*.

Acknowledgments

This material is based upon work supported by the National Science Foundation under Grant No. 2013692 [W.E.B]; National Research Council Postdoctoral Fellowship [L.E.V.]. University of Miami's College of Arts and Sciences [A.C.D. & W.E.B.].

References

1. Ryan JF, Pang K, Schnitzler CE, Nguyen A-D, Moreland RT, Simmons DK, Kock BJ, Francis WR, Havlak P, NISC Comparative Sequencing Program, Smith SA, Putnam NH, Haddock SHD, Dunn CW, Wolfsberg TG, Mullikin JC, Martindale MQ, Baxevanis AD (2013) The genome of the ctenophore *Mnemiopsis leidyi* and its implications for cell type evolution. Science 342(6164):1242592. https://doi.org/10.1126/science.1242592
2. Dunn CW, Leys SP, Haddock SHD (2015) The hidden biology of sponges and ctenophores. Trends Ecol Evol 30:282–291. https://doi.org/10.1016/j.tree.2015.03.003
3. Li Y, Shen X-X, Evans B, Dunn CW, Rokas A (2021) Rooting the animal tree of life. Mol Biol Evol 38:4322-4333. https://doi.org/10.1093/molbev/msab170
4. Hernandez-Nicaise ML (1991) Ctenophora. In: Harrison FW (ed) Microscopic anatomy of the invertebrates, vol 2. Wiley-Liss, New York, pp 359–418
5. Presnell JS, Vandepas LE, Warren KJ, Swalla BJ, Amemiya CT, Browne WB (2016) The presence of a functionally tripartite through-gut in Ctenophora has implications for metazoan character trait evolution. Curr Biol 26(20):2814–2820. https://doi.org/10.1016/j.cub.2016.08.019
6. Vandepas LE, Warren KJ, Amemiya CT, Browne WE (2017) Establishing and maintaining primary cell cultures derived from the ctenophore *Mnemiopsis leidyi*. J Exp Biol 220:1197–1201. https://doi.org/10.1242/jeb.152371
7. Traylor-Knowles N, Vandepas LE, Browne WE (2019) Still enigmatic: innate immunity in the ctenophore *Mnemiopsis leidyi*. Integr Comp Biol 59(4):811–818. https://doi.org/10.1093/icb/icz116
8. Vandepas LE, Stefani C, Traylor-Knowles N, Goetz FW, Browne WE, Lacy-Hulbert A (2020) Ctenophore immune cells produce chromatin traps in response to pathogens and NADPH-independent stimulus. bioRxiv 2020.06.09.141010. https://doi.org/10.1101/2020.06.09.141010
9. Sebé-Pedrós A, Chomsky E, Pang K, Lara-Astiso D, Gaiti F, Mukamel Z, Amit I, Hejnol A, Degnan BM, Tanay A (2018) Early metazoan cell type diversity and the evolution of multicellular gene regulation. Nat Ecol Evol 2:1176–1188. https://doi.org/10.1038/s41559-018-0575-6
10. Bely AE, Nyberg KG (2010) Evolution of animal regeneration: re-emergence of a field. Trends Ecol Evol (Amst) 25(3):161–170. https://doi.org/10.1016/j.tree.2009.08.005
11. Coonfield B (1936) Regeneration in *Mnemiopsis leidyi* Agassiz. Biol Bull 71:421–428
12. Henry JQ, Martindale MQ (2000) Regulation and regeneration in the ctenophore *Mnemiopsis leidyi*. Dev Biol 227(2):720–733. https://doi.org/10.1006/dbio.2000.9903
13. Marindale MQ (2016) The onset of regenerative properties in ctenophores. Curr Opin Genet Dev 40:113-119. https://doi.org/10.1016/j.gde.2016.06.017
14. Ramon-Mateu J, Ellison ST, Angelini TE, Martindale MQ (2019) Regeneration in the ctenophore *Mnemiopsis leidyi* occurs in the absence of a blastema, requires cell division, and is temporally separable from wound healing. BMC Biol 17:80. https://doi.org/10.1186/s12915-019-0695-8
15. Srivastava M, Mazza-Curll KL, van Wolfswinkel JC, Reddien PW (2014) Whole-body Acoel regeneration is controlled by Wnt and bmp-Admp signaling. Curr Biol 24(10):1107–1113. https://doi.org/10.1016/j.cub.2014.03.042
16. Cao P-L, Kumagai N, Inoue T, Agata K, Makino T (2019) JmjC domain-encoding genes are conserved in highly regenerative metazoans and are associated with planarian whole-body regeneration. Genome Biol Evol 11(2):552–564. https://doi.org/10.1093/gbe/evz021
17. Cary GA, Wolff A, Zueva O, Pattinato J, Hinman VF (2019) Analysis of sea star larval regeneration reveals conserved processes of whole-body regeneration across the metazoa. BMC

Biol 17:16. https://doi.org/10.1186/s12915-019-0633-9

18. Kassmer SH, Nourizadeh S, De Tomaso AW (2019) Cellular and molecular mechanisms of regeneration in colonial and solitary ascidians. Dev Biol 448(2):271–278. https://doi.org/10.1016/j.ydbio.2018.11.021
19. Sánchez Alvarado A, Tsonis PA (2006) Bridging the regeneration gap: genetic insights from diverse animal models. Nat Rev Genet 7(11):873–884. https://doi.org/10.1038/nrg1923

Open Access This chapter is licensed under the terms of the Creative Commons Attribution 4.0 International License (http://creativecommons.org/licenses/by/4.0/), which permits use, sharing, adaptation, distribution and reproduction in any medium or format, as long as you give appropriate credit to the original author(s) and the source, provide a link to the Creative Commons license and indicate if changes were made.

The images or other third party material in this chapter are included in the chapter's Creative Commons license, unless indicated otherwise in a credit line to the material. If material is not included in the chapter's Creative Commons license and your intended use is not permitted by statutory regulation or exceeds the permitted use, you will need to obtain permission directly from the copyright holder.





Chapter 19

Analysis of Spatial Gene Expression at the Cellular Level in Stony Corals

Nikki Traylor-Knowles and Madison Emery

Abstract

Scleractinians, or stony corals, are colonial animals that possess a high regenerative capacity and a highly diverse innate immune system. As such they present the opportunity to investigate the interconnection between regeneration and immunity in a colonial animal. Understanding the relationship between regeneration and immunity in stony corals is of further interest as it has major implications for coral reef health. One method for understanding the role of innate immunity in scleractinian regeneration is in situ hybridization using RNA probes. Here we describe a protocol for in situ hybridization in adult stony corals using a digoxigenin (DIG)-labeled RNA antisense probe which can be utilized to investigate the spatial expression of immune factors during regeneration.

Key words Coral reefs, Coral, Cnidaria, Regeneration, Innate immunity, Wound healing, In situ hybridization

1 Introduction

Scleractinian corals are stony corals that build coral reefs. They are part of Cnidaria, a diverse phylum that possesses over >10,000 known species and is the sister group to Bilateria. It is estimated that these groups split approximately 604–748 million years ago (Fig. 1) [1]. Stony corals are primarily colonial consisting of many clonal polyps that are interconnected through a web of gastrovascular canals [2]. Stony corals are known to possess a high capacity for tissue regeneration which is hypothesized to be driven by stem cell differentiation and proliferation. However, the mechanisms of this regeneration are still not well understood (Fig. 2) [3]. They also possess a highly diversified innate immune system [4, 5]. From the available coral genomes, we understand that many corals possess a high diversity of immune factors which originated both from neo- and subfunctionalization events. This indicates that a complex interaction of immune factors and regenerative factors may be involved in whole body regeneration [6–10].

Simon Blanchoud and Brigitte Galliot (eds.), *Whole-Body Regeneration: Methods and Protocols*, Methods in Molecular Biology, vol. 2450, https://doi.org/10.1007/978-1-0716-2172-1_19, © The Author(s) 2022

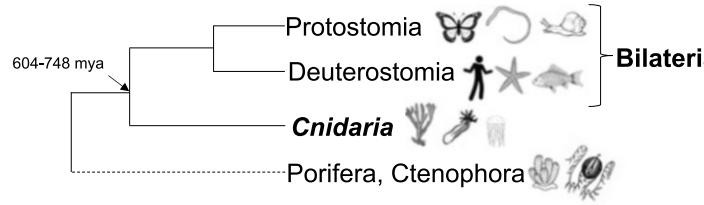


Fig. 1 Cnidarian phylogenetic tree. Scleractinians, or stony corals, are part of the phylum Cnidaria. This phylum is a diverse primarily marine phylum and is important for evolutionary study due to its placement as the sister group to Bilateria. The split between Bilateria and Cnidaria is estimated to have occurred 604–748 million years ago

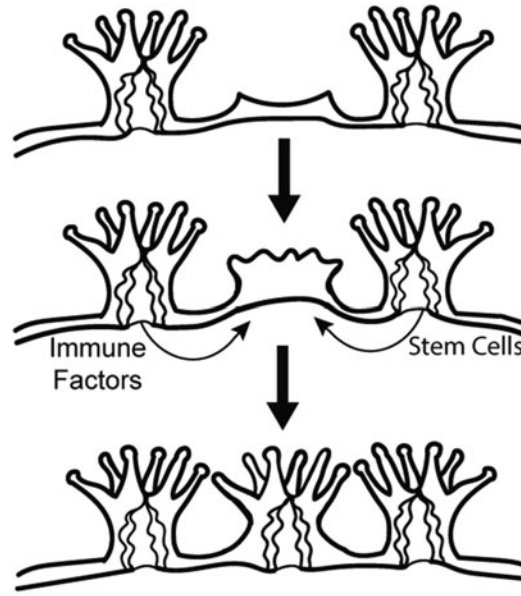


Fig. 2 Schematic of whole-body regeneration in a colonial coral. During whole body regeneration of a colonial coral polyp, immune and stem cell factors are upregulated in response to the injury, and initiate regeneration of the body. Communication between the adjacent polyps and the regenerating polyp are critical for whole body regeneration. Stem and immune cells from adjacent polyps are presumed to migrate into the regenerating polyp area. Depending on the coral species and environmental conditions whole polyp regeneration can take 7–30+ days [3]

The underlying functional mechanisms of whole-body regeneration in stony corals is not as well understood as in other cnidarian models such as *Nematostella* and *Hydra* [3]. This is due to a historical emphasis within coral rsearch to focus on the heat stress response, challenges of manipulating the porous stony skeleton, and the high amounts of obligate microbial symbioses [11–13]. But with recent advances in sequencing technologies and cell

biological techniques many of these challenges are starting to be addressed and tools to study whole-body regeneration are being developed [14–16]. Many genes and proteins have now been identified as involved in whole-body regeneration and immunity in corals, however the functional mechanisms of many of these genes are not known (Table 1) [3, 6].

One of the ways to investigate the interplay of innate immunity and regeneration is to use the method in situ hybridization (ISH) of RNA probes to assess the spatial gene expression of specific genes of interest. ISH is a very versatile technique because the RNA probes can be designed for any gene that is expressed. This method was first developed for the study of embryogenesis and has been further developed to understand the spatial gene expression across different live stages and stress response of many different organisms [17]. This method can be done by using many different types of probes labeled with nonradioactive nucleotides such as digoxigenin (DIG), fluorophores, or radioactive nucleotides [17–19]. The power of this technique is that it can detect and visualize small amounts of RNA at a cellular level. This is particularly useful for nonmodel organisms where the link between cell types and specific gene expression may not be understood.

To use this technique to study immunity during whole body regeneration, immune stimulation can be performed using synthetic elicitors such as lipopolysaccharides, peptidoglycans or exposure to known pathogens such as *Vibrio* to target immune and stem cell related genes that may be expressed during regeneration (Table 1) [20–24]. Additionally, no immune stimulator may be necessary if investigating the early process of regeneration, as the early signals of regeneration are early wound healing gene related to innate immunity [25].

In preparation for this method, DIG-labeled RNA antisense probe, and its accompanying sense control probe should already be designed and ready for use. Additionally, serial sections of paraffin embedded tissue should be prepared for testing both the sense and antisense probes. The sense probe is used as a control for nonspecific binding. If the sense probe has positive staining, then it will indicate that your antisense probe is not targeting the intended RNA. DIG-labeled probes are highly sensitive and can be developed from expressed RNAs for many different stressors [26–30]. It can also be applied to a wide range of tissues and organisms. This technique is not new, however, the application of it on adult stony coral tissues is an emerging technique that has promise for understanding the spatial expression of genes associated with whole-body regeneration. While this technique has primarily been used to assess the expression of developmental genes in cnidarians embryos and larvae, it has recently been modified to be used for adult cnidarians including stony corals [29]. In this book chapter we will outline the steps for performing in situ hybridization on stony coral tissue slices

Table 1
Summary of immune factors implicated in regeneration assays in corals

Immune factor	Function	Type	Method	Citation
Zinc metalloproteinase	Inflammatory factor, extracellular matrix degradation and immune signaling that modulates stem cells	Protein	Proteomics	[6]
Catalase	Antioxidant	Protein	Proteomics	[6]
HSP 90	Molecular chaperone, immune response	Protein	Proteomics	[6]
Mucin	Glycoprotein component of mucus	Protein	Proteomics	[6]
Melanin	Product of melanization cascade	Protein	Enzymatic assay	[31]
Phenol oxidase	Terminal enzyme of melanization cascade	Protein	Enzymatic assay	[31]

to yield cellular level resolution. This procedure could be easily modified for other cnidarians such as *Nematostella* and *Aiptasia*.

2 Materials

All solutions and dilutions should be made using molecular grade, RNase-free reagents, equipment and consumables. This procedure is highly sensitive to RNase contamination which can degrade the RNA probe.

2.1 Removal of Paraffin

1. Thin-sectioned paraffin-embedded slides.
2. 100% xylene.
3. Glass Coplin jars (*see* **Note 1**).
4. 100% ethanol.
5. 80% (v/v) ethanol.
6. 70% (v/v) ethanol.
7. 60% (v/v) ethanol.
8. Sterile slide mailer.
9. Hot water bath set to 100 °C.
10. 37 °C incubator.
11. 10× phosphate buffered saline (PBS): 2.56 g NaH_2PO_4, 11.94 g Na_2HPO_4, 102.2 g NaCl in 1 L. The phosphates should initially be mixed in 800 mL of water for a 1 L volume. pH should be 7.4 ± 0.4, if not, adjust pH to 7.4 with NaOH or HCl. After pH is adjusted, autoclave the solution. Once autoclaved, add NaCl and the last of the water to bring the final volume to 1 L.

12. 1× PBS: 100 mL 10× PBS, 900 mL water.
13. 10 mg/mL proteinase K stock solution: 10 mg proteinase K in 10 mL 1× PBS. Aliquot and store at −20 °C for later use.
14. Proteinase K working solution: 90 µL proteinase K stock solution, 18 mL 1× PBS. Prepare fresh (*see* **Note 2**).
15. 20× saline sodium citrate (SSC): 175.3 g NaCl, 88.2 g $Na_3C_6H_5O_7$, 800 mL water. Adjust pH to 4.5 using HCl, bring to a final volume of 1.0 L and autoclave.
16. 50× Denhardt's: 1% (w/v) Ficoll 400, 1% (w/v) polyvinylpyrrolidone (PVP), 1% (w/v) bovine serum albumin (BSA). Bring to a final volume of 100 mL using water. Dissolve all components in the water by stirring with a magnetic stirrer and filter any particulates. Store at −20 °C prior to use.
17. 20% (v/v) Tween 20: 20 mL Tween 20, 80 mL water. Mix Tween 20 in water using a stir plate. Store at 4 °C prior to use.
18. 20% (w/v) sodium dodecyl sulfate (SDS): 900 mL water, 200 g SDS. Bring this mixture to 68 °C and stir using a magnetic stirrer. Adjust the pH to 7.2 using HCl. Once the solution is completely mixed, adjust the volume to 1 L using water and store at room temperature.
19. Prehybridization (prehybe) buffer: 20 mL formamide, 12.5 mL 20× SSC, 100 µL 20 mg/mL heparin, 5 mL 50× Denhardt's, 20% (v/v) Tween 20, 20% (v/v) SDS, 2 mL of denatured salmon sperm DNA, 4.4 mL water. Aliquot in 50 mL tubes and keep at −20 °C for future use (*see* **Note 3**).
20. Ice bath.
21. 0.2% (w/v) glycine–PBS solution: 1 g glycine, 45 mL 10× PBS, 405 mL water. Mix at room temperature using a stir plate to make sure that the glycine is fully dissolved.
22. 2× SSC solution: 20 mL 20× SSC, 180 mL water.

2.2 Hybridization of RNA Probe

1. Hybridization buffer: 25 mL formamide, 12.5 mL 20× SSC, 100 µL 20 mg/mL heparin, 5 mL 50× Denhardt's, 500 µL 20% (v/v) Tween 20, 500 µL 20% (w/v) SDS, 2 mL denatured salmon sperm DNA, 1 mL RNase-free water (*see* **Note 3**). Aliquot in 50 mL tubes and store at −20 °C for future use.
2. RNA Probe (*see* **Note 4**).
3. Hybridization-probe solution: 0.5 µL probe, 24.5 µL hybridization buffer. Prepare just prior to probe hybridization.
4. Heat block set to 86–90 °C.
5. PAP pen.
6. Plastic coverslips.
7. Slide moisture chamber.

8. 1× SSC solution: 10 mL 20× SSC, 190 mL water.
9. 0.5× SSC solution: 5 mL 20× SSC, 195 mL water.
10. 50% formamide: 250 mL formamide, 250 mL water.
11. 4× SSC + 50% formamide: 6 mL 20× SSC, 24 mL 50% formamide. Prepare fresh under a hood just prior to use.

2.3 Visualization of RNA Probe

1. NaCl–Tris solution: 0.5 M NaCl, 0.5 M Tris. Bring total volume up to 50 mL in water.
2. Alkaline phosphatase buffer (AP-buffer) without $MgCl_2$: 20 mL NaCl–Tris solution, 500 μL Tween 20. Bring total volume up to 100 mL in water. Prepare just prior to use.
3. AP-buffer: 50 mM $MgCl_2$ in AP-buffer without $MgCl_2$. Prepare just prior to use.
4. DIG Nucleic Acid Detection Kit (e.g., Roche). Typically, all solutions should be prepared fresh just prior to use.
5. AP Substrate Solution: 25 mL AP-Buffer, 82.5 μL nitro blue tetrazolium chloride (NBT), 82.5 μL 5-bromo-4-chloro-3-indolyl phosphate (BCIP). Made in the low light conditions and prepared just prior to use in a 50 mL tube. Cover with foil to keep in dark (*see* **Note 5**).
6. Tris-EDTA (TE) buffer: 10 mM EDTA, pH 8.0, 1 mM Tris–HCl, pH 8.0, 98.8 mL water.
7. Glycerol mounting medium: 80 μL 1× PBS, 20 μL glycerol.

3 Methods

All manipulations should be done using sterilized equipment and at room temperature, unless otherwise stated.

3.1 Removal of Paraffin

1. Under a well-ventilated fume hood, pour 50 mL of 100% xylene into a sterile glass Coplin jar.
2. Place tissue slides into the Coplin jar carefully.
3. Allow 10 min for dewaxing to occur.
4. Fill four sterile glass Coplin jars with 100% ethanol, 80% (v/v) ethanol, 70% (v/v) ethanol, and 60% (v/v) ethanol respectively.
5. Soak slides in 100% ethanol for 10 min.
6. Replace the 100% ethanol with fresh 100% ethanol.
7. Incubate for 10 min.
8. Move the slides, using sterile tweezers to the Coplin jar with 80% (v/v) ethanol.
9. Incubate for 1 min.

10. Move the slides, using sterile tweezers to the Coplin jar with 70% (v/v) ethanol.
11. Incubate for 1 min.
12. Move the slides, using sterile tweezers to the Coplin jar with 60% (v/v) ethanol.
13. Incubate for 1 min.

3.2 Slide Pretreatment and Prehybe Preparation

1. Set your incubator to 37 °C and turn on the hot water bath to 100 °C.
2. Prepare the prehybe buffer by placing it in a boiling water bath for 15 min.
3. Place the prehybe buffer in an ice bath for 5 min.
4. Turn on your hybridization oven to the hybridization temperature (*see* **Note 6**).
5. Add 18 mL of prehybe buffer to a new sterile slide mailer.
6. Warm the slide mailer in the hybridization oven.
7. Remove slides from the 60% (v/v) ethanol incubation using sterile tweezers.
8. Place slides in a sterile slide mailer filled with 18 mL of 1× PBS.
9. Wash for 5 min on an orbital shaker set to 100–150 rpm.
10. Replace 1× PBS with 10 mL of proteinase K working solution to the slide mailer.
11. Incubate without shaking for 15 min at 37 °C (*see* **Note 7**).
12. Replace the proteinase K working solution in the slide mailer with 18 mL of 2× SSC solution.
13. Incubate at 100–150 rpm for 10 min at room temperature.
14. Transfer the slides to the slide mailer filled with the warmed prehybe buffer.
15. Incubate the slides with the prehybe buffer at hybridization temperature for 1 h.
16. Set the heat block to 86–90 °C.

3.3 RNA Probe Hybridization

1. Prepare the hybridization-probe solution.
2. Heat the hybridization-probe solution at 86–90 °C for 12 min using a heat block.
3. Cool hybridization-probe solution for 1 min on ice.
4. Remove the slide mailer from the hybridization oven.
5. Carefully remove slides one by one using sterile tweezers, laying them flat on a paper towel.
6. Remove excess prehybe buffer around samples.
7. Use a PAP pen to encircle the tissue.

8. Gently cover the tissue within the circle with 25 μL of hybridization-probe solution.
9. Cover with plastic coverslip (*see* **Note 8**).
10. Fill the bottom of the slide moisture chamber with 4× SSC + 50% formamide solution.
11. Place slides on the slide moisture chamber.
12. Place the slide moisture chamber in the hybridization oven set to 50–60 °C, depending on the hybridization of temperature of the probe (*see* **Note 6**).
13. Incubate for 24 h.
14. Carefully remove the slide moisture chamber from the hybridization oven.
15. Open the slide moisture chamber, and carefully remove the coverslips from each slide using sterile tweezers, taking care to not displace the tissue (*see* **Note 9**).
16. Rinse the slide with 1000 μL of 2× SSC solution by gently pipetting the solution to the tissue area using a pipette. Thoroughly rinse to ensure that all excess probes have been washed away to reduce nonspecific binding (*see* **Note 10**).
17. Fill a sterile slide mailer with 18 mL of 2× SSC solution.
18. Place each washed slide in the slide mailer.
19. Incubate at room temperature for 5 min with gentle rotation on an orbital shaker.
20. Replace the 2× SSC solution with 18 mL of 1× SSC solution.
21. Incubate at room temperature for 5 min with gentle rotation on an orbital shaker.
22. Set the incubator to 42 °C.
23. Replace 1× SSC solution with 18 mL of fresh 1× SSC solution.
24. Incubate at room temperature for 5 min with gentle rotation on the orbital shaker.
25. Replace 1× SSC solution with 18 mL of 0.5× SSC.
26. Incubate at 42 °C for 10 min without shaking.
27. Replace 0.5× SSC solution with 18 mL of fresh 0.5× SSC solution.
28. Incubate at 42 °C for 10 min without shaking.

3.4 RNA Probe Visualization

1. Incubate slides for 1 min in 18 mL of AP-buffer without $MgCl_2$ at room temperature.
2. Block the slides overnight at 4 °C on an orbital shaker according to the DIG Nucleic Acid Detection Kit manufacturer's instructions (*see* **Note 11**).

3. Conjugate DIG for 3 h at room temperature with gentle shaking in a sterile slide mailer according to the kit's instructions.
4. Replace the conjugate buffer with 18 mL of AP-buffer without $MgCl_2$.
5. Incubate for 5 min at room temperature with gentle shaking.
6. Replace the AP-buffer without $MgCl_2$ with 18 mL of AP-buffer.
7. Wash for 5 min at room temperature with gentle rotating on an orbital shaker.
8. Replace AP-buffer with 18 mL of fresh AP-buffer.
9. Wash for 5 min at room temperature with gentle rotating on an orbital shaker.
10. Transfer slide mailer to a dark room.
11. Replace the AP-buffer with 18 mL AP Substrate Solution.
12. Incubate in the dark at room temperature.
13. Check for purple color development every half hour (*see* **Note 12**).
14. Once color development is present, transfer slides to a new sterile slide mailer with 18 mL TE buffer to stop color development.
15. Incubate at room temperature in the dark for 5 min.
16. Replace the TE buffer with 18 mL of RNase-free water.
17. Incubate for 1 min at room temperature in the dark.
18. Remove slides from the water, drying around the edges of the tissue.
19. Add glycerol mounting medium and cover with coverslip.
20. Store slides at 4 °C in the dark until images are taken (Fig. 3).

4 Notes

1. Use glass jars for this step because xylene will melt plastic. Sterilize glass Coplin jar by autoclaving prior to use.
2. Diluted proteinase K can degrade quickly so use a fresh aliquot each time.
3. The salmon sperm needs to be denatured prior to adding to the prehybe buffer. To do this, boil an aliquot of the salmon sperm on a heat block for 5 min.
4. RNA probes, both sense and antisense should be made prior to starting this protocol [29].
5. As a substitute, BM Purple (Sigma-Aldrich, Germany) can be used. Keep in low light conditions.

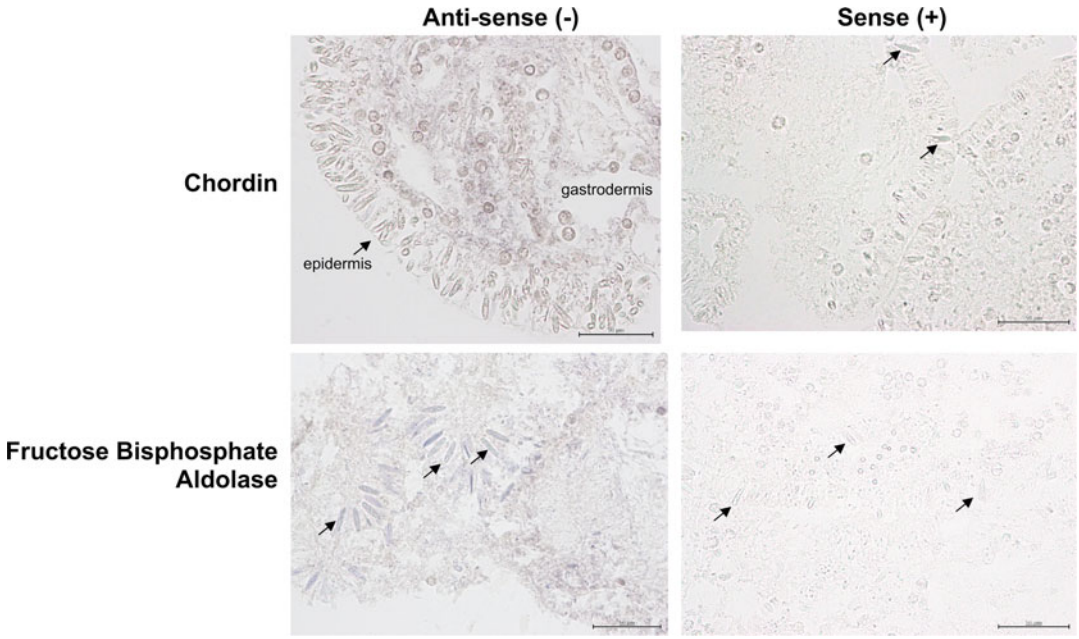


Fig. 3 Representative example of in situ hybridization results in the pacific stony coral, *Acropora hyacinthus* to demonstrate general outcomes of specific and nonspecific binding. (**a**) This panel shows the staining of Chordin, a marker expressed during cnidarian regeneration [20] in *Acropora hyacinthus* tissue which has been exposed to a heat stress. The expression the antisense (−) probe for Chordin was found throughout the gastrodermis, and in gastrodermal cells. The sense (+) control probe showed some staining within the cnidocytes indicating nonspecific binding of cnidocytes. Cnidocytes are indicated by black arrows. (**b**) This panel shows the staining of Fructose Bisphosphate Aldolase again in *Acropora hyacinthus* tissue exposed to heat stress. The antisense (−) probe had primary staining within the cnidocyte cells in the epidermis. Cnidocytes are indicated by black arrows. The sense (+) control had no nonspecific staining indicating that the cnidocyte staining in the antisense (−) probe was specific

6. Hybridization temperatures vary greatly due to the probe that is being used. Most hybridization temperatures range from 50–60 °C. During this step make sure to work quickly so that you do not dry out the sample. Also be extremely careful to not touch the tissue sample. The tissue is still very delicate, and touching it, can disrupt the tissue integrity. Folding a paper towel or a Kimwipes, gently pat the area around the tissue to soak up the excess prehybe buffer.
7. Do not shake the tissue samples at this step, as it can lead to damage of the tissue integrity.
8. For best results use plastic coverslips. They are more flexible and easier to manipulate then glass coverslips.
9. Each slide should be done one at a time, while the other slides are kept in the moisture chamber in the hybridization oven. Keeping the slides at room temperature with the probe still present will allow for more nonspecific binding.

10. This step can be done over a sink or over a container to catch the 2× SSC solution. Gently pipette the solution over the slide, and let it rinse the slide. Make sure to rinse thoroughly, as the residual presence of a probe can lead to more nonspecific binding.
11. A minimum of 1 h at room temperature with gentle shaking can also be done if constrained by time.
12. In some cases, probe visualization may take longer than 24 h. If this the case, develop the sample at 4 °C checking every 12–24 h to see if probe development has progressed.

Acknowledgments

This work is supported by startup funds provided by University of Miami, Rosenstiel School of Marine and Atmospheric Sciences and by NSF-1951826. The authors would like to thank Traylor-Knowles Lab, as well as thank Bradford Dimos and Emily Buckley for discussions concerning the chapter development.

References

1. Ryan JF, Burton PM, Mazza ME, Kwong GK, Mullikin JC, Finnerty JR (2006) The cnidarian-bilaterian ancestor possessed at least 56 homeoboxes: evidence from the starlet sea anemone, *Nematostella vectensis*. Genome Biol 7:R64. https://doi.org/10.1186/gb-2006-7-7-r64
2. Gladfelter EH (1983) Circulation of fluids in the gastrovascular system of the reef coral *Acropora cervicornis*. Biol Bull 165:619–636. https://doi.org/10.2307/1541469
3. Henry LA, Hart M (2005) Regeneration from injury and resource allocation in sponges and corals—a review. Int Rev Hydrobiol 90:125–158. https://doi.org/10.1002/iroh.200410759
4. Palmer CV, Traylor-Knowles NG (2018) Cnidaria: anthozoans in the hot seat. In: Advances in comparative immunology. Springer, Cham, pp 51–93
5. Palmer CV, Traylor-Knowles N (2012) Towards an integrated network of coral immune mechanisms. Proc R Soc B Biol Sci 279:4106–4114. https://doi.org/10.1098/rspb.2012.1477
6. Horricks RA, Herbinger CM, Lillie BN, Taylor P, Lumsden JS (2019) Differential protein abundance during the first month of regeneration of the Caribbean star coral *Montastraea cavernosa*. Coral Reefs 38:45–61. https://doi.org/10.1007/s00338-020-01952-4
7. Cunning R, Bay RA, Gillette P, Baker AC, Traylor-Knowles N (2018) Comparative analysis of the *Pocillopora damicornis* genome highlights role of immune system in coral evolution. Sci Rep 8:16134. https://doi.org/10.1038/s41598-018-34459-8
8. Shinzato C, Shoguchi E, Kawashima T et al (2011) Using the *Acropora digitifera* genome to understand coral responses to environmental change. Nature 476:320. https://doi.org/10.1038/nature10249
9. Voolstra CR, Li Y, Liew J et al (2017) Comparative analysis of the genomes of *Stylophora pistillata* and *Acropora digitifera* provides evidence for extensive differences between species of corals. Sci Rep 7:17583. https://doi.org/10.1038/s41598-017-17484-x
10. Shumaker A, Putnam HM, Qiu H et al (2019) Genome analysis of the rice coral *Montipora capitata*. Sci Rep 9:2571. https://doi.org/10.1038/s41598-019-39274-3
11. Blackall LL, Wilson B, van Oppen MJH (2015) Coral—the world's most diverse symbiotic ecosystem. Mol Ecol 24:5330–5347. https://doi.org/10.1111/mec.13400
12. Cziesielski MJ, Schmidt-Roach S, Aranda M (2019) The past, present, and future of coral

heat stress studies. Ecol Evol 9:10055–10066. https://doi.org/10.1002/ece3.5576

13. Parkinson JE, Baker AC, Baums IB et al (2020) Molecular tools for coral reef restoration: beyond biomarker discovery. Conserv Lett 13: e12687. https://doi.org/10.1111/conl.12687
14. Rosental B, Kozhekbaeva Z, Fernhoff N et al (2017) Coral cell separation and isolation by fluorescence-activated cell sorting (FACS). BMC Cell Biol 18:30. https://doi.org/10.1186/s12860-017-0146-8
15. Nowotny JD, Connelly MT, Traylor-Knowles N (2021) Novel methods to establish whole-body primary cell cultures for the cnidarians *Nematostella vectensis* and *Pocillopora damicornis*. Sci Rep 11:4086. https://doi.org/10.1038/s41598-021-83549-7
16. Levy S, Elek A, Grau-Bové X, Menéndez-Bravo S, Iglesias M, Tanay A, Mass T, Sebé-Pedrós A (2021) A stony coral cell atlas illuminates the molecular and cellular basis of coral symbiosis, calcification, and immunity. Cell 184:2973–2987.e18. https://doi.org/10.1016/j.cell.2021.04.005
17. Lehmann R, Tautz D (1994) Chapter 30. *In situ* hybridization to RNA. In: Methods in cell biology. Academic Press, New York, pp 575–598. https://doi.org/10.1016/S0091-679X(08)60933-4
18. Jin L, Lloyd RV (1997) *In situ* hybridization: methods and applications. J Clin Lab Anal 11: 2–9. https://doi.org/10.1002/(SICI)1098-2825(1997)11:1
19. Levsky JM, Singer RH (2003) Fluorescence *in situ* hybridization: past, present and future. J Cell Sci 116:2833–2838. https://doi.org/10.1242/jcs.00633
20. Connelly MT, McRae CJ, Liu P, Traylor-Knowles N (2020) Lipopolysaccharide treatment stimulates *Pocillopora* coral genotype-specific immune responses but does not alter coral-associated bacteria communities. Dev Comp Immunol 109:103717. https://doi.org/10.1016/j.dci.2020.103717
21. Kvennefors ECE, Leggat W, Kerr CC, Ainsworth TD, Hoegh-Guldberg O, Barnes AC (2010) Analysis of evolutionarily conserved innate immune components in coral links immunity and symbiosis. Dev Comp Immunol 34:1219–1229. https://doi.org/10.1016/j.dci.2010.06.016
22. Vidal-Dupiol J, Ladrière O, Meistertzheim AL, Fouré L, Adjeroud M, Mitt AG (2011) Physiological responses of the scleractinian coral *Pocillopora damicornis* to bacterial stress from *Vibrio coralliilyticus*. J Exp Biol 214:1533–1545. https://doi.org/10.1242/jeb.053165
23. Zhi Z, Shuimiao Z, Jia T, Zhaoqun L, Yibo W, Yan W, Senjie L (2019) Altered immune landscape and disrupted coral-symbiodinium symbiosis in the scleractinian coral *Pocillopora damicornis* by *vibrio coralliilyticus* challenge. Front Physiol 10:366. https://doi.org/10.3389/fphys.2019.00366
24. Takagi T, Yoshioka Y, Zayasu Y et al (2020) Transcriptome analyses of immune system behaviors in primary polyp of coral *Acropora digitifera* exposed to the bacterial pathogen *vibrio coralliilyticus* under thermal loading. Marine Biotechnol 22:748–759. https://doi.org/10.1007/s10126-020-09984-1
25. Gurtner G, Werner S, Barrandon Y et al (2008) Wound repair and regeneration. Nature 453: 314–321. https://doi.org/10.1038/nature07039
26. Darby IA, Bisucci T, Desmouliere A, Hewitson TD (2006) *In situ* hybridization using cRNA probes. In: Darby IA, Hewitson TD (eds) In situ hybridization protocols. Humana Press, Totowa, NJ. https://doi.org/10.1385/1-59745-007-3:17
27. Valentino KL, Eberwine JH, Barchas JD (1987) In situ hybridization. Oxford University Press, New York
28. Tautz D, Pfeifle C (1989) A non-radioactive *in situ* hybridization method for the localization of specific RNAs in *drosophila* embryos reveals translational control of the segmentation gene hunchback. Chromosoma 98:81–85. https://doi.org/10.1007/BF00291041
29. Traylor-Knowles N, Rose NH, Palumbi SR (2017) The cell specificity of gene expression in the response to heat stress in corals. J Exp Biol 220:1837–1845. https://doi.org/10.1242/jeb.155275
30. Wolenski FS, Layden MJ, Martindale MQ, Gilmore TD, Finnerty JR (2013) Characterizing the spatiotemporal expression of RNAs and proteins in the starlet sea anemone, *Nematostella vectensis*. Nat Protoc 8:900. https://doi.org/10.1038/nprot.2013.014
31. Palmer CV, Traylor-Knowles NG, Willis BL, Bythell JC (2011) Corals use similar immune cells and wound-healing processes as those of higher organisms. PLoS One 6:e23992. https://doi.org/10.1371/journal.pone.0023992

Open Access This chapter is licensed under the terms of the Creative Commons Attribution 4.0 International License (http://creativecommons.org/licenses/by/4.0/), which permits use, sharing, adaptation, distribution and reproduction in any medium or format, as long as you give appropriate credit to the original author(s) and the source, provide a link to the Creative Commons license and indicate if changes were made.

The images or other third party material in this chapter are included in the chapter's Creative Commons license, unless indicated otherwise in a credit line to the material. If material is not included in the chapter's Creative Commons license and your intended use is not permitted by statutory regulation or exceeds the permitted use, you will need to obtain permission directly from the copyright holder.



Chapter 20

Studying Stem Cell Biology in Intact and Whole-Body Regenerating *Hydra* by Flow Cytometry

Wanda Buzgariu, Jean-Pierre Aubry-Lachainaye, and Brigitte Galliot

Abstract

The freshwater *Hydra* polyp is a versatile model to study whole-body regeneration from a developmental as well as a cellular point of view. The outstanding regenerative capacities of *Hydra* are based on its three populations of adult stem cells located in the central body column of the animal. There, these three populations, gastrodermal epithelial, epidermal epithelial, and interstitial, continuously cycle in homeostatic conditions, and their activity is locally regulated after mid-gastric bisection. Moreover, they present an unusual cycling behavior with a short G1 phase and a pausing in G2. This particular cell cycle has been studied for a long time with classical microscopic methods. We describe here two flow cytometry methods that provide accurate and reproducible quantitative data to monitor cell cycle regulation in homeostatic and regenerative contexts. We also present a cell sorting procedure based on flow cytometry, whereby stem cells expressing a fluorescent reporter protein in transgenic lines can be enriched for use in applications such as transcriptomic, proteomic, or cell cycle analysis.

Key words *Hydra*, Cell cycle, Adult stem cells, Epithelial stem cells, Interstitial stem cells, Flow cytometry, GFP cell sorting, Click-iT EdU labeling of regenerating animals, Cell cycle analysis

1 Introduction

1.1 Hydra and the Unusual Properties of Its Stem Cells

The hydrozoan *Hydra* polyp, which belongs to Cnidaria, is well known for its robust regenerative abilities, thus providing an attractive model system for regenerative biology [1–5]. This freshwater polyp, which is about 1-cm long, reconstructs any missing part of its body, such as the basal (foot) or apical (head) regions, within a few days after amputation. The *Hydra* body exhibits a radial symmetry (Fig. 1a), with a cylindrical shape terminated at the apical pole by the head region centered on a unique opening called mouth, and at the basal pole by the basal disc, which helps the animal to adhere to various environmental substrates. The anatomy of *Hydra* is formed of two tissue layers, one epidermal, the other gastrodermal, held together by the mesoglea, a complex extracellular matrix that maintains their cohesion. This double-body wall

Simon Blanchoud and Brigitte Galliot (eds.), *Whole-Body Regeneration: Methods and Protocols*,
Methods in Molecular Biology, vol. 2450, https://doi.org/10.1007/978-1-0716-2172-1_20, © The Author(s) 2022

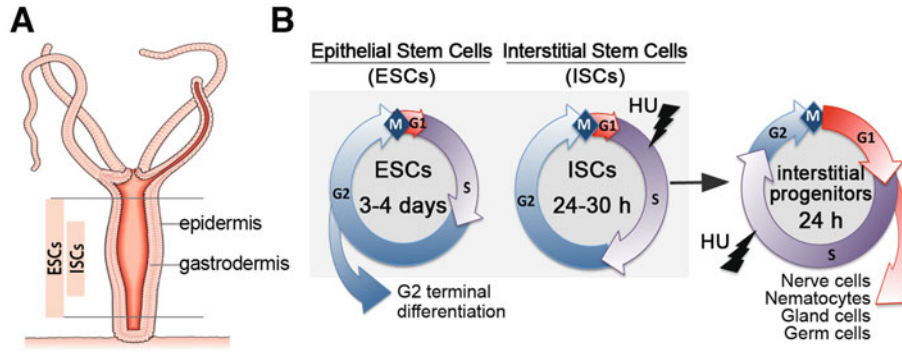


Fig. 1 *Hydra* anatomy and cycling properties of *Hydra* stem cells. (**a**) The *Hydra* polyp exhibits a radial symmetry centered on an oral–aboral axis. At the apical pole also called the head, a ring of tentacles surrounds a dome called hypostome that is centered on the mouth opening, while at the basal end called foot, the basal disc that produces mucus allows the animal to attach to substrates. The animal consists of two epithelial layers, the epidermis on the outside consisting of epidermal epithelial stem cells (eESCs), and the gastrodermis on the inside consisting of gastrodermal epithelial stem cells (gESCs). All epithelial cells along the gastric region are ESCs that terminally differentiate when they reach the extremities. Interstitial stem cells (ISCs) are abundant in the central region of the animal, interspersed with eESCs. (**b**) The cell cycle of ESCs lasts 3–4 days, while multipotent ISC cycle every 24–30 h. In each cycle, ISCs provide asymmetrically divided interstitial progenitors (IPs) that cycle faster than ISCs (less than 24 h). IPs are migratory cells that differentiate in G0 phase along the body axis and at the extremities. As for somatic derivatives, nematocytes are strictly located in the epidermis, nerve cells are found in both layers, and gland cells in the gastrodermis. Fast cycling cells such as ISCs and IPs are predominantly killed by hydroxyurea (HU) pulse treatment. In contrast, ESCs paused in G2 are resistant to such treatments. Passively moving toward the apical and basal poles, ESCs differentiate in G2 phase into head- and foot-specific epithelial cells. *Scheme adapted after* [6]

houses three populations of non-interchangeable adult stem cells: two populations of unipotent epithelial stem cells (ESCs), either epidermal or gastrodermal, and the multipotent interstitial stem cells (ISCs), which are found predominantly in the central body column [7–10] (Fig. 1a). By contrast, the tissue at both the ends of the animal consists mainly of differentiated cells, either epithelial or derived from ISCs, such as neurons and mechano-sensory cells called nematocytes [11, 12]. In addition, ISCs can also differentiate into glandular cells, distributed among the gastrodermal epithelial cells, and germ cells when the animal becomes sexual and differentiates gonads [9, 13].

Hydra tissue is characterized by a dynamic homeostasis, as stem cells from the central body region from all three lineages are continuously self-renewing, replacing every 20 days the differentiated cells that progressively get sloughed off at the extremities [14]. The length of the cell cycle of these adult stem cells differs between ESCs that divide every 3–4 days and ISCs that progress faster through the cell cycle, dividing every 24–30 h (Fig. 1b) [15, 16]. Intriguingly, all three stem cell populations share quite unusual features, i.e., a very short G1 phase that lasts 1 h, and an extended G2 phase that ranges from 24 up to 72 h for ESCs [6, 15,

17] and from 6 up to 22 h for ISCs [15, 16]. As a consequence, pulse treatments with drugs that block DNA synthesis such as hydroxyurea (HU) preferentially target the fast cycling cells, the ISCs, and their progenitors (Fig. 1b). Typically, three 24-h periods of HU exposure, each separated by a 12-h drug-free period, suffice to selectively deplete the interstitial cell line and, after a few weeks, produce animals that are purely epithelial. These animals, which have lost their nervous system, cannot catch preys yet can survive for months and years if manually force-fed. In such conditions, the epithelial tissues get properly renewed and the animals retain their developmental potential, i.e., are able to bud and regenerate [18, 19].

The continuous self-renewal of *Hydra* stem cells in the central part of the body column indicates that this region can be considered as a *pro-blastema* where stem cells paused in G2-phase are ready to differentiate, divide, and proliferate immediately after amputation [20, 21]. Similar to other cnidarians [22–24], proliferating cells play an important role in the regeneration of apical structures, and a synchronous cell division event is actually rapidly induced upon amputation [20, 25]. Seventeen evolutionarily conserved cell cycle genes are then synchronously upregulated (*Shox1, E2F7, TFDP1, POLQ, CCNF, PLK4, CCNE1, CCND2, CDC7, SIPA1L3, MCM5, DLEC1, MCM9, CDC6, CCNA2, CCNB3, PLK1*) [20], and a local wave of cell proliferation follows at an early-late stage (around 24 h post-amputation) [26]. When the S-phase progression is blocked with HU prior to amputation, it alters apical regeneration, although only partially, as the stock of epithelial cells stopped in G2 can differentiate without entering a final mitosis [21]. In summary, the regenerative capacity of *Hydra* relies on large stocks of continuously cycling stem cells, whose unusual properties explain their immediate contribution to the regenerative process, which is achieved in few days.

1.2 Stem Cell Sorting and Methods to Monitor the Cell Cycle Activity in Hydra

The cell cycling behavior of *Hydra* stem cells was intensively studied by classical microscopical methods that either analyze the incorporation of thymidine analogs (e.g., ^{3}H-thymidine, BrdU 5′-bromo-deoxyuridine) into replicating DNA, or evaluate the DNA content microfluorimetrically, or allow the counting of mitotic figures [16, 17, 27]. Among these methods, the counting of BrdU-labeled nuclei detected with anti-BrdU antibody allows the establishment of a precise BrdU-labeling index [26, 28]. However, these methods are time-consuming, and the quantitative results are obtained on a rather small number of analyzed cells. To overcome these limitations, we have applied to *Hydra* flow cytometric methods that are commonly used in model organisms such as algae, sea anemones, planarians, flies, as well as in mammalian cells, to address a variety of biological questions [29–33].

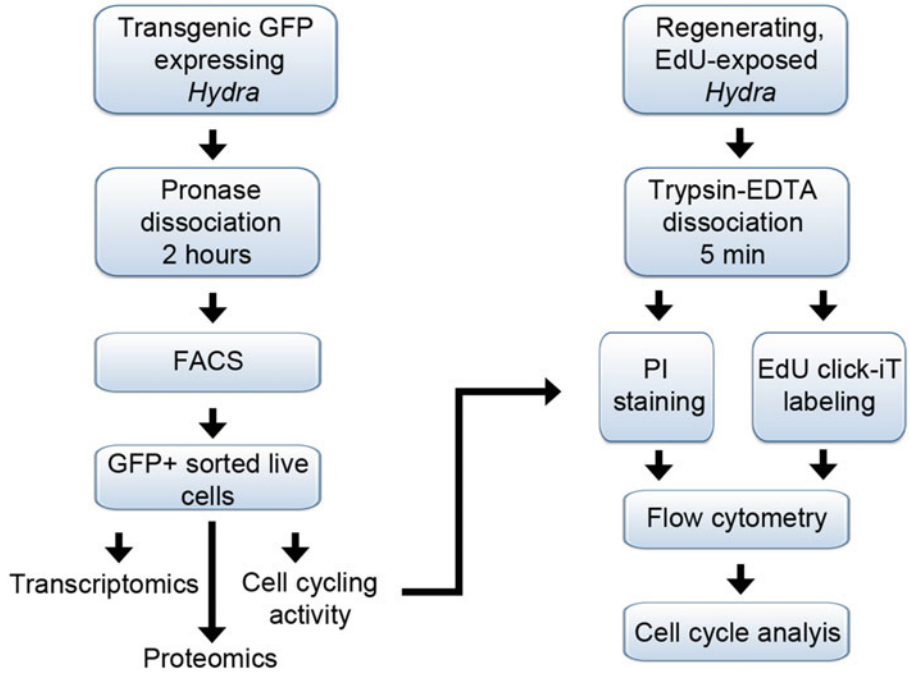


Fig. 2 Schematic view of the flow cytometry protocols presented in this chapter. In this study, two distinct protocols were used to dissociate the *Hydra* tissues, the first one is based on pronase activity and the second on trypsin–EDTA activity. Pronase dissociation is suitable because it provides living, viable *Hydra* cells that can be sorted by flow cytometry (*see* Subheading 3.2). The trypsin–EDTA dissociation is fast and convenient to use when rapid dissociation is needed as required to analyze the cell cycle activity (*see* Subheadings 3.3 and 3.4)

As a general definition, flow cytometry is a laser-based technology that allows the characterization of properties of cells in suspension, i.e., their size, volume, morphological complexity, and fluorescence-labeled components. This technology ensures that a large number of cells are analyzed quantitatively in a very short time. Advances of the flow cytometry-based cell sorting methodology (FACS, fluorescent-activated cell sorting) opened large possibilities for downstream applications such as transcriptomic [34, 35], proteomic [36], biochemical, or cellular [33] analyses. In this context, the production of transgenic lines in *Hydra* that constitutively express green fluorescent protein (GFP) in one or the other stem cell population, e.g., *ecto-GFP* [37], *endo-GFP* [38], or *Cnnos1*-GFP [39], opened the possibility to study the molecular signatures of each population after cell sorting [39–41]. The two first sections in this chapter describe how to sort *Hydra* stem cells based on their selective GFP expression (Figs. 2 and 3).

The flow cytometry methodology is also applied in *Hydra* to measure the modulations of the cell cycle behavior in homeostatic, regenerative, or ecotoxicological contexts [6, 20, 42–44]. A simple and easy method to characterize the distribution of cell populations in the different phases of the cell cycle is to measure the DNA

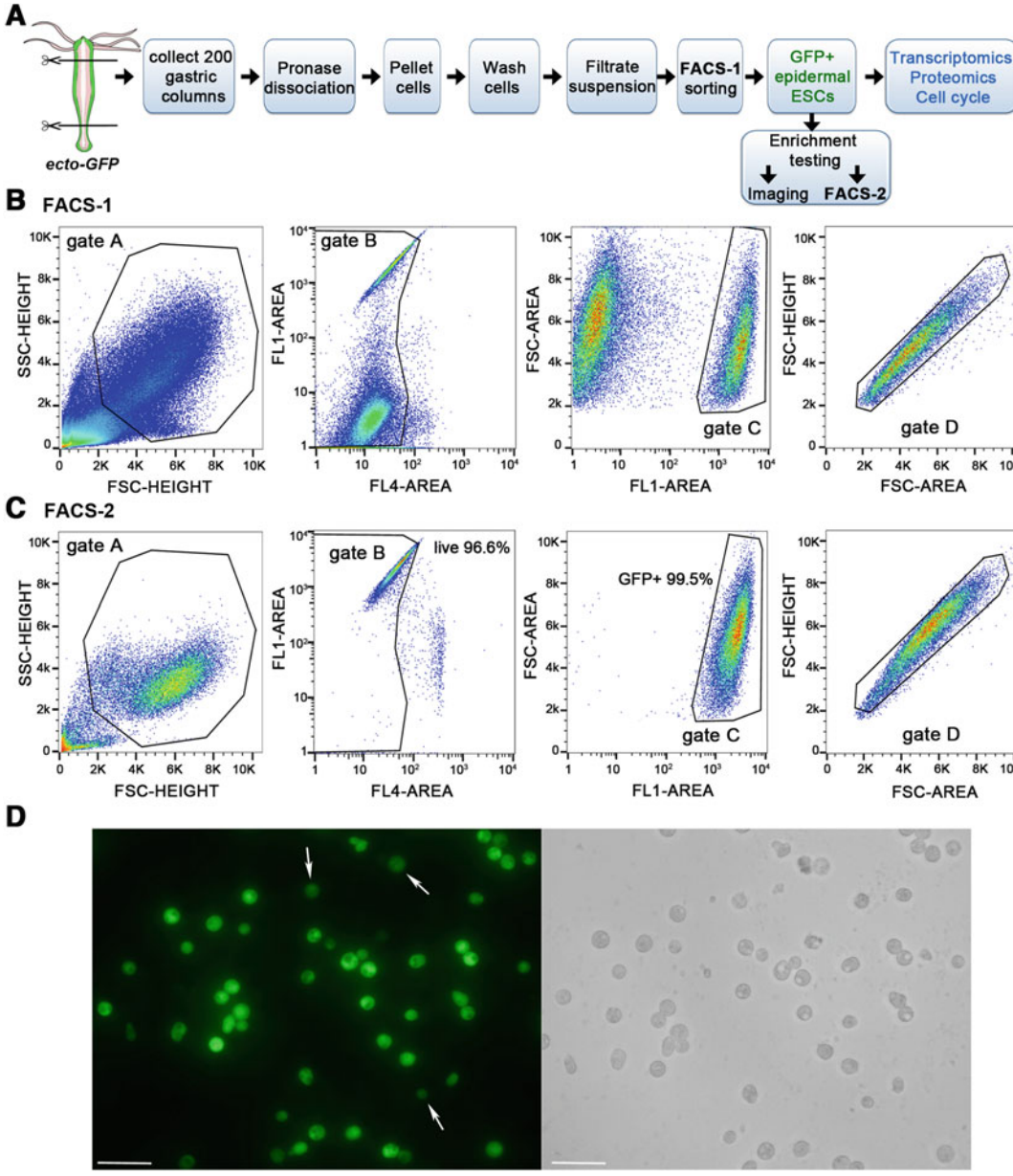


Fig. 3 Fluorescence-activated cell sorting (FACS) of epidermal ESCs constitutively expressing GFP. (**a**) Scheme depicting the FACS procedure to obtain live GFP-positive epidermal ESCs (eESCs) from *ecto-GFP* transgenic polyps [37] (*see* Subheadings 3.1 and 3.2). (**b**) Gating strategy: The cells are first gated based on the forward scatter (FSC-H) and side scatter (SSC) properties (gate A). Next, the intact, viable cell population is selected based on the intensity of Draq7 fluorescence, detected on the FL4-Area channel (gate B). Subsequently, the GFP-positive cells are identified considering the GFP fluorescence collected on the FL1 channel (gate C) and sorted after exclusion of cell doublets, based on the area and height of the FSC signal (gate D). (**c**) Analysis of the enrichment score of the GFP+ eESCs after re-running the sorted cells on the flow cytometer (FACS-2). Note that 96.6% of sorted cells are viable (gate B) and 99.5% are GFP-positive (gate C). The sorting was done with a Biorad cell sorter S3. (**d**) Microscopical control of the enrichment of the GFP+ eESCs after sorting. Green fluorescence (left panel) and bright field (right panel) images were acquired with a Leica DM5500 fluorescence microscope 3 h after sorting. Arrows point to cells with low GFP fluorescence. Scale bars: 75 μm

content that doubles during S-phase and is divided by twofold at the end of the G2-phase upon mitosis. The DNA content can be assessed quantitatively from staining with propidium iodide (PI), a DNA intercalating dye whose fluorescence is enhanced upon insertion between the bases [45]. This method is widely used to estimate the relative distribution of the cells between the G0/G1, S, or G2/M phases of the cell cycle, as shown in mammalian [46] or invertebrate cells from *Drosophila* [47], planarians [48], or *Daphnia* [49]. The DNA staining protocol presented here integrates a fast dissociation step of the tissue with trypsin–EDTA enzymatic digestion, followed by PI DNA labeling in a hypertonic staining solution in the presence of detergents [50]. This method allows the successful analysis of very small tissue fragments and the processing of a large number of samples in parallel while obtaining good quality DNA histograms as shown by the good coefficient of variations (CV) measured across the G0/G1 peak [6] (Fig. 4).

As an alternative, the monitoring of cell proliferation with the click-iT EdU detection assay was developed by Invitrogen. Similar to BrdU, EdU (5-ethynyl-2′-deoxyuridine) is a thymidine analog that gets incorporated into the newly synthesized DNA chain during the replication phase. In contrast to the antibody-based BrdU detection, the click-iT reaction consists of the chemical detection of EdU after a 30-min reaction between EdU and an Alexa photostable dye catalyzed by copper [51, 52]. This method, which can provide a dynamic view of the progression of DNA replication during the S-phase when several time-points are compared, is faster and easier than BrdU immunodetection because neither DNA denaturation nor immunodetection are needed. However, in *Hydra*, the cellular absorption of EdU in intact animals is low when compared to BrdU, and the number of S-phase cells detected with the click-iT EdU proliferation kit is not reliable. During regeneration, the tissues of amputated animals absorb well the thymidine analogue, and the EdU labeling procedure is well suited for monitoring cell proliferation (Fig. 5).

In this chapter, we report two distinct flow cytometry procedures to detect the cell cycle distribution in homeostatic or regenerative contexts. The first procedure analyses nuclei whose DNA is stained with PI after tissue dissociation while the second procedure relies on the pulse labeling of S-phase nuclei with EdU, a DNA-labeling process that takes advantage of the physiological replication process occurring in live animals. The protocols presented here rely on two distinct procedures for tissue dissociation that precedes flow cytometry. The relatively slow pronase dissociation is well suited to sort fluorescent cells by FACS, whereas the fast trypsin–EDTA dissociation is well suited for cell cycle analysis such as PI labeling or EdU click-iT labeling (Fig. 2). As this latter method discriminates between the cells in G1 or G2 from those in early or late S-phase, it provides a dynamic assessment of the

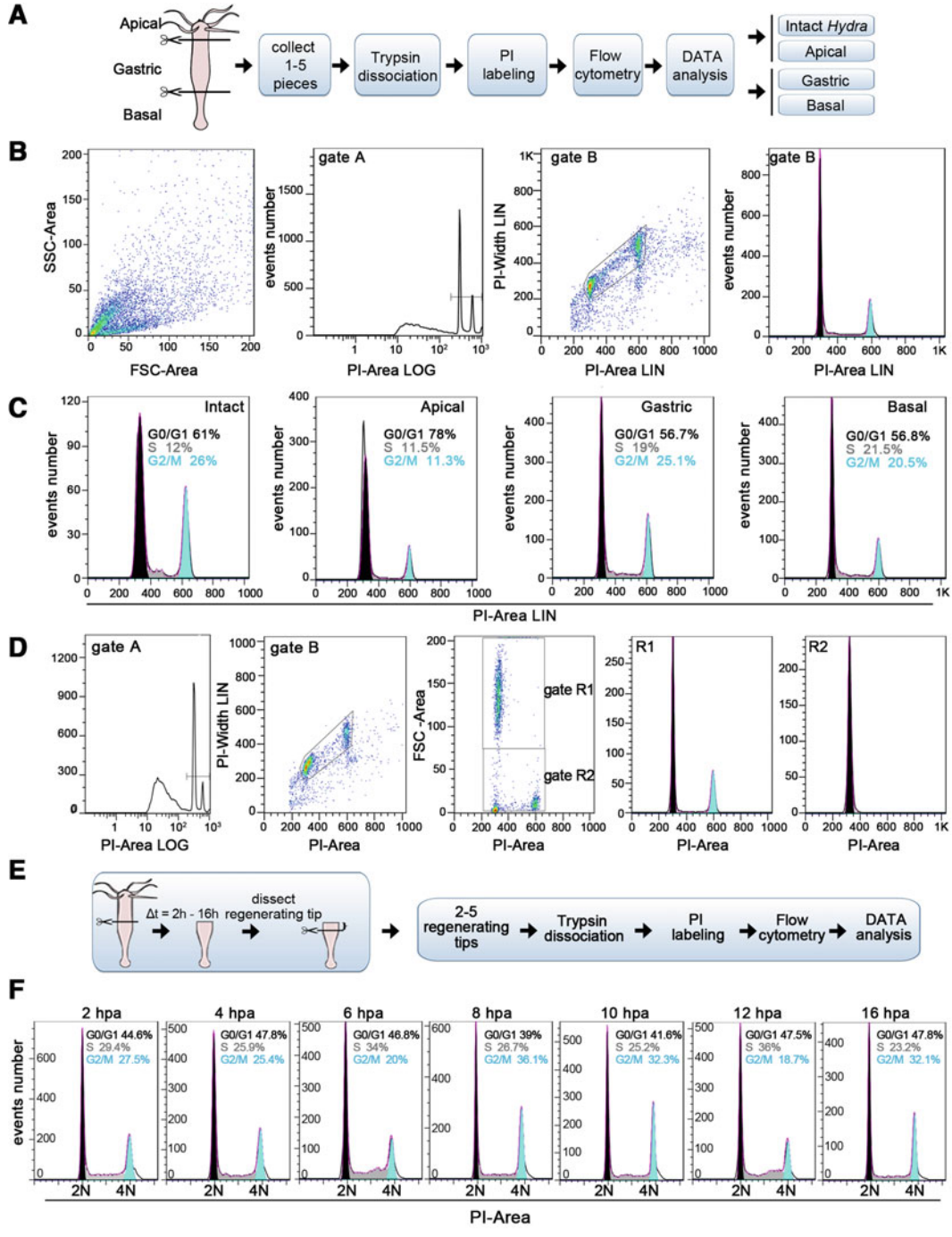


Fig. 4 DNA content measurement in *Hydra* cells after PI staining. (**a**) Workflow of the flow cytometry method used to analyze the cell cycle distribution after PI staining of DNA (*see* Subheading 3.3). (**b**) Typical successive gating procedure where the events are acquired based on the FSC/SSC parameters, then gated first on the channel that detects the PI fluorescence (gate A), followed by doublets and clumps exclusion after setting up a singlet discrimination PI-Area/PI-Width window (gate B). The cell cycle distribution (right panel) is deduced from the DNA content reflected by the intensity of the PI-Area signals of PI-labeled cells in gate B. (**c**) Cell cycle distribution in samples obtained after dissociation of whole animals (intact) or from different *Hydra* regions

number of cells progressing through the S-phase, when samples corresponding to different labeling periods are compared. In contrast, the PI labeling method, which is cheaper and faster, only provides a static view of the DNA content, allowing to deduce the cellular distribution between the different phases of the cell cycle at the time tissues were dissociated. Depending on the context and the experimental objective, these two flow cytometry methods are valuable tools for quantifying the rate of proliferating cells and the cell cycle progression during whole-body *Hydra* regeneration.

2 Materials

All stocks and working solutions are prepared with ultrapure, deionized MilliQ water in screw-capped bottles, sterilized either by autoclaving or filtration using a 0.22-μm filter. The bottles are stored at 4 °C or room temperature (RT) as indicated below. Check stock solutions regularly for any sign of contamination, discard them, and replace them with fresh ones when needed. To prepare the working solutions (1×), dilute any concentrated stock (10× or 20×) with ultrapure MilliQ water.

2.1 Dissociation of Hydra Live Cells

1. A transgenic *Hydra* strain constitutively expressing GFP (*see* **Note 1**).
2. Wild-type AEP *Hydra* strain.
3. 500× *Hydra* Medium Stock solution A: 60.57 g Tris–base–HCl in 900 mL H_2O, pH 7.7, bring to 1000 mL with H_2O. Sterilize by autoclaving, store at 4 °C for several weeks.

Fig. 4 (continued) (apical, gastric column, and basal). Note that the broader G0/G1 peak detected in samples from intact animals or apical region corresponds to a double G0/G1 peak formed by two different cell populations. (**d**) To identify these two distinct G0/G1 cell populations, a specific gating procedure was applied to the samples obtained after dissociation of tissues obtained from the apical region or from the whole animal. An additional gating based on the FSC-Area and PI-Area parameters allows the identification of these two populations as gate R1 and gate R2. Sorting of the nuclei from gate R1 revealed that this population is mainly composed of terminally differentiated nematocytes arrested in the G0 phase (data not shown), which are mainly found in the apical region. (**e**) Scheme depicting the flow cytometric procedure applied to head-regenerating tips (*see* Subheading 3.3). Animals bisected at the mid-gastric level were allowed to regenerate. At indicated time-points after bisection, the head regenerating tips were excised and prepared for analysis as shown in (**a**). (**f**) Cell cycle profiles measured in *H. magnipapillata* animals undergoing head regeneration. Five regenerating tips about 500 μm long were processed and analyzed as above. Note the increase in S-phase cells between 4 and 6 h post-amputation (hpa), followed by an increase in the G2 population at 8 hpa as previously reported [20]. The samples were run on a Gallios flow cytometer (Beckman Coulter) (**b–d**) or a BD FACSCalibur (**f**), and the data were analyzed with the FlowJo software and subjected to Watson's mathematical model to calculate the proportion of cells in each phase of the cell cycle

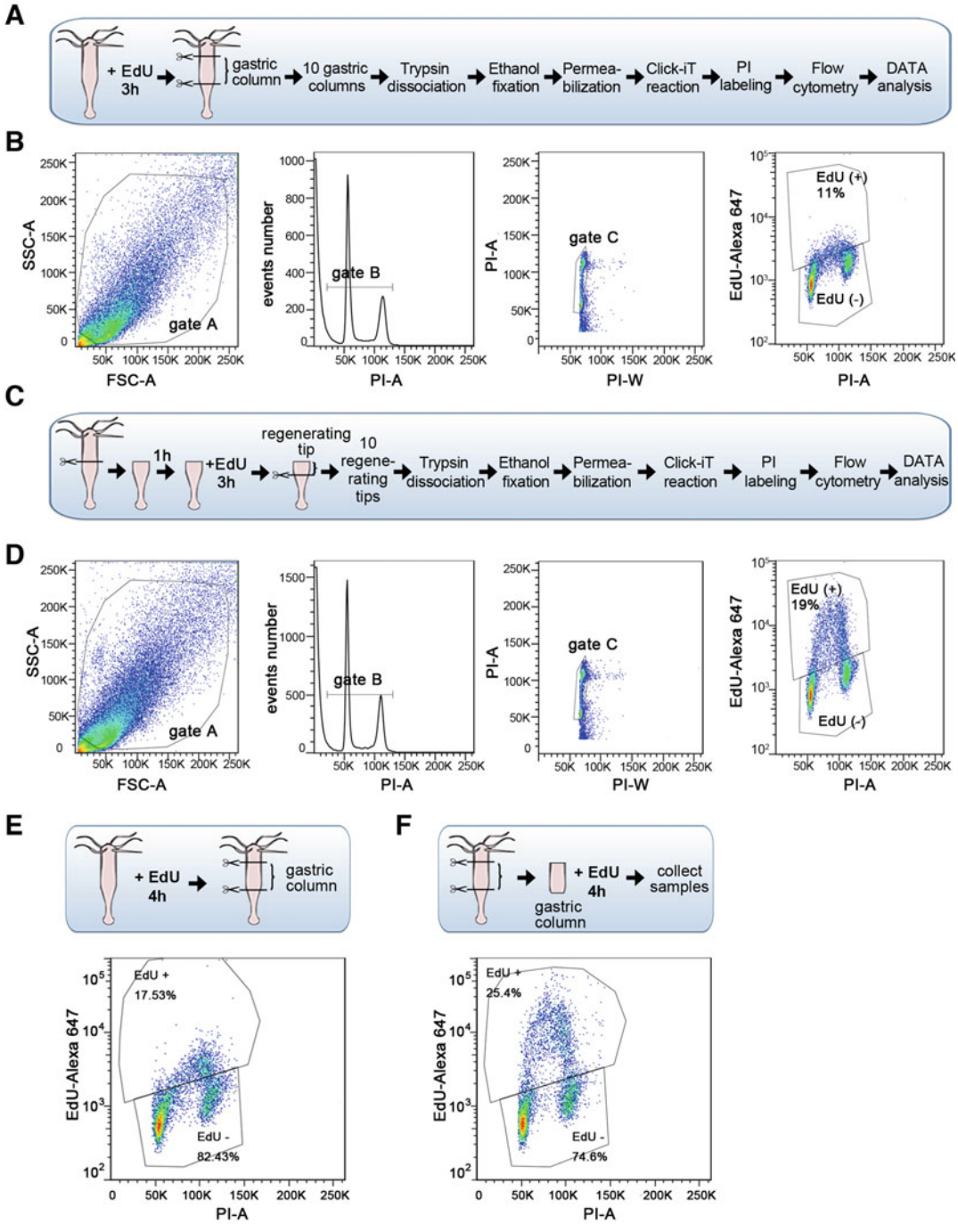


Fig. 5 Flow cytometry analysis of DNA replication in EdU-labeled Hydra cells. (**a**, **c**) Scheme illustrating the workflow of the flow cytometry procedure performed on samples obtained after dissociation of intact (**a**) or head-regenerating polyps (**c**) taken 4 h after bisection and incubated in EdU (5 mM) for 3 h. (**b**, **d**) To analyze cell proliferation, the cells were labeled with the click-iT EdU-Alexa 647 kit, the samples were run on a Fortessa flow cytometer, and the data collected based on the FSC and SSC signals (gate A). Next, the debris were removed from gate A by applying a second gating based on the PI-Area (PI-A) signal. The singlet cells were separated in a PI-Width (PI-W) and PI-A window, which helps to exclude the doublets (gate C). Finally, the

4. 500× *Hydra* Medium Stock solution B: 54.77 g $CaCl_2$•$6H_2O$, 14.6 g NaCl, 1.85 g KCl in 400 mL H_2O. Bring to 500 mL with H_2O. Sterilize by autoclaving, store at 4 °C for several weeks.
5. 10,000× *Hydra* Medium Stock solution C: 61.6 g $MgSO_4$•$7H_2O$ in 200 mL H_2O. Bring to 250 mL with H_2O. Sterilize by autoclaving, store at 4 °C for several weeks.
6. *Hydra* medium (HM): 2 mL stock solution A, 2 mL stock solution B, 100 µL stock solution C, 996 mL H_2O (*see* **Note 2**).
7. Dissociation medium (DM): 1.08 g KCl, 5.256 g $CaCl_2$•$6H_2O$, 1.184 g $MgSO_4$•$7H_2O$, 7.04 g sodium citrate, 2.748 g sodium pyruvate, 4.32 g glucose, 20 g TES-NaOH, pH 6.9 in 3.8 L H_2O. Bring to 4 L with H_2O, filter-sterilize, store at 4 °C (*see* **Note 3**).
8. Pronase E: 10 mg pronase E in 2 mL DM (*see* **Note 4**). Use immediately.
9. Membrane impermeable DNA dye (e.g., 0.3 mM Draq7, Biostatus).

2.2 PI Nuclei Staining for Cell Cycle Analysis

1. Trypsin–EDTA solution: 40 mg KCl, 6 mg KH_2PO_4, 35 mg $NaHCO_3$, 0.8 g NaCl, 9 mg Na_2HPO_4•$7H_2O$, 20 mg EDTA•4Na•$2H_2O$, 1 mg Phenol Red, 50 mg trypsin in 90 mL H_2O. Bring to 100 mL, filter-sterilize, aliquot, store at −20 °C (*see* **Note 5**).

Fig. 5 (continued) cells selected from gate C were analyzed in a PI/ EdU-Alexa Fluor 647 dot-plot area, where the negative and positive EdU gates are defined by the fluorescence intensity in the EdU-Alexa 647 channel. Thus, cells in S-phase, which have incorporated EdU, form the EdU(+) population, while cells in G0/G1 or G2/M correspond to the EdU(−) population. Note the lower percentage of EdU(+) cells and the lower fluorescence intensity on the Alexa 647 channel when intact animals (**b**) were incubated with the EdU solution compared to the regenerating ones (**d**). This result indicates that EdU incorporation is lower in gastric cells when intact *Hydra* are exposed to EdU compared to the regenerating ones. Beside a regulation linked to regeneration, this difference might actually be artefactual, reflecting the barrier effect of the *Hydra* cuticle to EdU in intact animals when compared to the wounded ones. This hypothesis is supported by the fact that the observed proportion of EdU-labeled cells (11%) after a 3-h labeling is lower than that measured by microscopic analysis after BrdU incorporation or by flow cytometry after PI staining method [6, 17, 20, 25, 26]. Indeed, in starved conditions, about 20% of the cells are cycling in gastric tissues from intact animals (*see* Fig. 4c). (**e**, **f**) Comparison between two experimental conditions: one where intact animals were exposed to EdU for 4 h before the central gastric tissue is dissected (**e**), another where the extremities of the animal are first amputated and then the severed gastric pieces are incubated in EdU for 4 h (**f**). After washing, the samples from both experiments were treated as described in Subheading 3.4. Analysis of the EdU-Alexa 647/PI-A data graph (**a** and **b**, lower panels) shows that the percentage of EdU-Alexa 647-positive cells is 50% higher when the central gastric pieces are amputated before EdU incubation compared to that obtained in gastric pieces amputated after EdU incubation. Note also that prolonging EdU incubation improves the fraction of EdU (+) cells: 17.5% after 4 h vs. 11% after 3 h

2. Fetal bovine serum (FBS) from commercial sources. Aliquot, store at −20 °C.
3. 10× PBS stock solution: 80 g NaCl, 2 g KCl, 29 g Na_2H-PO_4•$12H_2O$, 2 g KH_2PO_4 in 900 mL H_2O, pH 6.8. Bring to 1000 mL with H_2O. Sterilize by autoclaving, store at RT (*see* **Note 6**).
4. EDTA solution: 0.931 g EDTA in 40 mL H_2O, pH 8. Bring to 50 mL with H_2O. Filter-sterilize, store at RT.
5. Tris–HCl solution: 0.606 g Tris–base–HCl in 90 mL H_2O, pH 8, bring to 100 mL with H_2O. Sterilize by autoclaving, store at 4 °C.
6. Propidium iodide (PI) solution: 25 mg PI in 25 mL H_2O. Store at 4 °C up to 1 year protected from light (*see* **Note 7**).
7. RNase A solution: 200 mg RNase A in 10 mL Tris–HCl 50 mM. Store at 4 °C.
8. Hypertonic NP-40 buffer: 10 mL 10× PBS, 0.5 mL Nonidet NP-40 substitute, 100 µL 0.5 mM EDTA in 89.4 mL H_2O, Filter-sterilize, store at 4 °C (*see* **Note 8**).
9. Labeling solution (LB): 140 µL PI solution, 35 µL RNAse A solution in 2.8 mL hypertonic NP-40 buffer. Prepare freshly, keep on ice until use (*see* **Note 9**).

2.3 Click-iT EdU-Detection of Proliferating Hydra Cells

1. Click-iT Plus EdU Flow Cytometry Assay kit (C10634) (*see* **Note 10**).
2. 2× 5-ethynyl-2′-deoxyuridine (EdU) solution: 25.23 mg EdU, 10 µL DMSO in 10 mL HM. Prepare freshly (*see* **Note 11**).
3. 1× EdU solution: 1.5 mL of 2× EdU solution, 1.5 mL HM. Enough for one experimental condition, increase accordingly.
4. 1× PBS: 50 mL 10× PBS stock solution, 450 mL H_2O (*see* **Note 6**).
5. 1% Bovine albumin serum (BSA) solution: 1 g BSA in 100 mL 1× PBS. Filter-sterilize, store at 4 °C for up to 1 week (*see* **Note 12**).
6. 100% cold ethanol: 50 mL absolute ethanol, store at −20 °C.
7. Permeabilization and wash buffer (PWB): 5 mL Component E (C10634), 45 mL 1% BSA solution. Store at 4 °C for 1 week.
8. 10× buffer additive stock: 400 mg Component G (C10634) in 2 mL H_2O. Aliquot, store at −20 °C.
9. 1× buffer additive: 5 µL of 10× buffer additive stock, 45 µL H_2O for one sample. Prepare freshly. Multiply by the number of desired samples plus one.

10. Click-iT EdU detection cocktail: 10 μL Copper protectant (component F), 2.5 μL fluorescent Alexa picolyl azide (component B), 50 μL 1× buffer additive, 438 μL 1× PBS. Use within 15 min.
11. DNA staining solution: 12.5 μL PI solution, 5 μL RNase A, 483 μL PWB for one sample. Multiply by the number of desired samples plus one.

2.4 Equipment

1. Stereomicroscope (for example Olympus SZX10 with a 1.25× objective).
2. Pasteur glass pipette.
3. Borosilicate Pyrex 25 × 20 cm rectangular dishes (Pyrex dishes for alimentation).
4. Surgical scalpel No. 3.
5. Surgical blades No. 10.
6. Non-coated plastic petri dish.
7. Silicon bulbs, 5 mm diameter for Pasteur pipette.
8. Mini cell strainer, 70-μm mesh size.
9. Nylon mesh 100-μm pore size.
10. 5-mL polystyrene tubes for flow cytometry.
11. Digital dry bath.
12. Steriflip and steritope (0.22 μm) for filtration.
13. Mini vacuum pump.
14. Flow cytometer equipped with appropriate lasers.
15. Cell sorter equipped with 488 and 561 nm lasers.

3 Methods

3.1 Live Hydra Cell Suspension

1. Collect 250 GFP-expressing transgenic animals with the help of a glass Pasteur pipette (*see* **Note 13**) in a Pyrex dish.
2. Collect 50 wild-type *H. vulgaris AEP* non-transgenic animals with the help of a glass Pasteur pipette in a plastic petri dish.
3. Wash the animals with HM.
4. Check the green fluorescence at the stereomicroscope.
5. Removes animals with a weak or mosaic fluorescence.
6. Dispatch the transgenic animals in five plastic petri dishes (9 cm diameter), 50 animals per dish.
7. Wait 1–2 min for the animals to relax under the light and extend at their maximal length (*see* **Note 14**).

8. Cut with a scalpel the animals of a given dish twice to remove both the apical and the basal part (Fig. 3a).
9. Collect the remaining 50 central body columns in a 1.5-mL tube.
10. Remove as much as possible of the HM liquid from the 1.5-mL collection tube.
11. Add 400 µL of pronase E solution to the collection tube (*see* **Note 15**).
12. Transfer the tube to ice.
13. Repeat **steps 7–12** to cut the animals of all the dishes.
14. Carefully pool all the gastric regions into one tube using a clean Pasteur pipette.
15. Repeat **steps 7–12** with 50 wild-type AEP animals.
16. Transfer the tubes to RT.
17. Leave the samples to dissociate for 1 h.
18. Mix the samples by gently pipetting up and down several times.
19. Wait for 15 min.
20. Repeat **steps 18** and **19** three more times.
21. Centrifuge the samples at 100 rcf for 5 min at 4 °C.
22. Gently replace the supernatant with 1 mL of DM.
23. Slightly resuspend the pellet by pipetting up and down several times.
24. Re-centrifuge the samples at 100 rcf for 5 min at 4 °C.
25. Remove the supernatant and resuspend the pellet in 3 mL DM (*see* **Note 16**).
26. Filter the cell suspension using a mini PluriStrainer of 70-µm pore diameter (*see* **Note 17**).
27. Collect the filtrate in a 15-mL tube.
28. Dilute 15 µL of filtrated cell suspension into 135 µL of DM.
29. Load 10 µl of the diluted cells in each chamber of a hemocytometer.
30. Count four squares from the upper and lower chambers.
31. Calculate the cell density (number of cells/mL) by multiplying the obtained average cell number with 10^5.
32. Adjust the cell density to 10^6 cells/mL with DM.
33. Keep the samples on ice until sorting.

Table 1
Basic terminology used in this chapter related to flow cytometry and cell cycle analysis

Glossary	
Event	A single particle or cell detected by the flow cytometer
FL1	The fluorescence detected and amplified by the photomultiplier tube (PMT) FL1, in the green range of the spectrum (500–565 nm)
FL1-A	The area of the electric pulse (signal) generated by the PMT corresponding to FL1
FL2	The fluorescence detected and amplified by the PMT FL2, in the yellow range of the spectrum (565–590 nm)
FL3	The fluorescence detected and amplified by the PMT FL3, in the orange range of the spectrum (590–625 nm)
FL4	The fluorescence detected and amplified by the PMT FL4, in the red range of the spectrum (625–700 nm)
FL4-area	The area of the electric pulse (signal) generated by the PMT corresponding to FL4
FSC (forward scatter)	This measurement discriminates cells or nuclei according to their size based on the light scattered at an angle of less than 10° as the cells cross the laser beam [62, 63]
FSC-area	Area of the FSC signal
FSC-height	Height of the FSC signal
GATE	A frame or outline that delimitates a subset or sub-population of events. This boundary is drawn by the experimenter on the graph representing the data set [63]
GATING	The process of plotting a gate, the boundaries of a set of events on a diagram or histogram [63]
LIN	Linear scale
LOG	Logarithmic scale
PI-width	Width of the peak signal generated by the PI fluorescence detected on FL2 or FL3 according to the flow cytometer
PI-area	Area of the peak signal generated by the PI fluorescence detected on FL2 or FL3 according to the flow cytometer
SSC (side scatter)	This measurement discriminates cells or nuclei according to their granularity based on the light scattered at an angle of 90° as the cells cross the laser beam [62, 63]

3.2 Flow Cytometry Sorting of Hydra GFP-Expressing Stem Cell (FACS Protocol)

1. Replace the sheath fluid from the FACS sorter with DM (*see* **Note 18**).
2. Add Draq7 to the cell suspension to a final concentration of 0.3 μM.
3. Incubate for 10 min at RT (*see* **Note 19**).
4. Set up the gating windows by selecting first the viable cells from the debris (FSC-H/SSC-H window, Table 1), next the Draq7-negative cells, then the GFP-positive population and finally by excluding the cell doublets among the GFP-positive stem cells (Fig. 3b).

5. Collect the GFP fluorescence on the corresponding detector with a 525/30 nm band pass filter and the Draq7 fluorescence on the far red detector with a 655 long pass filter (Fig. 3b).
6. Set the cell-sorting rate at 1500 cells/s and use a 100-μm nozzle to pass the cells. On the Biorad S3 sorter, the pressure is set up at 20 psi. These cell-sorting conditions were optimized for a density of 1×10^6 cells/mL (*see* **Note 20**).
7. Add 60 μL of DM into a 1.5-mL collection tube (*see* **Note 21**).
8. Sort the GFP-positive stem cells into the tube filled with DM.
9. Check the enrichment factor by diluting 25 μL of sorted cells into 275 μL of DM and re-running the sample again on the sorter (Fig. 3c, *see* **Note 22**).
10. Centrifuge the tubes with the sorted cells at 100 rcf for 5 min at 4 °C.
11. Resuspend the pellet in the requested buffer for the desired application (RNA extraction, proteomics, etc., *see* **Note 23**) or in labeling buffer (LB) to proceed with cell cycle measurements by starting at **step 15** in Subheading 3.3.

3.3 Cell Cycle Measurement: PI Staining of Trypsin-Dissociated Cells

1. Place up to 20 animals in a 10-cm plastic petri dish pre-filled with 50 mL HM for each regenerating time point.
2. Wait 1–2 min to let the animals to relax and extend at their maximal length under the light.
3. When different body regions are analyzed, cut the animals to the desired level (Fig. 4a) using a scalpel (*see* **Note 14**) and continue with **step 8**.
4. For regeneration experiment, cut the animals at mid-gastric position (Fig. 4e).
5. Transfer the lower halves that will regenerate their head to a new pre-filled dish with HM.
6. Let the animals regenerate at 18 °C for 0–72 h.
7. Cut off at selected time-points the regenerating tip (about 200 μm thick) from two to five animals (Fig. 4e).
8. Collect the regenerating tips into a 1.5-mL tube.
9. Repeat **steps 7** and **8** at least three times to be able to analyze at least three replicates per time-point (*see* **Notes 24** and **25**).
10. Remove the maximum amount of HM with a micro-pipette from each tube.
11. Add 50 μL of Trypsin–EDTA solution to each tube.
12. Heat the tube for 5 min at 37 °C in a block-heater.
13. Dissociate the tissue by gently mixing the samples about 20 times up and down with a micropipette (*see* **Note 26**).

14. Add 20 μL of FBS and place the tube on ice (*see* **Note 27**).
15. Repeat **steps 10–14** to dissociate the next tube.
16. Add 430 μL of LB (*see* **Notes 28** and **29**).
17. Incubate the samples for 30 min in the dark at RT (*see* **Note 30**).
18. Transfer the samples into 5-mL flow cytometry tubes and store them on ice protected from light.
19. Run the samples on a regular flow cytometer using a low flow rate (*see* **Note 31**).
20. Set up the threshold on the PI channel and detect the PI fluorescence after linear amplification on the corresponding channel according to your flow cytometer (FL2 or FL3) as shown in Fig. 4 (*see* **Note 32**).
21. Gate the nuclei by separating the debris from the PI-labeled nuclei (PI-Area (LOG)/Events number) and by excluding the doublets and clumps (PI-Area (LIN)/PI-Width (LIN)) (Fig. 4b, *see* **Note 33**).
22. Acquire between 10,000 and 20,000 events for each sample.
23. Analyze the cell cycle profiles by using the software either available on your flow cytometer or commercially available such as FlowJo (*see* **Note 34**).
24. Clean the flow cytometer according to the washing/cleaning procedures of the supplier (*see* **Note 35**).

3.4 Cell Cycle Measurement: Click-iT EdU Labeling of Hydra Cells Replicating Their Genomic DNA (S-Phase)

1. Follow **steps 1** and **2** in Subheading 3.3.
2. Cut 10–15 animals at the mid-gastric level (Figs. 4e and 5c).
3. Collect the regenerating halves in a 2-mL tube.
4. Adjust the volume to 1 mL with HM.
5. Add 1 mL of 2× EdU solution.
6. Transfer the animals into a 12-well plate.
7. Add 3 mL of 1× EdU solution to each well containing animals (*see* **Note 36**).
8. Let the animals regenerate for the required time.
9. Transfer the animals into a 1.5-mL tube at the selected time-points.
10. Wash out the EdU solution by replacing five times the medium with fresh HM.
11. Follow **steps 10–13** in Subheading 3.3.
12. Add 20 μL of FBS and 650 μL of PBS to each tube.
13. Centrifuge the samples at 350 rcf, 5 min at 4 °C.

14. Gently aspire the supernatant without touching the sediment with the help of a pipette connected to a vacuum pump.
15. Add 200 µL of PBS to each tube.
16. Gently resuspend the pellet.
17. Add drop by drop 800 µL of pre-chilled 100% ethanol while vortexing the tubes at medium speed.
18. Fix the samples on ice for 1 h and overnight at 4 °C.
19. Centrifuge the samples next day at 650 rcf for 5 min at 4 °C.
20. Resuspend the pellet in 1% BSA.
21. Transfer the samples in a 5-mL flow cytometry tube.
22. Repeat **step 19**.
23. Resuspend the pellet in 1 mL of PWB.
24. Incubate the samples at RT for 15 min.
25. Follow **step 19**.
26. Gently resuspend the sample in 100 µL of PWB.
27. Add 500 µL of click-iT EdU detection cocktail to each tube.
28. Mix gently.
29. Incubate the tubes in the dark for 30 min (*see* **Note 37**).
30. Add 1 mL of PWB to each tube.
31. Re-centrifuge the tubes as in **step 19**.
32. Resuspend the pellet in the DNA-staining solution.
33. Incubate the samples at RT for 30 min protected from light.
34. Prepare two control tubes: one with cells only exposed to the DNA-staining solution and another with cells only exposed to the click-iT EdU detection cocktail (*see* **Notes 30** and **38**).
35. Filtrate the samples into a new flow cytometry tube using a cell strainer (70-µm mesh).
36. Collect the EdU-Alexa dye fluorescence according to the selected Alexa fluorochrome, on the corresponding detector: here the Alexa 647 dye was collected on a 660/20 band pass filter.
37. Detect the PI fluorescence after linear amplification on the corresponding channel according to your flow cytometer (FL2 or FL3) as shown in Fig. 5.
38. Set up the gating windows (Fig. 5b): select first the cells based on the FSC/SSC parameters, remove the debris by gating the cells labeled with PI (PI-A/events number histogram), remove the doublets by gating singlet cells in a PI-W/PI-A window, open a PI/EdU-Alexa 647 dot-plot.

39. Analyze the data with available software and estimate the percentage of EdU-positive cells that correspond to the proliferating population based on the EdU-Alexa 647 fluorescence intensity (Fig. 5b, d–F).

4 Notes

1. In the protocol described here, we used the *ecto-GFP* strain [37], a transgenic line produced in the laboratory of T. Bosch (Kiel, Germany) that constitutively expresses GFP in the epidermal epithelial stem cells. In a previous work [40], we also applied flow cytometry to *Hydra* transgenic strains that express GFP in gastrodermal epithelial cells from the *endo*-GFP line [38] or interstitial cells from the *cnnos1*-GFP strain [39]. These strains can be obtained from the Transgenic Hydra Facility at the University of Kiel (http://transgenic-hydra.org).
2. Here the *Hydra* medium is prepared according to [53].
3. The dissociation medium (DM), is a hyperosmotic solution (70 mOsm) used to dissociate the *Hydra* polyps and obtain live cells, which was initially used for reaggregation studies [54]. The protocol indicates that it is necessary to prepare a large volume of DM (4 L), as DM is also used to replace the classical fluid sheath in the sorter (*see* **Note 18**).
4. Pronase E is a mixture of several proteases obtained from *Streptomyces griseus*; it can be stored as powder at −20 °C. Select a product that is similar to P6911 from Sigma and has an enzymatic activity higher than 4 U/mg (the P6911 product is unfortunately discontinued).
5. The indicated trypsin–EDTA solution is used for mammalian cell culture. Therefore, any commercially available solution with the indicated concentration can be used to dissociate *Hydra* tissue.
6. It is not necessary to adjust the pH of the 10× PBS stock solution, because after dilution to 1× PBS, the pH reaches 7.4.
7. Always wear gloves when working with PI as PI is a DNA intercalating agent with mutagenic properties. Dispose the PI wastes according to the safety procedure established in your lab.
8. Nonidet NP-40 substitute is a viscous detergent that must be carefully aspirated during pipetting. Gently stir the labeling buffer to avoid foaming and bubbles.
9. The indicated PI and RNase-A concentrations correspond to the final concentration obtained after mixing the dissociated *Hydra* cells with the labeling buffer.

10. Different Click-iT Plus EdU Flow Cytometry kits have been developed by Invitrogen, which only differ by the Alexa fluorophores that have distinct spectral properties among the kits. Choose the right combination for the laser equipment available on your flow cytometer. The kit used here (Click-iT plus Alexa Fluor 647 flow cytometry assay kit, ref. C10634) is compatible with the detection of cell cycle dyes, GFP and mCherry. The protocol can be adapted to monitor the proliferation of a population of fluorescent reporter-expressing cells.
11. EdU is a potentially hazardous agent because it readily gets incorporated into the genome. It must therefore be handled with care while wearing gloves. To increase the solubility and uptake of EdU by *Hydra* cells, it is necessary to add DMSO to the EdU solution, however at a concentration not exceeding 0.5%, as DMSO above 1% affects the organization of epithelial cells [55].
12. To prepare the BSA solution, first transfer the powder to a 50-mL tube and then add the required volume of PBS. Mix the solution by gentle stirring to avoid foaming and bubble formation.
13. The number of transgenic animals required to isolate GFP-positive cells should be defined according to the expected number of GFP-positive cells obtained after sorting. We usually obtain 10^5 GFP-positive sorted cells from 100 gastric columns. Avoid taking animals that have been fed on the same day, as the gastrodermal epithelial cells would be full with digestive vacuoles, fragile, and thus easy to break. Moreover, the content of those digestive vacuoles is labeled by nuclei dyes, thus increasing the debris and noise level in the measurements.
14. To cut the animal at the correct position along the axis, let the animals relax under the stereomicroscope for about a minute. Apply the scalpel perpendicular to the body column and cut quickly. Change the blade regularly as it rusts easily.
15. *Hydra* epithelial cells are highly adhesive and re-aggregate rapidly after tissue dissociation [54]. The formation of clumps is a serious problem for flow cytometry as the clumps can clog the nozzle. For this reason, we prefer enzymatic dissociation with pronase-E than mechanical dissociation as initially established by Gierer and colleagues in 1972. The enzymatic method allows mesoglea lysis and tissue disintegration, producing viable cells that have lost their adhesiveness [56].
16. *Hydra* epithelial stem cells are large cells with a cuboidal or columnar shape, and they show a large cytoplasm and a high cytoplasm to nucleus ratio. They are highly sensitive to centrifugal forces; therefore, the centrifugation steps should be performed at a low speed to prevent their disruption. By contrast,

ISCs are much smaller than ESCs, and they show a higher nuclear to cytoplasmic ratio and a better resistance to centrifugation [56]. If ISCs are considered for sorting, an additional centrifugation step at 300 rcf is requested.

17. Always filtrate the cell suspension to separate the undigested small tissues fragments that can block the tubing or nozzle. For the filtration of volumes greater than 1 mL, use a 70-μm Pluristrainer. For small volumes, a homemade filter can be manufactured with a nylon mesh with a porosity of 70–100 μm. Use a plastic conical tip for 1-mL pipette, cut it about 1 cm from the top, cover the tip with a 1.5 × 1.5 cm piece of nylon mesh and insert it into a new intact conical tip. Transfer the cell suspension into the sectioned tip, firmly insert the micropipette, then gently press the micropipette plunger resulting in filtering the cell suspension through the nylon mesh, collecting the filtrate into a new tube.
18. The ProFlow sheath fluid, used in the flow cytometer fluidics to transport and focus the samples in the flow chamber, is usually the saline solution PBS, which is isotonic for mammalian cells but highly hypertonic for *Hydra* cells given their low osmolarity, lower than 10 mOsm [54, 57, 58]. Consequently, to prevent drastic shrinkage of the *Hydra* cells by water leakage, PBS should be replaced by DM, which has a much lower osmolarity (70 mOsm) than PBS (285–315 mOsm). The DM medium was previously tested in flow cytometry on beads (Spherotec) and the eight sorted peaks were found to be perfectly pure. Therefore, DM ensures the correct hydrodynamic focusing, the correct formation of the core stream, and the deflection of the droplets in the sorting flow chamber.
19. Draq7 is a nuclear far-red fluorescent dye that labels only dead or permeabilized cells as it cannot enter intact live cells. As consequence, Draq7 staining allows to exclude the damaged cells and to sort only viable cells.
20. Sorting conditions should be adjusted to run about 1×10^3 cells/s, and optimal conditions are depending on the initial density of the cell suspension. Depending on the available cell sorter, the pressure of the fluid sheath must be set at a minimum level so as not to damage the integrity of the cells. The best balance must be established between cell density, flow pressure, and sorting time.
21. The size of the collection tube and the amount of recovery medium should be adapted to the expected number of sorted cells and the objective of the experiment. According to our experience, on a Biorad S3 sorter, 1×10^5 cells are separated in about 400 μL of medium. If a higher cell yield is required ($4–5 \times 10^5$ cells), use larger tubes such as 5-mL flow cytometry

tubes or similar tubes available for your sorter. For RNA extraction, a high RNA yield (1 mg) was obtained with the minikit RNAeasy Plus (Qiagen) from 3×10^5 sorted cells.

22. The level of enrichment of GFP-positive cells among the sorted cells can be tested by re-running the sorted samples on the flow cytometer. In our hands, the re-analyzed samples are viable and the percentage of Draq7-positive cells is low (Fig. 3c). These Draq7-positive cells have a damaged cell membrane and show an intermediate GFP fluorescence profile, probably because cytoplasmic GFP can leak. An example of low GFP and broken membrane cells is shown in Fig. 3d, where the re-sorted cells were imaged under a fluorescent microscope. The sorted samples can also be analyzed with the Tali image-based cytometer (Invitrogen), which indicates the size and viability of the sorted cells.
23. To avoid damage to the sorted cells, process the samples quickly for the desired application. If transcriptomic analysis is planned, resuspend the cells in RNA extraction buffer and, if possible, process them immediately according to the supplier's instructions. Alternatively, the cells can be resuspended in the RNA protect Cell Reagent (Qiagen) and stored for a short period before RNA extraction.
24. The head-regenerating tip is the area located immediately below the bisection plan. It regenerates the head and is about 200 μm long. It is important to allow the animals to relax for a few minutes before sectioning to properly estimate the size of the slice to be cut. Indeed, cells behave differently in the head-regenerating tip than in the underlying tissue [25], and amputation of contracted polyps leads to the removal of larger slices where the regenerating tissue is diluted with homeostatic tissue.
25. The presented procedure (Fig. 4c, f) is adapted to allow the analysis of the cell cycle profile from very small tissue fragments containing a low number of cells (10^4) up to large tissue samples comprising 5×10^5 cells, corresponding to four or five medium-sized animals [6]. If a larger number of cells is to be analyzed, the volume of the labeling solution should be increased to adjust the cell density to a maximum of 1×10^6 cells/mL.
26. The established procedure (Fig. 4c, f) is based on a quick and easy method of tissue dissociation, which combines enzymatic dissociation by trypsin–EDTA with mechanical rupture. This method ensures complete dissociation of *Hydra* tissues, including the mesoglea and clusters of nematoblasts [6].

27. FBS contains protease inhibitors such as alpha 1-antitrypsin and is routinely used in mammalian cell culture to inactivate trypsin activity [59].
28. Incubation in the DNA-staining solution, which is hypertonic to *Hydra* cells and contains a substitute for NP-40 detergent, induces complete rupture of cell membranes [50]. As a result, this method provides mainly nuclei and very few cell clusters, which reduces sample preparation time since there is no need to filtrate the samples prior to flow cytometry.
29. The quality of the samples is determined by a low coefficient of variation (CV) across the G0/G1 peak. If too high, the accuracy of the measurement is limited. One parameter that can influence the CV is the stoichiometry of DNA labeling with PI. To ensure homogenous DNA staining, excess PI should be added. The concentration of 50 μg/mL has been shown to be appropriate for efficient labeling of different cell types and for a maximum cell density of 2×10^6 cells/mL [60].
30. PI is a DNA intercalating dye that binds to both DNA and double-strand RNA. Therefore, the labeling solution must contain RNase-A (100–200 μg/mL), which digests the RNA present in the sample. An incubation step of up to 30 min at RT is sufficient to degrade the RNA; subsequently, the tubes can be kept on ice for up to 2 h without altering the quality of the samples.
31. When the DNA content is measured by flow cytometry, the flow rate should be kept low, and the number of events should not exceed 200/s for optimal analysis of the sample with the best possible resolution (CV) of the PI fluorescence.
32. *Hydra* tissues contain about 12 different cell types that vary greatly in size and shape, with nuclei ranging from 5 to 15 μm [61]. To take into account this heterogeneity and to avoid the loss of small events/nuclei on the FSC channel, the threshold value should be set on the PI detector. In this way, only unwanted debris or noise is removed, and all intact nuclei stained with PI are acquired.
33. The name of acquisition parameters might slightly vary between the different types of flow cytometers. The acquisition should be done on the linear (LIN) and logarithmic scale (LOG) of the PI detector. The flow cytometry terms used in this chapter are presented in Table 1.
34. In general, CV values for samples taken from the central body column or from the basal region are below 3, which is acceptable given the heterogeneity of the *Hydra* tissue (Fig. 4c). However, we noted that when head region or intact animal is analyzed, a very wide G0/G1 peak is observed in the histogram (Fig. 4c). This wide peak actually consists of a double G0/G1

peak that corresponds to two different populations of nuclei. Therefore, to avoid misestimation of the S phase, we apply a different gating procedure to analyze the cell cycle profile of samples taken from the apical part of the animal (Fig. 4d), where the CV value did not exceed 3.0.

35. At the end of the acquisition, the flow cytometer must be cleaned immediately according to the protocol established in your facility, as PI is very adherent and persists in the tubing, contaminating subsequent acquisitions. Usually a 5 min wash with BDFACS Clean (bleach solution), followed by a 5 min wash with BDFACS Rinse (detergent solution) and a 5 min wash with H_2O is sufficient to clean the system.
36. The volume of the 5 mM EdU solution should be calculated considering that the standard conditions for regeneration are to maintain one regenerating animal in a minimal volume of 0.5 mL medium.
37. According to the supplier, the incubation time of 30 min with the click-iT EdU cocktail should not be exceeded.
38. Use unstained cells to set up the PMT voltage of each detector and use cells labeled with a single fluorophore to precisely adjust the voltage required for sample acquisition. If the emission spectra of DNA and Alexa dyes overlap, adjust the compensation voltage. The combination of Alexa Fluor 647 and PI does not require any compensation (Fig. 5b, d–f), since the spillover between the two fluorochromes is limited. However, if PI and Alexa Fluor 488 are selected, appropriate fluorescence compensations are required for correct sample acquisition.

Acknowledgments

This work was supported by the Swiss National Science Foundation (SNF grants 31003A_149630, 31003_169930, and 310030_189122), the Claraz donation, and the Canton of Geneva.

References

1. Steele RE (2002) Developmental signaling in Hydra: what does it take to build a "simple" animal? Dev Biol 248(2):199–219. pii: S001216060290744X
2. Bosch TC (2007) Why polyps regenerate and we don't: towards a cellular and molecular framework for Hydra regeneration. Dev Biol 303(2):421–433. https://doi.org/10.1016/j.ydbio.2006.12.012
3. Galliot B, Ghila L (2010) Cell plasticity in homeostasis and regeneration. Mol Reprod Dev 77(10):837–855. https://doi.org/10.1002/mrd.21206
4. Galliot B (2012) Hydra, a fruitful model system for 270 years. Int J Dev Biol 56(6–8):411–423. https://doi.org/10.1387/ijdb.120086bg
5. Vogg MC, Galliot B, Tsiairis CD (2019) Model systems for regeneration: Hydra. Development 146(21):dev177212. https://doi.org/10.1242/dev.177212

6. Buzgariu W, Crescenzi M, Galliot B (2014) Robust G2 pausing of adult stem cells in Hydra. Differentiation 87(1–2):83–99. https://doi.org/10.1016/j.diff.2014.03.001
7. David CN, Plotnick I (1980) Distribution of interstitial stem cells in Hydra. Dev Biol 76(1): 175–184. https://doi.org/10.1016/0012-1606(80)90370-x
8. Bosch TC (2009) Hydra and the evolution of stem cells. Bioessays 31(4):478–486. https://doi.org/10.1002/bies.200800183
9. David CN (2012) Interstitial stem cells in Hydra: multipotency and decision-making. Int J Dev Biol 56(6–8):489–497. https://doi.org/10.1387/ijdb.113476cd
10. Hobmayer B, Jenewein M, Eder D, Eder MK, Glasauer S, Gufler S, Hartl M, Salvenmoser W (2012) Stemness in Hydra - a current perspective. Int J Dev Biol 56(6–8):509–517. https://doi.org/10.1387/ijdb.113426bh
11. David CN, Murphy S (1977) Characterization of interstitial stem cells in hydra by cloning. Dev Biol 58(2):372–383. https://doi.org/10.1016/0012-1606(77)90098-7
12. Holstein TW, David CN (1990) Putative intermediates in the nerve cell differentiation pathway in hydra have properties of multipotent stem cells. Dev Biol 142(2):401–405. https://doi.org/10.1016/0012-1606(90)90361-l
13. Bode HR (1996) The interstitial cell lineage of hydra: a stem cell system that arose early in evolution. J Cell Sci 109(pt 6):1155–1164. https://jcs.biologists.org/content/joces/109/6/1155.full.pdf
14. Campbell RD (1967) Tissue dynamics of steady state growth in Hydra littoralis. II. Patterns of tissue movement. J Morphol 121(1):19–28. https://doi.org/10.1002/jmor.1051210103
15. David CN, Campbell RD (1972) Cell cycle kinetics and development of Hydra attenuata. I. Epithelial cells. J Cell Sci 11(2): 557–568. https://jcs.biologists.org/content/joces/11/2/557.full.pdf
16. Campbell RD, David CN (1974) Cell cycle kinetics and development of Hydra attenuata. II. Interstitial cells. J Cell Sci 16(2):349–358. https://jcs.biologists.org/content/joces/16/2/349.full.pdf
17. Holstein TW, David CN (1990) Cell cycle length, cell size, and proliferation rate in hydra stem cells. Dev Biol 142(2):392–400. https://doi.org/10.1016/0012-1606(90)90360-u
18. Bode HR, Flick KM, Smith GS (1976) Regulation of interstitial cell differentiation in Hydra attenuata. I. Homeostatic control of interstitial cell population size. J Cell Sci 20(1):29–46. https://doi.org/10.1007/BF00848421
19. Marcum BA, Campbell RD (1978) Development of Hydra lacking nerve and interstitial cells. J Cell Sci 29:17–33. https://jcs.biologists.org/content/joces/29/1/17.full.pdf
20. Buzgariu W, Wenger Y, Tcaciuc N, Catunda-Lemos AP, Galliot B (2018) Impact of cycling cells and cell cycle regulation on Hydra regeneration. Dev Biol 433(2):240–253. https://doi.org/10.1016/j.ydbio.2017.11.003
21. Dubel S, Schaller HC (1990) Terminal differentiation of ectodermal epithelial stem cells of Hydra can occur in G2 without requiring mitosis or S phase. J Cell Biol 110(4):939–945. https://doi.org/10.1083/jcb.110.4.939
22. Passamaneck YJ, Martindale MQ (2012) Cell proliferation is necessary for the regeneration of oral structures in the anthozoan cnidarian Nematostella vectensis. BMC Dev Biol 12:34. https://doi.org/10.1186/1471-213X-12-34
23. Amiel AR, Johnston HT, Nedoncelle K, Warner JF, Ferreira S, Rottinger E (2015) Characterization of morphological and cellular events underlying oral regeneration in the Sea Anemone, Nematostella vectensis. Int J Mol Sci 16(12):28449–28471. https://doi.org/10.3390/ijms161226100
24. Bradshaw B, Thompson K, Frank U (2015) Distinct mechanisms underlie oral vs aboral regeneration in the cnidarian Hydractinia echinata. Elife 4:e05506. https://doi.org/10.7554/eLife.05506
25. Chera S, Ghila L, Dobretz K, Wenger Y, Bauer C, Buzgariu W, Martinou JC, Galliot B (2009) Apoptotic cells provide an unexpected source of Wnt3 signaling to drive hydra head regeneration. Dev Cell 17(2):279–289. https://doi.org/10.1016/j.devcel.2009.07.014
26. Holstein TW, Hobmayer E, David CN (1991) Pattern of epithelial cell cycling in hydra. Dev Biol 148(2):602–611. https://doi.org/10.1016/0012-1606(91)90277-a
27. David CN, Gierer A (1974) Cell cycle kinetics and development of Hydra attenuata. III. Nerve and nematocyte differentiation. J Cell Sci 16(2):359–375
28. Plickert G, Kroiher M (1988) Proliferation kinetics and cell lineages can be studied in whole mounts and macerates by means of BrdU/anti-BrdU technique. Development 103(4):791–794. https://dev.biologists.org/content/develop/103/4/791.full.pdf
29. Veal DA, Deere D, Ferrari B, Piper J, Attfield PV (2000) Fluorescence staining and flow

cytometry for monitoring microbial cells. J Immunol Methods 243(1–2):191–210. https://doi.org/10.1016/s0022-1759(00)00234-9

30. Rosental B, Kozhekbaeva Z, Fernhoff N, Tsai JM, Traylor-Knowles N (2017) Coral cell separation and isolation by fluorescence-activated cell sorting (FACS). BMC Cell Biol 18(1):30. https://doi.org/10.1186/s12860-017-0146-8
31. Hayashi T, Agata K (2018) A subtractive FACS method for isolation of planarian stem cells and neural cells. Methods Mol Biol 1774:467–478. https://doi.org/10.1007/978-1-4939-7802-1_19
32. Dutta D, Buchon N, Xiang J, Edgar BA (2015) Regional cell specific RNA expression profiling of FACS isolated Drosophila intestinal cell populations. Curr Protoc Stem Cell Biol 34: 2F.2.1–2F.2.14. https://doi.org/10.1002/9780470151808.sc02f02s34
33. Cossarizza A et al (2019) Guidelines for the use of flow cytometry and cell sorting in immunological studies (second edition). Eur J Immunol 49(10):1457–1973. https://doi.org/10.1002/eji.201970107
34. Defaye A, Perrin L (2014) Tissue specific RNA isolation in Drosophila embryos: a strategy to analyze context dependent transcriptome landscapes using FACS. Methods Mol Biol 1196: 183–195. https://doi.org/10.1007/978-1-4939-1242-1_11
35. Huo X, Li H, Li Z, Yan C, Agrawal I, Mathavan S, Liu J, Gong Z (2019) Transcriptomic profiles of tumor-associated neutrophils reveal prominent roles in enhancing angiogenesis in liver tumorigenesis in zebrafish. Sci Rep 9(1):1509. https://doi.org/10.1038/s41598-018-36605-8
36. Ly T, Whigham A, Clarke R, Brenes-Murillo AJ, Estes B, Madhessian D, Lundberg E, Wadsworth P, Lamond AI (2017) Proteomic analysis of cell cycle progression in asynchronous cultures, including mitotic subphases, using PRIMMUS. Elife 6:e27574. https://doi.org/10.7554/eLife.27574
37. Anton-Erxleben F, Thomas A, Wittlieb J, Fraune S, Bosch TC (2009) Plasticity of epithelial cell shape in response to upstream signals: a whole-organism study using transgenic Hydra. Zoology 112(3):185–194. https://doi.org/10.1016/j.zool.2008.09.002
38. Wittlieb J, Khalturin K, Lohmann JU, Anton-Erxleben F, Bosch TC (2006) Transgenic Hydra allow in vivo tracking of individual stem cells during morphogenesis. Proc Natl Acad Sci U S A 103(16):6208–6211. https://doi.org/10.1073/pnas.0510163103
39. Hemmrich G, Khalturin K, Boehm AM, Puchert M, Anton-Erxleben F, Wittlieb J, Klostermeier UC, Rosenstiel P, Oberg HH, Domazet-Loso T, Sugimoto T, Niwa H, Bosch TC (2012) Molecular signatures of the three stem cell lineages in hydra and the emergence of stem cell function at the base of multicellularity. Mol Biol Evol 29(11):3267–3280. https://doi.org/10.1093/molbev/mss134
40. Wenger Y, Buzgariu W, Galliot B (2016) Loss of neurogenesis in Hydra leads to compensatory regulation of neurogenic and neurotransmission genes in epithelial cells. Philos Trans R Soc Lond B Biol Sci 371(1685):20150040. https://doi.org/10.1098/rstb.2015.0040
41. Siebert S, Farrell JA, Cazet JF, Abeykoon Y, Primack AS, Schnitzler CE, Juliano CE (2019) Stem cell differentiation trajectories in Hydra resolved at single-cell resolution. Science 365(6451):eaav9314. https://doi.org/10.1126/science.aav9314
42. Ulrich H, Tarnok A (2005) Quantification of cell-cycle distribution and mitotic index in Hydra by flow cytometry. Cell Prolif 38(2): 63–75. https://doi.org/10.1111/j.1365-2184.2005.00331.x
43. Colasanti M, Mazzone V, Mancinelli L, Leone S, Venturini G (2009) Involvement of nitric oxide in the head regeneration of Hydra vulgaris. Nitric Oxide 21(3–4):164–170. https://doi.org/10.1016/j.niox.2009.07.003
44. Zeeshan M, Murugadas A, Ghaskadbi S, Ramaswamy BR, Akbarsha MA (2017) Ecotoxicological assessment of cobalt using Hydra model: ROS, oxidative stress, DNA damage, cell cycle arrest, and apoptosis as mechanisms of toxicity. Environ Pollut 224: 54–69. https://doi.org/10.1016/j.envpol.2016.12.042
45. Crissman HA, Steinkamp JA (1973) Rapid, simultaneous measurement of DNA, protein, and cell volume in single cells from large mammalian cell populations. J Cell Biol 59(3): 766–771. https://doi.org/10.1083/jcb.59.3.766
46. Krishan A (1975) Rapid flow cytofluorometric analysis of mammalian cell cycle by propidium iodide staining. J Cell Biol 66(1):188–193. https://doi.org/10.1083/jcb.66.1.188
47. Shcherbata HR, Althauser C, Findley SD, Ruohola-Baker H (2004) The mitotic-to-endocycle switch in Drosophila follicle cells is executed by Notch-dependent regulation of G1/S, G2/M and M/G1 cell-cycle transitions. Development 131(13):3169–3181. https://doi.org/10.1242/dev.01172

48. Kang H, Sanchez Alvarado A (2009) Flow cytometry methods for the study of cell-cycle parameters of planarian stem cells. Dev Dyn 238(5):1111–1117. https://doi.org/10.1002/dvdy.21928
49. Gomez M, Mayo I, Torres S (2001) Flow cytometry of cell proliferation through the incorporation of bromodeoxyuridine as an index of growth rate in the water flea, Daphnia magna (Crustacea, Cladocera). Cytometry 44(3):264–271. https://doi.org/10.1002/1097-0320(20010701)44:3<264::aid-cyto1119>3.0.co;2-%23
50. Vindelov LL, Christensen IJ, Nissen NI (1983) A detergent-trypsin method for the preparation of nuclei for flow cytometric DNA analysis. Cytometry 3(5):323–327. https://doi.org/10.1002/cyto.990030503
51. Salic A, Mitchison TJ (2008) A chemical method for fast and sensitive detection of DNA synthesis in vivo. Proc Natl Acad Sci U S A 105(7):2415–2420. https://doi.org/10.1073/pnas.0712168105
52. Buck SB, Bradford J, Gee KR, Agnew BJ, Clarke ST, Salic A (2008) Detection of S-phase cell cycle progression using 5-ethynyl-2′-deoxyuridine incorporation with click chemistry, an alternative to using 5-bromo-2-′-deoxyuridine antibodies. Biotechniques 44(7):927–929. https://doi.org/10.2144/000112812
53. Loomis WF, Lenhoff HM (1956) Growth and sexual differentiation of hydra in mass culture. J Exp Zool 132(3):555–573. https://doi.org/10.1002/jez.1401320309
54. Gierer A, Berking S, Bode H, David CN, Flick K, Hansmann G, Schaller H, Trenkner E (1972) Regeneration of hydra from reaggregated cells. Nat New Biol 239(91):98–101. https://doi.org/10.1038/newbio239098a0
55. Bolzer A, Melzer RR, Bosch TC (1994) A SEM analysis of DMSO treated hydra polyps. Biol Cell 81(1):83–86. https://doi.org/10.1016/0248-4900(94)90059-0
56. Greber MJ, David CN, Holstein TW (1992) A quantitative method for separation of living Hydra cells. Roux Arch Dev Biol 201(5):296–300. https://doi.org/10.1007/BF00592110
57. Lilly S (1955) Osmoregulation and ionic regulation in Hydra. J Exp Biol 32:423–439. https://jeb.biologists.org/content/jexbio/32/2/423.full.pdf
58. Prusch RD, Benos DJ, Ritter M (1976) Osmoregulatory control mechanisms in freshwater coelenterates. Comp Biochem Physiol A Comp Physiol 53(2):161–164. https://doi.org/10.1016/s0300-9629(76)80048-5
59. Phelan MC (2007) Basic techniques in mammalian cell tissue culture. Curr Protoc Cell Biol Chapter 1:Unit 1 1. https://doi.org/10.1002/0471143030.cb0101s36
60. Ormerod MG (2005) Analysis of DNA - general methods. In: Ormerod MG (ed) Flow cytometry - a practical approach, 3rd edn. Oxford University Press, Oxford
61. David CN (1973) A quantitative method for maceration of hydra tissue. Wilhelm Roux Arch Dev Biol 171:259–268. https://doi.org/10.1007/BF00577724
62. FlowJo tutorial. https://www.flowjo.com/learn/flowjo-university/flowjo/getting-started-with-flowjo/58
63. Janis V. Giorgi Flow Cytometry Laboratory UCLA General Flow Cytometry Glossary and Cell cycle Analysis Terminology. https://web.archive.org/web/20041205055418/http://cyto.mednet.ucla.edu/Protocols/flow.htm

Open Access This chapter is licensed under the terms of the Creative Commons Attribution 4.0 International License (http://creativecommons.org/licenses/by/4.0/), which permits use, sharing, adaptation, distribution and reproduction in any medium or format, as long as you give appropriate credit to the original author(s) and the source, provide a link to the Creative Commons license and indicate if changes were made.

The images or other third party material in this chapter are included in the chapter's Creative Commons license, unless indicated otherwise in a credit line to the material. If material is not included in the chapter's Creative Commons license and your intended use is not permitted by statutory regulation or exceeds the permitted use, you will need to obtain permission directly from the copyright holder.



Chapter 21

Noninvasive Intravascular Microtransfusion in Colonial Tunicates

Lluìs Albert Matas Serrato, Alessandro Bilella, and Simon Blanchoud

Abstract

Tunicates are a diverse group of worldwide marine filter-feeders that are vertebrates' closest invertebrate relatives. Colonial tunicates are the only know chordates that have been shown to undergo whole-body regeneration (WBR). *Botrylloides* in particular can regenerate one fully functional adult from a minute fragment of their vascular system in as little as 10 days. This regenerative process relies on the proliferation of circulating stem cells, likely supported by the activity of some of the 11 identified types of hemocytes. To study and challenge WBR, it is thus important to have the capacity to isolate, analyze, and manipulate hemolymph in regenerating colonies. Here we present a microtransfusion technique that permits the collection of pure hemocytes, the quantification of their purity, their labeling, and reinjection into colonial tunicates. To exemplify our approach, we present in addition a protocol to analyze the isolated hemocytes using flow cytometry. Our approach is minimally invasive, does not induce lethality, and therefore allows repeated transfusion into exactly the same colony with minimal disruption to the process being studied.

Key words Hemolymph, Transfusion, Colonial ascidians, *Botrylloides*, Tunicates

1 Introduction

Tunicates are a group of worldwide highly diverse marine invertebrates separated into three classes that include over 3000 known extant species [1, 2]. Most tunicates are benthic sessile animals that reproduce sexually through a motile tadpole larval stage [3, 4]. In addition, a number of tunicate species are able to reproduce asexually through budding [5, 6]. Budding in tunicates typically leads to the formation of colonies where animals, called zooids, are interconnected by an external vascular system (Fig. 1a). Furthermore, some species of colonial tunicates are able to undergo whole-body regeneration (WBR) [7–9]. This is the only known occurrence of WBR among chordates [10].

In the *Botrylloides* genus, WBR is completed in as little as 10 days following the isolation of a fragment of their external vascular system [11]. WBR starts with the healing of the injury

Simon Blanchoud and Brigitte Galliot (eds.), *Whole-Body Regeneration: Methods and Protocols*,
Methods in Molecular Biology, vol. 2450, https://doi.org/10.1007/978-1-0716-2172-1_21, © The Author(s) 2022

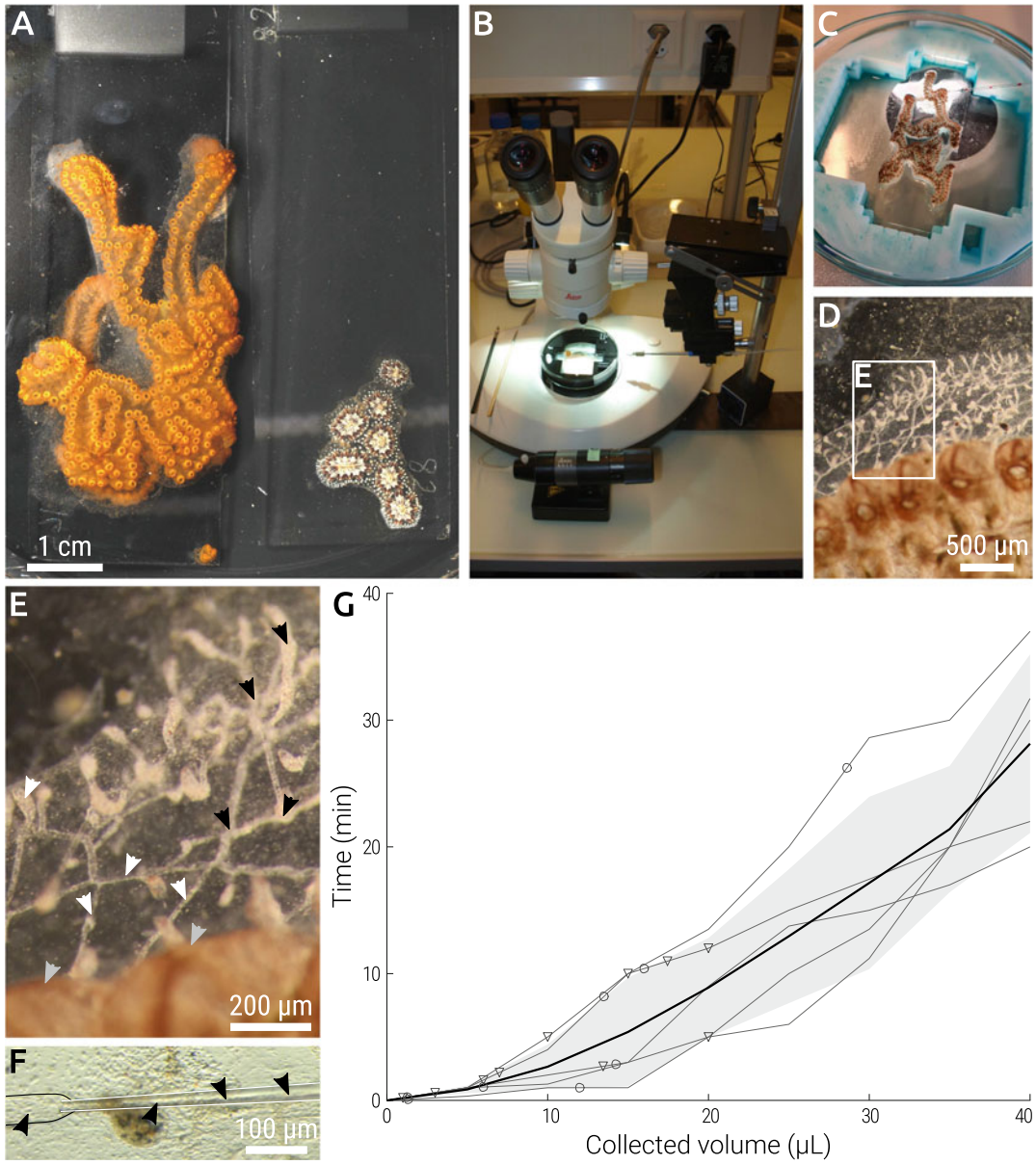


Fig. 1 Collecting hemocytes in the vascular system of *Botrylloides diegensis*. (**a**) A top-view of a colony of *Botrylloides diegensis* (left) and *Botryllus schlosseri* (right) growing on a microscopy glass slide. (**b**) Microinjection setup with a colony holder, a stereoscope, a microinjector, and the micromanipulator. (**c**) Close-up of the microtransfusion setup, with a colony placed on the colony holder and the marked micropipette close to the insertion point. (**d**) The external vasculature of the colony. (**e**) Magnification of the area delimited by the white rectangle in (**d**). Good candidate points for transfusion are indicated using black arrows, subendostylar points using gray arrows, and bad transfusion points using white arrows. (**f**) Microcollection of hemocytes. Micropipette is inserted inside the vessel lumen through the tunic and hemocytes (arrows) are flowing in. (**g**) Average collection rate over time ($n = 5$). Changes in collection point are indicated using circles, while changes in micropipette using triangles. Display are the individual collections (thin), the average collection (thick), and the corresponding standard deviation (gray)

sites followed by a major remodeling of the isolated vascular system [12]. Circulating stem cells are then mobilized to regeneration niches, i.e., a discrete regeneration locus within the vascular system. These niches compete through a yet undetermined process that consistently leads to the development of a single adult zooid, while all other niches are resorbed by the vascular system [12].

In addition to this role during regeneration [12], hemocytes are involved in numerous biological processes in colonial tunicates, including immune response [13–15], allorecognition [16–18], and asexual reproduction [19–21]. Colonial tunicates' hemolymph is typically composed of less than a dozen 4- to 25-μm-wide cell types classified into four functional classes: undifferentiated, phagocytic, cytotoxic, and storage cells [22–25]. For instance, in *Botrylloides leachii*, 11 different cell types ranging from 5 to 20 μm have been described [12], as well as the two additional mast-like and transport functional classes. Hemolymph extraction, manipulation, and alteration are thus essential tools for analyzing as well as challenging the functions of hemocytes. A large palette of approaches have been established for this purpose in colonial tunicates. Extracted hemolymph has been used for starting primary cultures of hemocytes [26], its cell composition studied through histological staining [12] as well as flow cytometry [27], and specific hemocyte populations sorted by fluorescently activated cell sorting [28]. Hemocytes have been labeled and injected in a recipient colony [29, 30], a variety of staining solutions delivered into the vasculature [31–33] and functional characterization undertaken by injection of small interfering RNA probes [33, 34] as well as chemical compounds [35, 36].

The most common approach for performing hemolymph collection is by mechanical injury of the vessel of an anti-clotting-treated colony. Hemolymph is then collected with a syringe or a glass micropipette as it bleeds out from the colony [12, 14, 22]. When larger amounts of hemolymph are required, mechanical dissociation of the entire colony is often used [21, 28–30, 37]. In both the approaches, the colony thus bears severe injuries and material exogenous to the hemolymph can contaminate the samples.

Here we describe a microtransfusion technique that allows to collect hemolymph intravascularly with high purity. We also present methods to characterize cytologically the hemolymph, label its hemocytes, and reinject them using the same setup used for the collection. This process can be routinely performed in the same colony with minimal damage, making it useful for long-term in vivo experiments aimed to study the role of the hemolymph in colonial tunicates.

2 Materials

All reagents are prepared with deionized water and stored at room temperature unless otherwise stated.

1. 10× K-depleted phosphate-buffered saline (K-PBS): 90 g NaCl, 10.6 g $NaH_2PO_4•H_2O$, 3.3 g Na_2HPO_4 in 1 L H_2O (*see* **Note 1**). Adjust pH to 7.8 with NaOH. Use within 2 months.
2. 3.3× K-PBS: 300 mL 10× K-PBS, 600 mL H_2O (*see* **Note 2**).
3. Marine Anti-Clotting solution (MAC): 0.38% (w/v) sodium citrate-NaOH, 10 mM L-cysteine, pH 7.5, in 3.3× K-PBS. Prepare fresh.
4. MAC-BSA-EDTA solution (MBE): 0.1% (w/v) bovine serum albumin (BSA), 10 mM ethylenediaminetetraacetic acid (EDTA) in MAC, 0.22-μm sterile filtered. Prepare fresh (*see* **Note 3**).
5. Purity assessment solution (PAS): 1% (v/v) Brilliant Blue FCF in MAC (*see* **Notes 4** and **5**).
6. Microtransfusion setup: Stereoscope, micromanipulator, microinjector capable of uptake (e.g., Cell-Tram Air, Eppendorf).
7. Collection support: Glass petri dish, high-profile 3D-printed colony holder (Fig. 1b, *see* **Note 6**).
8. Glass capillaries: Borosilicate glass capillaries compatible with the microinjector, 0.76 mm internal diameter (*see* **Note 7**).
9. Glass micropipettes: glass capillaries pulled using a microforge (e.g., Micropipette Puller P-87, Sutter Instrument), marked each 5 μL (i.e., each 11.02 mm for 0.76 mm ID capillaries).
10. Hematocytometer.
11. 2× brightfield cell viability dye (e.g., 0.4% (w/v) Trypan blue in 3.3× K-PBS).
12. Purity scale (*see* **Note 8**): 100% (100 μL MBE), 90% (90 μL MBE, 10 μL PAS), 70% (70 μL MBE, 30 μL PAS), 50% (50 μL MBE, 50 μL PAS), 30% (30 μL MBE, 70 μL PAS), 0% (100 μL PAS).
13. Microvolume spectrophotometer (e.g., NanoDrop, Thermo Fisher Scientific).
14. 200× live labeling dye (e.g., MemGlow 640, Cytoskeleton) (*see* **Note 9**).
15. 20× cell viability dye (e.g., 10 μg/mL Calcein Violet, eBioscience).

16. 500× DNA live labeling dye (e.g., 5 mM DRAQ5, Thermo Fisher Scientific).
17. 40-μm cell strainer (e.g., pluriStrainer, pluriSelect).
18. Calibration fluorescent beads (e.g., QbSure, Cytek).
19. 2× Fixation solution: 2% (w/v) $C_{12}H_{22}O_{11}$ (sucrose), 2% (v/v) $C_5H_8O_2$ (glutaraldehyde) in 3.3× K-PBS.

3 Methods

3.1 Intravascular Collection of Hemolymph

This protocol has been developed for *Botrylloides leachii* colonies, but has been successfully applied to *Botryllus schlosseri* as well. We thus expect it to work similarly well in all colonial ascidian species presenting an external vascular system accessible through a moderately soft tunic (*see* **Note 10**). This protocol typically yields in 30 min 40 μL (Fig. 1f) of 93% pure hemolymph (Fig. 2c) containing >99% viable hemocytes at a concentration around 300,000 cells/mL (*see* **Note 11**).

1. Select a colony to be used for hemolymph collection (*see* **Note 12**).
2. Transfer the colony on its transparent support into a container filled with 3.3× K-PBS.
3. Brush the colony with a fine paint brush under a stereoscope to remove debris and dirt.
4. Transfer the colony to another clean container filled with 3.3× K-PBS.
5. Trim a glass micropipette using a sharp razor blade to obtain a tip diameter of 17–30 μm (*see* **Note 13**).
6. Load 200 μL of MBE into a cut P200 pipette tip (*see* **Note 14**).
7. Insert the rear opening of the trimmed glass micropipette into the pipette tip.
8. Load the glass micropipette by slowly pipetting the MBE into it.
9. Remove the glass micropipette from the tip.
10. Mount the loaded glass micropipette into the holder of the microinjection device following the manufacturer's instructions.
11. Assemble the needle onto the micromanipulator.
12. Pipette 200 μL of MBE in the 1.5-mL tube to be used for collecting the hemocytes.
13. Vortex the tube for 5 s to coat its internal surface.
14. Wait 5 min for the coating to take effect.

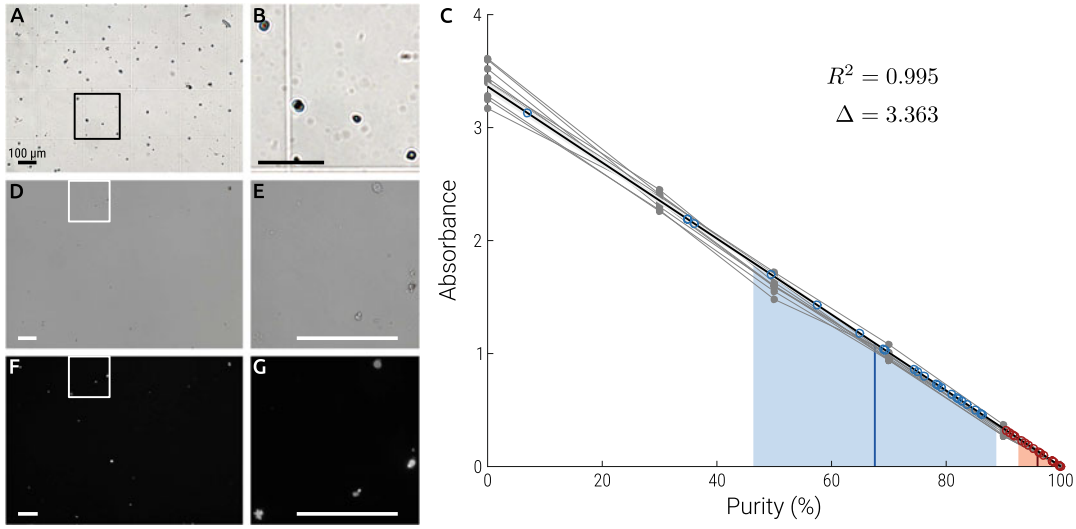


Fig. 2 Manipulating hemocytes. (**a**) Counting cells on a hemocytometer using Trypan blue to detect dead cells (none visible) with (**b**) a magnification of the area delimited in (**a**) where five cells are visible. (**c**) Measuring the purity of a collection using a linear regression of the absorbance of a purity scale. Absorbance of the reference samples are depicted using gray dots, purity scales as gray lines, the linear regression as a bold black line, and its 95% confidence interval by a light gray surface. Samples used to measure medium ($n = 23$) and high ($n = 18$) purity are depicted in blue and red, respectively. Their corresponding average values and standard deviation are shown as a bold line overlapping a light area. R^2 is the regression coefficient and Δ the slope of the regression. (**d**) Labeled hemocytes with (**e**) a magnification of the area delimited in (**d**) and (**f**) the corresponding fluorescence of the lipophyllic dye (MemGlow 640) with (**g**) the corresponding magnification. All scale bars are 100 µm

15. Remove the MBE from the tube.
16. Transfer the colony into a container filled with MAC.
17. Wait 5 min for the anticlotting to operate (*see* **Note 15**).
18. Submerge the colony into a container filled with PAS solution for 30 s.
19. Transfer the colony to an empty collection support.
20. Blot gently the colony using paper tissues.
21. Fill the collection support with 50 mL PAS to completely submerged the colony.
22. Retrieve the PAS solution into a container for later use (*see* **Note 16**).
23. Place the collection support in the microtransfusion setup (Fig. 1c).
24. Choose a collection point using the stereomicroscope (Fig. 1d, e, *see* **Note 17**).
25. Move the needle close to the target collection point using the micromanipulator (*see* **Note 18**).

26. Empty the needle from the MBE.
27. Insert the needle into the tunic towards the vessel lumen until the hemolymph enters the needle (Fig. 1f).
28. Apply negative pressure in the needle to compensate for reductions in the flow rate of hemocytes (*see* **Note 19**).
29. Gently rock forward/backward the needle inside the vessel to prevent hemocytes from attaching to the needle (*see* **Note 20**).
30. Alternate the release of the pressure with increases in negative pressure for collecting hemolymph (*see* **Note 21**).
31. Collect as much hemolymph as required (Fig. 1g, *see* **Note 22**).
32. Release the pressure valve in the microinjector.
33. Retract the needle form the vessel.
34. Empty the glass micropipette into the previously coated tube.
35. Unmount and discard the used glass micropipette.
36. Keep this hemolymph at RT until use (*see* **Note 23**).

3.2 Characterization of Hemolymph Collection

Depending on the downstream application, careful characterization of the sample needs to be undertaken. Here we measure the purity of the collection, the amount of collected cells, the viability of these hemocytes and calculate the in vivo cell concentration and hemolymph volume.

1. Incubate a P2 tip and a P200 tip in MBE for 5 min (*see* **Note 24**).
2. Pipette 200 µL of MBE in a 1.5-mL tube.
3. Vortex the tube for 5 s to coat its internal surface.
4. Wait for 5 min for the coating to take effect.
5. Remove the MBE from the tube.
6. Pipette 8 µL of MBE in the coated tube.
7. Pipette slowly the hemolymph ten times using the emptied coated P200 tip to mix it.
8. Transfer 2 µL of hemolymph to the coated tube using the emptied coated P2 tip.
9. Add 10 µL of 2× brightfield cell viability dye to the diluted cells.
10. Load 10 µL of cell mix in each side of the hematocytometer.
11. Wait for 5 min for all cells to settle at the bottom of the chamber.
12. Measure the concentration of viable and dead cells in both the wells according to the manufacturer's instructions (Fig. 2a, b).
13. Multiply the obtained average cell concentration by 10 to calculate the concentration of the collected sample (*see* **Note 11**).

14. Spin the collected hemolymph 12 min at 800 rcf.
15. Transfer the supernatant to a new 1.5-mL tube.
16. Measure the total amount of supernatant.
17. Multiply the determined cell concentration by the volume of supernatant to determine the total number of collected cells.
18. Add 20 μL of MBE to the pelleted cells.
19. Resuspend the collected hemocytes by pipetting ten times the bottom of the tube using the coated P200 tip (*see* **Note 25**).
20. Initialize the microvolume spectrophotometer according to the manufacturer's instructions using MBE as blank.
21. Calibrate the microvolume spectrophotometer to measure absorption at 630 nm.
22. Measure absorbance of 2 μL of the hemolymph supernatant.
23. Measure absorbance of 2 μL of each dilution of the purity scale (*see* **Note 26**).
24. Repeat **steps 21** and **22** two more times.
25. Perform a linear regression on the measurements of the absorption of the purity scale.
26. Use the regression to infer the purity of the collected hemolymph (Fig. 2c, *see* **Note 13**).
27. Divide the previously determined cell concentration by the inferred purity to obtain the in vivo cell concentration (*see* **Note 24**).
28. Multiply the volume of collected supernatant with the inferred purity to obtain the in vivo volume of hemolymph.
29. Keep the hemocytes at RT until use (*see* **Note 22**), freeze the serum and store at −80 °C (*see* **Note 27**).

3.3 Flow Cytometry Analysis of Hemolymph

As described in the introduction, hemolymph has been used for a variety of applications in a number of publications. Here we present our protocol to label hemocytes, analyze them using flow cytometry, and fix them for morphological purposes.

1. Transfer the desired amount of cells into a coated 1.5-mL tube (*see* **Note 28**).
2. Spin the hemocytes for 12 min at 800 rcf.
3. Remove the supernatant.
4. Resuspend the pellet by gently pipetting using a coated P200 tip in 20 μL of MBE.
5. Add 0.1 μL of the live cell labeling dye to the cells.
6. Mix by pipetting ten times using a coated P200 tip.
7. Wrap the tube in aluminum foil.

8. Leave 30 min to incubate at RT.
9. Spin the hemocytes for 12 min at 800 rcf.
10. Remove the supernatant.
11. Resuspend the cells in 47.4 μL of MBE (Fig. 2d–g).
12. Add 2.5 μL of the cell viability dye.
13. Add 0.1 μL of the DNA live labeling dye.
14. Mix by pipetting ten times using a coated P200 tip.
15. Keep the tube in aluminum foil at RT.
16. Transfer 20 μL of unstained cells into a coated 1.5-mL tube as negative control.
17. Pipette the cells through a cell strainer to remove cell aggregates.
18. Dilute the calibration beads in the unstained cells according to the manufacturer's instructions.
19. Initialize the flow cytometer according to the manufacturer's instructions.
20. Calibrate the voltage and the gain of each detector using the negative control (*see* **Note 29**).
21. Run 10 μL of stained cells to calibrate the gain in the fluorescent channels where signal is expressed.
22. Gate relevant events as single cells, DNA-positive, and live cells (*see* **Note 30**).
23. Record 10,000 events of labeled hemocytes (*see* **Note 31**).
24. Gate subpopulations of hemocytes in the forward vs. side scatter to quantify their relative proportions (*see* **Note 32**).
25. Add an equal volume of the fixative solution to the leftover cells for morphological fixation.
26. Mix by pipetting ten times using a coated P200 tip.
27. Incubate the cells for 30 min at 4 °C.
28. Spin the hemocytes 12 min at 800 rcf.
29. Replace the supernatant with 3.3× K-PBS.
30. Resuspend the cells by pipetting ten times using a P200 pipette.
31. Store fixed cells at 4 °C, use within 6 months.

3.4 Injection of Compounds and Cells

Given that the vasculature is a closed system, there is a limitation in the volume and rate of injection that can be achieved, which depends on the size of the colony. This protocol typically yields to the injection of 40 μL of solution in 15 min in colonies composed of more than five adults (Fig. 3c, *see* **Notes 33** and **34**).

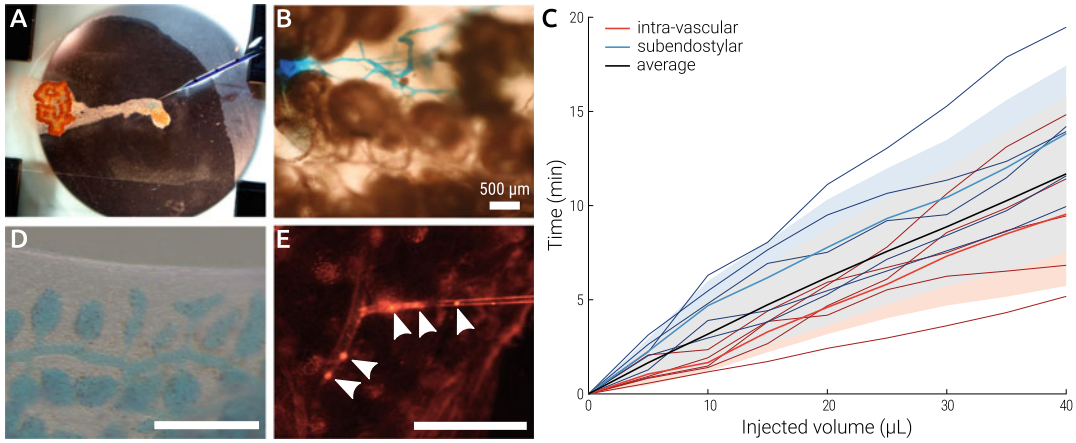


Fig. 3 Microinjections in *Botrylloides diegensis*. (**a**) Vascular system with a micropipette inserted in the vessel lumen loaded with PAS. (**b**) Properly inserted micropipette starting to inject a dyed solution. (**c**) Average injection rate over time, separated between intravascular (red, $n = 5$) and subendostylar (blue, $n = 5$), overlaid with the global average (black). Display are the individual collections (thin), the average collection (thick), and the corresponding standard deviation (light area). (**d**) Systemic distribution of the injected medium 5 min after the end of the microinjection. (**e**) Injection of labeled hemocytes (arrows) in the recipient colony. All scale bars are 500 µm

1. Follow **steps 1–4**, Subheading 3.1, to prepare a colony for injection.
2. Trim a glass micropipette using a sharp razor blade to obtain a tip diameter of 17–30 µm (*see* **Note 13**).
3. Load 200 µL of PAS into a cut P200 pipette tip (*see* **Notes 35** and **36**).
4. Follow **steps 7–11**, Subheading 3.1, to prepare the injection equipment.
5. Transfer the colony to an empty collection support.
6. Place the collection support in the microtransfusion setup.
7. Choose a collection point using the stereomicroscope (*see* **Note 37**).
8. Move the needle close to the target collection point using the micromanipulator (*see* **Note 18**).
9. Insert the needle into the tunic toward the vessel lumen until the hemolymph enters the needle (Fig. 3a, *see* **Note 38**).
10. Slowly increase the pressure to carefully inject a small amount of the solution (<1 µL).
11. Observe the dye spreading through the surrounding vasculature (Fig. 3b, *see* **Note 39**).
12. Continue increasing the pressure to inject the required amount of solution (Fig. 3c, *see* **Note 33**).

13. Follow **steps 32–35**, Subheading 3.1, to remove the micropipette from the colony.
14. Leave the colony resting for at least 5 min to allow systemic distribution of the stain through all the vasculature (Fig. 3d, *see* **Note 40**).
15. Load 20 μL of labeled cells into a trimmed glass micropipette.
16. Repeat **steps 4–14** to reinject labeled hemocytes (Fig. 3e).

4 Notes

1. Alternatively, natural sea water or artificial seawater could replace K-PBS after 0.22-μm sterile filtration. However, we have observed reduced hemocyte clotting in potassium- and magnesium-depleted media.
2. Adapt the salt concentration and the pH of the K-PBS to the culturing conditions used for your colonial ascidians. In our lab, *Botrylloides diegenesis* is cultured at 32 ppt salinity and pH 8.2.
3. Although we have used MBE up to 2 days old with success, we have observed that crystals and debris start forming after 6–10 h. We thus advice to prepare this medium fresh every time.
4. Brilliant Blue FCF is usually marketed as E133 food dye [38], a non-toxic, inexpensive and hydrophilic dye that contrasts well with the typical orange color of our colonies. Other dyes, and food dyes in particular, can be used instead. Fluorescent dyes could also be used, but phototoxicity during imaging should be carefully monitored.
5. Concentration has been empirically determined as the highest amount of dye that permits the visualization of the vessels on our microscope (Leica MS5), other setups might require different concentrations. Different batches of dye may have different initial concentrations.
6. The 3D-printed profile accommodates a standard 75 × 25 mm glass slide onto four supports located in each corner of the slide within a disk that fits tightly in a petri dish. These supports allow the convenient handling of colonies, including those with systems growing on the sides and back of the glass slide. Colonies can be maintained submerged and in a fixed position for long durations. Standard triangle language (STL) file of the 3D model is available upon request.
7. We have used capillaries with and without filament with similar results. Capillaries without filament have been preferred as they are cheaper.

8. The purity of hemolymph is inversely proportional to the percentage of PAS present in the collected samples. We use MBE as substitute to the hemolymph for our calibration scale.
9. We have tried Vybrant DiO (Molecular Probes) as alternative live labeling dye. We obtained good labeling and fluorescence, but it induced cell aggregation.
10. Important factors for accessibility are the possibility to visualize and identify vessels adequate for puncture, sufficient room around the puncture point to manipulate the needle and an internally soft tunic. In the case of *B. schlosseri*, the outer tunic is pretty tough, but a small incision using a micro knife gives access to the soft inner tunic.
11. On average, we have observed a concentration of 278,000 ± 31,000 ($n = 16$) viable cells. An almost three times higher cell concentration has been observed in colonies undergoing takeover. No dead cells should be present in a control sample.
12. Bigger colonies can yield higher amounts of hemolymph and allow larger injection volumes. However, the accessibility of good collection points is the main factor for good collections and injections.
13. Using our capillaries (TW100-6, World Precision Instruments), the diameter of the glass micropipette for the collection of the hemolymph can vary between 17 and 30 μm. Be aware that by using a small diameter (17–20 μm), the collected hemolymph is pure (96%) but the volume will be low (2–5 μL) before the tip clots. A glass micropipette with a larger diameter (20–30 μm) allows to collect a larger volume of hemolymph with a lower grade of purity (67%). Larger is the diameter, higher is the possibility that the PAS surrounding the colony goes inside the micropipette but greater is the amount of hemolymph collected.
14. The trimmed tip should fit snugly onto the rear of the capillary. Excess trimming of the P200 will leak MBE, preventing the loading of the capillary. New tip will have to be trimmed. Insufficient trimming will prevent the capillary to enter the tip; additional careful trimming should be done.
15. Anticlotting efficiency might vary in different species of colonial ascidians. We have observed an improved efficiency in *B. schlosseri* compared to *B. diegenesis*. Longer incubation times can be used to improve the anticlotting effect. We have soaked animals in MAC for up to 30 min without any noticeable deleterious effect.
16. Although PAS should be prepared fresh, multiple collections taking place on the same day can use the same medium.

17. Favor the following conditions for collection and injection: vessels with a big diameter (longer suction times, less clotting), Y-shaped vessel junctions, vessels embedded in a thick tunic (increases purity by reducing leakage into the glass micropipette).
18. Favor the lowest angle possible between the needle and the colony. The objective is that the needle goes through as much tunic as possible before puncturing the vessel to provide natural isolation with the PAS.
19. It is easier to properly monitor the flow of hemocytes inside the microneedle than at its tip.
20. Movement should be restricted within the vessel to preserve the purity of the sample. Excessive movements might puncture the other side of the vessel or create a gap between the entry site and the needle, thus allowing PAS to enter the vessel.
21. Excessive negative pressure will lead to the collapse of the vessel, preventing collection altogether. Vessel will ultimately recover but this is particularly inefficient. Low negative pressure will collect hemocytes at a reduced speed that will allow them to clot in the tightest portion of the needle.
22. Select a new collection point when the hemolymph inside the vessels is not circulating any more. This very likely indicates that a clot has formed in a near vascular junction to deviate the circulation to other vessels. If the tip is clogged, try increasing the negative pressure drastically to force it through the pipette. If that does not work, it is necessary to change the pipette.
23. Viability tests of hemocytes using Trypan Blue have shown that when kept in MBE, half of the total amount of cells die every 24 h. Storage of hemolymph at 4 °C did not show any significant differences compared to the storage at RT.
24. All handling of hemocytes should be done with coated tips. Reusing coated tips as much as possible is our preferred approach. Alternatively, coating multiple tips is possible. To coat multiple tips in parallel, we soak them loaded with MBE in a 50-mL glass beaker filled with MBE.
25. Avoid vortexing hemocytes as we have observed increased cell death after such treatment.
26. In our setup (NanoDrop One, Thermo Fisher Scientific), absorptions of the reference samples of our purity scale are remarkably constant between different measures made on different days (Fig. 2c). For new samples, we thus measure only a fresh 90% and 30% reference samples to confirm that the previously measured purity scale can be used for these values.
27. We have been successfully using the Simultaneous Metabolite, Protein, Lipid Extraction (SIMPLEX) approach [39] to

process freeze-dried samples for metabolomic and proteomic analysis.

28. Samples from different histocompatible colonies can be pooled to reach the desired amount of cells, if it exceeds the total amount of cells collected in one microtransfusion. Working with subclones of the same colony is even simpler. Note that the blastogenic cycle of isolated subclones can slowly diverge. Make sure that the pooled samples are in the same blastogenic stage if that is relevant for the experiment.
29. Hemocytes in *Botrylloides* have a size ranging between 5 and 35 μm in diameter [12]. Use the calibration beads to determine the minimum limit for the Forward Scatter (FSC). Use the signal of the unstained cells to set the voltage for all detectors. Note that colonial tunicate's hemocytes do have a significant amount of autofluorescence.
30. Although we favor the combination of dyes DRAQ5/Calcein Violet for their quantitativity, DAPI/propidium iodide is a very popular and functional alternative.
31. A total of 10,000 events is typically considered as the minimal number of events required to produce a flow cytometry plot. For higher resolution and better analysis, this number should be increased up to 50,000 events. For a quantitative analysis of expression and labeling, multiple controls need to be acquired together with the sample of interest. In particular, a negative control and single-label samples [40].
32. In *Botryllus schlosseri*, seven subpopulations of hemocytes have been gated successfully using the forward vs. side scatter [28]. Specific labeling further subdivided hemocytes into 11 populations.
33. The injections can be done either intravascularly or directly into a zooid's subendostylar sinus. To avoid leakages, rates of injection should not exceed 2 μL/min intravascularly and 5 μL/min into the sinus.
34. The maximal value that we have been able to inject in one isolated zooid without leakage is 15 μL. Consequently, even very small system of more than three zooids allow the injection of the 40 μL contained in the glass micropipette.
35. Injecting PAS is being used here as an example and has no additional application than transiently highlighting the vasculature. However, we suggest using it as a general marker for injections as injecting transparent solutions is more difficult to monitor and control.
36. Loading solutions can be done by several means. Loading using a cut P200 tip is the fastest and cheapest but requires large volumes of solution. Loading using microcapillary pipette

tips is pretty fast too, but these tips are relatively expensive. Alternatively, mounting the empty micropipette on the microinjection setup and loading it through its tip by applying negative pressure are slow but inexpensive.

37. Good injection points are similar to good collection points (*see* **Note 14**), with the addition of the possibility to inject even faster through the subendostylar sinus (*see* **Note 29**).
38. Make sure there is no hemolymph leaking around the puncture site, otherwise the injected material will mostly leak outside of the vascular system.
39. Failure for the solution to diffuse properly is a sign that the needle is not well inserted in the vessel lumen. Most typically, using a new injection point will be necessary to allow a leak-less injection.
40. PAS will diffuse through the vessel epithelium and the tunic and will be completely eliminated from the colony in less than 30 min.

Acknowledgments

Funding support was provided by the Swiss National Science Foundation (SNSF) grant number PZ00P3_173981 as well as by the European COST Action MARSITEM CA16203 short-term scientific mission grants (STSM) 40760 and 43747. We would like to thank Francesca Cima and Loriano Ballarin for the numerous discussions and advice; Sefano Tiozzo for hosting LAMS during his STSMs and for the help setting up microtransfusions; Aude Blanchoud for proofreading the manuscript.

References

1. WoRMS Editorial Board (2017) World Register of marine species. http://www.marinespecies.org at VLIZ. http://www.marinespecies.org/imis.php?dasid=1447&doiid=170. Accessed 29 Sept 2020. https://doi.org/10.14284/170
2. Shenkar N, Swalla BJ (2011) Global Diversity of Ascidiacea. PLoS One 6:e20657. https://doi.org/10.1371/journal.pone.0020657
3. Millar RH (1971) The biology of Ascidians. In: Advances in marine biology. Elsevier, Amsterdam, pp 1–100. https://doi.org/10.1016/S0065-2881(08)60341-7
4. Goodbody I (1975) The physiology of Ascidians. In: Advances in marine biology. Elsevier, Amsterdam, pp 1–149. https://doi.org/10.1016/S0065-2881(08)60457-5
5. Brown FD, Swalla BJ (2012) Evolution and development of budding by stem cells: Ascidian coloniality as a case study. Dev Biol 369:151–162. https://doi.org/10.1016/j.ydbio.2012.05.038
6. Alié A, Hiebert LS, Scelzo M et al (2020) The eventful history of nonembryonic development in tunicates. J Exp Zool B Mol Dev Evol 336:250. https://doi.org/10.1002/jez.b.22940
7. Rinkevich B, Shlemberg Z, Fishelson L (1995) Whole-body protochordate regeneration from totipotent blood cells. Proc Natl Acad Sci 92:7695–7699. https://doi.org/10.1073/pnas.92.17.7695
8. Voskoboynik A, Simon-Blecher N, Soen Y et al (2007) Striving for normality: whole body regeneration through a series of abnormal

generations. FASEB J 21:1335–1344. https://doi.org/10.1096/fj.06-7337com

9. Brown FD, Keeling EL, Le AD et al (2009) Whole body regeneration in a colonial ascidian, *Botrylloides violaceus*. J Exp Zool B Mol Dev Evol 312B:885–900. https://doi.org/10.1002/jez.b.21303
10. Bely AE, Nyberg KG (2010) Evolution of animal regeneration: re-emergence of a field. Trends Ecol Evol 25:161–170. https://doi.org/10.1016/j.tree.2009.08.005
11. Blanchoud S, Rinkevich B, Wilson MJ (2018) Whole-body regeneration in the colonial tunicate *Botrylloides leachii*. Results Probl Cell Differ 65:337–355. https://doi.org/10.1007/978-3-319-92486-1_16
12. Blanchoud S, Zondag L, Lamare MD et al (2017) Hematological analysis of the Ascidian *Botrylloides leachii* (Savigny, 1816) during whole-body regeneration. Biol Bull 232:143–157. https://doi.org/10.1086/692841
13. Cha IS, del Castillo CS, Nho SW et al (2011) Innate immune response in the hemolymph of an ascidian, *Halocynthia roretzi*, showing soft tunic syndrome, using label-free quantitative proteomics. Dev Comp Immunol 35:809–816. https://doi.org/10.1016/j.dci.2011.01.011
14. Ballarin L, Cima F, Sabbadin A (1993) Histoenzymatic staining and characterization of the colonial ascidian *Botryllus schlosseri* hemocytes. Bolletino Zool 60:19–24. https://doi.org/10.1080/11250009309355786
15. Rosental B, Raveh T, Voskoboynik A et al (2020) Evolutionary perspective on the hematopoietic system through a colonial chordate: allogeneic immunity and hematopoiesis. Curr Opin Immunol 62:91–98. https://doi.org/10.1016/j.coi.2019.12.006
16. Shirae M, Hirose E, Saito Y (1999) Behavior of hemocytes in the allorejection reaction in two compound Ascidians, *Botryllus scalaris* and *Symplegma reptans*. Biol Bull 197:188–197. https://doi.org/10.2307/1542614
17. Cima F, Sabbadin A, Ballarin L (2004) Cellular aspects of allorecognition in the compound ascidian *Botryllus schlosseri*. Dev Comp Immunol 28:881–889. https://doi.org/10.1016/j.dci.2004.02.001
18. Nydam ML (2020) Evolution of allorecognition in the tunicata. Biology 9:129. https://doi.org/10.3390/biology9060129
19. Ballarin L, Menin A, Tallandini L et al (2008) Haemocytes and blastogenetic cycle in the colonial ascidian *Botryllus schlosseri*: a matter of life and death. Cell Tissue Res 331:555–564. https://doi.org/10.1007/s00441-007-0513-4
20. Franchi N, Ballin F, Manni L et al (2016) Recurrent phagocytosis-induced apoptosis in the cyclical generation change of the compound ascidian *Botryllus schlosseri*. Dev Comp Immunol 62:8–16. https://doi.org/10.1016/j.dci.2016.04.011
21. Kassmer SH, Rodriguez D, Langenbacher AD et al (2015) Migration of germline progenitor cells is directed by sphingosine-1-phosphate signalling in a basal chordate. Nat Commun 6:8565. https://doi.org/10.1038/ncomms9565
22. Cima F, Perin A, Burighel P et al (2001) Morpho-functional characterization of haemocytes of the compound ascidian *Botrylloides leachi* (Tunicata, Ascidiacea). Acta Zool 82:261–274. https://doi.org/10.1046/j.1463-6395.2001.00087.x
23. Cima F, Peronato A, Ballarin L (2017) The haemocytes of the colonial aplousobranch ascidian *Diplosoma listerianum*: structural, cytochemical and functional analyses. Micron 102:51–64. https://doi.org/10.1016/j.micron.2017.08.007
24. Ballarin L, Cima F (2005) Cytochemical properties of *Botryllus schlosseri* haemocytes: indications for morpho-functional characterisation. Eur J Histochem 49:255–264. https://doi.org/10.4081/952
25. Ballarin L, Kawamura K (2009) The hemocytes of *Polyandrocarpa mysakiensis*: morphology and immune-related activities. Invertebr Surviv J 6:154–161
26. Rinkevich B, Rabinowitz C (1993) In vitro culture of blood cells from the colonial protochordate *Botryllus schlosseri*. Vitro Cell Dev Biol Anim 29:79–85. https://doi.org/10.1007/BF02634375
27. Donaghy L, Hong H-K, Park K-I et al (2017) Flow cytometric characterization of hemocytes of the solitary ascidian, *Halocynthia roretzi*. Fish Shellfish Immunol 66:289–299. https://doi.org/10.1016/j.fsi.2017.05.009
28. Rosental B, Kowarsky M, Seita J et al (2018) Complex mammalian-like haematopoietic system found in a colonial chordate. Nature 564:425–429. https://doi.org/10.1038/s41586-018-0783-x
29. Laird DJ, De Tomaso AW, Weissman IL (2005) Stem cells are units of natural selection in a colonial ascidian. Cell 123:1351–1360. https://doi.org/10.1016/j.cell.2005.10.026
30. Kassmer SH, Langenbacher AD, De Tomaso AW (2020) Integrin-alpha-6+ Candidate stem cells are responsible for whole body

regeneration in the invertebrate chordate *Botrylloides diegensis*. Nat Commun 11:4435. https://doi.org/10.1038/s41467-020-18288-w

31. Rodriguez D, Braden BP, Boyer SW et al (2017) In vivo manipulation of the extracellular matrix induces vascular regression in a basal chordate. Mol Biol Cell 28:1883–1893. https://doi.org/10.1091/mbc.e17-01-0009
32. Rodriguez D, Nourizadeh S, De Tomaso AW (2019) The biology of the extracorporeal vasculature of *Botryllus schlosseri*. Dev Biol 448: 309–319. https://doi.org/10.1016/j.ydbio.2018.10.013
33. Tiozzo S, Voskoboynik A, Brown FD et al (2008) A conserved role of the VEGF pathway in angiogenesis of an ectodermally-derived vasculature. Dev Biol 315:243–255. https://doi.org/10.1016/j.ydbio.2007.12.035
34. Rosner A, Paz G, Rinkevich B (2006) Divergent roles of the DEAD-box protein BS-PL10, the urochordate homologue of human DDX3 and DDX3Y proteins, in colony astogeny and ontogeny. Dev Dyn 235:1508–1521. https://doi.org/10.1002/dvdy.20728
35. Braden BP, Taketa DA, Pierce JD et al (2014) Vascular regeneration in a basal chordate is due to the presence of immobile, bi-functional cells. PLoS One 9:e95460. https://doi.org/10.1371/journal.pone.0095460
36. Gasparini F, Caicci F, Rigon F et al (2015) Testing an unusual in vivo vessel network model: a method to study angiogenesis in the colonial tunicate *Botryllus schlosseri*. Sci Rep 4: 6460. https://doi.org/10.1038/srep06460
37. Corey DM, Rosental B, Kowarsky M et al (2016) Developmental cell death programs license cytotoxic cells to eliminate histocompatible partners. Proc Natl Acad Sci 113: 6520–6525. https://doi.org/10.1073/pnas.1606276113
38. Avazpour M, Shiri S, Delpisheh A et al (2014) Simultaneous determination of Brilliant Blue FCF and carmoisine in food samples by aqueous two-phase system and spectrophometric detection. Ilam Univ Med Sci 1:56–65
39. Coman C, Solari FA, Hentschel A et al (2016) Simultaneous metabolite, protein, lipid extraction (SIMPLEX): a combinatorial multimolecular omics approach for systems biology. Mol Cell Proteomics 15:1453–1466. https://doi.org/10.1074/mcp.M115.053702
40. Roederer M (2001) Spectral compensation for flow cytometry: visualization artifacts, limitations, and caveats. Cytometry 45:194–205. https://doi.org/10.1002/1097-0320(20011101)45:3<194::AID-CYTO1163>3.0.CO;2-C

Open Access This chapter is licensed under the terms of the Creative Commons Attribution 4.0 International License (http://creativecommons.org/licenses/by/4.0/), which permits use, sharing, adaptation, distribution and reproduction in any medium or format, as long as you give appropriate credit to the original author(s) and the source, provide a link to the Creative Commons license and indicate if changes were made.

The images or other third party material in this chapter are included in the chapter's Creative Commons license, unless indicated otherwise in a credit line to the material. If material is not included in the chapter's Creative Commons license and your intended use is not permitted by statutory regulation or exceeds the permitted use, you will need to obtain permission directly from the copyright holder.



Part IV

Genetic Approaches



Chapter 22

Gene Manipulation in *Hydractinia*

Eleni Chrysostomou, Febrimarsa, Timothy DuBuc, and Uri Frank

Abstract

The ability to regenerate lost body parts is irregularly distributed among animals, with substantial differences in regenerative potential between and within metazoan phyla. It is widely believed that regenerative animal clades inherited some aspects of their capacity to regenerate from their common ancestors but have also evolved new mechanisms that are not shared with other regenerative animals. Therefore, to gain a broad understanding of animal regenerative mechanisms and evolution, a broad sampling approach is necessary. Unfortunately, only few regenerative animals have been established as laboratory models with protocols for functional gene studies. Here, we describe the methods to establish transgenic individuals of the marine cnidarian *Hydractinia*. We also provide methods for transient gene expression manipulation without modifying the genome of the animals.

Key words Hydractinia, Transgenesis, CRISPR-Cas9

1 Introduction

The phylum Cnidaria comprises some 11,000 species of rather diverse animals [1] that share a unique cell type—the cnidocyte, also known as nematocyte or stinging cell. These cells, which belong to the neural lineage, are used for prey capture, defense, and adhesion [2, 3]. Phylogenetically, members of the Cnidaria are divided between two main clades, Anthozoa (e.g., corals, sea anemones, and sea pens) and Medusozoa (e.g., hydrozoans, scyphozoans, and cubozoans), plus a group of parasitic cnidarians, the Myxozoa, that are a sister taxon to Medusozoa [4]. Anthozoans are being characterized by the lack of a medusa stage, which has been lost and gained multiple times in the Medusozoa clade. As a result, many modern medusozoans lack the medusa stage in their life cycle.

Cnidarians possess a remarkable regenerative ability, being able to regrow whole bodies from small tissue fragments, and in some cases also from reaggregated cell suspensions [5–7]. However, the mechanisms used for regeneration are different not only between

Simon Blanchoud and Brigitte Galliot (eds.), *Whole-Body Regeneration: Methods and Protocols*,
Methods in Molecular Biology, vol. 2450, https://doi.org/10.1007/978-1-0716-2172-1_22, © The Author(s) 2022

species but also within different body parts of single species [8, 9]. Hence, to gain full understanding of the mechanisms driving regeneration in such a diverse group, it is necessary to study regeneration in as many species and contexts as possible. The main challenge in doing so at the molecular level is the enormous effort required to develop transgenic technologies for each studied species. Contrary to common sense, it appears that substantially different protocols are required to obtain transgenic animals even within one phylum [10–13]. Here, we present the current protocols used to manipulate gene expression in the colonial hydrozoan *Hydractinia*.

The genus *Hydractinia* is represented in the literature primarily by two North Atlantic sibling species, *H. echinata and H. symbiolongicarpus*. Despite the similarity between the two, they do not readily hybridize [14] and differ in genome size (774 and 514 Mb, respectively) as well as in some aspects of post-metamorphosis growth form. Both the species can be grown in artificial seawater tanks, but selected laboratory strains are only available in *H. symbiolongicarpus* [15, 16].

Hydractinia is one of only four cnidarian genera for which transgenesis technologies have been well established (Fig. 1) [10, 11, 17, 18]; the other three being *Hydra, Nematostella,* and *Clytia*. First steps to generate transgenic *Aiptasia* have been reported recently [19]. Transient gene knockdown protocols using short hairpin RNA, RNAi, and morpholino oligonucleotides have been established in *Hydractinia* as well [20–22]. Transient ectopic/overexpression experiments can be achieved with mRNA injection into embryos [15].

Hydractinia has been primarily used to study stem/germ cells [15, 20], regeneration [19], neurogenesis [23], and allorecognition [24]. However, recent developments by the *Hydractinia* research community call for expansion of the usage of this tractable animal model to other disciplines as well.

2 Materials

2.1 Animal Maintenance, Spawning, and Metamorphosis

1. Artificial or filtered natural seawater (FSW): 28–32 ppm, 0.22 μm-filtered, pH 8.15–8.35.
2. CsCl stock solution: 580 mM CsCl in deionized H_2O (diH_2O).
3. Embryonic water: 20% (v/v) CsCl stock solution in FSW.
4. Self-made oyster puree.
5. Brine shrimp artemia cyst.
6. Brine shrimp hatcher.
7. Culture seawater tank system (Fig. 2).

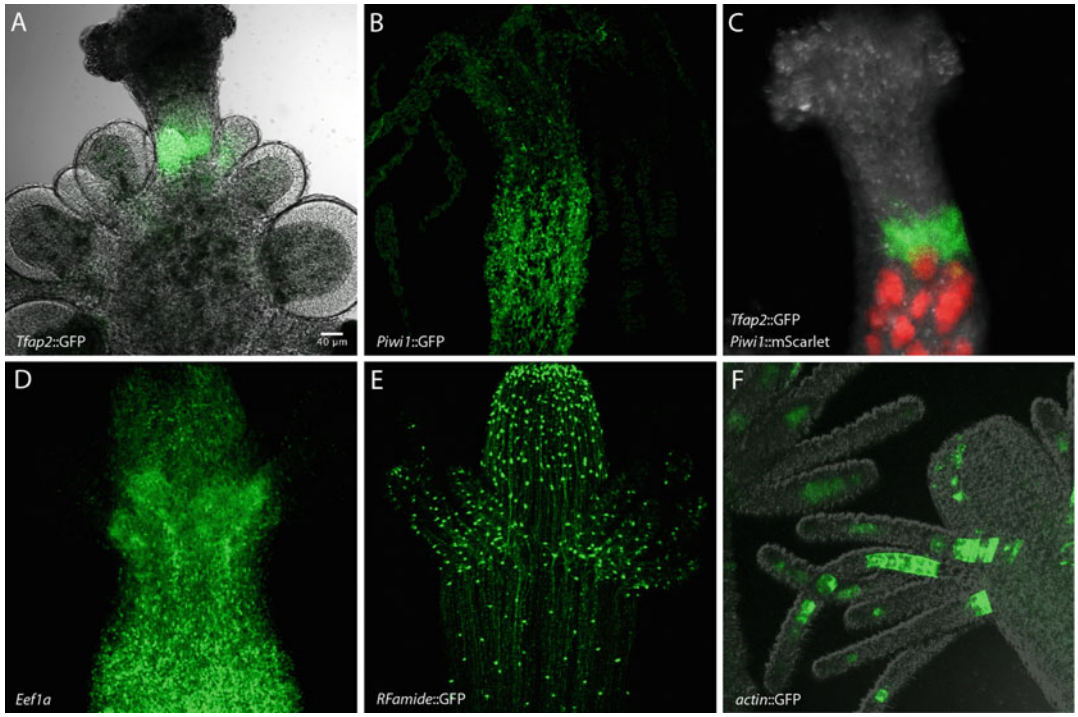


Fig. 1 A selection of transgenic reporter animals. (**a**) *Tfap2*::GFP. This male sexual polyp expresses GFP in early germ cells. (**b**) *Piwi1*::GFP. This animal expresses GFP in i-cells and germ cells. The image shows a feeding polyp with no germ cells. (**c**) A double transgenic female obtained by crossing a *Tfap2*::GFP animal with a *Piwi1*::mScarlet partner. (**d**) A CRISPR-Cas9 knockin animal in which GFP has been inserted in-frame in to the *Ef1a* endogenous coding sequence. (**e**) A *Rfamide*::GFP reporter animal. A subset of neurons express GFP. (**f**) A G0, *Actin1*:: GFP mosaic reporter animal. This transgene is epithelial specific. All images were taken from live animals

2.2 Embryo Microinjection

1. Injection plate: 35-mm petri dish with 180–200 µm plankton net attached.
2. Injection capillaries with filament: made by flaming micropipette puller.
3. Fluorescence tracer dye (e.g., Dextran AF555 200 ng/µL [ex/em: 555/565 nm], Lucifer Yellow CH 200 ng/µL [ex/em: 428/536 nm]).
4. Injection stock buffer: 2 M KCl in diH_2O.
5. Three axis coarse/fine joystick micro-manipulator.
6. Fluorescence stereo microscope.
7. Microinjector.
8. Vannas scissors, curved, 80 mm (e.g., Ted Pella; 1341).
9. Flaming micropipette puller (e.g., Sutter Instrument Co; P-97).

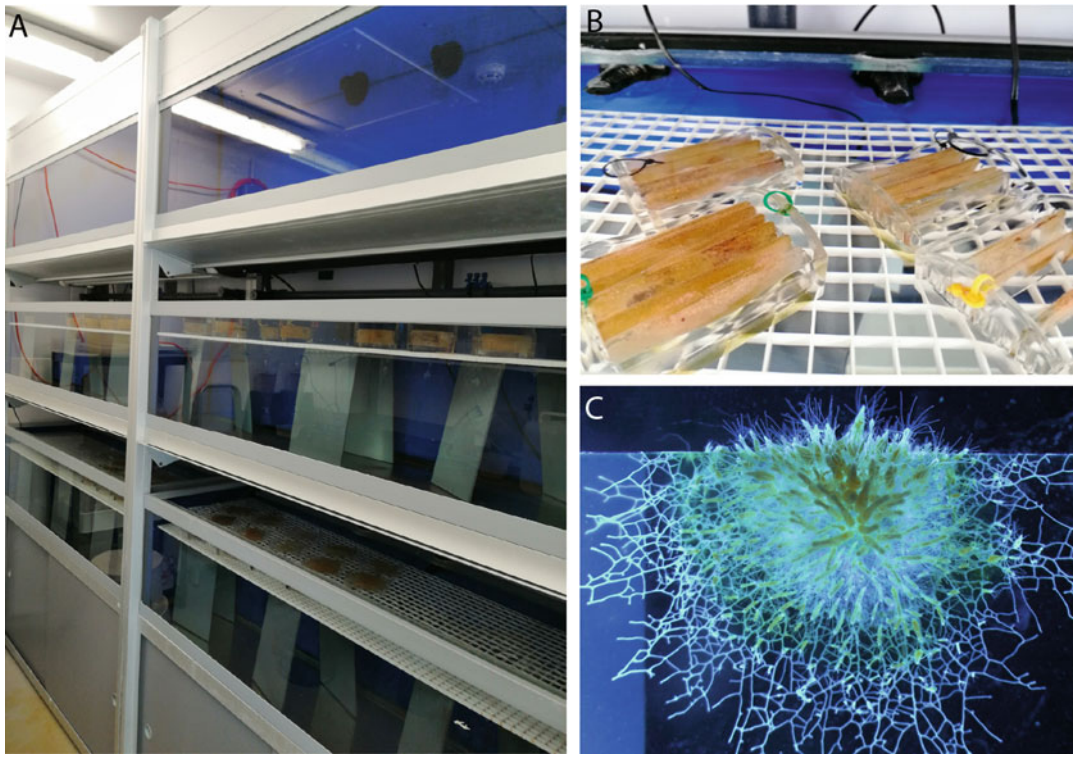


Fig. 2 *Hydractinia* culture. (**a**) Overview of a commercial tank system used in our laboratory. (**b**) A close-up on the slides-in-a-staining-rack system. (**c**) A close up on a colony growing on a microscope slide

2.3 shRNA

Prepare all solutions using ultrapure nuclease-free water (prepared by purifying deionized water, to attain a resistivity of 18 MΩ/cm at 25 °C) and analytical grade reagents. Diligently follow all waste disposal regulations when disposing waste materials.

1. T7-based in vitro transcription kit (e.g., NEB Arca/NTP T7 mRNA synthesis with poly A tailing).
2. Silica membrane column with 2-mL collection tube.
3. Wash-r1: 1 M Gu-HCl, 10 mM Tris–HCl, pH 7.0.
4. Wash-r2: 10 mM Tris–HCl, pH 7.5, 60 mM potassium acetate in 80% ethanol.
5. 3 U/μL DNaseI.
6. DNA digestion buffer: 40 mM Tris–HCl, pH 8.0, 10 mM NaCl, 6 mM $MgCl_2$, 10 mM $CaCl_2$.
7. DNA extraction kit (e.g., Qiagen, Cat. #69504).
8. High-Fidelity DNA Polymerase.
9. Taq polymerase.

10. A/T cloning vector (e.g., pGEM® T-easy Vector System, Promega).
11. Restriction endonuclease.
12. Gel extraction kit.

2.4 CRISPR-Cas9 Editing and Genotyping

CRISPR RNAs (crRNA) for gene targeting experiments are synthesized commercially (e.g., Integrated DNA Technologies, IDT). crRNAs need to be hybridized to tracer RNA (tracr RNA) prior to use and can be stored at −20 °C after hybridization. Cas9 enzyme aliquots are stored at −80 °C and are mixed with crRNAs:tracrRNA prior to use.

1. crRNA targeting sequences (two for performing deletions, *see* **Note 1**).
2. tracrRNA and hybridization buffer.
3. Cas9 enzyme.
4. 100 g/mL ampicillin in LB broth.
5. LB agar plates: 1.5% (w/v) agar in LB broth. Heat to dissolve, pour hot in petri dishes, store at 4 °C.
6. Plasmid miniprep kit (e.g., GenElute™ Plasmid Miniprep kit, Sigma-Aldrich).

3 Methods

3.1 Animal Maintenance, Spawning and Metamorphosis

1. Stable clones of wild-type/transgenic animals are grown on glass microscope slides at 20–22 °C in artificial seawater (Fig. 2) under a 14:10 light:dark regime (*see* **Note 2**).
2. Feed four times a week with freshly hatched Artemia and once a week with oysters (*see* **Note 3**).
3. Transfer the *Hydractinia* colonies to be spawned in water bowls filled with FSW outside of the tanks to facilitate embryo collection. The animals spawn about 90 min after being exposed to light.
4. Collect embryos into a water bowl filled with FSW using a Pasteur pipette (*see* **Note 4**).
5. Wait for 3 days for the embryos to reach planula larval stage.
6. Transfer the larvae into a water bowl filled with 110 mM CsCl in FSW.
7. Wait for 3 h.
8. Line a container with the desired substratum (e.g., glass slides) for the larvae to settle onto.
9. Fill the settling container with FSW.

10. Transfer the contracted larvae using a Pasteur pipette into the settling container.
11. Wait for 30 min for the larvae to settle.
12. Metamorphosis is completed within 24 h.

3.2 Capillaries' Preparation and Injection

1. Fill injection pump with pressurized air and adjust it to 60 psi.
2. Fill the pulled needle with injection solution (*see* **Note 5**) using a microloader pipette tip by inserting pipette tip from the back end as deep as possible into the tip of the needle and slowly release the injection solution.
3. Insert filled needle into the holding capillary, which is in turn secured in the capillary holder connected to the injector.
4. Cut/break the edge of the capillary, turn injection pump on, balance and adjust injection pressure/time (*see* **Note 6**).
5. Transfer embryos using a glass Pasteur pipette into to the injection plate filled with 4 °C pre-chilled ASW.
6. Place injection plate containing embryos on the stage of the dissection microscope.
7. Once the embryos are in the field of view, make sure they have settled into the pockets of the plankton net (*see* **Note 7**).
8. Lower the capillary holder until the tip of the needle becomes visible (through the binoculars) and submerged in ASW.
9. Cut the end of the needle with fine scissors until droplet is visible (*see* **Note 8**).
10. Inject embryos by placing the needle in the middle of the embryo. By moving the capillary holder up and down, you will be able to see the needle penetrating the embryo (*see* **Note 9**).
11. Move to the next embryo by moving the injection plate—not the capillary stage.
12. Transfer the injected embryos to a petri dish filled with ASW and place in a 16–18 °C incubator.

3.3 Strategy for Reporter Line Cloning

Reporter vector constructs are generated by inserting upstream regulatory sequence (URS) and downstream regulatory sequence (DRS) upstream and downstream of the fluorescent protein coding sequence (CDS), respectively (*see* **Note 10**). Cloning of the fragments can be achieved by restriction enzyme-based approach or by Gibson assembly. By using the former method, you can easily remove and add different URS and DRS fragments. All the vectors generated in our lab have the same restriction recognition sites (*see* **Note 11**; Fig. 3A).

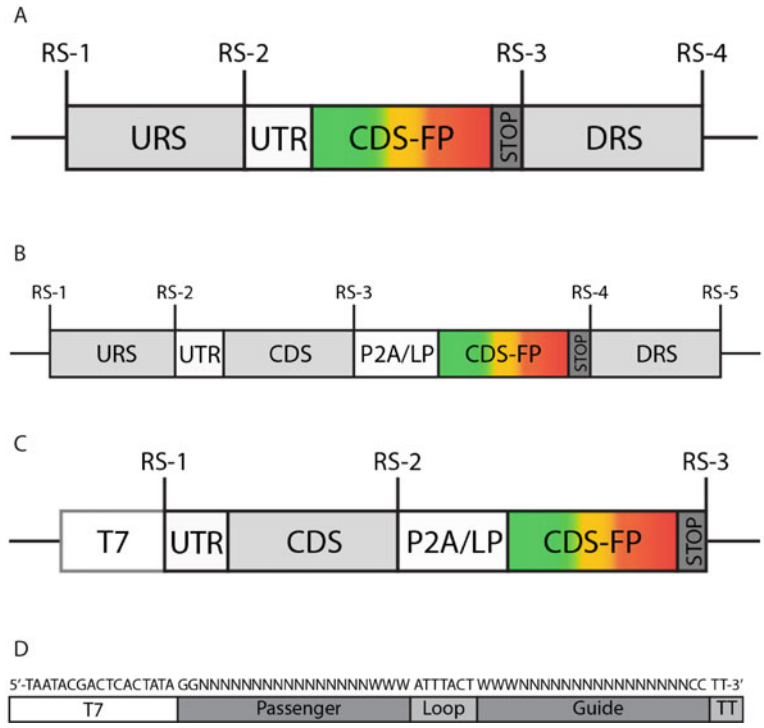


Fig. 3 Constructs structure. (**a**) Reporter construct. (**b**) Ectopic expression construct. (**c**) mRNA synthesis template. (**d**) shRNA synthesis template. *RS* restriction site, *P2A* self-cleavage P2A peptide coding sequence 5′GGTTCAGGT GCTACAAATTTTTCATTATTAAAACAAGCTGGTGATGTTGAAGAAAATCCAGGTCCA 3′, LP: linker peptide coding sequence 5′TGGCCAGGAGGCTCCGGCTCC3′, *UTR* untranslated region 5′ TGCAGCCCCGGTAGAAAAA3′. URS: upstream regulatory sequence; DRS: downstream regulatory sequence

1. Generate reporter vector by standard molecular cloning.
2. Transfect chemically/electro-competent XL1 Blue *E. coli* bacteria according to standard protocols.
3. Grow the bacteria and extract plasmids using a commercially available mini-prep kit or use a self-made one (*see* **Note 12**).
4. Inject embryos—*see* Subheading 3.2.
5. Transfer injected embryos from injection plate to large glass petri dishes and washed carefully with ASW.
6. Transfer to an 18 °C incubator.
7. Check for fluorescence the next day using a fluorescence stereomicroscope.
8. Transgenic larvae are separated from the non-injected ones and kept in the 18 °C incubator until metamorphosis induction.
9. Follow **steps 6–12** in Subheading 3.1. to induce metamorphosis.

10. Select transgenic animals based on the expected gene expression pattern from previous mRNA in situ hybridization or protein immunofluorescence.
11. Once transgenic animals reach sexual maturity, cross them with wild-type animals to produce G1 non-chimeric transgenic animals (*see* **Note 13**).

3.4 Strategy for Ectopic Expression Construct Cloning

Vectors for transgenic reporter lines can be used to ectopically express or overexpress your gene of interest. URS and DRS regions of the reporter line do not change and a cassette containing UTR + CDS + P2A peptide is inserted upstream of the fluorescence protein (Fig. 3B).

1. Design primers to clone a cassette containing UTR + the coding sequence of your gene of interest + a P2A peptide.
2. Follow the same procedure as in Subheading 3.3 in order to generate the vector.
3. Inject embryos as in Subheading 3.2.
4. Evaluate and maintain transgenic animals as described in Subheading 3.3.

3.5 Designing mRNA Constructs

1. Design template construct (TC) for mRNA synthesis (*see* **Note 14**).
2. Use target gene protein sequence from other animals as query to search the homologous transcripts from *Hydractinia symbiolongicarpus*.
3. Perform TBLASTN search at https://blast.ncbi.nlm.nih.gov/ against transcriptome shotgun assembly (TSA) database (do not use the default nr database) of *Hydractinia symbiolongicarpus*. Limit the search by TSA project and type in "GAWH: TSA: Hydractinia symbiolongicarpus, transcriptome shotgun assembly" into the box.
4. From the TBLASTN results page, retrieve the top hit *Hydractinia* transcript sequence. This is the coding sequence of gene of interest (CDS-GOI).
5. Retrieve the coding sequence of a fluorescence of protein (CDS-FP, e.g., eGFP or mScarlet) from a public database or use the available fluorescence protein sequence that you have already in an existing plasmid in your lab.
6. Codon optimize FP sequences for *Hydractinia symbiolongicarpus* using http://genomes.urv.es/ OPTIMIZER /. Codon usage table can be found at http://www.kazusa.or.jp/codon/cgi-bin/showcodon.cgi?species=13093.
7. Arrange these two CDS according to the scheme shown in Fig. 3C (*see* **Note 15**).

3.6 Synthesizing the mRNA Template Construct

There are three ways to synthesize the actual fragment: [1] design a plasmid with the construct as insert; [2] PCR several fragments and assembled it with Gibson Assembly process; [3] commercial synthesis. Synthesizing through a commercial service is the easier option, but the other two are more cost effective. We explain the two first options below. Both use plasmids that contain T7 promotor region flanking the insertion site (we use pGEM-T-easy vector plasmid).

3.6.1 Generating Plasmid for Template Construct

1. Design a primer pair to amplify CDS-GOI.
2. Add RS-1 and UTR sequences to the 5′ end of the forward primer and RS-2 to the 3′ end of the reverse primer for CDS-GOI.
3. Amplify CDS-GOI using high-fidelity DNA polymerase using *Hydractinia* cDNA library as template and the pair of primers design above.
4. Extract the amplicon from agarose gel and add an A-tail to the fragment by Taq polymerase.
5. Perform TA cloning of the A-tailed amplicon inserted into pGEM-T-easy vector.
6. Confirm and assess the plasmid by Sanger sequencing ensure to choose the correct in frame insertion of CDS-GOI to the 3′ region of the T7 promotor.
7. Keep the correct plasmid at −20 °C for **step 17**.
8. Design a primer pair to amplify CDS-FP.
9. Add RS-2 and P2A/LP sequence to the 5′end of the forward primer and add RS-3 (*see* **Note 16**).
10. Amplify CDS-FP using high-fidelity DNA polymerase, plasmid with FP and pair of primers design as in **steps 8** and **9**.
11. Run the amplicons on an agarose gel.
12. Extract the fragment using standard protocols.
13. Add A-tail to it by Taq polymerase.
14. Perform TA cloning of the A-tailed amplicon inserted into A/T vector.
15. Confirm and assess the plasmid by Sanger sequencing ensure to choose the correct in frame insertion of CDS-FP.
16. Keep the correct plasmid at −20 °C for **step 17**.
17. Digest plasmid from **steps 6** to **7** (pGOI) and from **steps 15** to **16** (pFP) with restriction endonuclease corresponding to RS-2 and RS-3. Ligate the small FP fragment from pFP digestion into the backbone fragment from pGOI digestion.

18. Confirm and assess the plasmid by Sanger sequencing and choose the plasmid with correct in-frame ligated template construct as described in Fig. 3C at the 3′ region of the T7 promotor sequence (pTC).
19. Digest and linearize pTC with restriction endonuclease corresponding with RS-3.
20. Extract the linearize pTC with gel extraction system and use this purified fragment as DNA template for in vitro transcription.

3.6.2 Synthesizing Gibson Assembled dsDNA Fragment for Template Construct

1. Design a primer pair to amplify CDS-GOI.
2. Add RS-1 (for Gibson assembly replace the restriction site with 20 nt sequence from the 5′ region of insertion site of your vector plasmid) and UTR sequence to the 5′end of the forward primer for CDS-GOI and add RS-2 and P2A/LP sequence to the 3′end of the reverse primer for CDS-GOI.
3. Amplify CDS-GOI using high-fidelity DNA polymerase, *Hydractinia* cDNA library as template and pair of primers design as in **steps 1** and **2**.
4. Keep the PCR mixture at 4 °C until electrophoresis.
5. Design a primer pair to amplify CDS-FP.
6. Add RS-2 and P2A/LP sequence (*see* **Note 17**) to the 5′end of the forward primer and add RS-3 and 3′ region of insertion site from the plasmid (*see* **Note 18**) to the 3′ end of the reverse primer for CDS-FP.
7. Amplify CDS-FP using high fidelity DNA polymerase, plasmid with *fp* and pair of primers design as in **steps 4** and **5**.
8. Keep the PCR mixture at 4 °C until electrophoresis.
9. Electrophorase the PCR mixture from **steps 3** and **6** in agarose gel.
10. Extract the amplicons from agarose gel.
11. Use both fragments and a backbone of plasmid for performing Gibson assembly following the manufacturer's instruction.
12. Transform competent *E. coli*, grow the colonies, and extract the plasmid.
13. Confirm and assess the plasmid by Sanger sequencing and ensure to choose the plasmid with correct in frame ligated template construct as described in Fig. 3C at the 3′ region of the T7 promotor sequence (pTC).
14. Digest and linearize pTC with restriction endonuclease corresponding with RS-3.
15. Extract the linearize pTC with gel extraction system and use this purified fragment as DNA template for in vitro transcription.

3.7 T7 In Vitro Transcription mRNA Synthesis, Microinjection, and Evaluation

1. Perform T7 in vitro transcription system according to the manufacturer's instruction to synthesize mRNA.
2. Purify the mRNA with an RNA column system or LiCl.
3. Run the yielded mRNA before and after poly-A-tailing in a formalin-agarose gel and assess the size of the mRNA before injection.
4. Inject the mRNA at 0.8–1.2 μg/μL according to Subheading 3.2.
5. Assess and evaluate the expression of the mRNA by checking the fluorescent protein. Phenotype can best be assessed between 5 and 96 h post injection.

3.8 Short-Hairpin RNA Interference

1. Use target gene protein sequence from other animals as query to search the orthologous transcripts from *Hydractinia symbiolongicarpus*.
2. Perform TBLASTN search at https://blast.ncbi.nlm.nih.gov/ against transcriptome shotgun assembly (TSA) database (do not use the default nr database) of *Hydractinia symbiolongicarpus*. Limit the search set by TSA project and type in "GAWH: TSA: Hydractinia symbiolongicarpus, transcriptome shotgun assembly" to the filling box.
3. From the tblastn results page, retrieve the top hit *Hydractinia*'s transcript sequence (only the sequence and not in fasta format).
4. Use the top hit sequence to find siRNA motif at http://www.invivogen.com/sirnawizard/design.php. Choose the desired motif size (21 nt is the default). Leave blanks the option of mRNA database and miRNA SEED database.
5. Choose several sequences from the motif outputs with higher GC content, 5′ GG, and 3′ AT-rich stretches (*see* **Note 19**).
6. Perform BLASTN on several motif output sequences against the *Hydractinia symbiolongicarpus* TSA with loose parameter (e.g., expected value 1) to confirm specificity (*see* **Note 20**).
7. Create the shRNA design by converting the selected 21-nt motif (passenger sequence) into RNA by replacing any T with U.
8. Add the reverse-complemented sequence (guide sequence) to the 3′ end and separate them by loop sequences [5-′-AUUUACU-3′].
9. Add "UU" to the 3′ of the sequence to create overhang.
10. Select sequences that are not predicted to form secondary structures using http://rna.tbi.univie.ac.at/cgi-bin/RNAWebSuite/RNAfold.cgi. Add one or two mismatches in the middle of the passenger sequence (but not to the guide sequence).

Table 1
Injection solution recipe for shRNA/mRNA injection

	Volume [μL]	Final concentration
Nuclease-free water	9-x	NA
Fluorescent tracer	0.5	10 ng/μL (*see* **Note 22**)
KCl (2 mM)	0.5	0.1 mM
shRNA/mRNA	x	250–900 ng/μL for shRNA or 0.8–1.2 μg/μL for mRNA (*see* **Note 23**)

11. Revert the RNA sequence back to DNA by replacing U to T and add T7 promoter [5′-TAATACGACTCACTATA-3′] to the 5′ (Fig. 3).
12. This sequence is the forward oligonucleotides. Create the reverse oligonucleotides sequence by reverse-complementing the forward oligonucleotides sequence. Synthesize the forward and reverse oligonucleotides using commercial services.
13. Dissolve forward and reverse oligonucleotides separately in ultrapure nuclease free water to a final concentration of 100 μM.
14. Dilute these 100 μM oligonucleotides 1:10 in nuclease-free H_2O while combining forward and reserved oligos.
15. Denature the combined oligonucleotides at 98 °C for 5 min.
16. Cool it down at room temperature for 10 min; this is the template for T7-based in vitro transcription (IVT) of shRNA.
17. Follow the manufacturer's protocol for IVT reaction; however, triple the total IVT volume to get enough yield.
18. The IVT reaction mix will turn viscous after the incubation. Thus, dilute the IVT suspension with nuclease-free H_2O to made up 100 μL solutions.
19. Add 1 volume of ethanol absolute into the solutions and mix them well.
20. Transfer the whole solution into an RNA column in 2-mL collection tube and bind the RNA into the column-membrane by centrifugation at 8000 rcf for 2 min then discard the flow-through.
21. Add 400 μL of Wash-r1 buffer into the column and centrifuge the column at 11,000 rcf for 1 min, then discard the flow-through.
22. Add 80 μL DNaseI solution into the center of the column and incubate it at room temperature for 1–3 h.

23. Wash the column with 400 μL of Wash-r1 buffer.
24. Further wash the column with 750 μL of Wash-r2 buffer.
25. Dry the column by one more centrifugation at maximum speed for 2 min.
26. Elute the RNA from the column with 40 μL ultrapure nuclease-free water by ≥11,000 rcf centrifugation for 1 min.
27. Assess the eluted RNA solution by miRNA assay of Qubit fluorometer, Nanodrop RNA mode, and RNA-gel electrophoresis using low molecular weight RNA marker (*see* **Note 21**).
28. Prepare the mixture of tracer dye in 1 M KCl.
29. Prepare shRNA for microinjection solution with the recipes described at Table 1.
30. Perform microinjection following the standard procedure in Subheading 3.2 (*see* **Note 22**).
31. Incubate the injected embryos in a 16 °C incubator until required for phenotype assessment.
32. Confirmation of shRNA-mediated knockdown can be performed by several methods including Western blot, given the antibody for the specific gene is available; utilizing the similar antibody, immunofluorescence can also be performed; if an antibody is not available, RT-qPCR is possible; performing mRNA ectopic expression of a fluorescence protein tagged with the shRNA target sequence, co-injected with specific shRNA, and using shRNA mock as control.
33. Once the shRNA-mediated knockdown in confirmed, phenotype evaluation can be performed as soon as 3–4 h after injection until 10–15 days post injection [15].
34. shRNA action will still be effective after metamorphosis; hence, it can be used to delay reporting the expression of a transgene if its embryonic expression is lethal [15].

3.9 CRISPR/Cas9 Design, Microinjection, and Genotyping

1. Design crRNAs using Geneious or other software.
2. BLAST crRNAs against the *Hydractinia* genome to confirm their specificity and exclude those with multiple matches in the genome.
3. Hybridize the crRNA with tracrRNA before use to create a viable short guide RNA (sgRNA) that can work with Cas9 for editing. Alternatively, obtain sgRNAs from a commercial supplier.
4. Incubate crRNA:tracrRNA with Cas9 enzyme for 15 min on ice prior to use.
5. Dilute Cas9 to 1 μg/μL and crRNA:tracrRNA to 500 ng/μL.

6. Use the protocol for microinjection described in Subheading 3.2.
7. Keep only injected animals, identified by dextran-AlexaFluor 555 co-injection.
8. Raise and metamorphose all injected embryos.
9. Obtain DNA samples from each individual approximately 10–14 days after metamorphosis by removing a single polyp from the colony and extracting DNA using an extraction kit. Remove excess seawater prior to beginning the extraction protocol.
10. Designed primers for PCR amplification to anneal over 100 bp away from the crRNA cut sites. In rare cases, regions as large as 1000 bp immediately around a single cut site can be deleted by resection. In these cases, multiple primer sets may be necessary for understanding the extent of a deletion.
11. Use a two-step PCR approach for initial amplification of DNA fragments. (denaturation = 98 °C, 3 min; denaturation = 98 °C, 30 s; annealing/extension = 68 °C, 1 min 15 s for 1–2 kb fragments).
12. Use high-fidelity DNA polymerase for the first round of PCR, followed by a short A-tailing step using Taq polymerase.
13. Ligate fragments into the A/T cloning vector.
14. Transform into DH5-alpha *E. coli* bacteria.
15. Plate on LB-agar plates.
16. Grow overnight at 37 °C.
17. Culture individual clones overnight in LB-broth with ampicillin.
18. Extract plasmid DNA using the plasmid miniprep kit.
19. Sequence plasmid DNA using pGEM primers for T7 or SP6 sequences.
20. Due to the mosaic nature of these experiments, genotyped animals should be crossed to generate non-mosaic knockout individuals for proper characterization of phenotypes.

4 Notes

1. Two crRNA can be selected to delete a specific segment in a gene to increase the probability of loss-of-function mutations.
2. *Hydractinia* can grow at nearly any light:dark cycle; choose the one most convenient to your work cycle. Several hours of darkness followed by light trigger spawning.
3. Both fresh or frozen oyster puree can be used.

4. Once the embryos are collected, they can be immediately stored in 4 °C for up to 4 h to halt their development, providing a wider timeframe for injections. At room temperature, they will start dividing after 30–60 min.
5. For the generation of transgenic reporter animals, 3–4 μg/μL of plasmid is mixed with 400 mM KCl in 1:5 ratio for better distribution of the plasmid, resulting in lower mosaicism.
6. We use injection pressure around 40–50 psi, but this may depend on the system used and should be determined empirically.
7. If the embryos are not secured in the net's pockets, injection will be difficult as they will keep rolling around in the plate.
8. Cut the needle bit by bit until a small droplet is visible. Be careful not to cut the needle too high because the solution will then come all out and be lost. When you press the petal, you should be able to see an increase in the droplet.
9. One way to discriminate between injected and uninjected embryos is size: injected ones are bigger. One can also use a fluorescence tracer. Two optional tracer dyes were successfully used in *Hydractinia*: Dextran-AF555 (Ex/Em: 555/565) and Lucifer yellow CH (Ex/Em: 428/536). Pay attention to the emission spectrum and avoid overlapping with the fluorescent protein used in the co-injected cassettes.
10. 5′ URS and 3′ DRS regions are usually identified based on the coding sequence of the gene of interest and forward and reverse primers are designed empirically. Based on the ORFs and by aligning *H. echinata* and *H. symbiolongicarpus* genomes, the conserved regions are usually selected for cloning.
11. 5′ URS is flanked upstream by BamHI and downstream by NotI. Fluorescence protein CDS is flanked upstream by NotI and downstream by SacI, and 3′ DRS is flanked upstream by SacI and downstream by PacI.
12. Miniprep commercially available kit is used for small-scale cultures in order to sequence the plasmids. Once the presence of the construct is confirmed, large-scale cultures are prepared in order to achieve high yield extracted plasmids.
13. Based on the observations from various transgenic reporter animals raised in our lab, second-generation animals (G1) tend to exhibit lower—or no mosaicism. Mosaicism in G1 probably reflect epigenetic factors.
14. mRNA synthesis can also be done using a PCR fragment as template. However, we recommended to construct a plasmid instead, as it will be more sustainable for long-term experimental plan. This design and plasmid construction is based on the TA-cloning system by Promega (pGEM-T-easy vector).

15. One can choose between P2A or LP to separate CDS-GOI and CDS-FP. LP is a small glycine rich peptide that will allow necessary distance between FP and GOI for correct folding, thus required only if the two proteins are meant to be fused in vivo. P2A is chosen if the two proteins need to be separated in vivo. UTR is a short, AT rich sequence that is necessary for the translational machinery in *Hydractinia* to effectively initiate translation in vivo. The CDS-GOI can be arranged in CDS-1 or CDS-2 position.
16. Restriction site 3 has to be the same as the restriction site available at the 3′ region of the plasmid insertion site and added to the 3′ end of the reverse primer for CDS-FP.
17. RS-2 and P2A/LP sequences act as the overlapping region for Gibson assembly.
18. Add some 20 nucleotides from the 3′ region of the insertion site of the backbone plasmid to create the overlapping region for the Gibson assembly to be successful.
19. GG dinucleotides at the 5′ is required to optimize the T7 IVT reaction. GGG would be better but GG or GC also work. At 3′ region, AT richness is necessary to enable the cell distinguishing passenger from guide sequence that will be use by the endogenous Argonaut.
20. BLASTN against the *Hydractinia* TSA database is necessary to prevent off-target effect, i.e., ensure that there is no other targets except the one intended.
21. For the first synthesis of shRNA, confirmation of the shRNA on a gel is recommended. Subsequent syntheses of shRNA from the same oligonucleotide will only require miRNA Qubit measurement.
22. The concentration of injected shRNA depends on the abundance of the target mRNA. For highly expressed gene such as Ef1α, it requires a concentration as high as 900 ng/μL. We have not tested higher concentrations.

Acknowledgments

Research in the Frank lab is supported by the SFI-HRB-Wellcome Research Partnership (grant No. 210722/Z/18/Z) and by National Science Foundation (grant No. 1827635).

References

1. Zapata F, Goetz FE, Smith SA, Howison M, Siebert S, Church SH, Sanders SM, Ames CL, McFadden CS, France SC, Daly M, Collins AG, Haddock SHD, Dunn CW, Cartwright P (2015) Phylogenomic analyses support traditional relationships within Cnidaria. PLoS One

10(10):e0139068. https://doi.org/10.1371/journal.pone.0139068

2. Technau U, Steele RE (2011) Evolutionary crossroads in developmental biology: Cnidaria. Development 138:1447–1458. https://doi.org/10.1242/dev.048959
3. Bosch TC, Klimovich A, Domazet-Loso T, Grunder S, Holstein TW, Jekely G, Miller DJ, Murillo-Rincon AP, Rentzsch F, Richards GS, Schroder K, Technau U, Yuste R (2017) Back to the basics: cnidarians start to fire. Trends Neurosci 40(2):92–105. https://doi.org/10.1016/j.tins.2016.11.005
4. Chang ES, Neuhof M, Rubinstein ND, Diamant A, Philippe H, Huchon D, Cartwright P (2015) Genomic insights into the evolutionary origin of Myxozoa within Cnidaria. Proc Natl Acad Sci U S A 112(48): 14912–14917. https://doi.org/10.1073/pnas.1511468112
5. Holstein TW, Hobmayer E, Technau U (2003) Cnidarians: an evolutionarily conserved model system for regeneration? Dev Dyn 226:257. https://doi.org/10.1002/dvdy.10227
6. DuBuc TQ, Traylor-Knowles N, Martindale MQ (2014) Initiating a regenerative response; cellular and molecular features of wound healing in the cnidarian Nematostella vectensis. BMC Biol 12(1):24. https://doi.org/10.1186/1741-7007-12-24
7. Vogg MC, Galliot B, Tsiairis CD (2019) Model systems for regeneration: Hydra. Development 146(21):dev177212. https://doi.org/10.1242/dev.177212
8. Chera S, Ghila L, Dobretz K, Wenger Y, Bauer C, Buzgariu W, Martinou J-C, Galliot B (2009) Apoptotic cells provide an unexpected source of Wnt3 signaling to drive *hydra* head regeneration. Dev Cell 17(2): 279–289
9. Bradshaw B, Thompson K, Frank U (2015) Distinct mechanisms underlie oral vs aboral regeneration in the cnidarian *Hydractinia echinata*. eLife 4:e05506. https://doi.org/10.7554/eLife.05506
10. Renfer E, Amon-Hassenzahl A, Steinmetz PRH, Technau U (2009) A muscle-specific transgenic reporter line of the sea anemone, Nematostella vectensis. Proc Natl Acad Sci 107(1):104–108. https://doi.org/10.1073/pnas.0909148107
11. Künzel T, Heiermann R, Frank U, Müller WA, Tilmann W, Bause M, Nonn A, Helling M, Schwarz RS, Plickert G (2010) Migration and differentiation potential of stem cells in the cnidarian *Hydractinia* analysed in GFP-transgenic animals and chimeras. Dev Biol 348:120–129
12. Klimovich A, Wittlieb J, Bosch TCG (2019) Transgenesis in Hydra to characterize gene function and visualize cell behavior. Nat Protoc 14(7):2069–2090. https://doi.org/10.1038/s41596-019-0173-3
13. Rentzsch F, Renfer E, Technau U (2020) Generating transgenic reporter lines for studying nervous system development in the Cnidarian Nematostella vectensis. Methods Mol Biol 2047:45–57. https://doi.org/10.1007/978-1-4939-9732-9_3
14. Buss LW, Yund PO (1989) A sibling species group of Hydractinia in the north-eastern United States. J Mar Biol Assoc UK 69(4): 857–874. https://doi.org/10.1017/S0025315400032215
15. DuBuc TQ, Schnitzler CE, Chrysostomou E, McMahon ET, Febrimarsa, Gahan JM, Buggie T, Gornik SG, Hanley S, Barreira SN, Gonzalez P, Baxevanis AD, Frank U (2020) Transcription factor AP2 controls cnidarian germ cell induction. Science 367(6479): 757–762. https://doi.org/10.1126/science.aay6782
16. Frank U, Nicotra ML, Schnitzler CE (2020) The colonial cnidarian Hydractinia. EvoDevo 11(1):7. https://doi.org/10.1186/s13227-020-00151-0
17. Wittlieb J, Khalturin K, Lohmann JU, Anton-Erxleben F, Bosch TCG (2006) From the cover: transgenic Hydra allow in vivo tracking of individual stem cells during morphogenesis. PNAS 103(16):6208–6211. https://doi.org/10.1073/pnas.0510163103
18. Quiroga Artigas G, Lapébie P, Leclère L, Takeda N, Deguchi R, Jékely G, Momose T, Houliston E (2018) A gonad-expressed opsin mediates light-induced spawning in the jellyfish Clytia. eLife 7:e29555. https://doi.org/10.7554/eLife.29555
19. Jones VAS, Bucher M, Hambleton EA, Guse A (2018) Microinjection to deliver protein, mRNA, and DNA into zygotes of the cnidarian endosymbiosis model Aiptasia sp. Sci Rep 8(1): 16437. https://doi.org/10.1038/s41598-018-34773-1
20. Millane RC, Kanska J, Duffy DJ, Seoighe C, Cunningham S, Plickert G, Frank U (2011) Induced stem cell neoplasia in a cnidarian by ectopic expression of a POU domain transcription factor. Development 138(12): 2429–2439. https://doi.org/10.1242/dev.064931
21. Flici H, Schnitker N, Millane RC, Govinden G, Houlihan A, Boomkamp SD, Shen S,

Baxevanis AD, Frank U (2017) An evolutionarily conserved SoxB-Hdac2 crosstalk regulates neurogenesis in a cnidarian. Cell Rep 18: 1395–1409. https://doi.org/10.1016/j.celrep.2017.01.019

22. Karadge UB, Gosto M, Nicotra ML (2015) Allorecognition proteins in an invertebrate exhibit homophilic interactions. Curr Biol 25: 2845–2850. https://doi.org/10.1016/j.cub.2015.09.030

23. Steven MS, Zhiwei M, Julia MH, Brooke MR, Gregory AG, Alan MW, Hakima F, Uri F, Christine ES, Andreas DB, Matthew LN (2018) CRISPR/Cas9-mediated gene knockin in the hydroid Hydractinia symbiolongicarpus. BMC Genomics 19(1) https://doi.org/10.1186/s12864-018-5032-z

24. Kanska J, Frank U. Novel roles for Nanos in neural cell fate determination revealed by studies in a cnidarian. J Cell Sci https://doi.org/10.1242/jcs.127233

Open Access This chapter is licensed under the terms of the Creative Commons Attribution 4.0 International License (http://creativecommons.org/licenses/by/4.0/), which permits use, sharing, adaptation, distribution and reproduction in any medium or format, as long as you give appropriate credit to the original author(s) and the source, provide a link to the Creative Commons license and indicate if changes were made.

The images or other third party material in this chapter are included in the chapter's Creative Commons license, unless indicated otherwise in a credit line to the material. If material is not included in the chapter's Creative Commons license and your intended use is not permitted by statutory regulation or exceeds the permitted use, you will need to obtain permission directly from the copyright holder.





Chapter 23

Manipulation of Gene Activity in the Regenerative Model Sea Anemone, *Nematostella vectensis*

Eric M. Hill, Cheng-Yi Chen, Florencia del Viso, Lacey R. Ellington, Shuonan He, Ahmet Karabulut, Ariel Paulson, and Matthew C. Gibson

Abstract

With a surprisingly complex genome and an ever-expanding genetic toolkit, the sea anemone *Nematostella vectensis* has become a powerful model system for the study of both development and whole-body regeneration. Here we provide the most current protocols for short-hairpin RNA (shRNA)-mediated gene knockdown and CRISPR/Cas9-targeted mutagenesis in this system. We further show that a simple Klenow reaction followed by in vitro transcription allows for the production of gene-specific shRNAs and single guide RNAs (sgRNAs) in a fast, affordable, and readily scalable manner. Together, shRNA knockdown and CRISPR/Cas9-targeted mutagenesis allow for rapid screens of gene function as well as the production of stable mutant lines that enable functional genetic analysis throughout the *Nematostella* life cycle.

Key words *Nematostella vectensis*, Cnidaria, CRISPR, shRNA, Mutagenesis, Electroporation, Knockdown, Cas9, Microinjection, Genome editing

1 Introduction

As a member of phylum Cnidaria, the sister group to Bilateria, the starlet sea anemone *Nematostella vectensis* is an important model for the study of animal development and evolution (Fig. 1) [1–4]. More recently, *Nematostella* has also become a popular system for the study of whole-body regeneration [5–7]. *Nematostella* polyps are highly regenerative, capable of replacing all missing parts through cellular proliferation in approximately 1 week (Fig. 2) [8, 9]. The presence of similar capabilities throughout most cnidarian species [10] makes whole-body regeneration a potentially shared characteristic of basal metazoans and uniquely positions *Nematostella* as a model to study the molecular and

Cheng-Yi Chen, Florencia del Viso, Lacey R. Ellington, Shuonan He, and Ahmet Karabulut contributed equally to this work.

Simon Blanchoud and Brigitte Galliot (eds.), *Whole-Body Regeneration: Methods and Protocols*, Methods in Molecular Biology, vol. 2450, https://doi.org/10.1007/978-1-0716-2172-1_23, © The Author(s) 2022

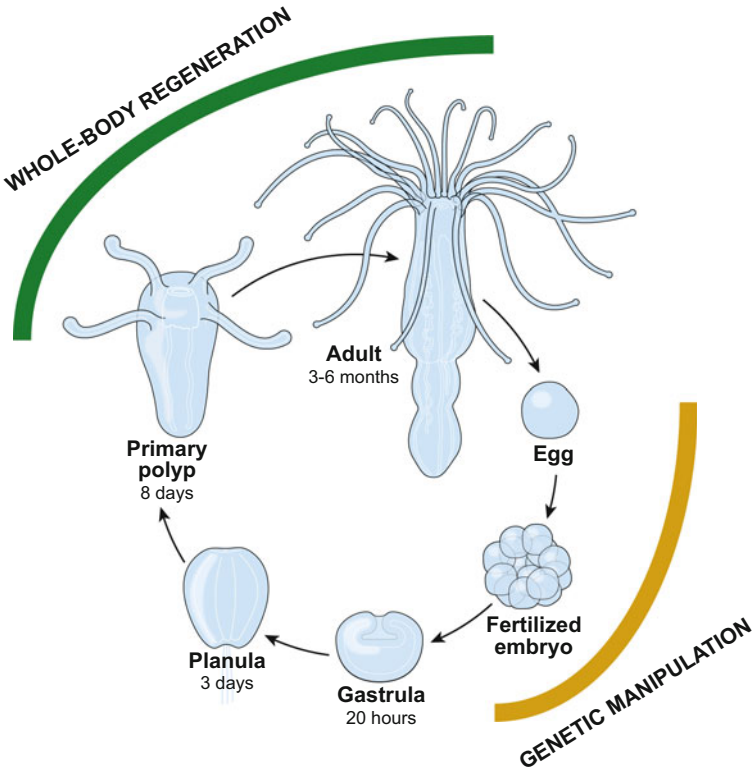


Fig. 1 Life cycle of *Nematostella vectensis.* The lifecycle of *Nematostella vectensis* is an example of indirect development. Eggs divide rapidly following fertilization and gastrulate to set up the germ layers of the animals and form a transient stage called a gastrula. The planula stage comes next. The planula is a motile larva that moves due to a ciliary organ called the apical tuft. After a few days, the planula undergoes metamorphosis to become a primary polyp. Growth from feeding causes the primary polyp to grow to a sexually mature adult polyp. Both primary and adult polyps are capable of whole-body regeneration. Currently, the egg and blastomeres formed by early mitotic cleavages are the most readily available stages for genetic manipulation

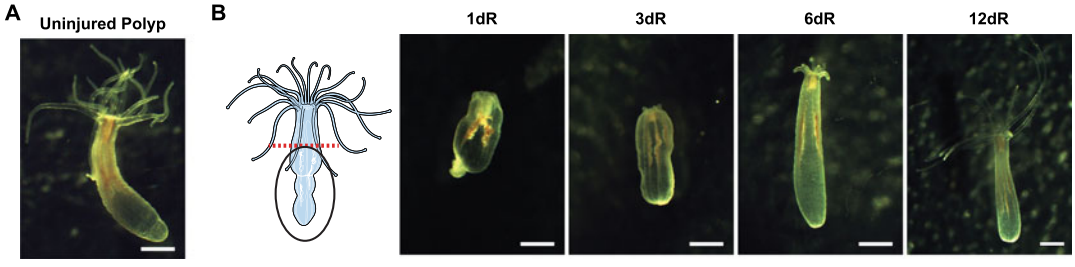


Fig. 2 Regeneration in *Nematostella vectensis*. (**a**) An uninjured *Nematostella vectensis* polyp. (**b**) Time course of oral regeneration after amputation aboral to the pharynx. All missing tissue is restored by 6 days of regeneration (6 dR). Tentacle growth continues for approximately an additional week (12 dR). Scale bar – 400 μm

genetic basis for ancient and conserved mechanisms of regeneration.

Gene-specific knockdown by shRNA was only recently reported in *Nematostella* [11]. The Cnidarian microRNA pathway most commonly regulates target mRNAs by cleavage, similar to the mechanism of small interfering RNAs and allows for highly specific knockdown of individual genes [11–13]. For shRNA design, a free web-based interface or downloadable programs support algorithms that can be used to design gene-specific 19-mer targeting motifs. Optimal targeting motifs are then incorporated into a standardized oligo design that allows for cost-effective DNA template production and in vitro transcription of shRNAs by T7 RNA polymerase (Fig. 3a, a′). Additionally, DNA templates for shRNA production can be produced from standard commercially produced oligonucleotides making it cost effective. Once produced, shRNA can be delivered either by microinjection or electroporation of eggs [11, 14]. The method we describe produces micrograms of shRNA per in vitro transcription (IVT), making each reaction suitable for hundreds of microinjections or multiple electroporation experiments.

Initial genome editing efforts in *Nematostella* used TALENs (Transcription Activator-Like Effector Nucleases) or multistep, cloning-based methods for CRISPR sgRNA production [15]. We have recently adopted a method for sgRNA production leveraging sgRNA design using CRISPRscan [16, 17] followed by T7-mediated transcription from a DNA template produced by a one-step Klenow extension reaction (Fig. 3b, b′). As with shRNA, this method produces micrograms of sgRNA molecules that can be used for hundreds of microinjection experiments. While the current preferred method for targeted mutagenesis is the injection of preloaded ribonucleoproteins (RNPs) of sgRNA and Cas9 protein, similar mutation rates can be achieved using a *Nematostella* codon-optimized Cas9 mRNA and slightly lower mutation rates can be obtained with a zebrafish codon-optimized Cas9 mRNA [18].

Although current methods for the introduction of functional RNA molecules are limited to early embryogenesis (Fig. 1), the future is bright for functional genetic analysis restricted only to polyp stage animals. A functional heat shock promoter [16] as well as the increased efficacy of genetic insertions by homology-directed repair [16, 19] will likely soon lead to the establishment of transgenic lines containing spatially and temporally controlled genetic tools, such as inducible site-specific DNA recombinase systems (e.g., Cre:*Lox* and FLP:*FRT*) or other synthetic conditional alleles found in traditional model organisms [20–24]. Continued development of the *Nematostella* toolkit will not only allow the functional interrogation of the genetic requirements of whole-body

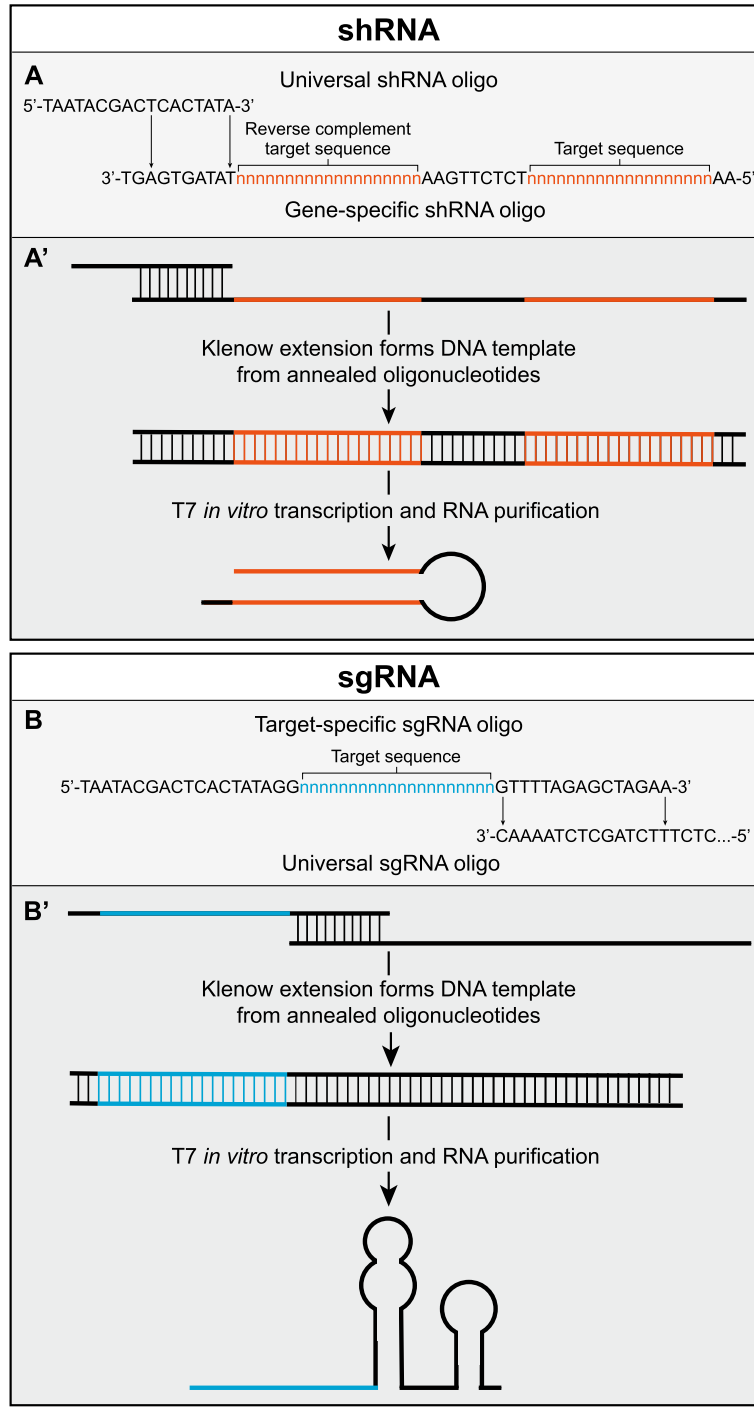


Fig. 3 Design and production of shRNAs and sgRNAs. (**a**) Schematic of universal shRNA and gene-specific shRNA oligonucleotides design. (**a′**) Graphic outline of shRNA production protocol. (**b**) Schematic of universal sgRNA and target-specific sgRNA oligonucleotides designed using CRISPRscan [14]. (**b′**) Graphic outline of sgRNA production protocol

regeneration but will also enable the direct comparison of embryogenesis and regeneration in the same animal.

Here, we discuss current strategies for functional genetic analysis by shRNA-mediated knockdown and CRISPR/Cas9-targeted mutagenesis in *Nematostella*. Both the shRNA knockdown and CRISPR/Cas9-targeted mutagenesis protocols detailed here have four main steps: (1) Design; (2) Production; (3) Delivery; and (4) Screening and Care. While the general methods for these two protocols are similar, their purposes are complementary and allow for genetic analysis throughout the life cycle of the animal.

2 Materials

All solutions should be prepared with molecular biology grade and nuclease-free reagents unless otherwise stated.

2.1 shRNA Production

1. shRNA candidate sequence prediction algorithm or web-based tool (*see* **Note 1**).
2. shRNA gene-specific reverse strand oligonucleotide with the following structure:

   5′-AA-[19 bp shRNA candidate sequence]- TCTCTTGAA -[reverse complement candidate sequence]- TATAGT GAGT-3′ (Fig. 3a).
3. Non-targeting shRNA oligonucleotide.
4. *Universal shRNA forward oligonucleotide* with T7 promoter sequence:

   5′-TAATACGACTCACTATA-3′.
5. N-terminal truncated DNA polymerase I (e.g., Klenow fragment).
6. 10× DNA polymerase buffer: 50 mM NaCl, 10 mM Tris–HCl, 10 mM $MgCl_2$, 1 mM dithiothreitol (DTT), pH 7.9 (*see* **Note 2**).
7. 10 mM dNTP mixture.
8. High-yield T7 in vitro transcription kit (e.g., AmpliScribe™ T7-Flash™ transcription kit, Lucigen).
9. RNA purification kit.
10. shRNA annealing mix solution: 3 μL 100 μM universal shRNA forward oligonucleotide, 4 μL nuclease-free water.
11. Template extension reaction: 2 μL 10× DNA polymerase buffer, 1 μL 10 mM dNTP, 1 μL N-terminal truncated DNA polymerase I (5000 U/mL), 6 μL nuclease-free water.

2.2 CRISPR/Cas9 Targeted Mutagenesis

1. CRISPRscan (http://crisprscan.org): sgRNA candidate sequence design web portal (*see* **Note 3**).
2. sgRNA target-specific oligonucleotide with the following structure:

   5′-TAATACGACTCACTATA-[target-specific region, 20 bp]-GTTTTAGAGCTAGAA-3′ (Fig. 3b).
3. Universal sgRNA reverse strand tail oligonucleotide: 5′-AAA AGCACCGACTCGGTGCCACTTTTTCAAGTTGATAACG GACTAGCCTTATTTTAACTTGCTATTTCTAGCTC TAAAAC-3′.
4. sgRNA annealing mix solution: 3 μL 100 μM universal sgRNA reverse strand tail oligonucleotide, 4 μL nuclease-free water.
5. Fluorometer.
6. Fluorometer assay tubes.
7. High-abundance RNA quantification kit (e.g., Qubit RNA BR, Invitrogen).
8. 1.25 μg/μL Cas9 protein with nuclear localization sequence stock solution.
9. High-fidelity PCR kit.
10. Forward and reverse primers designed to amplify genomic locus surrounding sgRNA target site.
11. DNA extraction lysis buffer (e.g., QuickExtract™ DNA extraction solution lysis buffer, Lucigen).
12. PCR cloning kit.
13. Liquid bacterial cultures for plasmid amplification.
14. DNA plasmid miniprep kit.
15. pCS2-nCas9n plasmid for the expression of zebrafish codon optimized *Cas9* mRNA (Addgene #47929).
16. pBS-Nvec-codonopti-Cas9-2xNLS plasmid for the expression of a *Nematostella vectensis* codon-optimized *Cas9* mRNA (Addgene #141108).
17. mRNA synthesis kit.

2.3 Microinjection

1. De-jellied *Nematostella* eggs (*see* **Notes 4–6**).
2. *Nematostella* sperm water (*see* **Note 7**).
3. 5/6-Fluorescein isothiocyanate (FITC) stock solution: 20 mg/mL in Tris–HCl, pH > 9.5.
4. Long-term labeling dextran conjugate (e.g., Dextran Texas Red™, 3000 molecular weight) stock solution: 20 mg/mL in nuclease-free water.
5. Filamented thin wall glass capillary needles: 100 mm length, 1 mm diameter, 0.25 mm thickness (*see* **Note 8**).

Table 1
CRISPR/Cas9 mutagenesis injection conditions.

	Suggested starting point	Functional experimental range	Troubleshooting
sgRNA	500 ng/μL	150–500 ng/μL	If no cutting is observed with minimal toxicity, increase sgRNA concentration If phenotype is too severe at low levels of Cas9 protein, reduce sgRNA concentration
Cas9 recombinant protein (PNA bio CP02)	500 ng/μL	150–500 ng/μL	If phenotype is too severe, reduce Cas9 protein. Mosaicism within individuals may be higher but more animals will survive to potentially transmit mutation to F1
Cas9 zebrafish codon-optimized mRNA (Addgene #47929)	50 ng/μL	25–100 ng/μL	mRNA injections can be highly toxic. If toxicity is observed the day after injection, reduce mRNA. Be sure to confirm DNA cutting still occurs
Cas9 *Nematostella* codon-optimized mRNA (*see* **Note 56**) (Addgene #141108)	20 ng/μL	10–50 ng/μL	Cas9 mRNA using *Nematostella* codon-optimized sequence typically has a higher mutagenesis rate than zebrafish codon-optimized This reagent can also be even more toxic than a typical mRNA injection. If toxicity is observed the day after injection, reduce mRNA. Be sure to confirm DNA cutting still occurs
Post-injection incubation (overnight)	Cas9 protein: 24 °C *Cas9* mRNA: 18 °C	Cas9 protein: 21–27 °C *Cas9* mRNA: 18–22 °C	Lower temperatures are better for embryo survival, but mutation rate is slightly better at higher temperatures Survival can be difficult if using *Cas9* mRNA. We see reduced toxicity at or below 18 °C overnight incubation

6. Needle puller (e.g., Sutter P-97).
7. Micropipette capillary tips.
8. Programmable microinjector.
9. 0.01 mm micrometer for needle calibration.
10. 60 mm petri dishes: BD Falcon – 351007 (*see* **Note 9**).
11. 12 ppt artificial sea water (ASW): 12 g/L artificial sea salt (e.g., Sea Salt, Instant Ocean™).

12. Injection tracer dye solution: 1-part FITC stock solution: 1-part long-term labeling dextran conjugate solution (*see* **Note 10**).
13. shRNA injection mixture: 0.5 μL injection tracer dye solution, *x* μL shRNA (to a final concentration of 500 ng/μL), nuclease-free water up to a total volume of 5 μL. Prepare fresh, keep on ice until ready for use.
14. Ribonucleoprotein (RNP) injection mixture: 2 μL Cas9 protein with nuclear localization sequence, *x* μL sgRNA (to a final concentration of 500 ng/μL), nuclease-free water up to a total volume of 4.5 μL.
15. Cas9 mRNA injection mixture: 0.5 μL injection tracer dye solution, *x* μL sgRNA (to a final concentration of 500 ng/μL), *y* μL *Cas9* mRNA (*see* Table 1 for final suggested final concentrations), nuclease-free water up to a total volume of 5 μL.

2.4 Electroporation of shRNA

1. Polysucrose 400 (e.g., Ficoll PM 400, Sigma Aldrich).
2. Square wave electroporation system with electroporation cuvette chamber (e.g., ECM 830 Electro Square Porator, BTX; Gene Pulser Xcell ShockPod Cuvette Chamber, Bio-Rad).
3. 4 mm electroporation cuvettes.
4. Electroporation Solution: 15% polysucrose 400 in 12 ppt ASW (*see* **Note 11**).

3 Methods

3.1 shRNA Production

1. Identify the coding sequence (CDS) region for each gene of interest (*see* **Note 12**).
2. Search the CDS for 19-mer shRNA candidate sequences using the shRNA prediction algorithm (*see* **Notes 13** and **14**).
3. Select 3–5 candidate shRNA sequences for each gene, ensuring the selected sequences span different regions of target gene CDS.
4. BLAST search each candidate in the *Nematostella* transcriptome using an expectation threshold of 1.0E-2 to compensate for shorter sequence inputs (*see* **Note 15**).
5. To ensure the specificity of shRNAs, discard each candidate sequence that has more than one match in the transcriptome.
6. Design gene-specific shRNA reverse oligos for 3–5 candidate shRNA sequences per gene using the following structure: 5′-AA-[shRNA candidate sequence, 19 bp]- TCTCTTGAA -

[reverse complement of shRNA candidate sequence, 19 bp]-TATAGTGAGT-3′ (Fig. 3a, *see* **Notes 16–18**).

7. Order the synthesized gene-specific shRNA oligos.
8. Dilute universal shRNA primer and gene-specific reverse primer to 100 μM.
9. Add 3 μL 100 μM gene-specific reverse primer to 7 μL shRNA annealing mix solution.
10. Incubate annealing reaction at 70 °C for 2 min in a thermocycler.
11. Hold annealing reaction at room temperature for 5 min.
12. Add 10 μL of DNA template extension solution to 10 μL of annealing reaction.
13. Incubate at 37 °C for 30 min.
14. Incubate at 70 °C for 20 min to deactivate the DNA polymerase enzyme. This reaction mixture is the DNA Template and will be directly used for in vitro transcription.
15. Use 5.5 μL DNA Template as starting product in a 20 μL in vitro transcription reaction per manufacturer's instructions (*see* **Note 19**).
16. Incubate in vitro transcription reaction at 37 °C for 5 h (*see* **Note 20**).
17. Add 1 μL of RNase-free DNaseI to in vitro transcription reaction (*see* **Note 21**).
18. Incubate at 37 °C for another 15 min to digest the DNA template.
19. Purify shRNA using the RNA purification kit according to the manufacturer's instructions (*see* **Note 22**).
20. Add 80 μL nuclease-free water to expand the reaction mixture to 100 μL.
21. Add 100 μL of ice cold 100% ethanol.
22. Mix well by pipetting.
23. Add the mixture into the RNA purification column.
24. Centrifuge for 30 s at 10,000 rcf.
25. Replace the flow-through with 700 μL of RNA wash buffer.
26. Centrifuge for 30 s at 10,000 rcf.
27. Discard flow-through.
28. Centrifuge for 2 min at max speed to completely remove the RNA wash buffer.
29. Transfer the column to a new microcentrifuge tube.
30. Carefully add 35 μL of nuclease-free water to the membrane of the column.

31. Wait for 1 min to allow the elution water to incubate on membrane at RT.
32. Centrifuge for 1 min at maximum speed to elute RNA product.
33. Quantify shRNA concentration using a spectrophotometer (*see* **Note 23**).
34. shRNA can be stored at −20 °C for at least a month. For long-term storage, store at −80 °C for up to a year.

3.2 shRNA Microinjection

An alternative protocol for shRNA delivery using electroporation is provided in Subheading 3.3. When choosing which shRNA delivery method, it can be important to consider your experiment. The main benefit of microinjection is consistent shRNA delivery due to calibrated injection volumes and the use of long-term labeling injection dyes. Therefore, ideal experiments for shRNA microinjection may include functional screening of a single or a small number of genes of interest or optimization of a consistent shRNA phenotype for production of a consistent samples for further analysis.

1. Load 2.2 μL shRNA injection mixture into a pulled capillary needle.
2. Let the mixture fall to the tip of the needle (*see* **Note 24**).
3. Insert the loaded needle into the capillary holder of the microinjector**.**
4. Gently transfer 200–400 de-jellied eggs to the center of a 60-mm petri dish using a 1.5-mL transfer pipette. Eggs should adhere to the surface of the petri dish (*see* **Note 25**).
5. Trim needle using forceps (*see* **Note 26**).
6. Calibrate injection parameters to allow for an injection volume of ~60–80 pL (~1.5% volume of the egg) using a 0.01 mm micrometer. Injection parameters will differ for individual microinjector setups. A well-calibrated needle should repeatedly produce an injection volume 5 μm in diameter as measured using a micrometer (*see* **Notes 27–29**).
7. Inject approximate number of eggs needed for experiment.
8. Remove un-injected eggs from the dish with a 1.5-mL transfer pipette being careful to avoid injected eggs.
9. Collect sperm water using a transfer pipette.
10. Fertilize injected eggs by completely filling 60 mm dish.
11. Repeat **steps 1–10** to deliver non-targeting shRNA for the mock treatment group.
12. Fertilize remaining de-jellied, untreated eggs to serve as a negative control.
13. Incubate the fertilized embryos at room temperature (21–25 °C) overnight.

3.3 shRNA Electroporation

An alternative to this shRNA delivery method using microinjection is provided in Subheading 3.2.

When choosing which shRNA delivery method, it can be important to consider your experiment. The main benefits of electroporation are ease of shRNA delivery, rapid delivery to a large number of eggs, higher throughput genetic screening, low equipment cost, and potential applicability for use with other Cnidarian species where shRNA injection is very difficult or impossible [25]. Therefore, ideal experiments for shRNA electroporation may include genetic screening of a large number of genes as well as the opportunity for evolutionary comparison of gene function across different Cnidarian species.

1. Transfer de-jellied *Nematostella* eggs into a 15-mL tube.
2. Add 5 mL *Nematostella* sperm water.
3. Fertilize for 30 min at room temperature by laying the tube horizontal and gently agitating every 5–10 min (*see* **Note 30**).
4. Place the tube upright.
5. Wait for the eggs to settle.
6. Remove sperm water with transfer pipette.
7. Wash the fertilized eggs 3 times with 10 mL of 12 ppt ASW.
8. Transfer eggs in ~1 mL 12 ppt ASW to a clean microcentrifuge tube.
9. Wait for eggs to settle.
10. Resuspend eggs in electroporation solution to reach a dilution of 2–5 eggs/μL (*see* **Notes 31** and **32**).
11. Gently pipette 100 μL of eggs suspension into a 4 mm electroporation cuvette using a p200 pipette with a disposable tip widened by cutting the end off.
12. Add purified shRNA to a final concentration of 300 ng/μL directly to egg suspension in the cuvette.
13. Mix gently by manually agitating the cuvette for approximately 15–20 s (*see* **Note 33**).
14. Turn on electroporator.
15. Insert cuvette into electroporation chamber.
16. Set desired electroporation conditions (50 V, 25 ms, 1 pulse) (*see* **Note 34**).
17. Press the start button to initiate electroporation.
18. Confirm that the electroporation charge was successfully dispatched across the sample visually by checking for bubbles on the side of the cuvette near the meniscus of the electroporation solution.

19. Remove the cuvette from chamber.
20. Transfer eggs to a 60-mm petri dish using a transfer pipette.
21. Use fresh 12 ppt ASW to rinse the cuvette of any remaining eggs into the 60-mm dish.
22. Repeat **step 21** until all eggs have been transferred into the 60-mm dish (*see* **Note 35**).
23. Gently swirl dish to disperse electroporated eggs (*see* **Note 36**).
24. Repeat **steps 11–23** to deliver non-targeting shRNA for the mock treatment group.
25. Fertilize remaining de-jellied, untreated eggs to serve as a negative control.
26. Incubate the dishes at room temperature overnight.

3.4 Screening and Care of shRNA-Treated Animals

1. Gently transfer developing blastula embryos into new 60 mm dishes filled with fresh 12 ppt ASW using a 1.5-mL transfer pipette.
2. Discard unhealthy, unfertilized, or lysed animals as well as debris.
3. Repeat **steps 1** and **2** daily.
4. As development proceeds, morphological, molecular or cellular phenotypes may begin to appear. Always compare experimental shRNA-treated groups to both mock treatments as well as to untreated *wild type* controls from the same spawning group (*see* **Notes 37–41**).

3.5 sgRNA Production for CRISPR/Cas9-Targeted Mutagenesis

1. Identify the genomic region of interest (*see* **Note 42**).
2. Copy and paste DNA sequence into the CRISPRscan Sequence Submission web interface (https://www.crisprscan.org/?page=sequence), select "Cas9 – NGG" and "In vitro T7 promoter" from dropdown menus and click "Get sgRNAs" button (*see* **Notes 43–45**).
3. The program will suggest many different sgRNA sequences (in upper case) and will automatically design necessary oligo sequences for production by T7 in vitro transcription for each (Fig. 3b).
4. Select 3–5 candidate sgRNA sequences for each DNA sequence (*see* **Note 46**).
5. BLAST search each sgRNA sequence (upper case only from CRISPRscan-designed oligos) in the *Nematostella* genome using an expectation value of 1.0E-2 to compensate for shorter sequence inputs. Each candidate sequence should only have one match in the genome. Additionally, it is important to confirm that the sgRNAs avoid intron–exon junctions (*see* **Notes 15** and **47**).

6. Order synthesized target-specific sgRNA oligos.
7. Dilute universal sgRNA tail reverse and target-specific sgRNA oligos to 100 μM.
8. Add 3 μL 100 μM target-specific sgRNA oligonucleotide to 7 μL sgRNA annealing mix solution.
9. Complete sgRNA production by following **steps 10–32** from Subheading 3.1 (Fig. 3b′).
10. Quantify the concentration using fluorometer and high abundance RNA concentration kit (*see* **Notes 48** and **49**).
11. Separate purified sgRNAs into 2–4 μL aliquots to avoid frequent freeze–thaw cycles. Aliquots can be stored at −20 °C for several weeks or moved to −80 °C for longer term storage if desired.

3.6 sgRNA/Cas9 Delivery by Microinjection

1. Incubate RNP Injection Mixture at 37 °C for 10 min.
2. Add 0.5 μL of injectable tracer dye solution.
3. Mix by pipetting.
4. Keep reaction at room temperature and protected from light until injection (*see* **Note 50**).
5. Load 2.2 μL RNP injection mixture into a pulled capillary needle.
6. Let the mixture fall to the tip of the needle.
7. Insert the loaded needle into the capillary holder of the microinjector.
8. Follow **steps 4–12** from Subheading 3.2 to complete the injection of eggs.
9. Incubate all experimental embryos at 18–27 °C overnight (see **Note 51**; Table 1).
10. Follow **steps 1–4** from Subheading 3.4 to observe potential phenotypes (*see* **Notes 52** and **53**).

3.7 Genotypic Screening and Care of CRISPR/Cas9 Injected Animals

Genotypic screening by standard PCR and molecular biology techniques is required to confirm DNA cutting and genomic mutagenesis.

1. Collect 8–16 individual larvae (72 h post-fertilization or later) in PCR tubes, making sure to note those with an observable candidate phenotype. Be sure to include injection control and *wild-type* animals for downstream genotypic analysis.
2. Carefully remove as much 12 ppt ASW as possible.
3. Add 12 μL of DNA extraction lysis buffer (*see* **Note 54**).
4. Lyse sample by incubating for 1 h at 65 °C.
5. Incubate 3 min at 98 °C.

6. Ensure tissue is fully lysed before placing tube on ice (*see* **Note 55**).
7. Perform 50 μL PCR for each sample with high-fidelity PCR kit and gene-specific primers designed to amplify the region surrounding the target cut site.
8. Run 2 μL of PCR product on a 1% agarose gel.
9. Note reactions with a band of the correct size.
10. Purify the remaining 48 μL of any positive PCR by column clean up.
11. Submit PCR product to standard Sanger sequencing.
12. Upon receipt of sequencing results, look for loss of base-calling quality and reduction of chromatogram peaks near target cut site. As these injected animals are F0, you can expect them to be mosaic and harbor several different alleles of genomic region of interest if mutagenesis was successful (*see* **Note 56**).
13. Use Sanger sequencing information to correlate genotypic and phenotypic information if possible.
14. Feed and raise the remaining F0 animals from injection series that show genotypic indications of successful mutagenesis (*see* **Notes 57** and **58**).
15. If only a small number of CRISPR/Cas9-injected F0 animals show evidence of genomic cutting at this step, repeat Subheading 3.6 with increased concentration of sgRNA, Cas9 protein, or both in the RNP injection mixture (*see* **Note 59**; Table 1). If this increase is unsuccessful too, consider using Cas9 mRNA injection mixture in targeted mutagenesis experiments (*see* **Notes 60–64**; Table 1).
16. Upon sexual maturation, isolate F0 animals in individual wells of a six-well untreated tissue culture plate.
17. Spawn F0 animals in individual wells.
18. Cross to either WT sperm or WT eggs to obtain heterozygous progeny. F1 animals resulting from this cross will not be individually mosaic, but some will be germline heterozygous carriers for the allele of interest (+/−).
19. The population of F1 animals will likely exhibit many different mutant alleles as well as the wild-type allele. To ensure that a loss of function allele is identified, screen for and identify specific alleles for downstream functional characterization (*see* **Note 65**).
20. Feed and raise F1 progeny from populations that showed genotypic evidence of desired mutant alleles (*see* **Note 66**).

21. When F1 animals mature to the juvenile polyp stage (6–8 tentacle), separate individuals into wells of a six-well tissue culture plate.
22. Cut 1–2 tentacles from each animal and transfer cut tissue to PCR tube for genotypic identification of specific mutant alleles. Be sure to maintain correlating information between tissue sample and animal (*see* **Note 67**).
23. Lyse tissue in 15 μL lysis buffer by incubating at 65 °C for 3 h followed by 98 °C for 3 min (*see* **Note 68**).
24. Perform a 50 μL PCR reaction on each sample with specific forward and reverse primers to amplify the target cut site and surrounding genomic region.
25. Run 2 μL of each PCR product on a gel.
26. Note reactions with a band of the correct size.
27. Ligate PCR products of correct size into a cloning vector.
28. Amplify 4–8 copies of the vector by liquid bacterial cultures.
29. Perform miniprep of liquid cultures per manufacturer's suggestions to isolate plasmid DNA containing genomic PCR insert of interest.
30. Identify heterozygous carriers of mutant allele by Sanger sequencing (*see* **Note 69**).
31. Continue raising F1 progeny with sequence-confirmed mutant alleles until sexual maturity (*see* **Note 70**).
32. Identify F1 heterozygous animals of different sexes that carry the same mutant allele.
33. If unable to identify F1 heterozygous animals of different sexes that carry the same allele, trans-heterozygous crosses of different mutant alleles of same gene can also be informative for gene function and phenotypic specificity (*see* **Note 71**).
34. Spawn animals and cross to generate F2 animals.
35. Separate individual F2 embryos and quantify morphological phenotypes. For a recessive mutant allele, approximately 25% of F2 animals should be homozygous mutant for the genomic region of interest (*see* **Note 72**).
36. Perform genotypic analysis of phenotypically quantified F2 animals by repeating **steps 4–13** to identify homozygous mutant animals and confirm mendelian segregation. Be sure to maintain individual information to correlate genotypic and phenotypic information (*see* **Notes 73** and **74**).
37. Heterozygous F1 founders as well as heterozygous or homozygous F2 animals (and any generations beyond) can be maintained for future experiments or to share with other researchers (*see* **Notes 75** and **76**).

4 Notes

1. The authors prefer the web-based tool siRNA Wizard™ from InvivoGen (https://www.invivogen.com/sirnawizard/design_advanced.php); however, any web-based or downloadable siRNA/shRNA design software should work.
2. Commercially provided buffers that come with DNA polymerase (e.g., New England BioLabs 10× Buffer 2 or 10× Buffer 2.1) will also work.
3. There are currently many websites and offline resources available for designing sgRNAs for use in the CRISPR/Cas9 system. We have had success with "CRISPRscan" and have structured this protocol on the design and output from this specific tool. Other websites should also work in this pipeline however it is important to confirm that the final target-specific sgRNA oligo structure detailed here is maintained.
4. A sex-sorted bowl containing only confirmed sexually mature female *Nematostella* should be used as the source for *Nematostella* eggs.
5. Induction of spawning and de-jellying of eggs have been previously reported in detail in previous protocols [15, 26] and should be consulted prior to the completion of any experimental protocols detailed here.
6. Contamination of eggs during spawning or de-jellying process will result in induction of fertilization prior to completion of experimental manipulations which could have deleterious effects on experimental performance and outcome.
7. It is not critical that the spawning bowl used for sperm water be only male *Nematostella* animals. If egg sacs are present in the spawned male bowl, avoid collecting those egg sacs when transferring sperm water for fertilization.
8. Using a Sutter Model P-97 Horizontal Needle Puller, the following settings can serve as a good starting point for needle production. Heat = Ramp Test Value +15, Pull = 175, Velocity = 90, Time = 50, Pressure = 500.
9. In general, eggs adhere best to polystyrene dishes. However, the authors suggest using BD Falcon—catalog number #351007 for 60 mm dishes specifically for any injection experiments as these dishes have provided consistent and robust egg adherence.
10. FITC is a green, non-toxic, short-term tracer dye which allows direct visualization of the injection mix for up to 5 h inside experimental embryos. This enables control of the injection volume and allows for the easy elimination of un-injected eggs.

Dextran Texas Red™ is a red, non-toxic, long-term tracer dye that will last for at least 7 days within injected animals. However, since it is much harder to visualize injection in the red channel of a fluorescent dissecting scope, it is generally recommended to add FITC to the mixture even when using Dextran as a long-term tracer. Alternatively, Dextran AlexaFluor488 (Thermo Fisher, D34682; Stock Concentration = 8.3 μg/μL) can be used as single long-term dye that works well for injection. However, it should be noted that primary polyps frequently exhibit endogenous green autofluorescence surrounding the pharynx which may make long-term labeling with this green dextran conjugates less ideal for many experiments.

11. Polysucrose 400 can be difficult to dissolve for the Electroporation Solution. Heating can help or the solution can be left to nutate overnight. The Electroporation Solution should be clear and transparent [15].
12. Double check the accuracy of the annotated gene model for your genomic locus or mRNA sequence by PCR or by cross-referencing with published RNA-seq results. shRNAs designed within intronic regions or against exon–intron junctions typically exhibit no knockdown effect.
13. Most shRNA design tools will provide many candidate shRNA sequences. Select for shRNA sequences with the following features: (1) overall GC content between 40% and 55%; (2) low 3′ GC percentage; and (3) reasonable sequence complexity, as defined as a Shannon entropy value greater than or equal to 2 (many shRNA design algorithms will perform this part of the selection automatically, but if unsure, there are webtools (e.g., https://planetcalc.com/2476/) that can be helpful in quantifying this value).
14. Sequences starting with GG or GGG usually have higher yields than sequences starting with GN. This is due to the nature of the T7 RNA polymerase. The composition of the initial sequence, however, does not seem to affect the effectiveness of shRNA.
15. At the time of publication, the most readily accessible genomic resources for *Nematostella vectensis* through the Joint Genome Institute (https://mycocosm.jgi.doe.gov/Nemve1/Nemve1.home.html). Originally published in 2007 [27], this genome is a powerful resource for the identification of putative gene homologs and has served the field well for over a decade. However, users should also be mindful that this genome assembly is non-contiguous, containing reads from numerous individual animal genotypes and existing across almost 11,000 scaffolds and, therefore, potentially imperfect in some of its

more formal annotations. As improved genomic resources for *Nematostella vectensis* emerge, this protocol can and should be used with the most up-to-date and trusted assemblies.

16. We suggest designing 3–5 candidate sequences to try to increase the likelihood of finding 2 or more shRNAs that specifically and effectively knockdown the target gene of interest.
17. A brief summary of each component of the gene-specific oligos and their functional importance. 5′-AA: after in vitro transcription, this generates a 3′-UU overhang, which mimics the terminator sequence of endogenous pre-microRNA. The 9 nt loop sequence, TCTCTTGAA , was first designed by Brummelkamp et al. (2002) and is crucial for shRNAs to be recognized and cleaved by the Dicer complex in vivo [28]. The 3′ sequence, TATAGTGAGT, reverse complements part of the T7 promoter sequence, enabling the Klenow reaction to generate a double-stranded DNA template for in vitro transcription.
18. Gene-specific oligonucleotides should be exactly 59 bp long, which is below the length limit for standard oligonucleotide synthesis reactions of most companies, reducing costs.
19. Make sure all components of the kit (with the exception of the T7 polymerase and RNase Inhibitor) are thawed to room temperature before use. The 10× transcription buffers can sometimes form a white precipitate at the bottom of the tube during this process. Vortex or invert the tube to completely dissolve the precipitant before adding the buffer to the reaction mix. Add all components according to the order listed in the manufacturer's protocol. Due to the high salt concentration in the T7 reaction buffer, NTPs will precipitate if they are added to the buffer directly. Instead, add the reaction buffer last before adding the enzyme and quickly pipette to ensure homogenous distribution of the buffer without precipitating NTPs. If precipitation is observed in the transcription reaction mix, heat the mixture to 37 °C for 5–10 min then proceed with in vitro transcription reaction preparation and incubation.
20. Incubation beyond 5 h does not significantly increase production yield for most commercially available kits. However, the reaction can be kept in the thermocycler at 4 °C overnight.
21. By the end of the in vitro transcription reaction, white precipitate is frequently visible at the bottom of the tube. When adding the RNase-free DNaseI, make sure to pipette until the precipitate forms an even suspension.
22. The kit suggests using any type of TRI reagent® (TRIzol®, RNAzol®, QIAzol®, etc.) for transcription reaction purification, which we found to be optional in the case of shRNA. In

fact, incomplete removal of the TRI reagent can affect the quality of shRNA (an abnormally low 260/280 reading) and result in injection toxicity. If the user decides to use TRI reagent®, simply expand the reaction to 100 μL and add 300 μL of TRI reagent®. Mix well and add another 400 μL of 100% ethanol before proceeding according to the instruction from the kit. If no TRI reagent® is being used, the user can safely skip the first two washes with RNA prewash buffer as detailed in this protocol. Empirical testing in our laboratory of RNA purification of IVT reactions described here have shown no significant reduction in product yield when omitting the TRI reagent®; however, individual users may want to confirm this on their own.

23. The concentration of shRNA by spectrophotometer after purification is usually 2000–3500 ng/μL, with a 260/280 ration above 1.9. A single transcription reaction typically yields a total of 60–100 μg of shRNA. This is sufficient for 50–100 rounds of injection or at least 1 round of electroporation, depending on the concentration needed.
24. Bubbles in the injection mix can impair injection efficiency. If any bubbles are present in the mixture after loading, attempt to remove them by gently agitating the needle prior to mounting on microinjector. If bubbles cannot be eliminated, reload a new needle.
25. For injection, gently eject de-jellied eggs from a transfer pipet into a 60-mm polystyrene dish filled with 12 ppt ASW and allow them to adhere on their own. Eggs will only adhere once, so be careful not to jostle them once plated.
26. For initial needle trimming, trim needle tip just above to the "curvy" part that forms during pulling. A well-trimmed needle should show minimal wavering when moved.
27. This calibration protocol is based on an injection volume of approximately 60–80 pL per egg, or ~1.5% total egg volume. Empirically, we have defined this as a 5 μm diameter bubble as measured by injecting into a drop of mineral oil on top of a 0.01 mm micrometer (diameter of 5 hashmarks).
28. Microinjector setting will need to be determined on each machine and each injection session. Typical starting settings for an Eppendorf Femtojet are within the following ranges and could serve as a starting point for all microinjector models: injection pressure: 400–1200 hectopascals (hPa); injection duration: 0.1–0.7 s; compensation pressure: 5–30 hPa. In all instances, increasing a parameter increases injection volume and bubble size. "Injection Duration" seems to be the condition that can be most readily changed without damage to eggs.

29. Additionally, to achieve and maintain the ~80 pL target volume while keeping the needle opening as narrow as possible, we regularly clean the needle using the microinjector "Clean" function, raising the needle out of the water, and by gently scraping the side of the needle using jeweler's forceps. It is important to be careful not to trim or damage the needle once it is calibrated. If the needle is damaged or trimmed, recalibration will need to be performed.
30. Electroporation of shRNA can also be performed on unfertilized eggs if desired. This can be particularly helpful if you are unsure of sperm quality/amount or wish to fertilize with multiple different male animals. If using unfertilized eggs, the protocol is the same except plenty of sperm water from the spawned males should be used for egg transfer and added to each dish following electroporation at **step 21** in Subheading 3.3.
31. The volume of egg suspension in electroporation solution should be determined by the number of electroporation experiments to be performed. In general, it is good to aim for at least 200 eggs in a volume of 100 μL for each electroporation experiment. For example, for three experiments, at least 500 μL of eggs in electroporation solution would be needed (including controls).
32. The purpose of the polysucrose 400 supplement is to keep eggs in suspension for optimal electroporation. However, even with this supplement added, eggs can still settle to the bottom of the tube. If this happens, gently tap or rock the tube to resuspend the eggs.
33. Electroporation requires substantially more shRNA than microinjection as the total delivery volume is ~100 μL (i.e., 300 ng/μL × 100 μL = 30 μg total). shRNA concentrations less than 2000 ng/μL are likely not sufficiently concentrated for electroporation. Consider repeating IVT with a smaller elution volume.
34. These electroporation conditions have been experimentally validated for shRNA delivery into *Nematostella* eggs. Electroporation conditions for other stages of development in *Nematostella* have not been determined at time of this publication. Recently, parameters were reported for the electroporation of shRNA into the eggs of another Cnidarian, *Hydractinia symbiolongicarpus* [25], suggesting this could be a useful means of shRNA delivery in all Cnidarians.
35. In addition to visual check in **step 18** Subheading 3.3, some eggs should be morphologically abnormal (resembling the shmoo of a fission yeast) following transfer into a 60-mm petri dish. This is expected and a good sign that the eggs

were successfully electroporated. Eggs should recover and return to normal morphology within 30–60 min.

36. All *Nematostella* eggs can fuse during early embryogenesis, but electroporated eggs seem to be more prone to fusion than non-electroporated. For this reason, it is important to be sure to disperse the eggs throughout the dish prior to overnight incubation.
37. Even under normal conditions, a certain percentage of *Nematostella* larvae and juveniles will look abnormal. It is recommended to keep a dish of non-injected or non-electroporated wild-type embryos as a negative biological control. Multiple shRNAs targeting the same gene should consistently result in similar phenotypes with high penetrance in comparison to the negative technical control of non-targeted shRNA injection. Additionally, delivery of shRNA can sometimes result in a slight delay of embryogenesis compared to untreated controls.
38. *Nematostella* embryogenesis and development to the primary polyp stage takes approximately 7 days at room temperature (22 °C). Information regarding the expression pattern and expression level of the gene of interest (in situ hybridization, qPCR, or cross-referencing published RNA-seq results) can be extremely helpful when considering when and where to focus on potential phenotypes.
39. If no phenotypes are readily apparent, we have observed that higher shRNA concentrations are more effective at knocking down genes expressed at later stages of development or at very high levels. At room temperature, gene knockdown by shRNA typically does not last longer than 7–10 days. If the gene of interest is expressed at the late stages of larval development or at primary polyp stage, shRNA injection may not have an effect, and it may be better to consider CRISPR/Cas9-targeted mutagenesis.
40. Different genes may exhibit different sensitivity toward shRNA knockdown. Interestingly, shRNA does not cause obvious toxicity. Even when embryos were injected with 1500 ng/μL shRNA, >80% of injected embryos were viable. The exact working concentration for each shRNA may have to be determined empirically. We have observed gene-specific phenotypes at shRNA concentrations ranging from 100 to 1500 ng/μL.
41. It can also be helpful to have primer sequences to generate positive and negative control shRNAs, their working concentrations, and observable phenotype [11, 15]:

    shAnthox1a_R:

    5′-AAGGTCTGACGACGAATGTGATCTCTTGAATCACATTCGTCGTCAGACCTATAGTGAGT-3′;

Working injection concentration: 500 ng/μL;
Working electroporation concentration: 900 ng/μL;
Observable phenotype: loss of endodermal segment s5, tentacle fusion at polyp stage.

shβ-catenin_R:

5′- AAGTGGCACCAAACGTATCATTCTCTTGAAAT GATACGTTTGGTGCCACTATAGTGAGT-3′;
Working injection concentration: 100 ng/μL;
Working electroporation concentration: 300 ng/μL;
Observable phenotype: gastrulation failure, disruption of epithelial tissue and lethal at 4 dpf.

sheGFP_R:

5′- AAGACGTAAACGGCCACAAGTTCTCTT GAAACTTGTGGCCGTTTACGTCTATAGTGAGT-3′;
Working injection concentration: 100–1000 ng/μL;
Working electroporation concentration: 200 ng/μL;
Observable phenotype: reduction of GFP in transgenic animals. Knockdown effect lasts to 7 dpf when used at 1000 ng/μL.

Scrambled_R:

5′- AAGCAACACGCAGAGTCGTAATCTCTTGAAT TACGACTCTGCGTGTTGCTATAGTGAGT-3′;
Working concentration: negative control, always match your test shRNA;
Observable phenotype: no observable phenotype when used under 1500 ng/μL. Slight developmental delay when used at 2000 ng/μL.

42. If possible, it can be a good idea to double check the accuracy of a genomic locus by PCR. Additionally, be aware of potential exon-intron boundaries as these are typically not ideal candidates to target for mutagenesis for functional analysis of gene function.
43. The T7 promoter sequence (TAATACGACTCACTATA) at 5′ end is to allow for amplification of sgRNA by T7 RNA polymerase. Reverse complement of universal sgRNA tail oligo (G TTTTAGAGCTAGAA) is located 3′ to the target-specific sequence and allows for DNA template production suitable for IVT by Klenow reaction.
44. Selecting "Sea anemone- *Nematostella vectensis"* from the drop-down menu will use JGI genome sequence information to detect potential off-target effects. However, if the *exact* sequence is not found in the JGI genome version (perhaps due to SNPs), CRISPRscan will display an error message.
45. CRISPRscan is a predictive algorithm designed to predict in vivo cutting efficacy from previous data generated using

>1000 sgRNAs injected in zebrafish [14]. sgRNAs are given scores to predict their ability to cut genomic DNA. Scores above 0.55 are termed "efficient for cutting" and above 0.70 are called "highly efficient for cutting *(17)*." In general, the direct correlation between CRISPRscan score and cutting efficiency holds true in *Nematostella*. However, it is worth noting that we have seen productive mutagenesis using sgRNAs with scores as low as 40 and when considering which sgRNA to use, the genomic location of the target with regard to ideal site for the experiment should be weighted more heavily than a CRISPRscan score. Both canonical ("GG18") and non-canonical ("Gg18," "GG17," etc.) will work for cutting [14].

46. If attempting to create frameshift mutations by non-homologous end-joining, choose 3–4 sgRNAs close to the start codon of the gene, within a known promoter region, or within the DNA sequence for key protein domains. sgRNAs targeting regions far from the transcription start site may be more likely to leave active or partially active gene products.
47. "Sea anemone—*Nematostella vectensis*" can be selected from the species dropdown menu on the CRISPRscan website genome; however, this source has no annotated information from the JGI genome and can only be used to show potential off target effects by sequence similarity, not to confirm functionality of a sgRNA target site.
48. A spectrophotometer could also be used to quantify sgRNA concentration. However, in practice, we typically use a fluorometer and high-abundance RNA detection kit for sgRNA measurement as this method is more sensitive and sgRNAs as RNPs appear more toxic than shRNAs.
49. Ideally, the original concentration should be above 2500 ng/μL. Additionally, if desired, sgRNA integrity can be check by electrophoresis. A clear ~100 bp band should appear for a good quality sgRNA.
50. sgRNA/Cas9 protein mixtures can be reused at least two times if stored at −80 °C.
51. Lower temperatures may be better for embryo survival, but the mutation rate of Cas9 protein increases with temperature. We have tried culturing embryos at temperatures as high as 29 °C and seen productive cutting. *See* Table 1 for additional information.
52. It can be helpful to reference expression data for the targeted gene of interest when determining the best plan for observing phenotypes. shRNA knockdown data can also be helpful in this pursuit. However, as sgRNA/Cas9 animals will be mosaic, not

all individuals harboring mutant alleles will show a phenotype as F0 animals.

53. If injected embryos present with very low viability (10% survival) the day after injection, consider reducing the concentration of Cas9 protein in the RNP injection mixture. If injected embryos present with very high viability (>90% or similar to un-injected controls), consider increasing sgRNA concentrations as cutting may be low. A measurable reduction in viability can be a good indicator of efficient DNA cutting. *See* Table 1 for more information.
54. The volume of lysis buffer can range from 5 to 15 μL depending on the developmental stage. In general, embryonic stages (blastula or gastrula) will require less lysis buffer (5–10 μL) than later planula or primary polyp stages (12–15 μL).
55. Check tubes for any remaining tissue. If intact tissue is still present, pipette vigorously to help with lysis or, if that fails, incubate longer (up to overnight) at 65 °C.
56. This step DOES NOT identify a specific allele or alleles present in the F0. Instead, this is a simple test to see if any evidence of genome cutting can be detected at the target site. Always compare sgRNA/Cas9-injected samples to *wild-type* or control-injected samples from the same experiment as SNPs or other natural genomic heterogeneity can exist in *Nematostella*. There are programs that can be used to try and predict the most prevalent mutant allele (i.e., TIDE, ICE, etc.), if desired. At this stage, the most important goal is to detect efficient DNA cutting. If allele-specific information is required at this stage, we would suggest cloning the PCR product into a cloning vector and sequencing many colonies (at least 12–16 colonies/PCR sample) from the resulting transformed bacteria. Ideal candidates for loss-of-function alleles are nonsense mutations that introduce a premature stop codon or large insertion or deletions that disrupt codon usage (e.g., insertions or deletions of a number of base pairs indivisible by 3). It should be noted though that presence or absence of a specific allele at this stage does not guarantee transmission to the F1 generation.
57. It can be helpful to sort out the animals that present with a visible phenotype that is correlated with a genotype and see if they grow. Phenotypically abnormal animals are good candidates for transmission if the phenotype does not disrupt growth and sexual maturation.
58. It can be helpful to use positive and negative control sgRNA examples when beginning CRISPR/Cas9-targeted mutagenesis. The following examples are from published work and adapted for the protocol described here as necessary

[11, 29]. It should be noted that different genomic loci very regularly require individually optimized injection mixtures.

eGFP sgRNA (negative control for wild type animals):

5′-taatacgactcactataGGTCAGGGTGGTCACGAGGGgttttagagctagaa-3′;

Working sgRNA injection concentration: 250–500 ng/μL;

Working Cas9 protein injection concentration: 500 ng/μL;

Observable F0 phenotype: No observable phenotype in wild-type animals; reduction or loss of fluorescent protein expression in GFP transgenic lines [11].

eGFP genotyping oligo Forward: 5′- AAGGCGTTATGGTCGGTATG-3′

eGFP genotyping oligo Reverse: 5′-TGCTTGTCGGCCATGATATAG-3′,

APC (positive control for wild-type animals):

5′-taatacgactcactataGGGGGGCCCTAGTCAGCAGGgttttagagctagaa-3′;

Working sgRNA injection concentration: 500 ng/μL;

Working Cas9 protein concentration: 500 ng/μL;

Observable F0 phenotype: Formation of ectopic oral structures (tentacles and pharynx) at primary polyp stage, 7–10 dpf [27].

APC genotyping oligo Forward: 5′- AGAATCCTGCAGAAGATGAACA-3′

APC genotyping oligo Reverse: 5′- CCTGGCATACAAAGGTGACA-3’.

59. In general, it is a good practice to attempt increasing sgRNA concentration before Cas9 protein to limit nonspecific toxicity as well as maintain an easy to work with RNP injection mixture. If increased sgRNA concentration alone does not increase genomic mutagenesis, increase both sgRNA and Cas9 protein. If injected embryo survival is significantly affected (0–20% viability), reduce Cas9 protein concentration until embryo viability returns to approximately 50% survival. The inherent differences in RNP cutting efficiency is why it is always best to start with 3–5 sgRNAs for the same target gene of interest.

60. Cas9 recombinant protein is the first choice for targeted mutagenesis as high levels of nonspecific toxicity is observed with the injection of *Cas9* mRNA. However, in instances where no phenotypes were observed with the injection of Cas9 protein, the injection of mRNA has resulted in targeted mutations. If you consistently see no DNA cutting across a range of sgRNA/Cas9 protein conditions, consider using *Cas9* mRNA. Both

zebrafish codon-optimized *Cas9* mRNA and *Nematostella* codon-optimized *Cas9* mRNA are functional in *Nematostella* embryos. *Nematostella* codon-optimized *Cas9* mRNA exhibits mutagenesis rates similar to Cas9 protein and higher than the zebrafish codon-optimized version. However, again, it must be stressed that toxicity is often high with any *Cas9* mRNA. *See* Table 1 for additional information.

61. *Nematostella vectensis* codon-optimized Cas9 was designed by computationally determining the codon usage rate for each amino acid from the coding regions of all transcripts found in published *Nematostella* transcriptomes. Each codon in the Cas9 CDS was replaced with the most-frequently occurring codon for that amino acid, as determined above.
62. Omit **step 1** from Subheading 3.6 as no pre-injection incubation is necessary if using *Cas9* mRNA.
63. At **step 4** in Subheading 3.6, store injection mixtures containing any *Cas9* mRNA on ice until use.
64. At **step 9** in Subheading 3.6, incubate *Cas9* mRNA injected embryos at 18 °C for higher viability.
65. If desired, F1 embryos can undergo same genotypic analysis as done previously for F0 animals (**steps 4–13** from Subheading 3.7). Base-calling may not be as reduced at target site as with F0 mosaic animals, but if a mutation has been transmitted sequencing errors should still be frequent after the target site. Again, this type of analysis is only to determine if any genomic editing has occurred. Specific alleles are not likely to be identified by this step.
66. Make note and continue to care for any F0 animals that transmitted mutant alleles to their F1 progeny. Transmitting F0 animals can be useful to generate additional F1 animals for genotypic screening or for preliminary experiments.
67. Other small amounts of adult tissue, such as part of the physa, can be used for genotyping if desired. However, it is important that the animal is still able to continue feeding and growing after tissue is taken.
68. Adult tissue takes longer to lyse than tissue from earlier developmental stages. If tissue is not completely lysed following incubation, mix vigorously with a pipette and/or incubate sample longer.
69. This is the step where specific mutant alleles will be identified. We suggest sequencing at least four colonies as this will give you an approximately 95% probability of identifying a mutant allele if present ($(1 - (0.5)^4) \times 100\% = 93.75\%$). Sequencing eight colonies gives a > 99% probability of identifying a potential mutant allele ($(1 - (0.5)^8) \times 100\% = 99.61\%$).

70. It is a good practice to raise more than one mutant allele if possible. This will increase the likelihood of identifying a loss of function mutation. Additionally, testing multiple alleles that show the same phenotype confirms specificity.
71. Trans-heterozygous crosses cross can be performed with F1 founder animals of different mutant alleles or even transmitting F0 animals. However, if crossing transmitting F0 animals, genotypic analysis must be performed following the cloning of the allelic PCR into a plasmid, as in **steps 17–25** from Subheading 3.7, except using embryonic tissue instead of juvenile/adult tissue for DNA extraction.
72. Based on F0 mutagenesis, shRNA knockdown or other experiments, a more detailed phenotypic analysis by immunohistochemistry or in situ hybridization analysis may be desired. We have successfully extracted DNA for PCR from samples post-antibody staining and post-in situ hybridization using the protocol described here in **steps 4–13** from Subheading 3.7.
73. A quantitative phenotypic analysis and corresponding genotypic confirmation of phenotype at F2 generation is the gold standard of all CRISPR/Cas9-targeted mutagenesis experiments. All resulting genotypes of F1 heterozygous cross can be readily identified from Sanger sequencing of a purified PCR product. Homozygous mutant animals will possess only one mutant allele, *wild-type* animals will possess only one non-mutant allele, and heterozygous animals will show loss of base-calling confidence at or after the target site indicating the presence of two alleles.
74. Genotypic and phenotypic analysis will likely need to be performed for each experiment resulting from a F1 heterozygote cross.
75. If homozygous mutants are viable and can become sexually mature, homozygous mutant F2 animals will be most helpful for future experiments as subsequent genotypic analysis is unnecessary.
76. Animals not being actively used can be maintained at room temperature or 18 °C for years with weekly or biweekly feeding. Be sure to always clean 1–2 days after any feeding. For induction of spawning, move animals to 18 °C at least 1 week prior to target spawn date and feed heavily (every 1 or 2 days).

Acknowledgments

We thank all Gibson Lab members past and present for their help in the development and optimization of the protocols detailed here. We thank Mark Miller for illustrations. We also thank the Stowers

Institute Molecular Biology Core, especially Kym Delventhal, MaryEllen Kirkman, and Kyle Weaver, for help with screening design as well as the Stowers Institute Reptile and Aquatics Core facility for animal husbandry help. This study was supported by NIH F32 GM131522 (EMH) and the Stowers Institute for Medical Research (MCG).

References

1. Technau U, Genikhovich G, Kraus JEM (2015) Cnidaria. In: Wanninger A (ed) Evolutionary developmental biology of invertebrates 1. Springer-Verlag, Wien, pp 115–163
2. Genikhovich G, Technau U (2017) On the evolution of bilaterality. Development 144: 3392–3404
3. Technau U, Steele RE (2011) Evolutionary crossroads in developmental biology: Cnidaria. Development 138:1447–1458
4. Layden MJ, Rentzsch F, Röttinger E (2016) The rise of the starlet sea anemone Nematostella vectensis as a model system to investigate development and regeneration. Wiley Interdiscip Rev. Dev Biol 5:408–428
5. Warner JF, Guerlais V, Amiel AR et al (2018) NvERTx: a gene expression database to compare embryogenesis and regeneration in the sea anemone Nematostella vectensis. Development 145:dev162867
6. Amiel AR, Johnston HT, Nedoncelle K et al (2015) Characterization of Morphological and Cellular Events Underlying Oral Regeneration in the Sea Anemone. Nematostella vectensis. Int J Mol Sci 16(28449–28):471
7. Bossert PE, Dunn MP, Thomsen GH (2013) A staging system for the regeneration of a polyp from the aboral physa of the anthozoan Cnidarian Nematostella vectensis. Dev Dyn 242: 1320–1331
8. Passamaneck YJ, Martindale MQ (2012) Cell proliferation is necessary for the regeneration of oral structures in the anthozoan cnidarian Nematostella vectensis. BMC Dev Biol 12:34
9. Bossert P, Thomsen GH (2017) Inducing Complete Polyp Regeneration from the Aboral Physa of the Starlet Sea Anemone Nematostella vectensis. J Vis Exp 119:e54626
10. Bely AE, Nyberg KG (2010) Evolution of animal regeneration: re-emergence of a field. Trends Ecol Evol 25:161–170
11. He S, del Viso F, Chen C-Y et al (2018) An axial Hox code controls tissue segmentation and body patterning in Nematostella vectensis. Science 361:1377–1380
12. Moran Y, Fredman D, Praher D et al (2014) Cnidarian microRNAs frequently regulate targets by cleavage. Genome Res 24:651–663
13. Moran Y, Agron M, Praher D et al (2017) The evolutionary origin of plant and animal microRNAs. Nat Ecol Evol 1:0027
14. Karabulut A, He S, Chen C-Y et al (2019) Electroporation of short hairpin RNAs for rapid and efficient gene knockdown in the starlet sea anemone, Nematostella vectensis. Dev Biol 448:7–15
15. Ikmi A, McKinney SA, Delventhal KM et al (2014) TALEN and CRISPR/Cas9-mediated genome editing in the early-branching metazoan Nematostella vectensis. Nat Commun 5: 5486
16. Moreno-Mateos MA, Vejnar CE, Beaudoin J-D et al (2015) CRISPRscan: designing highly efficient sgRNAs for CRISPR-Cas9 targeting in vivo. Nat Methods 12:982–988
17. Vejnar CE, Moreno-Mateos MA, Cifuentes D et al (2016) Optimized CRISPR-Cas9 system for genome editing in zebrafish. Cold Spring Harb Protoc 2016(10). https://doi.org/10.1101/pdb.prot086850
18. Jao L-E, Wente SR, Chen W (2013) Efficient multiplex biallelic zebrafish genome editing using a CRISPR nuclease system. Proc Natl Acad Sci U S A 110(13904–13):909
19. Sunagar K, Columbus-Shenkar YY, Fridrich A et al (2018) Cell type-specific expression profiling unravels the development and evolution of stinging cells in sea anemone. BMC Biol 16:108
20. Xu T, Rubin GM (1993) Analysis of genetic mosaics in developing and adult Drosophila tissues. Development 117:1223–1237
21. Golic KG, Lindquist S (1989) The FLP recombinase of yeast catalyzes site-specific recombination in the drosophila genome. Cell 59:499–509
22. Dang DT, Perrimon N (1992) Use of a yeast site-specific recombinase to generate embryonic mosaics in Drosophila. Dev Genet 13: 367–375

23. Lakso M, Sauer B, Mosinger B et al (1992) Targeted oncogene activation by site-specific recombination in transgenic mice. Proc Natl Acad Sci U S A 89:6232–6236
24. Orban PC, Chui D, Marth JD (1992) Tissue- and site-specific DNA recombination in transgenic mice. Proc Natl Acad Sci U S A 89:6861–6865
25. Quiroga-Artigas G, Duscher A, Lundquist K et al (2020) Gene knockdown via electroporation of short hairpin RNAs in embryos of the marine hydroid Hydractinia symbiolongicarpus. Sci Rep 10:12806
26. Genikhovich G, Technau U (2009) Induction of spawning in the starlet sea anemone Nematostella vectensis, in vitro fertilization of gametes, and dejellying of zygotes. Cold Spring Harb Protoc 2009(9). https://doi.org/10.1101/pdb.prot5281
27. Putnam NH, Srivastava M, Hellsten U et al (2007) Sea anemone genome reveals ancestral eumetazoan gene repertoire and genomic organization. Science 317:86–94
28. Brummelkamp TR, Bernards R, Agami R (2002) A System for Stable Expression of Short Interfering RNAs in Mammalian Cells. Science 296:550–553
29. Kraus Y, Aman A, Technau U et al (2016) Pre-bilaterian origin of the blastoporal axial organizer. Nat Commun 7:11694

Open Access This chapter is licensed under the terms of the Creative Commons Attribution 4.0 International License (http://creativecommons.org/licenses/by/4.0/), which permits use, sharing, adaptation, distribution and reproduction in any medium or format, as long as you give appropriate credit to the original author(s) and the source, provide a link to the Creative Commons license and indicate if changes were made.

The images or other third party material in this chapter are included in the chapter's Creative Commons license, unless indicated otherwise in a credit line to the material. If material is not included in the chapter's Creative Commons license and your intended use is not permitted by statutory regulation or exceeds the permitted use, you will need to obtain permission directly from the copyright holder.





Chapter 24

Monitoring Telomere Maintenance During Regeneration of Annelids

Nithila A. Joseph, Chi-Fan Chen, Jiun-Hong Chen, and Liuh-Yow Chen

Abstract

Telomere shortening is a hallmark of aging and eventually constrains the proliferative capacity of cells. The protocols discussed here are used for monitoring telomeres comprehensively in *Aeolosoma viride*, a model system for regeneration studies. We present methods for analyzing the activity of telomerase enzyme in regenerating tissue by telomeric repeat amplification protocol (TRAP) assay, for comparing telomere length between existing tissue and newly regenerated tissue by telomere restriction fragment (TRF) assay, as well as for visualizing telomeres by fluorescence in situ hybridization (FISH).

Key words *Aeolosoma viride*, Telomere maintenance, Regeneration, TRAP assay, TRF assay, Telomere FISH

1 Introduction

Regeneration aids in repairing or rebuilding damaged tissue or entire body parts in animals. The ability to regenerate is not uniform among animals. For instance, metazoans like planarians can regenerate entirely with symmetry and proportion from tiny fragments of their existing body using adult somatic stem cells called neoblasts [1]. Advanced mammals like humans can only regenerate certain body parts like liver after partial resection [2]. Salamanders like axolotls and newts can regenerate several body parts including limbs or tail by activating progenitor cells [3]. While axolotls lose the ability to regenerate eye lens around 2 weeks after birth, newts can regenerate lens without being limited by age [4]. Observations akin to this implicate aging as one of the factors that affect regeneration potential. Although the real mechanism of how age affects wound healing and regeneration is not clear, most people accept that wound healing is affected by aging.

This raises questions about the aging situation of the regenerated tissues. Are the regenerated tissues similar to the existing tissue or younger than them? Does regeneration evoke rejuvenation?

Simon Blanchoud and Brigitte Galliot (eds.), *Whole-Body Regeneration: Methods and Protocols*,
Methods in Molecular Biology, vol. 2450, https://doi.org/10.1007/978-1-0716-2172-1_24, © The Author(s) 2022

Aging is a complicated life phenomenon, and it is quite difficult to evaluate the age of animals especially that of invertebrates. Length of telomere, one of characteristics to realize aging in animals, was chosen as the parameter to figure out the relationship between aging and regeneration. The inability of DNA replication mechanism to fully replicate the lagging strand of chromosomes causes progressive shortening of telomeres [5].

Telomerase is a ribonucleoprotein composed of TERC (RNA component) and TERT (reverse transcriptase) to lengthen telomeres. Expression of telomerase is varied among organisms. Remarkably, certain species of animals with good regenerative ability have upregulated telomerase expression [6, 7]. Also, regenerative ability waning with age supports the notion that shorter telomeres contribute to diminished proliferation.

Established model animals for regeneration studies, such as amphibians and reptiles, usually have long life spans, which disallows the exploration of age as a factor restricting regeneration. To circumvent this problem, we used *Aeolosoma viride*, a freshwater annelid as a new model for regeneration and aging-related research. Annelids are well known for their ability to restore anterior and posterior ends from few of their body segments. Lifespan of *A. viride* is approximately 2 months, making it an appealing model for aging-related study.

A. viride of varying age groups when observed for regeneration showed that regeneration declines as age of the worm increases [8]. Telomere length was maintained at the regeneration sites after amputation of the head [8].

Here, we describe protocols to monitor the telomere maintenance in *A. viride* during tissue regeneration. We discuss three main strategies: (1) PCR-based telomeric repeat amplification protocol (TRAP) assay for analyzing the activity of telomerase in regenerating sites (2). Telomere restriction fragment (TRF) assay (3). Telomere fluorescence in situ hybridization (FISH).

2 Materials

All solutions are prepared using filtered and deionized ultrapure water at room temperature (RT) and analytical grade reagents (unless otherwise indicated).

2.1 Telomeric Repeat Amplification Protocol (TRAP) Assay

1. Regenerating *Aeolosoma viride*.
2. Artificial spring water (ASW): 48 mg/L $NaHCO_3$, 24 mg/L $CaSO_4 \cdot 2H_2O$, 30 mg/L $MgSO_4 \cdot 7H_2O$, 2 mg/L KCl in ddH_2O.
3. Telomerase detection kit (e.g., TRAPeze, Millipore).

4. 1× CHAPS lysis buffer: 10 mM Tris–HCl, pH 7.5, 1 mM $MgCl_2$, 1 mM EGTA, 0.1 mM benzamidine, 5 mM β-mercaptoethanol, 0.5% (v/v) 3-[(3-cholamidopropyl) dimethylammonio]-1-propanesulfonate (CHAPS), 10% (v/v) glycerol. Store at −20 °C.
5. Total protein concentration kit (e.g., Bradford reagent).
6. 10× TRAP reaction buffer: 200 mM Tris–HCl, pH 8.3, 15 mM $MgCl_2$, 630 mM KCl, 0.5% (v/v) Tween 20, 10 mM EGTA. Store at −20 °C.
7. 50× dNTP mix: 2.5 mM each of dATP, dTTP, dGTP, dCTP. Store at −20 °C.
8. TS primer. Store at −20 °C (*see* **Note 1**).
9. TRAP primer mix: reverse primer (RP), internal control forward primer (e.g., FP K1 in TRAPeze, Millipore), internal control template (e.g., TSK1 in TRAPeze, Millipore) (*see* **Note 2**). Store at −20 °C.
10. PCR grade water: protease, DNase and RNase free deionized water. Store at −20 °C.
11. DNA polymerase (e.g., Platinum™ Taq, Invitrogen). Store at −20 °C (*see* **Note 3**).
12. Acrylamide solution: 40% acrylamide/bis-acrylamide 19:1 (e.g., Bio-Rad).
13. Tetramethylethylenediamine (TEMED).
14. 10% (w/v) Ammonium persulfate (APS).
15. 0.5 M ethylenediaminetetraacetic acid (EDTA): 186.1 g disodium EDTA in 800 mL ddH_2O. Adjust pH to 8.0 with NaOH to completely dissolve EDTA.
16. 5× TBE solution: 54 g Tris base, 27.5 g boric acid, 20 mL 0.5 M EDTA, pH 8.0 in 1 L ddH_2O. Adjust to pH 8.3 using NaOH.
17. DNA fluorescent loading dye (e.g., FluoroDye™, SMOBIO).
18. 10% (w/v) non-denaturing polyacrylamide gel: 3.75 mL acrylamide solution, 3 mL 5× TBE solution, 200 μL 10% APS, 10 μL tetramethylethylenediamine (TEMED). Bring final volume to 15 mL with ddH_2O.
19. Polyacrylamide gel visualization setup (e.g., FluorChem M system, Protein Simple).

2.2 Terminal Restriction Fragment (TRF) Assay

1. Nuclei lysis buffer (e.g., Wizard Genomic DNA Purification Kit Promega).
2. 4 mg/mL RNase solution.
3. Protein precipitation solution (e.g., Wizard Genomic DNA Purification Kit Promega).

4. Nucleic acid quantification setup (e.g., NanoDrop ND-1000, Thermo Scientific).
5. 50× TAE stock: 242 g Tris base, 600 mL ddH_2O. Add 57.1 mL glacial acetic acid and 100 mL 0.5 M EDTA. Bring final volume to 1 L with ddH_2O.
6. TAE buffer: 20 mL 50× TAE stock, 980 mL ddH_2O.
7. 1% (w/v) agarose gel: 1 g agarose, 100 mL TAE buffer, melt and cool at 60 °C. Add nucleic acid stain according to the manufacturer's instructions. Pour the gel into a gel tank and insert a comb.
8. 6× DNA loading buffer: 30% (v/v) glycerol, 0.25% (w/v) bromophenol blue.
9. *Rsa*I restriction endonuclease.
10. *Hinf*I restriction endonuclease.
11. Restriction enzyme buffer.
12. Depurination solution: 0.25 N HCl.
13. Denaturing solution: 0.5 N NaOH, 1.5 M NaCl.
14. Neutralizing solution: 1.5 M NaCl, 1 M Tris–HCl.
15. Nylon membrane (e.g., Immobilon-Ny + Membrane; Millipore).
16. 10× SSC buffer: 1 M NaCl, 300 mM sodium citrate. Adjust pH to 7.0 by gradually adding HCl, dropwise. Autoclave.
17. UV cross-linker.
18. Hybridization oven.
19. Hybridization tube.
20. Church buffer: 0.5 M $NaPO_4$, 1 mM EDTA, 7% (w/v) sodium dodecyl sulfate (SDS), 1% (w/v) bovine serum albumin (BSA) in nuclease-free water.
21. $(TTAGGG)_4$ and $(CCCTAA)_4$ primers to generate double-stranded $(TTAGGG)_n$.
22. RadPrime™ DNA labeling system (Invitrogen).
23. 20% (w/v) SDS in nuclease-free water.
24. 4× SSC/0.1% SDS: 400 mL 10× SSC, 5 mL 20% SDS, 595 mL ddH_2O.
25. 2× SSC/0.1% SDS: 200 mL 10× SSC, 5 mL 20% SDS, 795 mL ddH_2O.
26. Phosphor screen.

1. 0.02% (w/v) colchicine in ASW.
2. Carnoy's fixative: 750 mL methanol, 250 mL glacial acetic acid.

2.3 Telomere Fluorescence In Situ Hybridization (Telomere FISH)

3. 60% (v/v) acetic acid.
4. 10× phosphate-buffered saline (PBS) stock: 80 g NaCl, 2 g KCl, 14.4 g Na_2HPO_4, 2.4 g KH_2PO_4 in 800 mL ddH_2O. Adjust pH to 7.4 using HCl and bring volume to 1 L with ddH_2O. Autoclave.
5. 1× PBS: 100 mL 10× PBS stock, 900 mL ddH_2O.
6. 4% paraformaldehyde (PFA): 40 g PFA in 800 mL 60 °C heated 1× PBS. Stir, add 1 N NaOH dropwise until PFA is dissolved. Bring volume of solution to 1 L with 1× PBS. Cool the solution and filter sterilize.
7. Hybridization mix: 70% (v/v) formamide, 0.5% (v/v) blocking agent (e.g., Roche), 250 nM $(CCCTAA)_3$ Peptide Nucleic Acid (PNA) probe (e.g., Panagene), 10 mM Tris–HCl, pH 7.5.
8. Wash buffer I: 70% (v/v) formamide, 10 mM Tris–HCl, pH 7.5.
9. Wash buffer II: 150 mM NaCl, 0.08% (v/v) Tween-20, 100 mM Tris–HCl, pH 7.5.
10. Counterstain: 0.3 μM DAPI.
11. Antifading mounting medium (e.g., ProLong® Gold, Molecular Probes).

3 Methods

3.1 Protein Extraction from Regenerating Tissues of Aeolosoma Viride

1. Bisect the anterior most segment of the regenerating site with needles from 100 regenerating annelids.
2. Pool the bisected tissue in ice-cold 1× CHAPS lysis buffer.
3. Homogenize the tissue by pipetting.
4. Incubate on ice for 30 min.
5. Centrifuge at 12,000 rcf for 20 min at 4 °C.
6. Collect the supernatant.
7. Measure the concentration of the total protein extract using the kit.
8. Store protein extract at −80 °C.

3.2 Telomeric Repeat Amplification Protocol (TRAP) Assay

1. Heat inactivate control samples at 85 °C for 10 min (*see* **Note 4**).
2. Set up TRAP reaction with 200 ng of protein extract.
3. Each TRAP reaction contains 2.5 μL of 10× TRAP reaction buffer, 0.5 μL of 50× dNTP mix, 0.5 μL of TS primer, 0.5 μL of TRAP primer mix, 0.2 μL of DNA polymerase and ddH_2O to make up volume to 25 μL.

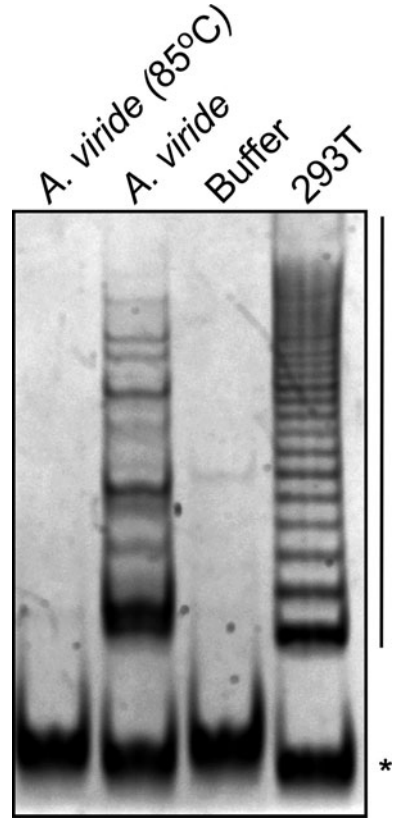


Fig. 1 TRAP assay of *A. viride* extract. Crude and heat-inactivated (85 °C) *A. viride* extracts were used for TRAP reaction. Lysate from human 293 T cells was used for positive control reaction and lysis buffer for negative control reaction. A ladder pattern indicates telomerase-extended products. Asterisk indicates internal control products. (Adapted from [8]).

4. Incubate the reaction mixtures for extension at 30 °C for 30 min.
5. Set up PCR with telomerase extended products by following these conditions: 95 °C for 2 min, 30 cycles of 94 °C for 15 s, 59 °C for 30 s, and 72 °C for 1 min.
6. Mix the PCR products with the DNA loading dye.
7. Resolve the products for 2 h on the 10% polyacrylamide gel at 150 V.
8. Visualize the products by imaging the gel (Fig. 1).
9. Analyze TRAP products (*see* **Note 5**).
10. Use the internal control band as normalization to quantify relative telomerase activity between samples.

3.3 Genomic DNA Extraction from Regenerating Tissues

1. Bisect the most anterior segment from 200 amputated worms with needles at desired time points after amputation.
2. Pool the tissues in 600 μL ice-cold nuclei lysis solution.
3. Store at −20 °C until extraction.
4. Homogenize the tissue in the nuclei lysis buffer with a micropestle.
5. Incubate at 65 °C for 5 min.
6. Mix the tissue lysate with 3 μL RNase solution.
7. Incubate at 37 °C for 5 min.
8. Cool down the sample to RT.
9. Add 200 μL of protein precipitation solution.
10. Mix thoroughly by vortexing.
11. Chill on ice for 5 min.
12. Centrifuge at 13,000 rcf for 4 min to precipitate the proteins.
13. Transfer the supernatant to a new tube.
14. Add an equal volume of isopropanol.
15. Mix by inverting the tube until thread-like aggregates of DNA form.
16. Centrifuge at full speed for 1 min at RT.
17. Discard the supernatant.
18. Add 1 mL of 75% ethanol to wash the DNA pellet.
19. Centrifuge at full speed for 1 min.
20. Remove the supernatant carefully.
21. Air-dry the DNA pellet.
22. Rehydrate by adding 100 μL nuclease-free water.
23. Measure concentration and quality of the isolated DNA.
24. Check DNA integrity by running a 1% agarose gel (*see* **Note 6**).

3.4 Terminal Restriction Fragment (TRF) Assay

1. Digest 700 ng of genomic DNA with 1 U/μL of *Rsa*I and 1 U/μL *Hinf*I at 37 °C overnight.
2. Resolve the digested DNA overnight on 1% agarose gel at 40 volts.
3. Stain the gel with the DNA staining dye.
4. Confirm complete digestion under UV source (*see* **Note 7**).
5. Soak the gel in depurination solution for 15 min.
6. Rinse the gel with ddH_2O to remove HCl.
7. Soak the gel in denaturing solution for 15 min.
8. Rinse with ddH_2O.
9. Soak the gel again in denaturing solution for 15 min.

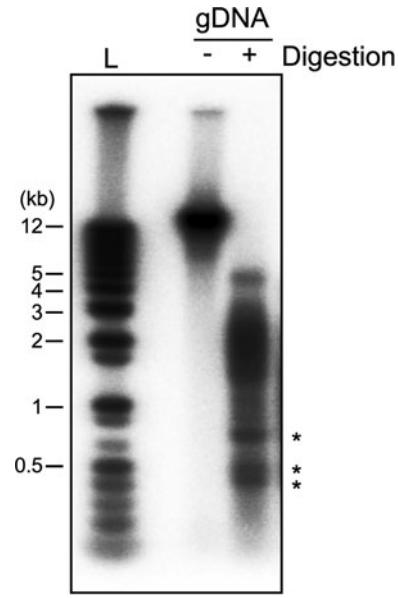


Fig. 2 TRF assay of *A. viride* genomic DNA. Intact (−) and restriction digested (+) genomic DNA were resolved by agarose gel electrophoresis for southern blotting. Restriction fragments of telomeric DNA shows a span of 0.2–5 kb in length. Asterisks indicate internal repetitive sequences. Sizes of selected bands of DNA ladder (L) are indicated on the left. (Adapted from [8]).

10. Rinse with ddH_2O.
11. Soak the gel in neutralizing solution for 15 min, twice.
12. Blot the DNA fragments onto a nylon membrane overnight by capillary transfer in 10× SSC buffer (*see* **Note 8**).
13. Rinse the blotted membrane briefly with 10× SSC buffer.
14. Air-dry the membrane until completely dry.
15. Crosslink by exposing it to 120 mJ/cm^2 UV light.
16. Place the membrane into a hybridization tube containing 45 °C pre-warmed Church buffer.
17. Pre-hybridize at 45 °C for 1 h.
18. While the membrane is incubating, generate double-stranded $(TTAGGG)_n$ DNA by self-priming PCR using $(TTAGGG)_4$ and $(CCCTAA)_4$ primers (*see* **Note 9**).
19. Generate ^{32}P-labeled probes with [α-^{32}P] dCTP using the DNA labeling system.
20. Column purify the probes.
21. Heat the probes for 10 min.
22. Chill on ice.
23. Add 500 µL of fresh Church buffer.

24. Discard the used Church buffer after pre-hybridization.
25. Add 50 mL fresh Church buffer containing double-stranded TTAGGG probe.
26. Hybridize overnight at 50 °C.
27. Discard the used Church buffer and wash the membrane with 4× SSC at 45 °C for 15 min.
28. Discard and wash membrane twice with 4× SSC/0.1% SDS at 45 °C for 15 min.
29. Discard and wash membrane twice with 2× SSC/0.1% SDS at 45 °C for 15 min.
30. Briefly rinse the membrane with 4× SSC and expose membrane to a phosphor screen overnight.
31. Image the phosphor screen (Fig. 2).

3.5 Telomere Fluorescence in Situ Hybridization (Telomere FISH)

1. Treat the regenerating worms with 0.02% colchicine overnight.
2. Place the colchicine-treated worms in distilled water for 20 min to cause hypotonic shock.
3. Harvest the regenerating tails in ice-cold Carnoy's fixative.
4. Incubate on ice for 1 h to fix them.
5. Replace used fixative with fresh fixative.
6. Store the sample at 4 °C overnight.
7. Dissociate the fixed tissue in 60% acetic acid with needles on a coverslip.
8. Place the coverslip on a heating plate at 70 °C for 1 min.
9. Air-dry the coverslip at RT overnight.
10. Rehydrate the sample briefly in 5 mL 1× PBS.
11. Fix in 4% PFA at RT for 10 min.
12. Wash the sample twice in 1× PBS for 30 s.
13. Dehydrate the sample using an ethanol series (70%, 95%, and 100%) for 5 min in each.
14. Air-dry the sample thoroughly.
15. Turn the coverslip upside down and place it over a drop of hybridization mix on a slide.
16. Place the slide on a heating plate at 80 °C for 3 min.
17. Incubate the slide at RT overnight in darkness (*see* **Note 10**).
18. Pick up the coverslip containing the cell spreads and wash by immersing it in wash buffer I twice at RT for 5 min (*see* **Note 11**).
19. Wash the coverslip with wash buffer II thrice at RT for 5 min.
20. Counterstain the sample with 0.3 μM DAPI.

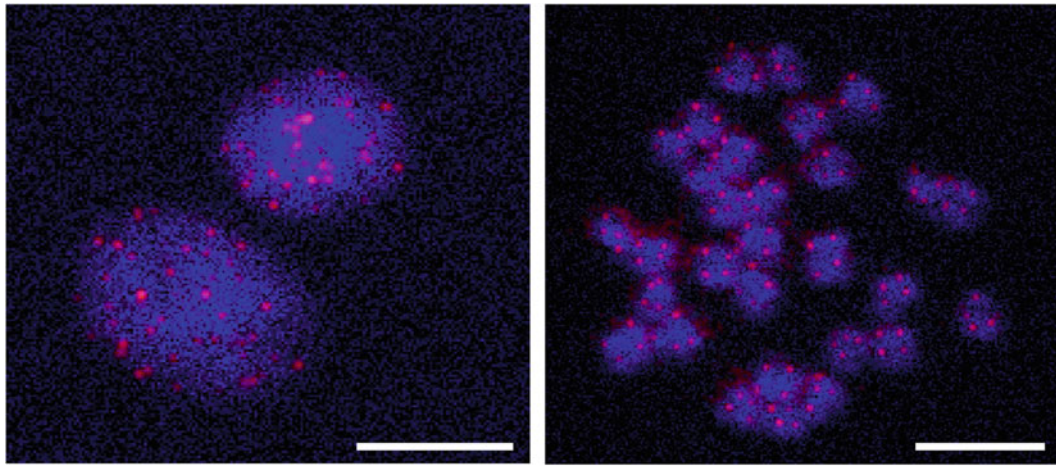


Fig. 3 FISH images of *A. viride* interphase nuclei (left) and metaphase spread (right) stained with telomeric PNA probes (red) and DAPI (blue). Scale bars: 10 μm. (Adapted from [8]).

21. Dehydrate the sample in ethanol series (70%, 95%, and 100%) for 5 min each.
22. Air-dry the sample thoroughly.
23. Mount the sample on a slide in antifade mounting medium.
24. Visualize telomeres with a fluorescence microscope equipped with 63× or 100× objective (Fig. 3) (*see* **Note 12**).

4 Notes

1. TS primer is non-telomeric synthetic oligonucleotide that is recognized by telomerase. If the prepared sample has active telomerase, new "TTAGGG" telomere repeats will be added to the 3′ end of the TS primer. Sequence of TS primer is 5′-AATCCGTCGAGCAGAGTT-3′.
2. Reverse primer (RP) is used in the downstream PCR to amplify the products of extension reaction. Reverse primer is complementary to telomere repeat sequence.

   Additionally, each reaction benefits from the addition of internal controls. This is done by adding a forward primer (e.g., K1in TRAPeze Telomerase Detection Kit) and an internal control template (e.g., TSK1 in TRAPeze Telomerase Detection Kit). Together with the TS primer, K1 and TSK1 amplify an internal control standard (a 36 bp amplicon in TRAPeze Telomerase Detection Kit). The internal control band is an indicator of PCR amplification efficiency.
3. TRAP reaction in its classical form uses a wax barrier to prevent CX primer from mixing with the other reaction components.

This was later simplified by the use of "hot start" Taq DNA-polymerase such as Platinum™ *Taq* DNA polymerase. The "hot start" Taq DNA-polymerase enzyme is activated when the sample is heated to 95 °C for 2 min before PCR cycling.

4. Heat-inactivated controls: Prepare heat-inactivated controls by heating 2 μL of the extracted test samples at 85 °C for 10 min. Add this to the reaction mix in place of the protein extract. Since telomerase is heat sensitive, heat-inactivated samples serve as negative controls.
5. ImageJ [9] is used to analyze TRAP products. Bands on positive control lanes are designated the standard, and intensity of bands from other reactions are compared to the standard (Fig. 1).
6. Evaluating the integrity of DNA must not be skipped prior to digestion. A quality DNA sample when visualized after agarose gel electrophoresis will appear as a single compact band. If the sample presents as a smear, it is an indication of possible degradation, and the sample is unsuitable for TRF assay. DNA integrity is vital in obtaining reliable telomere length, as a degraded sample may provide inaccurate measurements.
7. TRF assay relies on telomeric DNA being unaffected by restriction digestion with *RsaI/HinfI* due to lack of restriction sites, while genomic DNA is completely digested. After digestion with restriction enzymes, genomic DNA runs as a smear below 800 bp marker. Anything above 800 bp points to incomplete digestion of the genomic DNA. If incomplete digestion is observed, prolong the duration of digestion.
8. A tank is filled with 1 L 10× SSC buffer, and a platform to support the blot setup is placed in the tank. Wet the platform with 10× SSC buffer and place a filter paper (e.g., Whatman™ 3MM) on the support. Gently pour more 10× SSC buffer over the filter paper and remove air bubbles. Place the gel on top. Wet a nylon membrane (big enough to completely cover the gel) with ddH_2O and place it over the gel taking care to remove air bubbles in between. Wet few filter papers with 10× SSC buffer and place them over the nylon membrane. Lay a stack of paper towels over the filter paper and place a weight over it. Capillary transfer at RT overnight.
9. Preparation of ^{32}P-labeled TTAGGG probes is described from **steps 19** to **24** of Subheading 3.4. These steps can be performed during the incubation period of the prehybridization. There is ample time for the probe preparation during this time.
10. All the steps following hybridization are to be performed in a dark environment.

11. Post hybridization washes are performed by simply immersing the coverslips in the wash buffers for the specified amount of time without agitation or shaking. When wash time is over, the coverslip is picked up and placed into the next wash.
12. Interphase nuclei are identified as circular DAPI-stained areas in ~7.5–15 μm diameter (Fig. 3, left). Metaphase chromosomes (~1–2 μm) containing four telomeres are clustered together (Fig. 3, right).

References

1. Baguna J, Salo E, Auladell C (1989) Regeneration and pattern formation in planarians III. Evidence that neoblasts are totipotent stem cells and the source of blastema cells. Development 107:77–86
2. Michalopoulos GK (2007) Liver regeneration. J Cell Physiol 213:286–300. https://doi.org/10.1002/jcp.21172
3. Li Q, Yang H, Zhong TP (2015) Regeneration across metazoan phylogeny: lessons from model organisms. J Genet Genomics 42:57–70. https://doi.org/10.1016/j.jgg.2014.12.002
4. Tsonis PA, Madhavan M, Tancous EE, Del Rio-Tsonis K (2004) A newt's eye view of lens regeneration. Int J Dev Biol 48:975–980. https://doi.org/10.1387/ijdb.041867pt
5. Watson JD (1972) Origin of concatemeric T7 DNA. Nat New Biol 239(94):197–201. https://doi.org/10.1038/newbio239197a0
6. Alibardi L (2015) Immunodetection of telomerase-like immunoreactivity in normal and regenerating tail of amphibians suggests it is related to their regenerative capacity. J Exp Zool A Ecol Genet Physiol 323(10):757. https://doi.org/10.1002/jez.1989
7. Anchelin M, Murcia L, Alcaraz-Perez F, Garcia-Navarro EM, Cayuela ML (2011) Behaviour of telomere and telomerase during aging and regeneration in zebrafish. PLoS One 6(2): e16955. https://doi.org/10.1371/journal.pone.0016955
8. Chen CF, Sung TL, Chen LY, Chen JH (2018) Telomere maintenance during anterior regeneration and aging in the freshwater annelid Aeolosoma viride. Sci Rep 8:18078. https://doi.org/10.1038/s41598-018-36396-y
9. Rasband WS. ImageJ, U. S. National Institutes of Health, Bethesda, MD. https://imagej.nih.gov/ij/, 1997-2018

Open Access This chapter is licensed under the terms of the Creative Commons Attribution 4.0 International License (http://creativecommons.org/licenses/by/4.0/), which permits use, sharing, adaptation, distribution and reproduction in any medium or format, as long as you give appropriate credit to the original author(s) and the source, provide a link to the Creative Commons license and indicate if changes were made.

The images or other third party material in this chapter are included in the chapter's Creative Commons license, unless indicated otherwise in a credit line to the material. If material is not included in the chapter's Creative Commons license and your intended use is not permitted by statutory regulation or exceeds the permitted use, you will need to obtain permission directly from the copyright holder.





Chapter 25

Analysis of DNA Double-Stranded Breaks Using the Comet Assay in Planarians

Paul G. Barghouth, Salvador Rojas, Lacey R. O'Dell, Andrew M. Betancourt, and Néstor J. Oviedo

Abstract

Comet assay provides the opportunity to detect and characterize DNA strand breaks. Cellular lysing followed by embedding in agarose slide is used to visualize under an electrical current migration patterns corresponding to DNA fragments of different sizes. Here we describe the process of detecting and characterizing DNA damage by Comet assay on planarians, which is a model organism commonly used to understand the process of whole-body regeneration, stem cell regulation, and adult tissue maintenance.

Key words Alkaline Comet Assay, Planarian, Double-stranded breaks, DNA damage

1 Introduction

Single-cell gel electrophoresis or Comet assay is an attractive tool to assess the integrity of DNA molecules [1–4]. DNA maintains its structure through its negatively charged supercoils around the histone core. DNA strand breaks may result from endogenous and exogenous sources (e.g., ROS and ionizing radiation), leading to the disruption of DNA integrity [5]. The Comet assay takes advantage of the relaxation of DNA supercoils to assess the levels of DNA strand breaks. Briefly, cell suspensions are embedded in agarose-coated slides and are lysed with detergent (i.e., Triton-X 100) to remove nuclear membranes and DNA histone structures, resulting in gel-embedded nucleoid bodies [4]. Increases in DNA breaks and subsequent relaxation in its loops can be exposed when an electric field is applied, and a comet tail-like structure is formed in relation to the amount of damaged DNA. Higher amounts of DNA strand breaks yield more prominent comet tail-like structures [3, 4, 6–8]. After the initial comet protocols were established in 1980s [1, 2], many variations to the protocols have been established (e.g., Comet-FISH, Comet-BrdU) [6–10]. However, the

Simon Blanchoud and Brigitte Galliot (eds.), *Whole-Body Regeneration: Methods and Protocols*, Methods in Molecular Biology, vol. 2450, https://doi.org/10.1007/978-1-0716-2172-1_25, © The Author(s) 2022

Comet assay under alkaline conditions (i.e., pH >13) has remained the most widely used method by converting all types of DNA damage (i.e., crosslinks, strand breaks, adducts, etc.) to double-stranded DNA breaks [2–4, 11].

Detection of DNA damage and its repair can be studied in a variety of ways in planarian flatworms. These include immunohistochemistry and Western blot techniques to assess the expression of markers associated with the DNA damage response (i.e., RAD51, H2AX, and PARP) [12–15]. Planarian stem cells known as neoblasts are the only cells with replicative capacity in planarians. Techniques to assess neoblast chromosomal stability and telomeric maintenance have been established [12, 16, 17]. Recent research implemented the use of Comet assay in planarians to characterize the extent of DNA strand breaks [12, 14–16]. The procedure can be guided toward specific cell types by using flow cytometry to sort cells (e.g., neoblasts) or may involve evaluation of different cell types obtained by the dissociation of whole animals. Future adaptations of the Comet assay may also involve double labeling with immunostaining, gene expression probes, and BrdU, which altogether may facilitate characterization of DNA damage and repair on specific cell types.

The Comet assay not only provides a qualitative representation of the extent of DNA strand breaks but can also be used to obtain a precise quantification between different degrees of damage and repair. Here we demonstrate that Comet assay can be used to efficiently detect the extent of DNA strand breaks in a variety of conditions using the highly regenerative planarian model. This includes exposure to gamma irradiation, knockdown of genes, and pharmacological treatments with genotoxic compounds.

2 Materials

2.1 Handling Equipment

1. Electronic pipette.
2. Cell strainer, 70 μm.
3. Carbon steel blade.
4. Anti-static wipes.
5. Dissecting microscope.
6. Black round filter paper.
7. Superfrost microscope slides.
8. Scintillation vials.
9. DNA electrophoresis chamber.
10. Nucleic acid gel stain.
11. Fluorescent microscope.

12. Camera.
13. Imaging software.
14. Data processing software.

2.2 Comet Assay Solutions

All the solutions are prepared with Nanopure water unless otherwise stated.

1. Stock lysing solution: 2.5 M NaCl, 100 mM EDTA, 10 mM Tris–NaOH in 700 mL H_2O. Stir mixture. Add ~8 g of pelletized NaOH, allow the mixture to go into solution (~30 min). Adjust the pH to 10.0 with NaOH, bring to 900 mL using H_2O, filter (*see* **Note 1**). Store at room temperature for up to 6 months.
2. Final lysing solution: 36 mL stock lysing solution, 4 mL DMSO, 0.4 mL Triton x-100 (*see* **Note 2**). Refrigerate the solution at 4 °C for 60 minutes, allowing the solution to go from opaque to clear.
3. 1× TE Buffer: 200 mL H_2O, 0.395 g Tris–HCl, 0.0925 g EDTA, pH 7.5. Bring volume to 250 mL with H_2O. Store at room temperature.
4. 200 mM EDTA solution: 150 mL H_2O, 14.89 g EDTA, stir, adjust pH to 10 by using NaOH pellets (*see* **Note 3**). Adjust final volume to 200 mL (*see* **Note 4**). Refrigerate the solution at 4 °C.
5. 10 N NaOH solution: 450 mL H_2O, 200 g NaOH, stir and bring the volume to 500 mL (*see* **Notes 4** and **5**). Store at room temperature.
6. 1× electrophoresis buffer: 10 mL 10 N NaOH solution, 5 mL 200 mM EDTA solution in 700 mL H_2O. Adjust pH to more than 13 using NaOH dropwise, bring volume to 1 L (*see* **Note 6**). Refrigerate solution at 4 °C.
7. 0.4 M Tris neutralization buffer: 48.5 g Tris–HCl in 800 mL H_2O, pH 7.5. Adjust final volume to 1 L, store at 4 °C (*see* **Note 7**). Refrigerate solution at 4 °C.
8. Calcium- and magnesium-free (CMF) medium: 15 mL H_2O, 0.0100 g NaH_2PO_4, 0.0200 g NaCl, 0.0300 g KCl, 0.0200 g $NaHCO_3$, 0.0060 g Dextrose, 0.2500 g BSA, 0.0890 g HEPES-HCl, pH 7.3. Bring final volume to 25 mL. Filter the medium with a 0.22-μm filter and store at 4 °C for up to 7 days.
9. 10,000× nucleic acid gel stain: Add the stain (e.g., SYBR Gold Nucleic Acid Gel Stain, Invitrogen) according to the manufacturer's instructions to reach 10,000× of the recommended final concentration. Make aliquots in dark tubes, store at −20 °C. Use within 24 h after thawing.

10. 10× commercially available phosphate-buffered saline (PBS).
11. 0.5% low melting point agarose (LMPA): 0.25 g LMPA in 50 mL 10× PBS (*see* **Note 8**). Aliquot into scintillation vials and refrigerate solution at 4 °C.
12. 1% normal melting point agarose (NMPA): 0.5 g normal melting point agarose, 50 mL 10× PBS, boil until agarose is dissolved. Allow agarose to equilibrate in a 65 °C bath 30 minutes prior to coating slides (*see* **Note 9**). Make fresh when needed.

3 Methods

3.1 Agarose Slide Preparation

1. Pour dissolved and equilibrated 1% NMPA into a 50-mL conical tube.
2. While still hot, slowly dip in 3/4 of the superfrosted plus slide twice (5 mm thick) into the agarose.
3. With a tissue, remove excess agarose from the back of the slide.
4. Lay slides in a flat surface to air dry overnight or use a slide warmer (Fig. 1a) (*see* **Note 10**).
5. Once dry, store slides within a slide box at room temperature in dry low humidity.

3.2 Planarian Dissociation and Cell Recovery

1. Place 10 large planarians (i.e., control or experimental) onto a chilled 10 mm polystyrene petri dish lid on a Peltier cooler (alternatively, ice wrapped in plastic would work), located under a dissecting microscope (Fig. 1b).
2. Remove all excess liquid using anti-static wipes.
3. Finely cut the pool of worms with a carbon steel razor blade by applying rapid movements until tissues look like a homogenous paste of macerated tissues (Fig. 1c) (*see* **Note 11**).
4. Rinse homogenate, razorblade, and petri dish with ice-cold CMF medium.
5. Place suspension into a 15-mL conical tube.
6. Repeat washes until conical tube is filled with 10 mL of suspension.
7. Rock cell suspension at 4 °C for 25–45 min (*see* **Note 12**).
8. Filter cells using a 70-μm mesh.
9. Centrifuge suspension at 2230 rcf for 5 min at 4 °C.
10. Resuspend pellet in 2 mL of CMF media.
11. Calculate a cell density of 50,000 cells/mL using a hemocytometer; mix a 1:1 (5 μL:5 μL) ratio of Trypan Blue and cell suspension.

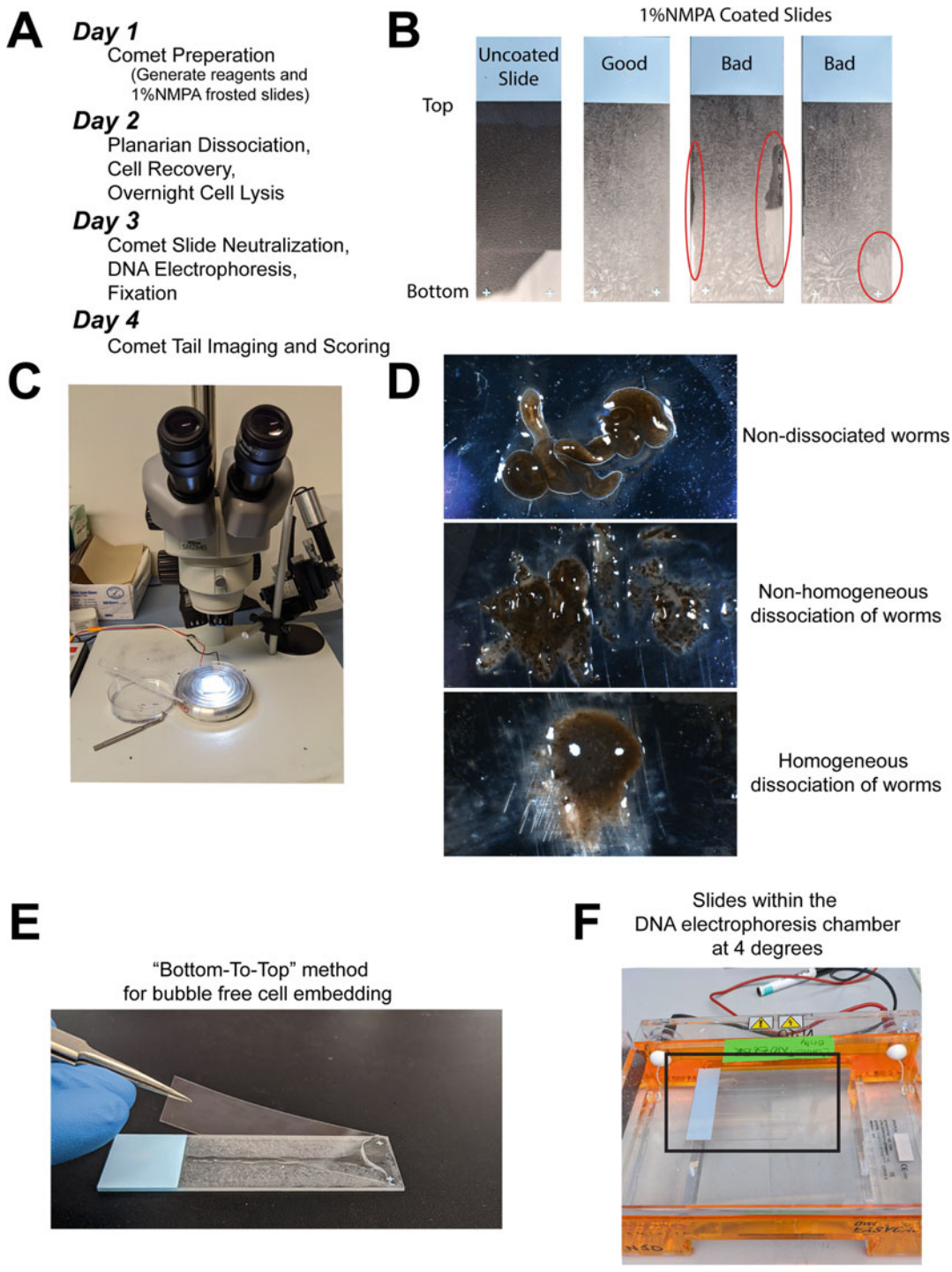


Fig. 1 Comet protocol preparation and visual protocol. (**a**) Comet workflow and timeline. (**b**) Representative images of unfrosted and 1% NMPA-coated slides. A good slide to conduct the Comet protocol with alongside coated slides that are not usable due to voids in agarose (i.e., red circles). (**c**) Setup for planarian dissociation. Needed a dissecting microscope, Peltier cooler, petri dish, and tweezer with a razor blade. (**d**) Representative images of steps in worm dissociation. Note that by the end of the dissociation process, the end product should look homogenous void of remaining tissue structures. (**e**) Image showing the "bottom-to-top" method to

12. Aliquot 50,000 cells/mL into 1.5 mL snap cap tubes; volume determined by cell density (*see* **Note 13**).
13. Allow cells to recover at 37 °C for 2 h (*see* **Note 14**).

3.3 Slide Preparation

1. Microwave and equilibrate 30 mL 0.5% LMPA to 37 °C for 30–60 min.
2. Centrifuge the recovered cells at 3725 rcf for 2 min.
3. Aspirate supernatant leaving ~40 μL of CMF medium on the pellet.
4. Dissolve the pellet by adding 100 μL of warm 0.5% LMPA.
5. Immediately, pipette the suspension to the coated 1% NMPA slide (*see* **Note 15**).
6. Immediately place a coverslip (24 × 50 mm) on top of solution and avoid air bubbles by starting at the bottom of the slide and slowly allow the coverslip to fall toward the top (i.e., plus sign to label of slide, respectively) (Fig. 1d).
7. Allow agarose to solidify in refrigerator at 4 °C for at least 15–20 min (*see* **Note 16**).

3.4 Cell Lysis

1. Remove coverslip using a tweezer to gently push toward one slide, the remaining steps in Subheading 3.3 must be conducted on ice.
2. Place 40 mL of cooled transparent final lysing solution in a Coplin jar.
3. Gently insert slides in the filled Coplin jar.
4. Protect slides from light by wrapping Coplin jar with aluminum foil.
5. Place Coplin jars in the 4 °C refrigerator overnight (*see* **Note 17**).

3.5 Comet Slide Electrophoresis

1. Refrigerate 500 mL of 1× electrophoresis buffer at 4 °C for 30 min.
2. Place the Coplin jar on ice.
3. Gently discard the lysing solution from the Coplin jar.
4. Remove the remaining solution by wadding a wipe and securing slides with it before inverting the Coplin jar.
5. Neutralize the slides with 40 mL cooled 0.4 M Tris neutralization buffer for 5 min maximum at 4 °C.

Fig. 1 (continued) prepare cell embedded slides without the generation of bubbles. (**f**) Electrophoresis setup within the 4 °C fridge connected to a voltage power source. The slides are aligned tightly side-by-side on the cathode side of the box

6. Gently discard neutralization buffer from the Coplin jar.
7. Invert the Coplin jar over a wipe.
8. Add 40 mL of 4 °C chilled 1× electrophoresis buffer into the Coplin jar.
9. Allow slides to equilibrate in buffer for 30 min at 4 °C (*see* **Note 18**).
10. With tweezer to gently place equilibrated slides in a precooled electrophoresis chamber (Fig. 1e).
11. Fill chamber with enough 4 °C chilled 1× electrophoresis buffer to cover slide by 3–5 mm (~800 mL) (*see* **Note 19**).
12. Run electrophoresis chamber for 30 min within the fridge. Set current to 12 V and 300 mA.

3.6 Comet Slide Neutralization and Fixation

1. Return slides from the electrophoresis chamber to an empty Coplin jar.
2. Invert the Coplin jar over a wipe.
3. Neutralize the slides with 40 mL cooled 0.4 M Tris neutralization buffer for 5 minutes maximum at 4 °C.
4. Gently discard neutralization buffer from the Coplin jar.
5. Invert the Coplin jar over a wipe.
6. Add 40 mL pre-cooled (−20 °C) 100% ethanol into the Coplin jar.
7. Store it in the −20 °C refrigerator for 5 min.
8. Remove slides from Coplin jar and drain excess ethanol by dabbing the bottom of each slide with a wipe.
9. Place the slides with agarose facing upward on a paper towel and allow to dry overnight in low humidity, at room temperature (*see* **Note 20**).

3.7 Comet Slide Staining and Visualization

1. Thaw 10,000× Nucleic Acid Gel Stain working solution.
2. Add 130–200 μL of Nucleic Acid Gel Stain solution on top of each dried slide.
3. Immediately place a coverslip (24 × 50 mm) on top of solution and avoid air bubbles by slowly placing the coverslip onto the slide with a top-down approach.
4. Place slides in a dark slide box.
5. Image each slide using a fluorescent microscope which contains optics recommended by the DNA stain's manufacturer.
6. The total amount of images taken should account for 200–500 randomly selected individual nuclei (i.e., comets) per slide. For statistical purposes, image a large sample size of comets and

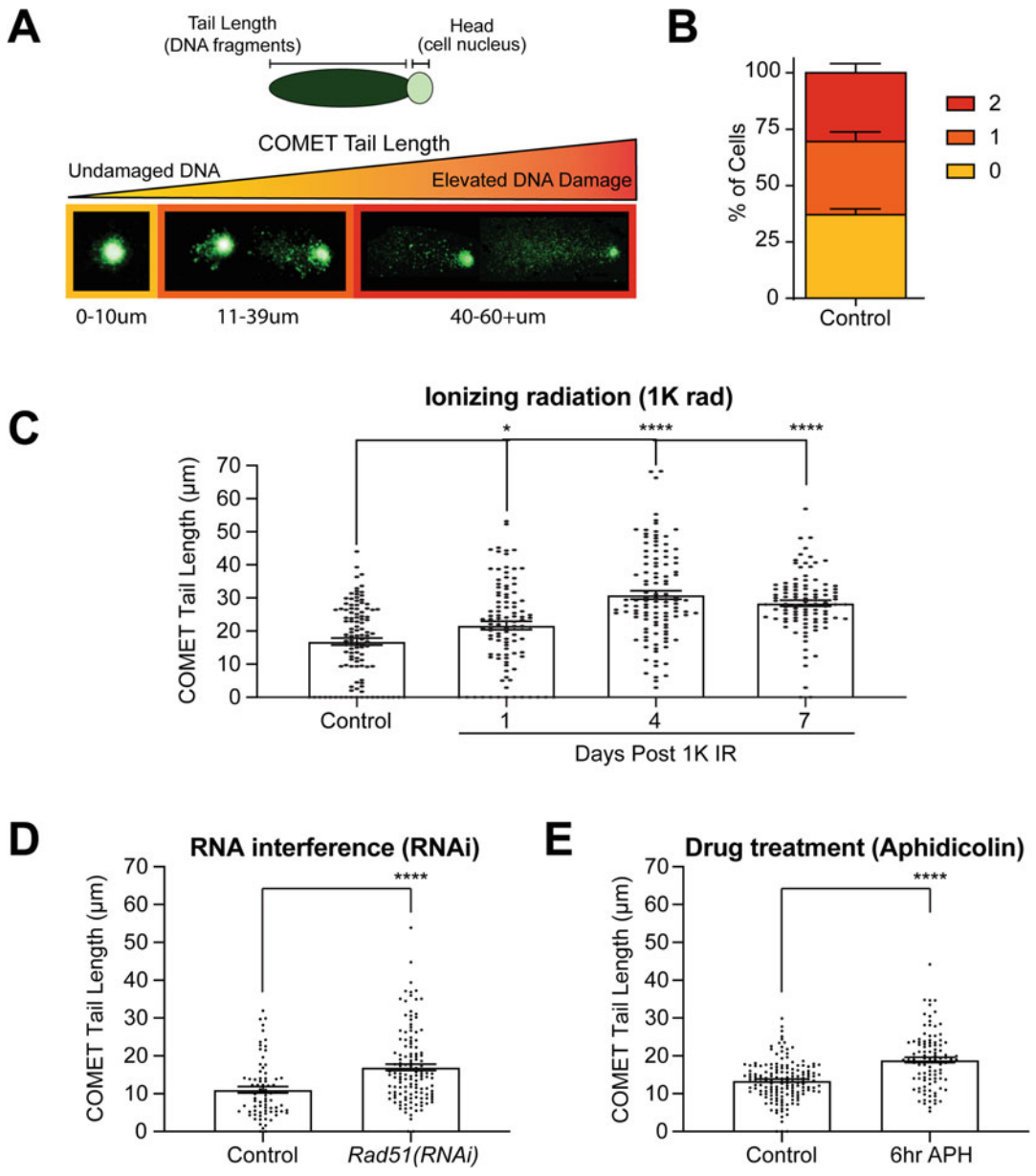


Fig. 2 The effect of various treatments on DNA damage using the Comet assay. (**a**) Visual representation of single nuclei post alkaline Comet electrophoresis and staining. Nuclei are stained with DNA dye (i.e., SYBR green) and imaged using florescent microscopy, revealing the severity of DNA damage per cell. Tail length can be ranked, categorizing cells as undamaged, moderate, and severe damage (e.g., yellow (0), orange [1], and red [2], respectively). (**b**) Quantification of three independent Comet assays using the ranking score method on 7-day starved animals. Approximately 40% of planarian cells contain undamaged DNA (i.e., score of 0) and is consistent with other experimental models [18]. (**c**) Comet-tail length after exposure to 1 K rad gamma irradiation (sub-lethal) in a 7-day time course post treatment. Planarian stem cells are lost by 1–2 days post sub-lethal irradiation due to increased DNA damage. However, by days 4–5 post irradiation, planarian stem cell begin to repopulate, and this is accompanied by an increase in DNA damage and DNA repair proteins as shown previously [12]. By day 7 post radiation, DNA integrity begins to reestablish. (**d**) Increase in DNA damage can be achieved through RNA interference (RNAi). Graph represents comet-tail length of 30-day

repeat each experiment in triplicated form for each independent biological replicate.

7. Measure the comet-tail length from the edge of the comet-head to the edge of the comet-tail using imaging software (e.g., ImageJ). Rank comet-tail lengths from 0 to 2, where a score of 0 shows little DNA damage, 1 moderate, and 2 is a dispersed tail with no nucleus visible (i.e., 0–10 μm, 11–39 μm, and 40–60 μm, respectively) (Fig. 2).

3.8 Comet Slide Storage

1. Remove coverslip.
2. Place in a Coplin jar.
3. Add 40 mL pre-cooled (−20 °C) 100% ethanol.
4. Store the Coplin jar in a − 20 °C refrigerator for 5 min.
5. Remove slides from Coplin jar and drain excess ethanol by dabbing the bottom of each slide with a wipe.
6. Place slide with agarose facing upward on a paper towel.
7. Allow to dry overnight in a region void of humidity, at room temperature.
8. Place slides in a slide box.
9. Store in a dark area with low humidity until the slides are no longer needed.
10. To re-stain the slides, follow Subheading 3.5. This re-stain process can occur multiple times as long as the gel is still present.

4 Notes

1. For the stock lysing solution, the remaining volume (100 mL) will be adjusted to 1 L when the final lysing solution is made as these components must be added fresh and prior to use.
2. Final lysing solution should be made fresh on the day of use and used only once. When generating final lysing solution, prepare

Fig. 2 (continued) starved animals for both the control and experimental group *Rad51(RNAi). Rad51(RNAi)* animals contain cells that harbor increased DNA damage and chromosomal abnormalities [13]. RAD51 is a key component in DSB repair within the planarian during homeostasis and pore-radiation stem cell repopulation. Chromosomal abnormalities. (**e**) Treatment with pharmacological agents such as Aphidicolin can result in increased DNA damage within the planarian model system. Aphidicolin (APH) is an inhibitor of DNA replication, blocking DNA polymerase Alpha and Delta during S-phase of the cell cycle. Comet assay was performed on animals exposed to DMSO and APH [0.5 mM] for 6 hours (i.e., control and experimental group, respectively). It is evident that APH treatment increases DNA DSBs within the planarian. (**c**–**e**) Each dot represents an individual planarian cell's comet-tail length. (**b**–**e**) All graphs represent mean ± s.e.m. Statistics were obtained by two-way ANOVA; * <0.05 and **** < 0.0001

a volume of 40 mL or an adequate volume to fill one Coplin jar. Increase volume depending on the number of Coplin jars required to hold all slides. Furthermore, this solution will turn opaque and requires cooling at 4 °C to turn clear. Solution must be clear prior to use.

3. NaOH pellets help increase pH and allow EDTA dissolve.
4. Both the 200 mM EDTA and 10 N NaOH solutions should be stored at 4 °C as it will increase their shelf life of 1 year. If left at room temperature, solutions will have a shelf life of 2 weeks.
5. 10 N NaOH solution is commercially available or can be made in the lab.
6. 1× electrophoresis buffer must be made fresh and cooled to 4 °C prior to use. It is important to have a pH greater or equal to 13. The high pH allows for proper alkaline Comet assay to occur by converting all types of DNA damage to double-stranded DNA strand breaks.
7. 1 M neutralization buffer is also commercially available and can be diluted into a 0.4 M solution.
8. Aliquot liquid 0.5% LMPA into scintillation vials and refrigerate at 4 °C until needed.
9. Microwave in small increments of time 25 s. Swirl the solution in between to aid in the dissolving process. Repeat until the mixture is fully dissolved.
10. The slides will look milky when dried, and this is normal (Fig. 1a). Avoid slides that look like they have pits, swirls, and gaps at the edges, resulting in an edge effect and distorting the shape of the comet when visualizing. To account for this during the coating process, dip ~50 slides to generate ~20 useable ones. Store the coated slides at room temperature until needed but avoid humidity to preserve the quality of the slides.
11. Make sure that animal dissociation results in a fine paste-like solution, lacking clumps of visible tissues (Fig. 1c). This process should be completed quickly (i.e., no longer than 10–15 min) to avoid excessive cellular lost due to the adverse conditions in which the process is performed (e.g., oxygen, pressure, media nutrients).
12. The time rocking cells post maceration depends on the general condition of the experimental group. Some RNA interference regimens or drug treatments are extremely harsh on animals. This could lead to friable tissues that can deteriorate prior to the start of the Comet assay. Therefore, reducing stress by limiting rocking time is advisable.

13. Generate 3–6 tubes per sample. This will account for the generation of at least two comet slides per group and handling error in losing cell pellet in subsequent steps. You will not need to generate all but two slides, the 3–6 tubes per sample are in place for backup just in case the pellet is lost during the subsequent steps.
14. Allowing cellular resting time post maceration and centrifugation enhances cellular viability and is crucial for the quality of the assay.
15. Use one 0.5% LMPA vial at a time. Once the agarose can no longer be pipetted with ease, use the second vial and allow the initial vial to go back into solution at 37 °C.
16. To make sure that 0.5% LMPA plus cell mixture has solidified check resistance of slide by gently rotating the coverslip from side-to-side. If there are still bubbles present after coverslip has been removed, add an additional layer of 0.5% LMPA (~100 μL) and repeat the solidification step by placing a coverslip again.
17. Overnight lysis step works best but a minimum of 4 hours is possible. Furthermore, slides can remain in lysis solution for up to 2 weeks. However, the slides become more sensitive the longer they are in the refrigerator, and the slides must be handled with caution during the subsequent steps.
18. Incubate slides in the alkaline 1× electrophoresis buffer to allow DNA unwinding and the expression of alkali-labile damage.
19. Slides must be submerged no more than 3–5 mm with 1× electrophoresis buffer. Electrophoresis chambers normally include labels for a fill line, but only filling in 3–5 mm over the slides will suffice.
20. Once slides are fixed, this can be a stopping point. Store slides until they are ready for staining in an environment with low humidity. Slides may be stored for years.

Acknowledgments

This work was supported by the University of California Cancer Research Coordinating Committee (Award# CRR-18-525108) and the National Institutes of Health (NIH) National Institute of General Medical Sciences (NIGMS) award R01GM132753 to N.J. O.

References

1. Ostling O, Johanson KJ (1984) Microelectrophoretic study of radiation-induced DNA damages in individual mammalian cells. Biochem Biophys Res Commun 123(1): 291–298. https://doi.org/10.1016/0006-291x(84)90411-x
2. Singh NP, McCoy MT, Tice RR, Schneider EL (1988) A simple technique for quantitation of low levels of DNA damage in individual cells. Exp Cell Res 175(1):184–191. https://doi.org/10.1016/0014-4827(88)90265-0
3. Langie SA, Azqueta A, Collins AR (2015) The comet assay: past, present, and future. Front Genet 6:266. https://doi.org/10.3389/fgene.2015.00266
4. Olive PL, Banath JP (2006) The comet assay: a method to measure DNA damage in individual cells. Nat Protoc 1(1):23–29. https://doi.org/10.1038/nprot.2006.5
5. Lord CJ, Ashworth A (2012) The DNA damage response and cancer therapy. Nature 481(7381):287–294. https://doi.org/10.1038/nature10760
6. Glei M, Hovhannisyan G, Pool-Zobel BL (2009) Use of comet-FISH in the study of DNA damage and repair: review. Mutat Res 681(1):33–43. https://doi.org/10.1016/j.mrrev.2008.01.006
7. Rapp A, Hausmann M, Greulich KO (2005) The comet-FISH technique: a tool for detection of specific DNA damage and repair. Methods Mol Biol 291:107–119. https://doi.org/10.1385/1-59259-840-4:107
8. Zainol M, Stoute J, Almeida GM, Rapp A, Bowman KJ, Jones GD, Ecvag (2009) Introducing a true internal standard for the comet assay to minimize intra- and inter-experiment variability in measures of DNA damage and repair. Nucleic Acids Res 37(22):e150. https://doi.org/10.1093/nar/gkp826
9. Guo J, Hanawalt PC, Spivak G (2013) Comet-FISH with strand-specific probes reveals transcription-coupled repair of 8-oxoGuanine in human cells. Nucleic Acids Res 41(16): 7700–7712. https://doi.org/10.1093/nar/gkt524
10. Kawashima Y, Yamaguchi N, Teshima R, Narahara H, Yamaoka Y, Anai H, Nishida Y, Hanada K (2017) Detection of DNA double-strand breaks by pulsed-field gel electrophoresis. Genes Cells 22(1):84–93. https://doi.org/10.1111/gtc.12457
11. Collins AR (2004) The comet assay for DNA damage and repair: principles, applications, and limitations. Mol Biotechnol 26(3):249–261. https://doi.org/10.1385/MB:26:3:249
12. Barghouth PG, Thiruvalluvan M, LeGro M, Oviedo NJ (2019) DNA damage and tissue repair: what we can learn from planaria. Semin Cell Dev Biol 87:145–159. https://doi.org/10.1016/j.semcdb.2018.04.013
13. Peiris TH, Ramirez D, Barghouth PG, Ofoha U, Davidian D, Weckerle F, Oviedo NJ (2016) Regional signals in the planarian body guide stem cell fate in the presence of genomic instability. Development 143(10):1697–1709. https://doi.org/10.1242/dev.131318
14. Thiruvalluvan M, Barghouth PG, Tsur A, Broday L, Oviedo NJ (2018) SUMOylation controls stem cell proliferation and regional cell death through hedgehog signaling in planarians. Cell Mol Life Sci 75(7):1285–1301. https://doi.org/10.1007/s00018-017-2697-4
15. Sahu S, Sridhar D, Abnave P, Kosaka N, Dattani A, Thompson J, Hill MA, Aboobaker A (2019) Ongoing repair of migration-coupled DNA damage allows stem cells to reach wound sites. bioRxiv. https://doi.org/10.1101/746701
16. Barghouth PG, Karabinis P, Venegas A, Oviedo NJ (2020) Poly(ADP-ribose) Polymerase-3 regulates regeneration in planarians. Int J Mol Sci 21(3):875. https://doi.org/10.3390/ijms21030875
17. Tan TC, Rahman R, Jaber-Hijazi F, Felix DA, Chen C, Louis EJ, Aboobaker A (2012) Telomere maintenance and telomerase activity are differentially regulated in asexual and sexual worms. Proc Natl Acad Sci U S A 109(11): 4209–4214. https://doi.org/10.1073/pnas.1118885109
18. Sinha M, Jang YC, Oh J, Khong D, Wu EY, Manohar R, Miller C, Regalado SG, Loffredo FS, Pancoast JR, Hirshman MF, Lebowitz J, Shadrach JL, Cerletti M, Kim MJ, Serwold T, Goodyear LJ, Rosner B, Lee RT, Wagers AJ (2014) Restoring systemic GDF11 levels reverses age-related dysfunction in mouse skeletal muscle. Science 344(6184):649–652. https://doi.org/10.1126/science.1251152

Open Access This chapter is licensed under the terms of the Creative Commons Attribution 4.0 International License (http://creativecommons.org/licenses/by/4.0/), which permits use, sharing, adaptation, distribution and reproduction in any medium or format, as long as you give appropriate credit to the original author(s) and the source, provide a link to the Creative Commons license and indicate if changes were made.

The images or other third party material in this chapter are included in the chapter's Creative Commons license, unless indicated otherwise in a credit line to the material. If material is not included in the chapter's Creative Commons license and your intended use is not permitted by statutory regulation or exceeds the permitted use, you will need to obtain permission directly from the copyright holder.





Chapter 26

Random Integration Transgenesis in a Free-Living Regenerative Flatworm *Macrostomum lignano*

Jakub Wudarski, Kirill Ustyantsev, Filipa Reinoite, and Eugene Berezikov

Abstract

Regeneration-capable flatworms are highly informative research models to study the mechanisms of stem cell regulation, regeneration, and tissue patterning. Transgenesis is a powerful research tool for investigating gene function, but until recently, a transgenesis method was missing in flatworms, hampering their wider adoption in biomedical research. Here we describe a detailed protocol to create stable transgenic lines of the flatworm *M. lignano* using random integration of DNA constructs through microinjection into single-cell stage embryos.

Key words *Macrostomum lignano*, Flatworms, Regeneration, Transgenesis, Microinjection, Random integration, Irradiation

1 Introduction

Macrostomum lignano is a free-living marine flatworm capable of regeneration anterior to the brain and posterior to the pharynx [1]. During the last decade, the interest in this research model steadily increased [2]. Similar to other flatworms, regeneration in *M. lignano* is fueled by stem cells called neoblasts [3]. It is a small and transparent animal that is easy to culture in laboratory conditions. *M. lignano* is a non-self-fertilizing hermaphrodite with a short generation time of 2–3 weeks [4, 5]. When cultured in standard laboratory conditions, animals lay approximately one egg per day. Embryonic development takes 5 days, and hatchlings reach adulthood in about two weeks. The laid eggs are fertilized, relatively large (100 μm) and follow the archoophoran mode of development [4, 5], i.e., they have a large, and yolk-rich oocyte instead of a small oocyte supplied by dedicated yolk cells. These features, together with the recently reported genome and transcriptome assemblies [6–8], make *M. lignano* a versatile model organism for

Simon Blanchoud and Brigitte Galliot (eds.), *Whole-Body Regeneration: Methods and Protocols*, Methods in Molecular Biology, vol. 2450, https://doi.org/10.1007/978-1-0716-2172-1_26, © The Author(s) 2022

research on stem cells and regeneration [2, 9]. In addition, the availability of transgenic techniques renders this flatworm a unique research model among Platyhelminthes [8]. Here we present a method for transgenesis in *M. lignano* using microinjection of different components into single-cell stage embryos. The method includes preparation and maintenance of animal cultures, design of transgenic constructs, microinjection procedures, and selection of transgenic animals.

2 Materials

A typical *M. lignano* transgenesis work space is similar to configurations used for transgenesis in other animals, where DNA is delivered by microinjection into cells. It includes instruments for preparation of microinjection needles (a micropipette puller and a microforge), a stereomicroscope and an inverted microscope equipped with micromanipulators and a microinjector (Fig. 1).

1. *M. lignano* line suitable for laboratory culture (*see* **Note 1**).
2. Unicellular diatom *Nitzschia curvilineata* (Heterokontophyta, Bacillariophyceae). It is the main and only source of food for the flatworm.
3. Artificial sea water (ASW): 32 g/L commercially available sea salt (e.g., Red Sea) in an autoclaved and rinsed bottle of dH_2O. Shake until almost all salts are dissolved, autoclave, and cool down.
4. f/2 salt solutions: 3.58 g $MnCl_2 \cdot 4H_2O$, 0.44 g $ZnSO_4 \cdot 7H_2O$, 0.20 g $CoCl_2 \cdot 6H_2O$, 0.20 g $CuSO_4 \cdot 5H_2O$, 0.12 g $NaMoO_4$. Prepare each separately in 20 mL dH_2O.
5. f/2 medium stock solution I: 15 g $NaNO_3$ in 100 mL dH_2O. Autoclave for at least 20 min at 120 °C. Store in a cool and dark place. Use within 6 months. Discard if there are changes in transparency, color or if a precipitate occurs.
6. f/2 medium stock solution II: 1 g $NaH_2PO_4 \cdot H_2O$ in 100 mL dH_2O. Handle and store as stock solution I.
7. f/2 medium stock solution III: 3 g $Na_2SiO_3 \cdot 9H_2O$ in 100 mL dH_2O. Handle and store as stock solution I.
8. f/2 medium stock solution IV: 0.88 g Na_2–EDTA, 0.63 g $FeCl_3 \cdot 6H_2O$, 0.2 mL of each of five f/2 salt solutions. Handle and store as stock solution I.
9. f/2 medium vitamin solution: 50 mg thiamine–HCl (B1), 200 μg biotin, 200 μg cobalamin (B12) in 100 mL dH_2O.

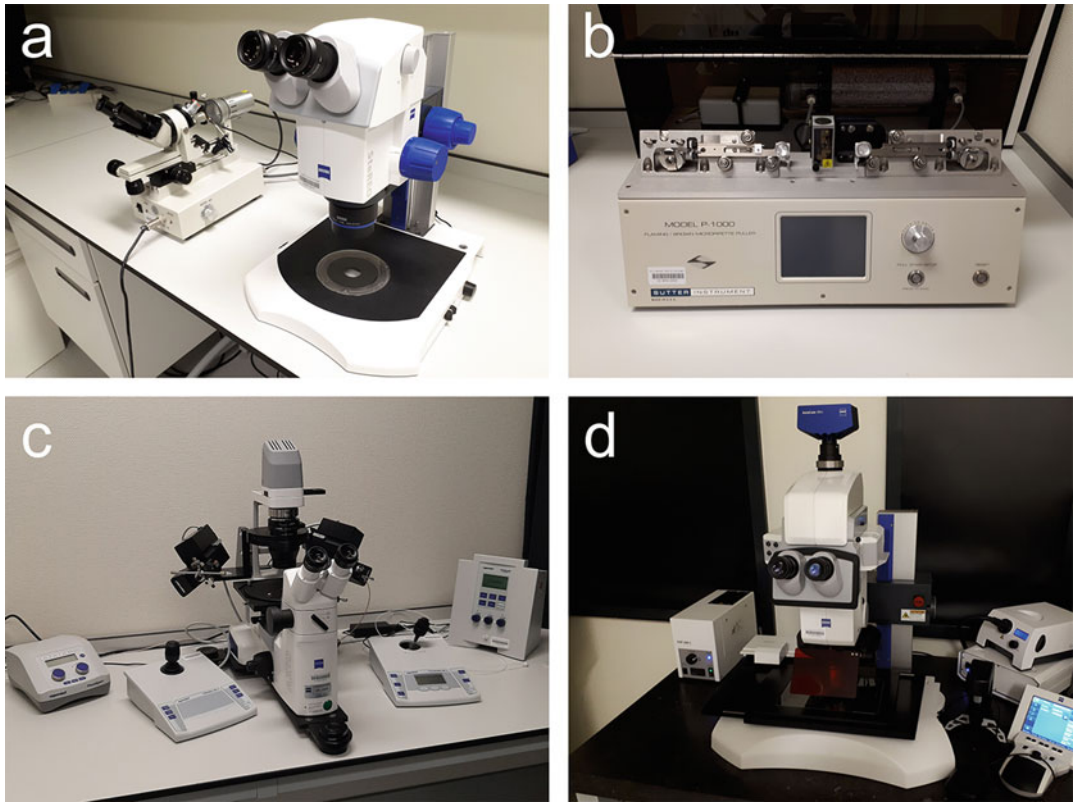


Fig. 1 Typical microinjection working station equipment. (**a**) On the right: a stereomicroscope for worm transferring and egg picking. On the left: a microforge for fine preparation of pulled microcapillaries into holders and/or needle opening. (**b**) A micropipette puller. (**c**) An inverted microscope equipped with micromanipulators and a microinjector. (**d**) A fluorescence stereomicroscope for the selection of eggs and worms positive for a transgene expression

10. Nutrient enriched ASW (Guillard's f/2 medium): 2 mL of each of the stock solutions (I-IV), 1 mL of the vitamin solution in 4 L ASW. Filter using a 0.22-μm filter.
11. Plastic petri dishes.
12. Climate chamber with possibility to use the following settings: 20 °C and 25 °C with constant aeration, a 14/10 h day/night cycle.
13. Food source: diatom grown on petri dishes with f/2 medium at 20 °C with constant aeration, and 14/10 h day/night cycle for 10–20 days to <100% confluency.
14. 30-mm round glass cover slides.
15. Plastic six-well plates.
16. Plastic 24-well plates.
17. Micropipette puller.

18. Aluminosilicate glass capillaries with filament.
19. Borosilicate glass capillaries without a filament.
20. Microforge (e.g., MF2).
21. Bunsen burner or spirit lamp.
22. Gamma-ray source.
23. Gel/PCR silica column-based DNA purification kit.
24. Stereomicroscope.
25. Inverted microscope.
26. Fluorescence stereomicroscope.
27. Micromanipulator to position the holding pipette.
28. Micromanipulator to position the injection pipette.
29. Microinjector (e.g., FemtoJet Express).
30. Piezo drill.
31. Microvolume spectrophotometer.
32. Microloader micropipette tips.
33. Low retention micropipette tips.

3 Methods

3.1 Setting Up Egg Producing Worm Cultures

1. Use a large population of worms (over 2000 in total) split into 4–6 separate petri dishes.
2. Transfer the worms to fresh food source using a 200-μL micropipette loaded with low retention tips (*see* **Note 2**).
3. Incubate at 25 °C for 2 days in the climate chamber. The worms should lay a substantial number (usually more than 4000) of eggs.
4. Transfer the worms to new petri dishes with fresh food (*see* **Note 3**) and incubate the plates with the laid eggs at 25 °C for an additional week to hatch the eggs.
5. Transfer between 300 and 500 hatchlings on a petri dish with fresh food and make a microinjection set consisting of six such petri dishes (*see* **Note 4**).
6. Incubate the hatchlings for an additional week at 25 °C.
7. Transfer to fresh food and keep at 20 °C, transferring to fresh food with intervals no longer than 4 days (*see* **Note 5**).

3.2 Preparing Single Wild-Type Worms for Crosses

Macrostomum lignano cannot self-fertilize and therefore requires a crossing partner. It is useful to have a number of worms dedicated for this purpose prepared in advance, so that crosses can be started as soon as transgenic founders are generated.

1. Select single wild-type hatchlings and put them separately in single wells in a 24-well plate with diatom.
2. Keep the worms at 20 °C until needed.
3. Transfer to a 24-well plate with fresh food every 2 weeks.

3.3 Preparation of Plastic Pickers for Egg Collection

M. lignano eggs are covered with a sticky mucus, which helps to fix the eggs on a surface. Most of the time, eggs are laid closely to each other and form clumps. Plastic pickers are used to separate eggs in the clumps. Additionally, the mucus around the eggs adheres to the tip of the picker, which helps to transfer the eggs from a petri dish to a microinjection slide and then attach them to the slide surface. A second picker is usually necessary to assist the release of the egg from the first picker. After that, the eggs can be easily manipulated to the desired location on the microinjection slide by gentle touching with the tip of the picker.

1. Take two plastic tips (preferably a microloader tip, because of their diameter; however, standard p10 pipette tips will work as well).
2. Set flame on a Bunsen burner or a spirit lamp.
3. Melt one of the tips by putting it on fire.
4. Extinguish the fire by blowing it off; the tip should be hot and melted at this moment.
5. Take the second tip and touch the melted fragment, it should melt as well.
6. Slowly start separating both the tips by pulling the second one away from the first. It should elongate into a thin plastic thread.
7. Check the size and shape of the picker; you can adjust it by cutting or bending using forceps or with your fingers. You can reuse the first tip for melting when pulling more than one picker (*see* **Note 6**). *See* Fig. 2a, b for a typical picker example.

3.4 Preparation of the Holders

1. Glass holders are pulled from borosilicate glass capillaries without a filament using the following settings (for a P-1000, Sutter Instrument, USA): Heat = ramp+18, Pull = 0, Velocity = 150, Time = 115, Pressure = 190.
2. Break the pulled glass capillary using a microforge to create a tip of approximately 140 μm outer diameter and 50 μm inner diameter.
3. Heat-polish the pipette tip to create smooth edges using the glass bead on the microforge filament.
4. Using the microforge, bend the tip to a ~20° angle. To do so, rotate the tip vertically and apply heat close to the point where the bend is needed. Do not touch the heat source to prevent

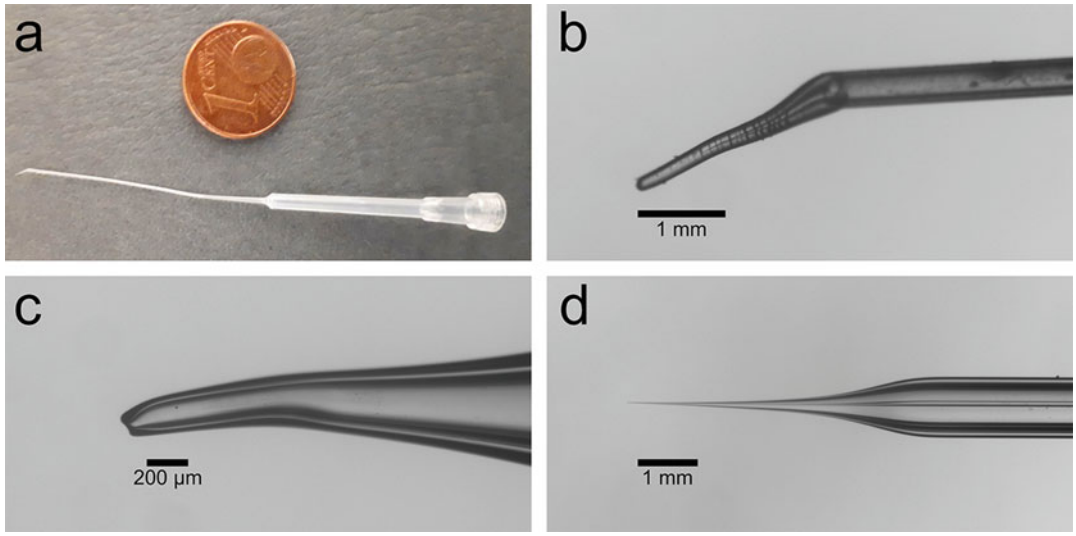


Fig. 2 Typical microinstruments used to manipulate and inject *M. lignano* eggs. (**a**) A plastic picker for egg collection made from a microloader tip. (**b**) A close up on the plastic picker tip. (**c**) A close up on the tip of a holder. (**d**) A close up on the taper and the tip of a microinjection needle. Note the filament inside

the glass from melting into the microforge. *See* Fig. 2c for a typical holder example.

3.5 Preparation of the Microinjection Needles

1. Use aluminosilicate glass capillaries with filament to prepare microinjection needles.
2. Pull the capillary using the following settings (for a P-1000, Sutter Instrument, USA): Heat = Ramp-17, Pull = 60, Velocity = 60, Time = 250, Pressure = 500, to produce two needles.
3. The tip of the freshly pulled needle is sealed. Use a microforge to break the tip of the needle and sharpen it by scratching against the glass bead on the microforge filament. Keep in mind that aluminosilicate glass breaks rather easily so not much force is required for this step (*see* **Note 7**). *See* Fig. 2d for a typical needle example.

3.6 Design of Transgenic Constructs

There are four necessary components that must be present in any transgenic construct planned for random integration: a promoter of the gene you want to study/use, a 5′ untranslated region (UTR), a protein-coding DNA sequence (CDS), and a 3′ UTR. Here we show an example of how to design a transgenic construct to study the expression pattern of the promoter of a gene of interest using the reporter green fluorescent protein (GFP) as the CDS.

1. Locate your gene of interest in the genome assembly using the *M. lignano* genome browser (http://gb.macgenome.org) either by entering the corresponding transcript ID in the

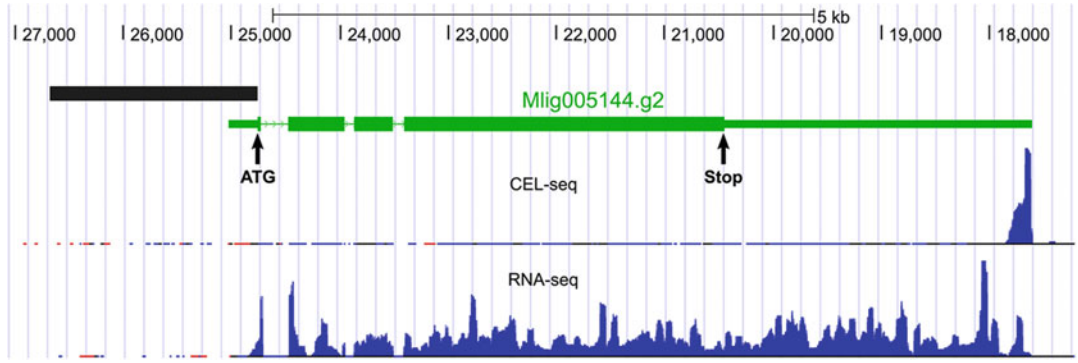


Fig. 3 Selection of the promoter for a gene of interest using *M. lignano* genome browser. A genomic region encompassing *Mlig005144.g2* gene (*APOB* homolog) shows the structure of the gene, and RNA-seq and CEL-seq tracks. Region selected for the promoter cloning is annotated as a black rectangular block upstream of the ATG

genome browser search field or by searching its sequence using the BLAT tool (*see* **Note 8**).

2. Identify the start and the end of the gene CDS, 5′ UTR, and 3′ UTR parts by looking at the Gene track in the genome browser (Fig. 3). Although the exact promoter boundaries can vary, the rule of the thumb is to start with a 1.5 kb region just upstream of the start codon of the CDS (*see* **Notes 9–11**).
3. Select two pairs of primers to PCR amplify this region and the 3′ UTR for later cloning into the plasmid vector with your preferred cloning strategy upstream and downstream of the GFP, respectively (*see* **Note 12**). GFP sequence itself can be directly cloned or PCR amplified from any existing vector, or ordered as a gene block with a codon optimized sequence for enhanced translation efficiency (*see* **Note 13**).

3.7 Microinjection Mix: DNA for Random Integration

The chosen DNA can be used in three different forms: as a circular plasmid, as a linearized plasmid, or as a PCR product. In the first case, a plasmid suspension in DNase/RNase-free water or TE-buffer with concentration of 150–300 ng/μL is recommended.

To prepare the cut plasmid:

1. Use the restriction sites flanking the desired region and digest approximately 3 μg of plasmid with the appropriate restriction enzyme(s).
2. Run the digested plasmid on an agarose gel and isolate the correct DNA fragment using gel purification silica-based column kit.
3. Estimate the concentration of the cut plasmid using the spectrophotometer. For microinjections, it should be around 50 ng/μL.

To prepare the PCR product:

1. Run a standard PCR of 200 μL.
2. Run a 1–5 μL aliquot on an agarose gel to check the size and integrity of the PCR product.
3. Clean the remaining PCR using silica-based column purification kit (*see* **Note 14**).
4. Estimate the concentration of the PCR product using the spectrophotometer. For microinjections, it should be around 50 ng/μL.

3.8 Microinjection Procedure

1. Transfer the worm culture to petri dishes with ASW (without diatom). The standard density of a microinjection plate is between 600 and 1000 worms per 6 cm petri dish. Fewer worms do not produce enough eggs and high number of worms seems not to start egg production at all (*see* **Note 15**).
2. Keep the transferred worms overnight at 20 °C to slightly starve them.
3. In the morning on the following day, transfer the worms again to fresh ASW and put them in the dark at 20 °C for approximately 2–3 h (can be in a shelf or a drawer at room temperature).
4. Move the worms into light (they can be returned to the incubator) and keep them there for 30 min.
5. Once the first eggs are laid, the egg collecting step can be started using a stereomicroscope.
6. Put a drop (150–200 μL) of ASW on a 30-mm non-treated round glass cover slide or any other glass slide that fits into a well of a six-well plate.
7. Use the plastic pickers to collect the laid eggs and transfer them to the drop of ASW (*see* **Notes 16–18**).
8. Put the slide with the eggs on the microinjection stage and focus the inverted microscope on the first egg using low magnification (5× or 10× objective) (Fig. 4a).
9. Mount the holder capillary on the micromanipulator and position it near the egg (Fig. 4a).
10. Load the microinjection needle with 1 μL of your choice of material-to-be-injected. There are no differences in the microinjection procedure in regard to the material used for injections (*see* **Note 19**). The needle can be loaded using a microloader tip or by capillary force by applying material to its back.
11. Mount the loaded needle on the micromanipulator and connect the pressure tube to the pressure supply unit of the microinjector.

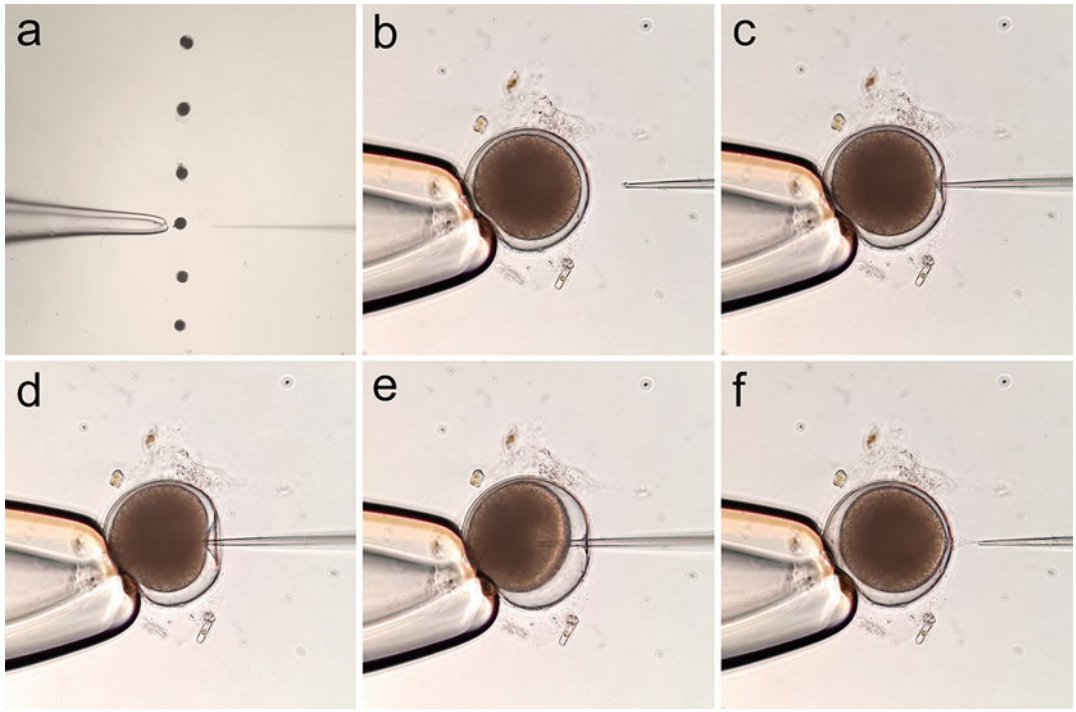


Fig. 4 Highlights of a typical microinjection procedure into the *M. lignano* single-cell eggs. (**a**) Positioning of the eggs, a loaded needle, and a holder under 5× objective of the inverted microscope. (**b**) The holder touching the edge of the egg, and the needle in the position to "clean" before the injection (40× objective). (**c**) The needle touching the egg shell before puncturing. (**d**) The needle puncturing through the egg shell. (**e**) The moment of injection is seen as a burst inside the egg. (**f**) The needle is removed from the successfully injected egg. Scale reference: *M. lignano* egg size ~100 μm

12. Make sure that the needle is opened, and there are no air bubbles in the tip. Use the microinjector's clean button if available (*see* **Note 20**).
13. Position the needle in the proximity of the egg (Fig. 4a).
14. Change the magnification to 40× objective and bring the egg, the holder, and the needle to focus (Fig. 4b) (*see* **Note 21**).
15. Position the needle so that it touches the edge of the egg (Fig. 4c) (*see* **Note 22**).
16. Pierce the egg shell with the needle, this moment should be clearly visible (Fig. 4d).
17. Push the needle deeper into the egg to pierce through the cell membrane (*see* **Note 23**).
18. Press the injection button and make sure you see a burst of the injected material appearing in the cell (*see* **Note 24)** (Fig. 4e).
19. Slowly remove the needle from the egg (*see* **Note 25**) (Fig. 4f).
20. Move the holder away from the egg.

21. Use the stage to position the next egg between the needle and the holder.
22. Repeat **steps 12–19** until all the eggs from the slide are injected.
23. Remove the slide from the microinjection stage and put it into one of the wells in a six-well plate filled with 3 mL of ASW.
24. Proceed to the next slide.
25. Repeat **steps 13–24** to process all slides.

3.9 Irradiation of Injected Eggs

Eggs can be exposed to gamma-ray radiation after injection of the desired construct to stimulate non-homologous recombination and increase integration rates [8]. Irradiate the six-well plate containing the injected eggs in ASW at a dose of 2.5 Gy of gamma-ray. This procedure should be carried out within 1-h post-injection, as long as the eggs are kept on ice until irradiation.

3.10 Transgenic Eggs Maintenance and Selection of Homozygous Lines

1. Incubate the injected eggs in an incubator at 25 °C until hatched (*see* **Note 26**).
2. Check the injected eggs for markers of positive injections (*see* **Note 27**) (Fig. 5a).
3. Use a glass pipette or a metal needle and kill all the negative eggs by pressing down the tip into the egg (*see* **Note 28**).
4. On the third day of incubation, add food to each of the wells containing a slide with injected eggs (*see* **Note 29**).
5. Worms will usually hatch between the fourth and fifth day. However, sometimes they need an additional day or two. The delay is caused by the damage inflicted during the injections.
6. Select the positive hatchlings and transfer them to single wells in a 24-well plate with diatom.
7. Cross the positive hatchlings with single wild-type worms (*see* Subheading 3.2).
8. Incubate at 25 °C until the worms start laying eggs (*see* **Note 30**).
9. Select the positive progeny and transfer to single wells in a 24-well plate (*see* **Note 30**).
10. Cross again with single wild-type worms.
11. Incubate at 25 °C until hatchlings appear (*see* **Note 31**).
12. Check the hatchlings. Homozygous worms will produce only positive offspring.
13. Select the homozygous worms and transfer them to single wells in a 24-well plate with diatom.
14. Incubate at 25 °C until the worms stop producing eggs (*see* **Note 32**).

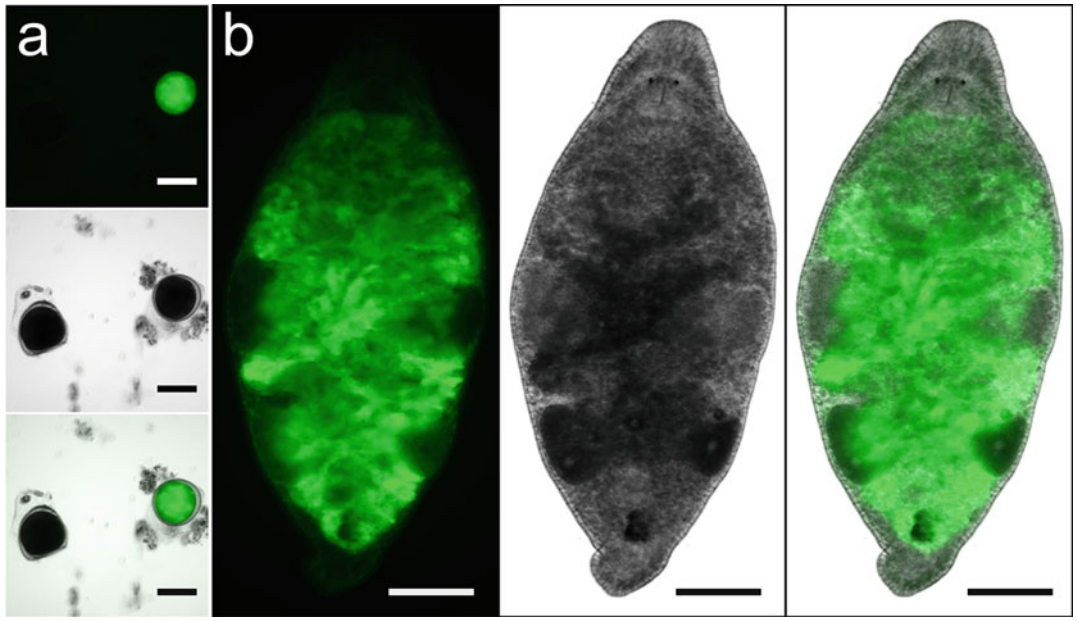


Fig. 5 An overview of an APOB::GFP::Ef1a_3′UTR transgene expression in *M. lignano* eggs and in the whole worm. (**a**) Comparison of positive and negative eggs under fluorescent stereomicroscope 1 day after the injection with the PCR DNA fragment encoding the transgene. From top to bottom: FITC channel, bright-field, and merged. Scale bars: 100 μm. (**b**) Promoter of the *M. lignano APOB* homolog (Mlig005144.g2) exhibits gut-specific expression pattern in the worm. From left to right: FITC channel, bright-field, and merged. Scale bars: 100 μm

15. Put the homozygous positive transgenic worms together in a six-well plate with food and incubate to produce offspring.
16. The line should reach the density of 100 worms within 2 months (*see* **Note 33**).
17. Use the transgenic line according to the needs (*see* **Note 34**) (Fig. 5b).

4 Notes

1. Any appropriate *M. lignano* line that can generate sufficient number of eggs can be used. For experiments in wild-type animals, we recommend NL12 line, which can be obtained from the Berezikov laboratory.
2. Regular micropipette tips should be avoided to prevent the worms from adhering to the inside walls of the tip, which can lead to the loss of animals. Worms that are adhering to the surface of the petri dish can be detached by discharging the liquid from the pipette close to the worm.

3. Put the transferred worms to 20 °C. They will not be used for microinjection but can be used for any other experiments.
4. Several microinjection sets can be maintained in parallel to ensure steady daily egg production.
5. The worms need a recovery period of 2 weeks after they are being starved to produce eggs for microinjections, keep that in mind when establishing a microinjection culture. If the culture is not dense enough, it will result in insufficient number of eggs laid, in which case you need to have more worms. If the culture is too dense, for example, if there are over 800 worms per petri dish, they will eat all the food very quickly, which will cause starvation. If the worms are not transferred regularly to fresh food, a new population of worms will hatch on the same plate. The hatchlings lower the overall egg production by competing with the adults for food and space. Keep the plates on food, regularly transferring the worms until the hatchlings become adults.
6. We use plastic pickers as they cause the least damage to the cells, are relatively cheap, easy, and fast to prepare. We strongly discourage using glass-based pickers, because of the damage they cause during the egg transfer.
7. The needle tips can also be broken using the holder when both the loaded needle and the holder are already mounted on the microinjection stage (*see* **steps 9–11** in Subheading 3.8 for mounting instructions).
8. Orientation of the transcript on the scaffold can be determined by the color of the mapped RNA-Seq reads indicated in the RNA-seq track: red—forward and blue—reverse. The position of the 3′ end can also be readily found by looking at the peak on the CEL-seq track of the genome browser.
9. If the selected 1.5 kb candidate promoter region spans another upstream gene or a large repeat element, it usually can be shortened by selecting the sequence between the end of this gene/repeat and the CDS start. The actual functional promoter sequences can be established in subsequent experiments by further truncating the initial promoter region that generated the expected expression pattern.
10. A substantial fraction of genes in *M. lignano* are trans-spliced [7, 10]. Whether the gene is trans-spliced can be determined by looking at the SL track in the genome browser, which reflects the mapping of RNA-seq reads containing SL sequences. Trans-spliced genes contain an SL peak at the beginning of their transcripts. The best strategy for promoter selection for trans-spliced genes remains to be investigated.

11. In many cases, the 3′UTR of *Ef1a* gene can be used instead of the native 3′UTR, but care should be taken in the interpretation of the resulting transgene expression patterns.
12. We find that monomeric fluorescent proteins mNeonGreen [11] and mScarlet-I [12] work well for the most of purposes.
13. The effect of codon optimization on transgene expression in *M. lignano* was not extensively investigated but an approach used for codon optimization in *Caenorhabditis elegans* is implemented and available at http://www.macgenome.org/codons.
14. If no size selection of the PCR product is required, we avoid the gel purification step, since gel-purified DNA tends to clog microinjection needles more. Instead, the PCR product can be cleaned-up directly on the columns following the manufacturer's protocol.
15. Try to avoid non-adult worms in microinjection cultures as they seem to lower the egg yield from microinjection cultures.
16. When transferring the eggs, we arrange them in a straight line to speed up the injection process and avoid double injection of the same egg.
17. When collecting the eggs, use the pickers to disperse worms that are forming ball-shaped clumps, usually there will be some freshly laid eggs inside.
18. Once picked, slides with eggs can be stored on ice or in a fridge to prevent them from dividing before starting the injections. In the meantime, you can continue picking eggs for new slides. Eggs in a fridge can be stored at least for 2 months without noticeable anomalies and can then be used right away for injections when necessary [5].
19. If the needle is clogged. The needle can be clogged by the viscosity of the injected material or by the sticky mucus surrounding the egg. If the injected material is expected to be viscous (e.g., proteins or mRNA), remember to spin down the mix. If this does not help, breaking the tip of the needle to create a larger opening might solve the problem, as well as applying higher pressure during the injections. If the mucus causes the clogging, using piezo pulses is the best solution. If the clog cannot be removed, the needle needs to be changed for a fresh one.
20. We use injection pressure (pi) of approximately 600–650 hPa and compensation pressure (pc) of 50–60 hPa. However, the settings are adjusted based on the amount of mucus and debris surrounding the eggs.
21. If the egg you want to inject is divided, chances of correctly delivering the material into a single cell decrease, and the

probability of generating mosaic animals increases. Thus, inject only an egg when it is in a single-cell stage.

22. If there is too much debris on the collected eggs, the best possible way to clean the eggs is to starve the worms. However, piezo pulses are also helpful in removing any sticky material from the needle.
23. This step is crucial. The needle needs to go through the cell membrane. You can use piezo pulses to assist this process.
24. We use manual control over the injection time. The usual value is around 0.1 s. However, it may vary. Use pedal or button for the desired time of injection, until you see a burst. If needed, repeat procedure to make sure material is delivered in the egg. Injection button corresponds to the function of foot or hand control. Foot control is used to speed up the injection procedure as both hands can be manipulating both needle and holder while the injection pulse occurs.
25. In order to prevent egg leakage, briefly stop at the point where needle leaves the egg shell.
26. Elevation of incubation temperature from 20 °C to 25 °C significantly speeds up the development of the eggs, as well as growth and maturation of the worms [5].
27. This depends on the material injected. Usually, first fluorescent signal appears after an overnight incubation, but it may take longer.
28. An egg is considered killed when the brown dark cell content is replaced by a light brown color (meaning that the cell membrane burst), or when the content of the egg clearly expelled outside the egg shell. Empty egg shells will not interfere with the subsequent procedures and can be left on the slide.
29. Use one petri dish with fresh diatom. Scratch quarter of the plate's surface using a pipette tip and resuspend the attached diatom in the ASW. Add equal volume of ASW to dilute the floating diatom. 50 μL of the diatom prepared in this way is sufficient for a single well.
30. Transfer to fresh food once a week, but keep the old plate in case of any eggs that were laid there.
31. If a heterozygous line is sufficient for further use, this step can be modified and all the positive progeny can be put together starting a line.
32. Transfer to fresh food once a week, the old plates can be discarded, as the offspring from the cross with the wild type animals will be heterozygous. This step can take up to 2 months.

33. When transferring to fresh food, keep the old plates with food, in order to incubate the laid eggs and select the hatchlings, adding them to the main culture.
34. *Macrostomum* eggs can be stored at 4 °C for at least 2 months [5]. Longer storage is possible but may affect the hatching rate of the stored eggs.

Acknowledgments

The work on the design of transgenic constructs and microinjection procedure was done at the Institute of cytology and Genetics SB RAS by KU and financially supported by Russian Science Foundation grant No. 19-74-00029. FR was supported by the UMCG Graduate School of Medical Sciences fellowship.

References

1. Egger B, Ladurner P, Nimeth K, Gschwentner R, Rieger R (2006) The regeneration capacity of the flatworm *Macrostomum lignano*—on repeated regeneration, rejuvenation, and the minimal size needed for regeneration. Dev Genes Evol 216:565–577. https://doi.org/10.1007/s00427-006-0069-4
2. Wudarski J, Egger B, Ramm SA, Schärer L, Ladurner P, Zadesenets KS, Rubtsov NB, Mouton S, Berezikov E (2020) The free-living flatworm *Macrostomum lignano*. EvoDevo 11:5. https://doi.org/10.1186/s13227-020-00150-1
3. Nimeth KT, Egger B, Rieger R, Salvenmoser W, Peter R, Gschwentner R (2006) Regeneration in *Macrostomum lignano* (Platyhelminthes): cellular dynamics in the neoblast stem cell system. Cell Tissue Res 327:637. https://doi.org/10.1007/s00441-006-0299-9
4. Morris J, Nallur R, Ladurner P, Egger B, Rieger R, Hartenstein V (2004) The embryonic development of the flatworm *Macrostomum* sp. Dev Genes Evol 214:220–239. https://doi.org/10.1007/s00427-004-0406-4
5. Wudarski J, Ustyantsev K, Glazenburg L, Berezikov E (2019) Influence of temperature on development, reproduction and regeneration in the flatworm model organism, *Macrostomum lignano*. Zool Lett 5:7. https://doi.org/10.1186/s40851-019-0122-6
6. Wasik K, Gurtowski J, Zhou X, Ramos OM, Delás MJ, Battistoni G, Demerdash OE, Falciatori I, Visozo DB, Smith AD, Ladurner P, Schärer L, McCombie WR, Hannon GJ, Schatz M (2015) Genome and transcriptome of the regeneration-competent flatworm, *Macrostomum lignano*. Proc Natl Acad Sci U S A 112:12462–12467. https://doi.org/10.1073/pnas.1516718112
7. Grudniewska M, Mouton S, Simanov D, Beltman F, Grelling M, de Mulder K, Arindrarto W, Weissert PM, van der Elst S, Berezikov E (2016) Transcriptional signatures of somatic neoblasts and germline cells in *Macrostomum lignano*. eLife 5:e20607. https://doi.org/10.7554/eLife.20607
8. Wudarski J, Simanov D, Ustyantsev K, De Mulder K, Grelling M, Grudniewska M, Beltman F, Glazenburg L, Demircan T, Wunderer J, Qi W, Vizoso D, Weissert P, Olivieri D, Mouton S, Guryev V, Aboobaker A, Schärer L, Ladurner P, Berezikov E (2017) Efficient transgenesis and annotated genome sequence of the regenerative flatworm model Macrostomum lignano. Nat Commun 8:2120. https://doi.org/10.1038/s41467-017-02214-8
9. Mouton S, Wudarski J, Grudniewska M, Berezikov E (2018) The regenerative flatworm *Macrostomum lignano*, a model organism with high experimental potential. Int J Dev Biol 62:551–558. https://doi.org/10.1387/ijdb.180077eb
10. Grudniewska M, Mouton S, Grelling M, Wolters AH, Kuipers J, Giepmans BN, Berezikov E (2018) A novel flatworm-specific gene implicated in reproduction in *Macrostomum*

lignano. Sci Rep 8:1–10. https://doi.org/10.1038/s41598-018-21107-4

11. Shaner NC, Lambert GG, Chammas A, Ni Y, Cranfill PJ, Baird MA, Sell BR, Allen JR, Day RN, Israelsson M, Davidson MW, Wang J (2013) A bright monomeric green fluorescent protein derived from *Branchiostoma lanceolatum*. Nat Methods 10:407–409. https://doi.org/10.1038/nmeth.2413
12. Bindels DS, Haarbosch L, van Weeren L, Postma M, Wiese KE, Mastop M, Aumonier S, Gotthard G, Royant A, Hink MA, Gadella TW Jr (2016) mScarlet: a bright monomeric red fluorescent protein for cellular imaging. Nat Methods 14:53–56. https://doi.org/10.1038/nmeth.4074

Open Access This chapter is licensed under the terms of the Creative Commons Attribution 4.0 International License (http://creativecommons.org/licenses/by/4.0/), which permits use, sharing, adaptation, distribution and reproduction in any medium or format, as long as you give appropriate credit to the original author(s) and the source, provide a link to the Creative Commons license and indicate if changes were made.

The images or other third party material in this chapter are included in the chapter's Creative Commons license, unless indicated otherwise in a credit line to the material. If material is not included in the chapter's Creative Commons license and your intended use is not permitted by statutory regulation or exceeds the permitted use, you will need to obtain permission directly from the copyright holder.





Chapter 27

RNAi Screening to Assess Tissue Regeneration in Planarians

Rachel H. Roberts-Galbraith

Abstract

Over the past several decades, planarians have emerged as a powerful model system with which to study the cellular and molecular basis of whole-body regeneration. The best studied planarians belong to freshwater flatworm species that maintain their remarkable regenerative capacity partly through the deployment of a population of adult pluripotent stem cells. Assessment of gene function in planarian regeneration has primarily been achieved through RNA interference (RNAi), either through the feeding or injection of double-stranded RNA (dsRNA). RNAi treatment of planarians has several advantages, including ease of use, which allows for medium-throughput screens of hundreds of genes over the course of a single project. Here, I present methods for dsRNA synthesis and RNAi feeding, as well as strategies for follow-up assessment of both structural and functional regeneration of organ systems of planarians, with a special emphasis on neural regeneration.

Key words Planarian, *Schmidtea mediterranea*, *Dugesia japonica*, RNAi, dsRNA synthesis, Screening, Regeneration, Functional genomics

1 Introduction

Planarian flatworms have grown popular as a study system for regeneration because they can regrow all cell types after nearly any injury. Over one hundred years ago, scientists determined that planarians can achieve whole-body regeneration starting with a small fragment of an adult animal. More recent work, mostly using the species *Schmidtea mediterranea* (Fig. 1a, b) and *Dugesia japonica* (*see* **Note 1**), revealed many important cellular and molecular contributors to planarians' regenerative capacity, including a population of adult, pluripotent stem cells, and constitutive body-wide axial polarity signaling (Fig. 1c, d; [7] and for reviews, see [2, 3, 8]). Planarians also possess diverse tissue types, allowing dissection of the molecular mechanisms that power structural and functional regeneration at the level of organ systems. The planarian body consists of: a tri-lobed intestine and a tube-shaped feeding

Simon Blanchoud and Brigitte Galliot (eds.), *Whole-Body Regeneration: Methods and Protocols*,
Methods in Molecular Biology, vol. 2450, https://doi.org/10.1007/978-1-0716-2172-1_27, © The Author(s) 2022

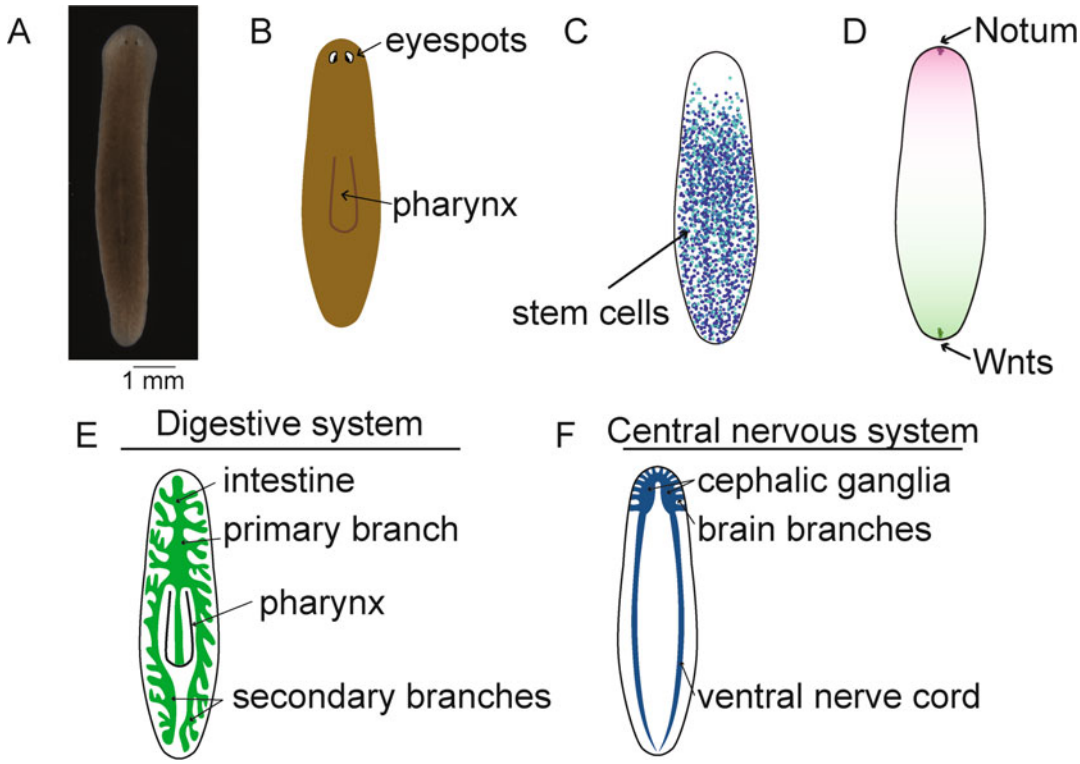


Fig. 1 Introduction to planarians. (**a**) A live planarian is pictured with its anterior (head) toward the top of the page. Eyespots are visible. (**b**) A planarian is diagrammed as pictured in **a**, with eyespots labeled. The pharynx (feeding organ) is tucked inside the body of the planarian when an animal is not feeding, but the outline of the pharynx can be faintly visible from the dorsal side. During feeding, the tube-shaped pharynx emerges from its pouch to extend through an opening on the ventral surface of the planarian body (not shown). (**c**) Planarian stem cells are a heterogeneous population, containing both pluripotent (dark blue) and specialized (light blue, teal) cells (reviewed in [1]). Stem cells are present throughout the planarian body, with two main exceptions. The pharynx has no resident stem cells, and few stem cells exist in the tip of the head (anterior to the eyespots). (**d**) A suite of polarity determinants regulates body patterning in the planarian (for review, see [2, 3]). The anterior/posterior axis of polarity signaling is depicted here. Wnt ligands (e.g., Wnt1, Wnt11-1, and Wnt11-2) are produced in the tail of the planarian. Wnt inhibitors (e.g., Notum, sFRP-1) are produced in the head to oppose Wnt signaling. Additional signaling molecules pattern the trunk of the planarian and pattern additional axes (e.g., dorsoventral) (for review, see [2, 3]). (**e**) The digestive system of the planarian is diagrammed, with the pharynx connecting to the intestine (green), which has one anterior primary branch and two posterior secondary branches. The intestine is composed of multiple cell types and is surrounded by enteric muscle [4, 5]. (**f**) The central nervous system of the planarian is diagrammed (for review, see [6]). Two ventral nerve cords connect with horseshoe-shaped cephalic ganglia which are also referred to as the planarian brain. Brain branches project outward from the cephalic ganglia to the edge of the planarian head

organ called a pharynx (Fig. 1e); muscle cells in many orientations throughout the body, which function to facilitate animal movement and produce signals for body patterning; a cephalized nervous system (Fig. 1f); osmoregulatory protonephridia; an epidermis, much of which is ciliated and promotes movement by gliding;

secretory organs that produce mucus; connective tissue called the parenchyma, within which stem cells are embedded; ovaries, testes, and other reproductive tissues; and other novel cell and tissue types still to be explored [4]. Even within these organ systems, an amazing degree of complexity is present. For example, the planarian nervous system is composed of dozens of neural cell types and glia, all arranged spatially within horseshoe-shaped cephalic ganglia that connect to two ventral nerve cords (Fig. 1f, [6]). Separate peripheral and pharyngeal nerve networks are also present.

As we have learned more about planarian regeneration and physiology, RNA interference has emerged as the most common tool with which to query gene function. Planarian biologists typically produce double-stranded RNA (dsRNA) either in bacteria or in vitro. dsRNA is administered to planarians by feeding, soaking, or injection to trigger RNAi [9–14]. This approach, often repeated several times, depending on the RNAi paradigm, causes a reduction in levels of the target mRNA that can range from nearly a 50% decrease to more than a 95% decrease [15]. The RNAi effect is even stronger in regenerated planarian tissues, which often experience a more penetrant reduction in mRNA [16]. The ease of performing RNAi in planarians allowed several screens of hundreds of genes within a single project (e.g., [15, 17]). Thus, this method is a powerful tool for medium-throughput analysis of gene function during whole-body regeneration and in the context of replacement of specific tissues or cell types after injury. In this chapter, I will outline typical methods for RNAi treatment by feeding of synthetic dsRNA in *Schmidtea mediterranea*. I will also present a range of possible approaches for assessment of regeneration downstream of RNAi.

Taken together, the following approaches can determine the extent to which regeneration occurs normally after gene perturbation by RNAi. dsRNA synthesis and feeding to achieve RNAi in planarians will be an accessible strategy for studies of regeneration, particularly those focused on whole-body regeneration, regeneration of complex organ systems or tissues, and brain regeneration in particular.

2 Materials

All solutions should be prepared with sterile, ultra-pure water, and stored at room temperature (RT) unless otherwise stated.

2.1 Template Preparation

1. RNase-free water (*see* **Note 2**).
2. 1 M Tris base, pH 9.5. Autoclave.
3. 10% Tween-20: 10% (v/v) Tween-20 in RNase-free water.
4. 1 M $MgCl_2$. Autoclave.

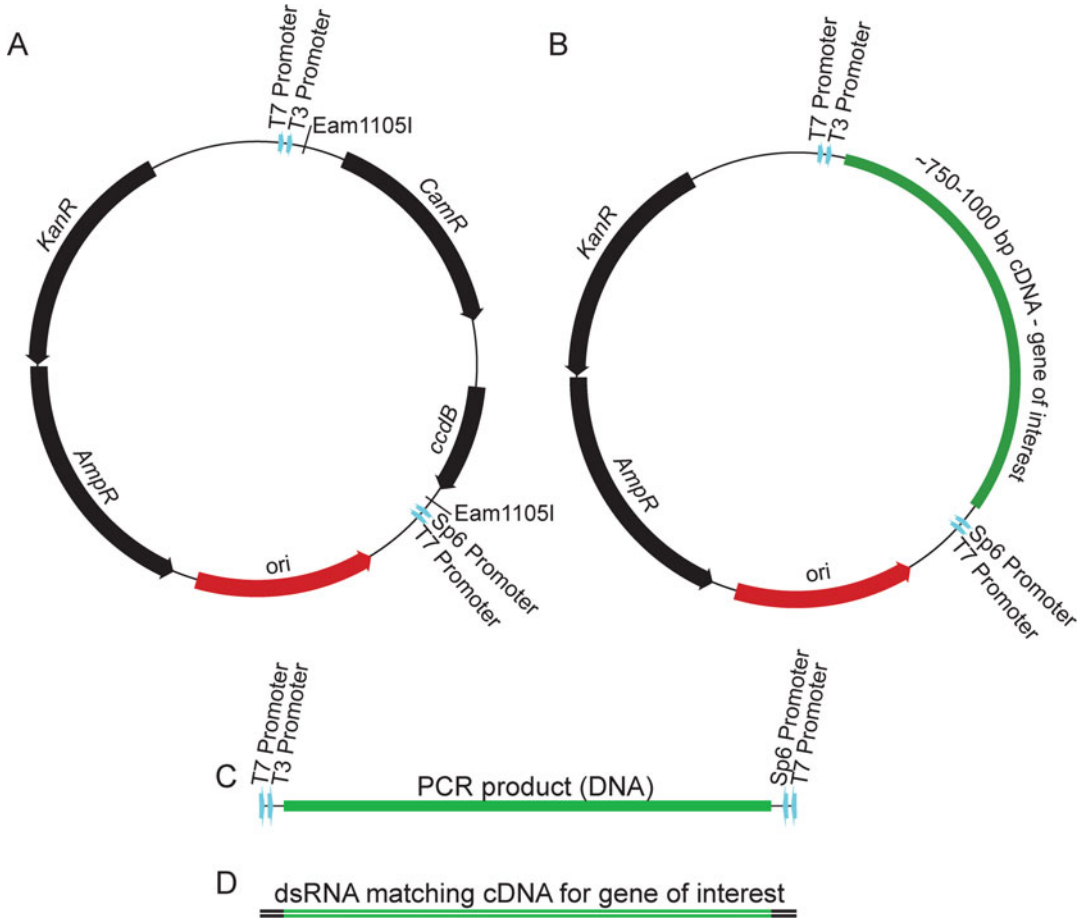


Fig. 2 Molecular strategy for dsRNA synthesis. (**a**) The pJC53.2 plasmid used for cloning upstream of dsRNA synthesis is pictured here [18]. This plasmid is digested with Eam1105I for TA cloning of PCR products generated from cDNA. (**b**) The resulting plasmids contain fragments of each gene of interest. These plasmids are subjected to PCR using a primer that recognizes the T7 promoter sequence to create an amplified product for each target and flanking promoters (**c**). The PCR products are used as a template for in vitro synthesis reactions using T7 RNA polymerase. Each in vitro synthesis reaction generates gene-specific dsRNA (**d**)

5. 35 mM $MgCl_2$. 35 μL 1 M $MgCl_2$ stock in 965 μL sterile water, aliquot 100 μL per tube and store at −20 °C.
6. 1 M ammonium sulfate. Sterile filter, aliquot 100 μL per tube and store at −20 °C.
7. Phosphoric acid (≥85%).
8. Hot start buffer: 500 μL 1 M Tris, pH 9.5, 100 μL 10% Tween-20 in 400 μL RNase-free water. Aliquot 200 μL per tube and store at −20 °C.
9. Hot start mix: 167 μL hot start buffer, 32 μL 1 M ammonium sulfate, 1 μL phosphoric acid. Made fresh or frozen only once.

10. 150–450 ng/μL template plasmid: ~750 bp target gene cloned from cDNA into the pJC53.2 vector. More on this vector can be found in [18]; cloning into this vector positions T7 polymerase sites on each side of the gene fragment (Fig. 2a, b, *see* **Note 3**).
11. dNTP mix: 10 mM dATP, 10 mM dGTP, 10 mM dCTP, 10 mM dTTP. Aliquot 100 μL and store at −20 °C.
12. 10 μM T7 primer: extended sequence GGATCCTAATAC GACTCACTATAGGG . Aliquot in 100 μL and store at −20 °C.
13. Recombinant Taq polymerase.
14. Kit for purification of polymerase chain reaction (PCR) products.
15. Gel electrophoresis setup: 1% (w/v) agarose gel, with ethidium bromide or equivalent, DNA ladder, loading dye, electrophoresis tank.
16. Thermocycler.
17. Gel imager.
18. Spectrophotometer.

2.2 dsRNA Synthesis

1. 1 M Tris base, pH 8.0. Autoclave.
2. 1 M spermidine. Filter sterilize, aliquot 500 μL per tube and store at −20 °C.
3. 1 M dithiothreitol (DTT). Filter sterilize, store at −20 °C.
4. 10× high yield transcription buffer: 4 mL 1 M Tris pH 8.0, 2 mL 1 M $MgCl_2$, 200 μL 1 M spermidine, 1 mL 1 M DTT, in 2.8 mL RNase-free water. Sterile filter, aliquot 200 μL per tube and store at −20 °C.
5. rNTP mix: 25 mM rATP, 25 mM rUTP, 25 mM rCTP, 25 mM rGTP. Aliquot 100 μL per tube and store at −20 °C.
6. T7 RNA polymerase.
7. Thermostable inorganic pyrophosphatase (TIPP) enzyme.
8. Ribonuclease (RNase) inhibitor (e.g., RNasin®).
9. Formaldehyde loading dye.
10. RNase-free DNase.
11. 5 M ammonium acetate. Prepare with RNase-free water. Sterile filter.
12. 100% ethanol.
13. 70% (v/v) ethanol. Prepare with RNase-free water.

2.3 RNAi Treatment and Amputation

1. ≥1 μg/μL purified dsRNA.
2. Planarians—*Schmidtea mediterranea*. 10 animals of 3–5 mm length per gene of interest, plus 10 animals of similar size for negative control.
3. 60–100 mm petri dishes.
4. Cafeteria trays.
5. 1x Montjuïc salts: 1.6 mM NaCl, 1 mM $CaCl_2$, 1 mM $MgSO_4$, 0.1 mM $MgCl_2$, 0.1 mM KCl, 1.2 mM $NaHCO_3$, pH 7.5 with HCl or NaOH.
6. Large bulb, wide mouth transfer pipettes (e.g., 8.6 mL).
7. Disposable pellet pestles.
8. Planarian food (e.g., liver puree prepared as per [19]).
9. Green food coloring.
10. Filter paper.
11. Low-lint science wipes.
12. Scalpel.
13. Dissecting microscope.
14. 50 mg/mL gentamicin sulfate solution.

3 Methods

3.1 Template Preparation by PCR

The starting material for template preparation is ~750 bp of each target gene cloned from cDNA into pJC53.2 vector (Fig. 2a, b, *see* **Note 3**). Positive and negative controls should also be included (*see* **Note 4**).

1. Prepare one PCR per template to be amplified (*see* **Note 5**).
2. Combine 5 μL of the hot start mix solution and 5 μL of 35 mM $MgCl_2$ in each tube.
3. Incubate for 15 min at RT to precipitate the $MgCl_2$.
4. Add to each tube: 32.5 μL sterile water; 1 μL template plasmid diluted 1:30 in water; 4 μL 10 μM T7 primer, which will serve as both forward and reverse primers in this reaction; 1.5 μL 10 mM dNTPs; 1 μL Taq polymerase.
5. Incubate the reactions in the thermocycler for the following program: incubation for 5 min at 95 °C; 35 cycles of the following three steps—30 s at 95 °C, 30 s at 55 °C, 1 min at 72 °C; incubation for 5 min at 72 °C; and hold at 4 °C.
6. Load 1.5 μL of each reaction into an agarose gel.
7. Run the gel electrophoresis setup on 120 V for 45 min.

8. Image the gel on the gel imager following the manufacturer's instructions to check for amplification.
9. Identify PCR products as single strong bands of 750–800 bp (insert plus promoter sequences) (*see* Fig. 2c).
10. Purify PCR products using a DNA clean-up kit, as per the manufacturer's protocol, except elute in 20 μL RNase-free water (*see* **Note 6**).
11. Determine the concentration of PCR products using a spectrophotometer.
12. Dilute with sterile water to a concentration of 50–150 ng/μL for in vitro dsRNA synthesis.

3.2 In Vitro dsRNA Synthesis

The starting material for dsRNA synthesis is template DNA with T7 promoter sequences on each side generated in Subheading 3.1 (*see* **Note 7**). For all steps in this section of the protocol, use RNase-free materials, including RNase-free filter tips and RNase-free tubes.

1. For each template, combine in a 1.5-mL tube: 10.5 μL template DNA; 2 μL 10× high yield transcription buffer; 5 μL rNTP mix (25 mM each); 1 μL T7 RNA polymerase; 1 μL TIPP; 0.5 μL RNase inhibitor. Total volume will be 20 μL.
2. Incubate at 37 °C overnight (>5 h).
3. Add the following to each tube: 8 μL RNase-free water; 1 μL 10× high yield transcription buffer; and 1 μL RNase-free DNase.
4. Mix well.
5. Incubate at 37 °C for 15 min.
6. To precipitate each reaction, add the following to each tube: 70 μL RNase-free water; 100 μL 5 M ammonium acetate; 400 μL 100% ethanol.
7. Mix well by inverting.
8. Incubate the mixture at −20 °C for >1 h.
9. Centrifuge samples for 15 min at 4 °C and at maximum speed (~20,000 rcf). A pellet should appear at the bottom of each tube. The pellets should be large and glassy or white in appearance.
10. Remove the supernatant carefully by pipetting with RNase-free filter tips. Be careful not to disturb the pellet.
11. Discard supernatant.
12. Add 500 μL 70% ethanol to each tube (containing precipitated dsRNA). This wash will help to remove any additional materials from the synthesis reaction.
13. Cap and invert tubes two times to mix.

14. Centrifuge samples to pellet for 5 min at 4 °C and at maximum speed.
15. Remove and discard *all* supernatant from tubes by pipetting.
16. Allow pellets to air dry on a bench-top for 5 min, with tubes uncapped and covered with a science wipe.
17. Resuspend pellets in 30 μL RNase-free water.
18. Cap and flick tubes with a finger to dislodge the pellets into the water.
19. Allow resuspension of pellets at RT until they are dissolved completely.
20. Anneal dsRNA with the following sequence of incubations: 95 °C for 5 min; 75 °C for 5 min; 50 °C for 5 min.
21. Allow to cool to RT for 5 min. The product will be well-annealed dsRNA (Fig. 2d).
22. Dilute each sample 1:10 by combining 1 μL of dsRNA with 9 μL RNase-free water.
23. Mix 1 μL of each 1:10 dilution with 8 μL RNase-free water and 1 μL of loading dye.
24. Run out these mixtures on a 1% agarose gel with a known volume of DNA ladder.
25. Image with a gel imager. Each dsRNA reaction should run as a clear band at approximately the expected molecular weight, with no degradation products smaller than the band. Occasionally, higher molecular-weight bands will be present; these are dsRNA with more complex secondary structure.
26. Using the ladder as a reference, estimate the concentration for each dsRNA sample (*see* **Note 8**).
27. Once purified, dsRNA can be stored at −20 °C for up to several months.

3.3 dsRNA Feeding for RNA Interference (RNAi)

Determine the design for the RNAi experiment. The time course frequently used in my laboratory is to complete three feedings every 5 days with 3–5 μg dsRNA per feeding for 10 planarians (Fig. 3a). We wait for 7 days after the last feeding and amputate animals pre-pharyngeally. After amputation, we wait for 7 days until observing or fixing animals for assessment of regeneration as detailed below. Other feeding paradigms, injection paradigms, dsRNA doses, and amputation strategies may be used (Fig. 3b–e, *see* **Note 9**).

1. Line a cafeteria tray with paper towels to absorb spills.
2. For each gene of interest, half-fill one Petri dish with 1x Montjuïc salts.

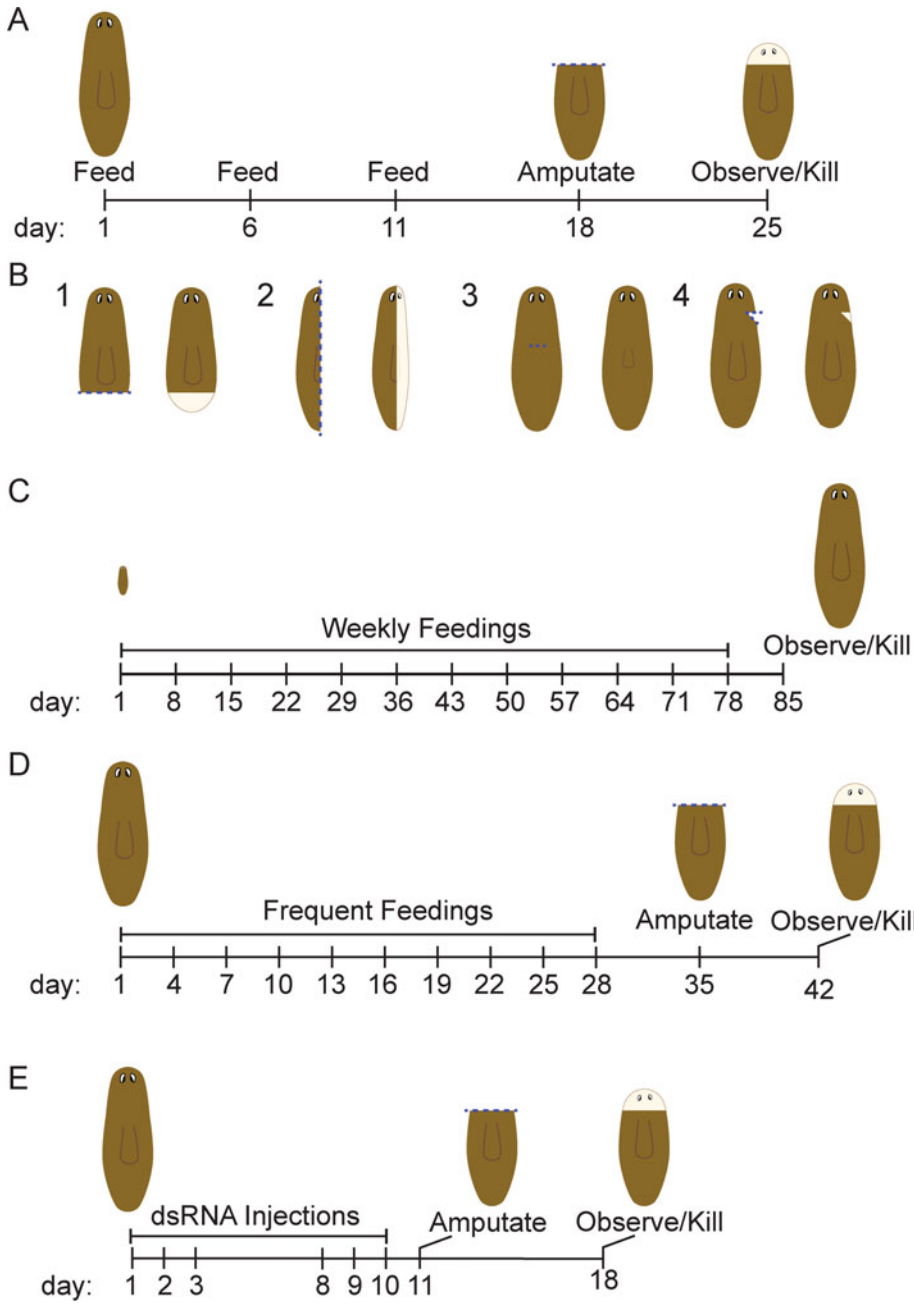


Fig. 3 Paradigms for RNAi. (**a**) The typical strategy used in my laboratory for dsRNA feedings and amputation is shown here. Planarians receive three feedings of dsRNA over the course of ~11 days. Pre-pharyngeal amputation occurs approximately 1 week after the final feeding and animals are observed for head or brain regeneration 1 week after amputation. (**b**) Additional amputation strategies are presented. Amputation is indicated with a dashed line on the left image of each pair and regeneration is diagrammed in the right image of each pair, with blastema tissue shown in a lighter color. (1) Animals can be amputated post-pharyngeally to observe tail regeneration. (2) Sagittal amputation can be used to observe regeneration of lateral structures and reestablishment of mediolateral patterning. (3) Chemical amputation can be used to remove the pharynx to observe pharyngeal regeneration [20]. (4) Other excisions can be made to determine local wound responses after minor injuries. (**c**) A long-term RNAi strategy with weekly dsRNA feedings can be used to determine

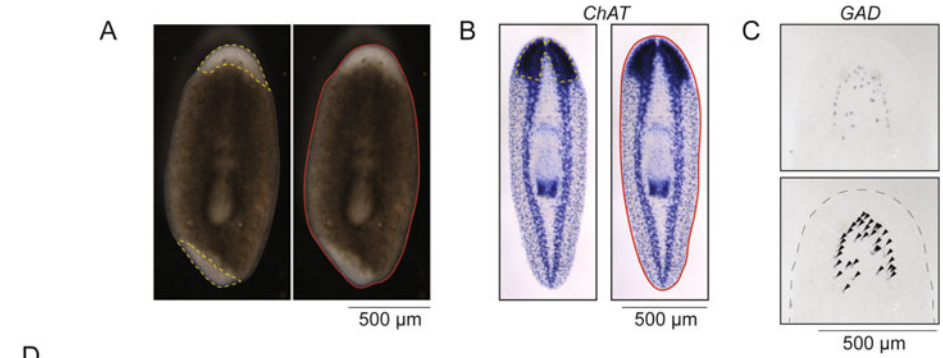
3. Include dishes for positive and negative controls (*see* **Notes 4** and **10**).
4. Label both the tray and each petri dish with experimental (tray) and sample (dish) information.
5. Add planarians to each dish. A 60-mm petri dish will fit 10 asexual planarians or a 100-mm deep-well petri dish can be used for 30 asexual planarians. Choose planarians that are ~5 mm long and that have been starved for ~1 week before the experiment. Details that follow are appropriate for experiments using 10 planarians.
6. In a 1.5-mL tube, mix 100 μL 1× Montjuïc salts per 400 μL planarian food.
7. Using a disposable pestle, mix the food and salts until the combination reaches a uniform consistency.
8. Pulse the tube in a centrifuge to pellet large pieces of tissue.
9. For each target of interest, aliquot 3–5 μg of purified dsRNA into a separate, labeled tube.
10. Add 1 μL green food coloring to each sample of dsRNA (*see* **Note 11**).
11. Pipet 30 μL of food mixture into each dsRNA-containing tube using a 200-μL pipette tip with the end cut off.
12. Using the same tip, stir until the food and coloring are evenly mixed.
13. Using the same tip, pipet the colored food and dsRNA mixture onto the bottom of a petri dish. The food mix should stay together well with a paste-like consistency and should not diffuse.
14. Repeat **steps 9–13** for each subsequent dsRNA sample.
15. Cover petri dishes with lids and cover the tray with a second tray or aluminum foil.
16. Allow planarians to eat for 1.5–2 h in near darkness. Planarians should appear green under a microscope after feeding, due to the food dye within their intestines.
17. Remove excess liver to a waste container using a transfer pipette.

Fig. 3 (continued) whether genes are required for growth or tissue maintenance under homeostatic (non-injury) conditions. (**d**) Frequent feeding strategies can be used to increase the efficiency of gene knockdown by RNAi and to improve phenotype penetrance. (**e**) Injection strategies can be used instead of or in addition to dsRNA feeding [13]. Though this strategy is more time-consuming, it can be especially valuable when gene knockdown interferes with proper feeding of the planarians

18. Using Montjuïc salts in a squirt bottle and a fresh transfer pipette for each plate, wash animals gently but thoroughly three times in the bottom of the petri dish.
19. Using the squirt bottle, add salts and pour to transfer the worms to the lid of the petri dish for three more washes.
20. After washes, transfer the planarians to fresh, labeled petri dishes half-filled with Montjuïc salts.
21. Incubate planarians in the dark at a constant, cool temperature (recommended incubation at 18 °C).
22. Wait for 5 days before feeding planarians.
23. Repeat **steps 6–22** two more times to induce a robust RNAi phenotype.
24. For paradigms that involve regeneration, amputation should occur 7 days after the last feeding.
25. Place two-folded science wipes on a solid metal block and then place one piece of filter paper on top of the science wipes.
26. Wet this setup until damp with Montjuïc salts.
27. Place this setup under a dissecting microscope to more precisely amputate the planarians.
28. Using a transfer pipette with a wide tip, transfer planarians from the petri dish onto the filter paper.
29. During the time in which planarians are on the filter paper, gently spray with Montjuïc salts as needed to keep planarians damp.
30. For head regeneration studies, use a clean scalpel to amputate planarians approximately 1/3 of the length of the body away from the tip of the head. This will remove the entire brain of the planarian (Fig. 3a).
31. Once all planarians from this dish are amputated, use a spray bottle of Montjuïc salts to rinse amputated pieces from the filter paper into a fresh petri dish.
32. Remove any unwanted pieces.
33. Fill the new petri dish half-full with 1x Montjuïc salts.
34. Repeat **steps 28–33** for each petri dish in the experiment.
35. Add gentamicin solution 1:1000 to prevent any bacterial growth.
36. Incubate planarians in the dark at a constant, cool temperature (18 °C) for regeneration.

3.4 Strategies for Assessing Regeneration After RNAi

Performing RNAi for 10 or more animals per sample is usually sufficient to assess whether significant differences exist between control and experimental RNAi-treated animals. After RNAi treatment and amputation, one or more of the following approaches may be used to assess and quantify regeneration: blastema



D

Cell type	Immunofluorescence	*in situ* hybridization
Stem cells	α-SMEDWI-1 ***(25)***, α-H3P(S10) ***(26)***	*smedwi-1* ***(30)***
Neurons (broad)	α-synapsin ***(22)***	*ChAT* ***(20)***, *PC2* ***(21)***, *nAChR*
Neural subsets	α-beta arrestin ***(40)***, α-5-HT ***(22)***	*gpas* ***(43)***, *TH* ***(44)***, *GAD* ***(35)***, *cintillo* ***(45)***, *CNG1* ***(13)***, *ppp-2* ***(16)***
Intestine	3G9 ***(46)***, 3F11 ***(24)***	*npc2*, *ctsla*, *slc22a6* ***(47)***, *dd2841*
Muscle	6G10 ***(23)***, 2G3 ***(23)***, 2H3 ***(24)***	*mhc* ***(48)***, *collagen* ***(49)***
Protonephridia	α-acetylated tubulin ***(50)***, 5B1 ***(23)***	*smedinx-10* ***(51)***, *cavII-1* ***(52)***, *rootletin* ***(53)***
Germ cells, etc.		*nanos* ***(54)***, *gH4* ***(54)***, *dmd-1* ***(55)***
Epidermis	3H3, 1E12 ***(24)***	*vim-1*, *laminB* ***(56)***, *rootletin* ***(57)***
Other cell types	α-IF-1 (glia) ***(58)***	*laminin* (pharynx) ***(31)***, *estrella* (glia) ***(13)***, *F-spondin* (parench) ***(13)***, many novel types ***(59-60)***

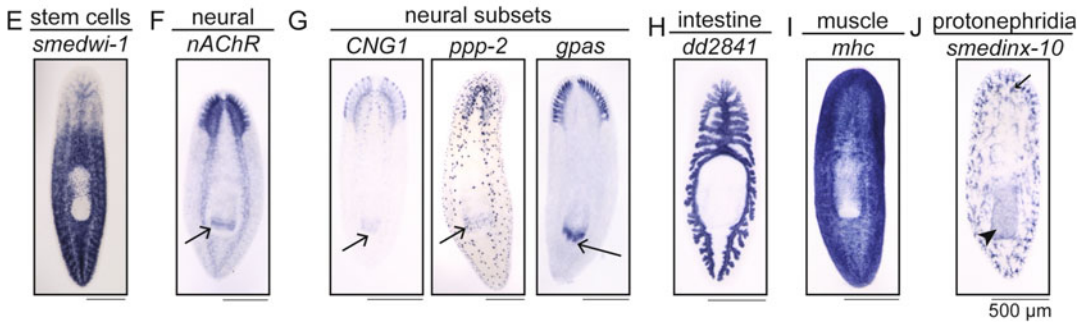


Fig. 4 Assessing regeneration phenotypes. (**a**) Blastema size can be measured by outlining the blastema (yellow dashed line) and measuring blastema area in ImageJ [30]. The body size can similarly be measured (red line). By dividing blastema size by body size to normalize for variable animal size, the resulting value can be compared across populations and RNAi treatments. (**b**) Similarly, I use in situ hybridization with a *choline acetyltransferase* (*ChAT*) riboprobe [23] to stain the central nervous system for measurement of brain size after regeneration (yellow dashed line). Brain size can also be normalized to body size (red line) for comparison of brain regeneration across RNAi treatments. (**c**) Some cell types are present in numbers low enough that they can be accurately counted, like cells expressing *glutamic acid decarboxylase* (*GAD*) [31]. Counting these cell types for regenerated animals following RNAi treatment would allow determination of genes that affect regeneration of GAD^+ cells. In the image shown, 34 cells are labeled (arrowheads). (**d**) This table lists some available antibodies and examples of riboprobes that can be used for staining diverse cell types or organ

measurement (*see* **Note 12**); in situ hybridization to examine specific organs or cell types ([21, 22], *see* **Note 13**); immunofluorescence to detect cell types or tissue regeneration ([23–29], *see* **Note 14**); reverse transcription and quantitative PCR (RT-qPCR) to examine gene expression (*see* **Notes 15** and **16**); functional assessment including behavioral assays (*see* **Note 17**). Potential data from these types of experiments are shown in Fig. 4.

4 Notes

1. This methods chapter describes the approach used in my laboratory to perform RNAi using the species *Schmidtea mediterranea*. RNAi has also been used to query gene function in other freshwater planarians including *Dugesia japonica* [11], *Procotyla fluviatilis* [52], *Phagocata kawakatsui* [53], and *Dendrocoelem lacteum* [54].
2. I use diethyl pyrocarbonate (DEPC) treatment as per the manufacturer's instructions to generate RNase-free water, but it can also be purchased directly.
3. The pJC53.2 vector was designed for TA cloning of cDNA fragments [18] (Fig. 2a, b). Cloning is performed to ligate PCR products amplified from cDNA into pJC53.2 which has been cut by Eam1105I. This strategy positions inserts so that they have T7 promoter sites on 5′ and 3′ ends to facilitate dsRNA synthesis. This vector also has an Sp6 promoter on one side of the insert and a T3 promoter on the other side of the insert. By cloning into this vector, one can use the same cloned fragment for dsRNA synthesis and for synthesis of antisense riboprobe for in situ hybridization. This vector is available from Addgene (plasmid #26536).
4. Prior to cloning, the pJC53.2 vector has two bacterial genes in the insert region, *ccdB* and *camR*. Thus, undigested pJC53.2 can be used to synthesize a dsRNA product that does not match planarian genes and can be used as a negative control. In my laboratory, we also routinely use *Aequoria green fluorescent protein* (*GFP*) cloned into pJC53.2 as a template for a

Fig. 4 (continued) systems [23–29, 32–51]. These approaches may be used to determine whether regeneration proceeds normally after RNAi, including the shape of organs and the renewed expression of key markers. (**e–j**) In situ hybridization examples are presented. These expression patterns could be used to explore regeneration of the following cell types, structures, and organs: stem cells (*smedwi-1* [32]); neurons (*nAChR*, *dd_Smed_v6_8058_0_1*); subsets of neurons (*CNG1* [15], *ppp-2* [18]) including brain branches (*gpas* [34]); the intestine (*dd_Smed_v6_2841_0_1*); muscle (*mhc* [39]); and protonephridia (*smedinx-10* [42]). Note some neural staining in the pharynx (arrows in **f** and **g**). *smedinx-10* also stains cells in the pharynx (arrowhead in **j**) and pigment cups of the eyespots (small arrow in **j**)

negative control. In parallel, for a positive control, I recommend that dsRNA be generated from a fragment of *Smedwi-2* or another gene for which RNAi produces a known phenotype. *Smedwi-2(RNAi)* causes lysis and death of the planarians in a short period of time [32]. Observation of this phenotype can help ensure that synthesis and dosage are appropriate and consistent.

5. I use a Hot Start PCR protocol for template amplification, but these steps could be exchanged for many other PCR protocols.
6. My laboratory uses Zymo Clean and Concentrator kits, but other kits or methods for DNA purification can be substituted. Take care to remove all ethanol during the purification of DNA products, as it can inhibit in vitro synthesis of RNA. For some kits, an extra drying spin after the wash steps can help to remove extra ethanol that is present in the wash buffer.
7. This protocol has been adapted from a previously published protocol for in vitro synthesis of dsRNA [12]. In this work, the authors also present helpful data on the effective timing and concentration for RNAi administered by dsRNA feeding.
8. Though a spectrophotometer can be used to estimate dsRNA concentration, I find that this approach typically overestimates the concentration of dsRNA. A falsely high spectrophotometer reading could be caused by residual rNTPs that are precipitated or retained during the purification steps. Determining dsRNA concentration based on the intensity of the band leads to more reproducible gene knockdown. For an example of this approach, if one compares a 1:10 dsRNA band and find that it is similar in intensity to 100 ng of the 1 kb band in the ladder, then one can estimate that our dsRNA concentration (undiluted) is ~1 μg/μL.
9. Here, I provide notes on experimental design for RNAi experiments. Three main variables must be chosen for RNAi experiments: dosage, frequency/duration of feeding, and method of dsRNA administration (injection vs. feeding). Our main experimental design is presented in the Methods section of this chapter (Fig. 3a). This paradigm is appropriate for most screening and assessment of gene effects on regeneration. Alternative amputation strategies to examine tail regeneration, lateral regeneration, pharyngeal regeneration [20], or regeneration after minor injuries are diagrammed (Fig. 3b). To observe the effects of long-term RNAi without amputation, I typically use a weekly feeding paradigm (Fig. 3c). Other approaches, including frequent feedings and injection (Fig. 3d, e), have been used for successful knockdown of genes of interest (e.g., [55] for frequent feedings, [56] for injections). Injection might be a preferred strategy in situations where a phenotype occurs

quickly or when the phenotype prevents feeding (e.g., paralysis, loss of pharynx).

10. Here, I provide notes for setup of RNAi experiments. Though cafeteria trays are convenient for organization, dropping a tray can be devastating. Be careful when transporting RNAi experiments and be cautious around other lab members when they are moving trays. I prefer deep-well 100-mm petri dishes for our bigger (30 worms) or long-term RNAi experiments *or* when I expect to use larger (1 cm) asexual planarians or sexual planarians. For especially large worms or large RNAi experiments, small Ziploc® containers may be used instead of petri dishes. The number of planarians per dish as well as animal size can be optimized for atypical RNAi paradigms. For example, I start with very small (<2 mm) worms for long-term experiments to avoid fissioning.
11. Though 3–5 μg per feeding (final concentration in liver mix of ~0.1–0.2 μg/μL) is sufficient for most of our experiments, the range of concentrations used in the planarian field is *very* broad. Concentration, as well as animal size and feeding paradigm, can impact the penetrance and speed of RNAi phenotypes [12]. In some experiments, I have combined knockdown of several genes to investigate whether genes work together or oppose one another (e.g., *activin* and *follistatin* [57]). In these experiments, I standardize both concentration and total mass of dsRNA across control, single knockdown, and double knockdown conditions.
12. Animals may be killed and fixed for blastema measurement (Fig. 4a) or observation of eyespots. Initially, regenerating tissue is unpigmented, which allows for the newly regenerated tissue within the blastema to be clearly observed and measured.
13. Animals may be killed and fixed for in situ hybridization using a riboprobe to mark specific organs or cell types [21, 22]. This allows one to assess the regeneration of a specific cell or tissue type (Fig. 4b–j). For example, in situ hybridization with *choline acetyltransferase* (*ChAT*) [23] marks cholinergic neurons and can be used to broadly mark the brain to measure brain size after regeneration [15] (Fig. 4b). Alternatively, with some in situ hybridization staining (e.g., *glutamic acid decarboxylase*, *GAD* [31]), cells can be counted (Fig. 4c).
14. Animals may be killed and fixed for immunofluorescence experiments to assess organ regeneration (Fig. 4d) [23–27]. Immunofluorescence is also useful for examining proteins that localize differently than their mRNA; for example, *smedwi-1* is present in dividing stem cells, but SMEDWI-1 protein is present in differentiating stem cells as well [28]. Immunofluorescence can also be used to detect protein

modifications. For example, histone H3 phosphorylated at Serine 10 is a marker of mitotic stem cells [29].

15. Animals may be killed and processed to purify mRNAs for downstream reverse transcription and quantitative PCR (RT-qPCR). This approach can be used to determine the effectiveness of RNAi knockdown or the effect of knockdown on other tissues using cell type-specific target genes (*see* **Note 12**, and for one example [15]).
16. When choosing primers for assessment of mRNA knockdown by RT-qPCR, it is best to choose a pair of primers that will recognize the target mRNA but not the dsRNA that is administered for RNAi. In some instances, the knockdown efficiency has seemed poor despite a strong phenotype, potentially due to a primer pair binding to and amplifying fragments of cDNA generated from both mRNA and dsRNA.
17. Animals may be subjected to functional analyses. For example, behavior could be assessed in a feeding assay [5, 15, 20, 58], which could give an indication of whether neural, intestinal, and/or pharyngeal regeneration has been achieved. Live imaging to assess movement or response to stimuli (touch, light, temperature) can indicate whether neural function and muscle function are normal after regeneration [33, 59, 60].

Acknowledgments

I would like to thank Bidushi (Tulip) Chandra and Jennifer Jenkins for constructive feedback on this chapter. I would like to thank our funding sources, including the Alfred P. Sloan Foundation and the McKnight Foundation, for financial support.

References

1. Reddien PW (2013) Specialized progenitors and regeneration. Development 140(5): 951–957. https://doi.org/10.1242/dev.080499
2. Ivankovic M, Haneckova R, Thommen A, Grohme MA, Vila-Farre M, Werner S, Rink JC (2019) Model systems for regeneration: planarians. Development 146(17). https://doi.org/10.1242/dev.167684
3. Reddien PW (2018) The cellular and molecular basis for planarian regeneration. Cell 175(2): 327–345. https://doi.org/10.1016/j.cell.2018.09.021
4. Roberts-Galbraith RH, Newmark PA (2015) On the organ trail: insights into organ regeneration in the planarian. Curr Opin Genet Dev 32:37–46. https://doi.org/10.1016/j.gde.2015.01.009
5. Forsthoefel DJ, Park AE, Newmark PA (2011) Stem cell-based growth, regeneration, and remodeling of the planarian intestine. Dev Biol 356(2):445–459. https://doi.org/10.1016/j.ydbio.2011.05.669
6. Ross KG, Currie KW, Pearson BJ, Zayas RM (2017) Nervous system development and regeneration in freshwater planarians. Wiley Interdiscip Rev Dev Biol 6(3). https://doi.org/10.1002/wdev.266
7. Wagner DE, Wang IE, Reddien PW (2011) Clonogenic neoblasts are pluripotent adult stem cells that underlie planarian regeneration.

Science 332(6031):811–816. https://doi.org/10.1126/science.1203983

8. Elliott SA, Sánchez Alvarado A (2018) Planarians and the history of animal regeneration: paradigm shifts and key concepts in biology. Methods Mol Biol 1774:207–239. https://doi.org/10.1007/978-1-4939-7802-1_4
9. Sánchez Alvarado A, Newmark PA (1999) Double-stranded RNA specifically disrupts gene expression during planarian regeneration. Proc Natl Acad Sci U S A 96(9):5049–5054. https://doi.org/10.1073/pnas.96.9.5049
10. Newmark PA, Reddien PW, Cebrià F, Sánchez Alvarado A (2003) Ingestion of bacterially expressed double-stranded RNA inhibits gene expression in planarians. Proc Natl Acad Sci U S A 100(Suppl 1):11861–11865. https://doi.org/10.1073/pnas.1834205100
11. Orii H, Mochii M, Watanabe K (2003) A simple "soaking method" for RNA interference in the planarian *Dugesia japonica*. Dev Genes Evol 213(3):138–141. https://doi.org/10.1007/s00427-003-0310-3
12. Rouhana L, Weiss JA, Forsthoefel DJ, Lee H, King RS, Inoue T, Shibata N, Agata K, Newmark PA (2013) RNA interference by feeding *in vitro*-synthesized double-stranded RNA to planarians: methodology and dynamics. Dev Dyn 242(6):C1. https://doi.org/10.1002/dvdy.23982
13. Shibata N, Agata K (2018) RNA interference in planarians: feeding and injection of synthetic dsRNA. Methods Mol Biol 1774:455–466. https://doi.org/10.1007/978-1-4939-7802-1_18
14. Adler CE, Sánchez Alvarado A (2018) Systemic RNA interference in planarians by feeding of dsRNA containing bacteria. Methods Mol Biol 1774:445–454. https://doi.org/10.1007/978-1-4939-7802-1_17
15. Roberts-Galbraith RH, Brubacher JL, Newmark PA (2016) A functional genomics screen in planarians reveals regulators of whole-brain regeneration. eLife 5:e17002. https://doi.org/10.7554/eLife.17002
16. Takano T, Pulvers JN, Inoue T, Tarui H, Sakamoto H, Agata K, Umesono Y (2007) Regeneration-dependent conditional gene knockdown (Readyknock) in planarian: demonstration of requirement for *Djsnap-25* expression in the brain for negative phototactic behavior. Develop Growth Differ 49(5):383–394. https://doi.org/10.1111/j.1440-169X.2007.00936.x
17. Reddien PW, Bermange AL, Murfitt KJ, Jennings JR, Sánchez Alvarado A (2005) Identification of genes needed for regeneration, stem cell function, and tissue homeostasis by systematic gene perturbation in planaria. Dev Cell 8(5):635–649. https://doi.org/10.1016/j.devcel.2005.02.014
18. Collins JJ 3rd, Hou X, Romanova EV, Lambrus BG, Miller CM, Saberi A, Sweedler JV, Newmark PA (2010) Genome-wide analyses reveal a role for peptide hormones in planarian germline development. PLoS Biol 8(10):e1000509. https://doi.org/10.1371/journal.pbio.1000509
19. Merryman MS, Sánchez Alvarado A, Jenkin JC (2018) Culturing planarians in the laboratory. Methods Mol Biol 1774:241–258. https://doi.org/10.1007/978-1-4939-7802-1_5
20. Adler CE, Seidel CW, McKinney SA, Sánchez Alvarado A (2014) Selective amputation of the pharynx identifies a *FoxA*-dependent regeneration program in planaria. eLife 3:e02238. https://doi.org/10.7554/eLife.02238
21. Pearson BJ, Eisenhoffer GT, Gurley KA, Rink JC, Miller DE, Sánchez Alvarado A (2009) Formaldehyde-based whole-mount in situ hybridization method for planarians. Dev Dyn 238(2):443–450. https://doi.org/10.1002/dvdy.21849
22. King RS, Newmark PA (2013) In situ hybridization protocol for enhanced detection of gene expression in the planarian *Schmidtea mediterranea*. BMC Dev Biol 13:8. https://doi.org/10.1186/1471-213X-13-8
23. Nishimura K, Kitamura Y, Taniguchi T, Agata K (2010) Analysis of motor function modulated by cholinergic neurons in planarian *Dugesia japonica*. Neuroscience 168(1):18–30. https://doi.org/10.1016/j.neuroscience.2010.03.038
24. Agata K, Soejima Y, Kato K, Kobayashi C, Umesono Y, Watanabe K (1998) Structure of the planarian central nervous system (CNS) revealed by neuronal cell markers. Zool Sci 15(3):433–440. https://doi.org/10.2108/zsj.15.433
25. Cebrià F (2008) Organization of the nervous system in the model planarian *Schmidtea mediterranea*: an immunocytochemical study. Neurosci Res 61(4):375–384. https://doi.org/10.1016/j.neures.2008.04.005
26. Ross KG, Omuro KC, Taylor MR, Munday RK, Hubert A, King RS, Zayas RM (2015) Novel monoclonal antibodies to study tissue regeneration in planarians. BMC Dev Biol 15:2. https://doi.org/10.1186/s12861-014-0050-9
27. Forsthoefel DJ, Waters FA, Newmark PA (2014) Generation of cell type-specific monoclonal antibodies for the planarian and

optimization of sample processing for immunolabeling. BMC Dev Biol 14:45. https://doi.org/10.1186/s12861-014-0045-6

28. Guo T, Peters AH, Newmark PA (2006) A *Bruno-like* gene is required for stem cell maintenance in planarians. Dev Cell 11(2): 159–169. https://doi.org/10.1016/j.devcel.2006.06.004
29. Newmark PA, Sánchez Alvarado A (2000) Bromodeoxyuridine specifically labels the regenerative stem cells of planarians. Dev Biol 220(2): 142–153. https://doi.org/10.1006/dbio.2000.9645
30. Schneider CA, Rasband WS, Eliceiri KW (2012) NIH image to ImageJ: 25 years of image analysis. Nat Methods 9(7):671–675
31. Nishimura K, Kitamura Y, Umesono Y, Takeuchi K, Takata K, Taniguchi T, Agata K (2008) Identification of *glutamic acid decarboxylase* gene and distribution of GABAergic nervous system in the planarian *Dugesia japonica*. Neuroscience 153(4):1103–1114. https://doi.org/10.1016/j.neuroscience.2008.03.026
32. Reddien PW, Oviedo NJ, Jennings JR, Jenkin JC, Sánchez Alvarado A (2005) SMEDWI-2 is a PIWI-like protein that regulates planarian stem cells. Science 310(5752):1327–1330. https://doi.org/10.1126/science.1116110
33. Inoue T, Kumamoto H, Okamoto K, Umesono Y, Sakai M, Sánchez Alvarado A, Agata K (2004) Morphological and functional recovery of the planarian photosensing system during head regeneration. Zool Sci 21(3): 275–283. https://doi.org/10.2108/zsj.21.275
34. Cebrià F, Kudome T, Nakazawa M, Mineta K, Ikeo K, Gojobori T, Agata K (2002) The expression of neural-specific genes reveals the structural and molecular complexity of the planarian central nervous system. Mech Dev 116(1–2):199–204
35. Nishimura K, Kitamura Y, Inoue T, Umesono Y, Sano S, Yoshimoto K, Inden M, Takata K, Taniguchi T, Shimohama S, Agata K (2007) Reconstruction of dopaminergic neural network and locomotion function in planarian regenerates. Dev Neurobiol 67(8): 1059–1078. https://doi.org/10.1002/dneu.20377
36. Oviedo NJ, Newmark PA, Sánchez Alvarado A (2003) Allometric scaling and proportion regulation in the freshwater planarian *Schmidtea mediterranea*. Dev Dyn 226(2):326–333. https://doi.org/10.1002/dvdy.10228
37. Forsthoefel DJ, James NP, Escobar DJ, Stary JM, Vieira AP, Waters FA, Newmark PA (2012) An RNAi screen reveals intestinal regulators of branching morphogenesis, differentiation, and stem cell proliferation in planarians. Dev Cell 23(4):691–704. https://doi.org/10.1016/j.devcel.2012.09.008
38. Forsthoefel DJ, Cejda NI, Khan UW, Newmark PA (2020) Cell-type diversity and regionalized gene expression in the planarian intestine. eLife 9:e52613. https://doi.org/10.7554/eLife.52613
39. Cebrià F, Vispo M, Bueno D, Carranza S, Newmark PA, Romero R (1996) *Myosin heavy chain* gene in *Dugesia (G.) tigrina*: a tool for studying muscle regeneration in planarians. Int J Dev Biol Suppl 1:177S–178S
40. Witchley JN, Mayer M, Wagner DE, Owen JH, Reddien PW (2013) Muscle cells provide instructions for planarian regeneration. Cell Rep 4(4):633–641. https://doi.org/10.1016/j.celrep.2013.07.022
41. Glazer AM, Wilkinson AW, Backer CB, Lapan SW, Gutzman JH, Cheeseman IM, Reddien PW (2010) The Zn finger protein iguana impacts hedgehog signaling by promoting ciliogenesis. Dev Biol 337(1):148–156. https://doi.org/10.1016/j.ydbio.2009.10.025
42. Oviedo NJ, Levin M (2007) *smedinx-11* is a planarian stem cell gap junction gene required for regeneration and homeostasis. Development 134(17):3121–3131. https://doi.org/10.1242/dev.006635
43. Rink JC, Vu HT, Sánchez Alvarado A (2011) The maintenance and regeneration of the planarian excretory system are regulated by EGFR signaling. Development 138(17):3769–3780. https://doi.org/10.1242/dev.066852
44. Scimone ML, Srivastava M, Bell GW, Reddien PW (2011) A regulatory program for excretory system regeneration in planarians. Development 138(20):4387–4398. https://doi.org/10.1242/dev.068098
45. Wang Y, Zayas RM, Guo T, Newmark PA (2007) *Nanos* function is essential for development and regeneration of planarian germ cells. Proc Natl Acad Sci U S A 104(14):5901–5906. https://doi.org/10.1073/pnas.0609708104
46. Chong T, Collins JJ 3rd, Brubacher JL, Zarkower D, Newmark PA (2013) A sex-specific transcription factor controls male identity in a simultaneous hermaphrodite. Nat Commun 4:1814. https://doi.org/10.1038/ncomms2811
47. Tu KC, Cheng LC, Vu HT, Lange JJ, McKinney SA, Seidel CW, Sánchez Alvarado A (2015) *Egr-5* is a post-mitotic regulator of planarian

epidermal differentiation. eLife 4:e10501. https://doi.org/10.7554/eLife.10501

48. van Wolfswinkel JC, Wagner DE, Reddien PW (2014) Single-cell analysis reveals functionally distinct classes within the planarian stem cell compartment. Cell Stem Cell 15(3):326–339. https://doi.org/10.1016/j.stem.2014.06.007
49. Wang IE, Lapan SW, Scimone ML, Clandinin TR, Reddien PW (2016) Hedgehog signaling regulates gene expression in planarian glia. eLife 5:e16996. https://doi.org/10.7554/eLife.16996
50. Fincher CT, Wurtzel O, de Hoog T, Kravarik KM, Reddien PW (2018) Cell type transcriptome atlas for the planarian *Schmidtea mediterranea*. Science 360(6391):eaaq1736. https://doi.org/10.1126/science.aaq1736
51. Plass M, Solana J, Wolf FA, Ayoub S, Misios A, Glazar P, Obermayer B, Theis FJ, Kocks C, Rajewsky N (2018) Cell type atlas and lineage tree of a whole complex animal by single-cell transcriptomics. Science 360(6391):eaaq1723. https://doi.org/10.1126/science.aaq1723
52. Sikes JM, Newmark PA (2013) Restoration of anterior regeneration in a planarian with limited regenerative ability. Nature 500(7460):77–80. https://doi.org/10.1038/nature12403
53. Umesono Y, Tasaki J, Nishimura Y, Hrouda M, Kawaguchi E, Yazawa S, Nishimura O, Hosoda K, Inoue T, Agata K (2013) The molecular logic for planarian regeneration along the anterior-posterior axis. Nature 500(7460):73–76. https://doi.org/10.1038/nature12359
54. Liu SY, Selck C, Friedrich B, Lutz R, Vila-Farre M, Dahl A, Brandl H, Lakshmanaperumal N, Henry I, Rink JC (2013) Reactivating head regrowth in a regeneration-deficient planarian species. Nature 500(7460):81–84. https://doi.org/10.1038/nature12414
55. Scimone ML, Wurtzel O, Malecek K, Fincher CT, Oderberg IM, Kravarik KM, Reddien PW (2018) *foxF-1* controls specification of non-body wall muscle and phagocytic cells in planarians. Curr Biol 28(23):3787–3801.e6. https://doi.org/10.1016/j.cub.2018.10.030
56. Fraguas S, Barberán S, Iglesias M, Rodríguez-Esteban G, Cebrià F (2014) *egr-4*, a target of EGFR signaling, is required for the formation of the brain primordia and head regeneration in planarians. Development 141(9):1835–1847. https://doi.org/10.1242/dev.101345
57. Roberts-Galbraith RH, Newmark PA (2013) Follistatin antagonizes Activin signaling and acts with notum to direct planarian head regeneration. Proc Natl Acad Sci U S A 110(4):1363–1368. https://doi.org/10.1073/pnas.1214053110
58. Miyamoto M, Hattori M, Hosoda K, Sawamoto M, Motoishi M, Hayashi T, Inoue T, Umesono Y (2020) The pharyngeal nervous system orchestrates feeding behavior in planarians. Sci Adv 6(15):eaaz0882. https://doi.org/10.1126/sciadv.aaz0882
59. Ross KG, Molinaro AM, Romero C, Dockter B, Cable KL, Gonzalez K, Zhang S, Collins ES, Pearson BJ, Zayas RM (2018) SoxB1 activity regulates sensory neuron regeneration, maintenance, and function in planarians. Dev Cell 47(3):331–347.e5. https://doi.org/10.1016/j.devcel.2018.10.014
60. Arenas OM, Zaharieva EE, Para A, Vásquez-Doorman C, Petersen CP, Gallio M (2017) Activation of planarian TRPA1 by reactive oxygen species reveals a conserved mechanism for animal nociception. Nat Neurosci 20(12):1686–1693. https://doi.org/10.1038/s41593-017-0005-0

Open Access This chapter is licensed under the terms of the Creative Commons Attribution 4.0 International License (http://creativecommons.org/licenses/by/4.0/), which permits use, sharing, adaptation, distribution and reproduction in any medium or format, as long as you give appropriate credit to the original author(s) and the source, provide a link to the Creative Commons license and indicate if changes were made.

The images or other third party material in this chapter are included in the chapter's Creative Commons license, unless indicated otherwise in a credit line to the material. If material is not included in the chapter's Creative Commons license and your intended use is not permitted by statutory regulation or exceeds the permitted use, you will need to obtain permission directly from the copyright holder.





Chapter 28

Monitoring Chromatin Regulation in Planarians Using Chromatin Immunoprecipitation Followed by Sequencing (ChIP-seq)

Divya Sridhar and Aziz Aboobaker

Abstract

Planarians are an accessible model system to study animal regeneration and stem cells. Over the last two decades, new molecular techniques have provided us with powerful tools to understand whole-body regeneration and pluripotent adult stem cells specifically. We describe a method for performing *Chromatin Immunoprecipitation followed by sequencing* (ChIP-seq) on planarian cells that relies on FACS to isolate different cell populations followed by immunoprecipitation and library preparation for next-generation sequencing. Whole-genome profiling of histone modifications enables a greater understanding of epigenetic mechanisms in development, pluripotency, and differentiation. This protocol adds to the growing list of functional genomic approaches to study whole-body regeneration in animals.

Key words Planarian, Chromatin, Immunoprecipitation, Epigenetic regulation, Pluripotency, FACS, Histone modifications

1 Introduction

Planarians are best known for their ability to regenerate their whole bodies and owe this remarkable ability to neoblasts, their sole population of pluripotent stem cells. Being the only dividing cell in planarians, neoblasts replace cells lost due to normal physiological turnover as well as injury [1–3]. Neoblasts are thus a promising model system to investigate the epigenetic regulation of pluripotency, stem cell function and differentiation, and tissue patterning during regeneration. Various studies have established conservation of key features of stem cell biology with other animals. Planarians also allow the study of stem cell heterogeneity and lineage progression from undifferentiated stem cells due to the availability of molecular markers for stem cells and their progeny [4, 5]. An advantage of using *Schmidtea mediterranea* as a model organism for studying epigenetics is the availability of an excellent array of genomic resources and tools to make these studies possible. These

Simon Blanchoud and Brigitte Galliot (eds.), *Whole-Body Regeneration: Methods and Protocols*,
Methods in Molecular Biology, vol. 2450, https://doi.org/10.1007/978-1-0716-2172-1_28, © The Author(s) 2022

include an excellent genome assembly [6], annotations [7], genome database [8], and a transcriptome repository [9]. Nevertheless, while planarians are a promising model system for in vivo stem cell biology, we are only beginning to understand the molecular principles governing the associated regulatory mechanisms. Further research into stem cells in planarians and other model organisms will help us understand fundamental stem cell properties, including disentangling pluripotency and self-renewal [10].

Our understanding of the epigenetic control of regeneration in planarian is in its relative infancy compared to other model organisms. As the epigenetic regulation of gene expression depends on DNA methylation, histone modifications, and overall chromatin organization, understanding these in pluripotent planarian stem cells is of interest to the community [10]. With respect to DNA methylation, a number of strong lines of evidence suggest that 5-methyl cytosine (the major form of DNA methylation in animals) is not part of epigenetic regulation in planarians [10, 11]. *S. mediterranea* was found to have only the conserved DNA methyltransferase 2 (DNMT2) that despite its name is only thought to methylate RNA [10]. DNA methylation is read by methyl binding domain (MBD) proteins that form key components of histone modifying and chromatin remodeling complexes. In planarians, a single MBD protein, called MBD2/3, has been described. This protein actually lacks the conserved residues known to contact methylated DNA and thus is unlikely to bind 5-methyl cytosine [11]. The absence of the 5-methyl cytosine modification in the *S. mediterranea* genome was also confirmed in various ways, including the lack of antibody staining against 5-methyl cytosine, and undetectable levels of 5-methyl cytosine in high-performance liquid chromatography mass spectrometry [11]. These different lines of evidence suggest that the function of planarian MBD2/3 is likely independent of DNA methylation, and that DNA methylation is not involved in the epigenetic control of planarian neoblasts. The MBD2/3 protein is known to function in the Nucleosome remodeling and Deacetylase (NuRD) complex in animals. In planarians MBD2/3 and the functions of four other NuRD components have been investigated by RNAi-mediated knockdown in planarians: Smed-HDAC1 [12–14] Smed-CHD [15], RbAp48 [16, 17], and GATAD2 (or p66) [18]. Knockdown of each of these genes affects stem cell differentiation.

The phenotypic effects of the loss of epigenetic regulators that control gene expression can be effectively assessed during planarian regeneration using RNAi. Stem cell survival and differentiation defects can be monitored with in situ hybridization using a growing list of markers. The phenotypes observed are caused by the mis-regulation of gene expression across the genome and often, the mis-regulation of a few key genes have a large effect with respect to the observed phenotype. With the advent of Chromatin

Immunoprecipitation followed by sequencing (ChIP-seq) on planarian cells, we can now correlate the phenotypic effects with epigenetic changes at loci across the genome by measuring changes in histone marks in populations of cells as a result of RNAi. By measuring changes in histone marks that induced by RNAi experiments and correlating these changes with gene expression, we can begin to identify epigenetic targets involved in normal stem cell regulation and regeneration. So far studies have confirmed that relationships between gene expression and the enrichment of particular histone marks on nucleosomes proximal to gene promoters present in other animals are conserved [19–21]. For example, as in other animals, higher levels of H3K4me3 are associated with the promoters of actively transcribed genes in planarian stem cells, while H3K27me3 is associated with the promoters of silenced genes [19–21].

ChIP-seq was first used on whole dissociated planarians to show that the histone methyl-transferase enzymes Set1 and MLL1/2, the main mediators of H3K4me3 in animals, target markedly different genomic loci in vivo, respectively [19]. Set1 targets were shown to be associated broadly with the maintenance of basic cell function and survival, while MLL1/2 targets were specifically enriched for genes involved in ciliogenesis. These observations correlate with loss of stem cells in *set1*(RNAi) animals and the specific loss of cilia and associated locomotion in *mll1/2*(RNAi) animals. Mihaylova et al. investigated the role of planarian orthologs of a third H3K4 methyltransferase enzymes MLL3/4 [20]. In mammals, loss of MLL3/4 function has been implicated in tumorigenesis [22–24]. RNAi of MLL3/4 in planarians led to the formation of tumor-like outgrowths, suggesting that this histone methyltransferase has tumor suppressor activity in planarians [20]. RNA-seq and ChIP-seq analyses performed on G2/M planarian stem cells from MLL3/4 knockdown animals indicate that genes downstream of MLL3/4 limit or promote stem cell proliferation during regeneration. The MLL3/4 protein plays a role in transcriptional regulation via mono- and/or tri-methylating H3K4 at promoters and enhancers [20] RNA-seq on the same cells revealed that a number of genes involved in cell proliferation and differentiation, including potential oncogenes, were significantly upregulated. The transcriptional changes of some genes following knockdown of planarian MLL3/4 correlate with differences in H3K4me1 peaks at the promoter region, suggestive of direct effect of MLL3/4.

A study by Dattani et al. applied an improved ChIP-seq protocol for neoblasts in *S. mediterranea* to generate genome-wide profiles for the active marks H3K4me3 and H3K36me3, and suppressive marks H3K4me1 and H3K27me3 [21] in order to look at epigenetic regulation of gene expression in neoblasts. As predicted from work in vertebrates and other protostomes, these marks

showed conserved patterns of association with active and suppressed gene expression in planarian neoblasts. Significantly, loci that have little or no transcriptional activity in the neoblast compartment and are known to activate transcriptionally in the post-mitotic progeny during differentiation show bivalent histone modifications, with both H3K4me3 and H3K27me3 marks at promoter regions. ChIP-seq also revealed high levels of paused RNA Polymerase II at the promoter-proximal region as further evidence that these genes are bivalent in neoblasts, becoming actively transcribed upon differentiation. These findings suggest that epigenetic regulation of potency through bivalency at promoter regions is conserved across bilaterians, rather than a special feature of vertebrates [21]. Overall, these studies have established that ChIP-seq can be efficiently used in neoblasts to investigate epigenetic regulation of stem cell fate.

In this chapter, we provide step-by-step robust protocols for cell dissociation and isolation of planarian cells, chromatin extraction and sonication, immunoprecipitation, and preparation of ChIP libraries (Fig. 1). We also outline a range of quality control steps that could be used at various stages of the protocol.

2 Materials

All solutions should be prepared using ultrapure water and analytical grade reagents. Reagents should be prepared and stored at the temperatures indicated. Local waste disposal regulations should be adhered to when disposing of chemical and plastic waste.

2.1 Cell Dissociation and Isolation of Stem Cells

1. 10× Calcium magnesium free (CMF) buffer: 25.6 mM $NaH_2PO_42H_2O$, 142.8 mM NaCl, 102.1 mM KCl, and 94.2 mM $NaHCO_3$. Add water up to 40 mL. Mix and adjust the pH to 7.2 using NaOH (*see* **Note 1**). Make up the volume to 50 mL. Store at 4 °C.
2. 150 mM HEPES: 1.78 g HEPES–NaOH, pH 7.2, 40 mL H_2O (*see* **Note 1**). Make up the volume to 50 mL and store at 4 °C.
3. 10% (w/v) glucose: 5 g glucose, 40 mL H_2O. Make up the volume to 50 mL and store at 4 °C until used. Make fresh for each use.
4. 10% (w/v) BSA: 5 g BSA, 40 mL H_2O. Make up the volume to 50 mL and store at 4 °C until used. Make fresh for each use.
5. 0.5 M EDTA: 0.5 M EDTA, pH 8.0 (store-bought).
6. $CMFHe^{2+}$: 250 μL 10% BSA, 2.5 mL 10% glucose, 5 mL 150 mM HEPES, 301 μL 0.5 M EDTA, 5 mL 10× CMF.

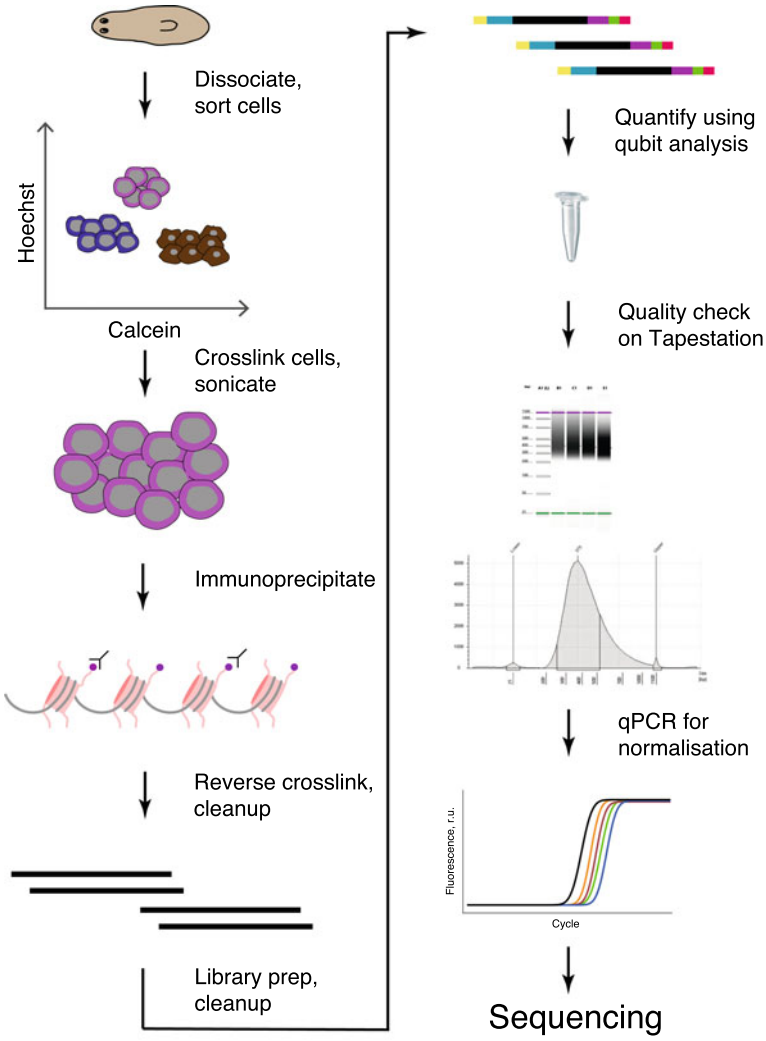


Fig. 1 An overview of the ChIP-seq workflow

Make up the volume to 50 mL using H_2O. Make fresh for each use (*see* **Note 2**).

7. Papain digestion solution: 1 mL 30 U/mL papain, 1 mL $CMFHe^{2+}$. Make fresh for each use (*see* **Note 3**).
8. 5 mL round bottom tubes.
9. 100 μm nylon net filter.
10. 35 μm pore-size cell strainer cap.
11. 20× live DNA stain stock solution (e.g., 1 mg/mL Hoechst 34580 in distilled water). Store at −20 °C.
12. 2000× live cytoplasmic stain stock solution (e.g., 0.2 μg/mL Calcein AM in DMSO). Store at −20 °C.

13. 1000× cell viability stain stock solution (e.g., 10 μg/mL in distilled water). Store at 4 °C in a dark 1.5-mL tube to protect from light.
14. Planaria water: 5 g commercial sea salts (e.g., Instant Ocean) in 10 L water.

2.2 Chromatin Extraction and Sonication

1. 10% NP-40: Molecular biology grade 10% NP-40 solution (store-bought).
2. 10% Triton X-100: Molecular biology grade 10% Triton X-100 solution (store-bought).
3. 1 M Tris–HCl pH 7.5 solution (store-bought).
4. 1 M $CaCl_2$: 11.1 g $CaCl_2$ in 100 mL H_2O. Store at 4 °C.
5. 1 M Sucrose: 17.1 g sucrose in 50 mL H_2O. Store at 4 °C.
6. 0.1 M DTT: 1.5 g DTT in 10 mL of H_2O. Aliquot and store at −20 °C.
7. Phosphatase cocktail inhibitor 2 (Sigma-Aldrich).
8. Phosphatase cocktail inhibitor 3 (Sigma-Aldrich).
9. Protease inhibitor tablets (cOmplete protease inhibitor cocktail, Roche).
10. Nuclei extraction buffer (NEB): 500 μL 10% NP-40, 250 μL 10% Triton X-100, 100 μL 1 M Tris, 30 μL 1 M $CaCl_2$, 2.5 mL 1 M sucrose, 100 μL 0.1 M DTT, 100 μL phosphatase cocktail inhibitor 2, 100 μL phosphatase cocktail inhibitor 3, 6.32 mL H_2O. Prepare the NEB fresh every time, although stock solutions of each components can be stored. Add inhibitors just before use.
11. 1× Phosphate Buffer Solution (PBS): 1.86 mM NaH_2PO_4, 8.41 mM Na_2HPO_4, 175.0 mM NaCl, pH 7.4.
12. PBS with protease inhibitors: One protease inhibitor tablet in 50 mL cold 1× PBS. Ideally make fresh, but will keep for 2–3 days at 4 °C.
13. 2.5 M glycine: 9.386 g glycine in 50 mL water. 2.5 M Glycine can be made in advance and stored at room temperature (RT). Do check for microbial growth if stored for more than 7 days.
14. 10% SDS (store-bought).
15. 1 M Tris–HCl, pH 8.0 solution (store-bought).
16. SDS-lysis buffer: 500 μL 10% SDS, 250 μL 1 M Tris–HCl, pH 8.0, 100 μL 0.5 M EDTA, 4.15 mL H_2O. Can be made in advance and will keep for 2–3 months at RT.
17. ChIP buffer stock: 10 μL 10% SDS, 24 μL 0.5 M EDTA, 167 μL 1 M Tris–HCl, pH 8.0, 334 μL 5 M NaCl, 9.46 mL H_2O. Can be prepared in advance and will keep for 1–2 weeks at RT.

18. ChIP dilution buffer: 2 mL ChIP buffer stock, 2 μL phosphatase cocktail inhibitor 2, 2 μL phosphatase cocktail inhibitor 3, 20 μL 0.1 M DTT. Make fresh and keep on ice.
19. High-precision, temperature-controlled, multiple samples, in sealed tubes sonicator (e.g., Bioruptor, Diagenode).
20. 16% formaldehyde: 16% (w/v) formaldehyde solution (store-bought).
21. DNA mini-elute PCR purification kit.
22. DNA electrophoresis equipment (e.g., TapeStation 2200, Agilent).
23. DNA concentration fluorometer (e.g., Qubit, Thermo Fisher Scientific).

2.3 Immunoprecipitation and Reverse Crosslinking

1. Protein-A covered beads.
2. Magnetic separation rack for 1.5-mL tubes.
3. Blocking solution: 0.5% BSA in 1× PBS.
4. ChIP-grade antibodies: 7 μg antibody per sample (*see* **Note 4**).
5. Commercial Drosophila S2 chromatin as internal immunoprecipitation control (store-bought, e.g., Active Motif).
6. ChIP wash buffer: 50 mM HEPES–KOH, pH 8, 0.5 M LiCl, 1 mM EDTA, 1% NP-40, 1% sodium deoxycholate, 1 protease inhibitors tablet. Make fresh for each use.
7. Tris–EDTA buffer (TE): 1× TE buffer (store-bought).
8. 0.1× TE: 10 μL TE, 90 μL water.
9. TE-SDS: 2% (v/v) SDS in 1× TE.
10. TE/NaCl: TE buffer, 50 mM NaCl.
11. Elution buffer: 50 mM Tris–HCl, pH 8, 10 mM EDTA, 1% SDS.
12. Phenol:chloroform:isoamyl alcohol: 25:24:1 (v/v/v) phenol, chloroform, isoamyl alcohol (store-bought).
13. RNAse A: 100 mg/mL RNAse A solution (store-bought).
14. Proteinase K: 20 μg/mL proteinase K solution (store-bought).
15. 5 M NaCl: 29.2 g NaCl in 100 mL H_2O.
16. 20 mg/mL glycogen: 20 mg/mL glycogen solution (store-bought).

2.4 Preparation of ChIP Libraries for Sequencing

1. NEBNext Ultra II DNA Library Prep kit (NEB): End Prep Enzyme Mix, End Prep Reaction buffer, adaptor, ligation master mix, ligation enhancer, USER enzyme. PCR amplification kit: master mix, i7 primer stock solution, i5 primer stock solution.
2. Agencourt AMPure XP beads (Beckman Coulter).

3. 80% ethanol: 40 mL molecular biology grade 100% ethanol, 10 mL H_2O.
4. Magnetic stand-96 (e.g., Ambion, Invitrogen).

3 Methods

3.1 Dissociation and Isolation of Stem Cells

1. Fill a 100-mm petri dish with ice.
2. Compact the ice to form an even surface.
3. Place two filter paper circles on top of the ice.
4. Wrap parafilm to keep the filter paper in place.
5. Place an aluminum foil circle on top to complete the "stage."
6. Select one 7- to 8-mm-long planarian per desired sample (*see* **Note 5**).
7. Place the worms on the aluminum foil.
8. Cut the worms using a razor blade.
9. Transfer the worms into a cold petri dish filled with 50 mL planaria water.
10. Replace planaria water with cold $CMFHe^{2+}$ (*see* **Note 2**).
11. Cut the worms as small as possible with a scalpel. Wipe the scalpel frequently in order to prevent the accumulation of mucus.
12. Carefully transfer worm pieces to 1.5-mL tubes with a plastic Pasteur pipette. Transfer pieces with a large amount of liquid to avoid adhesion to the walls of the pipette.
13. Wait 10 min for the worm pieces to settle.
14. Remove all $CMFHe^{2+}$.
15. Add 600 μL of papain digestion solution.
16. Incubate for 1 h at 25 °C. The solution should not be mixed, nor should the tubes be moved.
17. Mechanically dissociate the digested pieces by pipetting up and down using a P1000 for 20 strokes. Solution will turn cloudy.
18. Repeat **step 17** until no large pieces are visible.
19. Centrifuge at 500 rcf for 5 min at 4 °C to pellet the cells.
20. Replace the supernatant with 1 mL of $CMFHe^{2+}$.
21. Repeat **steps 19** and **20**.
22. Resuspend the pellet.
23. Filter the suspension through a 100-μm filter and another 35-μm filter into a 5-mL round bottom tube to remove undigested tissue fragments (*see* **Note 6**).

24. Add 50 μL of 20× live DNA stain stock solution and 0.5 μL of 2000× live cytoplasmic stain stock solution per 1 mL of filtered sample (*see* **Note 7**).
25. Incubate the samples in the dark for 1 h.
26. Add 1 μL of 1000× cell viability stain stock solution.
27. Create the proper gate for size and granularity in each cell population of interest.
28. Sort the cells (*see* **Note 8**) and collect cells into a tube containing ice-cold 1× PBS.

3.2 Chromatin Extraction and Sonication

1. Transfer cells from FACS tubes to protein low-binding 1.5-mL tubes.
2. Spin at 4000 rcf for 4 min at 4 °C.
3. Remove supernatant and pool tubes of sorted cells.
4. Repeat **steps 2** and **3** until all of the sample is pelleted in one single tube.
5. Remove supernatant and completely resuspend pellet in 1 mL of NEB by gently pipetting up and down 10 times.
6. Add 62.5 μL 16% formaldehyde.
7. Leave at RT on a rotator for 7 min.
8. Add 50 μL of 2.5 M glycine to quench the reaction.
9. Leave at RT on a rotator for 3 min.
10. Centrifuge at 4000 rcf for 4 min at 4 °C to pellet.
11. Replace gently the supernatant by 1 mL of ice-cold 1× PBS with protease inhibitors, without totally resuspending it.
12. Centrifuge at 4000 rcf for 4 min at 4 °C to pellet.
13. Repeat **steps 11** and **12** two more times.
14. Remove supernatant.
15. Resuspend the pellet in 120 μL cold SDS-lysis buffer by pipetting up and down.
16. Incubate on ice for 20 min.
17. Add 280 μL ChIP dilution buffer to make up the volume to 400 μL.
18. Sonicate the samples according to the manufacturer's instruction to obtain average chromatin fragments between 200 and 400 bp.
19. Add 40 μL of 10% Triton X-100.
20. Centrifuge at 20,000 rcf for 15 min at 4 °C to pellet debris (*see* **Note 9**).

21. Carefully transfer the supernatant containing sheared chromatin to be used for immunoprecipitation to fresh 1.5 mL protein low-binding tube (*see* **Note 10**).
22. Aliquot 50 μL of the sample to a new low-binding tube for a test de-crosslink reaction to assess fragment distribution and concentration.
23. Store the sheared chromatin at 4 °C overnight or at −80 °C for longer periods.
24. Thaw the aliquot on ice if retrieved from −80 °C.
25. Add 150 μL of TE-SDS.
26. Heat at 65 °C for 2 h.
27. Purify the DNA using a mini-elute kit according to the manufacturer's instructions (*see* **Note 11**).
28. Analyze the DNA fragment sizes with the DNA electrophoresis equipment (Fig. 2).

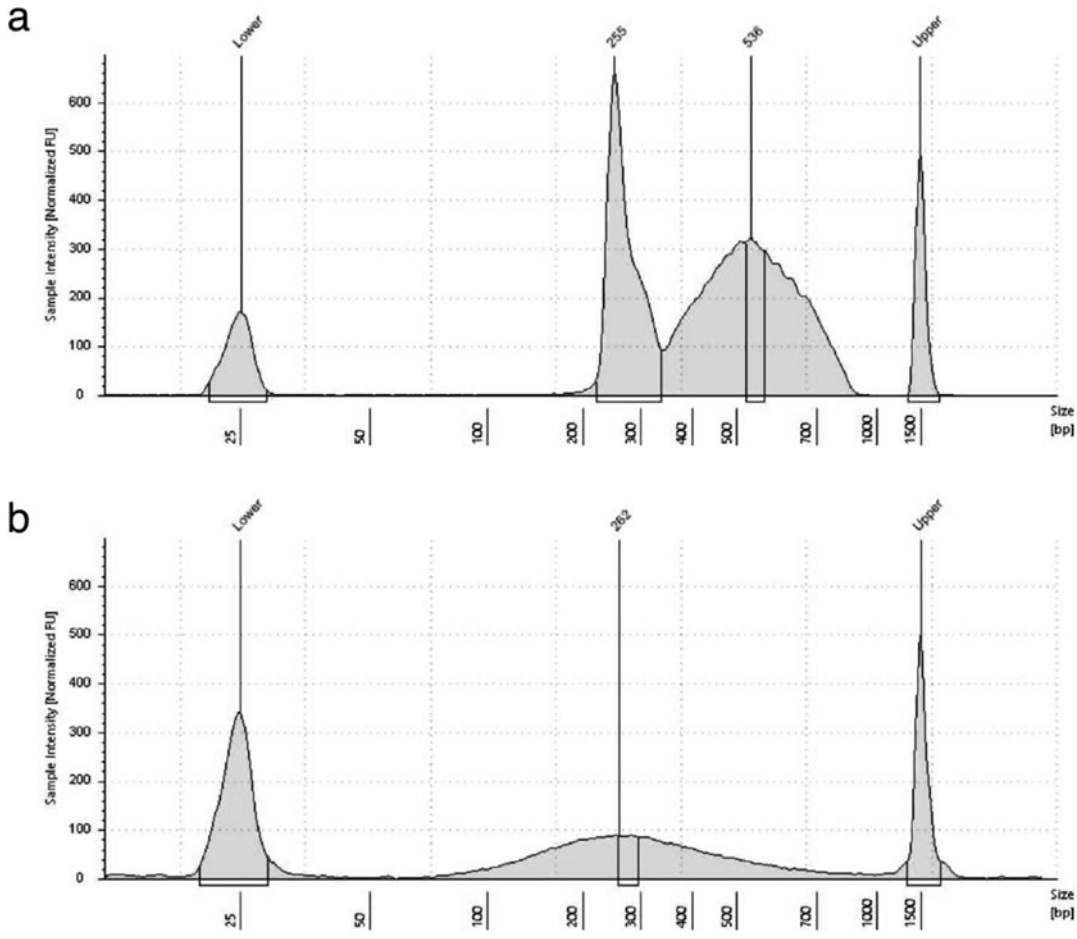


Fig. 2 Example fragment size distribution analyzed on TapeStation (**a**) after chromatin shearing, (**b**) after a test de-crosslink. The optimal chromatin size distribution for ChIP-seq is between 200 and 800 bp

29. Estimate the DNA concentration using the fluorometer following manufacturer's instructions.

3.3 Chromatin Immunoprecipitation

1. Transfer 50 μL of beads per sample into a low-binding 1.5-mL tube.
2. Wash the beads thrice with 1 mL 0.5% BSA/PBS using a magnetic rack to pellet the beads.
3. Resuspend beads in 125 μL of blocking solution.
4. Add 7 μg of antibody per reaction.
5. Incubate tubes overnight on a rotator at 4 °C.
6. Wash the beads three times using 1 mL 0.5% BSA/PBS using a magnetic rack to pellet the beads.
7. Resuspend the beads in 50 μL of blocking solution.
8. Add 100 μL of sheared chromatin from the end of Subheading 3.2 to the beads per antibody sample.
9. Add 5 μL of Drosophila S2 chromatin spike-in. The total amount of chromatin should 1–2% of the planarian chromatin (*see* **Note 12**).
10. Transfer a separate 50 μL aliquot of sheared chromatin with Drosophila S2 chromatin into a low-binding 1.5-mL tube without antibodies, to be used as input DNA control.
11. Incubate the tubes overnight on a rotator at 4 °C.
12. Wash six times with 1 mL ChIP wash buffer (*see* **Note 13**).
13. Resuspend beads in 800 μL TE/NaCl.
14. Place on a rotator at 4 °C for 3 min.
15. Pellet the beads using a magnetic rack.
16. Remove all of the supernatant (*see* **Note 14**).
17. Resuspend the beads in 250 μL elution buffer.
18. Place tubes at 65 °C for 15 min on a shaking block at 1400 rpm.
19. Centrifuge the beads at 16,000 rcf for 1 min at RT.
20. Transfer the supernatant to a fresh tube.
21. Incubate the supernatant as well as the Input DNA control tube at 65 °C overnight for reverse crosslinking.
22. Add 250 μL of TE to each tube.
23. Add 2 μL RNAse A to each sample.
24. Incubate at 37 °C for 1 h.
25. Add 4 μL Proteinase K.
26. Incubate at 55 °C for 1 h.
27. Add 500 μL of phenol:chloroform:isoamyl alcohol.

28. Vortex at maximum power for 2 min.
29. Centrifuge at max speed at RT for 5 min.
30. Transfer the upper aqueous phase to a new tube avoiding contamination of residual phenol (*see* **Note 15**).
31. Add 2 μL of 5 M NaCl, 1.5 μL of 20 mg/mL glycogen and 1.5 mL of −20 °C 100% ethanol.
32. Incubate at −80 °C for 1 h.
33. Centrifuge at max speed for 30 min at 4 °C.
34. Replace the supernatant with 1 mL 70% ethanol.
35. Centrifuge at max speed for 10 min at 4 °C.
36. Remove most of the supernatant with disturbing the bottom of the tube.
37. Leave the open tubes at room temperature for 1 h to dry.
38. Resuspend the DNA in 50 μL 1× TE.
39. Shake the tubes at 37 °C for 20 min.
40. Incubate the tubes at RT for 45 min to completely resuspend the DNA.

3.4 Preparation of ChIP Libraries for Sequencing

1. Transfer 50 μL of fragmented DNA to a PCR tube.
2. Add 3 μL NEBNext Ultra II End Prep Enzyme Mix and 7 μL NEBNext Ultra II End Prep Reaction buffer.
3. Pipette up and down at least 10 times 50 μL using a P200 to thoroughly mix the solution.
4. Briefly spin the tubes for 5 s at max speed to collect liquid from the sides of the tubes.
5. Place in a thermocycler with a heated lid.
6. Run a program at 20 °C for 30 min followed by 65 °C for 30 min.
7. Dilute the NEBNext Adaptor in Tris/NaCl, pH 8.0 according to the DNA concentration previously measured (*see* **Note 16**).
8. Add 2.5 μL of diluted adaptors to the reaction mix.
9. Add 30 μL of ligation master mix and 1 μL of ligation enhancer to the reaction mix.
10. Pipette up and down at least 10 times 80 μL using a P200 to thoroughly mix the solution.
11. Briefly spin the tubes 5 s at max speed to collect all the liquid from the sides.
12. Incubate at 20 °C for 15 min in a thermocycler with the heated lid off.
13. Add 3 μL of USER enzyme to the mixture.

14. Mix well and incubate at 37 °C for 15 min in a thermocycler with the heated lid set to 47 °C.
15. Samples can be stored at −20 °C overnight at this point.
16. Allow AMPure XP beads and the DNA samples to warm to RT for approximately 30 min.
17. Vortex the beads for 5 s at max speed.
18. Add 87 μL of the beads to the ligation mix.
19. Mix well by pipetting up and down at least 10 times.
20. Incubate the mix for 5 min at RT.
21. Transfer to a 96-well PCR plate.
22. Place the plate on a magnetic rack.
23. Wait for 5 min for the beads to separate from the supernatant.
24. Remove the supernatant carefully without disturbing the beads.
25. Add 180 μL of freshly prepared 80% ethanol to the tube while it is on the rack. 80% ethanol is added to the beads slowly, and the beads are not to be resuspended in it.
26. Incubate on the rack at RT for 30 s.
27. Carefully remove and discard the supernatant without disturbing the beads.
28. Repeat **steps 25–27** once. Be sure to remove all of the supernatant (*see* **Note 17**).
29. Air dry the beads for 5 min on the magnetic rack.
30. Remove the plate from the magnetic rack.
31. Add 17 μL 0.1× TE to each well.
32. Resuspend the beads fully by pipetting up and down 10 times.
33. Incubate the beads off the magnetic rack for 3 min at RT.
34. Place the plate on the magnetic rack for 5 min.
35. Transfer 15 μL of the supernatant to a fresh PCR plate.
36. Samples can be stored at −20 °C at this point.

3.5 PCR Enrichment and Purification of DNA

1. Allow samples to warm to RT for approximately 30 min.
2. Add 25 μL of Master mix, 5 μL of i7 primer stock solution, and 5 μL of i5 primer stock solution to each sample.
3. Pipette up and down at least 10 times 80 μL using a P200 to mix the solution thoroughly.
4. Place the tube on a thermocycler.
5. Perform PCR amplification as follows:

Initial denaturation at 98 °C for 30 s/N [denaturation at 98 °C for 10 s, annealing/extension at 65 °C for 75 s] followed by final extension at 65 °C for 5 min. $N = 3$–15 (*see* **Note 18**).

6. Allow AMPure XP beads to warm at room temperature for approximately 30 min.
7. Vortex the beads for 5 s at max speed.
8. Add 45 μL of beads to the ligation mix.
9. Pipette up and down at least 10 times.
10. Incubate the beads for 5 min at room temperature.
11. Place the plate on a magnetic rack and allow the beads to separate from the supernatant.
12. Wait for 5 min.
13. Repeat step until the solution is clear.
14. Carefully remove and discard the supernatant.
15. Add 180 μL of freshly prepared 80% ethanol to the tube while it is on the stand. 80% ethanol is added to the beads slowly, and the beads are not to be resuspended in it.
16. Incubate on the magnetic rack at room temperature for 30 s.
17. Carefully remove and discard the supernatant without disturbing the beads.
18. Repeat **steps 6–8** once. Be sure to remove all of the supernatant (*see* **Note 17**).
19. Air dry the beads for 5 min on the magnetic rack.
20. Remove the plate from the magnetic rack.
21. Add 35 μL of 0.1× TE to the beads to elute the DNA target.
22. Resuspend the beads fully by pipetting up and down 10 times.
23. Incubate the beads off the magnetic rack for at least 2 min at room temperature.
24. Place the plate back to the magnetic rack.
25. Wait for 5 min.
26. Repeat step until the solution is clear.
27. Transfer 30 μL of the supernatant to a fresh tube.
28. Aliquot the samples and/or dilute for different analysis (*see* **Note 19**).
29. Check the size distribution using the DNA electrophoresis equipment (Fig. 3).
30. The samples may need to be diluted before loading after normalizing concentrations of different libraries using a qPCR-based library quantification kit.
31. Process samples for paired-end sequenced on an Illumina NextSeq or other Illumina machine.

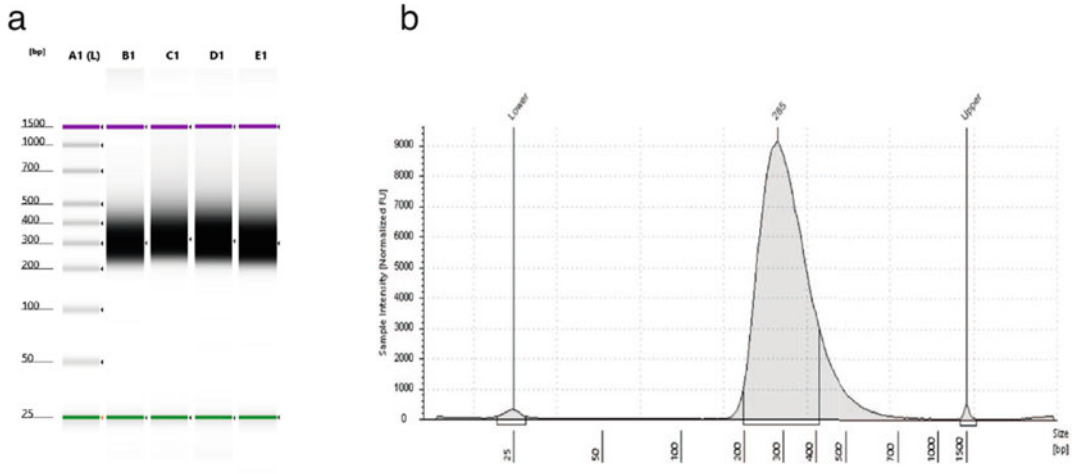


Fig. 3 Size distribution of (**a**) input along with 3 ChIP DNA libraries, (**b**) ChIP DNA library

4 Notes

1. Set pH of 10× CMF and HEPES very carefully, an extra drop of NaOH easily shoots the pH up.
2. Instead of $CMFHE^{2+}$, Holtfreter's solution diluted 5/8 in distilled water (5/8 Holtfreter; 21.88 g NaCl, 0.63 g $CaCl_2$, 0.31 g KCl, 1.25 g $NaHCO_3$ in 10 L distilled water, pH 7.4) or PBS containing 1 mM EDTA can also be used.
3. Papain can be substituted by other proteinases, such as 0.25% (w/v) trypsin or 1 mg/mL collagenase in $CMFHE^{2+}$. Digestion times will vary with different enzymes and their concentrations, and therefore digestion time must be standardized.
4. Typically, 3–7 μg of antibody is required for every 25 μg of chromatin. Using an optimal concentration of antibody can significantly reduce background. The amount of antibody required could be titrated by performing a ChIP experiment using different antibody concentrations. The different antibodies tested in our laboratory include H3K9ac, H3K27ac, H3K9me3, H3K4me3, H3K36me3, H3K4me1, H3K27me3, and RNAPII-Ser5P.
5. Select 30–40 of wild-type (a week starved) [25] or experimental (RNAi, irradiated, etc.) worms. The number of worms used depends on number of cells required for each experiment. Typically, at least 0.6–0.7 million stem cells are obtained per FACS session using 40 animals. Chromatin from these cells is used for 4 ChIP reactions (3 ChIP for histone marks antibodies with an input control).

6. Filtering the cell suspension removes any large debris and enriches neoblasts and neoblast progeny.
7. The amount of stain necessary will vary based on the number of cells/worms used. This must be worked out and the same amount should be added for all of the samples that are used in each experiment.
8. The first time the cell dissociation protocol is performed, it is advisable to check the cell suspension under a fluorescent microscope to confirm cell viability and optimal dissociation.
9. As the pellet can be small, the supernatant must be removed carefully without aspirating the pellet.
10. The cell debris in the pellet can be re-suspended in 400 μL ChIP dilution buffer and used in parallel as control in the test de-crosslink reaction.
11. It is important to determine the chromatin concentration for normalizing samples at the immunoprecipitation step, and hence, a test de-crosslink is performed.
12. Commercial Drosophila S2 chromatin is added as spike-in. Alternatively, S2 cells can be added before chromatin preparation. Drosophila S2 spike-in is added to the chromatin before immunoprecipitations simply as a method to normalize any technical differences in immunoprecipitations across replicate libraries [26].
13. Beads are often stuck on the tube caps, and the samples can be centrifuged very briefly to collect all the beads at the bottom of the tube.
14. If all the supernatant could not be removed, tubes can be centrifuged at 2000 rcf for 3 min at 4 °C to remove all the TE.
15. To avoid contamination of phenol, transfer the aqueous layer multiple times in small volumes. One can start with a P100 and then move to P20 or P10 to transfer the liquid.
16. This is based on the DNA concentration values from the end of Subheading 3.2. For 1 μg to 101 ng input, no adaptor dilution (15 μM final concentration), for 100 ng to 5 ng, 1:10 adaptor dilution (1.5 μM final concentration), for <5 ng, 1:25 adaptor dilution (0.6 μM final concentration).
17. Briefly spin the plate if necessary, place back on the magnetic stand, and remove traces of ethanol with a P10.
18. The number of cycles depends on DNA input and sample type. The number of cycles should be high enough to provide sufficient library fragments required for a successful sequencing run, but low enough to avoid PCR artefacts and over-cycling. The number of PCR cycles recommended can be found in

Table 1
Scaling of PCR amplification cycles based on input DNA. The ideal number of PCR cycles to amplify libraries for sequencing depends on the amount of DNA that goes into the end repair reaction (Subheading 3.4). In our experience, this can vary depending on the antibody used and the amount of chromatin used in immunoprecipitation

Input DNA into end prep reaction	Number of cycles required for library preparation
1 μg	3–4
500 ng	4–5
100 ng	6–7
50 ng	8–9
10 ng	10–11
5 ng	12–13

Table 1 and serve as a starting point to determine the number of PCR cycles best for standard library preparation.

19. Qubit, agarose gel, TapeStation or bioanalyzer can be used to test the suitability of the libraries for sequencing.

References

1. Aboobaker AA (2011) Planarian stem cells: a simple paradigm for regeneration. Trends Cell Biol 21:304–311. https://doi.org/10.1016/j.tcb.2011.01.005
2. Rink JC (2013) Stem cell systems and regeneration in planaria. Dev Genes Evol 223:67–84. https://doi.org/10.1007/s00427-012-0426-4
3. Adler CE, Sánchez Alvarado A (2015) Types or states? Cellular dynamics and regenerative potential. Trends Cell Biol 25:687–696. https://doi.org/10.1016/j.tcb.2015.07.008
4. Eisenhoffer GT, Kang H, Alvarado AS (2008) Molecular analysis of stem cells and their descendents during cell turnover and regeneration in the planarian Schmidtea mediterranea. Cell Stem Cell 3:1841–1850. https://doi.org/10.1016/j.stem.2008.07.002
5. van Wolfswinkel JC, Wagner DE, Reddien PW (2014) Single-cell analysis reveals functionally distinct classes within the planarian stem cell compartment. Cell Stem Cell 15:326–339. https://doi.org/10.1016/j.stem.2014.06.007
6. Grohme MA, Schloissnig S, Rozanski A, Pippel M, Young GR, Winkler S, Brandl H, Henry I, Dahl A, Powell S, Hiller M, Myers E, Rink JC (2018) The genome of Schmidtea mediterranea and the evolution of core cellular mechanisms. Nature 554(7690):56–61. https://doi.org/10.1038/nature25473
7. Cantarel BL, Korf I, Robb SMC, Parra G, Ross E, Moore B, Holt C, Alvarado AS, Yandell M (2008) MAKER: an easy-to-use annotation pipeline designed for emerging model organism genomes. Genome Res 18:188–196. https://doi.org/10.1101/gr.6743907
8. Robb SMC, Gotting K, Ross E, Alvarado AS (2015) SmedGD 2.0: the Schmidtea mediterranea genome database. Genesis 4:139–148. https://doi.org/10.1038/nmeth.2839.A
9. Brandl H, Moon HK, Vila-Farré M, Liu SY, Henry I, Rink JC (2016) PlanMine—a mineable resource of planarian biology and biodiversity. Nucleic Acids Res 44:D764–D773. https://doi.org/10.1093/nar/gkv1148
10. Dattani A, Sridhar D, Aboobaker AA (2018) Planarian flatworms as a new model system for understanding the epigenetic regulation of stem cell pluripotency and differentiation. Semin Cell Dev Biol 87:79–94. https://doi.org/10.1016/j.semcdb.2018.04.007
11. Jaber-Hijazi F, Lo PJKP, Mihaylova Y, Foster JM, Benner JS, Tejada Romero B, Chen C, Malla S, Solana J, Ruzov A, Aziz Aboobaker

A (2013) Planarian MBD2/3 is required for adult stem cell pluripotency independently of DNA methylation. Dev Biol 384:141–153. https://doi.org/10.1016/j.ydbio.2013.09.020

12. Ross KG, Omuro KC, Taylor MR, Munday RK, Hubert A, King RS, Zayas RM (2015) Novel monoclonal antibodies to study tissue regeneration in planarians. BMC Dev Biol 15:2. https://doi.org/10.1186/s12861-014-0050-9
13. Zhu SJ, Pearson BJ (2013) The Retinoblastoma pathway regulates stem cell proliferation in freshwater planarians. Dev Biol 373:442–452. https://doi.org/10.1016/j.ydbio.2012.10.025
14. Robb SMC, Alvarado AS (2014) Histone modifications and regeneration in the planarian Schmidtea mediterranea. Curr Top Dev Biol 108:71–93. https://doi.org/10.1016/B978-0-12-391498-9.00004-8
15. Scimone ML, Meisel J, Reddien PW (2010) The Mi-2-like Smed-CHD4 gene is required for stem cell differentiation in the planarian Schmidtea mediterranea. Development 137:1231–1241. https://doi.org/10.1242/dev.042051
16. Bonuccelli L, Rossi L, Lena A, Scarcelli V, Rainaldi G, Evangelista M, Iacopetti P, Gremigni V, Salvetti A (2010) An RbAp48-like gene regulates adult stem cells in planarians. J Cell Sci 2:690–698. https://doi.org/10.1242/jcs.053900
17. Hubert A, Henderson JM, Cowles MW, Ross KG, Hagen M, Anderson C, Szeterlak CJ, Zayas RM (2015) A functional genomics screen identifies an importin-α homolog as a regulator of stem cell function and tissue patterning during planarian regeneration. BMC Genomics 16:1–18. https://doi.org/10.1186/s12864-015-1979-1
18. Vásquez-Doorman C, Petersen CP (2016) The NuRD complex component p66 suppresses photoreceptor neuron regeneration in planarians. Regeneration 3:168–178. https://doi.org/10.1002/reg2.58
19. Duncan EM, Chitsazan AD, Seidel CW, Alvarado AS (2015) Set1 and MLL1/2 target distinct sets of functionally different genomic loci in vivo. Cell Rep 13:2741–2755. https://doi.org/10.1016/j.celrep.2016.09.071
20. Mihaylova Y, Abnave P, Kao D, Hughes S, Lai A, Jaber-hijazi F, Kosaka N, Aboobaker AA, Aziz A (2018) Conservation of epigenetic regulation by the MLL3/4 tumour suppressor in planarian pluripotent stem cells. Nat Commun 9:3633. https://doi.org/10.1038/s41467-018-06092-6
21. Dattani A, Kao D, Mihaylova Y, Abnave P, Hughes S, Lai A, Sahu S, Aboobaker AA (2018) Epigenetic analyses of planarian stem cells demonstrate conservation of bivalent histone modifications in animal stem cells. Genome Res 28:1543–1554. https://doi.org/10.1101/gr.239848.118
22. Thirman MJ, Gill HJ, Burnett RC, Mbangkollo D, McCabe NR, Kobayashi H, Ziemin-van der Poel S, Kaneko Y, Morgan R, Sandberg AA, Chaganti RSK, Larson RA, Le Beau MM, Diaz MO, Rowley JD (1992) Rearrangement of the MLL gene in acute lymphoblastic and acute myeloid leukemias with 11q23 chromosomal translocations. N Engl J Med 329:909–914
23. Sobulo OM, Borrow J, Tomek R, Reshmi S, Harden A, Schlegelberger B, Housman D, Doggett NA, Rowley JD, Zeleznik-Le NJ (1997) MLL is fused to CBP, a histone acetyltransferase, in therapy-related acute myeloid leukemia with a t(11;16)(q23;p13.3). Proc Natl Acad Sci U S A 94:8732–8737. https://doi.org/10.1073/pnas.94.16.8732
24. Chen C, Liu Y, Rappaport AR, Kitzing T, Schultz N, Shroff AS, Dickins RA, Vakoc CR, Bradner JE, Stock W, Lebeau MM, Shannon KM, Kogan S, Zuber J, Lowe SW (2014) MLL3 is a haploinsufficient 7q tumor suppressor in acute myeloid leukemia. Cancer Cell 25:652–665. https://doi.org/10.1016/j.ccr.2014.03.016.MLL3
25. Merryman MS, Alvarado AS, Jenkin JC (2018) Chapter 5 culturing planarians in the laboratory. Methods Mol Biol 1774:241–258. https://doi.org/10.1007/978-1-4939-7802-1
26. Orlando DA, Chen MW, Brown VE, Solanki S, Choi YJ, Olson ER, Fritz CC, Bradner JE, Guenther MG (2014) Quantitative ChIP-Seq normalization reveals global modulation of the epigenome. Cell Rep 9:1163–1170. https://doi.org/10.1016/j.celrep.2014.10.018

Open Access This chapter is licensed under the terms of the Creative Commons Attribution 4.0 International License (http://creativecommons.org/licenses/by/4.0/), which permits use, sharing, adaptation, distribution and reproduction in any medium or format, as long as you give appropriate credit to the original author(s) and the source, provide a link to the Creative Commons license and indicate if changes were made.

The images or other third party material in this chapter are included in the chapter's Creative Commons license, unless indicated otherwise in a credit line to the material. If material is not included in the chapter's Creative Commons license and your intended use is not permitted by statutory regulation or exceeds the permitted use, you will need to obtain permission directly from the copyright holder.





Chapter 29

Assessing Chromatin Accessibility During WBR in Acoels

Andrew R. Gehrke and Mansi Srivastava

Abstract

Dynamic gene expression seen during whole-body regeneration is likely controlled by genomic regulatory elements that dictate the spatiotemporal activity of the regeneration transcriptome. Identifying and characterizing these non-coding regulatory sequences are key to understanding how genes are connected into networks to deploy the process of whole-body regeneration. Here, we describe the application of the Assay for Transposase Accessible Chromatin (ATAC-seq) in the acoel *Hofstenia miamia* to identify regions of open chromatin that represent putative regulatory elements. Notably, when paired with gene knockdown techniques such as RNAi, ATAC-seq can be implemented in a functional genomics approach to validate putative regulatory elements. ATAC-seq requires no species-specific reagents, is amenable to small input cell numbers, and can be completed in a single day, making it an ideal assay to identify dynamic chromatin at high resolution during whole-body regeneration in virtually any species with a quality genome assembly.

Key words ATAC-seq, Chromatin, Gene regulation, Acoel, Whole-body regeneration

1 Introduction

The crucial role of regulatory elements that comprise the non-coding genome has been demonstrated in development, disease, and evolution [1, 2]. Advances in genomics (e.g., the ability to sequence and assemble myriads of animal genomes) and techniques in molecular biology have now made it possible to explore the role of the regulatory genome in the process of whole-body regeneration. Previous techniques to characterize regulatory elements have relied either on species-specific reagents or a large number of input cells, hindering the genome-wide identification of putative enhancers in emerging model systems. The Assay for Transposase Accessible Chromatin (ATAC-seq) [3], which is relatively wet-lab simple and requires a small amount of input material, has the potential to revolutionize the fields of functional genomics and evolutionary-developmental

The original version of this chapter was revised. The correction to this chapter is available at https://doi.org/10.1007/978-1-0716-2172-1_37

Simon Blanchoud and Brigitte Galliot (eds.), *Whole-Body Regeneration: Methods and Protocols*, Methods in Molecular Biology, vol. 2450, https://doi.org/10.1007/978-1-0716-2172-1_29, © The Author(s) 2022, corrected publication 2022

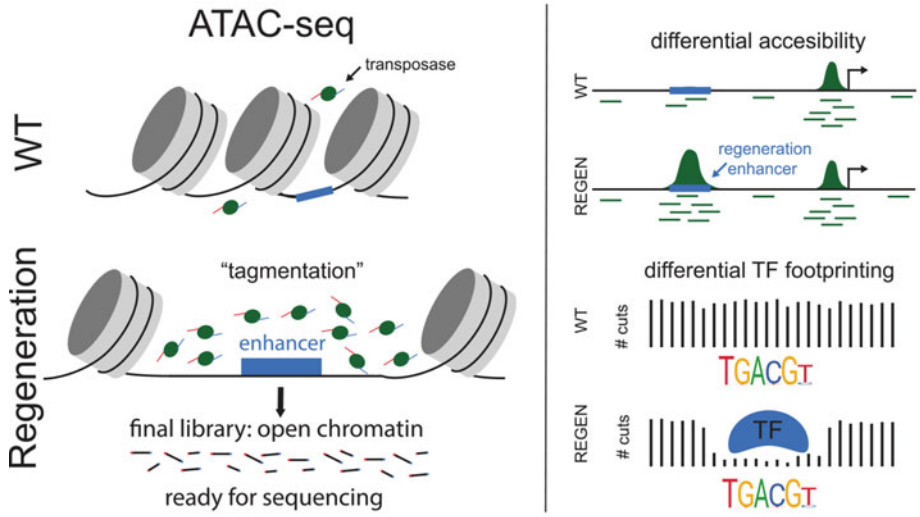


Fig. 1 Overview of an ATAC-seq seq experiment to assay regeneration-responsive chromatin. ATAC-seq involved applying a transposase (left panel) capable of cutting open chromatin and simultaneously ligating in sequencing primers ("tagmentation"). The transposase enzyme will integrate less in closed chromatin (WT) and will preferentially insert into open chromatin, e.g., a region that harbors an enhancer (blue) that opens during regeneration ("regen," bottom left). The final library consists of small regions of open chromatin that are ready to be sequenced. After alignment of these sequences to the genome (green lines, right panel), "peaks" of open chromatin (green) can be called and compared across regenerating samples (differential accessibility). Transcription factor (TF) binding can be inferred by viewing the number of transposase cutting events (# cuts) around TF binding sites. When a TF is bound, it occludes the transposase from inserting into that region and leaves a "footprint," which can be compared across samples ("differential TF footprinting")

biology by providing a method to identify putative enhancers at high resolution in emerging systems of study (Fig. 1).

ATAC-seq works by treating a small number of permeabilized cells or exposed nuclei to a transposase enzyme that preferentially accesses regions of open chromatin, simultaneously cutting DNA and inserting primers for sequencing ("tagmentation") (Fig. 1). Following sequencing, reads mapped to the genome provide information on open chromatin, nucleosome position, and transcription factor binding. The main benefits of the assay are (1) no species-specific reagents, (2) low input required, from 50,000 cells down to a few thousand, (3) reproducibility, in that replicates are highly concordant, and (4) speed, one can go from intact tissue to a sequencing-ready library in a single day.

Due to the experimental ease and high resolution of ATAC-seq, a number of methods papers have been published that describe the assay in detail. These include step-by-step instructions for cell lines [4], zebrafish [5, 6], echinoderms [7], xenopus [8], and plants [9]. Recent advances to the protocol ("Omni-ATAC") have improved the sensitivity of the assay and made it possible to perform in frozen tissues [10]. In addition to the wet-lab protocols for ATAC-seq, there are a number of methods papers that describe the bioinformatic data analysis portion of ATAC-seq [11–13]. The majority of

the wet and dry lab portions of ATAC-seq are quite similar across organisms and do not deviate much from the original methods paper describing the assay [4]. The critical factor when performing ATAC-seq in a "new" species is attaining the correct number of cells for proper transposition. Keeping this as a focus, here we describe step-by-step instructions for ATAC-seq in the acoel worm *Hofstenia miamia*. A defining step of this protocol is direct disruption of tissue in lysis buffer (as opposed to traditional dissociation and cell counting), followed immediately by transposition. This rapid processing of samples likely reduces background noise and better captures transcription factor binding as inferred by footprinting. We envision that this protocol will work robustly for all invertebrate animals that are generally easy to lyse or dissociate into single cells.

2 Materials

1. Octylphenoxypolyethoxyethanol (IGEPAL CA-630) (Sigma cat # I8896).
2. Tagment DNA enzyme 1 (TDE1) enzyme.
3. 2× Tagment DNA (TD) buffer (Illumina cat # 20034197) (*see* **Note 1**).
4. Mini kit for gel extraction and PCR clean up (e.g., Nucleospin, Macherey-Nagel cat # 740609).
5. High-fidelity 2× PCR master mix (New England Labs cat # M0541).
6. PCR primers (Table 1).
7. DNA concentration measurement equipment (e.g., Qubit, Thermo Fisher Scientific, cat # Q32851).
8. Automated electrophoresis tool (e.g., Tapestation, Agilent).
9. 0.40-μm cell strainer (Falcon cat # 352340).
10. Lysis buffer: 10 mM Tris–HCl, pH 7.4, 10 mM NaCl, 3 mM $MgCl_2$, 0.1% (v/v) IGEPAL CA-630. Prepare fresh, keep on ice.
11. Transposition reaction mix: 25 μL TD buffer, 2.5 μL TDE1 enzyme, 22.5 μL ddH_2O. Prepare fresh, keep on ice.
12. PCR reaction mix: 25 μL high-fidelity 2× PCR mix, 2.5 μL 25 μM universal PCR primer 1, 2.5 μL 25 μM barcoded PCR primer 2, 10 μL H_2O. Make fresh when performing the PCR amplification.
13. Samtools software version 1.10 [14].
14. Bowtie2 software version 2.3.2 [15].
15. Picard software version 2.24.0.
16. NGmerge software version 0.3 [16].

Table 1
Primer sequences. Primer sequences used for PCR, table reproduced from Supplementary Table 1 of [3]

Primer name	Sequence
Ad1_noMX	AATGATACGGCGACCACCGAGATCTACACTCGTCGGCAGCGTCAGATGTG
Ad2.1_TAAGGCGA	CAAGCAGAAGACGGCATACGAGATTCGCCTTAGTCTCGTGGGCTCGGAGATGT
Ad2.2_CGTACTAG	CAAGCAGAAGACGGCATACGAGATCTAGTACGGTCTCGTGGGCTCGGAGATGT
Ad2.3_AGGCAGAA	CAAGCAGAAGACGGCATACGAGATTTCTGCCTGTCTCGTGGGCTCGGAGATGT
Ad2.4_TCCTGAGC	CAAGCAGAAGACGGCATACGAGATGCTCAGGAGTCTCGTGGGCTCGGAGATGT
Ad2.5_GGACTCCT	CAAGCAGAAGACGGCATACGAGATAGGAGTCCGTCTCGTGGGCTCGGAGATGT
Ad2.6_TAGGCATG	CAAGCAGAAGACGGCATACGAGATCATGCCTAGTCTCGTGGGCTCGGAGATGT
Ad2.7_CTCTCTAC	CAAGCAGAAGACGGCATACGAGATGTAGAGAGGTCTCGTGGGCTCGGAGATGT
Ad2.8_CAGAGAGG	CAAGCAGAAGACGGCATACGAGATCCTCTCTGGTCTCGTGGGCTCGGAGATGT
Ad2.9_GCTACGCT	CAAGCAGAAGACGGCATACGAGATAGCGTAGCGTCTCGTGGGCTCGGAGATGT
Ad2.10_CGAGGCTG	CAAGCAGAAGACGGCATACGAGATCAGCCTCGGTCTCGTGGGCTCGGAGATGT
Ad2.11_AAGAGGCA	CAAGCAGAAGACGGCATACGAGATTGCCTCTTGTCTCGTGGGCTCGGAGATGT
Ad2.12_GTAGAGGA	CAAGCAGAAGACGGCATACGAGATTCCTCTACGTCTCGTGGGCTCGGAGATGT
Ad2.13_GTCGTGAT	CAAGCAGAAGACGGCATACGAGATATCACGACGTCTCGTGGGCTCGGAGATGT
Ad2.14_ACCACTGT	CAAGCAGAAGACGGCATACGAGATACAGTGGTGTCTCGTGGGCTCGGAGATGT
Ad2.15_TGGATCTG	CAAGCAGAAGACGGCATACGAGATCAGATCCAGTCTCGTGGGCTCGGAGATGT
Ad2.16_CCGTTTGT	CAAGCAGAAGACGGCATACGAGATACAAACGGGTCTCGTGGGCTCGGAGATGT
Ad2.17_TGCTGGGT	CAAGCAGAAGACGGCATACGAGATACCCAGCAGTCTCGTGGGCTCGGAGATGT
Ad2.18_GAGGGGTT	CAAGCAGAAGACGGCATACGAGATAACCCCTCGTCTCGTGGGCTCGGAGATGT

(continued)

Table 1
(continued)

Primer name	Sequence
Ad2.19_AGGTTGGG	CAAGCAGAAGACGGCATACGAGATCCCAACCTGTCTCGTGGGC TCGGAGATGT
Ad2.20_GTGTGGTG	CAAGCAGAAGACGGCATACGAGATCACCACACGTCTCGTGGGC TCGGAGATGT
Ad2.21_TGGGTTTC	CAAGCAGAAGACGGCATACGAGATGAAACCCAGTCTCGTGGGC TCGGAGATGT
Ad2.22_TGGTCACA	CAAGCAGAAGACGGCATACGAGATTGTGACCAGTCTCGTGGGC TCGGAGATGT
Ad2.23_TTGACCCT	CAAGCAGAAGACGGCATACGAGATAGGGTCAAGTCTCGTGGGC TCGGAGATGT
Ad2.24_CCACTCCT	CAAGCAGAAGACGGCATACGAGATAGGAGTGGGTCTCGTGGGC TCGGAGATGT

3 Methods

Care should be taken to move as quickly as possible from tissue extraction to dissociation to retain chromatin state at the appropriate timepoint. This protocol is based on the original ATAC-seq protocol [3]. Modifications that improve the assay have been described ("Omni-ATAC") [10], but use a detergent mixture that may be harmful to more sensitive cells. Thus, we suggest attempting the original protocol first and subsequently exploring the Omni-ATAC modifications to potentially improve the experiment.

3.1 Library Preparation

Determine the optimal tissue size of interest that contains ~50,000–100,000 cells (*see* **Note 2**).

1. Extract the desired tissue at timepoint of interest using sterile surgical blade (*see* **Notes 3** and **4**).
2. Transfer the sample to a 1.5-mL tube filled with ~25 μL of appropriate solution (e.g., PBS, sea water).
3. Replace the solution with 200 μL of cold lysis buffer.
4. Dissociate the tissue by gently pipetting using a p200 pipette until the fragment is completely in solution (~30 s) (*see* **Note 5**).
5. Filter the solution through a 40-μm filter into a new 1.5-mL tube.

6. Centrifuge the solution at 800 rcf for 10 min at 4 °C to pellet the cells/nuclei.
7. Gently remove the supernatant.
8. Resuspend the (invisible) pellet in 50 μL of the transposition reaction mix.
9. Incubate the cells at 37 °C for 30 min under 1000 rpm orbital shaking (e.g., thermomixer).
10. Purify the transposed DNA using extraction kit (*see* **Note 6**) according to the manufacturer's instructions.
11. Elute in 12 μL of elution buffer.
12. Store purified DNA at −20 °C.

3.2 PCR Amplification of Library and Sequencing

1. Add 10 μL of the eluted library to the 40 μL PCR reaction mix in a 0.2-mL PCR tube.
2. Run PCR using the following conditions (*see* **Note 7**): 1 cycle 5 min at 72 °C, 11 cycles 10 s at 98 °C, 30 s at 63 °C, 1 min at 72 °C, hold at 4 °C.
3. Purify the amplified DNA using the gel extraction and PCR clean up mini kit according to the manufacturer's instructions.
4. Elute in 22 μL of elution buffer.
5. Store-purified DNA at −20 °C.
6. Determine the concentration of library using the DNA concentration measurement equipment according to the manufacturer's instructions. We typically attain around ~10–20 ng/μL, but concentration can range from ~1 to 30 ng/μL.
7. Run purified DNA on the automated electrophoresis tool according to manufacturer's instructions (*see* **Note 8**, Fig. 2).
8. Pool libraries according to Illumina sequencing platform and desired ratio of reads (*see* **Note 9**).
9. Sequence using 50 bp paired-end on an Illumina platform at ~15 million mapped reads per Gb of genome (*see* **Note 10**).

3.3 Data Analysis

Raw reads should be backed up in at least two separate locations, ideally one physical and one cloud- or server-based. The following steps are designed to guide the user from raw reads to a processed alignment file, which is the most common input file for most downstream applications. Further example code and details for read processing and other applications (including differential peak analysis, *see* **Note 11**) can be found at https://github.com/agehrke6/ATAC_processing_analysis_guide. Note that the example code given below is designed as a starting point for the beginner user, and the manuals for each bioinformatic tool should be consulted for full explanation and detail.

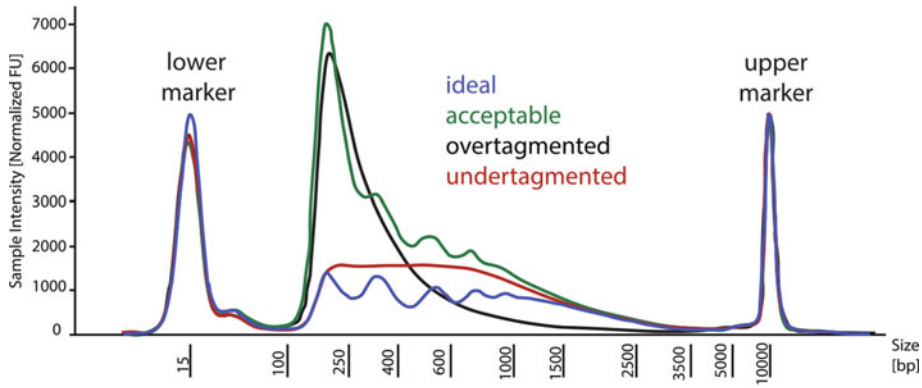


Fig. 2 Tapestation examples of different quality ATAC libraries. ATAC libraries were run on an Agilent Tapestation 2200 using an HD5000 tape. "Ideal" trace shows extensive nucleosomal "laddering," indicating a high-quality library. The "acceptable" trace also shows nucleosomal laddering, but with an extended sub-nucleosomal peak that may indicate slight "over-tagmentation" (over-cutting of the enzyme, likely due to too few cells in the reaction). If no "ideal" libraries are present this library is acceptable to sequence. "Overtagmented" shows no laddering and only a single peak, likely due to too few cells being added to the reaction. This library should not be sequenced, and the experiment should be repeated with more input cells. The "undertagmented" (insufficient cutting by the enzyme) trace shows no nucleosomal laddering but also no clear sub-nucleosomal peak, which could be the result of too many cells in the reaction. This library should not be sequenced, and the experiment should be repeated with fewer cells

1. Trim raw reads of adapters using NGmerge: *NGmerge -a -e 20 -n 4 -1 <sample>.R1.fastq.gz -2 <sample>.R2.fastq.gz -o <sample>_trimmed*. This command will output two files: *<sample>_trimmed.R1.fastq.gz* and *<sample>_trimmed.R2.fastq.gz*.
2. Index genome of interest with Bowtie2: *bowtie2-build <genome>.fasta <build_name>*.
3. Map trimmed reads to reference genome with Bowtie2: *bowtie2 -x <build_name> -X 2000 -1 <sample>_trimmed.R1.fastq.gz -2 <sample>_trimmed.R2.fastq.gz -p 31 | samtools view -b -S - | samtools sort - <sample>*. This command will create an alignment file (.bam).
4. Index the .bam file: *samtools index <sample>_nodups_nomulti.bam*. Quality libraries have a high percentage of mapped reads (>80%).
5. Remove PCR duplicates from alignment (.bam) file using Picard: *java -jar picard.jar MarkDuplicates I=<sample>.bam O=<sample>_nodups.bam M=<sample>_dups.txt REMOVE_DUPLICATES=true VALIDATION_STRINGENCY=LENIENT*.
6. Remove reads mapping to the mitochondrial genome from the de-duplicated alignment (.bam) file using samtools: *samtools view -h <sample>_nodups.bam | grep -v chrM | samtools sort -O bam -o <sample>_nodups_noMt.bam*. Note that *chrM* should be

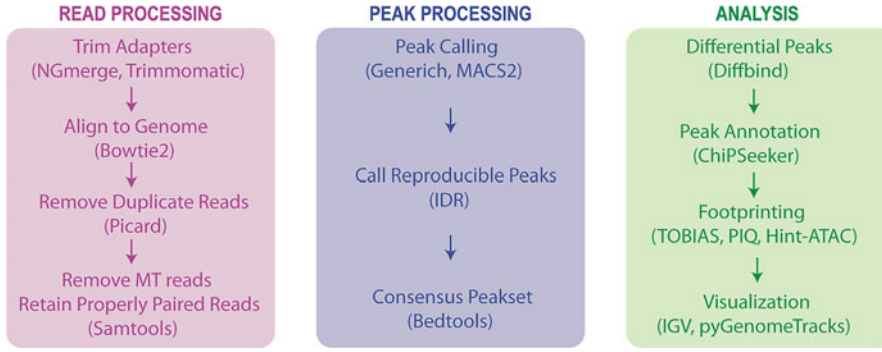


Fig. 3 Standard bioinformatic workflow for processing and analyzing ATAC-seq data. Raw reads are removed of adapters, then aligned to the genome of interest with no additional quality trimming. Duplicate reads are removed, as well as reads that map to the mitochondrial genome, and reads that are not properly paired. We use Genrich to call peaks on each biological replicate, and then use IDR to call reproducible peaks between replicates. Finally, we use bedtools merge on all peaksets from all samples to create a non-overlapping set of peaks that represents a consensus peakset. For analysis, we use Diffbind to call differentially accessible peaks between samples, ChIPseeker to make peak-to-gene connections, and TOBIAS for footprinting and bound site calling. Results are best visualized first using IGV, and then pyGenomeTracks to create publication-quality figures

changed to the designation of the mitochondrial genome in the input assembly (e.g., scaffoldX).

7. Remove multi-mapped reads using samtools (*see* **Note 12**): *samtools view -h -q 30 <sample>_nodups_noMt.bam > <sample>_nodups_noMt_nomulti.bam*.
8. Retain only properly paired reads using samtools (*see* **Note 12**): *samtools view -h -b -F 1804 -f 2 <sample>_nodups_noMt_nomulti.bam > <sample>_nodups_noMt_nomulti_filtered.bam*.
9. Sort the .bam file: *samtools sort <sample>_nodups_noMt_nomulti_filtered.bam* -o *<sample>_nodups_noMt_nomulti_filtered_sorted.bam*.
10. Index the final file using samtools: *samtools index <sample>_nodups_noMt_nomulti_filtered_sorted.bam*.
11. Use "clean" .bam file for peak calling and downstream analysis (*see* **Note 12**) (Fig. 3).

4 Notes

1. Alternatively, a homemade tagment buffer can be made: 20 mM Tris(hydroxymethyl)aminomethane; 10 mM $MgCl_2$; 20% (v/v) dimethylformamide [17]. Adjust pH to 7.6 with 100% acetic acid before adding dimethylformamide. Store at −20 °C for 6 months.

2. Determining the optimal number of cells is the most crucial and variable aspect of the ATAC-seq protocol. As a first step, we recommend excising different tissue sizes, dissociating cells, and then counting to determine the size that most likely contains 50,000–100,000 cells. Once the appropriate general tissue size is identified, subsequent ATAC-seq experiments can be run without having to take the time-sensitive step of preparing and counting cells. It is likely that the immediate lysis of tissue described in this protocol is key to producing high-quality data by capturing chromatin state as quickly as possible. If the "direct lysis" method continues to give substandard libraries, we recommend the standard protocol of attaining a single-cell suspension of live cells, counting and attaining ~50,000 cells, then proceeding with the remainder of the protocol using 50 μL volumes of reagents.
3. Design experiments so multiple samples can be processed at the same time, e.g., a 0 hour post amputation (hpa) sample can be processed alongside a 6 hpa sample that was cut 6 h prior (Fig. 4).
4. We aim to include three biological replicates during each ATAC experiment, eventually choosing the best two samples based on the Tapestation trace to sequence. Due to the speed of the ATAC-seq protocol and depending on the timepoints desired, multiple samples of a regeneration time-course can be completed in a single day. We typically cut the appropriate number of animals at the beginning of the day, and process samples as different timepoints of regeneration (e.g., 0 hpa, 1 hpa, 3 hpa, 6 hpa). Avoid processing more than ~4 samples at a time to ensure the speed of the assay.
5. Due to the delicate nature of *Hofstenia miamia* tissue, we are able to attain single-cell suspensions in less than 30 s of gentle pipetting, which are simultaneously made accessible to the transposase by performing this step in lysis buffer. Depending on the organism or tissue being used, attaining a single-cell suspension or lysis may be more challenging, and thus, we suggest species-specific protocols to attain single-cell suspensions if necessary.
6. A variety of DNA purification kits are acceptable, including the Qiagen minelute kit. After adding the buffer in the first step of the cleanup protocol, the solution can be frozen at −20 °C for purification at another time.
7. In order to determine the correct number of PCR cycles to avoid saturation and PCR-induced artifacts, it is advisable to run the first PCR for five cycles and then subsequently perform a qPCR reaction. This protocol is provided in detail in [4]. We found that our libraries nearly always converged on 11 cycles as

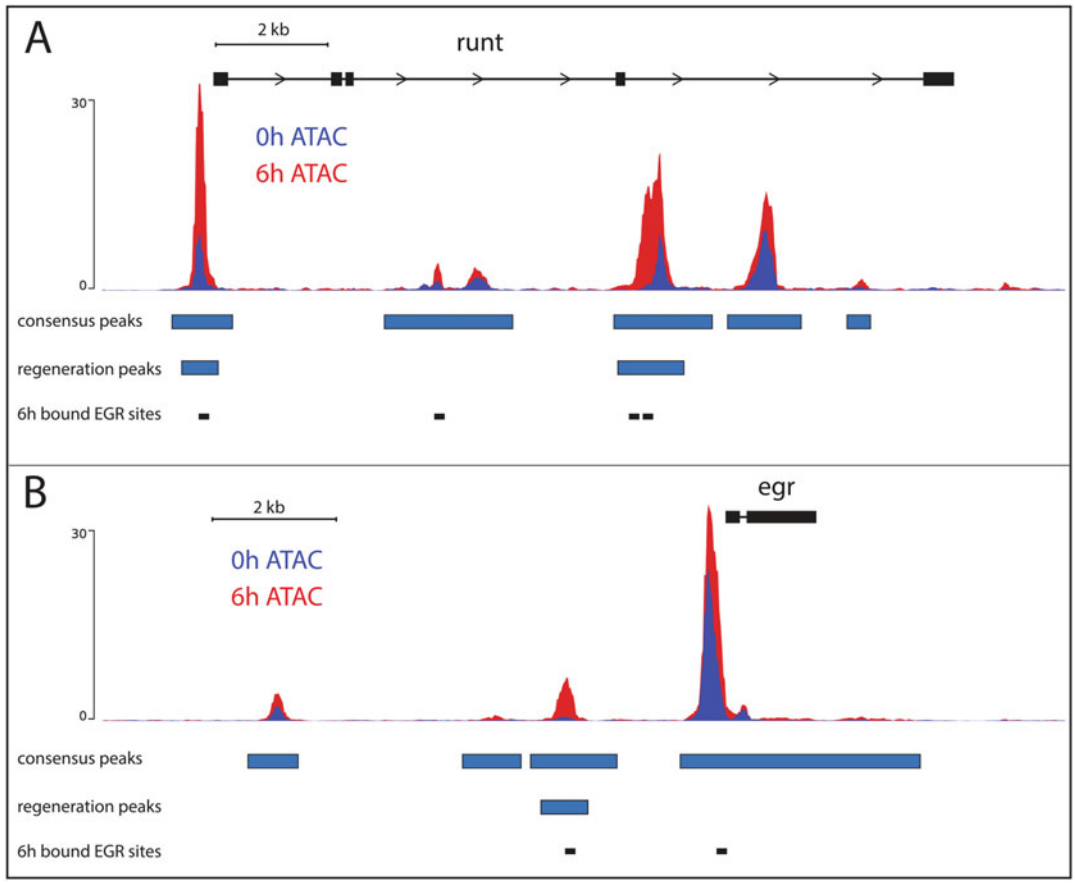


Fig. 4 Expected results. (**a**) ~15 kb region of the *Hofstenia* genome that encompasses a gene, *runt*, showing ATAC data for 0 h and 6 h, along with with the consensus peakset, Diffbind-called regeneration peaks, and sites that are bound by the TF egr at 6 h by TOBIAS. There are two major regeneration-responsive peaks (shown in red), the first being the promoter, and the second in an intron. Both the regeneration peaks have "bound" sites for egr. (**b**) A second region of the *Hofstenia* genome, this time showing an intergenic regeneration-responsive peak upstream of a putative target gene

the optimal number, and thus adopted this number as part of the protocol. When starting ATAC-seq with a new system, the optimal number of PCR cycles should be explored using the qPCR instructions found in [4].

8. The automated electrophoresis tool is used (in this case) to view the sizes of nucleic acids present in an ATAC-seq library. In a properly tagmented library, the transposase enzyme will insert into histone linker regions, creating a "nucleosomal ladder" rolling landscape where peaks correspond to varying numbers of nucleosomes. A proper nucleosomal ladder is the best indicator of a successful ATAC-seq experiment, and examples of the most common traces of varying quality are shown in Fig. 2.

9. Work with sequencing facility or Illumina representative to pool different barcoded ATAC libraries at the proper molar ratios for the desired model of sequencer. If desired, molar ratios can be adjusted to skew the number of reads to a more desired library.
10. The ENCODE standard for acceptable libraries states that human paired-end ATAC-seq libraries must have 50 million non-duplicate, non-mitochondrial aligned reads (i.e., 25 million fragments). For footprinting, recommended sequencing depths are much higher (>200 million mapped reads), though we have found emerging footprinting software [18] can reliably detect footprints at substantially less sequencing depth, though this need to be empirically determined for the species of interest.
11. With a clean alignment file in hand, a number of useful downstream applications can be performed. These include peak-calling with programs such as Genrich or MAC2, which will call sets of peaks for each replicate that can be narrowed down to reproducible peaks. In order to identify dynamic regions of chromatin (e.g., between different stages of regeneration), two common tools are Diffbind [19] and csaw [20]. Motif-finding algorithms such as HOMER [21] or GimmeMotifs [22] using significant peaks, or assigning regions-to-nearest-gene using ChIPseeker [23] can be useful ways to define candidate regulators. In addition to scanning regions for motif matches, regions of the genome that are protected by bound TFs will leave "footprints" that can be determined bioinformatically (Fig. 1). We use TOBIAS [18] to make bound/unbound calls for all predicted sites of a particular TF in the genome, as well as create aggregate plots that show overall binding differences between timepoints. *See* Fig. 3 for a genome browser example of these types of data combined.
12. Depending on downstream analysis, removing multi-mapped reads and retaining only properly paired reads may be unnecessary or detrimental (too few reads retained). For instance, peak-calling with Genrich can utilize both multi-mapped and unpaired alignments in generating peak calls. We recommend checking the documentation of software for the desired downstream application to determine how best to handle these reads.

Acknowledgments

We thank Jose Luis Gomez Skarmeta (Centro Andaluz de Biología del Desarrollo, Sevilla, Spain) and Elisa de la Calle-Mustienes (Centro Andaluz de Biología del Desarrollo, Sevilla, Spain) for

assistance with initial *Hofstenia* ATAC-seq experiments, performed at the Marine Biological Laboratories. We thank Kyle McCulloch for critical reading of the manuscript. A.R.G. is supported by the Simeon J. Fortin Charitable Foundation, Bank of America, N.A. Trustee, and the Helen Hay Whitney Foundation, M.S. is supported by the Milton Foundation of Harvard University and the National Science Foundation (award no.1652104).

References

1. Maeso I, Acemel RD, Gómez-Skarmeta JL (2017) Cis-regulatory landscapes in development and evolution. Curr Opin Genet Dev 43:17–22
2. Spitz F, Duboule D (2008) Global control regions and regulatory landscapes in vertebrate development and evolution. Adv Genet 61: 175–205
3. Buenrostro JD, Giresi PG, Zaba LC, Chang HY, Greenleaf WJ (2013) Transposition of native chromatin for fast and sensitive epigenomic profiling of open chromatin, DNA-binding proteins and nucleosome position. Nat Methods 10:1213–1218
4. Buenrostro JD, Wu B, Chang HY, Greenleaf WJ (2015) ATAC-seq: a method for assaying chromatin accessibility genome-wide. Curr Protoc Mol Biol 109:21.29.1–21.29.9. https://doi.org/10.1002/0471142727.mb2129s109
5. Fernández-Miñán A, Bessa J, Tena JJ, Gómez-Skarmeta JL (2016) Assay for transposase-accessible chromatin and circularized chromosome conformation capture, two methods to explore the regulatory landscapes of genes in zebrafish. Methods Cell Biol 135: 413–430. https://doi.org/10.1016/bs.mcb.2016.02.008
6. Doganli C, Sandoval M, Thomas S, Hart D (2017) Assay for transposase-accessible chromatin with high-throughput sequencing (ATAC-Seq) protocol for zebrafish embryos. Methods Mol Biol 1507:59–66. https://doi.org/10.1007/978-1-4939-6518-2_5
7. Shashikant T, Ettensohn CA (2019) Genome-wide analysis of chromatin accessibility using ATAC-seq. Methods Cell Biol 151:219–235
8. Bright AR, Veenstra GJC (2019) Assay for transposase-accessible chromatin-sequencing using Xenopus embryos. Cold Spring Harb Protoc 2019. https://doi.org/10.1101/pdb.prot098327
9. Bajic M, Maher KA, Deal RB (2018) Identification of open chromatin regions in plant genomes using ATAC-Seq. Methods Mol Biol 1675:183–201
10. Corces MR, Trevino AE, Hamilton EG, Greenside PG, Sinnott-Armstrong NA, Vesuna S et al (2017) An improved ATAC-seq protocol reduces background and enables interrogation of frozen tissues. Nat Methods 14:959–962
11. Miskimen KLS, Chan ER, Haines JL (2017) Assay for transposase-accessible chromatin using sequencing (ATAC-seq) data analysis. Curr Protoc Hum Genet 92:1.16.1
12. Yan F, Powell DR, Curtis DJ, Wong NC (2020) From reads to insight: a hitchhiker's guide to ATAC-seq data analysis. Genome Biol 21:22
13. Wei Z, Zhang W, Fang H, Li Y, Wang X (2018) esATAC: an easy-to-use systematic pipeline for ATAC-seq data analysis. Bioinformatics 34: 2664–2665
14. Li H, Handsaker B, Wysoker A, Fennell T, Ruan J, Homer N et al (2009) The Sequence Alignment/Map format and SAMtools. Bioinformatics 25:2078–2079
15. Langmead B, Salzberg SL (2012) Fast gapped-read alignment with Bowtie 2. Nat Methods 9: 357–359
16. Gaspar JM (2018) NGmerge: merging paired-end reads via novel empirically-derived models of sequencing errors. BMC Bioinformatics 19: 536
17. Magri MS, Jiménez-Gancedo S, Bertrand S, Madgwick A, Escrivà H, Lemaire P et al (2019) Assaying chromatin accessibility using ATAC-Seq in invertebrate chordate embryos. Front Cell Dev Biol 7:372
18. Bentsen M, Goymann P, Schultheis H, Petrova A (2019) Beyond accessibility: ATAC-seq footprinting unravels kinetics of transcription factor binding during zygotic genome activation. BioRxiv. https://www.biorxiv.org/content/10.1101/869560v1.abstract
19. Stark R, Brown GD (2011) DiffBind: differential binding analysis of ChIP-Seq peak data. Bioconductor (https://bioconductor.org/packages/release/bioc/html/DiffBind.html).

20. Lun ATL, Smyth GK (2016) csaw: a Bioconductor package for differential binding analysis of ChIP-seq data using sliding windows. Nucleic Acids Res 44:e45
21. Heinz S, Benner C, Spann N, Bertolino E, Lin YC, Laslo P et al (2010) Simple combinations of lineage-determining transcription factors prime cis-regulatory elements required for macrophage and B cell identities. Mol Cell 38:576–589
22. Bruse N, Van Heeringen SJ (2018) GimmeMotifs: an analysis framework for transcription factor motif analysis. BioRxiv. https://www.biorxiv.org/content/10.1101/474403v1.abstract
23. Yu G, Wang L-G, He Q-Y (2015) ChIPseeker: an R/Bioconductor package for ChIP peak annotation, comparison and visualization. Bioinformatics 31:2382–2383

Open Access This chapter is licensed under the terms of the Creative Commons Attribution 4.0 International License (http://creativecommons.org/licenses/by/4.0/), which permits use, sharing, adaptation, distribution and reproduction in any medium or format, as long as you give appropriate credit to the original author(s) and the source, provide a link to the Creative Commons license and indicate if changes were made.

The images or other third party material in this chapter are included in the chapter's Creative Commons license, unless indicated otherwise in a credit line to the material. If material is not included in the chapter's Creative Commons license and your intended use is not permitted by statutory regulation or exceeds the permitted use, you will need to obtain permission directly from the copyright holder.



Part V

OMICS Approaches



Chapter 30

Single-Cell Transcriptomic Analysis in the Regenerating Cnidarian *Nematostella vectensis*

Flora Plessier, Sandrine Schmutz, Sophie Novault, and Heather Marlow

Abstract

Cnidarians have historically served as excellent laboratory models for regenerative development given their capacity to regrow large portions of the adult organism. This capacity is notably absent or poorly developed in the powerful genetic laboratory models *Drosophila*, *C. elegans*, and mouse. Increasingly, development of genetic and genomic resources and the application of next-generation sequencing-based techniques in cnidarian systems has further expanded the potential of cnidarian regenerative models. Here, we present a workflow for the characterization of the regenerative response in the sea anemone *Nematostella vectensis* utilizing fluorescence-activated cell sorting and a plate-based single-cell RNA-sequencing pipeline. This approach can characterize the transcriptional response during regeneration in distinct populations of cells, thus providing a quantitative view of a whole organism process at cellular resolution.

Key words Single-cell RNA-seq, Cnidaria, *Nematostella vectensis*, Regeneration, Flow cytometry

1 Introduction

The ability to regenerate is widespread among marine invertebrates. Understanding the molecular and developmental basis of regeneration in a diversity of taxa has the potential to provide insight into shared principles of the regenerative response. Cnidarians (*Hydra*, jellyfish, sea anemones, corals) belong to one of the earliest-branching metazoan phyla and are well known for their extensive regenerative abilities [1–3]. The sea anemone *Nematostella vectensis* is an experimentally tractable Cnidarian species for studies into mechanisms of regeneration. Significant advances in genetic and genomic resources, ease of culture, and conservation of gene content with Bilaterian taxa contribute to the utility of this sea anemone as a developmental and regenerative model system [4–6].

An experimentally bisected *Nematostella vectensis* polyp can regenerate two whole animals in about a week [1]. How the sea anemone regenerates lost tissue, maintains axial coordinates, and generates the appropriate number and distribution of constituent

Simon Blanchoud and Brigitte Galliot (eds.), *Whole-Body Regeneration: Methods and Protocols*,
Methods in Molecular Biology, vol. 2450, https://doi.org/10.1007/978-1-0716-2172-1_30, © The Author(s) 2022

cell types during regeneration or asexual reproduction is not well understood. Studies focusing on the cellular dynamics following oral pole regeneration in juvenile polyps have highlighted the involvement of cellular proliferation and apoptosis [1, 7]. Whole-animal transcriptomic time-courses have been employed to uncover genes modulated during the regeneration process [8–10]. However, the behaviors of individual cell populations during regeneration have not been molecularly or functionally characterized in *Nematostella vectensis* thus far [11]. In order to better characterize the process of regeneration, additional tools that allow for the characterization of behaviors of single cells are needed. As regeneration is dynamic, gaining an understanding of the molecular events happening in individual cells throughout this process is critical.

Over the past few years, newly developed single-cell RNA-Sequencing (scRNA-Seq) techniques have enabled investigators to sample the transcriptome of single cells from complex tissues and whole organisms, to assess their developmental trajectories and reconstruct gene regulatory networks governing cell identity and function [12]. Different single-cell sequencing technologies have been developed ranging from plate-based, droplet or microfluidic platforms, each with distinct advantages and limitations [13]. Recently, single-cell RNA-Seq of whole *Nematostella vectensis* polyps and planula larvae via a plate-based approach, MARS-seq, has enabled the generation of a molecular atlas of the cell types present in the sea anemone [14]. In combination with targeted genetic labeling and trajectory inference methods, scRNA-Seq data from regenerating animals could enable the reconstruction of key cellular trajectories, as well as the relative contributions of different cell populations to the newly regenerated tissues.

From cell suspension, most scRNA-seq protocols rely on a similar workflow, where single cells are physically isolated and lysed, in wells or droplets, captured mRNA molecules are reverse transcribed and amplified, and multiplexed dsDNA libraries are generated and sequenced [13]. Complete, high-viability dissociation of starting tissue is a critical pre-requisite of scRNA-seq. Single cells can then be isolated through Fluorescence-activated cell sorting (FACS), which enables a single cell to be separated from a cell suspension with a high degree of purity. Following single-cell isolation, mature mRNAs are often captured through their polyadenylated tails using barcoded oligos bearing polyT stretches, then reverse transcribed into cDNAs before being amplified via PCR or in vitro transcription [15]. During capture or in subsequent steps, cell- and/or pool-specific barcodes are added, to enable attribution of the sequenced reads to a specific cell and sample of origin. To limit the impact of amplification artifacts, unique molecular identifiers (UMIs), short stretches of random DNA bases, are attached to the captured mRNA molecules [15, 16]. Duplicate reads from the same mRNA molecule can be merged by UMI. For data processing

and analysis, several quality control and clustering analysis packages have been developed [17–19].

In this protocol, we focus on a single-cell RNA-sequencing experiment in a regenerating *Nematostella vectensis* polyp including the dissociation of samples of interest into live single-cell suspensions, the flow cytometer parameters and gating strategy to sort live single cells into separate wells of a 384-well plate, as well as an overview of quality control steps after library sequencing, read demultiplexing and mapping, QCs, and general notes and considerations specific to single-cell RNA-Seq *Nematostella vectensis* data (Fig. 1). Briefly, polyps along a regeneration time-course following oral pole amputation are dissociated into single-cell suspensions at timepoints of interest (Fig. 1a), then live single cells are sorted on a flow cytometer into single wells of a 384-well plate (Fig. 1b). Following cell lysis and mRNA capture with barcoded oligonucleotides in individual wells, multiplexed cDNA libraries are generated using the MARS-Seq single-cell RNA-Seq method [15, 20] (Fig. 1c). The scRNA-seq library preparation method has been adapted from an established workflow and an extensive protocol detailing the experimental steps, and an associated computational pipeline has recently been published [20]. After library sequencing, reads are filtered, demultiplexed, and mapped using the MARS-Seq computational pipeline onto the *Nematostella* genome to generate count tables, listing the number of recovered molecules from each gene in each sequenced cell [20, 21] (Fig. 1d). The count tables can then be filtered and clustered using various clustering methods for biological analyses [22] (Fig. 1d). Here, we generate an example clustering using the MetaCell clustering package, a published pipeline for the analysis of scRNA-seq data [17].

2 Materials

All solutions should be prepared using ultrapure water and stored at room temperature (RT) unless otherwise stated.

1. *Nematostella* medium: 12.8 g/L artificial seawater salt in distilled water.
2. 24 h starved 5- to 8-week-old juvenile animals.
3. Six-well plates.
4. Sterile scalpel blades.
5. 3-mL plastic Pasteur pipets.
6. 7% (w/v) magnesium chloride solution in ultrapure water.
7. Low-binding 1.5-mL tubes (e.g., Biozym #710176).
8. Calcium-Magnesium-Free Artificial Seawater (CMFSW) for *Nematostella* dissociation medium: 495 mM NaCl, 9.7 mM

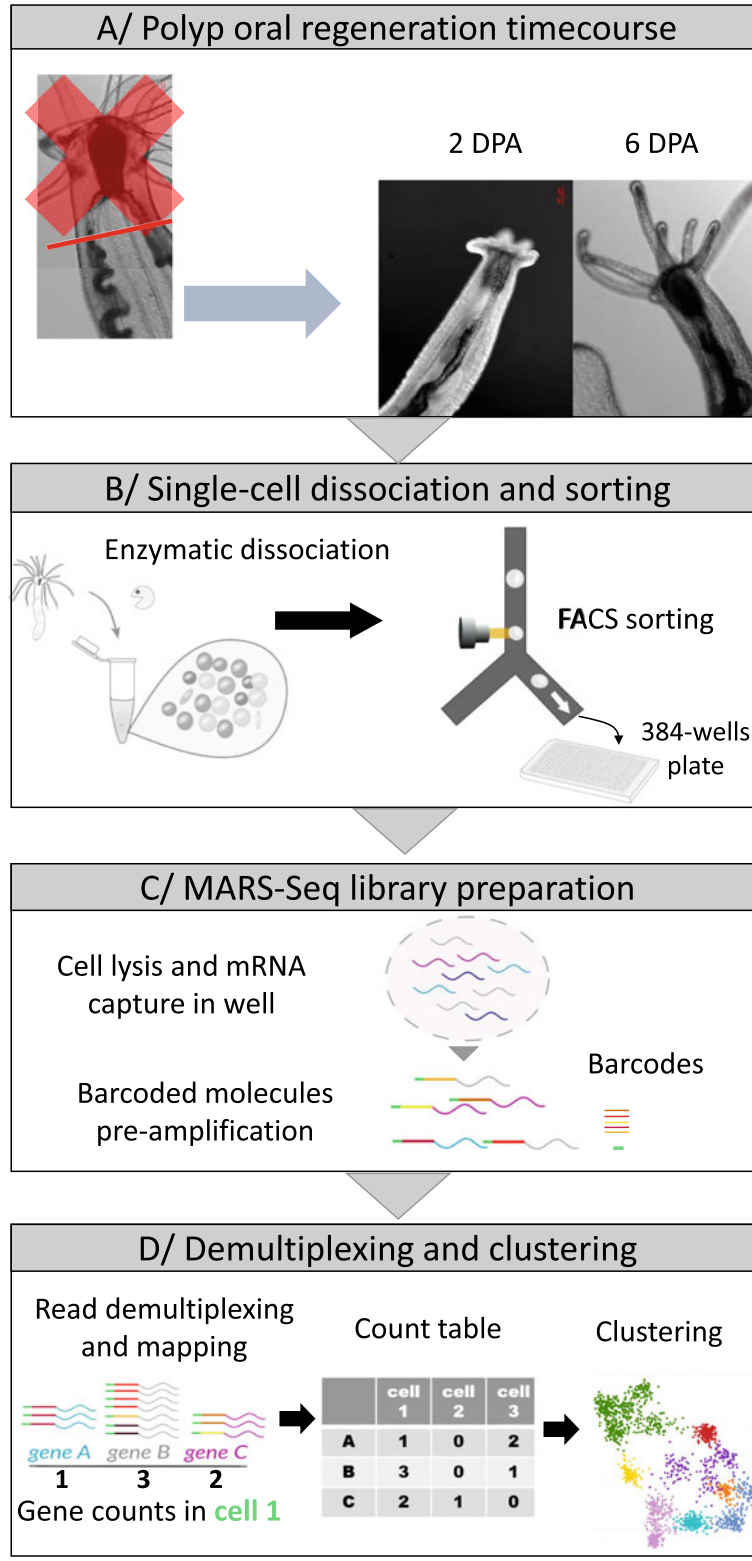


Fig. 1 Overview of single-cell RNA Sequencing in the regenerating sea anemone *Nematostella vectensis*. (**a**) DIC images of the oral region of uncut control, 2 and

KCl, 27.6 mM $NaHCO_3$, 50 mM Tris–HCl pH 8. Filter sterilize.

9. Live cell marker: 1 μg/μL calcein AM resuspended in dimethyl sulfoxide (DMSO). Protect from light and store at −20 °C (*see* **Note 1**).
10. Dead cell marker: 1 mg/mL propidium iodide ready-to-use solution. Protect from light and store at 4 °C (*see* **Note 1**).
11. Collagenase solution: 5 mg/mL LiberaseTM resuspended in nuclease-free water. Store aliquots at −20 °C.
12. Gelatin solution: 1 mg/mL gelatin. Heat to dissolve, filter.
13. Gelatin-coated P200 tips: pipette up and down gelatin solution, let the tips dry overnight, store at RT.
14. Gelatin-coated P1000 tips.
15. Trimmed P200 gelatin-coated tips: remove 1–2 mm of dry coated tip length using a scalpel blade.
16. Dissociation medium: 32.4 mL CMFSW, 17.6 mL ultrapure H_2O, filter at 0.4 μm. Check salinity against sample salinity.
17. Staining medium: 2 μL/mL live cell marker, 3 μL/mL dead cell marker in dissociation medium. Prepare fresh. Protect from light.
18. Fluorescence-Activated Cell Sorter (e.g., BD FACS ARIAIII), with laser/filters combinations appropriate for the dyes used (*see* **Note 2**).
19. Flow cytometer sizing beads: 1.34 μm, 3 μm, and 6 μm diameter.
20. Frozen cell capture plates: 384-wells plates filled with 2 μL polyT barcoded capture oligos in lysis solution stored at −80 °C (*see* **Note 3**).
21. *Nematostella vectensis* genome and gene annotation (*see* **Note 4**).
22. MARS-Seq library preparation pipeline (*see* **Note 5**).

Fig. 1 (continued) 6 day post-amputation (2 dpa and 6 dpa) juvenile *Nematostella vectensis* polyps (~5 weeks) at room temperature. Amputation site is indicated with a red line. (**b**) Enzymatic dissociation of sample into a single-cell suspension and single-cell FACS sorting into 384-well plates. (**c**) Simplified overview of the labeling strategy for single-cell-derived mRNA which includes barcoding for each cell in each well using capture oligonucleotides with a polyT-tract, a random unique molecular identifier (UMI) and a cell barcode. (**d**) Multiplexed single-cell RNA-seq short-read libraries are sequenced, reads are filtered, mapped, and demultiplexed to attribute recovered molecules, through their unique UMIs tags, to their cell of origin. Cells are then clustered using unsupervised clustering based on gene expression for downstream analyses

23. DNA electrophoresis equipment (e.g., TapeStation, Agilent).
24. DNA concentration fluorometer (e.g., Qubit, Thermo Fisher Scientific).
25. MARS-Seq computational pipeline (*see* **Note 6**).
26. scRNA-seq data clustering pipeline (*see* **Note 7**).

3 Methods

3.1 Cell Dissociation of Regenerated and Control Samples

1. Select 5- to 8-week-old siblings of similar size (*see* **Note 8**).
2. Transfer one polyp into the lid of a 5-cm plastic dish filled with 1.5 mL *Nematostella* medium.
3. Repeat **step 2** for the remaining siblings, in separate lids.
4. Wait for ~20 min for the polyp to relax, until the tentacles are fully extended.
5. Add drop-by-drop, on the side of the lid, 1.5 mL of 7% $MgCl_2$.
6. Wait for 30 s for full immobilization (*see* **Note 9**).
7. Amputate the oral end by cutting perpendicularly to the oral-aboral axis below the pharynx in one straight cut. *See* red line in Fig. 1a for the amputation plane used here.
8. Gently transfer the aboral end to a well of a six-well plate filled with ~3 mL *Nematostella* medium using a plastic Pasteur pipette with a wider opening (*see* **Note 10**).
9. Keep the plate at 22 °C.
10. Repeat **steps 5–8** three more times to transfer the replicates to separate wells.
11. Transfer the two control polyps to the remaining wells.
12. Keep the plate in an incubator at 22 °C.
13. Do not feed control or regenerating animals.
14. Wait until the desired timepoint is reached (*see* **Note 11**).
15. Transfer each sample in a separate 1.5-mL low-binding tube using a plastic pipette.
16. Spin down each sample by brief centrifugation (<1 s) on a tabletop centrifuge.
17. Remove the superficial liquid layer, while keeping each sample immersed.
18. Add 1 mL of dissociation medium to wash.
19. Repeat **steps 16–18** for another wash step.
20. Adjust total volume to 300 μL with dissociation medium (*see* **Note 12**).
21. Add 3 μL of thawed liberaseTM solution.

22. Gently pipette up and down slowly at RT (>1.5 s per pipetting cycle) using a trimmed P200 gelatin-coated tip (*see* **Note 13**). Use different tips for each sample to avoid cross-contamination.
23. Transition to an uncut gelatin-coated P200 tip with a narrower opening when the diameter of the remaining particles is small enough to pass through the new opening.
24. Add 30 μL of 0.5 M EDTA to stop the dissociation.
25. Add 420 μL of dissociation medium.
26. Gently pipette up and down slowly with gelatin-coated P1000 tips to homogenize.
27. Fill the P1000 tip with the cell suspension.
28. Place the tip directly atop the filtering cap of the 5-mL FACS tube, at an angle.
29. Gently eject the cell through the filter, aiming at the side of the tube (*see* **Note 14**).
30. Add 750 μL of staining medium.
31. Slowly pipette up and down with a gelatin-coated P1000 tip to mix.
32. Protect from light and place tubes in a tube holder atop ice.
33. Bring tubes to the flow cytometer facility (*see* **Note 15**).

3.2 Live Single-Cell Sorting Using Flow Cytometry for Single-Cell RNA-Sequencing

1. Initialize flow cytometer according to manufacturer's instructions, including laser alignment testing and time delay setup for sorting (*see* **Note 16**).
2. Adjust plate holder arm coordinates so that the sort stream deposits a single droplet within the center of each well of a cell capture plate (*see* **Note 17**).
3. Display the forward scatter-area (FSC-A) signal and side scatter-area (SSC-A) signal in the biexponential scale for all samples and adjust the photomultipliers (PMT) voltages and thresholds to visualize the dynamic range of particles (Fig. 2a, b) (*see* **Note 18**).
4. Select singlet particles from all the events by excluding multiplets based on their forward scatter-width vs. forward scatter-height signal (gated population is in blue in Fig. 2c).
5. Set the photomultiplier voltages for the channels associated to the live and dead cell dyes fluorescent channels using positive (stained) and negative (fluorescence-minus one—FMO) populations (*see* **Note 19**).
6. Select live singlet particles from the singlet population (in blue in Fig. 2c) by gating the populations according to the live cell

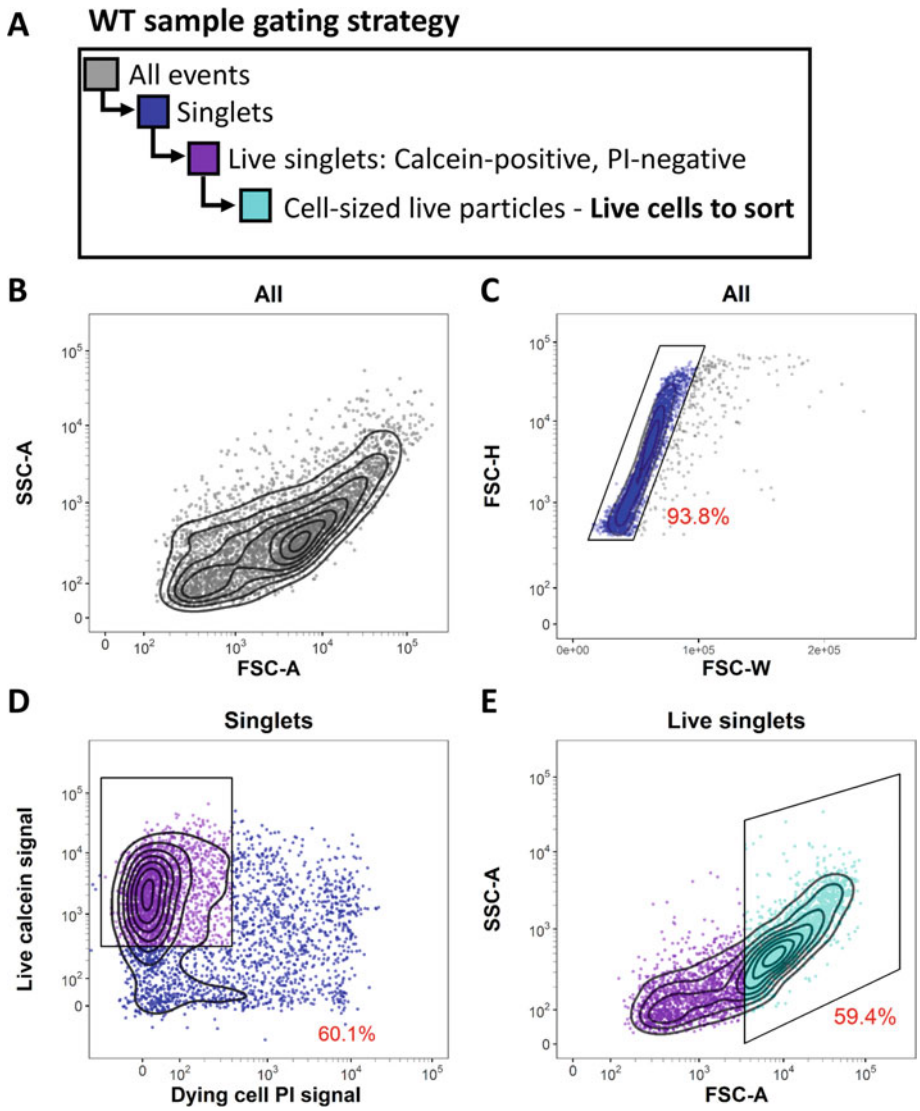


Fig. 2 FACS gating strategy for live cell-sized singlets with live/dead double-staining. (**a**) Gating strategy to select live single cells from sample stained with calcein AM and propidium iodide (PI). (**b**) Overall events SSC-A vs. FSC-A profile. Note that we are using bi-exponential scaling on both FSC-A and SSC-A because of the size heterogeneities in our samples. (**c**) Singlet gate to exclude multiplets based on FSC-H vs. FSC-W profile. Singlet proportion is usually in the 90–95% range. (**d**) From the singlet population, the live cell gating strategy is based on calcein (live) signal inclusion and propidium iodide (permeabilized dead cells) signal exclusion. (**e**) From the live singlet population, setup of the cell-sized particle gate, to keep only live single cells for sorting. For setting up this cell-sized gate boundaries, *see* Fig. 3a, g. The proportion of cells that fall within the represented gate is indicated in red

marker and dead cell marker (gated population in purple in Fig. 2d).

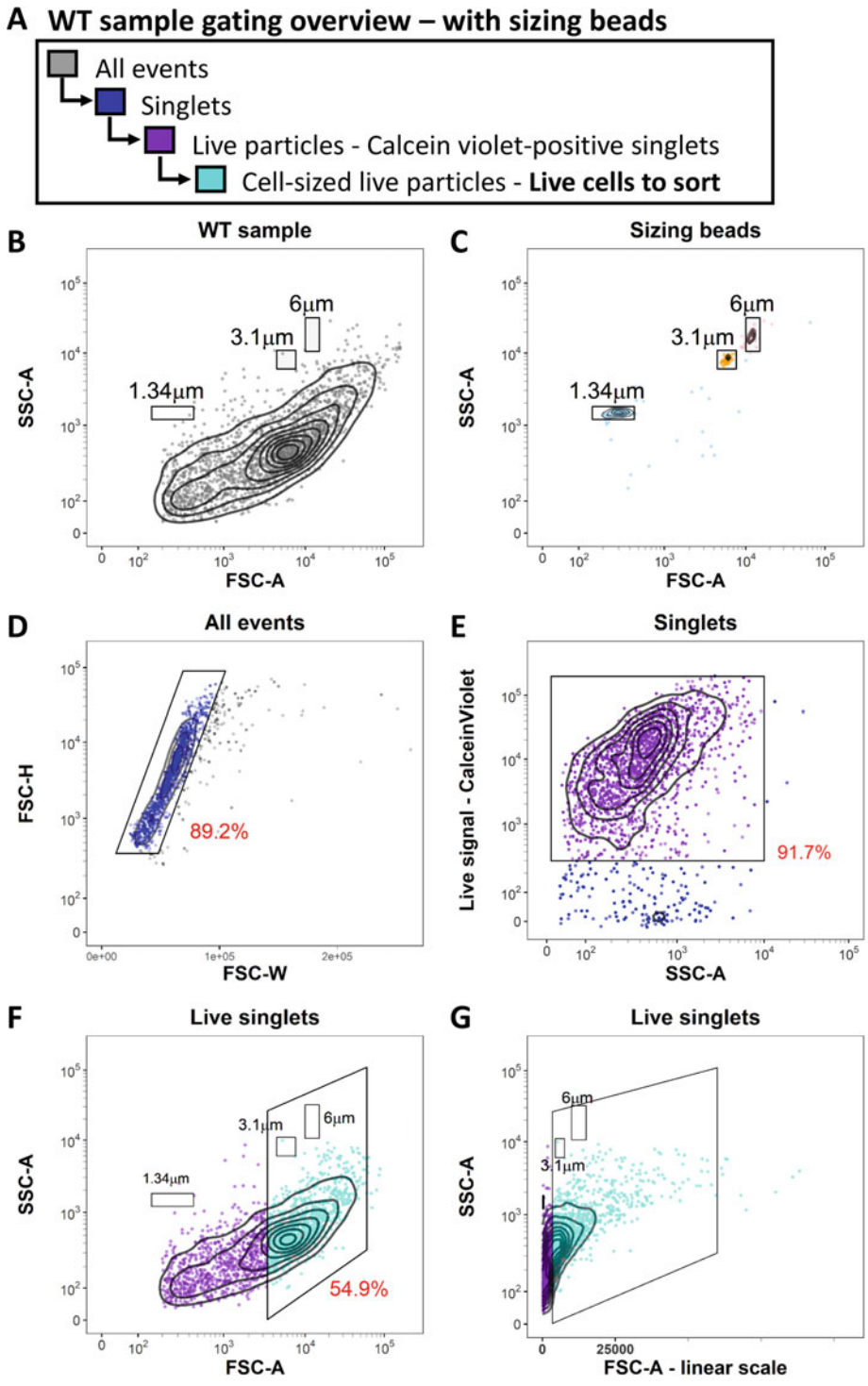


Fig. 3 FACS gating strategy setup for live cell-sized singlets with absolute size comparison. (**a**) Gating strategy to select live single cells. (**b**) All events gate from a whole animal cell suspension (SSC-A vs. FSC-A). Note that we are using bi-exponential scaling on both FSC-A (except in panel **g**) and SSC-A given the inherent size heterogeneities of *Nematostella vectensis* whole organism cell suspensions. (**c**) Overlay of three sizing beads FCS-A profiles (1.34 µm, 3.1 µm, and 6 µm beads) to set the FSC-A boundary of the cell-sized gate presented

7. Select the live single cell-sized particles (~3–20 μm) to sort from the live singlet population (in purple in Fig. 2d) based on their SSC-A vs. FSC-A signal (gated population in cyan in Fig. 2e). The setup of the cell-sized gate is presented in Fig. 3a–g (*see* **Note 20**).
8. Thaw the 384-well capture plates.
9. Sort one single cell of interest (precision mode: single cell with yield mask: 0, purity mask: 32 and phase mark: 16) per well in each 384-well capture plate, leaving four control wells empty.
10. Spin down the plate at 1000 rcf for 1 min and seal the plate.
11. Freeze on dry ice until the rest of the plates have been sorted.
12. Store at −80 °C until processing (*see* **Note 21**).

3.3 Single-Cell RNA-Seq Library Generation, QC, and Initial Characterization

1. Process plates through the MARS-Seq library preparation pipeline with $N = 17$ cycle of PCR amplification at the last step.
2. Check library fragment size distribution using the DNA electrophoresis equipment, according to manufacturer's instructions. MARS-Seq libraries should have a homogeneous fragment size distribution of around 410–440 bp (Fig. 4a for an example profile).
3. Check library concentration using the DNA concentration fluorometer, according to manufacturer's instructions. *Nematostella* libraries from a half-plate (190 cells) are routinely in the 1–5 ng/μL range, for a total yield of ~20–100 ng per library.
4. Pool libraries equimolarly and sequence using an high output sequencer according to the manufacturer's protocol (*see* **Note 22**).
5. Run the MARS-Seq computational pipeline to filter, demultiplex and map sequencing reads onto the *Nematostella* genome according to the user manual (*see* **Note 23**).
6. Check that sequencing depth across libraries is homogeneous (Fig. 4b). Library sequencing depth depends on the number of libraries pooled and on the sequencing kit used. Here, we sequenced libraries to a median depth of ~40,000 reads per well (*see* **Note 24**).
7. Check the distribution of UMIs in each library (Fig. 4c). Median cell UMI number in *Nematostella* samples is usually around 400–800 UMIs per library, depending on sequencing

Fig. 3 (continued) in panel **g**. (**d**) Singlet gate to exclude multiplets based on their FSC-H vs. FSC-W profile. (**e**) Live cell gating strategy based on calcein Violet signal to keep only cells with calcein (live) signal. (**f**) and (**g**) Cell-sized particle gate. Gate boundary is based on beads sizing gate, including all particles ~3 μm and above to maximize cells and minimize debris. Representation in a biexponential scale enables clearer demarcation of cell-sized live particles. The proportion of cells that fall within the represented gate is indicated in red.

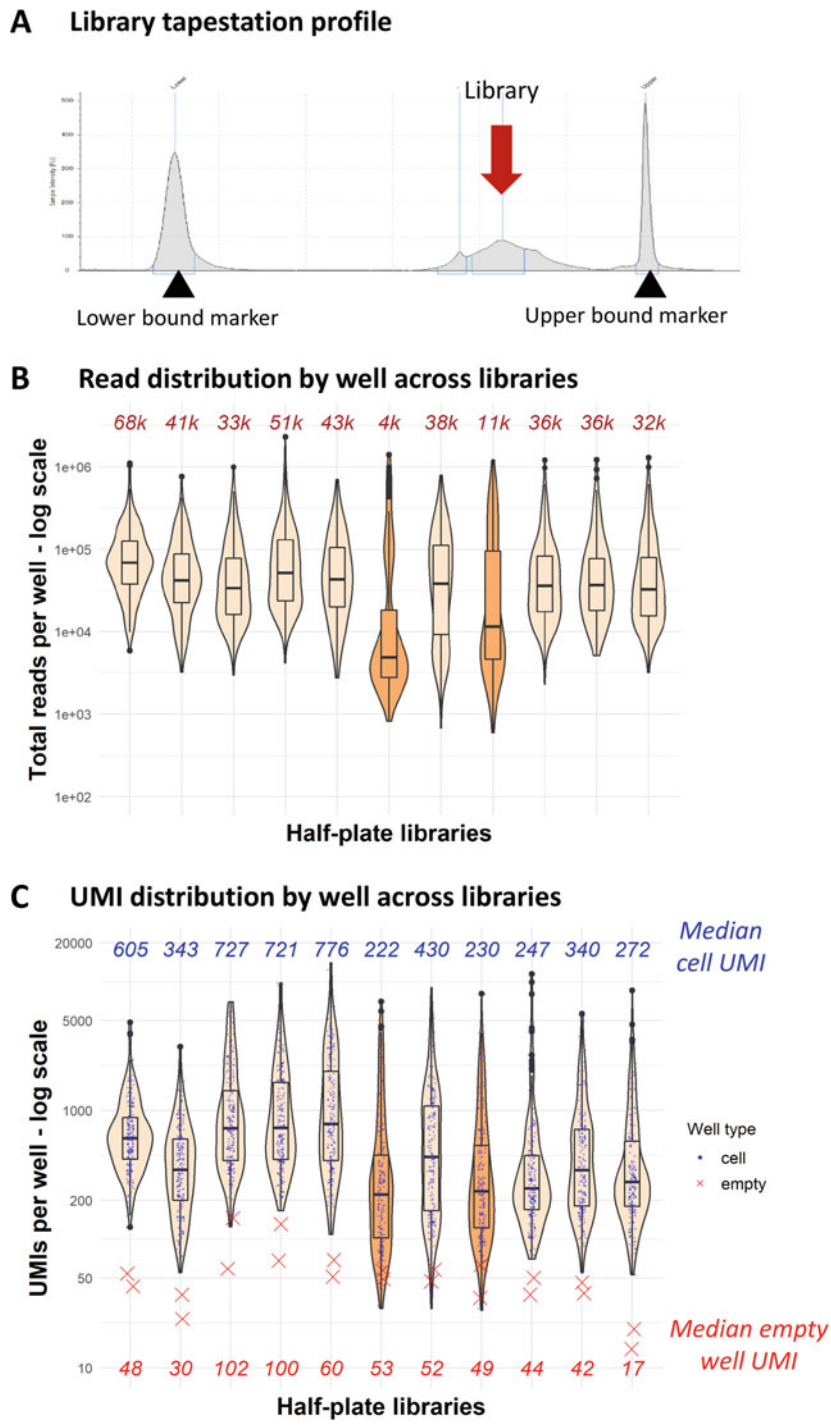


Fig. 4 Library quality metrics of a sequenced single-cell RNA-seq experiment. (**a**) Example of a typical library tapestation profile of a single MARS-Seq half-plate library (red arrow). Expected fragment size is usually in the 410–440 bp range. Black arrowheads indicate the upper and lower lane markers on a D1000 high sensitivity tape. (**b**) Sequencing depth statistics across sequenced libraries, by half-plate (192 cells) library. Median read depth per library is indicated in dark red at the top. Median sequencing depth target is 40,000 reads/cell when sequencing 32 MARS-Seq libraries on a NextSeq 500 high output kit. Note the two libraries flagged in orange

depth, cell, and sample type. UMI recovery per cell correlates with the overall cell size, with bigger cells yielding higher UMI counts.

8. Check noise level from the recovered UMIs in the control empty wells. UMI recovery from empty well are significantly lower than for wells with cells (red Xs on Fig. 4c).
9. Filter out cells based on a UMI threshold. Threshold should be over the noise level. We usually use 100–300 UMIs as a lower boundary. Here, boundaries were set at 120–3000 UMIs (Fig. 5a).
10. Cluster cells passing QC using the clustering pipeline, parameters will depend on cell number and sample cell type diversity. *See* 2D projection of a pilot experiment on ~1200 cells in Fig. 5b–d, with a subset of key known markers to propose a cell cluster annotation.

4 Notes

1. For cells labeled with a fluorophore overlapping with the calcein AM or propidium iodide (e.g., transgenic fluorescent reporter), it is possible to use the calcein violet (live dye) instead of calcein AM, and SytoxRed (dead cell dye) instead of propidium iodide.
2. For the calcein AM signal: fluorescein (FITC) channel, laser excitation: 488 nm, emission filters: LP 502 nm, and BP 530/30 nm. Propidium iodide (PI) signal: phycoerythrin (PE) channel, laser excitation: 561 nm, emission filters: BP 582/15 nm. If sorting mOrange-labeled cells, the following channel combinations can be used: calcein violet signal (live dye): laser excitation, 405 nm, emission filters: BP 450/40 nm. mOrange signal: phycoerythrin (PE) channel, laser excitation: 561 nm, emission filters: BP 582/15 nm. "Green" autofluorescence signal: fluorescein (FITC) channel, laser excitation: 488 nm, emission filters: LP 502 nm, and BP 530/30 nm. In that case, mOrange-positive cells should be sorted from live singlets from a mOrange signal/Green autofluorescence signal

Fig. 4 (continued) whose median sequencing depth is much lower, indicating potentially either a sample issue, or library undersequencing or library quality issues. As their matched other half-plates show the expected sequencing depth, it seems likely to be a technical issue arising during processing or library pooling. The other libraries pass this check. (**c**) Unique Molecular Identifiers (UMI) recovery statistics across half-plate libraries. Same libraries as shown in **b**. Note that flagged libraries (in orange in **b** and **c**) also display a lower UMI distribution compared to their other half-plate. The two empty wells kept as negative controls (red Xs) per half-plate display very low UMI recovery (noise) compared to wells that held one cell (blue dots)

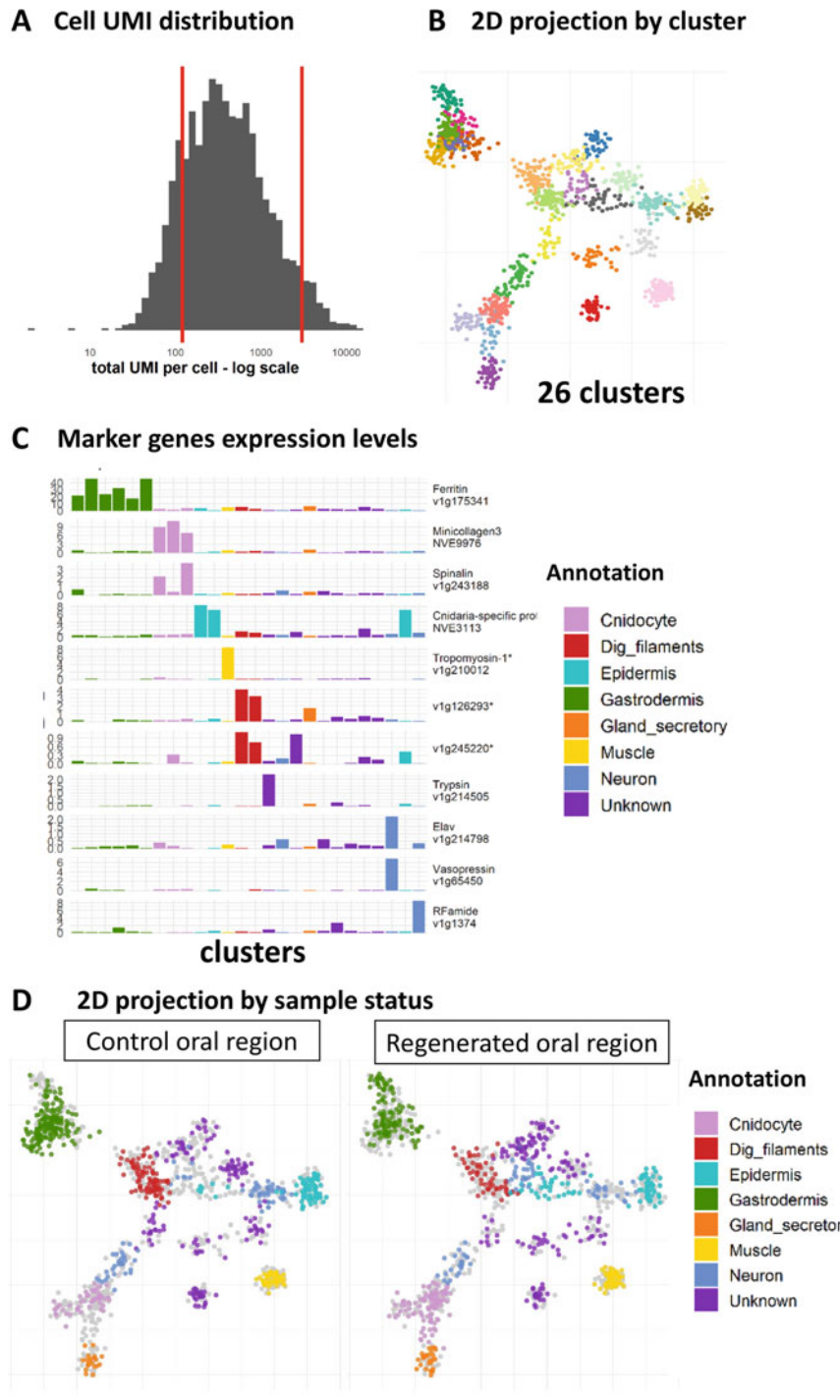


Fig. 5 UMI distribution in cells passing QC and clustering example from a *N. vectensis* regeneration experiment. (**a**) UMI distribution across all cells. Here, cells from which between 120 and 3000 (red lines) UMIs were recovered were kept for downstream analyses. (**b**) 2D-projection of 1300 cells clustered here using the MetaCell analysis package, colors are used to demarcate individual MetaCell clusters. (**c**) Gene expression (UMIs per 1000 UMIs in the cluster) for known marker genes from [14] are used to annotate the clusters. (**d**) 2D-projection of control and regenerated oral regions at 4/6 days post-amputation. Overall 2D clustering is

visualization, by selecting mOrange signal-positive cells that are not also GFP-like positive.

3. A detailed step-by-step protocol to efficiently prepare the MARS-Seq capture plates, with lysis buffer and specific poly-T barcoded capture oligos has been published previously [15].
4. Genome file [21] can be downloaded from the JGI website at https://genome.jgi.doe.gov/Nemve1/Nemve1.home.html. Annotation according to [17].
5. We have been following the step-by-step MARS-Seq 2.0 protocol published by the Amit and Tanay's labs [20] to generate sequencing-ready libraries.
6. This protocol uses MARS-seq2.0 [20] as provided on the website of Amos Tanay's group; http://compgenomics.weizmann.ac.il/tanay/?page_id=672.
7. We have been using MetaCell, a clustering algorithm based on K-nn graph partitioning [17].
8. A single polyp will yield ample cells to populate all the sixteen 384-well plates for a full MARS-seq run. However, as FACS-sorted plates can be associated with index information, multiple replicate polyps can be processed in the same sequencing run.
9. If the animal is not fully relaxed, wait for it to relax before adding $MgCl_2$. If the animal contracts upon $MgCl_2$ addition, wash it out of the $MgCl_2$ solution by moving it into bigger volumes of *Nematostella* medium and use another animal.
10. It is best to cut off the tip of a 3-mL plastic Pasteur pipette to avoid damaging the polyp with the smaller opening while transferring it.
11. 4 days and 6 days post-amputation and control non-amputated animals were used here.
12. For processing a larger amount of starting material, the dissociation volume can be scaled up as well as all the subsequent reagents, or/and samples can be split across several tubes.
13. Liberase activity is optimal at 37 °C; however, to avoid heat stress, all steps are carried out at RT (22–24 °C), and dissociation usually takes between 10 and 30 min depending on sample density, type, and stage.

Fig. 5 (continued) split by sample origin (control or regenerated), and colored according to a preliminary MetaCell annotation based on known markers published in the *N. vectensis* cell atlas [14]. Most cells are split according to their prospective cell state, with newly regenerated oral side samples falling within all broad cell types

14. If the cell suspension is very dense or large fragments of extracellular matrix remain, the filter may become clogged. In that case, changing the filter and rediluting the sample prior to refiltering is recommended.
15. Cell concentration, morphology, presence of multiplets, and viability should be checked on a ~10 μL aliquot of the cell suspension at a microscope prior to FACS-sorting.
16. It is recommended that the FACS be set up and calibrated prior to starting the dissociation. CS&T beads™ Fluorospheres (BD Biosciences) are used to perform optical QC (delay performance measurements) as well as establish laser delay. For additional settings for single-cell deposition, we have used Accudrop™ fluorescent beads. Sheath fluid—BD FACS Flow—was filtered twice through a 0.2-μm filter. The sheath flow formed stable droplets using a 70-μm nozzle.
17. Single-cell deposition efficiency in each well of the 384-well plate should be controlled prior to experiments using a colorimetric method [23]. Briefly, this uses 3,3′,5,5-′-tetramethylbenzidine (TMB) and horseradish peroxidase (HRP) to verify whether a droplet from the cell sorter has successfully reached the fluid in the bottom of the well. The droplet contains the enzyme HRP, which is deposited into a well containing the substrate TMB. When HRP and TMB come into contact, TMB is oxidized and rapidly turns to blue color. Parameters adjusted on the Aria III before single-cell deposition sorting include forward scatter area, side scatter area, and fluorescent area parameters. Forward scatter-area, forward scatter-width, forward scatter-height, side scatter-area, side scatter-width, and side scatter-height are used to exclude multiple cell containing droplets and ensure single cells were deposited. Higher acquisition rates will generally increase the likelihood that droplets will contain multiple cells; therefore, low flow rate is kept constant throughout sorting.
18. Using a biexponential scale for the FSC-A signal is usually more informative because of the very broad size range (~3–25 μm, with a majority of 4–15 μm cells) seen in *Nematostella* cells. The default FSC-A machine threshold may need to be lowered as some *Nematostella* cells are much smaller.
19. If sorting for a GFP-like fluorophore reporter, whose spectrum overlaps with the calcein AM live cell dye, the live dye can be substituted for calcein violet (e.g., 405 nm, emission filters: BP 450/40 nm), if there is no spectral overlap. Calcein AM and calcein violet signal are completely coherent (i.e., a double-stained sample will exhibit signal only in the diagonal in the calcein AM/calcein violet visualization plane).

20. Multiple sizing beads (ideally with 1, 3, 6, and 10 μm sizing beads) are used as an absolute size reference for the FSC-A signal, which correlates with particle size. On a FSC-A vs. SSC-A display, most live single cells should be in the 3–20 μm range, with the majority in the 4–15 μm range. Alternatively, a solution of freshly spawned *Nematostella vectensis* mature sperm displays a homogeneous FSC-A vs. SSC-A profile and can be used as a ~3 μm threshold reference.
21. Plates of captured sorted cells can be stored over at least several months at −80 °C as some samples have been processed and gave similar yields after more than 1.5 years in storage.
22. We routinely used a NextSeq500 high output kit from Illumina but similar coverage can be obtained using several Illumina HiSeq lanes.
23. The pipeline generates UMI count tables used for subsequent clustering as well as a quality control (QC) report whose panels are presented and commented in depth in the MARS-Seq protocol [20].
24. If specific libraries are undersequenced, that could indicate a library pooling issue, or a library quality issue. Repeat DNA electrophoresis analysis of the library to check library profile and re-assess library concentration, if the profile is as expected and the concentration in the expected range for the number of amplification cycles used, use the new concentration to repool and sequence with other libraries. If read number is heterogeneous within a library, that can be due to technical issues during cell sorting or plate processing. Check the distribution of reads or UMIs across the plate, sometimes plate borders or plate sides display overall lower recovered UMI counts linked to well localization on the plate because of a plate processing issue.

References

1. Amiel AR, Johnston HT, Nedoncelle K et al (2015) Characterization of morphological and cellular events underlying oral regeneration in the sea anemone, *Nematostella vectensis*. Int J Mol Sci 16:28449–28471
2. Bradshaw B, Thompson K, Frank U (2015) Distinct mechanisms underlie oral vs aboral regeneration in the cnidarian *Hydractinia echinata*. eLife 4:e05506
3. Vogg MC, Galliot B, Tsiairis CD (2019) Model systems for regeneration: Hydra. Development 146(21):dev177212
4. Layden MJ, Rentzsch F, Röttinger E (2016) The rise of the starlet sea anemone *Nematostella vectensis* as a model system to investigate development and regeneration. Wiley Interdiscip Rev Dev Biol 5:408–428
5. Rentzsch F, Juliano C, Galliot B (2019) Modern genomic tools reveal the structural and cellular diversity of cnidarian nervous systems. Curr Opin Neurobiol 56:87–96
6. Rentzsch F, Technau U (2016) Genomics and development of *Nematostella vectensis* and other anthozoans. Curr Opin Genet Dev 39: 63–70
7. Amiel AR, Foucher K, Ferreira S et al (2019) Synergic coordination of stem cells is required to induce a regenerative response in anthozoan cnidarians. bioRxiv 2019.12.31.891804

8. Schaffer AA, Bazarsky M, Levy K et al (2016) A transcriptional time-course analysis of oral vs. aboral whole-body regeneration in the Sea anemone *Nematostella vectensis*. BMC Genomics 17:718
9. Warner JF, Guerlais V, Amiel AR et al (2018) NvERTx: a gene expression database to compare embryogenesis and regeneration in the sea anemone *Nematostella vectensis*. Development 145(10):dev162867
10. Warner JF, Amiel AR, Johnston H et al (2019) Regeneration is a partial redeployment of the embryonic gene network. bioRxiv:658930
11. Watanabe H, Hoang VT, Mättner R et al (2009) Immortality and the base of multicellular life: lessons from cnidarian stem cells. Semin Cell Dev Biol 20:1114–1125
12. Kolodziejczyk AA, Kim JK, Svensson V et al (2015) The technology and biology of single-cell RNA sequencing. Mol Cell 58:610–620
13. Ziegenhain C, Vieth B, Parekh S et al (2017) Comparative analysis of single-cell RNA sequencing methods. Mol Cell 65:631–643.e4
14. Sebé-Pedrós A, Saudemont B, Chomsky E et al (2018) Cnidarian cell type diversity and regulation revealed by whole-organism single-cell RNA-seq. Cell 173:1520–1534.e20
15. Jaitin DA, Kenigsberg E, Keren-Shaul H et al (2014) Massively parallel single-cell RNA-seq for marker-free decomposition of tissues into cell types. Science 343:776–779
16. Kivioja T, Vähärautio A, Karlsson K et al (2012) Counting absolute numbers of molecules using unique molecular identifiers. Nat Methods 9:72–74
17. Baran Y, Bercovich A, Sebe-Pedros A et al (2019) MetaCell: analysis of single-cell RNA--seq data using K-nn graph partitions. Genome Biol 20(1):206
18. Stuart T, Butler A, Hoffman P et al (2019) Comprehensive integration of single-cell data. Cell 177:1888–1902.e21
19. Kiselev VY, Kirschner K, Schaub MT et al (2017) SC3: consensus clustering of single-cell RNA-seq data. Nat Methods 14:483–486
20. Keren-Shaul H, Kenigsberg E, Jaitin DA et al (2019) MARS-seq2.0: an experimental and analytical pipeline for indexed sorting combined with single-cell RNA sequencing. Nat Protoc 14:1841–1862
21. Putnam NH, Srivastava M, Hellsten U et al (2007) Sea anemone genome reveals ancestral eumetazoan gene repertoire and genomic organization. Science 317:86–94
22. Satija R, Farrell JA, Gennert D et al (2015) Spatial reconstruction of single-cell gene expression data. Nat Biotechnol 33:495–502
23. Rodrigues OR, Monard S (2016) A rapid method to verify single-cell deposition setup for cell sorters. Cytometry A 89:594–600

Open Access This chapter is licensed under the terms of the Creative Commons Attribution 4.0 International License (http://creativecommons.org/licenses/by/4.0/), which permits use, sharing, adaptation, distribution and reproduction in any medium or format, as long as you give appropriate credit to the original author(s) and the source, provide a link to the Creative Commons license and indicate if changes were made.

The images or other third party material in this chapter are included in the chapter's Creative Commons license, unless indicated otherwise in a credit line to the material. If material is not included in the chapter's Creative Commons license and your intended use is not permitted by statutory regulation or exceeds the permitted use, you will need to obtain permission directly from the copyright holder.





Chapter 31

Characterization of Soluble Cell-Free Coelomic Fluid Proteome from the Starfish *Marthasterias glacialis*

Laidson Paes Gomes, Catarina Gouveia e Silva, Jean-Charles Gaillard, Jean Armengaud, and Ana Varela Coelho

Abstract

Proteomics combined to advanced bioinformatics tools is acquiring a pivotal role in the comprehensive understanding of living organism's biology, in particular for non-model organisms, which includes most marine and aquatic invertebrates. Depicting of protein composition in a whole organ/organism followed by their assembling in functional protein association networks promotes the understanding of key biological processes. Here, we provide a detailed description of the extraction procedure of cell-free coelomic fluid soluble proteins and the characterization of the proteome of the starfish *Marthasterias glacialis*. Due to coelomic fluid richness in glycoproteins, which complicates protein identification, extracts of soluble proteins are deglycosylated prior to tandem mass spectrometry. This experimental approach is useful at improving knowledge on the coelomic fluid physiological role and deciphering its involvement in regeneration of starfish body parts when comparing different regeneration conditions.

Key words Starfish, *Marthasterias glacialis*, Coelomic fluid, Proteomics, Tandem mass spectrometry

1 Introduction

Proteomics is the study of multiple protein systems with focus on the interplay of multiple, distinct proteins, and their roles as part of a larger system or network [1]. Mass spectrometry (MS), coupled to liquid chromatography (LC–MS), is the most used well-established methodology for proteome investigations [2]. A mass spectrometer measures the mass/charge ratio (m/z) of generated peptide molecular ions and their relative abundances allowing to characterize, identify, and quantify peptides and proteins. Protein extracts rich in glycoproteins can be enzymatically deglycosylated prior to LC-MS analysis to extend the number of identified proteins [3]. To make sense of the extensive sets of identified proteins by proteomics, a functional analysis is required. It tends to organize the identified proteins in biochemical, cellular, biological, and disease-related categories according to the process that they are

Simon Blanchoud and Brigitte Galliot (eds.), *Whole-Body Regeneration: Methods and Protocols*, Methods in Molecular Biology, vol. 2450, https://doi.org/10.1007/978-1-0716-2172-1_31, © The Author(s) 2022

associated with. These different steps are hampered in non-model organisms due to the lack of biological knowledge and complete genome information.

Regenerative potential is expressed to a maximum extent in echinoderms. Starfish are capable of reconstructing external appendages and internal organs often subjected to amputation, self-induced or traumatic, rapidly followed by complete successful re-growth of lost parts. *Marthasterias glacialis* (Linné 1758) is a fairly common asteroid echinoderm widely distributed throughout the northern Europe; it is often found on the Atlantic coast of central/northern Portugal due to its preference for glacial waters. This spiny starfish, which surface is covered with thorns, can be found in waters up to 200 m in a variety of habitats from muddy, protected locations to rock exposed waves [4]. *M. glacialis* normally reaches 25–30 cm in diameter, has five arms, each having three rows of thorns, and differs in color from dark brown to greenish gray. It is a voracious predator feeding on various animals, dead or alive, such as mollusks, fishes, crustaceans, or other echinoderms [5]. Starting from only one fifth of the central disc, *M. glacialis* can survive and regenerate a new individual [4]. However, its regeneration process is slow and complex. Its arm tip regeneration, or even of an entire arm lost by autotomy, can take from a couple of weeks to several months [4]. This species can be seen as an important model for the study of regeneration due to 70% genome similarity with humans [4], its extraordinary regeneration ability [6], and its easy collection from the wild and maintenance in aquaria.

The coelomic fluid circulates the water vascular system, an internal network composed of channels that contacts their internal organs. The liquid part of the coelomic fluid consists of seawater and is extremely rich in secreted molecules. This fluid is responsible for the transport of circulating cells (coelomocytes), nutrients, and metabolites bathing the internal organs [7]. Major coelomocyte morphotypes have the primary function of mediating immune responses, being able to recognize and neutralize foreign material [8, 9]. Humoral responses on echinoderms are represented by a great variety of molecules, like lectins, perforins, and cytokines, secreted by coelomocytes or surrounding tissues, and promoting cell migration, agglutination, and healing [9]. Recently, the *Asterias rubens* coelomocyte-free coelomic fluid proteome was characterized by LC-MALDI tandem mass spectrometry, identifying 91 proteins [10]. The most represented functional categories were pattern recognition receptors and peptidase inhibitors. Proteins known to be involved in the process of sea cucumber intestinal regeneration, such as ependymin, β-microseminoprotein, serum amyloid A and avidin-like proteins, have also been identified. Proteome characterization of cell-free coelomic fluid soluble proteins suggests that this fluid plays an important role in cell signaling,

transport, and responses to injury in starfish, constituting a relevant tissue to be studied to deeply elucidate the molecular processes associated with starfish organ regeneration. The protocol presented here below can be easily applied to other invertebrate fluids and to quantitative differential proteomics studies involving regeneration or other physiological challenges.

Figure 1 summarizes the shotgun proteomics experimental workflow for the characterization of the soluble proteome of cell-free coelomic fluid (CFF) from *M. glacialis*. In order to extend the number of identified proteins, half of the precipitated protein extract is deglycosylated with Peptide-N-Glycosidase F (PNGase F). PNGase F enzymatic treatment removes the N-linked oligosaccharides from glycoproteins since it cleaves between the innermost N-acetylglucosamine (GlcNAc) and asparagine residues of high mannose, hybrid, and complex oligosaccharides [3]. Since this step can reduce the sensitivity of the analytical procedure, the non-deglycosylated extract is also assayed. Proteins are in-gel digested with trypsin previous to identification by LC-MSMS analysis. Functional analysis of the identified proteins, including prediction of N-glycosylation sites [11], is used to allow a comprehensive description of the metabolic and biological processes occurring in this tissue.

2 Materials

Use bidistilled water and room temperature unless otherwise stated.

2.1 Sample Preparation

1. Adult wild *Marthasterias glacialis* (*see* **Notes 1** and **2**).
2. Venipuncture needle (e.g., Venofix Safety, B Braun).
3. Protein precipitation solution: 40% (w/v) trichloroacetic acid, 0.028% (v/v) β-mercaptoethanol.
4. −20 °C cold acetone pro-analysis grade.
5. 50 mM ammonium bicarbonate (AB).
6. Protein solubilization solution: 6 M urea, 50 mM AB.
7. Total protein quantification kit (e.g., BCA assay).
8. Peptide-N-Glycosidase F (PNGase F) Kit (New England Biolabs, Fisher Scientific): containing 500 mM sodium phosphate and 10% (w/v) NP-40.

2.2 Denaturing Polyacrylamide Gel Electrophoresis (SDS-PAGE)

1. Resolution gel buffer: 1.5 M Tris–HCl, pH 8.8, 0.1% (w/v) sodium dodecyl sulfate (SDS).
2. Stacking gel buffer: 0.5 M Tris–HCl, pH 6.8, 0.1% (w/v) SDS.

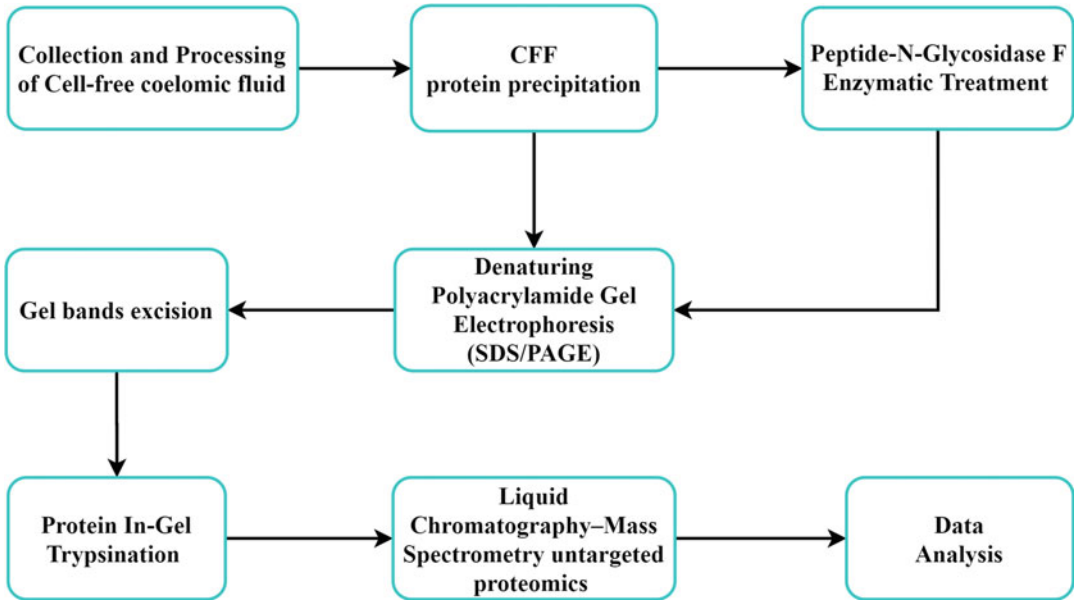


Fig. 1 Experimental workflow for the characterization of CFF soluble proteome from *M. glacialis*. Each step of this protocol is described in text boxes and the workflow follows the sequence of events indicated by the arrows

3. 40% (w/v) acrylamide/bis-acrylamide (crosslinker ratio 29:1): 38.67% (w/v) acrylamide, 1.33% (w/v) bis-acrylamide.
4. 10% (w/v) SDS.
5. 10% (w/v) ammonium persulfate (APS).
6. Tetramethylethylenediamine (TEMED).
7. 12.5% (w/v) acrylamide resolution gel solution: 4.2 mL water, 2.5 mL resolution gel buffer, 3.1 mL 40% (w/v) acrylamide/bis-acrylamide, 100 μL 10% (w/v) SDS, 100 μL 10% (w/v) APS, 5 μL of TEMED.
8. 5% (w/v) Acrylamide resolution gel solution: 3.18 mL water, 1.26 mL resolution gel buffer, 500 μL 40% (w/v) acrylamide/bis-acrylamide, 50 μL 10% (w/v) SDS, 50 μL 10% (w/v) APS, 5 μL TEMED.
9. 4× sample loading buffer: 0.25 M Tris–HCl pH 6.8, 10% (v/v) β-mercaptoethanol, 8% (w/v) SDS, 0.02% (w/v) bromophenol blue, 30% (v/v) glycerol.
10. 1× SDS-PAGE running buffer: 25 mM Tris–HCl, 192 mM glycine, 0.1% (w/v) SDS.
11. Coomassie staining solution: 0.05% (w/v) Coomassie brilliant blue R-250, 50% (v/v) ethanol, 10% (v/v) acetic acid.
12. Destaining solution: 30% (v/v) ethanol, 10% (v/v) acetic acid.

13. Polyacrylamide gel electrophoresis system (e.g., Mini-PROTEAN® Tetra system, Bio-Rad).
14. Polyacrylamide gel electrophoresis system power supply (e.g., Amersham BioSciences Electrophoresis EPS 301).

2.3 Protein In-Gel Trypsination

1. Trypsin solution: 0.01 μg/μL mass spectrometry grade trypsin (e.g., Trypsin Gold, Promega) in 0.01% (v/v) trifluoroacetic acid.
2. Enhancer of trypsin enzymatic performance: 0.01% (v/v) ProteaseMax™ in AB.
3. 50% (v/v) methanol in AB.
4. Acetonitrile pro-analysis grade (ACN).
5. 50% (v/v) ACN in AB.
6. 25 mM DTT in AB.
7. 55 mM iodoacetamide in AB.
8. 5% (v/v) trifluoroacetic acid.

2.4 Untargeted Proteomics and Data Analysis

1. Nanoscale liquid chromatography system (e.g., nano LC system, UltiMate 3000 RSLC, Dionex).
2. High-resolution tandem mass spectrometer incorporating an ultra-high-field Orbitrap analyzer (e.g., Q Exactive HF Hybrid Quadrupole-Orbitrap™, ThermoFisher Scientific).
3. Desalt reversed-phase (RP) C18 trapping column (e.g., Acclaim PepMap 100, 5 μm, 100 Å, 300 μm id × 5 mm, ThermoFisher Scientific).
4. RP C18 analytical column (e.g., Acclaim PepMap 100, 3 μm, 100 Å, 75 μm id × 500 mm, ThermoFisher Scientific).
5. Solvent A: 0.1% (v/v) formic acid (FA).
6. Solvent B: 80% (v/v) ACN, 0.1% (v/v) FA.
7. Feature extraction software: ProteomeDiscoverer 2.3 (Thermo) for .RAW file to .MGF file conversion.
8. Protein identification software: MASCOT 2.5.1 (Matrix Science).
9. Protein sequences database (*see* **Note 3**).
10. Protein similarity search tool: BLAST [12].
11. Pathway Database: KEGG [13].
12. Protein molecular interaction open source software STRING [14].
13. Prediction of N-glycosylation sites in proteins tool: NetNGlyc [11].

3 Methods

3.1 Cell-Free Coelomic Fluid Collection and Protein Precipitation

1. Transfer a wild starfish onto the bench (*see* **Note 4**).
2. Puncture the starfish arm tip with a Venipuncture needle.
3. Hold the animal with the punctured arm hanging.
4. Place a 15-mL tube below the arm with the Venipuncture capillary inside it.
5. Collect 15 mL of the coelomic fluid by gravity into the tube.
6. Centrifugate the sample at 1000 rcf for 5 min at 4 °C (*see* **Note 5**).
7. Transfer the supernatant, the Cell-Free Coelomic Fluid (CFF), to a new 15-mL tube.
8. Discard the circulant cells (pellet).
9. Transfer 7.5 mL of CFF into a 15-mL tube.
10. Add to both the tubes 7.5 mL of protein precipitation solution (*see* **Note 6**).
11. Incubate both the tubes overnight at 4 °C.
12. Centrifugate the tubes at 10,000 rcf for 30 min at 4 °C.
13. Discard the supernatant.
14. Add 10 mL of ice-cold acetone to one of the tubes.
15. Resuspend the protein pellets by pipetting up and down 20 times.
16. Transfer the resuspended protein pellet to the second tube.
17. Repeat **steps 12–15** to remove the residual trichloroacetic acid and β-mercaptoethanol.
18. Dry the protein pellet under a N_2 flux.
19. Add 20 μL of protein solubilization solution.
20. Vortex the tube 30 s to solubilize the pellet.
21. Repeat **steps 19** and **20** until complete pellet solubilization (*see* **Note 7**).
22. Measure the total protein concentration following the kit manufacturer's instructions.

3.2 Peptide-N-Glycosidase F Enzymatic Treatment and SDS-PAGE Sample Preparation

1. Transfer 40 μg of the CFF protein extract to a 1.5-mL tube.
2. Denature the proteins by heating at 99 °C for 10 min (*see* **Note 8**).
3. Add 8 μL of 500 mM sodium phosphate, 8 μL of 10% NP-40, 4 μL of PNGase F.
4. Adjust the final volume of the mixture to 82 μL adding ultrapure water.

5. Incubate the reaction mixture at 37 °C for 1.5 h.
6. Concentrate four times the deglycosylated protein extract in a vacuum centrifuge.
7. Transfer 40 μg of the CFF protein extract to a 1.5-mL tube.
8. Add 5 μL of the 4× sample loading buffer to each protein sample, either deglycosylated or not (*see* **Note 9**).
9. Vortex the sample mixture for 30 s.
10. Heat the sample mixture for 5 min at 99 °C.

3.3 Denaturing Polyacrylamide Gel Electrophoresis (SDS-PAGE): Gel Casting and Sample Running

1. Cast the gel using the polyacrylamide gel electrophoresis system and following the manufacturer's instructions (Fig. 2).
2. Assemble the gel cassette using 7-cm glass plates and 1.0-mm spacers.
3. Fill up the space between the glass plates to below the bottom of the comb position with the acrylamide resolution gel solution.
4. Add a small layer of water to the top of the gel (*see* **Note 10**).
5. Leave it 30 min till the completion of the acrylamide polymerization process.
6. Remove the water layer from the top of the resolution gel.
7. Add the acrylamide stacking gel solution until the inter plates space in the casting chamber is completely full.
8. Insert the comb between the plates in the upper part of the gel cassette.
9. Leave the casting system for 30 min till the completion of the acrylamide polymerization process.
10. Remove the gel cassette from the casting stand.
11. Place the gel cassette in the electrode assembly together with a dummy gel cassette.
12. Remove the comb from the gel cassette.
13. Pour 1× SDS-PAGE running buffer into the opening of the casting frame between the gel cassettes, until it fills the wells of the gel.
14. Fill the region outside the frame with 1× SDS-PAGE running buffer.
15. Load 40 μg of each non-digested and PNGase F digested CFF protein samples into different gel well.
16. Conduct the protein separation by electrophoresis at 200 V, 60 mA (for our Amersham BioSciences Electrophoresis Power Supply EPS 301) until the samples migrate 2 cm (*see* **Note 11**).

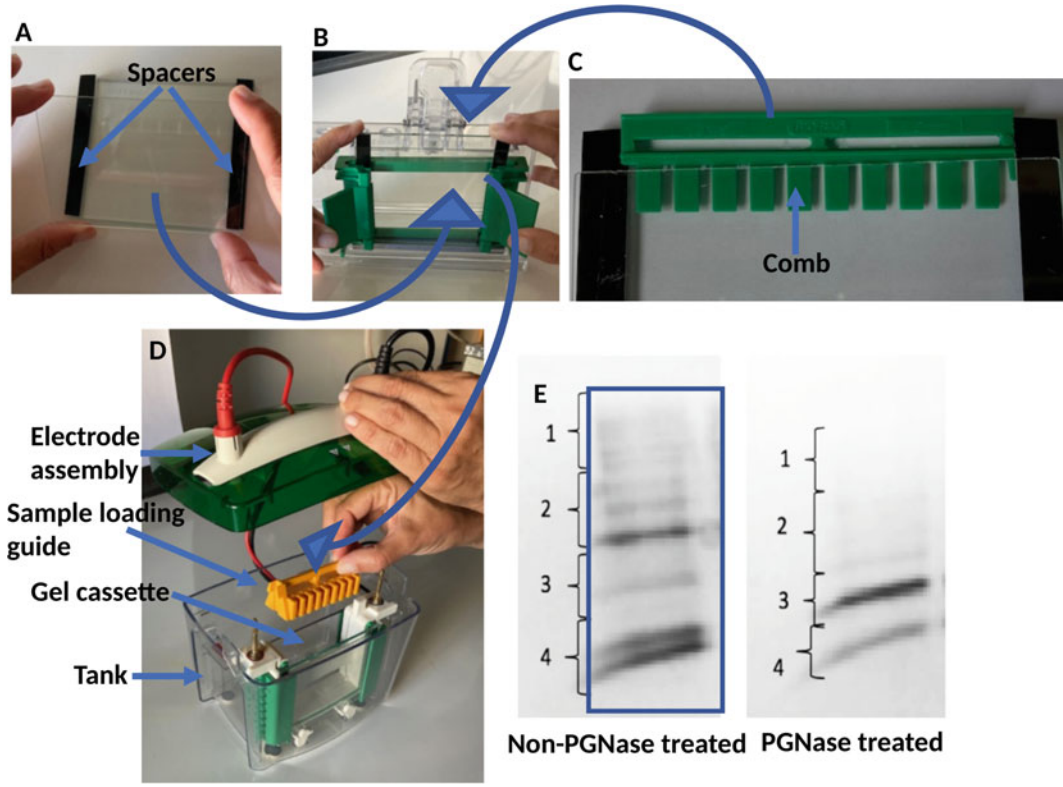


Fig. 2 Polyacrylamide gel electrophoresis: gel casting and sample running. (**a**, **b**) Assembling the gel cassette using two glass plates and two spacers. (**c**) The comb is introduced between the two glass plates after pouring the acrylamide stacking gel solution. (**d**) The gel cassette with the polymerized acrylamide (polyacrylamide) is included in the electrode assembly before introducing it inside the tank of the electrophoresis system. (**e**) Protein bands stained with Coomassie Blue after 2 cm migration of the non-deglycosylated and deglycosylated CFF total protein extract. The rectangle delimits the region of the gel to be excised and divided in four strips, here defined by the square brackets, before in-gel trypsinization

3.4 Coomassie Blue Gel Staining

1. Disassemble the polyacrylamide gel electrophoresis system.
2. Separate the glasses of the gel cassette.
3. Transfer the gel into a glass recipient and wash it with ultrapure water (*see* **Note 12**).
4. Cover the gel with the Coomassie staining solution.
5. Leave it overnight.
6. Remove the staining solution.
7. Add the destaining solution to the gel.
8. Renew the destaining solution until removing the blue background (Fig. 2e).
9. Substitute the destaining solution by water.
10. Keep the gel at 4 °C to avoid dehydration.

3.5 Protein In-Gel Trypsination

1. Cut each gel band by the limit of gel wells, between the front of migration and the well bottom in 0.5 cm height bands with a scalpel.
2. Transfer the bands to separate 1.5-mL tubes.
3. Add 200 μL of 50% (v/v) methanol in AB.
4. Vortex for 1 min at 500 rpm.
5. Repeat **steps 3** and **4** to destain the gel bands.
6. Replace the solution with 200 μL 50% (v/v) ACN in AB.
7. Vortex for 5 min at 500 rpm.
8. Replace the solution with 100% acetonitrile.
9. Vortex for 1 min at 500 rpm.
10. Remove the supernatant.
11. Dry the gel bands in a vacuum centrifuge.
12. Add 100 μL of 25 mM DTT in 50 mM AB.
13. Incubate for 10 min at 56 °C under 500 rpm agitation in a ThermoMixer® to rehydrate the gel and reduce the proteins persulfate bonds.
14. Add 100 μL of 55 mM iodoacetamide in 50 mM AB.
15. Incubate for 10 min in the dark to alkylate the proteins thiol groups.
16. Wash twice the gel bands with water as in **steps 9** and **10**.
17. Dehydrate the gel bands as described in **step 11**.
18. Incubate the dried in-gel digests with 40 μL 0.01 μg/μL trypsin in 0.01% (v/v) trifluoroacetic acid for 15 min on ice.
19. Discard the supernatant.
20. Add 70 μL of the enhancer of trypsin enzymatic performance solution.
21. Incubate for 1 h at 50 °C.
22. Stop the proteolysis by adding 5 μL of 5% (v/v) trifluoroacetic acid (*see* **Note 13**).

3.6 Liquid Chromatography–Mass Spectrometry Untargeted Proteomics Analysis

1. Load 3 μL of each tryptic peptide mixture to be online desalted on the RP C18 trapping column.
2. Resolve the tryptic peptides on the RP C18 analytical column at a flow rate of 200 nL/min with a 90 min gradient of 4–25% of solvent A in 75 min and 25–40% of solvent B in 15 min (*see* **Notes 14** and **15**).
3. The mass spectrometer is operated in data-dependent method consisting in a scan cycle initiated with a full scan of peptide ions, followed by selection of the precursor molecular ion, high energy collisional dissociation, and MS/MS scans on the

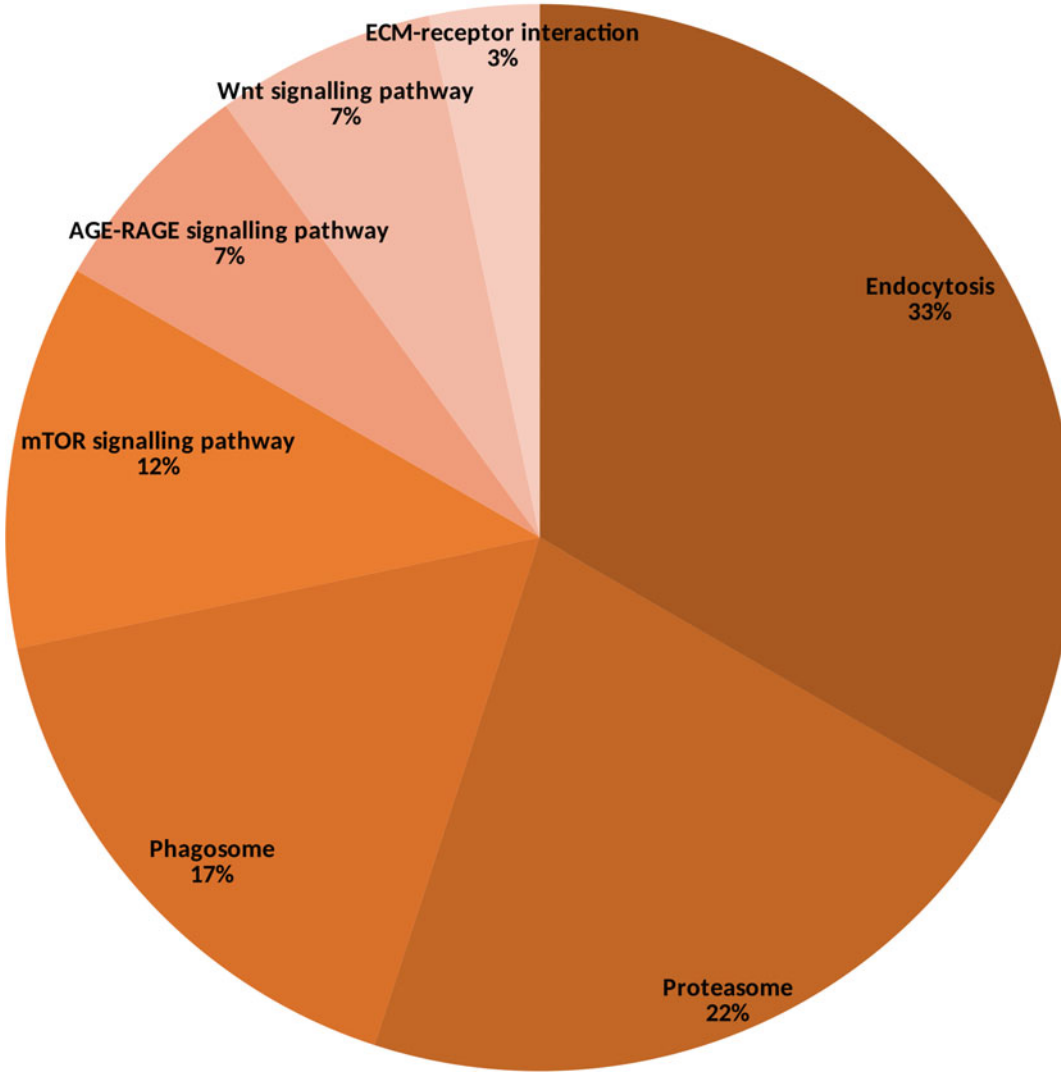


Fig. 3 Pie chart illustrating chosen relevant KEGG pathways from STRING. A total of 51proteins were classified in seven biological processes other than carbon metabolism

20 most abundant precursor ions. Full scan mass spectra are acquired from m/z 350–1500 with a resolution of 60,000. Each MS/MS scan is acquired with a threshold intensity of 83,000, on potential charge states of 2+ and 3+ after ion selection performed with a dynamic exclusion of 10 s, maximum IT of 60 ms and an m/z isolation window of 2.

4. MS/MS spectra at a resolution of 15,000 are search against the established echinoderm assembled protein database using MASCOT 2.5.1 software. The peptide matches with a MASCOT peptide score below a p-value of 0.05 were filtered and assigned to proteins.

5. Additionally, the following parameters are used for MS/MS spectra assignation: full-trypsin specificity, maximum of two missed cleavages, mass tolerances of 5 ppm on the parent ion, fixed modification of carbamidomethyl cysteine (+57.0215), and oxidized methionine (+15.9949) and deamidated asparagine/glutamine (NQ) (0.9840) as dynamic modifications. The mass tolerance for the MS scans is 0.02 Da (*see* **Note 16**).
6. Proteins are validated with the MASCOT decoy search mode, considering a valid protein when at least two different specific peptides are detected in the best sample with a false discovery rate below 1% (*see* **Note 17**).
7. Abundance of each protein is calculated with the sum of spectra assigned to the corresponding peptides (*see* **Note 18**).
8. Functional analysis of identified proteins is performed with the STRING web interface, using *Strongylocentrotus purpuratus* as the homologous organism and a minimum required interaction score with high confidence (0.7).
9. For the proteins not assigned to KEGG pathway classifications in STRING, a protein Blast sequence homology search is performed, using Echinodermata as a taxonomy restriction. Any protein with less than 50% query cover and 70% identity or more than 1×10^{-20} e-value is dismissed, and the best match is chosen (*see* **Note 19**, Fig. 3).
10. Some proteins are identified only in the deglycosylated samples with an asparagine residue to aspartic acid modification, and so with potentially glycosylated peptides, suggesting these are originally glycoproteins. Use NetNGlyc [11] to predict the eventual existence of N-glycosylation sites, thus further validating the results interpretation (*see* **Note 20**).

4 Notes

1. Collect wild starfish at low tides on suitable rocky beaches from the European Atlantic Coast. We collect our *Marthasterias glacialis* on the west coast of Portugal (38.701850° N, 9.392015° W).
2. *Marthasterias glacialis* specimens can be kept for 1 year in open-circuit tanks with recirculating sea water, at 15 °C and 33‰ and fed ad libitum with a diet of mussels.
3. If a homology search has to be performed, namely due to the unavailability of a quality genome sequence for the species under study or for an homologous organism, a compilation of the available proteomes for the close taxonomic related species should be done and used as the protein search database. Since *M. glacialis* genome sequence is not available, protein

identification was performed using the protein sequences available from other echinoderm specimens. This database was constructed compiling protein data from several databases, such as NCBI (https://www.ncbi.nlm.nih.gov/protein/), UniProt (https://www.uniprot.org/), and Echinobase (https://www.echinobase.org/entry/).

4. In order to avoid contamination of coelomic fluid samples with human proteins, in particular keratins, it is strongly advised to wear powder-free nitrile gloves till ending the protein trypsination step.
5. Low speed centrifugation avoids the coelomocytes lysis, that will cause a contamination of CFF with the circulating cell proteins.
6. Further details on the mechanism of protein precipitation by TCA can be found in reference [15].
7. The necessary volume of protein solubilization solution will be dependent on the amount of precipitated protein. In order to keep a high protein concentration, the minimum amount of the protein solubilization solution should be used. Although, it is very important to assure that the whole pellet was solubilized before proceed to the quantification step.
8. PNGase F (Peptide-N-Glycosidase F) treatments are performed using the PNGase F Kit (New England Biolabs, Fisher Scientific) following the manufacturer's instructions with some adjustments. In order to maximize the amount of protein to be digested, the addition of the denaturant solution is substituted by heat denaturation. This procedure adjustment do not make significant changes to the efficiency of protein deglycosylation.
9. Description of the role of 4× sample loading buffer compounds follows. SDS is an anionic detergent that promotes protein denaturation by binding to the vast majority of proteins and breaking the majority of the non-covalent interactions. The SDS-desaturated protein bound formed give every protein the same charge-to-mass ratio. Additionally, and since gels have sieving properties, mobility becomes a parameter for protein discrimination as a function of molecular mass [16]. 2-Mercaptoethanol is added to the protein sample to break up persulfate bonds and to prevent oxidation of cysteines. The denaturation process is extended by overheating the sample at 100 °C. Bromophenol blue is a dye used to help visualizing protein sample load in the well and tracking its progress through the gel. Glycerol has a higher mass density than water, causing the sample to fall to the bottom of the well, avoiding overflow and consequent loss of the sample. 4× sample loading buffer is added in a proportion 1:4 (v:v) to the total protein extract.

10. The water layer will prevent the diffusion of oxygen that acts as an inhibitor of acrylamide polymerization.
11. This SDS-PAGE step allows to clean the protein sample from eventual interferents of the LC-MS assay. Additionally, it is used to obtain less complex protein samples to extend the number of identified proteins.
12. In order to avoid contamination with non-CFF proteins, dedicated plastic containers or glass containers should be used in this step.
13. The final volume of the tryptic peptide mixture is 50 μL.
14. Conditions and parameters are provided for the separation of tryptic peptide mixtures in an UltiMate 3000 RSLCnano LC system (Dionex) and analyzed with a Q Exactive HF high-resolution tandem mass spectrometer (ThermoFisher Scientific), incorporating an ultra-high-field Orbitrap analyzer. Sample running conditions and parameters could need adjustments if another high-resolution LC-MS/MS system is used for this assay.
15. The average total protein concentration in the CFF is 9 ± 3 μg/mL. Considering its minimum concentration (6 μg/mL), the volume of collected coelomic fluid (15 mL) will allow to assay two replicates by SDS-PAGE (40 μg/each run that generates 50 μL of tryptic peptide mixture/replicate) and a total of 15 LC-MSMS assays (3 μL/each run).
16. The specified amino acid modifications are originated during the in-gel protein trypsinization protocol depicted in Subheading 3.6. Fixed modifications are expected to affect all cysteine residues, while dynamic modifications can happen in some methionine, asparagine, or glutamine residues. The carbamidomethylation of cysteine results from the alkylation reaction promoted by iodoacetamide.
17. Using the herein described workflow based on shotgun proteomics, it was possible to identify in total 1717 proteins of which 380 were certified with at least two non-ambiguous peptides.
18. The abundance of each protein is not used for proteome characterization, but for differential proteomics studies aiming to compare the levels of each detected protein in diverse experimental conditions, namely for regeneration studies. Multi- and univariate analyses should be performed to determine the discriminant proteins among experimental conditions.
19. From the 380 proteins identified in *M. glacialis* coelomic fluid using the herein described protocol, 51 proteins were classified into pathways not included in the central metabolism (endocytosis, proteasome, phagosome, extracellular matrix-receptor

interaction, mTOR, AGE-RAGE, and Wnt signaling pathways).

20. PNGase F removes the internal *N*-linked oligosaccharides from glycoproteins. This enzyme catalyzes the cleavage between N-acetyl-D-glucosamine and asparagine residues. The asparagine residue from which the oligosaccharide is removed is deaminated to aspartic acid. For *M. glacialis* coelomic fluid 43 proteins were only detected after PNGase F treatment and with an asparagine residue to aspartic acid modification. Thirty-seven out of these proteins had glycosylation site predictions, and 31 had more than one glycosylation site predictions.

References

1. Liebler DC (2001) Introduction to proteomics: tools for the new biology. Springer Science & Business Media
2. Schubert OT, Röst HL, Collins BC, Rosenberger G, Aebersold R (2017) Quantitative proteomics: challenges and opportunities in basic and applied research. Nat Protoc 12(7):1289–1294. https://doi.org/10.1038/nprot.2017.040
3. Maley F, Trimble RB, Tarentino AL, Plummer TH Jr (1989) Characterization of glycoproteins and their associated oligosaccharides through the use of endoglycosidases. Anal Biochem 180(2):195–204. https://doi.org/10.1016/0003-2697(89)90115-2
4. Franco C.d.M.F. (2011) Proteomics based approach to understand tissue regeneration. Dissertation, Universidade Nova de Lisboa
5. Bay-Nouailhat A (2005) Description of *Marthasterias glacialis*. European Marine Life. http://www.european-marine-life.org/30/marthasterias-glacialis.php. Accessed 06 Aug 2013
6. Tuya F, Duarte P (2012) Role of food availability in the bathymetric distribution of the starfish *Marthasterias glacialis* (Lamk.) on reefs of northern Portugal. Sci Mar 76(1):9–15. https://doi.org/10.3989/scimar.2012.76n1009
7. Wahltinez SJ, Newton AL, Harms CA, Lahner LL, Stacy NI (2020) Coelomic fluid evaluation in *Pisaster ochraceus* affected by sea star wasting syndrome: evidence of osmodysregulation, calcium homeostasis derangement, and coelomocyte responses. Front Vet Sci 7:131
8. Franco C, Soares R, Pires E, Koci K, Almeida AM, Santos R et al (2013) Understanding regeneration through proteomics. Proteomics 13(3–4):686–709. https://doi.org/10.1002/pmic.201200397
9. Ramírez-Gómez F, García-Arrarás J (2010) Echinoderm immunity. Invertebr Surviv J 7(2):211–220
10. Shabelnikov SV, Bobkov DE, Sharlaimova NS, Petukhova OA (2019) Injury affects coelomic fluid proteome of the common starfish, *Asterias rubens*. J Exp Biol 222(6). https://doi.org/10.1242/jeb.198556
11. Gupta R, Brunak S (2002) Prediction of glycosylation across the human proteome and the correlation to protein function. Pac Symp Biocomput 322:310–322
12. Camacho C, Coulouris G, Avagyan V, Ma N, Papadopoulos J, Bealer K et al (2009) BLAST+: architecture and applications. BMC Bioinformatics 10:1–9. https://doi.org/10.1186/1471-2105-10-421
13. Kanehisa M, Furumichi M, Tanabe M, Sato Y, Morishima K (2017) KEGG: new perspectives on genomes, pathways, diseases and drugs. Nucleic Acids Res 45(D1):D353–D361. https://doi.org/10.1093/nar/gkw1092
14. Szklarczyk D, Gable AL, Lyon D, Junge A, Wyder S, Huerta-Cepas J et al (2019) STRING v11: protein-protein association networks with increased coverage, supporting functional discovery in genome-wide experimental datasets. Nucleic Acids Res 47(D1):D607–D613. https://doi.org/10.1093/nar/gky1131

15. Sivaraman T, Kumar T, Jayaraman G, Yu C (1997) The mechanism of 2, 2, 2-trichloroacetic acid-induced protein precipitation. J Protein Chem 16(4):291–297. https://doi.org/10.1023/A:1026357009886

16. Reynolds JA, Tanford C (1970) Binding of dodecyl sulfate to proteins at high binding ratios. Possible implications for the state of proteins in biological membranes. Proc Natl Acad Sci 66(3):1002–1007. https://doi.org/10.1073/pnas.66.3.1002

Open Access This chapter is licensed under the terms of the Creative Commons Attribution 4.0 International License (http://creativecommons.org/licenses/by/4.0/), which permits use, sharing, adaptation, distribution and reproduction in any medium or format, as long as you give appropriate credit to the original author(s) and the source, provide a link to the Creative Commons license and indicate if changes were made.

The images or other third party material in this chapter are included in the chapter's Creative Commons license, unless indicated otherwise in a credit line to the material. If material is not included in the chapter's Creative Commons license and your intended use is not permitted by statutory regulation or exceeds the permitted use, you will need to obtain permission directly from the copyright holder.





Chapter 32

Using RNA-Seq for Transcriptome Profiling of *Botrylloides* sp. Regeneration

Michael Meier and Megan J. Wilson

Abstract

The decrease in sequencing costs and technology improvements has led to the adoption of RNA-sequencing to profile transcriptomes from further non-traditional regeneration model organisms such as the colonial ascidian *Botrylloides leachii*. The relatively unbiased way in which transcripts are identified and quantified makes this technique suitable to detect large-scale changes in expression, and the identification of novel transcripts and isoforms. Of particular interest to many researchers is the discovery of differentially expressed transcripts across different treatment conditions or stages of regeneration. This protocol describes a workflow starting from processing raw sequencing reads, mapping reads, assembly of transcripts, and measuring their abundance, creating lists of differentially expressed genes and their biological interpretation using gene ontologies. All programs used in this protocol are open-source software tools and freely available.

Key words Regeneration, Sequencing, RNA-seq, Ascidian

1 Introduction

Ascidians, also known as tunicates or sea squirts, are marine invertebrate filter-feeding animals. They belong to the Tunicata subphylum, an extant sister clade of the vertebrate clade in the chordate phylum. The close evolutionary relationship is most evident during embryo development where ascidians share vertebrate morphological features such as a notochord and a neural tube. Broadly, ascidians can be classified as solitary or colonial and whether they are pelagic or sessile. Botrylloid colonial ascidians have become an important model organism to study whole-body regeneration, chordate evolution, immunobiology, and allorecognition [1–7]. Fueled by recent advances in next-generation sequencing technology, RNA-sequencing has become a standard tool to characterize entire transcriptomes of cells, tissues, and whole organisms. This protocol uses publicly available RNA-seq data from a regeneration time course experiment in *Botrylloides leachii* [1]. Additionally, with

Simon Blanchoud and Brigitte Galliot (eds.), *Whole-Body Regeneration: Methods and Protocols*,
Methods in Molecular Biology, vol. 2450, https://doi.org/10.1007/978-1-0716-2172-1_32, © The Author(s) 2022

the availability of a sequenced genome [8], a wider range of software tools (for sequenced organisms) are now also available to analyze this RNA-seq data from *B. leachii*.

Despite the wide use of RNA-seq, data analysis workflows are equally numerous and not yet standardized [9]. RNA-seq can provide a snapshot of all transcripts present in a cell or tissue of interest. Often though, the research questions are centered around quantifying changes in gene expression across time points or treatment conditions. To accurately compare different samples to each other important post-processing steps of RNA-seq data must be done before meaningful conclusions can be drawn. The focus of this chapter is to provide the user with a workflow to produce a table of differentially expressed genes (DEGs) from an RNA-seq experiment. The dataset used in this protocol has been previously published by our lab and consists of eight samples, each consisting of pooled RNA from multiple regenerating fragments isolated during a regeneration time-course [1]. Although no replicates were included in this earlier study, limiting differential expression analysis of lowly expressed genes, this protocol includes a "simulated" workflow for DESeq2 [10] to obtain a list of differentially expressed genes across stages of regeneration. We also provide an overview of library preparation strategies and overall experimental design.

Figure 1 presents a general workflow for species with a sequenced and annotated genome.

In principle, this protocol can also be applied to RNA-seq datasets generated from other organisms. Although a genome reference is needed when following the protocol described here, we also suggest software to quantify gene expression without such a reference.

2 Materials

One of the challenges in conducting RNA-seq analysis or any other bioinformatic task is the installation and maintenance of various software packages and programs which can represent a major hurdle for users new to this field. Commands written in shell will be indicated by the "$" prefix, commands in R will be proceeded by ">" and outputs by "#".

1. RNA-seq data (*see* **Notes 1**–**4**).
2. Reference genome (*see* **Notes 5** and **6**).
3. Genome annotations and gene ontology information (*see* **Notes 6**–**8**).
4. A medium to high-performance computer (*see* **Note 9**).
5. A terminal access to that computer (*see* **Note 10**).

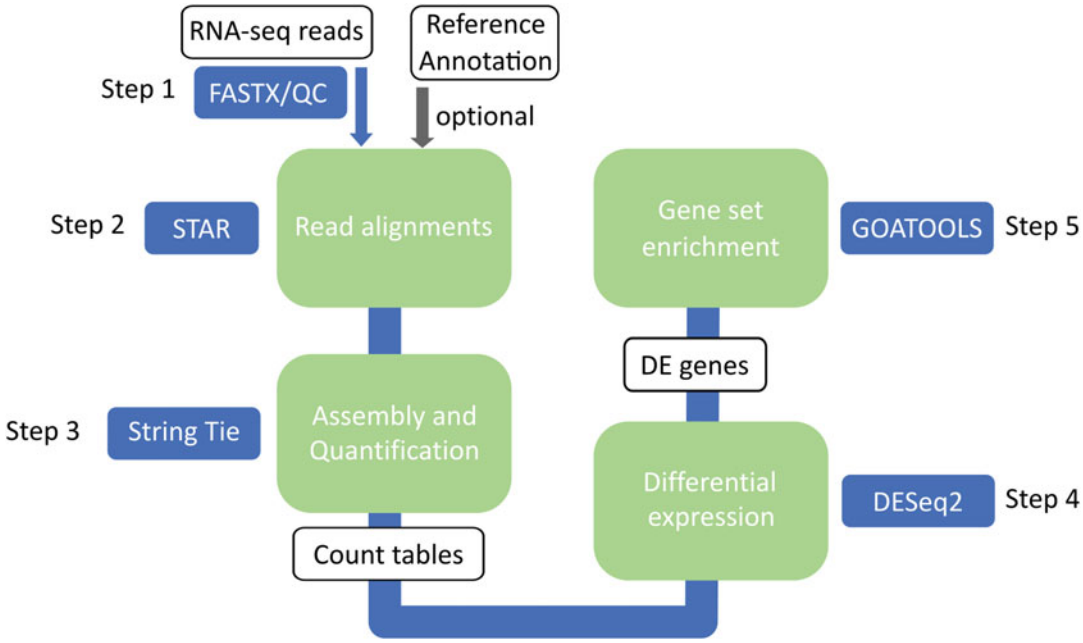


Fig. 1 Overview over the protocol. The first step in a typical RNA-seq workflow is removal of low quality and adapter sequences (step 1). Reads are mapped to the genome either using STAR where it is optional to include a transcriptome reference annotation (step 2). Star maps, assembles and quantifies transcripts simultaneously producing count tables (step 3). Count tables are then used as input for differential gene expression analysis with DESeq2 which produces tables of differentially expressed (DE) genes (step 4). Gene ontology analysis of DE genes is performed with GOATOOLS

6. A scientific software management environment: Bioconda (*see* **Notes 11** and **12**).
7. An RNA sequence mapper: STAR (*see* **Note 12**).
8. Differential expression software: DESeq2 (*see* **Note 12**).
9. Command-line access to the sequence read archive (SRA): SRA-Tools (*see* **Note 13**).
10. Gene Ontology (GO) analysis toolkit: GOATOOLS (*see* **Note 14**).
11. R statistical computing environment (*see* **Note 15**).

3 Methods

This protocol will be exemplified using our paired RNA-seq data of regeneration in *B. leachii* [1]. This dataset consists of eight samples which are listed in Table 1 and can be retrieved from the SRA archive SRP064769 (*see* **Note 16**).

Table 1
RNA-seq sample list from SRA archive SRP064769

Run	Sample name	Short identifier
SRR2729873	Embryos	embr
SRR2641158	Whole colony	wcol
SRR2641167	Vascular tissue (WBR Stage:0)	reg_0
SRR2641168	Vascular tissue (WBR Stage:1)	reg_1
SRR2729836	Vascular tissue (WBR Stage:2)	reg_2
SRR2729869	Vascular tissue (WBR Stage:3)	reg_3
SRR2729871	Vascular tissue (WBR Stage:4)	reg_4
SRR2729872	Vascular tissue (WBR Stage:5)	reg_5

3.1 Quality Control and Trimming

First, before mapping can be done, quality and adapter trimming should be performed.

1. Open a terminal on the computer.
2. Change directory to the folder containing the RNA-seq data to be analyzed:

```
$ cd /Users/yourusername/projectfolder/RNAseqdata
```

3. Quality control (QC) paired-end data by running the following command:

```
$ trim_galore --paired --fastqc embr_1.fq embr_2.fq
```

4. QC single-ended data run this command instead:

```
$ trim_galore --fastqc embr.fq
```

5. Open the newly created embr.fastqc file using a web browser.
6. If there are persistent QC issues with the sequencing data additional filtering steps might be necessary (*see* **Note 17**).
7. Otherwise, proceed to mapping the reads to the reference genome.

3.2 Mapping

Before we can align the reads to the reference genome, we have to build a genome index using STAR [11]. Then samples will be mapped and gene expression values will be calculated and expressed as a raw gene count number.

1. In terminal create a folder for the reference genome files (*see* **Note 18**).

2. Create the genome index (*see* **Note 19**):

```
$ STAR --runMode genomeGenerate --runThreadN 4 --genomeDir genome_Boleac --genomeFastaFiles Boleac_SBv3_genome.fasta --sjdbGTFfile Boleac_transcripts.gtf
```

3. Align the reads (*see* **Notes 20** and **21**):

```
$ STAR --runMode alignReads --genomeDir genome --outFileNamePrefix BL_regeneration/reg_0 --sjdbGTFfile Boleac_transcripts_v5.gtf --quantMode GeneCounts --runThreadN 4 --outSAMtype BAM SortedByCoordinate --readFilesIn reg_0_1_val_1.fq reg_0_2_val_2.fq
```

4. Repeat for other samples (*see* **Note 22**).

3.3 Normalizing Count Data with DESeq2

1. Start R software environment [12].
2. Set the working directory to the path where your STAR output files are contained.

```
> setwd("path to your local folder")
```

3. Load DESeq2 by typing:

```
> library(DESeq2)
```

4. Concatenate count files by typing (*see* **Notes 23** and **24**):

```
> ff <- list.files( path = "./", pattern = "*ReadsPerGene.out.tab$", full.names = TRUE )
> counts.files <- lapply( ff, read.table, skip = 4 )
> counts <- as.data.frame(sapply( counts.files, function(x) x[ , 4 ]))
> ff <- gsub( "[.]ReadsPerGene[.]out[.]tab", "", ff )
> ff <- gsub( "[.]/counts/", "", ff )
> colnames(counts) <- c("embr","wcol","reg_0","reg_1","reg_2","reg_3","reg_4","reg_5")
> row.names(counts) <- counts.files[[1]]$V1
```

5. DESeq2 requires a sample information sheet (*see* **Note 25**) that can be created using a spreadsheet software such as MS Excel and imported into R by typing:

```
coldata <- read.csv(file="coldata.csv", row.names=1)
```

6. Generate a dds object which normalizes all count data across samples to library size by typing:

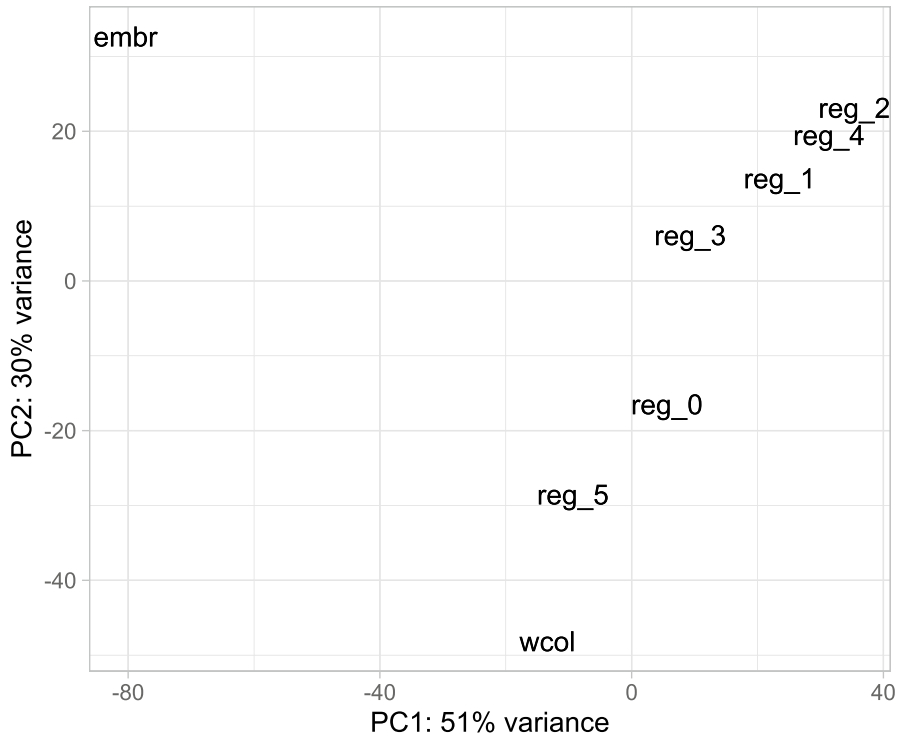


Fig. 2 PCA plot created from the top 500 variable genes among samples

```
 > dds <- DESeqDataSetFromMatrix(countData = counts,colData =
coldata,design = ~ stage)
  > dds <- DESeq(dds)
```

7. Create a sample distance matrix type (*see* **Note 26**):

```
> res <- results(dds)
> vsd <- vst(dds, blind=FALSE)
> sampleDists <- dist(t(assay(vsd)))
> data <- plotPCA(vsd, returnData=TRUE)
> percentVar <- round(100 * attr(data, "percentVar"))
```

8. Load ggplot2 by typing:

```
> library(ggplot2)
```

9. Plot the principal component analysis (PCA) of your data (Fig. 2) with:

```
 > p<-ggplot(data, aes(PC1, PC2)) + geom_text(label=rownames
(data), nudge_x=0.25, nudge_y=0.25,check_overlap=T) + xlab
(paste0("PC1: ",percentVar[1],"% variance")) + ylab(paste0
("PC2: ",percentVar[2],"% variance")) + theme_light()
 > p
```

3.4 Differential Gene Expression Analysis Using DESeq2

To extract differentially expressed genes (DEGs) between conditions (stages 1 and 2 and 0, arbitrarily chosen), we define the contrasts we are interested in with the results() function from DESeq2 (*see* **Note 27**).

1. To get differentially expressed genes between stages 1 and 0, we type:

```
> res1_0 <- results(dds, contrast=c("stage","1","0"))
```

2. We then using the subset function to generate result tables of differentially up- and down-regulated at an adjusted *p*-value also described as false discovery rate (FDR) of 5%.

```
> res_1_0_sig<-subset(res1_0, padj < 0.05)
> res_1_0_sig_up<-subset(res_1_0_sig, log2FoldChange > 0.5)
 > res_1_0_sig_up_order<-res_1_0_sig_up[order(res_1_0_sig_up
$padj),]
 > write.csv(res_1_0_sig_up_order, file="res_1_0_sig_up_or-
der.csv")
> res_1_0_sig_down<-subset(res_1_0_sig, log2FoldChange < 0.5)
 > res_1_0_sig_down_order<-res_1_0_sig_down[order(re-
s_1_0_sig_down$padj),]
 > write.csv(res_1_0_sig_down_order, file="res_1_0_sig_dow-
n_order.csv")
```

3. To view the results table (Table 2):

```
> head(res_1_0_sig_up_order)
```

4. Perform the same process to generate results for comparing stages 2 and 0.

```
> res2_0 <- results(dds, contrast=c("stage","2","0"))
> res_2_0_sig<-subset(res2_0, padj < 0.05)
> res_2_0_sig_up<-subset(res_2_0_sig, log2FoldChange > 0.5)
 > res_2_0_sig_up_order<-res_2_0_sig_up[order(res_2_0_sig_up
$padj),]
 > write.csv(res_2_0_sig_up_order, file="res_2_0_sig_up_or-
der.csv")
> res_2_0_sig_down<-subset(res_2_0_sig, log2FoldChange < 0.5)
 > res_2_0_sig_down_order<-res_2_0_sig_down[order(re-
s_2_0_sig_down$padj),]
 > write.csv(res_2_0_sig_down_order, file="res_2_0_sig_dow-
n_order.csv")
```

Table 2
List of DEGs ordered by increasing significance

	baseMean	log2FoldChange	lfcSE	stat	pvalue	padj
	<numeric>	<numeric>	<numeric>	<numeric>	<numeric>	<numeric>
Boleac.CG.SB_v3.S61.g12353	2501.94	5.36293	0.458323	11.7012	1.26E-31	8.03E-28
Boleac.CG.SB_v3.S266.g06290	4143.94	3.54434	0.353969	10.01313	1.33E-23	4.26E-20
Boleac.CG.SB_v3.S591.g12038	2316.12	4.05544	0.419868	9.65886	4.51E-22	1.15E-18
Boleac.CG.SB_v3.S16.g03334	1978.72	4.38938	0.493055	8.90241	5.46E-19	5.82E-16
Boleac.CG.SB_v3.S119.g01518	3800.73	4.51266	0.515569	8.75278	2.08E-18	1.90E-15
Boleac.CG.SB_v3.S99.g15805	2917.23	4.5493	0.540179	8.42184	3.71E-17	2.96E-14

3.5 Gene Ontology Enrichment Analysis

To get more insight into the biological significance of DE genes we obtained in the above step, we will assign gene ontologies and perform Gene Ontology (GO) enrichment analysis using goatools [13].

1. In R create a list of gene IDs from the result file:

```
> gene_ids_up<-rownames(res_1_0_sig_up_order)
> write.table(gene_ids_up,file="gene_ids_up.csv", row.names=FALSE, quote = FALSE, col.names=FALSE)
```

2. Repeat this step for all the result output files created.
3. Define our background gene list:

```
> res1_0_universe<-subset(res1_0, baseMean > 10)
> gene_ids_univ<-rownames(res1_0_universe)
> write.table(gene_ids_univ,file="gene_ids_univ.txt", row.names=FALSE, quote = FALSE, col.names=FALSE)
```

4. Modify the GAF file so the identifiers match the gene IDs in our lists:

```
> gaf<-read.table(file="Boleac_slimTunicate.gaf",skip=5, sep="\t")
> gaf_red<-gaf_new[ ,c("V6","V5")]
> gaf_red_col<-aggregate(V5 ~V6, gaf_red, paste, col-
```

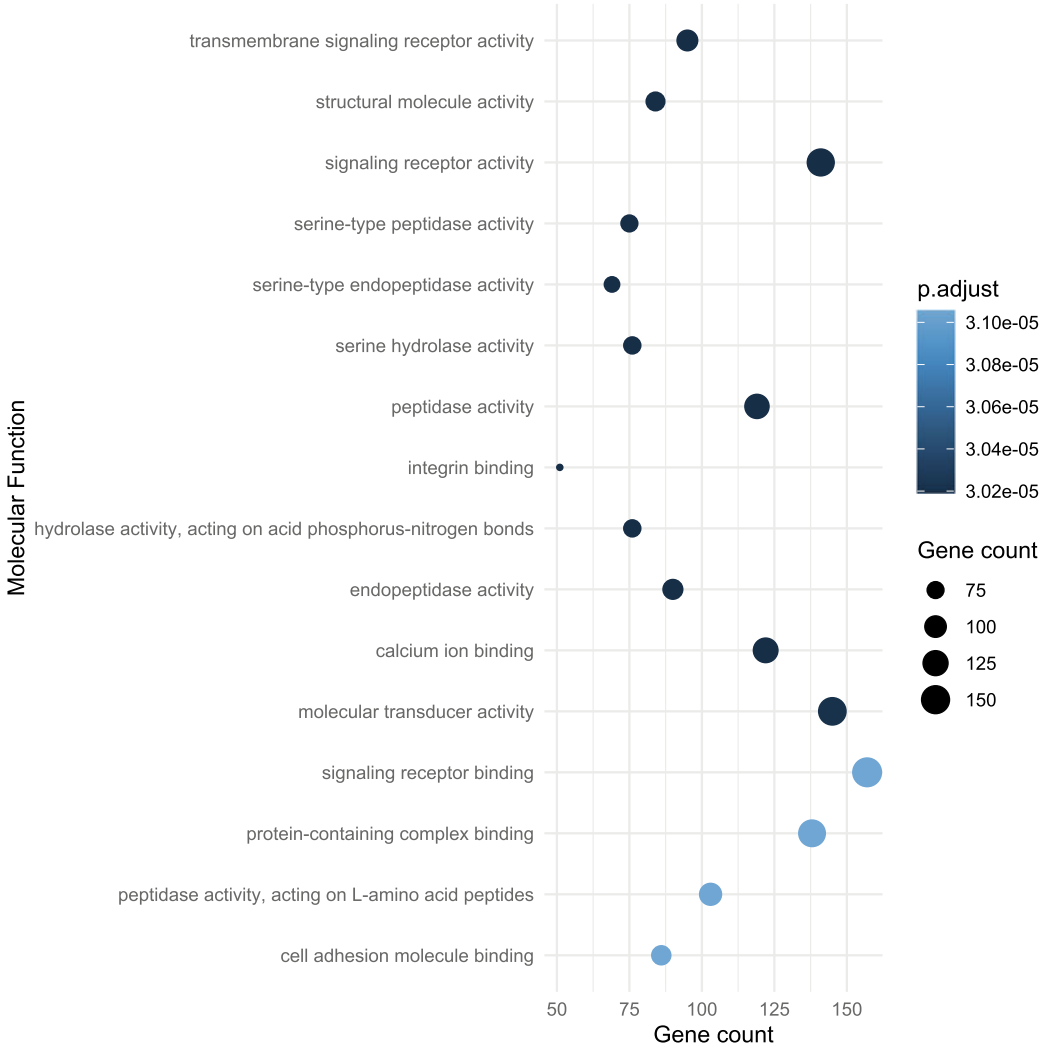


Fig. 3 Example of a GO plot for molecular function terms overrepresented using the list of stage 1 upregulated genes. The dotplot generated using ggplot shows the 15 most significant (adjusted *p*-value < 0.05) enriched GO terms within the molecular function (MF) category

```
lapse=";")
 > write.table(gaf_red_col,file="ids2go_BL.txt", row.name-
s=FALSE, quote = FALSE, col.names=FALSE)
```

5. Find enrichments with a python script run in terminal (*see* **Note 28**).

```
$ find_enrichment.py gene_ids_up.txt gene_ids_univ.txt ids2-
go_BL.txt --pval=0.05 --method=fdr_bh --pval_field=fdr_bh --
outfile=results_id2gos_1_0_up.xlsx
```

6. Plot top 15 enriched terms of each category (*see* **Notes 29** and **30**, Fig. 3).

```
> library("readxl")
> go<-readxl::read_excel("results_id2gos_1_0_up.xlsx")
> go_MF<-subset(go, NS=="MF")
> go_MF_15<-go_MF[1:15, ]
 > b<-ggplot(go_MF_15, aes(x=reorder(name, -p_fdr_bh),
y=study_count,color=p_fdr_bh,size=study_count))+geom_point()
+coord_flip()
 > b + theme_minimal() + labs(x="Molecular Function",y="Gene
count",color="p.adjust", size="Gene count")
```

4 Notes

1. Although this protocol focuses largely on the analysis of RNA-seq data, a few important considerations about the study design are mentioned here. How many reads per sample and how many biological replicates should an RNA-seq experiment have? As a general rule, biological replicates should be prioritized over-read depth. To better estimate the number of reads needed, Illumina offers a read coverage calculator called Scotty (https://support.illumina.com/downloads/sequencing_coverage_calculator.html). This web-based tool is designed to use user data from a small trial experiment consisting of at least two biological replicates per condition to estimate the number of replicates and sequencing depth needed. Alternatively, publicly available datasets closely resembling the user's data can be used. The higher the expected biological variation the more replicates and the higher the sequencing depth needed to identify DEGs.
2. Due to the high sensitivity of RNA-seq, so-called batch-effects created during sample or library preparation can have negative implications on identifying DEGs stemming from "true" biological variation. To control for these effects, processing (e.g., RNA-extraction) of samples and library prep should ideally happen at the same time.
3. This experiment used an RNA-seq library preparation method generating strand-specific paired-end reads which are recommended when no reference genome is available. Strand-specific information is also useful if anti-sense transcripts such as long-non-coding RNAs are of interest. If the goal is to simply measure differential gene expression between conditions, then an un-stranded library can be sufficient although the

price difference in stranded vs. non-stranded kits almost warrants a stranded kit.

4. RNA quality is very important and should be assessed using Bioanlayzer (Agilent Technologies) which gives an RNA integrity number (RIN) based on the ratio of the major ribosomal RNA fractions. Especially samples that are widely different from the average RIN of other samples should be reconsidered. Most sequencing providers will recommend a certain threshold above which they will process a sample (>7.0). Ascidians biosynthesize cellulose which is incorporated into their protective tunic imposes the use of relatively harsh methods to extract RNA, which can lead to degradation of the RIN in some samples. We have had success using plant RNA extraction kits to circumvent this issue.
5. If there is no genomic sequence available to map RNA-seq reads, programs such as Trinity [14] or SOAPdenovo [15] can be used to assemble and quantify transcripts.
6. Download the genome sequence (FASTA) and annotation files (GTF and GAF) for *B. leachii* can be obtained from Aniseed https://www.aniseed.cnrs.fr/aniseed/download/download_data. This can be done directly in terminal using the commands:

```
$ wget https://www.aniseed.cnrs.fr/aniseed/download/?file=-
data%2Fboleac%2FBoleac_SBv3_genome_gff3_fasta.zip
$ wget https://www.aniseed.cnrs.fr/aniseed/download/?file=-
data%2Fboleac%2FBoleac.gaf.gz
```

7. Download the gene annotation and gene ontology files in terminal by typing:

```
$ wget https://www.aniseed.cnrs.fr/aniseed/download/?file=-
data%2Fboleac%2FBoleac_slimTunicate.gaf.gz -O Boleac_slimTu-
nicate.gaf.gz
$ gunzip Boleac_slimTunicate.gaf.gz
$ wget http://purl.obolibrary.org/obo/go/go-basic.obo -O go--
basic.obo
```

8. If there is no genome annotation available, it is possible to perform automated genome annotation. However, this analysis lies outside of the scope of this protocol. For a generic pipeline for performing such an analysis, *see* Blanchoud et al. [8].
9. A computer with more than 4 GB RAM is required for analysis. The most memory-intensive step is the alignment of the reads to the genome which scales with the genome size of the

organism. This step could be also performed on a high-capacity server more suitable for this task.

10. We recommend that you familiarize yourself with basic command line use (e.g., https://ubuntu.com/tutorials/command-line-for-beginners#1-overview) to create, rename, and navigate folders and files.
11. To also make RNA-seq analysis more reproducible, we recommend using a software manager called Bioconda [16]. This protocol will be using software available in this environment, but similar software could be installed from other sources too.
12. To install Miniconda (a version of Anaconda which supports Bioconda) on a computer, run the following commands:

```
$ curl -O https://repo.anaconda.com/miniconda/Miniconda3-
latest-${ARCH}.sh
$ sh Miniconda3-latest-${ARCH}.sh
```

    where the environment variable ARCH should be set to the type of your local operating system (e.g., Linux-ppc64le, Linux-x86_64, MacOSX-x86_64, Windows-x86). This installation includes software tools used in this protocol such as STAR [11], statistical environment R [12], and DESeq2 [10]. For a full list of installed packages run:

```
$ conda list
$ conda install -c bioconda bioconductor-deseq2
```

13. To install SRA-Tools run:

```
$ conda install -c bioconda sra-tool
```

    Detailed instructions and information on setting up downloads from SRA archives can be found on the website https://ncbi.github.io/sra-tools/

14. Install goatools [13] by typing the code below in terminal.

```
$ conda install -c bioconda goatools
```

15. Go to R project website (http://www.r-project.org/), download, and install an up-to-date R version [12].
16. Individual files from the archive SRP064769 can be downloaded using the fastq-dump command:

```
$ fastq-dump --split-files SRR2729873
```

This will create two FASTQ files for each sample, rename all files with their short identifier according to Table 3, e.g., SRR2729873 to embr before proceeding.

17. A detailed explanation of FastQC and examples of good/bad datasets and what to look for in the reports created can be found here on the website: http://www.bioinformatics.babraham.ac.uk/projects/fastqc/.
18. To create the directory that will contain the genome index, use the command:

```
$ mkdir genome_Boleac
```

19. The option "--genomeDir" specifies where the generated indexes are stored. The path to the FASTA file is specified with "–genomeFastaFiles" and the GTF annotation file with "–sjdbGTFfile." In this case, the annotation file is supplied in GFF format "–sjdbGTFtagExonParentTranscript," Parent option can be used instead. "–runThreadN" option defines the number of threads used for parallelization.
20. This commands give paths to genome indexes (--genomeDir), the GTF file (--sjdbGTFfile), the trimmed FASTQ files (–readFilesIn), and will quantify transcripts(--quantMode GeneCounts). This step is computationally intensive and can take several hours.
21. The option—quantMode GeneCounts—produces a file named ReadsPerGene.out.tab with four columns specified in Table 3: geneID; 2: counts for unstranded RNA; 3: counts for first strand; 4: counts for second strand. Additionally, the number of unmapped and multi-mapping reads are in the header. If the

Table 3
An example of a text file showing the first few lines of gene raw count data

N_unmapped	2,393,088	2,393,088	2,393,088
N_multimapping	795,113	795,113	795,113
N_noFeature	3,338,541	16,620,277	3,570,148
N_ambiguous	242,875	284	24,093
Boleac.CG.SB_v3.S0.g00001	59	0	59
Boleac.CG.SB_v3.S0.g00002	262	0	262
Boleac.CG.SB_v3.S0.g00003	666	3	663
Boleac.CG.SB_v3.S0.g00004	1132	3	1129
Boleac.CG.SB_v3.S0.g00005	235	0	235

percentage of unmapped reads is higher than 25% of total reads, the sample is problematic and should be reconsidered.

22. This command detailed in **step 3** of Subheading 3.2 is only for sample `reg_0`. For other samples, the "–outFileNamePrefix" as well as "–readFilesIn" part needs to be altered. Again, specify a directory for the output files (*see* **Note 20**), and give paths to genome indexes (--genomeDir) as well as GTF file (--sjdbGTFfile).
23. For subsequent analysis, using DESeq2 read counts must be selected based on the library preparation protocol was used, unstranded or stranded. To identify the library preparation method and sequencing strategy of the sample, the number of reads for each strand and in total can be counted using the awk function:

```
 $ grep -v "N_" reg_0ReadsPerGene.out.tab | awk '{unst+=$2;
forw+=$3;rev+=$4}END{print\ unst,forw,rev}'
```

which results in "$ 8842238 508841 8718480." This is interpreted as 8,718,480 reads map to the reverse or second strand and only 508,841 reads map to the first strand, which indicates a stranded library was made and the reverse strand was sequenced.

24. Depending on the library preparation method, it is crucial to select the right column in this step. In our case, second-strand synthesis was used, so column 4 was selected for further analysis.

```
> counts <- as.data.frame( sapply( counts.files, function(x) x
[ , 4 ))
```

25. To define which condition or time-points samples are associated, we create a coldata object which can be made in a text-editor or Microsoft Excel and saved in a CSV file format in the working directory specified earlier. In this example, the coldata object has a unique identifier for each sample (column 1) and one column specifying conditional information (Table 4). The unique identifier of samples must be identical in the coldata object as well as in the counts object. To check if that is the case type:

```
> all(rownames(coldata) == colnames(counts))
```

In this case, the counts object column names can be replaced with the sample identifiers in coldata. Please note that the condition in this chosen arbitrary is for demonstration purposes only.

Table 4
Coldata object with sample information

	Stage
embr	E
wcol	A
reg_0	0
reg_1	1
reg_2	1
reg_3	2
reg_4	2
reg_5	5

26. A principal component plot (PCA) is a useful tool to assess if and how individual samples cluster and if the variation in the expression of the most heterogeneously expressed genes can be explained by the nature of the sample (e.g., samples clustering along developmental time).

    In this case, we can see (Fig. 2) a strong separation of the embryonic stage (explaining most of the variation) and separation of regeneration stages and the whole colony as the second-largest component of variation.

27. It is not recommended to perform differential gene expression analysis on data sets without biological replicates. In our case and for demonstration purposes only, we arbitrarily pooled samples from reg_1 and reg_2 (Stage 1) and reg_3 and reg_4 (Stage 2) to compare it to reg_0 (Stage 0) in the coldata object (Table 4) when running DESeq2 in **step 6** of Subheading 3.3. To get differentially expressed genes between these conditions, we need to specify which comparison we want to make.

28. The results of the goatools enrichment analysis contains GO terms which are found significantly (Benjamini/Hochberg: fdr_bh at a 5% false discovery rate) overrepresented in the differentially expressed genes compared to the GO terms of all expressed genes in the samples. The resulting file contains terms for three major categories such as biological process (BP), cellular component (CC), and molecular function (MF).

29. To import xls files back into R, install the library "readxl":

```
> install.packages("readxl")
```

30. To plot the other categories or more terms, you can change the subset and name the output accordingly.

Acknowledgments

This work is supported by a Royal Society of New Zealand grant (UOO1713) to M.J.W. We would like to thank Berivan Temiz for critical reading of the manuscript.

References

1. Zondag LE, Rutherford K, Gemmell NJ, Wilson MJ (2016) Uncovering the pathways underlying whole body regeneration in a chordate model, Botrylloides leachi using de novo transcriptome analysis. BMC Genomics 17: 114
2. Zondag L, Clarke RM, Wilson MJ (2019) Histone deacetylase activity is required for Botrylloides leachii whole-body regeneration. J Exp Biol 222:jeb203620
3. Ballarin L, Zaniolo G (2007) Colony specificity in Botrylloides leachi. II. Cellular aspects of the non-fusion reaction. Invert Surviv J 4:38–44
4. Blanchoud S, Rinkevich B, Wilson MJ (2018) Whole-body regeneration in the colonial tunicate Botrylloides leachii. Results Probl Cell Differ 65:337–355
5. Paz G, Rinkevich B (2002) Morphological consequences for multi-partner chimerism in Botrylloides, a colonial urochordate. Dev Comp Immunol 26:615–622
6. Burighel P, Caicci F, Zaniolo G, Gasparini F, Degasperi V, Manni L (2008) Does hair cell differentiation predate the vertebrate appearance? Brain Res Bull 75:331–334
7. Hirose E, Saito Y, Watanabe H (1997) Subcuticular rejection: an advanced mode of the allogeneic rejection in the compound ascidians Botrylloides simodensis and B. fuscus. Biol Bull 192:53–61
8. Blanchoud S, Rutherford K, Zondag L, Gemmell NJ, De Wilson MJ (2018) Novo draft assembly of the Botrylloides leachii genome provides further insight into tunicate evolution. Sci Rep 8:5518
9. Mortazavi A, Williams BA, McCue K, Schaeffer L, Wold B (2008) Mapping and quantifying mammalian transcriptomes by RNA-Seq. Nat Methods 5:621–628
10. Love MI, Huber W, Anders S (2014) Moderated estimation of fold change and dispersion for RNA-seq data with DESeq2. Genome Biol 15:550
11. Dobin A, Davis CA, Schlesinger F, Drenkow J, Zaleski C, Jha S, Batut P, Chaisson M, Gingeras TR (2013) STAR: ultrafast universal RNA-seq aligner. Bioinformatics 29:15–21
12. R Core Team (2021). R: A language and environment for statistical computing. R Foundation for statistical computing. Vienna, Austria. https://www.R-project.org/
13. Klopfenstein DV, Zhang L, Pedersen BS, Ramirez F, Warwick Vesztrocy A, Naldi A, Mungall CJ, Yunes JM, Botvinnik O, Weigel M, Dampier W, Dessimoz C, Flick P, Tang H (2018) GOATOOLS: a Python library for Gene Ontology analyses. Sci Rep 8:10872
14. Grabherr MG, Haas BJ, Yassour M, Levin JZ, Thompson DA, Amit I, Adiconis X, Fan L, Raychowdhury R, Zeng QD, Chen ZH, Mauceli E, Hacohen N, Gnirke A, Rhind N, di Palma F, Birren BW, Nusbaum C, Lindblad-Toh K, Friedman N, Regev A (2011) Full-length transcriptome assembly from RNA-Seq data without a reference genome. Nat Biotechnol 29:644–652
15. Xie YL, Wu GX, Tang JB, Luo RB, Patterson J, Liu SL, Huang WH, He GZ, Gu SC, Li SK, Zhou X, Lam TW, Li YR, Xu X, Wong GKS, Wang J (2014) SOAPdenovo-Trans: de novo transcriptome assembly with short RNA-Seq reads. Bioinformatics 30:1660–1666
16. Gruning B, Dale R, Sjodin A, Chapman BA, Rowe J, Tomkins-Tinch CH, Valieris R, Koster J, Bioconda T (2018) Bioconda: sustainable and comprehensive software distribution for the life sciences. Nat Methods 15:475–476

Open Access This chapter is licensed under the terms of the Creative Commons Attribution 4.0 International License (http://creativecommons.org/licenses/by/4.0/), which permits use, sharing, adaptation, distribution and reproduction in any medium or format, as long as you give appropriate credit to the original author(s) and the source, provide a link to the Creative Commons license and indicate if changes were made.

The images or other third party material in this chapter are included in the chapter's Creative Commons license, unless indicated otherwise in a credit line to the material. If material is not included in the chapter's Creative Commons license and your intended use is not permitted by statutory regulation or exceeds the permitted use, you will need to obtain permission directly from the copyright holder.



Part VI

Integrative Approaches

Chapter 33

Studying Mechanical Oscillations During Whole-Body Regeneration in *Hydra*

Jaroslav Ferenc and Charisios D. Tsiairis

Abstract

Cells of the freshwater cnidarian *Hydra* possess an exceptional regeneration ability. In small groups of these cells, organizer centers emerge spontaneously and instruct the patterning of the surrounding population into a new animal. This property makes them an excellent model system to study the general rules of self-organization. A small tissue fragment or a clump of randomly aggregated cells can form a hollow spheroid that is able to establish a body axis de novo. Interestingly, mechanical oscillations (inflation/deflation cycles of the spheroid) driven by osmosis accompany the successful establishment of axial polarity. Here we describe different approaches for generating *Hydra* tissue spheroids, along with imaging and image analysis techniques to investigate their mechanical behavior.

Key words Tissue spheroids, Mechanical oscillations, De novo axis formation, Symmetry breaking, Self-organization

1 Introduction

Hydra is a simple freshwater animal composed of two epithelial layers, gastrodermis and epidermis, and organized along a single oral/aboral axis. Its regenerative capacities and amenability to experimental manipulation have made it a rich source of insights about regenerating missing body parts already at the dawn of modern experimental biology [1]. Experiments where regeneration has been challenged, as well as transplantation experiments, have substantially shaped the theories of biological pattern formation [2, 3]. Importantly, *Hydra* does not only offer a platform for manipulating existing patterns but also for observing their emergence de novo. This was shown when cells from dissociated body columns were reaggregated, and they managed to recreate functional animals in a few days [4, 5]. Astonishingly, unlike organoid systems, they are able to do so without the external addition of signaling factors (*see* ref. 1 for further comparison with organoids).

Simon Blanchoud and Brigitte Galliot (eds.), *Whole-Body Regeneration: Methods and Protocols*,
Methods in Molecular Biology, vol. 2450, https://doi.org/10.1007/978-1-0716-2172-1_33, © The Author(s) 2022

Initially, the cells in the aggregates sort to re-establish the epidermal and gastrodermal layers, thus creating a symmetric hollow epithelial spheroid composed of cells whose positional identity along the main body axis is to be specified [6]. After approximately 24 h, symmetry is broken and Wnt-expressing organizing centers start to emerge. These centers guide the appearance of head structures at the oral end of the axis [7]. The role of Wnt signaling as a key driver of oral identity is well established both in the homeostatic conditions and in regenerating *Hydra* [8, 9]. Depending on the size of the aggregates and the axial origin of dissociated tissue, one or more organizing centers can appear [10]. A similar fate awaits spheroids created from small tissue fragments [11]. When a small piece of the body column tissue is excised, it will fold into a hollow spheroid, visually indistinguishable from the one created from reaggregated cells. Since all the cells have a shared identity, body poles need to be defined in this case as well. Wnt signaling centers will emerge and eventually develop into new animal heads.

Interestingly, regenerating spheroids of any origin experience cycles of inflations and deflations on the way to symmetry breaking [12]. These mechanical oscillations are osmotically driven and appear to be important for proper regeneration [13]. Water from the hypotonic medium is entering the cells, which pump it inside the spheroid cavity to maintain their osmotic balance [14]. As a result, the whole spheroid inflates until reaching a threshold of tissue rupture. The accumulated liquid is thus released, the spheroid deflates, and the cycle is repeated. During the spheroid development, the profile of oscillations changes. Initial high-amplitude and low-frequency oscillations (termed Phase I oscillations) eventually transition to faster cycles with lower amplitude (Phase II oscillations). This is a hallmark of symmetry breaking and reflects the emergence of a stable mouth opening that releases the accumulated liquid under lower pressures [15].

Spheroids prepared from small tissue fragments or by single-cell re-aggregation (Fig. 1) are useful to study these mechanical events during regeneration. However, one method might suit specific experimental demands better than the other. Making reaggregates is more laborious, yet offers better control of the spheroid size by using a fixed number of cells. In addition, different cell populations (e.g., expressing different fluorescent markers) can be mixed in one aggregate. Cut tissue pieces, on the other hand, preserve tissue integrity, close faster, and allow better selection of original tissue axial position. Importantly, such spheroids also retain supracellular actin myofibers, which have been recently implicated in mechanically guiding the axis emergence [16]. These structures dissolve upon tissue dissociation and begin to reappear with random orientation in the aggregates. Moreover, they only seem to align and reorient after the symmetry has been broken [17]. This

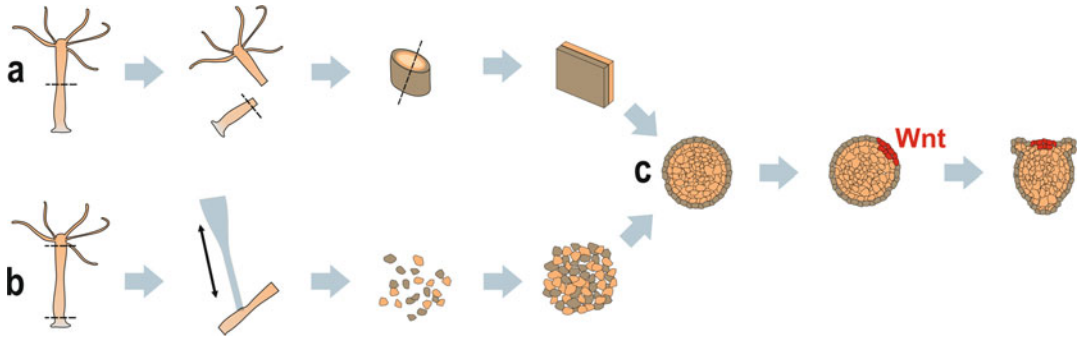


Fig. 1 Overview of spheroid preparation and development. (**a**) Using cut pieces as starting material, (**b**) using cells from dissociated body columns, (**c**) both methods generate spheroids that will break symmetry and regenerate into full animals

difference thus offers an opportunity to dissect the impact of these actin structures on the tissue mechanical and biological properties.

Importantly, *Hydra* spheroids as an experimental model system do not only offer versatile starting conditions. Additional advantages include short regeneration time, simple culture conditions, amenability to imaging, and experimental manipulations. Perturbing the osmolarity by adding solutes, such as sucrose or sorbitol, to the medium allows slowing down the oscillations in a concentration-dependent manner [13]. Different small molecules (e.g., cytoskeleton-affecting drugs) have also been used to perturb the oscillation dynamics. For example, treatment with the Rho-kinase inhibitor Y-27632 results in a sigmoidal rather than linear inflation behavior [18]. Furthermore, since similar oscillations occur in many other cyst-like structures [19], *Hydra* spheroids offer a unique system to tackle the biological significance of such phenomena. In the following protocols, we detail techniques for making *Hydra* spheroids from both cells originating from dissociated animals and cut tissue pieces (Fig. 1). Instructions and tools for live imaging and computational extraction of basic oscillation characteristics from the acquired image data are also provided.

2 Materials

Use distilled water to prepare all the solutions. If not indicated otherwise, solutions can be stored at room temperature.

2.1 Culture Media and Animal Handling

1. M-solution: 0.1 M Tris–HCl, 0.1 M $NaHCO_3$, 0.01 M KCl, 0.01 M $MgCl_2$, pH 7.4. Filter sterilize.
2. Calcium chloride solution: 1 M $CaCl_2$. Filter sterilize.
3. *Hydra* medium: 2 mL M-solution, 1 mL calcium chloride solution in 1 L water (*see* **Note 1**).

4. Handling pipettes: Flame the tip of Pasteur pipettes for a few seconds using a Bunsen burner to blunt the edges.
5. Agarose gel: 1% (w/v) agarose boiled in *Hydra* medium. Can be stored for 1–2 weeks.
6. Imaging chamber: Multi-chamber glass-bottom imaging slides covered with 2 mm of Agarose gel (*see* **Note 2**).

2.2 Cutting and Dissociating Animals

1. Microsurgical scalpel (e.g., MICRO FEATHER 15° or 45° ophthalmic incision scalpels, *see* **Note 3**).
2. Stereomicroscope.
3. Dissociation medium: 3.6 mM KCl, 6 mM $CaCl_2$, 1.2 mM $MgSO_4$, 6 mM sodium citrate, 6 mM sodium pyruvate, 4 mM glucose, 12.5 mM TES-HCl, pH 6.9. Add antibiotics (0.05 g/L kanamycin, 0.1 g/L streptomycin) and filter sterilize. This solution can be stored at 4 °C for a month.
4. Reaggregate medium 1: A 1:3 mixture of *Hydra* medium and dissociation medium.
5. Reaggregate medium 2: A 1:1 mixture of *Hydra* medium and dissociation medium.
6. Reaggregate medium 3: A 3:1 mixture of *Hydra* medium and dissociation medium.
7. Dissociation pipettes: Flame Pasteur pipettes to obtain a narrow opening smaller than 1 mm in diameter. This requires some practice.
8. 0.4-mL microcentrifuge tubes (e.g., APEX Scientific mini).

3 Methods

3.1 Spheroid Preparation from Cut Tissue Pieces

1. Fill the lid of a 90-mm Petri dish with *Hydra* medium.
2. Transfer a few animals into the dish using a handling pipette.
3. Orient the animals with the help of the handling pipette so that they are lying flat and wait until they relax (*see* **Note 4**).
4. Bisect the body column in 50% of its length with a swift movement of the blade (*see* **Notes 5** and **6**).
5. Allow the bisected halves to relax again. The tissue immediately next to the cut should appear slightly swollen.
6. Make a second cut just below the swelling to obtain a ring of tissue (Fig. 2a). Rings can be taken from both halves of the animal.
7. Cut the ring open.
8. Perform another cut in the middle of the resulting tissue stripe to create two pieces of equal size (Fig. 2b, *see* **Notes 7** and **8**).

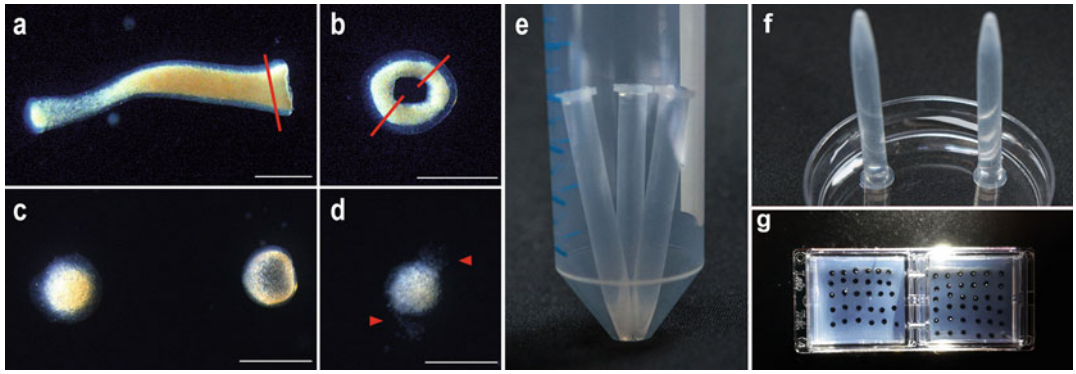


Fig. 2 Critical steps in spheroid preparation protocols. (**a**) foot half of a bisected animal (note the slight tissue swelling next to the cut side), red line indicates the position of the next cut, (**b**) ring of tissue, red lines indicate the positions of cuts to prepare fragments of equal size that will give rise to spheres, (**c**) properly closed spheroids just after closing (left), and after inflation begun (right), (**d**) improperly closed spheroid releasing cells (arrowheads), (**e**) tubes with cell suspension positioned in a 50-mL tube and ready for centrifugation, (**f**) tubes standing in a dish of dissociation medium before the release of aggregates, (**g**) spheroids mounted in the agarose wells in imaging chamber. All scale bars correspond to 500 μm

9. Transfer the pieces into a 35-mm Petri dish with *Hydra* medium (*see* **Note 9**).
10. Let them close for 2–2.5 h (*see* **Note 10**).

3.2 Spheroid Preparation from Dissociated Body Tissue

1. Fill the lid of a 90-mm Petri dish with *Hydra* medium.
2. Transfer ~30 *Hydra* individuals into the dish using a handling pipette.
3. Orient the animals with the help of the pipette so that they are lying flat and wait until they relax (*see* **Note 4**).
4. Cut away the heads of the animals (cut below the tentacles).
5. Cut away the feet (cut above the less pigmented zone) of the animals (*see* **Note 11**).
6. Transfer the resulting body columns into a 15-mL tube with 3 mL of dissociation medium.
7. Vortex briefly and wait until the body columns settle at the bottom of the tube.
8. Remove as much of the medium as possible.
9. Add 3 mL of dissociation medium.
10. Slowly pipette the medium in and out of a dissociation pipette (approximately 20 times) to begin dissociating the body column. Avoid introducing any bubbles. The medium should become cloudy.
11. Let the suspension sit for about 2 min to allow the sedimentation of bigger tissue pieces.

12. Carefully transfer as much of the cell suspension as possible to a new 15 mL tube without disturbing the sediment.
13. Repeat **steps 9–12** twice with the leftover sediment. Pool all cell suspensions in one tube. You should have collected 9–10 mL of the cell suspension after the third round of dissociation.
14. Centrifuge the collected cell suspension for 5 min at 4 °C and 150 rcf.
15. Discard most of the supernatant (leave just enough to cover the pellet).
16. Resuspend the pellet in 3 mL of dissociation medium (*see* **Note 12**).
17. Cut the caps of the 0.4-mL microcentrifuge tubes away.
18. Fill the tubes with 400 μL of the cell suspension. Pipette the liquid slowly down the side of the tube to avoid creating bubbles. If there is a bubble at the bottom of the tube, tap the tube to release it (*see* **Note 13**).
19. Position a maximum of four 0.4-mL tubes per 50-mL tubes.
20. Centrifuge the 50-mL tubes for 5 min at 4 °C and 150 rcf (Fig. 2e, *see* **Note 14**).
21. Carefully remove the microcentrifuge tubes from tubes using forceps.
22. Add a small amount of dissociation medium to slightly overfill the tube.
23. Fill a 90-mm Petri dish with 40 mL of dissociation medium.
24. Invert the tubes upside down and place them into the dish with dissociation medium. The tubes should be standing upright with openings completely submerged in the liquid (Fig. 2f, *see* **Note 15**).
25. Wait for 10–30 min for the aggregates to detach from the tubes and descend into the dish (*see* **Note 16**).
26. Gently remove the microcentrifuge tubes from the Petri dish.
27. Wait for 1 h and carefully transfer the aggregates into the reaggregate medium 3 using a handling pipette.
28. Wait for 1 h and transfer the aggregates into the reaggregate medium 2.
29. Wait for 1 h and transfer the aggregates into the reaggregate medium 1 (*see* **Notes 17** and **18**).
30. Culture the aggregates in *Hydra* medium at 18–23 °C until regeneration is complete.

3.3 Imaging

1. Boil the 1% agarose gel (*see* **Note 19**).
2. Pipette the agarose to the imaging chambers. The agarose layer should cover the flat bottom of the chamber and be approximately 2-mm thick (*see* **Note 20**).
3. Incubate the chambers at 4 °C until the gel solidifies.
4. Create wells in the imaging chamber using a 1000-μL micropipette with the tip attached (*see* **Note 21**): Depress the plunger and push the tip through the agarose layer. Rotate the pipette slightly to make sure that the agarose is cut. Release the plunger to suck out the cut piece and take the tip out of the agarose. Create as many wells as necessary for the number of spheroids you intend to image (*see* **Note 22**).
5. Fill the chambers up with *Hydra* medium (*see* **Note 23**). If air becomes trapped in the wells, release the bubbles by flushing them with a stream of medium from a pipette.
6. Select properly formed spheroids (Fig. 2c, d, *see* **Notes 24** and **25**).
7. Using a handling pipette, carefully transfer spheres to individual wells in agarose (*see* **Note 26**). Take care to avoid getting the spheroids in contact with the liquid/air interface, as they will be torn apart by the surface tension. Instead of forcing the spheroids into the wells, hover them over, and wait for them to descend by gravity (Fig. 2g).
8. Cover the imaging chamber with a lid and place it on the microscope stage.
9. Image in transmitted light with an inverted microscope at temperatures below 23 °C (*see* **Notes 27** and **28**). Use magnification that allows fitting the whole agarose well into the field of view. Adjust the light settings so that the spheroid has good contrast against the background—the center of the spheroid will become more transparent as it inflates (Fig. 3a).

3.4 Image Segmentation and Quantification of Oscillation Parameters

1. Load the acquired images into ImageJ and apply a coarse median filter (radius = 75 μm, *see* **Note 29**).
2. Use the Phansalkar segmentation method (radius = 65 μm, parameter 1 and 2 = 0, parameters 1 and 2 correspond to the k and r values in the Phansalkar thresholding method, respectively [20]) in "Auto Local Threshold" function (*see* **Note 30**).
3. Apply the "Fill holes" function.
4. Apply a median filter with a radius of 25 μm.
5. Visually inspect the accuracy of the segmentation (Fig. 3b, *see* **Note 31**). ImageJ macro for batch segmentation that follows this protocol is provided in Table 1.

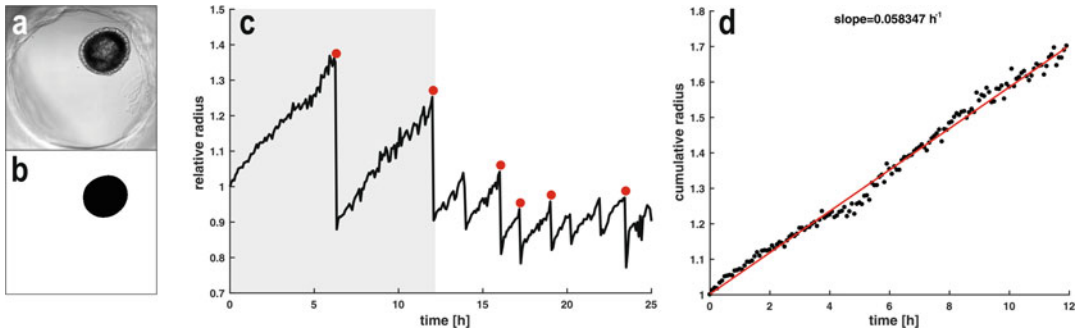


Fig. 3 Imaging setup and image analysis. (**a**) Proper imaging setup, (**b**) the image from (**a**) segmented using the described strategy, (**c**) example of a relative radius trace, shaded area indicates Phase I oscillations, deflation points detected by the "findcollapse" function with a threshold of 1.15 are shown as red dots, (**d**) plot generated using the "sphereslope" function for the Phase I data in **c**, black dots indicate the corrected radius (note the absence of deflation), the fitted line is shown in red

Table 1
Image segmentation macro that can be used for batch processing in ImageJ. Adjust the parameters to fit the pixel size of your images as described in Note 29

```
run("8-bit");
run("Median...", "radius=60 stack");
run("Auto Local Threshold", "method=Phansalkar radius=50 parameter_1=0
  parameter_2=0 white stack");
run("Fill Holes", "stack");
run("Median...", "radius=20 stack");
```

6. Use the "Analyze Particles" function to measure the size of segmented objects. Include particles bigger than 5000 μm^2.
7. Load the area measurements into Matlab (*see* **Note 32**).
8. Convert the area measurement into radius according to the formula $r = (S/\pi)^{1/2}$, where S is the measured area and r is the estimated radius.
9. Normalize the radius data per sample by dividing them with the respective initial values.
10. Use the "findcollapse" function (Table 2) to detect the time and amplitude of spheroid deflations (*see* **Note 33**).
11. Use the "sphereslope" function (Table 3, *see* **Note 34**) to extract the inflation slope.

4 Notes

1. The stock solutions should not be mixed before adding them to the water. This will cause the salts to precipitate.

Table 2
The "findcollapse" function. This function identifies deflations and outputs for each instance the time (as frame of the time course) and the amplitude (as the difference of relative radius). Inputs: rad—relative radius data as a column vector, threshold—threshold for detecting the collapse. We recommend a threshold of 1.15 for Phase I oscillations

```
function [frame,amplitude]=findcollapse(rad,threshold)
if ~iscolumn(rad)
 error('expect rad to be a column vector');
end
amplitude = -diff(rad);
b = rad(1:end-1)./rad(2:end);
frame = (2:(length(rad)))';
frame(b <= threshold) = [];
amplitude(b <= threshold) = [];
end
```

2. We use Lab-Tek (Nunc) or μ-Slide (ibidi) chambers for imaging. Multiwell plates can also be used; however, they are more prone to medium evaporation. Evaporation changes the osmolarity of the medium and impacts on the characteristics of the oscillations.
3. Microsurgical blades from different manufacturers are suitable for cutting. The angle of the blade is a matter of experimenters' preference.
4. Use non-budding animals. Be consistent with the feeding status of animals used for experiments since this can influence the results. We typically use animals starved for 24 h.
5. If reusing the scalpel, clean the blade with 70% ethanol beforehand. The blade should be sharp and cut through the tissue effortlessly. Use a new scalpel if the blade is damaged. Cut edges that appear squeezed or release threads of cells are an indication of a worn-out blade.
6. Body columns can be bisected at different levels, depending on the experimental requirements, for example, to assess the influence of axial position on regeneration.
7. It is not recommended to cut the ring in two pieces with a single cut. This usually creates more damage to the resulting pieces than necessary.
8. Depending on the proportions of the ring, the animal, and the desired spheroid size, adapt the number of pieces that are cut from one ring. We typically use tissue pieces with the shorter side of ~100–150 μm and the longer side of ~300–500 μm. Animals of some strains (e.g., 105) are thinner, and dividing the ring into two equally sized pieces might result in spheroids that are too small to develop properly. In that case, trim the open ring to the desired size and discard the smaller piece.

Table 3
The "sphereslope" function. This function extracts the slope of inflation for a specified period of the time course and plots the fit if requested. Inputs: rad—relative radius data as a column vector, threshold—threshold for detecting the collapse, tinterval—time step of imaging in minutes, frstart—defines the beginning (frame in the time course) of the measured interval, frstop—defines the end of the measured interval, varargin—use either "plot" or "noplot" depending on your preferences. If nothing is specified for varargin, the default option is no plot

```
function slope = sphereslope(rad,threshold,tinterval,frstart,frstop,
  varargin)
if ~isempty(varargin)
 switch varargin{1}
 case 'plot'
 gen_plot = true;
 case 'noplot'
 gen_plot = false;
 otherwise
 error('plot options are plot and noplot')
 end
else
 gen_plot = false; % default plot option
end
if ~iscolumn(rad)
 error('expect rad to be a column vector');
end
% detecting collapses and correcting for them
a = -diff(rad);
b = rad(1:end-1)./(rad(2:end));
corrad = rad + [0;cumsum(a.*(b > threshold))];
% linear fit
time = ((0:(length(rad)-1))*(tinterval/60))';
P = polyfit(time(frstart:frstop),corrad(frstart:frstop),1);
slope = P(1);
% plot result
if gen_plot
 scatter(time(frstart:frstop),corrad(frstart:
  frstop),15,'k','o','filled')
 yfit = P(1)*time + P(2);
 title(['slope=',num2str(slope),'h-1'])
 ylabel('cumulative radius')
 xlabel('time [h]')
 hold on;
 plot(time(frstart:frstop),yfit(frstart:
  frstop),'r','LineWidth',2);
 hold off;
end
end
```

Similarly, rings with big diameter can be divided into three or more pieces.

9. Repeat **steps 4–6** in Subheading 3.1 if you want to obtain more rings/spheres from the same animal.

10. Tissue pieces from the AEP strain close better than the 105 or Basel strains. To increase the success of closing, dissociation medium can be used instead of the *Hydra* medium.
11. **Steps 1–5** in Subheading 3.2 can be omitted but we highly recommend cutting the differentiated parts away before starting the experiments.
12. To ensure having a single-cell suspension, the resuspended cells can be passed through a cell strainer (30 μm pore size).
13. Less than 400 μL of cell suspension can be used, depending on the desired aggregate size and dissociation efficiency. Always fill up the rest of the tube with dissociation medium.

    For better reproducibility among experiments, cell concentration should be determined using a counting chamber and aggregates prepared with the same number of cells. In our experience, a few thousands of epithelial cells should be used to prepare an aggregate of a final size comparable to a cut spheroid.
14. To achieve proper pellet formation, the tubes should be almost vertical during centrifugation. Different rotors might allow for such arrangements even without the use of 50 mL tubes as we describe here. If you want to prepare aggregates with patches of different cells (e.g., expressing two different fluorescent markers), centrifuge first the smaller population of cells, which should form the patch. Then replace the supernatant with the suspension of the other cell population and repeat the centrifugation step.
15. The liquid column inside the tubes should be continuous with the medium inside the dish. If you notice any bubbles created at the interface while positioning the tubes, remove them from the dish, add dissociation medium as in **step 22** in Subheading 3.2, and place them back into the dish.
16. Some aggregates may take longer to detach. These samples often do not develop as well as the faster detaching ones.
17. While performing **steps 27–29** in Subheading 3.2, you should see the cells sorting and reestablishing the epithelial layers. If you want to image cell sorting, start imaging after the transfer to reaggregate medium 2 and keep the aggregates in this solution.
18. The aggregates should stay in the reaggregate medium 1 for 1–2 h before starting the imaging. By this time, the epidermal and gastrodermal layers should be reestablished, which is a sign of successfully completed cell sorting. Depending on the size of the aggregates, cell type ratios, and *Hydra* strain, the sorting might take longer. In that case, we recommend prolonging the second incubation (reaggregate medium 2). The duration is

best determined empirically. Ultimately, the epidermal layer should be continuous, flat, and cells should not be released from spots in the surface.

19. Even though the agarose gel can be stored in a closed flask and re-melted when needed, imaging chambers with agarose should always be prepared fresh (e.g., while the spheroids are closing). This prevents the gel in the chamber from drying out and shrinking. Always change tips when pipetting warm agarose to prevent volume changes as the tip heats up.
20. It is important to compensate for the presence of agarose in the well when doing chemical treatments. Thermostable compounds (e.g., sucrose) can be added directly to the agarose. Prepare 2% agarose in *Hydra* medium and mix it, after boiling, with an equal volume of 2× concentrated compound solution. Pipette into the chambers as described. If this approach is not feasible (e.g., for thermolabile molecules), adjust the concentration of the compound, taking the total volume of medium plus agarose into account.
21. The wells prevent the spheroids from escaping the field of view during imaging. However, they are spacious enough to allow spheroid expansion without imposing any mechanical constrains.
22. You can use a 1000-μL pipette tip or a Pasteur pipette connected to suction to punch the wells and suck out the excess agarose. Alternatively, wells can also be cast using the 200-μL tips or similar custom-made inserts. Position the inserts immediately after pouring liquid agarose into the chambers and make sure they are touching the bottom of the slide. Let the agarose solidify and release the insert afterward by carefully wiggling it out of the gel.
23. Various osmolytes (such as sucrose and sorbitol) can be used to osmotically alter the properties of the oscillations. For example, adding 30 mM sucrose approximately doubles the period of Phase I oscillations. If using sucrose or sorbitol, we recommend adding antibiotics to the medium (0.05 g/L kanamycin, 0.1 g/L streptomycin) and filter sterilizing it.
24. Properly closed cut spheroids should not be releasing threads of cells and should appear round. The typical size range varies between 300 and 500 μm in diameter. If the spheroids seem to be closing, but the closure point is still visible as a furrow, extend the closing time by 30 min. If you are using *Hydra* medium for closing the spheroids, some of them may already start inflating after the tissue closes (Fig. 2c). The success rate of closing is strain dependent. We typically observe about 70–95% of successfully closed spheroids in *Hydra* medium for the AEP strain but a much lower percentage (50–75%) for the

105 strain. The usual causes of unsuccessful closing include cutting with a blunt blade, damage while handling the cut pieces, and poor health of the animals.

25. Properly formed spheroids from dissociated cells should be indistinguishable from the spheroids prepared from tissue pieces. Similarly, if the aggregates appear fluffy and/or are releasing threads of cells, they should not be used for further experiments.
26. If the imaging medium is not identical with the closing medium, include an additional washing step. Put the spheroids first into a dish with the imaging medium and only then transfer them to the imaging chambers to avoid changing the composition of medium there. Alternatively, the medium in the chamber can also be exchanged after positioning all the spheres in agarose.
27. Adjust the parameters of imaging to fit your experimental needs. We routinely image for 60 h with a time step of 10 min.
28. This setup is also useful for fluorescence imaging. The bottom half of the sphere can be imaged with good results using a confocal microscope.
29. The filter radii are given in μm to be universally applicable. However, the functions in ImageJ require values in pixels. Calculate those according to the pixel size of your image.
30. Global segmentation can also be used, but this algorithm tends to outperform it in more challenging situations.
31. Common segmentation challenges include cells extruded by the spheroid, agarose pieces in the wells and uneven illumination. Depending on the specific sample, it might be possible to alleviate these issues by adjusting brightness and contrast of the image before segmentation, applying shading and background corrections, or using trainable segmentation algorithms. It is also helpful to only perform the segmentation on the area inside of the agarose well.
32. The analysis pipeline can also be implemented in other environments using the information on the algorithm rationale in the following notes and comments within the respective Matlab functions.
33. The collapses are detected by dividing the radius values of neighboring time points. For this, the function requires specifying a threshold, which also allows adjusting the sensitivity of detection. We usually use a threshold of 1.15 for Phase I oscillations (Fig. 3c). The amplitude is then calculated as the difference between these points when a collapse is detected.
34. This function uses the same deflation detection method as "findcollapse" and uses the amplitude values to correct for

the shifts created by spheroid deflations. A straight line is then fitted to the corrected data. This allows measuring the overall slope for long periods, such as the whole Phase I duration (Fig. 3d). To enable slope measurements for different time windows (e.g., one oscillation), the function requires the user to specify an interval for this measurement.

Acknowledgments

We thank Jacqueline Ferralli for useful additions to the protocols and Melinda Liu Perkins (UC Berkeley) for helpful suggestions on the Matlab functions. Our research is supported by the Novartis Research Foundation and by the Schweizerischer Nationalfonds zur Förderung der Wissenschaftlichen Forschung (grant 31003A_182674).

References

1. Vogg MC, Galliot B, Tsiairis CD (2019) Model systems for regeneration: Hydra. Development 146(21):dev177212
2. Wolpert L, Hornbruch A, Clarke MRB (1974) Positional information and positional signalling in Hydra. Am Zool 14(2):647–663
3. Meinhardt H (1993) A model for pattern formation of hypostome, tentacles, and foot in hydra: how to form structures close to each other, how to form them at a distance. Dev Biol 157(2):321–333
4. Noda K (1971) Reconstitution of dissociated cells of hydra. Zool Mag 80:99–101
5. Gierer A, Berking S, Bode H et al (1972) Regeneration of hydra from reaggregated cells. Nat New Biol 239(91):98–101
6. Technau U, Holstein TW (1992) Cell sorting during the regeneration of Hydra from reaggregated cells. Dev Biol 151(1):117–127
7. Sato M, Sawada Y (1989) Regulation in the numbers of tentacles of aggregated hydra cells. Dev Biol 133(1):119–127
8. Hobmayer B, Rentzsch F, Kuhn K et al (2000) WNT signalling molecules act in axis formation in the diploblastic metazoan Hydra. Nature 407(6801):186–189
9. Lengfeld T, Watanabe H, Simakov O et al (2009) Multiple Wnts are involved in Hydra organizer formation and regeneration. Dev Biol 330(1):186–199
10. Technau U, von Laue CC, Rentzsch F et al (2000) Parameters of self-organization in Hydra aggregates. Proc Natl Acad Sci 97(22):12127–12131
11. Bode PM, Bode HR (1984) Formation of pattern in regenerating tissue pieces of Hydra attenuata: II. Degree of proportion regulation is less in the hypostome and tentacle zone than in the tentacles and basal disc. Dev Biol 103(2):304–312
12. Fütterer C, Colombo C, Jülicher F et al (2003) Morphogenetic oscillations during symmetry breaking of regenerating Hydra vulgaris cells. Europhys Lett 64(1):137
13. Kücken M, Soriano J, Pullarkat PA et al (2008) An osmoregulatory basis for shape oscillations in regenerating hydra. Biophys J 95(2):978–985
14. Benos DJ, Kirk RG, Barba WP et al (1977) Hyposmotic fluid formation in Hydra. Tissue Cell 9(1):11–22
15. Soriano J, Colombo C, Ott A (2006) Hydra molecular network reaches criticality at the symmetry-breaking axis-defining moment. Phys Rev Lett 97(25):258102
16. Livshits A, Shani-Zerbib L, Maroudas-Sacks Y et al (2017) Structural inheritance of the actin cytoskeletal organization determines the body axis in regenerating hydra. Cell Rep 18(6):1410–1421
17. Seybold A, Salvenmoser W, Hobmayer B (2016) Sequential development of apical-basal and planar polarities in aggregating epithelio-muscular cells of Hydra. Dev Biol 412(1):148–159
18. Sander H, Pasula A, Sander M et al (2020) Highly coordinated mechanical motion mediated by the microtubule cytoskeleton is a

pivotal element of de-novo symmetry breaking in hydra spheroids. bioRxiv

19. Ruiz-Herrero T, Alessandri K, Gurchenkov BV et al (2017) Organ size control via hydraulically gated oscillations. Development 144(23): 4422–4427
20. Phansalkar N, More S, Sabale A, Joshi M (2011) Adaptive local thresholding for detection of nuclei in diversity stained cytology images. In: 2011 international conference on communications and signal processing. IEEE, pp 218–220

Open Access This chapter is licensed under the terms of the Creative Commons Attribution 4.0 International License (http://creativecommons.org/licenses/by/4.0/), which permits use, sharing, adaptation, distribution and reproduction in any medium or format, as long as you give appropriate credit to the original author(s) and the source, provide a link to the Creative Commons license and indicate if changes were made.

The images or other third party material in this chapter are included in the chapter's Creative Commons license, unless indicated otherwise in a credit line to the material. If material is not included in the chapter's Creative Commons license and your intended use is not permitted by statutory regulation or exceeds the permitted use, you will need to obtain permission directly from the copyright holder.



Chapter 34

Combining RNAi-Mediated β-Catenin Inhibition and Reaggregation to Study *Hydra* Whole-Body Regeneration

Matthias Christian Vogg and Brigitte Galliot

Abstract

In addition to its ability to regenerate any amputated body part, the *Hydra* freshwater polyp shows the amazing ability to regenerate as a full polyp after a complete dissociation of its tissues. The developmental processes at work in reaggregates undergoing whole-body regeneration can be investigated at the molecular level by RNA interference (RNAi). Here we provide a protocol that combines β-*catenin* RNAi with reaggregation. This protocol serves as a basis to generate "RNAi-reaggregates," followed by the extraction of high-quality RNA for the precise quantification of gene expression by real-time PCR. This protocol is efficient, providing both a molecular signature, with the significant downregulation of β-*catenin* and *Wnt3*, as well as a robust phenotype, the lack of axis formation, which is observed in all reaggregates.

Key words *Hydra*, Reaggregation, Whole-body regeneration, siRNA electroporation, Gene knockdown, β-catenin, Wnt3, qPCR, Patterning

1 Introduction

Hydra is a small freshwater organism that belongs to the phylum Cnidaria (Fig. 1a). The animals exhibit a tube shape with a head at the apical pole and a foot (basal disk) at the basal one. The head region is composed of an apical dome-shaped structure centered around the mouth opening, named hypostome, and at its base, a ring of tentacles (Fig. 1b). When a *Hydra* is cut into two halves, each half will regenerate within 3–4 days a new complete body, including a fully functional head from the lower half and a foot from the upper half [2]. This is achieved through the rapid formation of an organizer (a group of cells that can induce and pattern adjacent cells) at the regenerating tip as reviewed in [3]. Over the last two decades, it has been demonstrated that Wnt/β-catenin signaling is a component of the head organizer, with the growth factor Wnt3 acting as a head activator [4–8]. In brief, *Wnt3* is mainly expressed in the hypostome, is the earliest upregulated

Simon Blanchoud and Brigitte Galliot (eds.), *Whole-Body Regeneration: Methods and Protocols*, Methods in Molecular Biology, vol. 2450, https://doi.org/10.1007/978-1-0716-2172-1_34, © The Author(s) 2022

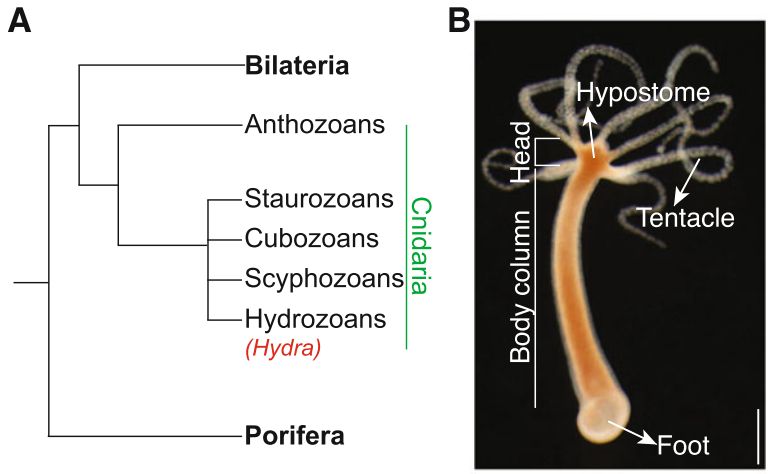


Fig. 1 Phylogenetic position and *Hydra* anatomy. (**a**) *Hydra* is a member of the phylum Cnidaria and the class Hydrozoa. Phylogenetic tree, after Collins et al. [1]. (**b**) The *Hydra* head is composed of a hypostome (dome-shaped structure surrounding the mouth opening) with a mouth opening at the apex and a tentacle ring at the basis. The body column separates the head from the basal region with the basal disk also named foot. Scale bar: 500 μm

Wnt gene during head regeneration, and acts in an auto-regulatory loop to maintain Wnt/β-catenin activity in the apical region [6, 7]. Noteworthy, *Wnt3* expression and thus head formation outside the head region are suppressed by the transcription factor Sp5 [8]. At the basal pole, BMP signaling seems to play a key role in basal regeneration [9]. Overall, two regulatory networks organize each pole of a regenerating *Hydra*.

The extreme regenerative capacity of *Hydra* culminates in the regeneration from reaggregates. The phenomenon of *Hydra* cells to self-organize into a new animal has fascinated researchers since its discovery in the 1970s [10, 11]. Once *Hydra* tissues are dissociated into a single-cell suspension, reaggregates either form spontaneously by keeping the cells at a high density or can be induced by mechanically compacting the cells in capillary tubes or by gentle centrifugation [10]. In the first immediate phase of the reaggregation process, epidermal and gastrodermal cells sort out to re-establish the original cell layers [10]. Over the next days, new polyps emerge from the mass of cells, equipped with tentacles, and a hypostome at the apical pole that become fully functional (i.e., able to feed) around day 6 [10]. At a later stage, a basal disk develops on each polyp, which will eventually detach 1–4 weeks later. The number of polyps that develop from a given reaggregate depends on the initial number of cells that form the reaggregate (classically several polyps emerge from a 70,000-cell reaggregate).

Hydra reaggregates can be seen as the forefather of organoids as they share common features, i.e., their formation relies on

self-organization and requires Wnt/β-catenin signaling for symmetry breaking [2]. In *Hydra* reaggregates, the transition from a ball shape to an elongated shape of the reaggregate is a critical first axis-defining step, characterized by the emergence of *Wnt3* expressing clusters that will develop into apical poles [12]. To functionally assess the involvement of genes that act in the patterning of a reaggregate, RNA interference (RNAi) serves as a powerful tool to silence gene expression.

RNAi can be induced in intact *Hydra* by electroporating small interfering RNAs (siRNAs) [8, 13]. In short, siRNAs are loaded onto an RNA-induced silencing complex (RISC), whereas the "passenger" strand is removed by Argonaute-2 (Ago-2). This leads to an activation of the RISC complex with a single-stranded "guide" RNA molecule that targets mRNAs in a sequence-specific manner. Due to the action of the RNase-H like activity of Ago-2, mRNAs are degraded, which results in gene silencing [14, 15]. We recently demonstrated that gene silencing persists over several days even when RNAi animals are dissociated to a single-cell level, which has opened up new perspectives to study the developmental processes at work in reaggregates [8].

In this chapter, we provide a detailed protocol that combines RNAi-mediated gene silencing with reaggregation (Fig. 2). The effectiveness of this protocol is illustrated by the case of β-*catenin*, leading to a failure of axis formation. Indeed, the quantification of β-*catenin* transcripts, in reaggregates exposed to β-*catenin* siRNAs, by real-time PCR (qPCR) shows a significant downregulation of β-*catenin*. In addition, these β-*catenin* RNAi reaggregates show a reduced *Wnt3* expression and do not develop axes, which is consistent with a function of Wnt/β-catenin signaling in the formation of the *Hydra* body axis.

2 Materials

Prepare all solutions with ultrapure water (Milli-Q system 18.2 MΩ-cm at 25 °C) at room temperature except noted otherwise.

2.1 Electroporation and Reaggregation

1. *Hydra* medium (HM) stock solution A: 109.54 g $CaCl_2$•6 H_2O, 29.2 g NaCl, 3.7 g KCl in 1 L water. Autoclave and store at 4 °C.
2. HM stock solution B: 60.57 g Tris–HCl, pH 7.7 in 1 L water. Autoclave and store at 4 °C.
3. HM stock solution C: 246.5 g $MgSO_4$•7 H_2O in 1 L water. Autoclave and store at 4 °C.

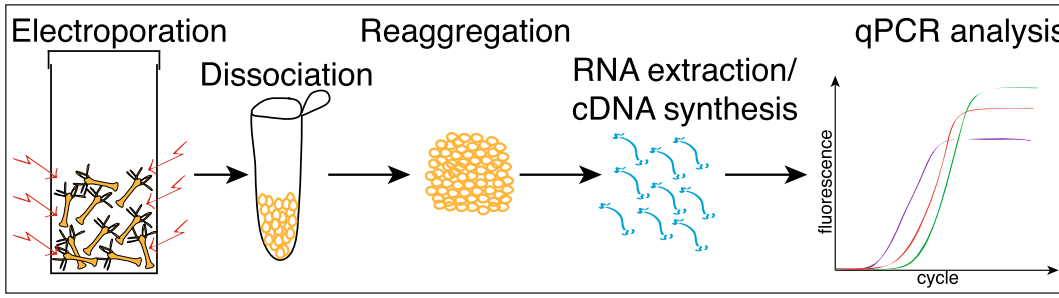


Fig. 2 Method overview. *See* text for details

4. *Hydra* medium (HM): 2 mL stock solution A, 2 mL stock solution B, 0.1 mL stock solution C in 1 L water. Store at 18 °C.
5. Electroporation dissociation medium (E-DM): 0.27 g KCl, 1.31 g $CaCl_2$•6 H_2O, 0.30 g $MgSO_4$•7 H_2O, 1.77 g Na-citrate•2 H_2O, 0.66 g Na-pyruvate, 1.08 g glucose, 2.87 g TES in 950 mL water. Stir until all components are dissolved and adjust pH to 6.9 with HCl. Fill up to 1 L and store at 4 °C.
6. 121.5 mM rifampicin stock solution: 0.1 g rifampicin in 1 mL DMSO. Store at −20 °C.
7. Restoration medium (RM): 40 mL HM, 10 mL E-DM, 4.9 µL 121.5 mM rifampicin stock solution.
8. HEPES solution: 10 mM HEPES–HCl, pH 7.0. Sterile filter and store at RT.
9. Reaggregation dissociation medium (R-DM): 0.2684 g KCl, 0.6647 g $CaCl_2$, 0.296 g $MgSO_4$•7 H_2O, 1.765 g Na-citrate•2 H_2O, 0.666 g Na-pyruvate, 0.721 g glucose, 2.865 g TES in 950 mL water. Stir until all components are dissolved and adjust pH to 6.9 with HCl. Add 0.05 g rifampicin, 0.10 g streptomycin, and 0.05 g kanamycin. Make up to 1 L with water and stir for 2 h (*see* **Note 1**). Store at 4 °C.
10. 70% R-DM: 35 mL R-DM, 15 mL HM.
11. 50% R-DM: 25 mL R-DM, 25 mL HM.

2.2 RNA Extraction, Small Interfering RNAs, and Real-Time PCR

1. 70% Ethanol (EtOH) solution: 35 mL 100% EtOH, 15 mL nuclease-free water.
2. 40 µM β-*catenin* siRNA-1 stock solution: dissolve the lyophilized oligonucleotide UCA ACC UAA CAG ACA A in nuclease-free water and store at −20 °C.
3. 40 µM β-*catenin* siRNA-2 stock solution: UGA GGA GCU AUA CUU AUG A in nuclease-free water, stored at −20 °C.
4. 40 µM β-*catenin* siRNA-3 stock solution: ACG ACU CUC UGU UGA AUU A in nuclease-free water, stored at −20 °C.

5. 40 μM *scramble* siRNA stock solution: AGGUAGU GUAAUCGCCUUG in nuclease-free water, stored at −20 °C.
6. β-*catenin* siRNA working solution: 6.7 μL 40 μM β-*catenin* siRNA-1 stock solution, 6.7 μL 40 μM β-*catenin* siRNA-2 stock solution, 6.7 μL 40 μM β-*catenin* siRNA-3 stock solution in 180 μL 10 mM HEPES solution. Prepare fresh before use, keep at 18 °C.
7. *Scramble* siRNA working solution: 20 μL 40 μM *scramble* siRNA in 180 μL 10 mM HEPES solution. Prepare fresh before use, keep at 18 °C.
8. 10 μM β-*catenin* forward primer: dissolve the lyophilized oligonucleotide TACGCAATGTTGTTGGTGCT in nuclease-free water and store at −20 °C.
9. 10 μM β-*catenin* reverse primer: GCTTCAATTCGATGGCC TAA in nuclease-free water, stored at −20 °C.
10. 10 μM *Wnt3* forward primer: GAGTTGACGGTTGC GAACTT in nuclease-free water, stored at −20 °C.
11. 10 μM *Wnt3* reverse primer: ACATGAAACCTTGCAA CACCA in nuclease-free water, stored at −20 °C.
12. 10 μM TATA-box binding protein (*TBP*) forward primer: AA GCGATTTGCAGCAGTTAT in nuclease-free water, stored at −20 °C.
13. 10 μM *TBP* reverse primer: GCTCTTCACTTTTTGCTCCA in nuclease-free water, stored at −20 °C.

2.3 Kits and Equipment

1. Total RNA extraction kit (e.g., E.Z.N.A., Omega Bio-Tek).
2. 7.5 M lithium chloride precipitation solution.
3. 10,000 U DNase I recombinant.
4. cDNA synthesis kit (e.g., qScript cDNA SuperMix, Quantabio).
5. Master mix for real-time PCR detection (e.g., SYBR® Select Master Mix for CFX).
6. 4-mm electroporation cuvettes.
7. 1.5-mL nuclease-free microcentrifuge tubes.
8. Pasteur pipettes 150 mm.
9. 1-mL single-use syringes.
10. 23G × 1 needles (0.6 × 25 mm).
11. Real-time PCR detection system.
12. Electroporation system.

3 Methods

3.1 Hydra Electroporation

For one electroporation experiment, use 20 animals. All steps are performed at 18 °C.

1. Rinse the *Hydras* three times in Milli-Q water (*see* **Note 2**).
2. Incubate animals for 45 min in Milli-Q water (*see* **Note 3**).
3. Transfer animals by suction with a Pasteur pipette into a 4-mm electroporation cuvette.
4. Remove all the Milli-Q water with the Pasteur pipette from the cuvette (*see* **Note 4**).
5. Add either β-*catenin* or *scramble* siRNA working solution into the cuvette (*see* **Note 5**).
6. Tap the cuvette three times gently to evenly distribute the animals (*see* **Note 6**).
7. Place the cuvette into the shocking chamber of the electroporation system.
8. Wait for 3 min until all animals are relaxed (*see* **Note 7**).
9. Set the following electroporation parameters: Voltage: 150 V; Pulse length: 50 ms; Number of pulses: 2; Pulse intervals: 0.1 s (*see* **Note 8**).
10. Press the pulse button.
11. Immediately after the electroporation, add 200 μL RM into the cuvette.
12. Transfer all animals with a Pasteur pipette into a six-well plate filled with 5 mL of RM.
13. Keep animals for 24 h in RM.
14. Transfer them to HM.
15. Wait for 24 h.
16. Repeat **steps 1–15** a second time (*see* **Note 9**).

3.2 Hydra Dissociation and Reaggregation

For one reaggregation experiment, use 80 RNAi animals, which will give four reaggregates (*see* **Note 10**). **Steps 1–16** are performed on ice at 18 °C. All the remaining steps are performed at 18 °C unless stated otherwise.

1. Transfer 80 electroporated animals into a 15-mL tube (Tube 1) and remove all HM from the tube (*see* **Note 11**).
2. Add 3 mL of R-DM.
3. Gently pipette up and down 30 times with a burned Pasteur pipette (*see* **Note 12**).
4. Wait 5 min to let tissue pieces sediment.

5. Transfer supernatant into a new 15-mL tube (Tube 2) (*see* **Note 13**).
6. Add 3 mL of R-DM into Tube 1.
7. Pipette up and down 30 times.
8. Wait for 5 min to let tissue pieces sediment.
9. Transfer supernatant into Tube 2.
10. Add 3 mL of R-DM into Tube 1 and pipette up and down 50 times (*see* **Note 14**).
11. Wait for 5 min to let tissue pieces sediment.
12. Transfer supernatant into Tube 2.
13. Add 1 mL of R-DM into Tube 1.
14. Pipette up and down 50 times.
15. Wait for 5 min to let tissue pieces sediment.
16. Transfer supernatant into Tube 2.
17. Centrifuge at 245 rcf for 45 min at 4 °C (*see* **Note 15**).
18. Carefully remove supernatant.
19. Resuspend cell pellet in 2 mL R-DM.
20. Distribute cell suspension into 1.5-mL tubes (500 μL per tube).
21. Centrifuge at 209 rcf for 45 min at 4 °C (*see* **Note 15**).
22. Horizontally lay down tubes on a bench.
23. Wait until reaggregates detach from the bottom of the tubes (*see* **Note 16**).
24. Transfer reaggregates into a six-well plate filled with 75% R-DM.
25. Keep them for 16 h in 70% R-DM (*see* **Note 17**).
26. Transfer reaggregates into a six-well plate filled with 50% R-DM.
27. Keep them for 4 h in 50% R-DM (*see* **Note 18**).
28. Transfer reaggregates into HM.
29. Change HM daily (*see* **Notes 19** and **20**).

3.3 RNA Extraction and Real-Time PCR (qPCR)

1. Transfer a reaggregate into a 1.5-mL tube.
2. Add 350 μL of the RNA extract kit's lysis buffer.
3. Pass the lysate 15 times through a 23G × 1 needle fixed to a single-use syringe.
4. Perform RNA extraction following the manufacturer's instructions.
5. Elute RNA in 30 μL nuclease-free water.

6. Add 4 μL of 10× DNase buffer, 2 μL of DNase, and 4 μL of nuclease-free water to the eluted RNA.
7. Incubate at 37 °C for 15 min (*see* **Note 21**).
8. Add 27 μL 7.5 M lithium chloride precipitation solution.
9. Incubate for 2 h at −80 °C (*see* **Note 22**).
10. Centrifuge full speed for 30 min at 4 °C.
11. Carefully remove supernatant.
12. Add 500 μL ice-cold 70% EtOH.
13. Gently wash the pellet by pipetting up and down (*see* **Note 23**).
14. Centrifuge full speed for 30 min at 4 °C.
15. Carefully remove 70% EtOH.
16. Air-dry RNA for 5 min (*see* **Note 24**).
17. Resuspend RNA in 20 μL nuclease-free water.
18. Store at −80 °C or short term on ice for cDNA synthesis (*see* **Note 25**).
19. Transcribe 500 ng of purified RNA into cDNA in a total volume of 20 μL following the kit manufacturer's instructions.
20. Adjust the cDNA concentration to 3.2 ng/μL by mixing 9 μL of cDNA template with 61 μL of nuclease-free water (*see* **Note 26**).
21. Add 16 ng of cDNA template (5 μL of the 3.2 ng/μL cDNA solution) into as many wells of a 96-well plate as qPCR to be done.
22. Per well, add 10 μL of master mix, 0.6 μL of 10 μM qPCR forward primer (300 nM final), 0.6 μL of 10 μM qPCR reverse primer (300 nM final), and 3.8 μL nuclease-free water (*see* **Note 27**).
23. Perform qPCR in the 96-well plate following the manufacturer's instructions (*see* **Note 28**).

4 Notes

1. Rifampicin is very hard to dissolve. Stir R-DM for at least 2 h after adding rifampicin.
2. Cool down Milli-Q water to 18 °C prior to usage.
3. Water is hypotonic, which leads to a swelling of the cells. Do not exceed an incubation time of 1 h 15 min as this leads to excessive tissue loss.
4. Remaining HM will dilute the siRNAs. If necessary, use a micropipette to remove the HM.

5. Do not keep siRNA dilutions on ice. The animals will not relax when a cold solution is added onto them. Always keep siRNA dilutions at 18 °C until the electroporations are performed.
6. The electroporation efficiency will be reduced when the animals clump and are not evenly distributed in the cuvette.
7. The surface of the relaxed animals is greater than that of the contracted ones, and thus more siRNAs can be taken up by relaxed *Hydra*. Never perform an electroporation on contracted animals, as this will reduce the electroporation efficiency. We never use any chemical for relaxing the animals prior to electroporation. *Hydras* spontaneously relax in in the siRNA dilution after 3 min.
8. The electroporation conditions are optimized to obtain a 100% survival rate for *Hydra magnipapillata*. Depending on the species used, the conditions might need to be adjusted.
9. The more often animals are electroporated the smaller they get as tissue loss occurs. We do not recommend performing more than two electroporations as the animals become too small to perform a reaggregation experiment.
10. To obtain four reaggregates from wild-type *Hydra magnipapillata*, 60 animals are sufficient. However, over the electroporations, the animals slightly shrink as tissue loss occurs and thus the number of animals should be increased to 80. In comparison, 120 electroporated *Hydra vulgaris* of the Basel strain are necessary to obtain four reaggregates [8].
11. 24 h after the second electroporation, RNAi animals can also be drug treated for 18 h, i.e., with Alsterpaullone to enhance certain phenotypes, which is then directly followed by reaggregation [8].
12. The sharp end of a Pasteur pipette can easily destroy the *Hydra* cells. Always slightly burn the Pasteur pipette so that the end is smooth. Excessive pipetting up-and-down can also cause damage to cells. Pipetting up-and-down 30 times is sufficient to dissociate the *Hydra* tissue.
13. Tissue pieces that are a sign of incomplete dissociation should never be transferred into tube 2. If necessary, increase the sedimentation time to obtain a better separation of single cells (supernatant) from tissue pieces.
14. At that stage, we recommend to start pipetting up-and-down 50 times to achieve a complete dissociation of any remaining tissue pieces.

15. The centrifugation time can be adjusted depending on the centrifuge used. In our hands, a centrifugation of less than 45 min leads to partial cell collection.
16. Do not use a rotating wheel to detach the reaggregates as this leads to excessive cell loss.
17. A critical step in ensuring a 100% reaggregate survival is a long incubation in 70% R-DM. After 16 h in R-DM, the surface of the reaggregates should be smooth (*see* 1 d time point of Fig. 3), which indicates a successful separation of the two cell layers, epidermis and gastrodermis.
18. The incubation time can be reduced to 1 h if the cell layers are already separated. If not, extend the incubation to 4 h, which will further promote the separation of the cell layers and thus the smoothening of the reaggregates.
19. To prevent any infection, the reaggregates should always be kept in clean HM.
20. We have successfully combined RNAi and reaggregation. Note that axis formation is not visible after silencing β-*catenin* (Fig. 3).
21. DNase treatment is performed to remove any remaining genomic DNA traces that might falsify the qPCR result. Note that SYBR interacts with any double-stranded DNA.
22. Lithium chloride offers the advantage over other precipitation methods that it does not precipitate contaminants such as DNA, carbohydrates, and proteins [16].
23. Be careful not to lose the RNA pellet. The RNA has a white color and is hard to see.
24. Do not over-dry RNA as this will cause its degradation.
25. The RNA yield of four reaggregates is approximately 700 ng.
26. We recommend using low retention tips in all steps to reduce the adhesion of DNA to the tip surface.
27. We have used qPCR to validate the silencing of β-*catenin* and to test the expression of *Wnt3*. We demonstrate a successful silencing of β-*catenin* and a downregulation of *Wnt3* gene expression (Fig. 4). Note that the expression of *Wnt3* in β-*catenin* RNAi reaggregates can also be tested by in situ hybridization as described in [8].
28. The analysis was carried out as described in [17].

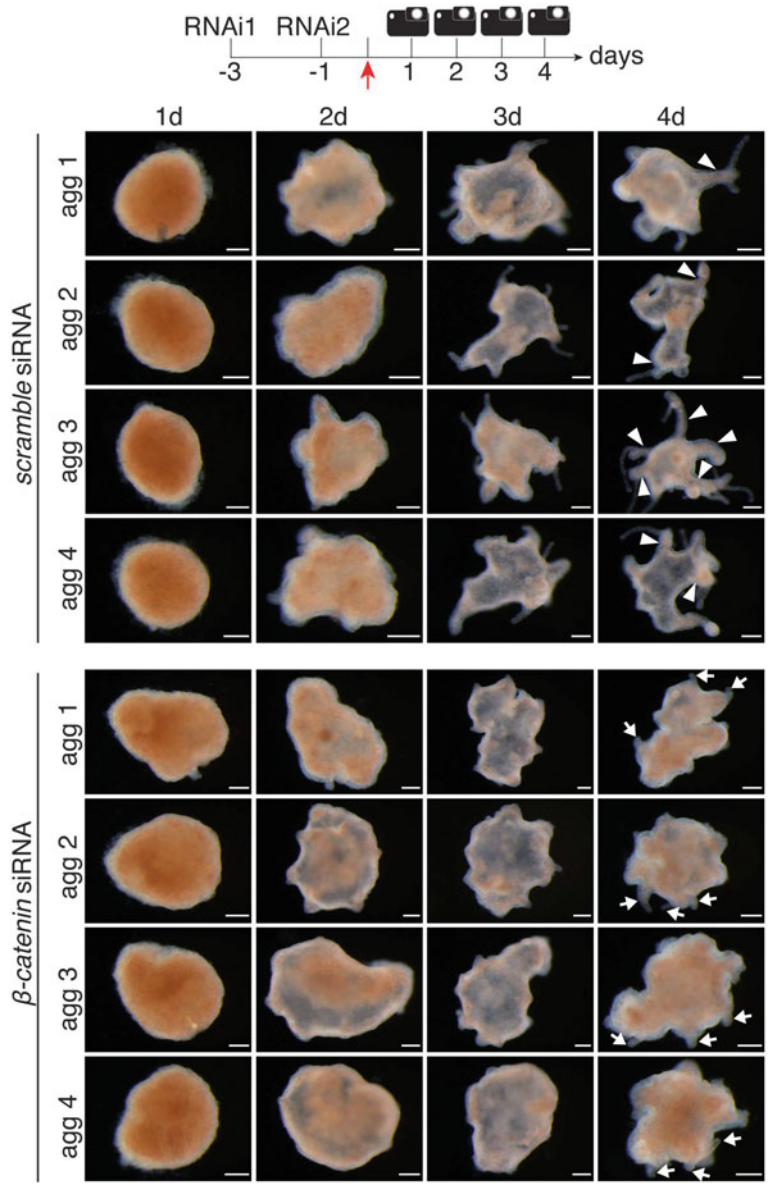


Fig. 3 Regeneration of *Hydra* body axes from reaggregated cells after silencing β-*catenin*. The reaggregation experiment was performed with animals exposed twice (RNAi1, RNAi2) to *scramble* (top) and β-*catenin* (bottom) siRNAs. Shown are four representative reaggregates (agg 1–4). Reaggregates were imaged at indicated time points. The red arrow indicates the time point of animal dissociation, taken as t0 for reaggregation. Note that axes are clearly visible in control RNAi reaggregates on day 4 (white arrowheads), while β-*catenin* RNAi reaggregates fail to develop axes while forming a few tentacles (white arrows). Scale bars: 200 μm

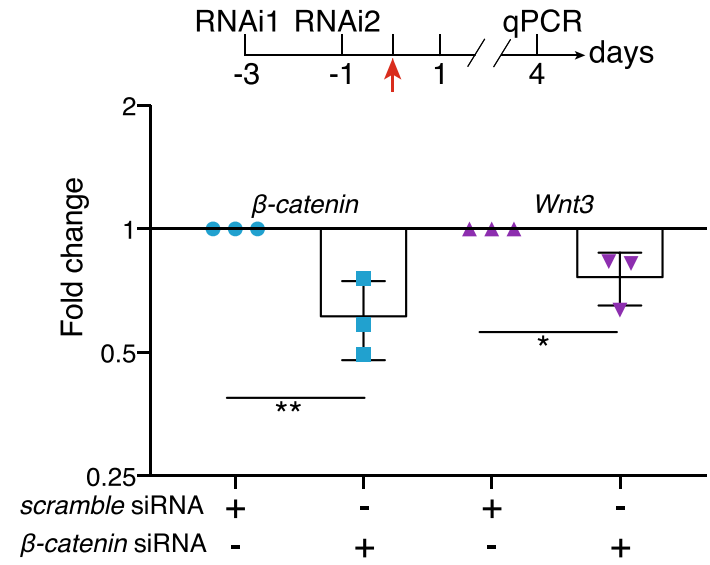


Fig. 4 Real-time PCR of RNAi reaggregates. RNAi was performed as depicted in the scheme. The red arrow indicates the time point of animal dissociation, taken as t0 for reaggregation. RNA was extracted on day 4 of the reaggregation process, followed by real-time PCR (qPCR) to measure the expression of β-*catenin* (blue symbols) and *Wnt3* (purple symbols) in control and β-*catenin* RNAi reaggregates. Each data point represents one biologically independent experiment. Statistical *p*-values: * ≤ 0.05, ** ≤ 0.01 (unpaired *t*-test)

Acknowledgments

The authors thank Charisios Tsiairis for helpful comments and discussions. The research in the Galliot laboratory is supported by the Swiss National Science Foundation (SNF 310030_189122), the Canton of Geneva, and the Claraz donation.

References

1. Collins AG, Schuchert P, Marques AC, Jankowski T, Medina M, Schierwater B (2006) Medusozoan phylogeny and character evolution clarified by new large and small subunit rDNA data and an assessment of the utility of phylogenetic mixture models. Syst Biol 55(1):97–115. https://doi.org/10.1080/10635150500433615
2. Vogg MC, Galliot B, Tsiairis CD (2019) Model systems for regeneration: Hydra. Development 146 (21). https://doi.org/10.1242/dev.177212
3. Vogg MC, Wenger Y, Galliot B (2016) How somatic adult tissues develop organizer activity. Curr Top Dev Biol 116:391–414. https://doi.org/10.1016/bs.ctdb.2015.11.002
4. Hobmayer B, Rentzsch F, Kuhn K, Happel CM, von Laue CC, Snyder P, Rothbacher U, Holstein TW (2000) WNT signalling molecules act in axis formation in the diploblastic metazoan Hydra. Nature 407(6801):186–189. https://doi.org/10.1038/35025063
5. Chera S, Ghila L, Dobretz K, Wenger Y, Bauer C, Buzgariu W, Martinou JC, Galliot B (2009) Apoptotic cells provide an unexpected source of Wnt3 signaling to drive hydra head regeneration. Dev Cell 17(2):279–289.

https://doi.org/10.1016/j.devcel.2009.07.014

6. Lengfeld T, Watanabe H, Simakov O, Lindgens D, Gee L, Law L, Schmidt HA, Ozbek S, Bode H, Holstein TW (2009) Multiple Wnts are involved in Hydra organizer formation and regeneration. Dev Biol 330(1):186–199. https://doi.org/10.1016/j.ydbio.2009.02.004
7. Nakamura Y, Tsiairis CD, Ozbek S, Holstein TW (2011) Autoregulatory and repressive inputs localize Hydra Wnt3 to the head organizer. Proc Natl Acad Sci U S A 108(22):9137–9142. https://doi.org/10.1073/pnas.1018109108
8. Vogg MC, Beccari L, Iglesias Olle L, Rampon C, Vriz S, Perruchoud C, Wenger Y, Galliot B (2019) An evolutionarily-conserved Wnt3/beta-catenin/Sp5 feedback loop restricts head organizer activity in Hydra. Nat Commun 10(1):312. https://doi.org/10.1038/s41467-018-08242-2
9. Wenger Y, Buzgariu W, Perruchoud C, Loichot G, Galliot B (2019) Generic and context-dependent gene modulations during Hydra whole body regeneration. bioRxiv:587147. https://doi.org/10.1101/587147
10. Gierer A, Berking S, Bode H, David CN, Flick K, Hansmann G, Schaller H, Trenkner E (1972) Regeneration of hydra from reaggregated cells. Nat New Biol 239(91):98–101
11. Noda K (1971) Reconstruction of dissociated cells of hydra. Zool Mag 80:27–31
12. Technau U, Cramer von Laue C, Rentzsch F, Luft S, Hobmayer B, Bode HR, Holstein TW (2000) Parameters of self-organization in Hydra aggregates. Proc Natl Acad Sci U S A 97(22):12127–12131. https://doi.org/10.1073/pnas.97.22.12127
13. Watanabe H, Schmidt HA, Kuhn A, Hoger SK, Kocagoz Y, Laumann-Lipp N, Ozbek S, Holstein TW (2014) Nodal signalling determines biradial asymmetry in Hydra. Nature 515(7525):112–115. https://doi.org/10.1038/nature13666
14. Kim D, Rossi J (2008) RNAi mechanisms and applications. BioTechniques 44(5):613–616. https://doi.org/10.2144/000112792
15. Pratt AJ, MacRae IJ (2009) The RNA-induced silencing complex: a versatile gene-silencing machine. J Biol Chem 284(27):17897–17901. https://doi.org/10.1074/jbc.R900012200
16. Barlow JJ, Mathias AP, Williamson R, Gammack DB (1963) A simple method for the quantitative isolation of undegraded high molecular weight ribonucleic acid. Biochem Biophys Res Commun 13:61–66. https://doi.org/10.1016/0006-291x(63)90163-3
17. Pfaffl MW (2001) A new mathematical model for relative quantification in real-time RT-PCR. Nucleic Acids Res 29(9):e45

Open Access This chapter is licensed under the terms of the Creative Commons Attribution 4.0 International License (http://creativecommons.org/licenses/by/4.0/), which permits use, sharing, adaptation, distribution and reproduction in any medium or format, as long as you give appropriate credit to the original author(s) and the source, provide a link to the Creative Commons license and indicate if changes were made.

The images or other third party material in this chapter are included in the chapter's Creative Commons license, unless indicated otherwise in a credit line to the material. If material is not included in the chapter's Creative Commons license and your intended use is not permitted by statutory regulation or exceeds the permitted use, you will need to obtain permission directly from the copyright holder.





Chapter 35

Creating a User-Friendly and Open-Access Gene Expression Database for Comparing Embryonic Development and Regeneration in *Nematostella vectensis*

Olivier Croce and Eric Röttinger

Abstract

The sea anemone *Nematostella vectensis* has emerged as a powerful research model to understand at the gene regulatory network level, to what extend regeneration recapitulates embryonic development. Such comparison involves massive transcriptomic analysis, a routine approach for identifying differential gene expression. Here we present a workflow to build a user-friendly, mineable, and open-access database providing access to the scientific community to various RNAseq datasets.

Key words Database, Data mining, Open-access, RNAseq, Cnidarian, *Nematostella vectensis*, Regeneration, Embryonic development

1 Introduction

The anthozoan cnidarian *Nematostella vectens*is (Fig. 1) has initially been developed as a research model organism to gain insights into the evolution of developmental mechanisms and novel cell types/biological features as it is easily cultivable under laboratory conditions [4]. The first cnidarian genome to be sequenced was the one from *Nematostella* that has revealed astonishing similarities with the ones from mammalians [5, 6]. Since then, a wealth of resources and tools have been developed ranging from embryonic RNAseq datasets [1, 2] to meganuclease-induced transgenesis [7], as well as functional approaches for gene know-downs [8–11] and CRISPR/CAS9 mediated knock-outs and knock-ins [11–13].

More recently, *Nematostella* is emerging as a powerful and complementary whole-body regeneration model, as it is able to regrow missing body parts within days after amputation [14–18]. In combination with its historical use as an embryogenesis research model, *Nematostella* is thus very well suited to compare embryonic development and whole-body regeneration within the

Simon Blanchoud and Brigitte Galliot (eds.), *Whole-Body Regeneration: Methods and Protocols*,
Methods in Molecular Biology, vol. 2450, https://doi.org/10.1007/978-1-0716-2172-1_35, © The Author(s) 2022

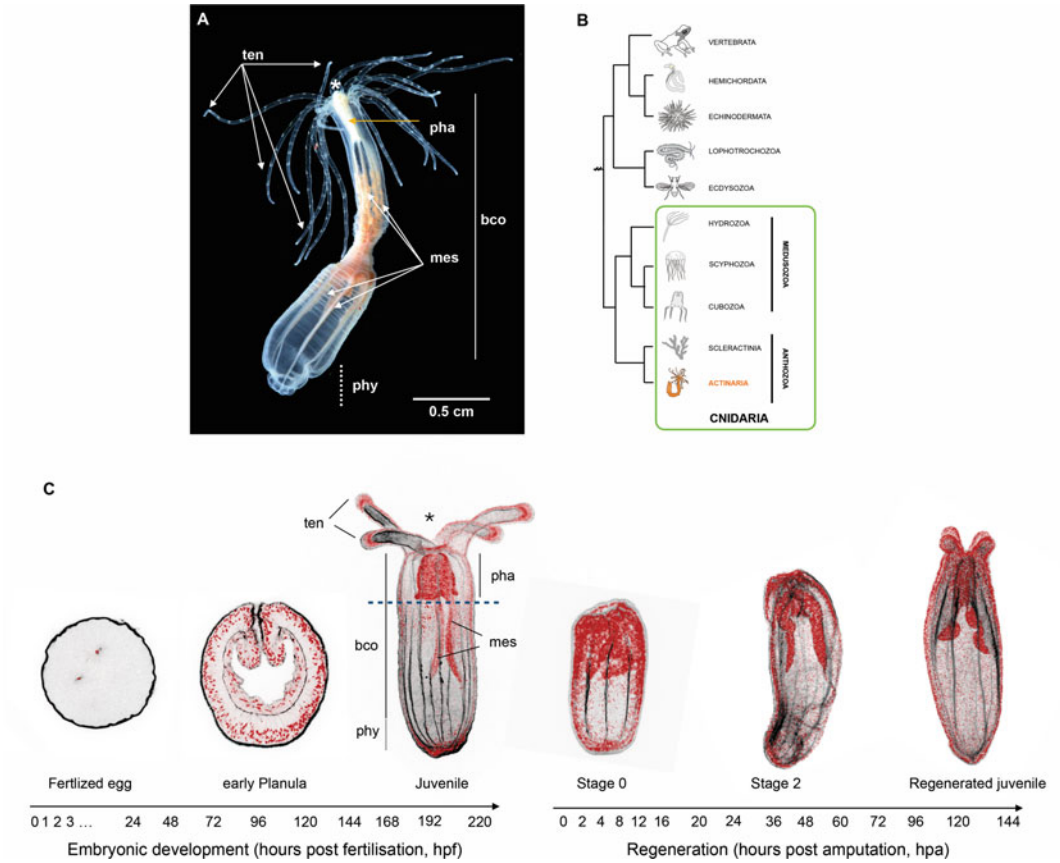


Fig. 1 *Nematostella vectensis*, a research model to assess the relationship between embryonic development and regeneration. (**a**) General anatomy of the sea anemone *Nematostella*. The body of this small anthozoan cnidarian (<5 cm) is organized along an oral/aboral axis. The oral region is formed by tentacles (ten) that surround the mouth (*) and a pharynx (pha). The body column (bco) contains internal structures called mesenteries (mes) that end at the aboral most region with the so-called physa (phy). (**b**) Schematic representation of the phylogenetic position of cnidarians (including *Nematostella*, indicated in orange) within the metazoan tree of life. (**c**) Confocal images (phalloidin/actin filaments in black, DAPI/nuclei in red) of representative stages of *Nematostella* embryonic development and regeneration. Depicted below are the time points for which published RNAseq samples [1–3] are present in the NvERTx database

same organism [3, 17, 19]. This is particularly convenient not only to determine to what extent regeneration recapitulates the gene regulatory program deployed during embryonic development—addressing one of the long-lasting questions in regeneration biology [20], but importantly to highlight if regeneration is controlled by specific toolkits only present in differentiated tissues.

Several studies have performed global gene expression analysis during embryonic development [1–3, 6, 21] or regeneration [3, 22]. In the present chapter, we describe the methods we used to create *NvERTx*, a gene expression database for comparing embryonic development and regeneration gene expression data in

Nematostella vectensis [3, 23]. This database features transcriptomic data combining 22 time points during embryonic development and 16 time points during regeneration (Fig. 1c). In addition, we have developed a web interface to facilitate the manipulation of the data contained in this database. This website simplifies data mining and can generate some figures such as graphs to compare groups of sequences. This interface also integrates various common online tools like Blast to retrieve all transcripts homologous for a given sequence entered by the user. Building such in silico tool is a mean to make RNAseq data accessible to the larger scientific community and enable additional usage of the vast amount of data that were initially produced for a given scientific question.

The workflow presented in this protocol is only a general framework for developing an open-access scientific database. More in-depth knowledge of various aspects of programming and of computer science theory in general might be necessary to implement such tool. Although collaborations will bring together knowledge about the biology to be incorporated and the technology to deploy it online, skills to develop such database can be acquired through a wealth of documentation and literature.

2 Materials

The protocol and material presented here is the one that was used to develop NvERTx, a website to access and mine quantitative transcriptomic data from the sea anemone *Nematostella vectensis* [3]. The protocol will need to be adapted to develop websites presenting other types of data as well as to take into account the unavoidable evolution of software and data format. Yet, this protocol provides a generic and flexible framework to make data accessible and usable to the larger scientific community. In addition to programming skills, we here detail the basic material/data/tools required for the development of a user-friendly transcriptome data mining website. Data implemented in the developed database and website is assumed existent. Refer to [23] for a recent protocol describing a standard workflow for quantifying and performing initial analysis of next-generation sequencing (NGS) reads from an RNA-seq analysis.

2.1 Data Resource Requirements

1. Reference genome (e.g., Nemve1, Table 1).
2. Genome annotations (*see* **Note 1**): Annotations should be provided as a single file in GTF or GFF3 format. These files can be downloaded from each genome-related repository (Genbank or specific website, e.g., Nemve1, Table 1) and do not intend to be generated (or re-generated) by the user. However, it is also possible to perform a gene prediction

Table 1
Genomic and transcriptomic resources for *Nematostella vectensis*

Name	Type	Version	URL	References
Nemve1	Genome, gene models, transcript models, annotations	2.0	https://mycocosm.jgi.doe.gov/pages/search-for-genes.jsf?organism=Nemve1	[5]
Nvec200	Genome, gene models, transcript models, annotations	2.0	https://simrbase.stowers.org/starletseaanemone	[24]
NVE	Gene models, transcript models	2.0	https://figshare.com/articles/Nematostella_vectensis_transcriptome_and_gene_models_v2_0/807696	[25]
NvERTx	Transcript models, annotations	1.0	http://nvertx.kahikai.org or nvertx.ircan.org	[3]

(using AUGUST, Prodigal, or common ORFing prediction tools) if no annotation is available in public databases.

3. Assembled reference transcriptome (e.g., NvERTx, Table 1): Preferably download and use a transcriptome from a public repository (*see* **Note 2**).
4. Transcriptome annotations: We encourage to provide the annotations as GTF or GFF3 files (*see* **Note 3**).
5. Quantified RNA-seq data (e.g., different time-points of WBR, NvERTx, Table 1): The results data from RNA-seq experiments must be easily readable by a script to be stored as records of the database. This implies that the values should have to be sorted in rows and columns in a CSV or text file format.

2.2 Technical Requirements

1. Web server: We used the Apache web server under a Linux computer. A valid domain name and an openly accessible internet access are mandatory. We recommend integrating the website and the database into a Docker container for a reliable security and for more flexibility.
2. Database management system: Database management should follow a relational model. The model organizes data into many tables with a unique key identifying each row. Queries can be performed using the SQL that is the reference language since many decades. We encourage to use MySQL (*see* **Note 4**).
3. Web framework: A modern web development requires to use a robust and reusable syntax. We used Django which is a high-level Python web framework that encourages rapid development and clean, pragmatic design (https://www.djangoproject.com/). Moreover, Django facilitates the communication with the database directly or through additional

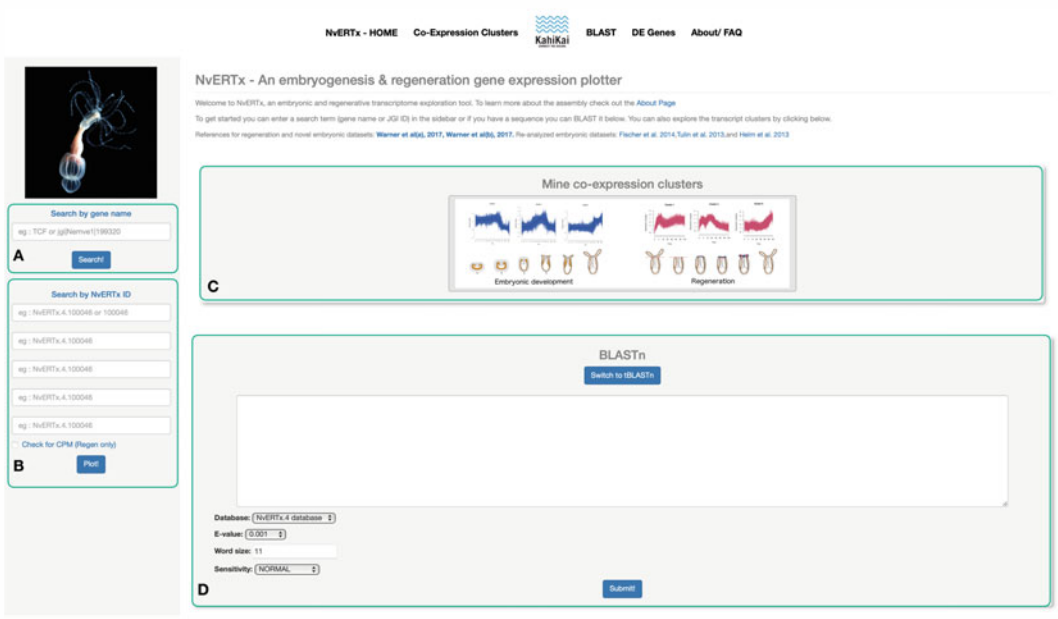


Fig. 2 Screenshot of the NvERTx homepage. (**a**) Users can search for genes using the gene name, Nemve1 accession number, NCBI GenBank accession number. (**b**) NvERTx IDs can also be used to directly obtain the temporal expression profiles for the genes of interest. Multiple, up to five, transcripts can be queried simultaneously. (**c**) Users can also directly explore co-expression clusters from embryonic development and regeneration to identify groups of co-expressed genes. (**d**) The transcriptome can also be searched using BLASTn or tBLASTn

libraries such as SQL-Alchemy (https://www.sqlalchemy.org) (*see* **Note 5**). For the design of the site, we have used "Bootstrap" (https://getbootstrap.com) which is an additional framework. It facilitates the creation of web interfaces (HTML + JavaScript) and avoids display problems that can occur between web browsers.

4. Data mining software suite: The web interface of NvERTx includes online software to perform basic manipulations of the RNA-seq sequences (Fig. 2). We added the BLAST suite to facilitate the search of all transcripts of the NvERTx database homologous to a given sequence entered by the user. The aligner MUSCLE was also added to visually compare a group of similar sequences (SNPs, indels, etc.). The integration of these tools in the Django code is facilitated by some specific API such as PyBlast (https://pypi.org/project/pyblast/) or django-blastplus (https://github.com/michalstuglik/django-blastplus).

3 Methods

3.1 Defining the Scope and Application of the Tool

An important aspect for developing a database for internal use or for the scientific community is to define the scope and intended use of the tool. Some preliminaries are therefore required to be clearly defined such as:

1. List the scientific goals of the tool (e.g., Mining transcriptomic data).
2. Define the community for which the tool is intended (e.g., scientists, students, laymen).
3. Define the level of expertise required to use this tool as a user and/or database manager.
4. Determine the time and budget allocated for this project.
5. Determine the functionalities that the users might want to use on the website to query the data (*see* **Note 6**).

3.2 Setup the Relational Database

3.2.1 Database Design

Prior to starting the building of the database and the website per se, the probably most important aspect of the process is to take time to conceptualize the database regarding its intended usage. Taken this into account will make this online tool user-friendly and as useful as possible for the scientific community.

To do so, we encourage you to make an exhaustive inventory of all information and meta-information that will have to be integrated into the database (*see* **Note 7**). This information consists of the biological resources acquired from experiments such as RNA-seq results, but also include every data or metadata that could be related to the numerical values: annotations (genes, go-terms, pathways, etc.), information of the experiments protocol itself (samples sources, extraction method, library preparation, sequencer device used), general or user comments, image descriptions. The data inventory should also include the external sources of information that could be useful to associate: GSEA, ontologies, PubMed, websites of collaborators, etc.

It is also necessary to consider other information that are not directly related to the biological data, but which will be useful for the management of the database and the website: e.g., a table grouping the users with their respective access permissions (guest, administrator, permissions to read or modify part of the data in the database, etc.) (*see* **Note 8**).

3.2.2 Build the Database Structure

A popular method to build databases is based on a relational model that uses linked tables. Depending on the size of the expected database, it is advisable to create a model before directly building the Tables. A database model is a way to set a representation of the

data and its relations understandable by a non-expert and independent from any further technical choice of development.

There are several tools or methods to make this model. For example, the Merise method is a general-purpose modeling methodology in the field of information systems development. Merise proceeds to separate treatment of data and processes, where the data-oriented view is modeled in three stages, from conceptual, logical through to physical. The UML (Unified Modeling Language) is also a general-purpose, developmental, modeling language in the field of software engineering that is intended to provide a standard way to visualize the design of a system. A model built using UML proposes a diagram structure representation that can be easily interpreted.

An intermediate solution is to use a graphical table construction and visualization. This type of software allows the biologist to visually verify that all the information is present in the database and in the right place. Also, the relationships between tables can be represented with this type of tools. Once the database schema is finalized, the tool can automatically generate the tables in SQL format for import into a MySQL system for instance. Among these tools, we can mention "MySQL Workbench" which is a free tool and both simple and powerful (https://www.mysql.com/products/workbench/).

Finally, the design of the database must prioritize the independence from the technical solutions that will be used to make the GUI. It must be sufficiently modular to not constrain the use of a specific coding language. It should be possible to interact with the database via an external website, a scripting API, or any interfacing solution that can be developed later (*see* **Note 9**).

3.2.3 Populate the Database

There are several possibilities to populate the database. The most direct is to fill the data directly in SQL command lines or through an external graphical tool like "PHP MyAdmin" (https://www.phpmyadmin.net) which facilitates the access and the management of a database.

Some recurring operations will be easier by using some dedicated scripts that will have to be developed. For example, importing data from RNA-Seq to populate the database is almost impossible to do without using a script that retrieves the values from a raw file and converts them into SQL entries. It will then be necessary to develop a series of scripts, in Python or in a language familiar to the database manager.

If the database is extended, it will be necessary to develop several scripts and to check that the logic of filling the database is respected: some tables must be filled before others, some records must be mandatory, others optional (*see* **Note 10**).

3.3 Build the Website

3.3.1 Design and Create the Main Webpages

In addition to the classical sections such as a Home page describing the project and an About page displaying the various contact details, the important parts of the website will have to be decided in close collaboration with the main end-users. In our example, NvERTx presents a dedicated page for displaying the data of co-expression clusters of embryogenesis versus regeneration and a dedicated page displaying RNA-Seq differential expression by sample type. Each of these webpages are linked to selection menus allowing to display specific information.

Forms to search information must be clearly visible. The entry boxes to search using terms like gene names or by IDs will be often used. They must be accessible directly, e.g., from the left or top main menu. The development of the frontend will be done via the chosen framework (*see* **Note 11**).

3.3.2 Implementing Data Visualization and Mining Tools

It is necessary to establish the list of features that will be required to achieve the project (e.g., count tables, expression plots, expression clusters). These functionalities can be classified into two sets: tools to visualize the data and tools to mine the data.

1. Tools to visualize the data are a way to make the content of the database user-friendly. This interface will be important to enhance the data (gene expression profiles at different time-points, co-expression clusters, images, annotations, etc.), but also for editing the data. Through interactive forms, this will be a graphical way for a user to add or modify certain information contained in the database as additional annotations or new entries. For NvERTx, expression profiles and volcano plots are generated dynamically using the Plotly javascript library (https://plot.ly/javascript/), a free and open-source graphing library (Figs. 3 and 4).
2. Mining tools are a way to extend the use of the data. A user can experiment two kind of actions: deep information searches, usually for nucleotides/proteins sequences, and comparisons between sets. Sequence searches are done either by entering keywords, usually annotations related to the sequence searched, or by homology by entering a given sequence and asking the system to match all the sequences like it. This last type of search is performed using tools that evaluate the degree of homology of sequences pairwise. BLASTn (used by NvERTx, Fig. 2d) is the most popular tool for this kind of applications, but there are other tools like BLAT, USEARCH, GHOSTX, or GHOSTM which can be used, and which are generally faster. For sequence comparisons, there is a multitude of tools that can be integrated to a web GUI. The simplest ones can consist in multiple sequence aligners like MUSCLE but can be more elaborate like using specific suite as Shiny (https://shiny.rstudio.com) or Ploty (https://plot.ly/javascript/)

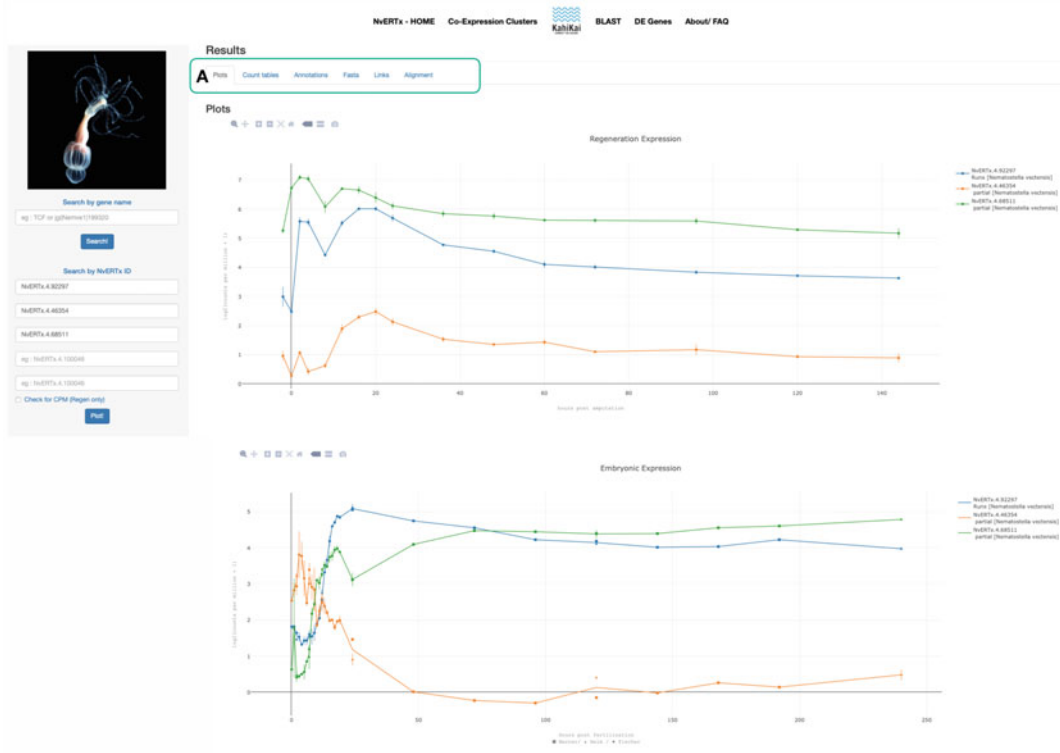


Fig. 3 Screenshot of the expression plots. Shown are plots for regeneration (top) and embryonic development (bottom) for *Nematostella runx* (NvERTx.4.92297), *tcf/lef* (NvERTx.4.46364), c-ets1B (NvERTx.4.68511). Selecting the tabs in (**a**) enables the users to obtain (1) count data from each of the data sets, (2) transcript annotations, (3) sequences in FASTA format, (4) bibliographical resources including PubMed links and PaperBlast queries (if available), and (5) MUSCLE alignment to compare similar transcripts

which allows to mix different sets of value to generate online graphics (3D histograms, heatmaps, or more sophisticated representations).

3.4 Data and Services Availability

3.4.1 Accessibility

If the website is hosted on a local web server, unless for a strict internal use, you will need external access permissions for the site to be visible to the rest of the world. The database itself does not necessarily need to have an open access to the outside because it will go through the website. It is recommended to have a real domain name associated with the website to improve its visibility.

The NvERTx website is freely and openly accessible to the community (http://nvertx.kahikai.org). The source code for the website can be found at https://github.com/IRCAN/NvER_plotter_django. Data sets from the database can be found at http://nvertx.ircan.org/ER/ER_plotter/about.

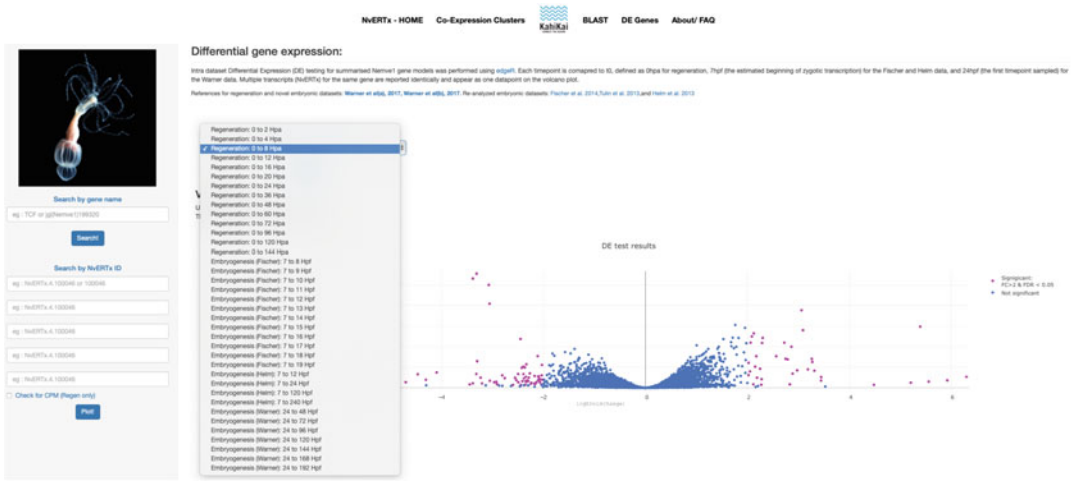


Fig. 4 Screenshot of the differential gene expression (DE Genes) feature from NvERTx. A scroll down menu indicates all possible differential gene expression analysis, whose results are represented by volcano plots. Selecting a given dot will provide additional information such as the NvERTx ID, nr_hits, and fold change values

3.4.2 *Maintenance*

It is highly recommended to use a Docker container system (https://www.docker.com) or similar. This system allows to encapsulate the database, the site, and all the technical requirements in a single file. This makes the project independent of the native server environment and avoids compatibility problems between different versions or other websites hosted on the same server. Moreover, a container is easily exportable and installable on another server without complicated technical modifications. NvERTx uses a Docker container (https://hub.docker.com/repository/docker/ircan/nvertx).

We recommend depositing all the developments of the project (database structure, website code, API, documents) on a source code development (SCM) platform such as GitHub. This has the advantage of making the code open-source and usable by anyone. Moreover, this kind of sharing platform facilitates collaborative development of IT projects: people who want to improve the project can contribute by modifying the code. The latest version of the project can be made available from this platform. Note that this does not concern the data of the database itself, but only the main source code related to the project.

3.4.3 *Documentation*

Several documents must be provided. These documents can be text files included at the root level of the GitHub project for example. There will be a README file giving the main lines of the project, an INSTALL detailing the technical procedure to install the database and the associated code of this project, a CHANGELOG specifying the modifications made since the last update of the

code. Moreover, a document specific to the practical use of the database and the website is strongly recommended. It could be a pdf that can be downloaded directly from the site detailing the data available and all the items/tools available on the site or an "how to" tutorial.

3.4.4 Evaluating the Impact of the Database

User feedback is the best way to evaluate the usage and user friendliness of a given database. Those feedbacks may not only help to improve the database usefulness itself but also for the development of any potential upgrade or future in silico database. Several tools exist to gain information on the statistics such as number, origin, session durations, etc. of the database users (e.g., GOOGLE analytics). However, certainly the most valuable evaluation factor for scientific databases is its referenced usage by the larger scientific community, i.e., the resulting citations or collaborations. Thus, providing information on how to cite the database is crucial and should be implemented in the webpage (e.g., the FAQ section).

4 Notes

1. A unique file containing genome sequence + annotations (.gbk or .embl) could also be provided instead, but is less useful since the integrated webtools usually needs fasta or gff as separate files, i.e., the blast database indexing requires fasta format only.
2. If no transcriptome is available or if the database manager prefers to use its own transcriptome, the file must be a single fasta file. Each entry in the file has to be a single transcript sequence and the related description should preferably contain some useful IDs to be used for crossing with other databases (e.g., Ensembl, ReSeq, nt).
3. It is possible to add usual short annotations directly into the description lines of the transcriptome fasta file: GeneSymbol name, ortholog names/IDs, GO term ID, or other information specific to the transcript.
4. MySQL is an open-source relational database management system widely used in the biology field. Its capabilities allow to support a high number of entries as well as a powerful engine for complex queries. For small databases is also possible to use SQLite instead, having the advantage to be lighter and using an independent file system for storing data. Like the webserver, prefer to install and run your database server into a separate Docker container.
5. Another option is to use "Ruby on Rails" (https://rubyonrails.org) instead of Django. This framework is similar to Django

with some differences like a fully object-oriented language with a more powerful frontend part. Ruby is probably slightly more difficult to handle for beginner developers.

6. Start from your personal / the labs' needs and exchange with the community to determine additional functionalities to be added. Often additional functionalities arise during the test phase of the database/website. Once launched, consider taking users' feedback for a future update of the data mining tools.
7. Some data require high amount of space storage such as raw sequence or high-definition images. They can be stored outside the database, in files. Exporting this big data will keep the database quite light; however, it will be required to add links to these external files into the database (system directory paths, external URLs, etc.).
8. The database should be modular enough to allow additional tables or fields in the future.
9. Apply the traditional rules of database design, i.e., to avoid redundancy, to propose unique keys for each table, to organize the data in the different tables in a way that is neither too large nor too small, and to create intermediate tables containing the keys of the tables whose records are to be crossed. We advise to carefully read up some documentation on relational database conception to avoid certain errors because it can be very difficult to modify the structure of the database once it contains the data and starts to be used.
10. The development of these small pipelines can be organized in such a way that it will constitute a real Application Programming Interface (API), which can be reused during the construction of the website.
11. The code and the SQL queries generated when validating the forms must be clear and modular. The possible APIs developed to fill the database can be reused here. The developer can use free existing templates and CSS files to build the site, or he can decide to develop the site from scratch. He can also use a content management system (CMS) to set up the website (such as Zope for Django), but we do not advise this solution as these CMS are not appropriate for very specialized sites like NvERTx.

Acknowledgments

The authors thank Jacob Warner and Vincent Guerlais for the development of NvERTx as well as Boris Meyer for technical support after the launch of the online database. This work was supported by the French Government (National Research Agency, ANR) through the grant RENEW (ANR-19-PRC) to E.R.

References

1. Fischer, Antje HL, Smith J (2013) Nematostella High-density RNAseq time-course, 2013-06-14.
2. Helm RR, Siebert S, Tulin S, Smith J, Dunn CW (2013) Characterization of differential transcript abundance through time during Nematostella vectensis development. BMC Genomics 14(1):266
3. Warner JF, Guerlais V, Amiel AR, Johnston H, Nedoncelle K, Röttinger E (2018) NvERTx: a gene expression database to compare embryogenesis and regeneration in the sea anemone Nematostella vectensis. Development 145(10): dev162867
4. Hand C, Uhlinger KR (1992) The culture, sexual and asexual reproduction, and growth of the sea anemone Nematostella vectensis. Biol Bull 182(2):169–176. https://www.researchgate.net/
5. Putnam NH, Srivastava M, Hellsten U, Dirks B, Chapman J, Salamov A et al (2007) Sea anemone genome reveals ancestral eumetazoan gene repertoire and genomic organization. Science 317(5834):86–94
6. Schwaiger M, Schonauer A, Rendeiro AF, Pribitzer C, Schauer A, Gilles AF et al (2014) Evolutionary conservation of the eumetazoan gene regulatory landscape. Genome Res 24(4): 639–650
7. Renfer E, Amon-Hassenzahl A, Steinmetz PRH, Technau U (2010) A muscle-specific transgenic reporter line of the sea anemone, Nematostella vectensis. Proc Natl Acad Sci U S A 107(1):104–108
8. Layden MJ, Röttinger E, Wolenski FS, Gilmore TD, Martindale MQ (2013) Microinjection of mRNA or morpholinos for reverse genetic analysis in the starlet sea anemone, Nematostella vectensis. Nat Protoc 8(5):924–934
9. Röttinger E, Dahlin P, Martindale MQ (2012) A framework for the establishment of a Cnidarian gene regulatory network for "Endomesoderm" specification: the inputs of ß-catenin/TCF signaling. PLoS Genet 8(12):e1003164
10. Rentzsch F, Fritzenwanker JH, Scholz CB, Technau U (2008) FGF signalling controls formation of the apical sensory organ in the cnidarian Nematostella vectensis. J Embryol Exp Morphol 135(10):1761–1769
11. Servetnick MD, Steinworth B, Babonis LS, Simmons D, Salinas-Saavedra M, Martindale MQ (2017) Cas9-mediated excision of Nematostella brachyury disrupts endoderm development, pharynx formation and oral-aboral patterning. Development 144(16):2951–2960
12. Ikmi A, McKinney SA, Delventhal KM, Gibson MC (2014) TALEN and CRISPR/Cas9-mediated genome editing in the early-branching metazoan Nematostella vectensis. Nat Commun 5:5486
13. Kraus Y, Aman A, Technau U, Genikhovich G (2016) Pre-bilaterian origin of the blastoporal axial organizer. Nat Commun 7:11694
14. Bossert PE, Dunn MP, Thomsen GH (2013) A staging system for the regeneration of a polyp from the aboral physa of the anthozoan cnidarian Nematostella vectensis. Dev Dyn 242: 1320–1331
15. Amiel A, Johnston H, Nedoncelle K, Warner J, Ferreira S, Röttinger E (2015) Characterization of morphological and cellular events underlying oral regeneration in the sea anemone, Nematostella vectensis. Int J Mol Sci 16(12):28449–28471
16. Passamaneck YJ, Martindale MQ (2012) Cell proliferation is necessary for the regeneration of oral structures in the anthozoan cnidarian Nematostella vectensis. BMC Dev Biol 12(1):1
17. Reitzel A, Burton P, Krone C, Finnerty J (2007) Comparison of developmental trajectories in the starlet sea anemone Nematostella vectensis: embryogenesis, regeneration, and two forms of asexual fission. Invertebr Biol 126(2):99–112
18. Amiel AR, Röttinger E (2021) Experimental tools to study regeneration in the sea anemone Nematostella vectensis. Methods Mol Biol 2219:69–80

19. Warner JF, Amiel AR, Johnston H, Röttinger E (2019) Regeneration is a partial redeployment of the embryonic gene network. bioRxiv 121: 658930
20. Morgan TH (1901) Regeneration, Columbia University Biological series, vol 279. Macmillan, New York, NY
21. Tulin S, Aguiar D, Istrail S, Smith J (2013) A quantitative reference transcriptome for Nematostella vectensis early embryonic development: a pipeline for de novo assembly in emerging model systems. EvoDevo 4(1):16
22. Schaffer AA, Bazarsky M, Levy K, Chalifa-Caspi V, Gat U (2016) A transcriptional time-course analysis of oral vs. aboral whole-body regeneration in the sea anemone Nematostella vectensis. BMC Genomics 17(1):718
23. Warner JF, Röttinger E (2021) Transcriptomic analysis in the sea anemone Nematostella vectensis. Methods Mol Biol 2219:231–240
24. Zimmermann B, Robb SMC, Genikhovich G, Fropf WJ, Weilguny L, He S et al (2020) Sea anemone genomes reveal ancestral metazoan chromosomal macrosynteny. bioRxiv 2020.10.30.359448
25. Fredman D, Schwaiger M, Rentzsch F, Rentzsch F, Technau U (2013) Nematostella vectensis transcriptome and gene models v2.0

Open Access This chapter is licensed under the terms of the Creative Commons Attribution 4.0 International License (http://creativecommons.org/licenses/by/4.0/), which permits use, sharing, adaptation, distribution and reproduction in any medium or format, as long as you give appropriate credit to the original author(s) and the source, provide a link to the Creative Commons license and indicate if changes were made.

The images or other third party material in this chapter are included in the chapter's Creative Commons license, unless indicated otherwise in a credit line to the material. If material is not included in the chapter's Creative Commons license and your intended use is not permitted by statutory regulation or exceeds the permitted use, you will need to obtain permission directly from the copyright holder.





Chapter 36

Formalizing Phenotypes of Regeneration

Daniel Lobo

Abstract

Regeneration experiments can produce complex phenotypes including morphological outcomes and gene expression patterns that are crucial for the understanding of the mechanisms of regeneration. However, due to their inherent complexity, variability between individuals, and heterogeneous data spreading across the literature, extracting mechanistic knowledge from them is a current challenge. Toward this goal, here we present protocols to unambiguously formalize the phenotypes of regeneration and their experimental procedures using precise mathematical morphological descriptions and standardized gene expression patterns. We illustrate the application of the methodology with step-by-step protocols for planaria and limb regeneration phenotypes. The curated datasets with these methods are not only helpful for human scientists, but they represent a key formalized resource that can be easily integrated into downstream reverse engineering methodologies for the automatic extraction of mechanistic knowledge. This approach can pave the way for discovering comprehensive systems-level models of regeneration.

Key words Formalization, Modeling, Inference, Regeneration

1 Introduction

The resultant phenotypes of regeneration experiments can include complex morphologies, spatial patterns, anatomical manipulations, and temporal dynamics—an extraordinary rich dataset to aid in the understanding of the mechanisms of regeneration [1–3]. Organisms such as planarian worms can regenerate any body part after almost any amputation, including new heads, eyes, brain, etc., and produce aberrant morphologies after genetic perturbations [4–7]. Amphibians and insects can regenerate their amputated limbs and appendages by re-growing them from the rest of their bodies, and perturbations can result in ectopic segments [8–10]. In addition, grafting experiments surgically transplanting tissue or appendages to different locations can highlight the system response to ectopic signals and result in the regeneration of a completely new anterior–posterior axis, such as with an inverted graft in planaria [11], or the regeneration of supernumerary limbs, as in the case of graft rotations in axolotl [12] and cockroach [13]. These experiments are

Simon Blanchoud and Brigitte Galliot (eds.), *Whole-Body Regeneration: Methods and Protocols*,
Methods in Molecular Biology, vol. 2450, https://doi.org/10.1007/978-1-0716-2172-1_36, © The Author(s) 2022

essential to discern the spatial localizations of the signals dictating the tissue organization during regeneration.

However, the experimental perturbations and the anatomical features of the regenerated morphologies are usually characterized in the literature with microscopy images containing much variability between similar phenotypes [14] and described in natural language, which can be ambiguous and miss crucial details [15, 16]. As a result, these rich and large datasets cannot be readily analyzed by neither human scientists nor computational methods for the extraction of mechanistic knowledge. Instead, a first step formalizing the experimental procedures and the phenotypes of regeneration is needed to encode both their qualitative and quantitative features in a standardized way.

For the unambiguous formalization of regeneration phenotypes, we have developed mathematical formalisms that can precisely describe anatomical structures, organ locations, and overall morphological shapes. We have developed such formalisms for encoding the regeneration phenotypes of planaria whole-body morphology [17], and salamander, frog, crustacean, insect, and arachnid limb and appendages [18]. These formalisms are based on mathematical graphs, where the nodes of the graph represent morphological regions or organs, such as the head or tail of a planarian worm, and the edges represent the connections and topological information between these regions, such as the segments forming a limb. Importantly, the topological information of the graphs can be extended with quantitative data regarding the overall shapes and sizes of the morphological structures, their angles of interconnection, and the localization vectors and rotations of the organs, a process that removes the unimportant differences between individual organisms. These formalizations can also include unambiguous descriptions of the experiments that produce the resultant phenotypes. A mathematical tree can define how different amputations, graftings, and irradiations are performed in a particular experiment. In this way, these formal descriptions based on mathematical structures can encode unambiguously both the experimental procedures and the resultant phenotypes of regeneration.

To facilitate working with these formalizations, we have developed user-friendly tools that allows any user to easily encode the phenotypes of regeneration. Planform [19] is a software tool for the formalization of regeneration experiments and phenotypes of planarian worms. Any user without special training can easily create the mathematical formalisms with the provided drag-and-drop interface for the specification of the different types of worm regions, sizes, and overall shapes. Similarly, the interface allows the definition of precise surgical manipulations, the grafting of pieces between worms, and the total or partial irradiation of regions of the worm body. For the formalization of limb regeneration

experiments, we have developed Limbform [20], a similar software tool with a user-friendly interface. Limbform can be used to define experiments and phenotypes for salamander, frog, crustacean, insect, and arachnid. The number and position of each anatomical structure, such as digits and ectopic limbs, can be easily defined. Importantly, these tools automatically produce from the graph encodings the cartoon diagrams of the created reference morphologies, which can guide the user during the formalization of complex morphologies. The morphologies, experiments, and expression patterns formalized with these tools are stored in a centralized local database file. Using this protocol, we have curated a database of planarian regeneration with more than 1500 different experiments from the literature (*see* **Note 1**). In addition, we have curated a database of limb regeneration experiments with more than 800 different experiments (*see* **Note 2**). Both databases are freely available resources for the community, and the tools include a search functionality to find particular regeneration phenotypes resulting from any manipulation, gene, and drug of interest included in these large databases.

Gene expression patterns represent another fundamental phenotype in regeneration experiments. In situ hybridization [21, 22] and immunohistochemistry [23–25] assays can reveal the spatial gene expression pattern of a specific gene at the level of the whole organism. Gene expression patterns through space and time can reveal the genetic regulation of the key elements controlling regeneration. We have developed PlanGexQ [26] as a user-friendly software tool to formalize planarian gene expression patterns in standard reference morphologies. The spatial localization of gene expression patterns can be easily input into a standard 2D worm morphology defined with a similar mathematical graph formalism as in Planform. Predefined expression patterns for organs are also available for the user to select, which transfers directly to the current standard morphology. In addition, the tool automatically assigns gene ontology terms from the Planarian Anatomy Ontology [27] by scanning the spatial locations of the gene expression in the reference morphology as well as searching for keywords in the entered captions and descriptions.

Crucially, the mathematical nature of these formalized datasets can be integrated in a reverse-engineering methodology for the inference of mechanistic models or regeneration directly from experimental phenotypes [28] (*see* **Note 3**). Figure 1 illustrates the main steps of this iterative methodology and its integration with the formalization of phenotypes. First, functional experiments are performed at the bench to obtain morphological phenotypes from surgical, pharmacological, and genetic perturbations. These experiments and phenotypes are then formalized with the methodology presented in this chapter. Mathematical models based on ordinary or partial differential equations are built to include the

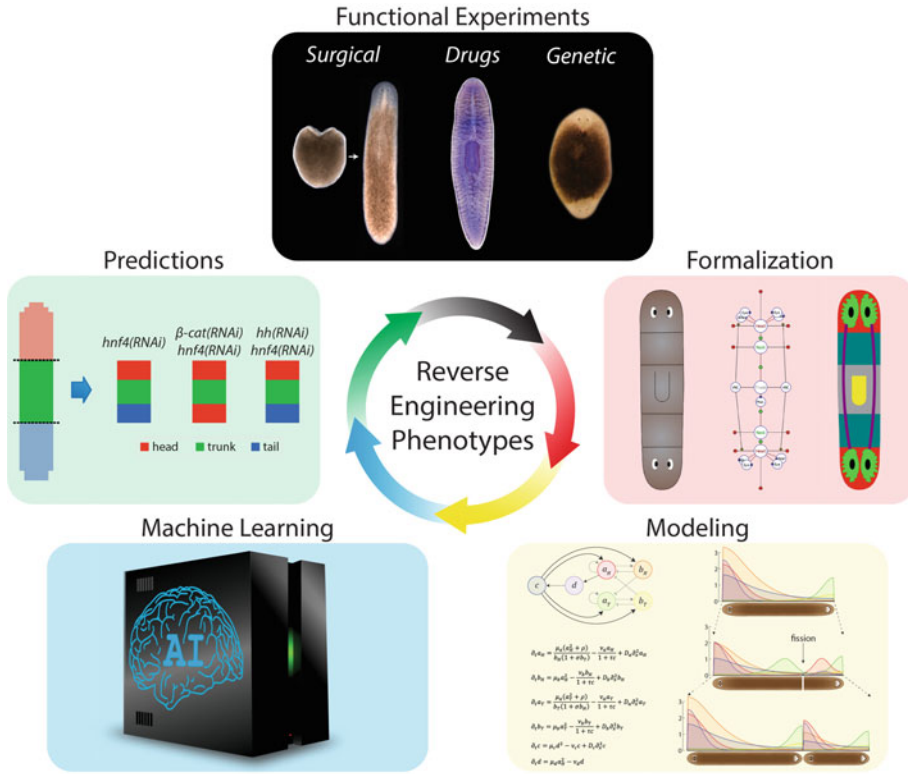


Fig. 1 The formalization protocol presented in this chapter can be integrated as a key component in an iterative methodology for the reverse engineering of the phenotypes of regeneration. Functional experiments at the bench provide the input datasets, which need to be formalized before knowledge can be computationally extracted. Mathematical models based on dynamical systems are designed to include the relevant regulatory networks and biophysical interactions. The model parameters, regulatory interactions, and particular equations can be discovered by machine learning to infer a mechanistic hypothesis explaining the input experimental dataset. Predictions are made with the model, which are then tested with new experiments, closing the methodology loop

main components of the system, their regulations, and the relevant cell and tissue biophysical forces [29–31]. Features of the model such as the parameters and the particular interactions in the regulatory network can be automatically inferred from the experimental datasets with a machine learning approach [32–34]. Finally, the inferred mechanistic model can be employed to formulate testable predictions in terms of novel phenotypes, genes, and perturbations that can be validated with further experiments at the bench [35–37], closing the reverse engineering cycle. In this way, the phenotypes of regeneration formalized with the presented protocols can be computationally analyzed toward the inference of mechanistic knowledge directly extracted from them.

This chapter presents detailed protocols for the formalization of regeneration experiments and phenotypes using user-friendly interactive tools (*see* **Note 4**). The first protocol aims to formalize

planarian regeneration. The curation process includes the definition of experimental details, detailed spatial manipulation procedures, and morphological outcomes—body configurations, organ positions, and geometric properties. The second protocol can be used to formalize limb regeneration experiments for a variety of model organisms. Complex amputation and grafting procedures can be unambiguously encoded together with the precise limb and appendage configurations during regeneration. Finally, the last protocol details a procedure to encode planarian gene expression patterns using reference morphologies. This methodology facilitates the curation of a formal dataset of standardized and ontologically annotated gene patterns that can streamline their comparative analysis and downstream mechanistic inference. Practical notes are included for clarifying key steps and implementation details.

2 Materials

1. Personal computer with Windows, Mac OS X, or Linux operating systems.
2. PlanForm software tool installed in the computer. Planform is freely available at https://lobolab.umbc.edu/planform/. The user-friendly program is compatible with Windows, Mac OS X, and Linux operating systems.
3. LimbForm software tool installed in the computer. Limbform is freely available at https://lobolab.umbc.edu/limbform/. The user-friendly program is compatible with Windows, Mac OS X, and Linux operating systems.
4. PlanGexQ software tool installed in the computer. PlanGexQ is freely available at https://lobolab.umbc.edu/plangexq/. The user-friendly program is compatible with Windows, Mac OS X, and Linux operating systems.
5. Microscopy images of planarian or limb regeneration phenotypes and the experimental and manipulation details used to obtain them.
6. Planarian gene expression pattern phenotypes from in situ microscopy images and the experimental and manipulation details used to obtain them.

3 Methods

This protocol includes detailed instructions to formalize a planarian experimental phenotype with the Planform software tool. Start by executing the program and continue with the following steps.

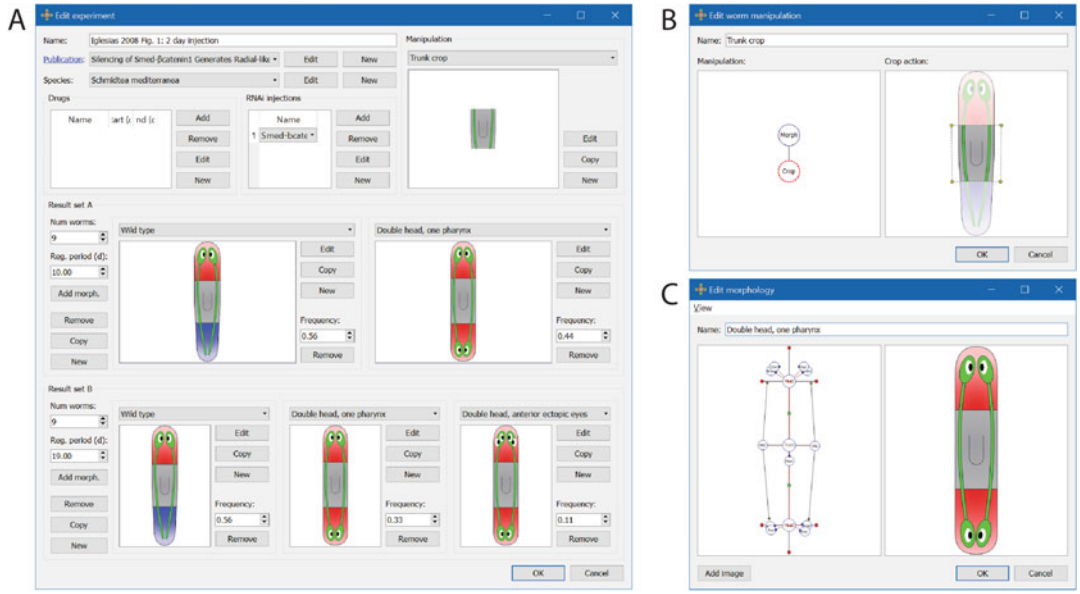


Fig. 2 Screenshots of the user-friendly software tool Planform for the curation and formalization of experimental procedures and resultant phenotypes of planarian regeneration. (**a**) An experiment formalization includes procedure details, manipulations, and the resultant morphologies. (**b**) Manipulations are unambiguously defined as a hierarchy of simpler actions, such as amputations and graftings. (**c**) Worm morphologies are defined with a mathematical graph, where the nodes represent worm regions and organs

3.1 Formalizing Planarian Regeneration Phenotypes with Planform

1. Create a new database by clicking *File* and then *New database*. Input a new file name in any computer folder when prompted (*see* **Note 5**). Alternatively, open any existing database already created or downloaded with *Open database* (*see* **Note 6**).
2. Within the *Experiments* tab in Planform main window, click *New*. A form appears to enter the experimental conditions and resultant regeneration phenotypes (Fig. 2a).
3. Type the name of the experiment (*see* **Note 7**).
4. Select from the drop-down list, or create new, the publication (*see* **Note 8**), and planarian species used for the experiment.
5. Indicate the drugs, if any, used in the experiment and the time period of its application relative to the worm manipulation time (considered day 0). Use negative numbers to indicate days pre-manipulation. Multiple drugs and time periods can be specified clicking *Add*. The database stores a list of drugs used in the experiments, which can be modified with the *Edit*, and *New* buttons.
6. Indicate the genes that were knockdown, if any, with RNA interference (RNAi) treatments during the experiment. Similar to drugs, multiple knockdown genes can be specified in a single experiment.

7. Specify a new manipulation clicking *New* or copy or edit an existing one from the drop-down menu by clicking *Edit* or *Copy* (*see* **Notes 9** and **10**). If the manipulation is already created in the database, select it from the dropdown menu and continue with **step 21**.
8. Give a descriptive name to the new manipulation.
9. A manipulation is defined as a hierarchical combination (represented as a mathematical tree) of simpler actions and base worm morphologies (Fig. 2b). First, create a new base morphology for the manipulation. If the appropriate morphology is already present in the database, select it from the drop-down menu and continue with **step 18**.
10. A new morphology can be created starting from an empty morphology (clicking *New*) or from an existing one by directly editing it (clicking *Edit*) or by copying into a new morphology (clicking *Copy*) (*see* **Note 11**).
11. A morphology is defined as a network of connected worm regions (represented as a mathematical graph), their organs, and parameters to define their shape and size (Fig. 2c).
12. Type a descriptive name for the new morphology.
13. Optionally, a worm microscopy image of the corresponding morphology can be added clicking *Add image* and then selecting an image file from the local computer. This image will be also stored in the database.
14. Add new region and organ nodes by right clicking an existing region node and selecting the region or organ type to connect. Place the region or organ in the correct location by dragging the node (*see* **Note 12**).
15. Define the relative positions between the regions by dragging the corresponding nodes (green circles) (*see* **Note 13**).
16. Define the size and orientation parameters of regions and organs by dragging the corresponding parameter nodes (small red and blue circles) (*see* **Note 14**).
17. The cartoon diagram shows in real-time a representation of the defined morphology to aid in the formalization (*see* **Note 15**). To save the resultant morphology, click *OK* (*see* **Note 16**).
18. Select the appropriate manipulation actions performed in the experiment using the right-click menu (*see* **Note 17**). The actions available are surgical manipulations, such as crops, removals, and joins (grafts), and complete or partial irradiations (*see* **Note 18**).
19. Specify the parameters of the manipulation action with the drag-and-drop interface within the cartoon visualization. The areas of surgical and irradiation manipulations are defined with

polygons with an arbitrary number of points (vertices), which can be edited with the right-click menu. The position and orientation of grafting manipulations can be defined as well with the drag-and-drop cartoon interface. Clicking and dragging a grafted piece translates it with respect the host morphology, while clicking and dragging on empty space rotates the graft.

20. Repeat **steps 18** and **19** until all the manipulation actions in the experiment are defined. Then click *OK*.
21. Specify the set of resultant morphologies obtained in the experiment. Multiple time points can be defined to formalize a time series of morphological outcomes. For each time point to formalize in the experiment, click *New* and then define the number of worms in the experiment (*N*) as well as the regeneration period as days after the manipulation.
22. For each regeneration period, define a set of morphological outcomes and their frequency. To add a new resultant morphology, click *Add morph.* and indicate the ratio of worms (frequency) that resulted in that regeneration phenotype (*see* **Note 19**).
23. For each resultant morphology, specify the phenotype by selecting it from the drop-down menu. If the morphology is not already created in the database, create a new one following **steps 10–17**.
24. Repeat **steps 21–23** for each resultant phenotype obtained in the experiment. Then click *OK* to save the formalized experiment in the database (*see* **Note 20**).

3.2 Formalizing Limb Regeneration Phenotypes with Limbform

Limbform follows the same general design than Planform, but for the formalization of regeneration phenotypes of salamander, frog, crustacean, insect, and arachnid limb and appendages. To formalize a new phenotype, follow the same procedure as with Planform except for the following steps.

1. Define all treatments, such as drug injections, using a unified list and include for each of them the time period of its application relative to the limb manipulation time (considered day 0). Use negative numbers to indicate days pre-manipulation (Fig. 3a).
2. The list of actions that define a manipulation (Fig. 3b) are extended with relocation and reverse actions. Use a relocation action to define together an amputation of a limb section and its graft in an ectopic location. Use a reverse action to define similarly an amputation of a limb section and its graft in an ectopic location, but where the graft is 180° rotated around the proximal–distal axis.

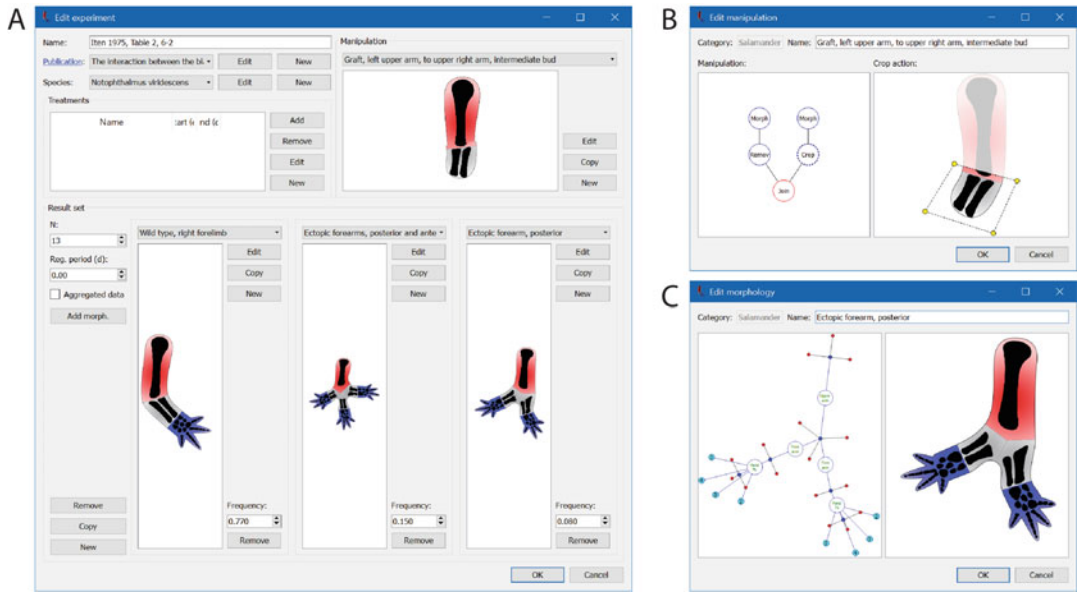


Fig. 3 Screenshots of the software tool Limbform for the curation and formalization of salamander, frog, crustacean, insect, and arachnid limb and appendage regeneration experiments and morphologies. (**a**) Example of a formalized grafting experiment with salamander resulting in multiple ectopic forearms. (**b**) User-friendly interface for the formalization of a grafting experiment from the left to the right arm. (**c**) Limb phenotype with ectopic forearms, including details such as the number of bones in each limb segment and digit

3. Formalize limb morphologies by defining with the interactive interface limb segments as the edges of the graph and their joints as the vertices of the graph (Fig. 3c) (*see* **Note 21**).
4. Define the type of each segment (which is particular to the animal species) and the body side it developed or regenerated (left or right) by right clicking on each node. In a similar way, define for each segment whether they are reversed (180° rotation around the proximal–distal axis) or inverted (swap of the proximal–distal segment ends) (*see* **Note 22**).
5. For salamander and frog limbs, define the number of bones for each segment as well as for their digits. These options are also available in the right-click menu. The selected number of bones and digits are also shown in the cartoon diagram (Fig. 3c).
6. Finally, for salamander and frog limbs, optionally define nerves as a segmented line through the limb morphology. Use the right-click menu to add and remove points in a nerve.

3.3 Formalizing Planarian Gene Expression Patterns with PlanGexQ

PlanGexQ is a software tool for the formalization of planarian gene expression patterns into standard morphologies. Start by executing the program and continue with the following steps.

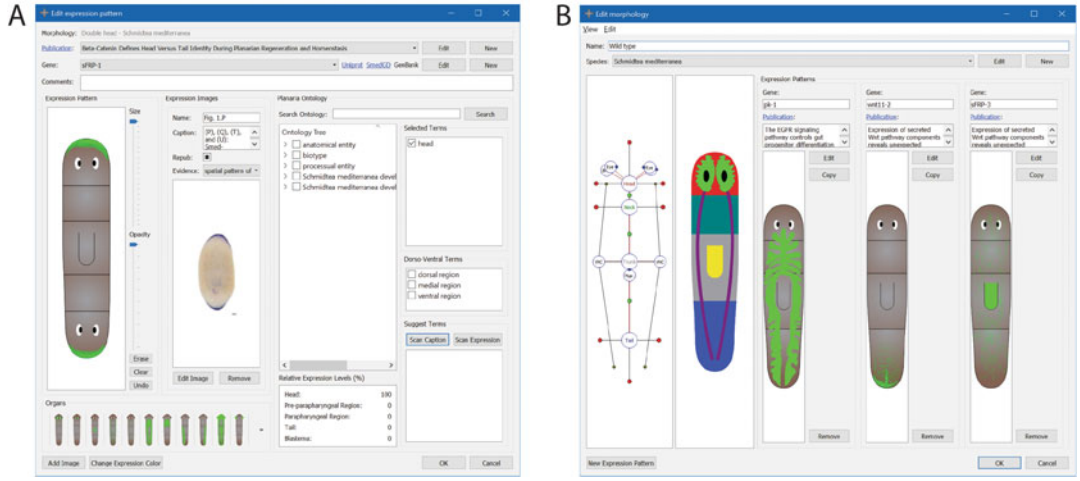


Fig. 4 Screenshots of the software tool PlanGexQ for the registration and ontological annotation of gene expression patterns in planarian worms. (**a**) Interface for the curation of a gene expression pattern in a double head regeneration phenotype, including the original microscopy image and ontology terms. (**b**) Formalized standard morphology together with curated gene expression patterns. Registering expression patterns in standard morphologies facilitates their downstream analysis with machine learning tools

1. Create a new database by clicking *File* and then *New database*. Input a new file name in any computer folder when prompted (*see* **Note 23**). Alternatively, open any existing database already created or downloaded with *Open database*.
2. Before curating a new gene expression pattern, make sure that the corresponding worm morphology exists in the *Morphologies* tab. To create a new standard morphology, select the *Morphologies* tab, and click *New*. The procedure to create new worm morphologies is similar than for Planform (*see* **steps 11–17** in Subheading 3.1).
3. Within the *Expression Patterns* tab in PlanGexQ main window, click *New*. A new form appears to select the standard morphology of the worm to formalize among those stored in the database. After selecting a morphology, a new form appears to enter the gene expression pattern details (Fig. 4a).
4. Select from the drop-down list, or create new, the publication where the gene expression pattern is being curated from, if any.
5. Select from the drop-down list, or create new, the gene reported in the expression pattern. For new genes, additionally input their accession number from the Uniprot [38], SmedGD [39], and GenBank [40] databases (*see* **Note 24**).
6. Define the gene expression pattern in the cartoon reference morphology with the interactive tool. An automated registration method to map the gene expression patterns in the reference morphology directly from microscopy images is available

starting from v.3.0 of the tool. If the expression pattern includes specific organs, click on their diagram to directly include their expression pattern. Optionally, select a different expression color by clicking *Change Expression Color*.

7. Add one or more microscopy images of the gene expression pattern clicking *Add Image*. For each image, input a name and a caption. Optionally, select from the drop-down menu the type of evidence as a term from the Evidence and Conclusion Ontology [41]. In particular, gene expression patterns obtained with in situ hybridization assays can be annotated with the term ECO_0000047, *spatial pattern of transcript expression evidence*.
8. Scan the caption and expression pattern to automatically assign ontology terms from the Planarian Anatomy Ontology [27] to the gene expression pattern by clicking *Scan Caption* and *Scan Expression* (*see* **Note 25**).
9. If needed, assign additional ontology terms by clicking them on the complete ontology tree hierarchy shown in the interface. The tree can be easily searched typing keywords in the *Search Ontology* box (*see* **Note 26**).
10. When finished, click *OK* to save the gene expression pattern information in the database.

4 Notes

1. A curated database of planarian regeneration experiments is freely available at https://lobolab.umbc.edu/planform/download/ and can be opened and explored with the latest version of Planform in any of the compatible operating systems.
2. A curated database of limb regeneration experiments is freely available at https://lobolab.umbc.edu/limbform/download/ and can be opened and explored with the latest version of Limbform in any of the compatible operating systems.
3. A simulation software including reverse-engineered models of planarian regeneration is freely available at https://lobolab.umbc.edu/planarianmodels/. These models were automatically inferred directly from regeneration phenotypes formalized following the first protocol presented in this chapter. In addition, a methodology for inferring dynamic gene regulatory network models from spatial expression patterns (including an open source software implementation) is available at [34].
4. The formalization tools used in this chapter (Planform, Limbform, and PlanGexQ) were developed in C++ using the Qt libraries (The Qt Company; https://www.qt.io/). This approach allows the implementation of highly customized

native tools that are multiplatform, as the same code can be compiled for Windows, Mac OS X, and Linux operating systems. The Qt libraries are especially useful for implementing the user interface—including forms, widgets, menus, and any other graphical element—and abstracting the access to the database file. Importantly, Qt also provides a Graphics View Framework, which was used for the visualization and interaction with the morphology and manipulation graphs as well as for the worm and limb cartoon diagrams. This framework provides a surface for displaying interactive custom-made 2D graphical items and support zooming and rotation. In this way, the nodes and lines of a morphological graph can be shown as interactive objects for the user to easily formalize a worm, limb, or expression pattern. Furthermore, the framework supports the creation of custom shapes using Bézier curves, which was used to implement the dynamic real-time generation of worm and limb cartoon diagrams directly from the corresponding graph formalization.

5. The file extension for Planform databases is *edb* and for Limbform databases is *ldb*. During the installation of the tools, file types and extension associations are automatically created in the operating system so that double clicking database files automatically open them in their respective tools. To guarantee compatibility with external tools, these database files are locally stored in the SQLite version 3 (public domain) format, the most used database engine in the world.
6. A database is stored in a single file containing all the data in a centralized fashion. This approach facilitates the sharing of information between researchers. In addition, Planform, Limbform, and PlanGexQ include functionality to import the data from one database into another. For this, open the target database and select the *Import* command in the *File* menu. Using the file selection window that popups, select the database file with the source data. The program then compares all the data from both databases and shows all the elements that are modified, new, or deleted. The user can then select the specific data to import.
7. The experiment name must be unique within a database. The name convention in the public curated Planform database is the first author last name, year of publication, and the figure panel in the paper where the resultant phenotype is reported.
8. A publication includes the title, year, and URL that links to the full manuscript text. To maximize long-term accessibility, we recommend using the DOI link when possible.
9. To create a complex manipulation, it is recommended to copy an existing one already in the database and change the steps

that differ, rather than starting completely from a new empty manipulation.

10. When editing an element in the database, such as a manipulation or morphology, the new changes will be reflected in all experiments containing such element. If that behavior is not desired, copy the element instead, and assign a new name.
11. It is recommended to create a new morphology by first copying an existing one already in the database and change the region and organs that differ. Intact wild-type morphologies are automatically created in a new database.
12. A link can be added between two existent regions by holding the shift key and selecting both nodes followed by right click. Links can be deleted between regions by right clicking on the link and selecting the appropriate menu option.
13. The spatial location of each region is defined relative to the other regions, and hence, a morphology is invariant under translations or rotations. The spatial location and orientation of organs are defined relative to the region they are linked to. In this way, region translations do not affect the relative location of the organs within the region.
14. For more precise control and placement of nodes, a user can zoom in and out the graph and cartoon representations in both morphologies and manipulations by holding the Ctrl key (key on a Mac) and moving the mouse wheel. If any part of the morphology or graph is not visible in the current view, scroll bars appear to translate the visualization. In addition, vertical scrolling can be achieved by holding the Shift key and moving the mouse wheel. Horizontal scrolling can be achieved by holding the Alt key (Option key on a Mac) and moving the mouse wheel.
15. Cartoon diagrams and graph representations can be exported as image files by right-clicking on any empty space and then selecting *Save image*.
16. Clicking *OK* on any form in the tool saves the changes made in that form into the local database file without the need of any further command in the *File* menu. To save and continue using a new copy of the database file, select *Save database as* in the *File* menu.
17. The manipulation actions form together a tree structure, where the root of the tree represents the final manipulated worm, and the leaves represent the starting worm morphologies. In this way, complex manipulations can be unambiguously formalized with the interface by combining multiple actions (e.g., multiple graftings from different source worms).

18. Notice that a crop action amputates a section of the morphology and discards the rest of the morphology (e.g., amputating the head region to produce a head fragment). In contrast, a removal action amputates a section from the morphology, discards it, and keeps the rest of the morphology (e.g., removing the tail region and keeping the head and trunk regions).
19. The sum of all the frequencies in a regeneration period must be one.
20. Researchers are encouraged to contribute their curated experiments to the centralized databases of Planform and Limbform. For this, please follow the instructions in the submission page of their respective websites.
21. While both worm and limb morphologies are defined with mathematical graphs, notice that the nodes of the graph define regions in a worm but joints in a limb.
22. A limb segment can have four configurations: normal, reversed, inverted, and reversed and inverted. When formalizing a limb morphology, these attributes are defined directly on each segment. When formalizing a limb manipulation, the reverse action affects the entire morphology (to reverse a smaller section, apply a crop action previous to the reverse action), and rotations can be freely applied to any graft using the join and relocation actions.
23. The file extension for PlanGexQ databases is *.gdb*. During the installation of PlanGexQ, a file type and extension association are automatically created in the operating system so that double clicking PlanGexQ database files automatically open them in the PlanGexQ tool. Similar to Planform and Limbform, these database files are locally stored in the SQLite version 3 (public domain) format.
24. The form to input new genes facilitates the search of their accession number from the Uniprot, SmedGD, and GenBank databases. After writing the gene name in the *Name* field, a link is shown that directly searches Uniprot and GenBank within the appropriate planarian species for the gene name entered. The link to SmedGD directs to the general search in that database. After entering the appropriate accession number from these databases, the link changes to a direct access to the appropriate gene information page. These direct links are also shown in the main expression pattern form.
25. The *Scan Caption* function searches in the caption from all the images for relevant keywords that are related to anatomical ontology terms and then suggest them for inclusion in the annotation. In addition, this function can suggest gene names for the experiment as found in the caption using a pattern matching approach. The *Scan Expression* function suggests

anatomical ontology terms according to the worm regions that include gene expression as currently input in the standard morphology. This function also updates the relative gene expression levels for each worm region of the current expression pattern.

26. The check marks in the ontology tree terms, selected terms, and suggested terms are always synchronized so it is clear which terms are assigned to the current expression pattern. To facilitate the annotation process, hovering the mouse over a term shows the description of the ontology term.

Acknowledgments

I thank the members of the Lobo Lab for their dedicated work and discussions. This work was supported by the National Institute of General Medical Sciences of the National Institutes of Health under award number R35GM137953. The content is solely the responsibility of the authors and does not necessarily represent the official views of the National Institutes of Health.

References

1. Li Q, Yang H, Zhong TP (2015) Regeneration across metazoan phylogeny: lessons from model organisms. J Genet Genomics 42:57–70. https://doi.org/10.1016/j.jgg.2014.12.002
2. Lobo D, Beane WS, Levin M (2012) Modeling planarian regeneration: a primer for reverse-engineering the worm. PLoS Comput Biol 8: e1002481. https://doi.org/10.1371/journal.pcbi.1002481
3. Rubin BP, Brockes J, Galliot B et al (2015) A dynamic architecture of life. F1000Research 4. https://doi.org/10.12688/f1000research.7315.1
4. Sánchez Alvarado A (2006) Planarian regeneration: its end is its beginning. Cell 124:241–245
5. Ivankovic M, Haneckova R, Thommen A et al (2019) Model systems for regeneration: planarians. Development 146:dev167684. https://doi.org/10.1242/dev.167684
6. Birkholz TR, Van Huizen AV, Beane WS (2019) Staying in shape: planarians as a model for understanding regenerative morphology. Semin Cell Dev Biol 87:105–115. https://doi.org/10.1016/j.semcdb.2018.04.014
7. Reddien PW (2018) The cellular and molecular basis for planarian regeneration. Cell 175:327–345. https://doi.org/10.1016/j.cell.2018.09.021
8. Brockes JR, Kumar A (2008) Comparative aspects of animal regeneration. Annu Rev Cell Dev Biol 24:525–549. https://doi.org/10.1146/annurev.cellbio.24.110707.175336
9. Joven A, Elewa A, Simon A (2019) Model systems for regeneration: salamanders. Development 146(14):dev1677000. https://doi.org/10.1242/dev.167700
10. Miller BM, Johnson K, Whited JL (2019) Common themes in tetrapod appendage regeneration: a cellular perspective. Evodevo 10:1–13. https://doi.org/10.1186/s13227-019-0124-7
11. Kato K, Orii H, Watanabe K et al (1999) The role of dorsoventral interaction in the onset of planarian regeneration. Development 126:1031–1040. https://doi.org/10.1242/dev.126.5.1031
12. Maden M, Turner RN (1978) Supernumerary limbs in the axolotl. Nature 273:232–235. https://doi.org/10.1038/273232a0
13. French V (1976) Leg regeneration in the cockroach, Blatella germanica. II. Regeneration from a noncongruent tibial graft/host junction. J Embryol Exp Morphol 35:267–301
14. Mace DL, Varnado N, Zhang W et al (2009) Extraction and comparison of gene expression

patterns from 2D RNA in situ hybridization images. Bioinformatics 26:761–769. https://doi.org/10.1093/bioinformatics/btp658

15. Deans AR, Lewis SE, Huala E et al (2015) Finding our way through phenotypes. PLoS Biol 13. https://doi.org/10.1371/journal.pbio.1002033
16. Christiansen JH, Yang Y, Venkataraman S et al (2006) EMAGE: a spatial database of gene expression patterns during mouse embryo development. Nucleic Acids Res 34: D637–D641. https://doi.org/10.1093/nar/gkj006
17. Lobo D, Malone TJ, Levin M (2013) Towards a bioinformatics of patterning: a computational approach to understanding regulative morphogenesis. Biol Open 2:156–169. https://doi.org/10.1242/bio.20123400
18. Lobo D, Feldman EB, Shah M et al (2014) A bioinformatics expert system linking functional data to anatomical outcomes in limb regeneration. Regeneration 1:37–56. https://doi.org/10.1002/reg2.13
19. Lobo D, Malone TJ, Levin M (2013) Planform: an application and database of graph-encoded planarian regenerative experiments. Bioinformatics 29:1098–1100. https://doi.org/10.1093/bioinformatics/btt088
20. Lobo D, Feldman EB, Shah M et al (2014) Limbform: a functional ontology-based database of limb regeneration experiments. Bioinformatics 30:3598–3600. https://doi.org/10.1093/bioinformatics/btu582
21. Broitman-Maduro G, Maduro MF (2011) In situ hybridization of embryos with antisense RNA probes. In: Rothman JH, Singson A (eds) Caenorhabditis elegans: molecular genetics and development. Academic Press, Waltham, MA, pp 253–270. https://doi.org/10.1016/B978-0-12-544172-8.00009-8
22. King RS, Newmark PA (2018) Whole-mount in situ hybridization of planarians. In: Rink JC (ed) Planarian regeneration: methods and protocols. Humana Press, New York, pp 379–392. https://doi.org/10.1007/978-1-4939-7802-1_12
23. Adell T, Barberán S, Sureda-Gómez M et al (2018) Immunohistochemistry on paraffin-embedded planarian tissue sections. In: Rink JC (ed) Planarian regeneration: methods and protocols. Humana Press, New York, pp 367–378. https://doi.org/10.1007/978-1-4939-7802-1_11
24. Forsthoefel DJ, Ross KG, Newmark PA et al (2018) Fixation, processing, and immunofluorescent labeling of whole mount planarians. In: Rink JC (ed) Planarian regeneration: methods and protocols. Humana Press, New York, pp 353–366. https://doi.org/10.1007/978-1-4939-7802-1_10
25. Ramos JA (2005) Technical aspects of immunohistochemistry. Vet Pathol 426:405–426. https://doi.org/10.1354/vp.42-4-405
26. Roy J, Cheung E, Bhatti J et al (2020) Curation and annotation of planarian gene expression patterns with segmented reference morphologies. Bioinformatics 36:2881–2887. https://doi.org/10.1093/bioinformatics/btaa023
27. Nowotarski SH, Davies EL, Robb SMC et al (2020) The planarian anatomy ontology: a resource to connect data within and across experimental platforms. Running title Keywords. bioRxiv. https://doi.org/10.1101/2020.08.14.251579
28. Lobo D, Levin M (2017) Computing a worm: reverse-engineering planarian regeneration. In: Adamatzky A (ed) Advances in unconventional computing, vol 2: prototypes, models and algorithms. Springer, Cham, pp 637–654. https://doi.org/10.1007/978-3-319-33921-4_24
29. Herath S, Lobo D (2020) Cross-inhibition of Turing patterns explains the self-organized regulatory mechanism of planarian fission. J Theor Biol 485:110042. https://doi.org/10.1016/j.jtbi.2019.110042
30. Ko JM, Lobo D (2019) Continuous dynamic modeling of regulated cell adhesion: sorting, intercalation, and involution. Biophys J 117:2166–2179. https://doi.org/10.1016/j.bpj.2019.10.032
31. García-Quismondo M, Levin M, Lobo D (2017) Modeling regenerative processes with Membrane Computing. Inf Sci (Ny) 381:229–249. https://doi.org/10.1016/j.ins.2016.11.017
32. Lobikin M, Lobo D, Blackiston DJ et al (2015) Serotonergic regulation of melanocyte conversion: a bioelectrically regulated network for stochastic all-or-none hyperpigmentation. Sci Signal 8:ra99. https://doi.org/10.1126/scisignal.aac6609
33. Lobo D, Levin M (2015) Inferring regulatory networks from experimental morphological phenotypes: a computational method reverse-engineers planarian regeneration. PLoS Comput Biol 11:e1004295. https://doi.org/10.1371/journal.pcbi.1004295
34. Mousavi R, Konuru SH, Lobo D (2021) Inference of dynamic spatial GRN models with multi-GPU evolutionary computation. Brief Bioinform 22(bbab104):1–11. https://doi.org/10.1093/bib/bbab104

35. Lobo D, Lobikin M, Levin M (2017) Discovering novel phenotypes with automatically inferred dynamic models: a partial melanocyte conversion in Xenopus. Sci Rep 7:41339. https://doi.org/10.1038/srep41339
36. Lobo D, Morokuma J, Levin M (2016) Computational discovery and in vivo validation of hnf4 as a regulatory gene in planarian regeneration. Bioinformatics 32:2681–2685. https://doi.org/10.1093/bioinformatics/btw299
37. Lobo D, Hammelman J, Levin M (2016) MoCha: molecular characterization of unknown pathways. J Comput Biol 23:291–297. https://doi.org/10.1089/cmb.2015.0211
38. UniProt Consortium (2019) UniProt: a worldwide hub of protein knowledge. Nucleic Acids Res 47:D506–D515. https://doi.org/10.1093/nar/gky1049
39. Robb SMC, Gotting K, Ross E et al (2015) SmedGD 2.0: the Schmidtea mediterranea genome database. Genesis 53:535–546. https://doi.org/10.1002/dvg.22872
40. Sayers EW, Cavanaugh M, Clark K et al (2019) GenBank. Nucleic Acids Res 47:D94–D99. https://doi.org/10.1093/nar/gky989
41. Giglio M, Tauber R, Nadendla S et al (2019) Eco, the evidence & conclusion ontology: community standard for evidence information. Nucleic Acids Res 47:D1186–D1194. https://doi.org/10.1093/nar/gky1036

Open Access This chapter is licensed under the terms of the Creative Commons Attribution 4.0 International License (http://creativecommons.org/licenses/by/4.0/), which permits use, sharing, adaptation, distribution and reproduction in any medium or format, as long as you give appropriate credit to the original author(s) and the source, provide a link to the Creative Commons license and indicate if changes were made.

The images or other third party material in this chapter are included in the chapter's Creative Commons license, unless indicated otherwise in a credit line to the material. If material is not included in the chapter's Creative Commons license and your intended use is not permitted by statutory regulation or exceeds the permitted use, you will need to obtain permission directly from the copyright holder.

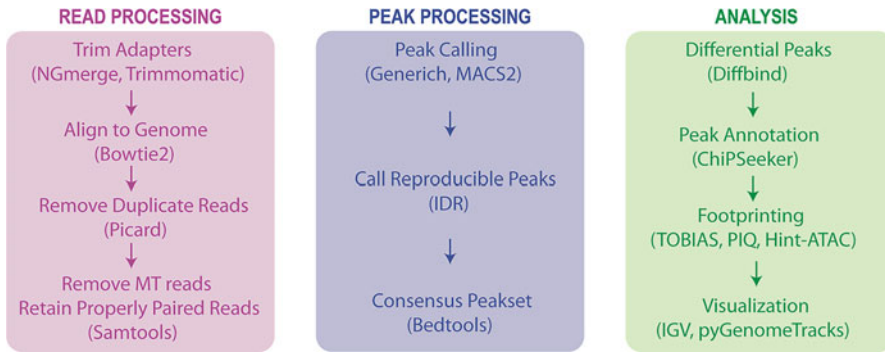


Correction to: Assessing Chromatin Accessibility during WBR in Acoels

Andrew R. Gehrke and Mansi Srivastava

Correction to:
Chapter 29 in: Simon Blanchoud and Brigitte Galliot (eds.), ***Whole-Body Regeneration: Methods and Protocols,*** **Methods in Molecular Biology, vol. 2450,**
https://doi.org/10.1007/978-1-0716-2172-1

In the original version of this book, Figure 3 in Chapter 29 was inadvertently published with some errors. This has been rectified in the updated version of this book.



The updated version of this chapter can be found at
https://doi.org/10.1007/978-1-0716-2172-1_29

Simon Blanchoud and Brigitte Galliot (eds.), *Whole-Body Regeneration: Methods and Protocols*,
Methods in Molecular Biology, vol. 2450, https://doi.org/10.1007/978-1-0716-2172-1_37, © The Author(s) 2022

INDEX

A

Acropora hyacinthus 368
Adaptations 5, 18, 85, 231, 315, 480
Aeolosoma viride 179–193, 468, 471, 472, 474, 476
Algae cultures 126, 142, 143, 147
Alkaline-comet assay 488
Anatomy 15, 53, 70, 154, 373, 374, 636, 650, 665, 673
Anesthesia 41, 147, 221, 306
Animal collection 297, 298
Annelida 137, 179–193, 195–204, 207–225
Antibody stainings 253, 258, 530
Apoptosis 73, 83, 84, 88, 89, 313, 566
Archeocytes 335, 336, 345
Arm explants 263–290
Ascidians 10, 18, 27–44, 312, 313, 325, 599, 609
Asexual reproductions 5, 17, 28, 32, 40, 70, 179, 245, 264, 293, 312, 401, 566
Assay for Transposase Accessible Chromatin sequences (ATAC-seq) 13, 549–551, 553, 555, 556, 559, 560

B

Barentsia benedeni 135, 137, 138, 141, 142, 147
Biomarkers 196
Botrylloides
anceps 311–330
diegensis 35, 36, 39, 312, 400, 408, 410
leachii 35, 36, 39, 43, 312, 401, 403, 599, 601, 609
Breeding ..... vi, 209, 227
Brown bodies 152, 154
Bryozoa 136, 151, 153
Budding 6, 12, 13, 28, 32, 39, 136, 153–155, 246, 312, 399

C

Cas9 ..... 423, 430, 439, 442–444, 448–450, 459–462
Cell cycle 73, 82, 89, 216, 374–376, 378–380, 382, 383, 386–391, 393, 395, 487
Cell cycling activity ..... vi, 375
Cell extraction ..... vi, 175, 350
Cell proliferation 6, 9, 33, 73, 82, 83, 88, 89, 96, 108, 115, 116, 181, 184, 216, 223, 375, 378, 381, 531
Characters 7–10, 12, 13, 137, 326
Chordates 28, 44, 263, 293, 311, 399, 599
Chromatin 529–545, 549–560
Chromatin Immunoprecipitation Followed by Sequencing (ChIP-seq) 529–545
Cnidaria 359, 360, 373, 419, 437, 635, 636
Coelomic fluid 583–596
Collections 36, 77, 98–100, 111, 138, 141, 147, 155, 156, 158, 159, 166, 197, 202, 229, 231–234, 238, 239, 266, 267, 269, 270, 279, 280, 285, 287, 294, 297, 299, 313, 314, 317, 325, 385, 387, 392, 400–406, 408, 410, 411, 413, 422, 423, 430, 497, 498, 584, 588, 644
Colonial ascidians 13, 17, 32, 35, 36, 38–41, 43, 44, 315, 325, 403, 408, 410, 599
Colonial circulatory system 28, 30, 35, 37, 39, 40
Comet assays 479–489
Corals 15, 18, 158, 208, 294, 303, 305, 313, 359–369, 419, 565
CRISPR/Cas9 ..... 430, 432, 442, 443, 449–451, 649
Cryptomonas baltica 147
Ctenophora 95, 96, 347
Culture 32, 33, 52, 53, 55–58, 63, 64, 76, 79, 86, 98, 100, 103–107, 112–114, 122, 126–128, 130, 131, 135–148, 152, 155–157, 162–164, 169–171, 174, 181, 183, 184, 191, 192, 197, 199, 200, 203, 210, 212, 220, 221, 224, 234–241, 246, 247, 252, 254, 257, 264, 266, 305, 313, 325, 347–357, 390, 394, 401, 409, 420, 422, 432, 433, 442, 450, 451, 493, 494, 496, 500, 504, 505, 507, 565, 621–622, 624

Simon Blanchoud and Brigitte Galliot (eds.), *Whole-Body Regeneration: Methods and Protocols*, Methods in Molecular Biology, vol. 2450, https://doi.org/10.1007/978-1-0716-2172-1,

© The Editor(s) (if applicable) and The Author(s) 2022

D

Databases 185, 238, 326, 425, 429, 434, 530, 586, 592, 594, 649–661, 665, 668–670, 672, 673
Data mining 651, 653, 660
De novo axis formation 619
Developments 5–8, 18, 32, 35, 40, 41, 53, 70, 113, 154, 207, 216, 219, 222, 224, 225, 254, 294, 311, 312, 344, 367, 369, 401, 420, 433, 437–439, 448, 456, 457, 463, 493, 506, 549, 599, 620, 621, 651, 652, 655, 656, 658–661
Differential expression 600, 601, 656
DIG-labeled RNA probes 296, 341, 361
Diopatra neapolitana 195–204
DNA barcoding 313, 314, 316, 317, 325, 326
DNA damage 480, 486–488
DNA electrophoresis 480, 535, 538, 542, 570, 572, 580
DNA extraction 137, 238, 246, 256, 306, 422, 442, 449, 463, 473
Double strand breaks 479–489
Drug treatment ..... vi, 488
DsRNA synthesis 511, 512, 515, 516, 521
Dugesia japonica 509, 521

E

Echinaster sepositus 263–290
Echinodermata 263–289, 593
Ecology 15, 17, 18, 195, 196, 231, 294, 335
EdU labeling 33, 34, 116, 180, 186, 192, 216, 218, 223, 259, 378, 388–390
Electron microscopy 38, 71, 73, 81, 87, 155, 165, 264
Electroporation 183, 186, 428, 439, 443, 445, 447, 453, 455, 456, 458, 637–640, 643
Embryonic development 223, 493, 649–660
Endpoints 58, 59
Entoprocta 136
Environmental alterations 195–204
Ephydatia fluviatilis 335–345
Epigenetic regulation 529–532
Epithelial stem cells (ESCs) 374, 377, 389, 391, 392
Evisceration 32, 34, 41, 42
Evolution 5, 8–13, 15, 17–19, 69, 137, 207, 225, 263, 294, 335, 348, 437, 549, 599, 649, 651
Extracts 62, 144, 147, 192, 233, 286, 350, 425, 427, 428, 432, 471, 472, 477, 553, 583, 585, 588–590, 594, 605, 609, 626, 628, 641

F

Feedings 17, 27, 63, 96, 97, 104, 105, 107, 112, 114, 115, 123, 135, 137, 142, 143, 147, 152, 153, 155, 156, 162, 169, 171, 172, 186, 190, 193, 213, 221, 235, 236, 238–240, 257, 259, 305, 313, 314, 421, 438, 462, 463, 509–511, 516–519, 522–524, 584, 627
Fixations 79–82, 85, 87, 109, 129, 137, 139, 144, 163, 174, 175, 184, 210, 213, 215, 216, 218, 223, 246, 251, 253, 258, 267, 270–272, 275, 276, 329, 403, 407, 485
Flatworms 10, 15, 227, 480, 493–507, 509
Flow cytometry 349, 354, 373–395, 401, 406, 407, 412, 480, 571, 574
Fluorescence-activated cell sorting (FACS) 36, 373, 376–378, 386, 387, 537, 542, 566, 569, 571–573, 579
Formalizations 664–666, 668, 669, 671
Functional genomics 549

G

Gene expression 36, 44, 54, 193, 222, 231, 259, 293, 294, 304, 306, 336, 347, 349, 359–369, 420, 426, 480, 521, 530–532, 569, 577, 600–602, 605, 607, 613, 637, 644, 649–660, 665, 667, 671–673, 677
Gene knockdown 420, 457, 518, 522
Gene ontology (GO) 600, 601, 606–609, 613, 659, 665
Genotyping 423, 430, 432, 461, 462
Gonads 18, 28, 29, 31, 34, 35, 41, 69, 96, 113, 374
Growth 5, 16–18, 52, 54, 55, 57–59, 62–64, 70, 72, 111, 141, 147, 154, 155, 157, 162, 164, 167, 171, 180, 184, 208–210, 214, 216, 222, 241, 246, 285, 348, 354–356, 420, 438, 460, 506, 518, 519, 533, 635

H

Hemichordata 293–308
Hemolymph 399, 401, 403–408, 410, 411, 413
Histological sectioning
  semithin sectioning 268, 273–276, 279–282, 287, 289
  ultrathin sectioning 268, 274, 276, 279, 282–284, 289
Histology 13, 34, 36, 37, 155, 157, 163, 266, 321
Histone modifications 530, 532
Hofstenia miamia 10, 245, 551, 558
Homology 8, 10, 13, 592, 593, 656

Husbandry 98, 100, 104, 106, 183, 267, 269, 295, 313, 317, 318, 320, 321, 325, 327, 464
Hydractinia 419–434, 456
Hydra vulgaris 384, 643

I

Image analysis 55, 626
Image quantification ..... vi, 625–626
Immunohistochemistry 34, 36, 37, 71, 327, 463, 480, 665
Immunoprecipitations 529–545
Inference 239, 566, 665–667
Injections 36, 41, 42, 54, 59, 60, 64, 191, 401, 407–413, 420, 421, 424, 425, 429–431, 433, 439, 443–445, 447, 449, 450, 453, 455, 457, 458, 460–462, 496, 500, 501, 503, 505, 506, 511, 516, 518, 522, 668
Injuries 6, 7, 13, 14, 17, 18, 32, 52, 54, 57, 58, 64, 70, 110, 154, 195, 208, 221, 228, 312, 360, 399, 401, 509, 511, 517, 522, 529, 585
Innate immunity 361
In situ hybridisation
FISH 336, 342, 344, 345, 468, 476
Interstitial stem cells (ISCs) 336, 374, 375, 392
Intertidal 155, 169, 196, 202, 229, 231–233, 238, 294, 315
Irradiation 33, 37, 480, 486, 501, 664, 669
Isodiametra pulchra 10, 245–260

K

Kamptozoa 135–137, 141, 147, 148
Knockdown 36, 37, 431, 439, 441, 453, 454, 457–459, 463, 480, 522–524, 530, 531, 668

L

Larvae 18, 43, 99, 104, 105, 107, 111, 112, 114, 135, 136, 155, 162, 168, 172–174, 213, 220, 224, 361, 423–425, 449, 457, 566
Leucosolenia sp. 69–91
Lineus sanguineus 227–242
Live imaging 34, 36, 41, 96, 108, 110, 115, 117, 524, 621

M

Macrostomum lignano 493–507
Marthasterias glacialis 264, 583–596
Mazes 53–55, 58, 59
Mechanical oscillations 619–632
Microinjections 36, 114, 189–191, 193, 400, 403, 408, 413, 421, 429–432, 439, 442–445, 447, 449, 456, 494–502, 504, 505, 507
Microscopy 36, 54, 55, 59, 60, 64, 71, 73, 109, 122, 127, 155, 272, 276, 313, 314, 321, 343, 400, 486, 664, 667, 669, 672, 673
Mnemiopsis leidyi 95–117, 347–357
Modeling 54, 655
Musashi 335, 336, 345
Mutagenesis 439, 441–443, 448–450, 457–463

N

NBT/BCIP staining 188, 211, 297, 339–341
Nematostella vectensis 437–463, 565–580, 649–661
Nemertea 137, 227–242
Neoblast stem cells 246
Networks 8, 32, 51–55, 57, 59–63, 65, 511, 566, 583, 584, 636, 666, 669
Neural complex 28, 29, 31, 34, 35, 41

O

Open-access 649–660

P

Partial regeneration 6, 28, 35, 37, 39–41, 43
Patterning 14, 54, 266, 325, 510, 517, 529, 637
Phalloidin 139, 248, 249, 255, 650
Pharmacological inhibitors 219, 223
Phylogenies 8, 12, 15–17, 137, 153
Physarum polycephalum 51–65
Pilidiophora 229
Piwi 10, 36, 247, 335, 336, 421
Placozoa 121
Planarians 10, 12, 15, 235, 336, 345, 374, 378, 467, 479–489, 509–524, 529–544, 663–665, 667, 668, 671, 673
Platyhelminthes 10, 494
Platynereis dumerilii 207–225
Pluripotency 335, 529, 530
Polychaetes 136, 141, 180, 195–197, 202, 203
Porifera 9, 69
Posterior regeneration 180, 184, 201, 216, 222, 306
Preabsorbed antibodies 295, 301, 303
Primary cell cultures 348, 349, 352, 354, 356
Proliferation 9, 10, 52, 53, 73, 116, 312, 348, 356, 359, 378, 391, 437, 468, 566

Protein extraction 6, 471, 477, 583, 585, 588–590
Proteomics 362, 376, 387, 412, 583, 585, 586, 591, 593, 595
Protista 51
Ptychodera flava 293–308

Q

QPCR 36, 37, 457, 559, 637, 641, 642, 644, 646

R

Random integration 498–500
Reaggregation 9, 71, 73, 78, 86, 124, 129, 130, 389, 635–646
Real time PCR 637–639, 641, 642, 646
Regeneration 3–19, 27–44, 51–65, 69–91, 95–117, 121–131, 137, 139, 143, 151, 154, 155, 162, 169, 171, 179–193, 195–204, 207–225, 227–242, 245–260, 263–289, 293–308, 311–330, 348, 359–362, 368, 375, 378, 380, 382, 387, 395, 399, 401, 419, 420, 437–439, 441, 467–478, 493, 494, 509–524, 529–531, 549–560, 565–567, 577, 584, 585, 595, 599–614, 619–632, 635–646, 649–660, 663–677
Regression 18, 40, 152, 154, 212, 404, 406
RNA extraction 139, 144, 246, 247, 255, 256, 269, 284, 285, 306, 387, 393, 607, 609, 638, 639, 641, 642
RNA interference 180, 183, 186, 246, 250, 253, 429, 486, 488, 511, 516, 518, 519, 637, 668
RNA sequencing 44, 54, 566–568, 571, 574, 599–613
RNA synthesis 337, 339, 344

S

Schmidtea mediterranea 235, 509, 511, 514, 521, 529–531
Screening 98, 354, 441, 445, 447–451, 462, 464, 509–524
Self-organization 636
Sequencing 146, 148, 256, 314, 319, 326, 349, 360, 427, 428, 450, 451, 460, 462, 463, 529–545, 550, 554, 559, 566, 567, 572, 575, 576, 578, 599, 602, 607, 609, 612, 651
Serum 174, 181, 211, 249, 295, 296, 301, 302, 349, 350, 352, 363, 383, 402, 406, 470, 584
Settlement 141, 157, 168, 172, 173, 196
ShRNAs 422, 425, 429–431, 434, 439–441, 443–448, 450, 453–459, 463
Signaling 13, 36, 38, 52, 219, 223, 264, 348, 362, 509, 510, 584, 596, 619, 620, 635–637
Single-cell RNA-seq 566, 567, 569, 572, 575, 576
Siphons 28–31, 33, 35, 37, 38, 40–42, 311, 325, 327
siRNA electroporation 637, 638
Slime moulds 51–53
Spawning 15, 100, 106, 112, 113, 162, 170, 172, 420, 423, 432, 448, 450, 463
Spiralia 227
Sponges 9, 10, 15, 18, 69–91, 141, 227, 325, 335–345
Stainings 34, 36, 73, 87–90, 115, 128, 137, 139, 144, 165, 174, 182, 188, 211, 217, 222, 223, 246, 249, 251, 253–255, 259, 268, 274–276, 280, 282–284, 294, 297, 303, 307, 308, 313, 314, 316–318, 320, 329, 330, 338, 343, 361, 368, 378, 379, 382–384, 387, 388, 392, 394, 401, 463, 473, 485–487, 489, 520, 521, 523, 569, 571, 586, 590
Starfish 263, 264, 266, 267, 269–271, 279, 287, 583–596
Stem cells 11, 13, 16, 27, 32, 33, 40, 54, 122, 129, 154, 208, 209, 246, 247, 312, 335–345, 360, 362, 373–395, 401, 467, 480, 486, 487, 493, 494, 509–511, 521, 523, 524, 529–545
Surgery 43, 71, 73, 77–79, 96, 101, 107, 114, 115
Suspension culture 347–356
Symmetry breaking 620, 637

T

Tandem mass spectrometry 584
Telomere FISH 471, 474, 476
Telomere maintenance 467–478
Telomere monitoring 467–478
TEM grid staining 283
Thorax 28, 31, 33, 40, 42
Time-lapse 58, 59, 71, 73, 79, 86, 96, 99, 110, 111, 116, 117, 129
Tissue dissociation 71, 73, 378, 391, 393, 620
Tissue spheroids 623, 624
Transfusion 400
Transgenesis 44, 420, 439, 493–507, 649
Transmission electron microscopy (TEM) 34, 36, 37, 71, 72, 79–81, 87, 175, 266, 268, 270, 271, 275, 276, 279, 282–284, 287–289
Transplantation 33, 124, 125, 130, 619
TRAP assay 472
TRF assay 474, 477

Trichoplax adhaerens 121–131
Tunic 28, 30–34, 37, 40, 41, 43, 311, 328, 400, 403, 405, 408, 410, 411, 413, 609
Tunicata 27, 311–330, 599

U

Ultrastructure 123, 168, 266

V

Vascular budding 39, 312
Vital stainings 128

W

Whole-mount in situ hybridization (WISH) 162, 180, 182, 185, 193, 308, 336, 342, 344, 456
Wnt3 ..... 635–637, 639, 644, 646
Wound healing 8, 13, 73, 96, 101, 107, 110, 111, 115, 117, 124, 129, 195, 214, 300, 347, 348, 354, 361, 467

X

Xenacoelomorpha 10, 12, 245–260